APR1400
DESIGN CONTROL DOCUMENT TIER 2

CHAPTER 15
TRANSIENT AND ACCIDENT ANALYSES

APR1400-K-X-FS-13002
REVISION 0
SEPTEMBER 2013

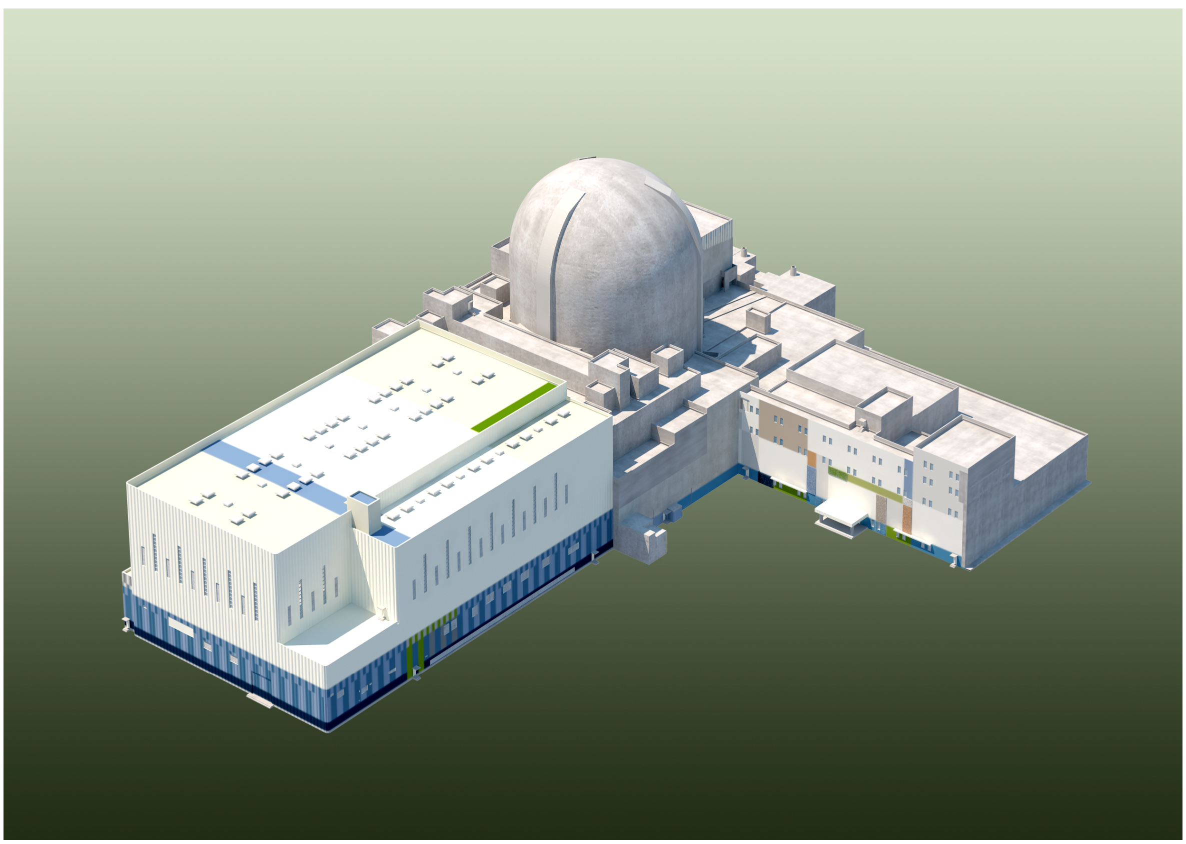

KOREA ELECTRIC POWER CORPORATION
KOREA HYDRO & NUCLEAR POWER CO., LTD

CHAPTER 15 – TRANSIENT AND ACCIDENT ANALYSES

TABLE OF CONTENTS

LIST OF TABLES

LIST OF FIGURES

ACRONYM AND ABBREVIATION LIST

AB	Auxiliary Building
AC	Alternation Current
ADV	Atmospheric Dump Valve
AFAS	Auxiliary Feedwater Actuation Signal
AFW	Auxiliary Feedwater
AOO	Anticipated Operational Occurrence
APR1400	Advanced Power Reactor 1400
ARSAP	Advanced Reactor Severe Accident Program
ASI	Axial Shape Index
AST	Alternative Source Term
ATWS	Anticipated Transient Without Scram
BOC	Beginning of Cycle
BWR	Boiling Water Reactor
CCW	Component Cooling Water
CEA	Control Element Assembly
CEAC	Control Element Assembly Calculator
CEAE	Control Element Assembly Ejection
CEDE	Committed Effective Dose Equivalent
CEDM	Control Element Drive Mechanism
CEDMCS	Control Element Drive Mechanism Control System
CHF	Critical Heat Flux
CIAS	Containment Isolation Actuation Signal
CLVPS	Containment Low Volume Purge System
COL	Combined License
COLR	Core Operating Limits Report
COLSS	Core Operating Limit Supervisory System
CPC	Core Protection Calculator
CPCS	Core Protection Calculator System
CPIAS	Containment Purge Isolation Actuation Signal

CS	Containment Spray
CSAS	Containment Spray Actuation Signal
CSS	Containment Spray System
CVCS	Chemical and Volume Control System
DBA	Design Basis Accident
DBE	Design Basis Event
DCF	Dose Conversion Factor
DDE	Deep Dose Equivalent
DE	Dose Equivalent
DEG/PD	Double-ended Guillotine at the Pump Discharge
DF	Decontamination Factor
DNB	Departure from Nucleate Boiling
DNBR	Departure from Nucleate Boiling Ratio
DPS	Diverse Protection System
DVI	Direct Vessel Injection
EAB	Exclusion Area Boundary
ECC	Emergency Core Cooling
ECCS	Emergency Core Cooling System
EDE	Effective Dose Equivalent
EFPD	Effective Full Power Day
EOC	End of Cycle
EOP	Emergency Operating Procedure
ESF	Engineered Safety Feature
ESFAS	Engineered Safety Features Actuation System
ESF-CCS	Engineered Safety Features Component Control System
FF	Flash Fraction
FHA	Fuel Handling Accident
FHAEVAS	Fuel Handling Area Emergency Ventilation Actuation Signal
FLB	Feedwater Line Break
FMEA	Failure Modes and Effects Analysis
FTC	Fuel Temperature Coefficient

FWCS	Feedwater Control System
GDC	General Design Criteria
GIS	Generated Iodine Spike
GSI	Generic Safety Issue
HEPA	High Efficiency Particulate Air
HFP	Hot Full Power
HPPT	High Pressurizer Pressure Trip
HSGL	High Steam Generator Level
HVAC	Heating Ventilating and Air Conditioning
HZP	Hot Zero Power
ICC	Inadequate Core Cooling
ICRP	International Commission on Radiological Protection
IOSGADV	Inadvertent Opening of a Steam Generator Atmospheric Dump Valve
IRWST	In-containment Refueling Water Storage Tank
ITC	Isothermal Temperature Coefficient
LBLOCA	Large Break Loss-of-Coolant Accident
LCO	Limiting Conditions for Operation
LDLB	Letdown Line Break
LFW	Loss of Normal Feedwater Flow
LHGR	Linear Heat Generation Rate
LHR	Linear Heat Rate
LOAC	Loss of Nonemergency AC Power
LOCA	Loss-of-Coolant Accident
LOCV	Loss of Condenser Vacuum
LOF	Loss of Flow
LOFW	Loss of Normal Feedwater Flow
LOOP	Loss of offsite Power
LPD	Local Power Density
LPLD	Low PZR Pressure and Low DNBR
LPZ	Low Population Zone
LSGL	Low Steam Generator Level

LTC	Long-Term Cooling
LTOP	Low Temperature Overpressure Protection
MCR	Main Control Room
MDNBR	Minimum Departure from the Nucleate Boiling Ratio
MFS	Main Feedwater System
MSIS	Main Steam Isolation Signal
MSIV	Main Steam Isolation Valve
MSLB	Main Steam Line Break
MSSV	Main Steam Safety Valve
MTC	Moderator Temperature Coefficient
NRC	Nuclear Regulatory Commission
NSSS	Nuclear Steam Supply System
PA	Postulated Accident
PAMI	Post-accident Monitoring Instrumentation
PCMI	Pellet Cladding Mechanical Interaction
PCT	Peak Cladding Temperature
PIS	Pre-accident Iodine Spike
PLCS	Pressurizer Level Control System
PLHGR	Peak Linear Heat Generation Rate
POL	Power Operating Limit
POSRV	Pilot Operated Safety and Relief Valve
PPCS	Pressurizer Pressure Control System
PPS	Plant Protection System
P-T-S	Primary-to-Secondary
PWR	Pressurized Water Reactor
RADTRAD	Radionuclide Transport, Removal, and Dose
RCFC	Reactor Containment Fan Cooler
RCGVS	Reactor Coolant Gas Vent System
RCP	Reactor Coolant Pump
RCPB	Reactor Coolant Pressure Boundary
RCS	Reactor Coolant System

RHR	Residual Heat Removal
RIA	Reactivity-initiated Accident
RMI	Reflective Metal Insulation
RMS	Radiation Monitoring System
RPCS	Reactor Power Cutback System
RPS	Reactor Protection System
RRS	Reactor Regulating System
RTO	Reactor Trip Override
RTP	Return to Power
RV	Reactor Vessel
SAFDL	Specified Acceptable Fuel Design Limit
SBCS	Steam Bypass Control System
SBLOCA	Small Break Loss-of-Coolant Accident
SCS	Shutdown Cooling System
SDC	Shutdown Cooling
SDM	Shutdown Margin
SER	Safety Evaluation Report
SF	Single Failure
SFP	Spent Fuel Pool
SG	Steam Generator
SGTR	Steam Generator Tube Rupture
SI	Safety Injection
SIAS	Safety Injection Actuation Signal
SIP	Safety Injection Pump
SIRCP	Startup of an Inactive Reactor Coolant Pump
SIS	Safety Injection System
SIT-FD	Safety Injection Tank with Fluidic Device
SIT	Safety Injection Tank
SLB	Steam Line Break
SLBFP	Large Steam Line Break during Full Power Operation
SLBZP	Large Steam Line Break during Zero Power Operation

SRM	Source Range Monitoring
SRP	Standard Review Plan
SRS	Simple Random Sampling
SRSS	Square-root-sum-of-the-squares
TBV	Turbine Bypass Valve
TEDE	Total Effective Dose Equivalent
TSC	Technical Support Center
TS	Technical Specification
UGS	Upper Guide Structure
USEPA	U.S. Environmental Protection Agency
USI	Unresolved Safety Issue
VOPT	Variable Overpower Trip

CHAPTER 15 – TRANSIENT AND ACCIDENT ANALYSES

15.0 Introduction: Transient and Accident Analyses

15.0.0 General Information for Safety Analyses

This chapter presents the analysis of the response of the Advanced Power Reactor 1400 (APR1400) nuclear steam supply system (NSSS) to postulated transients in process variables and to postulated malfunctions or failures of equipment. Such incidents (or events) are postulated, and their consequences are analyzed despite the many precautions that are taken in the design, construction, quality assurance, and plant operation to prevent their occurrence. The effects of the incidents are examined to determine their consequences and to evaluate the capability of the plant design to control or accommodate such failures and conditions.

The incidents analyzed in this chapter are presented in accordance with the guidance in References 1 and 2. The subsections that address the incidents are numbered as described in Table 15.0-1. The documents that are cited in Chapter 15 are listed in Subsection 15.0.5.

Tables 15.0-11, 15.0-12, and 15.0-13 show how the APR1400 complies with the applicable TMI-related requirements, unresolved safety issues (USIs) and generic safety issues (GSIs), and the operating experience insights in Generic Letters and bulletins, respectively.

15.0.0.1 Transient and Accident Classification

The event frequency category is indicated in Table 15.0-5 for each design basis event and event combination considered. The two major event frequency categories are as follows:

a. Anticipated operational occurrence (AOO): “conditions of normal operation which are expected to occur one or more times during the life of the nuclear power unit and include but are not limited to loss of power to all recirculation pumps, tripping of the turbine generator set, isolation of the main condenser, and loss of all offsite power” (10 CFR 50, Appendix A).

   The current Standard Review Plan (SRP) for Chapter 15 uses the term AOO to refer to the events that are categorized in Nuclear Regulatory Commission (NRC) RG

1.206 as incidents of moderate frequency (i.e., events that are expected to occur several times during the life of the plant) and infrequent events (i.e., events that may occur during the life of the plant).

b. Postulated accident (PA): Events that are not expected to occur during the life of the nuclear power unit but are postulated because they pose the potential for the release of a significant amount of radioactivity.

AOOs and PAs for the APR1400 fall into one of the following event categories:

a. Increase in heat removal by the secondary system

b. Decrease in heat removal by the secondary system

c. Decrease in reactor coolant system (RCS) flow rate

d. Reactivity and power distribution anomaly

e. Increase in RCS inventory

f. Decrease in RCS inventory

g. Radioactive release from a subsystem or component

15.0.0.1.1 Normal Operation and Anticipated Operational Occurrences

Normal operation includes general categories corresponding to the operating modes in which they occur such as plant heatup and cooldown, power level increases, and load decreases. These types of normal operational occurrences have historically not been addressed in accident analyses.

AOOs are the conditions that may occur one or more times during the life of the plant. The occurrences that are considered are single component or control system failures resulting in transients that may require protective action.

The fuel design and reactor coolant pressure boundary (RCPB) limits used in the reactor protection system (RPS) design for the AOOs are as follows:

a. The departure from the nucleate boiling ratio (DNBR) in the limiting coolant channel in the core is not less than the DNBR safety limit of 1.29

b. The hot fuel pellet in the core does not experience centerline melting. Maintaining the peak linear heat rate (LHR) less than 656 W/cm (20 kW/ft) provides reasonable assurance that fuel centerline melt will not occur during an AOO.

c. The RCS pressure does not exceed the established pressure boundary limits (110 percent of design pressure)

15.0.0.1.2 Postulated Accidents

PAs are unanticipated occurrences. The following are examples of PAs in pressurized water reactors (PWRs):

a. Major rupture of a pipe containing reactor coolant up to and including double-ended rupture of the largest pipe in the RCPB

b. Ejection of a control rod assembly

c. Major secondary system pipe rupture up to and including double-ended rupture

d. Single reactor coolant pump locked rotor

The basic criteria for PAs are as follows:

a. Pressures in the reactor coolant and main steam systems are maintained below the acceptable design limits.

b. Fuel cladding integrity is maintained by providing reasonable assurance that the minimum DNBR remains above the 95/95 DNBR limit. If the minimum DNBR does not meet this limit, the fuel is assumed to have failed.

c. The release of radioactive material does not result in offsite doses in excess of the guidelines in 10 CFR 50.34. Any event-specific accident limits for allowable radiological releases are described in the appropriate sections.

d. The postulated accident does not by itself result in a consequential loss of required functions of systems needed to cope with the fault, including those of the RCS and the reactor containment system.

For reactivity-initiated accidents (RIAs), SRP 4.2, Appendix B (Interim Acceptance Criteria and Guidance for the Reactivity Initiated Accidents), provides the following additional acceptance criteria regarding core coolability, which are considered an extension of criterion d above:

a. Peak radial average fuel enthalpy remains below 230 cal/g.

b. Peak fuel temperature remains below incipient fuel melting conditions.

c. Mechanical energy generated as a result of non-molten fuel-to-coolant interaction and fuel rod burst is addressed with respect to pressure boundary, reactor internals, and fuel assembly structural integrity.

d. No loss of coolable geometry occurs from fuel pellet or cladding fragmentation or dispersal or from fuel rod ballooning.

15.0.0.2 Plant Characteristics and Initial Conditions Assumed in the Accident Analysis

15.0.0.2.1 Design Plant Conditions

AOOs and PAs are considered to occur over a safety analyses range of initial plant operating conditions. The range is chosen to bound all steady-state operational configurations. These values are used to establish the limits for the Technical Specifications with appropriate allowances for surveillance intervals and instrument uncertainties.

Each event considers the status of the control systems, which are the steam bypass, feedwater, pressurizer pressure, and pressurizer level. If a control system is used to mitigate a transient, the analysis of the transient assumes that the control system is in the manual mode of operation. Control systems are assumed to be in the automatic mode of operation if the control system makes the consequences of a transient more adverse.

15.0.0.2.2 Initial Conditions

The events described in this chapter were analyzed over a range of initial values for the principal process variables. The ranges were chosen to encompass all steady-state operational configurations.

The analyses performed over a range of initial conditions are compatible with the monitoring function performed by the core operating limit supervisory system (COLSS), which is addressed in Subsection 7.7.1.4, and the flexibility of plant operation that the COLSS allows. This flexibility is produced by allowing parameter trade-offs by monitoring the principal process variables, synthesizing the margin to fuel thermal design limits, and displaying the core power operating limit to the reactor operator. Table 15.0-3 contains the range of values of each principal process variable that is considered in the event analyses, and Table 15.0-6 contains the initial conditions for the event analyses.

15.0.0.2.3 Reactivity Coefficients

Doppler Coefficient

The fuel temperature coefficient of reactivity (Doppler coefficients) is addressed in Subsection 4.3.2.3.1. The safety analysis uses a more negative or less negative Doppler feedback coefficient including uncertainties in order to produce a more adverse result that is closer to the analytical acceptance criteria.

Moderator Temperature Coefficient

The events analyzed in this chapter model moderator reactivity as a function of moderator temperature instead of a moderator temperature coefficient. The moderator temperature coefficients corresponding to the moderator reactivity functions range from 0.0×10^{-4} $\Delta\rho$/°C (0.0×10^{-4} $\Delta\rho$/°F) to -5.4×10^{-4} $\Delta\rho$/°C (-3.0×10^{-4} $\Delta\rho$/°F) at nominal full power condition (T_{avg}

= 308.9 °C or 588 °F). These values include all uncertainties and bound the expected moderator temperature coefficients for first cycle burnup power level, control element assembly (CEA) configurations, and boron concentrations.

The most conservative moderator temperature coefficient is assumed for each analysis.

Shutdown CEA Reactivity

The shutdown reactivity is dependent on the CEA worth available on reactor trip and the axial power distribution. For most transient analyses, conservative total CEA worths of −8.0 %Δρ and −5.5 %Δρ are used for hot full power and hot zero power (HZP), respectively. For some events, more conservative values are used. However, in steam line break events, a CEA worth of −9.3 %Δρ is used for the full power cases. The values include uncertainties, the most reactive CEA stuck in the fully withdrawn position, and the effect of temperature on CEA worth for events initiated from the HZP (Subsection 4.3.2.4.3).

The shutdown reactivity worth versus position curve that is used in most of the Chapter 15 analyses is shown in Figure 15.0-1 and is applicable for an axial shape with an axial shape index (ASI) of +0.3. The shutdown worth versus position curve yields a conservatively slower rate of negative reactivity insertion than is expected to occur during the majority of operations, including power maneuvering. Accordingly, it is a conservative representation of shutdown reactivity insertion rates for the reactor trips that occur as a result of the events that are analyzed. For some events, a dynamic axial power function is used based on the HERMITE code (Subsection 15.0.2.2.5).

15.0.0.2.4 CEA Insertion Characteristics

The control element drive mechanism (CEDM) is designed to function during and after all normal plant transients. The CEA drop time for a 90 percent insertion rate is a maximum of 4.0 seconds. The drop time is defined as the interval between the time the power is removed from the CEDM coils and the time the CEA has reached 90 percent of its fully inserted position.

15.0.0.2.5 Residual Decay Heat

Total Residual Decay Heat

The ANS 5.1-1979 standard decay heat model is used to calculate the decay heat generation in large-break loss-of-coolant accident (LBLOCA) analyses, and the ANS 5.1-1971 decay heat model is applied to small-break loss-of-coolant accident (SBLOCA) and the post-loss-of-coolant accident (LOCA) long-term cooling analyses. The non-LOCA analyses use the ANS 5.1-1973 decay heat curve with uncertainties.

Distribution of Decay Heat Following a Loss-of-Coolant Accident

Neutron, gamma, and beta energy fission products are generated during normal operation. In a LOCA, there are no neutron-induced chain reactions because the reactor is tripped either by void formation or by CEA insertion. Only gamma and beta radiation is created during a LOCA. During a LOCA, some gamma radiation is released from the fuel rod into another fuel rod, the reactor coolant, or the core structure while the beta radiation remains stored in the fuel rods, resulting in a redistribution of the core heat after the LOCA.

15.0.0.3 Reactor Trip System and Engineered Safety Feature Systems Analytical Limit and Delay Times

During any event, various systems operate in response to the event. The sequence of events and systems operations include information about systems operations. The systems that may operate in an event are (1) electrical, instrumentation, and control systems that are designed to perform a safety function, which are systems that operate during an event to mitigate the consequences and (2) systems that are not required to perform a safety function. Refer to Sections 7.2 through 7.6 and Section 7.7, respectively.

The RPS is described in Section 7.2. Table 15.0-2 lists the RPS trips for which credit is taken in the analyses that are described in Chapter 15, including the setpoint and response times associated with each trip. The analyses take into consideration the response times of actuated devices after the value of the monitored parameter at the sensor has equaled or exceeded the trip setpoint. The relevant reactor trip functions and engineered safety feature (ESF) functions for each event are shown in Table 15.0-7, and the specified reactor

trip setpoints and ESF actuations are provided in the sequence of events for the relevant event.

The RPS total response time is the sum of the RPS sensor response time and the reactor trip delay time. The sensor response time is defined as the difference of the value of the monitored parameter when the sensor equals or exceeds the reactor protection system trip setpoint and when the sensor output equals or exceeds the trip setpoint. The sensor response is modeled by using a transfer function for the relevant sensor. The reactor trip delay time is defined as the difference of the sensor output when it equals or exceeds the trip setpoint and when the reactor trip breakers are fully open. The interval between the following two points is assumed to be 0.50 second: (1) the opening of the trip breaker and (2) when the magnetic flux of the CEA holding coils has decayed enough to allow CEA motion.

The engineered safety feature actuation systems (ESFASs) and electrical, instrumentation, and control systems required for safe shutdown are addressed in Sections 7.3 and 7.4, respectively. The manner in which the systems function during events is addressed in the description of the event. The instrumentation that is required to be available to the operator to assist with evaluating the nature of the event and determining the required action is addressed in Section 7.5. The operator's use of the instrumentation is addressed in each event description.

Other systems that function during events are addressed in Chapters 6 and 9. The use of these systems is specified in the appropriate event descriptions.

Systems that may perform safety functions but are not required to are addressed in Section 7.7. These systems include various control systems and the COLSS. In general, the normal automatic operation of these control systems is assumed unless manual operation would make the consequences of the event more adverse.

15.0.0.4 Component Failures

Component failures could cause events such as a steam system piping failure. Components are discrete items from which a system is assembled. Examples of components are wires, transistors, switches, motors, relays, solenoids, pipes, fittings, pumps,

tanks, and valves. The accident analyses assume that any equipment that can be failed as a consequence of the initiating event is not available for the accident mitigation.

According to 10 CFR 50, Appendix A, a single failure is an occurrence that results in the loss of the capability of a component to perform its safety functions. Multiple failures from a single occurrence are considered a single failure. Fluid and electrical systems are considered to be designed against an assumed single failure if the following failures do not result in a loss of the capability of the system to perform its safety functions: (1) a single failure of any active component (assuming passive components function properly) and (2) a single failure of a passive component (assuming active components function properly).

An active component is a component in which mechanical movement occurs in order to accomplish the nuclear safety function of the component. A passive component is a component that is not an active component. Active and passive failures are described in more detail in the following two subsections.

15.0.0.4.1 Active Failures

An active failure is a malfunction, excluding passive failure, of a component that relies on mechanical movement to complete its intended nuclear safety function on demand. Examples of active failures are the failure of a valve or check valve to move to its correct position and the failure of a pump, fan, or diesel generator to start.

Examples of an active failure in mechanical components are:

a. Failure of an item of equipment whose operation requires a mechanical movement by one of its components in order to carry out an operation on demand

b. Incomplete actuation of an item of equipment with the consequence that the intended safety function is not fulfilled

c. Spurious actuation of a powered component originating from its instrumentation and control system (unless design features or operating restrictions preclude such spurious action)

d. Single incorrect or omitted action by a human operator attempting to perform a safety-related action according to written operating instructions in response to an initiating event

15.0.0.4.2 Passive Failures

A passive failure is a breach of a fluid pressure boundary or blockage of a process flow path. Blockage of a process flow path could occur, for example, due to separation of a valve disc from its stem.

Examples of passive failures are:

a. Rupture of a pipeline or tank

b. Blockage of the containment sump due to heat insulation material of the primary circuit

15.0.0.4.3 Limiting Single Failure or Operator Errors

For event combinations that require a single failure, the limiting failure is selected from those listed in Table 15.0-4. Pre-existing failures are equipment failures that occur before the event is initiated and that are not revealed until called on to function during the event (e.g., failure of an auxiliary feedwater pump). High-probability occurrences are included in the event analysis if they would result in an adverse impact. Interactive control system failures are not more limiting than the active failures listed.

According to 10 CFR 50, Appendix A, a single failure is an occurrence that results in the loss of the capacity of a component to perform its intended safety functions. However, failures are considered not only of safety-related systems whose operation may be required but also of nonsafety-related systems whose failure could produce results more severe than the failure of a safety system. If a nonsafety-related system is used to mitigate a transient, the analysis of the transient assumes that the system is in the manual mode of operation. Nonsafety-related systems are assumed to be in the automatic mode of operation if the system would make the consequences of a transient more adverse.

The purpose of the single failure list is to identify the single failures that could create the most adverse conditions during a given transient, regardless of the safety-related status of that component or system. In most cases, the automatic action of safety-related systems overrides the operation of nonsafety-related systems. The justification for choosing the most limiting single failure is explained further in the analyses in this chapter.

Operator error, in the context of a single failure criterion, is a single incorrect action or omitted action by a human operator attempting to perform a nuclear safety-related manipulation in response to an initiating occurrence. Operator errors are considered potential single failures for actions that are expected or directed by emergency procedures but are not accounted for in the accident analysis.

15.0.0.5 Nonsafety-Related Systems Assumed in the Analysis

Nonsafety-related systems are not required to mitigate the consequences of events discussed in Chapter 15. Only safety-related systems are credited in the APR1400 safety analyses. Nominal control system characteristics are modeled (best estimate) in the accident analyses only if they would adversely affect the results.

15.0.0.6 Operator Action

Operator actions are required by plant emergency operating procedures following a design basis event (DBE) and when one or more actions are necessary to accomplish a safety-related function. Safety-related operator action is a manual action required by plant emergency operating procedures that is necessary to cause a safety-related system to perform its safety-related function during the DBE. The successful performance of a safety-related operator action may require discrete actions to be performed in a specific order.

Operator action is credited for the mitigation of postulated events in some analyses. In these analyses, the operator action is not credited until 30 minutes after event initiation even though the action can be performed from the main control room (MCR) within 30 minutes. In addition, operator errors are considered in developing event initiators and in limiting single failures (see Subsection 15.0.0.4.3 for a more detailed description).

Operator actions required to mitigate accidents are described in the event evaluation subsections.

15.0.0.7 Loss of Offsite Alternating Current (AC) Power

All event analyses resulting in a turbine generator trip consider the loss of offsite power (LOOP) while applying the same acceptance criteria for the event with and without LOOP. In the analyses for which the LOOP is assumed to result from a turbine trip, the time delay between the turbine trip and LOOP is assumed to be zero. However, a 3-second time delay can be assumed between reactor trip breakers opening and the turbine trip because of the turbine trip delay circuits. This time delay is assumed in the CEA misoperation and CEA ejection events while the other events do not use the time delay conservatively.

15.0.0.8 Long-Term Cooling

The operator can initiate a controlled system cooldown by using the auxiliary feedwater (AFW) system in conjunction with the atmospheric dump valves (ADVs). In the absence of a forced reactor coolant flow, RCS heat is removed by natural circulation along with the steam generators (SGs). After the reactor coolant temperature and pressure have been reduced to approximately 176.7 °C (350 °F) and 31.6 kg/cm^{2}A (450 psia), respectively, the shutdown cooling system (SCS) is put into operation to reduce the RCS temperature to the cold shutdown condition. Any event-specific assumptions for the transition to shutdown conditions using the SCS are described in the relevant event-specific safety analysis section.

15.0.0.9 Methodology for Determining Uncertainties

Existing uncertainties in an instrument signal are classified as random or bias errors. Random errors are basic measurement uncertainties or variations that exist in any repeated measurement. These errors are usually caused by the combination of numerous effects that exist in any measurement. An exact value of a random error cannot be predicted for a specific measurement. To account for the random errors, the unsystematic errors are enveloped by upper and lower limits, around the measured value, that bound the most probable value for the instrumentation output at any instance.

Bias errors do not exhibit random normal distribution characteristics; rather, they exhibit a correlated, predictable, fixed, or systematic behavior. A bias exists where there is a known offset of measurement from the ideal value. Both random and bias error effects of an

instrument measurement loop are evaluated. Uncertainties inherent in the signal communication process are accommodated by the method of setpoint calculation recommended by ANSI/ISA-67.04-1994, "Setpoints for Nuclear Safety-Related Instrumentation."

To establish the total uncertainty in an instrument or measurement, the various random and bias error effects are combined. The errors that are considered random are combined using statistical formulae such as the square-root-sum-of-the-squares (SRSS). Bias errors are algebraically combined. Finally, the resultant random and bias errors are algebraically combined to yield a total uncertainty.

Some events analyzed in the safety analysis result in a more severe environment for protection system equipment than others. As a result, the expected total equipment uncertainties can be event-specific, and a trip parameter can have an accident setpoint for each design basis event.

The setpoints presented in Table 15.0-2 are determined based on the methodology presented above. The main methodology for determining uncertainties and the detailed uncertainty values are provided in Reference 51, which is based on NRC RG 1.105, Rev. 3, "Setpoints for Safety-Related Instrumentation." The setpoint methodology for plant protection system is provided in Reference 77.

15.0.0.10 Thermal Conductivity Degradation

The effects of thermal conductivity degradation (TCD) on non-lOCA and LOCA evaluations, except for a CEA ejection accident and LBLOCA, are negligible. The effects are provided in Reference 78.

The results of the evaluation of a CEA ejection accident and LBLOCA are provided in Subsections 15.4.8.3 and 15.6.5.3, respectively.

15.0.1 Radiological Consequence Analysis Using Alternative Source Terms

A radiological consequence analysis using alternative source terms is not applicable to the APR1400 because it is prepared to review the application for the initial implementation of an alternative source terms (AST) methodology at the plants for which an operating license

was issued prior to January 10, 1997. The radiological consequences in the analyses of the APR1400 are addressed in Subsection 15.0.3 and Appendix 15A.

15.0.2 Review of Transient and Accident Analysis Methods

15.0.2.1 Analysis Methods

The NSSS response to various events is simulated using computer programs and analytical methods. The documents that are relevant to the safety analysis methodologies in Chapter 15 are as follows:

a. Non-LOCA Safety Analysis Methodology, APR1400-Z-A-NR-13006-P, Rev. 00, September 2013

b. LBLOCA BE Analysis Methodology, APR1400-F-A-TR-12004-P, Rev. 00, December 2012

c. SBLOCA Evaluation Model, APR1400-F-A-NR-12003-P, Rev. 00, October 2012

d. Post-LOCA LTC Evaluation Model, APR1400-F-A-NR-12002-P, Rev. 00, October 2012

The reports listed above address compliance with conditions and limitations in the relevant NRC safety evaluation reports (References 17 and 79).

15.0.2.2 Computer Codes Used

Information about the computer codes used for analyzing events is provided in the following subsections. Any specialized modeling capabilities that are unique to a specific event are provided in the relevant event analysis subsection.

15.0.2.2.1 CESEC-III

CESEC-III is used to simulate the NSSS unless otherwise specified for an event. CESEC-III is a version of CESEC that incorporates the anticipated transient without scram (ATWS) model modifications documented in References 10 through 14 and includes additional improvements that extend the range of applicability of the models. CESEC-III models the

steam void formation and collapse in the upper head region of the reactor vessel. It also includes a detailed thermal hydraulic model that simulates the mixing in the reactor vessel from asymmetric transients, an RCS flow model that calculates the time-dependent reactor coolant mass flow rate in each loop, a wall heat model, a 3-D reactivity feedback model, a safety injection tank model, and a primary-to-secondary (P-T-S) heat transfer model that calculates the heat transfer for each steam generator node rather than for a steam generator as a whole. The CESEC-III is documented in References 15 and 16 and approved in Reference 17.

CESEC-III computes key system parameters during a transient including core heat flux, pressures, temperatures, and valve actions. A partial list of the dynamic functions included in this NSSS simulation is as follows: point kinetics neutron behavior, Doppler and moderator reactivity feedback, boron and CEA reactivity effects, multi-node average thermal hydraulics, reactor coolant pressurization and mass transport, reactor coolant system safety valve behavior, steam generation, steam generator water level, turbine bypass, main steam safety and turbine admission valve behavior, as well as alarm, control, protection, and engineered safety feature systems. The steam turbines, condensers, and associated controls are not included in the simulation. Steam generator feedwater enthalpy and flow rate are provided as input to CESEC-III.

During the simulation, CESEC-III obtains steady-state and transient solutions to the set of equations that mathematically describe the physical models of the subsystems mentioned above. Simultaneous numerical integration of a set of first-order differential equations with time-varying coefficients is carried out by means of a simultaneous solution. As the time variable evolves, edits of the principal systems parameters are printed at prespecified intervals. An extensive library of the thermodynamic properties of uranium dioxide, water, and zircaloy is incorporated into the program. Symmetric and asymmetric plant response over a wide range of operating conditions can be determined by using CESEC-III.

15.0.2.2.2 COAST

COAST is used to calculate the reactor coolant flow coastdown transient for any combination of active and inactive pumps and forward or reverse flow in the hot or cold legs. The program is described in Reference 18, referenced in Reference 3, and approved in Reference 19.

The equations of conservation of momentum are written for each flow path in the COAST model assuming unsteady one-dimensional flow of an incompressible fluid. The equation of conservation of mass is written for the appropriate nodal points. Pressure losses due to friction and geometric losses are assumed to be proportional to the flow velocity squared. Pump dynamics are modeled using a head-flow curve for a pump at full speed and using four-quadrant curves, which are parametric diagrams of pump head and torque on coordinates of speed versus flow for a pump at other than full speed.

15.0.2.2.3 STRIKIN-II

STRIKIN-II is used to simulate the heat conduction in the reactor fuel rods and associated surface heat transfer. STRIKIN-II is described in Reference 20.

STRIKIN-II provides a single- or dual-closed channel model of a core flow channel to calculate the clad and fuel temperatures for an average or hot fuel rod and the extent of the zirconium water reaction for a cylindrical geometry fuel rod. STRIKIN-II includes:

a. Incorporation of all major reactivity feedback mechanisms

b. Maximum of six delayed neutron groups

c. Both axial (maximum of 20) and radial (maximum of 20) segmentation of the fuel element

d. Control rod scram initiation on high neutron power

15.0.2.2.4 TORC and CETOP

The TORC code is used to simulate the three-dimensional fluid conditions within the reactor core. The TORC code is addressed in References 24 and 25, referenced in Reference 3, and approved in Reference 26.

Results from the TORC code include the core radial distribution of the relative channeled axial flow rate that is used to calibrate CETOP, described in Reference 7 and approved in Reference 27. Transient core heat flux and thermal-hydraulic conditions from CESEC-III

are input to CETOP, which uses the KCE-1 critical heat flux correlation described in Reference 28.

15.0.2.2.5 HERMITE

The HERMITE code solves the few-group, space-group and time-dependent neutron diffusion equation in order to consider the integral effect of space and time in the transient state. The HERMITE code uses a closed-channel model or an open-channel model in the TORC code as the thermal-hydraulic model to calculate the feedback effects of fuel temperature, coolant temperature, coolant density, xenon distributions, and control rod motion. The one-dimensional, two-dimensional and three-dimensional neutron diffusion equation is solved with nodal expansion method. The fuel temperature model represents the pellet, gap, and clad. The heat conduction equations are solved by a finite difference method. The HERMITE code is addressed in Reference 6 and approved in Reference 29.

15.0.2.2.6 HRISE

The HRISE code is used to predict the transient DNBR for the thermal-hydraulic conditions beyond the range of applicability for the KCE-1 critical heat flux correlation used in the TORC and CETOP codes. The HRISE code is described in Reference 30 and approved in Reference 31.

The HRISE code performs thermal-hydraulic calculations using a closed-channel model and calculates DNBR with various critical heat flux (CHF) correlations including the Macbeth correlation, which is approved by the NRC for the post-trip steam line break analysis.

15.0.2.2.7 Reactor Physics

Numerous computer programs are used to produce the input reactor physics parameters required by the NSSS simulation and reactor core programs previously described. These reactor physics programs are addressed in Chapter 4.

15.0.2.2.8 RADTRAD

RADionuclide Transport, Removal, And Dose (RADTRAD) (Reference 59) is designed to calculate doses at offsite locations, such as the exclusion area boundary (EAB), the low

population zone (LPZ), and in the MCR. The code is capable of modeling fission product release to the containment. As the material is transported through the containment and other buildings, credit is given for several natural and engineered fission product removal mechanisms. Containment sprays remove aerosols, elemental iodine, and organic iodine fission products. The flow of the fission products between buildings or rooms may be through high-efficiency particulate air (HEPA) filters, and leakage to the environment may occur. Aerosols can deposit on surfaces within rooms and also in connecting paths. Computer models are included for the different removal mechanisms. Alternatively, the time-dependent values for the fission product removal coefficient may be selected as inputs. After transporting the nuclides to different locations, RADTRAD calculates the dose at user-specified locations. Additional details are discussed in Appendix 15A.

15.0.2.2.9 RELAP5/MOD3.3

The RELAP5 code (Reference 65) was developed for the best-estimate transient simulation of light-water-reactor coolant systems. The code has been used worldwide for analyzing large- and small-break LOCAs and operational transients, such as anticipated transient without scram, loss of offsite power, loss of feedwater, and loss of flow. A generic modeling approach is used to model as much of a particular system as necessary. Control system and secondary system components are included to permit modeling of plant controls, turbines, condensers, and secondary feedwater conditioning systems.

The RELAP5/MOD3.3 code is based on a non-homogeneous, non-equilibrium model for the two-phase system that is solved by a fast, partially implicit numerical scheme to permit economical calculation of system transients. The objective of the RELAP5 development from the outset is to produce a code that includes important first-order effects necessary for the accurate prediction of system transients but that is sufficiently simple and cost-effective so that parametric or sensitivity studies can be conducted.

15.0.2.2.10 CONTEMPT4/MOD5

The CONTEMPT4/MOD5 code (Reference 66) is a containment analysis code that describes the response of multi-compartment containment systems subjected to postulated LOCA conditions. The program can accommodate both PWR and boiling water reactor (BWR) containment systems. Also, both design basis accident (DBA) and degraded core type LOCA conditions can be analyzed. This code includes water pool pressure

suppression system modeling, hydrogen tracking and burn capability, a gas radiation heat transfer model, a user-specified junction (leakage) area as a function of pressure or time, an alternative containment spray model, and containment spray carryover capability.

The code calculates the time variation of compartment thermodynamic state, heat structure temperature distribution, and mass and energy inventories in response to postulated LOCA conditions described by the user input, taking into the account inter-compartment exchange of mass and energy. Containment spray, fan/pump, fan cooler, and hydrogen burn analytical models are provided. Any compartment can have both a liquid pool region and a vapor atmosphere region.

15.0.2.2.11 CEFLASH-4AS

The CEFLASH-4A code (Reference 69) calculates the blowdown thermal-hydraulic response of a water-cooled reactor system during a LOCA. The CEFLASH-4AS code was modified from CEFLASH-4A to enable the program to treat LOCAs that are characterized by phase separation. Many of the modifications involved translating the basic applicability from a homogeneous to a heterogeneous treatment of the primary system coolant. Major modifications included the development of a new flow path representation, core heat transfer method, and bubble rise model. The improved program is designated CEFLASH-4AS to identify the computations the version performs.

15.0.2.2.12 COMPERC-II

The COMPERC-II code (Reference 70) calculates the hydraulic response of a PWR during the reflood period of a small break LOCA. The COMPERC-II program is initialized when the annulus downflow with vessel pressure and core conditions is obtained from CEFLASH-4AS. This program is then run with emergency core cooling system (ECCS) simulation to determine vessel refill and reflood and to obtain the appropriate heat transfer coefficient for the hot channel. Together, CEFLASH-4AS and COMPERC-II completely describe the fluid hydraulics and thermodynamics of both the blowdown and the refill-reflood processes.

15.0.2.2.13 PARCH

The PARCH code (Reference 72) is applied to the evaluation of fuel rod temperatures during the period following initial reversal of the coolant flow at the core inlet. The

PARCH code is written for use in analysis of conditions that occur during small-break LOCAs. It describes the removal of heat from a fuel rod that is surrounded by a quasi-static fluid partially or totally covering the length of the fuel rod. Thus, the mechanisms for convective heat transfer are pool boiling below the two-phase fluid surface and forced convection to steam above the two-phase fluid surface.

15.0.2.2.14 CELDA

The CELDA code is used to determine the reactor system long-term primary system depressurization and refill for small breaks in the reactor coolant system. The analysis is initialized from the CEFLASH-4AS analysis that is performed for the early part of the accident.

15.0.2.2.15 BORON

The BORON code is used to compute the boric concentration in the core and determines whether the core flow is sufficient to prevent the solubility limit of boric acid from being exceeded. Steam removed from the core is calculated using decay heat curves. BORON is run as a subroutine of CELDA for small breaks and as a separate code for large breaks.

15.0.3 Design Basis Accident Radiological Consequence Analyses for Advanced Light Water Reactors

15.0.3.1 Introduction

This subsection identifies the models used to calculate offsite and MCR doses that would result from releases of radioactivity due to various DBAs. The DBAs are as follows:

a. Steam system piping failures outside the containment (Subsection 15.1.5.5)

b. Feedwater system pipe break (Subsection 15.2.8.5)

c. Reactor coolant pump (RCP) rotor seizure (Subsection 15.3.3.5)

d. CEA ejection (Subsection 15.4.8.5)

e. Failure of small lines carrying primary coolant outside containment (Subsection 15.6.2.5)

f. Steam generator tube rupture (SGTR) (Subsection 15.6.3.2.5)

g. LOCA (Subsection 15.6.5.5)

h. Fuel handling accident (Subsection 15.7.4)

The radiological consequences of each DBA listed above are analyzed based on assumptions and parameters used in the respective subsections.

Initial core and core gap activities, reactor coolant equilibrium concentrations in the Technical Specifications, pre-accident iodine spike primary coolant concentrations, and event-generated iodine spiking appearance rates are addressed in Appendix 15A, Subsection 15A.1.2. The releases to the environment resulting from each accident are presented in the respective subsections.

For all cases, the potential offsite doses are within the limits of 10 CFR 50.34 (Reference 57), while the potential doses for the MCR and technical support center (TSC) are within the limits of General Design Criterion (GDC) 19 (Reference 58).

15.0.3.2 Methodology

The radiological consequences of the DBAs are calculated at the EAB, outer boundary of LPZ, and MCR resulting from the fission products releases following DBAs, using the AST methodology as defined in NRC RG 1.183, “Alternative Radiological Source Terms for Evaluating Design Basis Accidents at Nuclear Power Reactors” (Reference 54), and the total effective dose equivalent (TEDE) methodology.

For the analysis of the radiological consequences of the DBAs, the RADTRAD computer code is used. The RADTRAD computer code (Reference 59) is designed to calculate doses at offsite locations, as well as onsite locations such as the MCR, due to postulated radioactivity releases from DBA conditions. The code calculates dose consequences for different time intervals based on user information on the amount, form, and species of the radioactive material released in the plant.

The time for release termination of an accident is determined based on the thermal-hydraulic conditions of the primary and secondary systems. The release typically ends when the release path is isolated or the plant is cooled down to the cold shutdown entry conditions. The release termination times for different events are given in Table 15.0-9.

The TEDE, which is the sum of the committed effective dose equivalent (CEDE) from inhalation and the deep dose equivalent (DDE) from external exposure, for each DBA does not exceed the guideline values in 10 CFR 50.34(a)(1) and GDC 19. Table 15.0-10 provides the results of radiological consequences of the APR1400 DBAs and the corresponding acceptable dose criteria for each accident. The potential doses to the MCR and TSC personnel are presented in Table 6.4-2.

The methodology and the analytical model for determining the doses are discussed in detail in Appendix 15A.

15.0.3.3 Source Terms

It is assumed that the inventory of fission products in the reactor core that is available for release to the containment is based on the maximum power level of 4,062.66 MWt corresponding to fuel enrichment and fuel burnup, which is 1.02 times the APR1400 thermal power of 3,983 MWt as specified in NRC RG 1.183, Regulatory Position 3.1 (Reference 54). The initial radioactivity inventory in the core is used for the events that cause failure of the fuel cladding or melting, which releases fission products from the fuel gap or pellets.

For DBA analysis, the core gap activities are based on the guidance provided in NUREG-1465 (Reference 53) and NRC RG 1.183. The noble gas, iodine, cesium, and rubidium inventories in the fuel gap region are dependent on the type of DBA. The chemical species of the iodine released into the containment are based on the guidance in NUREG-1465 (i.e., 95 percent in the form of particulate iodine, 4.85 percent in the form of elemental iodine, and 0.15 percent in the form of organic iodine).

The initial activities in the primary and secondary systems are also used as a source term for DBAs, which cause releases of primary or secondary coolant to the environment. The equilibrium activity concentrations in the RCS and the secondary coolant system are calculated assuming full power operation in the following cases: (1) nuclide-specific

distribution corresponding to 1.0 percent fuel defects specified in Section 11.1 and (2) the limiting concentrations in the Technical Specifications. The limiting conditions for operation (LCO) activities in the Technical Specifications are used in the analysis of the main steam line break, feedwater line break, RCP locked rotor accident, CEA ejection accident, failure of small lines carrying primary coolant outside the containment, feedwater line break, and steam generator tube rupture.

The Technical Specifications restrict the concentrations in the primary and secondary systems to 3.7×10^4 Bq/g (1.0 μCi/g) and to 3.7×10^3 Bq/g (0.1 μCi/g) dose equivalent (DE) I-131, respectively, and to 1.11×10^7 Bq/g (300 μCi/g) DE Xe-133 in the primary system.

For some accidents, the iodine concentrations in the reactor coolant are calculated based on the equilibrium coolant iodine concentrations augmented by iodine spiking as follows: the pre-accident iodine spike (PIS) and the event-generated iodine spike (GIS) models.

The PIS concentrations are determined by increasing the primary coolant iodine concentrations to 60 times the maximum value specified in the Technical Specifications.

The GIS is modeled by increasing the iodine release rates from fuel rods into the primary coolant to 500 times (or 335 times for steam generator tube rupture) the equilibrium iodine concentration release rates.

15.0.3.4 Dose Conversion Factors

The exposure-to-CEDE factors for inhalation of radioactive material are derived from the data in International Commission on Radiological Protection (ICRP) Publication 30, “Limits for Intakes of Radionuclides by Workers.” The CEDE dose conversion factors (DCFs) derived from the ICRP-30 are provided in the “effective” column of Table 2.1 of U.S. Environmental Protection Agency (USEPA) Federal Guidance Report 11, “Limiting Values of Radionuclide Intake and Air Concentration and Dose Conversion Factors for Inhalation, Submersion, and Ingestion” (Reference 55).

As discussed in NRC RG 1.183, the DDE is calculated using submergence in semi-infinite cloud assumptions with appropriate credit for attenuation by body tissue. The DDE is nominally equivalent to the effective dose equivalent (EDE) from external exposure if the

whole body is irradiated uniformly. Because this assumption is reasonable for submergence exposure situations, the EDE is used in lieu of the DDE to determine the contribution of external dose to the TEDE. This calculation models the EDE dose conversion factors in the "effective" column of Table III 1 of USEPA Federal Guidance Report 12, "External Exposure to Radionuclides in Air, Water, and Soil" (Reference 56). Radionuclide-specific CEDE and EDE DCFs are presented in Table 15A-10.

Control room doses are calculated using the offsite dose analysis dose conversion factors identified in NRC RG 1.183, Regulatory Position 4.1. The DDE from photons is corrected for the difference between finite cloud geometry in the control room and the semi-infinite cloud assumption used in calculating the dose conversion factors. The equation below is used in this analysis to correct the semi-infinite cloud dose, DDE_{∞}, to a finite cloud dose, DDE_{finite}, where the control room is modeled as a hemisphere with a volume (V) in cubic feet, equivalent to that of the control room (Reference 54):

$$DDE_{finite} = (DDE_{\infty} \times V^{0.338}) \ / \ 1{,}173$$

For the first 8 hours after the accident, the offsite breathing rate is assumed to be 3.5×10^{-4} m^3/sec. From 8 to 24 hours, the breathing rate is assumed to be 1.8×10^{-4} m^3/sec. Between 24 hours and the end of the accident, the rate is assumed to be 2.3×10^{-4} m^3/sec. For the MCR and TSC, the breathing rate of the individual is assumed to be 3.5×10^{-4} m^3/sec during the entire period of the accident.

15.0.3.5 Atmospheric Dispersion Factor

Accident atmospheric dispersion factors (χ/Q) for the EAB and the LPZ are used to calculate the potential offsite doses. The short-term χ/Q values at the EAB and LPZ are determined as described in Subsection 2.3.4 and are given in Table 2.3-1. The MCR and TSC χ/Q values are discussed in Subsection 2.3.4 and given in Tables 2.3-2 through 2.3-12. These χ/Q values are used in conjunction with dose conversion factors to calculate TEDE at receptor locations.

The atmospheric releases given in each accident subsection are used in conjunction with the appropriate χ/Q values to calculate the potential offsite and MCR and TSC doses for the corresponding accidents.

The combined license (COL) applicant is to perform the radiological consequence analysis using site-specific χ/Q values, unless the χ/Q values used in the DCD envelop the site-specific short-term or long-term χ/Q values of the DCD, and to show that the resultant doses are within the guideline values of 10 CFR 50.34 for EAB and LPZ and that of 10 CFR 50, Appendix A, GDC 19 for the MCR and TSC (COL 15.0(1)).

15.0.3.6 Analytical Models for Loss-of-Coolant Accidents

This section describes the brief analytical models used in the calculation of radiation doses resulting from a LOCA. Details are presented in Subsection 15.6.5.5. The doses are calculated for the following locations:

a. EAB

b. LPZ outer boundary

c. MCR and TSC

The CEDE due to inhalation and the DDE due to the emission of photons from the radioisotopes are computed. The TEDE, which is the sum of the CEDE and the DDE, is calculated and compared with the dose limits specified in 10 CFR 50.34(a)(1) and GDC 19.

The doses at the EAB are based on the total activity released for any 2 hours following a LOCA. The doses at the LPZ and in the MCR are based on the total activities released over 30 days in accordance with the requirements of NRC RG 1.183. The TEDE at a given location is calculated by summing the doses from various release paths to the atmosphere. These paths are as follows:

a. Containment leakage

b. Containment release through the containment low volume purge before isolation

c. Leakage from ESF system outside the containment

The assumptions used for the LOCA dose models are consistent with those in NUREG-1465 and NRC RG 1.183 as follows:

a. The radionuclide release to the containment from the primary system is divided into three phases. These are as follows:

   1) Coolant release phase, from t = 0 to t = 30 seconds

   2) Gap release phase, from t = 30 seconds to t = 0.5083 hours

   3) Early in-vessel release phase, from t = 0.5083 hours to t =1.8083 hours

   Therefore, the release to the containment is assumed to end at 1.8083 hours after the start of the accident. The release magnitudes for the gap and early in-vessel release phases as fractions of core inventory are presented in Table 15.0-8.

   The release rate is assumed to be uniform over the duration of the release phases. The doses at the EAB and the LPZ are calculated from the onset of the accident.

b. The chemical and physical form of the radionuclides released to the containment is discussed in NRC RG 1.183. The entire release has the chemical form of particulate except for the noble gases and 5 percent of the iodine. The dose analyses assume that 0.15 percent of iodine is organic and 4.85 percent of iodine is elemental.

c. Airborne radionuclides are removed by the operation of the containment sprays as described in Subsection 6.5.2, and the removed activity is assumed to mix into the in-containment refueling water storage tank (IRWST) inventory. The liquid is circulated through the various safety pumps in the ESF rooms. Leakage through the pump seals and valves results in an activity in the ESF rooms that vents to the atmosphere.

d. No credit is taken for depletion of the effluent plume due to deposition on the ground or radioactive decay during transport to the locations of interest.

e. Doses are calculated by the RADTRAD code using inputs for breathing rate, containment parameters, and MCR parameters.

15.0.3.7 Analytical Models for Non-Loss-of-Coolant-Accident Events

This subsection provides a brief description of analytical models for calculating offsite and MCR doses resulting from non-LOCA events. The models incorporate the guidelines in NRC RG 1.183 (Reference 54) for calculating radiological consequences and the use of conservative assumptions to maximize doses. The non-LOCA doses are calculated for the same receptor locations as for the LOCA.

In accordance with the guidelines of NUREG-0800, Subsection 15.0.3, the doses at the EAB are calculated based on the total activity released for any 2 hours (in general, the initial 2 hours for non-LOCA) following the initiation of the event. Similarly, the doses at the MCR, TSC, and LPZ are determined on the basis of the total activity released over the entire event. The total doses at a given location are derived from activities from various release paths to the atmosphere, as follows:

a. Main steam safety valves

b. Atmospheric dump valves

c. Auxiliary building emergency heating, ventilation, and air conditioning (HVAC) vent

d. Containment

The following assumptions are employed in the non-LOCA dose calculations to conservatively maximize radiological consequences.

a. Accident doses are calculated for the following three scenarios, as applicable, consistent with the guidelines of NRC RG 1.183:

    1) A GIS coincident with the initiation of the event

    2) A PIS

3) A failed fuel condition in the core

b. GIS calculations employ an iodine spiking factor of 335 for a steam generator tube rupture and 500 for other non-LOCAs.

c. For the PIS case, the iodine concentration is increased to 60 times the iodine concentration in the Technical Specifications.

d. The LCO concentrations in the Technical Specifications are employed for the initial iodine activity concentrations for the primary and secondary systems, which are 3.7×10^4 Bq/g (1.0 μCi/g) DE I-131 and 3.7×10^3 Bq/g (0.1 μCi/g) DE I-131, respectively. The initial noble gas concentrations in the primary side are conservatively assumed to be at 2.15×10^7 Bq/g (580 μCi/g) DE Xe-133, even though the LCO concentration in the Technical Specifications limits noble gas concentrations below 1.11×10^7 Bq/g (300 uCi/g) DE Xe-133.

e. The timing of an operator action may vary for each event. It is generally assumed that an operator action is not credited in the analysis before 30 minutes after event initiation unless an earlier operator action results in more adverse consequences.

f. An overall steam generator tube leakage of 2.27 L/min (0.6 gpm) is assumed for the duration of the transient.

g. Conservative partition coefficients for iodine and alkali metals are assumed for various occurrences as follows:

1) For primary coolant release via steam generator:

	With SG Dried-Out	Without SG Dried-Out
Flashed Portion	1	1
Unflashed Portion	1	100

2) For secondary coolant release via steam generator and condenser:

Release via steam generator		Release via condenser
With SG Dried-Out	Without SG Dried-Out	
1	100	100

3) For release evolving out of the spent fuel pool (fuel handling accident only):

Iodines		Other nuclides
Organic	Elemental	
1	500	Infinite

h. Pipe breaks in the primary or secondary systems outside the containment are assumed to be isolated 30 minutes after the accident. For a steam line break (SLB) upstream of the main steam isolation valve (MSIV), further steam releases are included beyond 30 minutes.

i. χ/Q provided in Subsection 2.3.4 are used.

j. The core inventory of all significant isotopes is provided in Appendix 15A, Table 15A-1.

k. No credit is taken for the radioactive decay of the isotopes during transit in the calculation.

15.0.3.8 Radiological Consequence

The analyses of the events described in Chapter 15 are generally terminated when the plant achieves a stable and controlled condition (i.e., the reactor is subcritical and remains subcritical, the core is covered, decay heat is being removed from the RCS, and secondary inventory levels are sufficient to maintain RCS temperatures). Subsequent actions, including cooldown, are addressed in plant-specific emergency operating procedures (EOPs). For the radiological consequence analysis, the release to the environment is calculated until the time for release termination. Table 15.0-9 presents the time for release termination for each DBA.

Offsite radiological consequences at the EAB and LPZ following the APR1400 DBAs are summarized in Table 15.0-10. Even with the conservative assumptions on the atmospheric dispersion factors, the offsite dose results for all DBAs are well within the dose limits in 10 CFR 50.34. Radiological consequences to the MCR personnel are summarized in Table 6.4-1. Similarly, the MCR doses for all DBAs meet the criteria of 10 CFR 50, Appendix A, GDC 19.

15.0.4 Combined License Information

COL 15.0(1) The COL applicant is to perform the radiological consequence analysis using site-specific χ/Q values, unless the χ/Q values used in the DCD envelop the site-specific short-term or long-term χ/Q values of the DCD, and to show that the resultant doses are within the guideline values of 10 CFR 50.34 for EAB and LPZ and that of 10 CFR 50, Appendix A, GDC 19 for the MCR and TSC.

15.0.5 References

1. NRC RG 1.206, "Combined License Applications for Nuclear Power Plants (LWR Edition)," Rev. 00, June 2007.

2. NUREG-0800, "Standard Review Plan for the Review of Safety Analysis Reports for Nuclear Power Plants," Rev. 03, March 2007.

3. "APR1400 Standard Safety Analysis Report," Chapter 15, May 7, 2002.

4. "Yonggwang Units 3&4 Safety Analyses Report," Appendix 15A: Loss of Primary Coolant Flow Methodology Description, KEPCO, 1993.

5. Letter from G.W. Knighton (NRC) to Arizona Public Service, "Amendment No. 24 to License No. NPF-41," October 21, 1987.

6. CENPD-188-A, "HERMITE A Multi-Dimensional Space-Time Kinetics Code for PWR Transients," July 1976, Proprietary Information.

7. CEN-214-P, "CETOP-D Code Structure and Modeling Methods for Arkansas Nuclear One-Unit 2," July 1982.

8. CENPD-190-A, “C-E Method for Control Element Assembly Ejection Analysis,” January 1976.

9. Letter from Olan D. Parr (NRC) to A.E. Scherer (CE), dated June 10, 1976.

10. CENPD-107, Supplement 1, “ATWS Model Modifications to CESEC,” September 1974, Proprietary Information.

11. CENPD-107, Supplement 5-P, “ATWS Models Modification to CESEC,” June 1976, Proprietary Information.

12. CENPD-107, Supplement 2, “ATWS Model for Reactivity Feedback and Effect of Pressure on Fuel,” September 1974, Proprietary Information.

13. CENPD-107, Supplement 3, “ATWS Model Modifications to CESEC,” August 1975.

14. CENPD-107, Supplement 4-P, “ATWS Model Modifications to CESEC,” December 1975, Proprietary Information.

15. CENPD-107, “CESEC Digital Simulation of a Combustion Engineering Nuclear Steam Supply System,” April 1974, Proprietary Information.

16. LD-82-001 (dated 1/6/82), “CESEC Digital Simulation of a Combustion Engineering Nuclear Steam Supply System,” Enclosure 1-P to letter from A. E. Scherer to D. G. Eisenhut, December 1981.

17. TAC No. 01142, Safety Evaluation Report, “CESEC Digital Simulation of a Combustion Engineering Nuclear Steam Supply System,” Enclosure to Letter from C.O. Thomas (NRC) to A.E. Scherer (C-E), April 3, 1984.

18. CENPD-98-A, “COAST Code Description,” April 1973, Proprietary Information.

19. Letter from Olan D. Parr (NRC) to F. M. Stern (CE), December 4, 1974.

20. CENPD-135, “STRIKIN-II, A Cylindrical Geometry Fuel Rod Heat Transfer Program,” April 1974 (Proprietary).

21. CENPD-263-P, “ATWS Early Verification,” November 1979, Proprietary Information.

22. CENPD-158, Rev. 01, “Analysis of Anticipated Transients Without Reactor Scram in CE NSSSs,” May 1976, Proprietary Information.

23. “Response to NRC Action Plan Item II.K.3.30 Justification of Small Break LOCA Methods” CEN-203-P, March 1982 (Proprietary).

24. CENPD-161-P, “TORC Code - A Computer Code for Determining the Thermal Margin of a Reactor Core,” July 1975, Proprietary Information.

25. CENPD-206-P-A, “TORC Code-Verification and Simplified Modeling Methods,” June 1981, Proprietary Information.

26. Letter from R. L. Tedesco (NRC) to A.E. Scherer (CE), “Acceptance for Referencing of Topical Report CENPD-206(P), TORC Code Verification and Simplified Modeling Methods,” December 11, 1980.

27. Letter from R. A. Clark (NRC) to W. Cavanaugh III (AP&L), “Operation of ANO-2 During Cycle 2,” July 21, 1981 (Safety Evaluation and Amendment No. 26 to Facility Operating License No. NPF-6 for ANO-2).

28. APR1400-F-C-TR-12002-P, Rev. 0, “KCE-1 Critical Heat Flux Correlation for PLUS7 Thermal Design,” November 2012.

29. CENPD-188-A, “HERMITE A Multi-Dimensional Space-Time Kinetics Code for PWR Transients,” March 1976, Reprinted July 1976. (NRC Approval Letter dated June 10, 1976).

30. CE-CES-159, Rev. 0-P, “HRISE User’s Manual,” December 1992.

31. Letter from C. B. Brinkman (NRC) to A. E. Scherer (CE), “Macbeth CHF Correlation Approval,” LD-WO-3900, August 2, 1983.

32. CENPD-183-A, “C-E Methods for Loss of Flow Analysis,” June 1984.

33. Proceedings of the Institute of Mechanical Engineers, Vol. 180, Pt 3c, pp. 37-50, “An Appraisal of Forced Convection Burn-out Data,” Macbeth, R.V., 1965-66.

34. A.E.E.W. Report R358, “Burn-out Analysis - Part 5: Examination of Published World Data for Rod Bundles,” Macbeth, R.V., 1964.

35. "Ulchin Units 3&4 Final Safety Analysis Report," Subsection 15.1.5 and Appendix 15B: Steam System Piping Failure Inside and Outside Containment, KEPCO, 1996.

36. Safety Evaluation Report Related to the Final Design of the Standard Nuclear Steam Supply Reference System CESSAR System 80, Docket No. STN 50-470, NUREG-0852, Supplement 2, Appendix G, September 1983.

37. Journal of Heat Transfer, Transactions of the ASME, "The Two Phase Critical Flow of One-Component Mixtures in Nozzles, Orifices and Short Tubes," R.E. Henry and H.K. Fauske, May 1971.

38. NRC NUREG-0800, "U.S. Nuclear Regulatory Commission Standard Review Plan, Subsection 15.0.3, Radiological Consequence Analyses Using Alternative Source terms," Rev. 0, July 2000.

39. "Licensing Design Basis Source Term Update for the Evolutionary Advanced Light Water Reactor," Advanced Reactor Severe Accident Program (ARSAP) Source Term Expert Group, September 1990.

40. NRC NUREG-0800, "Nuclear Regulatory Commission Standard Review Plan, Subsection 6.5.2, Containment Spray as a Fission Product Cleanup System," Rev. 2, December 1988.

41. NRC NUREG-0800, "Nuclear Regulatory Commission Standard Review Plan, Section 6.4, Control Room Habitability Systems," Rev. 2, 1981.

42. NRC NUREG-0800, "Nuclear Regulatory Commission Standard Review Plan, Section 11.3, Branch Technical Position ESTB 11-5," Rev. 2, 1981.

43. NRC NUREG-0800, "Nuclear Regulatory Commission Standard Review Plan," Subsection 9.1.5, "Overhead Heavy Load Handling Systems," Rev.2, 1981.

44. ANSI-N14.6, "American National Standard for Special Lifting Devices for Shipping Containers Weighing 10,000 Pounds (4500 kg) or More for Nuclear Materials," 1993.

45. NRC NUREG-0612, "Control of Heavy Loads at Nuclear Power Plant," July 1980.

46. ANSI/ANS-57.2, "Design Requirements for Light Water Reactor Spent Fuel Storage Facilities at Nuclear Power Plants," 1983.

47. ANSI/ANS-57.1, “Design Requirements for Light Water Reactor Fuel Handling Systems,” 1992.

48. NRC NUREG-0554, “Single Failure Proof Cranes for Nuclear Power Plants,” May 1979.

49. Advanced Light Water Reactor Utility Requirements Document, “Fueling and Refueling Systems,” Electric Power Research Institute, Rev. 09, February 2008.

50. NRC RG 1.25, “Assumptions Used for Evaluating the Potential Consequences of a Fuel Handling Accident in the Fuel Handling and Storage Facility for Boiling and Pressurized Water Reactors,” March 1972.

51. APR1400-R-I-T(NR)-11003-P, “Technical Report for Uncertainty and Application for Instrumentation,” Rev. 00, May 2012.

52. Oak Ridge National Laboratory C00545/MNYCD00, SCALE 4.4 “Modular Code System for Performing Standardized Computer Analyses for Licensing Evaluation for Workstation and Personal Computer,” 1998.

53. NRC NUREG-1465, “Accident Source Terms for Light Water Nuclear Power Plants,” February 1995.

54. NRC RG 1.183, “Alternative Radiological Source Terms for Evaluating Design Basis Accidents at Nuclear Power Reactors,” July 2000.

55. USEPA, Federal Guidance Report No. 11, EPA 520/1-88-020, “Limiting Values of Radionuclide Intake and Air Concentration and Dose Conversion Factors for Inhalation, Submersion, and Ingestion,” September 1993.

56. USEPA, Federal Guidance Report No. 12, EPA 402-R-93-081, “External Exposure to Radionuclides in Air, Water, and Soil,” September 1993.

57. 10 CFR 50.34, “Contents of Applications; Technical Information,” January 10, 1997.

58. 10 CFR 50, Appendix A, “General Design Criteria for Nuclear Power Plants,” January 24, 2000.

59. NUREG/CR-6604, “RADTRAD: A Simplified Model for RADionuclide Transport and Removal and Dose Estimation,” SNL, December 1997.

60. NRC Branch Technical Position 11-5, “Postulated Radioactive Release Due to Waste Gas System Leak or Failure,” March 2007.

61. NRC Branch Technical Position 11-6, “Postulated Radioactive Release Due to Liquid-Containing Tank Failure,” March 2007.

62. “Acceptance Criteria for Emergency Core Cooling Systems for Light Water-Cooled Nuclear Power Reactors,” 10 CFR 50.46, October 1988.

63. “Realistic Evaluation Methodology for Large-Break LOCA of the APR1400,” APR1400-F-A-TR-12004-P, December 2012 (Proprietary).

64. “Best-estimate calculations of emergency core cooling system performance,” NRC RG 1.157, May 1989.

65. “RELAP5/MOD3 Code Manual Vol. 6, Validation of Numerical Techniques in RELAP5/MOD3.0,” NUREG/CR-5535/Rev 1, December 2001.

66. “CONTEMPT4/MOD4, A Multicompartment Containment System Analysis Program,” NUREG/CR-3716, BNL-NUREG-51754, March 1984.

67. “Small Break LOCA Evaluation Model,” APR1400-F-A-NR-12003-P, October 2012.

68. Letter, O. D. Parr (NRC) to F. M. Stern (C-E), June 13, 1975.

69. “CEFLASH-4AS, A Computer Program for Reactor Blowdown Analysis of the Small Break Loss-of-Coolant Accident,” CENPD-133P, Supplement 1, August 1974 (Proprietary).

    “CEFLASH-4AS, A Computer Program for the Reactor Blowdown Analysis of the Small Break Loss-of-Coolant Accident,” CENPD-133, Supplement 3-P, January 1977 (Proprietary).

70. “COMPERC-II, A Program for Emergency Refill-Reflood of the Core,” CENPD-134P, August 1974 (Proprietary).

"COMPERC-II, A Program for Emergency Refill-Reflood of the Core (Modifications)," CENPD-134P, Supplement 1, February 1975 (Proprietary).

"COMPERC-II, A Program for Emergency Refill-Reflood of the Core," CENPD-134, Supplement 2, June 1985.

71. "STRIKIN-II, A Cylindrical Geometry Fuel Rod Heat Transfer Program," CENPD-135P, August 1974 (Proprietary).

"STRIKIN-II, A Cylindrical Geometry Fuel Rod Heat Transfer Program (Modifications)," CENPD-135P, Supplement 2, February 1975 (Proprietary).

"STRIKIN-II, A Cylindrical Geometry Fuel Rod Heat Transfer Program," CENPD-135, Supplement 4-P, August 1976 (Proprietary).

"STRIKIN-II, A Cylindrical Geometry Fuel Rod Heat Transfer Program," CENPD-135, Supplement 5-P, April 1977 (Proprietary).

72. "PARCH, A FORTRAN-IV Digital Program to Evaluate Pool Boiling, Axial Rod and Coolant Heatup," CENPD-138P, August 1974 (Proprietary).

"PARCH, A FORTRAN-IV Digital Program to Evaluate Pool Boiling, Axial Rod and Coolant Heatup (Modifications)," CENPD-138P, Supplement 1, February 1975 (Proprietary).

73. "Post-LOCA Long Term Cooling Evaluation Model," APR1400-F-A-NR-12002-P, October 2012.

74. "C-E Fuel Evaluation Model," CENPD-139-P-A, July 1974 (Proprietary).

"Improvements to Fuel Evaluation Model," CEN-161 (B)-P-A, August 1989 (Proprietary).

"Improvements to Fuel Evaluation Model," CEN-161 (B)-P, Supplement 1-P-A, January 1992 (Proprietary).

75. "Justification of Trip Two/Leave Two Reactor Coolant Pump Trip Strategy," CEN-268, Revision 1, Combustion Engineering, Inc., May 1987.

76. "Non-LOCA Safety Analysis Methodology," APR 1400-Z-A-NR-13006-P, Rev. 00, September 2013.

77. "Setpoint Methodology for PPS," APR1400-Z-J-13005-P, Rev. 00, April 2013.

78. "The Effect of Thermal Conductivity Degradation on APR1400 Design and Safety Analyses," APR 1400-F-A-NR-13002-P, Rev.0, September 2013.

79. NRC NUREG-1462, "Final Safety Evaluation Report Related to the Certification of the System 80+ Design Docket No. 52-002," Rev. 0, 1994.

Table 15.0-1

Chapter 15 Subsection Designation

Each subsection is identified as 15.W.X.Y, where:	
W =	1 Increase in heat removal by the secondary system
	2 Decrease in heat removal by the secondary system
	3 Decrease in reactor coolant system flow rate
	4 Reactivity and power distribution anomalies
	5 Increase in reactor coolant inventory
	6 Decrease in reactor coolant inventory
	7 Radioactive release from a subsystem or component (e.g., 1,2)
	8 Anticipated transient without scram
X =	Event title from Reference 1
Y =	1 Identification of causes and frequency classification
	2 Sequence of events and systems operation
	3 Core and system performance
	4 Barrier performance
	5 Radiological consequences
	6 Conclusions

Table 15.0-2

Reactor Protection System Trips Used in the Safety Analysis

Event	RPS	Analysis Setpoint [1]	Sensor Response Time	Reactor Trip Delay Time [2]
Events not Mentioned Below	High logarithmic Power Level	0.05 %	0 ms	550 ms
	Variable Overpower	116.5 %	0 ms	550ms
	CPC Variable Overpower	115 %	0 ms	650 ms
	High Pressurizer Pressure	169.7 kg/cm^{2}A (2,414 psia)	300 ms	550 ms
	Low Pressurizer Pressure	122.0 kg/cm^{2}A (1,735 psia)	600 ms	550 ms
	Low SG Pressure	57.1 kg/cm^{2}A (812 psia)	600 ms	550 ms
	Low SG Water Level	40.7 % wide range [3]	650 ms	600 ms
	High SG Water Level	95 % narrow range [4]	600 ms	550 ms
	Low Reactor Coolant Flow	80 % [5]	0 ms	1200 ms [7]
	CPC Low RCP Shaft Speed	94.83 %	0 ms	450 ms
	CPC Coincident Low Pressure/DNBR	140.6 kg/cm^{2}A (2,000 psia) /1.45 [6]	300 ms	650 ms
Feedwater and Steam Line Breaks	High Pressurizer Pressure	173.17 kg/ cm^{2}A (2,463 psia)	300 ms	550 ms
	Low Pressurizer Pressure	109.3 kg/cm^{2}A (1,555 psia)	600 ms	550 ms
	Low SG Pressure	52.7 kg/cm^{2}A (750 psia)	600 ms	550 ms
	Low SG Water Level	28.4 % wide range [3]	650 ms	600 ms
	High SG Water Level	95 % narrow range [4]	600 ms	550 ms
	Low Reactor Coolant Flow	60 % [5]	0 ms	850 ms [7]
	CPC Low RCP Shaft Speed	94.83 %	0 ms	450 ms
	CPC Variable Overpower	121 % [8]	0 ms	650 ms
	High Containment Pressure	0.28 kg/cm^{2}G (4 psig)	600 ms	550 ms

(1) Some Chapter 15 analyses assumed more conservative setpoints for specific events.

(2) Reactor protection system response time testing is discussed in Section 7.2.

(3) Percent of distance between the wide range instrument taps; the setpoint is valid at full power only (i.e., 100 − 102 % power).

(4) Percent of distance between the narrow range instrument taps

(5) Percent of hot leg flow

(6) Trip credited for 15.6.3 events

(7) The total response time is the sum of sensor response time and reactor trip delay time. For a shaft break event, a reactor trip is required 1.2 seconds after the flow in the hot leg reaches its analysis setpoint. For a steam line break (SLB) with a LOOP up to 30 minutes into the event, a reactor trip is required 0.85 second after the core flow reaches its analysis setpoint.

(8) For SLB outside the containment, an additional 6 percent is considered conservative.

Table 15.0-3

Initial Conditions

Parameter	Units	Range
Core power	% of 3,983 MWt	0 ~ 102
Axial shape index	—	−0.3 < ASI < + 0.3[(1)]
Reactor vessel inlet coolant flow rate	% of 1,689,429 L/min (% of 446,300 gpm)	95 ~ 116
Pressurizer water level	% distance (between upper tap and lower tap) above lower tap	21 ~ 60
Core inlet coolant temperature < 90 % power 90 % ~ 100 % power	 °C (°F) °C (°F)	 285.0 ~ 295.0 (545 ~ 563) 287.8 ~ 295.0 (550 ~ 563)
Pressurizer pressure	kg/cm^2A (psia)	152.9 ~ 163.5 (2,175 ~ 2,325)
Steam generator water level Low level High level	 % wide range [(2)] % narrow range [(3)]	 40.7 95.0

(1) ASI = (A – B) / C
Where:
A = Core power in lower half of core
B = Core power in upper half of core
C = Total core power
For power less than 20 %, −0.6 < ASI < +0.6 is used

(2) Percent of distance between the wide range instrument taps

(3) Percent of distance between the narrow range instrument taps

Table 15.0-4 (1 of 2)

Single Failures [(1)]

Part A: Safety and Electrical System

Main feedwater system
1. One main feedwater isolation valve fails to close (two valves exist in series)
2. One main feedwater isolation valve back-flow check valve fails to close (two valves exist in series)
Main steam system
3. One main steam isolation valve fails to close
4. One main steam isolation valve bypass valve fails to close
5. One atmospheric dump valve fails to open
6. One atmospheric dump valve fails to reclose
Auxiliary feedwater system
7. Failure of any one auxiliary feedwater pump to start or auxiliary feedwater valve to function
Safety injection system
8. Failure of one SI pump
Electrical power sources
9. Failure of one emergency diesel generator to start, run, or load (each SI pump is powered from each emergency diesel generator)

(1) Limiting single failure for each event is provided in the section on the identification of causes and frequency classification of the relevant event.

Table 15.0-4 (2 of 2)

Part B: Control System

Steam bypass control system
1. Excessive modulation of one or more TBVs
2. Failure to prevent CEA withdrawal due to failure of automatic withdrawal prohibit signal
3. Excessive steam bypass flow (one TBV fail to quick close)
Reactor regulating systems
4. Failure of automatic withdrawal prohibit demand signal (redundant to 2)
Reactor power cutback system
5. Loss of DRCS reactor trip signal
6. Failure to generate turbine runback, setback, turbine inhibit increase signals
Feedwater control system
7. Failure of reactor trip override
8. Failure of high level override
Turbine-generator control system
9. Failure to setback or runback turbine (redundant to 6)
10. Failure to trip the turbine (redundant to 5)
Pressurizer pressure control system
11. Insufficient pressurizer spray flow
12. Excessive pressurizer spray flow (after spray actuation)
13. Failure of backup heaters to turn on
14. Failure of backup heaters to turn off
Pressurizer level control system
15. Charging control valve fails to open
16. Charging control valve fails to close

Table 15.0-5 (1 of 3)

Initial Events and Frequencies

Section/ Subsection	Event	Frequency of Event
15.1	Increase in heat removal by the secondary system	—
15.1.1	Decrease in feedwater temperature	AOO
15.1.2	Increase in feedwater flow	AOO
15.1.3	Increase in steam flow	AOO
15.1.4	Inadvertent opening of a steam generator relief or safety valve	AOO
15.1.5	Steam system piping failures inside and outside the containment	PA
15.2	Decrease in heat removal by the secondary system	—
15.2.1	Loss of external load	AOO
15.2.2	Turbine trip	AOO
15.2.3	Loss of condenser vacuum	AOO
15.2.4	Closure of main steam isolation valve	AOO
15.2.5	Steam pressure regulator failure	N/A
15.2.6	Loss of nonemergency AC power to the station auxiliaries	AOO
15.2.7	Loss of normal feedwater flow	AOO
15.2.8	Feedwater system pipe break inside and outside the containment	PA
15.3	Decrease in reactor coolant system flow rate	—

Table 15.0-5 (2 of 3)

Section/ Subsection	Event	Frequency of Event
15.3.1	Loss of forced reactor coolant flow	AOO
15.3.2	Flow controller malfunctions	N/A
15.3.3	Reactor coolant pump rotor seizure	PA
15.3.4	Reactor coolant pump shaft break	PA
15.4	Reactivity and power distribution anomalies	—
15.4.1	Uncontrolled control rod assembly withdrawal from subcritical or low-power startup conditions	AOO
15.4.2	Uncontrolled control element assembly withdrawal at power	AOO
15.4.3	Control element assembly misoperation	AOO
15.4.4	Startup of an inactive reactor coolant pump	AOO
15.4.5	Flow controller malfunction causing an increase in BWR core flow rate	N/A
15.4.6	Inadvertent decrease in boron concentration in the reactor coolant system	AOO
15.4.7	Inadvertent loading and operation of a fuel assembly in an improper position	AOO
15.4.8	Spectrum of control element assembly ejection accidents	PA
15.5	Increase in reactor coolant inventory	—
15.5.1	Inadvertent operation of the emergency core cooling system that increases the reactor coolant inventory	AOO
15.5.2	Chemical and volume control system malfunction that increases the reactor coolant inventory	AOO

Table 15.0-5 (3 of 3)

Section/ Subsection	Event	Frequency of Event
15.6	Decrease in reactor coolant inventory	—
15.6.1	Inadvertent opening of a PWR pressurizer pressure relief valve	PA
15.6.2	Failure of small lines carrying primary coolant outside the containment	AOO
15.6.3	Steam generator tube failure	PA
15.6.4	Radiological consequences of main steam line failure outside the containment (BWR)	N/A
15.6.5	Loss-of-coolant accidents resulting from spectrum of postulated piping breaks within the RCPB	PA
15.7	Radioactive material release from a subsystem or component	—
15.7.1	Radioactive gas waste system leak or failure	PA
15.7.2	Radioactive liquid waste system leak or failure	N/A
15.7.3	Postulated radioactive releases due to liquid-containing tank failures	PA
15.7.4	Fuel handling accident	PA
15.7.5	Spent fuel cask drop accident	PA
15.8	Anticipated transient without scram	N/A

Table 15.0-6 (1 of 7)

Summary of Computer Codes and Initial Conditions

Events in Increase in Heat Removal by the Secondary System

Subsection	Event	Code	Initial Conditions			
			Core Power MWt	Core Flow Rate 10^6 kg/hr (10^6 lbm/hr)	Doppler Coefficient	MTC $\Delta\rho$/°C ($\Delta\rho$/°F)
15.1.1	Decrease in feedwater temperature	CESEC-III CETOP	—	—	—	—
15.1.2	Increase in feedwater flow	CESEC-III CETOP	—	—	—	—
15.1.3	Increase main steam flow	CESEC-III CETOP	—	—	—	—
15.1.4	Inadvertent opening of a steam generator relief or safety valve	CESEC-III CETOP	4,062.66	85.03 (187.46)	Least negative	-5.4×10^{-4} (-3.0×10^{-4})
15.1.5	Steam system piping failure inside and outside the containment	CESEC-III CETOP	4,062.66	69.64 (153.52)	Most negative	Most negative
			4,062.66	85.03 (187.46)	Least negative	Adjusted to minimum DNBR
			10	69.64 (153.52)	Most negative	Most negative

Table 15.0-6 (2 of 7)

Events in Decrease in Heat Removal by the Secondary System

Subsection	Event	Code	Initial Conditions			
			Core Power MWt	Core Flow Rate 10^6 kg/hr (10^6 lbm/hr)	Doppler Coefficient	MTC $\Delta\rho$/°C ($\Delta\rho$/°F)
15.2.1	Loss of external load	CESEC-III CETOP	—	—	—	—
15.2.2	Turbine trip	CESEC-III CETOP	—	—	—	—
15.2.3	Loss of condenser vacuum	CESEC-III CETOP	4,062.66	73.3 (161.6)	Least Negative	0.0
15.2.4	Main steam isolation valve closure	CESEC-III CETOP	—	—	—	—
15.2.6	Loss of nonemergency AC power to the station auxiliaries	CESEC-III CETOP	—	—	—	—
15.2.7	Loss of normal feedwater flow	CESEC-III CETOP	—	—	—	—
15.2.8	Feedwater system pipe breaks	CESEC-III CETOP	4,062.66	69.44 (153.52)	Least Negative	0.0 (0.0)

Table 15.0-6 (3 of 7)

Events in Decrease in Reactor Coolant Flow Rate

Subsection	Event	Code	Initial Conditions			
			Core Power MWt	Core Flow Rate 10^6 kg/hr (10^6 lbm/hr)	Doppler Coefficient	MTC $\Delta\rho$/°C ($\Delta\rho$/°F)
15.3.1	Loss of Forced Reactor Coolant Flow	CESEC-III CETOP HERMITE	4062.66	85.03 (187.46)	Least Negative	0.0 (0.0)
15.3.3	Reactor Coolant Pump Rotor Seizure	CESEC-III CETOP HERMITE TORC	4062.66	69.64 (153.52)	Least Negative	0.0 (0.0)
15.3.4	Reactor coolant pump shaft break with loss of offsite power	CESEC-III CETOP HERMITE TORC	—	—	—	—

Table 15.0-6 (4 of 7)

Events in Reactivity and Power Distribution Anomalies

Subsection	Event	Code	Initial Conditions: Core Power MWt	Core Flow Rate 10^6 kg/hr (10^6 lbm/hr)	Doppler Coefficient	MTC $\Delta\rho/°C$ ($\Delta\rho/°F$)
15.4.1	Uncontrolled CEA withdrawal from a subcritical or low power startup condition	CESEC-III CETOP	0.03983	69.64 (153.52)	Least Negative	0.9×10^{-4} (0.5×10^{-4})
15.4.2	Uncontrolled CEA withdrawal at power	CESEC-III CETOP	4062.66	69.64 (153.52)	Least Negative	0.0 (0.0)
15.4.3	CEA Misoperation	CESEC-III CETOP	4062.66	69.64 (153.52)	Most Negative	-5.4×10^{-4} (-3.0×10^{-4})
15.4.4	Startup of an inactive reactor coolant pump	N/A	—	—	—	—
15.4.6	Inadvertent decrease in boration concentration in the reactor coolant system	N/A	—	—	—	—
15.4.7	Inadvertent loading and operation of a fuel assembly in an improper position	N/A	—	—	—	—

Table 15.0-6 (5 of 7)

Events in Reactivity and Power Distribution Anomalies

Subsection	Event	Code	Initial Conditions			
			Core Power MWt	Core Flow Rate 10^6 kg/hr (10^6 lbm/hr)	Doppler Coefficient	MTC $\Delta\rho/°C$ ($\Delta\rho/°F$)
15.4.8	Spectrum of CEA Ejection accidents	STRIKIN-II CESEC-III CETOP	4,062.66	69.64 (153.52)	Least negative	0.00 (0.00)
			1991.50	69.64 (153.52)	Least negative	0.45×10^{-4} (0.25×10^{-4})
			796.60	69.64 (153.52)	Least negative	0.72×10^{-4} (0.40×10^{-4})
			1.00	69.64 (153.52)	Least negative	0.90×10^{-4} (0.50×10^{-4})

Table 15.0-6 (6 of 7)

Events in Increase in Reactor Coolant Inventory

Subsection	Event	Code	Initial Conditions			
			Core Power MWt	Core Flow Rate 10^6 kg/hr (10^6 lbm/hr)	Doppler Coefficient	MTC $\Delta\rho$/°C ($\Delta\rho$/°F)
15.5.1	Inadvertent operation of ECCS	N/A	—	—	—	—
15.5.2	CVCS malfunction	CESEC-III CETOP	4,062.66	73.30 (161.6)	Least Negative	-5.4×10^{-4} (-3.0×10^{-4})

Table 15.0-6 (7 of 7)

Events in Decrease in Reactor Coolant Inventory

Subsection	Event	Code	Initial Conditions: Core Power MWt	Initial Conditions: Core Flow Rate 10^6 kg/hr (10^6 lbm/hr)	Initial Conditions: Doppler Coefficient	Initial Conditions: MTC Δρ/°C (Δρ/°F)
15.6.1	Inadvertent opening of a pressurizer POSRV	N/A	—	—	—	—
15.6.2	Double-ended break of a letdown line outside containment	CESEC-III CETOP	4,062.66	69.64 (153.52)	—	—
15.6.3	Steam generator tube rupture	CESEC-III CETOP	4,062.66	73.30 (161.6)	Least negative	0.0
15.6.5	LOCA	CAREM	3,983.0	73.30 (161.6)	Least negative	0.9×10^{-4} (0.5×10^{-4})

Table 15.0-7 (1 of 5)

Plant Systems Used in the Accident Analysis

Incident	Reactor Trip Functions(1)	ESF Functions(2)	Other Equipment
15.1 Increase in Heat Removal by Secondary System			
15.1.1 Decrease in feedwater temperature	N/A	N/A	—
15.1.2 Increase in feedwater flow	N/A	N/A	—
15.1.3 Increase in steam flow	N/A	N/A	—
15.1.4 Inadvertent opening of an SG relief or safety valve	• Low DNBR • High LPD • High core power • Low SG pressure	• MSIS on low SG pressure • SIS actuation on low PZR pressure • MSIV closure on low SG pressure	• MSSVs
15.1.5 Steam system piping failure	• High core power • Low DNBR • CPC variable overpower • CPC low RCP shaft speed • Low SG pressure • Low PZR pressure • High containment pressure	• MSIVs and MFIVs closure on low SG pressure • SIS on low PZR pressure • AFW pumps actuation on low SG level or concurrent with reactor trip	—

Table 15.0-7 (2 of 5)

Incident	Reactor Trip Functions[(1)]	ESF Functions[(2)]	Other Equipment
15.2 Decrease in Heat Removal by Secondary System			
15.2.1 Loss of external load	N/A	N/A	—
15.2.2 Turbine trip	N/A	N/A	—
15.2.3 Loss of condenser vacuum	• High PZR pressure • Low SG level • Low RCP speed	• AFWS on low SG level	• POSRVs • MSSVs
15.2.4 Closure of an MSIV	N/A	N/A	—
15.2.6 Loss of nonemergency AC power	N/A	N/A	—
15.2.7 Loss of normal feedwater flow	N/A	N/A	—
15.2.8 Feedwater system pipe failure	• High PZR pressure • Low SG level • High containment pressure	• Auxiliary feedwater actuation by low SG level • Containment isolation by high containment pressure	• POSRVs • MSSVs

Table 15.0-7 (3 of 5)

Incident	Reactor Trip Functions(1)	ESF Functions(2)	Other Equipment
15.3 Decrease in Reactor Coolant System Flow Rate			
15.3.1 Loss of Forced Reactor coolant flow	• CPC low RCP shaft speed • High PZR pressure	N/A	• POSRVs • MSSVs
15.3.3 Reactor Coolant Pump Rotor Seizure	• Low reactor coolant flow • High PZR pressure	• AFW on low SG level	• POSRVs • MSSVs
15.4 Reactivity and Power Distribution Anomalies			
15.4.1 Uncontrolled CEA withdrawal from a subcritical or low power startup condition	• High logarithmic power level • Variable overpower • CPC variable overpower • High PZR pressure	N/A	N/A
15.4.2 Uncontrolled CEA withdrawal at power	• Variable overpower • CPC variable Overpower • Low DNBR • High LPD • High PZR pressure	N/A	N/A
15.4.3 CEA Misoperation	• Low DNBR • High LPD	N/A	N/A

Table 15.0-7 (4 of 5)

Incident	Reactor Trip Functions[(1)]	ESF Functions[(2)]	Other Equipment
15.4.4 Startup of an inactive reactor coolant pump	N/A	N/A	N/A
15.4.6 Inadvertent decrease in boron concentration in the reactor coolant system	N/A	N/A	• BDAS
15.4.7 Inadvertent loading and operation of a fuel assembly	N/A	N/A	N/A
15.4.8 Spectrum of CEA ejection accidents	• Variable overpower • CPC variable overpower • Low DNBR • High LPD • High PZR pressure	AFW on low SG level	• POSRVs • MSSVs

Table 15.0-7 (5 of 5)

Incident	Reactor Trip Functions(1)	ESF Functions(2)	Other Equipment
15.5 Increase in RCS inventory			
15.5.1 Inadvertent operation of the ECCS	N/A	N/A	—
15.5.2 CVCS malfunction that increase reactor coolant inventory	High PZR pressure	SIS/partial cooldown on low RCS pressure	—
15.6 Decrease in RCS inventory			
15.6.1 Inadvertent opening of a pressurizer relief valve	N/A	N/A	—
15.6.2 Letdown line break	• CPCS low PZR pressure and low DNBR (LPLD)	SIP actuation on low PZR pressure	—
15.6.3 SGTR	• Low DNBR • Low PZR pressure • High SG level • Low PZR pressure and low DNBR (LPLD) • CPCS hot leg saturation temperature	• MSIV closure on high SG level • SIP actuation on low PZR pressure • AFWS on low SG level	• MSSVs
15.6.5 Loss-of-coolant accident	• Low PZR pressure	• SIS/partial cooldown on RCS pressure	• RCP trip • MSSVs

(1) All reactor trip functions available

(2) All ESF functions available

Table 15.0-8

Core Fission Product Release Fraction Released into Containment for LOCA

Nuclide Group	Gap Release (0.0083 ~ 0.5083 hr)	Early In-vessel Release (0.5083 ~ 1.8083 hr)
Noble gases	0.05	0.95
Halogens	0.05	0.35
Alkali metals	0.05	0.25
Tellurium group	0	0.05
Barium, strontium	0	0.02
Noble metals	0	0.0025
Cerium group	0	0.0005
Lanthanides	0	0.0002

Table 15.0-9

Time for Release Termination of Design Basis Accidents

Events	Time for Release Termination
Loss-of-coolant accidents	• For containment and ESF leakage: 720 hr
Steam generator tube rupture	• For affected SG: time to isolation (1) • For unaffected SG: until shutdown cooling entry condition is established (2)
Steam system piping failure	• For affected SG: until cold shutdown is established (3) • For unaffected SG: until shutdown cooling entry condition is established (2)
Feedwater system pipe break	• For containment: 720 hr • For secondary side: until shutdown cooling entry condition is established (2)
Failure of small lines carrying primary coolant outside containment	• For auxiliary building: 8 hr • For secondary side: until shutdown cooling entry condition is established (2)
RCP rotor Seizure	• For secondary side: until shutdown cooling entry condition is established (2)
Control element assembly ejection	• For containment: 720 hr • For secondary side: until shutdown cooling entry condition is established (2)
Fuel handling accident	• For containment: 720 hr • For auxiliary building: 2 hr(4)

(1) The MSSVs in the affected SG side remain closed after the operator action is taken at 30 minutes by which the RCS is cooled down using ADVs in unaffected SG side.

(2) The cooldown capacity of the auxiliary feedwater system provides reasonable assurance that the shutdown cooling entry condition is reached before 8 hours. The radiological consequence analyses assume that the shutdown cooling condition is reached at 8 hours.

(3) P-T-S leakage is be assumed to continue until the primary system pressure is less than the secondary system or until the temperature of the leakage is less than 100 °C (XX °F), as specified in NRC RG 1.183. Cold shutdown condition (< 100 °C [< XX °F]) is reached due to the same reason given in Note (2).

(4) All the radioactive material that escapes from the fuel pool to the auxiliary building are assumed to be released to the environment over a 2-hour period, as specified in Appendix B of NRC RG 1.183.

Table 15.0-10

Results of Radiological Consequences of APR1400 Design Basis Accidents

Design Basis Accidents		TEDE (mSv)		Dose Criteria (mSv TEDE)
		EAB	LPZ	
Steam system piping failure	1.0 % Fuel Failure	3.33E+01	2.08E+01	2.50E+02
	Pre-accident spike	2.66E+00	1.57E+00	2.50E+02
	Event-generated spike	1.15E+01	6.20E+00	2.50E+01
Feedwater system pipe break		4.22E-01	2.22E-01	2.50E+01
RCP rotor seizure		2.09E+01	1.07E+01	2.50E+01
Control element assembly ejection	Containment	3.99E+01	3.77E+01	6.30E+01
	Steam generator	3.99E+01	2.23E+01	6.30E+01
Failure of small lines carrying primary coolant outside containment		1.36E+01	3.18E+00	2.50E+01
Steam generator tube rupture	Pre-accident spike	1.10E+01	2.53E+00	2.50E+02
	Event-generated spike	6.32E+00	1.57E+00	2.50E+01
Loss-of-coolant accidents		2.27E+02	2.37E+02	2.50E+02
Fuel handling accident		3.89E+00	8.56E+00	6.30E+01

Table 15.0-11 (1 of 3)

TMI Action Plan

Item #	Subject	Disposition for APR1400
I.C.1	NUREG-0737, I.C.1, Short-Term Accident Analysis and Procedures Revision	The ultimate responsibility for meeting NUREG-0737, Supplement 1 and Generic Letter 82-33, remains with the utility owner-operator. KHNP, however, assists the owner-operator in establishing these procedures and training the plant operators and staff by providing Emergency Operations Guidelines. KHNP provides analyses and guidance to assist the owner-operator in meeting the guidance of NUREG-0737, Supplement 1 and Generic Letter 82-33.
II.B.3	10 CFR 50.34(f)(2)(viii) Post-Accident Sampling System	The APR1400 includes the Primary Sampling System (see Section 9.3.2), which is designed to collect representative samples of liquids and gases in various process systems and deliver them to sample stations for chemical and radiological analyses. The Primary Sampling System fulfills the applicable requirements of 10 CFR 50.34 (f) and meets the guidance identified in NUREG-0737 and the Staff Requirements Memorandum of July 21, 1993.
II.E.1.1	10 CFR 50.34(f)(1)(ii) Evaluation of the Auxiliary Feedwater (AFW) System	The evaluation of the AFW system is presented in: • Subsection 10.4.9, Auxiliary Feedwater System • Section 19.1, Probabilistic Risk Assessment
II.E.1.2	10 CFR 50.34(f)(2)(xii) AFW Automatic Initiation and Flow Indication	The AFW system is actuated automatically by an auxiliary feedwater actuation signal (AFAS) from the ESF actuation system or by the auxiliary protection system (described in Subsection 7.3.1.3). In addition to this automatic feature, the AFAS can be manually initiated as described in Subsection 10.4.9. The auxiliary feedwater system, including its integral instrumentation and controls, fulfills the applicable requirements of 10 CFR50, Appendix A by meeting the guidance identified in NUREG-0737 and the design criteria in IEEE 603-1991.
II.E.5.1	10 CFR 50.34(f)(2)(xvi) ECCS and PS Actuation Cycles	Not applicable to the APR1400 (applicable to B&W designs only).

Table 15.0-11 (2 of 3)

Item #	Subject	Disposition for APR1400
II.F.1	10 CFR 50.34(f)(2)(xvii) Additional Accident Monitoring Instrumentation	Accident monitoring instrumentation, which meets NRC guidance, is addressed in Subsection 7.5.1.1. • Section 7.5, Information Systems Important to Safety
II.F.2	10 CFR 50.34(f)(2)(xviii) Instrumentation for Detecting Inadequate Core Cooling	Inadequate Core Cooling (ICC) monitoring instrumentation is part of the MCR and is designed to meet the intent of the guidance identified in NUREG-0737. The ICC monitoring instrumentation and displays provide sufficient information to permit the operator to evaluate the potential for core uncovery, and gross breach of protective barriers, including the resultant release of radioactivity to the environment. The ICC monitoring instrumentation is described in Subsection 7.5.1.2. The MCR is designed in accordance with the applicable codes, standards and regulations, (10 CFR 50, Appendix A) and meets the intent of Regulatory Guide 1.97, Rev. 4, and NUREG-0737, as previously described.
II.F.3	10 CFR 50.34(f)(2)(xix) Instrumentation for Monitoring Plant Conditions, including core damage	The MCR includes the post-accident monitoring instrumentation (PAMI). The PAMI is designed in accordance with the intent of the guidance in NRC RG Guide 1.97, Rev. 4. This instrumentation is itemized in Subsection 7.5.1.1.5 and Table 7.5-3. These instrumentation and information systems meet the intent of NRC RG 1.97, Rev. 4, and ANSI/ANS-4.5.
II.K.2.16	10 CFR 50.34(f)(1)(iii) Reactor Coolant Pump Seal Damage for SBLOCA	RCP seal integrity can be maintained by component cooling water (CCW). In the event of a loss of offsite ac power, power can be supplied to the CCW pumps, as presented in Subsection 9.2.2, Component Cooling Water System

Table 15.0-11 (3 of 3)

Item #	Subject	Disposition for APR1400
II.K.2.17	Voiding in the reactor vessel and the hot legs during normal anticipated transients (See item I.C.1).	See Disposition to I.C.1.
II.K.3.1	Auto PORV Isolation	The APR1400 DC has pressurizer pilot-operated safety relief valves (POSRVs) that incorporate relief capability. Because of the safety function, they are not isolatable. Refer to Subsection 5.4.14, Safety and Relief Valves.
II.K.3.5	Auto Trip of RCPs	The effects of automatic tripping of the RCPs on small-break LOCAs are reported in CEN-268 (Reference 75), which identifies the RCP trip methodology.
II.K.3.7	Evaluation of PORV Opening Probability	Not applicable to the APR1400. no PORV for the APR1400)
II.K.3.13	10 CFR 50.34(f)(1)(iii) HPCI and RCIC Initiation Levels	Not applicable to the APR1400 (applicable to BWRs only)
II.K.3.30	Small break LOCA methodology	This requirement is satisfied by CEN-203 (Reference 23 in Subsection 15.0.5.
II.K.3.31	Compliance with 10 CFR 50.46	Compliances with 10 CFR 50.46 is presented in: • Subsection 15.6.5, Loss-of-Coolant Accidents Resulting from the Spectrum of Postulated Piping Breaks within the Reactor Coolant Pressure Boundary
II.K.3.44	Evaluate Transients Considering Single Failures	The analyses of the transients presented in Chapter 15 consider single failures as required and described in the relevant sections, Identification of Causes and Frequency Classification
II.K.3.45	10 CFR 50.34(f)(1)(xi) Depressurization Methods	Not applicable to the APR1400 (applicable to BWRs only)

Table 15.0-12 (1 of 4)

Unresolved and Generic Safety Issues

Item #	Subject	Disposition for APR1400
USI-A-9	Anticipated Transients Without Scram	The requirements for the reduction of risk from ATWS events are given in 10 CFR 50.62, "Requirements for Reduction of Risk from Anticipated Transients without Scram Events for Light-Water-Cooled Nuclear Power Plants." The APR1400 design includes digital safety system and a diverse protection system (DPS) to comply with the ATWS rule as described in Section 15.8, Anticipated Transients without Scram
USI-A-47	Safety Implications of Control Systems	Consistent with the requirements and guidance of GL 89-19, the APR1400 incorporates: (1) SG overfill protection, and (2) an automatically initiated safety-grade Auxiliary Feedwater System. Furthermore, a Technical Specification for verifying overfill protection availability and emergency operations guidelines for an SBLOCA are established.
USI-B-17	Criteria for Safety-Related Operator Actions	APR1400 credits operation action in some analyses with the mitigation of postulated events. In these analyses, the action is not credited until 30 minutes after the event initiation. One significant improvement is the elimination of the ECCS realignment to the containment sump because the refueling water storage tank is inside containment and acts as the containment sump. Based on APR1400 design improvements and the more stringent safety analysis assumptions for operator action.
USI-C-4	Statistical Methods for ECCS Analyses	The APR1400 uses the statistical methodology to evaluate a large break LOCA (Reference 63 in Subsection 15.0.5).
USI-C-5	Decay Heat Model Update	The 1971 ANS 5.1 decay heat standard is used for the evaluation of small break LOCA (Reference 67 in Subsection 15.0.5). The 1979 ANS 5.1 decay heat standard is used for the evaluation of a large break LOCA (Reference 63 in Subsection 15.0.5).

Table 15.0-12 (2 of 4)

Issue #	Subject	Disposition for APR1400
USI-C-6	LOCA Heat Source	The methodologies for evaluating large break and small break LOCA (References 63 and 67 in Subsection 15.0.5) account for effects of power density, decay heat, stored energy, fission power decay, and their associated uncertainties as required.
USI-C-10	Effective Operation of Containment Spray	An automatically actuated containment spray system is conservatively assumed to be activated at time zero in LOCA minimum containment pressure analysis, as presented in Subsection 6.2.1.5, Minimum Containment Pressure Analysis for Performance Capability Studies of the Emergency Core Cooling System.
GSI-3	Instrumentation Setpoint Drift	The APR1400 includes safety-related instrumentation and controls with established setpoints to actuate safety functions (Chapter 7). Setpoints for safety related systems and components (e.g., the Plant Protection System), are established and maintained in accordance with the guidance given in NRC RG 1.105, Rev. 3, and conform to the criteria identified in ISA-S67.04-1994.
GSI-22	Detection of boron dilution events during shutdown and refueling	This requirement is satisfied through a safety-related system that monitors boron concentration in the RCS and isolates the CVCS if boron dilution is detected as described in Subsection 15.4.6, Inadvertent Decrease in Boron Concentration in the Reactor Coolant System
GSI-23	Reactor Coolant Pump Seal Failure	The APR1400 minimizes the possibility of core damage resulting from a small-break LOCA event caused by an RCP shaft seal failure by assuring seal integrity. Reasonable assurance of seal integrity is provided by seal and support systems design, which address susceptibility to station blackout. RCP seal integrity can be maintained by either of two independent sources of cooling water: the seal injection flow from the Chemical and Volume Control System (CVCS) or Component Cooling Water (CCW). In the event of a loss of offsite AC power or during a complete loss of AC power, power can be supplied to the charging pumps, auxiliary charging pump and CCW pumps, or auxiliary charging pump, respectively, as presented in: • Subsection 5.4.1, Reactor Coolant Pumps • Subsection 9.2.2, Component Cooling Water System • Subsection 9.3.4, Chemical and Volume Control System

Table 15.0-12 (3 of 4)

Issue #	Subject	Disposition for APR1400
GSI-24	Automatic ECCS Suction Switchover to Recirculation Mode	This requirement is not applicable to the APR1400. The source of safety injection water is the IRWST, which functions as the sump. Therefore, there is no need for a switchover to recirculation mode.
GSI-40	BWR Scram System Pipe Break	Not applicable to the APR1400 (applicable to BWRs only).
GSI-75	Generic Implications of ATWS Events at the Salem Nuclear Plant	This issue is therefore resolved for the APR1400.
GSI-125. II.7	Reevaluate Provision to Automatically Isolate Feedwater from Steam Generator During a Line Break	The APR1400 does not include automatic steam generator AFW isolation logic on low SG pressure. The calculated mass and energy release to the containment building as the result of a main steam line break (MSLB) includes the additional mass and energy introduced from auxiliary feedwater flow to the affected steam generator. This additional mass and energy addition is assumed to continue for at least 30 minutes after an MSLB.
GSI-135	Steam Generator and Steam Line Overfill	The thermal-hydraulic evaluation of an SGTR is presented in Subsection 15.6.3, Steam Generator Tube Failure. The affected steam generator does not overfill and cause liquid to enter the steam line. Additional provisions to prevent SG overfill are automatic termination of main and auxiliary feedwater flows on high SG water and operator action to secure the reactor coolant pumps in the affected loop. Additional design features such as the safety depressurization and vent system, automatic termination of feedwater on high steam generator water level, and longer allowable operator response time minimize the probability of overfill in an SGTR event. In summary, because the plant capabilities are consistent with the goals of the NRC's tasks in GSI 135,

Table 15.0-12 (4 of 4)

Issue #	Subject	Disposition for APR1400
GSI-185	Control of Recriticality Following SBLOCAs	GSI-185 is related to post-LOCA boron dilution accidents, which are beyond DBAs. In addition, this issue is satisfied by NUREG-0933. Therefore, it is not necessary to describe this issue in the APR1400.
GSI-191	PWR Sump Clogging	The APR1400 incorporates mitigative features to resolve this issue by applying advantage of the lessons learned from operating plants and on industry treads. Four strainers are installed in the IRWST, which have a large surface area to accommodate the small amount of debris that reaches it. The RCS piping and components, and other potentially insulated systems or components in the containment are insulated with reflective metal insulation (RMI), and or no fibrous or microporous insulation, to reduce potential sources of debris that would significantly increase head loss through the sumps. An evaluation of the susceptibility of the APR1400 design to debris blockage is performed in accordance with the guidance of NRC RG 1.82, Rev. 4. It is concluded that the APR1400 does not challenge long-term recirculation capability due to the strainer blockage resulting from deposition of debris on the strainers.

Table 15.0-13 (1 of 4)

NRC Generic Letters and Bulletins

Item #	Subject	Disposition for APR1400
GL-80-19	Resolution of Enhanced Fission Gas Release Concern	This GL is satisfied for the APR1400. Fission gas release at extended burnup is calculated by the fuel performance computer codes FATES3B described in Reference 74.
GL-80-35	Effect of a DC Power Supply Failure on ECCS Performance	The APR1400 provides 4 independent trains of ECCS with 4 EDGs. Because there are no effects on ECCS performance with a DC power supply failure, this issue is resolved for the APR1400.
GL-83-11	Licensee Qualification for Performing Safety Analysis in Support of Licensing Actions	Not Applicable to the APR1400 (not included in the APR1400 design requirements)
GL-83-22	Safety Evaluation of ‘Emergency Response Guidelines’	Not Applicable to the APR1400 (applicable to Westinghouse design only)
GL-83-32	NRC Staff Recommendations Regarding Operator Action for Reactor Trip and ATWS	Not applicable to the APR1400. However, the APR1400 complies with the requirements of 10 CFR 50.62 as described in Section 15.8, Anticipated Transients Without Scram.
GL-85-06	Quality Assurance Guidance for ATWS Equipment That Is Not Safety-Related	Not applicable to the APR1400 (not included in the APR1400 design requirements)
GL-85-16	High Boron Concentrations	Not applicable to the APR1400 (not included in the APR1400 design requirements)
GL-86-13	Potential Inconsistency between Plant Safety Analyses and Technical Specifications	The potential for inconsistency between the APR1400 Technical Specifications (TSs) and Chapter 15 analyses is avoided because safety analysis evaluated the complete operating ranges from power operation to cold shutdown and the TS are based on these safety analyses.
GL-86-16	Westinghouse ECCS Evaluation Models	Not Applicable to the APR1400 (applicable to Westinghouse design only)
GL-88-16	Removal of Cycle-Specific Parameter Limits from Technical Specifications	Fuel cycle specific parameter information is provided in the Core Operating Limits Report.

Table 15.0-13 (2 of 4)

Item #	Subject	Disposition for APR1400
GL-88-17	Loss of Decay Heat Removal	In accordance with the recommendations of GL 88-17, the APR1400 includes the relevant features to facilitate reduced inventory operations. The equipment and instrumentation are highly reliable and are described in Subsection 5.4.7, the shutdown cooling system (SCS). In addition to the design features, analysis of loss of RHR during mid-loop operation is performed to provide a basis for operating procedure guidelines. These include the relationships between time after shutdown and decay heat, RCS heatup rate and boil-off rate. Guidelines is provided for reduced inventory operating and administrative procedures, including verifying availability of equipment, avoiding concurrent operations that perturb the RCS, and initiation of containment isolation upon detection of the loss of RHR. Because the foregoing design features and guidelines for operations with reduced RCS inventory meet the intent of the recommendations in GL 88-17, this is resolved for the APR1400.
GL-93-04	Rod Control System Failure and Withdrawal of Rod Control Cluster Assemblies	Not applicable to the APR1400 (applicable to Westinghouse design only)
GL-97-01	Degradation of Control Rod Drive Mechanism Nozzle and Other Vessel Closure Head Penetrations	Control element assembly ejection is evaluated from a reactivity standpoint in Subsection 15.4.8. A failure in the reactor vessel head penetration that causes a SBLOCA is bounded by the analyses in Subsection 15.6.5.2.
GL-98-02	Loss of Reactor Coolant Inventory and Associated Potential for Loss of Emergency Mitigation Functions while in a Shutdown Condition	The safety injection system (SIS), which provides the emergency core cooling function for the APR1400, consists of four independent trains. Because the SIS does not use a common pump suction header for its emergency core cooling function, a common cause failure is precluded. All failure modes of SIS design are discussed in the failure modes and effects analysis (FMEA), Section 6.3, Safety Injection System.

Table 15.0-13 (3 of 4)

Item #	Subject	Disposition for APR1400
GL-2004-02	Potential Impact of Debris Blockage on Emergency Recirculation During Design Basis Accidents at Pressurized-Water Reactors	The APR1400 incorporates mitigative features to resolve this issue by applying advantage of the lessons learned from operating plants and on industry treads. Four strainers are installed in the IRWST, which have a large surface area to accommodate the small amount of debris that reaches it. The RCS piping and components, and other potentially insulated systems or components in the containment are insulated with reflective metal insulation (RMI), and or no fibrous or microporous insulation, to reduce potential sources of debris that would significantly increase head loss through the sumps. An evaluation of the susceptibility of the APR1400 design to debris blockage is performed in accordance with the guidance of NRC RG 1.82, Rev. 4. It is concluded that the APR1400 does not challenge long-term recirculation capability due to the strainer blockage resulting from deposition of debris on the strainers.
GL-2008-01	Managing Gas Accumulation in Emergency Core Cooling, Decay Heat Removal, and Containment Spray Systems	For the APR1400, design features preventing and controlling gas accumulation to acceptable levels are as follows: • Suction piping of SIS with continuous downward slope • Suction piping of SCS with continuous downward slope • Sump strainer in the IRWST to prevent vortex formation • Numerous safety-related pressure and level sensors on SIT • Elevation difference of more than XX m (10 ft) between SIT nozzle and SIT check valve • Continuous pressurization of the RCPB lines by the SITs • High point vents: precludes gas accumulation to unacceptable level in SIS/RHRS Therefore, this issue is resolved for the APR1400 DC.

Table 15.0-13 (4 of 4)

Item #	Subject	Disposition for APR1400
BL-80-04	Analysis of a PWR Main Steam Line Break with Continued Feedwater Addition	MSLB is evaluated in Subsection 6.2.1.4, Mass and Energy Release Analysis for Postulated Secondary System Pipe Ruptures Inside Containment, with a continued feedwater addition for the conservatism.
BL-80-18	Maintenance of Adequate Minimum Flow thru Centrifugal Charging Pumps Following Secondary Side High Energy Line Rupture	Not applicable to the APR1400 (the APR 1400 has separate charging pumps and safety injection pumps)
BL-86-03	Potential Failure of Multiple ECCS Pumps due to Single Failure of Air-operated Valve in Minimum Flow Recirculation Line	Not applicable to the APR1400 (not included in the APR1400 design requirements)
BL-93-02	Debris Plugging of Emergency Core Cooling Suction Strainers – Fibrous air filters and other temporary material appear to be likely sources of such fibrous material.	The APR1400 design avoids this issue by the installation of four strainers with a sufficient surface area and the exclusion of the fibrous material in containment.
BL-95-02	Unexpected Clogging of a Residual Heat Removal (RHR) Pump Strainer while Operating in Suppression Pool Cooling Mode	The APR1400 design avoids this issue by the installation of four strainers with a sufficient surface area and the exclusion of the fibrous material in containment.
BL-96-01	Control Rod Insertion Problems – operability of control rods in high burnup fuel assemblies	Not applicable to the APR1400 (applicable to Westinghouse design only)
BL-96-03	Potential Plugging of Emergency Core Cooling Suction Strainers by Debris in Boiling Water Reactors	Not applicable to the APR1400 (applicable to BWRs only)
BL-2001-01	Circumferential Cracking of Reactor Pressure Vessel Head Penetration Nozzles	Control element assembly ejection is evaluated from a reactivity standpoint in Section 15.4.8. A failure in the reactor vessel head penetration that causes an SBLOCA is bounded by the analyses in Subsection 15.6.5.

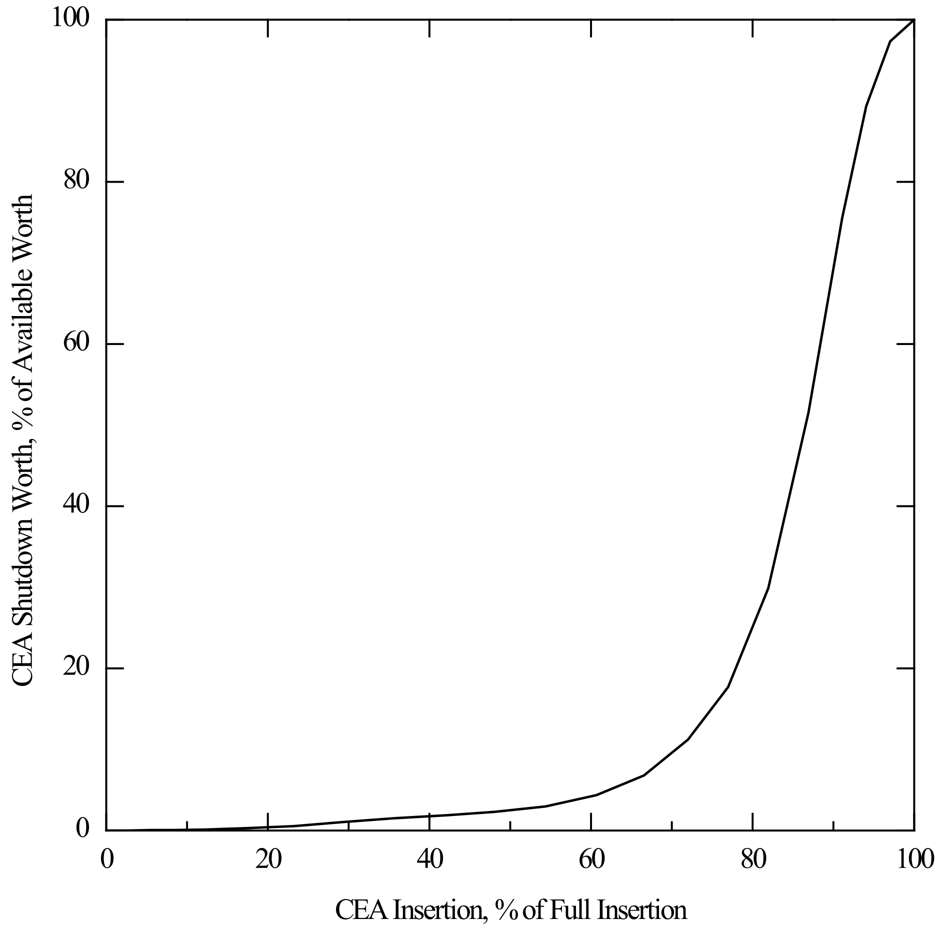

Figure 15.0-1   Shutdown Reactivity Worth vs. Position Curve.

15.1 Increase in Heat Removal by the Secondary System

This section describes analyses that have been performed for events that could result in an increase in the rate of heat removal by the secondary system, which could lead to a temperature decrease in the reactor coolant system (RCS).

Several anticipated operational occurrences (AOO) and one postulated accident (PA) result in an unplanned increase in heat removal by the secondary system. In these events, a decrease in reactor coolant temperature causes an increase in core reactivity that leads to an increase in core power. Detailed analyses of these RCS cooldown events are presented in this section. The events are:

a. Subsection 15.1.1 – Decrease in feedwater temperature

b. Subsection 15.1.2 – Increase in feedwater flow

c. Subsection 15.1.3 – Increase in steam flow

d. Subsection 15.1.4 – Inadvertent opening of a steam generator relief or safety valve

e. Subsection 15.1.5 – Steam system piping failure inside and outside the containment

15.1.1 Decrease in Feedwater Temperature

15.1.1.1 Identification of Causes and Frequency Classification

A decrease in feedwater temperature may result from a loss of feedwater heaters. The feedwater heaters may be lost due to isolation of one of two high-pressure feedwater heater trains. The maximum decrease in feedwater temperature due to a failure in the main feedwater system is less than 37.78 °C (100 °F). A LOOP concurrent with a turbine trip is considered a basic assumption.

A decrease in feedwater temperature event is classified as an AOO. Event frequency conditions are discussed in Subsection 15.0.0.1 and Table 15.0-5.

15.1.1.2 Sequence of Events and Systems Operation

A decrease in feedwater temperature causes an increase of heat transfer from the primary to the secondary system through the steam generators (SGs) and a decrease in the reactor coolant temperature. It also causes an increase in reactor power due to the negative moderator temperature coefficient and a decrease in the RCS and steam generator pressure. Detection of these conditions is accomplished by the RCS and SG low-pressure alarms and the high linear power alarm. Trip signals generated by the core protection calculators (CPCs) provide reasonable assurance that the low departure from nucleate boiling ratio (DNBR) or high local power density limits are not exceeded with the specified acceptable fuel design limit (SAFDL) approaching during the transient.

15.1.1.3 Core and System Performance

15.1.1.3.1 Evaluation Model

The evaluation model for the inadvertent opening of a steam generator atmospheric dump valve (IOSGADV) is applicable to a decrease in feedwater temperature (see Subsection 15.1.4.3.1).

15.1.1.3.2 Input Parameters and Initial Conditions

The input parameters and initial conditions used to analyze the nuclear steam supply system (NSSS) response to a decrease in feedwater temperature are bounded by the input parameters and initial conditions of an IOSGADV (Subsection 15.1.4.3.2).

15.1.1.3.3 Results

The core power increase from a decrease in feedwater temperature event is larger than that for an IOSGADV. However, a core power increase greater than obtained for the IOSGADV would cause an immediate CPC reactor trip on low DNBR or high local power density, which would terminate the degradation in fuel performance. Therefore, an analysis of the most adverse decreased feedwater temperature event shows that the minimum transient DNBR occurs with the decreased feedwater temperature concurrent with a loss of offsite power and a turbine trip following the reactor trip. These events are described in Subsection 15.1.4. Likewise, the results of these events in combination with a limiting single failure are less limiting than an IOSGADV event with a loss of offsite

power and the limiting single failure. These events are also described in Subsection 15.1.4.

15.1.1.4 Barrier Performance

A decrease in main feedwater temperature event is characterized by an initial cooldown of the primary and secondary systems and by decreasing RCS and steam generator pressures. The result is an insignificant increase in RCS pressure. The maximum RCS pressure is below 110 percent of the RCS design pressure. The maximum SG pressure is also below 110 percent of the SG design pressure.

15.1.1.5 Radiological Consequences

The radiological consequences of this event are bounded by the radiological consequences of the steam system piping failure described in Subsection 15.1.5.

15.1.1.6 Conclusions

The decreased feedwater temperature events result in DNBRs greater than 1.29 throughout the transient. Also, the RCS pressures remain below 193.34 kg/cm^2A (2,750 psia), and the steam generator pressures remain below 92.83 kg/cm^2A (1,320 psia).

15.1.2 Increase in Feedwater Flow

15.1.2.1 Identification of Causes and Frequency Classification

An increase in main feedwater flow could be caused by the further opening of a feedwater control valve or an increase in the feedwater pump speed. The maximum increase at full power is less than nominal flow for the main feedwater system. An increase in feedwater flow could be caused by the inadvertent actuation of an auxiliary feedwater pump. The auxiliary feedwater maximum flow of 3,596.14 L/min (950 gpm) is within a 10 percent of the rated main feedwater flow, including the effect of the lower enthalpy of the auxiliary feedwater.

An increase in feedwater flow event is classified as an AOO. Each frequency condition is described in Subsection 15.0.0.1 and Table 15.0-5.

15.1.2.2 Sequence of Events and Systems Operation

An increase in feedwater flow causes an increase of heat transfer from the primary to the secondary system through the steam generators, a decrease in the temperature of the reactor coolant, an increase in reactor power due to the negative moderator temperature coefficient, a decrease in the RCS and SG pressure, and an increase in SG water level. Detection of these conditions is accomplished by the RCS low pressure alarm and SG low pressure and high water level alarms. Protection against the violation of a SAFDL, as a consequence of an increase in feedwater flow, is provided by the reactor trip caused by CPC variable overpower or the high steam generator water level trips.

15.1.2.3 Core and System Performance

15.1.2.3.1 Evaluation Model

The evaluation model for the IOSGADV is applicable to this event (Subsection 15.1.4.3.1).

15.1.2.3.2 Input Parameters and Initial Conditions

The input parameters and initial conditions used to analyze the NSSS response to an increase in feedwater flow are bounded by those of an IOSGADV (Subsection 15.1.4.3.2).

15.1.2.3.3 Results

The minimum transient DNBR for this event with a loss of offsite power concurrent with a turbine trip following a reactor trip is greater than that for the IOSGADV event and for the IOSGADV event with a loss of offsite power concurrent with a turbine trip following a reactor trip, respectively, which are presented in Subsection 15.1.4. Likewise, the results of these events in combination with the limiting single failure are less limiting than those of the IOSGADV event and the IOSGADV event with a loss of offsite power in combination with the limiting single failure, respectively, which are also presented in Subsection 15.1.4.

15.1.2.4 Barrier Performance

An increase in main feedwater flow event is characterized by an initial cooldown of the primary and secondary systems, decreasing RCS and SG pressures, and increasing SG water level. Thus, the events of this section result in an insignificant increase in RCS pressure. The maximum RCS pressure is below 110 percent of the RCS design pressure.

The maximum SG pressure also is below 110 percent of the SG design pressure.

15.1.2.5 Radiological Consequences

The radiological consequences of this event are bounded by the radiological consequences of the steam system piping failure described in Subsection 15.1.5.

15.1.2.6 Conclusions

Increased feedwater flow events result in DNBRs greater than 1.29 throughout the transient. Also, the RCS pressure remains below 193.34 kg/cm^{2}A (2,750 psia), and the steam generator pressure remains below 92.83 kg/cm^{2}A (1,320 psia).

15.1.3 Increase in Steam Flow

15.1.3.1 Identification of Causes and Frequency Classification

An increase in main steam flow may be caused by an inadvertent increased opening of the turbine admission valves. This inadvertent opening may be caused by operator error or turbine load limit malfunctions and results in no more than an 11 percent increase over the nominal full power steam flow rate. An increase in the main steam flow can also result from the inadvertent opening of a turbine bypass valve or an atmospheric dump valve; these events are discussed separately in Subsection 15.1.4.

An increase in steam flow event is classified as an AOO. Each frequency condition is described in Subsection 15.0.0.1 and Table 15.0-5.

15.1.3.2 Sequence of Events and Systems Operation

An increase in the main steam flow causes an increase of heat transfer from the primary to the secondary system through the SG, a decrease in the temperature of the reactor coolant, an increase in core power and heat flux, and a decrease in reactor coolant system and SG pressure. Detection of these conditions is accomplished by the RCS and the SG low-pressure alarms and the high reactor power alarm. Trip signals generated by the CPCs provide reasonable assurance that the low DNBR or high local power density limits are not exceeded if the transient results in an approach to the SAFDL.

15.1.3.3 Core and System Performance

15.1.3.3.1 Evaluation Model

The evaluation model for an IOSGADV is applicable to this event (Subsection 15.1.4.3.1).

15.1.3.3.2 Input Parameters and Initial Conditions

The input parameters and initial conditions used to analyze the NSSS response to an increase in steam flow are bounded by those of an IOSGADV (Subsection 15.1.4.3.2).

15.1.3.3.3 Results

The maximum RCS temperature decrease for the increased main steam flow event is similar to that for an IOSGADV event. This is because both events cause an increase in main steam flow of no more than 11 percent, which is assumed for the IOSGADV event. The resultant power increase and the subsequent DNBR transient are also similar. The system operation described above is similar to the IOSGADV event described in Subsection 15.1.4.

The systems operation for the increased main steam flow event with a LOOP is similar to an IOSGADV event with a loss of offsite power, which is discussed in Subsection 15.1.4. These events in combination with a limiting single failure are no more severe than the IOSGADV event and the IOSGADV with a LOOP, combined with the limiting single failure, respectively, which are also described in Subsection 15.1.4.

15.1.3.4 Barrier Performance

All increased heat removal events analyzed in this section are characterized by decreasing RCS pressure due to the cooldown of the primary system. These events result in an insignificant increase in RCS pressure. The maximum SG pressure also is below 110 percent of the SG design pressure.

15.1.3.5 Radiological Consequences

The radiological consequences of this event are bounded by the radiological consequences of the steam system piping failure described in Subsection 15.1.5.5.

15.1.3.6 Conclusions

The increased main steam flow events result in a DNBR greater than 1.29 throughout the transient. Also, the RCS pressure remains below 193.34 kg/cm^{2}A (2,750 psia), and the SG pressures remain below 92.83 kg/cm^{2}A (1,320 psia).

15.1.4 Inadvertent Opening of a Steam Generator Relief or Safety Valve

15.1.4.1 Identification of Causes and Frequency Classification

An atmospheric dump valve (ADV) or a turbine bypass valve may be inadvertently opened by an operator or may open due to a failure of the control system that operates the valve. A SG safety valve remains open only as a result of a valve failure. The opening of any of these valves results in similar consequences because they relieve steam at the same maximum flow rate (no more than 11 percent of full power turbine flow rate). A LOOP concurrent with a turbine trip following a reactor trip is considered a basic assumption. As discussed in the previous subsections, the consequences of an IOSGADV event bound those of the increased main steam flow, decreased feedwater temperature, and increased feedwater flow events.

An IOSGADV event is classified as an AOO. Each frequency condition is described in Subsection 15.0.0.1 and Table 15.0-5.

For the events discussed in this section, the major parameter of concern is the minimum hot channel DNBR. This parameter establishes whether a fuel design limit has been violated and whether fuel cladding degradation is anticipated.

The factors that cause a decrease in a local DNBR are:

a. Increasing coolant temperature

b. Decreasing coolant pressure

c. Increasing local heat flux (including radial and axial power distribution effects)

d. Decreasing coolant flow

A single failure is assumed to be a failure that yields the minimum DNBR before the reactor trip and the greatest decrease in DNBR after initiation of a reactor trip signal.

The most limiting single failure for the events discussed in this section is determined to be the excessive feedwater flow after a turbine trip on a reactor trip based on an evaluation of the single failures listed in Table 15.0-4. The feedwater flow is not reduced after a reactor trip causing the primary and secondary system pressures continue to decrease after the reactor trip. The analysis assumes that the most reactive CEA is held in the fully withdrawn position following the reactor trip. The LOOP is postulated to occur due to the turbine generator trip and is conservatively assumed to occur with no time delay.

15.1.4.2 Sequence of Events and Systems Operation

Case 1: IOSGADV with a LOOP

The opening of a steam generator ADV increases the rate of heat removal by the steam generators, causing cooldown of the RCS. Because of the negative moderator temperature coefficient, the core power increases from the initial value of 102 percent of rated core power, reaching a new stabilized value of 113 percent. The feedwater control system, which is assumed to be in the automatic mode, supplies feedwater to the steam generators so that the steam generator water levels are maintained.

Acting on the large power mismatch between the reactor and turbine and the audible indication of steam blowdown, the reactor operator recognizes that the plant is in an abnormal state and manually trips the reactor. The analysis presented here assumes that the initial operator action is delayed until after 30 minutes following the event initiation. It is also conservatively assumed that a LOOP occurs immediately on the turbine trip. The reactor coolant pumps are therefore assumed to begin coasting down at the time of the turbine trip.

Following the generation of a turbine trip on a reactor trip and a concurrent LOOP, the normal feedwater flow to steam generators is terminated. The water level of both steam generators decreases following the reactor trip and falls below the point for auxiliary feedwater flow initiation. The main steam system pressures decrease steadily until the main steam isolation signal is generated. A decrease in core power and reactor coolant cooldown, which is due to cooling by ADV of the affected steam generator, maintains

natural circulation and decreases the coolant temperature. The main steam isolation signal (MSIS) results in the isolation of the unaffected steam generator from the flow path through the ADV, which is stuck open.

After tripping the reactor, the operator manually closes the inadvertently opened ADV, terminating the steam release to the atmosphere from the affected steam generator. The analysis conservatively assumes that the action to close the ADV is delayed 20 minutes beyond the operator's initial action to trip the reactor or a total of 50 minutes after event initiation. The operator is assumed to initiate plant cooldown 30 minutes after the manual reactor trip. RCS heat removal for plant stabilization and cooldown is accomplished by using the ADVs on the unaffected steam generator.

Case 2: IOSGADV with a loss of feedwater control system reactor trip override and a LOOP

Until the assumed reactor trip occurs, the transient due to the IOSGADV is identical with or without a single failure. For the IOSGADV+SF event, the reactor is manually tripped 30 minutes following the first indication of the event. A LOOP is assumed to occur, concurrent with the turbine trip following the reactor trip. Because of the single failure, it is assumed that the feedwater control system does not receive the reactor trip override (RTO) signal to cut back the feedwater flow. Therefore, primary and secondary pressures continue to decrease, and the main steam safety valves (MSSVs) fail to open. Primary pressure and temperatures decrease more rapidly after a reactor trip with a single failure.

The operator recognizes the incident based on a variety of indications and manually closes the ADV that had been inadvertently opened, terminating steam release to the atmosphere from the affected steam generator. The indications include the initial large power mismatch between the reactor and turbine, the steady decrease in steam generator pressure and water levels after reactor trip, the continued decrease in pressure in the affected steam generator after the MSIS, the low steam generator pressure alarms, and the audible indication of steam blowdown. The analysis assumes that the initial operator action to close the open ADV is delayed until 20 minutes after the operator's initial action to trip the reactor or a total of 50 minutes after event initiation. The operator is assumed to initiate plant cooldown 30 minutes after a manual reactor trip. RCS heat removal for plant stabilization and cooldown is accomplished by manual control of the ADVs on the unaffected SG.

15.1.4.3 Core and System Performance

15.1.4.3.1 Evaluation Model

The nuclear steam supply system response to the IOSGADV and the IOSGADV+SF with a LOOP was simulated using the CESEC-III described in Subsection 15.0.2.2.1. The time-dependent thermal margins on DNBR in the reactor core were calculated using the CETOP, which uses the KCE-1 critical heat flux correlation described in Reference 28 in Subsection 15.0.5.

15.1.4.3.2 Input Parameters and Initial Conditions

Table 15.1.4-3 lists the assumptions and initial conditions used for these analyses in addition to those discussed in Section 15.0. The initial conditions for the principal process variables are varied to determine the set of initial conditions that would produce the greatest overpower condition caused by the increase in steam flow. If the core power increases to more than 115 percent, the core protection calculators (CPCs) initiate a reactor trip and there is no further degradation in the thermal margin.

15.1.4.3.3 Results

Case 1: IOSGADV with a LOOP

The dynamic behavior of the NSSS parameters following an IOSGADV is presented in Figures 15.1.4-1.1 through 15.1.4-1.15. Table 15.1.4-1 summarizes the major events, times, and results for this transient.

The opening of an ADV increases the rate of heat removal by the steam generators, causing cooldown of the RCS. Because of the negative moderator reactivity coefficient, the core power increases from 102 percent of rated core power, reaching a new, stabilized value of 113 percent. The feedwater control system, which is assumed to be in the automatic mode, supplies feedwater to the steam generators so that the steam generator water levels are maintained.

At 1,800.1 seconds, the trip breakers open, the turbine trip is initiated, the LOOP is assumed to occur, and the RCPs begin to coast down. Because of the RCP coastdown, the

transient DNBR decreases, reaching a minimum value of 1.336, which is above the SAFDL value of 1.29 at 1,801.7 seconds, and then rapidly increases, as shown in Figure 15.1.4-1.15.

At 2,105.9 seconds, the steam generator pressure drops below the MSIS setpoint of 57.09 kg/cm^{2}A (812 psia). At 1,966.5 seconds, a void begins to form in the RV upper head. At 3,000 seconds, the operator manually closes the open ADV. The operator initiates plant cooldown at 3,600 seconds.

<u>Case 2: IOSGADV with single failure and a LOOP</u>

The dynamic behavior of the salient NSSS parameters after an IOSGADV with a LOOP and with a loss of the feedwater control system reactor trip override is presented in Figures 15.1.4-2.1 through 15.1.4-2.15. Table 15.1.4-2 summarizes the major events, times, and results for this transient.

The opening of an SGADV increases the rate of heat removal by the steam generators, causing a cooldown of the RCS. Because of the negative moderator reactivity coefficient, the core power increases from 102 percent of rated core power, reaching a new, stabilized value of 113 percent. The feedwater control system, which is assumed to be in the automatic mode, supplies feedwater to the steam generators so that the steam generator water levels are maintained.

During the IOSGADV+SF transient, the operator manually trips the reactor at 1,800 seconds. At 1,800.1 seconds, the trip breakers open, the turbine trip is initiated, the LOOP is assumed to occur, and the RCPs begin to coast down. Because of the RCP coastdown, the transient DNBR decreases, reaching a minimum value of 1.336, which is above the SAFDL value of 1.29 at 1,801.7 seconds, and then rapidly increases, as shown in Figure 15.1.4-2.15. The IOSGADV event plus the limiting SF does not result in DNB in fuel pins.

At 1,955.65 seconds, the steam generator pressure drops below the MSIS setpoint of 57.09 kg/cm^{2}A (812 psia). The MSIVs close by 1,962.0 seconds. The MFIVs close by 1,967.0 seconds. Voids begin to form in the upper head of the reactor vessel at 1,888.7 seconds. At 3,000 seconds, the operator manually closes the open ADV. The operator initiates plant cooldown at 3,600 seconds.

15.1.4.4 Barrier Performance

The IOSGADV event is characterized by an initial cooldown of the primary and secondary systems, decreasing RCS and steam generator pressures. Thus, the events describe in this subsection result in an insignificant increase in RCS pressure. The maximum RCS pressure is below 110 percent of the RCS design pressure. The maximum SG pressure also is below 110 percent of the SG design pressure.

15.1.4.5 Radiological Consequences

The radiological consequences of this event are bounded by the radiological consequences of the steam system piping failure described in Subsection 15.1.5.

15.1.4.6 Conclusions

In the IOSGADV with a LOOP event, a single failure does not have an effect on the consequence, and the fuel pins are not predicted to be in DNB. For all cases, the RCS pressure remains below 193.34 kg/cm^{2}A (2,750 psia), providing reasonable assurance that the integrity of the RCS is maintained. The steam generator pressure remains below 92.83 kg/cm^{2}A (1,320 psia), providing reasonable assurance that the integrity of the secondary system is maintained.

15.1.5 Steam System Piping Failure Inside and Outside the Containment

15.1.5.1 Identification of Causes and Frequency Classification

A steam line break (SLB) is defined as a pipe break in the main steam system that results in excessive RCS cooldown and causes the core reactivity to increase. Degradation in fuel cladding performance may result from this event, which is classified as an accident. SLB analysis cases are chosen to maximize potential for a post-trip return to power (RTP) to maximize the potential for degradation in fuel cladding performance and to maximize the doses at the EAB and LPZ. An SLB event is classified as a PA. Each frequency condition is described in Subsection 15.0.0.1 and Table 15.0-5. The SLBs presented are:

a. Cases chosen to maximize the potential for a post-trip RTP:

1) Case 1: A large SLB inside the containment during full power operation with a LOOP concurrent with the initiation of the event in combination with a single failure and a stuck CEA (SLBFPLOOP)

2) Case 2: A large SLB inside the containment during full power operation with offsite power available in combination with a single failure and a stuck CEA (SLBFP)

3) Case 3: A large SLB inside the containment during zero power operation with a LOOP concurrent with the initiation of event in combination with a single failure and a stuck CEA (SLBZPLOOP)

4) Case 4: A large SLB inside the containment during zero power operation with offsite power available in combination with a single failure and a stuck CEA (SLBZP)

b. Cases chosen to maximize the potential for a pre-trip degradation in fuel performance and doses at the EAB and LPZ:

1) Case 5: An SLB outside the containment upstream of the MSIV during full power operation with a LOOP concurrent with turbine trip following a reactor trip in combination with a single failure, Technical Specification SG tube leakage, and a stuck CEA (SLBFPD+LOOP)

2) Case 6: An SLB outside the containment upstream of the MSIV during zero power operation with a LOOP concurrent with the initiation of event in combination with a single failure, Technical Specification SG tube leakage, iodine spike, and a stuck CEA (SLBZPLOOPD)

The following are not presented because the event consequences are bounded by the event presented in Case 5: (1) an SLB outside the containment upstream of the MSIV during full power operation with a LOOP or without a LOOP concurrent with the initiation of event in combination with a single failure, (2) SG tube leakage at the allowable limit of the Technical Specifications, and (3) a stuck CEA. The case with a LOOP concurrent with

turbine trip after a reactor trip bounds all other cases because it presents the greatest degradation of DNBR and the greatest potential for large radiological doses.

The following produces the same radiological dose as the corresponding case with a LOOP (Case 6): an SLB outside the containment upstream of the MSIV during zero power operation with offsite power available in combination with a single failure, SG tube leakage at the allowable limit of the Technical Specifications, and a stuck CEA. Both cases result in doses that are within the 10 CFR 50.34 guidelines. In addition, the zero power cases are bounded by the full power SLB outside the containment case.

The largest possible size of SLB is the double-ended rupture of a steam line upstream of the MSIV. An integral flow restrictor exists in each SG outlet nozzle. The largest effective steam blowdown area for each steam line, which is limited by the flow restrictor throat area, is approximately 30 percent of the steam line cross-section area, or 0.119 m^2 (1.28 ft^2).

These SLB events are analyzed in two ways. The first analysis maximizes post-trip degradation in fuel performance by the RTP. For the first analysis (SLB Cases 1 through 4), the initial conditions are adjusted to maximize the post-trip degradation in fuel performance at approximately the time of maximum reactivity, which occurs several minutes after reactor trip. For Cases 1 through 4, post-trip RTP may occur. The DNBR and linear heat generation rate (LHGR) during the interval of post-trip RTP is verified not to violate the DNBR SAFDL and LHGR limit or justified that a limited amount of fuel failure would occur to maintain the core coolable geometry and that the radiological consequences are within 10 CFR 50.34 guidelines.

The second analysis maximizes pre-trip degradation in fuel performance (Cases 5 and 6). There is a potential for violating the transient DNBR limit during the pre-trip period. These cases are analyzed to maximize the potential for fuel damage near the time of the reactor trip. The final pre-trip analysis was performed in compliance with General Design Criteria (GDC) 17 (i.e., considering the event with and without LOOP). The limiting case analysis assumes that a LOOP that results from turbine trip occurs with no time delay.

Because there is a concern for an asymmetric temperature in the reactor core for a failure of a steam line at the Advanced Power Reactor 1400 (APR1400) with 2 loops, the isolation time of the main steam line is compared with the time of a minimum departure from the nucleate boiling ratio (MDNBR).

15.1.5.2 Sequence of Events and Systems Operation

SLBs are characterized as cooldown events due to an increased steam flow rate, which causes excessive energy removal from the SGs and the RCS. The excessive energy removal results in a decrease in temperature and pressure in the RCS and SG. The cooldown causes an increase in core reactivity due to the negative moderator and Doppler reactivity coefficients.

Detection of the cooldown is accomplished by the low pressurizer pressure alarm, low SG pressure alarm, high reactor power alarm, and low SG water level alarm. A reactor trip as a consequence of an SLB is provided by one of several available reactor trip signals including low SG pressure, low pressurizer pressure, low SG water level, high reactor power, low DNBR trip initiated by the CPCs, and, for inside containment breaks, high containment pressure. For an SLB that occurs with a LOOP concurrent with the initiation of the event, the events of turbine stop valve closure, termination of feedwater to both SGs, and coastdown of the RCPs are assumed to be initiated simultaneously.

The reactor trip can be provided by CPCs on low RCP shaft speed or reactor protection system (RPS) variable overpower trip (VOPT) for the conservative early trip.

Following the reactor trip, the most reactive control rod is conservatively assumed to be held in the fully withdrawn position. The auxiliary feedwater is assumed to be immediately activated to the SGs or only the affected SG. The depressurization of the affected SG results in the actuation of an MSIS. Actuation of an MSIS closes the MSIVs, isolating the unaffected SG from blowdown, and closes the MFIVs, terminating the main feedwater flow to both SGs. The pressurizer pressure decreases to the point where a safety injections actuation signal (SIAS) is initiated. The introduction of safety injection boron upon SIAS causes the core reactivity to decrease.

The operator, using the appropriate emergency procedures, may initiate plant cooldown by manual control of the ADVs, or if offsite power is available, by using the unaffected SG and the turbine bypass valves. The analysis presented here conservatively assumes that operator action is delayed until 30 minutes after the first indication of the event. The plant is then cooled to 176.7 °C (350 °F) and 31.64 kg/cm^{2}A (450 psia), at which point shutdown cooling is initiated.

Table 15.1.5-11 provides the results of a parametric study of single failures that would have an adverse impact on the SLB. For the full and zero power cases with a LOOP concurrent with the initiation of event (Cases 1 and 3), the failure of one emergency diesel generator to start or the failure of one MSIV on a steam line to close is assumed. The results demonstrate that the failure of one of the emergency diesel generators to start on the LOOP and the consequent loss of two safety injection (SI) pumps following SIAS have the most adverse effect. Consequently, two SI pumps are conservatively assumed to fail in these cases. For the full and zero power SLB without LOOP (Cases 2 and 4), a failure of one SI pump to start, or the failure of one MSIV to close, is assumed. The evaluation shows that the most adverse effect for the zero power case is caused by one MSIV that failed to close following the steam line isolation actuation signal. One MSIV failing to close is assumed to be a single failure in this case.

After the turbine trip and main steam isolation actuation signal concurrent with the reactor trip, the flow from the unaffected SG is assumed to be at a rate of a maximum 11 percent design steam flow rate of non-isolable steam flow. For one SI pump failure, this flow is terminated by an MSIV closure after the generation of an MSIS.

For Case 5 (SLBFPD+LOOP), there is no single failure that increases the potential for degradation in fuel cladding performance or that increases the offsite dose. The radiological consequences of an SLB outside the containment upstream of the MSIV are not affected by the failure of one MSIV in the unaffected SG. For the radiological consequences for this event, it is conservatively assumed that after the affected SG blowdown ends, the plant heats up to hot standby after which the operator initiates an orderly cooldown to shutdown cooling entry conditions by releasing steam to the environment through the ADVs. Without a LOOP, the transient minimum DNBR is higher, and the results are bounded by the conditions with a LOOP.

The SG level for Case 5 is initially at the low SG level trip setpoint. If the feedwater control system is in the automatic mode, the plant is at the normal water level, and with a larger SG inventory, the rate of SG depressurization and RCS cooldown is decreased, resulting in a slower increase in core power and hence higher minimum DNBRs.

The sequences of events for Cases 1 through 5 above are presented in Tables 15.1.5-1 through 15.1.5-5, respectively. The sequence of events for Case 6 is the same as for Case 3 (Table 15.1.5-3).

15.1.5.3 Core and System Performance

15.1.5.3.1 Evaluation Model

The NSSS response to the SLB was simulated using the CESEC-III that is described in Reference 16 (Subsection 15.0.5). For the SLB initiated from full power conditions, the pre-trip DNBR in the hot channel was calculated using the CETOP described in Subsection 15.0.2.2.4 with the KCE-1 critical heat flux (CHF) correlation (Reference 28 in Section 15.0.5).

The determination of DNBR for post-trip RTP conditions requires methods that differ from those applied to pre-trip cases because the verified range of the KCE-1 correlation used in the CETOP does not cover the post-trip RTP conditions (low pressures and low flow rates). The MacBeth DNBR correlation (References 33 and 34 in Subsection 15.0.5) has been selected to represent the margin to DNB during periods of RTP. HRISE (Subsection 15.0.2.2.6) using the MacBeth CHF correlation is used to calculate the transient DNBR during periods of RTP.

Open core calculations indicate that the local quality in the hot channel during SLB post-trip RTP conditions seldom exceeds a few percent, regardless of the fission power rate or core average mass flux. This occurs due to the assembly cross-flow effects. The presence of low-density liquid or of voids at the top of the hot channel causes post-trip power generation to occur near the bottom of the core. For RTP DNBR calculations, a three-dimensional peaking factor (F_q) for the core power distribution during the period of RTP is used for the APR1400 Design. Enthalpy as a function of height is computed by performing a closed-channel heat balance. Hot channel inlet enthalpy is set equal to the average enthalpy predicted by CESEC-III for the fluid at the core inlet for that half of the core on the side associated with the affected steam generator. Maximum enthalpy is limited to that corresponding to 25 percent quality at the system pressure to account for the cross-flow effect. The mathematical models and data transfer between codes used in the SLB analysis are identical to those presented in Reference 35 in Subsection 15.0.5.

15.1.5.3.2 Input Parameters and Initial Conditions

The initial conditions assumed in the analysis of the NSSS response to Cases 1 through 5 are presented in Tables 15.1.5-6 through 15.1.5-10, respectively. The initial conditions for

Case 6 are the same as those for Case 3. Justification of the selection of the initial conditions and input parameters follows.

a. Post-Trip RTP Cases

Degradation in fuel performance during the post-trip portion of SLB-initiated transients can occur only if there is an RTP. The primary consideration for maximizing post-trip degradation in fuel performance is to select the parameters and conditions that maximize the RTP. The magnitude of the RTP is determined by the value of the maximum post-trip reactivity, the timing of this reactivity peak, and the duration of the reactivity peak. The timing of the maximum post-trip reactivity has an important effect on the post-trip RTP. The same reactivity produces less RTP later in a transient because (1) the fission power will have decreased to a lower value prior to the RTP, requiring more multiplication to reach a given power level, and (2) the delayed neutron background will be lower, requiring more reactivity to produce a given, positive rate of change of power. The duration of reactivity peak is important in that this parameter determines how long the post-trip power will continue to rise (if an RTP occurs) before being turned around by decreasing reactivity. For transients that result in an RTP, the degradation in the post-trip fuel cladding performance is affected strongly by the core flow at the time of the RTP.

The core flow at the time of an RTP is primarily a function of the RCP coastdown. Initial conditions and possible single failures have little or no effect on the core flow. The effect of pressure and temperature upon post-trip DNBR is small compared with the impact of these parameters on fuel performance because of their effect on the magnitude of the RTP via the reactivity feedback.

The impact of the initial conditions on the potential for post-trip degradation in fuel performance is through their effect on the RTP via the magnitude, timing, and duration of the post-trip total reactivity peak. This effect acts through its contributions to the moderator reactivity, the Doppler reactivity, and the SI boron reactivity. The ranges of the parameters given in Table 15.0-3 are considered in establishing the most adverse initial plant state for an RTP. For the APR1400 design, the most adverse state has been found to be the maximum core power, most positive axial shape index (ASI), minimum core flow rate, maximum pressurizer water level, maximum core inlet coolant temperature, maximum RCS pressure, and

maximum water inventory in the SGs. If a post-trip RTP is to occur for the SLB transient, a conservative three-dimensional peaking factor will be used.

Maximizing the core power and core inlet temperature and minimizing the core flow affect the RTP adversely because of the effect of maximizing the RCS average temperature and core outlet temperature. Maximizing the RCS average temperature maximizes the rate of cooldown because it maximizes SG pressure. Maximizing the RCS (core) average temperature also causes the cooldown to occur over a more adverse portion of the moderator reactivity function. Maximizing the core outlet temperature maximizes the energy stored in the water and metal of the upper head region of the reactor vessel and also maximizes the saturation pressure of the water in this region.

As the RCS pressure falls below the saturation pressure of the liquid in the upper head region, the stored energy provides the energy necessary to vaporize the liquid, resulting in a low rate of decrease in the RCS pressure below the saturation pressure of the liquid in the upper head. The SI boron reactivity at the time of RTP is minimized because the SIAS is delayed and the SI pump flow is impeded by the higher transient pressures.

Use of the most positive ASI maximizes the delay in the insertion of CEA reactivity following the trip but little effect on the RTP. Maximizing pressurizer water level and pressure maximizes the energy stored in the pressurizer. This maximizes transient RCS pressures, delaying and impeding the SI flow. Maximizing the SG water level in the affected SG maximizes the amount of cooldown until the SG dries out, resulting in maximizing the insertion of positive moderator reactivity. Maximizing the water level in the unaffected SG maximizes the amount of steam blowdown from that SG before MSIS because a higher initial SG water level results in a lower rate of decrease in SG pressure, causing a lower rate of decrease in steam blowdown flow rate. Increasing the initial water level in the unaffected SG also increases the cooldown due to steam blowdown from this SG.

Use of the most negative moderator and the Doppler coefficients maximizes the reactivity feedbacks obtained during the cooldown, thereby maximizing the possibility of a post-trip RTP. Figure 15.1.5-0 presents the moderator reactivity as a function of moderator temperature, which is used for SLB analyses. The moderator reactivity function used for the post-trip SLB analyses is the most

adverse function expected for SLBs, which is for an all-rods-in condition, most reactive rod fully withdrawn, end-of-cycle state corresponding to the most negative moderator temperature coefficient allowed by the Technical Specifications (-5.4×10^{-4} %Δρ/°C [-3.0×10^{-4} %Δρ/°F]) at nominal full power conditions. This function includes both the moderator temperature and density effects and the loss of rod worth with temperature and is based on constant fuel temperature and xenon distributions. The most negative Doppler reactivity versus fuel temperature function is assumed to provide reasonable assurance that the calculation of the reactivity increase due to cooldown of the fuel is conservative. The minimum scram rod worth at each power level is assumed to be 9.3 percent Δρ at full power and 5.5 percent Δρ at zero power. These values assume that the most reactive CEA is stuck in the fully withdrawn position, which minimizes the negative reactivity of CEA and maximizes the possibility of a post-trip RTP.

If an auxiliary feedwater system is actuated during an SLB, it will contribute to the RCS cooldown and may have an adverse impact on the RTP. The maximum value of 3,596 L/min (950 gpm) auxiliary feedwater flow is assumed to be delivered until the operator takes manual action to isolate auxiliary feedwater and cooldown the plant to the shutdown cooling entry conditions. The auxiliary feedwater is assumed to be actuated at the time of the reactor trip even though the SG inventories are greater than the value at which the auxiliary feedwater is normally actuated. For the SLB case with offsite power available, the auxiliary feedwater is assumed to be actuated to both SGs. For the cases with a LOOP, the auxiliary feedwater is conservatively assumed to be actuated to the affected SG only simultaneously with the reactor trip.

b. Pre-Trip Degradation in Fuel Performance Cases

For the purposes of analyzing the pre-trip portion of the SLB event, the initial conditions chosen for RCS pressure, temperature, core flow, and power are:

1) To make an initial values of ASI and radial peaking factors near a power operating limit (POL)

2) To minimize the transient minimum DNBR

The value of the ASI and radial peaking factor (F_R) are chosen to maximize the fraction of fuel pins calculated to experience the DNB. The maximum initial core flow is assumed to maximize the RCS cooldown rate. Assumptions concerning the initial pressurizer water level have little or no impact on the transient DNBR.

The initial SG mass inventory is reduced to its minimum value to maximize the RCS cooldown before the MSIVs are closed. This lower initial inventory leads to a more rapid SG depressurization and temperature reduction. The lower secondary temperatures cause a correspondingly more rapid decrease in the RCS temperatures.

Different SG liquid inventories are used in the SLB inside and outside the containment because each analyses has a different objective. For an SLB inside the containment, the objective is to maximize the possibility of a post-trip RTP. For an SLB outside the containment, the objective is to maximize the pre-trip degradation in fuel performance. In the latter, this is achieved through minimizing the SG liquid inventory. The maximum cooldown rate of the RCS creates the most rapid power increase due to the reactivity feedback. This results in a more rapid decrease in the DNBR. Hence, a greater potential for fuel damage is given.

The Technical Specification tube leak scenario is the most limiting for doses to the environment following an SLB outside the containment because the dose is driven by the radioactivity transported from the primary to the secondary system. The minimum scram rod worth minimizes the rate of reactivity insertion upon a reactor trip and therefore maximizes the delay in core power decrease. Use of the least negative Doppler reactivity coefficient minimizes the insertion of negative reactivity during fuel heatup. Therefore, use of the minimum rod worth and of the least negative Doppler coefficient maximizes the core heat flux and minimizes the DNBR before and shortly after the reactor trip.

Using the most adverse moderator reactivity may be overly conservative because the most negative moderator cooldown reactivity will occur in the post-trip portion of the analysis. In this analysis, the moderator cooldown reactivity at the time of minimum DNBR is used for the full power case (Case 5), which is calculated between the moderator cooldown reactivity at all rods in and all rods out (Reference 35 in Subsection 15.0.5). The moderator cooldown reactivity is presented in Figure 15.1.5-0.

For Case 6, because the transient DNBR remains high with limited core power increase, there are no fuel rods experiencing DNB. Because the other initial conditions including the RCS flow rate have little impact on the secondary steam release, all of the initial conditions and assumptions for Case 6 are assumed to be the same as those for Case 3 to maximize the secondary steam release.

15.1.5.3.3 Results

Case 1: Large steam line break during full power operation with a loss of offsite power (SLBFPLOOP) concurrent with the initiation of event

The dynamic behavior of the NSSS parameters following the SLBFPLOOP is presented in Figures 15.1.5-1.1 through 15.1.5-1.16. Table 15.1.5-1 summarizes the major events, times, and results for this transient.

Concurrent with the SLB, a LOOP occurs. At this time, an actuation signal for the emergency diesel generators is initiated, and the assumed single failure is that one diesel generator fails to start. Because of the decreasing core flow following a loss of power to the RCPs, conditions exist for the CPC low DNBR trip or low RCP shaft speed trip. At 0.67 seconds, the RCP speed reaches the CPC low RCP shaft speed trip setpoint of 94.83 percent of full speed. At 1.02 seconds, the CPC generates a low RCP shaft speed trip signal. At 1.12 seconds, the reactor trip breakers open. At 9.98 seconds, voids begin to form in the upper head of the reactor vessel. At 14.08 seconds, the SG pressure drops below the MSIS setpoint of 52.73 kg/cm^2A (750 psia). The MSIVs and MFIVs are closed by 20.43 seconds and 25.43 seconds, respectively. At 193.45 seconds, the pressurizer empties. At 242.40 seconds, the pressurizer pressure drops below 109.32 kg/cm^2A (1,555 psia), generating SIAS. Within 40.0 seconds from the time of reaching the SI setpoint, the operable SI pumps are loaded on the diesels and reach full speed, and the SI valves are fully open. SI boron begins to reach the core at 329.96 seconds. At 356.96 seconds, the maximum core reactivity (-0.382 %$\Delta\rho$) occurs. Because there is no RTP, there is no potential for fuel performance degradation after the reactor trip.

At 30 minutes after the event initiation, the operator, using the appropriate emergency procedure, initiates plant cooldown by manual control of the ADVs,

assuming that offsite power has not been restored. Shutdown cooling is initiated when the RCS reaches 176.7 °C (350 °F) and 31.64 kg/cm^{2}A (450 psia).

Case 2: Large steam line break during full power operation with offsite power available (SLBFP)

The dynamic behavior of the NSSS parameters following the SLBFP is presented in Figures 15.1.5-2.1 through 15.1.5-2.16. Table 15.1.5-2 summarizes the major events, times, and results for this transient.

At 4.30 seconds, the core power reaches the RPS VOPT setpoint of 103.5 percent power. To maximize the post-trip core reactivity, the minimum RPS VOPT setpoint is conservatively assumed. The trip signal is generated at 4.75 seconds. At 4.85 seconds, the reactor trip breakers open. At 11.48 seconds, voids begin to form in the upper head of the reactor vessel. At 17.20 seconds, the SG pressure drops below the MSIS setpoint of 52.73 kg/cm^{2}A (750 psia), and one MSSV failure to close is assumed to be a single failure. The operable MSIVs and MFIVs are closed by 23.55 seconds and 28.55 seconds, respectively. At 84.90 seconds, the pressurizer empties. At 124.45 seconds, the pressurizer pressure drops below 109.32 kg/cm^{2}A (1,555 psia), generating SIAS. Within 40.0 seconds from the time of reaching the SI setpoint, the SI pumps reach full speed, and the SI valves are fully open. SI boron begins to reach the core at 202.95 seconds. At 278.25 seconds, the maximum core reactivity (−0.259 %Δρ) occurs. Because there is no RTP, there is no potential for fuel performance degradation after the reactor trip.

At 30 minutes after the event initiation, the operator, using the appropriate emergency procedure, initiates plant cooldown by manual control of the ADVs or by using the unaffected SG and turbine bypass valves. Shutdown cooling is initiated when the RCS reaches 176.7 °C (350 °F) and 31.64 kg/cm^{2}A (450 psia).

Case 3: Large steam line break during zero power operation with loss of offsite power concurrent with the initiation of event (SLBZPLOOP)

The dynamic behavior of the NSSS parameters following the SLBZPLOOP is presented in Figures 15.1.5-3.1 through 15.1.5-3.16. Table 15.1.5-3 summarizes the major events, times, and results for this transient.

Concurrent with the SLB, a LOOP occurs. At this time, an actuation signal for the emergency diesel generators is initiated, and one diesel generator is assumed to fail to start as a single failure. Because of the decreasing core flow following a loss of power to the RCPs, conditions exist for the CPC low DNBR trip or low RCP shaft speed trip. At 0.67 seconds, the RCP reaches the CPC low RCP shaft speed trip setpoint of 94.83 percent of full speed. At 1.02 seconds, the CPC generates a low RCP shaft speed trip signal. At 1.12 seconds, the reactor trip breakers open. At 11.56 seconds, the SG pressure drops below the MSIS setpoint of 52.73 kg/cm^{2}A (750 psia). The MSIVs and MFIVs are closed by 17.91 seconds and 22.91 seconds, respectively.

At 79.01 seconds, the pressurizer empties. At 83.60 seconds, the pressurizer pressure drops below 109.32 kg/cm^{2}A (1,555 psia) generating an SIAS. Within 40.0 seconds from the time of reaching the SI setpoint, the operable SI pumps are loaded on the diesels and reach full speed, and the SI valves are fully open. At 106.62 seconds, voids begin to form in the upper head of the reactor vessel. SI boron begins to reach the core at 148.72 seconds. At 189.22 seconds, the maximum core reactivity (−0.534 %$\Delta\rho$) occurs. Because there is no RTP, there is no potential for fuel performance degradation after the reactor trip.

At 30 minutes after the event initiation, the operator, using the appropriate emergency procedure, initiates plant cooldown by manual control of the ADVs, assuming that offsite power has not been restored. Shutdown cooling is initiated when the RCS reaches 176.7 °C (350 °F) and 31.64 kg/cm^{2}A (450 psia).

Case 4: Large steam line break during zero power operation with offsite power available (SLBZP)

The dynamic behavior of the salient NSSS parameters following the SLBZP is presented in Figures 15.1.5-4.1 through 15.1.5-4.16. Table 15.1.5-4 summarizes the major events, times, and results of this transient.

At 12.04 seconds after initiation of the SLB, the SG pressure drops below the low SG pressure trip and MSIS setpoint of 52.73 kg/cm^{2}A (750 psia). At 13.19 seconds, the reactor trip breakers open, and one MSSV failure to close is assumed as a single failure. The operable MSIVs and MFIVs are closed by 18.39 seconds and 23.39 seconds, respectively. At 59.85 seconds, the pressurizer empties. At

63.12 seconds, the pressurizer pressure drops below 109.32 kg/cm^{2}A (1,555 psia) generating an SIAS. Within 40.0 seconds from the time of reaching the SI setpoint, the operable SI pumps reach full speed, and the SI valves are fully open. At 73.26 seconds, voids begin to form in the upper head of the reactor vessel. SI boron begins to reach the core at 124.75 seconds. At 167.05 seconds, the maximum core reactivity (−0.424 %$\Delta\rho$) occurs. Because there is no RTP, there is no potential for a fuel performance degradation after the reactor trip.

At 30 minutes after the event initiation, the operator, using the appropriate emergency procedure, initiates plant cooldown by manual control of the MSIV bypass valves associated with the ADV or by using the unaffected SG and turbine bypass valves. Shutdown cooling is initiated when the RCS reaches 176.7 °C (350 °F) and 31.64 kg/cm^{2}A (450 psia).

Case 5: Steam line break outside the containment during full power operation with loss of offsite power concurrent with reactor/turbine trip (SLBFPD+LOOP)

The dynamic behavior of the NSSS parameters following a typical limiting SLBFPD with LOOP is presented in Figures 15.1.5-5.1 through 15.1.5-5.9. Table 15.1.5-5 summarizes the major events, times, and results for this transient. The largest break size yields the minimum DNBR. Therefore, the transient presented here results from the double-ended break of a main steam line.

A late trip with maximum setpoint is assumed to maximize core power at the time of the reactor trip, which reduces the minimum transient DNBR. No later than 6.63 seconds after initiation of the SLB, the core power reaches the maximum CPC VOPT setpoint of 121 percent power. The trip signal is generated at 7.18 seconds. At 7.28 seconds, the reactor trip breakers open. At 8.98 seconds, a minimum transient DNBR of 1.3229 is calculated to occur, after which the DNBR rapidly increases, as shown in Figure 15.1.5-5.9.

At 24.59 seconds, voids begin to form in the upper head of the reactor vessel. At 14.42 seconds, the SG pressure drops below the MSIS setpoint of 52.73 kg/cm^{2}A (750 psia). The MSIVs and the MFIVs are closed by 20.77 seconds and 25.77 seconds, respectively.

The failure of a steam line in the APR1400 with two loops causes asymmetric temperature within the reactor core. Because the isolation of the main steam line

(20.77 seconds) will occur after an MDNBR is reached (8.98 seconds), asymmetric core temperatures do not affect the DNBR analysis.

The subsequent events of this transient follow a sequence that is similar to the events of the SLBFPLOOP (Case 1).

Because the cooldown is less severe due to the smaller initial SG inventory, the potential for post-trip degradation in fuel cladding performance is less for this case (SLBFPD+LOOP) than for Case 1 (SLBFPLOOP).

At 30 minutes after the event initiation, the operator, using the appropriate emergency procedure, initiates plant cooldown by manual control of the ADVs assuming that offsite power has not been restored. Shutdown cooling is initiated when the RCS reaches 176.7 °C (350 °F) and 31.6 kg/cm^{2}A (450 psia).

At the point of the minimum transient DNBR, the fuel rods are not predicted to experience DNB. However, 1 percent of the fuel rods is conservatively assumed to experience DNB for radiological doses. All of the activity in the fuel gap for fuel rods that are assumed to fail is assumed to be uniformly mixed with the reactor coolant.

Assuming the Technical Specification SG tube leakage of 2.27 L/min (0.6 gpm), during the 2 hours after initiation of the SLBFPD with LOOP, the integral leakage from the RCS through the affected SG is 273 kg (601 lbm), which is assumed to be released to the atmosphere with a decontamination factor (DF) of 1.

The total steam released from the affected SG for 2 hours is 438,177 kg (966,015 lbm), which includes the steam release for 30 minutes and steam amount used to remove the decay heat and sensible heat for 2 hours. The affected SG empties within 2 hours. The unaffected SG releases less than 40,824 kg (90,002 lbm) of steam during a 30-minute period before the closure of the MSIV. During the SLBFPD with LOOP, the MSIVs isolate the unaffected SG and prevent it from emptying.

The doses are calculated by the methods described in Appendix 15A. Table 15.1.5-12 presents the major assumptions and parameters for this transient. The resultant offsite radiological consequences are given in Table 15.1.5-13.

Case 6: Large steam line break outside the containment during zero power operation with a loss of offsite power concurrent with the initiation of event (SLBZPLOOPD)

Case 6 is included in Case 3 because the break of the latter can be inside or outside the containment.

Assuming the Technical Specification SG tube leakage of 2.27 L/min (0.6 gpm), during the 2 hours after initiation of the SLBZPLOOPD, the integral leakage from the RCS through the affected SG is 273 kg (601 lbm).

The total steam released from the affected SG for 2 hours is 385,106 kg (849,014 lbm), which includes the steam release for 30 minutes and steam amount used to remove the decay heat and sensible heat for 2 hours. The affected SG empties within 2 hours.

Less than 39,010 kg (86,003 lbm) of steam from the unaffected SG is released within 2 hours. During the SLBZPLOOPD, the MSIVs isolate the unaffected SG and prevent it from emptying. The doses are calculated by the methods described in Appendix 15A. Table 15.1.5-12 presents the major assumptions and parameters used in evaluating the radiological consequences for this transient. The resultant offsite radiological consequences are given in Table 15.1.5-13.

15.1.5.4 Barrier Performance

The MSLB event is characterized by an initial cooldown of the primary and secondary systems, decreasing RCS and SG pressures. The events described in this subsection result in an insignificant increase in RCS pressure. The maximum RCS pressure is below 110 percent of the RCS design pressure. The maximum SG pressure also is below 110 percent of the SG design pressure.

Normally, the RCP seal is cooled by (1) seal injection water from chemical and volume control system (CVCS) and (2) the component cooling water system through a high-pressure seal cooler. The evaluations of the reactor coolant pumps presented in Subsections 5.4.1.2 and 5.4.1.3 show that the integrity of the RCPs is maintained with a loss of component cooling water (CCW) for at least 30 minutes.

The containment vessel response to steam piping failures inside containment is described and analyzed in Subsection 6.2.1.4.

15.1.5.5 Radiological Consequence

The radiological consequences are performed to determine EAB, LPZ, MCR, and TSC doses due to main steam line break (MSLB) accidents using the Alternative Source Term (AST) methodology; the total effective dose equivalent (TEDE) dose criteria; guidance in NRC RG 1.183, Appendix E; and the plant-specific bounding design information applicable to the APR1400.

15.1.5.5.1 Evaluation Model

The following transport models of radioactive materials are applied to evaluate radiological consequences due to MSLB accidents:

Release via the Containment

An RCS fluid is released to the in-containment refueling water storage tank (IRWST) located inside containment during the MSLB accident. The pressurizer pressure reaches the safety injection actuation signal (SIAS) after onset of a MSLB. Per Technical Specification LCO 3.3.5, the low pressurizer pressure actuates the safety injection actuation signal, which further actuates the containment isolation signal, and eventually the containment is isolated. The released RCS fluid has a negligible impact on the containment operating pressure that is the driving force for containment leakage in comparison to the hundreds of thousands of pounds of RCS mass released during a loss-of-coolant accident. Therefore, the activity released from the RCS is confined within the containment envelope during the MSLB accident and is not expected to release to the environment.

Release via the Affected Steam Generator

The post-MSLB thermal hydraulic condition in the affected SG is such that the primary-to-secondary (P-T-S) leakage is assumed to flash immediately to vapor in the affected SG, and the radioiodine and noble gases carried from the RCS to the affected SG are directly released to the environment without mitigation concurrently with the initiation of the

MSLB accident. During the SG dryout, the radioiodine in the affected SG liquid is assumed to be released to environment with steaming rates. The affected SG is assumed to be filled with the feedwater to cool down the RCS, and an iodine partition coefficient between the secondary liquid in the SG and the steam generated is used for the secondary liquid iodine steaming rates.

Release via the Unaffected Steam Generator

In the cases of unaffected SG, in which tubes are fully submerged by the secondary liquid, the P-T-S leakage is assumed to mix with the secondary water without flashing. The radioactivity in the bulk water is assumed to become vapor at a rate that is the function of the steaming rate and the partition coefficient.

Release via the Condenser

Prior to the LOOP, the contaminated secondary steam in the unaffected SG is released to the condenser. However, the steam release to the condenser is not considered in the post-MSLB activity release to the environment due to the tortuous path to the condenser via the turbines and moisture separators, and the condenser hold-up time.

Figure 15A-1 in Appendix 15A shows the leakage or transport of the activity released to the environment, MCR, and TSC during the MSLB accident.

15.1.5.5.2 Input Parameters and Initial Conditions

The design basis MSLB accident is analyzed using a conservative set of assumptions based on NRC RG 1.183, Appendix E, and the APR1400 design inputs. Input parameter values used for the MSLB radiological consequence evaluation are presented in Table 15.1.5-12.

Per the accident analyses performed for the APR1400, the radiological consequence analysis for the MSLB are performed for the two (2) cases out of six (6) cases: (1) SLBFPDLOOP and (2) SLBZPLOOPD, which are the most liming cases.

Consistent with NRC RG 1.183, Appendix E, Section 2, the activity assumed in the analysis is based on the activity associated with the projected fuel damage or the maximum Technical Specification values, whichever maximizes the radiological consequences. For

SLBZPLOOPD case (Case 6), since fuel damage is not postulated, the maximum Technical Specification values are used. For the SLBFPDLOOP case (Case 5), because 1 percent fuel damage is postulated, the activity due to the projected fuel damage (i.e., 1.0 percent fuel damage) is used. Therefore, two iodine spiking cases (pre-accident iodine spike and concurrent iodine spike) are analyzed for SLBZPLOOPD and the fuel damage case is analyzed for SLBFPDLOOP.

a. It is assumed for the pre-accident iodine spike that a reactor transient has occurred prior to the postulated MSLB and has raised the primary coolant iodine concentration to the maximum value of 2.22×10^6 Bq/g (60 μCi/g) DE I-131.

b. For the event-generated iodine spike that the primary system transient associated with the MSLB causes an iodine spike in the primary system. The increase in primary coolant iodine concentration is estimated using a spiking model that assumes that the iodine release rate from the fuel rods to the primary coolant increases to a value 500 times greater than the release rate corresponding to the equilibrium primary coolant iodine concentration of 3.7×10^4 Bq/g (1.0 μCi/g) DE I-131. The assumed iodine spike duration is 8 hours. It is assumed that the iodine activity released from the fuel to RCS is mixed instantaneously and homogeneously with the primary coolant. The event-generated iodine spike isotopic iodine activity appearance rates and resulting iodine activities in the RCS are presented in Table 15A-4.

c. The maximum RCS noble gas concentration for the APR1400 is 2.15×10^7 Bq/g (580 μCi/g) DE Xe-133.

The RCS is assumed to leak into the unaffected and affected SGs at 2.27 L/min (0.6 gpm). From 0 to 0.5 hours, one-half of the P-T-S leakage is into the affected SG, and one-half of the P-T-S leakage is into the unaffected SG. From 0.5 to 8 hours, the total 2.27 L/min (0.6 gpm) P-T-S leakage is into the affected SG. It is assumed that the P-T-S leakage continues until the primary system pressure is less than the secondary system pressure or until the temperature of the leakage is less than 100 °C and shutdown cooling is in operation.

The chemical forms of iodine released from the steam generators to the environment are assumed to be 97 percent elemental and 3 percent organic.

All noble gas radionuclides released from the primary system via the P-T-S leak are released to environment without reduction or mitigation.

The χ/Q values used in the analysis for EAB, LPZ, MCR, and TSC are described in Subsection 2.3.4 and are given in Tables 2.3-2 through 2.3-12; the breathing rates are given in Table 15A-11.

15.1.5.5.3 Results

The radiological consequences due to an MSLB accident are presented in Table 15.1.5-13. The results of the MSLB accident analyses indicate that the EAB and LPZ doses due to an MSLB accident with a pre-accident iodine spike, an event-generated iodine spike, and 1 percent fuel failure are within their allowable dose criteria limits, which are 100 percent, 10 percent, and 100 percent of the 10 CFR 50.34(a)(1) value, respectively.

The MCR and TSC doses for all cases are also within the dose limits in GDC 19.

15.1.5.6 Conclusions

A post-trip RTP does not occur in all cases so that the fuel integrity is not challenged by this event (an increase in heat removal by the secondary system). Consequently, the core remains in place and is unaffected with no loss of core cooling capability.

Also, the RCS pressures remain below 193.34 kg/cm^{2}A (2,750 psia), and the steam generator pressures remain below 92.83 kg/cm^{2}A (1,320 psia).

For pre-trip fuel degradation, the maximum potential for radiological releases due to fuel failure occurs in SLBs outside the containment with a LOOP concurrent with reactor/turbine trip (SLB Case 5). In this case, the maximum potential for degradation in fuel cladding performance occurs before and during the reactor trip. With the assumption of the Technical Specification SG tube leakage and the predicted fuel failure, the doses at the EAB, LPZ, and MCR are calculated to be within the criteria of 10 CFR 50.34 (a)(1) and GDC 19.

For a large SLB during zero power operation in combination with a LOOP and a Technical Specification SG tube leakage (SLB Case 6), the doses at the EAB, LPZ, and MCR are also within the criteria of 10 CFR 50.34 (a)(1) and GDC 19.

15.1.6 Combined License Information

No COL information is required with regard to Section 15.1.

Table 15.1.4-1

Sequence of Events of Full Power Inadvertent Opening of a Steam Generator Atmospheric Dump Valve (IOSGADV) with a Loss of Offsite Power

Time (sec)	Event	Setpoint or Value
0.0	One atmospheric dump valve opens fully	—
1,800	Operator initiates manual trip	—
1,800.10	Reactor trip breakers open/turbine trip/ loss of offsite power/RCPs begin to coast down	—
1,801.70	Minimum transient DNBR	1.336
1,963.45	Pressurizer pressure reaches safety injection actuation signal analysis setpoint, kg/cm^2A (psia)	121.98 (1,735)
1,966.50	Void begins to form in RV upper head	—
2,003.45	Safety injection flow begins	—
2,105.90	Steam generator pressure reaches main steam isolation signal analysis setpoint, kg/cm^2A (psia)	57.09 (812)
2,112.25	MSIVs close completely	—
2,117.25	MFIVs close completely	—
2,324.60	Steam generator water level reaches auxiliary feedwater actuation analysis setpoint, %WR	19.9
3,000	Operator manually closes ADV	—
3,600	Operator initiates plant cooldown	—

Table 15.1.4-2

Sequence of Events of Full Power Inadvertent Opening of a Steam Generator Atmospheric Dump Valve with a Single Failure (IOSGADV+SF) and with a Loss of Offsite Power

Time (sec)	Event	Setpoint or Value
0.0	One atmospheric dump valve opens fully	—
1,800	Operator initiates manual trip	—
1,800.10	Reactor trip breakers open/turbine trip/ loss of offsite power/RCPs begin to coast down	—
1,801.70	Minimum transient DNBR	1.336
1,887.90	Pressurizer pressure reaches safety injection actuation signal analysis setpoint, kg/cm^2A (psia)	121.98 (1,735)
1,888.70	Void begins to form in RV upper head	—
1,927.90	Safety injection flow begins	—
1,955.65	Steam generator pressure reaches main steam isolation signal analysis setpoint, kg/cm^2A (psia)	57.09 (812)
1,962.0	MSIVs close completely	—
1,967.0	MFIVs close completely	—
3,000	Operator manually closes ADV	—
3,600	Operator initiates plant cooldown	—

Table 15.1.4-3

Assumptions and Initial Conditions for Full Power Inadvertent Opening of an Atmospheric Dump Valve, Inadvertent Opening of an Atmospheric Dump Valve and a Single Failure (IOSGADV and IOSGADV+SF) with a Loss of Offsite Power

Parameter	Value
Initial core power level, MWt	4,062.66 (102 %)
Initial core inlet coolant temperature, °C (°F)	296.1 (565)
Initial core mass flow rate, 10^6 kg/hr (10^6 lbm/hr)	85.03 (187.46)
Initial pressurizer pressure, kg/cm^{2}A (psia)	163.46 (2,325)
Initial pressurizer water volume, m^3 (ft^3)	13.56 (478.80)
Initial steam generator inventory, kg per SG (lbm per SG)	127,131 (280,276)
CEA worth on trip, %Δρ	−8.0
Moderator temperature coefficient, Δρ/°C (Δρ/°F)	-5.4×10^{-4} (-3.0×10^{-4})
Core burnup	End of cycle
ASI	+0.3
Maximum radial peaking factor	2.0552
Doppler reactivity	Least negative

Table 15.1.5-1

Sequence of Events for a Large Steam Line Break During Full Power Operation with a Loss of Offsite Power Concurrent with the Initiation of Event (SLBFPLOOP)

Time (sec)	Event	Setpoint or Value
0.0	Steam line break and loss of offsite power occur	—
0.67	Reactor coolant pump reaches CPC low RCP shaft speed setpoint, % of full speed	94.83
1.02	CPC low RCP shaft speed trip signal generated and AFW flow initiated to the affected SG	—
1.12	Reactor trip breakers open	—
9.98	Voids begin to form in RV upper head	—
14.08	Steam generator pressure reaches main steam isolation signal analysis setpoint, kg/cm^2A (psia)	52.73 (750)
20.43	MSIVs close completely	—
25.43	MFIVs close completely	—
193.45	Pressurizer empties	—
242.40	Pressurizer pressure reaches safety injection actuation signal analysis setpoint, kg/cm^2A (psia)	109.32 (1,555)
282.40	Safety injection flow begins	—
329.96	Safety injection boron begins to reach reactor core	—
356.96	Maximum transient reactivity, %$\Delta\rho$	−0.382
1,800	Operator initiates cooldown	—

Table 15.1.5-2

Sequence of Events for a Large Steam Line Break During Full Power Operation with Offsite Power Available (SLBFP)

Time (sec)	Event	Setpoint or Value
0.0	Steam line break occurs	—
4.30	RPS variable overpower trip condition reached, % of full power	103.5
4.75	RPS variable overpower trip signal generated and AFW flow initiated to both SGs	—
4.85	Reactor trip breakers open	—
11.48	Voids begin to form in RV upper head	—
17.20	Steam generator pressure reaches main steam isolation signal analysis setpoint, kg/cm^2A (psia)	52.73 (750)
23.55	MSIVs close completely	—
28.55	MFIVs close completely	—
84.90	Pressurizer empties	—
124.45	Pressurizer pressure reaches safety injection actuation signal analysis setpoint, kg/cm^2A (psia)	109.32 (1,555)
164.45	Safety injection flow begins	—
202.95	Safety injection boron begins to reach reactor core	—
278.25	Maximum transient reactivity, $\%\Delta\rho$	−0.259
1,800	Operator initiates cooldown	—

Table 15.1.5-3

Sequence of Events for a Large Steam Line Break During Zero Power Operation with a Loss of Offsite Power Concurrent with the Initiation of Event (SLBZPLOOP and SLBZPLOOPD)

Time (sec)	Event	Setpoint or Value
0.0	Steam line break and loss of offsite power occur	—
0.67	Reactor coolant pump reaches CPC low RCP shaft speed setpoint, % of full speed	94.83
1.02	CPC low RCP shaft speed trip signal generated and AFW flow initiated to the affected SG	—
1.12	Reactor trip breakers open	—
11.56	Steam generator pressure reaches main steam isolation signal analysis setpoint, kg/cm^2A (psia)	52.73 (750)
17.91	MSIVs close completely	—
22.91	MFIVs close completely	—
79.01	Pressurizer empties	—
83.60	Pressurizer pressure reaches safety injection actuation signal analysis setpoint, kg/cm^2A (psia)	109.32 (1,555)
106.62	Voids begin to form in RV upper head	—
123.60	Safety injection flow begins	—
148.72	Safety injection boron begins to reach reactor core	—
189.22	Maximum transient reactivity, $\%\Delta\rho$	−0.534
1,800	Operator initiates cooldown	—

Table 15.1.5-4

Sequence of Events for a Large Steam Line Break
During Zero Power Operation with Offsite Power Available (SLBZP)

Time (sec)	Event	Setpoint or Value
0.0	Steam line break occurs	—
12.04	Steam generator pressure reaches reactor trip analysis setpoint and steam generator pressure reaches main steam isolation signal analysis setpoint, kg/cm^2A (psia)	52.73 (750)
13.09	Low steam generator pressure reactor trip signal generated and AFW flow initiated to both SGs	—
13.19	Trip breakers open	—
18.39	MSIVs close completely	—
23.39	MFIVs close completely	—
59.85	Pressurizer empties	—
63.12	Pressurizer pressure reaches safety injection actuation signal analysis setpoint, kg/cm^2A (psia)	109.32 (1,555)
73.26	Voids begin to form in RV upper head	—
103.12	Safety injection flow begins	—
124.75	Safety injection boron begins to reach reactor core	—
167.05	Maximum transient reactivity, $\%\Delta\rho$	−0.424
1,800	Operator initiates cooldown	—

Table 15.1.5-5

Sequence of Events for a Large Steam Line Break Outside Containment during Full Power Operation with a Loss of Offsite Power Concurrent with Reactor/Turbine Trip (SLBFPD+LOOP)

Time (sec)	Event	Setpoint or Value
0.0	Steam line break occurs	—
6.63	CPC variable overpower trip condition reached, % of full power	121.0
7.18	CPC variable overpower trip signal generated and AFW flow initiated to both steam generators	—
7.28	Reactor trip breakers open, loss of offsite power concurrent with turbine trip occurs and RCPs begin to coast down	—
8.98	Minimum transient DNBR	1.3229
14.42	Steam generator pressure reaches main steam isolation signal analysis setpoint, kg/cm^2A (psia)	52.73 (750)
20.77	MSIVs close completely	—
24.59	Voids begin to form in RV upper head	—
25.77	MFIVs close completely	—
144.25	Pressurizer pressure reaches safety injection actuation signal analysis setpoint, kg/cm^2A (psia)	109.32 (1,555)
184.25	Safety injection flow begins	—
236.03	Safety injection boron begins to reach reactor core	—
287.28	Affected steam generator empty	—
1,800	Operator initiates cooldown	—

Table 15.1.5-6

Assumptions and Initial Conditions for a Large Steam Line Break during Full Power Operation with a Loss of Offsite Power Concurrent with the Initiation of Event (SLBFPLOOP)

Parameter	Assumed Value
Initial core power level, MWt	4,062.66
Initial core inlet coolant temperature, °C (°F)	295 (563)
Initial core mass flow rate, 10^6 kg/hr (lbm/hr)	69.64 (153.52)
Initial pressurizer pressure, kg/cm^{2}A (psia)	163.46 (2,325)
Initial pressurizer water volume, m^3(ft^3)	39.91 (1,409.44)
Axial shape index	+0.3
CEA worth for trip, %Δρ	−9.3
Doppler coefficient	Most negative
Moderator coefficient	Most negative
Initial steam generator liquid inventory per SG, kg (lbm)	124,113 (273,623)
Two safety injection pumps powered by one emergency diesel generator	Inoperative
Core burnup	End of cycle
Blowdown fluid	Saturated steam
Blowdown area for each steam line, m^2 (ft^2)	0.119 (1.28)
Loss of offsite power	Assumed at event initiation

Table 15.1.5-7

Assumptions and Initial Conditions for a Large Steam Line Break During Full Power Operation with Offsite Power Available (SLBFP)

Parameter	Assumed Value
Initial core power level, MWt	4,062.66
Initial core inlet coolant temperature, °C (°F)	295 (563)
Initial core mass flow rate, 10^6 kg /hr (lbm/hr)	69.64 (153.52)
Initial pressurizer pressure, kg/cm^{2}A (psia)	163.46 (2,325)
Initial pressurizer water volume, m^3(ft^3)	39.91 (1,409.44)
Axial shape index	+0.3
CEA worth for trip, %$\Delta\rho$	−9.3
Doppler coefficient	Most negative
Moderator coefficient	Most negative
Initial SG liquid inventory per SG, kg (lbm)	124,113 (273,623)
One MSSV	Fail to close
Core burnup	End of cycle
Blowdown fluid	Saturated steam
Blowdown area for each steam line, m^2 (ft^2)	0.119 (1.28)
Loss of offsite power	Not assumed

Table 15.1.5-8

Assumptions and Initial Conditions for a Large Steam Line Break During Zero Power Operation with Concurrent Loss of Offsite Power

Parameter	Assumed Value
Initial core power level, MWt	10
Initial core inlet coolant temperature, °C (°F)	295 (563)
Initial core mass flow rate, 10^6 kg/hr (lbm/hr)	69.64 (153.52)
Initial pressurizer pressure, kg/cm^{2}A (psia)	163.46 (2,325)
Initial pressurizer water volume, m^3 (ft^3)	39.91 (1,409.44)
Doppler coefficient	Most negative
Moderator coefficient	Most negative
Axial shape index	+0.6
CEA worth for trip, %Δρ	−5.5
Initial steam generator liquid inventory per SG, kg (lbm)	190,331 (419,608)
Two safety injection pumps	Inoperative
Core burnup	End of cycle
Blowdown fluid	Saturated steam
Blowdown area for each steam line, m^2 (ft^2)	0.119 (1.28)
Loss of offsite power	Assumed at event initiation

Table 15.1.5-9

Assumptions and Initial Conditions for a Large Steam Line Break During Zero Power Operation with Offsite Power Available (SLBZP)

Parameter	Assumed Value
Initial core power level, MWt	10
Initial core inlet coolant temperature, °C (°F)	295 (563)
Initial core mass flow rate, 10^6 kg/hr (lbm/hr)	69.64 (153.52)
Initial pressurizer pressure, kg/cm^{2}A (psia)	163.45 (2,325)
Initial pressurizer water volume, m^3 (ft^3)	39.91 (1,409.44)
Axial shape index	+0.6
CEA worth for trip, %$\Delta\rho$	−5.5
Doppler coefficient	Most negative
Moderator coefficient	Most negative
Initial steam generator liquid inventory per SG, kg (lbm)	190,331 (419,608)
One MSSV	Fail to close
Core burnup	End of cycle
Blowdown fluid	Saturated steam
Blowdown area for each steam line, m^2 (ft^2)	0.119 (1.28)
Loss of offsite power	Not assumed

Table 15.1.5-10

Assumptions and Initial Conditions for the Steam Line Break Outside Containment During Full Power Operation with a Loss of Offsite Power Concurrent with Reactor/Turbine Trip (SLBFPD+LOOP)

Parameter	Assumed Value
Initial core power level, MWt	4,062.66
Initial core inlet coolant temperature, °C (°F)	296.1 (565)
Initial core mass flow rate, 10^6 kg/hr (lbm/hr)	85.03 (187.46)
Initial pressurizer pressure, kg/cm^{2}A (psia)	163.45 (2,325)
Initial pressurizer water volume, m^3 (ft^3)	39.91 (1,409.44)
Axial shape index	+0.3
Radial peaking factor (F_R)	2.0212
CEA worth for trip, %$\Delta\rho$	−9.3
Doppler coefficient	Least negative
Moderator coefficient	Adjusted to minimum DNBR
Initial steam generator liquid inventory per SG, kg (lbm)	53,738 (125,968)
Two safety injection pumps	Inoperative
Core burnup	End of cycle
Blowdown fluid	Saturated steam
Blowdown area for each steam line, m^2 (ft^2)	0.119 (1.28)
Loss of offsite power	Concurrent with reactor trip

Table 15.1.5-11

Effect of Single Failure of MSIV or SI Pump on Maximum Post-Trip Reactivity for Double-Ended Guillotine Main Steam Line Breaks with a Stuck CEA

Initial Power Level	Offsite Power	Single Failure	Maximum Post-Trip Reactivity (%Δρ)
Full	Unavailable	Two SI pumps	−0.382
		One MSIV	−0.626
	Available	One SI pump	−0.287
		One MSIV	−0.259
Zero	Unavailable	Two SI pumps	−0.534
		One MSIV	−0.548
	Available	One SI pump	−0.621
		One MSIV	−0.424

Table 15.1.5-12 (1 of 3)

Parameters Used in Evaluating the Radiological Consequences of the Steam Line Break Outside Containment

Parameter	Value
Source Terms	
Reactor Core Power Level	4,062.66 MWt
Percent of Fuel Assumed to Experience Departure from Nucleate Boiling (DNB)	1 % For SLBFPDLOOP 0 % For SLBZPLOOPD
Percent of Fuel Assumed to Melt	0 % For SLBFPDLOOP 0 % For SLBZPLOOPD
Radial Peaking Factor	1.80
Initial RCS Mass	274,392 kg (604,930 lbm) for SLBFPDLOOP 286,829 kg (632,340 lbm) for SLBZPLOOPD
Initial Steam Generator Liquid Mass per SG	54,592 kg (120,353 lbm) for SLBFPDLOOP 187,658 kg (413,709 lbm) for SLBZPLOOPD
Initial RCS Iodine Specific Activity	3.7×10^4 Bq/g (1.0 μCi/g) DE I-131
Initial Secondary Liquid Iodine Specific Activity	3.7×10^3 Bq/g (0.1 μCi/g) DE I-131
Initial RCS Noble Gas Specific Activity	2.15×10^7 Bq/g (580 μCi/g) DE Xe-133
RSC Iodine Specific Activity Used for Pre-accident Iodine Spike Case	2.22×10^6 Bq/g (60 μCi/g) DE I-131
Event-generated Iodine Spiking Factor	500
Duration of Event-generated Iodine Spike	8 hrs
Chemical Forms of Iodine Released from the SG to the Environment	97 % elemental and 3 % organic

Table 15.1.5-12 (2 of 3)

Parameter	Value
Secondary System Activity Transport Model	
Primary-to-secondary Leakage Rate through SGs	2.27 L/min (0.6 gpm) for two SGs
Integrated P-T-S Leakage 0 ~ 2 hrs 2 ~ 8 hrs	 272 kg (601 lbm) 818 kg (1,803 lbm)
Total Mass Release from Affected SG For SLBFPDLOOP 0 ~ 0.5 hrs 0.5 ~ 2 hrs 2 ~ 8 hrs For SLBZPLOOPD 0 ~ 0.5 hrs 0.5 ~ 2 hrs 2 ~ 8 hrs	 196,862 kg (434,000 lbm) 241,315 kg (532,000 lbm) 657,720 kg (1,450,000 lbm) 158,760 kg (350,000 lbm) 226,346 kg (499,000 lbm) 639,576 kg (1,410,000 lbm)
Total Mass Release from Unaffected SG For SLBFPDLOOP 0 ~ 0.5 hrs 0.5 ~ 8 hrs For SLBZPLOOPD 0 ~ 0.5 hrs 0.5 ~ 8 hrs	 40,824 kg (90,000 lbm) 0.0 kg (0.0 lbm) 39,010 kg (86,000 lbm) 0.0 kg (0.0 lbm)
Termination of Release from Affected SG	30 mins
Unaffected SG P-T-S Leak Duration, and Termination of Release from Unaffected SG	8 hrs
SG Liquid Iodine Partition Coefficient	100
Letdown System Flow Rate	18,100 kg/hr (39,842 lbm/hr)
RCS Fluid Released to IRWST	5,443 kg (12,000 lbm) For SLBFPDLOOP 2,948 kg (6,500 lbm) For SLBZPLOOPD

Table 15.1.5-12 (3 of 3)

Parameter	Value
MCR and TSC Model Parameters	
Envelope Volume	5,663 m^3 (200,000 ft^3)
Normal Ventilation Flow Rate (unfiltered)	105 m^3/min (3,700 cfm)
Emergency Ventilation Makeup Rate (filtered)	105 m^3/min (3,700 cfm)
Emergency Ventilation Recirculation Flow Rate (filtered)	122 m^3/min (4,300 cfm)
Emergency HVAC Delay Time	5 mins
Emergency Ventilation Charcoal Filter Efficiency (elemental and organic iodine removal)	99 %
Emergency Ventilation HEPA Filter Efficiency (particulate removal)	99 %
Unfiltered Inleakage	8.50 m^3/min (300 cfm)
Occupancy Factors 0 ~ 24 hrs 24 ~ 96 hrs 96 ~ 720 hrs	 100 % 60 % 40 %
Onsite χ/Qs	See Tables 2.3.2 ~ 2.3.12
Offsite Model Parameters	
χ/Qs	See Table 2.3-1
Breathing Rate	See Table 15A-11
Dose Conversion Factors	See Table 15A-10

Table 15.1.5-13 (1 of 2)

Radiological Consequences of Steam Line Breaks Outside Containment

Pre-accident Iodine Spike Case (SLBZPLOOPD)

Post-MSLB Activity Release Path	TEDE Dose (mSv)		
	MCR and TSC	EAB	LPZ
P-T-S Iodine Release	1.70E+00	2.18E+00	1.46E+00
P-T-S Noble Gas Release	1.38E-02	1.20E-02	8.55E-03
Secondary Liquid Iodine Release	4.27E-01	4.64E-01	1.04E-01
External Cloud	6.88E-01	0.00E+00	0.00E+00
Emergency Ventilation Filter Shine	1.34E-06	0.00E+00	0.00E+00
Total	2.83E+00	2.66E+00	1.57E+00
Allowable TEDE Limit	5.00E+01	2.50E+02	2.50E+02

Table 15.1.5-13 (2 of 2)

Event-generated Iodine Spike Case (SLBZPLOOPD)

Post-MSLB Activity Release Path	TEDE Dose (mSv)		
	MCR and TSC	EAB	LPZ
P-T-S Iodine Release	6.77E+00	1.11E+01	6.09E+00
P-T-S Noble Gas Release	1.38E-02	1.20E-02	8.55E-03
Secondary Liquid Iodine Release	4.27E-01	4.64E-01	1.04E-01
External Cloud	6.88E-01	0.00E+00	0.00E+00
Emergency Ventilation Filter Shine	1.34E-06	0.00E+00	0.00E+00
Total	7.90E+00	1.15E+01	6.20E+00
Allowable TEDE Limit	5.00E+01	2.50E+01	2.50E+01

1 % Fuel Failure Case (SLBFPDLOOP)

Post-MSLB Activity Release Path	TEDE Dose (mSv)		
	MCR and TSC	EAB	LPZ
P-T-S Iodine Release	2.26E+01	2.89E+01	1.96E+01
P-T-S Noble Gas Release	7.87E-01	1.14E+00	4.96E-01
Secondary Liquid Iodine Release	3.52E+00	3.18E+00	7.04E-01
External Cloud	6.88E-01	0.00E+00	0.00E+00
Emergency Ventilation Filter Shine	1.34E-06	0.00E+00	0.00E+00
Total	2.76E+01	3.33E+01	2.08E+01
Allowable TEDE Limit	5.00E+01	2.50E+02	2.50E+02

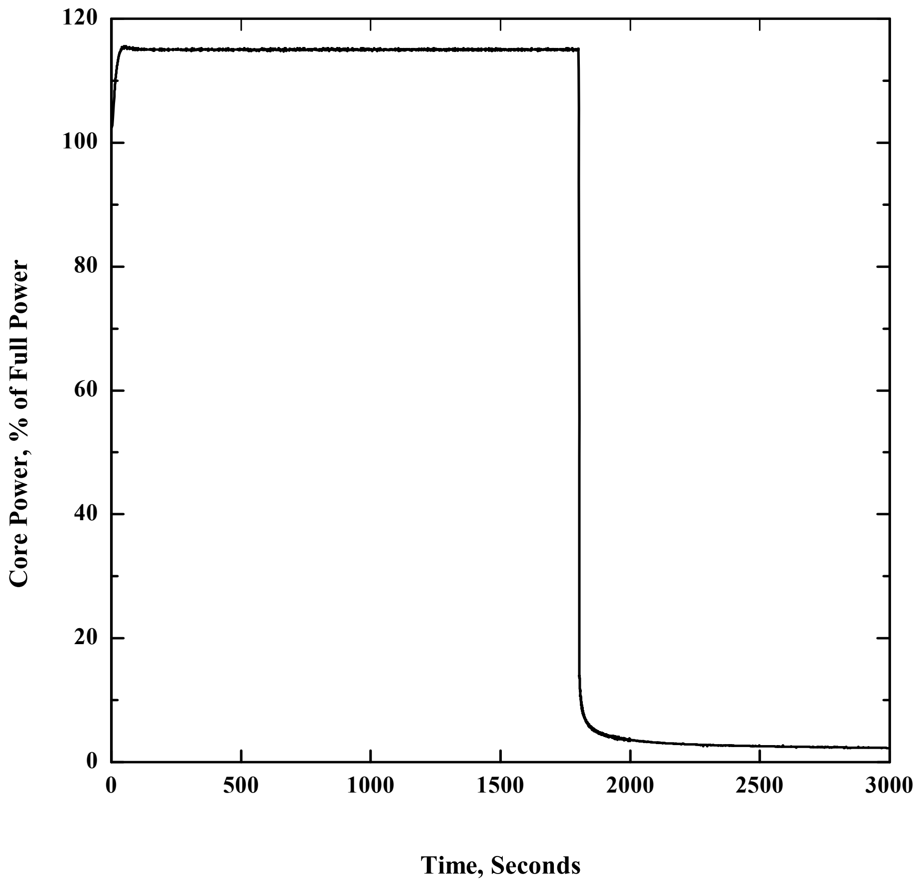

Figure 15.1.4-1.1 IOSGADV with LOOP: Core Power vs. Time

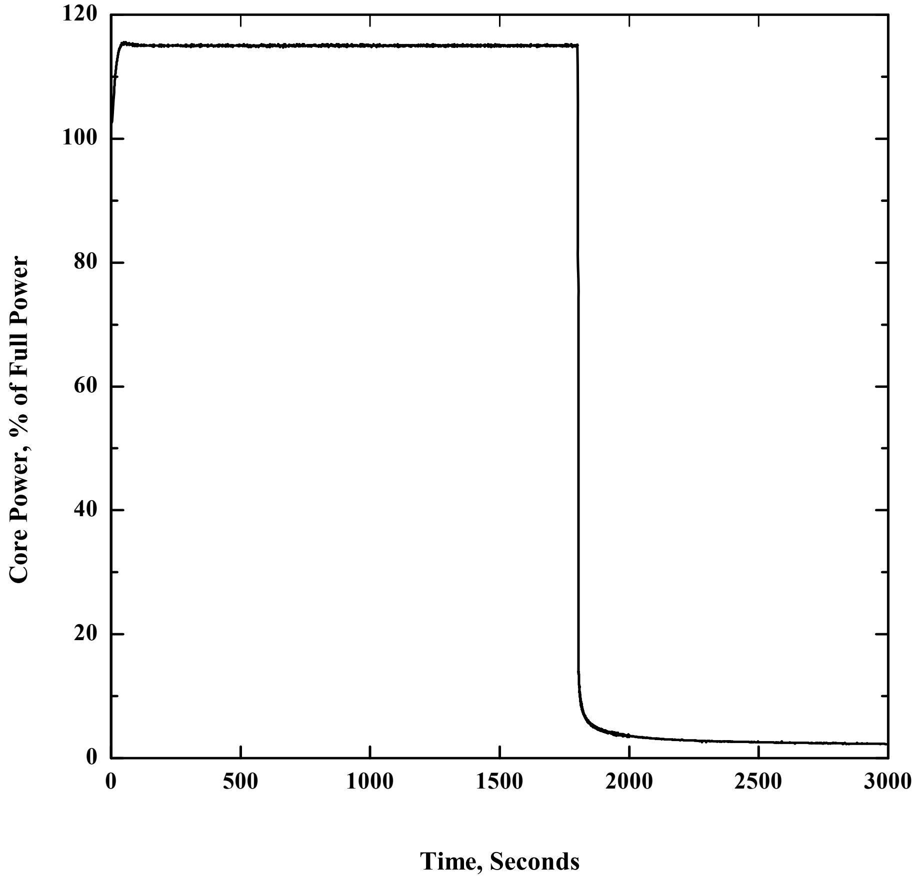

Figure 15.1.4-1.2 IOSGADV with LOOP: Core Average Heat Flux vs. Time

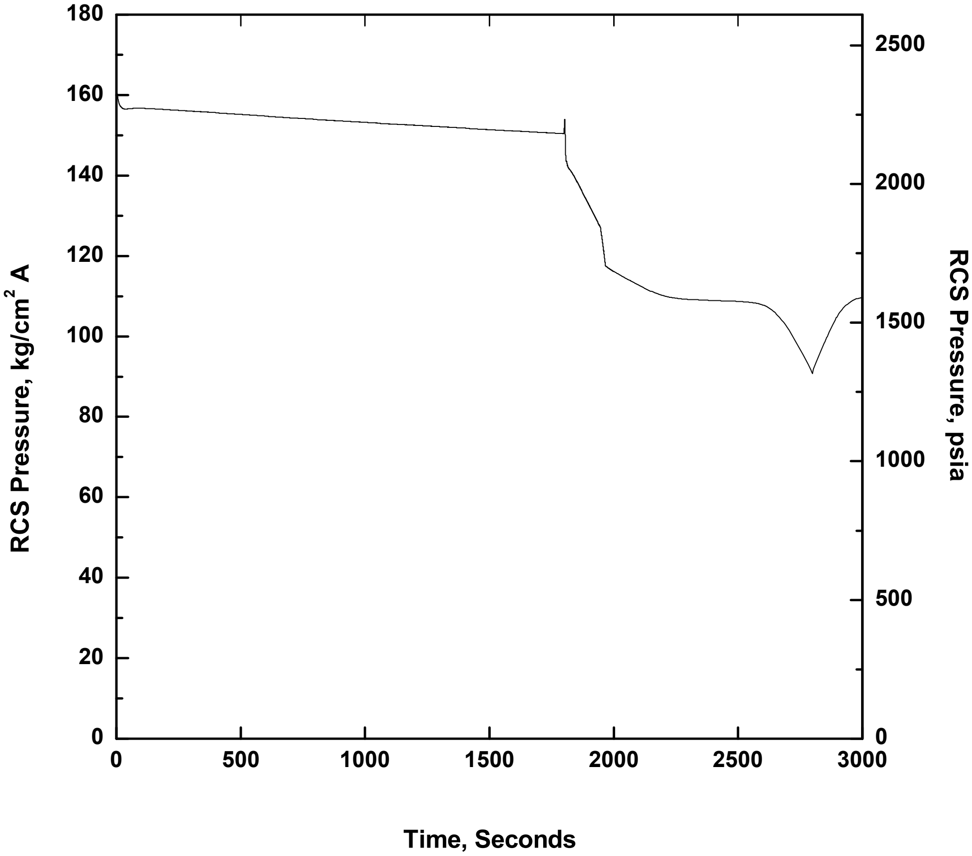

Figure 15.1.4-1.3 IOSGADV with LOOP:RCS Pressure vs. Time

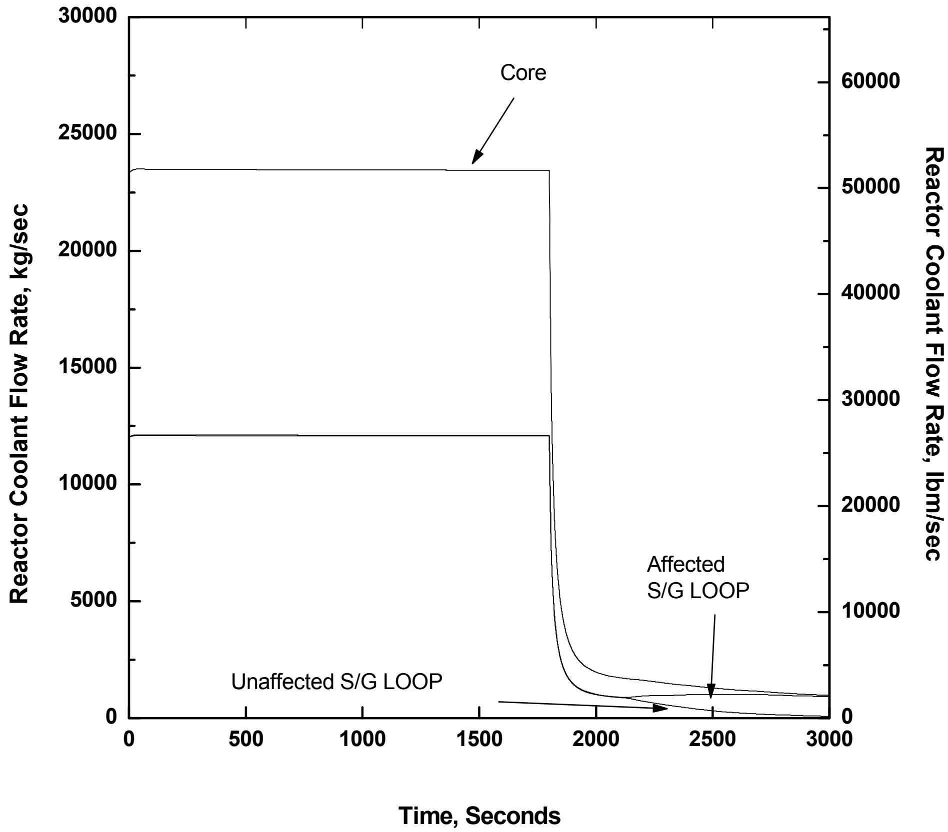

Figure 15.1.4-1.4 IOSGADV with LOOP:Reactor Coolant Flow Rates vs. Time

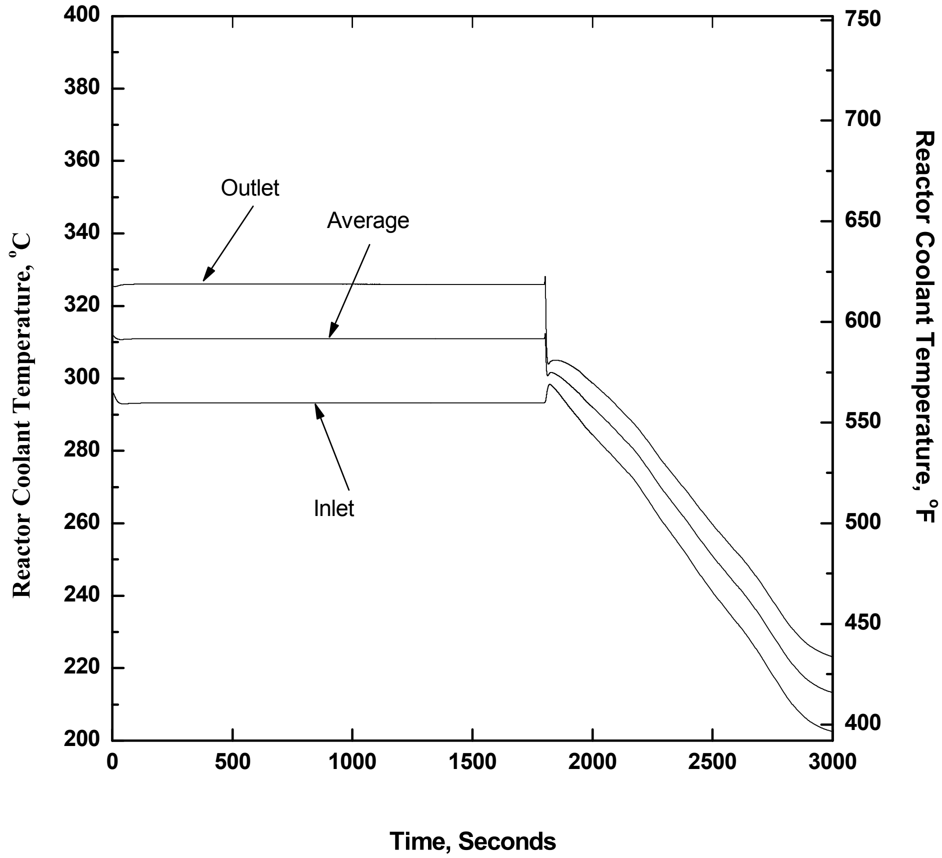

Figure 15.1.4-1.5A IOSGADV with LOOP:Reactor Coolant Temperature (A) vs. Time

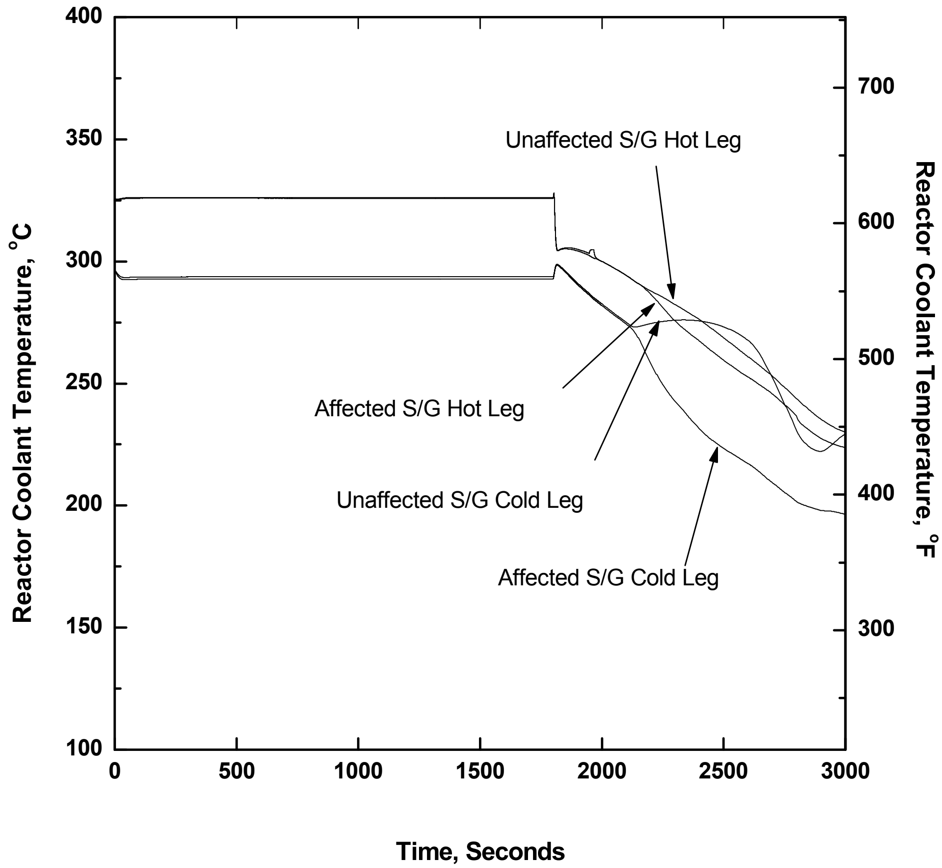

Figure 15.1.4-1.5B IOSGADV with LOOP:Reactor Coolant Temperature (B) vs. Time

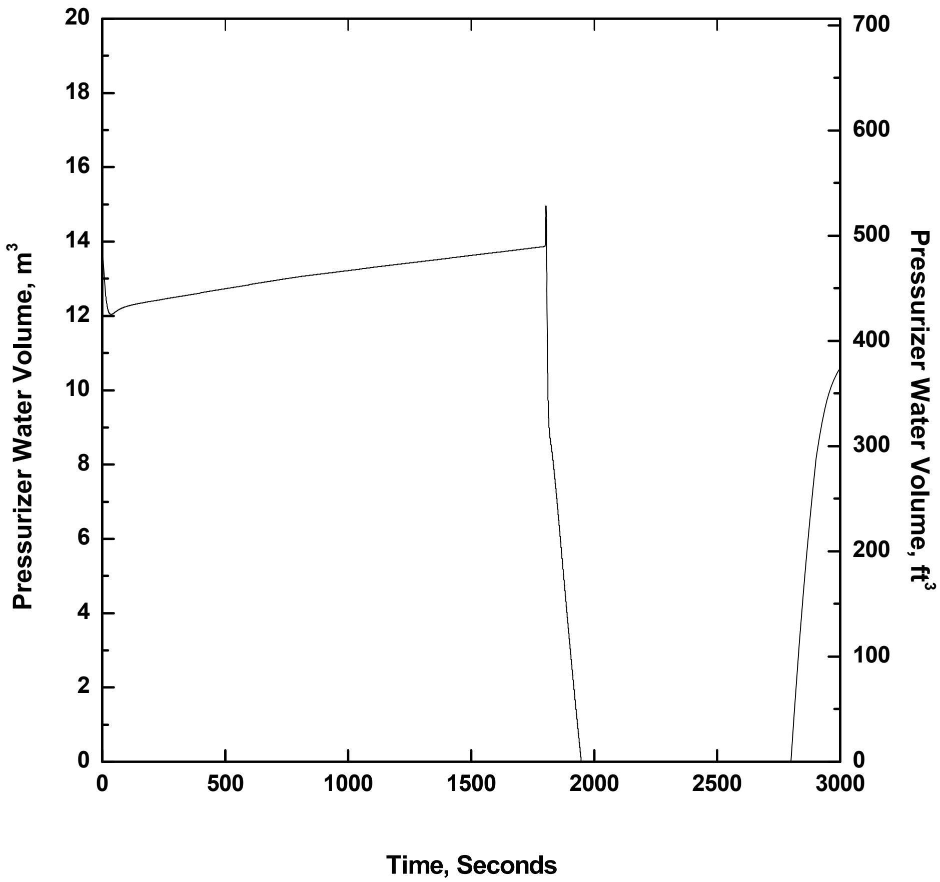

Figure 15.1.4-1.6 IOSGADV with LOOP : Pressurizer Water Volume vs. Time

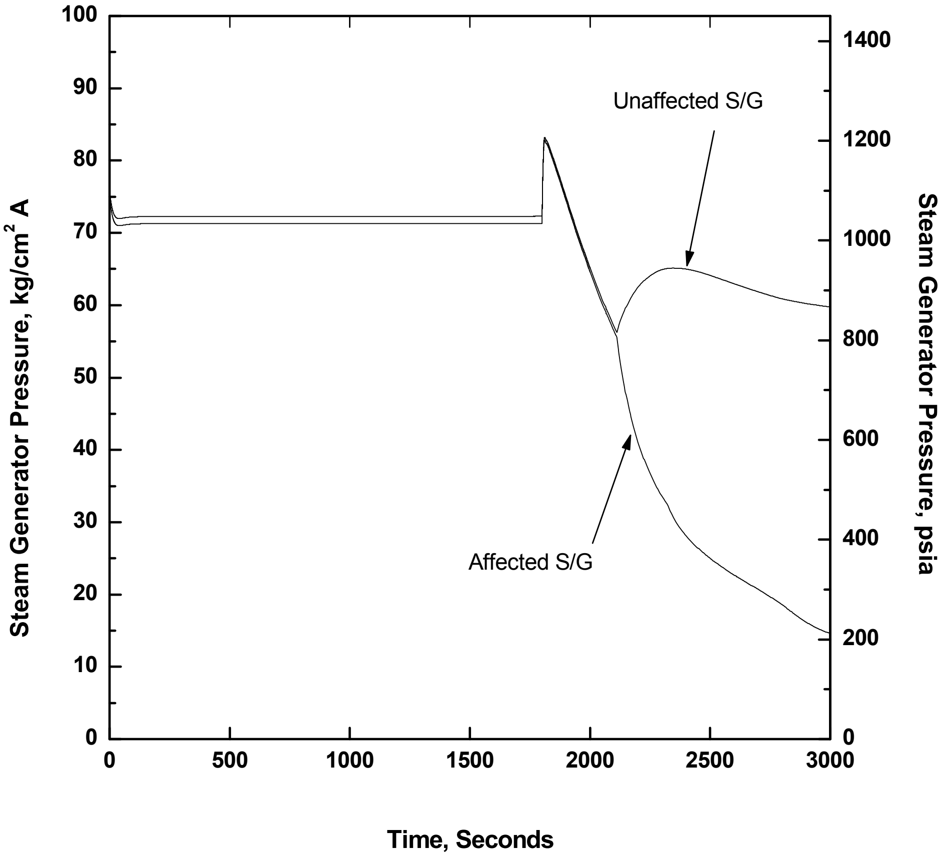

Figure 15.1.4-1.7 IOSGADV with LOOP : Steam Generator Pressure vs. Time

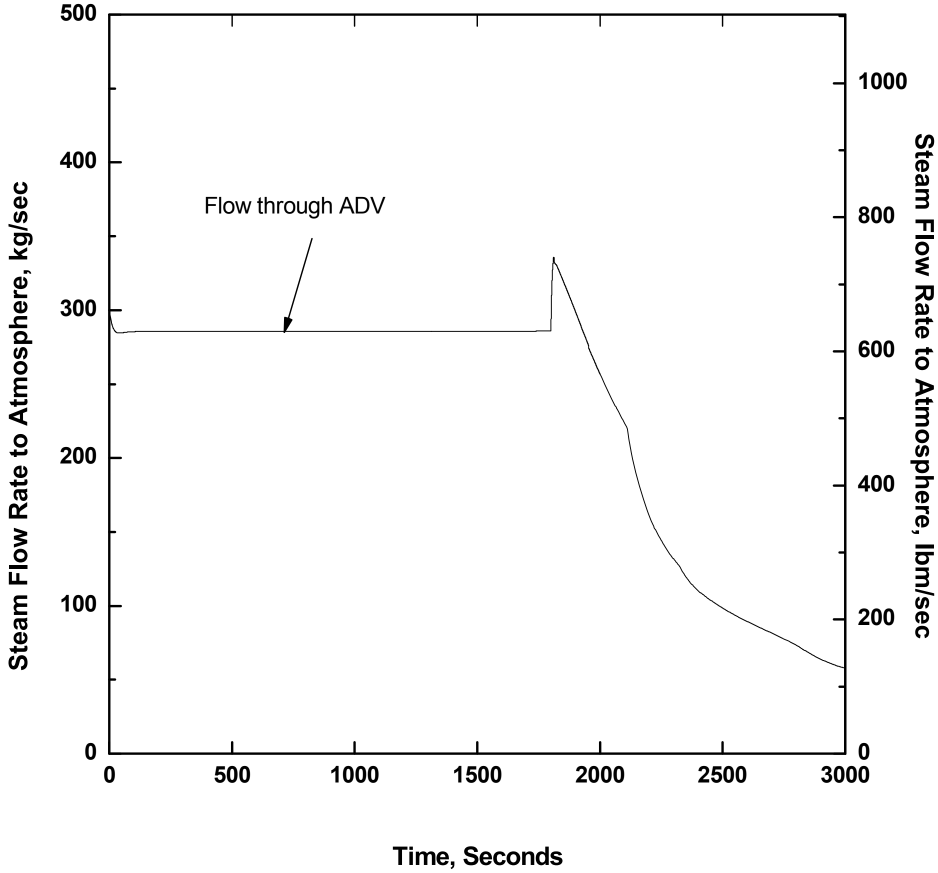

Figure 15.1.4-1.8 IOSGADV with LOOP : Steam Flow Rate to Atmosphere vs. Time

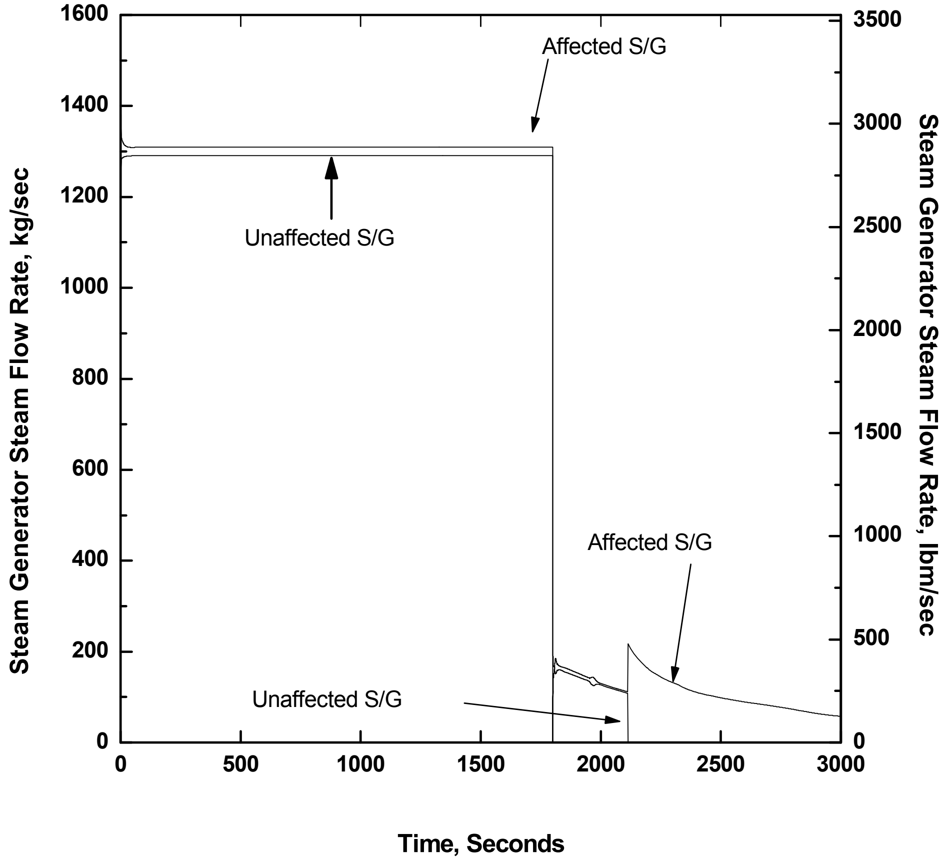

Figure 15.1.4-1.9 IOSGADV with LOOP : Steam Generator Steam Flow Rates vs. Time

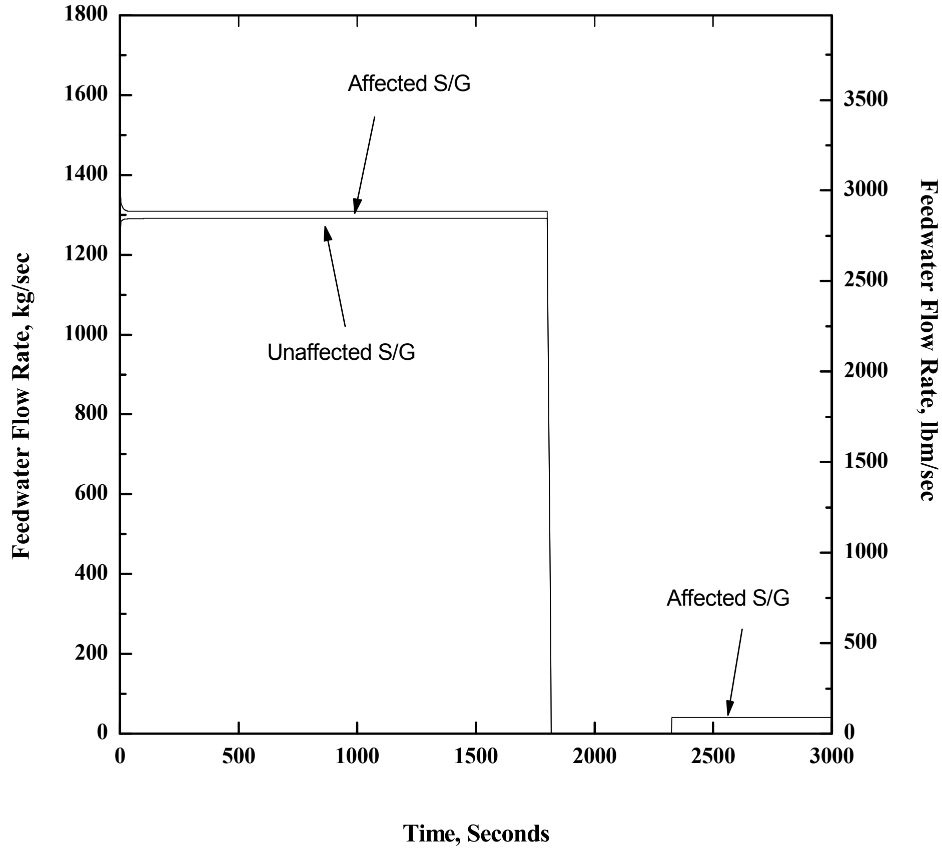

Figure 15.1.4-1.10 IOSGADV with LOOP:Feedwater Flow Rates vs. Time

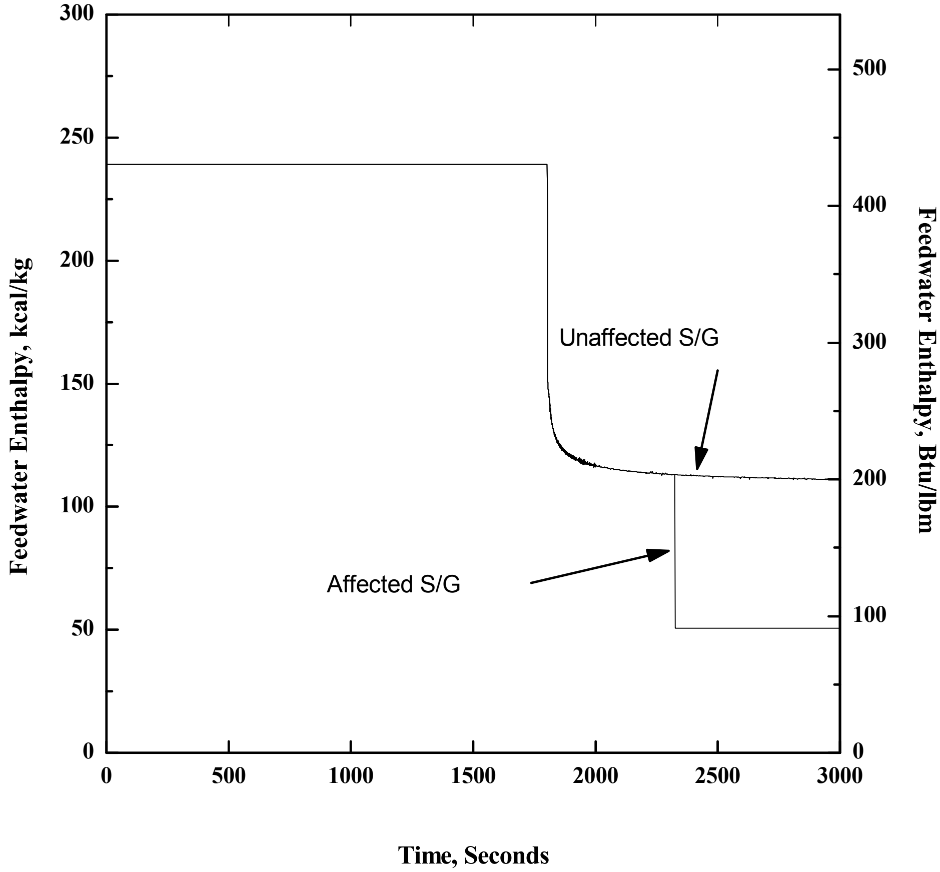

Figure 15.1.4-1.11 IOSGADV with LOOP:Feedwater Enthalpy vs. Time

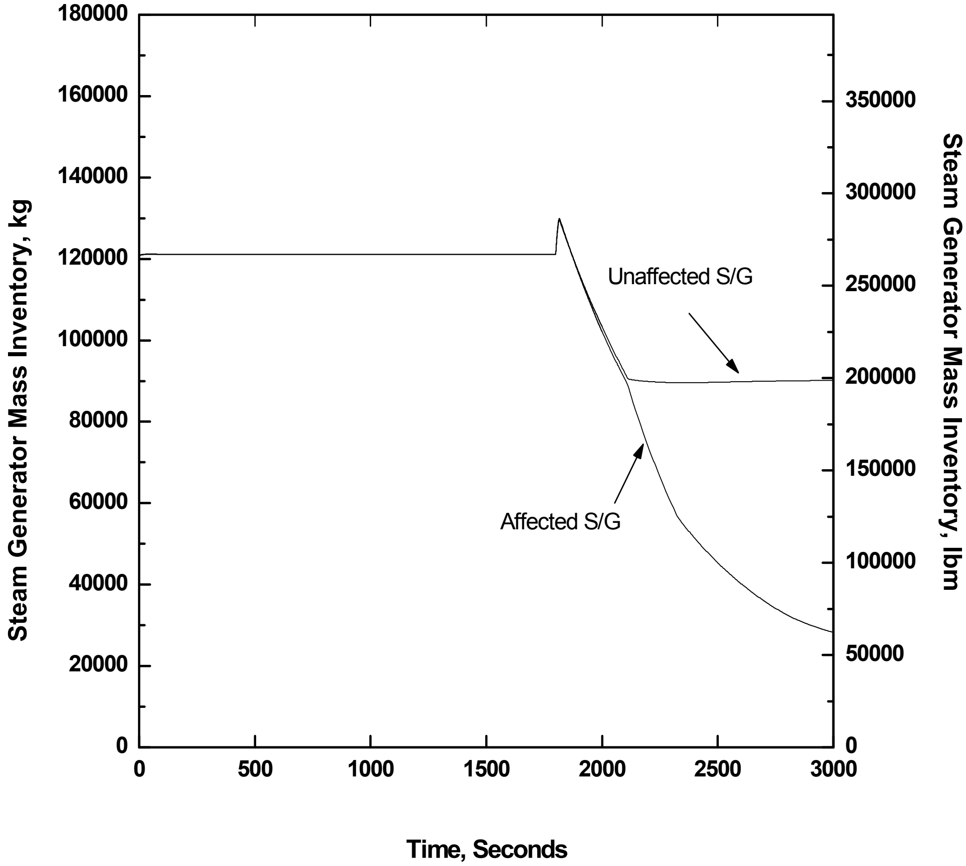

Figure 15.1.4-1.12 IOSGADV with LOOP:Steam Generator Mass Inventories vs. Time

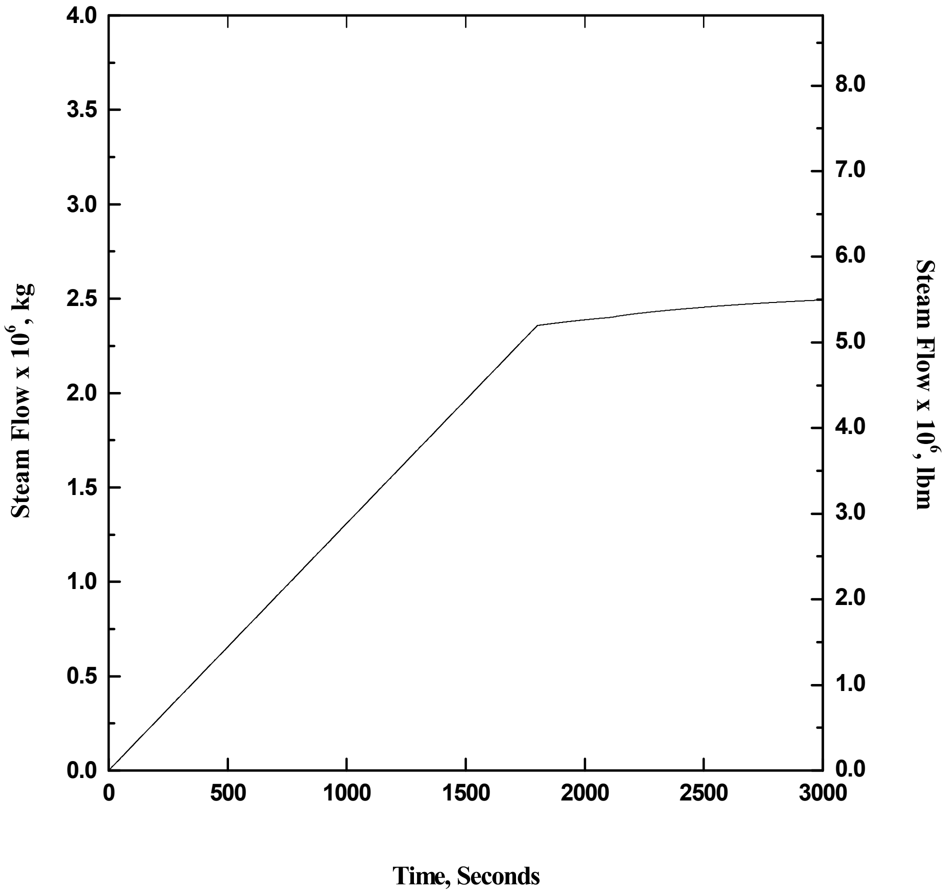

Figure 15.1.4-1.13 IOSGADV with LOOP:Integrated Steam Mass Release Through Break vs. Time

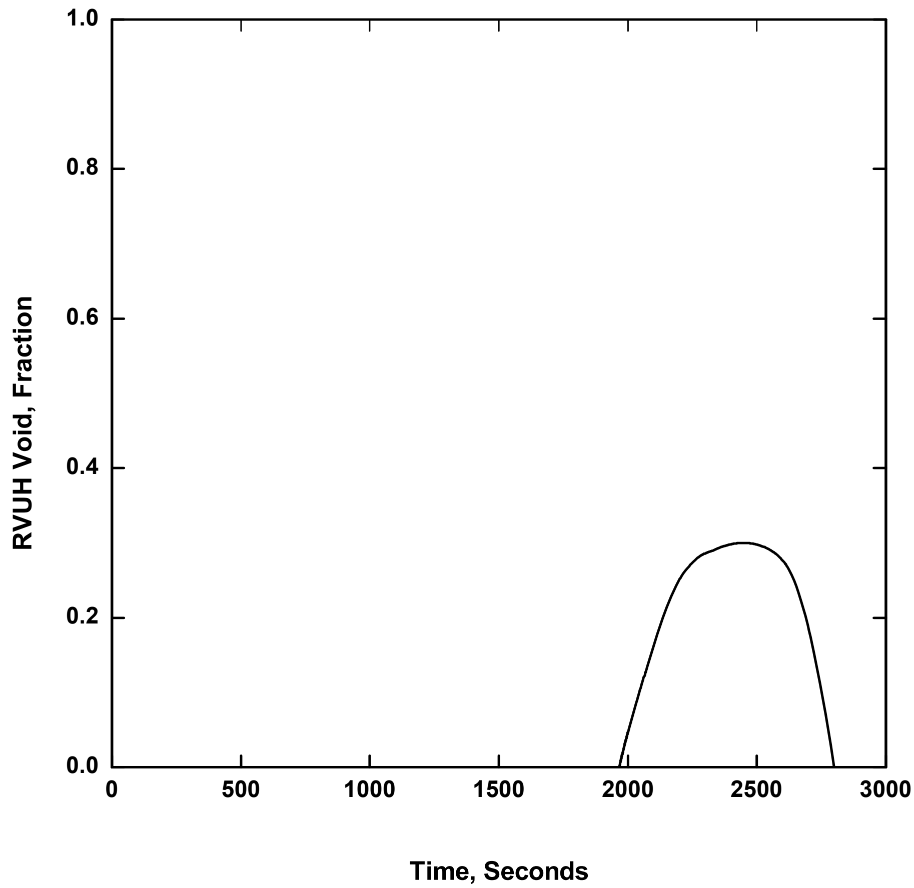

Figure 15.1.4-1.14 IOSGADV with LOOP:RV Upper Head Void Fraction vs. Time

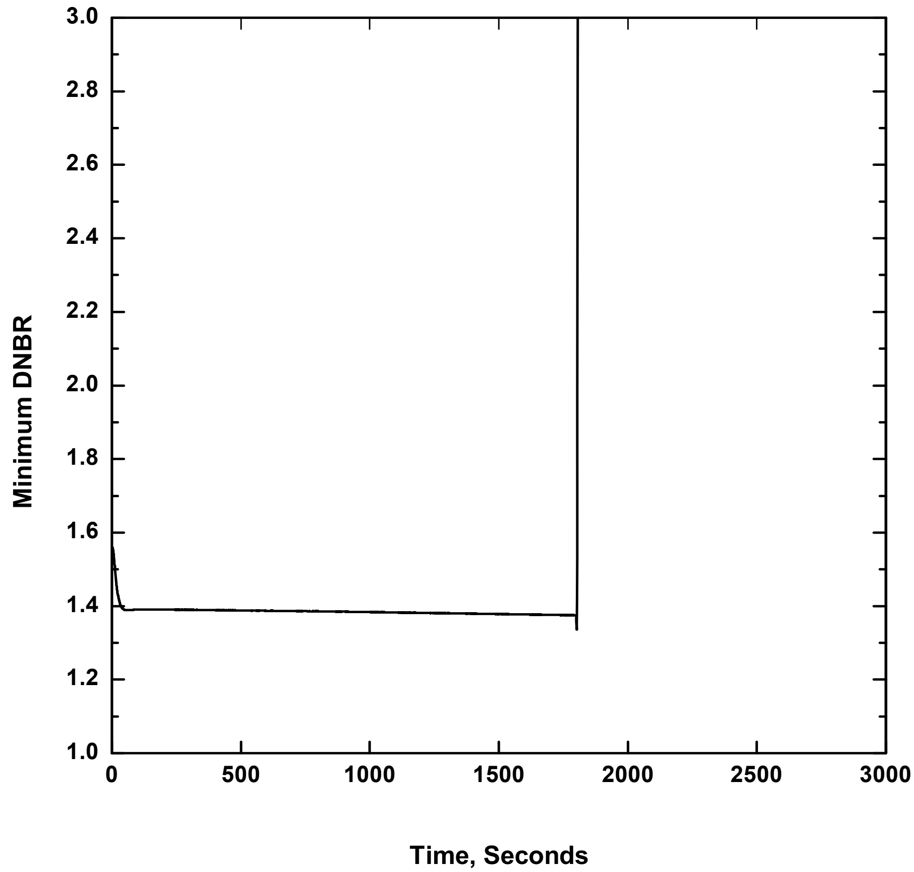

Figure 15.1.4-1.15 IOSGADV with LOOP:Minimum DNBR vs. Time

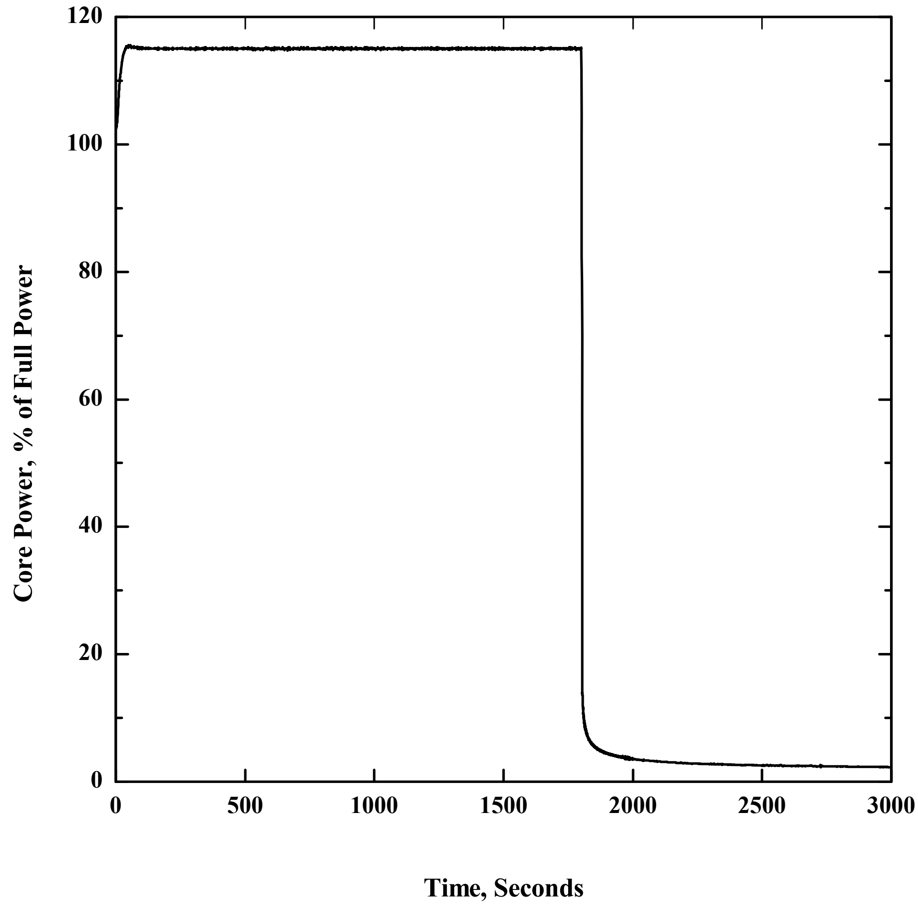

Figure 15.1.4-2.1 IOSGADV with Single Failure and LOOP:Core Power vs. Time

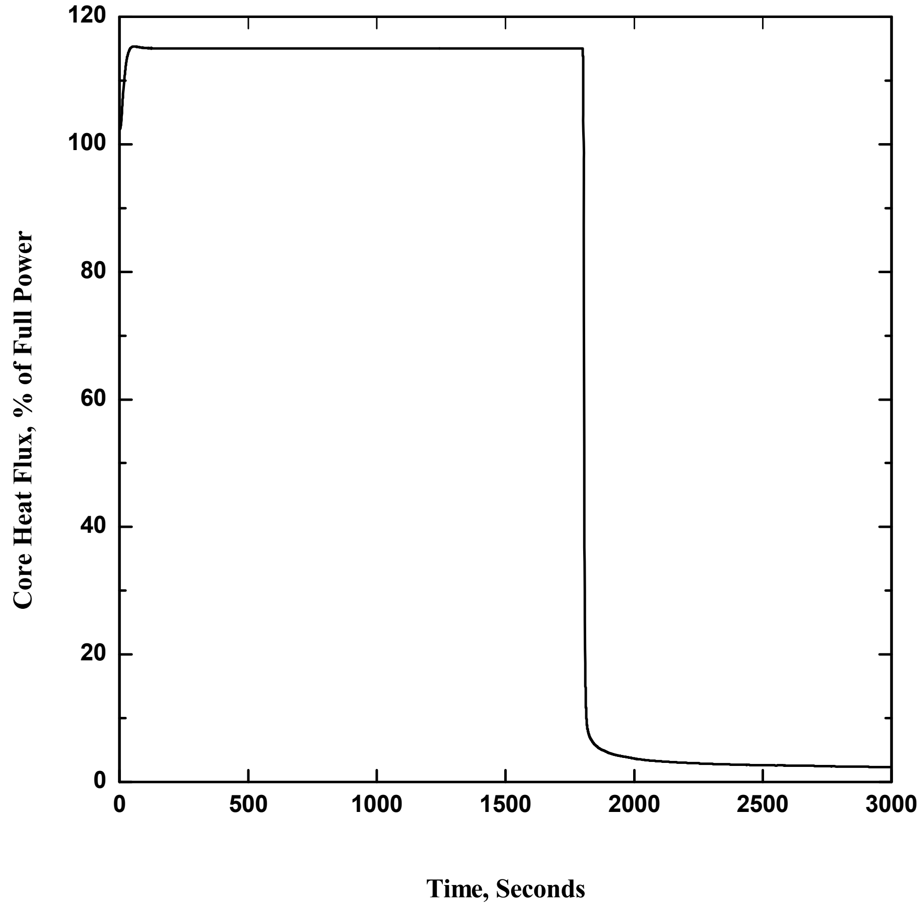

Figure 15.1.4-2.2 IOSGADV with Single Failure and LOOP:Core Heat Flux vs. Time

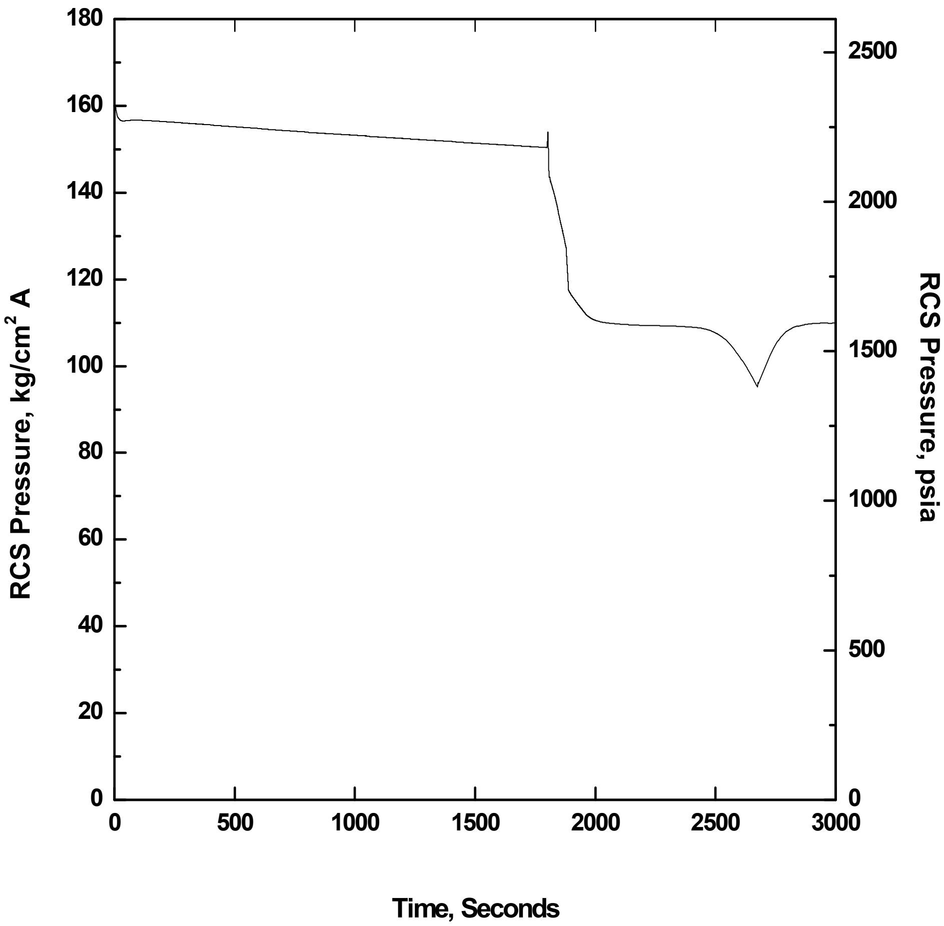

Figure 15.1.4-2.3 IOSGADV with Single Failure and LOOP:RCS Pressure vs. Time

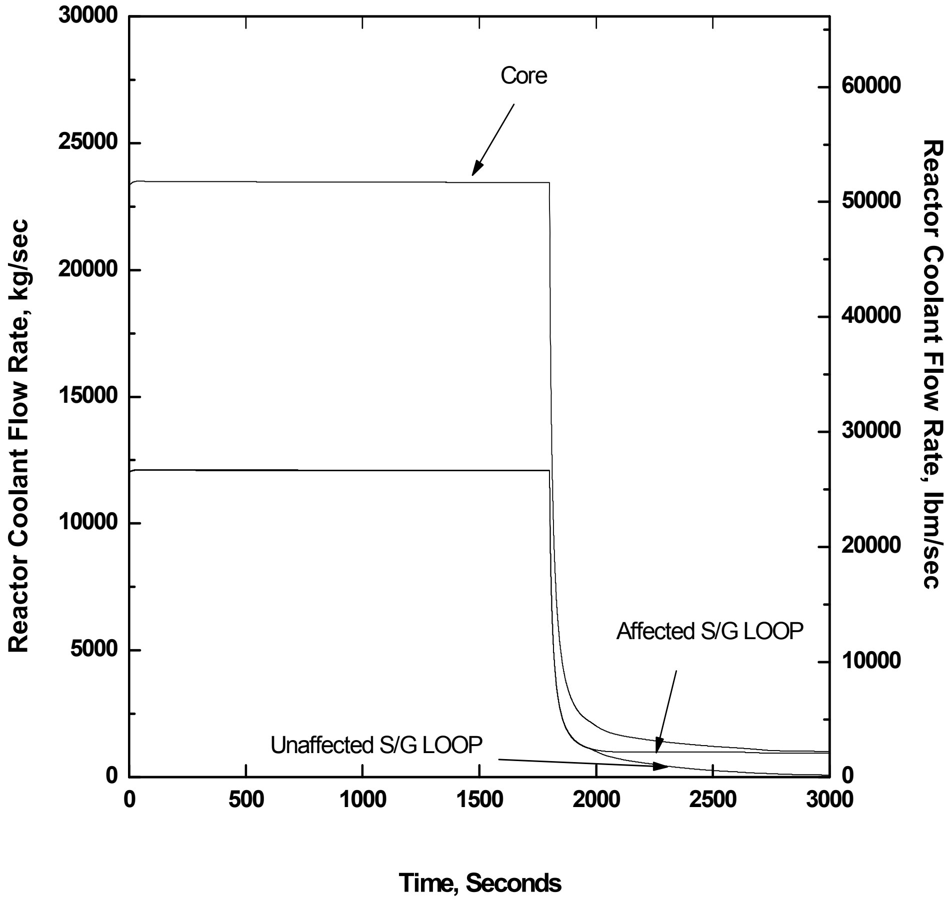

Figure 15.1.4-2.4 IOSGADV with Single Failure and LOOP: Reactor Coolant Flow Rates vs. Time

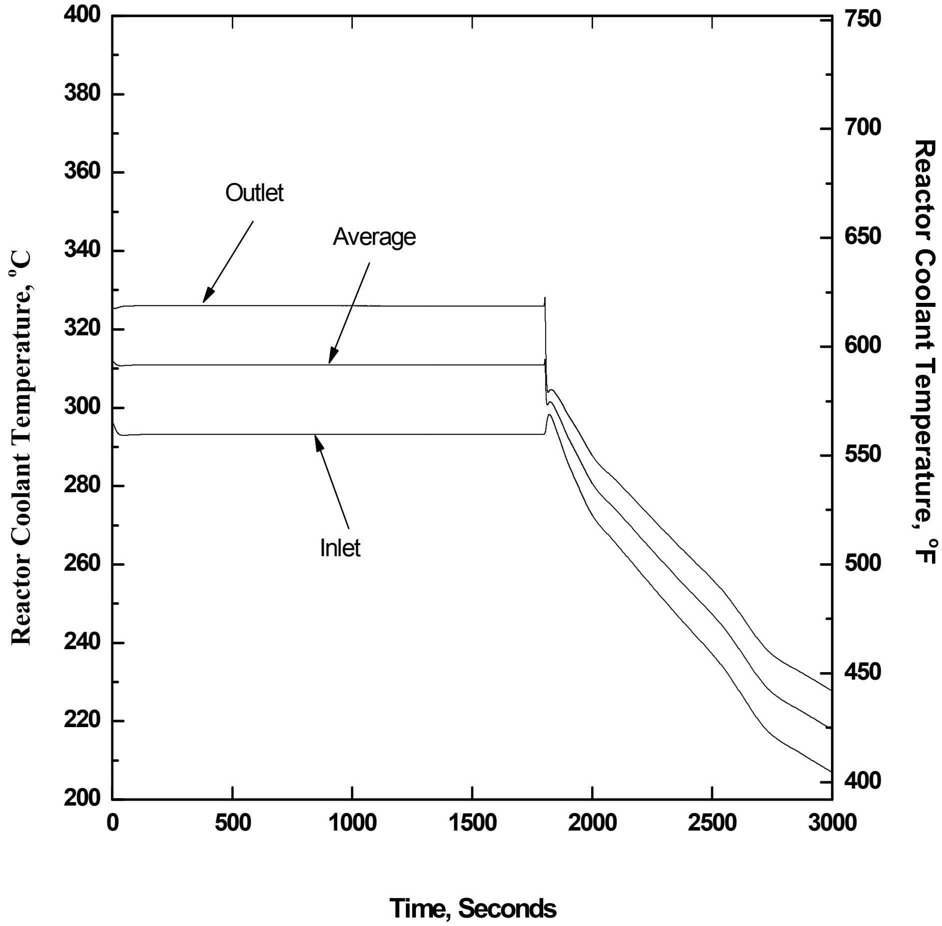

Figure 15.1.4-2.5A IOSGADV with Single Failure and LOOP: Reactor Coolant Temperature (A) vs. Time

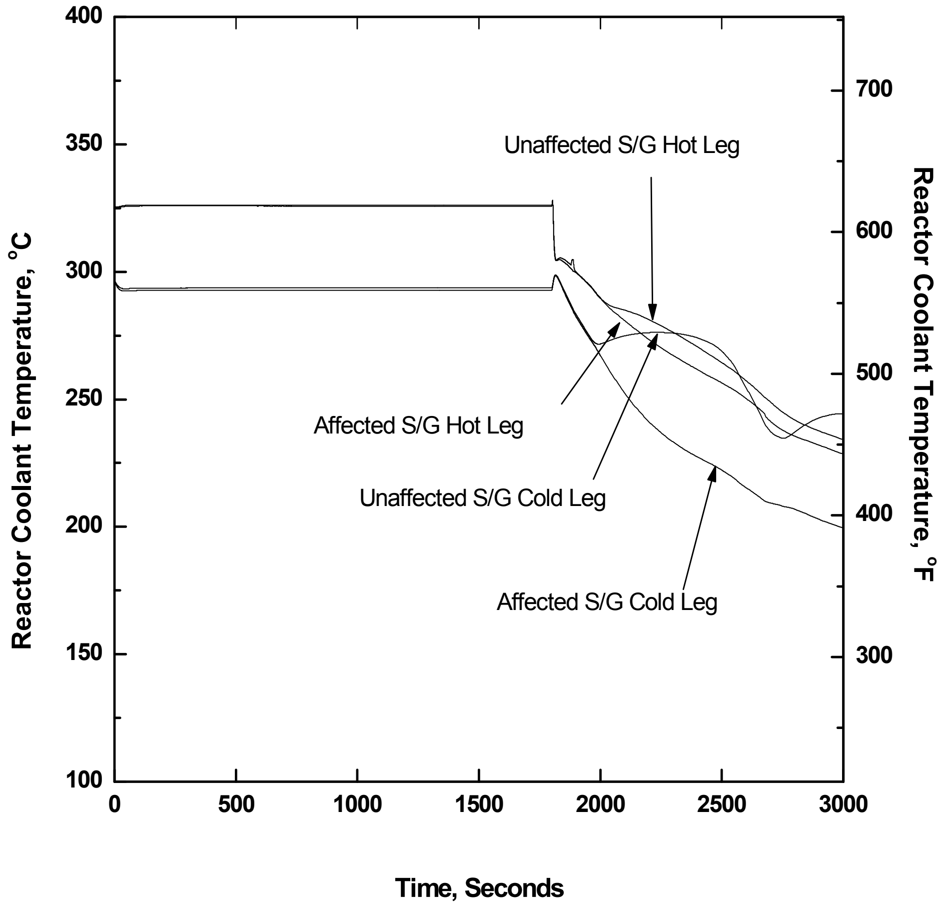

Figure 15.1.4-2.5B IOSGADV with Single Failure and LOOP: Reactor Coolant Temperature (B) vs. Time

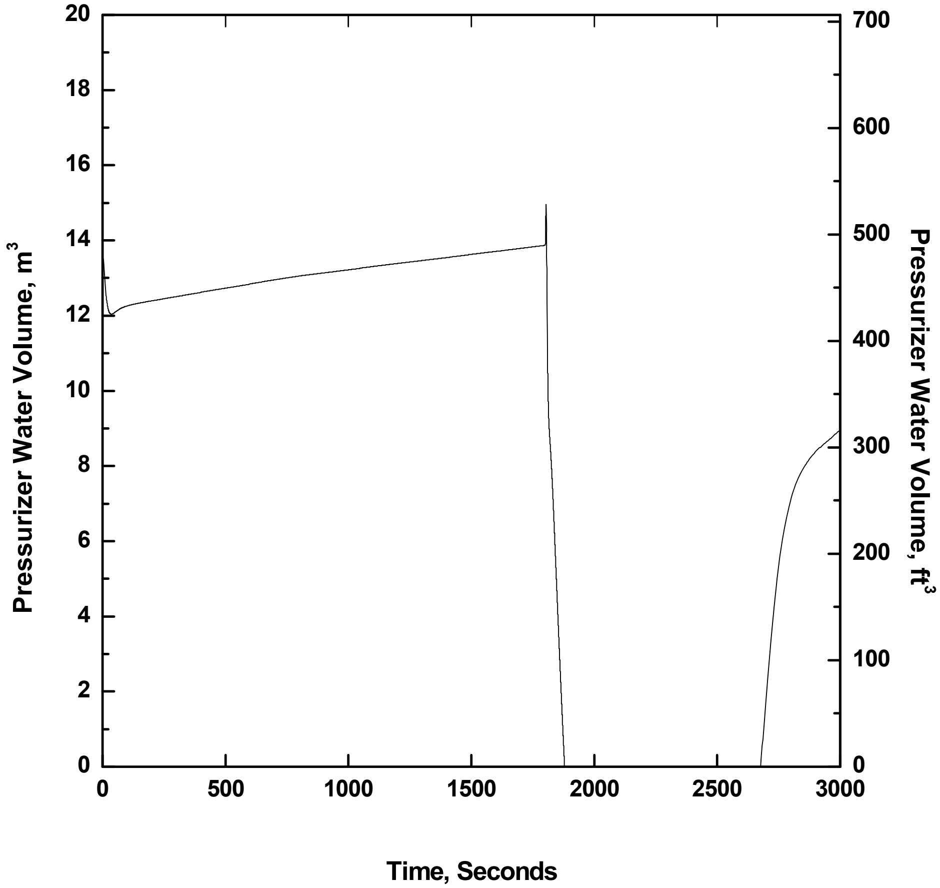

Figure 15.1.4-2.6 IOSGADV with Single Failure and LOOP: Pressurizer Water Volume vs. Time

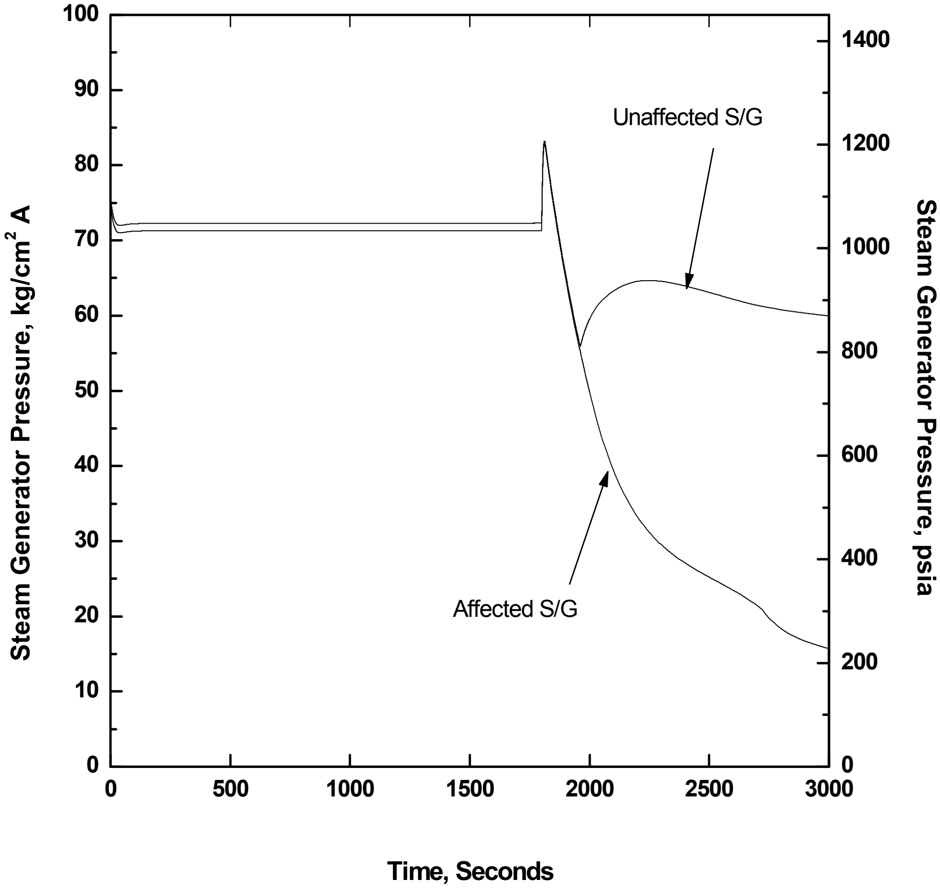

Figure 15.1.4-2.7 IOSGADV with Single Failure and LOOP: Steam Generator Pressure vs. Time

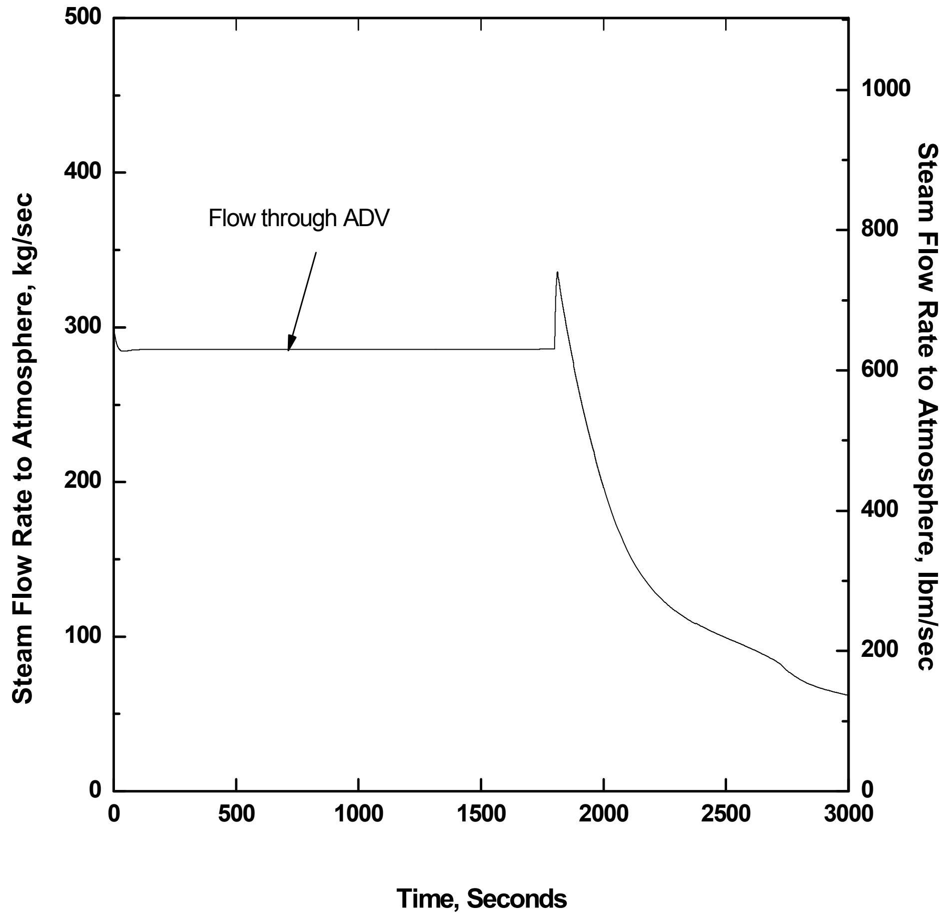

Figure 15.1.4-2.8 IOSGADV with Single Failure and LOOP: Steam Flow Rate to Atmosphere vs. Time

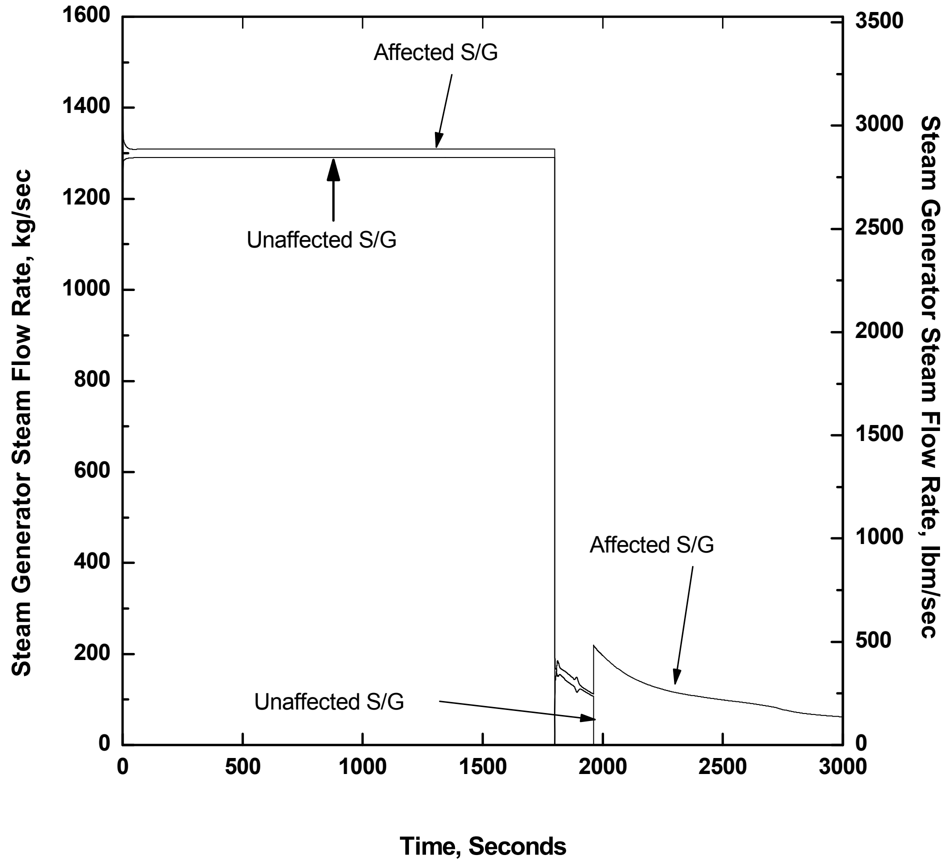

Figure 15.1.4-2.9 IOSGADV with Single Failure and LOOP: Steam Generator Steam Flow Rates vs. Time

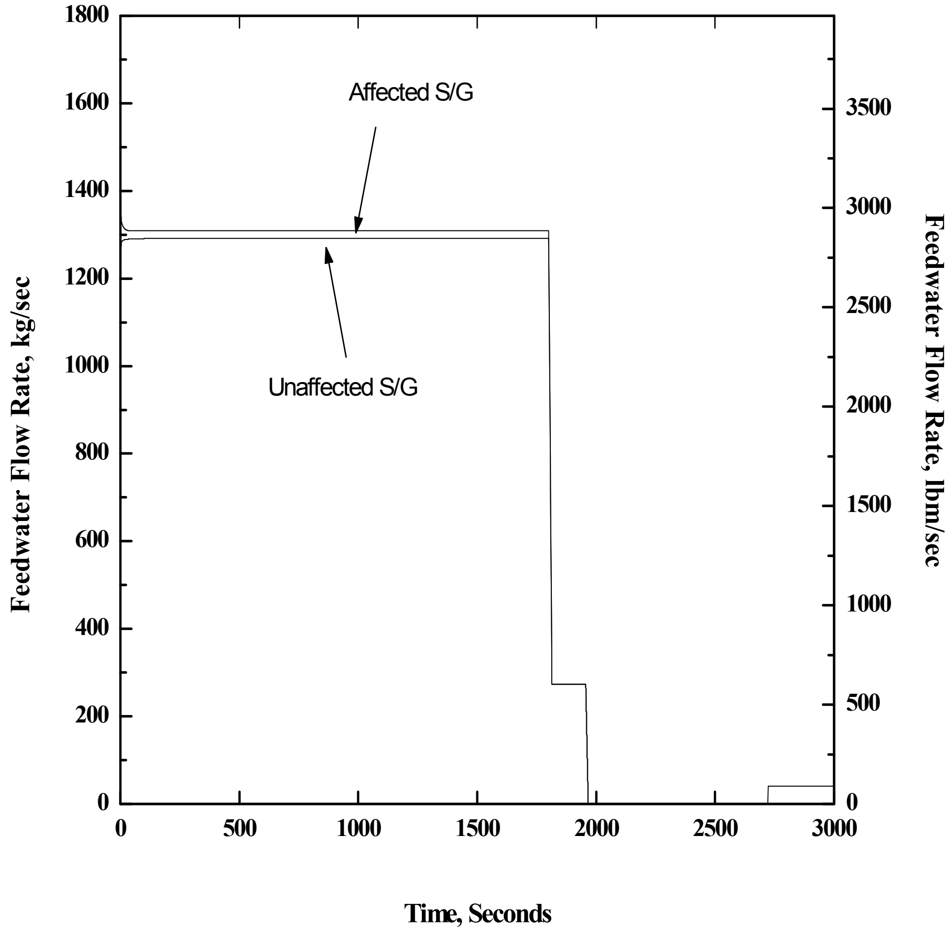

Figure 15.1.4-2.10 IOSGADV with Single Failure and LOOP: Feedwater Flow Rates vs. Time

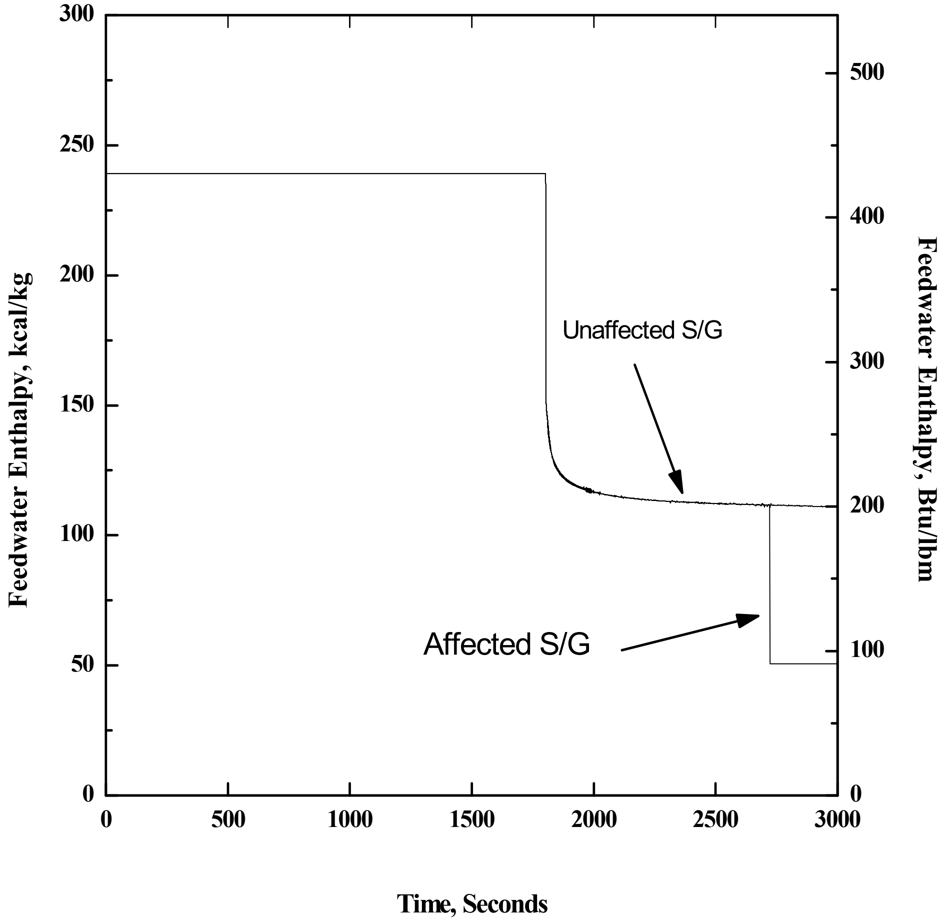

Figure 15.1.4-2.11 IOSGADV with Single Failure and LOOP:Feedwater Enthalpy vs. Time

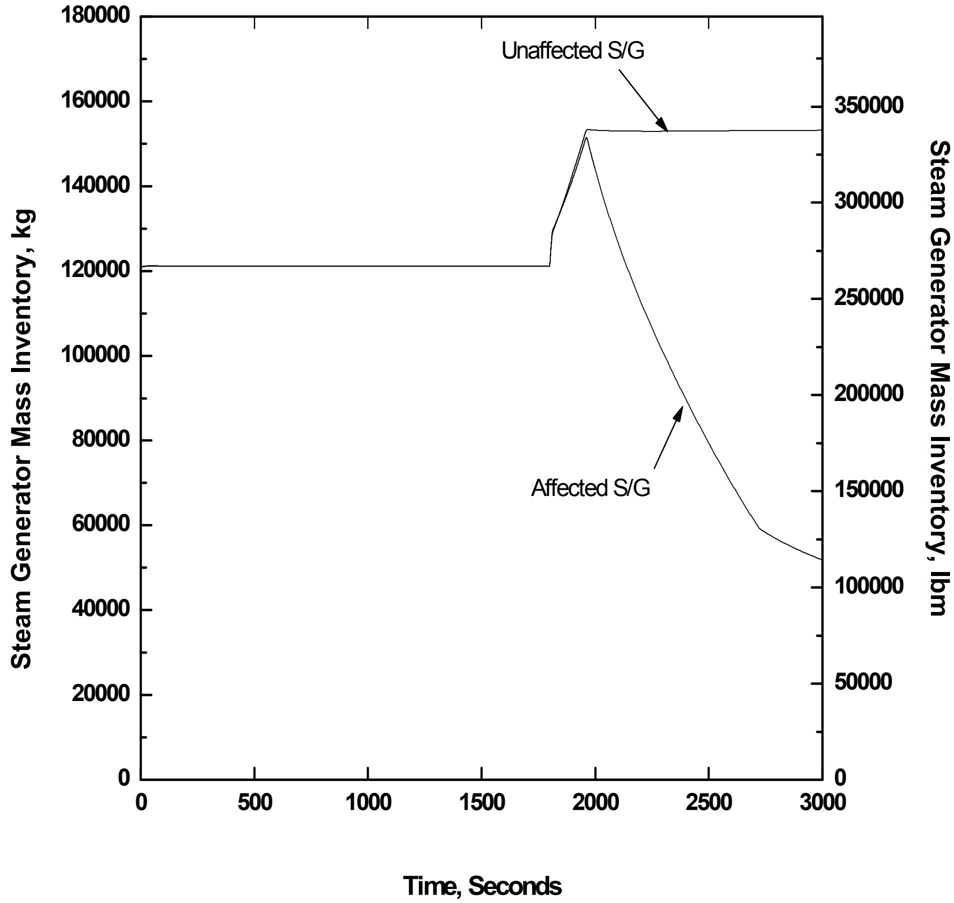

Figure 15.1.4-2.12 IOSGADV with Single Failure and LOOP: Steam Generator Mass Inventories vs. Time

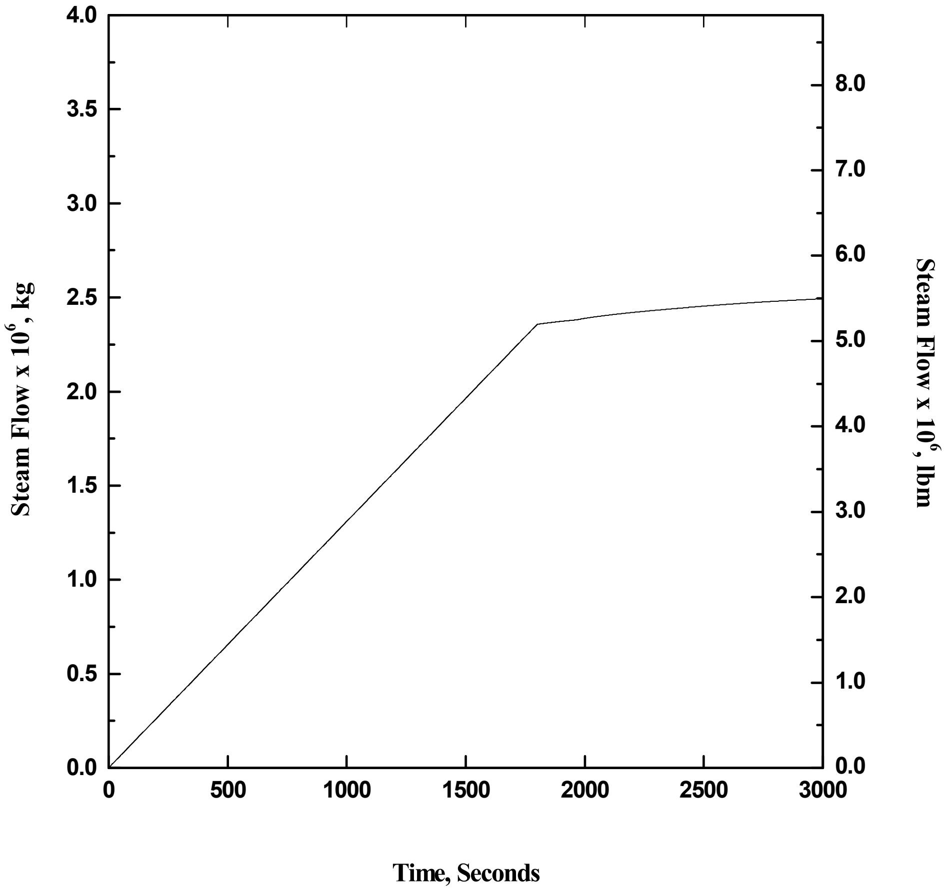

Figure 15.1.4-2.13 IOSGADV with Single Failure and LOOP: Integrated Steam Mass vs. Time

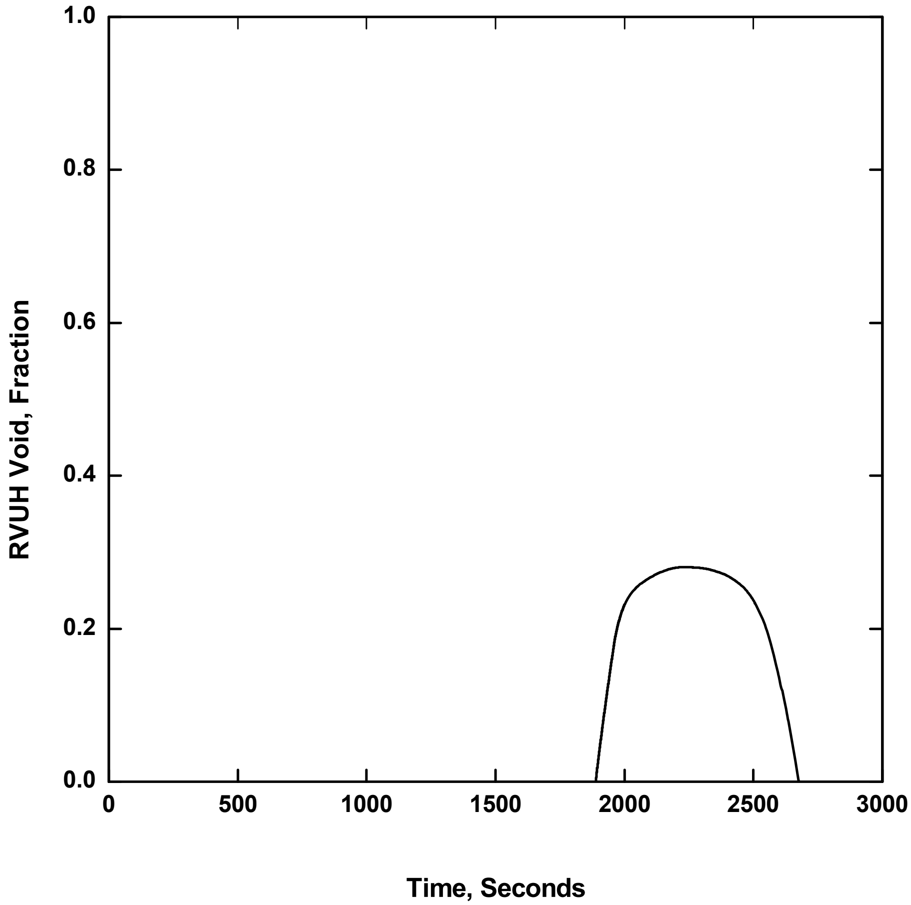

Figure 15.1.4-2.14 IOSGADV with Single Failure and LOOP: RV Upper Head Void Fraction vs. Time

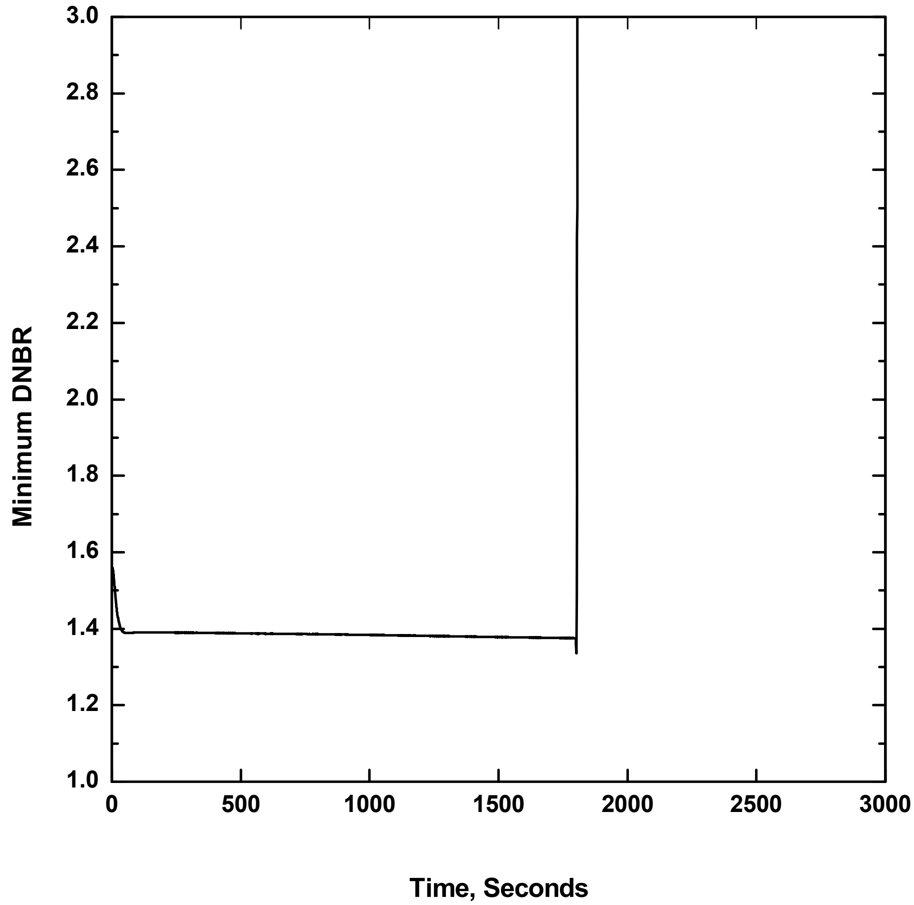

Figure 15.1.4-2.15 IOSGADV with Single Failure and LOOP:Minimum DNBR vs. Time

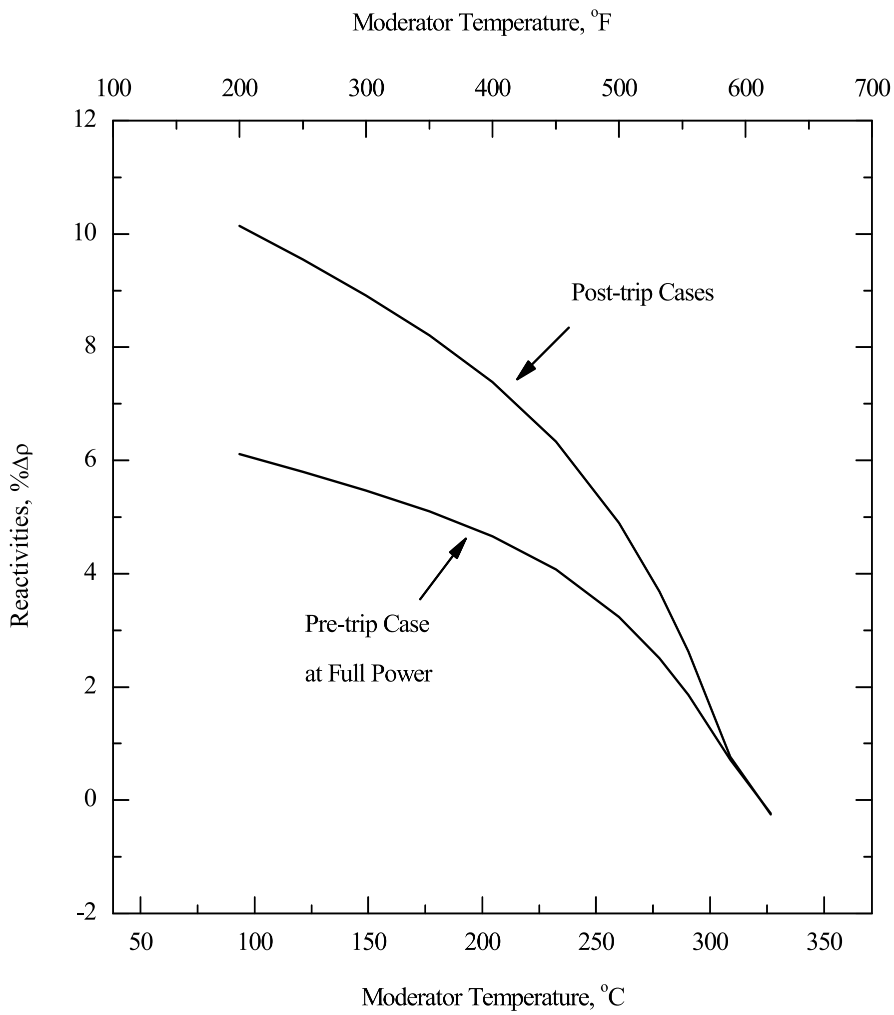

Figure 15.1.5-0 Moderator Temperature Reactivity vs. Temperature

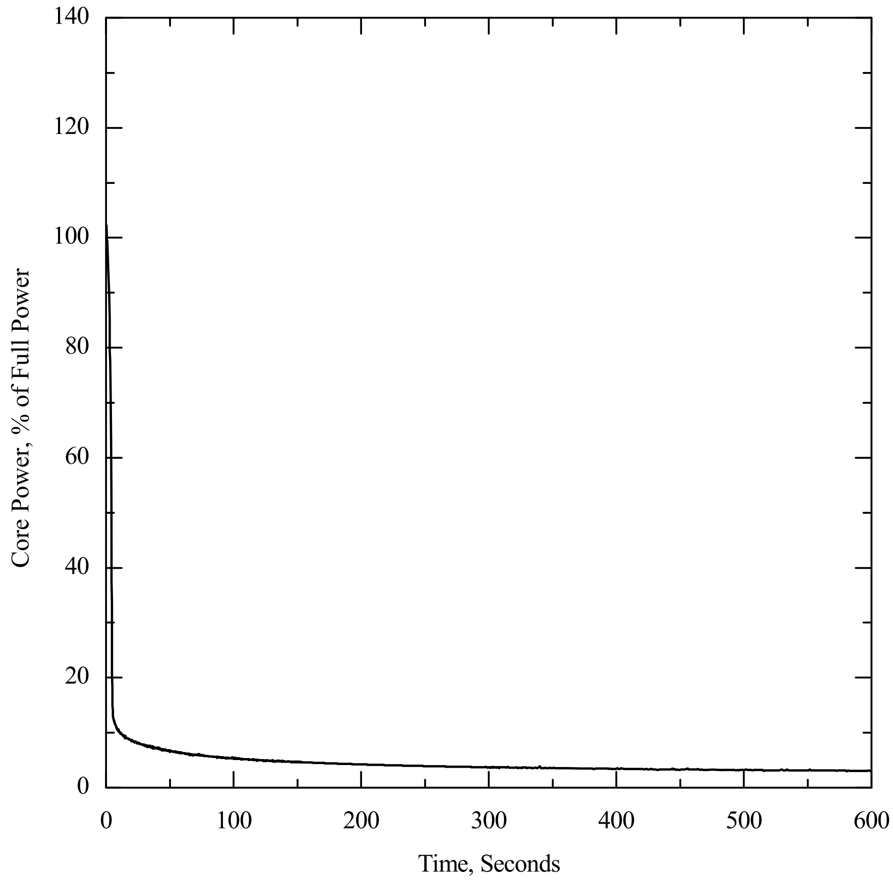

Figure 15.1.5-1.1 Full Power Large Steam Line Break with Concurrent LOOP: Core Power vs. Time

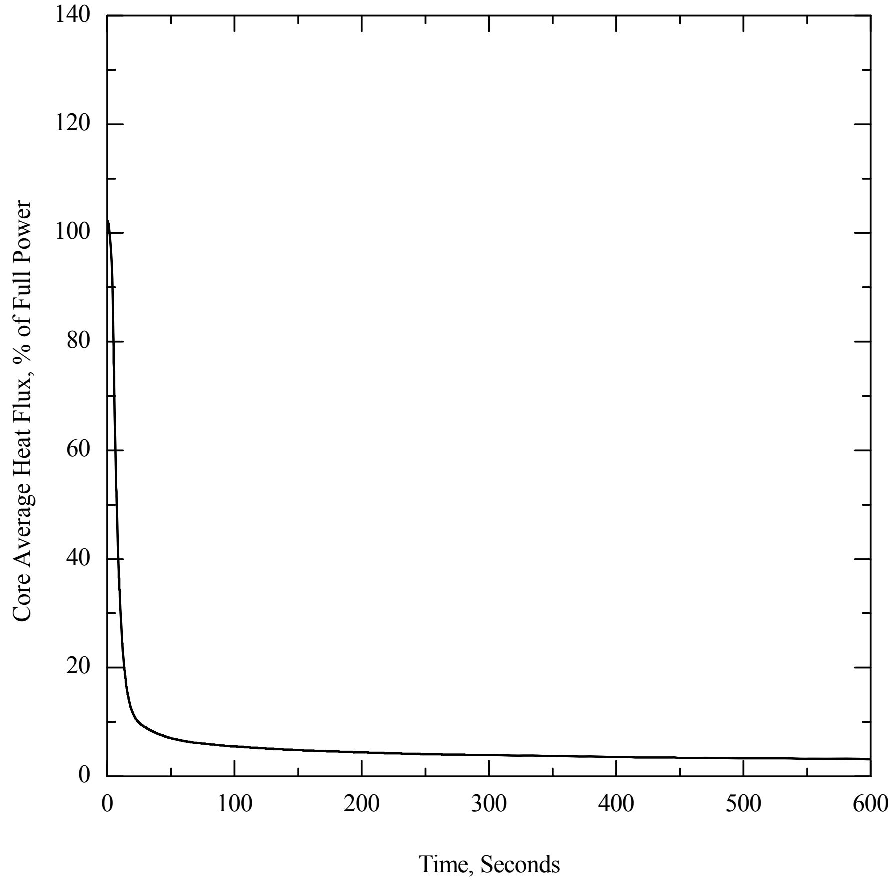

Figure 15.1.5-1.2 Full Power Large Steam Line Break with Concurrent LOOP: Core Average Heat Flux vs. Time

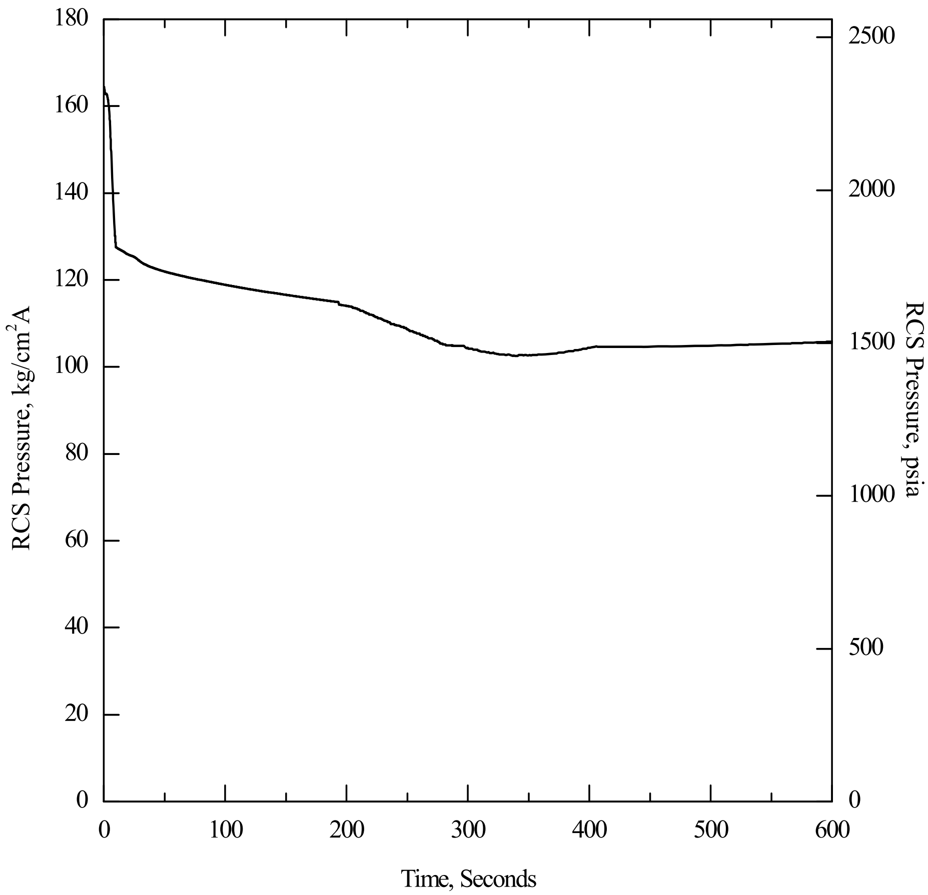

Figure 15.1.5-1.3 Full Power Large Steam Line Break with Concurrent LOOP: RCS Pressure vs. Time

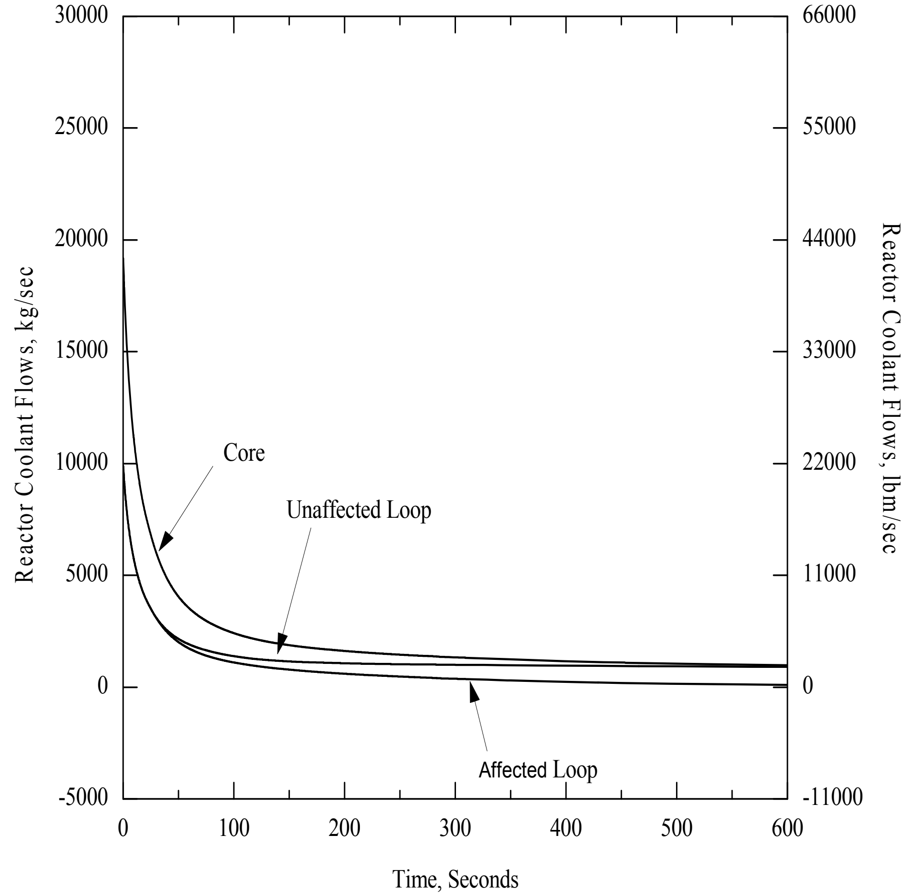

Figure 15.1.5-1.4 Full Power Large Steam Line Break with Concurrent LOOP: Reactor Coolant Flow Rates vs. Time

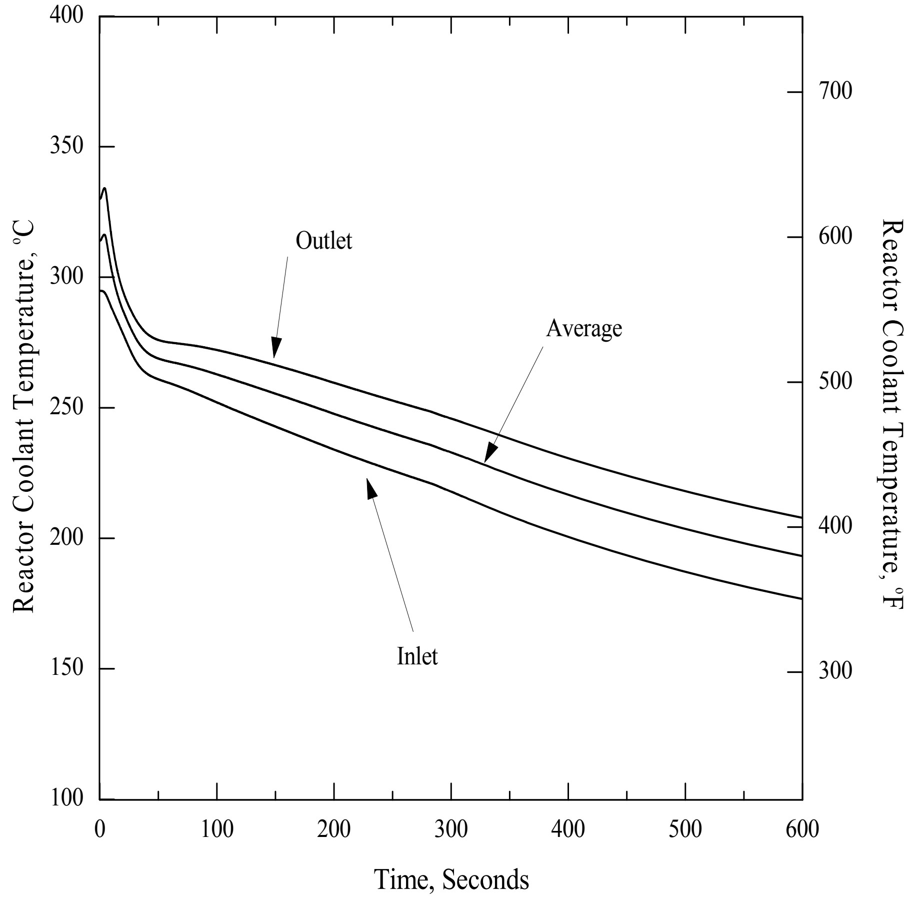

Figure 15.1.5-1.5 Full Power Large Steam Line Break with Concurrent LOOP: Reactor Coolant Temperature (A) vs. Time

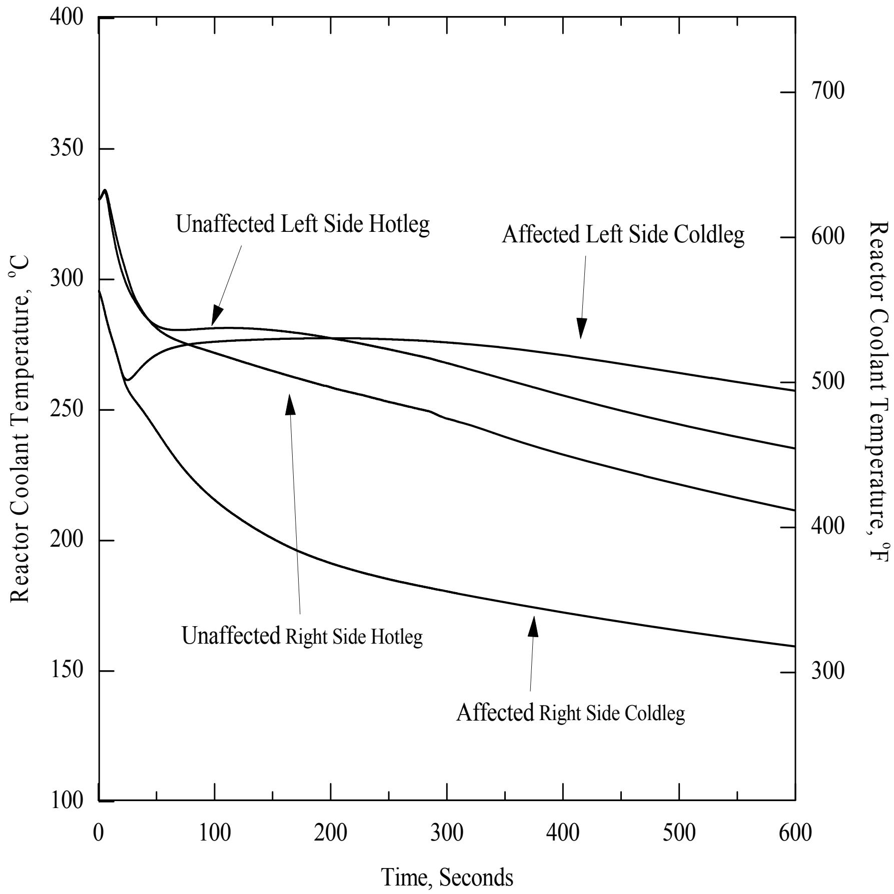

Figure 15.1.5-1.6 Full Power Large Steam Line Break with Concurrent LOOP: Reactor Coolant Temperature (B) vs. Time

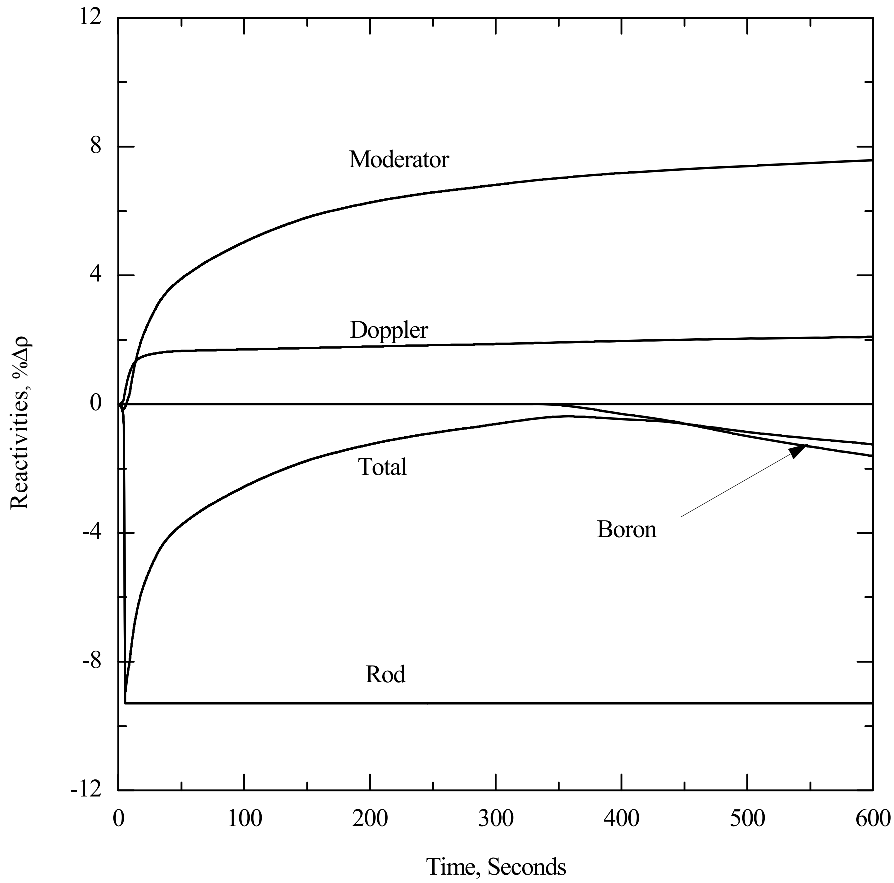

Figure 15.1.5-1.7 Full Power Large Steam Line Break with Concurrent LOOP: Reactivity vs. Time

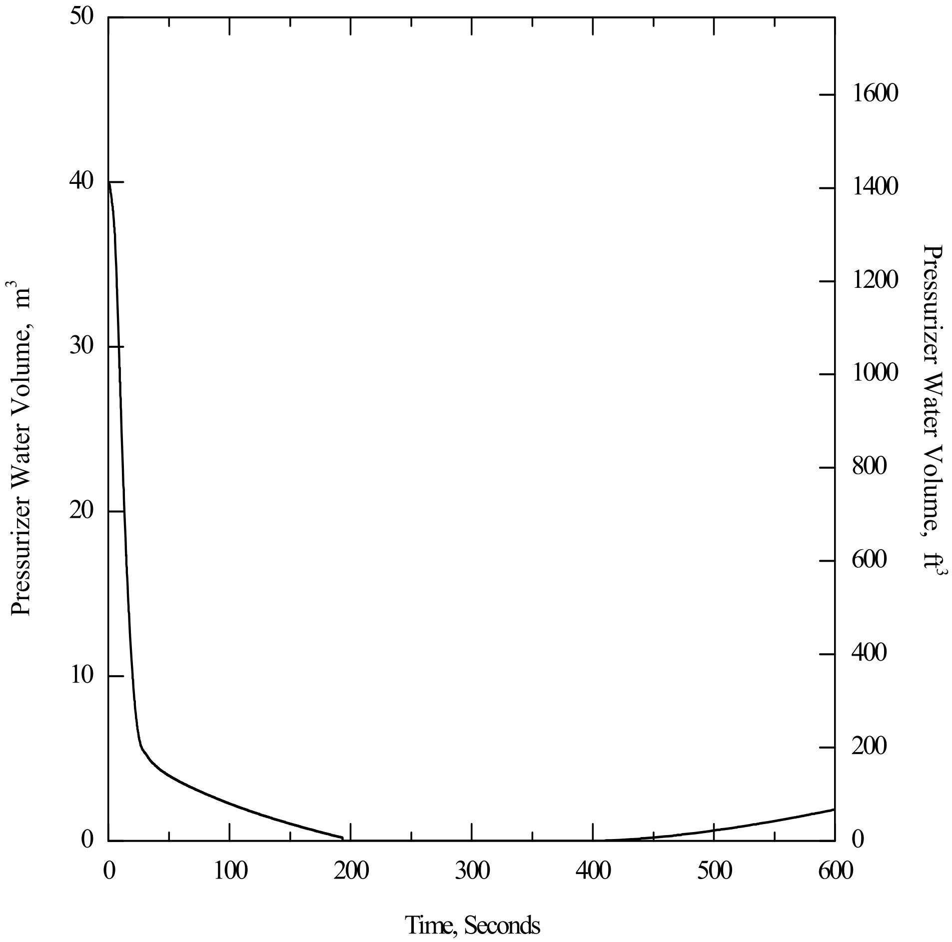

Figure 15.1.5-1.8 Full Power Large Steam Line Break with Concurrent LOOP: Pressurizer Water Volume vs. Time

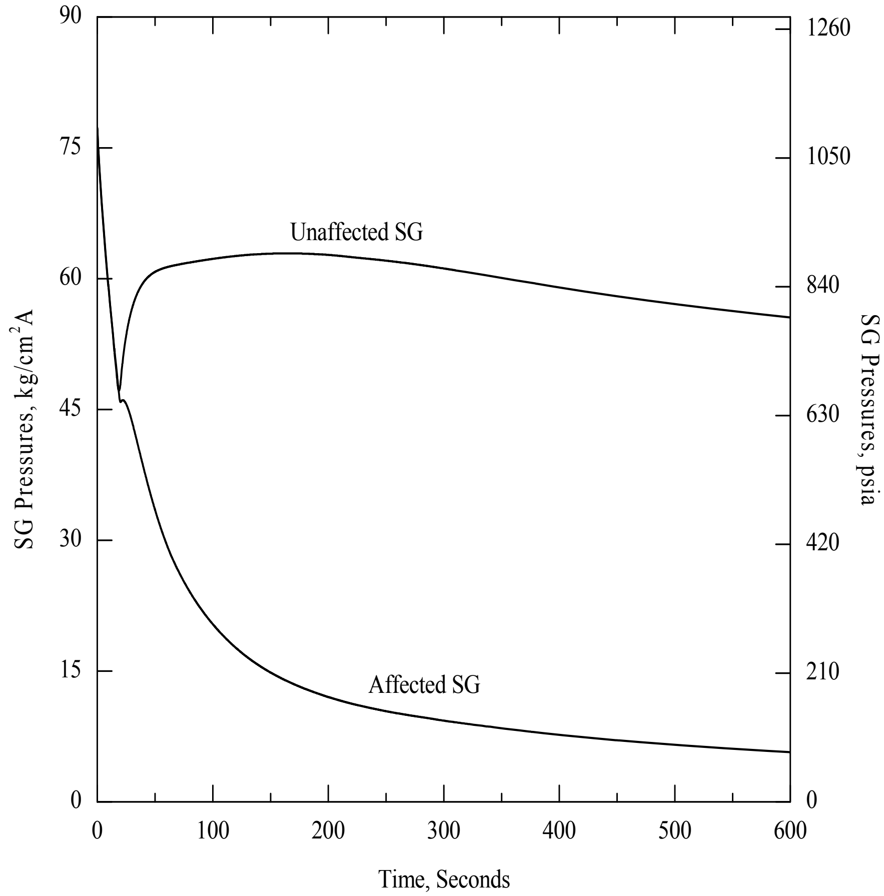

Figure 15.1.5-1.9 Full Power Large Steam Line Break With Concurrent LOOP: Steam Generator Pressure vs. Time

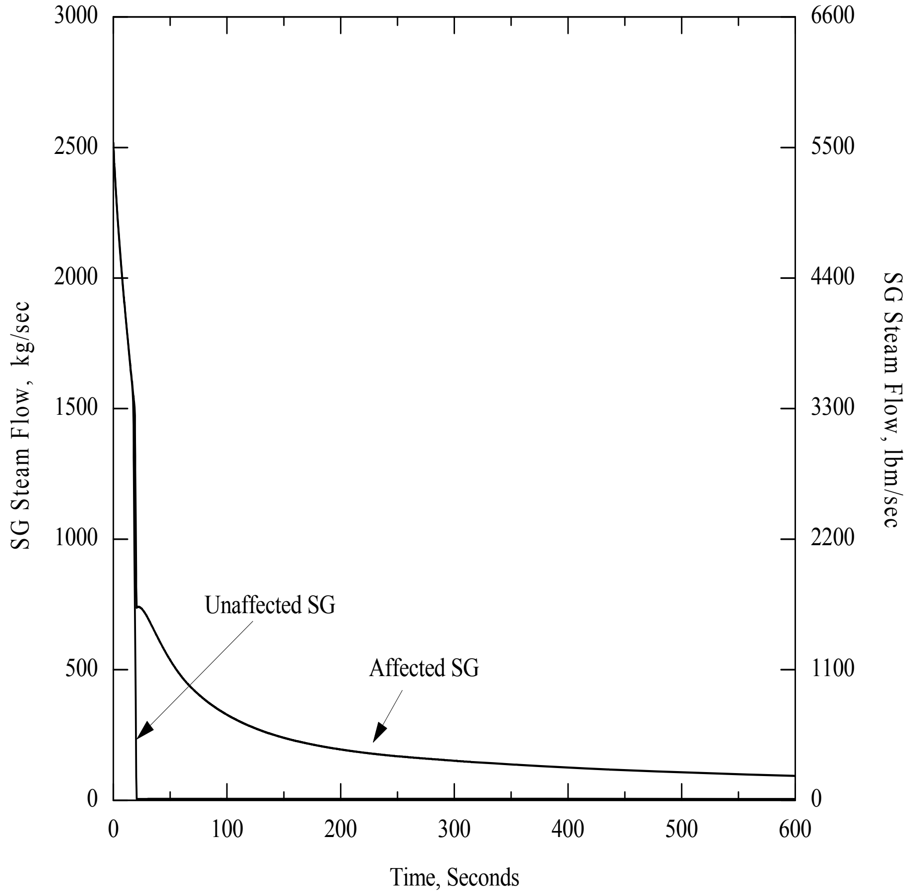

Figure 15.1.5-1.10 Full Power Large Steam Line Break with Concurrent LOOP: Steam Generator Flow Rates vs. Time

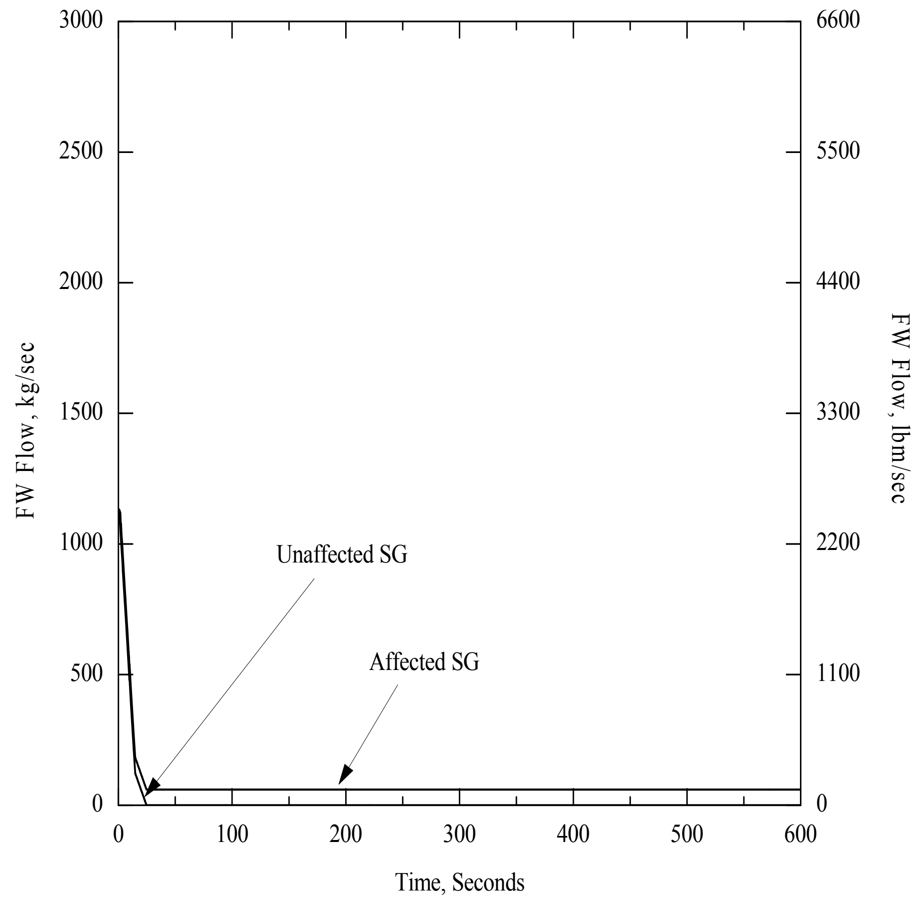

Figure 15.1.5-1.11 Full Power Large Steam Line Break with Concurrent LOOP: Feedwater Flow Rates vs. Time

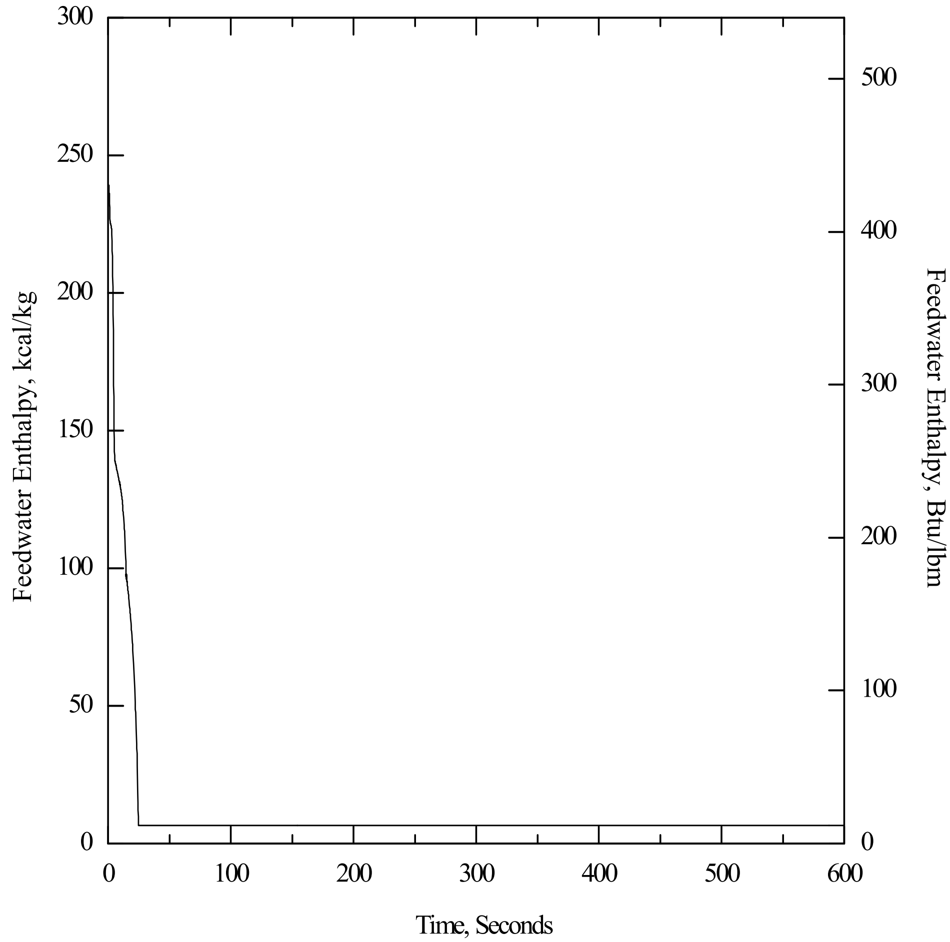

Figure 15.1.5-1.12 Full Power Large Steam Line Break with Concurrent LOOP: Feedwater Enthalpy vs. Time

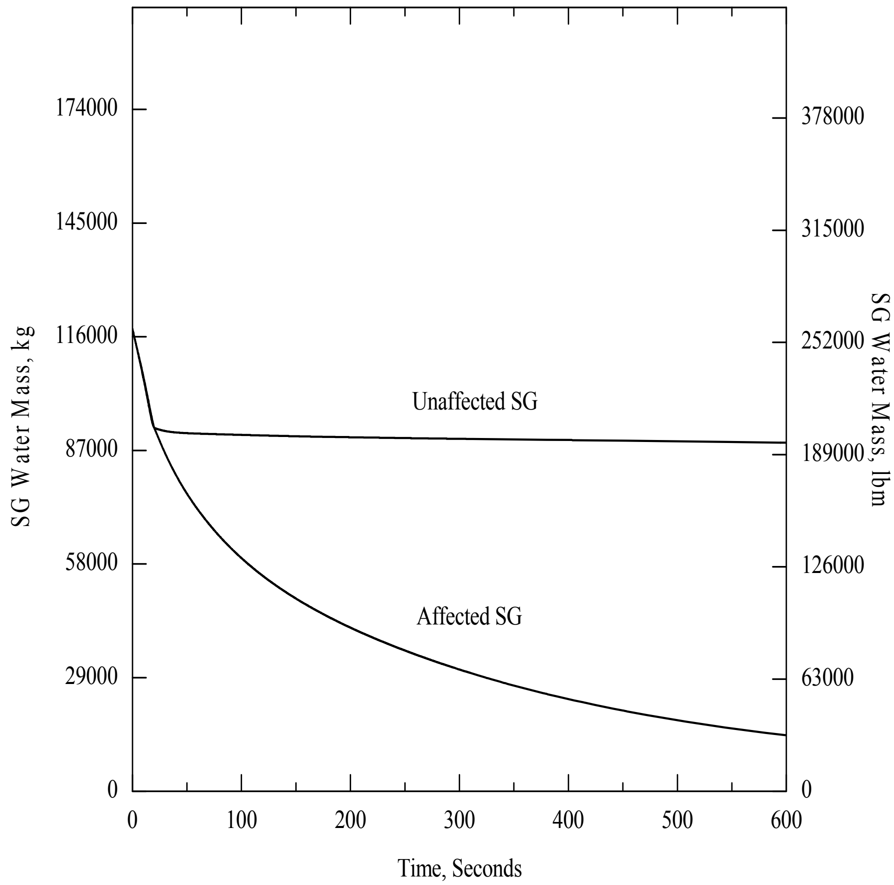

Figure 15.1.5-1.13 Full Power Large Steam Line Break with Concurrent LOOP: Steam Generator Mass Inventories vs. Time

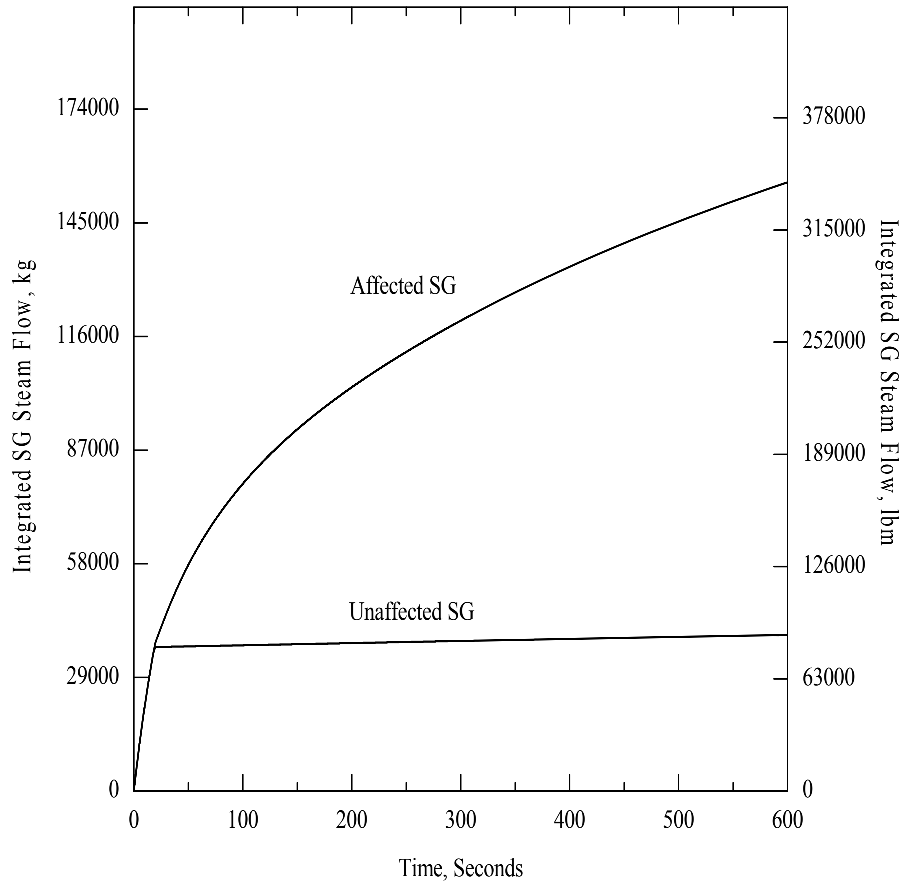

Figure 15.1.5-1.14 Full Power Large Steam Line Break with Concurrent LOOP: Integrated Steam Mass Release Through Break vs. Time

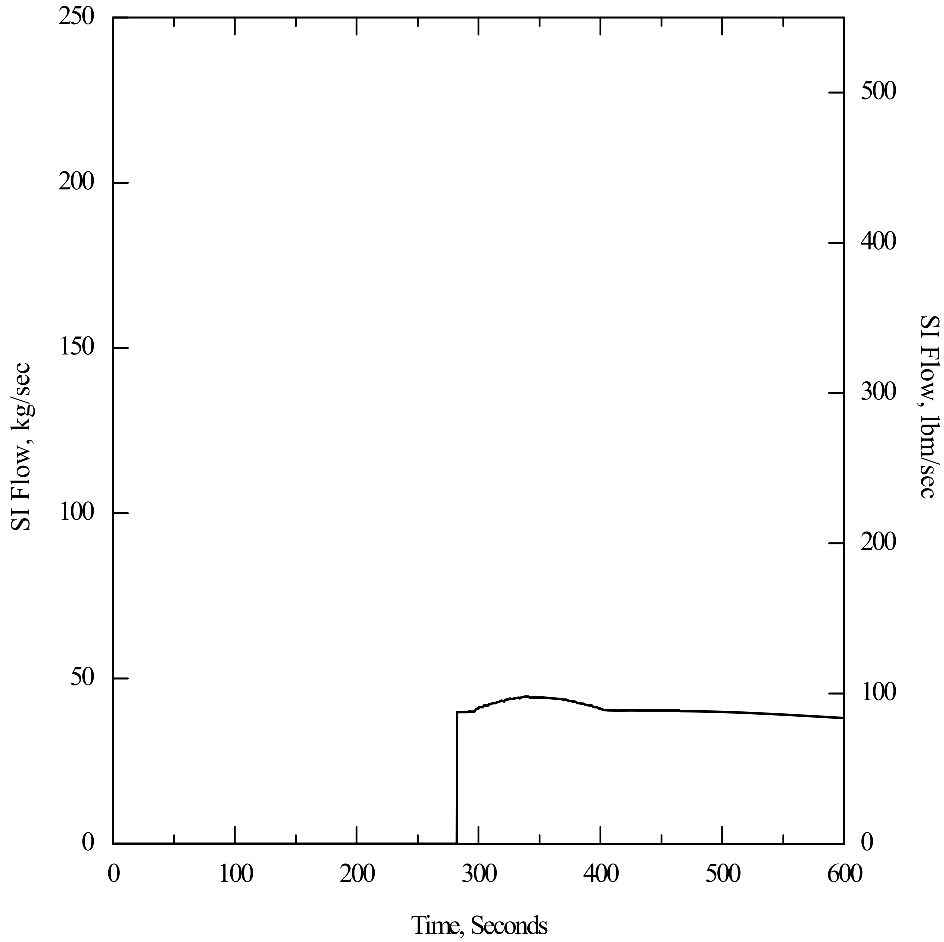

Figure 15.1.5-1.15 Full Power Large Steam Line Break with Concurrent LOOP: Safety Injection Flow Rates vs. Time

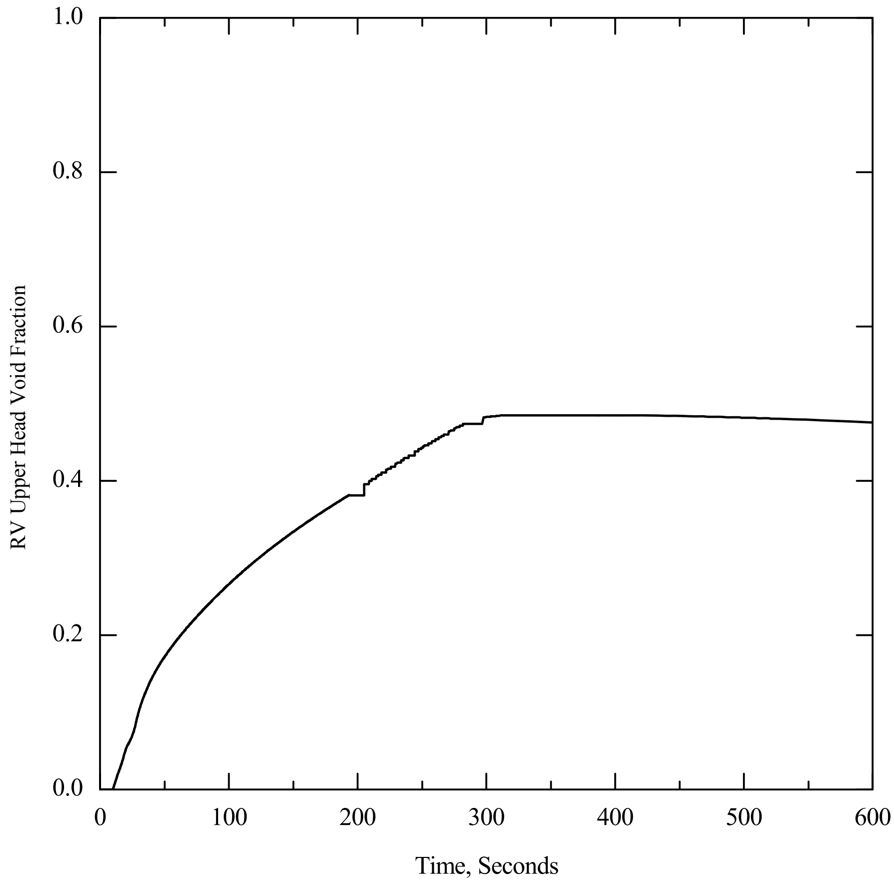

Figure 15.1.5-1.16 Full Power Large Steam Line Break with Concurrent LOOP: RV Upper Head Void Fraction vs. Time

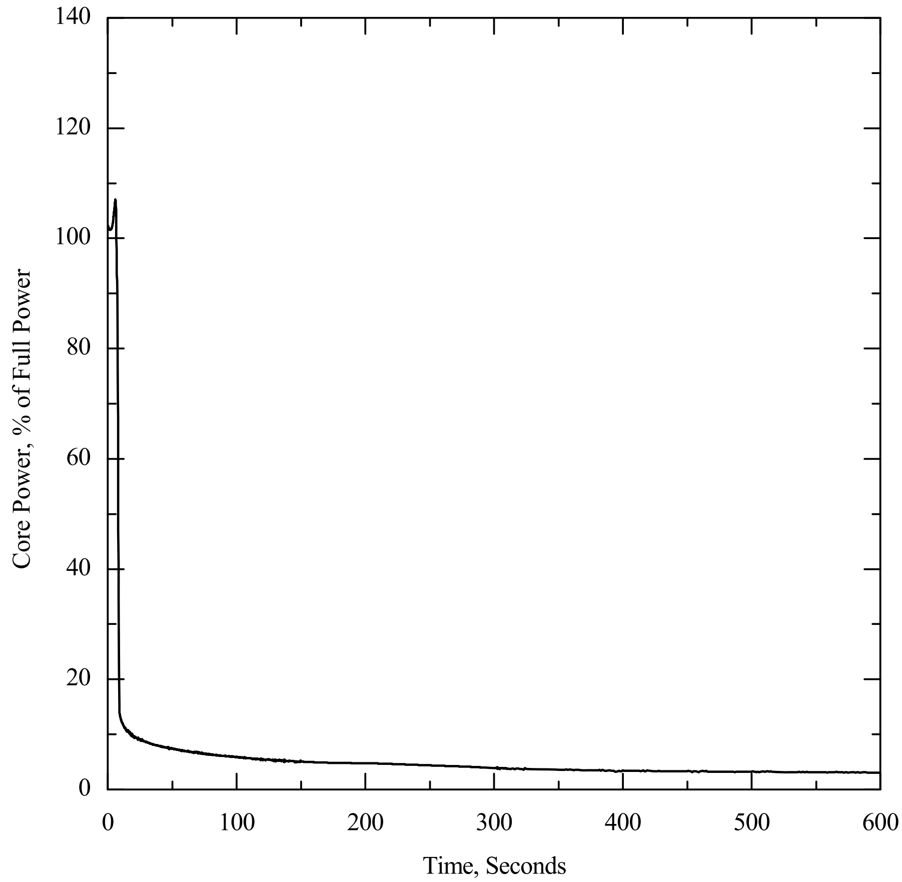

Figure 15.1.5-2.1 Full Power Large Steam Line Break with Offsite Power Available: Core Power vs. Time

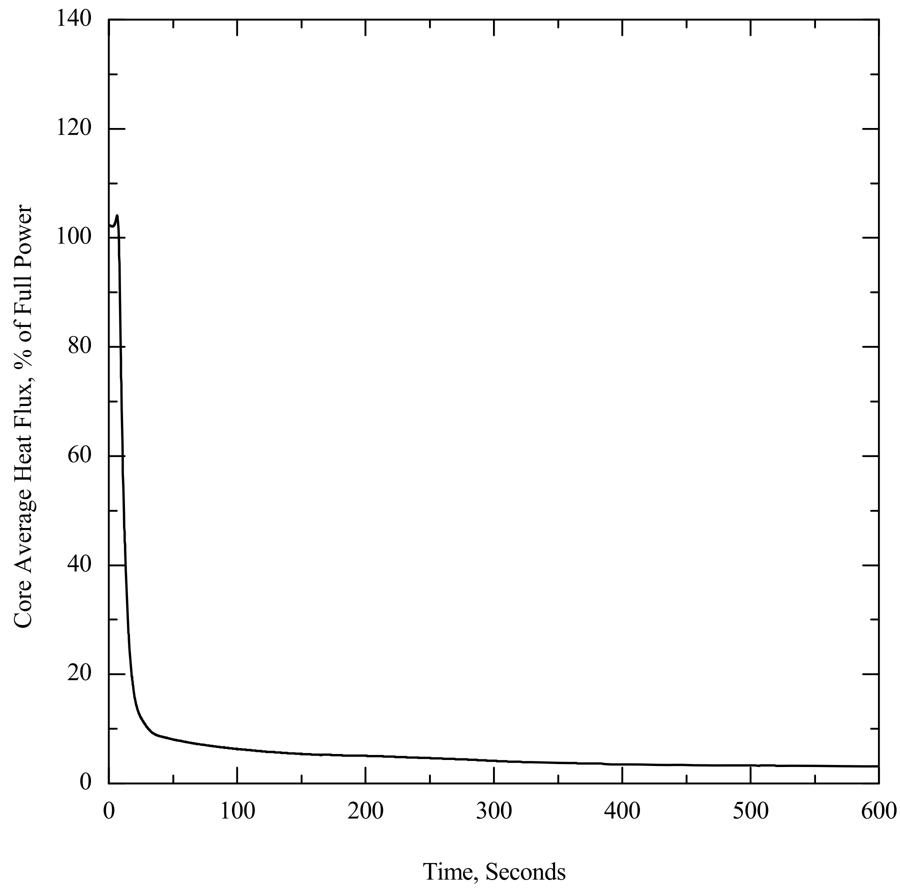

Figure 15.1.5-2.2 Full Power Large Steam Line Break with Offsite Power Available: Core Average Heat Flux vs. Time

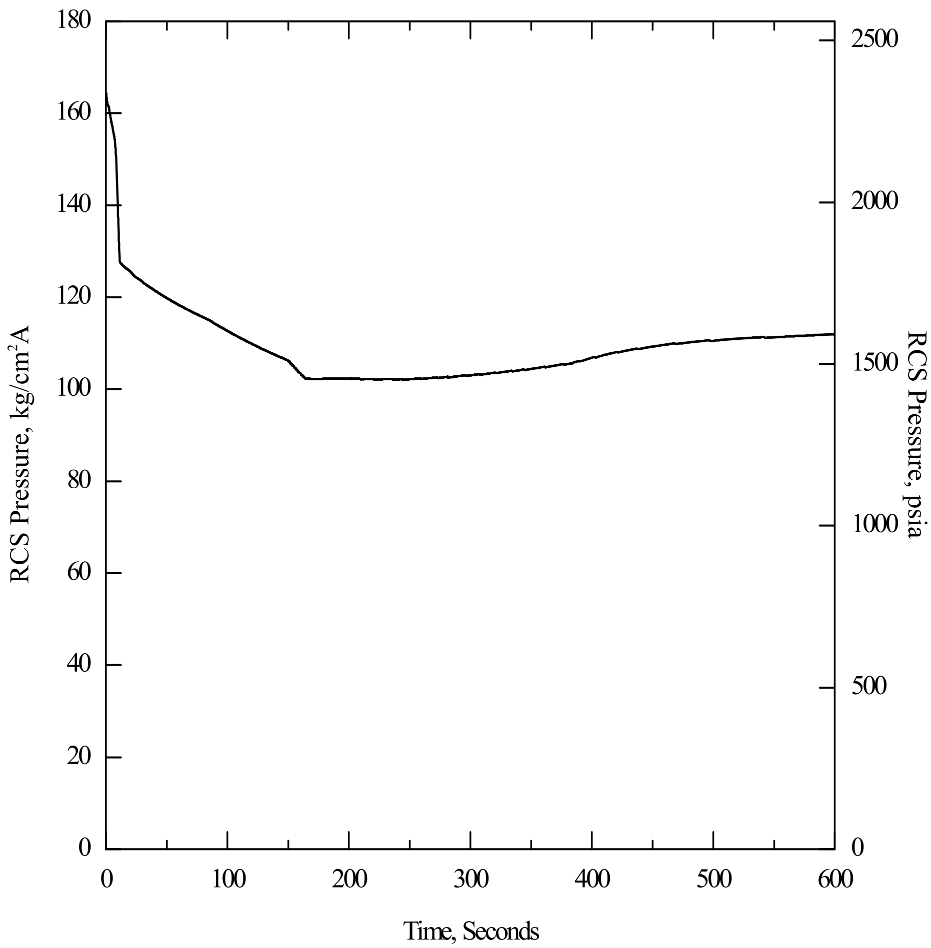

Figure 15.1.5-2.3 Full Power Large Steam Line Break with Offsite Power Available: RCS Pressure vs. Time

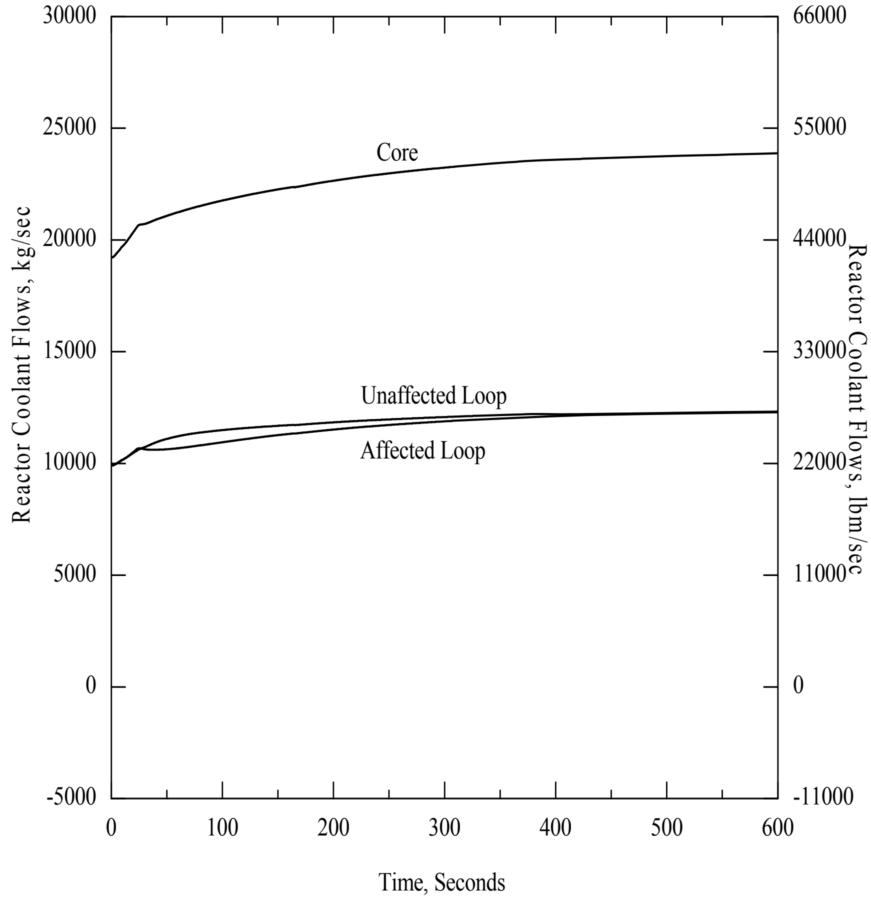

Figure 15.1.5-2.4 Full Power Large Steam Line Break with Offsite Power Available: Reactor Coolant Flow Rates vs. Time

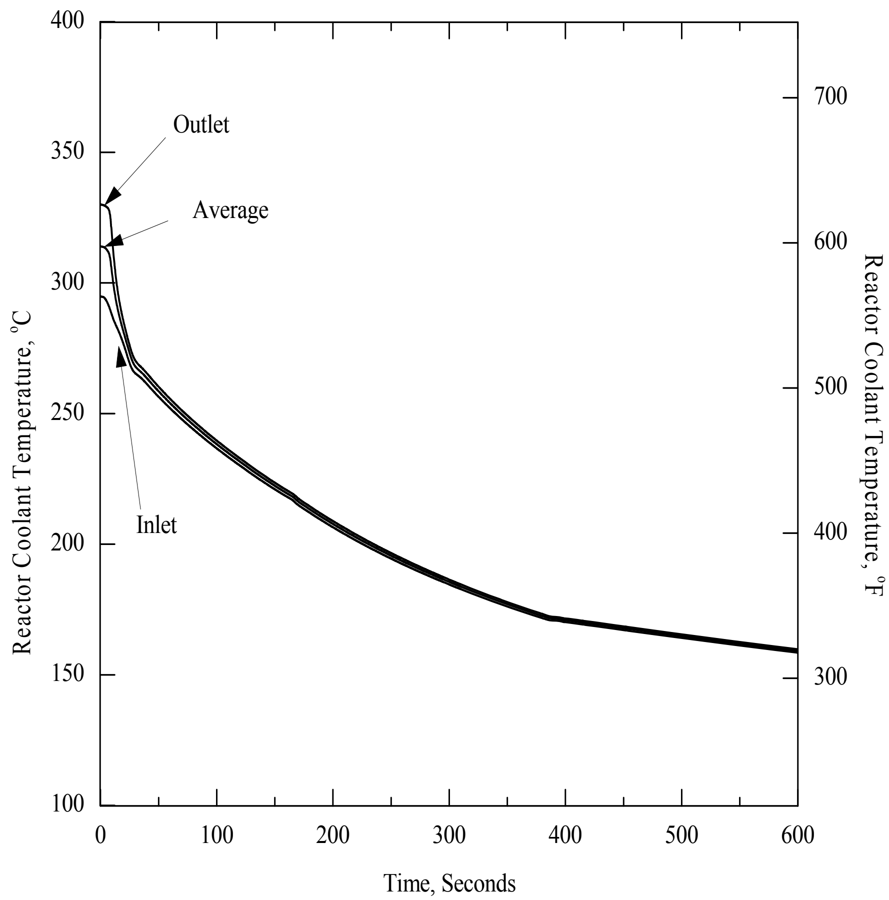

Figure 15.1.5-2.5 Full Power Large Steam Line Break with Offsite Power Available: Reactor Coolant Temperature (A) vs. Time

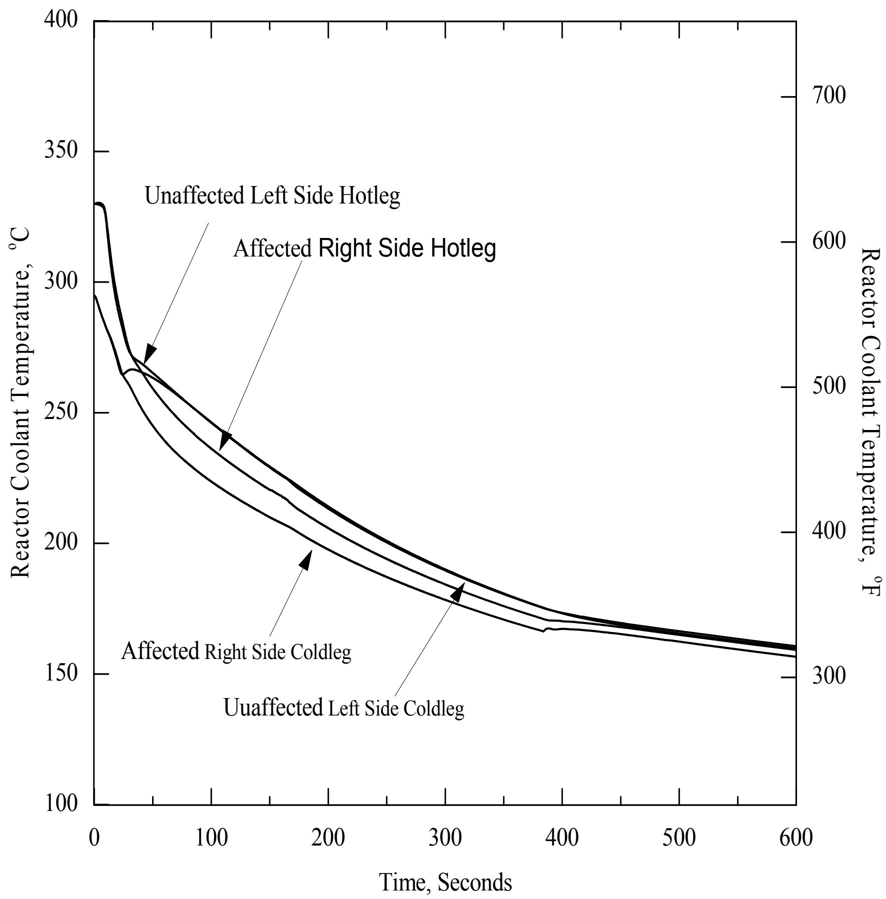

Figure 15.1.5-2.6 Full Power Large Steam Line Break with Offsite Power Available: Reactor Coolant Temperature (B) vs. Time

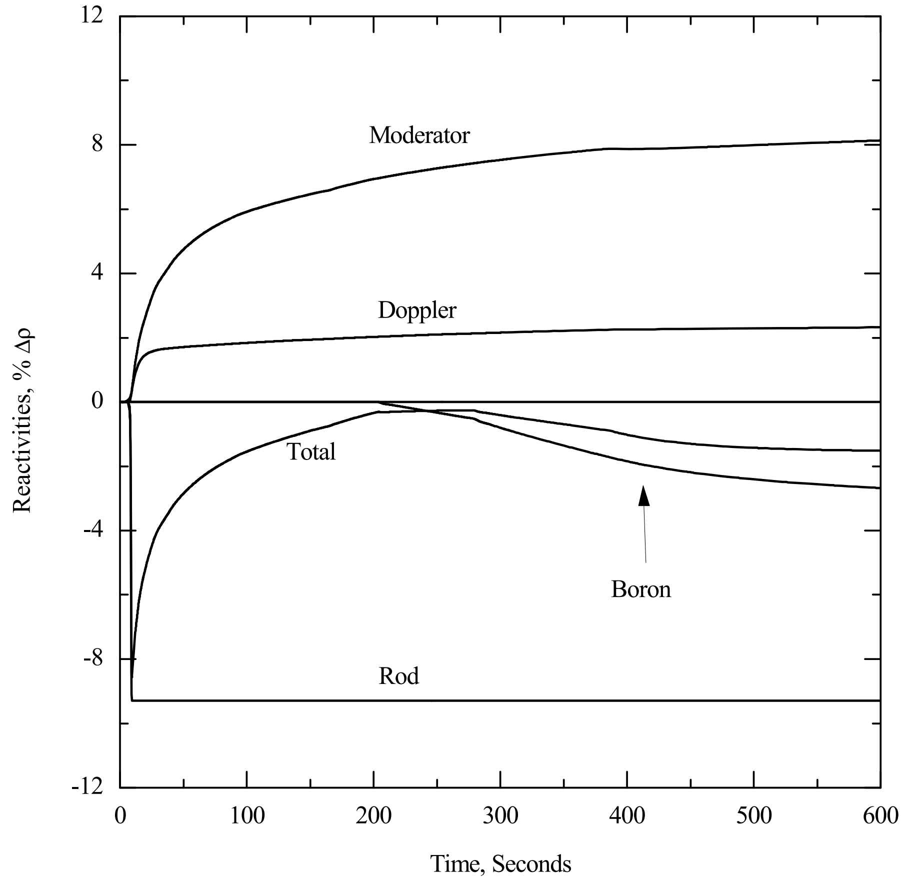

Figure 15.1.5-2.7 Full Power Large Steam Line Break with Offsite Power Available: Reactivity vs. Time

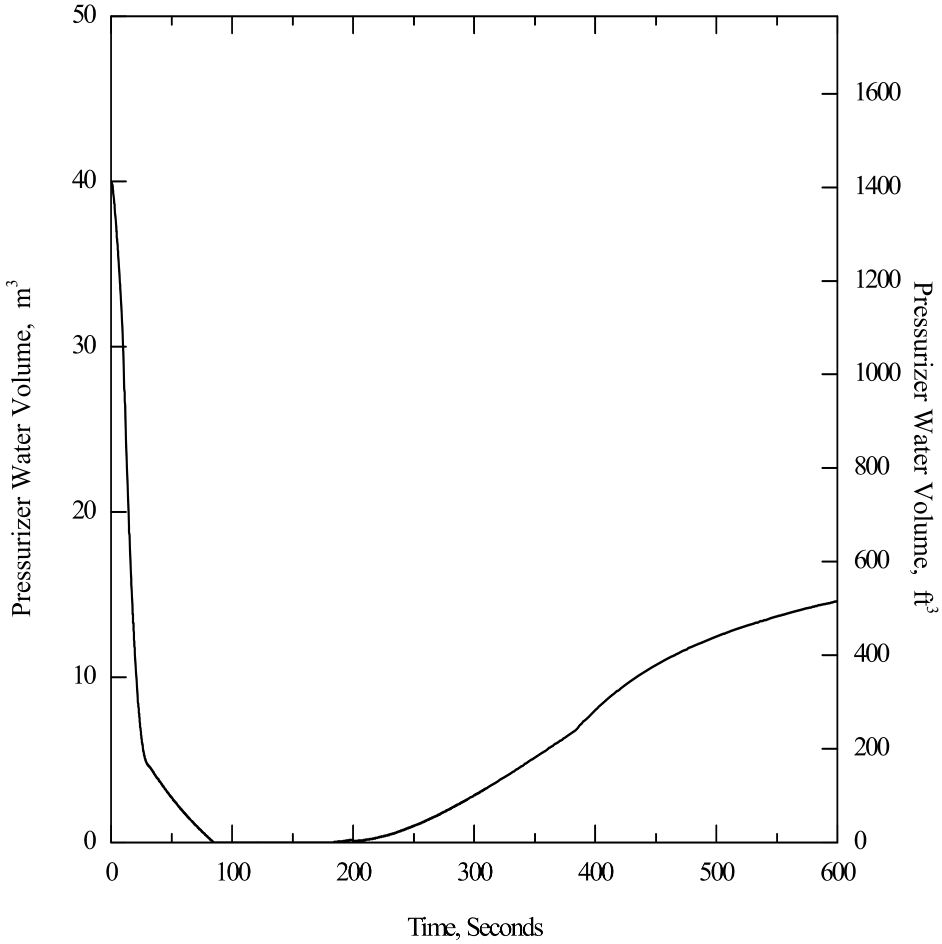

Figure 15.1.5-2.8 Full Power Large Steam Line Break with Offsite Power Available : Pressurizer Water Volume vs. Time

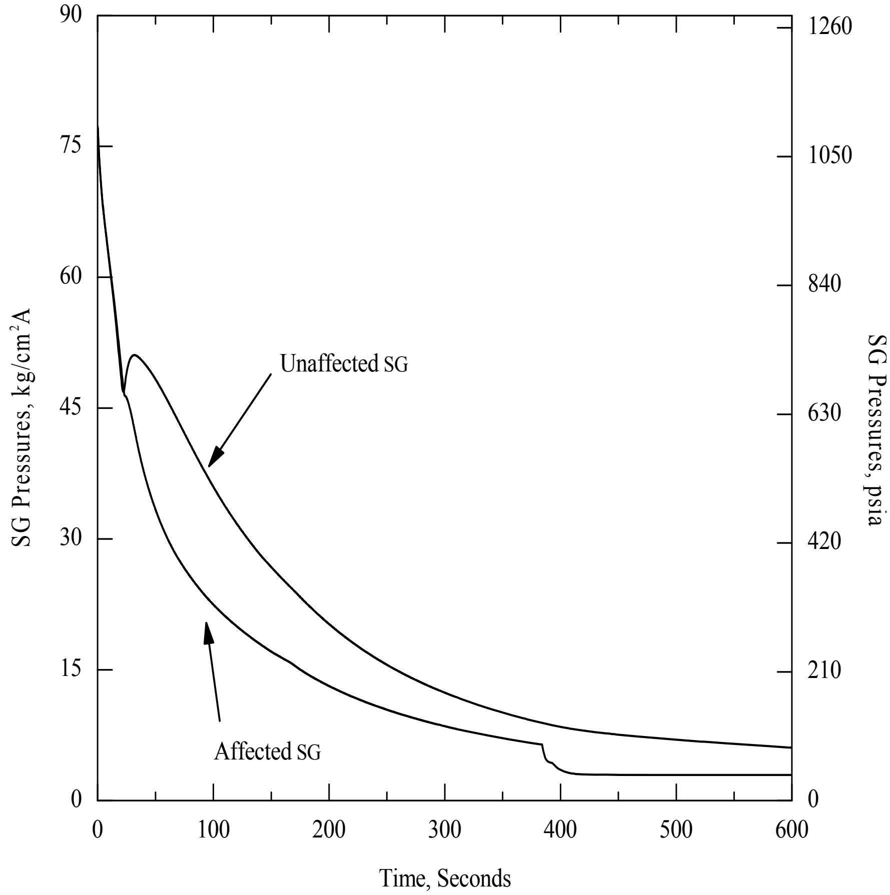

Figure 15.1.5-2.9 Full Power Large Steam Line Break with Offsite Power Available : Steam Generator Pressure vs. Time

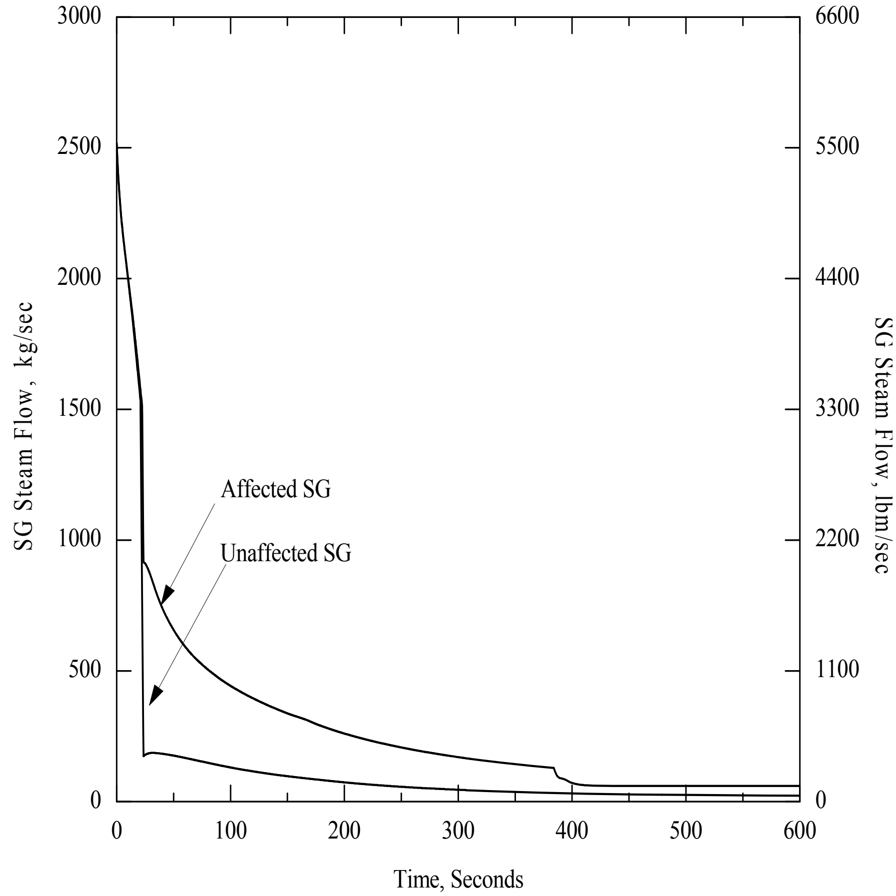

Figure 15.1.5-2.10 Full Power Large Steam Line Break with Offsite Power Available : Steam Generator Steam Flow Rates vs. Time

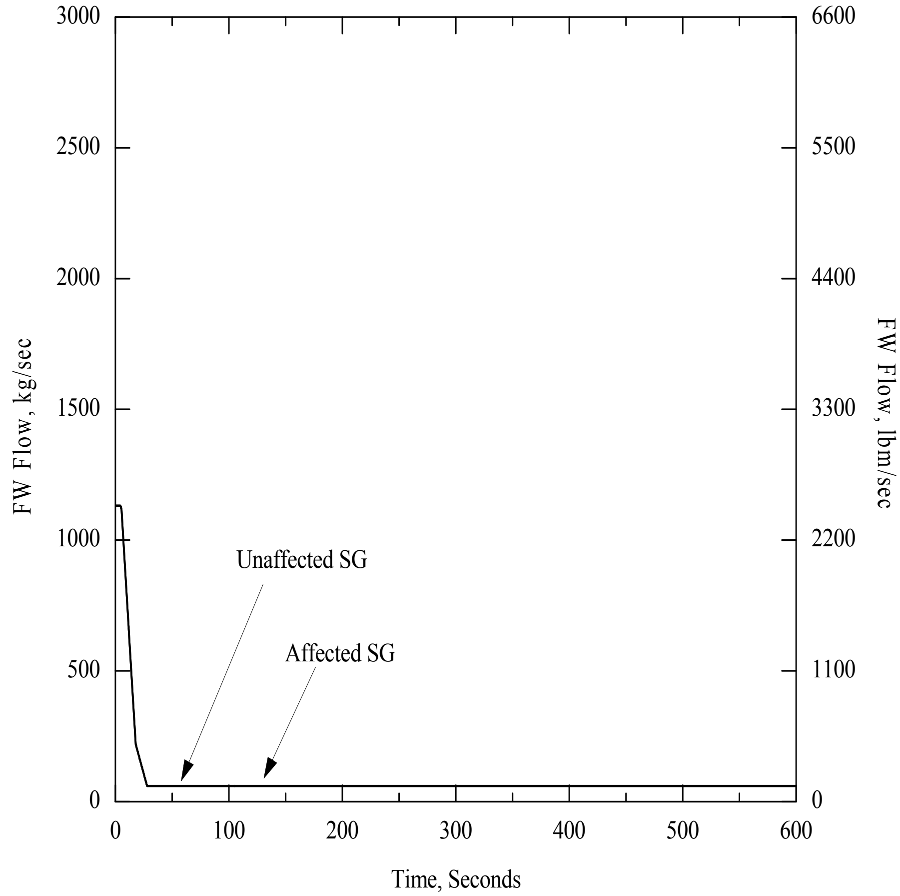

Figure 15.1.5-2.11 Full Power Large Steam Line Break with Offsite Power Available : Feedwater Flow Rates vs. Time

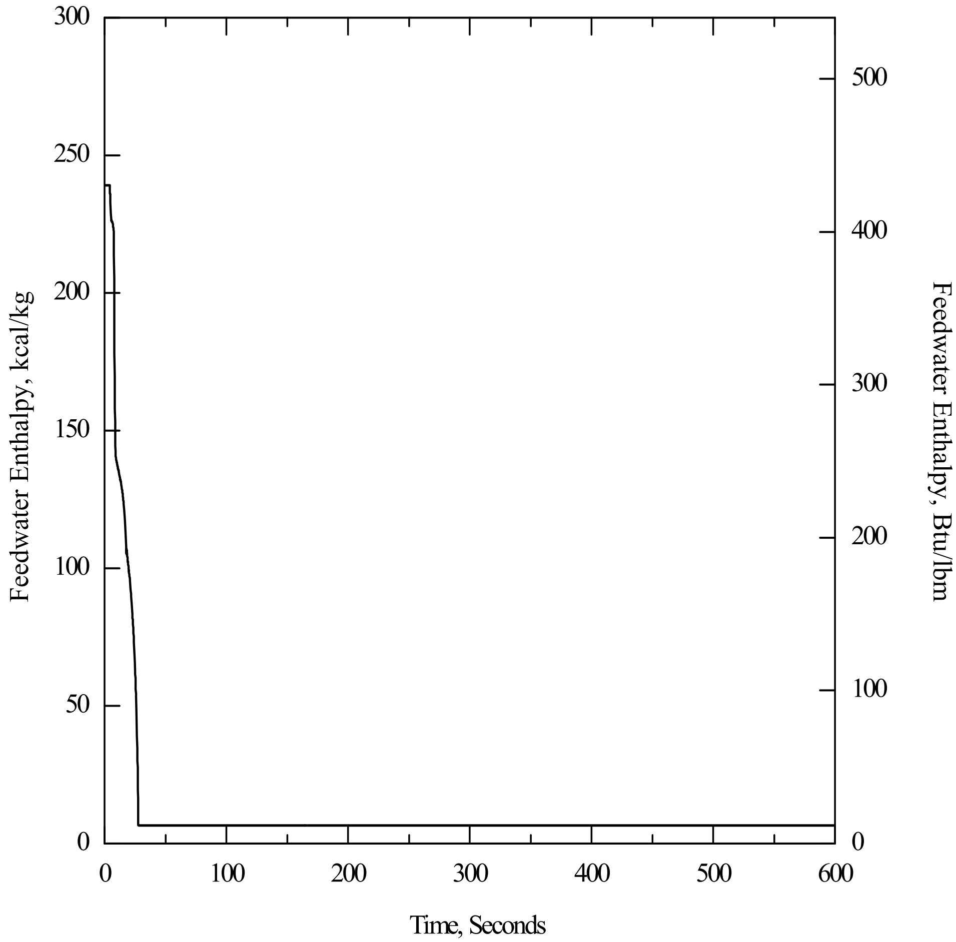

Figure 15.1.5-2.12 Full Power Large Steam Line Break with Offsite Power Available : Feedwater Enthalpy vs. Time

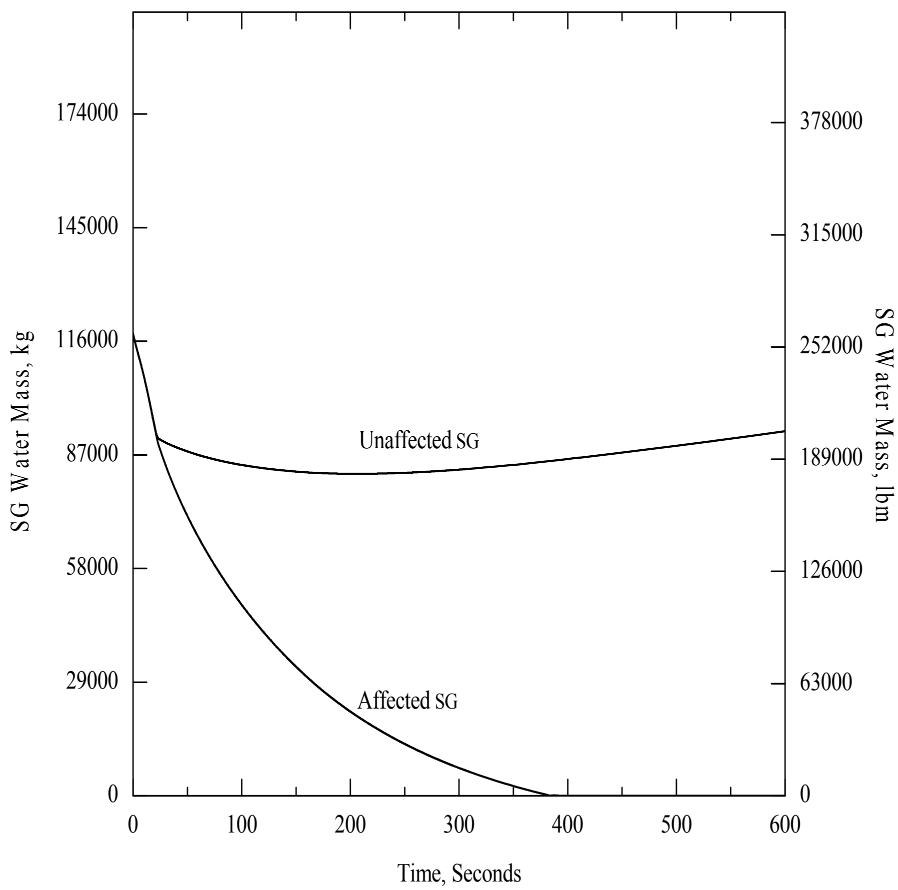

Figure 15.1.5-2.13 Full Power Large Steam Line Break with Offsite Power Available : Steam Generator Mass Inventories vs. Time

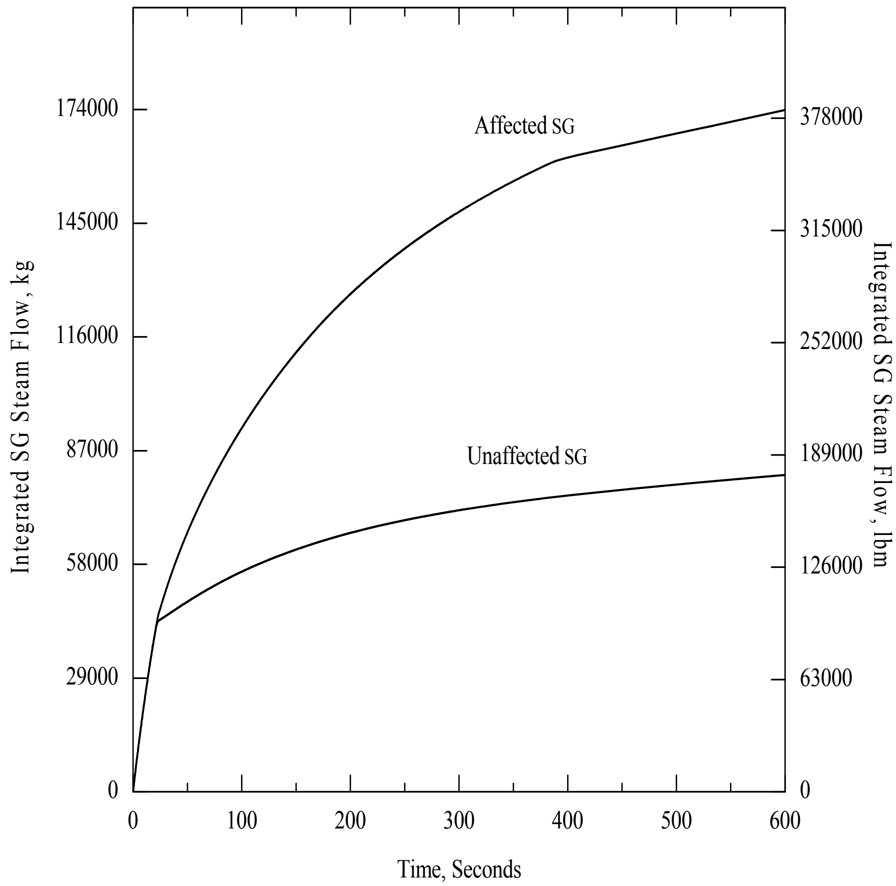

Figure 15.1.5-2.14 Full Power Large Steam Line Break with Offsite Power Available : Integrated Steam Mass Release Through Break vs. Time

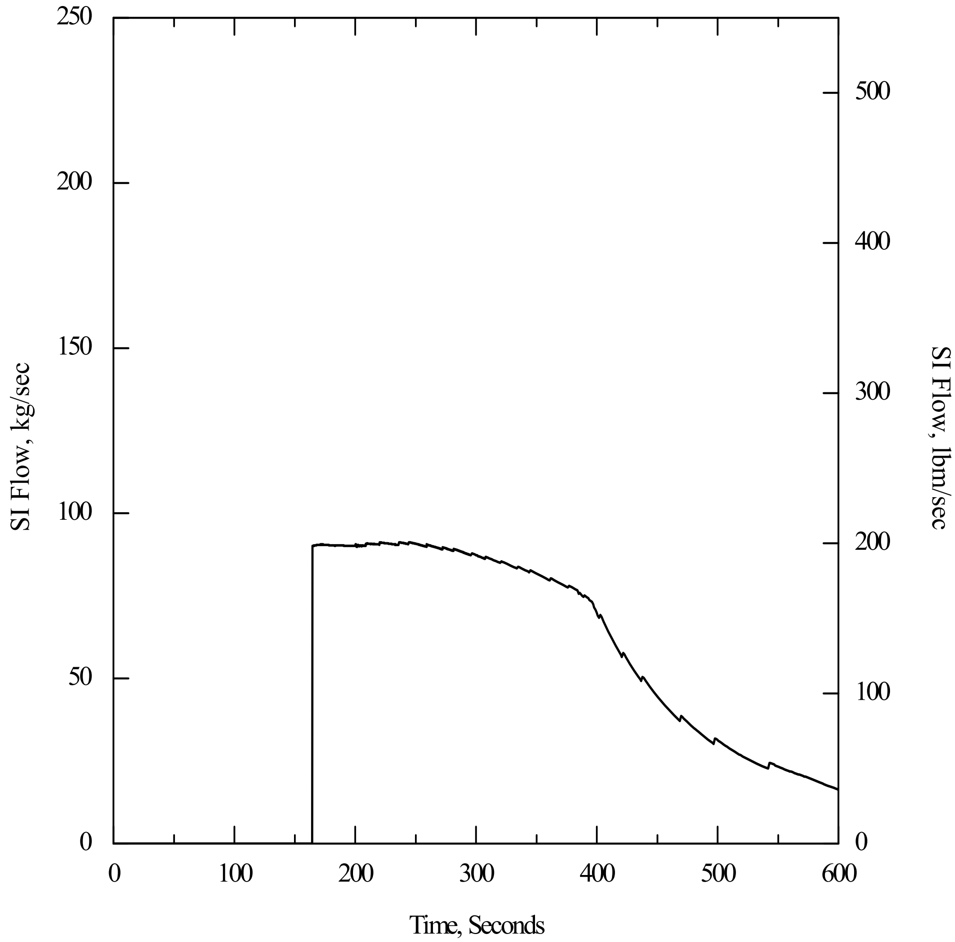

Figure 15.1.5-2.15 Full Power Large Steam Line Break with Offsite Power Available: Safety Injection Flow Rates vs. Time

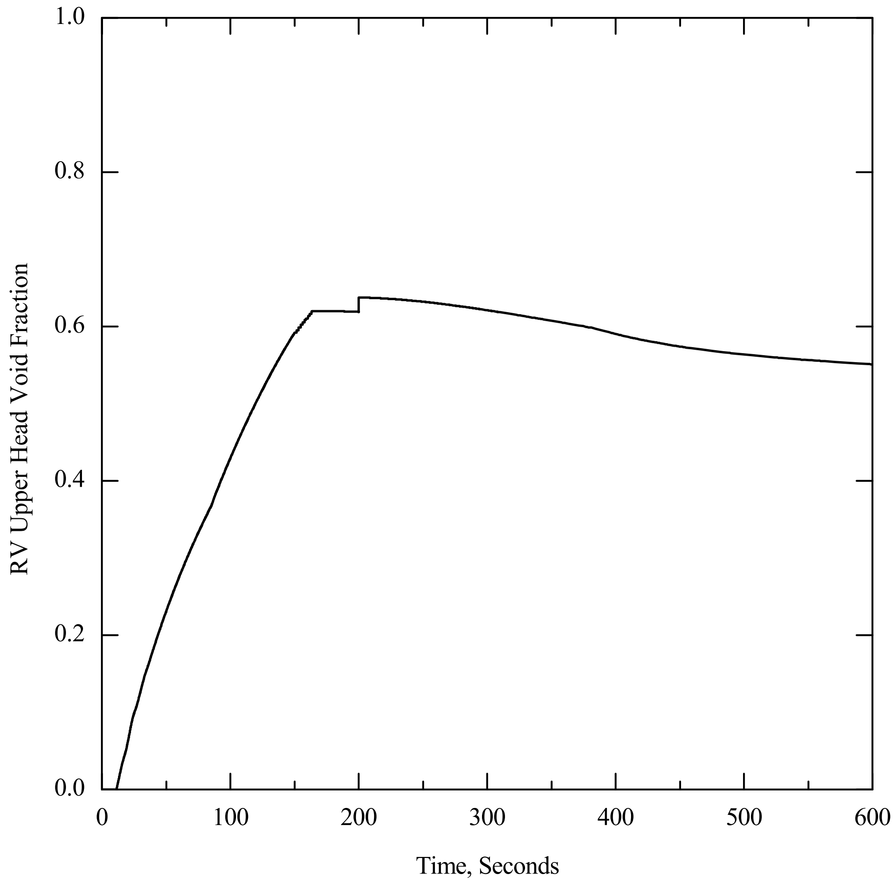

Figure 15.1.5-2.16 Full Power Large Steam Line Break with Offsite Power Available: RV Upper Head Void Fraction vs. Time

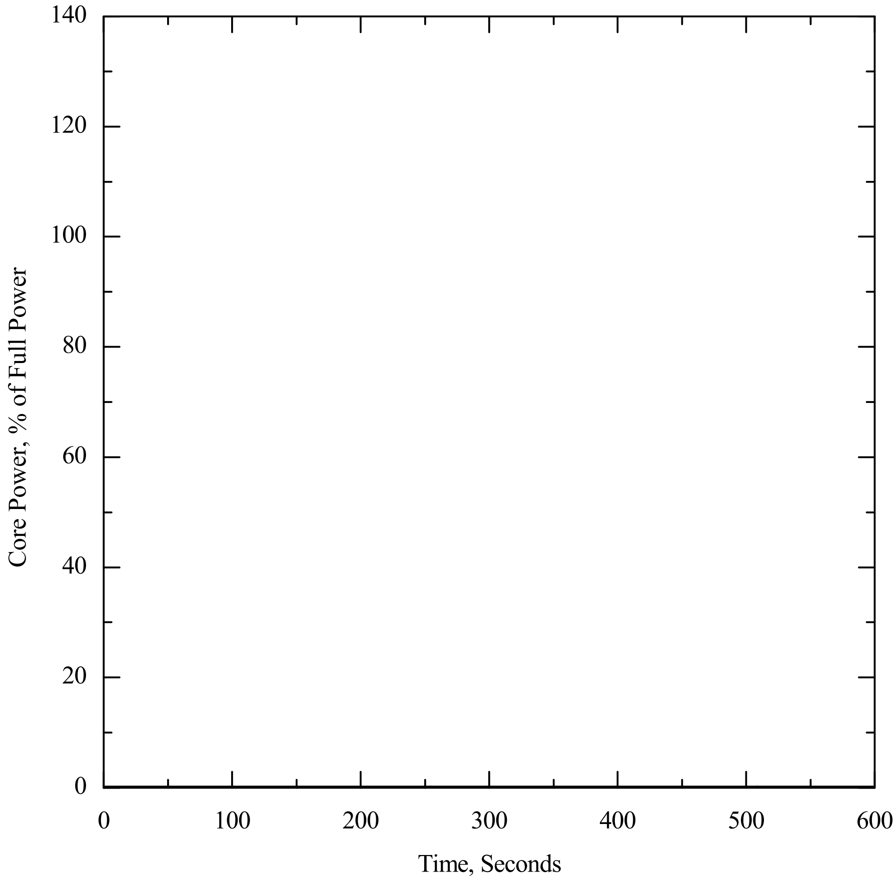

Figure 15.1.5-3.1 Zero Power Large Steam Line Break with Concurrent LOOP:Core Power vs. Time

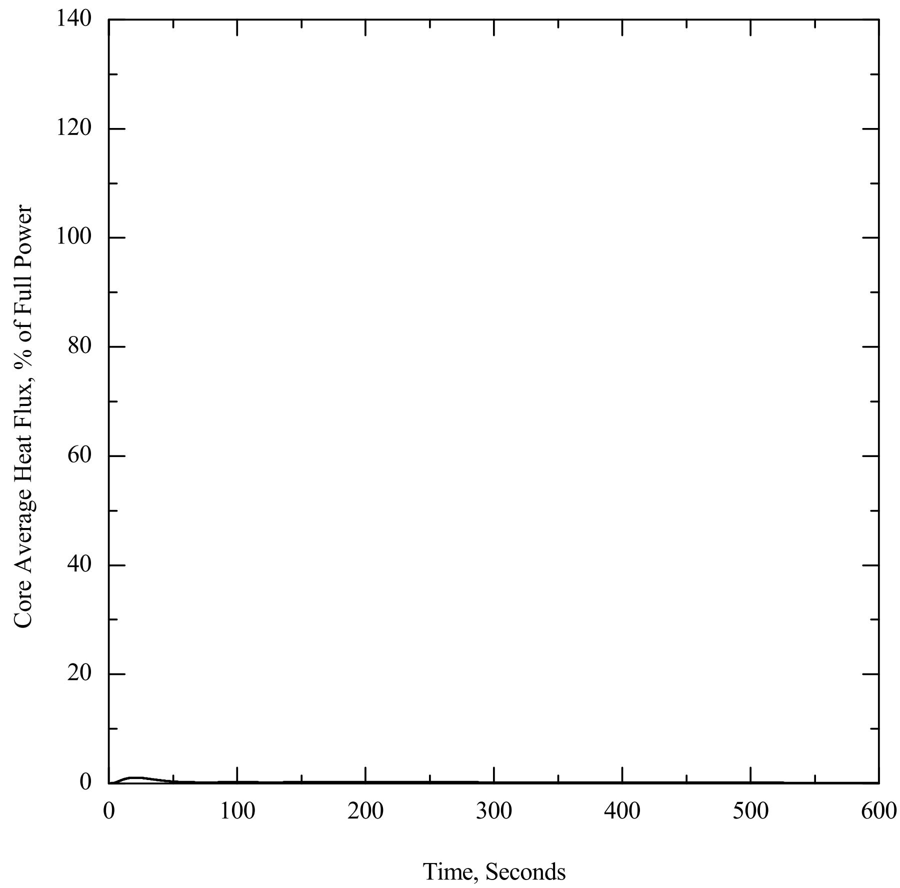

Figure 15.1.5-3.2 Zero Power Large Steam Line Break with Concurrent LOOP: Core Average Heat Flux vs. Time

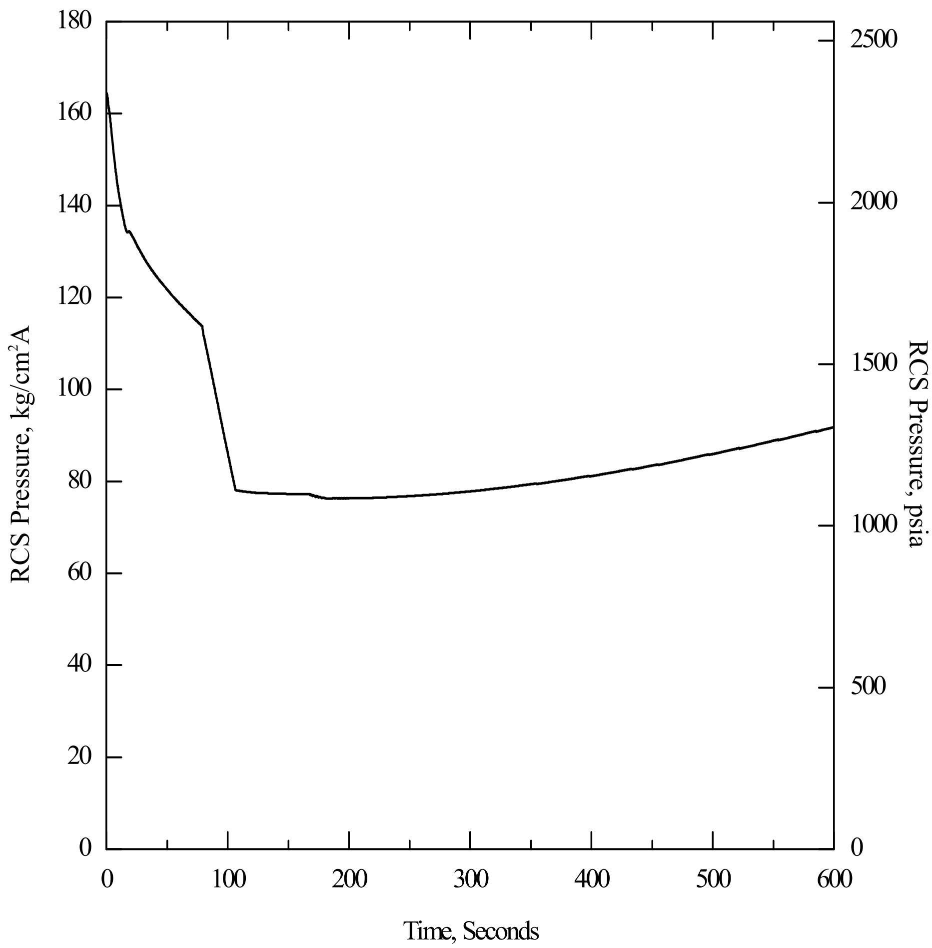

Figure 15.1.5-3.3 Zero Power Large Steam Line Break with Concurrent LOOP : RCS Pressure vs. Time

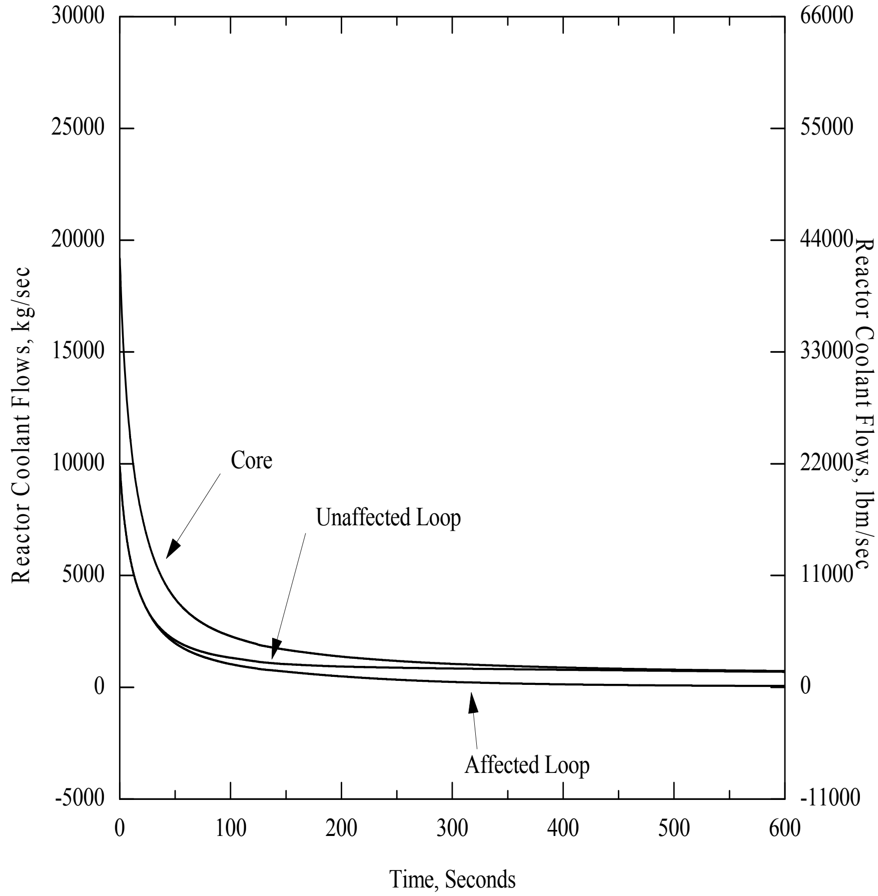

Figure 15.1.5-3.4 Zero Power Large Steam Line Break with Concurrent LOOP: Reactor Coolant Flow Rates vs. Time

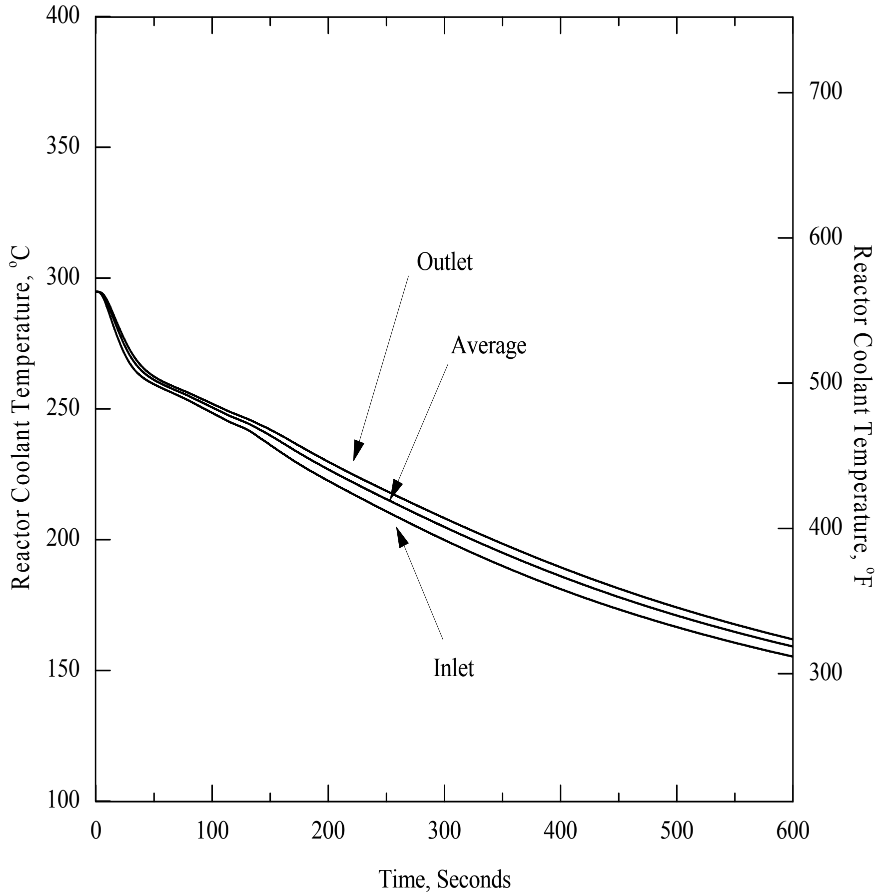

Figure 15.1.5-3.5 Zero Power Large Steam Line Break with Concurrent LOOP: Reactor Coolant Temperature (A) vs. Time

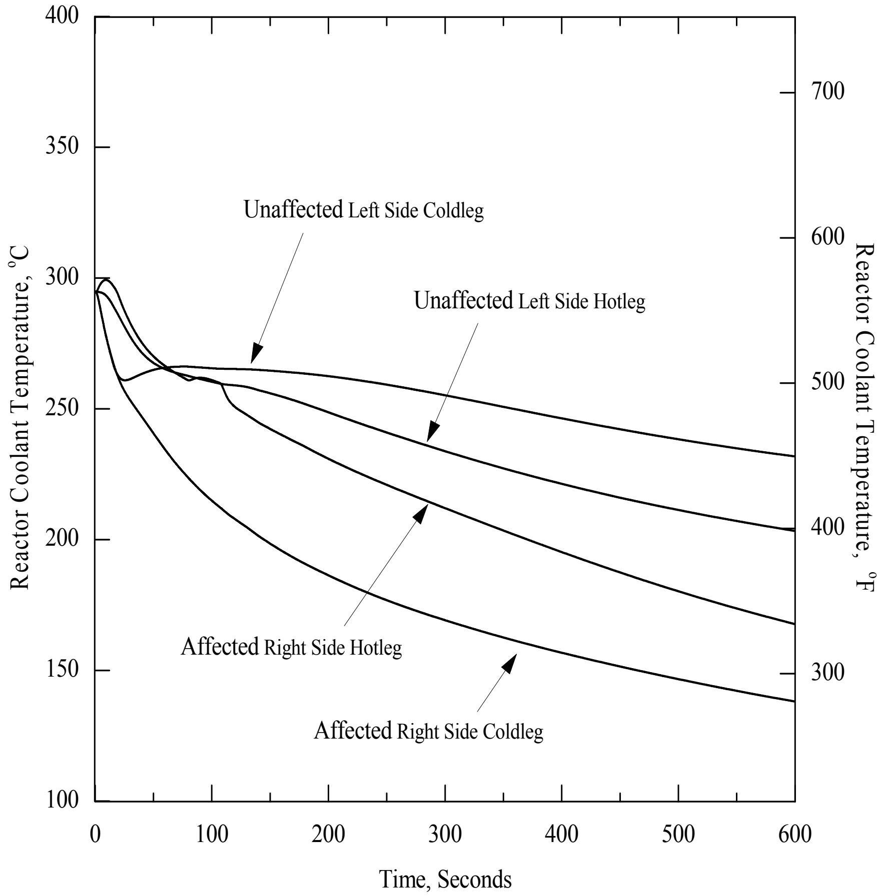

Figure 15.1.5-3.6 Zero Power Large Steam Line Break with Concurrent LOOP: Reactor Coolant Temperature (B) vs. Time

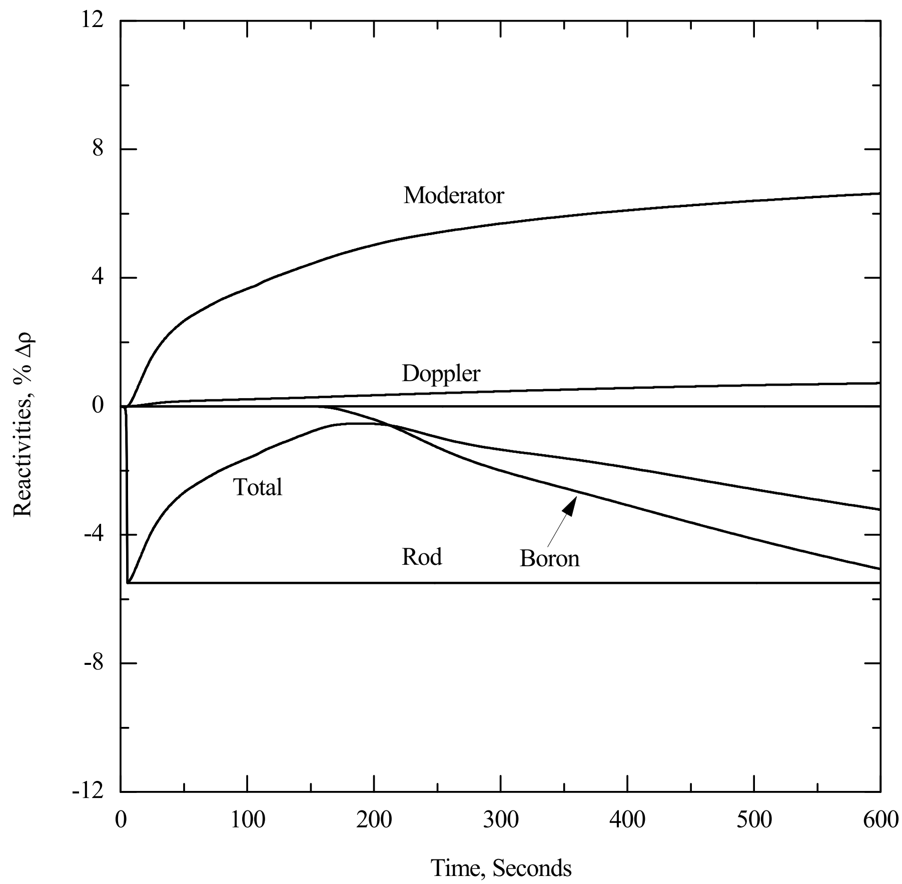

Figure 15.1.5-3.7 Zero Power Large Steam Line Break with Concurrent LOOP : Reactivity vs. Time

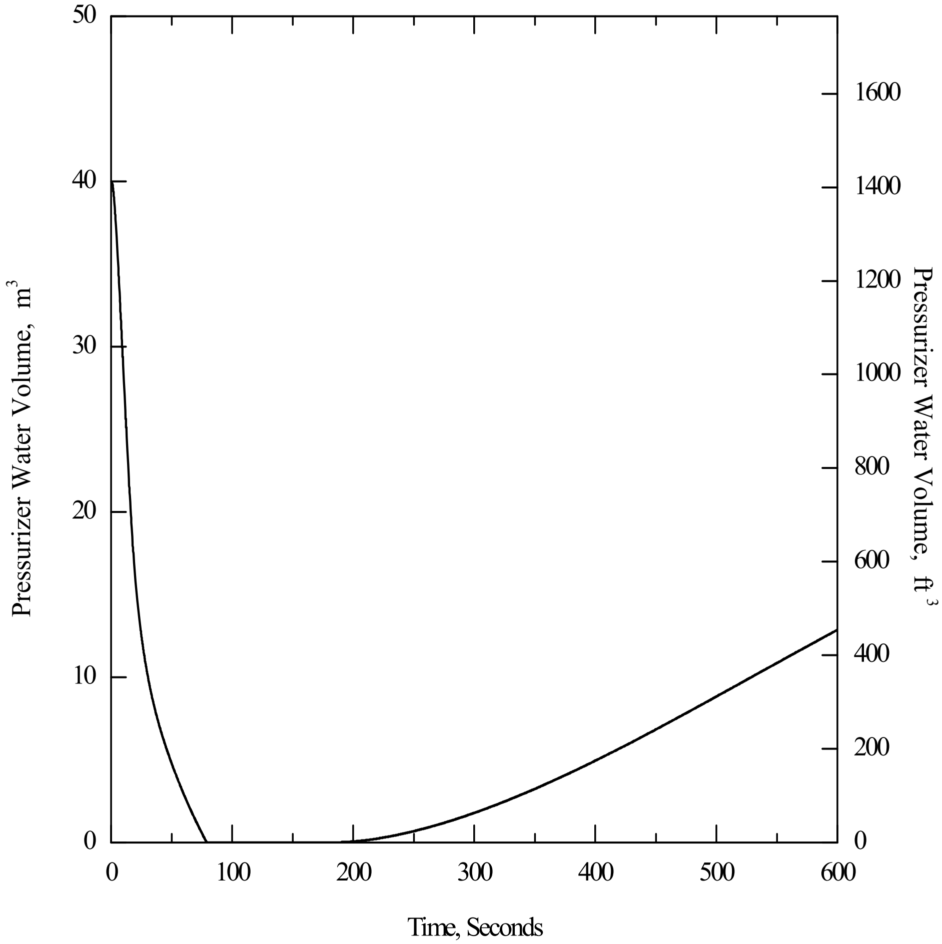

Figure 15.1.5-3.8 Zero Power Large Steam Line Break with Concurrent LOOP: Pressurizer Water Volume vs. Time

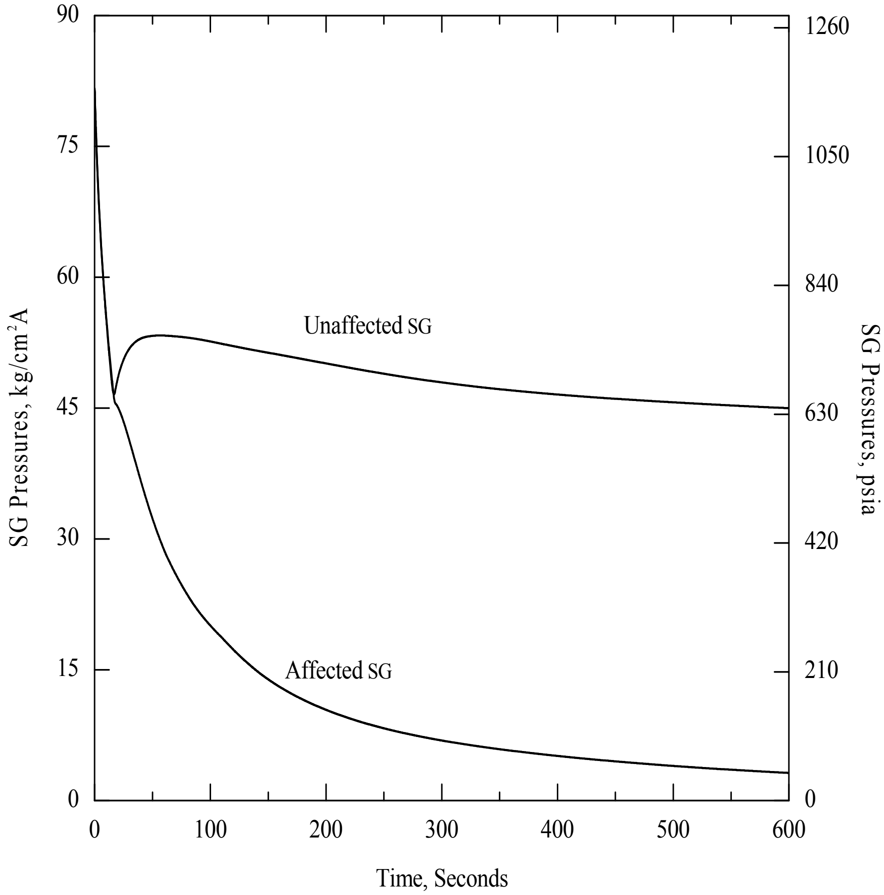

Figure 15.1.5-3.9 Zero Power Large Steam Line Break with Concurrent LOOP: Steam Generator Pressure vs. Time

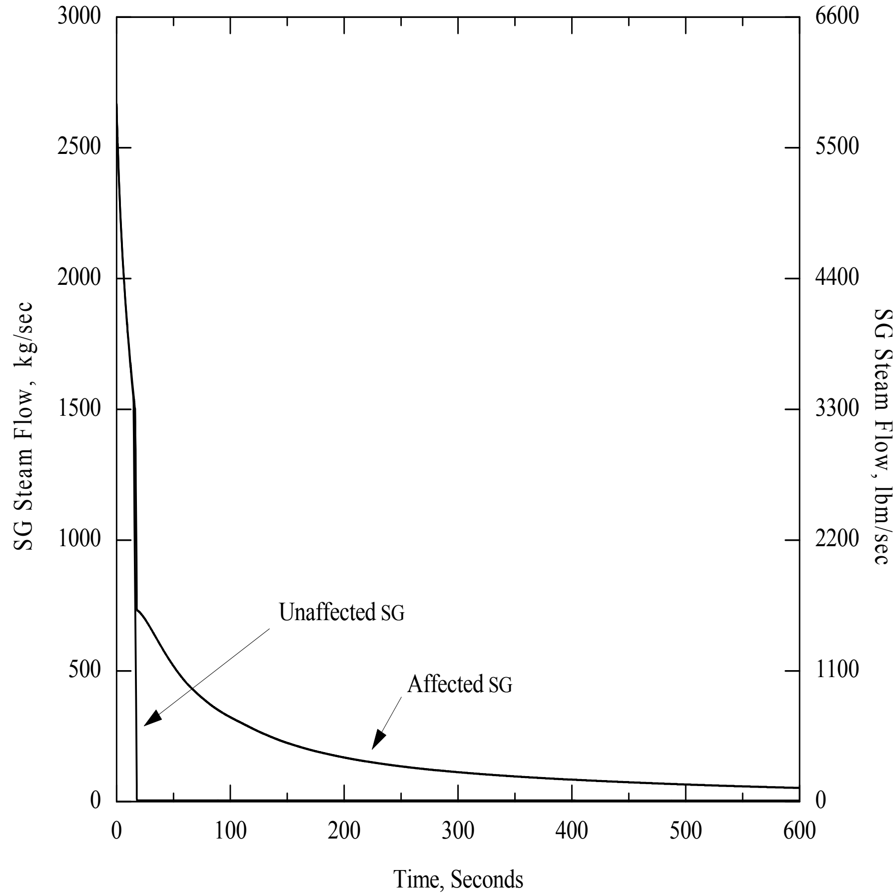

Figure 15.1.5-3.10 Zero Power Large Steam Line Break with Concurrent LOOP: Steam Generator Flow Rates vs. Time

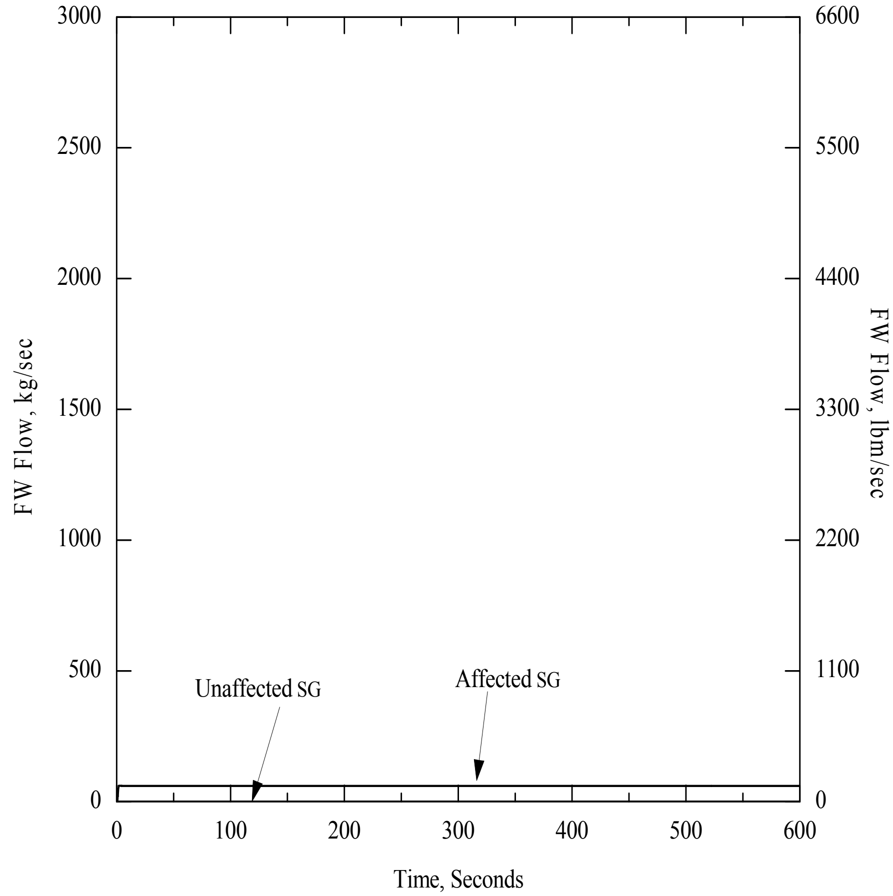

Figure 15.1.5-3.11 Zero Power Large Steam Line Break with Concurrent LOOP: Feedwater Flow Rates vs. Time

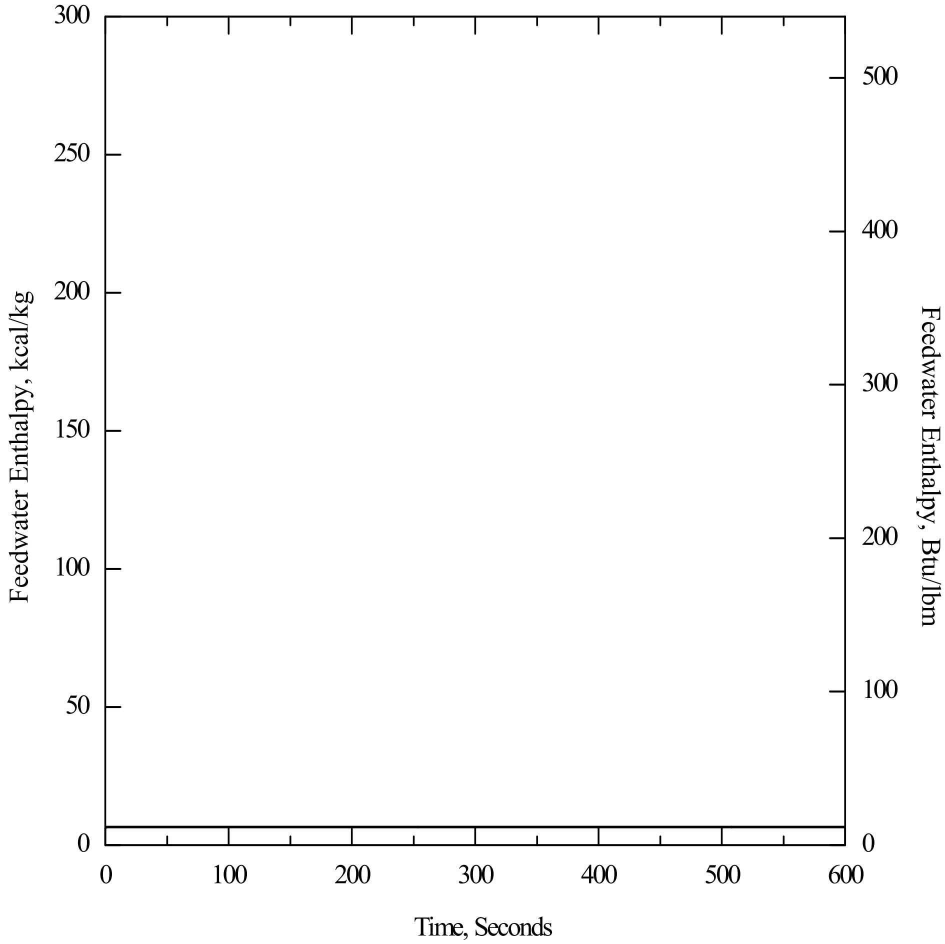

Figure 15.1.5-3.12 Zero Power Large Steam Line Break with Concurrent LOOP: Feedwater Enthalpy vs. Time

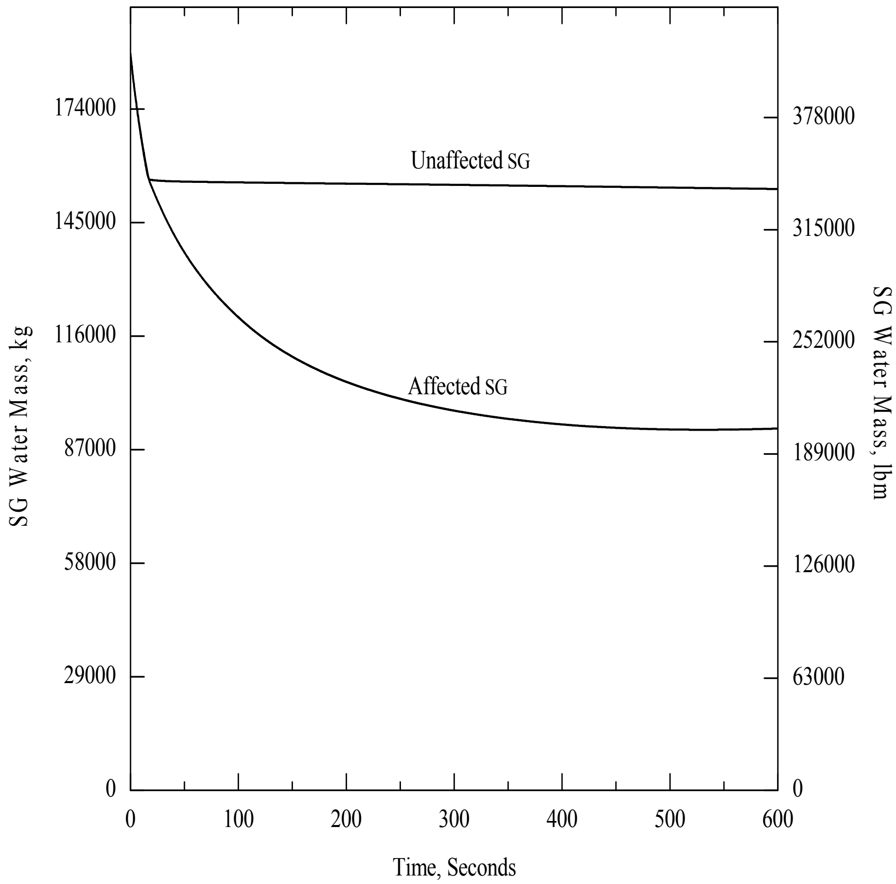

Figure 15.1.5-3.13 Zero Power Large Steam Line Break with Concurrent LOOP: Steam Generator Mass Inventories vs. Time

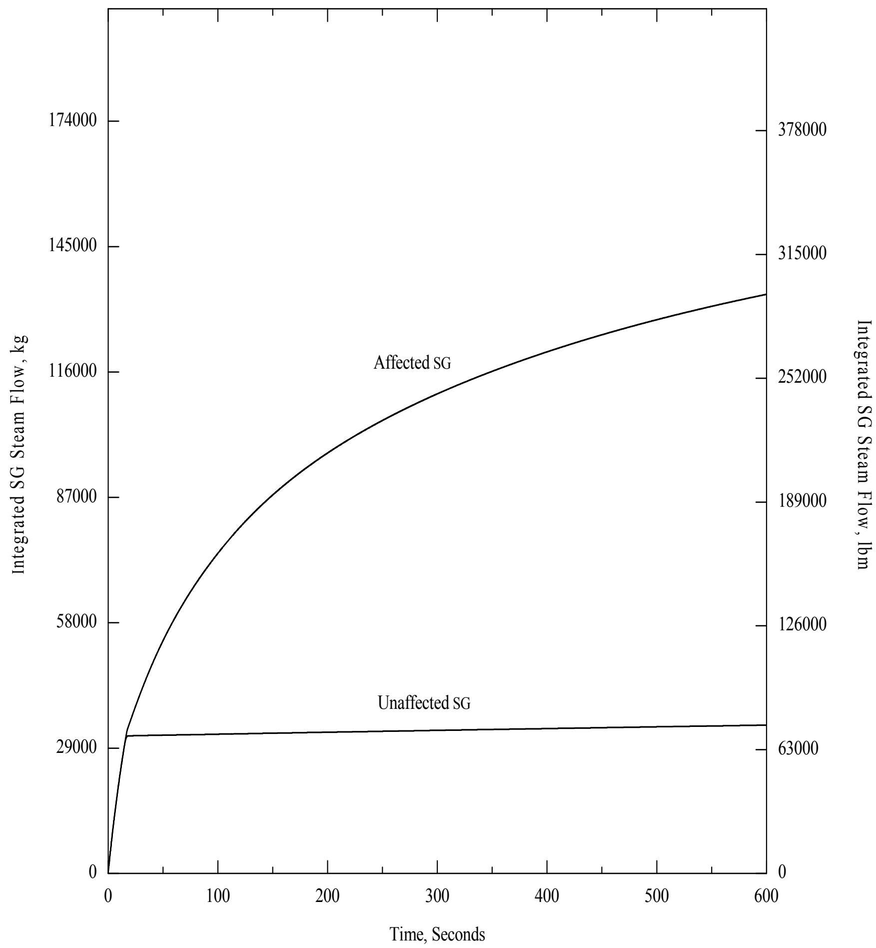

Figure 15.1.5-3.14 Zero Power Large Steam Line Break with Concurrent LOOP : Integrated Steam Release Through Break vs. Time

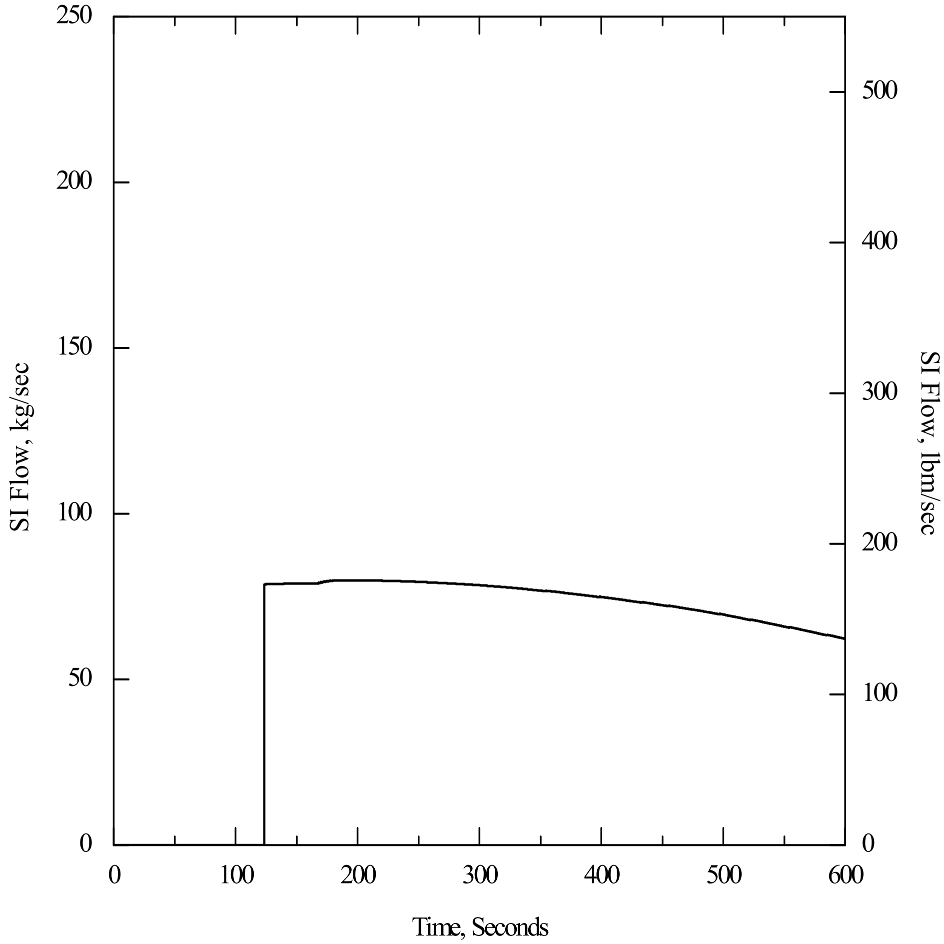

Figure 15.1.5-3.15 Zero Power Large Steam Line Break with Concurrent LOOP: Safety Injection Flow Rate vs. Time

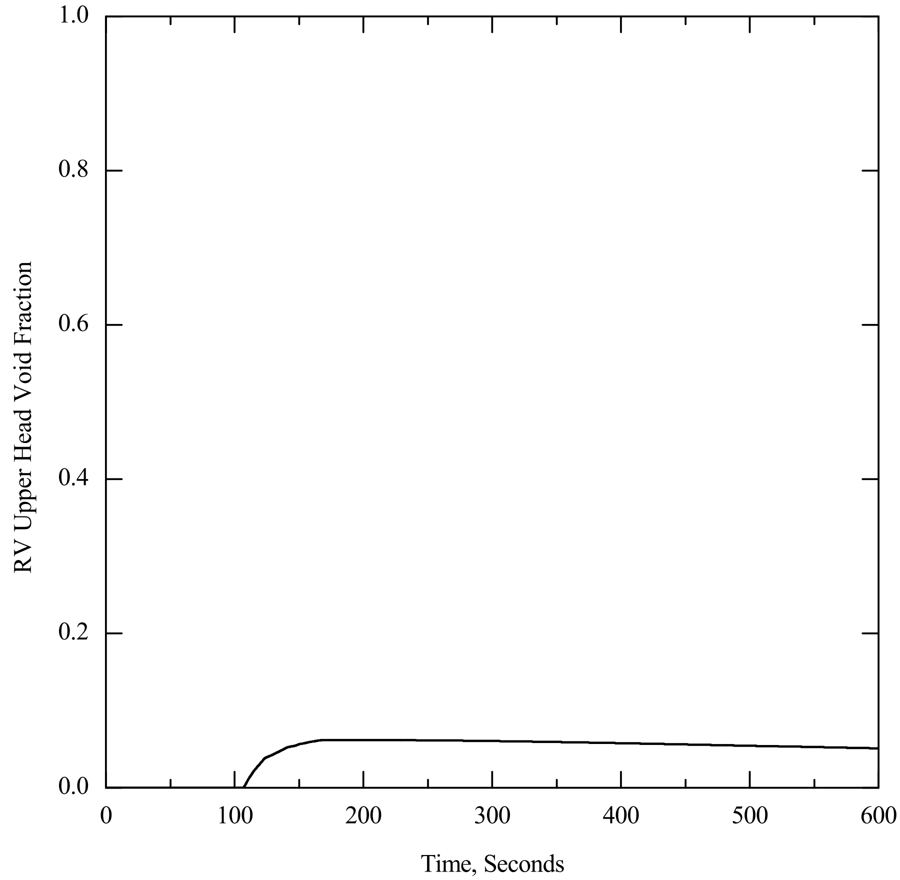

Figure 15.1.5-3.16 Zero Power Large Steam Line Break with Concurrent LOOP: RV Upper Head Void Fraction vs. Time

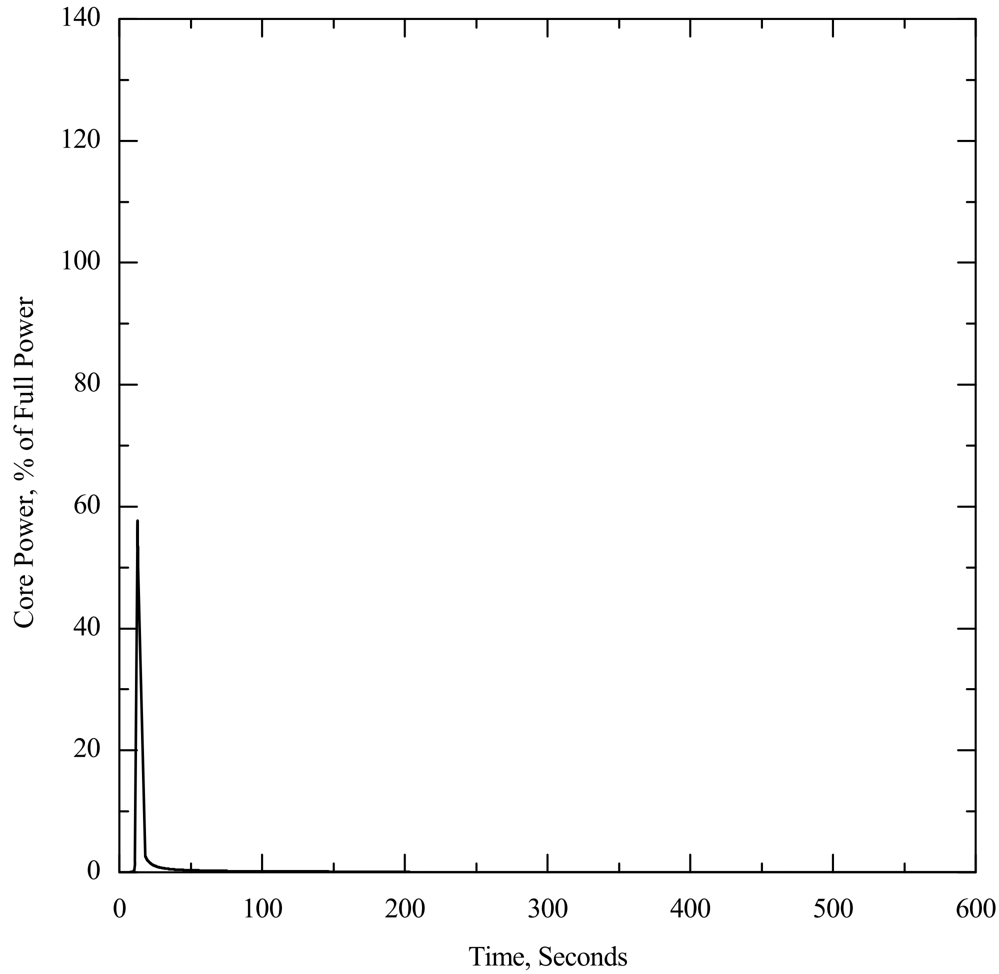

Figure 15.1.5-4.1 Zero Power Large Steam Line Break with Offsite Power Available: Core Power vs. Time

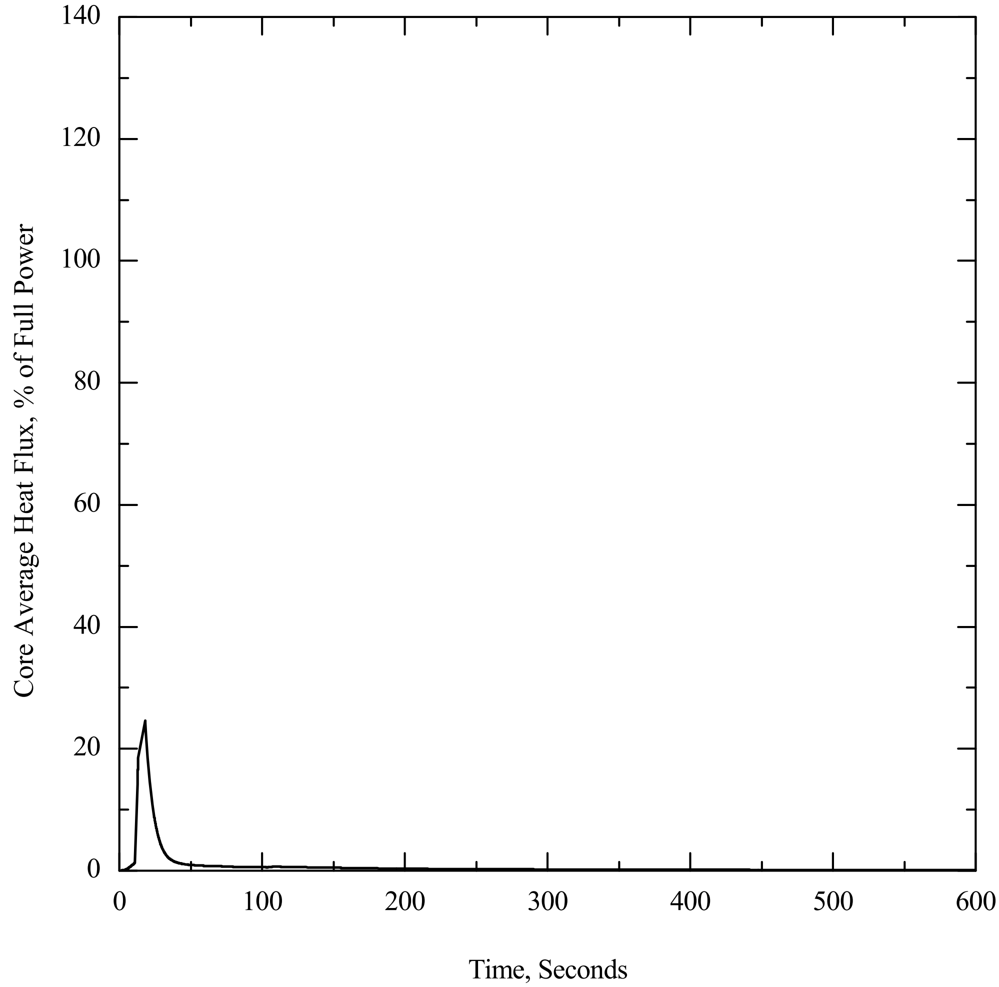

Figure 15.1.5-4.2 Zero Power Large Steam Line Break with Offsite Power Available: Core Average Heat Flux vs. Time

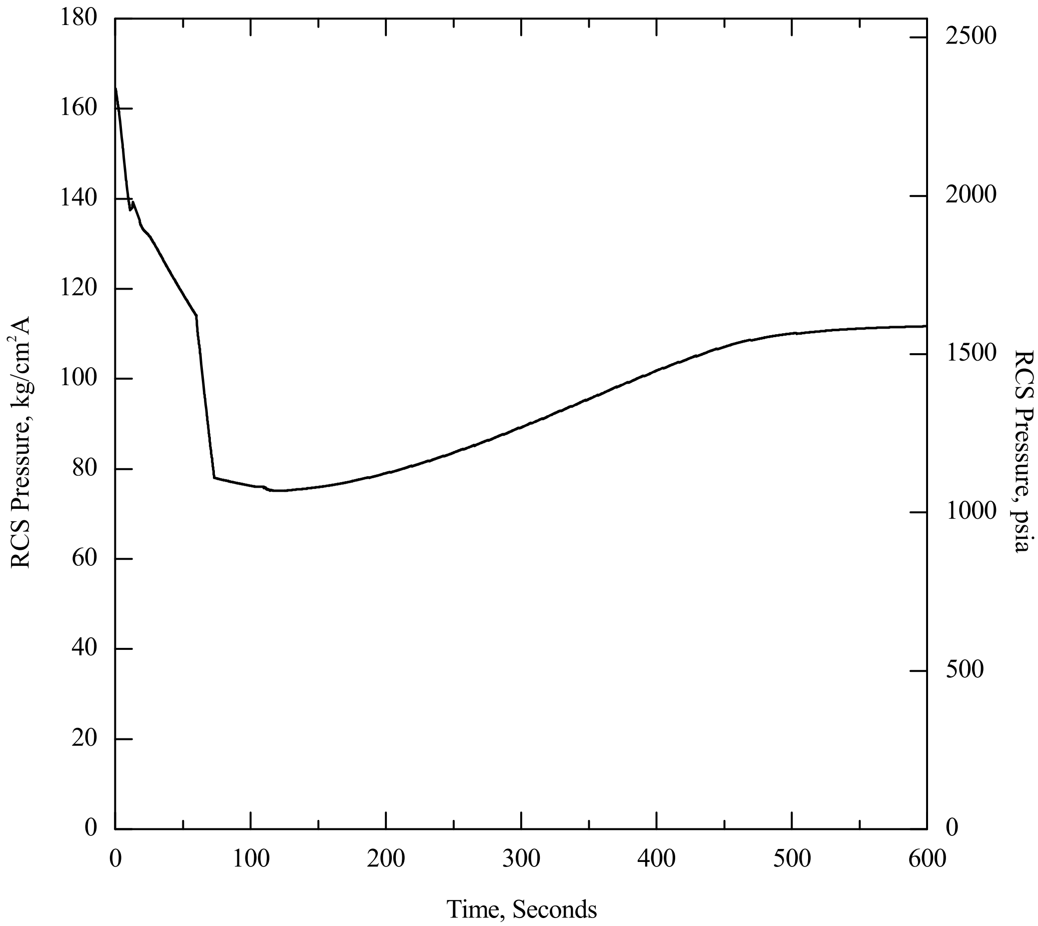

Figure 15.1.5-4.3 Zero Power Large Steam Line Break with Offsite Power Available: RCS Pressure vs. Time

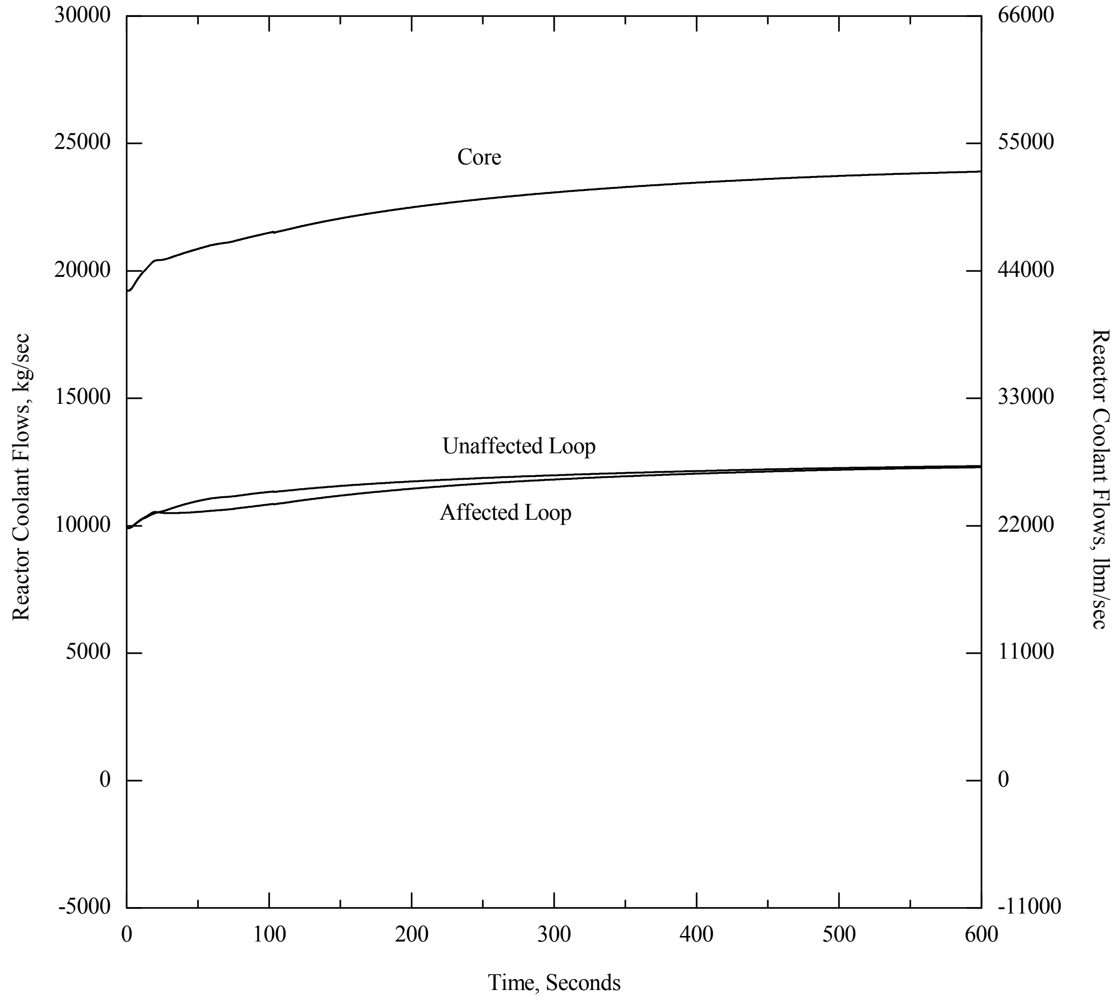

Figure 15.1.5-4.4 Zero Power Large Steam Line Break with Offsite Power Available: Reactor Coolant Flow Rates vs. Time

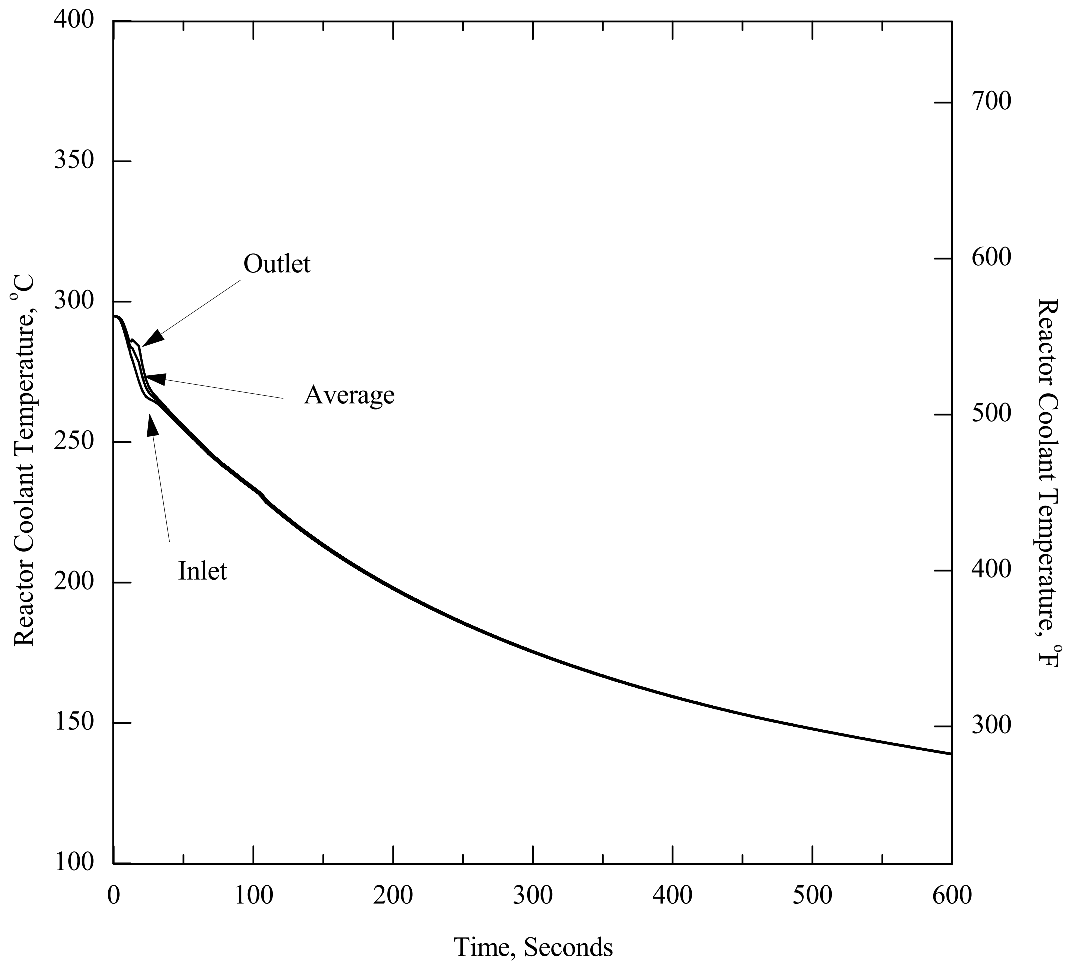

Figure 15.1.5-4.5 Zero Power Large Steam Line Break with Offsite Power Available: Reactor Coolant Temperatures (A) vs. Time

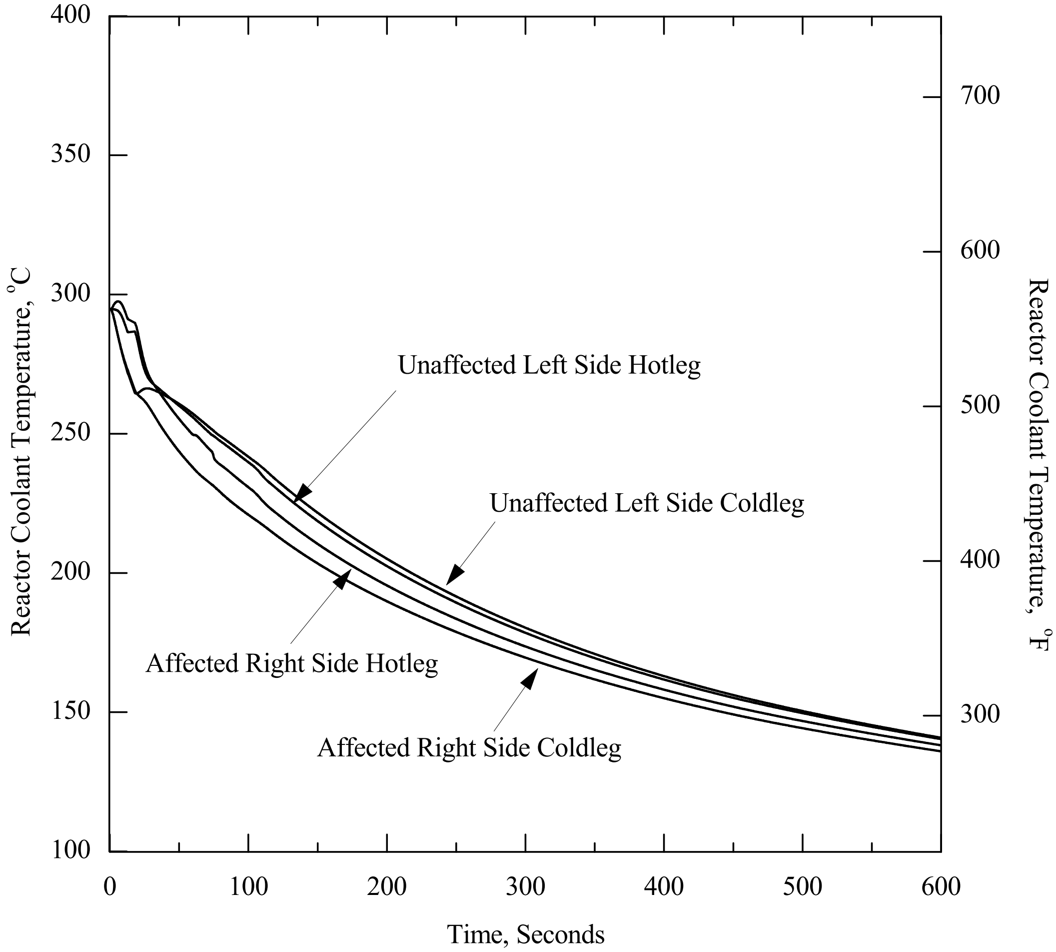

Figure 15.1.5-4.6 Zero Power Large Steam Line Break with Offsite Power Available: Reactor Coolant Temperatures (B) vs. Time

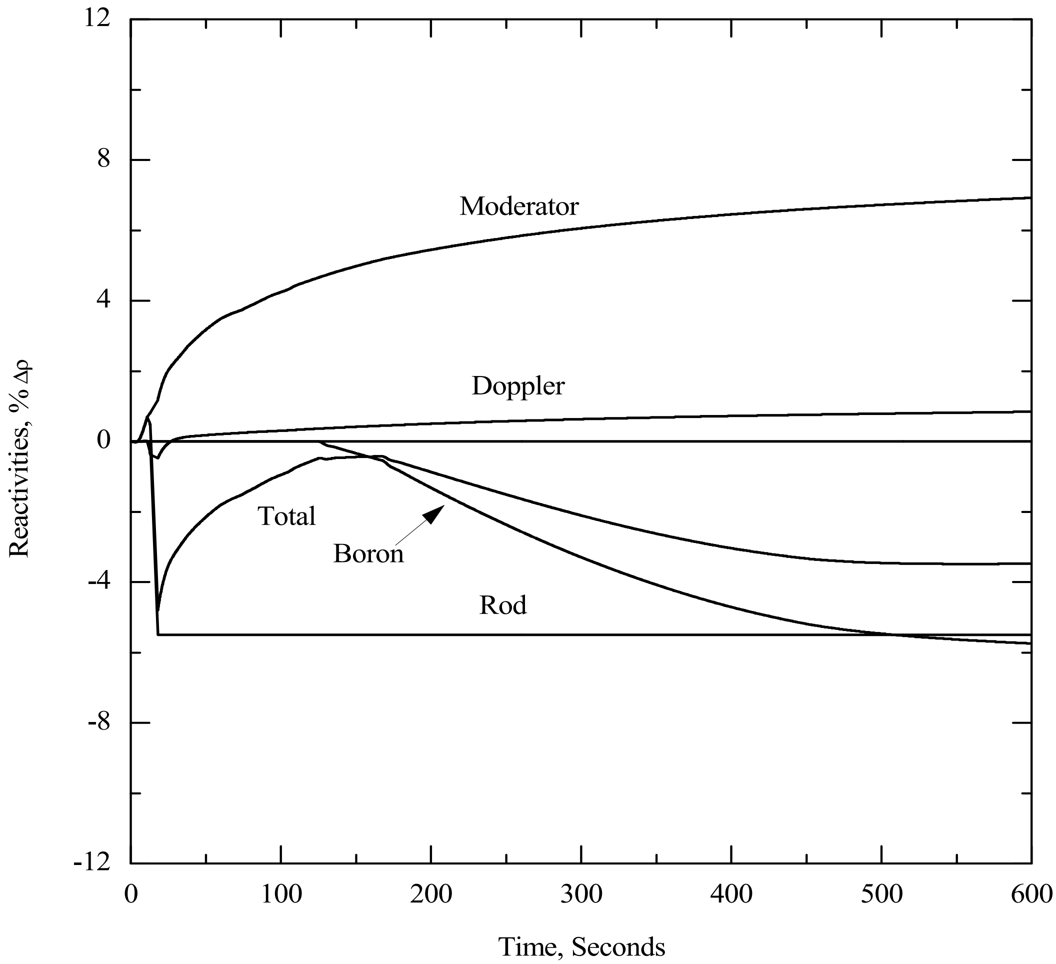

Figure 15.1.5-4.7 Zero Power Large Steam Line Break with Offsite Power Available: Reactivity vs. Time

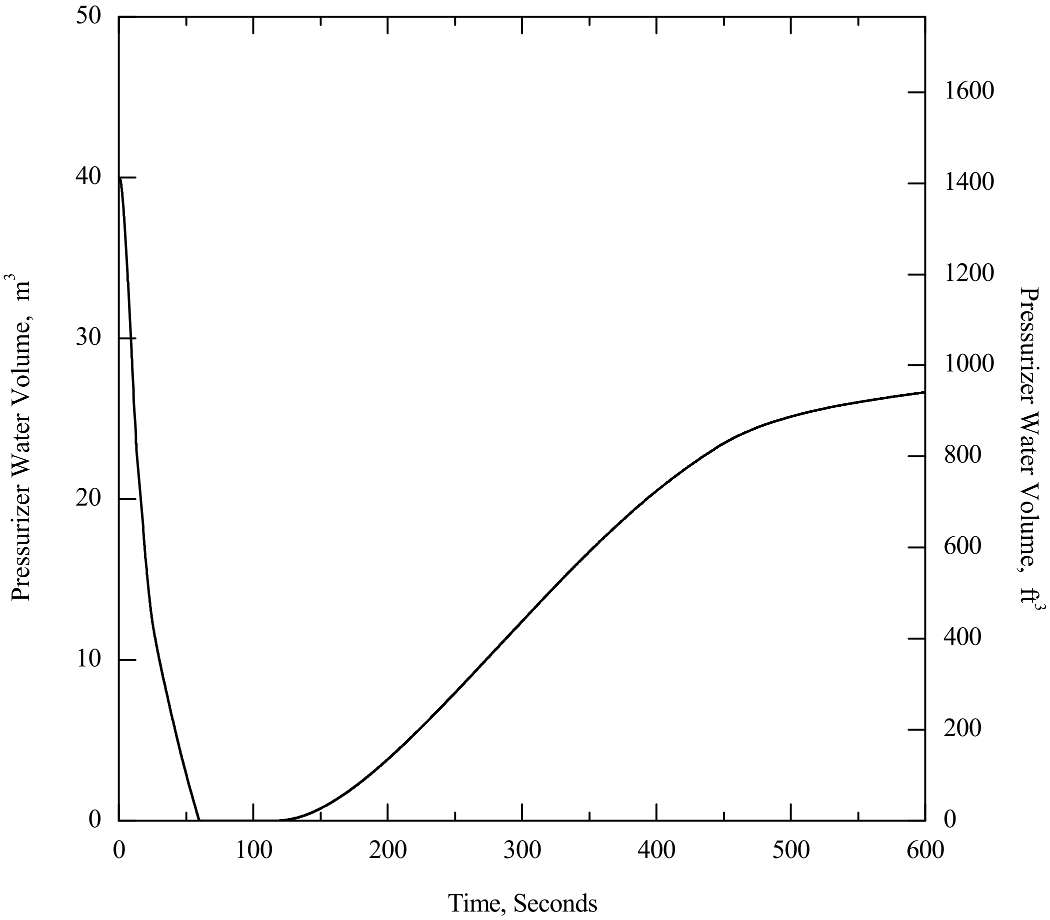

Figure 15.1.5-4.8 Zero Power Large Steam Line Break with Offsite Power Available: Pressurizer Water Volume vs. Time

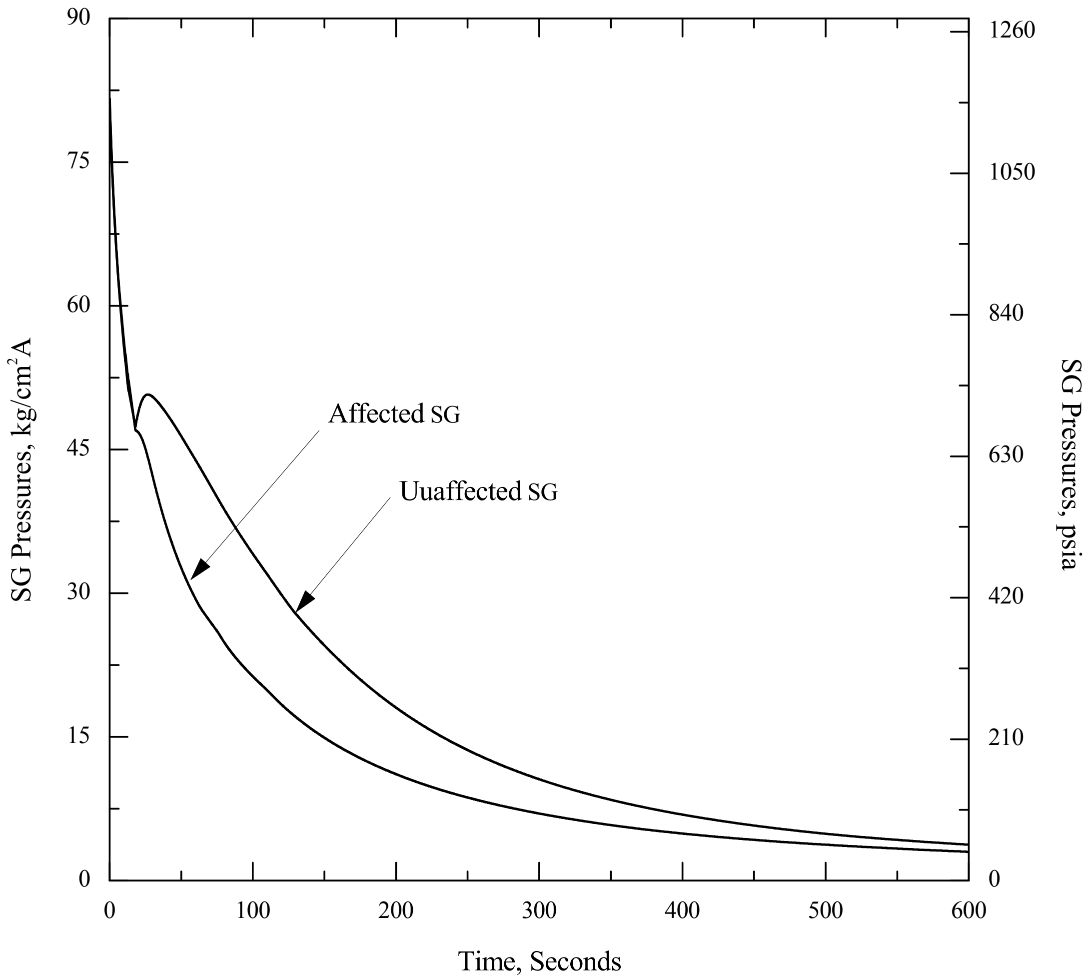

Figure 15.1.5-4.9 Zero Power Large Steam Line Break with Offsite Power Available: Steam Generator Pressure vs. Time

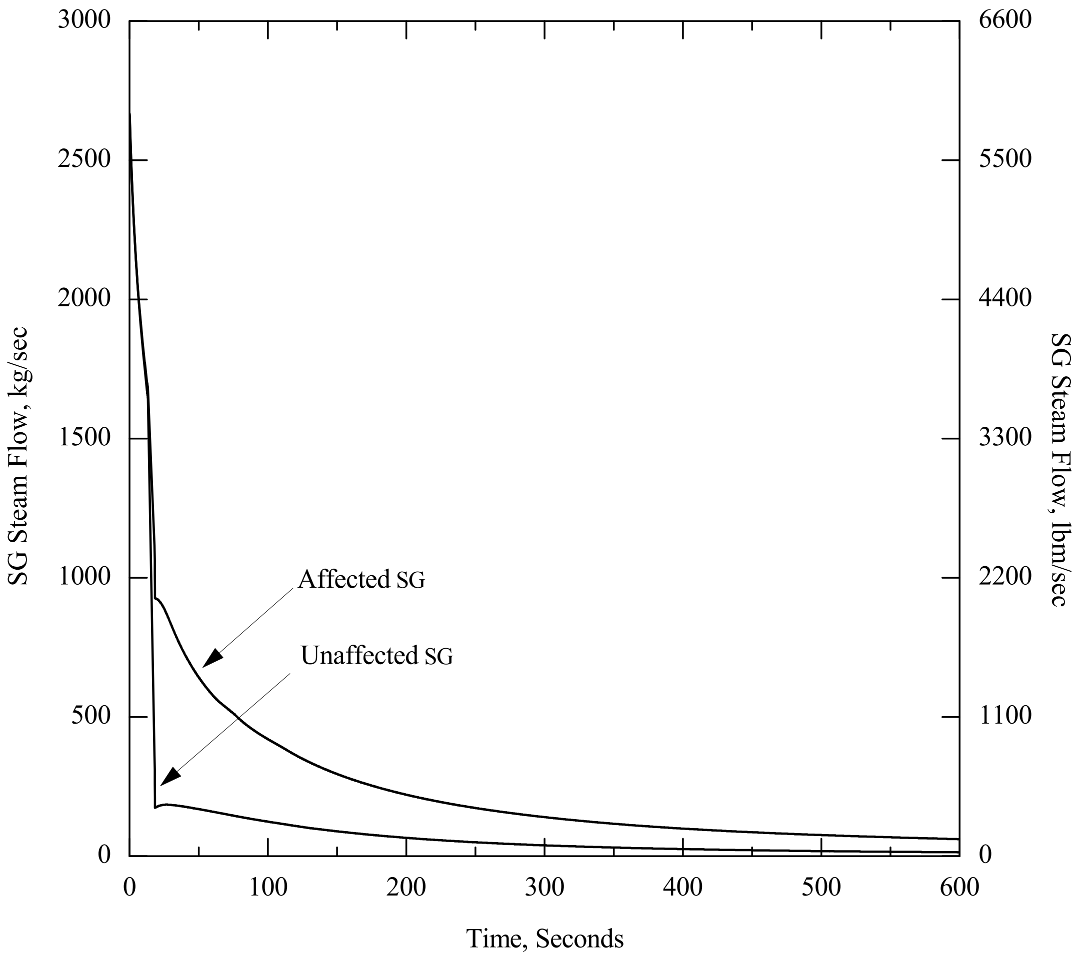

Figure 15.1.5-4.10 Zero Power Large Steam Line Break with Offsite Power Available: Steam Generator Steam Flow Rates vs. Time

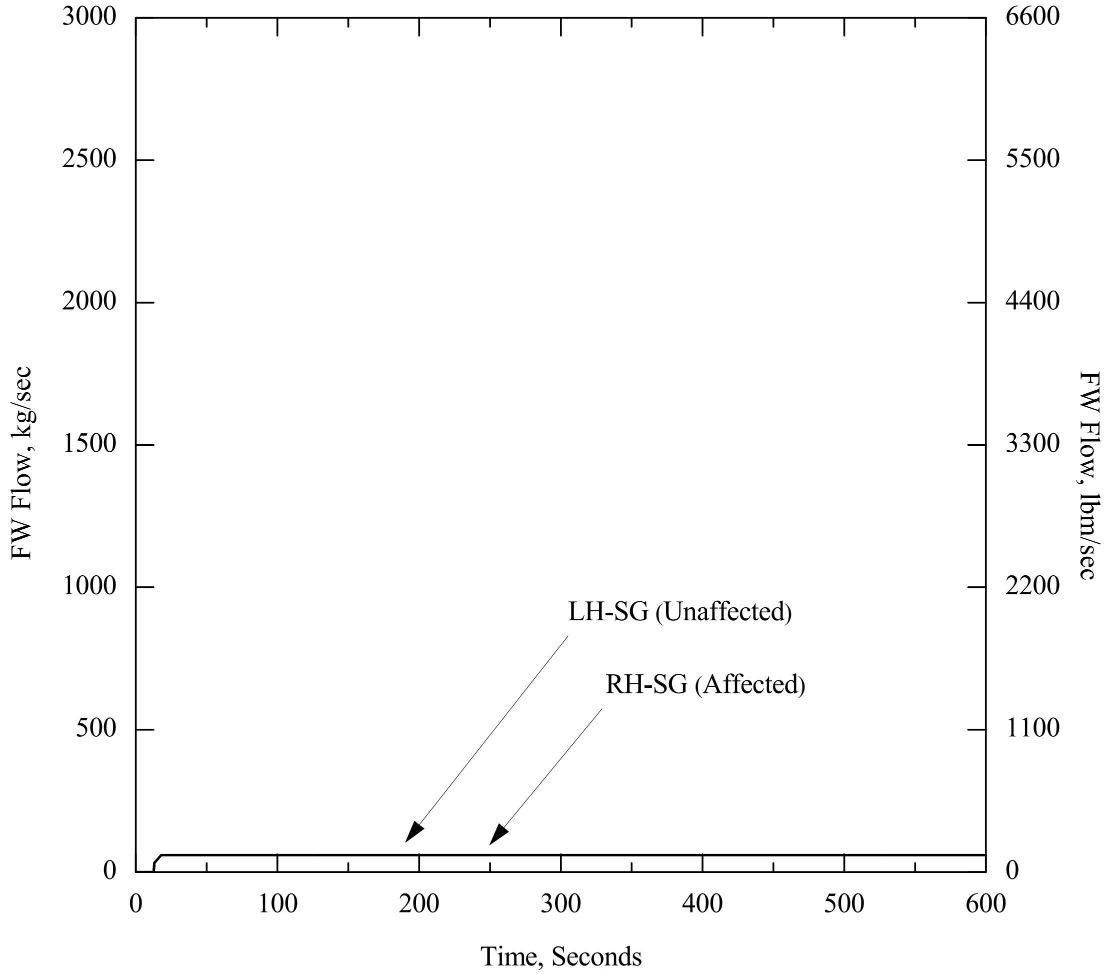

Figure 15.1.5-4.11 Zero Power Large Steam Line Break with Offsite Power Available: Feedwater Flow Rates vs. Time

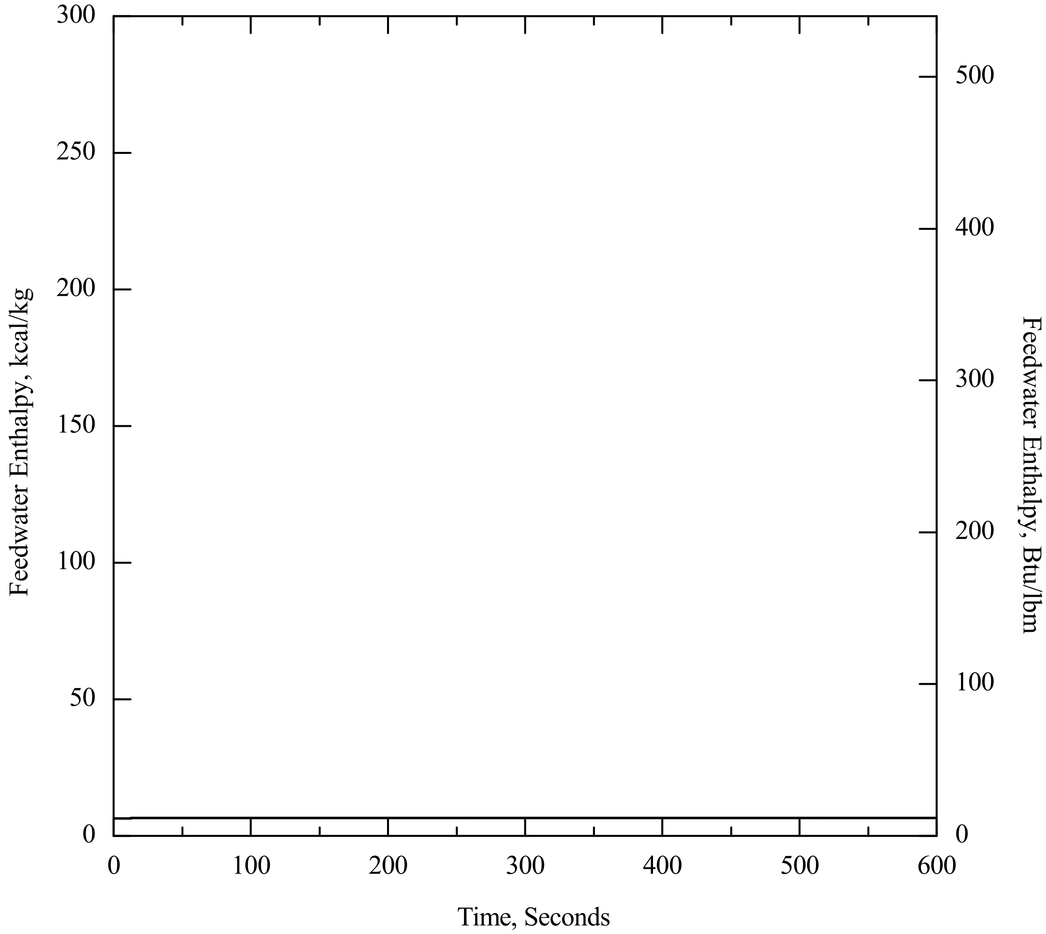

Figure 15.1.5-4.12 Zero Power Large Steam Line Break with Offsite Power Available: Feedwater Enthalpy vs. Time

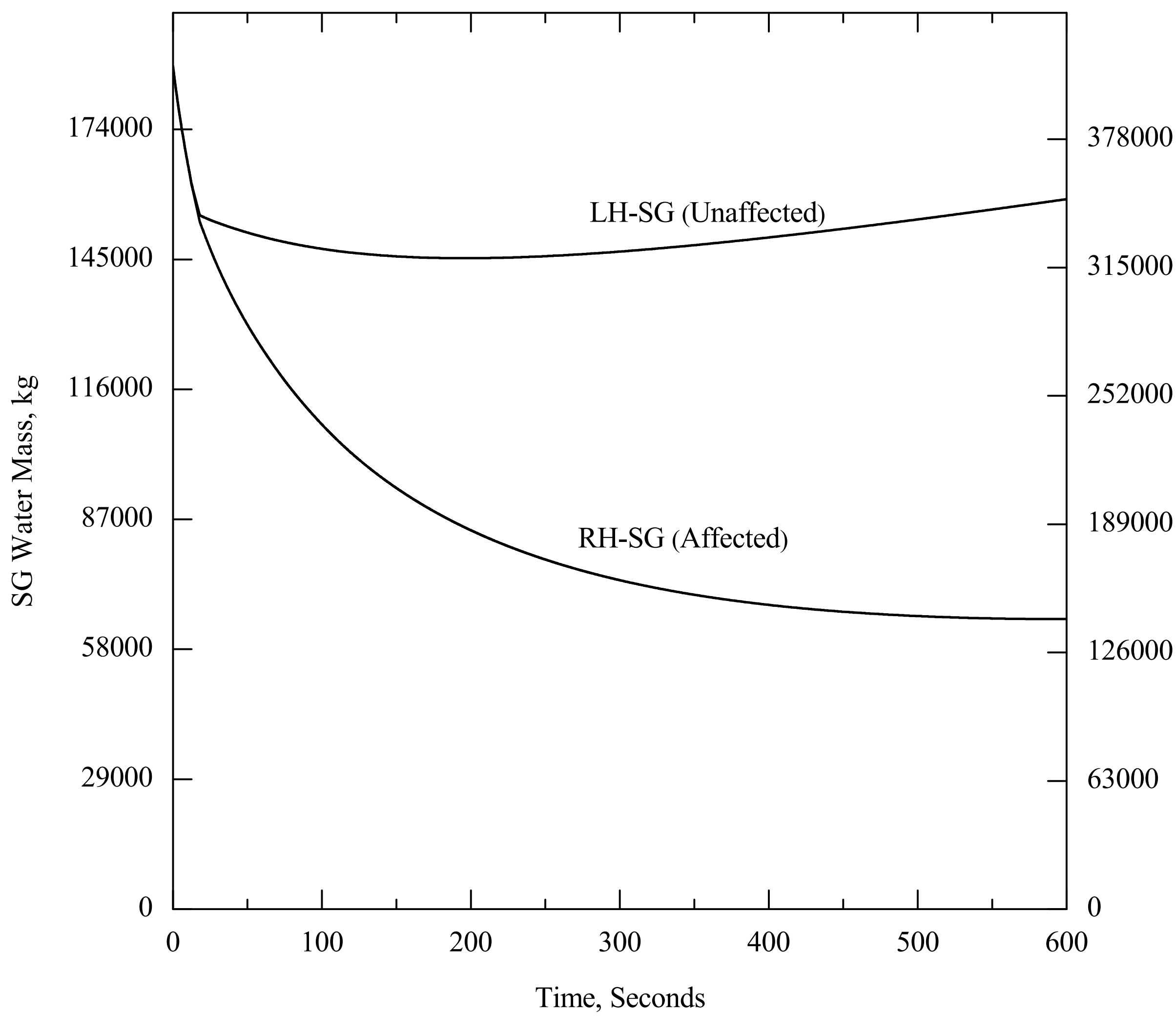

Figure 15.1.5-4.13 Zero Power Large Steam Line Break with Offsite Power Available : Steam Generator Mass Inventories vs. Time

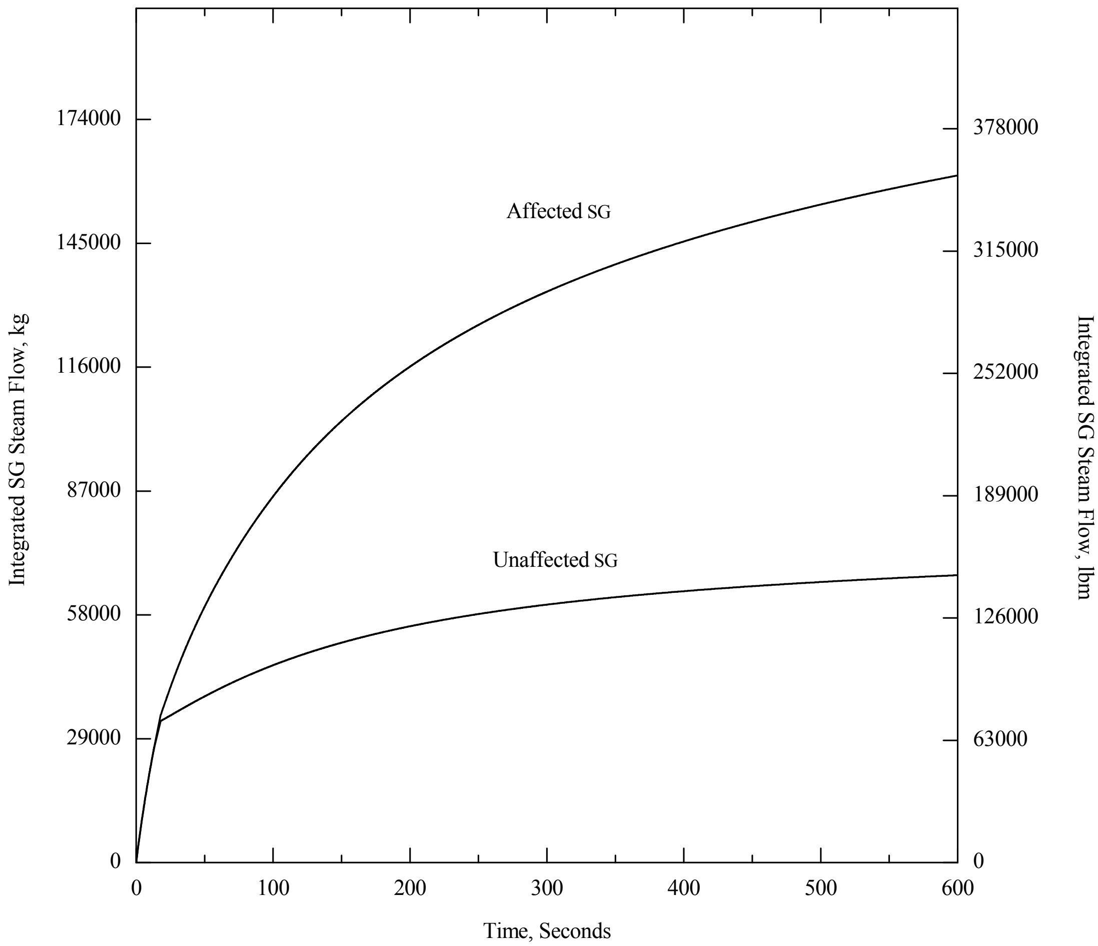

Figure 15.1.5-4.14 Zero Power Large Steam Line Break with Offsite Power Available: Integrated Steam Mass Release Through Break vs. Time

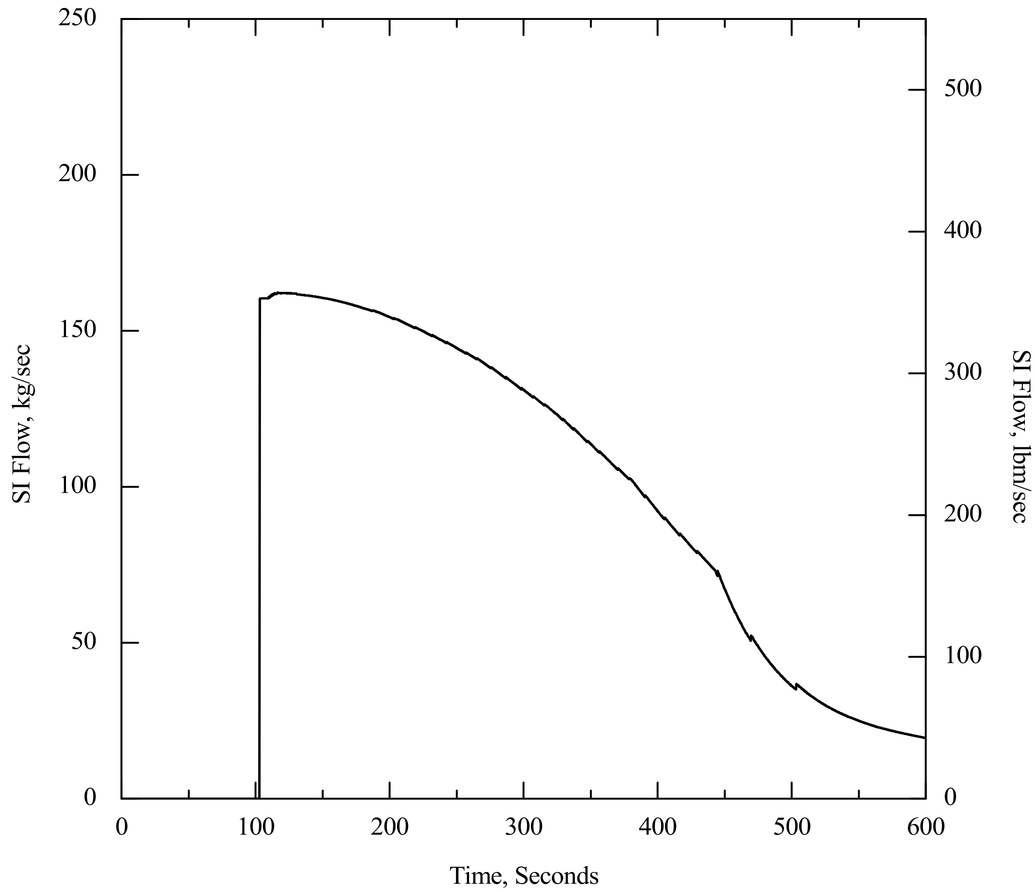

Figure 15.1.5-4.15 Zero Power Large Steam Line Break with Offsite Power Available: Safety Injection Flow Rate vs. Time

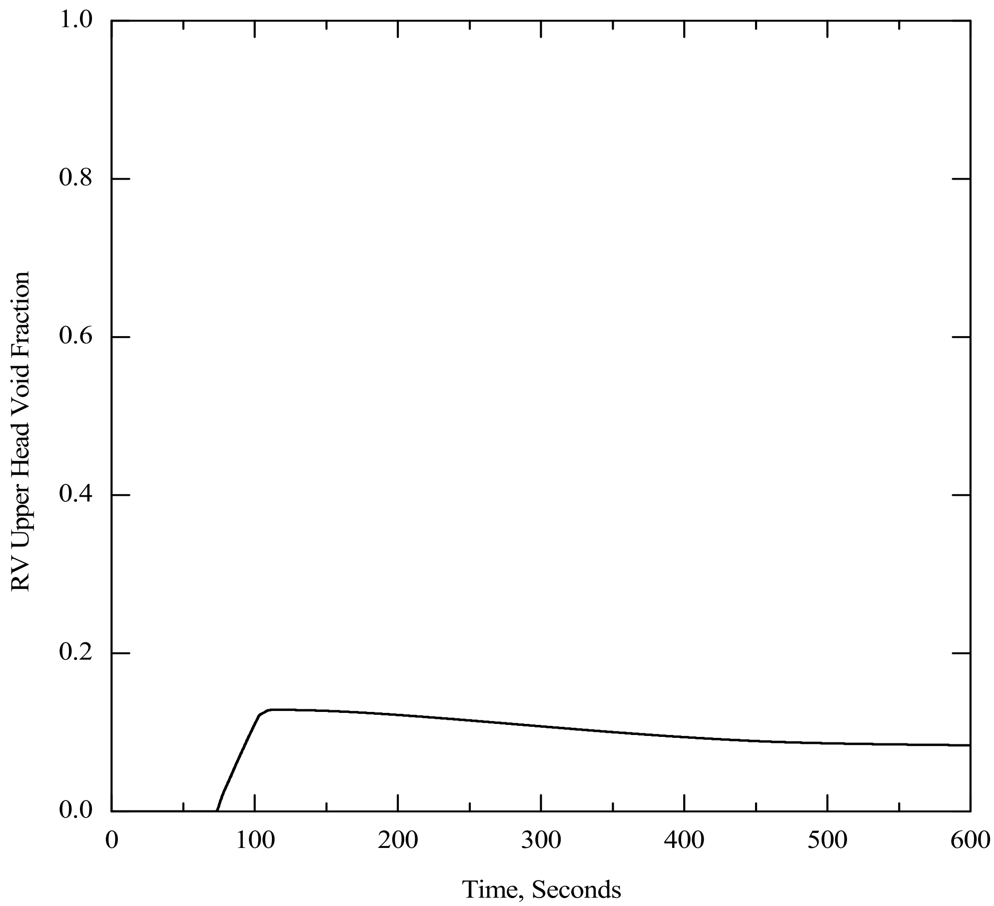

Figure 15.1.5-4.16 Zero Power Large Steam Line Break with Offsite Power Available: RV Upper Head Void Fraction vs. Time

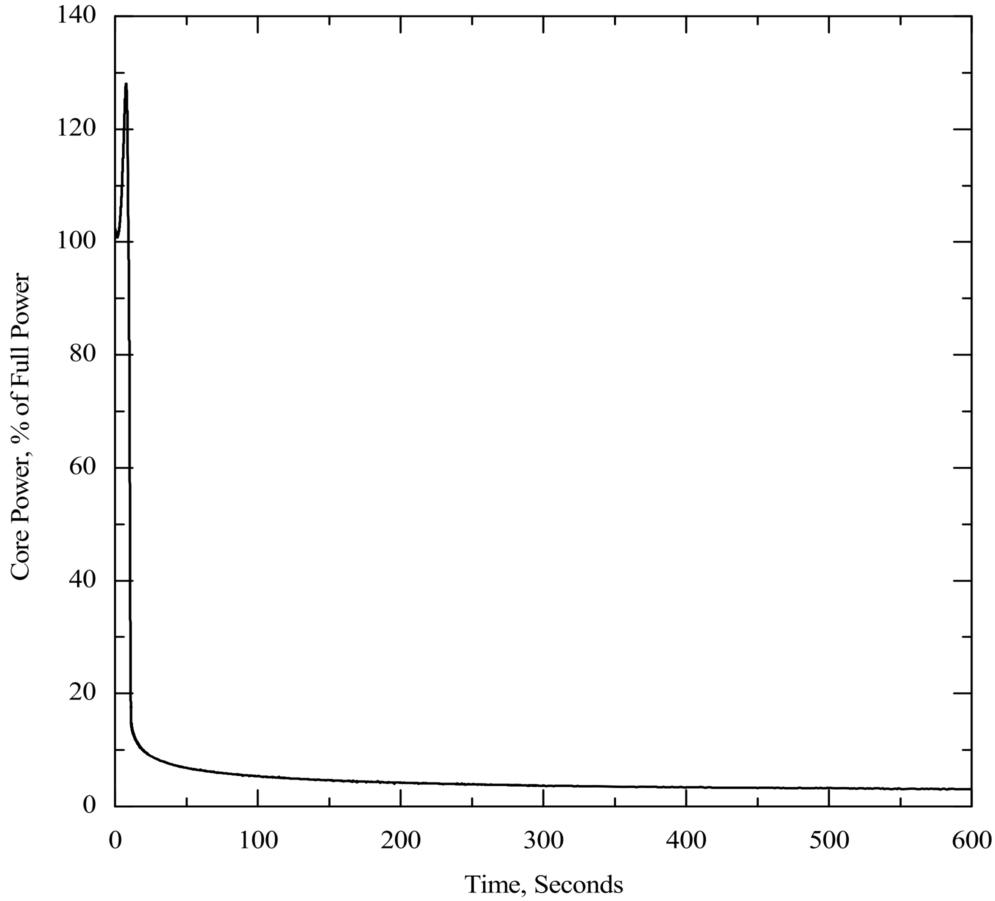

Figure 15.1.5-5.1 Full Power Steam Line Break with LOOP: Core Power vs. Time

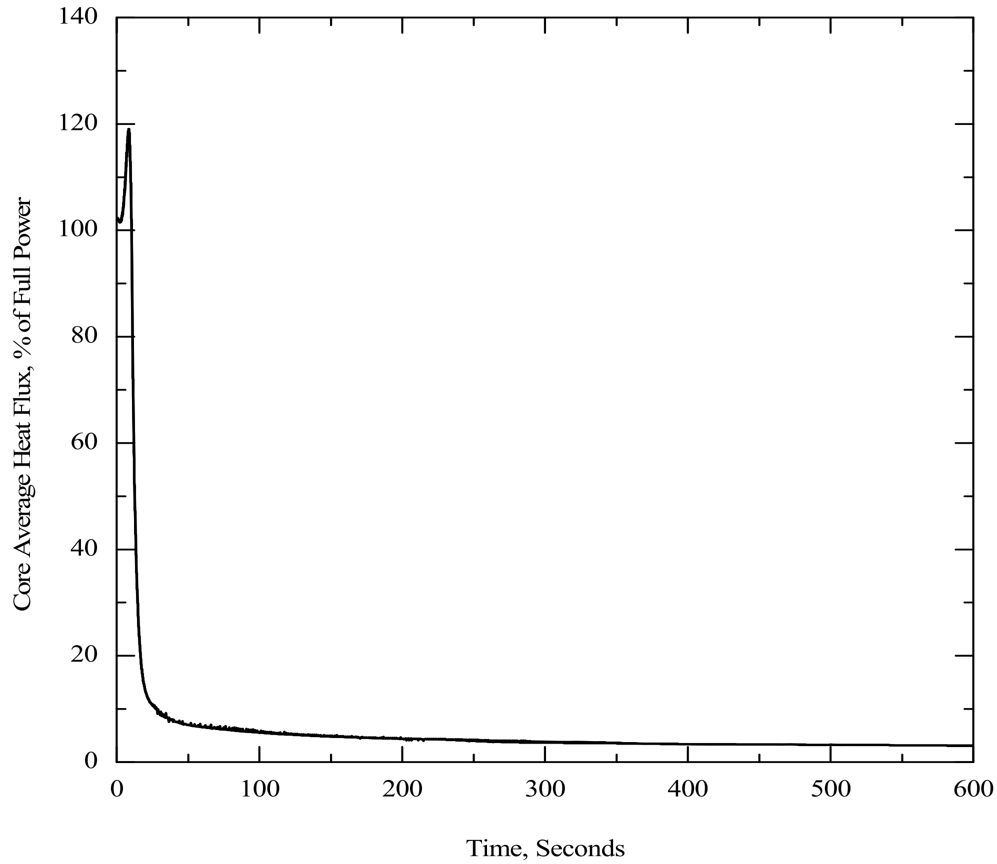

Figure 15.1.5-5.2 Full Power Steam Line Break with LOOP: Core Average Heat Flux vs. Time

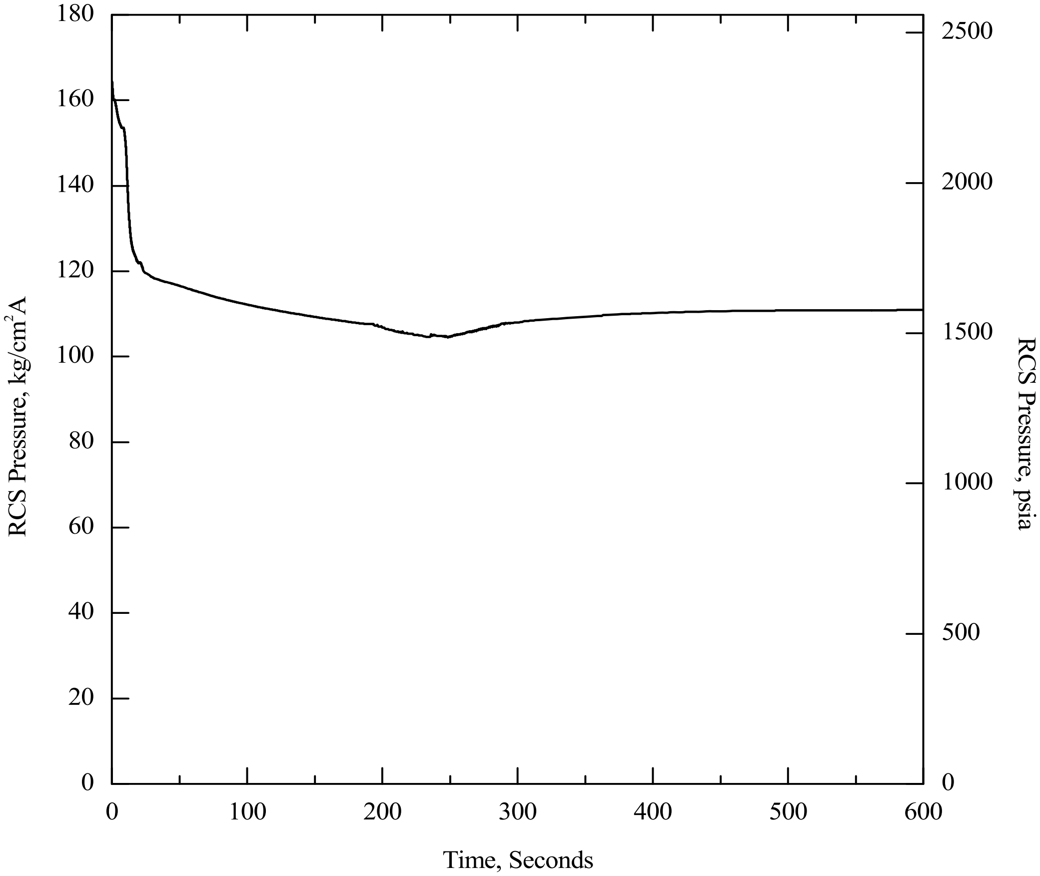

Figure 15.1.5-5.3 Full Power Steam Line Break with LOOP: RCS Pressure vs. Time

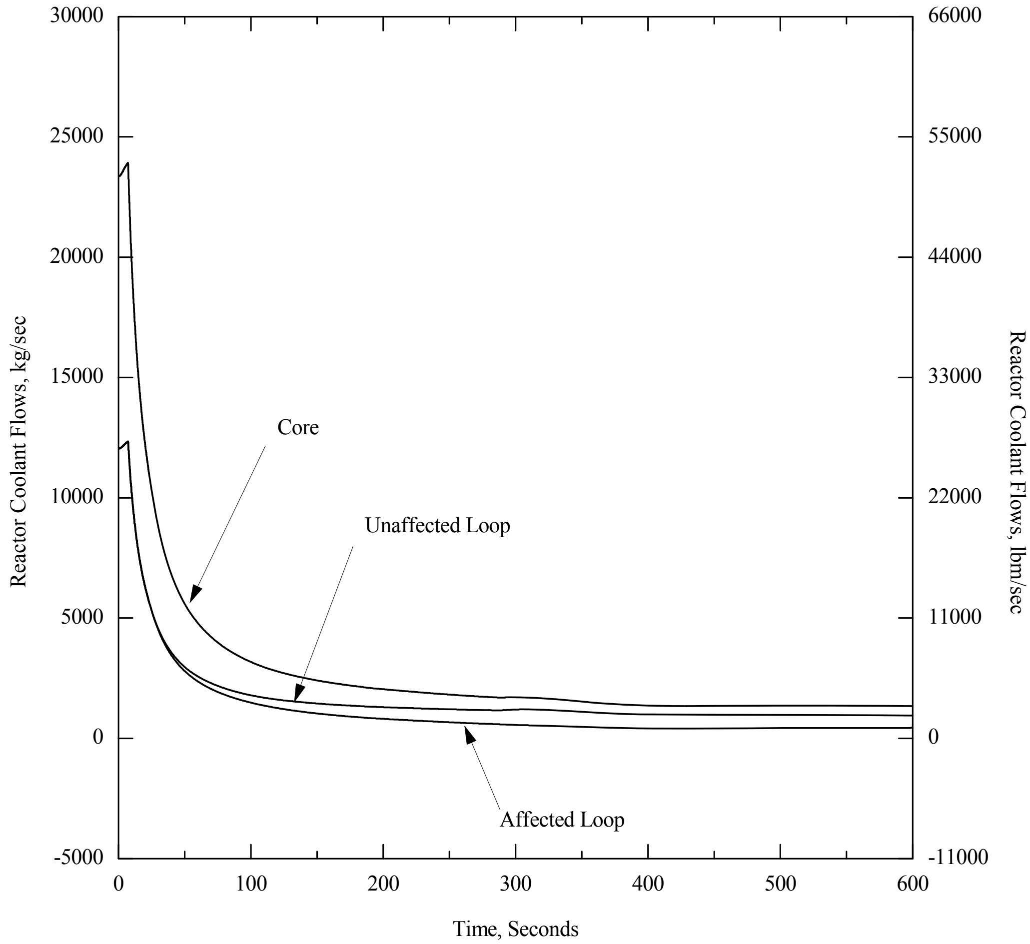

Figure 15.1.5-5.4 Full Power Steam Line Break with LOOP: Reactor Coolant Flow Rates vs. Time

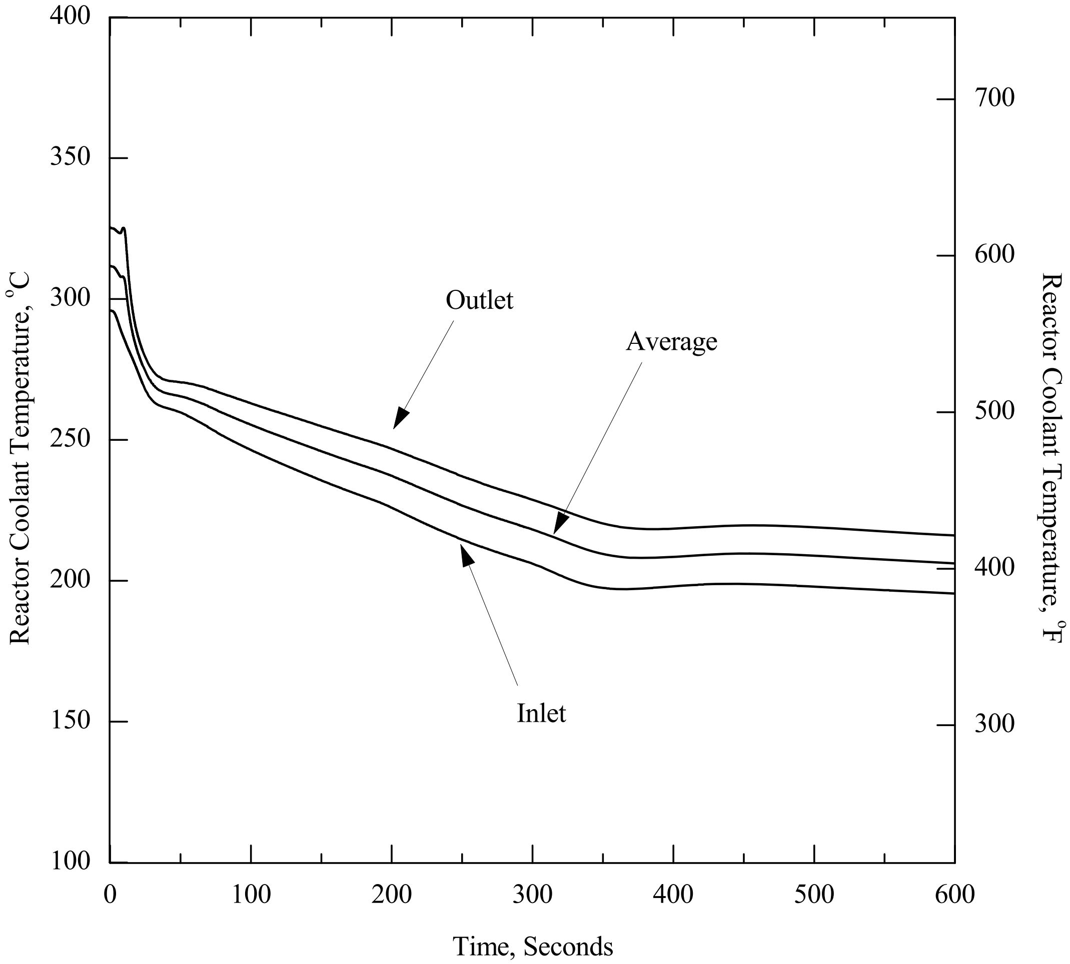

Figure 15.1.5-5.5 Full Power Large Steam Line Break with LOOP: Reactor Coolant Temperatures vs. Time

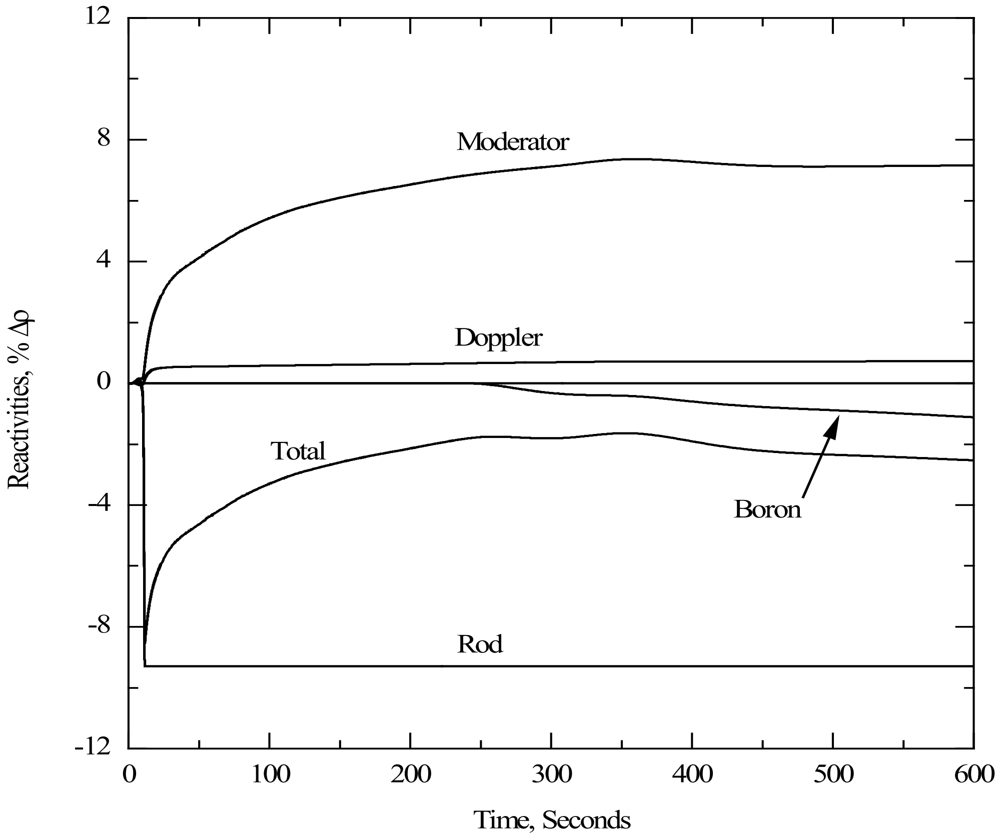

Figure 15.1.5-5.6 Full Power Large Steam Line Break with LOOP: Reactivity vs. Time

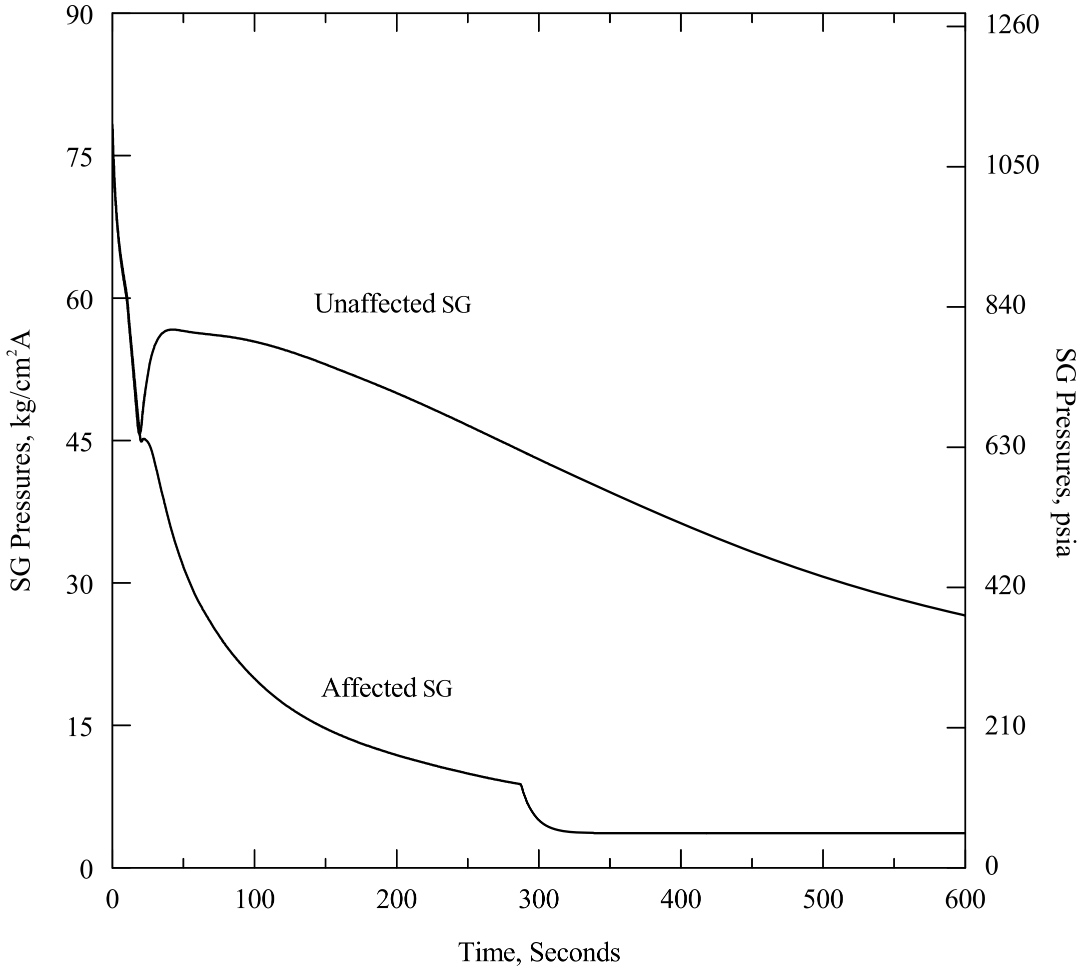

Figure 15.1.5-5.7 Full Power Steam Line Break with LOOP: Steam Generator Pressure vs. Time

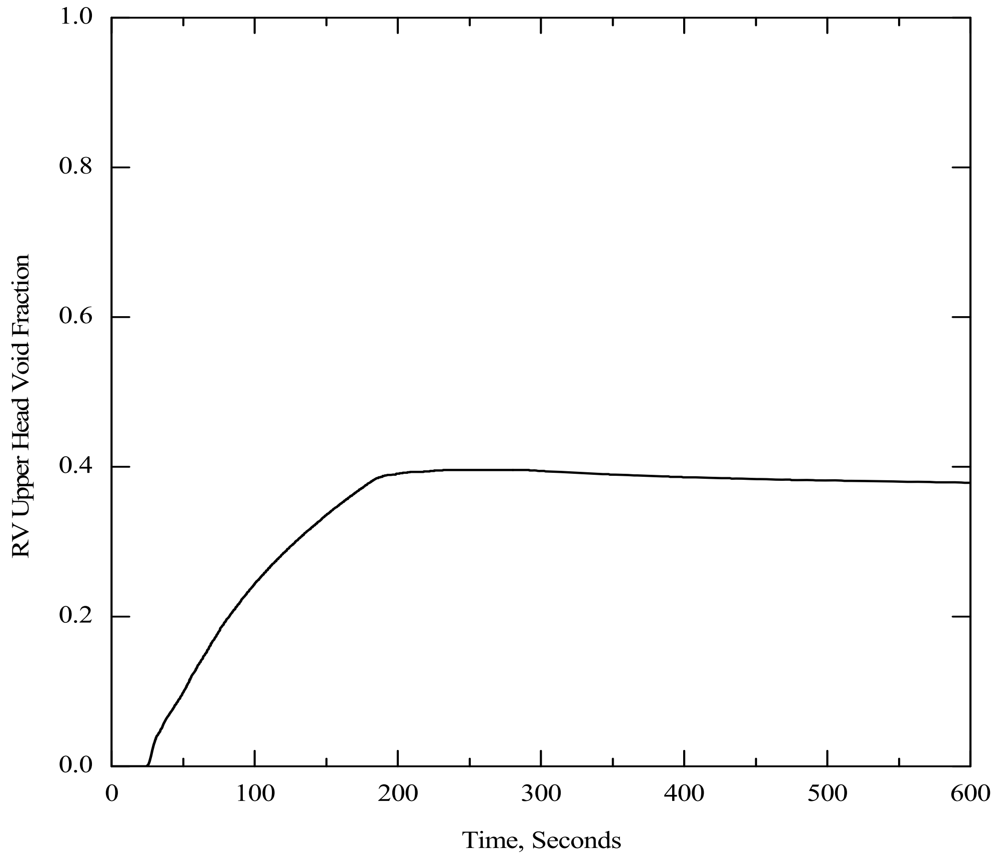

Figure 15.1.5-5.8 Full Power Large Steam Line Break with LOOP: RV Upper Head Void Fraction vs. Time

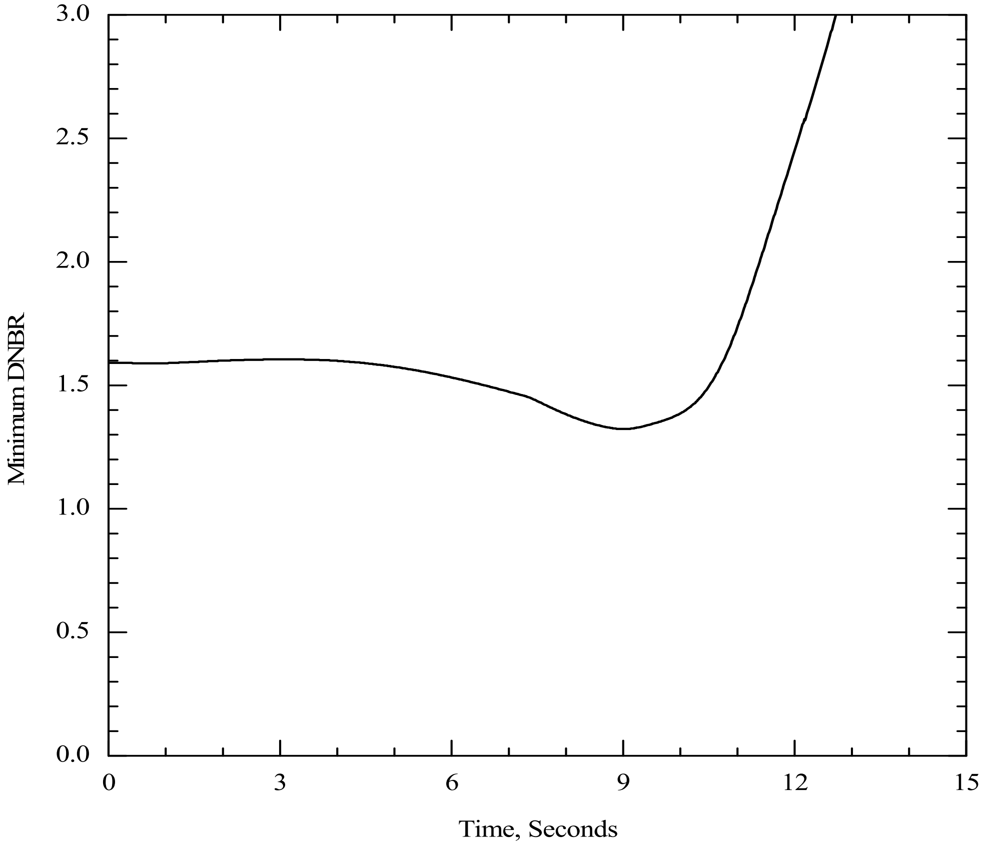

Figure 15.1.5-5.9 Full Power Large Steam Line Break with LOOP: Minimum DNBR vs. Time

15.2 Decrease in Heat Removal by the Secondary System

This section describes the analyses that have been performed for events that could result in a decrease in heat removal by the secondary system. By decreasing the heat removal capability of the secondary system, the temperature in the primary reactor coolant system (RCS) is increased.

Several anticipated operational occurrences (AOO) and one postulated accident (PA) result in an unplanned decrease in heat removal by the secondary system. These events are described in the following subsections:

a. Subsection 15.2.1 – Loss of external load

b. Subsection 15.2.2 – Turbine trip

c. Subsection 15.2.3 – Loss of condenser vacuum

d. Subsection 15.2.4 – Closure of main steam isolation valve

e. Subsection 15.2.5 – Steam pressure regulator failure (not applicable to the APR1400)

f. Subsection 15.2.6 – Loss of nonemergency ac power to the station auxiliaries

g. Subsection 15.2.7 – Loss of normal feedwater flow

h. Subsection 15.2.8 – Feedwater system pipe break inside and outside the containment

The events listed above are AOOs with the exception of the feedwater line break (FLB), which is classified as a PA.

The LOCV results in a turbine trip. This larger reduction in heat removal capability results in a higher peak RCS pressure and lower minimum DNBR for the LOCV. The results of the LOCV are limiting compared to those of the relevant events such as the loss

of external load, the turbine trip, the closure of the main steam isolation valve and the loss of normal feedwater flow.

15.2.1 Loss of External Load

15.2.1.1 Identification of Causes and Frequency Classification

The loss of external load is caused by the disconnection of the turbine generator from the electrical distribution grid. A loss of external load event is classified as an AOO. Each frequency condition is described in Subsection 15.0.0.1 and Table 15.0-5.

15.2.1.2 Sequence of Events and Systems Operation

A loss of external load generates a turbine trip that results in isolating the steam flow from the steam generators to the turbine due to the closure of the turbine stop valves. The steam bypass control system (SBCS) and reactor power cutback system (RPCS) are both normally in automatic mode and are available upon turbine trip to accommodate the load rejection without necessitating a reactor trip or the opening of the main steam safety valves (MSSVs). If a turbine trip occurs with these systems in manual mode, an isolation of main steam flow and reactor trip occurs on high pressurizer pressure (assuming the control grade reactor trip on turbine trip with the RPCS in manual is available but not credited). If no credit is taken for immediate operator action, the MSSVs open to limit the main steam system pressure increase. The operator can initiate a controlled system cooldown using the SBCS or the steam generator (SG) atmospheric dump valves any time after the reactor trip occurs.

15.2.1.3 Core and System Performance

15.2.1.3.1 Evaluation Model

The evaluation model for the loss of condenser vacuum (LOCV) is applicable to this event (Subsection 15.2.3.3.1).

15.2.1.3.2 Input Parameters and Initial Conditions

The input parameters and initial conditions used to analyze the nuclear steam supply system (NSSS) response to a loss of external load are bounded by those of an LOCV (Subsection 15.2.3.3.2).

15.2.1.3.3 Results

The LOCV results in a turbine trip; however, feedwater flow instantaneously terminates following an LOCV whereas the flow ramps down following the loss of external load. This larger reduction in heat removal capability results in a higher peak RCS pressure and lower minimum DNBRs for the LOCV. There are no concurrent single failures, which, when combined with the loss of external load, result in consequences more severe than the LOCV with a concurrent single failure event with respect to RCS pressurization and fuel performance. The results of the loss of external load event are no more limiting with respect to RCS pressurization than those of the loss of condenser vacuum (LOCV) event presented in Subsection 15.2.3.

15.2.1.4 Barrier Performance

For the loss of external load event and the loss of external load event with a coincident LOOP, and these events in combination with a single failure, the maximum RCS pressure remains below 110 percent of the RCS design pressure. The maximum SG pressure also is below 110 percent of the SG design pressure.

15.2.1.5 Radiological Consequences

This event is bounded by the feedwater system piping failure event described in Subsection 15.2.8 for the radiological consequences.

15.2.1.6 Conclusions

For a loss of external load event and a loss of external load event with a coincident LOOP, and these events in combination with a single failure, the maximum RCS pressure remains below 193.34 kg/cm^2A (2,750 psia), providing reasonable assurance of primary system integrity. The maximum steam generator pressure remains below 92.83 kg/cm^2A (1,320 psia), providing reasonable assurance of secondary system integrity. The minimum DNBR remains above 1.29, thus providing reasonable assurance of fuel cladding integrity.

15.2.2 Turbine Trip

15.2.2.1 Identification of Causes and Frequency Classification

A turbine trip can be the result of a number of conditions that cause the turbine generator control system to initiate a turbine trip signal. A turbine trip initiates closure of the turbine stop valves.

A turbine trip event is classified as an AOO. Each frequency condition is described in Subsection 15.0.0.1. Also see Table 15.0-5.

15.2.2.2 Sequence of Events and Systems Operation

A turbine trip results in isolating the steam flow from the steam generators to the turbine because of the closure of the turbine stop valves. The SBCS and RPCS are both normally in automatic mode and are available upon turbine trip to accommodate the load rejection without necessitating a reactor trip or the opening of the MSSVs. If a turbine trip occurs with these systems in manual mode, an isolation of main steam flow results and a reactor trip occurs on high pressurizer pressure (assuming the control grade reactor trip on the turbine trip with the RPCS in manual is available but not credited). If no credit is taken for immediate operator action, the MSSVs open to limit the main steam system pressure increase. The operator can initiate a controlled system cooldown using the SBCS or SG atmospheric dump valves any time after the reactor trip occurs.

15.2.2.3 Core and System Performance

15.2.2.3.1 Evaluation Model

The evaluation model for the LOCV is applicable to this event (Subsection 15.2.3.3.1).

15.2.2.3.2 Input Parameters and Initial Conditions

The input parameters and initial conditions used to analyze the NSSS response to a loss of external load are bounded by those of an LOCV (Subsection 15.2.3.3.2).

15.2.2.3.3 Results

The LOCV results in a turbine trip. The feedwater flow instantaneously terminates following a LOCV, but it ramps down following the turbine trip. This larger reduction in heat removal capability results in a higher peak RCS pressure and lower minimum DNBR for the LOCV.

There are no concurrent single failures, which, when combined with the loss of external load, result in consequences more severe than the LOCV with a concurrent single failure event with respect to RCS pressurization and fuel performance. The results of the turbine trip event are no more limiting with respect to RCS pressurization than those of the LOCV event presented in Subsection 15.2.3.

15.2.2.4 Barrier Performance

For the turbine trip event, and the turbine trip event with a coincident loss of offsite power, as well as these events in combination with a single failure, the maximum RCS pressure remains below 110 percent of the RCS design pressure. The maximum SG pressure also is below 110 percent of the SG design pressure.

15.2.2.5 Radiological Consequences

This event is bounded by the feedwater system piping failure event described in Subsection 15.2.8 for the radiological consequences.

15.2.2.6 Conclusions

For the turbine trip event, and the turbine trip event with a coincident LOOP, as well as these events in combination with a single failure, the maximum RCS pressure remains below 193.34 kg/cm^{2}A (2,750 psia), providing reasonable assurance of primary system integrity. The maximum steam generator pressure remains below 92.83 kg/cm^{2}A (1,320 psia), providing reasonable assurance of secondary system integrity. The minimum DNBR remains above 1.29, thus providing reasonable assurance of fuel cladding integrity.

15.2.3 Loss of Condenser Vacuum

15.2.3.1 Identification of Causes and Frequency Classification

A loss of condenser vacuum (LOCV) may occur due to the failure of the circulating water system to supply cooling water, failure of the main condenser evacuation system to remove non-condensable gases, or excessive in-leakage of air. Immediate cessation of feedwater flow is assumed, and the turbine is assumed to trip immediately coincident with the occurrence of the cause for the loss of condenser vacuum.

When in automatic mode, the RPCS will function to reduce the SG and RCS pressure increases during a loss of condenser vacuum if the offsite power is available. However, in this analysis the reactor power cutback system (RPCS) is assumed to be in manual mode and credit is not taken for its functioning. Also, the control grade reactor trip on turbine trip with the RPCS in manual is assumed to be available but not credited.

Consideration of the influence of a LOOP and of single failures is addressed in Subsection 15.2.3.4.

An LOCV event is classified as an AOO. Each frequency condition is described in Subsection 15.0.0.1. Also see Table 15.0-5.

15.2.3.2 Sequence of Events and Systems Operation

Table 15.2.3-1 presents the chronological sequence of events that occur following the LOCV until operator action is initiated.

The LOCV concurrent with LOOP results in a complete reduction in steam flow to the turbine and feedwater flow to the SGs. The complete steam flow reduction and termination of the feedwater flow cause a reactor trip on high pressurizer pressure due to reduced RCS cooling, a reactor trip on RCP low speed due to LOOP, and the pressurizer POSRVs open to limit the primary system pressure increase. The steam discharged from the pressurizer POSRVs is released to the inside-containment refueling water storage tank (IRWST). The LOCV concurrent with turbine trip results in a main steam system pressure increase, and the MSSVs open to limit the main steam system pressure increase. Auxiliary feed water recovers the decreased steam generator water level.

After reactor trip, the RCS pressure decreases and stabilizes. If a SIAS is generated on low pressurizer pressure, additional negative reactivity is inserted when the borated safety injection water reaches the core.

The operator can initiate a controlled system cooldown using the atmospheric dump valves 30 minutes after the event initiation. RCS heat removal is accomplished utilizing the RCPs and SGs. When the loss of offsite power concurrent with turbine trip is assumed, RCS heat removal is accomplished by natural circulation along with the steam generators. During cooldown, the pressurizer pressure and level control systems can be manually operated to regulate pressure and level in the primary system.

The shutdown cooling system (SCS) is manually actuated when RCS temperature and pressure have been reduced to the shutdown cooling entrance condition of 176.7 °C (350 °F) and 31.6 kg/cm^{2}A (450 psia).

15.2.3.3 Core and System Performance

15.2.3.3.1 Evaluation Model

The NSSS response to an LOCV was simulated using the CESEC-III computer program described in Subsection 15.0.2.2.1. The DNBR was calculated using the CETOP-D computer code (Subsection 15.0.2.2.4), which uses the KCE-1 CHF correlation.

15.2.3.3.2 Input Parameters and Initial Conditions

The fuel integrity analysis uses the initial core inlet temperature of 290.56 °C (555 °F), and the initial pressurizer pressure of 158.19 kg/cm^2 (2,250 psia), and all other initial conditions and assumptions are listed in Table 15.2.3-2.

15.2.3.3.3 Results

Initiating the LOCV with a loss of offsite power event with initial conditions selected to minimize the transient DNBR results in a minimum DNBR of 1.43 at 3.29 seconds as presented on Figure 15.2.3-13. The minimum DNBR remains above 1.29, providing reasonable assurance of fuel cladding integrity.

15.2.3.4 Barrier Performance

15.2.3.4.1 Evaluation Model

The barrier performance evaluation for peak RCS pressure employs the same CESEC-III evaluation model as in the core and system performance analysis described in Subsection 15.2.3.3.1.

15.2.3.4.2 Input Parameters and Initial Conditions

The input parameters and initial conditions used to analyze the NSSS response are given in Table 15.0-3. Table 15.2.3-2 contains the initial conditions and assumptions used for the limiting event with respect to RCS peak pressure. The initial conditions for the principal process variables are varied within the ranges given in Table 15.0-3 to determine the set of initial conditions that would produce the most adverse consequences following an LOCV. Various combinations of initial core inlet temperature, core inlet flow, pressurizer pressure, pressurizer water level, and steam generator water level are considered in order to evaluate the effects on peak reactor coolant system pressure.

Decreasing the initial core inlet temperature reduces the initial steam generator pressure, thereby delaying the heat removal associated with the opening of the MSSVs. The initial core inlet temperature for this event is the minimum of 287.78 °C (550 °F).

The reactor vessel flow rate at the rated condition causes a conservative consequence. The flow rate does not have a significant impact on the consequences of the event.

The minimum initial SG water mass minimizes the heat removal capacity; therefore, less SG inventory causes greater increase in RCS peak pressure. If the initial SG inventory is too small, RCS peak pressure is decreased because an SG low-level trip occurs quickly causing minimum SG inventory at the value that a pressurizer high-pressure reactor trip occurs, which is slightly earlier than an SG low-level reactor trip. Parametric studies show that RCS peak pressure is obtained when the initial SG level is 65 percent wide range.

The lower initial pressurizer pressure results in a delayed pressurizer POSRV opening and a delayed reactor trip on high pressurizer pressure. A higher initial pressurizer water level results in a faster increase in pressure, but also a faster pressurizer POSRV opening. Parametric studies show the RCS peak pressure is obtained when MSSVs opening is

slightly earlier than the pressurizer POSRV opening. Based on the results of these parametric studies, the initial conditions that resulted in the highest RCS peak pressures are presented in Table 15.2.3-2.

The LOCV with a LOOP is assumed to abruptly and completely terminate both main steam and feedwater flow.

For the LOCV event without a LOOP, the operation of reactor coolant pump is available, thus, the P-T-S heat transfer is more active than the LOCV with a LOOP such that the consequence would be more conservative considering peak pressure in coolant system. Initiation time of LOOP also has an influence on peak pressure. A LOOP concurrent with LOCV causes early reactor trip on RCP low speed. If the initiation time of LOOP is delayed, it does not affect the peak pressure due to the reactor trip following pressurizer high pressure. As a result of parametric studies of LOOP initiation times, the highest peak pressure occurs when initiation time of a LOOP has some delay after the beginning of an LOCV.

The LOCV event coincident with LOOP is similar to the loss of nonemergency power to the station auxiliaries described in Subsection 15.2.6. These events have the same effects as the loss of forced reactor coolant flow event, which is discussed in Subsection 15.3.1.

With respect to peak pressure criteria, there are no single failures that, when combined with the event, result in a more severe peak pressure than the LOCV by itself. Similarly, with regard to fuel performance, there are no single failures that, when combined with the event, result in a more severe minimum DNBR than the event by itself.

15.2.3.4.3 Results

With respect to peak pressure criteria, the dynamic behavior of important NSSS parameters following the loss of condenser vacuum is presented on Figures 15.2.3-1 through 15.2.3-12.

The sudden reduction of steam flow, caused by the LOCV, leads to a reduction of the P-T-S heat transfer. The moderator reactivity is constant prior to reactor trip due to a zero moderator temperature coefficient (MTC), even though the average core temperature increased from the initial conditions. The RCS is rapidly heated up, and there is a CPC low pump shaft speed trip condition at 6.67 seconds. At 7.02 seconds, a CPC low pump

shaft speed trip signal is generated. The reactor trip breakers open at 7.12 seconds, limiting the maximum core power to 102 percent of full power.

The pressurizer POSRVs open at 8.46 seconds, and the maximum RCS pressure of 193.0 kg/cm^2A (2,745 psia) is reached at 9.33 seconds. The MSSVs open at 7.20 seconds, and the maximum secondary pressure of 91.0 kg/cm^2A (1,294.04 psia) is reached at 10.79 seconds.

The RCS pressure then decreases rapidly due to the combined effects of reactor trip and opening of primary and secondary safety valves. The pressurizer POSRVs fully close at 12.56 seconds. Auxiliary feedwater automatically begins at 102.25 seconds. Thirty minutes after initiation of the event, the operator commences a reactor cooldown using the atmospheric dump valves to release steam.

15.2.3.5 Radiological Consequences

This event is bounded by the feedwater system piping failure event described in Subsection 15.2.8 for the radiological consequences.

15.2.3.6 Conclusions

For the LOCV, the maximum RCS pressure remains below 193.34 kg/cm^2A (2,750 psia) providing reasonable assurance of primary system integrity. The maximum steam generator pressure remains below 92.83 kg/cm^2A (1,320 psia) providing reasonable assurance of secondary system integrity. The minimum DNBR remains above 1.29 providing reasonable assurance of fuel cladding integrity.

15.2.4 Closure of the Main Steam Isolation Valve

15.2.4.1 Identification of Causes and Frequency Classification

The main steam isolation valve closure event is initiated by the closure of all MSIVs due to a spurious closure signal. A closure of the MSIV event is classified as an AOO. Each frequency condition is described in Subsection 15.0.0.1 and Table 15.0-5.

15.2.4.2 Sequence of Events and Systems Operation

The closure of all MSIVs results in the termination of all main steam flow. The decreased heat removal results in increased primary and secondary temperatures and pressure. Reactor trip occurs on high pressurizer pressure. The pressure increases in the primary and secondary systems are limited by the pressurizer POSRVs and the MSSVs, respectively. The operator can initiate a system cooldown using the SG atmospheric dump valves after reactor trip occurs.

15.2.4.3 Core and System Performance

15.2.4.3.1 Evaluation Model

Evaluation model for the loss of condenser vacuum (LOCV) is applicable to this event (Subsection 15.2.3.3.1).

15.2.4.3.2 Input Parameters and Initial Conditions

The input parameters and initial conditions used to analyze the NSSS response to the closure of MSIV are bounded by those of an LOCV (Subsection 15.2.3.3.2).

15.2.4.3.3 Results

The MSIV closure event also results in the termination of all main steam flow. The main steam flow is terminated more rapidly during the LOCV because the closure time for the turbine stop valves is much shorter than for the MSIVs resulting in a higher peak RCS pressure for the LOCV event.

With respect to fuel performance, the DNBR increases during the MSIV closure event due to the increasing RCS pressure. The initial DNBR is also the minimum DNBR for the MSIV closure event. The MSIV closure event is similar to the loss of normal AC power discussed in Subsection 15.2.6.

There are no concurrent single failures that, when combined with the MSIV closure event, will result in RCS pressurization and fuel performance consequences more severe than the LOCV event. The results of the MSIV closure event are no more limiting with respect to

RCS pressurization and fuel performance than those of the LOCV event presented in Subsection 15.2.3.

15.2.4.4 Barrier Performance

For the MSIV closure event and the MSIV closure with coincident loss of offsite power, as well as these events in combination with a single failure, the maximum RCS pressure remains below 110 percent of the RCS design pressure, providing reasonable assurance of primary system integrity. The maximum SG pressure also is below 110 percent of the SG design pressure.

15.2.4.5 Radiological Consequences

This event is bounded by the feedwater system piping failure event described in Section 15.2.8 for the radiological consequences.

15.2.4.6 Conclusions

For the MSIV closure event and the MSIV closure with coincident loss of offsite power, as well as these events in combination with a single failure, the maximum RCS pressure remains below 193.34 kg/cm^2A (2,750 psia), providing reasonable assurance of primary system integrity. The maximum steam generator pressure remains below 92.83 kg/cm^2A (1,320 psia), providing reasonable assurance of secondary system integrity. The minimum DNBR remains above 1.29, providing reasonable assurance of fuel cladding integrity.

15.2.5 Steam Pressure Regulator Failure

This event does not apply to the APR1400 design, and therefore, is not presented.

15.2.6 Loss of Nonemergency AC Power to the Station Auxiliaries

15.2.6.1 Identification of Causes and Frequency Classification

The loss of nonemergency AC power to the station auxiliaries (LOAC) may be the result of a complete loss of the external grid or a loss of the onsite AC distribution system. An LOAC is presented as the initiating event for the four RCPs loss of flow (LOF) events discussed in Subsection 15.3.1.

An LOAC event is classified as an AOO. Each frequency condition is described in Subsection 15.0.0.1 and Table 15.0-5.

15.2.6.2 Sequence of Events and Systems Operation

When all normal AC power is assumed to be lost, the turbine stop valves close, and it is assumed that the area of the turbine control valves is instantaneously reduced to zero. Also, the feedwater flow to both steam generators is instantaneously assumed to stop. The reactor coolant pumps coast down and the reactor coolant flow begins to decrease. A CPC reactor trip will occur as a result of a low pump shaft speed as the flow coastdown begins. The pressure increases in the RCS, and steam generators are limited by the pressurizer POSRVs and the MSSVs, respectively.

The loss of all normal AC power is followed by automatic startup of the standby diesel generators of which power output is sufficient to supply electrical power to all necessary engineered safety feature systems and to maintain the plant in a safe shutdown condition. Subsequent to the reactor trip, stored and fission product decay energy is dissipated by the RCS and main steam system. In the absence of forced reactor coolant flow, core heat removal occurs by natural circulation in the RCS. Initially, the residual water inventory in the steam generators is used as a heat sink, and the resultant steam is released to the atmosphere by the MSSVs. With the availability of standby diesel power, auxiliary feedwater is automatically initiated on a low steam generator water level signal. Plant cooldown is operator controlled using the atmospheric dump valves until offsite power is restored at which time the steam bypass control system and the condenser are utilized for the remainder of the cooldown.

15.2.6.3 Core and System Performance

15.2.6.3.1 Evaluation Model

Evaluation model for the loss of flow (LOF) is applicable to this event (Subsection 15.3.1.3.1).

15.2.6.3.2 Input Parameters and Initial Conditions

The input parameters and initial conditions used to analyze the NSSS response to a LOAC are bounded by those of an LOF (Subsection 15.3.1.3.2).

15.2.6.3.3 Results

During the LOCV event the plant experiences simultaneous losses of steam and feedwater flow and condenser availability and a complete loss of forced reactor coolant flow at the initiation of the event. The loss of forced reactor coolant flow results in an earlier reactor trip for the LOAC event compared to the reactor trip for the LOCV event. The earlier trip promotes a less severe P-T-S heat imbalance and results in a lower RCS peak pressure for the LOAC event.

There are no single failures that, when combined with LOAC event, result in consequences more severe than the LOCV event with respect to the RCS pressurization.

The fuel performance for the LOAC is no more limiting than that for the LOF event discussed in Subsection 15.3.1. The LOAC is the initiating event for the LOF so the fuel performance results of the LOF event are directly applicable to the LOAC event. The results of the LOAC event are identical to those of the LOF presented in Subsection 15.3.1 and are no more limiting with respect to RCS pressurization than the results of the LOCV event presented in Subsection 15.2.3.

15.2.6.4 Barrier Performance

For the LOAC event and the LOAC with a concurrent single failure, the RCS pressure remains below 110 percent of the RCS design pressure providing reasonable assurance of primary system integrity.

The maximum SG pressure also is below 110 percent of the SG design pressure.

15.2.6.5 Radiological Consequences

This event is bounded by the feedwater system piping failure event described in Subsection 15.2.8 for the radiological consequences.

15.2.6.6 Conclusions

For the LOAC event and the LOAC with a concurrent single failure, the RCS pressure remains below 193.34 kg/cm^{2}A (2,750 psia), which provides reasonable assurance of primary system integrity. The steam generator pressure remains below 92.83 kg/cm^{2}A

(1,320 psia), providing reasonable assurance of secondary system integrity. The minimum DNBR remains above 1.29, providing reasonable assurance of fuel cladding integrity.

15.2.7 Loss of Normal Feedwater Flow

15.2.7.1 Identification of Causes and Frequency Classification

The loss of normal feedwater flow (LFW) event may be initiated by losing two or more of the three operating main feedwater pumps or by a spurious signal being generated by the feedwater control system resulting in a closure of the feedwater control valve(s).

An LFW event is classified as an AOO. Each frequency condition is described in Subsection 15.0.0.1 and Table 15.0-5.

15.2.7.2 Sequence of Events and Systems Operation

LFW results in decreased water level and increased pressure and temperature in the steam generators. The RCS pressure and temperature also rise until a reactor trip occurs from either low steam generator water level or high pressurizer pressure. Assuming the SBCS is in the manual mode of operation, termination of main steam flow due to closure of the turbine stop valves following reactor trip temporarily causes steam generator and RCS pressurization. The decrease in core heat rate after insertion of the CEAs in combination with the MSSVs opening restores the RCS to a new steady-state condition. Auxiliary feedwater flow is automatically initiated on a low steam generator water level, providing reasonable assurance of sufficient steam generator inventory for core decay heat removal and cooldown to shutdown cooling entry conditions. The cooldown is operator-controlled using the SBCS and the condenser.

15.2.7.3 Core and System Performance

15.2.7.3.1 Evaluation Model

The evaluation model for the loss of condenser vacuum (LOCV) is applicable to this event (Subsection 15.2.3.3.1).

15.2.7.3.2 Input Parameters and Initial Conditions

The input parameters and initial conditions used to analyze the NSSS response to the loss of normal feedwater flow are bounded by those of an LOCV (Subsection 15.2.3.3.2).

15.2.7.3.3 Results

A LOCV event results in the termination of main steam flow prior to reactor trip in addition to the total loss of normal feedwater flow. This additional condition aggravates RCS pressurization and the impact on fuel performance by further reducing the rate of P-T-S heat transfer.

With respect to fuel performance, the DNBR increases during the LFW event due to the increasing pressure. The initial DNBR is also the minimum DNBR for the LFW event.

There are no concurrent single failures that, when combined with LFW, result in consequences more severe than the LOCV event with a single failure with respect to RCS pressurization and fuel performance.

Events with a loss of offsite power coincident with a turbine trip or a single failure result in an event with less severe consequences than an LOCV event with a loss of offsite power or with a loss of offsite power in combination with a single failure. The maximum RCS pressure and fuel performance for the LWF event are less limiting than the results for the LOCV event presented in Subsection 15.2.3.

15.2.7.4 Barrier Performance

For the loss of feedwater flow event and the loss of feedwater flow event with LOOP as well as these events in combination with a single failure, the RCS pressure remains below 110 percent of the RCS design pressure, providing reasonable assurance of primary system integrity. The maximum SG pressure also is below 110 percent of the SG design pressure.

15.2.7.5 Radiological Consequences

This event is bounded by the feedwater system piping failure event described in Subsection 15.2.8 for the radiological consequences.

15.2.7.6 Conclusions

For the loss of feedwater flow event and the loss of feedwater flow event with LOOP as well as these events in combination with a single failure, the RCS pressure remains below 193.3 kg/cm^{2}A (2,750 psia), providing reasonable assurance of primary system integrity. The steam generator pressure remains below 92.8 kg/cm^{2}A (1,320 psia), providing reasonable assurance of secondary system integrity. The minimum DNBR remains above 1.29, thus providing reasonable assurance of fuel cladding integrity.

15.2.8 Feedwater System Pipe Break Inside and Outside the Containment

15.2.8.1 Identification of Causes and Frequency Classification

The feedwater line break (FLB) accident is initiated by a break in the main feedwater system (MFS) piping. Depending on the break size and location and response of the MFS, the effects of a break can vary from a rapid heatup to a rapid cooldown of the NSSS. In the consideration of the possible effects, breaks are categorized as “small” if the associated discharge flow is within the excess capacity of the MFS, and other breaks are categorized as “large.” The main feedwater line is connected to downcomer nozzle and economizer nozzle where the break is assumed to occur. Break locations are identified with respect to the feedwater line reverse flow check valves, which are located between the steam generator feedwater nozzles and the containment penetrations. For a break upstream of the valves, the closure of these valves maintains the integrity of the steam generator by preventing reverse flow from the nearest steam generator.

Breaks upstream of the check valves can initiate one of the following transients. If the MFS is unavailable following the pipe failure, a total loss of normal feedwater flow (LOFW) occurs. With the MFS remaining in operation, no reduction in feedwater flow to the steam generators occurs for small breaks, while large breaks impose either a partial LOFW or a total LOFW, if the area is sufficient to discharge the entire feedwater pump flow capacity.

In addition to the possibility of partial or total LOFW events, breaks downstream of the check valves have the potential to establish reverse flow from the nearest steam generator (referred to as the “affected” steam generator) back to the break. Reverse flow occurs when the MFS is not operating subsequent to a pipe break or when the MFS is operating

but without sufficient capacity to maintain pressure at the break above the steam generator pressure. This analysis deals primarily with the breaks that develop reverse flow.

Depending on the enthalpy of the reverse flow and the affected steam generator's heat transfer characteristics, the reverse flow may induce either an RCS heatup or cooldown. Excessive heat removal through the break is not considered in this analysis because the cooldown potential is less than that of the steam line break accidents. The maximum break size is smaller for FLB accidents than for SLB accidents. In addition, SLBs have a greater potential for discharging high enthalpy fluid due to the location of steam piping above feedwater piping within the steam generator. An FLB could cause an instant reduction in feedwater flow unlike an SLB, which would result in a reduced heat removal capacity due to the lower liquid inventory. An FLB can cause a rapid depletion of affected steam generator liquid mass, reducing the heat transfer capability and causing a rapid RCS heatup and pressurization.

In compliance with GDC 17, which considers the accident with and without a LOOP, the limiting FLB analysis presented in this section assumes a LOOP coincident with a turbine trip following a reactor trip.

An FLB event is classified as a PA. Each frequency condition is described in Subsection 15.0.0.1 and Table 15.0-5.

15.2.8.2 Sequence of Accidents and Systems Operation

Table 15.2.8-2 presents the chronological sequence of accidents that occurs following an FLB until operator action is initiated.

A general description of the limiting FLB accident follows and assumes a break downstream of the check valves, inoperability of the MFS, and low enthalpy break discharge.

The loss of subcooled feedwater flow to both steam generators causes increasing steam generator temperatures and decreasing liquid inventories and water levels. The increasing secondary temperatures reduce the P-T-S heat transfer and force a heatup and pressurization of the RCS. The heatup becomes more severe as the affected steam generator experiences a further reduction in its heat transfer capability due to insufficient liquid inventory as the

break discharge continues. This initial sequence of accidents culminates with a reactor trip on high pressurizer pressure, low steam generator water level, or high containment pressure. RCS heatup can continue after trip due to a total loss of heat transfer in the affected steam generator as it empties. Eventually, the decreasing core power following the reactor trip reduces the core heat rate to the heat removal capacity of the unaffected steam generator.

15.2.8.3 Core and System Performance

15.2.8.3.1 Evaluation Model

Analysis of the FLB accident is performed using the CESEC-III program described in Subsection 15.0.2 along with several simplifying assumptions that, with respect to RCS overpressurization, conservatively model the break discharge flow and enthalpy and the affected steam generator water level and heat transfer. Sensitivity of the RCS overpressurization and DNBR to changes in various plant initial conditions is evaluated to provide reasonable assurance of acceptable results with the most adverse initial conditions for the FLB accident.

Blowdown of the steam generator nearest the feedwater line break is modeled assuming frictionless critical flow as calculated by the Henry-Fauske/Moody correlation. Although the enthalpy of the blowdown physically depends upon the location of the break relative to fluid conditions within the affected steam generator, it is assumed that saturated liquid is discharged until no liquid remains. With respect to RCS overpressurization, these assumptions result in conservatively high mass flow and conservatively low energy flow from the steam generator to the break, thereby minimizing the affected generator heat removal capacity.

In the case of a LOOP, no credit is taken for a low water level trip condition in the affected steam generator until the generator is emptied of liquid. This conservatively delays the time of the reactor trip, prolonging the RCS heatup and overpressurization.

An instantaneous closure of the turbine stop valve is assumed to occur at the time of the reactor trip. This maximizes the main steam system pressure resulting in RCS heatup. No credit is taken for the high containment pressure trip because it occurs after the high pressurizer pressure trip.

In order to determine the sensitivity of the RCS overpressurization to the affected steam generator heat transfer characteristics without implementing a detailed steam generator model, the effective heat transfer area is assumed to decrease linearly from the design value to zero as the steam generator liquid mass decreases from a selected value through a specified increment. The mass difference where heat transfer area decreases linearly from the design value to zero is defined as ΔM. Thus, the heat transfer area decreases rapidly as ΔM decreases. ΔM is assumed to be 0 kg (0 lbm) to conservatively apply the sensitivity study results.

Sensitivity studies are used to establish the most adverse set of initial operating and transient parameters with respect to RCS overpressurization. These parameters include initial pressurizer pressure, break size, initial reactor vessel flow, initial pressurizer liquid volume, initial core inlet temperature, and initial steam generator level. Among these parameters, initial pressurizer pressure, break size, and initial steam generator level are chosen for the sensitivity study in this analysis.

Table 15.0-4 is used to determine the limiting single failure of the FLB accident with a LOOP. There are no single failures identified in this table that can adversely impact the consequences (i.e., pressurization) associated with the FLB accident.

As a result of the evaluation method applied to the FLB accident analysis, mitigation of the RCS pressurization is associated with the pressurizer POSRVs, the reactor coolant flow, the MSSVs, and P-T-S system heat transfer. There are no credible failures that can degrade pressurizer POSRV or MSSV capacity and no any credible failures that can reduce steam flow to the affected steam generator. A decrease in P-T-S heat transfer due to reactor coolant flow coastdown can only be caused by a LOOP following a turbine trip. The failure of one auxiliary feedwater pump to start is assumed in order to minimize the long-term decay heat removal capability.

15.2.8.3.2 Input Parameters and Initial Conditions

The fuel integrity analysis uses the initial core inlet temperature of 296.11 °C (565 °F), and the initial pressurizer pressure of 163.46 kg/cm^2 (2,325 psia). All other initial conditions and assumptions are listed in Table 15.2.8-1.

A spectrum of break sizes is analyzed using the methodology described in the preceding paragraphs to determine the limiting break size. The results of this analysis are provided on Figure 15.2.8-1, which plots maximum primary pressure versus break size; as it illustrates, a 0.0093 m^2 (0.1 ft^2) break is determined to be limiting for DNBR.

15.2.8.3.3 Results

A separate FLB case is run to minimize the DNBR for this transient based on the break area for the lowest peak RCS pressure. The limiting break area for this case is 0.0093 m^2 (0.1 ft^2), and the minimum DNBR versus time, as shown on Figure 15.2.8-17, remains above 1.29 throughout the transient. No fuel cladding failure occurs.

15.2.8.4 Barrier Performance

15.2.8.4.1 Evaluation Model

The barrier performance evaluation for peak RCS pressure employs the same CESEC-III evaluation model as the core and system performance analysis described in Subsection 15.2.8.3.1.

15.2.8.4.2 Input Parameters and Initial Conditions

The input parameters and initial conditions used to analyze the NSSS response are discussed in Section 15.0. The initial conditions considered are given in Table 15.0-3. The initial conditions used in the analysis are shown in Table 15.2.8-1.

In addition to conservatively delaying steam generator low-level trip coincident with the assumed heat transfer degradation, the initial primary system pressure is adjusted within the range specified in Table 15.0-3 to achieve, where possible, a coincident reactor trip signal on high pressurizer pressure. This maximizes the primary pressurization potential of the accident by maximizing the primary system pressure at the time of the coincident reactor trip signal.

A spectrum of break sizes is analyzed using the methodology described in the preceding paragraphs to determine the limiting break size. The results of this analysis are provided on Figure 15.2.8-1, which plots maximum primary pressure versus break size. As is illustrated, the limiting break size is the 0.0372 m^2 (0.4 ft^2) break for overpressurization.

15.2.8.4.3 Results

The sequence of accidents and the dynamic response of the important NSSS parameters following the FLB with LOOP are provided in Table 15.2.8-2 and Figures 15.2.8-2 through 15.2.8-16, respectively.

A 0.0372 m^2 (0.4 ft^2) crack in the main feedwater line is assumed to instantaneously terminate feedwater flow to both steam generators and establish critical flow (about 1,814.37 kg/sec [4,000 lbm/sec] of saturated liquid) from the affected steam generator nearest the break. The absence of subcooled water and pressurization of the steam generators while the affected SG is empty reduces the P-T-S heat transfer rate, causing a reactor coolant temperature and pressure increase. Due to fuel temperature reactivity feedback during this period, the core power decreases slightly from 102.0 percent of design full power.

Due to the loss of feedwater and the increase in pressure in the SG, pressurizer pressure reaches the high pressurizer pressure condition at 26.38 seconds, and high pressurizer pressure trip occurs at 27.13 seconds. The trip breakers are opened at 27.23 seconds. At 27.50 seconds, the affected steam generator is assumed to instantaneously lose all heat transfer capability due to total depletion of its liquid inventory by boil-off and the break discharge flow. This initiates a rapid heatup and pressurization of the RCS and depressurization of the steam generators. The rate of RCS pressurization is further aggravated at 27.23 seconds when closure of the turbine stop valves leaves the pipe break as the only steam relief path. This reduces the energy flow from the unaffected steam generator to below that of the primary-to-secondary heat transfer rate. The resulting steam generator pressurization reduces the temperature difference between primary and secondary, further degrading heat transfer. The loss of reactor coolant flow following the loss of electrical power decreases the heat transfer coefficient of the coolant in the steam generator tubes.

The high insurge flow to the pressurizer raises the pressurizer pressure to the pressurizer POSRV setpoint at 28.37 seconds. The RCS pressure continues to increase to a maximum of 196.57 kg/cm^2A (2,795.88 psia) at 29.43 seconds.

The rate of RCS heatup decreases subsequent to core heat flux decay and causes the primary system pressure to drop. The unaffected generator pressure is forced to reach a

maximum value of 89.17 kg/cm^{2}A (1,268.30 psia). The P-T-S heat transfer mismatch is reduced sufficiently by 33.25 seconds to allow closure of the pressurizer POSRVs. The RCS experiences a cooldown under the influence of steam blowdown through the affected steam generator to the break.

Main steam isolation is initiated at 163.05 seconds on low steam generator pressure, which closes the main steam isolation valves decoupling the unaffected steam generator from the affected steam generator and the break. The unaffected steam generator repressurizes, thereby reducing heat transfer and eventually causing a primary system heatup. With the MSSVs of the unaffected steam generator open at 392.80 seconds, the primary-to-secondary heat imbalance is eliminated. Thereafter, the NSSS enters into a quasi-steady-state with a very gradual cooldown and depressurization due to decreasing core decay heat, cycling of the MSSVs, and auxiliary feedwater flow, which is initiated at 116.09 seconds maintaining an adequate liquid inventory within the unaffected steam generator for heat removal. Thirty minutes after the initiation of the accident, the operator initiates a controlled cooldown to shutdown cooling using the atmospheric dump valves.

The low steam generator water level trip is a PPS trip function provided with each steam generator. The trip signal is produced using the wide range steam generator level sensors that are seismically and environmentally qualified in accordance with the methodology discussed in Section 3.11.

Since steam generator pressure is increasing in the time period up to and past the time of reactor trip and the time of peak RCS pressure, there is no tendency for level swell in the steam generator to occur or to affect the low water level signal. Consequently, there are no level fluctuations that will have an adverse influence on the instrumentation. The 28.4 percent wide range level corresponding with the minimum analysis setpoint of the RPS is a conservative reactor trip setpoint for the FLB accident.

The influence of offsite power and credit for the harsh environment low steam generator water level trip setpoint in the affected steam generator result in a substantial reduction of the peak RCS pressure from 196.57 kg/cm^{2}A (2,795.88 psia) to 187.34 kg/cm^{2}A (2,664.57 psia) and an increase in peak steam generator pressure from 89.17 kg/cm^{2}A (1,268.30 psia) to 91.0 kg/cm^{2}A (1,294.32 psia). Both effects are due to the continually forced circulation in the RCS and delay of dryout in the affected steam generator. The later steam generator

dryout also delays backflow of steam from the unaffected steam generator into the affected steam generator until after the core power is decreased by the reactor trip.

The RCS pressure response and the responses of parameters following the FLB with offsite power are provided on Figures 15.2.8-18 through 15.2.8-23. These figures show a substantial change from the case with loss of offsite power.

Instantaneous termination of feedwater flow to both steam generators, along with a 0.0372 m^2 (0.4 ft^2) break, increases steam generator pressure as the steam generators boil off liquid inventory. The absence of subcooled water and the pressurization of the steam generators reduce the P-T-S heat transfer, which increases primary temperature and pressure.

The turbine stop valves close simultaneously with reactor trip, causing the steam generator pressures and the RCS temperatures and pressures to increase more rapidly until the MSSVs open at 24.55 seconds and the pressurizer POSRVs open at 24.80 seconds. The peak RCS pressure is 187.34 kg/cm^2A (2,664.57 psia) at 25.18 seconds, and the peak steam generator pressure is 91.0 kg/cm^2A (1,294.32 psia) at 26.60 seconds.

Pressure and temperature decrease, trailing the decrease in reactor power. There is a momentary increase in RCS temperatures and pressures when the affected steam generator reaches the dryout condition at 40.14 seconds. The reactor power is low at this time, and the loss of heat transfer in the affected steam generator is inconsequential.

During the first 30 minutes following the initiation of this FLB accident, mass releases from the system amount to 72,666 kg (160,200 lbm) and 180,409 kg (239,000 lbm) of steam, which is assumed to be released to the atmosphere and into the containment, respectively. Between 30 minutes and 8 hours, the steam releases are 970,688 kg (2,140,000 lbm).

Without credit for offsite power, the maximum RCS pressure is slightly above 110 percent of design, which is less than 120 percent of design. This meets the overpressurization acceptance criteria for very low probability accidents.

With credit for offsite power, the maximum RCS pressure and the maximum steam generator pressures remain below 110 percent of design pressure.

Normally, the RCP seal is cooled by (1) seal injection water from chemical and volume control system (CVCS) and (2) the component cooling water system through a high-pressure seal cooler. The evaluations of the reactor coolant pumps presented in Subsections 5.4.1.2 and 5.4.1.3 show that the integrity of RCPs is maintained with a loss of CCW for at least 30 minutes.

15.2.8.5 Radiological Consequences

The radiological consequences are performed to determine EAB, LPZ, MCR, and TSC doses due to main feedwater line break (FLB) accident using the AST methodology, TEDE dose criteria, guidance in SRP 15.0.3, and the plant-specific bounding design information applicable to the APR1400.

15.2.8.5.1 Evaluation Model

The following transport models of radioactive materials are applied to evaluate radiological consequences due to an FLB accident.

Release via the Containment

The secondary coolant is released from the affected SG into the containment building through the feedwater line break and from there is released directly to the environment as a result of the containment leakage. The RCS fluid is released to the IRWST through the pilot operated safety and relief valve (POSRV) or reactor coolant gas vent system (RCGVS) and from there, released directly to the environment due to the containment leakage. The flashing fraction for radioiodine is conservatively assumed to be 1.

Release via Affected Steam Generator

At the beginning of the FLB event, one-half of the total P-T-S leakage entering the affected SG is released to the environment through the MSSVs. When the MSIV is closed due to low SG pressure after closure of MSSVs, P-T-S leakage is released to the containment through the broken feedwater line of the affected SG. It is conservatively assumed that the P-T-S leakage is released with no mitigation or dilution. During the period of SG dryout due to the FLB event, the radioiodine in one-half of the total P-T-S leakage entering

the affected SG is assumed to flash to vapor and is leaked into the containment through the break in the feedwater line without crediting any holdup in the affected SG.

Release via the Unaffected Steam Generator

During the first 30 minutes of the FLB event, the iodine activity in the P-T-S leakage is mixed with the SG liquid and assumed to become vapor at a rate that is a function of the steaming rate and an iodine partition coefficient, which is released through the MSSVs of the unaffected SG. At 30 minutes, operator action is taken to open the unaffected SG ADV to cool down the RCS. The radioactivity in the bulk water is assumed to become vapor at a rate that is the function of the steaming rate and the partition coefficient. The steam release from the unaffected SG continues for 8 hours until the shutdown cooling system is aligned to dissipate heat.

Release via the Condenser

Prior to the LOOP, the contaminated secondary steam in the unaffected and affected SGs is released to the condenser. The steam release to the condenser is not considered in the post-FLB activity release to the environment due to the tortuous path to the condenser through the turbines and moisture separators, and condenser hold-up time.

Figure 15A-2 in Appendix 15A shows the leakage paths and transport of the activity released to environment, MCR, and TSC during an FLB event.

15.2.8.5.2 Input Parameters and Initial Conditions

The design basis FLB accident is analyzed using a conservative set of assumptions based on NRC RG 1.183 and the APR1400 design inputs. Input parameter values used for an FLB radiological consequence evaluation are presented in Table 15.2.8-3.

No fuel damage is postulated for the FLB accident. The iodine activity in the RCS is assumed to be the maximum coolant activity allowed by the Technical Specifications including effect of event-generated iodine spike that increases the equilibrium fission product activity release rate from fuel by a factor of 500. The event-generated iodine spike case is considered to evaluate the resulting EAB, LPZ, MCR, and TSC doses because:

a. The iodine release due to the event-generated iodine spike by a factor of 500 is higher than the pre-accident iodine spike of 2.22×10^6 Bq/g (60 μCi/g).

b. The offsite allowable dose limits for the event-generated iodine spike are limiting in comparison to the offsite dose limits for the pre-accident iodine spike per SRP 15.0.3, Table 1.

It is assumed that the primary system transient associated with the FLB causes an iodine spike in the primary system. The increase in primary coolant iodine concentration is estimated using a spiking model that assumes that the iodine release rate from the fuel rods to the primary coolant increases to a value 500 times greater than the release rate corresponding to the equilibrium primary coolant iodine concentration of 3.7×10^4 Bq/g (1.0 μCi/g) DE I-131. The assumed iodine spike duration is 8 hours. The iodine activity released from the fuel to RCS is assumed to be mixed instantaneously and homogeneously with the primary coolant. The event-generated iodine spike isotopic iodine activity appearance rates in the RCS are calculated in Table 15A-7.

The maximum RCS noble gas concentration is 2.15×10^7 Bq/g (580 μCi/g) DE Xe-133.

The RCS is assumed to leak into both the affected and unaffected SGs at a total P-T-S leak rate of 2.27 L/min (0.6 gpm). It is assumed that the P-T-S leakage into the SGs continues until the primary system pressure is less than the secondary system pressure, or until the temperature of the leakage is less than 100 °C (212 °F) and shutdown cooling is in operation. The RCS is assumed to leak into the SGs for 8 hours until the shutdown cooling system is initialized.

The chemical forms of iodine released from the SGs to the environment are assumed to be 97 percent elemental and 3 percent organic.

All noble gas radionuclides released from the primary system via the P-T-S leak are released to environment without reduction or mitigation.

The χ/Q values used in the analysis for EAB, LPZ, MCR, and TSC are described in Subsection 2.3.4 and are provided in Tables 2.3-2 through 2.3-12; the breathing rates are given in Table 15A-11.

15.2.8.5.3 Results

The radiological consequences due to FLB accident are presented in Table 15.2.8-4. The results of the FLB accident analyses indicate that the EAB and LPZ doses due to an FLB accident with an event-generated iodine spike are within their allowable dose criteria limits, which is 10 percent of the 10 CFR 50.34(a)(1) value as specified in SRP 15.2.8. The MCR and TSC doses are also within the dose limit in GDC 19.

15.2.8.6 Conclusions

The limiting overpressurization case of the FLB accident (0.0372 m^2 [0.4 ft^2] break) assumes a coincident LOOP, which is considered a very low probability accident, and produces an NSSS transient with a maximum pressure slightly above 110 percent of the design 193.34 kg/cm^2A (2,750 psia). This is less than 120 percent (210.92 kg/cm^2A [3,000 psia]) of design in the RCS and less than 110 percent (92.83 kg/cm^2A [1,320 psia]) of design in the steam generators. This meets the overpressurization acceptance criteria for very low probability accidents. With credit for offsite power, the maximum RCS pressure and the maximum steam generator pressures remain below 110 percent of design pressure.

In a case run specifically to minimize DNBR, the minimum DNBR is shown to remain above 1.29. Therefore, there is no fuel cladding failure.

The results of the FLB accident analyses indicate that the EAB, LPZ, MCR, and TSC doses due to an FLB accident with an event-generated iodine spike are within their allowable dose criteria limits.

15.2.9 Combined License Information

No COL information is required with regard to Section 15.2.

Table 15.2.3-1

Sequence of Events for an LOCV

Time (sec)	Event	Setpoint or Value
0.0	Loss of condenser vacuum	—
6.0	A loss of offsite power occurred	—
6.67	CPC low shaft speed trip condition reached, %	94.83
7.02	CPC low shaft speed trip signal generated	—
7.12	Trip breakers open	—
7.20	First MSSV open, kg/cm^2A (psia)	86.88 (1,235.66)
8.46	Pressurizer POSRVs opening setpoint reached, kg/cm^2A (psia)	177.13 (2,519.4)
8.63	Second MSSV open, kg/cm^2A (psia)	89.14 (1,267.9)
9.33	Maximum RCS pressure, kg/cm^2A (psia)	193.0 (2,745)
10.70	Third MSSV open, kg/cm^2A (psia)	90.97 (1,293.9)
10.79	Maximum steam generator pressure, kg/cm^2A (psia)	91.0 (1,294.04)
12.56	Pressurizer POSRVs closure, kg/cm^2A (psia)	159.32 (2,266)
24.54	Third MSSV close, kg/cm^2A (psia)	81.87 (1,164.51)
40.50	Second MSSV close, kg/cm^2A (psia)	80.23 (1,141.11)
40.80	Auxiliary feedwater actuation signal generated, %WR	19.9
75.45	First MSSV close, kg/cm^2A (psia)	78.19 (1,112.09)
102.25	Auxiliary feedwater flow initiated, liter/min (gpm)	2,460.52 (650)
1,800.00	Operator initiates plant cooldown	—

Table 15.2.3-2

Initial Conditions for an LOCV

Parameter	Value
Initial core power level, MWt	4,062.66
Initial core inlet coolant temperature, °C (°F)	287.8 (550)
Initial core mass flow, 10^6 kg/hr (10^6 lbm/hr)	73.3 (161.6)
Initial pressurizer pressure, kg/cm^{2}A (psia)	152.92 (2,175)
Initial pressurizer water volume, m^3 (ft^3)	13.56 (478.8)
Initial steam generator water level, %WR	65.0
CEA worth for trip, 10^{-2} $\Delta\rho$	−8.0
Moderator temperature coefficient, 10^{-4} $\Delta\rho$/°C ($\Delta\rho$/°F)	0.0 (0.0)
Doppler reactivity	Least negative

Table 15.2.8-1

Initial Conditions for the Limiting Case Feedwater Line Break

Parameter	Assumed Value
Initial core power, MWt	4,062.66
Initial core inlet temperature, °C (°F)	296.11 (565)
Initial core mass flow rate, 10^6 kg/hr (10^6 lbm/hr)	69.44 (153.52)
Initial pressurizer pressure, kg/cm^{2}A (psia)	159.60 (2,270)
Fuel gas gap heat transfer coefficient, kcal/hr-m^2-°C (Btu/hr-ft^2-°F)	3,156.82 (647)
Pressurizer pilot operated safety relief valves rated flow rate per valve, kg/hr (lbm/hr)	244,940 (540,000)
Initial pressurizer liquid volume, m^3 (ft^3)	39.91 (1,409.44)
Initial steam generator inventory, kg (lbm)	97,046 (213,950)
Initial feedwater enthalpy, kcal/kg (Btu/lbm)	233.06 (419.5)
Steam bypass control system	Manual
Normal onsite or offsite electrical power after turbine trip	Unavailable
Feedwater pipe break area, m^2 (ft^2)	0.0372 (0.4)
CEA worth at trip, 10^{-2} $\Delta\rho$	−8.0
Moderator temperature coefficient, 10^{-4} $\Delta\rho$/°C ($\Delta\rho$/°F)	0.0 (0.0)
Doppler reactivity	Least negative

Table 15.2.8-2 (1 of 2)

Sequence of Events for the Limiting Case Feedwater Line Break

Time (sec)	Accident	Setpoint or Value
0.0	Break in the main feedwater line, m^2 (ft^2)	0.0372 (0.4)
0.0	Instantaneous loss of all feedwater flow to both steam generators	—
0.0	Instantaneous development of critical flow from the affected steam generator to the break	—
26.38	Pressurizer pressure reached to analysis setpoint, kg/cm^2A (psia)	173.17 (2,463)
27.13	High pressurizer pressure trip signal generated	—
27.23	Trip breakers open	—
27.23	Instantaneous closure of the turbine stop valves	—
27.23	Loss of offsite power	—
27.50	Instantaneous loss of all heat transfer to the affected steam generator	—
28.37	Pressurizer POSRVs opening setpoint reached, kg/cm^2A (psia)	177.13 (2,519.40)
29.39	Main steam safety valves open, unaffected loop, kg/cm^2A (psia)	86.88 (1,235.66)
29.43	Maximum reactor coolant system pressure, kg/cm^2A (psia)	196.57 (2,795.88)
30.69	Maximum pressurizer surge line flow, kg/sec (lbm/sec)	1,260.56 (2,779.05)
33.25	Pressurizer POSRVs closing setpoint reached, kg/cm^2A (psia)	159.32 (2,266)
33.37	Maximum steam generator pressure, kg/cm^2A (psia)	89.17 (1,268.3)

Table 15.2.8-2 (2 of 2)

Time (sec)	Accident	Setpoint or Value
54.54	Main steam safety valves close, unaffected loop, kg/cm^2A (psia)	78.19 (1,112.09)
54.64	Steam generator water level reaches auxiliary feedwater actuation analysis setpoint in the unaffected generator, %WR	5
116.09	Auxiliary feedwater flow initiated to the unaffected steam generator, L/min (gpm)	2,460.52 (650)
156.60	Steam generator pressure reaches main steam isolation signal analysis setpoint, kg/cm^2A (psia)	52.73 (750)
163.05	Main steam isolation valves closed	—
168.05	Main feedwater isolation valves closed	—
392.80	Main steam safety valves reopened, kg/cm^2A (psia)	86.88 (1,235.66)
455.80	Pressurizer POSRVs opening setpoint reached, kg/cm^2A (psia)	177.13 (2,519.40)
458.32	Pressurizer POSRVs closing setpoint reached, kg/cm^2A (psia)	159.32 (2,266)
1,800.00	Operator opens the atmospheric steam dump valves to begin plant cooldown to shutdown cooling	—

Table 15.2.8-3 (1 of 3)

Parameters Used in Evaluating the Radiological Consequences of a Feedwater Line Break

Parameter	Value
Source Terms	
Reactor Core Power Level	4,062.66 MWt
Percent of Fuel Assumed to Experience Departure from Nucleate Boiling (DNB)	0 %
Percent of Fuel Assumed to Melt	0 %
Initial RCS Mass	288,086 kg (635,120 lbm)
Initial Steam Generator Liquid Mass	89,721 kg/SG (197,802 lbm/SG)
Initial RCS Iodine Specific Activity	3.7×10^4 Bq/g (1.0 μCi/g) DE I-131
Initial Secondary Liquid Iodine Specific Activity	3.7×10^3 Bq/g (0.1 μCi/g) DE I-131
Initial RCS Noble Gas Specific Activity Limit	2.15×10^7 Bq/g (580 μCi/g) DE Xe-133
Event-generated Iodine Spiking Factor	500
Duration of Event-generated Iodine Spike	8 hrs
Chemical Forms of Iodine Released from the SG to the Environment	97 % elemental and 3 % organic

Table 15.2.8-3 (2 of 3)

Parameter	Value
Secondary System Activity Transport Model	
Integrated P-T-S leakage 0 – 2 hrs 0 – 8 hrs	 272 kg (601 lbm) 818 kg (1,803 lbm)
Release from affected SG through MSSV Total liquid mass Duration of release	 2,810 kg (6,200 lbm) 20 secs
Total mass released from affected SG to containment through the break in the feedwater line (0 – 0.5 hrs)	1,080 kg (239,000 lbm)
Total steam mass release from intact SG 0 – 0.5 hrs 0.5 – 2 hrs via ADV 2 – 8 hrs via ADV	 69,800 kg (154,000 lbm) 481,000 kg (1,060,000 lbm) 490,000 kg (1,080,000 lbm)
FLB isolation time	30 minutes
Primary-to-secondary Leakage Rate through SGs	2.27 L/min (0.6 gpm)
Termination of intact SG P-T-S leak	8 hrs
SG liquid iodine partition coefficient	100
Letdown system flow rate	18,100 kg/hr 10^4 (39,842 lbm/hr)
RCS Fluid Released to IRWST	1,660 kg (3,651 lbm)
Duration of RCS Fluid Released to IRWST	1 min

Table 15.2.8-3 (3 of 3)

Parameter	Value
MCR and TSC Model Parameters	
Envelope Volume	5,663 m^3 (200,000 ft^3)
Normal Ventilation Flow Rate (unfiltered)	105 m^3/min (3,700 cfm)
Emergency Ventilation Makeup Rate (filtered)	105 m^3/min (3,700 cfm)
Emergency Ventilation Recirculation Flow Rate (filtered)	122 m^3/min (4,300 cfm)
Emergency HVAC Delay Time	5 min
Emergency Ventilation Charcoal Filter Efficiency (elemental and organic iodine removal)	99 %
Emergency Ventilation HEPA Filter Efficiency (particulate removal)	99 %
Unfiltered Inleakage	8.50 m^3/min (300 cfm)
Occupancy Factors 0 – 24 hrs 24 – 96 hrs 96 – 720 hrs	 100 % 60 % 40 %
Onsite χ/Qs	See Tables 2.3.2 ~ 2.3.12
Offsite Model Parameters	
χ/Qs	See Table 2.3-1
Breathing Rate	See Table 15A-11
Dose Conversion Factors	See Table 15A-10

Table 15.2.8-4

Radiological Consequences of Feedwater Line Break

Post-FLB Activity Release Path	TEDE Dose (mSv)		
	MCR and TSC	EAB	LPZ
Containment Leakage	6.78E-03	7.17E-03	3.03E-02
P-T-S Iodine Release	1.48E-01	2.80E-01	1.37E-01
P-T-S Noble Gas Release (Unaffected SG)	6.63E-03	5.98E-03	4.28E-03
P-T-S Noble Gas Release (Containment)	9.22E-08	1.20E-07	4.09E-07
Secondary Liquid Iodine Release	6.95E-02	1.29E-01	5.08E-02
External Cloud	6.88E-01	0.00E+00	0.00E+00
Containment Shine	0.00E+00	0.00E+00	0.00E+00
Emergency Ventilation Filter Shine	0.00E+00	0.00E+00	0.00E+00
Total	9.19E-01	4.22E-01	2.22E-01
Allowable TEDE Limit	5.00E+01	2.50E+01	2.50E+01

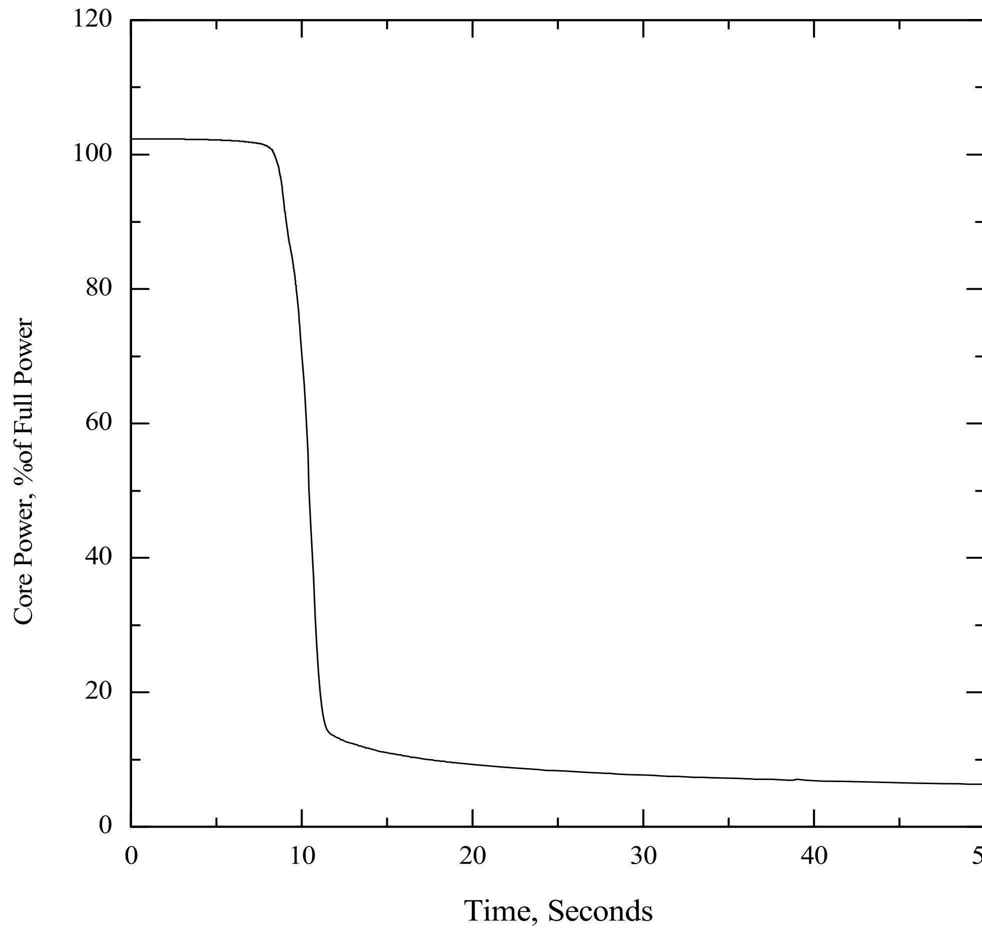

Figure 15.2.3-1 Loss of Condenser Vacuum: Core Power vs. Time

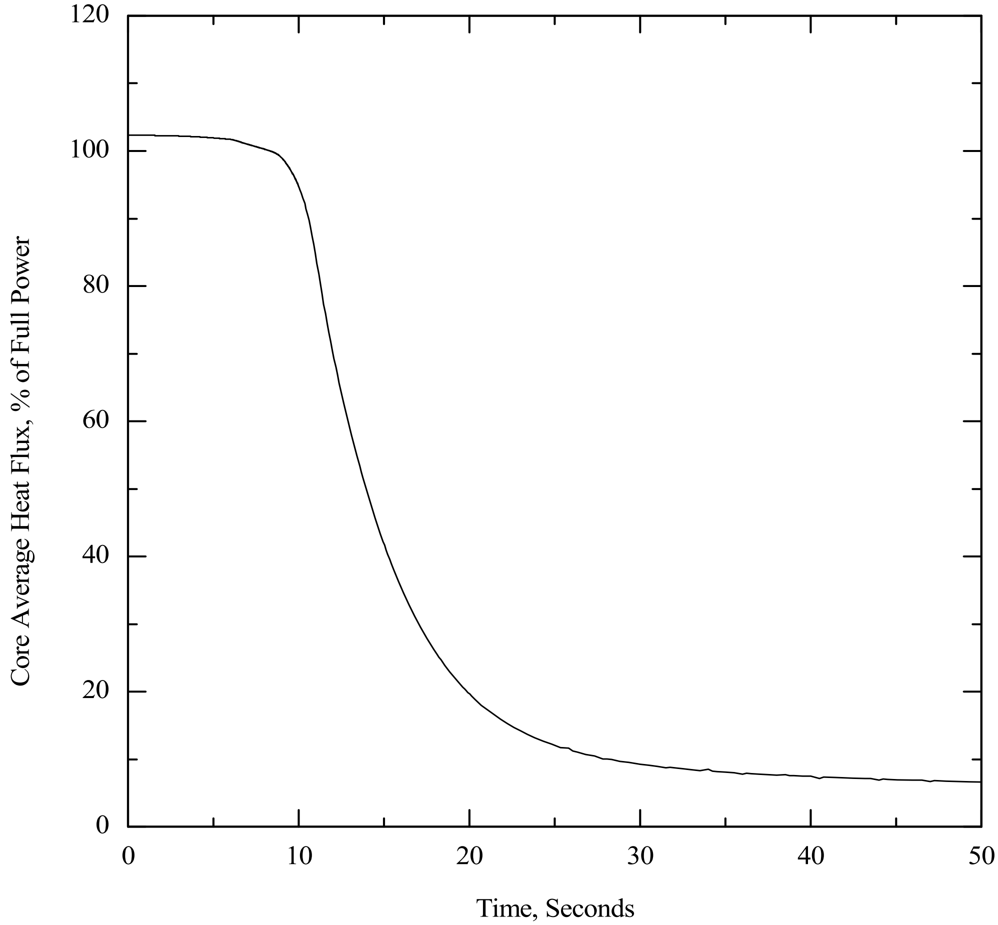

Figure 15.2.3-2 Loss of Condenser Vacuum:Core Average Heat Flux vs. Time

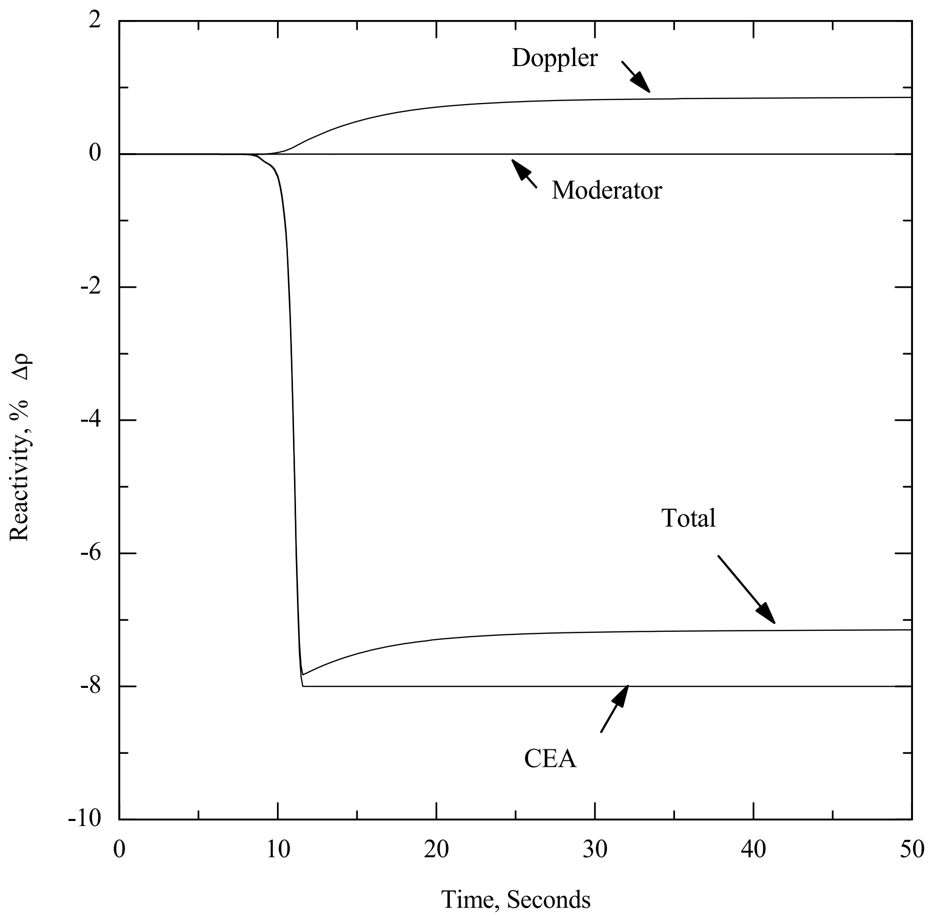

Figure 15.2.3-3 Loss of Condenser Vacuum: Reactivity vs. Time

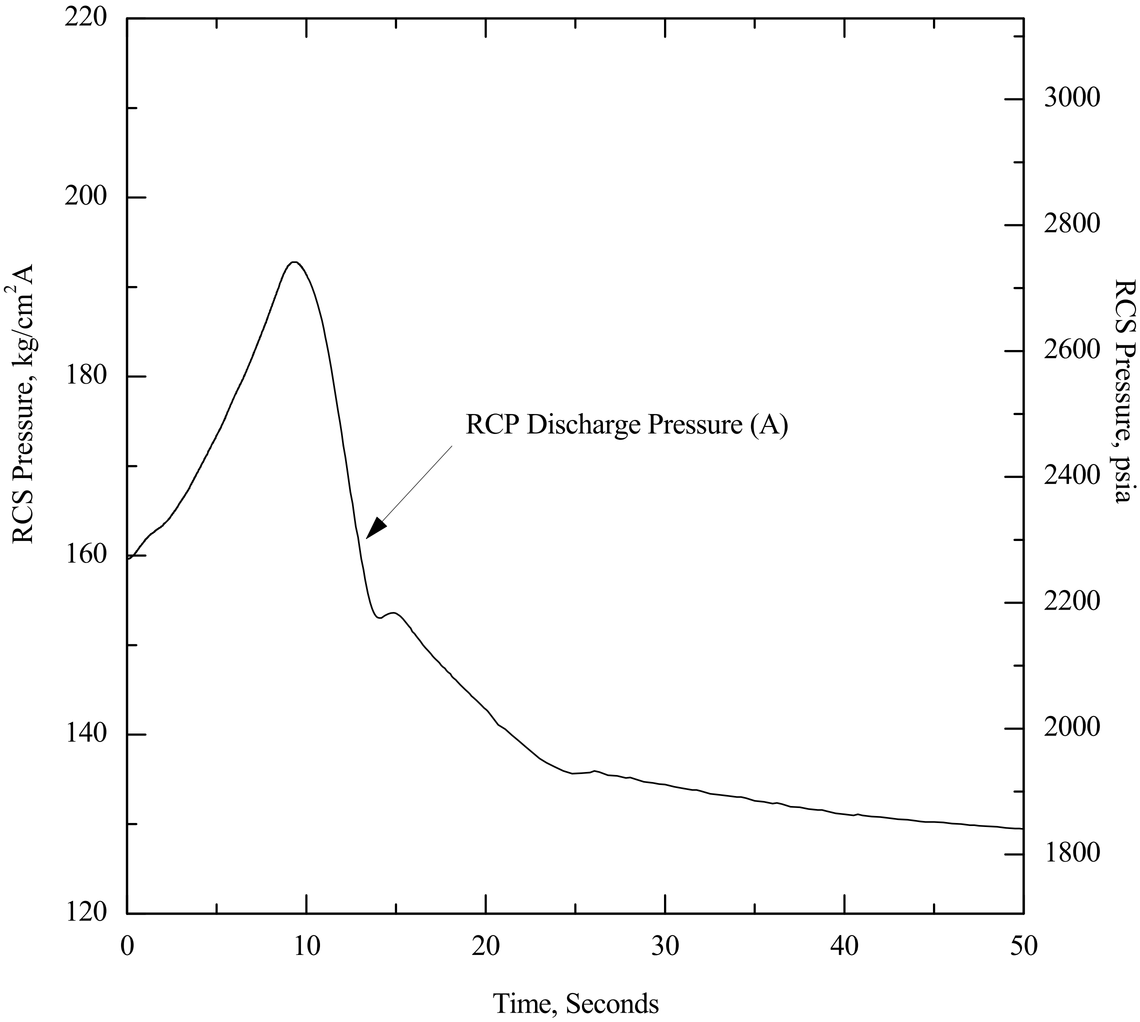

Figure 15.2.3-4 Loss of Condenser Vacuum: RCS Pressure (A) vs. Time

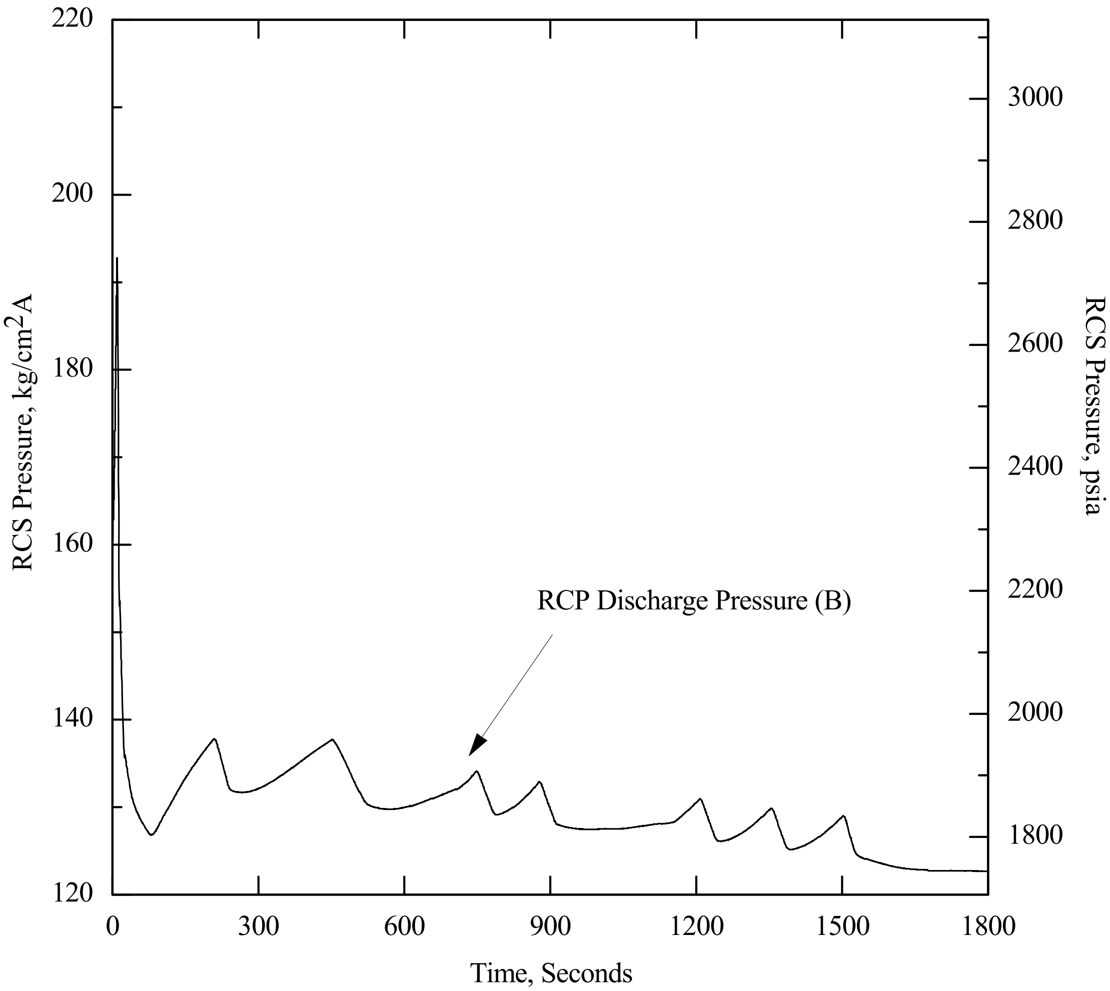

Figure 15.2.3-5 Loss of Condenser Vacuum: RCS Pressure (B) vs. Time

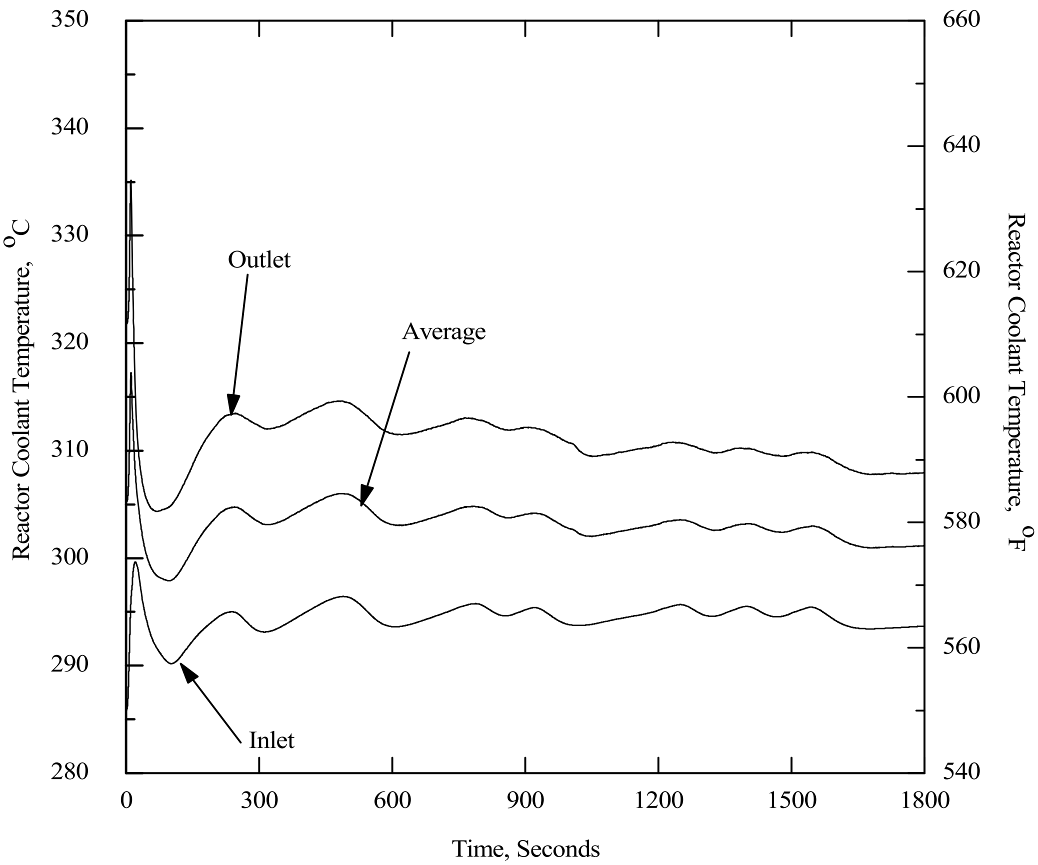

Figure 15.2.3-6   Loss of Condenser Vacuum: Reactor Coolant Temperatures vs. Time

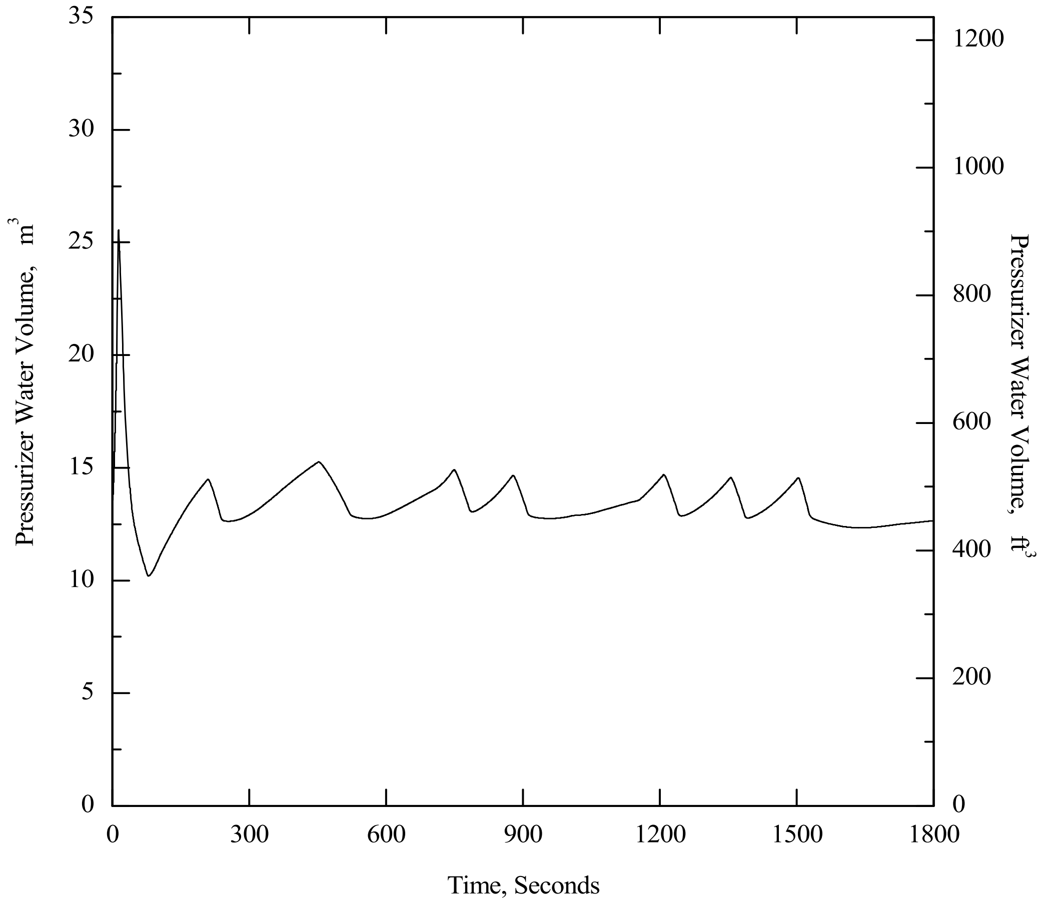

Figure 15.2.3-7 Loss of Condenser Vacuum: Pressurizer Water Volume vs. Time

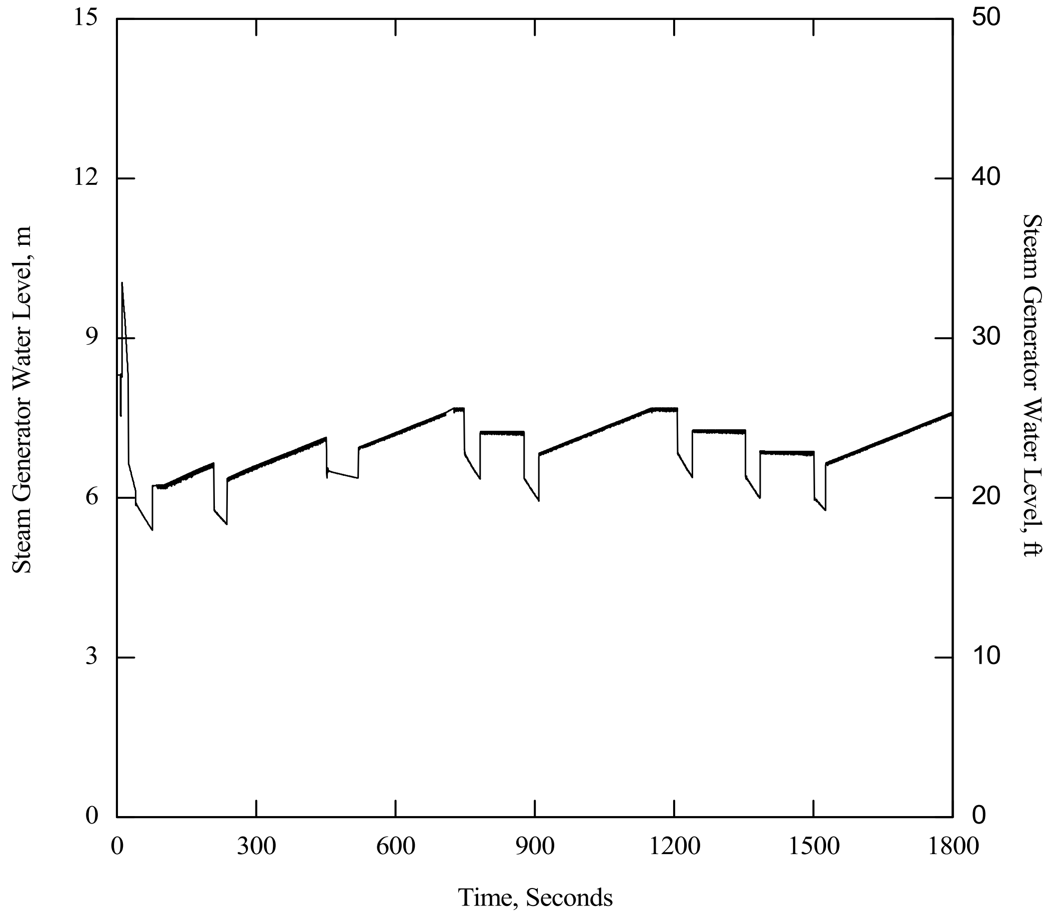

Figure 15.2.3-8 Loss of Condenser Vacuum: Steam Generator Water Level vs. Time

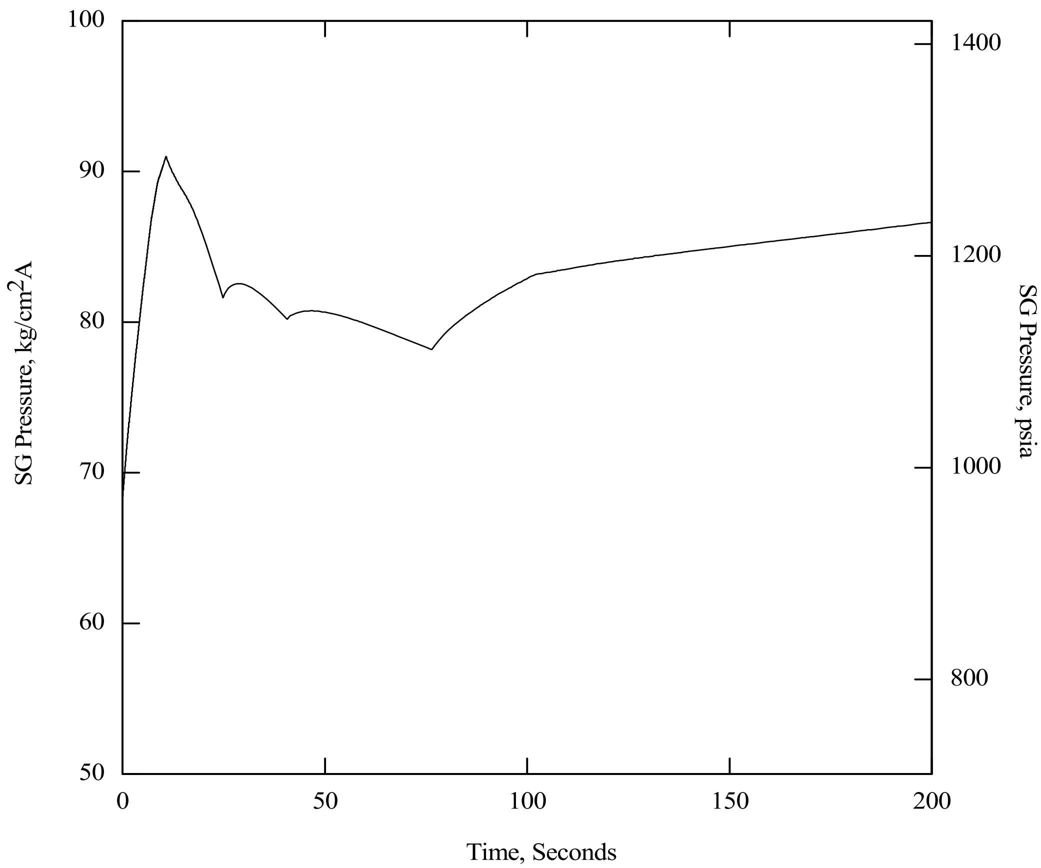

Figure 15.2.3-9 Loss of Condenser Vacuum: Steam Generator Pressure (A) vs. Time

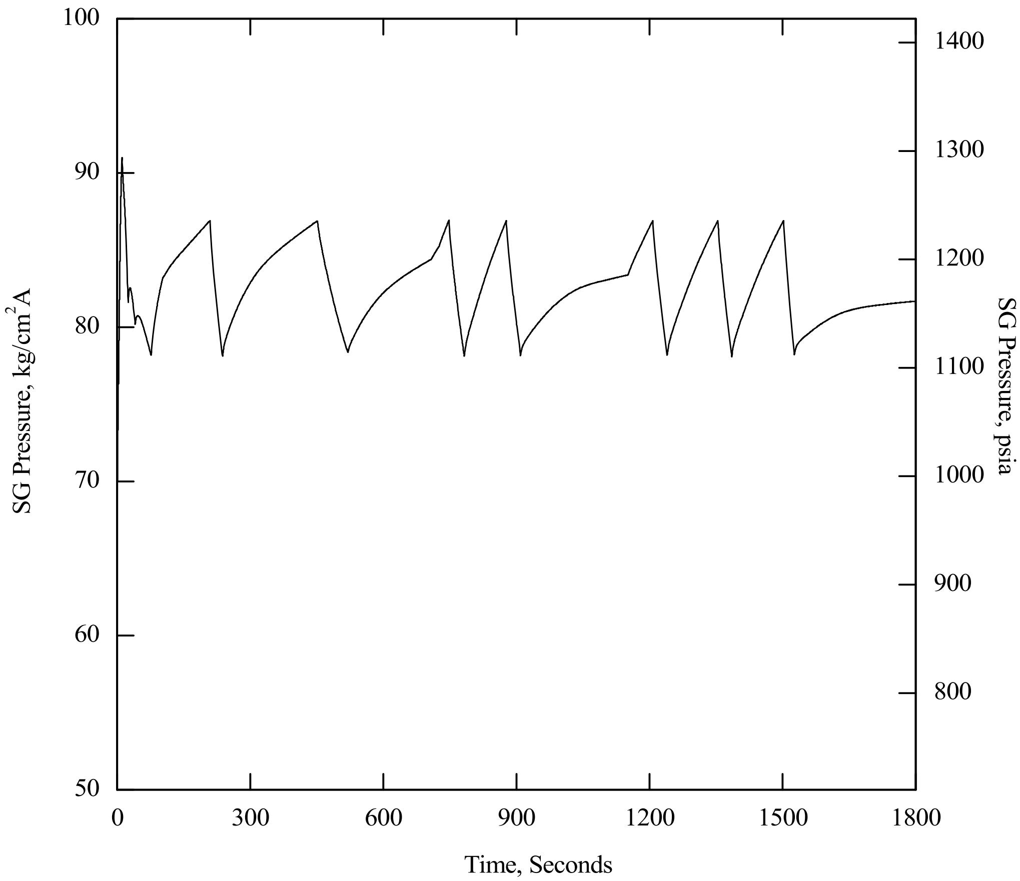

Figure 15.2.3-10 Loss of Condenser Vacuum:Steam Generator Pressure (B) vs. Time

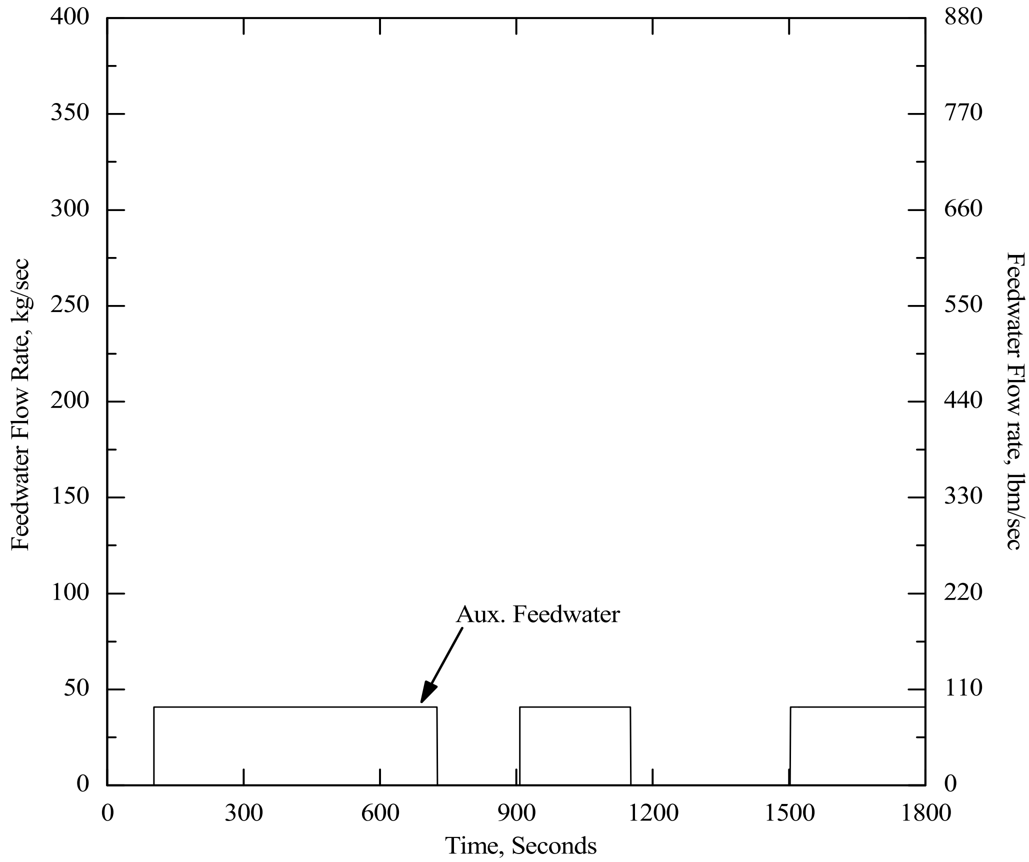

Figure 15.2.3-11 Loss of Condenser Vacuum:Feedwater Flow Rate vs. Time

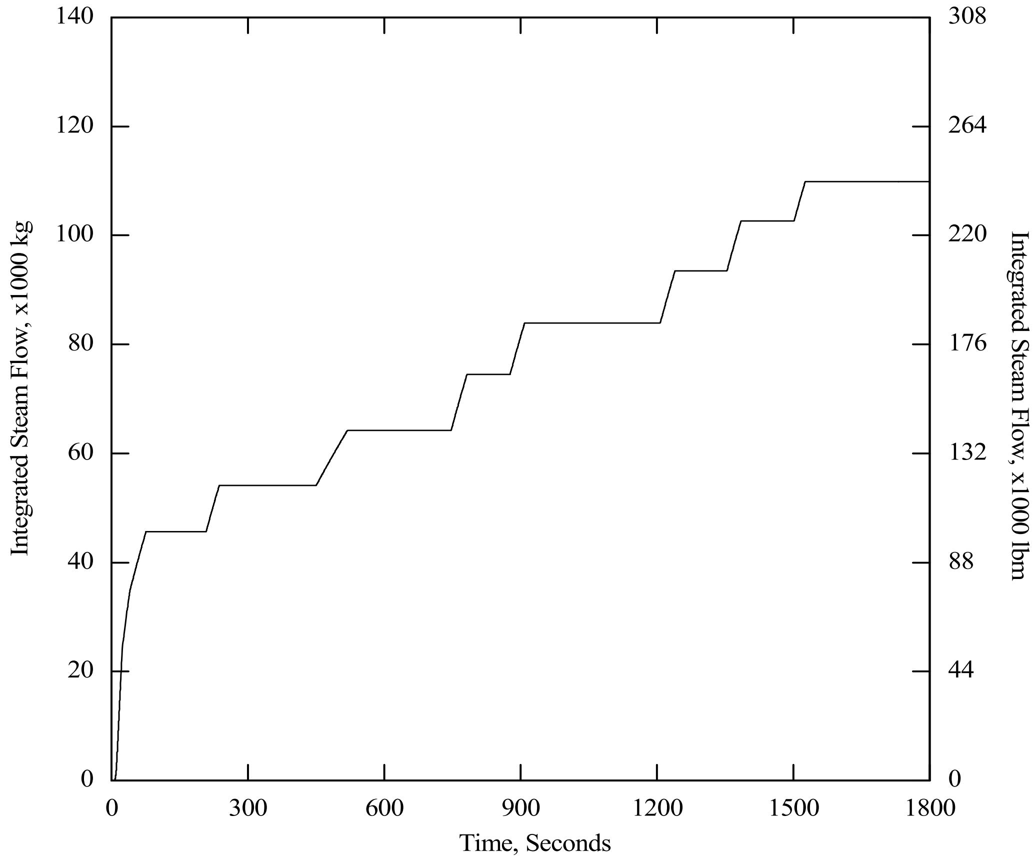

Figure 15.2.3-12 Loss of Condenser Vacuum:Integrated Steam Flow vs. Time

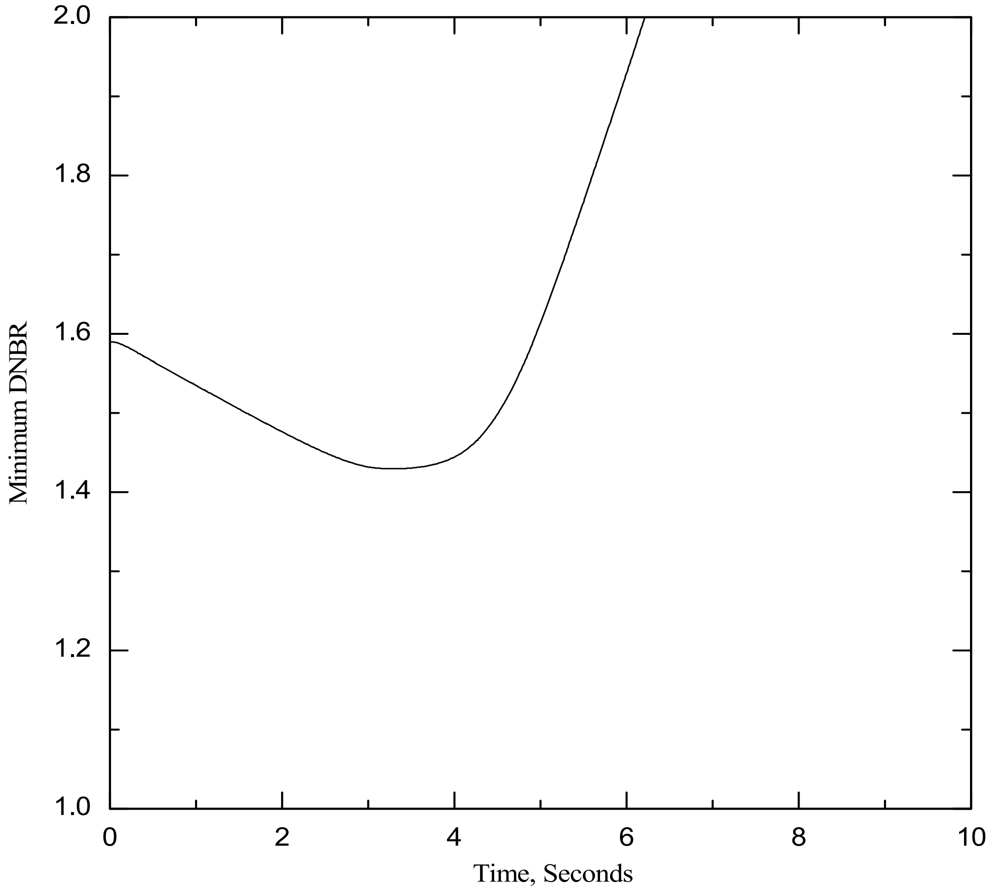

Figure 15.2.3-13 Loss of Condenser Vacuum: Minimum DNBR vs. Time

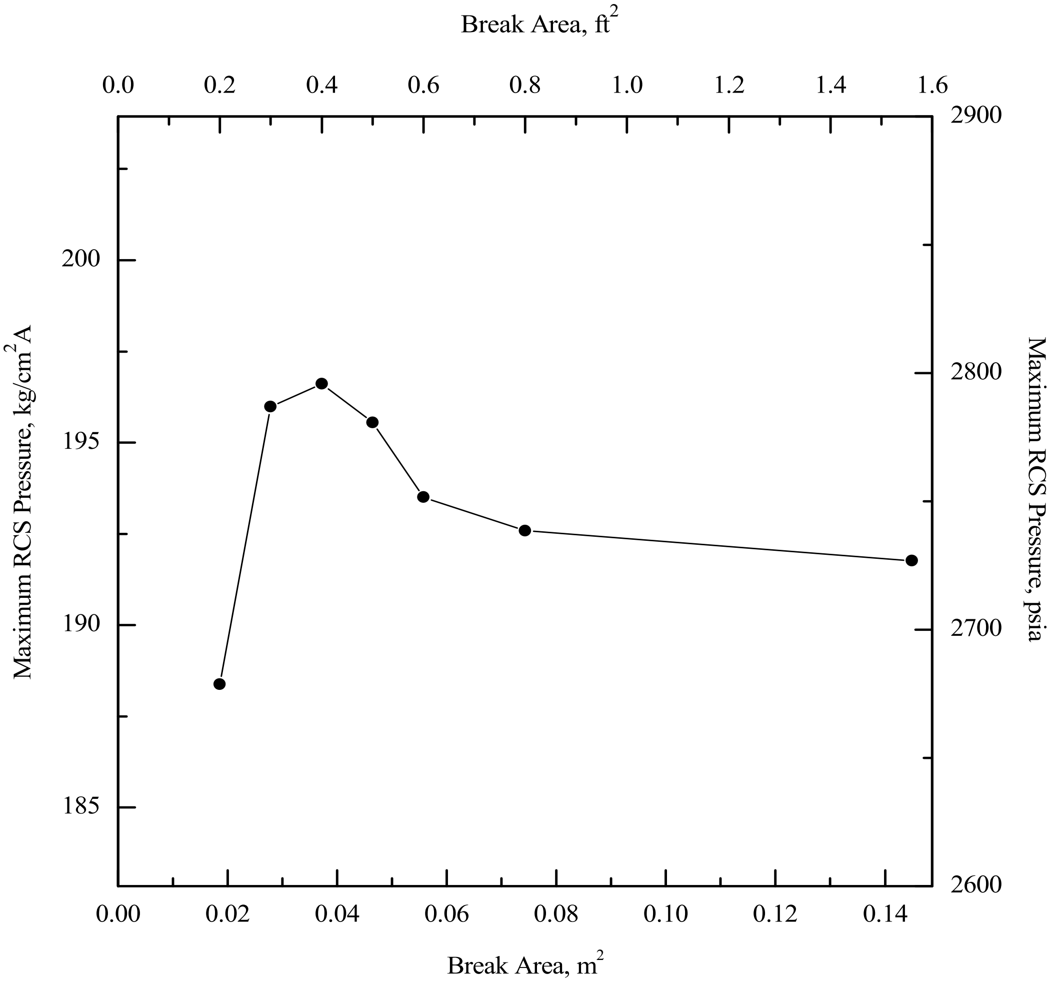

Figure 15.2.8-1 Main Feedwater Line Break With Concurrent LOOP: Maximum RCS Pressure vs. Break Area

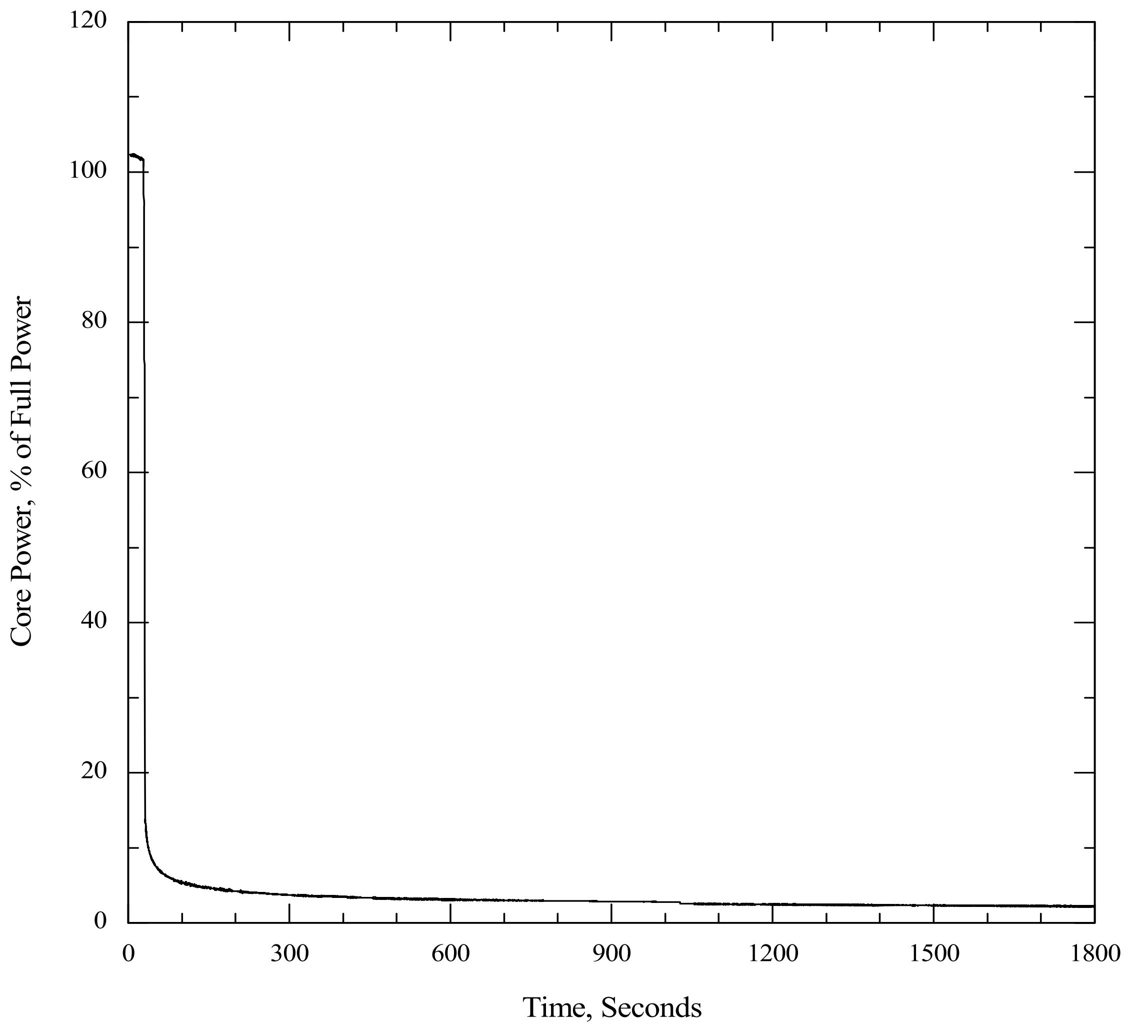

Figure 15.2.8-2 Main Feedwater Line Break With Concurrent LOOP: Core Power vs. Time

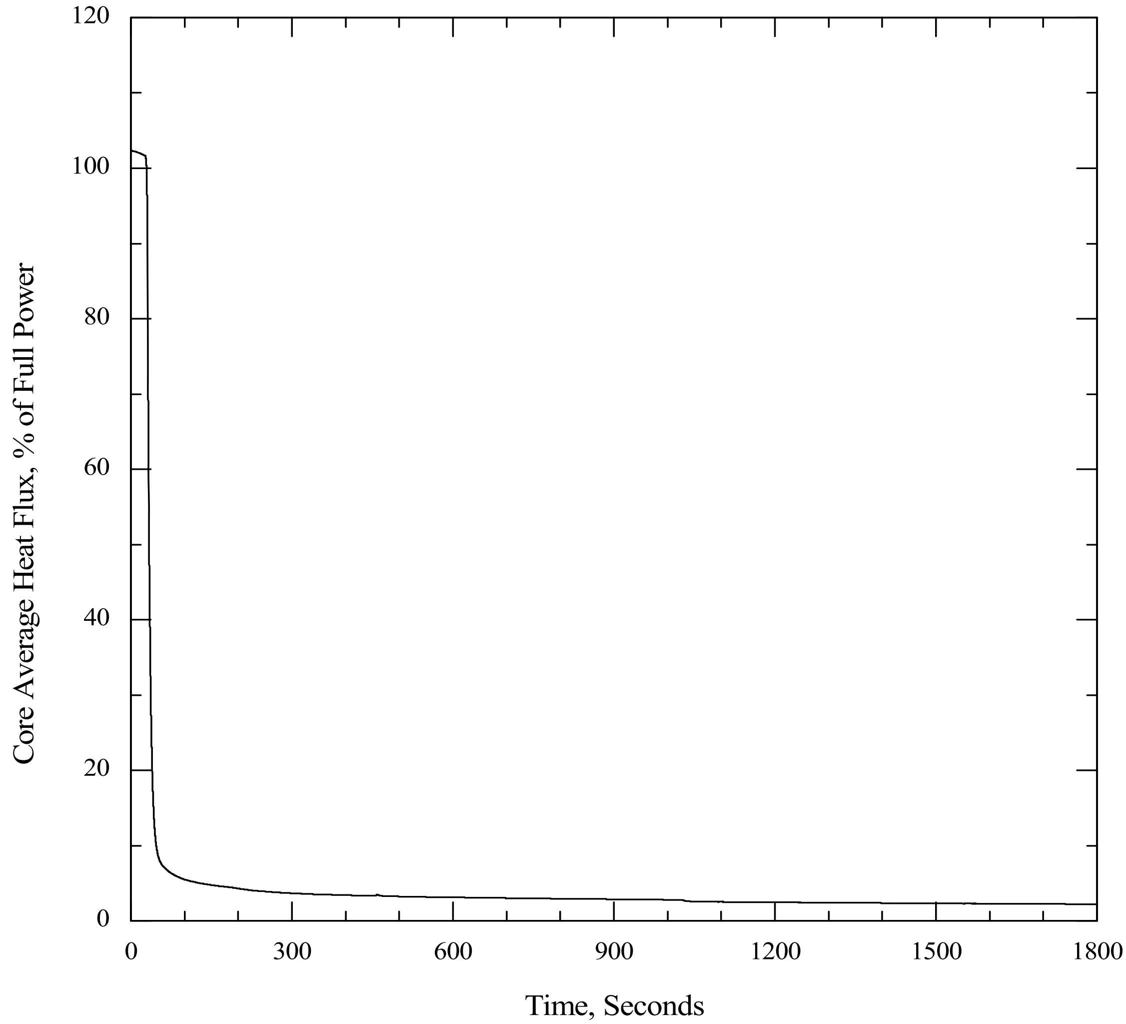

Figure 15.2.8-3 Main Feedwater Line Break With Concurrent LOOP: Core Average Heat Flux vs. Time

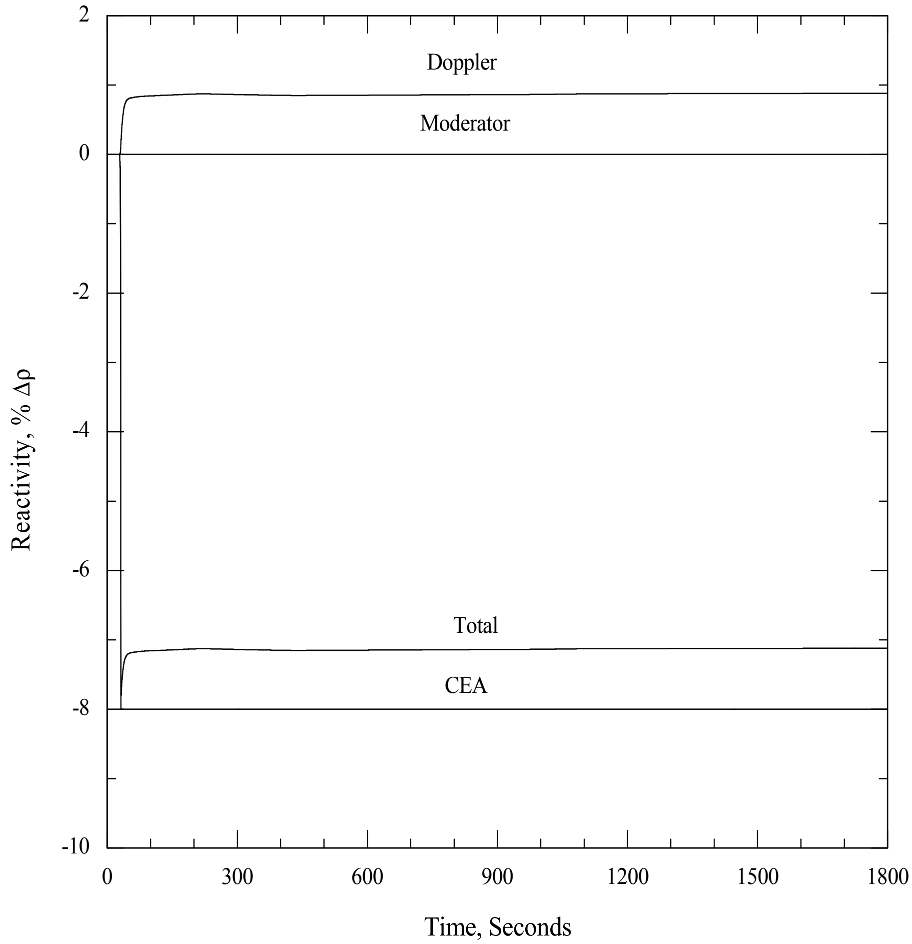

Figure 15.2.8-4 Main Feedwater Line Break With Concurrent LOOP:Reactivity vs. Time

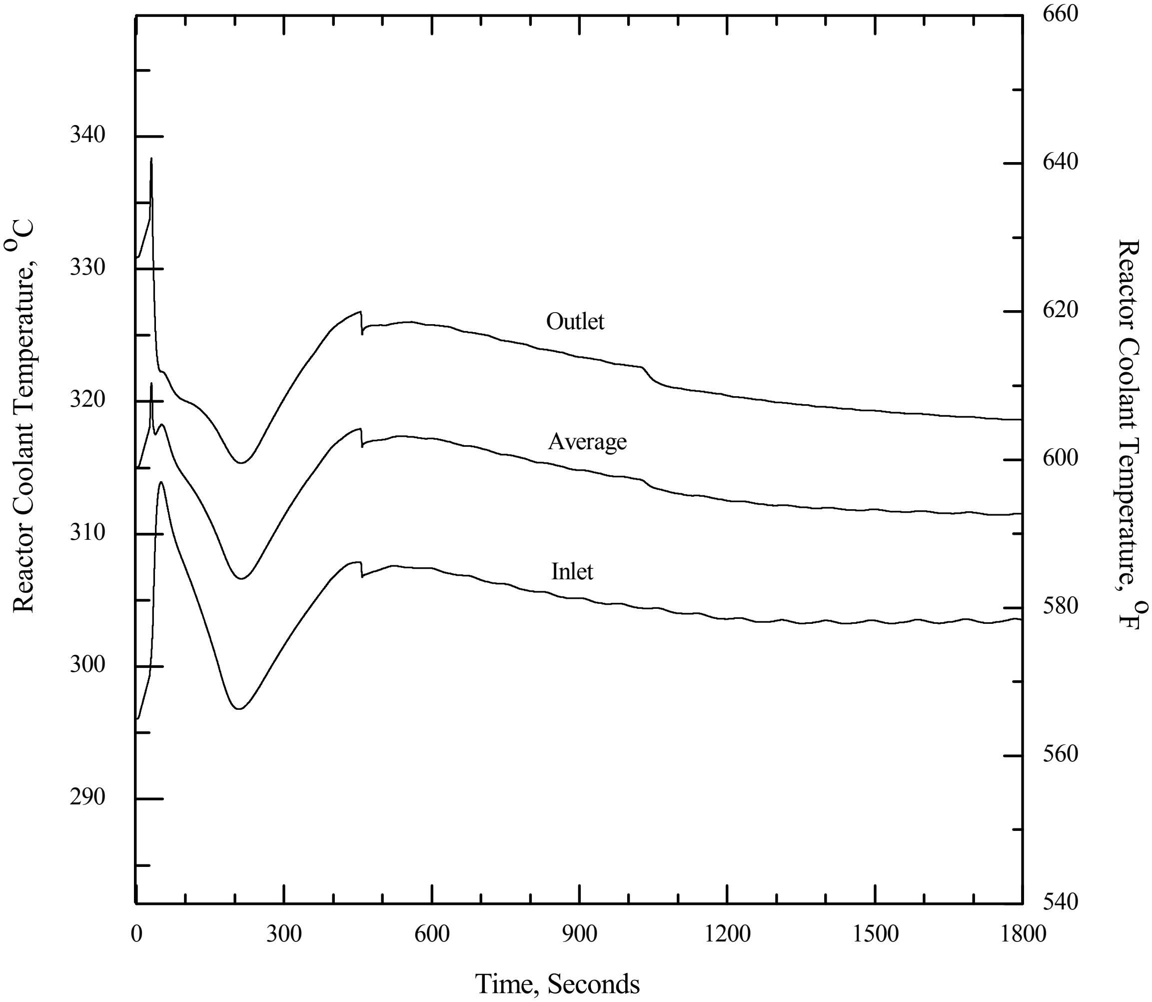

Figure 15.2.8-5 Main Feedwater Line Break With Concurrent LOOP: Reactor Coolant Temperature vs. Time

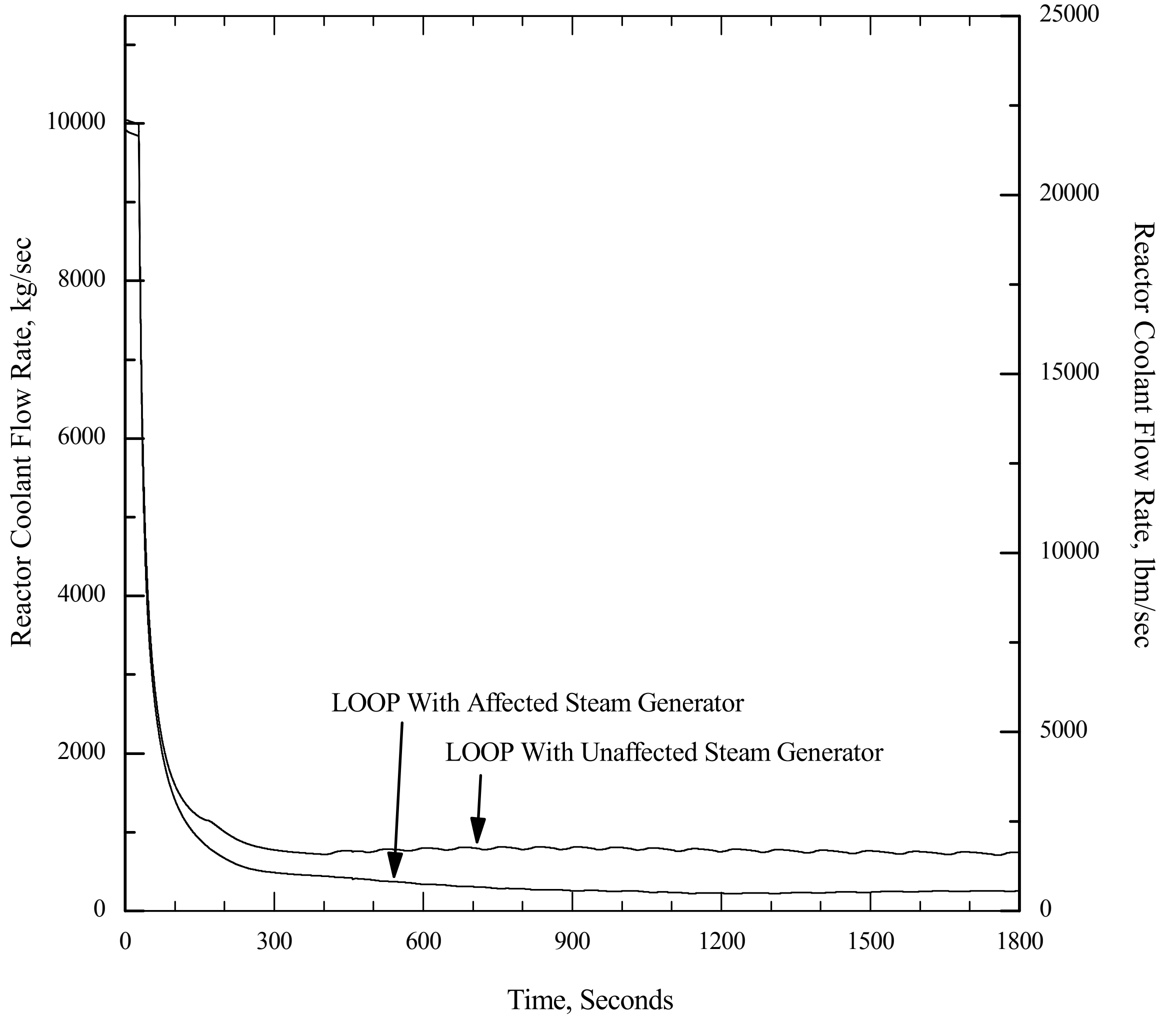

Figure 15.2.8-6 Main Feedwater Line Break With Concurrent LOOP: Reactor Coolant Flow Rates vs. Time

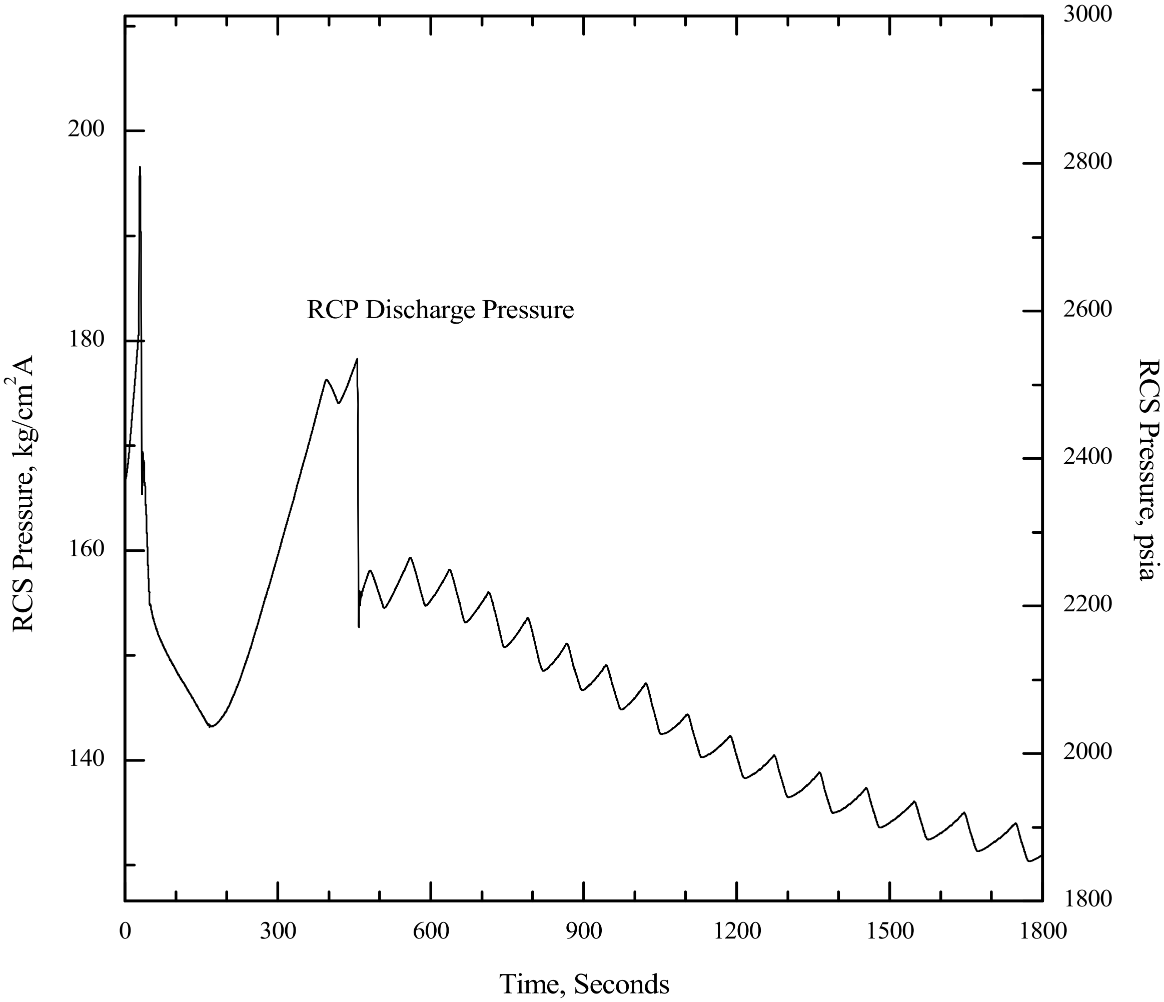

Figure 15.2.8-7 Main Feedwater Line Break With Concurrent LOOP: RCS Pressure vs. Time

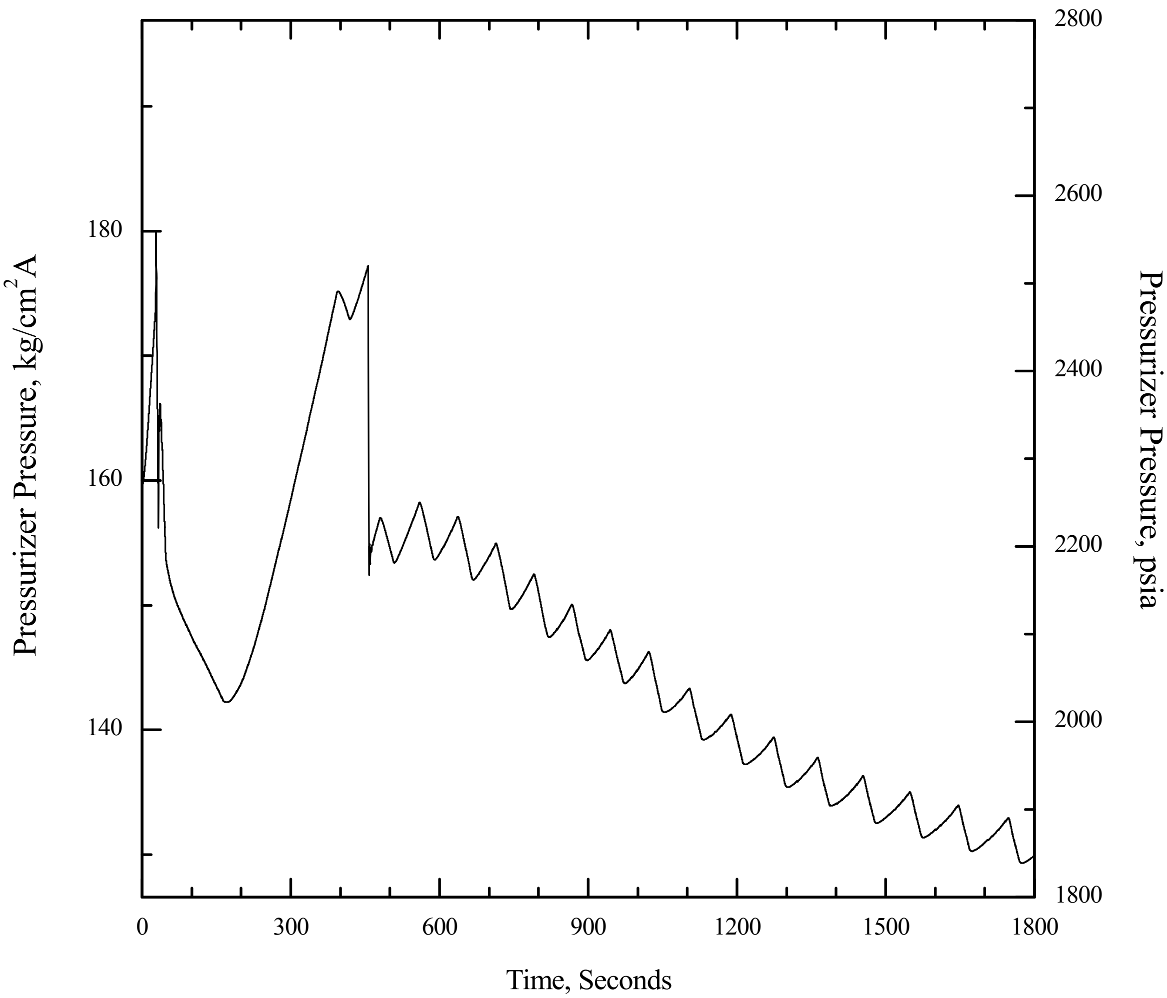

Figure 15.2.8-8 Main Feedwater Line Break With Concurrent LOOP : Pressurizer Pressure vs. Time

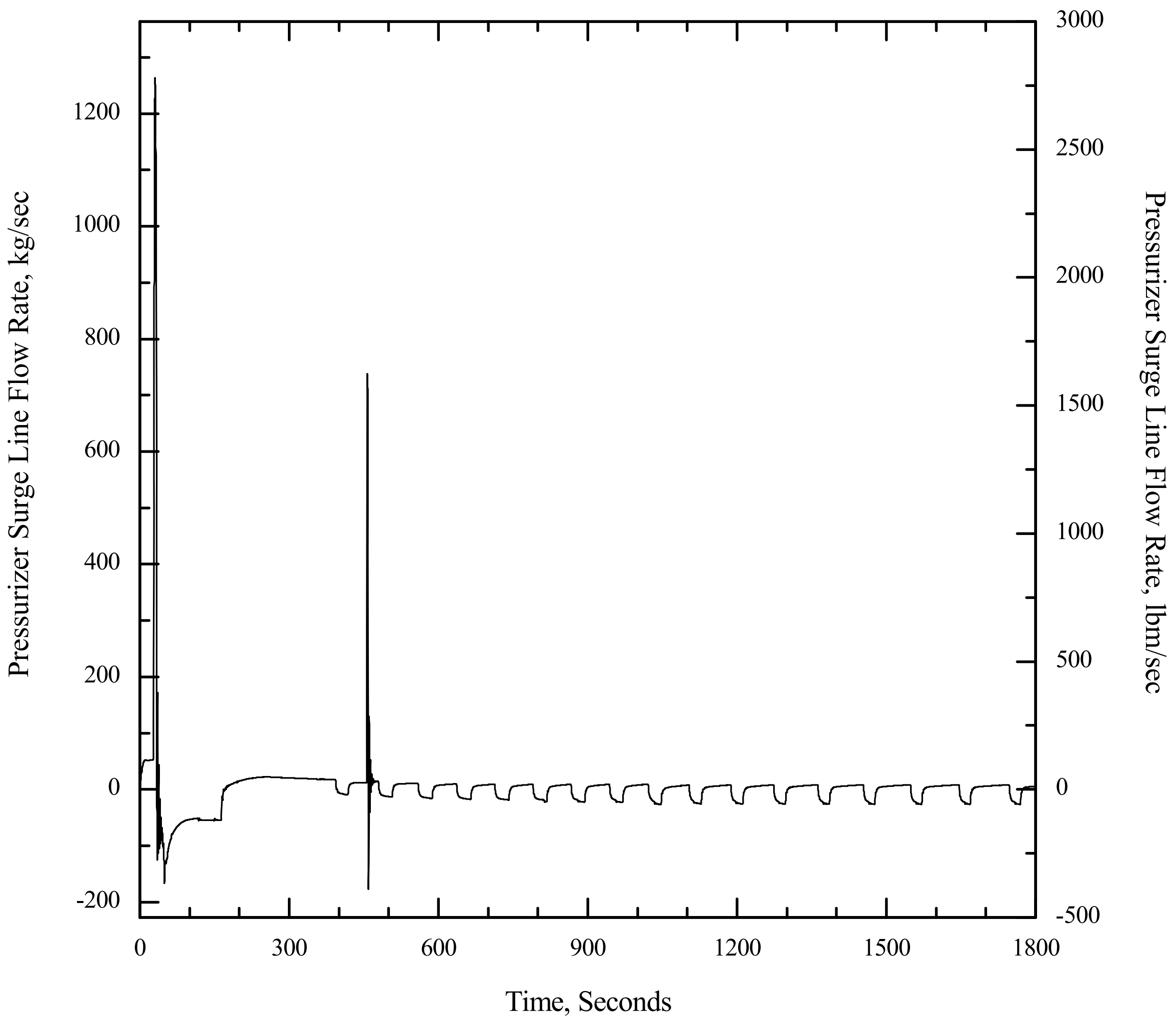

Figure 15.2.8-9 Main Feedwater Line Break With Concurrent LOOP : Pressurizer Surge Line Flow Rates vs. Time

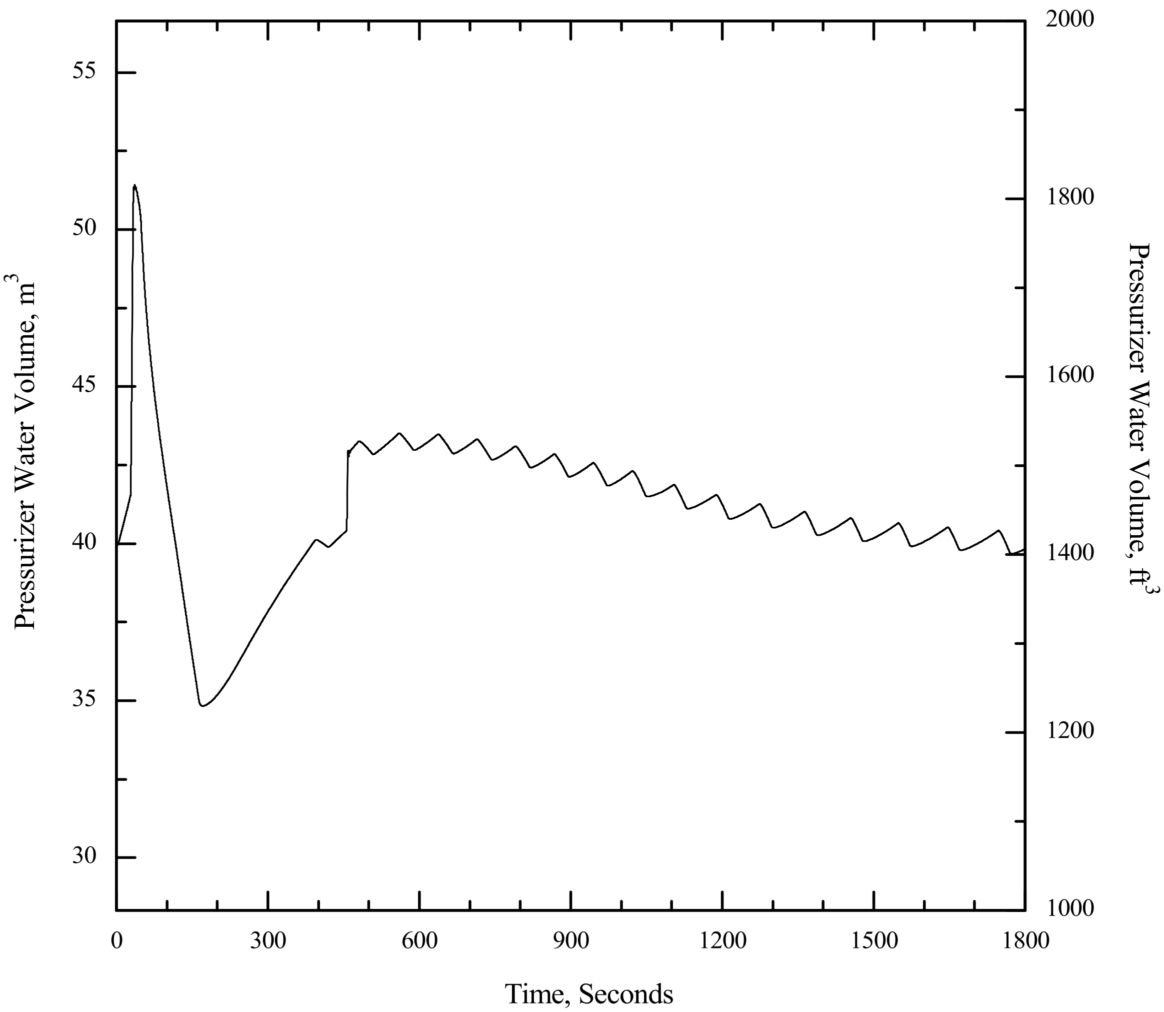

Figure 15.2.8-10 Main Feedwater Line Break With Concurrent LOOP: Pressurizer Water Volume vs. Time

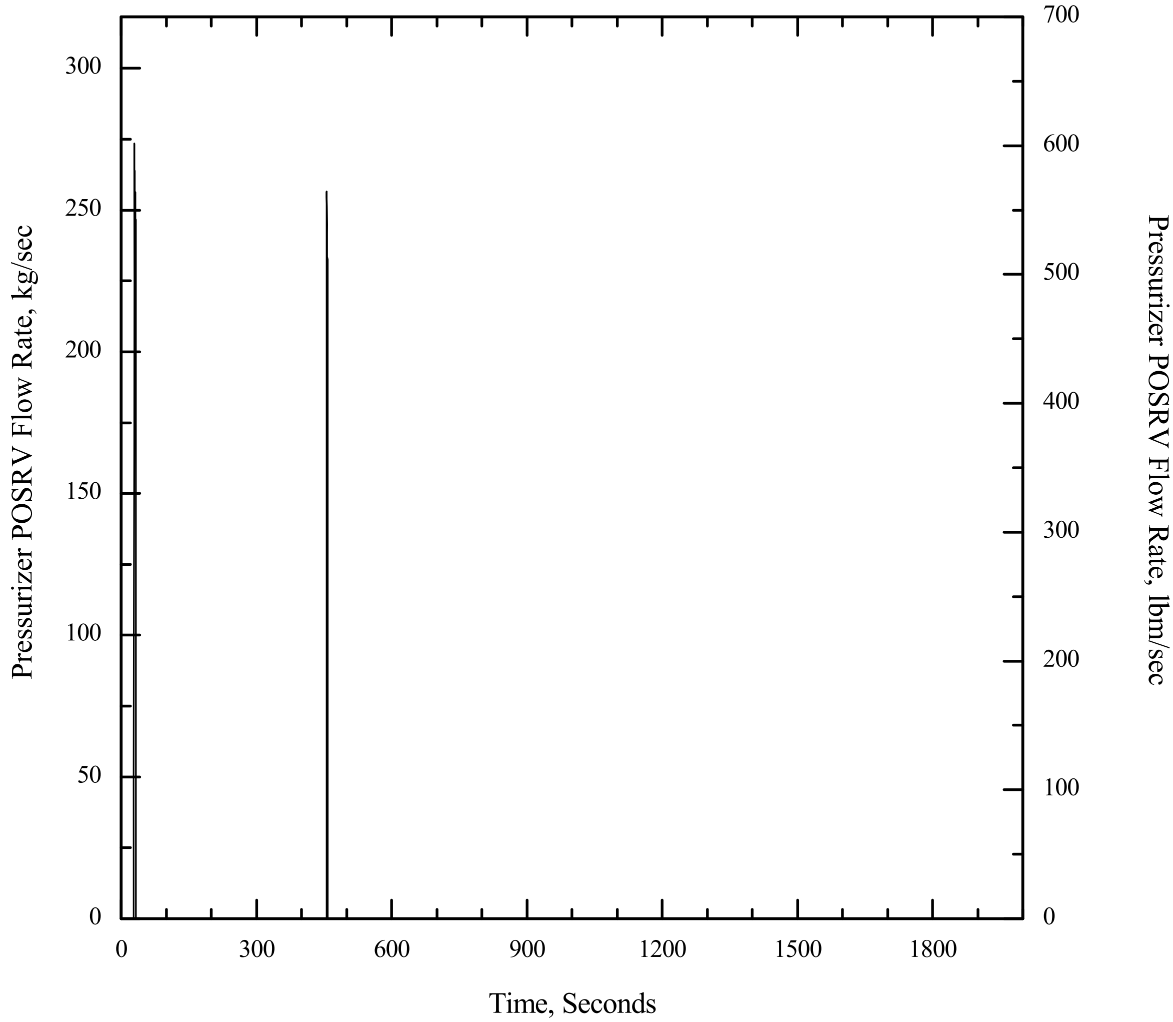

Figure 15.2.8-11 Main Feedwater Line Break With Concurrent LOOP: Pressurizer POSRV Flow Rate vs. Time

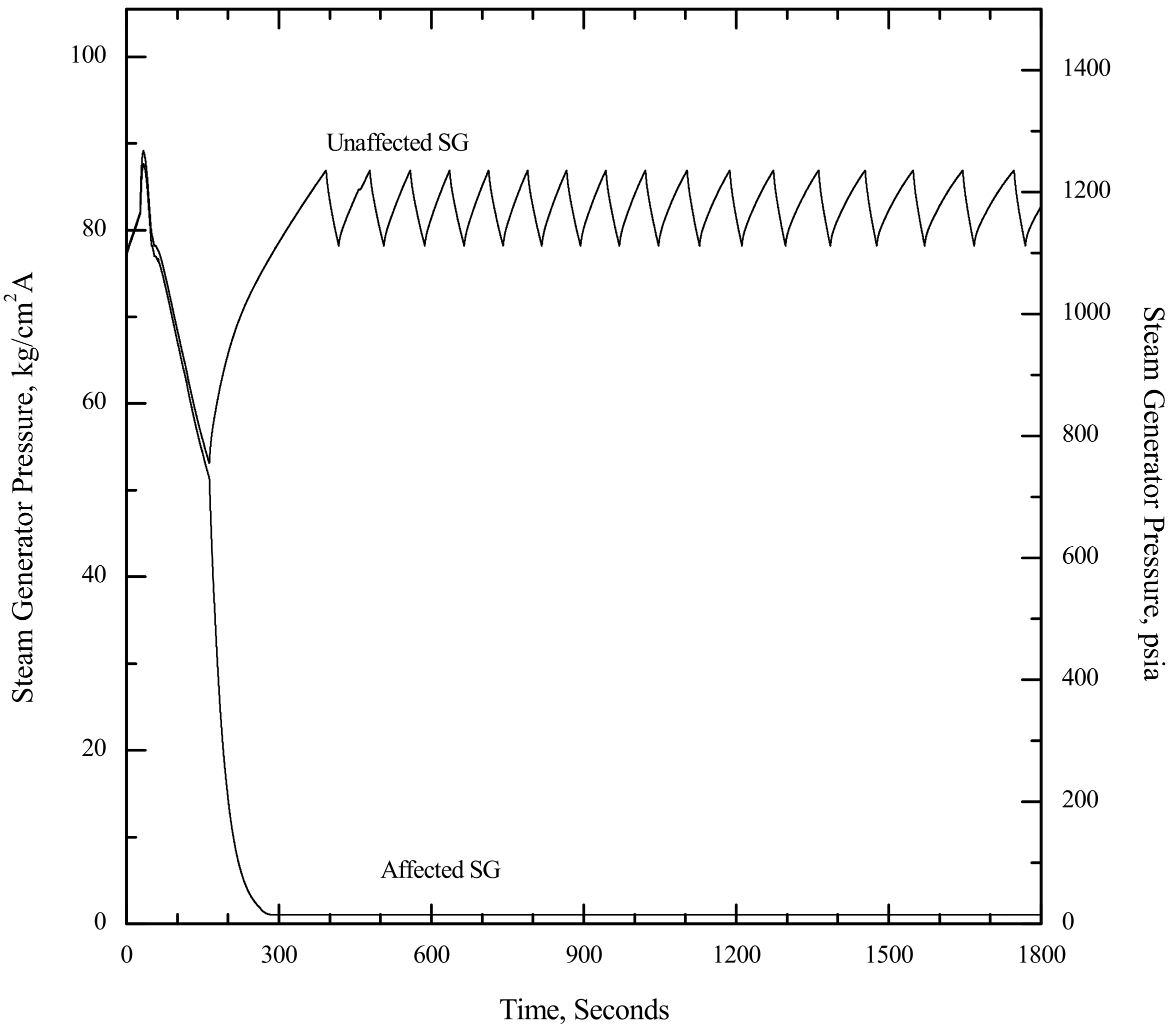

Figure 15.2.8-12 Main Feedwater Line Break With Concurrent LOOP: Steam Generator Pressure vs. Time

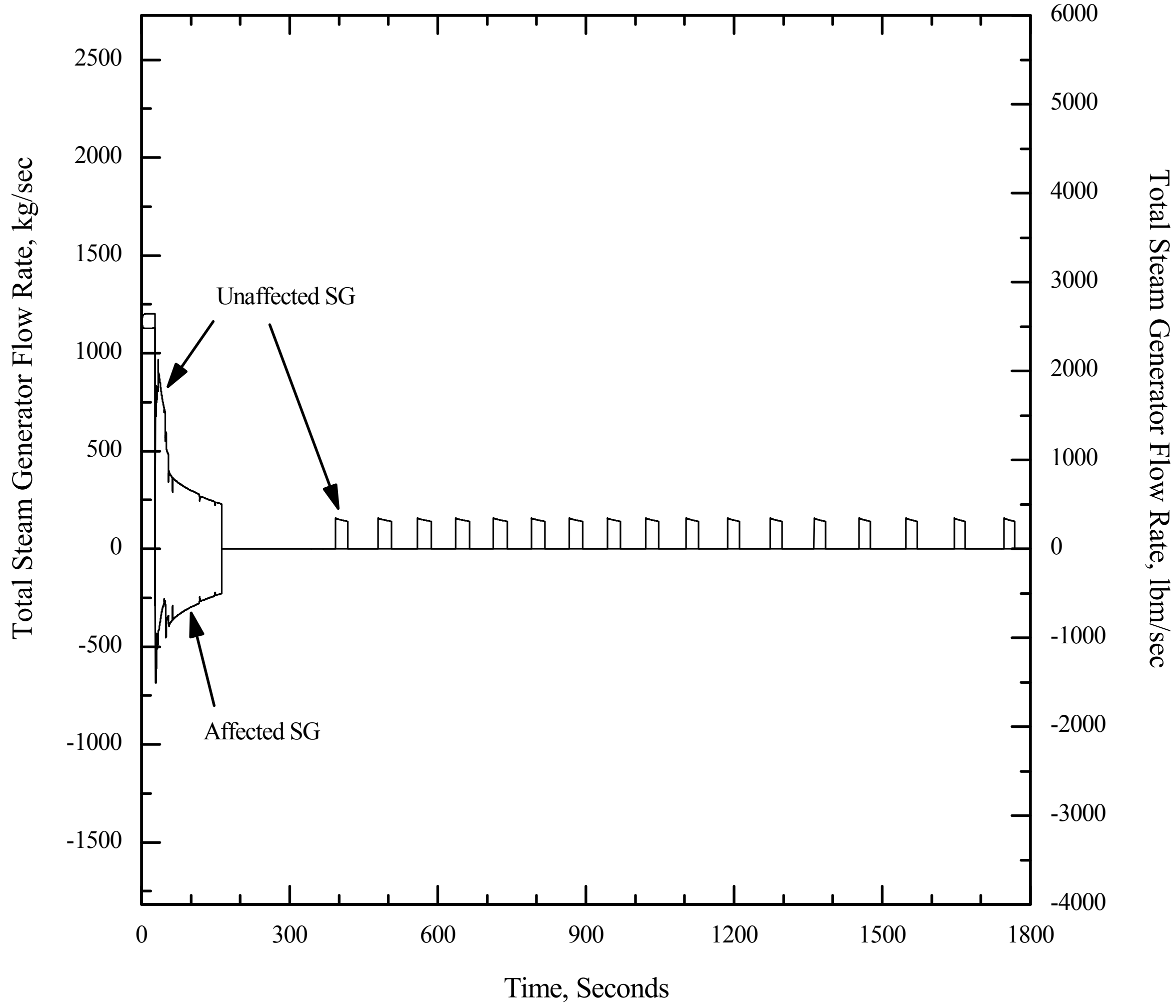

Figure 15.2.8-13 Main Feedwater Line Break With Concurrent LOOP: Total Steam Flow Rate vs. Time

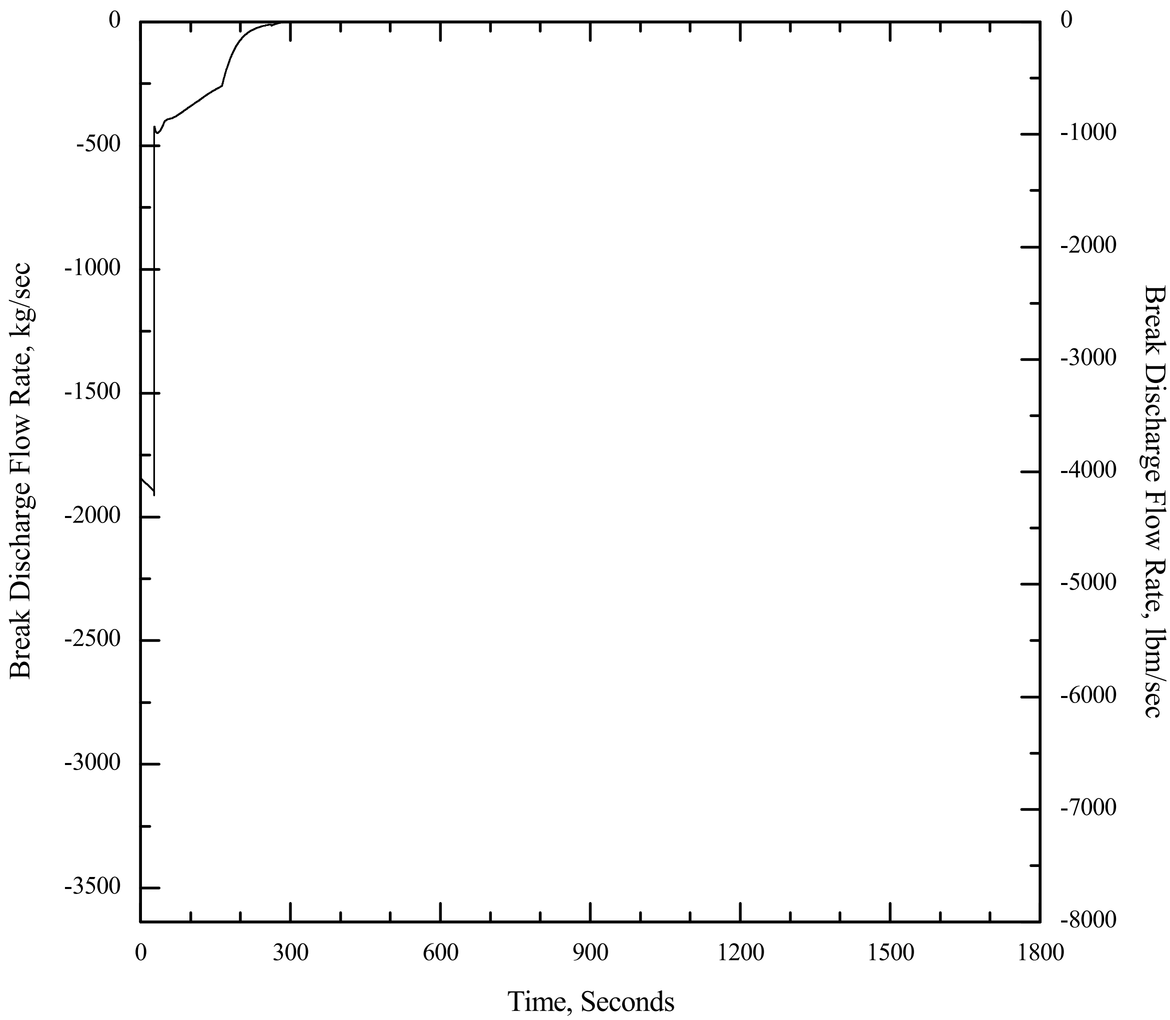

Figure 15.2.8-14 Main Feedwater Line Break With Concurrent LOOP : Break Discharge Flow Rate vs. Time

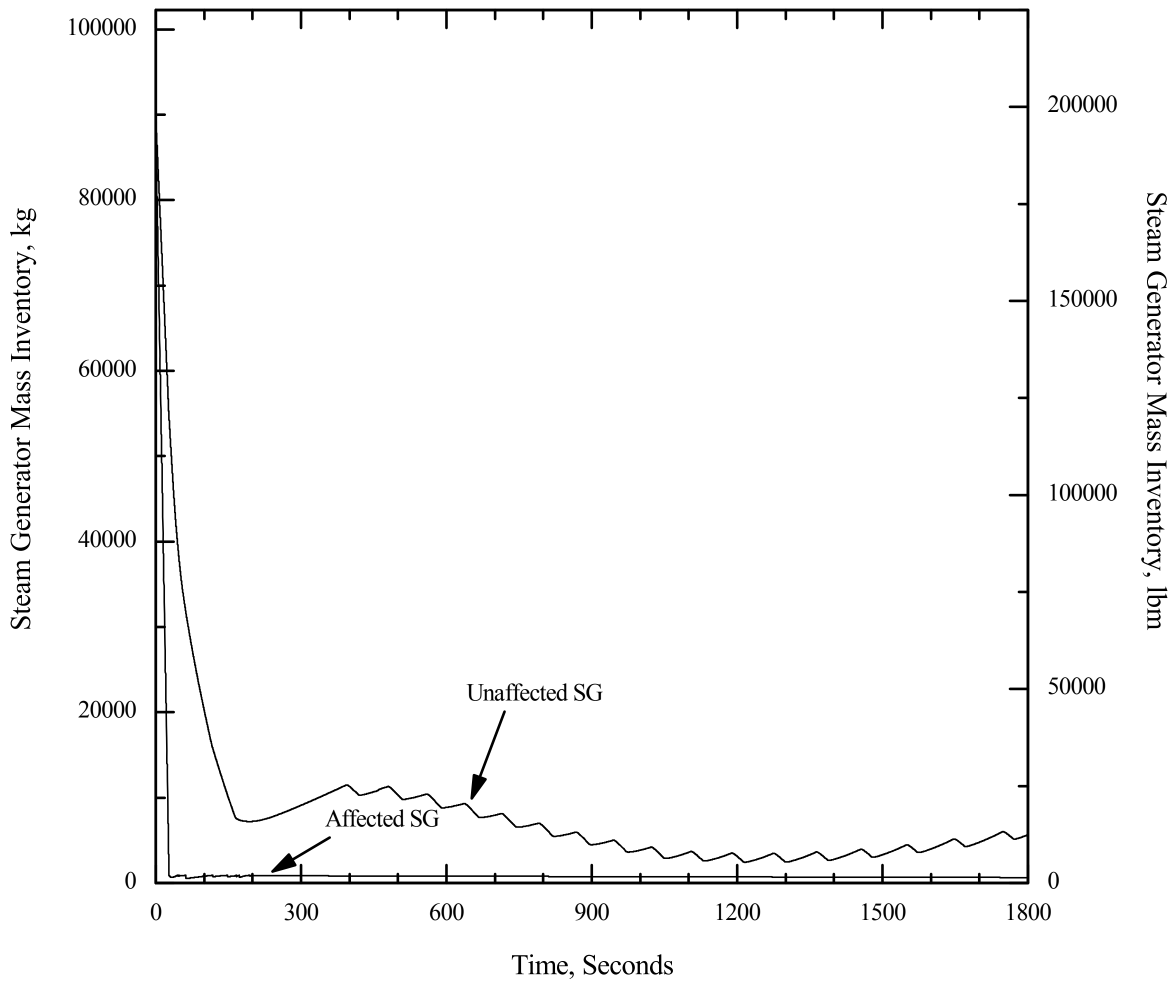

Figure 15.2.8-15 Main Feedwater Line Break With Concurrent LOOP: Steam Generator Mass Inventories vs. Time

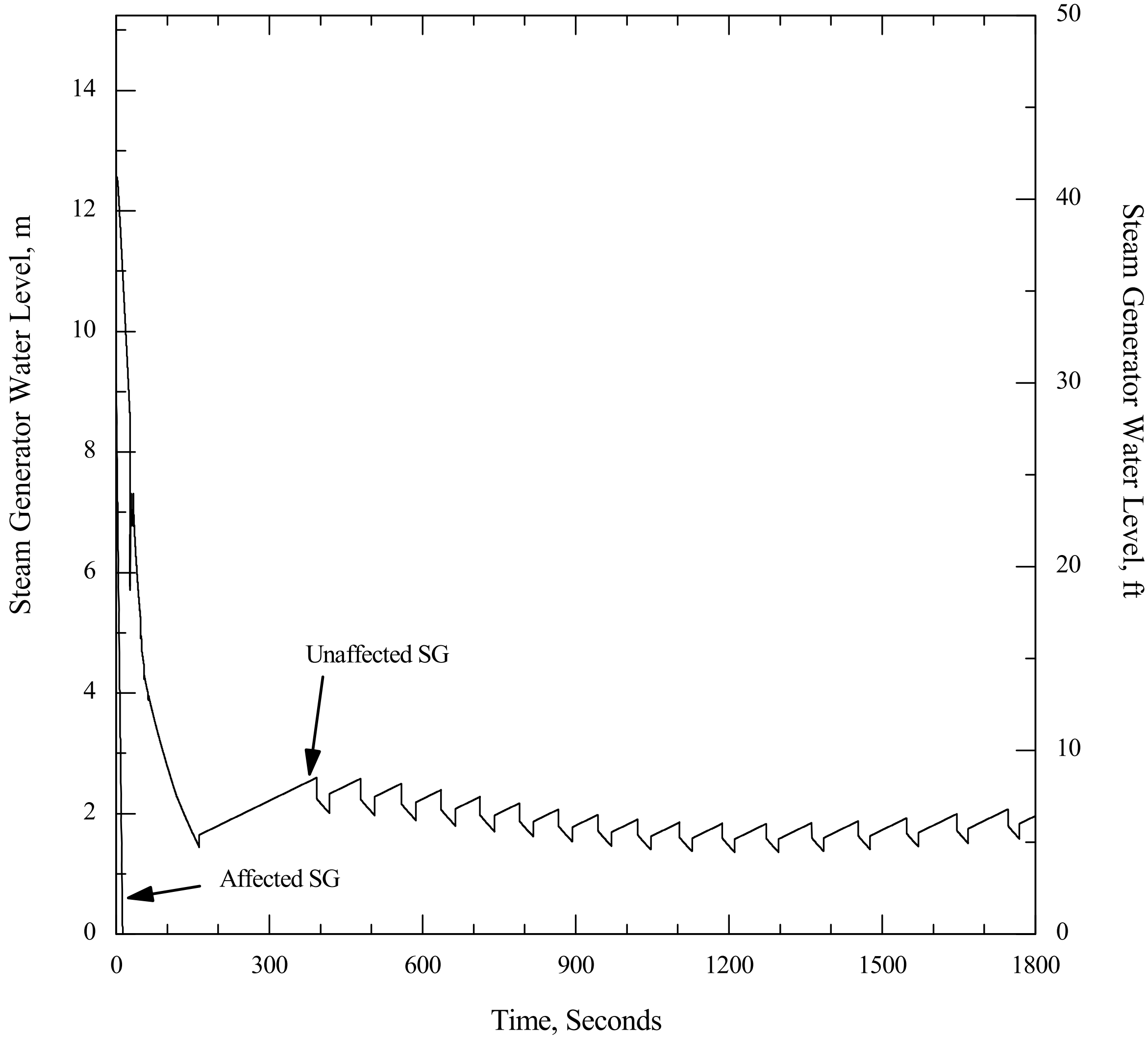

Figure 15.2.8-16 Main Feedwater Line Break With Concurrent LOOP: Steam Generator Water Level vs. Time

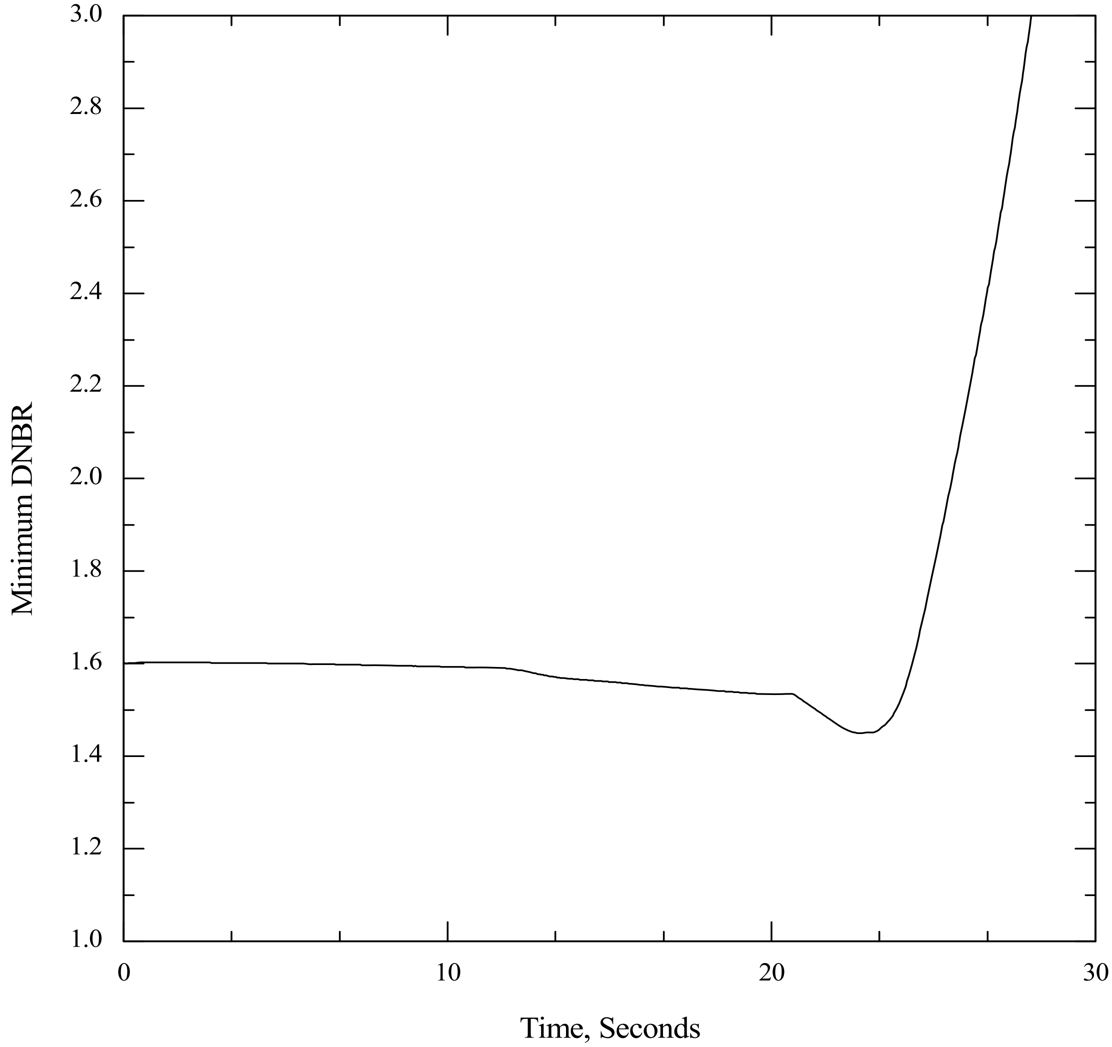

Figure 15.2.8-17 Main Feedwater Line Break With Concurrent LOOP: Minimum DNBR vs. Time

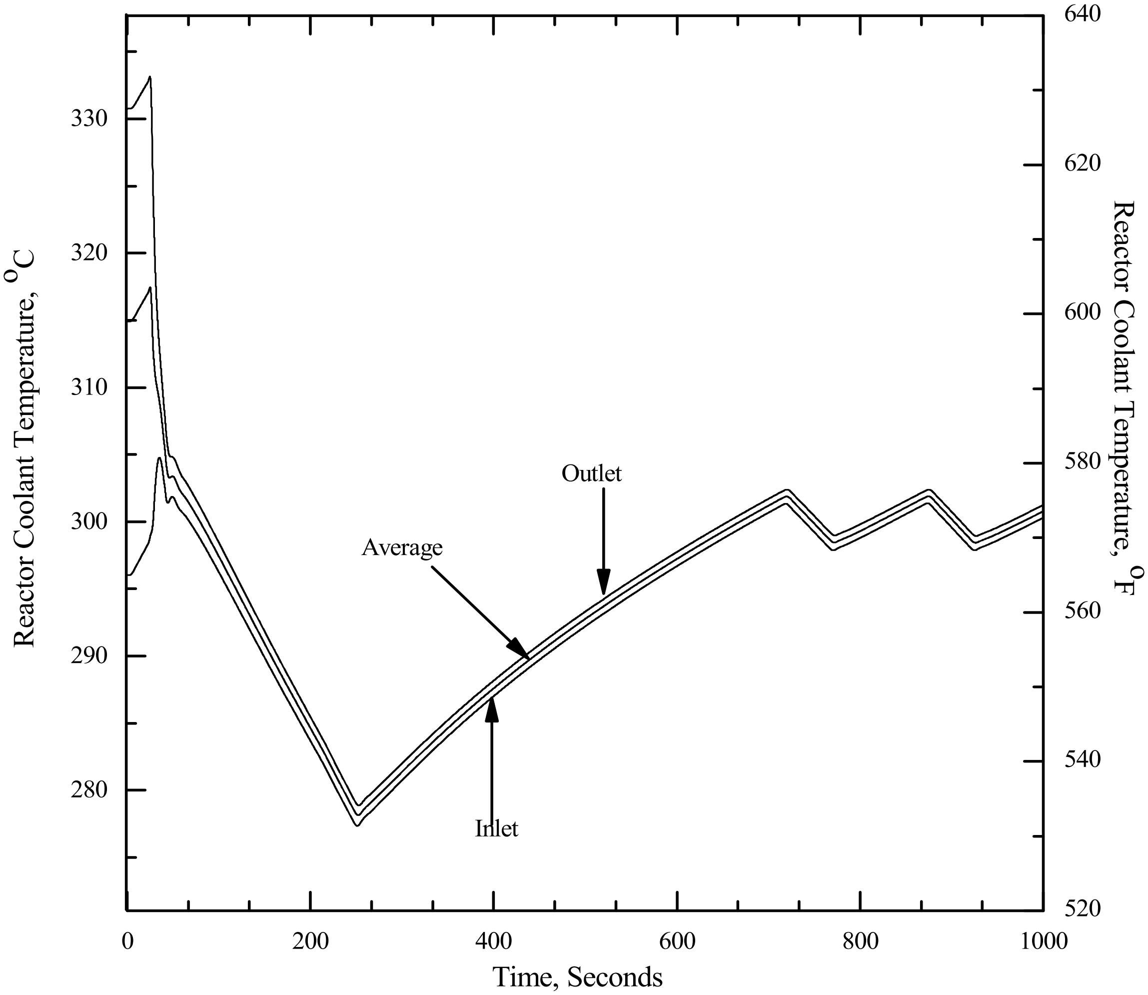

Figure 15.2.8-18 Main Feedwater Line Break With Offsite Power: Reactor Coolant Temperatures vs. Time

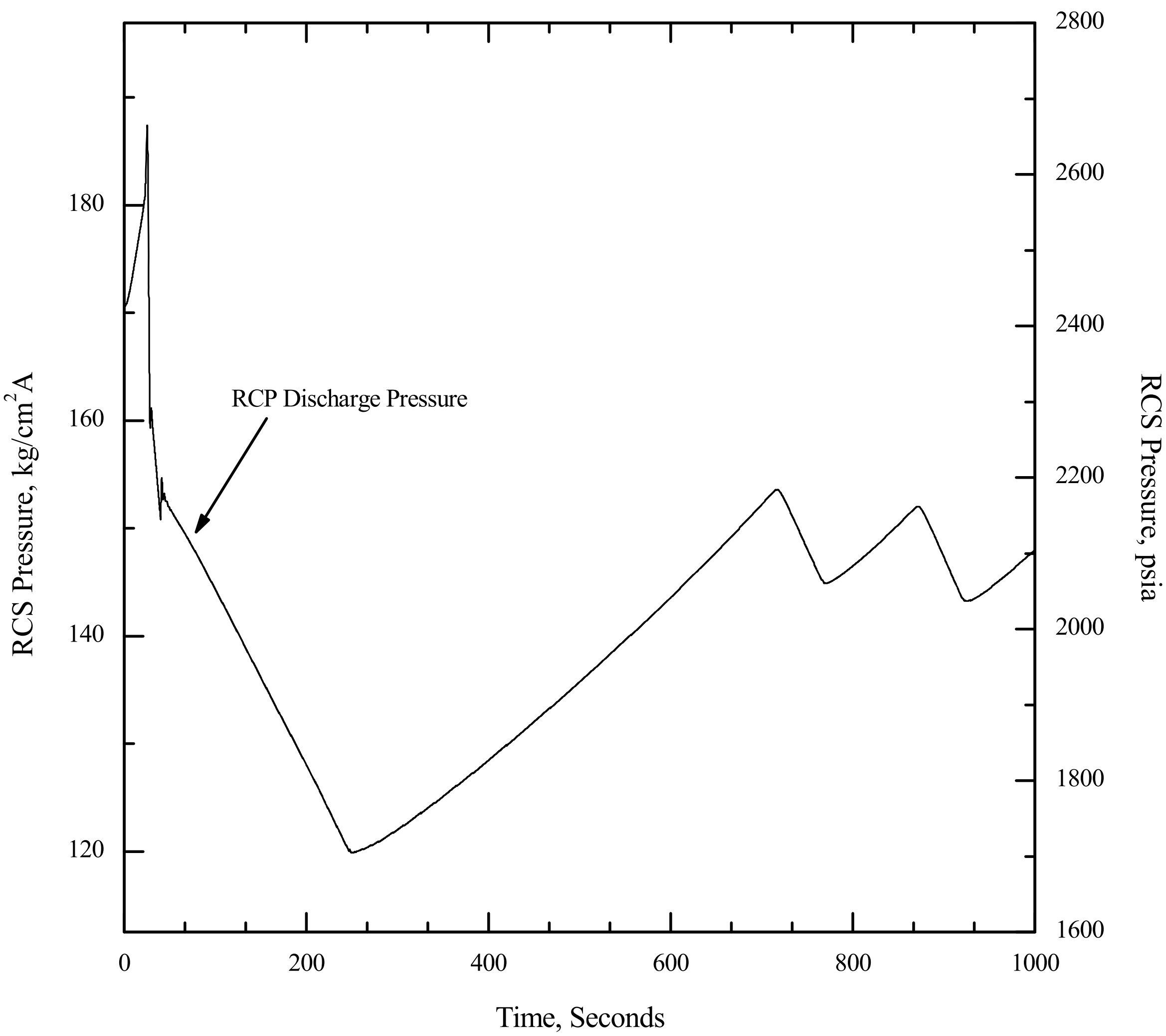

Figure 15.2.8-19 Main Feedwater Line Break With Offsite Power : RCS Pressure vs. Time

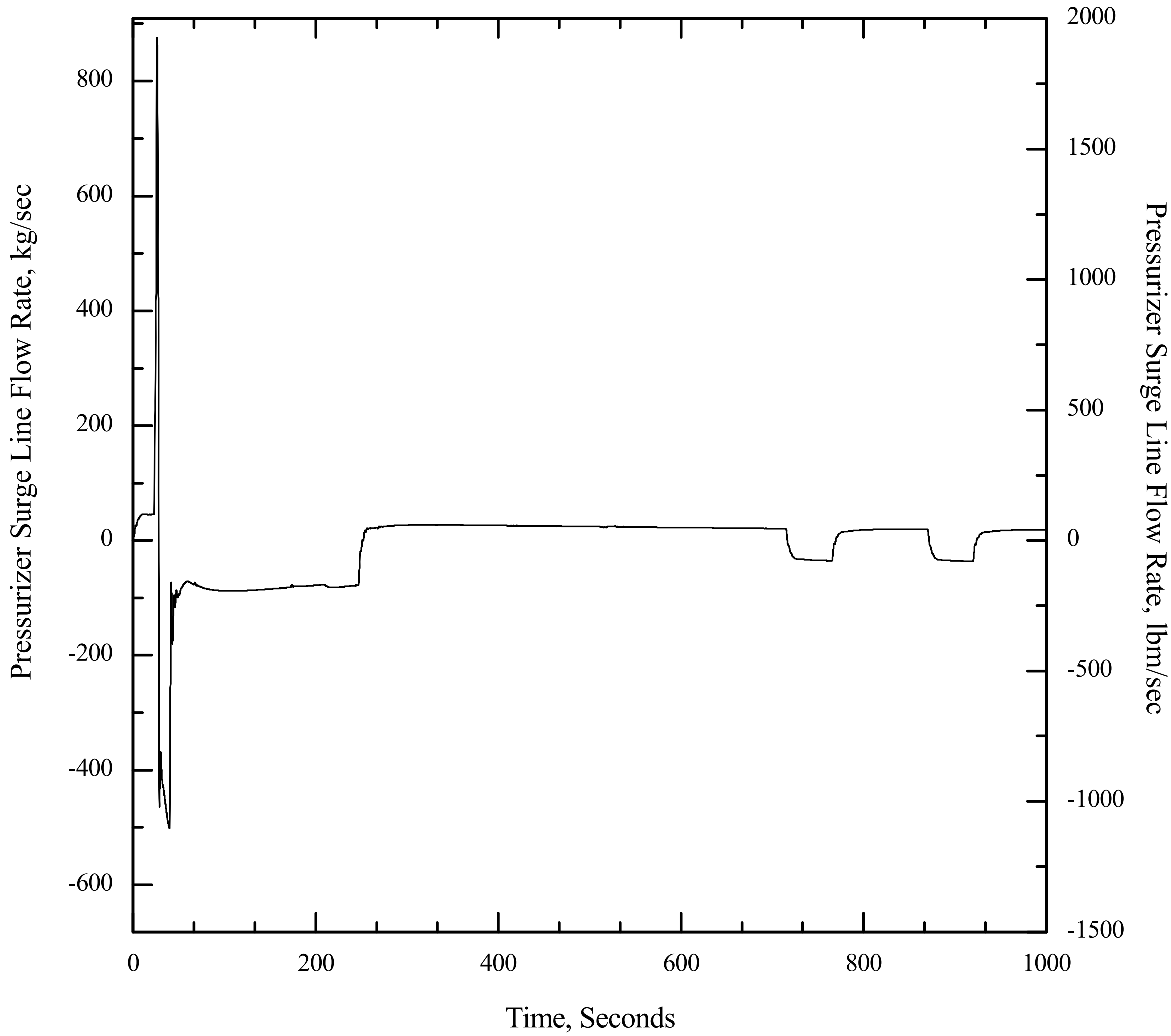

Figure 15.2.8-20 Main Feedwater Line Break With Offsite Power: Pressurizer Surge Line Flow Rate vs. Time

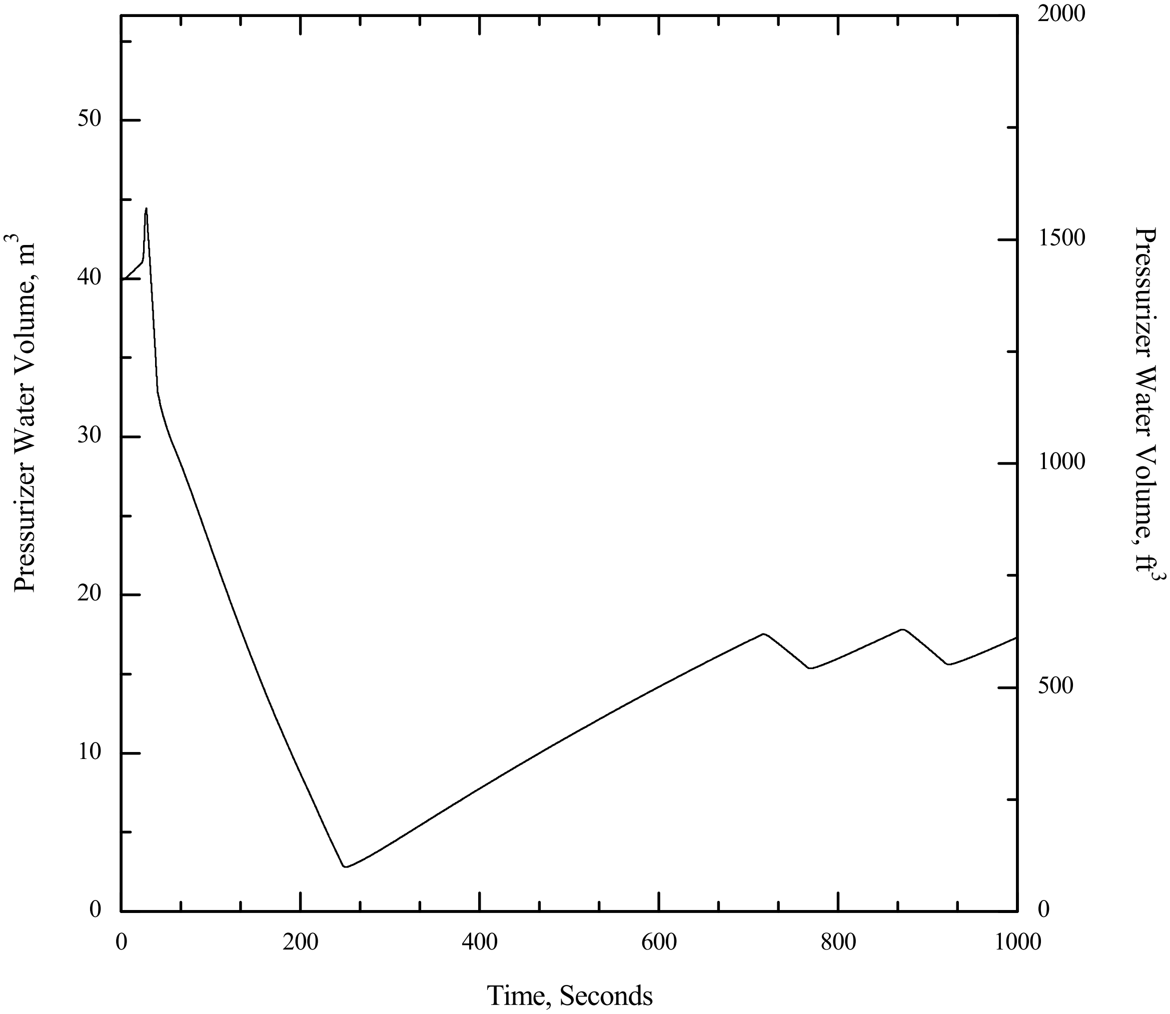

Figure 15.2.8-21 Main Feedwater Line Break With Offsite Power: Pressurizer Water Volume vs. Time

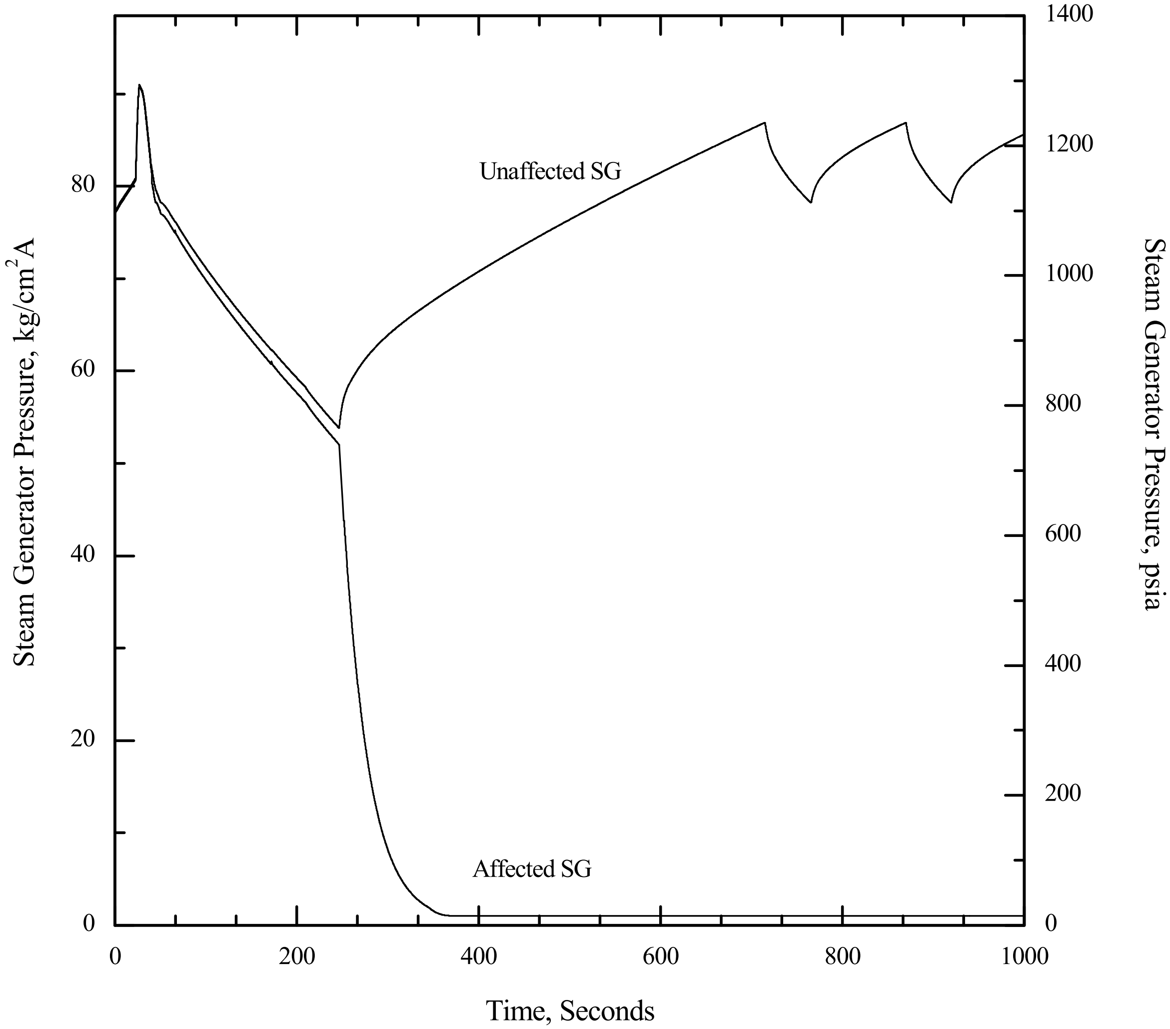

Figure 15.2.8-22 Main Feedwater Line Break With Offsite Power: Steam Generator Pressure vs. Time

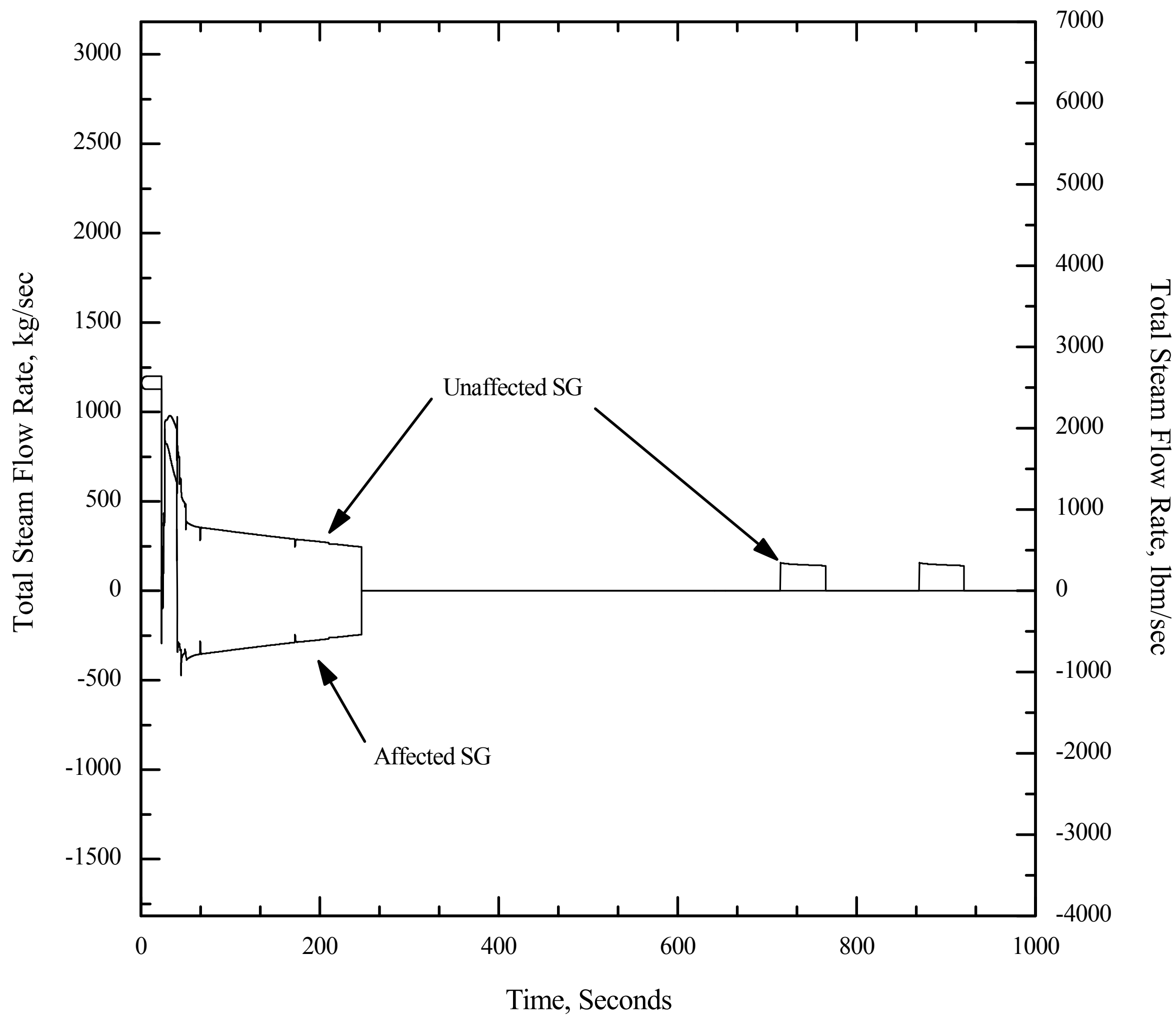

Figure 15.2.8-23 Main Feedwater Line Break With Offsite Power: Total Steam Flow rates vs. Time

15.3 Decrease in Reactor Coolant System Flow Rate

This section describes the analyses that have been performed for events that could result in a decrease in the reactor coolant system (RCS) flow rate.

One anticipated operational occurrence (AOO) and two postulated accidents (PAs) result in a decrease in reactor coolant flow. The analyses of these events are described in the following subsections:

a. Subsection 15.3.1 – Loss of Forced Reactor Coolant Flow

b. Subsection 15.3.2 – Flow Controller Malfunctions (not applicable to the APR1400)

c. Subsection 15.3.3 – Reactor Coolant Pump Rotor Seizure

d. Subsection 15.3.4 – Reactor Coolant Pump Shaft Break

15.3.1 Loss of Forced Reactor Coolant Flow

15.3.1.1 Identification of Causes and Frequency Classification

A complete loss of forced reactor coolant flow results from the simultaneous loss of electrical power to all reactor coolant pumps (RCPs). The only credible failure that can result in a simultaneous loss of power is a complete loss of offsite power.

A complete loss of forced reactor coolant flow produces a minimum departure from nucleate boiling ratio (DNBR) more adverse than any partial loss of forced reactor coolant flow event, since the reactor will trip at the same time for both cases; though, the partial loss of flow has a slower flow coastdown. This event is classified as an AOO as defined in Subsection 15.0.0.1.

15.3.1.2 Sequence of Events and Systems Operation

A loss of electric power to all four RCPs produces a reduction of coolant flow through the reactor core that causes an increase in core average coolant temperature, system pressure, and a decrease in margin to DNB. Table 15.3.1-1 presents a chronological list and time of system actions that occur during the complete loss of reactor coolant flow event.

The core protection calculator (CPC) generates reactor trip when any one of the four RCP shaft speeds drops to 95 percent of normal speed. The CPC trip provides reasonable assurance that the event induced minimum DNBR value will remain above the specified acceptable fuel design limit (SAFDL) for DNBR.

The combination of loss of primary heat sink (due to loss of offsite power causing a loss of load on turbine, turbine trip and closure of turbine admission valves) with a reduction of reactor coolant flow results in an increase in RCS pressure that is limited by the pilot operated safety and relief valves (POSRVs).

The steam bypass control system also becomes unavailable due to loss of offsite power, which results in a loss of condenser vacuum and termination of main feedwater to the steam generators. This sequence of system interactions leads to the opening of the main steam safety valves (MSSVs), which limits the secondary side pressure and removes heat stored in the core and the RCS.

The loss of offsite power is followed by automatic startup of the standby diesel generators whose power output is sufficient to supply electrical power to all necessary engineered safety features and to maintain the plant in a safe shutdown condition. Subsequent to the reactor trip, stored and fission product decay energy is dissipated by the RCS and main steam system. In the absence of forced reactor coolant flow, core heat removal occurs by natural circulation in the RCS. Initially, the residual water inventory in the steam generators is used as a heat sink, and the resultant steam is released to atmosphere by the MSSVs. With the availability of standby diesel power, auxiliary feedwater is automatically initiated on a low steam generator water level signal. Plant operators initiate cooldown after the event induced reactor trip occurs by using the auxiliary feedwater system (AFWS) and atmospheric dump valves (ADVs).

The loss of offsite power event plus a single failure will not result in a lower DNBR than that calculated for the loss of offsite power event alone. For decreasing reactor coolant flow events, the major parameter of concern is the minimum DNBR. This parameter establishes whether a fuel design limit has been violated and whether fuel damage might be anticipated.

Factors that cause a decrease in local DNBR are as follows:

a. Increasing coolant temperature

b. Decreasing coolant pressure

c. Increasing local heat flux

d. Decreasing coolant flow

For the loss of offsite power event, the minimum DNBR occurs during the first few seconds of the transient and the reactor is tripped by the CPCs on the approach to the DNBR limit. Therefore, any single failure that would result in a lower DNBR during the transient would have to affect at least one of the above parameters during the first few seconds of the event. None of the single failures listed in Table 15.0-4 has any effect on the transient minimum DNBR during this period of time.

None of the single failures listed in Table 15.0-4 has any effect on the peak primary system pressure. The loss of offsite power makes unavailable any systems whose failure could affect the calculated peak pressure.

A loss of offsite power event with a single failure is no more adverse than the loss of offsite power event in terms of the minimum DNBR and peak primary system pressure.

Non safety-related systems are not assumed to mitigate the consequences of this event as discussed in Subsection 15.0.0.5.

15.3.1.3 Core and System Performance

15.3.1.3.1 Evaluation Model

The total loss of reactor coolant flow methodology is described in Subsection 15.0.2.

The computer programs employed are CESEC-III, HERMITE, and CETOP as described in Subsection 15.0.2. The nuclear steam supply system (NSSS) response to a complete loss of reactor coolant flow is simulated using the CESEC-III computer program. The

minimum DNBR is calculated using the HERMITE and CETOP computer programs. The CETOP computer program uses the KCE-1 critical heat flux (CHF) correlation.

15.3.1.3.2 Input Parameters and Initial Conditions

The ranges of initial conditions considered are given in Table 15.0-3. Table 15.3.1-2 gives the initial conditions used in the analysis of the complete loss of flow event.

The principal process variables that determine thermal margin to DNB in the core are monitored by core operating limit supervisory system (COLSS). COLSS computes a power operating limit (POL) that assists the operator in maintaining the thermal margin in the core greater than that needed to cause the minimum DNBR to remain greater than DNBR SAFDL for a complete loss of flow. COLSS is addressed in Subsection 7.7.1.4. Based on the parametric studies, the most adverse combinations of initial conditions are selected to minimize the DNBR. A high primary system pressure, a low core inlet temperature, and high reactor coolant flow are chosen in conjunction with the radial peaking factor compatible with these initial conditions, to initiate the event from a POL allowed by COLSS.

The moderator temperature coefficient is assumed to have the maximum value as defined in Subsection 15.0.0.2. The Doppler coefficient is assumed to have the minimum value, as defined in Subsection 15.0.0.2. Use of these values maximizes the heat flux in the initial stage of the transient. The minimum shutdown control element assembly (CEA) worth is assumed as defined in Subsection 15.0.0.2.

15.3.1.3.3 Results

The typical responses of key parameters as a function of time are presented in Figures 15.3.1-1 to 15.3.1-8 for this event. The loss of offsite power causes the plant to experience a simultaneous turbine trip, loss of main feedwater, condenser inoperability, and coastdown of four RCPs. As a result of the RCP coastdown, the CPC generates a trip signal and the CEAs start to drop into the core.

Since there is no power excursion during the transient, the complete loss of forced reactor coolant event does not challenge the linear heat generation rate limit of 656 W/cm (20 kW/ft) and, consequently, the fuel temperature remains below the fuel melting temperature.

The minimum DNBR is greater than the DNBR SAFDL value of 1.29 (see Figure 15.3.1-8). Fuel cladding damage is not predicted for this event.

15.3.1.4 Barrier Performance

15.3.1.4.1 Evaluation Model

The barrier performance evaluation for peak RCS pressure is performed using the CESEC-III as in the core and system performance analysis described in Subsection 15.3.1.3.1.

15.3.1.4.2 Input Parameters and Initial Conditions

The ranges of initial conditions considered are given in Table 15.0-3. Input parameters and initial conditions are modified in order to maximize the primary and secondary system pressure. The peak pressure analysis used the initial core inlet temperature of 295 °C (563 °F), and the initial steam generator pressure of 75.86 kg/cm^{2}A (1,079 psia), with all other initial condition parameter values as listed in Table 15.3.1-2.

15.3.1.4.3 Results

The typical responses of key parameters as a function of time are presented in Figures 15.3.1-9 to 15.3.1-12 for this event.

The loss of steam flow due to closure of the turbine stop valves results in a rapid increase in the steam generator pressure. A sharp reduction in P-T-S heat transfer follows and in conjunction with the loss of forced reactor coolant flow, causes a rapid heatup of the primary coolant. The RCS pressure decreases rapidly as the combination of reactor trip, POSRVs and MSSVs opening reduce the reactor coolant system energy.

The maximum RCS pressure is 188.8 kg/cm^{2}A (2,685 psia) (see Figure 15.3.1-9), which is less than 193.3 kg/cm^{2}A (2,750 psia) (110 percent of RCS design pressure). The maximum secondary system pressure is 91.12 kg/cm^{2}A (1,296 psia) (see Figure 15.3.1-10), which is less than 92.81 kg/cm^{2}A (1,320 psia) (110 percent of secondary design pressure).

15.3.1.5 Radiological Consequences

This event is bounded by the reactor coolant pump rotor seizure event described in Subsection 15.3.3 for the radiological consequences.

15.3.1.6 Conclusions

The minimum DNBR remains above the SAFDL, thereby providing reasonable assurance of fuel cladding integrity. The initial margin required as a result of this analysis is preserved by the limiting condition of operation on DNBR margin.

The maximum RCS and secondary system pressure remain within 110 percent of their design values following the complete loss of forced reactor coolant flow event.

The event is mitigated and the plant is maintained in a stable condition through the automated response of safety-related equipment, avoiding a more serious plant condition.

15.3.2 Flow Controller Malfunctions

This event is categorized as a Boiling Water Reactor event in SRP 15.3.2, and will not be analyzed.

15.3.3 Reactor Coolant Pump Rotor Seizure

15.3.3.1 Identification of Causes and Frequency Classification

A reactor coolant pump (RCP) rotor seizure is caused by the seizure of either the upper or the lower RCP thrust-journal bearings. Loss of offsite power (LOOP) may be caused by a complete loss of the external electrical grid triggered by the turbine generator trip.

Event frequency conditions are described in Subsection 15.0.0.1. The reactor coolant pump rotor seizure is a PA.

15.3.3.2 Sequence of Events and Systems Operation

Table 15.3.3-1 presents a chronological list and time of system actions that occur following the RCP rotor seizure event for initial conditions selected to minimize the DNBR and

maximize the radiological release. A separate case is analyzed to determine the maximum pressure transient in Subsection 15.3.3.3.4.

The loss of offsite power is assumed to occur due to grid instability. No delay between the time of turbine trip and the time of loss of offsite power is assumed.

The event analysis presented demonstrates that the operator can cool the plant down to cold shutdown during the event.

Following seizure of an RCP rotor, the core flow rapidly decreases to the value that would occur with only three RCPs operating. The rapid reduction in primary coolant flow rate causes an increase in the average coolant temperature in the core, a corresponding reduction in the margin to DNB, and an increase in the primary system pressure. A low coolant flow reactor trip is generated by the reactor protection system (RPS). Analytical setpoints and response times associated with the RPS trip functions and engineered safety features actuation system (ESFAS) functions are consistent with, or conservative with respect to, numerical values delineated in Subsection 15.0.0.3. The RPS trip conservatively assumes the largest possible delay time for sensor delay, calculation period, control element drive mechanism (CEDM) dead time, and CEDM coil decay time.

The reactor heat removal takes place by means of natural circulation in the reactor coolant system following the coastdown of the unfailed RCPs. The steam generator provides P-T-S heat transfer.

After the loss of offsite power, the plant experiences a simultaneous loss of feedwater flow, condenser inoperability, and a coastdown of all RCPs. The steam generator pressure does not exceed the safety limits because the increased pressure in both steam generators results in the opening of the MSSVs. The MSSVs close when the steam generator pressure drops. Water levels in each of the steam generators begin decreasing immediately after the loss of main feedwater flow and an auxiliary feedwater (AFW) actuation signal is generated on low steam generator water level. The auxiliary feedwater actuation system setpoint is first reached in the steam generator in the unaffected loop. This leads to the startup of the auxiliary feedwater pumps.

After 30 minutes, the operator initiates cooldown of the RCS by using the atmospheric dump valves (ADVs) and the auxiliary feedwater system. Plant cooldown is accomplished by using the AFW system in conjunction with the ADVs until shutdown cooling entry conditions are reached.

The shutdown cooling system (SCS) is manually actuated when the RCS temperature and pressure have been reduced to the shutdown cooling entry conditions. This system provides sufficient cooling to bring the RCS to cold shutdown. For decreasing reactor coolant flow events, the major parameter of concern is the minimum hot channel DNBR. This parameter establishes whether a fuel design limit has been violated and, whether fuel damage could be anticipated. The factors that cause a decrease in local DNBR are as follows:

a. Increasing coolant temperature

b. Decreasing coolant pressure

c. Increasing local heat flux

d. Decreasing coolant flow

For the RCP rotor seizure event, the minimum DNBR occurs during the first few seconds of the transient, and the reactor is tripped by the RPS on low reactor coolant flow. Any single failure that would result in a lower DNBR during the transient would have to affect at least one of the above parameters during the first few seconds of the event.

The single failures that have been postulated are listed in Table 15.0-4.

None of the single failures listed in Table 15.0-4 will result in a more adverse transient minimum DNBR than that predicted for the RCP rotor seizure event. None of the single failures listed in Table 15.0-4 has any effect on the peak primary system pressure.

15.3.3.3 Core and System Performance

15.3.3.3.1 Evaluation Model

The NSSS response to an RCP rotor seizure with loss of offsite power concurrent with turbine trip is simulated using the CESEC-III described in Subsection 15.0.2.2.1. The HERMITE Code, described in Subsection 15.0.2.2.5, is used to determine the short-term response of the reactor core during the postulated RCP rotor seizure event. The DNBR is calculated using the TORC and CETOP computer codes (Subsection 15.0.2.2.4), which use the KCE-1 CHF correlation.

15.3.3.3.2 Input Parameters and Initial Conditions

The ranges of initial conditions considered are given in Table 15.0-3. Table 15.3.3-2 gives the initial conditions used in the analysis of the RCP rotor seizure event.

Based on the parametric studies, the most adverse combination of initial conditions is selected to maximize the amount of failed fuel. Using the highest core power maximizes the RCS heatup, which is the driving force of the secondary steam release. A high primary system pressure, a low core inlet temperature, and low reactor coolant flow are chosen in conjunction with the radial peaking factor compatible with these initial conditions, to initiate the event from a power operating limit (POL) allowed by core operating limit supervisory system (COLSS).

The moderator temperature coefficient is assumed to have the maximum value as defined in Subsection 15.0.0.2.3. The Doppler coefficient is assumed to have the least negative value, as defined in Subsection 15.0.0.2.3. Use of these values maximizes the heat flux in the initial stage of the transient. The minimum shutdown CEA worth is assumed as defined in Subsection 15.0.0.2.3.

15.3.3.3.3 Results

The responses of key parameters as a function of time are presented in Figures 15.3.3-1 to 15.3.3-12 for this event.

Table 15.3.3-1 summarizes the sequence of events and significant results of the event.

The RCP rotor seizure event results in a flow coastdown in the affected loop, a consequent reduction in flow through the core, an increase in the average coolant temperature in the core, a corresponding reduction in the margin to DNB, and an increase in the primary system pressure. A reactor trip on low reactor coolant flow is generated by the RPS. The reactor trip causes the turbine generator to trip. At the time of the turbine generator trip, the loss of offsite power is assumed to occur. The remaining RCPs begin their normal coastdown after the loss of offsite power. The loss of offsite power also causes a loss of main feedwater and condenser inoperability. The turbine trip with the steam bypass control system and the condenser unavailable leads to a rapid buildup in secondary system pressure and temperature. This increase in pressure is shown in Figure 15.3.3-10. The opening of the MSSVs limits this pressure increase.

The increasing temperature of the secondary system leads to a reduction of the P-T-S heat transfer. Concurrently, the failed RCP and the three RCPs coasting down result in a lower RCS flow (Figure 15.3.3-9), which further reduces the heat transfer capability of the RCS. This decrease in heat removal from the RCS leads to an increase in the core coolant temperatures as shown in Figure 15.3.3-6. The core coolant temperatures peak shortly after the time of reactor trip.

During the first few seconds of the transient, the combination of decreasing flow rate and increasing RCS temperatures results in a decrease in the fuel pin DNBR. The transient minimum DNBR and the time it occurs are indicated in Table 15.3.3-1. Figure 15.3.3-12 shows the variation of the minimum DNBR with time. The negative CEA reactivity inserted after reactor trip causes a rapid power and heat flux decrease, which causes DNBR to increase again.

The percentage of the fuel pins that are calculated for this event to experience DNB is less than 7 percent. All fuel pins that experience DNB are conservatively assumed to fail. The fuel rod failures do not propagate to the surrounding rods. The evaluation of rod internal pressure and the effect of ballooning are described in Subsection 4.2.3.1.2. The fuel rod failures are sufficiently limited to maintain core-cooling capability.

15.3.3.4 Barrier Performance

15.3.3.4.1 Evaluation Model

The barrier performance evaluation for peak RCS pressure uses the same CESEC-III evaluation model as in the core and system performance analysis described in Subsection 15.3.3.3.1.

15.3.3.4.2 Input Parameters and Initial Conditions

The ranges of initial conditions considered are given in Table 15.0-3. Input parameters and initial conditions are modified in order to maximize the primary and secondary system pressure. The peak pressure analysis uses the initial core inlet temperature of 295 °C (563 °F), and the initial steam generator pressure of 75.86 kg/cm^{2}A (1,079 psia), and all other initial condition parameter values are the same as listed in Table 15.3.3-2.

15.3.3.4.3 Results

The peak RCS and steam system pressure are 186.6 kg/cm^{2}A (2,655 psia) and 90.33 kg/cm^{2}A (1,285 psia), respectively. These values are less than 110 percent of design RCS and steam system pressure, respectively. The peak RCS pressure includes the pressure difference between the cold leg at RCP discharge and the surge line. The dynamic behaviors of important NSSS parameters following an RCP rotor seizure are presented in Figures 15.3.3-13 through 15.3.3-16.

The RCP seal is normally cooled by (1) seal injection water from chemical and volume control system (CVCS), and (2) the component cooling water (CCW) system through a high-pressure seal cooler. The evaluations of the RCPs presented in Subsections 5.4.1.2 and 5.4.1.3 show the integrity of RCPs would be maintained with a loss of CCW for at least 30 minutes.

15.3.3.5 Radiological Consequences

The radiological consequences are evaluated to determine EAB, LPZ, MCR, and TSC doses due to a reactor coolant pump (RCP) rotor seizure accident using the AST methodology, the TEDE dose criteria, the guidance in SRP 15.0.3, and the plant-specific bounding design information applicable to the APR1400.

15.3.3.5.1 Evaluation Model

Figure 15A-3 in Appendix 15A shows the leakage paths and transport of the activity released to environment and control room during RCP rotor seizure event.

Release via the Steam Generators

In this analysis, the affected steam generator (SG) is the SG associated with the RCS loop with the RCP rotor seizure. Both the affected and unaffected SG tubes are expected to be uncovered during the first 30 minutes of the RCP rotor seizure. During this period, the P-T-S leakage flashing fraction averages 15.0 percent. After 30 minutes, the tubes in both SGs are assumed to remain covered during the RCP rotor seizure event. Per NRC RG 1.183, the iodine activity in the P-T-S leakage is assumed to mix with SG coolant without flashing during the period of submergence, and an iodine partition coefficient of 100 is assumed. The RCS iodine release continues from 0 to 2 hours in the affected SG and from 0 to 8 hours for the unaffected SG until the shutdown cooling system is initialized at 8 hours.

Release via the Condenser

The release of fission products from the secondary system is evaluated with the assumption of a coincident LOOP. The offsite power is assumed to be lost so that the main steam condenser is not available for removal of the decay heat.

15.3.3.5.2 Input Parameters and Initial Conditions

The design basis RCP rotor seizure accident is analyzed using a conservative set of assumptions and the APR1400 design inputs. The analysis is performed using the guidance in NRC RG 1.183, Appendix G.

The APR1400 RCP rotor seizure analysis predicts that no more than 7 percent of the fuel in the core will fail due to DNBR, and no fuel will melt. The assumed inventory of fission products in the reactor core and available for release to the reactor coolant is based on the maximum power level of 4,062.66 MWt corresponding to current fuel enrichment and fuel burnup, which is 1.02 times the APR1400 licensed thermal power of 3,983 MWt. The

activity released from the fuel is assumed to be released instantaneously and homogeneously through the primary coolant.

The chemical forms of iodine released from the steam generators to the environment are 97 percent elemental and 3 percent organic. These iodine chemical forms are applied to iodine releases from the P-T-S leakage and from the secondary liquid.

The secondary coolant iodine concentration is limited to 3.7×10^3 Bq/g (0.1 μCi/g) DE I-131. The RCS DE I-131 isotopic concentration profile is multiplied by a factor of 0.1 representing the ratio of the secondary to primary limits to determine the secondary coolant iodine concentration. The secondary coolant iodine concentration is multiplied by the total coolant mass in both steam generators to calculate the total secondary coolant iodine inventory.

This analysis models the RCS leakage limit of 1.14 L/min (0.3 gpm) gpm of P-T-S leakage through each SG. The primary coolant density used in converting the volumetric P-T-S leak rates to mass leak rates is 1.0 g/cm^3 (62.4 lbm/ft^3). The P-T-S leakage continues until the primary system pressure is less than the secondary system pressure, or until the temperature of the leakage is less than 100 °C (212 °F), and the release of radioactivity is assumed to continue until shutdown cooling is in operation and releases from the steam generator have terminated. In this analysis, the RCS is conservatively assumed to leak into the affected SG for 0 to 2 hours and into unaffected SG for 0 to 8 hours until the shutdown cooling system is initialized. All noble gas radionuclides released from the primary system (through the P-T-S leak) are released to the environment without reduction or mitigation. Input parameter values used for RCP rotor seizure radiological consequence evaluation are presented in Table 15.3.3-3.

The χ/Q values used in the analysis for EAB, LPZ, MCR, and TSC are described in Subsection 2.3.4 and are in Tables 2.3-1 through 2.3-12; breathing rates are given in Table 15A-11.

15.3.3.5.3 Results

The radiological consequences due to RCP rotor seizure accident are presented in Table 15.3.3-4. The results of the RCP rotor seizure accident analyses indicate that the EAB and LPZ doses are within their allowable dose criteria limit, which is 10 percent of the 10 CFR

50.34(a)(1) value, as specified in SRP 15.0.3. The MCR and TSC doses are also within the dose limit in GDC 19.

15.3.3.6 Conclusions

The percentage of fuel pins that are calculated to experience DNB in this event is lower than the percentage that is assumed for the radiological dose analysis. The fuel rod failures are sufficiently limited to maintain core-cooling capability.

The maximum RCS and steam system pressure due to an RCP rotor seizure event in combination with LOOP coincident with turbine generator trip remain below 110 percent of their respective design values.

Only a small fraction of the fuel pins experience DNB and are conservatively assumed to fail. The doses at the EAB, LPZ, MCR, and TSC are within their allowable criteria limits.

15.3.4 Reactor Coolant Pump Shaft Break

15.3.4.1 Identification of Causes and Frequency Classification

A reactor coolant pump shaft break could be caused by mechanical failure of the pump shaft. This is assumed to result from a manufacturing defect in the shaft. Loss of offsite power following turbine generator trip may be caused by a complete loss of the external electrical grid triggered by the turbine generator trip.

Event frequency conditions are described in Subsection 15.0.0.1. This event is a PA.

15.3.4.2 Sequence of Events and Systems Operation

The sequence of events and system operations is similar to that for the reactor coolant pump rotor seizure event (see Subsection 15.3.3). For both the shaft break event and the pump rotor seizure event, the reactor is tripped by the RPS on a low reactor coolant flow condition. The loss of offsite power is assumed to occur due to grid instability. No delay between the time of the turbine trip and the time of the loss of offsite power is assumed to occur.

The flow coastdown for the reactor coolant pump rotor seizure event is faster than the coastdown for the reactor coolant pump shaft break event. For the reactor coolant pump shaft break event, the rotor is still capable of rotating, thereby offering less resistance to flow during the rapid flow decrease. This results in a less severe coastdown for the reactor coolant pump shaft break event than for the reactor coolant pump rotor seizure event. The trip time of the reactor coolant pump shaft break is later than the trip time of the reactor coolant pump rotor seizure. Despite the later trip time, the slower reactor coolant pump shaft break coastdown results in a higher minimum DNBR and less fuel failure for reactor coolant pump shaft break event than for the reactor coolant pump rotor seizure event.

15.3.4.3 Core and System Performance

The analysis performed for the RCP rotor seizure (Subsection 15.3.3) bounds the response and results for the reactor coolant pump shaft break.

15.3.4.4 Barrier Performance

The analysis performed for the RCP rotor seizure (Subsection 15.3.3) bounds the response and results for the reactor coolant pump shaft break.

15.3.4.5 Radiological Consequences

The radiological consequences due to steam released from the secondary system would be less than the consequences of the single RCP rotor seizure event as described in Subsection 15.3.3. Thus, the radiological consequences for the shaft break event with LOOP event are bounded by the values in Table 15.3.3-4.

15.3.4.6 Conclusions

The analysis performed for the reactor coolant pump rotor seizure (Section 15.3.3) bounds the response and results for the reactor coolant pump shaft break.

15.3.5 Combined License Information

No COL information is required with regard to Section 15.3.

Table 15.3.1-1

Sequence of Events for the Loss of Forced Reactor Coolant Flow

Time (sec)	Event	Setpoint or Value
0.00	Loss of offsite power Turbine trip Diesel generator starting signal Reactor coolant pumps coast down Main feedwater is lost	—
0.87	Core protection calculator (CPC) Low RCP shaft speed trip condition reached, % of full speed	94.8
1.22	CPC low RCP speed trip signal generated	—
1.32	CPC low RCP speed trip	—
3.9	Minimum transient DNBR	1.29
4.35	POSRV open setpoint reached, kg/cm^2 A (psia)	177.13 (2,519.4)
4.9	Maximum RCS pressure, kg/cm^2 A (psia)	184.4 (2,622.5)
9.05	MSSV open, kg/cm^2 A (psia)	86.88 (1,235.66)
13.6	Maximum steam generator pressure, kg/cm^2 A (psia)	89.48 (1,272.7)
1,800.0	Operator initiates plant cooldown	—

Table 15.3.1-2

Assumptions and Initial Conditions
for the Loss of Forced Reactor Coolant Flow

Parameter	Value
Core power level, MWt	4,062.66
Core inlet coolant temperature, °C (°F)	287.8 (550)
Reactor coolant system pressure, kg/cm^2A (psia)	163.45 (2,325)
Steam generator pressure, kg/cm^2A (psia)	75.86 (1,079)
Core Mass Flow, 10^6 kg/hr (10^6 lbm/hr)	85.03 (187.46)
Initial core minimum DNBR	1.53
Maximum radial peaking factor	2.10
CEA worth on trip, % $\Delta\rho$ (most reactive CEA stuck)	−8.0
Moderator temperature coefficient, $\Delta\rho$/°C ($\Delta\rho$/°F)	0.0 (0.0)
Doppler reactivity	Least negative

Table 15.3.3-1 (1 of 2)

Sequence of Events for the Reactor Coolant Pump Rotor Seizure

Time (sec)	Event	Setpoint or Value
0.0	Seizure of a single reactor coolant pump	—
0.3	Low reactor coolant flow trip condition reached, fraction of hot leg flow	0.80
1.5	Reactor trip breakers open	—
1.5	Turbine trip/generator trip	—
1.5	Loss of offsite power occurs	—
2.0	CEAs begin to drop	—
3.5	Minimum transient DNBR	1.08
4.4	POSRV open setpoint reached, kg/cm^2A (psia)	177.13 (2,519.4)
5.0	Maximum RCS pressure, kg/cm^2A (psia)	182.54 (2,596.3)
15.6	Main steam safety valves open, unaffected loop, kg/cm^2A (psia)	86.88 (1,235.66)
16.2	Main steam safety valves open, affected loop, kg/cm^2A (psia)	86.88 (1,235.66)
23.0	Maximum steam generator pressure, unaffected loop, kg/cm^2A (psia)	88.43 (1,257.7)
23.7	Maximum steam generator pressure, affected loop, kg/cm^2A (psia)	88.28 (1,255.6)
404.3	Steam generator water level reaches auxiliary feedwater actuation signal analysis setpoint in the unaffected loop, %WR	19.9
465.8	Auxiliary feedwater begins entering steam generator, unaffected loop, kg/sec (lbm/sec)	40.42 (89.10)

Table 15.3.3-1 (2 of 2)

Time (sec)	Event	Setpoint or Value
921.2	Steam generator water level reaches auxiliary feedwater actuation signal analysis setpoint in the affected loop, % Wide Range	19.9
982.7	Auxiliary feedwater begins entering steam generator, affected loop, kg/sec (lbm/sec)	40.42 (89.10)
1,627	Main steam safety valves close, all loops, kg/cm^2A (psia)	78.19 (1,112.09)
1,800	Atmospheric dump valves opened to initiate plant cooldown	—
28,800	Shutdown cooling initiated	—

Table 15.3.3-2

Assumptions and Initial Conditions
for Reactor Coolant Pump Rotor Seizure Analysis

Parameter	Value
Core power level, MWt	4,062.66
Core inlet coolant temperature, °C (°F)	287.8 (550)
Pressurizer pressure, kg/cm^{2}A (psia)	163.45 (2,325)
Steam generator pressure, kg/cm^{2}A (psia)	68.28 (971)
Core mass flow rate, 10^6 kg/hr (10^6 lbm/hr)	69.64 (153.52)
Maximum radial power peaking factor	1.76
CEA worth on trip, % Δρ (most reactive CEA stuck)	−8.0
Moderator temperature coefficient, $\Delta\rho\times10^{-4}$/°C ($\Delta\rho\times10^{-4}$/°F)	0.0 (0.0)
Doppler reactivity	Least negative

Table 15.3.3-3 (1 of 2)

Parameters Used in Evaluating the Radiological Consequences of the Reactor Coolant Pump Rotor Seizure

Parameter	Value
Source Terms	
Reactor Core Power Level	4,062.66 MWt
Percent of Fuel Assumed to Experience Departure from Nucleate Boiling (DNB)	7.0 %
Percent of Fuel Assumed to Melt	0 %
Radial Peaking Factor	1.80
RCS Mass	272,000 kg (600,000 lbm)
Initial RCS Iodine Specific Activity	3.7×10^4 Bq/g (1.0 μCi/g) DE I-131
Initial RCS Noble Gases Specific Activity	2.15×10^7 Bq/g (580 μCi/g) DE X-133
Initial Secondary Liquid Iodine Specific Activity	3.7×10^3 Bq/g (0.1 μCi/g) DE I-131
Secondary System Activity Transport Model	
Primary-to-Secondary Leak Rate through SGs	2.27 L/min (0.6 gpm) for two SGs
Density of P-T-S Leakage Measurement	1 g/cm^3 (62.4 lbm/ft^3)
Steam Mass Release from Affected SG 0 ~ 0.5 hrs 0.5 ~ 2 hrs 2 ~ 8 hrs	 56,800 kg (125,000 lbm) 193,000 kg (425,000 lbm) 0.0 kg (0.0 lbm)
Steam Mass Release from Unaffected SG 0 ~ 0.5 hrs 0.5 ~ 2 hrs 2 ~ 8 hrs	 53,900 kg (119,000 lbm) 199,000 kg (439,000 lbm) 609,000 kg (1,340,000 lbm)
Initial SG Liquid Mass	84,200 kg (186,000 lbm)
Primary-To-Secondary Leak Flashing Fraction	15.0 % average for 30 mins after onset of accident
SG Liquid Iodine Partition Coefficient for SG Liquid Iodine Release	100

Table 15.3.3-3 (2 of 2)

Parameter	Value
Chemical Form of Iodine Released from SG to Environment Elemental Organic	 97 % 3 %
MCR and TSC Model Parameters	
Envelope Volume	5,663 m^3 (200,000 ft^3)
Normal Ventilation Flow Rate (unfiltered)	105 m^3/min (3,700 cfm)
Emergency Ventilation Makeup Rate (filtered)	105 m^3/min (3,700 cfm)
Emergency Ventilation Recirculation Flow Rate (filtered)	122 m^3/min (4,300 cfm)
Emergency HVAC Delay Time	5 mins
Emergency Ventilation Charcoal Filter Efficiency (elemental and organic iodine removal)	99 %
Emergency Ventilation HEPA Filter Efficiency (particulate removal)	99 %
Unfiltered Inleakage	8.50 m^3/min (300 cfm)
Occupancy Factors 0 ~ 24 hrs 24 ~ 96 hrs 96 ~ 720 hrs	 100 % 60 % 40 %
Onsite χ/Qs	See Tables 2.3.2 ~ 2.3.12
Offsite Model Parameters	
χ/Qs	See Table 2.3-1
Breathing Rate	See Table 15A-11
Dose Conversion Factors	See Table 15A-10

Table 15.3.3-4

Radiological Consequences of the Reactor Coolant Pump Rotor Seizure

Post-RCP Rotor Seizure Activity Release Path	TEDE Dose (mSv)		
	MCR and TSC	EAB	LPZ
P-T-S Iodine Release	9.19E+00	1.29E+01	8.10E+00
P-T-S Noble Gas Release	3.94E+00	7.89E+00	2.57E+00
Secondary Liquid Iodine Release	5.03E-02	7.51E-02	3.70E-02
External Cloud	6.88E-01	0.00E+00	0.00E+00
MCR Filter Shine	1.34E-06	0.00E+00	0.00E+00
Total	1.39E+01	2.09E+01	1.07E+01
Allowable TEDE Limit	5.00E+01	2.50E+01	2.50E+01

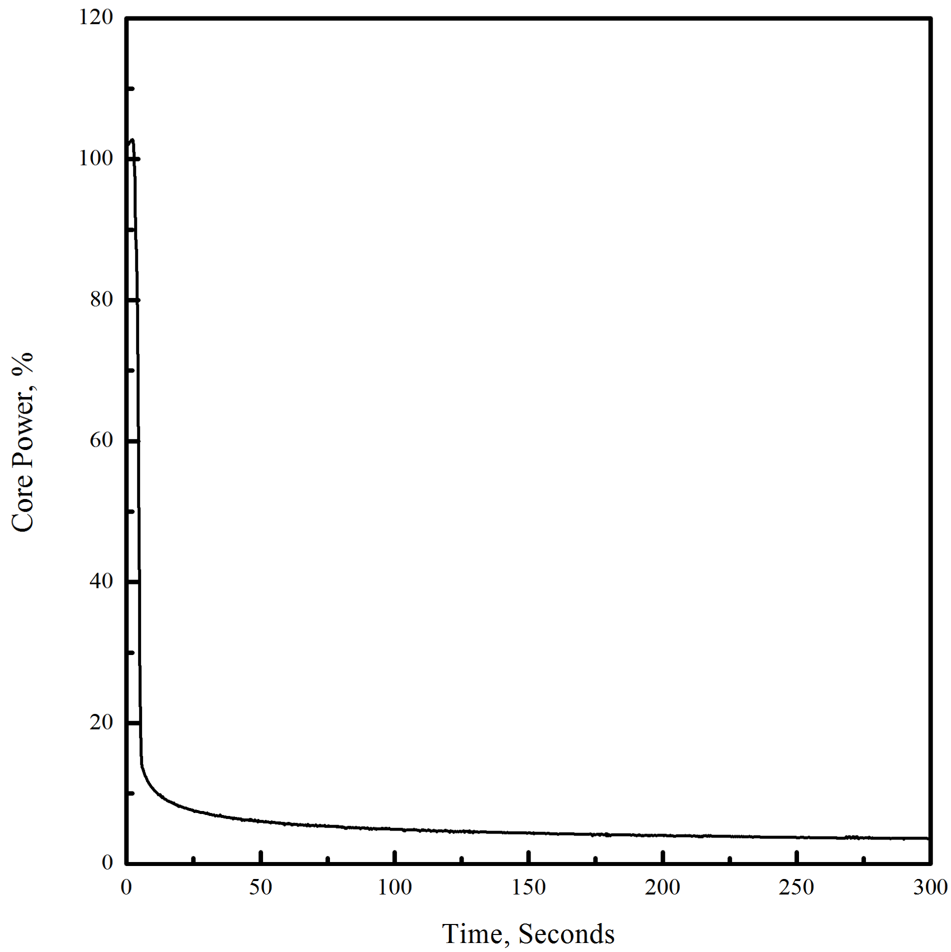

Figure 15.3.1-1 Loss of Forced Reactor Coolant Flow ; Core Power vs. Time

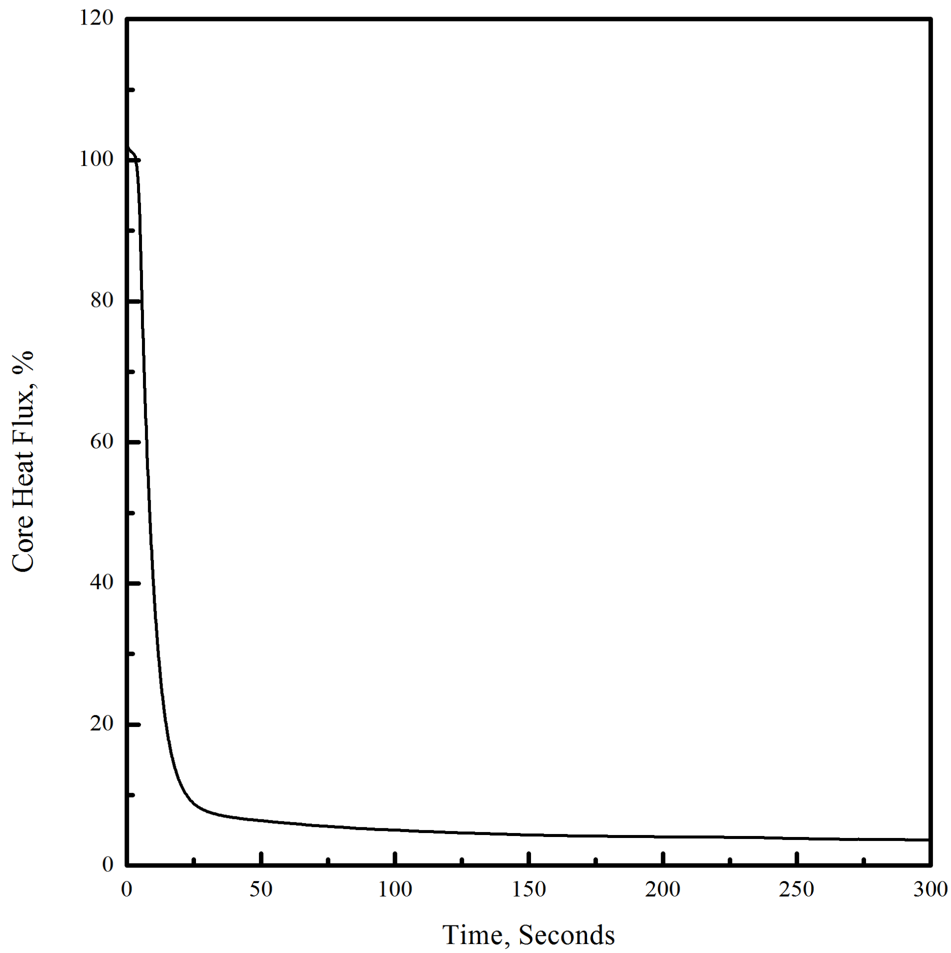

Figure 15.3.1-2 Loss of Forced Reactor Coolant Flow ; Core Average Heat Flux vs. Time

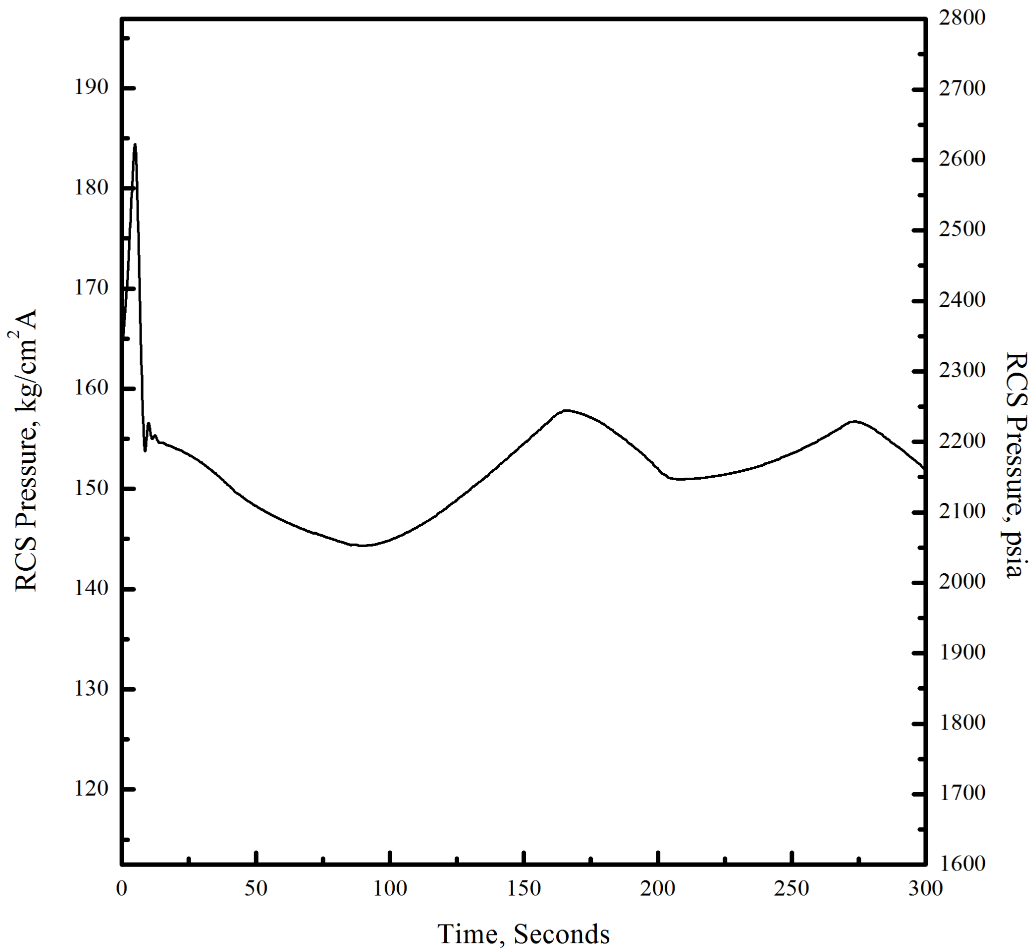

* The pressure difference between cold leg at the RCP discharge and the surge line is not included.

Figure 15.3.1-3 Complete Loss of Reactor Coolant Flow ; RCS Pressure vs. Time

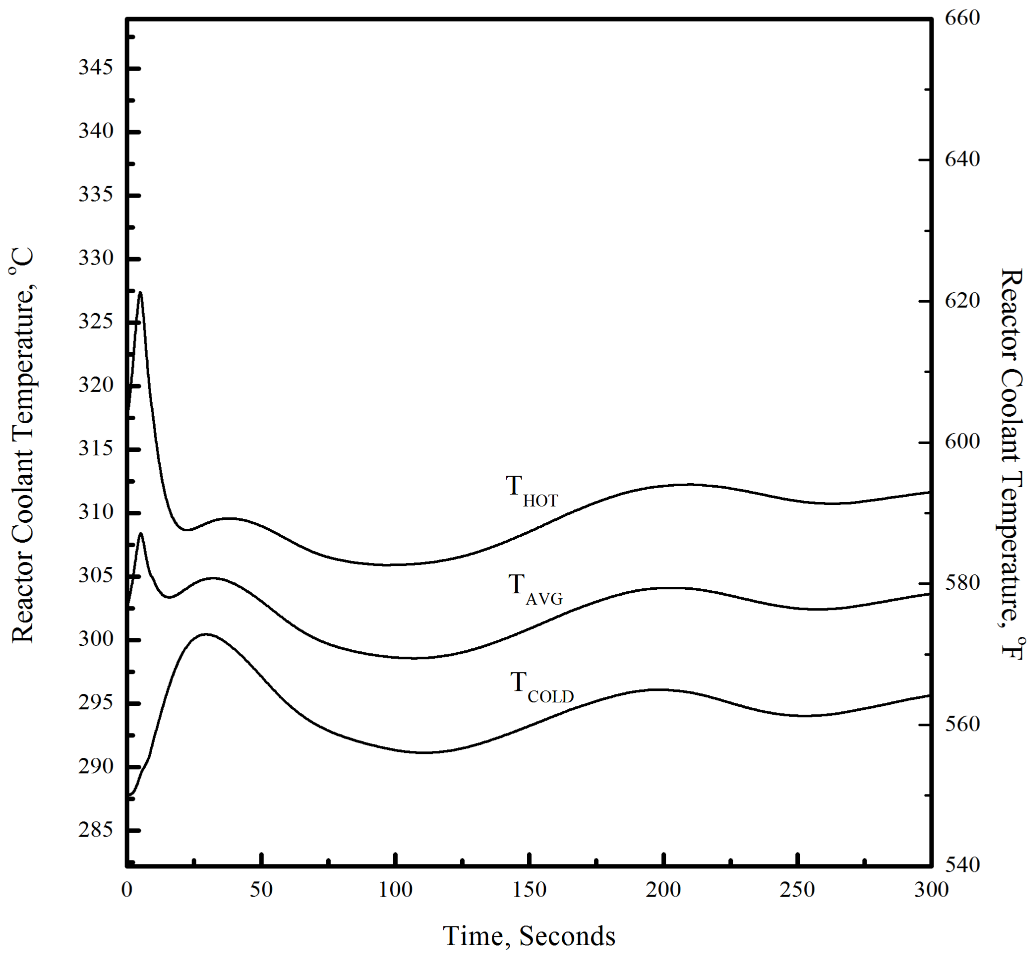

Figure 15.3.1-4 Loss of Forced Reactor Coolant Flow ; Reactor Coolant Temperature vs. Time

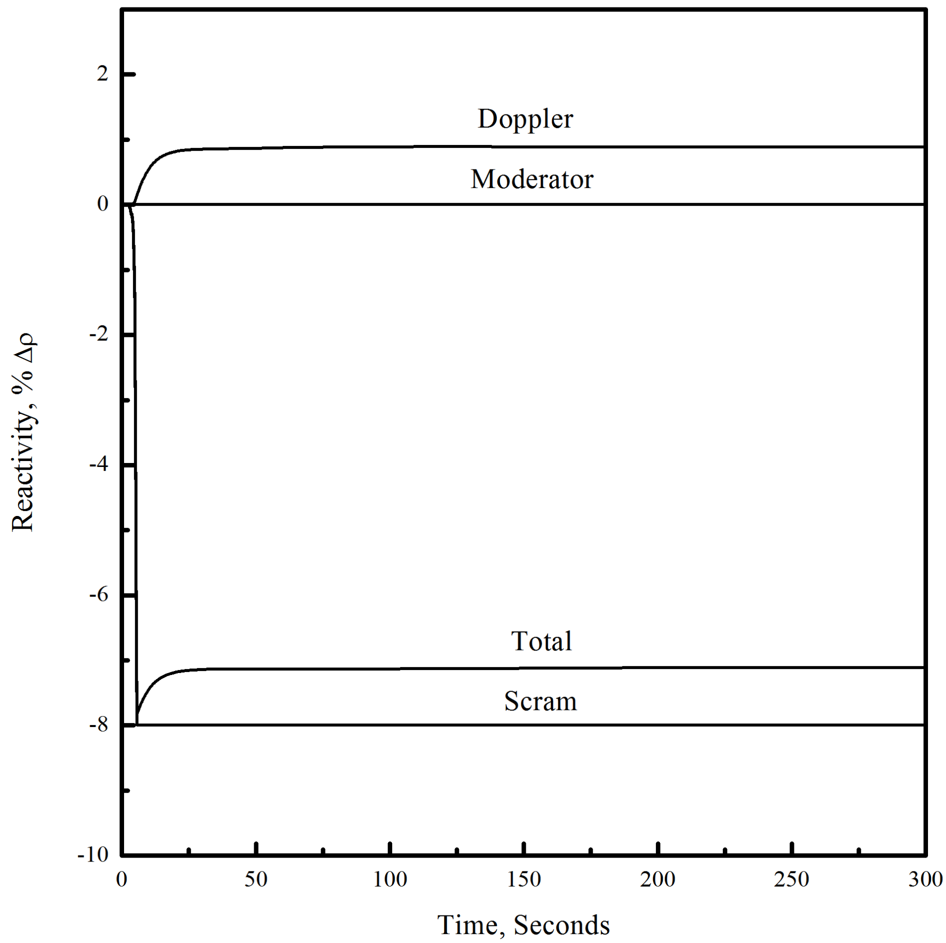

Figure 15.3.1-5 Loss of Forced Reactor Coolant Flow ; Reactivity vs. Time

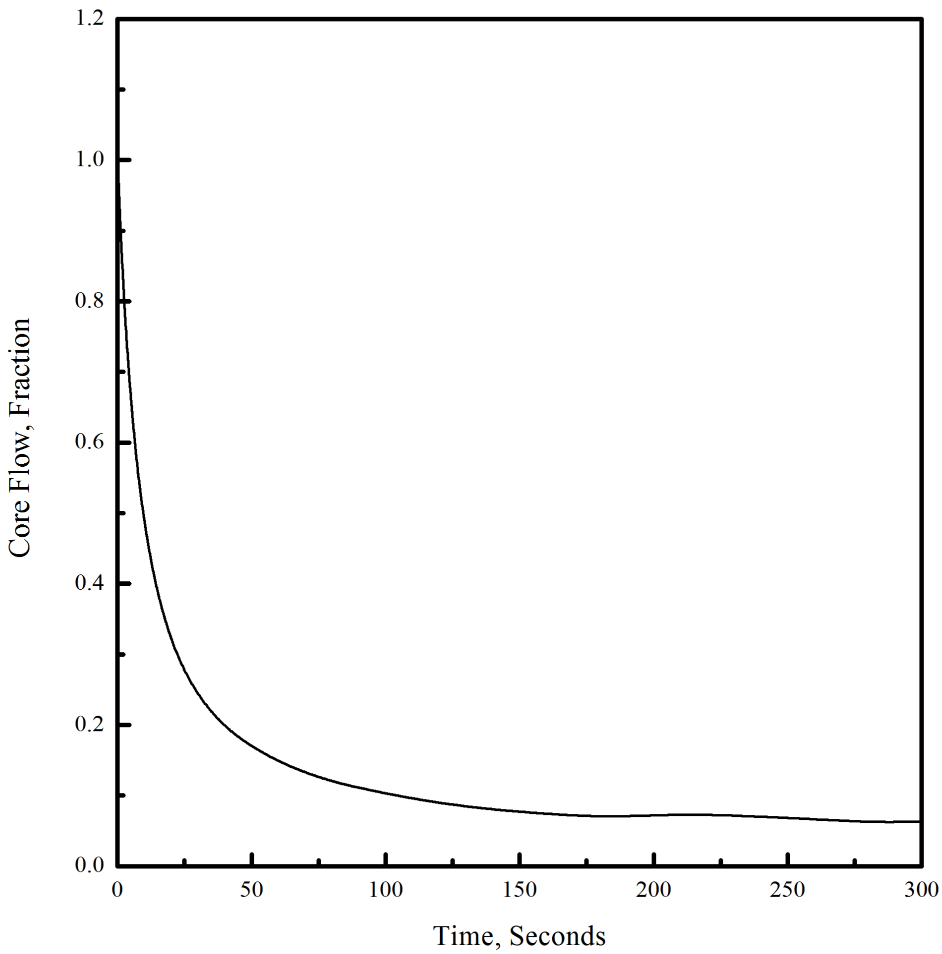

Figure 15.3.1-6 Loss of Forced Reactor Coolant Flow ; Core Flow vs. Time

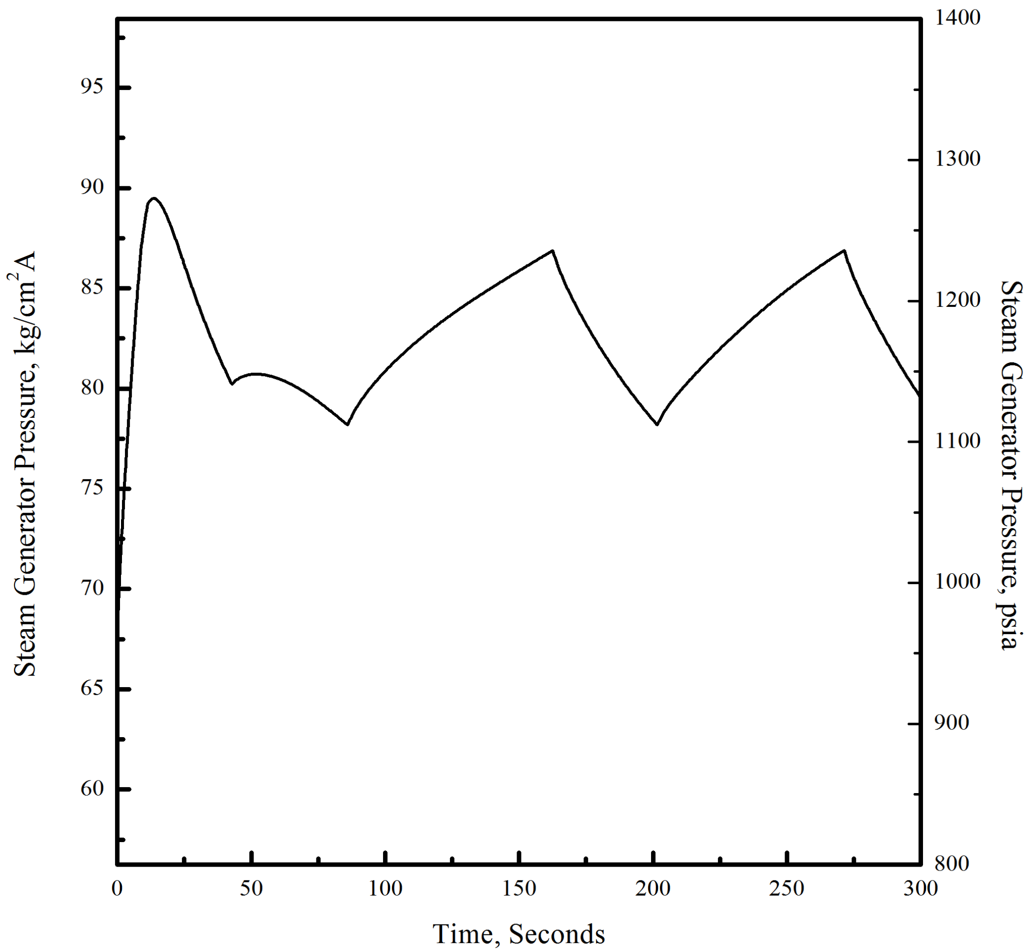

Figure 15.3.1-7 Loss of Forced Reactor Coolant Flow ; Steam Generator Pressure vs. Time

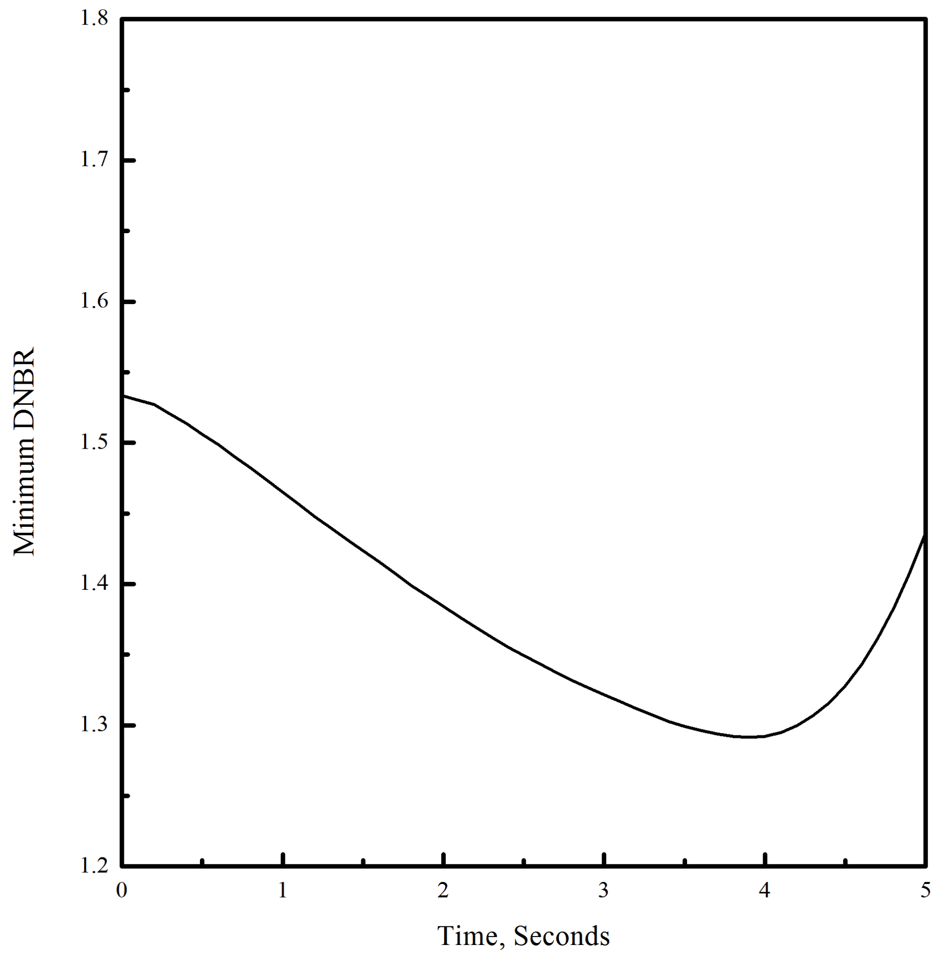

Figure 15.3.1-8 Loss of Forced Reactor Coolant Flow ; Minimum DNBR vs. Time

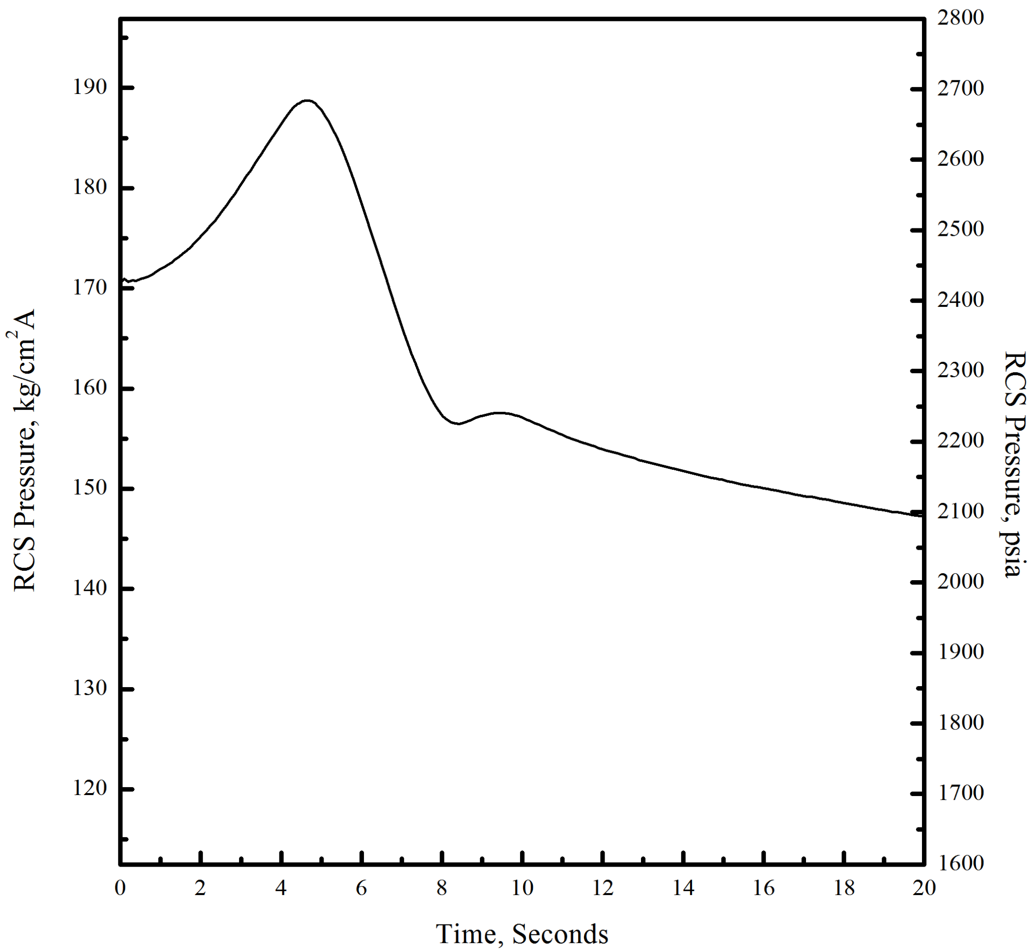

* The pressure difference between cold leg at the RCP discharge and the surge line is included.

Figure 15.3.1-9 Complete Loss of Reactor Coolant Flow ; Maximum RCS Pressure vs. Time (Peak Pressure Case)

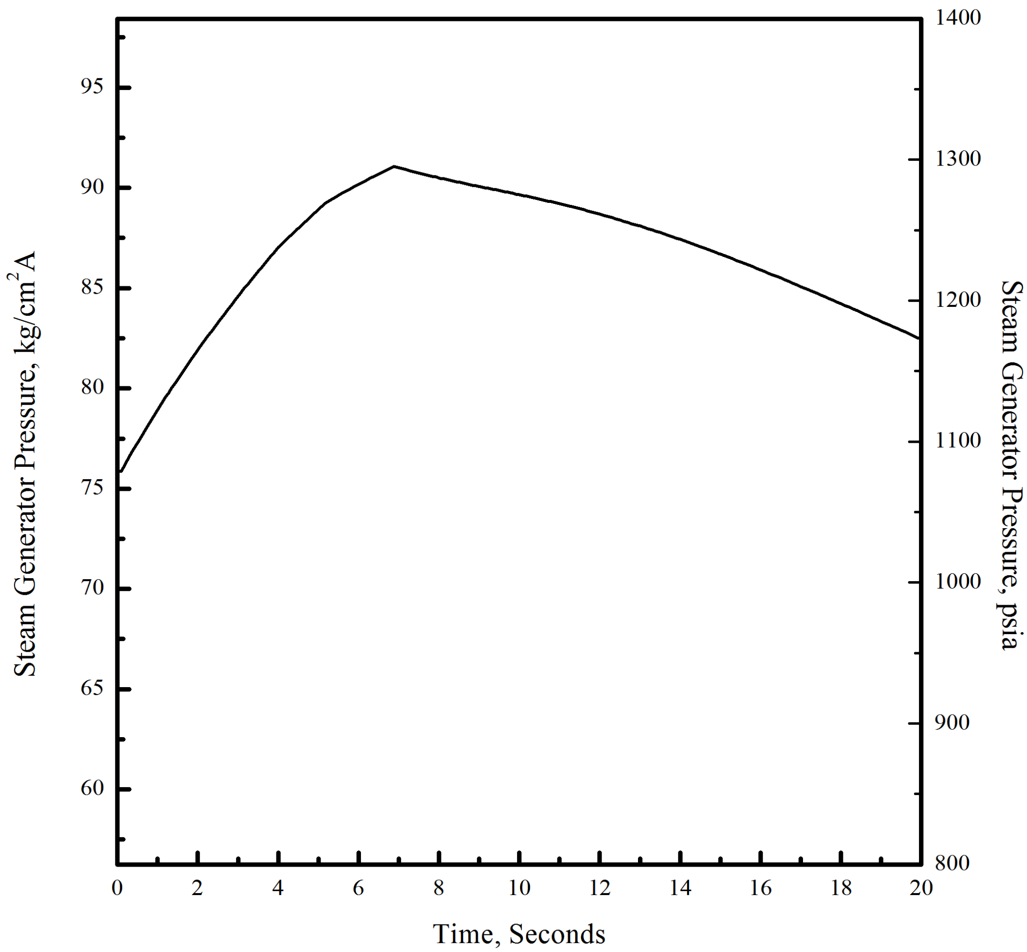

Figure 15.3.1-10 Loss of Forced Reactor Coolant Flow ; Steam Generator Pressure vs. Time (Peak Pressure Case)

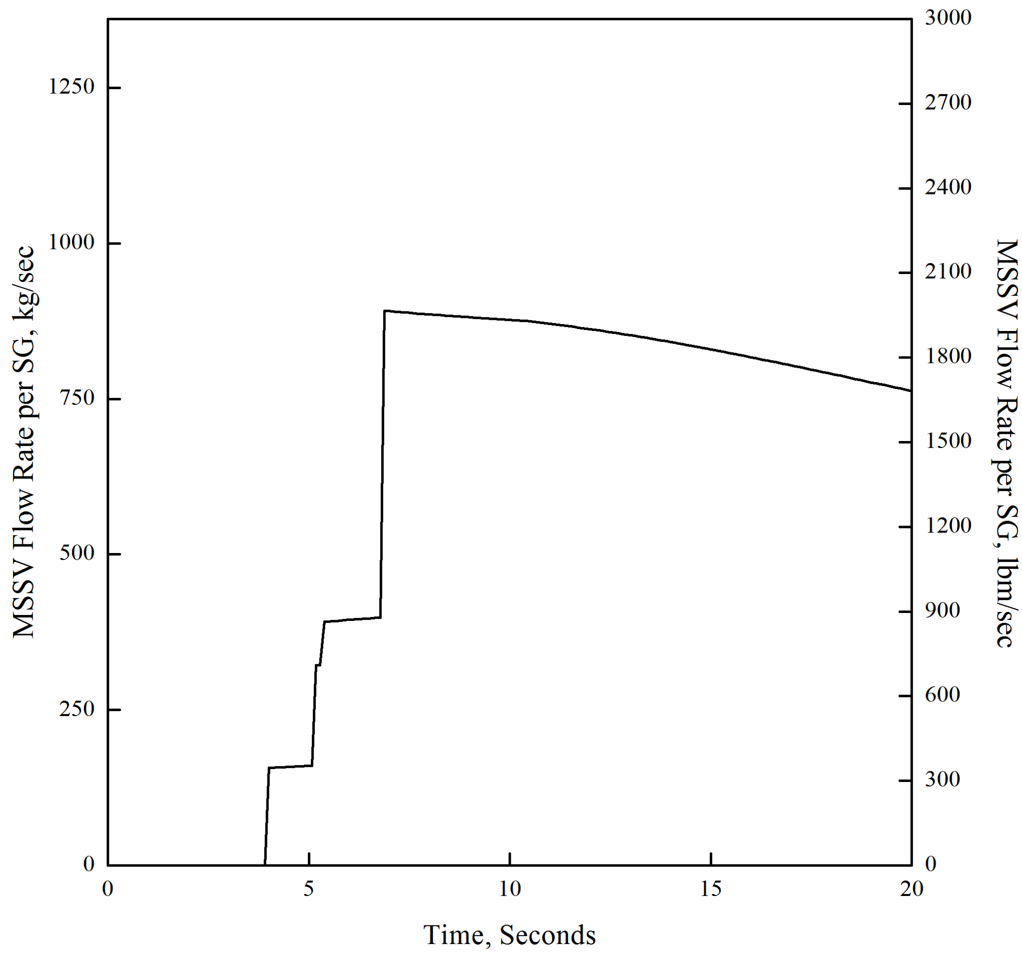

Figure 15.3.1-11 Loss of Forced Reactor Coolant Flow ; Main Steam Safety Valve Flow Rate per Steam Generator vs. Time (Peak Pressure Case)

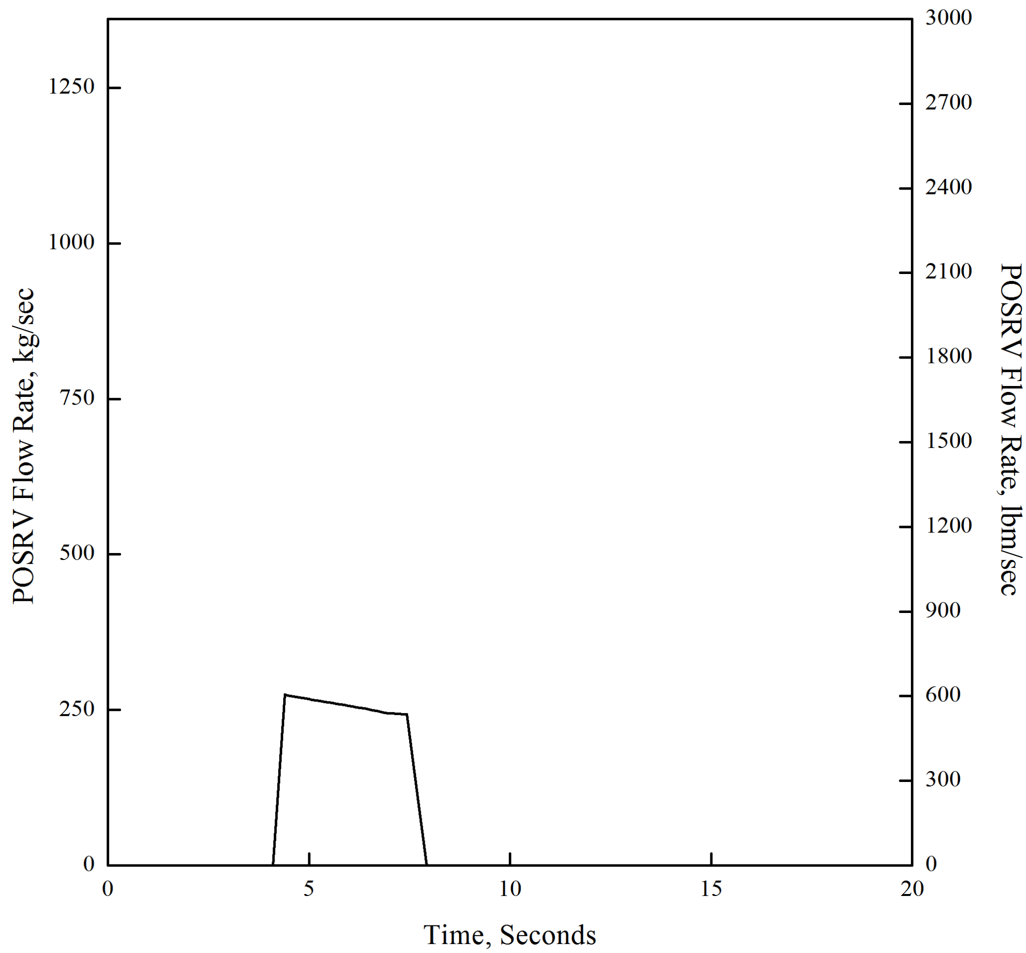

Figure 15.3.1-12 Loss of Forced Reactor Coolant Flow ; Pressurizer Pilot Operated Safety Relief Valve Flow Rate vs. Time (Peak Pressure Case)

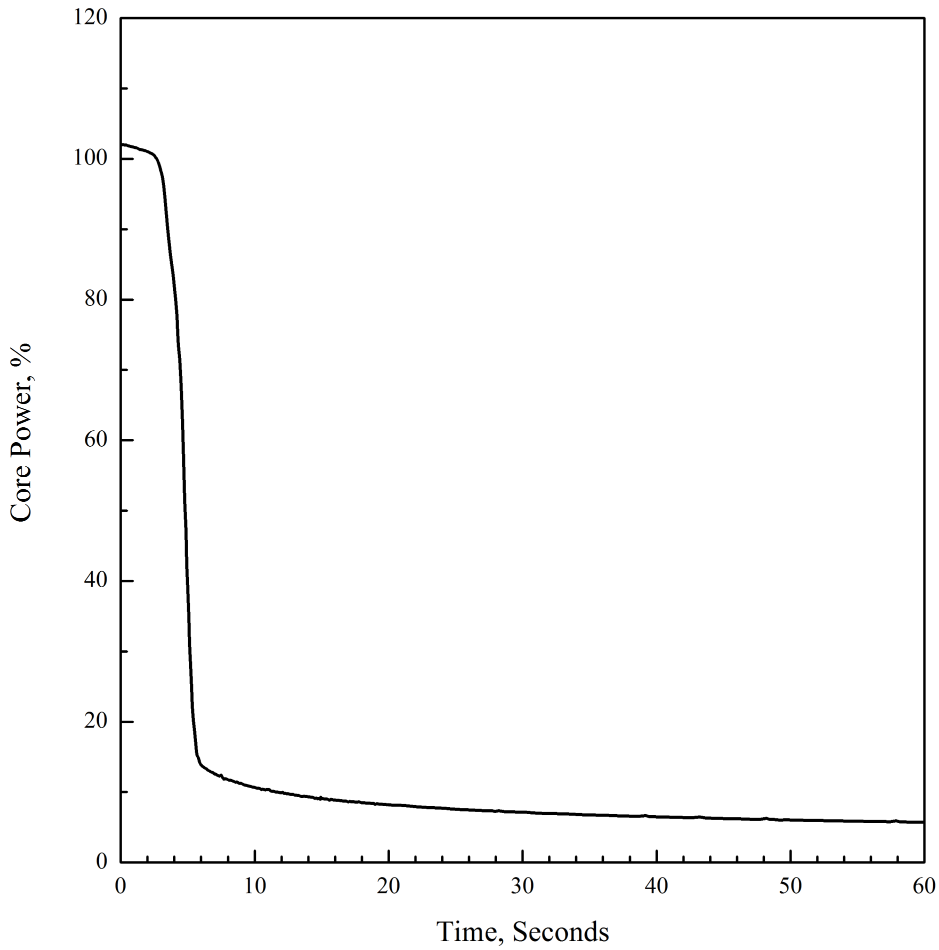

Figure 15.3.3-1 RCP Rotor Seizure ; Core Power vs. Time

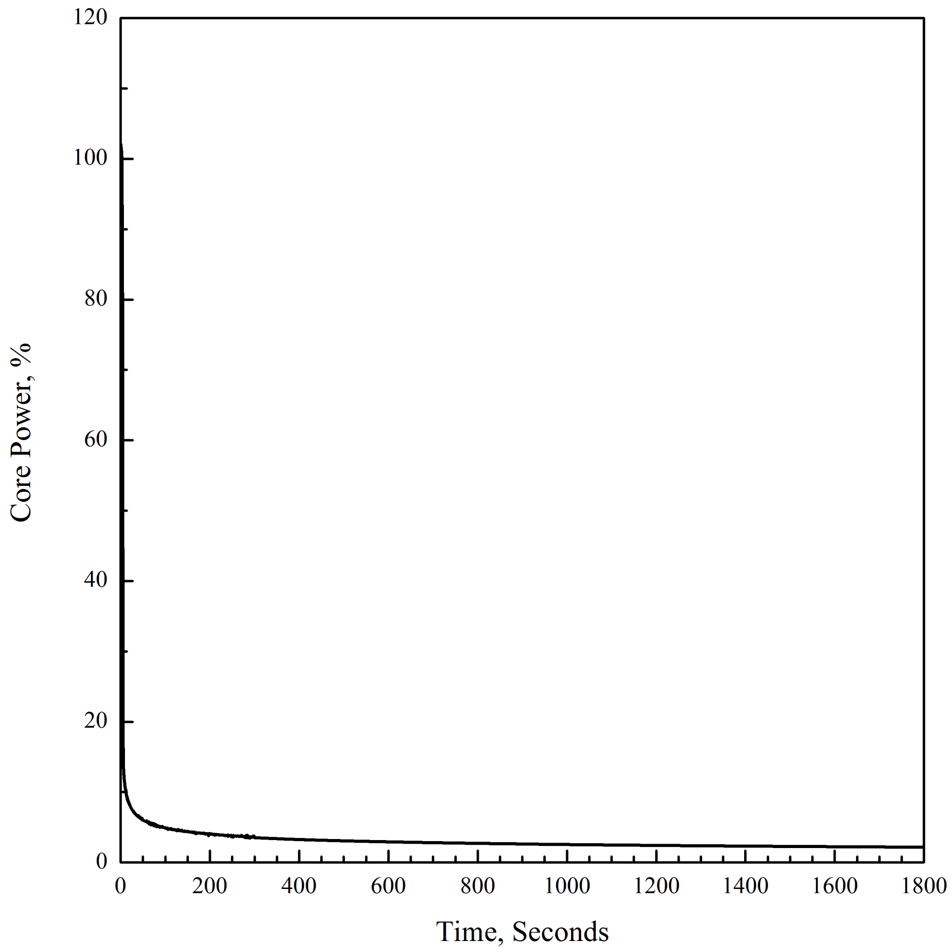

Figure 15.3.3-2 RCP Rotor Seizure ; Core Power vs. Time

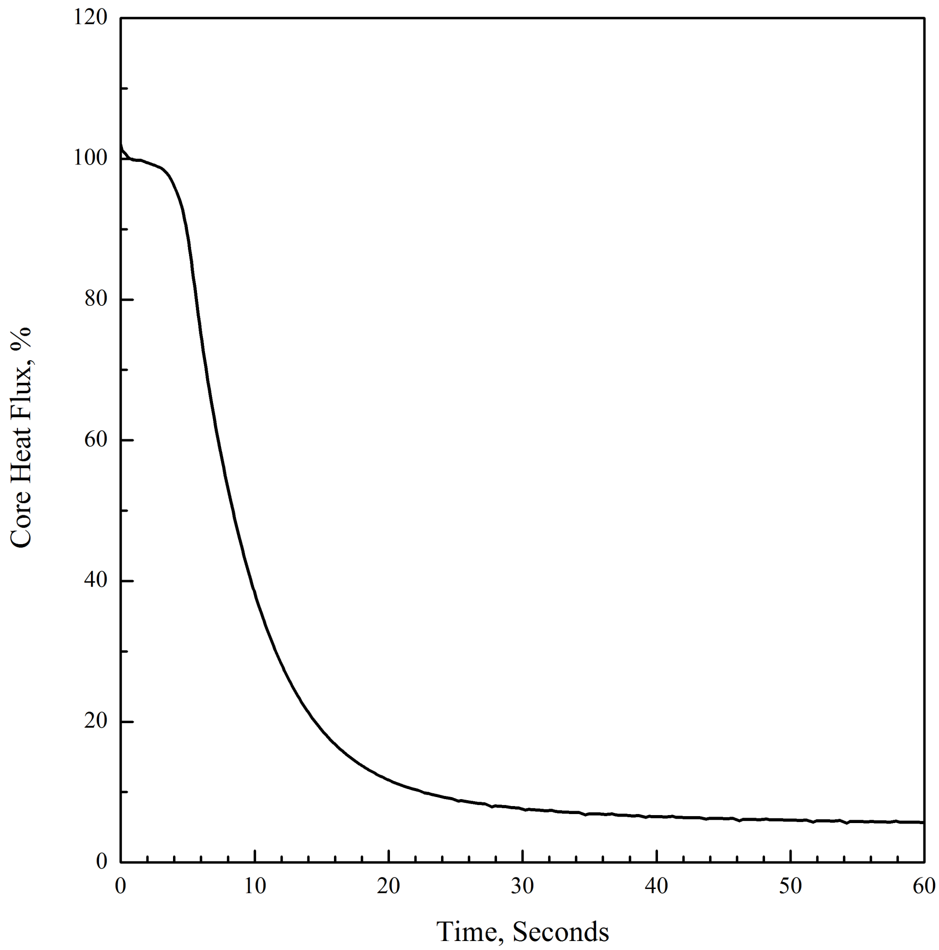

Figure 15.3.3-3 RCP Rotor Seizure ; Core Average Heat Flux vs. Time

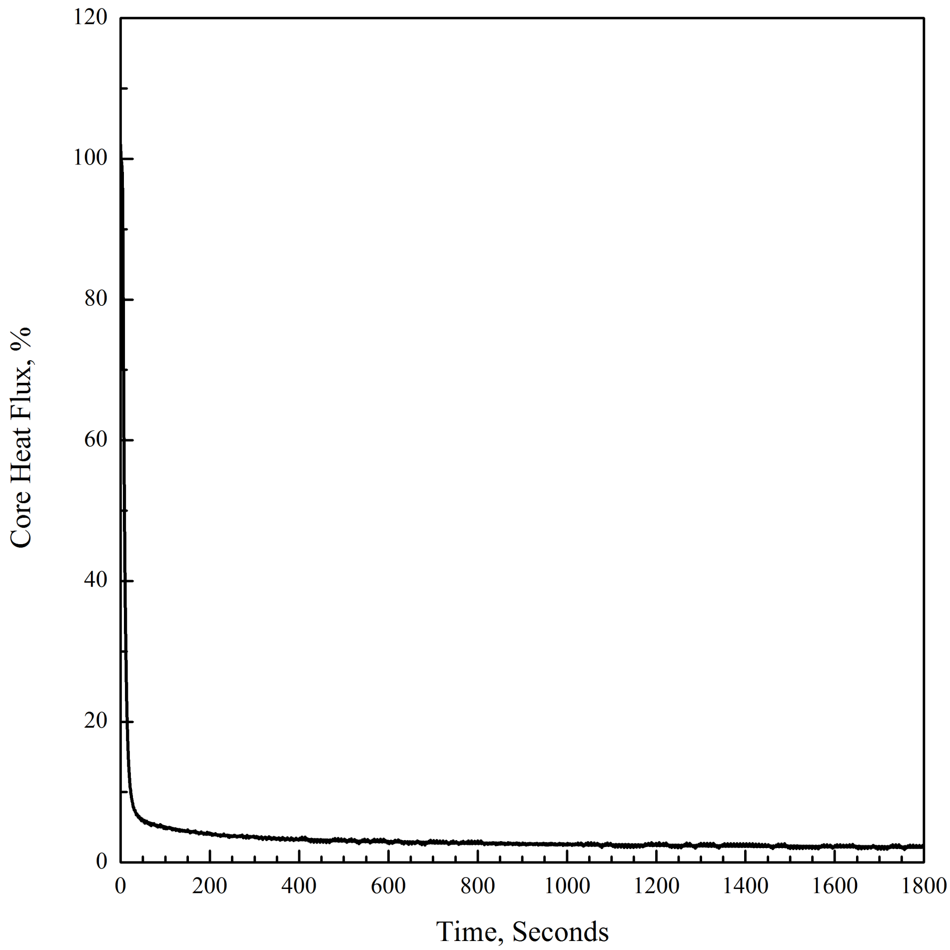

Figure 15.3.3-4 RCP Rotor Seizure ; Core Average Heat Flux vs. Time

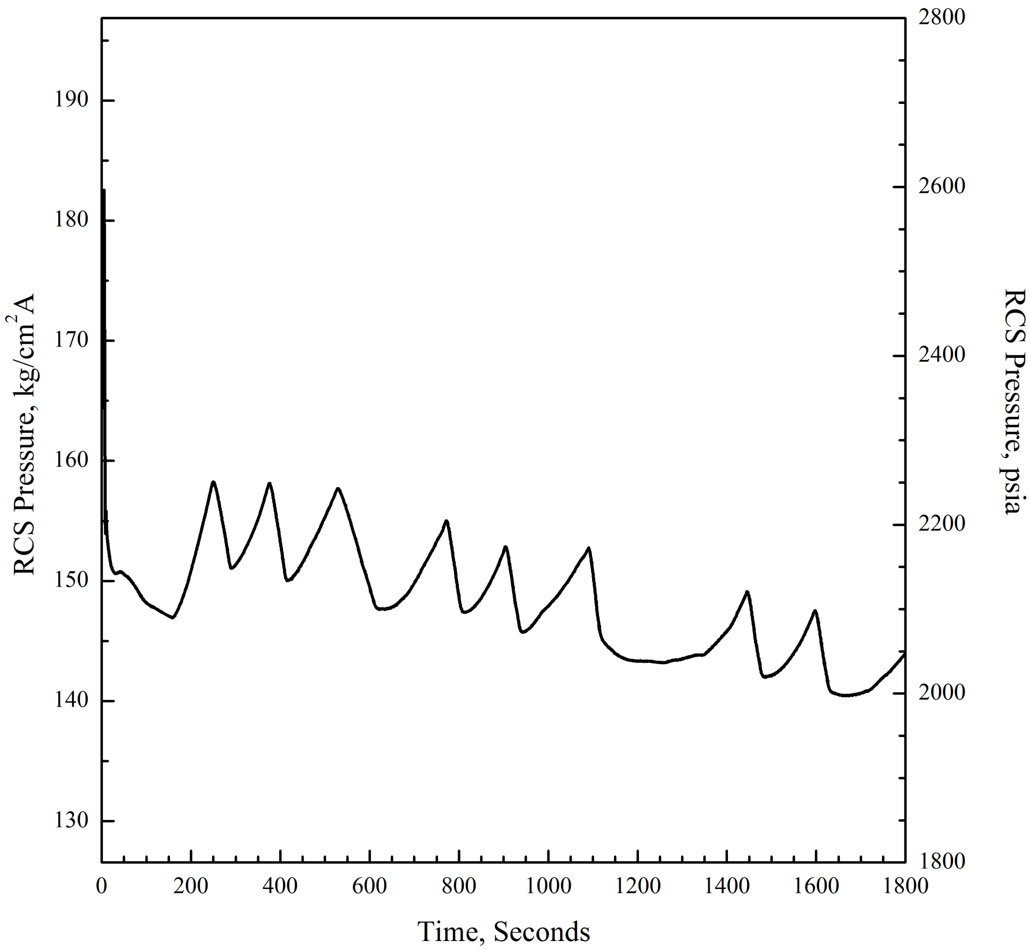

* The pressure difference between cold leg at the RCP discharge and the surge line is not included.

Figure 15.3.3-5 RCP Rotor Seizure ; RCS Pressure vs. Time

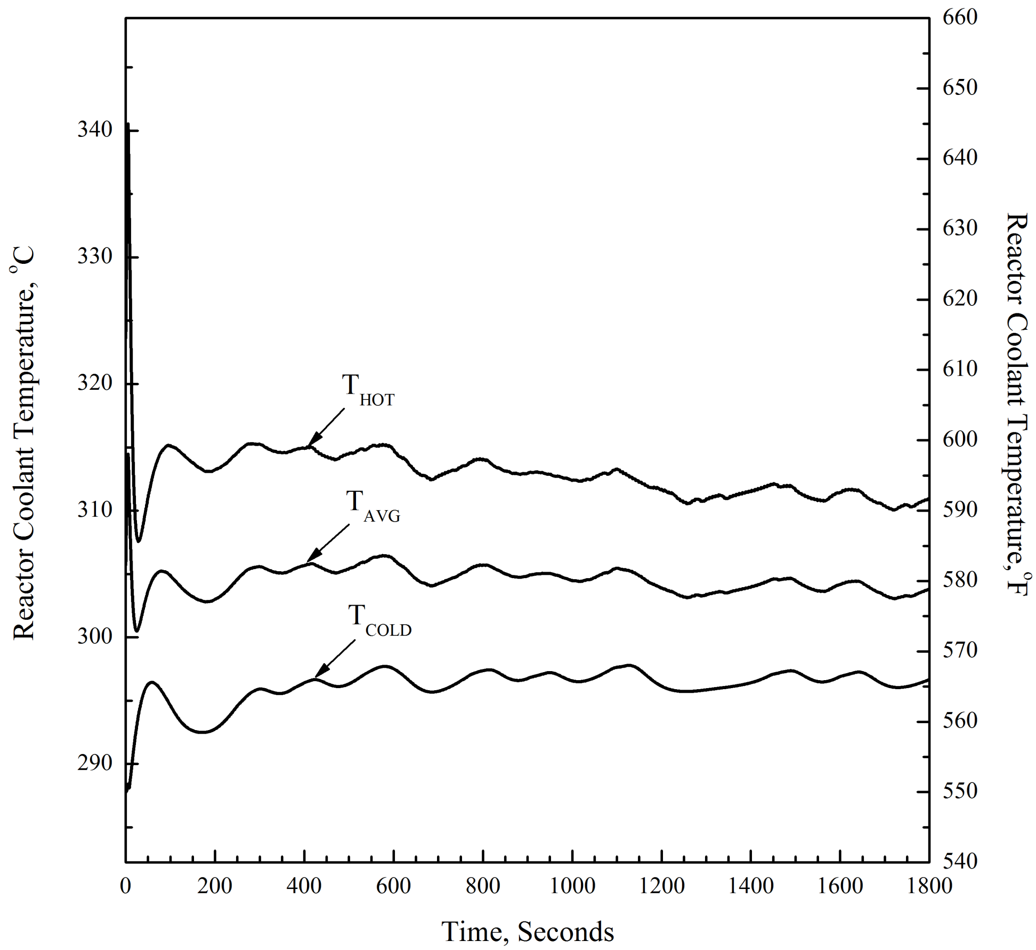

Figure 15.3.3-6 RCP Rotor Seizure ; Reactor Coolant Temperature vs. Time

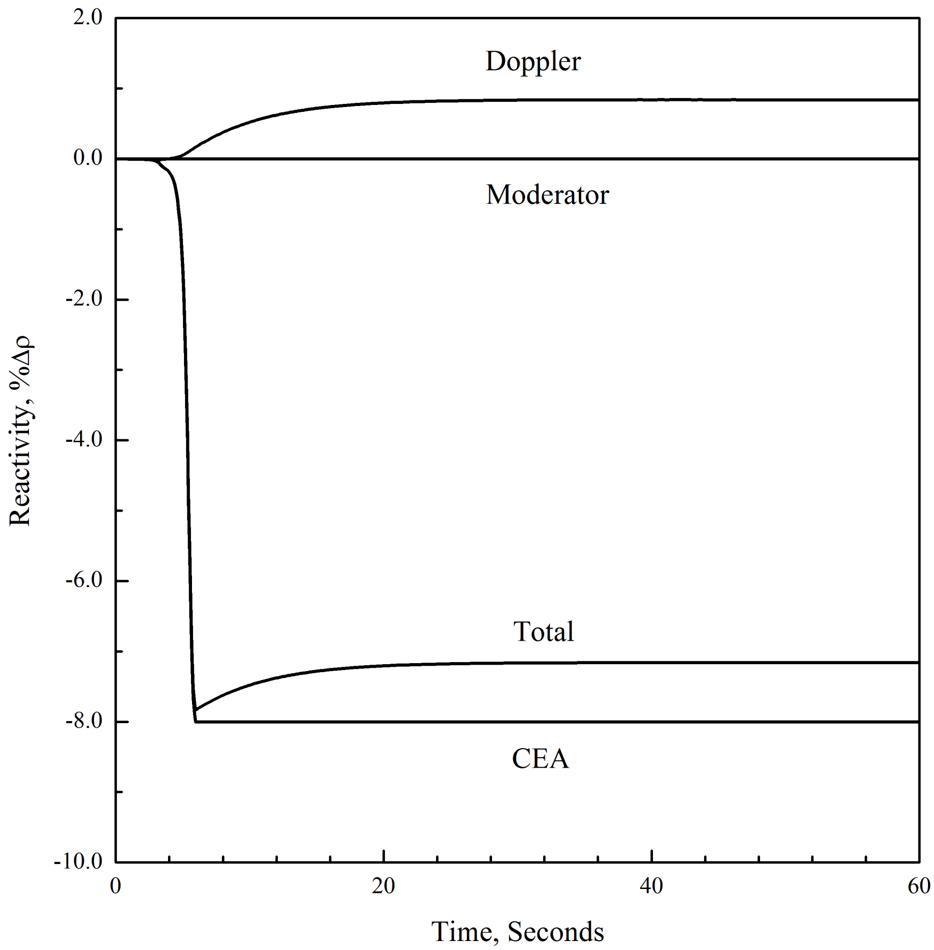

Figure 15.3.3-7 RCP Rotor Seizure ; Reactivity vs. Time

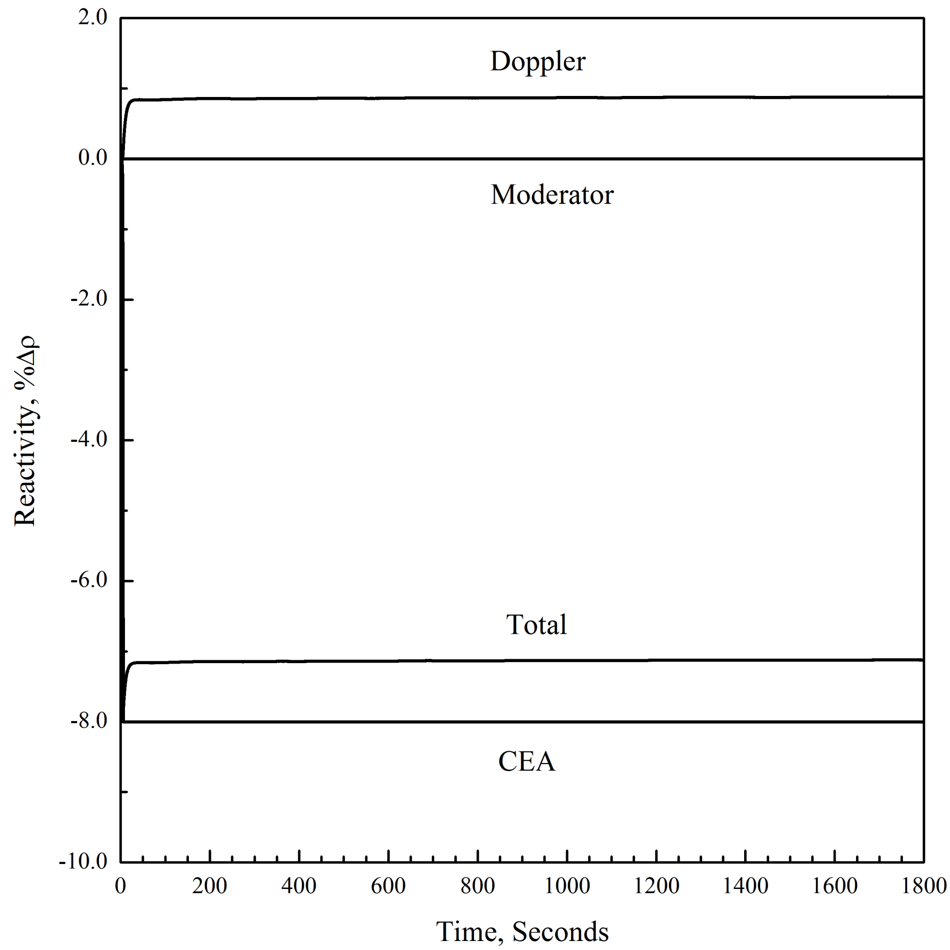

Figure 15.3.3-8 RCP Rotor Seizure ; Reactivity vs. Time

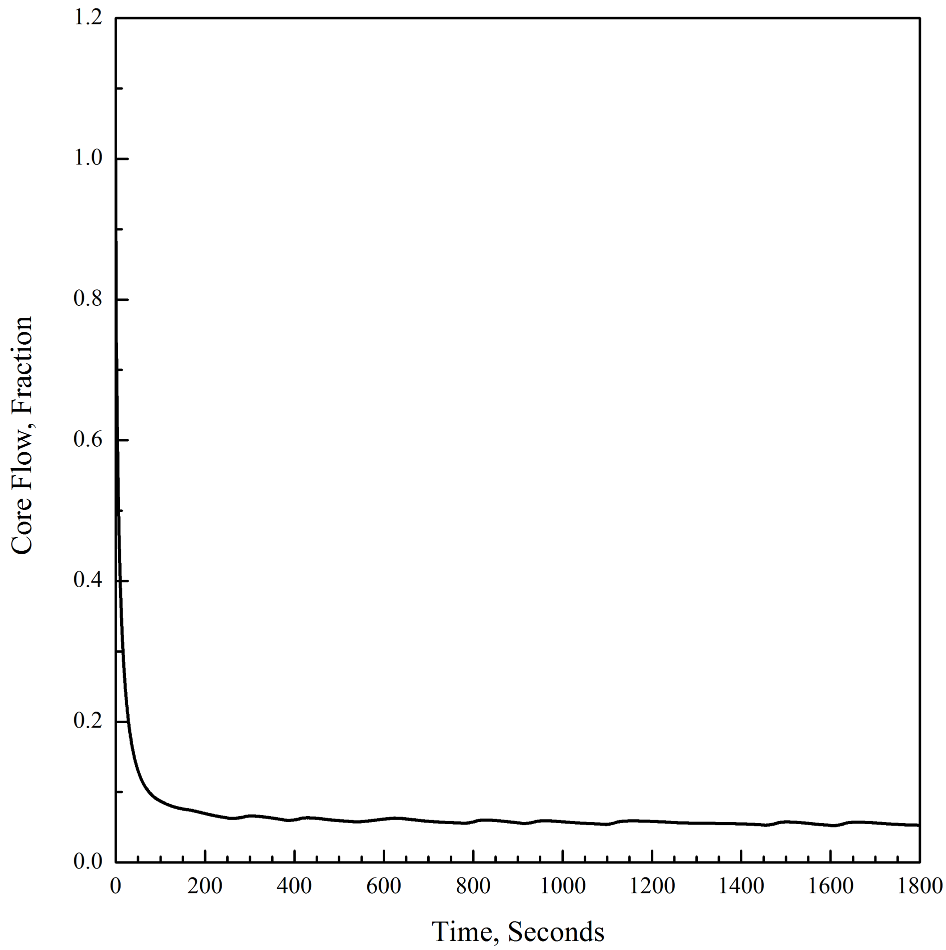

Figure 15.3.3-9   RCP Rotor Seizure ; Core Flow vs. Time

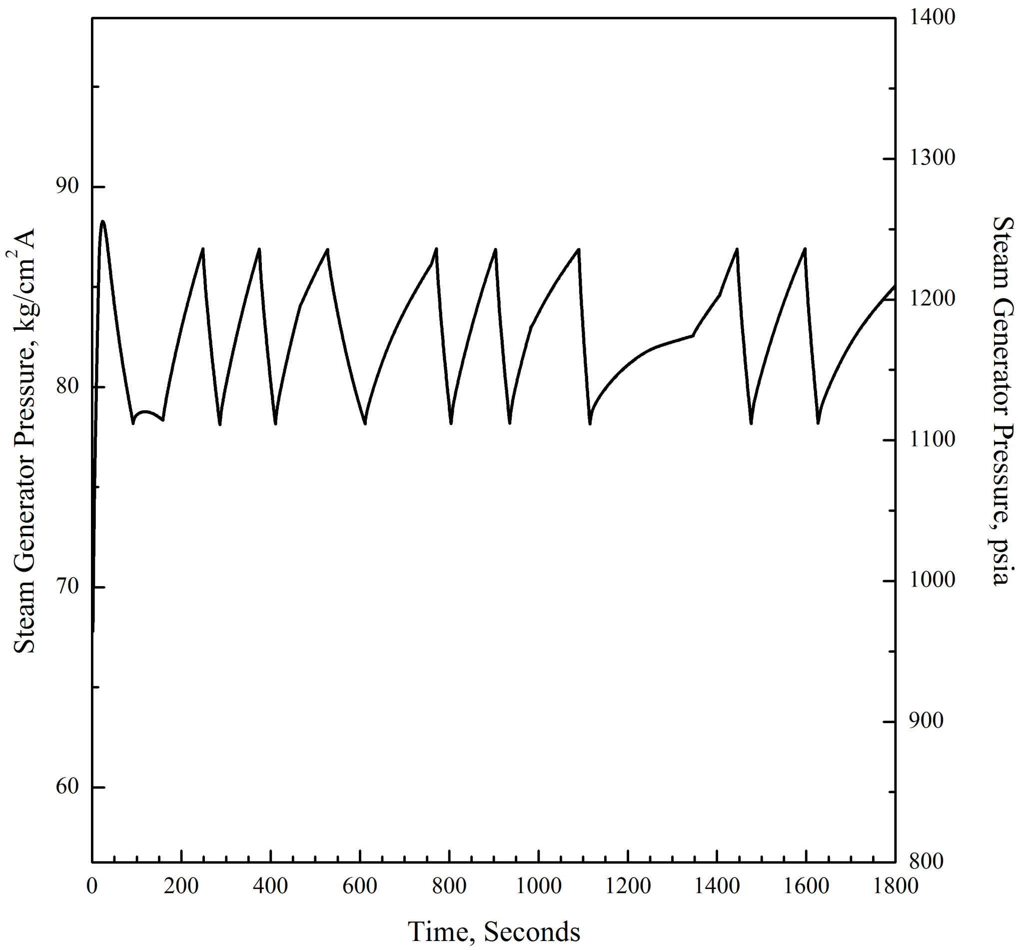

Figure 15.3.3-10 RCP Rotor Seizure ; Steam Generator Pressure vs. Time

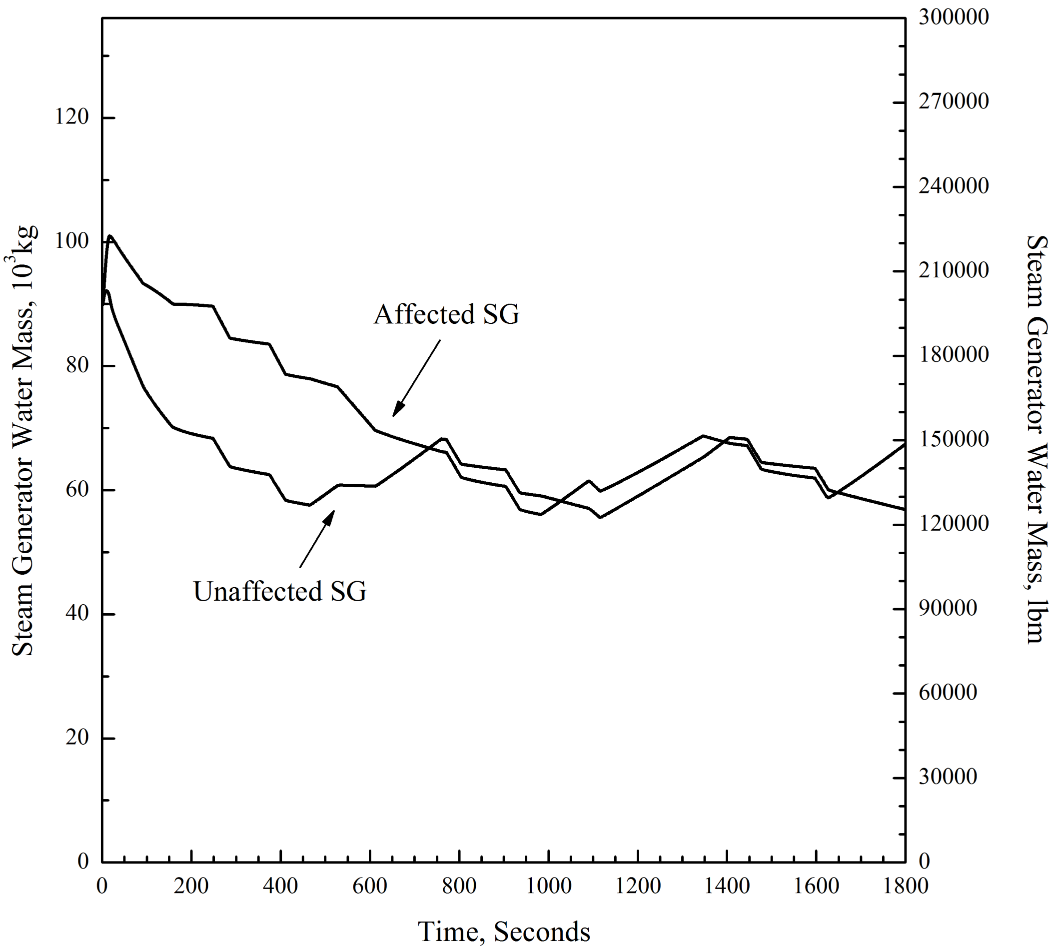

Figure 15.3.3-11   RCP Rotor Seizure ; Steam Generator Liquid Mass vs. Time

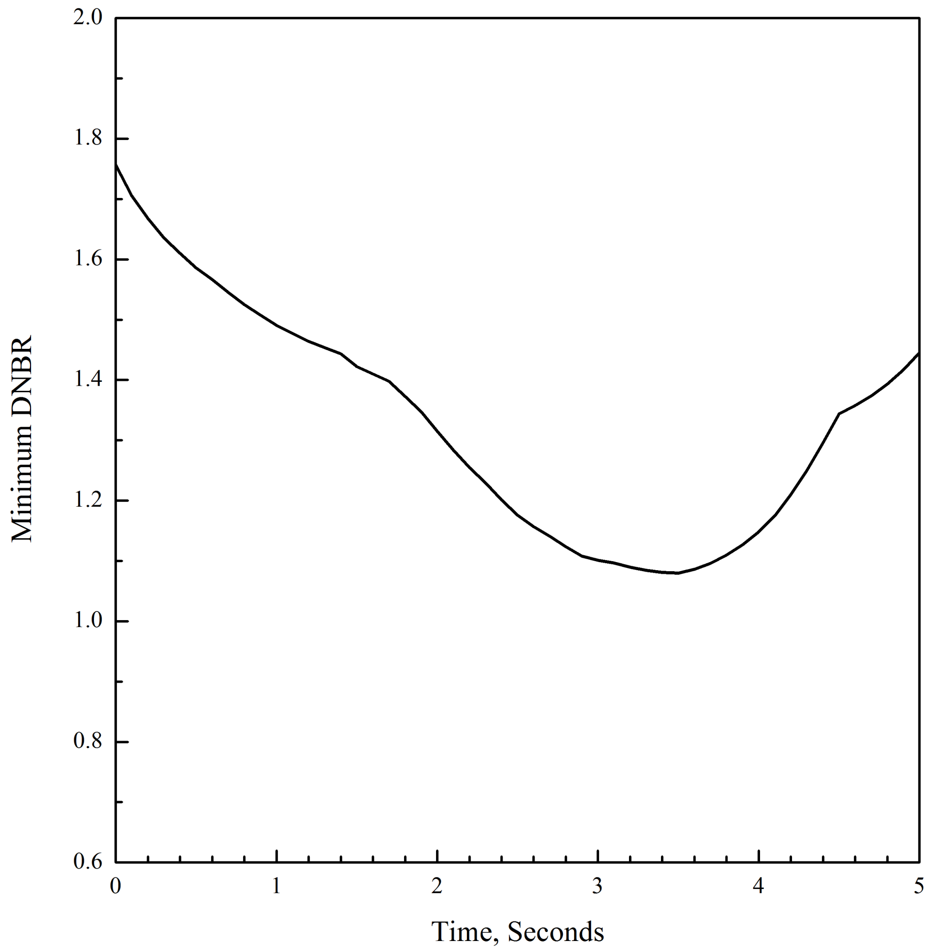

Figure 15.3.3-12   RCP Rotor Seizure ; Minimum DNBR vs. Time

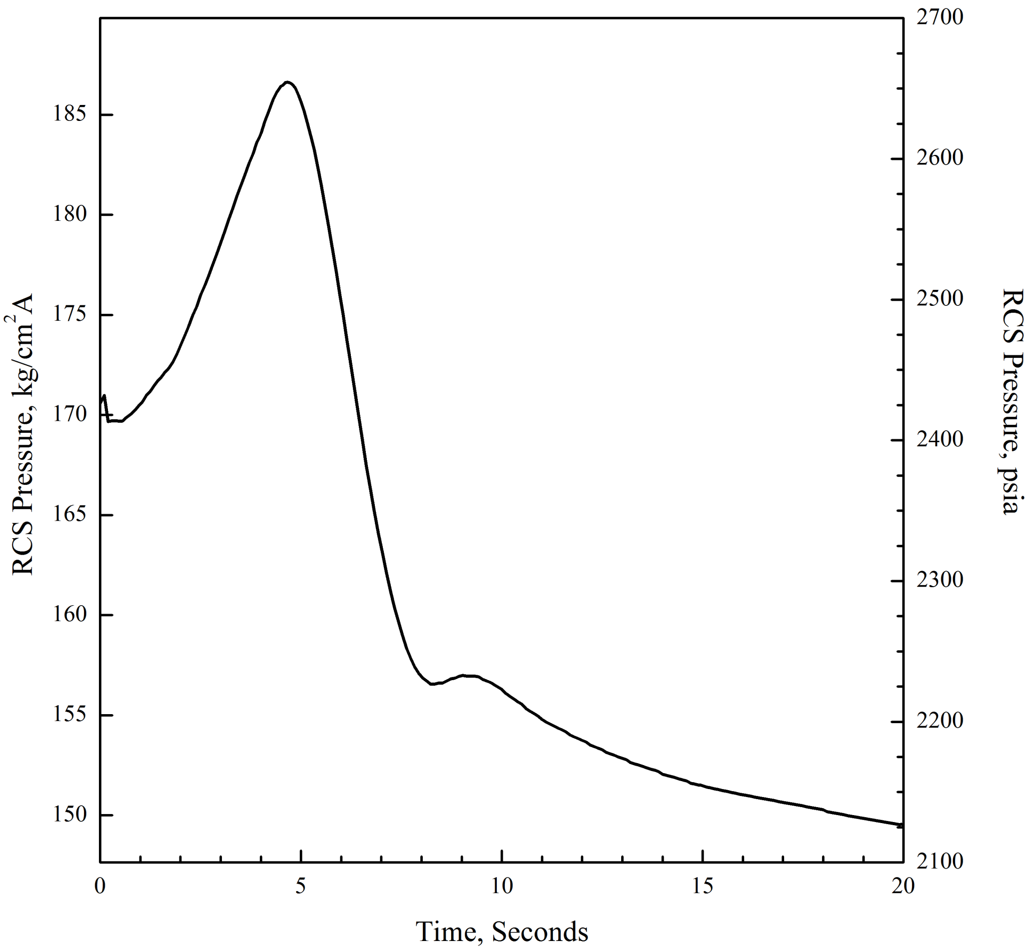

*The pressure difference between cold leg at the RCP discharge and the surge line is included.

Figure 15.3.3-13 RCP Rotor Seizure ; RCS Pressure vs. Time (Peak Pressure Case)

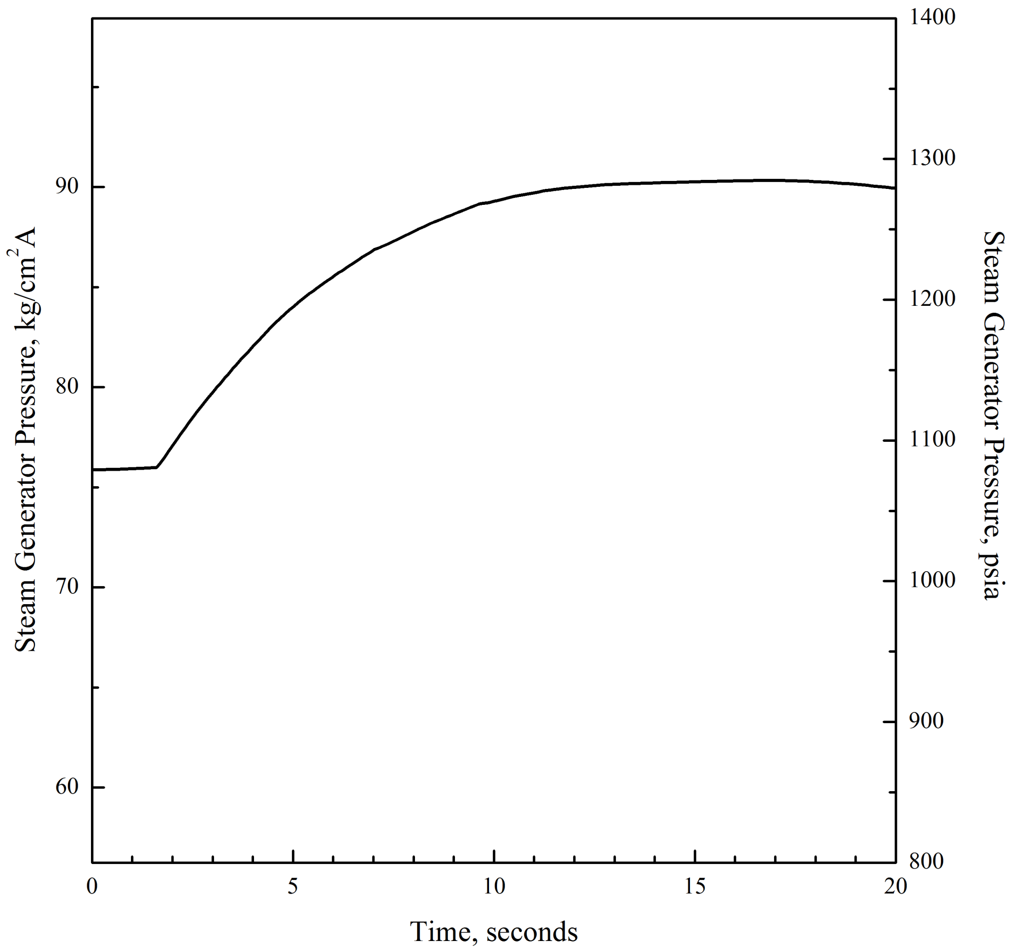

Figure 15.3.3-14 RCP Rotor Seizure ; Steam Generator Pressure vs. Time (Peak Pressure Case)

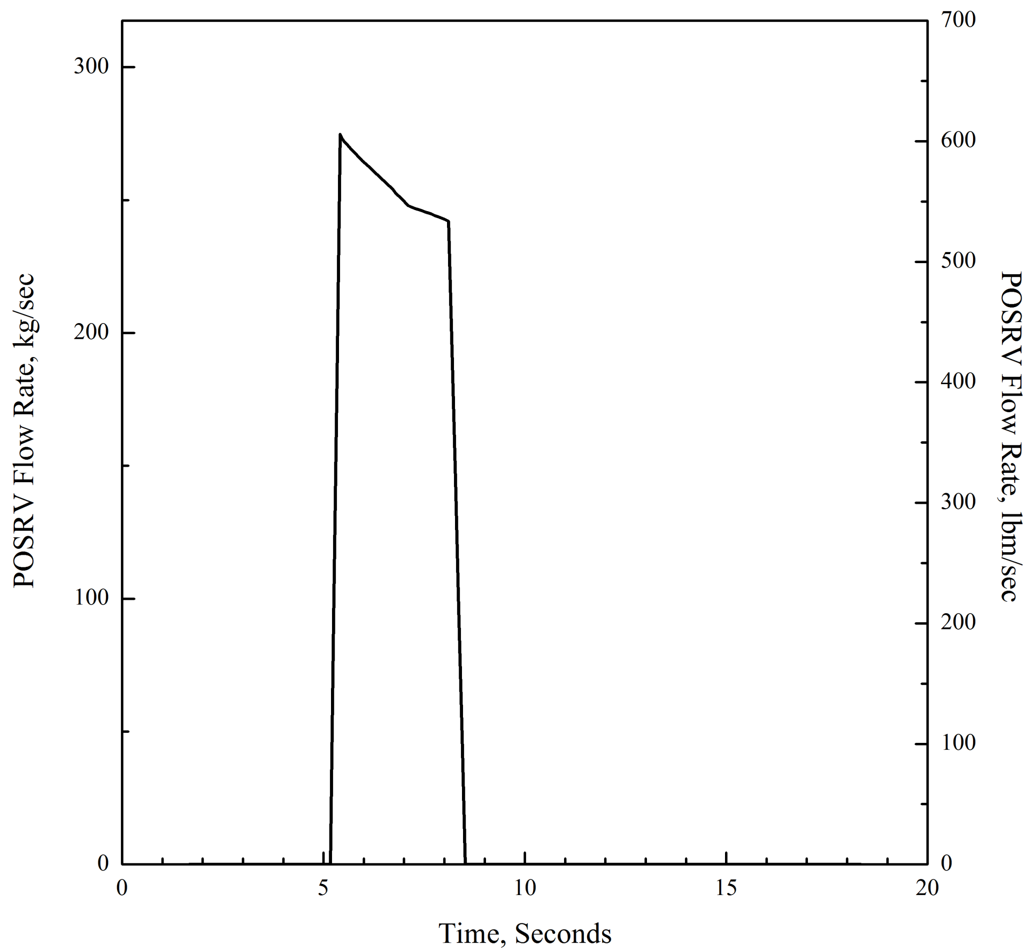

Figure 15.3.3-15 RCP Rotor Seizure ; POSRV Flow Rate vs. Time (Peak Pressure Case)

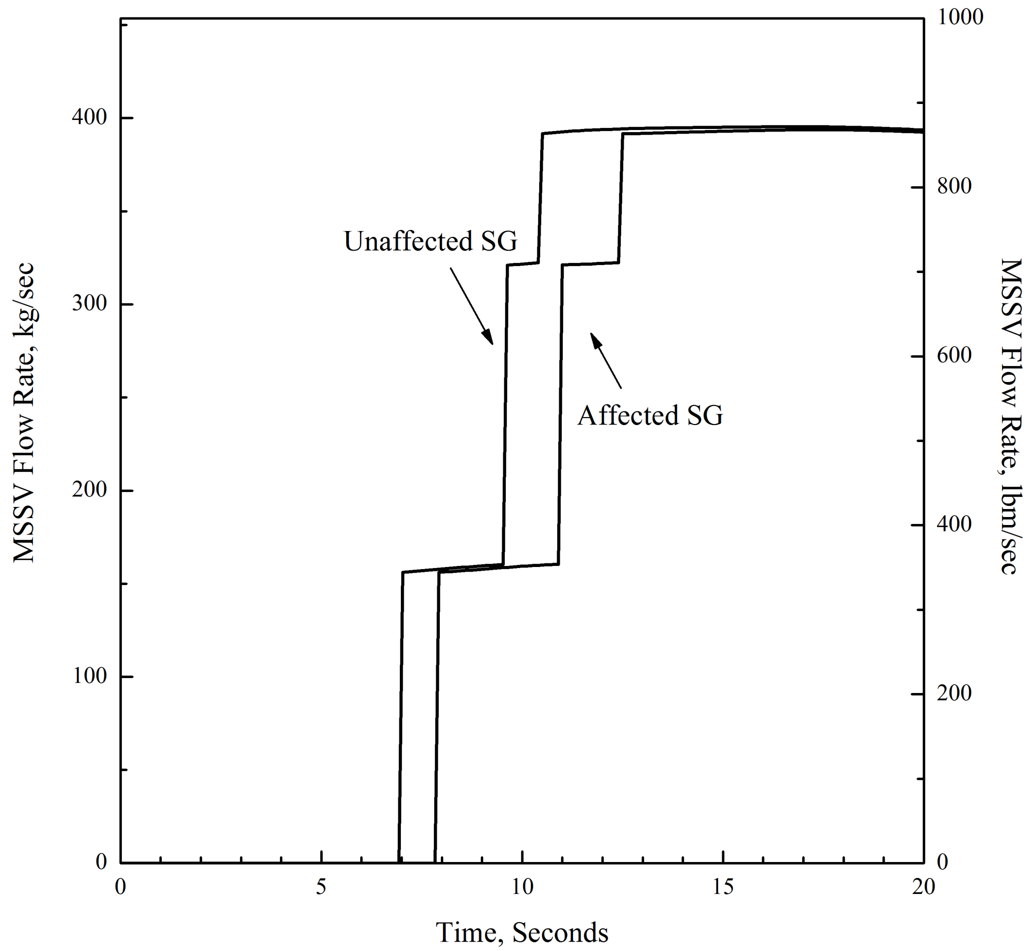

Figure 15.3.3-16 RCP Rotor Seizure ; MSSV Flow Rate vs. Time (Peak Pressure Case)

15.4 Reactivity and Power Distribution Anomalies

This section describes analyses that have been performed for events that could result in a reactivity and power distribution anomalies.

Several anticipated operational occurrences (AOO) and one postulated accident (PA) result in a reactivity and power distribution anomalies. These events are described in the following subsections of Section 15.4:

a. Subsection 15.4.1 – Uncontrolled Control Element Assembly Withdrawal from a Subcritical or Low Power Startup Condition

b. Subsection 15.4.2 – Uncontrolled Control Element Assembly Withdrawal at Power

c. Subsection 15.4.3 – Control Element Assembly Misoperation

d. Subsection 15.4.4 – Startup of an Inactive Reactor Coolant Pump

e. Subsection 15.4.5 – Flow Controller Malfunction Causing an Increase in BWR Core Flow Rate (not applicable to the APR1400)

f. Subsection 15.4.6 – Inadvertent Decrease in Boron Concentration in the Reactor Coolant System

g. Subsection 15.4.7 – Inadvertent Loading and Operation of a Fuel Assembly in an Improper Position

h. Subsection 15.4.8 – Spectrum of CEA Ejection Accidents

15.4.1 Uncontrolled Control Element Assembly Withdrawal from a Subcritical or Low-Power Startup Condition

15.4.1.1 Identification of Causes and Frequency Classification

An uncontrolled withdrawal of control element assemblies (CEAs) is assumed to occur as a result of a single failure in the control element drive mechanism (CEDM), control element

drive mechanism control system (CEDMCS), reactor regulating system (RRS), or as a result of operator error. In compliance with General Design Criterion (GDC) 17, the loss of offsite power (LOOP) is assumed to occur concurrent with a reactor trip.

This event is classified as an AOO as defined in Subsection 15.0.0.1.

15.4.1.2 Sequence of Events and Systems Operation

The withdrawal of CEAs from subcritical or low power conditions adds reactivity to the reactor core, causing both the core power level and the core heat flux to increase together with corresponding increases in reactor coolant temperatures and reactor coolant system (RCS) pressure. The withdrawal motion of CEAs also produces a time-dependent redistribution of core power. These transient variations in core thermal parameters result in a system approach to the specified fuel design limits, requiring the protective action of the reactor protection system (RPS). The total energy generated during the power excursion at low power is greater than during the subcritical case; therefore, only the low power case is presented here.

Table 15.4.1-1 gives the sequence of events for the limiting CEA withdrawal transient at low power with a LOOP identified in Subsection 15.4.1.3. A LOOP was assumed to be coincident with a turbine trip. The CEA withdrawal at low power with a LOOP was determined to be limiting relative to the CEA withdrawal at low power without a LOOP.

None of the single failures listed in Table 15.0-4 has any effect on this event.

15.4.1.3 Core and System Performance

15.4.1.3.1 Evaluation Model

The nuclear steam supply system (NSSS) response to a CEA sequential withdrawal from subcritical or low power conditions is simulated using the CESEC-III computer program described in Subsection 15.0.2.2.1. The thermal margin on departure from nucleate boiling ratio (DNBR) in the reactor core is simulated using the CETOP computer program described in Subsection 15.0.2.2.4 with the KCE-1 critical heat flux (CHF) correlation.

15.4.1.3.2 Input Parameters and Initial Conditions

The input parameters and initial conditions used to analyze the NSSS response are discussed in Table 15.0-4. In particular, parameters that were unique to the CEA withdrawal from subcritical or low power conditions discussed below are listed in Table 15.4.1-2.

a. The initial conditions and NSSS characteristics assumed in this analysis have been determined to be the limiting set of conditions allowed by the limiting conditions for operation (LCOs) specified by the Technical Specifications in terms of providing the closest approach to the fuel design limits for a CEA withdrawal at low power.

b. The initial conditions that provide the closest approach to the fuel design limits correspond to low power, maximum core inlet temperature of 295 °C (563 °F), minimum core inlet flow of 95 percent of design flow, and minimum RCS pressure of 152.91 kg/cm^2A (2,175 psia).

c. A bottom peaked axial power shape (i.e., +0.6 ASI) is used to model scram reactivity insertion.

d. A three-dimensional peaking factor of 5.94 including uncertainties is conservatively assumed for this analysis. The three-dimensional peaking factor is the highest peak expected for any CEA configuration and time in core lifetime at low power.

e. An initial power level of 1×10^{-3} percent of rated core power, 0.03983 MWt, results in the closest approach to the fuel design limits during the CEA withdrawal transient. Subcritical or zero power CEA withdrawal transients initiated from below 1×10^{-3} percent rated power are terminated by the high logarithmic power trip.

f. Transients initiated from power levels above 1×10^{-3} percent of rated power are terminated sooner by the variable overpower trip, resulting in less limiting consequences than the case presented here.

g. The most positive moderator temperature coefficient, 0.9×10^{-4} $\Delta\rho$/°C (0.5×10^{-4} $\Delta\rho$/°F), is assumed for this analysis to maximize the power increase. The least negative Doppler coefficient is also assumed to maximize the power increase.

h. The regulating CEA positions are initially in the fully inserted position when the CEA withdrawal is initiated. Based on calculated differential control CEA bank worth (0.00925 % $\Delta\rho$/cm) and the maximum CEA withdrawal rate (76.2 cm/min) of the CEA drive system, the reactivity insertion is the maximum expected rate of 1.175×10^{-4} $\Delta\rho$/sec.

15.4.1.3.3 Results

The dynamic behaviors of important NSSS parameters following a CEA withdrawal from low power conditions are presented in Figures 15.4.1-1 through 15.4.1-8.

The withdrawal of CEAs from low power (0.03983 MWt) conditions adds reactivity to the reactor core, causing both the core power and the core heat flux to increase. The power transient causes increasing temperature and pressure transients, which produce the closest approach to the specified acceptable fuel design limit on DNBR. A variable overpower trip setpoint is reached at 29.19 seconds. The CEAs begin dropping into the core and terminate the transient. The minimum DNBR reached during the transient remains above the 95/95 design limit.

The sequence of events for this accident is listed in Table 15.4.1-1. With the reactor tripped, the plant returns to a stable condition and is subsequently brought to cold shutdown by the appropriate normal plant shutdown procedures.

The peak linear heat generation rate during the transient remains less than 656 W/cm (20 kW/ft).

15.4.1.4 Barrier Performance

This event is bounded by uncontrolled CEA withdrawal at power event described in Subsection 15.4.2.4 for barrier performance.

15.4.1.5 Radiological Consequences

The radiological consequence of this event is bounded by the CEA ejection accident described in Subsection 15.4.8.

15.4.1.6 Conclusions

The uncontrolled CEA withdrawal from subcritical or low power conditions with a LOOP meets GDC 20 and 25. These criteria require that the specified acceptable fuel design limits are not exceeded and the protection system action is initiated automatically. The withdrawal of CEAs from low power conditions with a LOOP meet the following fuel design limits, which serve as the acceptance criteria for this event: (1) the transient terminates with a minimum DNBR greater than or equal to 1.29, and (2) the peak linear heat generation rate during the transient is less than 656 W/cm (20 kW/ft).

The reactor coolant system pressure remains within 110 percent of its system design pressure. Therefore, the integrity of the reactor coolant pressure boundary is maintained.

15.4.2 Uncontrolled Control Element Assembly Withdrawal at Power

15.4.2.1 Identification of Causes and Frequency Classification

An uncontrolled sequential withdrawal of CEAs is assumed to occur as a result of a single failure in the control element drive mechanism control system (CEDMCS), reactor regulating system (RRS), or as a result of operator error. In compliance with General Design Criteria (GDC) 17, the loss of offsite power (LOOP) is assumed to occur concurrent with a reactor trip.

This event is classified as an AOO as defined in Subsection 15.0.0.1.

15.4.2.2 Sequence of Events and Systems Operation

The uncontrolled withdrawal of a CEA at power conditions adds reactivity to the core, causing both the core power level and the core heat flux to increase, followed by corresponding increases in reactor coolant temperatures and reactor coolant system (RCS) pressure. The withdrawal of CEAs also produces a time-dependent redistribution of core power. These transient variations in core thermal parameters may result in an approach to the specified acceptable fuel design limits (SAFDLs) on DNBR and fuel centerline melt temperatures, requiring the protective action of the reactor protection system (RPS).

The net reactivity insertion rate accompanying the uncontrolled CEA withdrawal is dependent upon the CEA withdrawal rate and reactivity feedback mechanisms present at

the time of the CEA withdrawal at power conditions. Depending on the reactivity insertion rate and the system initial conditions, the uncontrolled CEA withdrawal transient at power is terminated by a core protection calculator (CPC) variable overpower trip (VOPT), CPC low DNBR trip, CPC high local power density (LPD) trip, or the high pressurizer pressure trip (HPPT).

Table 15.4.2-1 presents a chronological sequence of events that occur during a sequential CEA group withdrawal transient. A LOOP is assumed to be coincident with a turbine trip. The CEA withdrawal at power with a LOOP is determined to be limiting relative to the CEA withdrawal at power without a LOOP.

None of the single failures listed in Table 15.0-4 has any effect on this event.

15.4.2.3 Core and System Performance

15.4.2.3.1 Evaluation Model

The nuclear steam supply system (NSSS) response to a CEA withdrawal at power conditions was simulated using the CESEC-III computer program described in Subsection 15.0.2.2.1. The thermal margin on DNBR in the reactor core was simulated using the CETOP computer program described in Subsection 15.0.2.2.4 with the KCE-1 CHF correlation.

15.4.2.3.2 Input Parameters and Initial Conditions

Table 15.4.2-2 lists the assumptions and initial conditions used for this analysis in addition to those discussed in Subsection 15.0.0.1. These initial conditions (i.e., radial power peak, core flow, inlet temperature) are chosen to minimize the minimum DNBR.

The following assumptions are utilized to calculate conservative DNBR transient results for an uncontrolled CEA bank withdrawal at power event:

a. The initial conditions and NSSS characteristics used in this analysis yield the minimum DNBR for the CEA bank withdrawal with a LOOP incident. The core inlet temperature, pressurizer pressure, core flow, and radial peaking factor are chosen so that the reactor is operating at a power operating limit (POL) at the initiation of the event.

b. The power level from which the withdrawal is initiated is assumed to be 102 percent of core thermal power. This power level is for a typical case. Initial power levels from low to full power are analyzed in COLSS/CPCS design stage.

c. The initial core average axial power distribution for this analysis is a shape characterized by an axial shape index equal to -0.3. This ASI is used as the limiting axial power shape for only DNBR calculations.

d. A bottom peaked axial power shape (i.e., +0.3 ASI) is used to model scram reactivity insertion.

e. Other input parameters that are important to this analysis are the moderator temperature coefficient (MTC) and fuel temperature coefficient (FTC) of reactivity. The most positive MTC and the least negative FTC were assumed in this analysis, which corresponds to beginning of cycle core conditions to maximize the peak power.

f. The regulating CEA position from which the CEA withdrawal is initiated corresponds to the power dependent insertion limit. This particular insertion was selected based on the calculated CEA worth and associated uncertainties to produce the worst transient. Based on calculated differential CEA worth (0.00248 %Δρ/cm) and the maximum CEA withdrawal rate (76.2 cm/min) of the CEA drive system, the reactivity insertion is the maximum expected rate of 0.315×10^{-4} Δρ/sec. This maximum reactivity insertion rate is used for a typical case. Reactivity insertion rates from very low to maximum possible for the control system, including allowance for uncertainties, are analyzed in COLSS/CPCS design stage.

15.4.2.3.3 Results

The dynamic behaviors of important NSSS parameters following an uncontrolled CEA withdrawal are presented in Figures 15.4.2-1 through 15.4.2-12.

The withdrawal of CEAs causes a positive reactivity change, resulting in an increase in the core power and heat flux. As a consequence, the reactor coolant temperature and pressurizer pressure increase. The reactor is immediately tripped at the CPC variable overpower analysis setpoint of 115 percent of nominal power and the trip breakers are

opened. Also at this time, the turbine is assumed to trip resulting in an instantaneous LOOP. Subsequently, the CEAs begin dropping into the core and terminate the transient.

The minimum DNBR reached during the transient remains above the 95/95 design limit. The peak linear heat generation rate during the transient remains less than 656 W/cm (20 kW/ft).

15.4.2.4 Barrier Performance

15.4.2.4.1 Evaluation Model

The evaluation model is identical to that used to evaluate core performance as described in Subsection 15.4.2.3.1. The CESEC-III code is used to analyze the core average power histories and to calculate the RCS pressure transient following CEA withdrawal at power conditions.

15.4.2.4.2 Input Parameters and Initial Conditions

The assumptions for the barrier performance case for peak RCS pressure are similar to the core and system performance analysis provided in Subsection 15.4.2.3.2; the differences between the two are described below.

a. The initial conditions and NSSS characteristics assumed in this analysis have been determined to maximize the primary and secondary system pressures. The peak pressure analysis used the initial core inlet temperature of 295 °C (563 °F), and the initial steam generator pressure of 75.86 kg/cm^{2}A (1,079 psia), with all other initial condition parameter values as listed in Table 15.4.2-2

b. It is assumed that pressurizer spray does not initiate in order to maximize the peak pressure during the event

15.4.2.4.3 Results

The dynamic behaviors of important NSSS parameters following an uncontrolled CEA withdrawal are presented in Figures 15.4.2-13 through 15.4.2-15.

The reactor coolant pump (RCP) outlet pressure, the highest pressure in the RCS, does not exceed the reactor coolant pressure boundary limits. Figure 15.4.2-13 shows that the reactor coolant system pressure remains within 110 percent of the system design pressure and that the integrity of the reactor coolant pressure boundary is maintained. The main steam system pressure is not challenged by this event.

15.4.2.5 Radiological Consequences

The radiological consequences of this event are bounded by a CEA ejection accident as described in Section 15.4.8.

15.4.2.6 Conclusions

The uncontrolled CEA withdrawal event with a LOOP meets GDC 20 and 25. These criteria require that the specified acceptable fuel design limits are not exceeded and the protection system action is initiated automatically. The withdrawal of CEAs from full power conditions with a LOOP meet the following fuel design limits, which serve as the acceptance criteria for this event: (1) the transient terminates with minimum DNBR greater than or equal to 1.29, and (2) the peak linear heat generation rate during the transient is less than 656 W/cm (20 kW/ft).

The reactor coolant system pressure remains within 110 percent of the system design pressure. Therefore, the integrity of the reactor coolant pressure boundary is maintained.

15.4.3 Control Element Assembly Misoperation

The types of AOOs that include one or more CEAs moving or displaced from normal or allowed control bank positions are as follows:

a. Dropped CEA or CEA subgroup

b. Statically misaligned CEA

c. Single CEA withdrawal

The core protection calculator system (CPCS) provides the low DNBR trip and the high LPD trip by applying penalty factors for these occurrences with an exception of a four-

finger CEA drop, a statically misaligned CEA within deadband, and a single CEA withdrawal within deadband. The detailed descriptions for the CPCS penalty factors during CEA misoperation are provided in Section 7.2.

In cases of a four-finger CEA drop, a statically misaligned CEA within deadband, and a single CEA withdrawal within deadband, the control element assembly calculator (CEAC) does not provide deviation penalties to the CPCS for DNBR or LPD calculations. For these events, reasonable assurance of acceptable results is provided because the initial thermal margin is preserved through the Technical Specifications limiting conditions for operation (LCOs).

The initial thermal margin required for a four-finger CEA drop, a statically misaligned CEA within deadband, and a single CEA withdrawal within deadband is not affected by the assumption of a LOOP following a turbine trip since a delay is implemented in the RPS design that the turbine trip signal occurs 3 seconds following a reactor trip.

Four-finger single CEA drop is the limiting case regarding to the required thermal margin and described in the following subsection.

15.4.3.1 Identification of Causes and Frequency Classification

A single CEA drop results from an interruption in the electrical power to the control element drive mechanism (CEDM) holding coil of a single CEA. This interruption can be caused by a holding coil failure or loss of power to the holding coil. The limiting case is the single CEA drop that does not cause a reactor trip to occur but results in an approach to the specified acceptable fuel design limit (SAFDL) on the departure from DNBR.

This event is classified as an AOO as defined in Subsection 15.0.0.1.

15.4.3.2 Sequence of Events and Systems Operation

Table 15.4.3-1 presents a chronological list of events that occur during the single CEA drop transient, from initiation to the attainment of steady-state conditions.

The transient is initiated by the release and subsequent drop of a single CEA. The transient initiates a reduction in core power and a P-T-S side power to load mismatch. The

mismatch results in a cooldown of the RCS due to excess heat removal by the secondary system. In the presence of a negative moderator temperature coefficient (MTC), the cooldown adds positive reactivity, and the core power tends to return to initial power level.

The resultant increase in the hot pin radial peaking factor coupled with a return to initial power (following a temporary power depression) results in a power distribution distortion. The power distribution distortion increases with time as xenon redistributes. After core power recovers the initial level, the core maintains certain transient states without shutdown and a minimum DNBR that remains above the DNBR SAFDL. By 1,800 seconds, the operator is assumed to have reduced power if the CEA has not been realigned. Operation at reduced power is allowed for a limited period to allow the CEA to be realigned.

None of the single failures listed in Table 15.0-4 has any effect on this event.

15.4.3.3 Core and System Performance

15.4.3.3.1 Evaluation Model

The nuclear steam supply system (NSSS) response to the single CEA drop transient was simulated using the CESEC-III computer program described in Subsection 15.0.2.2.1. The thermal margin on DNBR in the reactor core was simulated using the CETOP code described in Subsection 15.0.2.2.4 with the KCE-1 CHF correlation.

15.4.3.3.2 Input Parameters and Initial Conditions

Table 15.4.3-2 lists the assumptions and initial conditions used for this analysis in addition to those provided in Table 15.0-3. These initial conditions (i.e., radial power peak, core flow, inlet temperature) were chosen to minimize the hot channel minimum DNBR.

The initial conditions and NSSS characteristics used in this analysis yield the minimum DNBR for the single CEA drop event. The core inlet temperature, pressurizer pressure, core flow, and radial peaking factor were chosen so that the reactor was operating at a power operating limit (POL) at the initiation of the event.

a. The power level from which the CEA drop is initiated was assumed to be 102 percent of core thermal power.

b. The initial conditions that provide the closest approach to the fuel design limits are core inlet temperature of 295 °C (563 °F), core inlet flow of 95 percent of design flow, and minimum RCS pressure of 152.91 kg/cm^{2}A (2,175 psia).

c. The initial core average axial power distribution for this analysis is a shape characterized by an axial shape index equal to –0.3.

d. Other input parameters that are important to this analysis are the moderator temperature coefficient (MTC) and fuel temperature coefficient (FTC) of reactivity. The most negative MTC and FTC were assumed in this analysis, which corresponds to end of cycle core conditions. The MTC and FTC cause a positive reactivity insertion that brings the core back to initial power.

e. For this analysis, the mode of reactor regulating system is inconsequential because there would be no regulating bank motion if the system was in manual mode. In the automatic mode, the CEA withdrawal prohibit, actuated on the CEA calculator (CEAC) based rod deviation, prevents the motion of any regulating bank.

f. The maximum radial peak distortion following a four-finger CEA drop is assumed to be 1.205.

15.4.3.3.3 Results

Table 15.4.3-1 presents the sequence of events for the single CEA drop event initiated at the condition described in Table 15.4.3-2. The dynamic behavior of important NSSS parameters following the drop of a single CEA is presented in Figures 15.4.3-1 through 15.4.3-11. The CEA drop is characterized by a prompt decrease in core average and local power followed by an increasing distortion in radial power distribution. Then the reactivity feedbacks due to the decreasing core inlet and average temperatures cause the power, which was initially depressed immediately following the drop, to rise. The greater radial peaking factor, coupled with the core average power returning to its initial value, causes a decrease in DNBR.

For the case in which a trip does not occur, a minimum DNBR is always greater than 1.29. If the maximum rod radial peaking factor occurs in the region of the axial power peak, the

peak linear heat generation rate during the transient remains less than 656 W/cm (20 kW/ft), providing reasonable assurance of no centerline melt.

15.4.3.4 Barrier Performance

The single CEA drop event does not result in exceeding the reactor coolant pressure boundary design limits. The results of the core and system performance evaluation case demonstrate that the reactor coolant system pressure remains below 110 percent of system design pressure. The main steam pressure cannot challenge the main steam system pressure design limit, as shown in Figure 15.4.3-8. A single CEA drop event maintains the integrity of the reactor coolant pressure boundary and the main steam system pressure boundary.

15.4.3.5 Radiological Consequences

The radiological consequences of this event are bounded by CEA ejection accident described in Subsection 15.4.8.

15.4.3.6 Conclusions

The single CEA drop event meets GDC 20 and 25 criteria. These criteria require that the specified acceptable fuel design limits are not exceeded and the protection system action is initiated automatically. The drop of a CEA meets the following fuel design limits, which serve as the acceptance criteria for this event: (1) the transient terminates with a hot channel minimum DNBR greater than or equal to 1.29, and (2) the peak linear heat generation rate during the transient is less than 656 W/cm (20 kW/ft).

15.4.4 Startup of an Inactive Reactor Coolant Pump

15.4.4.1 Identification of Causes and Frequency Classification

The startup of an inactive reactor coolant pump (SIRCP) during power operation is not applicable because power operation with an inactive reactor coolant pump is not allowed by the Technical Specifications. The SIRCP is presented here with respect to potential loss of minimum required shutdown margin during Modes 3 through 6.

This event is classified as an AOO as defined in Subsection 15.0.0.1.

15.4.4.2 Sequence of Events and Systems Operation

SIRCP can either increase or decrease core average coolant temperature. The average temperature can be decreased by increased heat transfer to the steam generators caused by increased core coolant flow and by colder primary system water in the steam generators being forced into the core. The core average temperature can be increased by increased heat transfer from the steam generators to the RCS as a result of increased core coolant flow and by hotter primary system water in the steam generators being forced into the core.

The SIRCP event that reduces the core average temperature (the cooldown event) combined with a negative isothermal temperature coefficient (ITC) produces a positive reactivity insertion. The SIRCP event that increases core average temperature (the heatup event), combined with a positive ITC, produces an increase in reactor coolant system (RCS) pressure and a positive reactivity insertion.

The RCS boron concentration in Modes 3 through 6 is always very high to maintain the shutdown margin (SDM) required by the Technical Specifications. Therefore, the core does not reach criticality due to a reactor coolant pump startup.

For Modes 3 and 4, when the RCS is above the conditions requiring low temperature overpressure protection (LTOP), the pressurizer pilot operated safety and relief valves (POSRVs) are designed to maintain the RCS below 110 percent of design pressure. During Modes 4, 5, and 6, when the RCS is in the LTOP mode, overpressure protection is provided by the shutdown cooling system relief valves. The shutdown cooling system design bases are presented in Subsection 5.4.7. None of the single failures listed in Table 15.0-4 has any effect on this event.

15.4.4.3 Core and System Performance

15.4.4.3.1 Evaluation Model

The reactivity added to the core during a heatup or cooldown SIRCP event is determined using conservative ITCs with a maximum uncertainty applied. These ITCs are used with the maximum core temperature increase or decrease to determine the maximum reactivity inserted during SIRCP. This reactivity insertion is compared to the total amount of subcriticality.

15.4.4.3.2 Input Parameters and Initial Conditions

The initial conditions considered for this event range from a positive to a negative temperature difference between the secondary and primary system. Assuming a primary system temperature is greater than the secondary temperatures (a positive temperature difference) results in RCS cooling. Assuming the secondary system temperature is initially greater than the primary temperature (a negative temperature difference) results in RCS heating. Cooling the RCS increases reactivity if there is a negative ITC. Heating the RCS increases reactivity and RCS pressure if there is a positive ITC.

To conservatively calculate the reactivity added to the core during SIRCP, the most negative or positive ITCs are used with uncertainties applied in the most conservative direction.

The following assumptions are made:

a. Prior to SIRCP, all reactor coolant pumps are off. Normally at least one RCP is running (or one shutdown cooling train during shutdown cooling operation). The Technical Specifications allow operation without any pumps running for up to 1 hour. This assumption maximizes the change in temperature during SIRCP.

b. Following SIRCP, the core average temperature (1) drops to the coldest temperature of the steam generator for the cooldown event or (2) increases to the hottest temperature of the steam generator for the heatup event. This conservatively bounds the maximum change in core temperature that can occur during this event.

15.4.4.3.3 Results

The results show that the maximum temperature change during SIRCP, when used with the most conservative ITCs, does not result in a loss of subcriticality. Because the shutdown margin is not lost during the event, there is no increase in heat flux and therefore the minimum DNBR in the hot channel does not decrease.

15.4.4.4 Barrier Performance

The maximum temperature change during SIRCP does not result in a loss of subcriticality as discussed in Subsection 15.4.4.3.3. As stated in Subsection 5.2.2, the overpressure

protection for steam generators and the reactor coolant system is in accordance with the requirements set forth in ASME Section III. When the RCS is above the conditions requiring LTOP, the pressurizer POSRV, main steam safety valves, and reactor protection system are designed to maintain the RCS below 110 percent of design pressure during worst pressure transients. While the RCS is in the LTOP mode, overpressure protection is provided by the shutdown cooling system relief valves.

Therefore, the integrity of the reactor coolant pressure boundary and the main steam system pressure boundary are maintained.

15.4.4.5 Radiological Consequences

The radiological consequence of this event is bounded by the CEA ejection accident described in Subsection 15.4.8.

15.4.4.6 Conclusions

The SIRCP does not result in a loss of shutdown margin. There is no increase in core heat flux and no fuel damage. The increase in pressure during this event will not result in peak pressures greater than the applicable limits.

15.4.5 Flow Controller Malfunction Causing an Increase in BWR Core Flow Rate

Not applicable to the APR1400.

15.4.6 Inadvertent Decrease in Boron Concentration in the Reactor Coolant System

15.4.6.1 Identification of Causes and Frequency Classification

The inadvertent decrease in reactor coolant boron concentration event is presented here with respect to time available for operator corrective action prior to the loss of minimum required shutdown margin. Fuel integrity is not challenged by this event since the reactivity excursions by this event in Modes 1 and 2 are less than those of CEA withdrawal events, and the critical core condition is not reached in Modes 3 through 6.

The inadvertent decrease in reactor coolant boron concentration event may be caused by improper operator action or by a failure in the boric acid makeup flow path, which reduces the flow of borated water to the charging pump suction. Either cause can produce a boron concentration of the charging flow, which is below the concentration of the reactor coolant.

Event frequency conditions are described in Section 15.0.0.1. This event is classified as an AOO.

NUREG-0800, Subsection 15.4.6, states if operator action is required to terminate the transient, the following minimum time intervals must be available between the time an alarm announces an unplanned moderator dilution and the time shutdown margin is lost: (1) during refueling: 30 minutes, or (2) during startup, cold shutdown, hot shutdown, hot standby, and power operation: 15 minutes. However, in this analysis, the operator action time of 30 minutes is conservatively assumed for all operation modes (Modes 1 through 6).

Analysis of the inadvertent decrease in reactor coolant boron concentration event initiated during each of the six operational modes defined in the Technical Specifications is performed. These analyses show that Mode 4 (hot shutdown) results in the least time available for detection and termination of the event as shown in Table 15.4.6-1.

15.4.6.2 Sequence of Events and Systems Operation

The inadvertent decrease in reactor coolant boron concentration event is evaluated during all modes of operation including Modes 1 through 6.

Table 15.4.6-1 provides a summary of the operating parameters and conditions for the inadvertent decrease in reactor coolant boron concentration event for the APR1400.

The indications and/or alarms available to alert the operators that the inadvertent decrease in reactor coolant boron concentration event is occurring in each of the operational modes are outlined below.

a. For Modes 1 and 2: (1) a high power or, for some set of conditions, a high pressurizer pressure trip in Mode 1 and (2) a high logarithmic power level trip in Mode 2. Furthermore, a high T_{AVG} alarm may also occur prior to trip.

b. In Modes 3, 4, and 5 with RCS full and at least one of the reactor coolant pumps (RCPs) operating, a neutron flux alarm on the startup flux channel will provide indication of any inadvertent decrease in reactor coolant boron concentration event.

c. In Modes 4 and 5 with the RCS full and all RCPs idle, the primary coolant volume available for mixing consists of only the volume of the reactor vessel up to the top of the hot legs, the volume of the shutdown cooling system, the volume of one hot leg, the volume of two discharge legs, and the volume from the top of the annulus to the bottom of the upper guide structure support plate. The rest of the RCS volume is not included because of the possibility of stagnation. The neutron flux alarm on the startup flux channel will provide indication of any inadvertent decrease in reactor coolant boron concentration event.

d. In Mode 5 with the RCS partially drained for system maintenance, the volume available for mixing consists of only the volume of the reactor vessel up to the midplane of the hot legs, the volume of the shutdown cooling system, half the volume of one hot leg, and half the volume of two discharge legs. The neutron flux alarm on the startup flux channel will provide indication of any inadvertent decrease in reactor coolant boron concentration event.

e. In Mode 6, with the reactor upper head removed and the CEAs fully withdrawn, the coolant is maintained at a boron concentration of at least 2,150 ppm before entering this mode. In this condition, deboration is prohibited. The neutron flux alarm on the startup flux channel or the reactor makeup water flow alarm (backup only) provides indication of any inadvertent decrease in reactor coolant boron concentration event. In Mode 6, this event is prevented by administrative controls that isolate the RCS from the potential source of unborated water. The associated valve in the CVCS is locked closed during Mode 6 to block the flow paths that could allow unborated makeup to reach the RCS.

An inadvertent decrease in reactor coolant boron concentration event when the reactor is critical (Modes 1 and 2), results in a slow increase in core power and RCS temperature. This event is slower than other reactivity excursions analyzed (e.g., CEA withdrawals), and the reactor will trip in time to prevent violation of any safety limit. This trip provides reasonable assurance of a second dilution period, during which the operator is notified of

any ongoing deboration at least 30 minutes before the reactor achieves criticality. Therefore, Modes 1 and 2 do not have to be analyzed further with respect to an inadvertent decrease in reactor coolant boron concentration event.

For Modes 3, 4, 5, and 6, operation time is calculated from event initiation to loss of shutdown margin. For these modes, 30 minutes is conservatively subtracted from this time to determine the latest allowable time for alarm actuation. In these modes, it is calculated that at 30 minutes prior to loss of shutdown, the source range monitoring (SRM) ratio exceeds its setpoint. An operator response time of at least 30 minutes is demonstrated.

The operator can identify a boron dilution through a neutron flux alarm on the startup flux channel, reactor makeup flow rate, sampling or boric acid flow rate. The operator turns off the charging pump in order to stop further boron dilution. Next, the operator increases the RCS boron concentration by implementing the emergency boration procedure.

None of the single failures listed in Table 15.0-4 has any effect on this event in Modes 1 through 6.

15.4.6.3 Core and System Performance

15.4.6.3.1 Evaluation Model

Assuming complete mixing of boron in the RCS, the rate of change of boron concentration during dilution is described by the following equation.

$$M\frac{dC}{dt} -WC \qquad \text{(Eq. 15.4-1)}$$

Where:

M = RCS mass

C = time-dependent RCS boron concentration

W = charging mass flow rate of unborated water

dC/dt is maximized by maximizing W and minimizing M

Assuming W is equal to the maximum possible value and choosing M equal to the minimum value occurring during the boron dilution incident, the solution of Equation 15.4-1 can be written as follows:

$$C(t) = C_0 e^{-t/\tau} \qquad \text{(Eq. 15.4-2)}$$

Where:

$C(t)$ = boron concentration at time t

C_0 = initial boron concentration

τ = M/W = boron dilution time constant

The time required to dilute to criticality is given by:

$$T = \tau \ln \frac{C_0}{C_{crit}} \qquad \text{(Eq. 15.4-3)}$$

Where:

C_{crit} = critical boron concentration

For Modes 3, 4, and 5 operations, total dilution time is calculated from the Equation 15.4-3. Alarm time is determined by subtracting 30 minutes from this total dilution time. Using the boron concentration at this time and the initial boron concentration, the setpoint of the SRM ratio is determined.

The neutron flux alarm is activated when the SRM ratio exceeds its setpoint. The SRM ratio is defined as follows:

$$\text{SRM ratio} = \frac{\text{Source range signal at time t}}{\text{Source range signal at start of dilution}} \qquad \text{(Eq.15.4-4)}$$

15.4.6.3.2 Input Parameters and Initial Conditions

The inadvertent deboration is assumed to proceed at the maximum possible rate. For this to occur, the charging pump is on, the reactor makeup water tank is aligned with the charging pump suction, a reactor makeup water pump is on, letdown flow is diverted from the volume control tank, and a failure in the boric acid makeup water flow path (e.g., flow control valve failing in the closed position) terminates borated water flow to the charging pump suction.

Analysis of inadvertent decrease in reactor coolant boron concentration event initiated during operational Modes 1 through 6 (defined in the Technical Specifications) was performed. These analyses show that the Mode 4 (hot shutdown) configuration results in the shortest available time for detection and termination of the event. Therefore, the initial conditions and analysis parameters are chosen for the hot shutdown operational mode to minimize the interval from initiation of dilution to the time at which criticality is reached. This results in the least amount of time between detection and criticality.

The following are the analysis assumptions for Mode 4:

a. The core operating limits report (COLR) lower limit on shutdown margin for hot shutdown is assumed to be 6.5 %$\Delta\rho$.

b. The most adverse initial core condition is for an initial K_{eff} corresponding to 6.5 %$\Delta\rho$ subcritical and assuming subcriticality is maintained by boron concentration only.

c. The cold reactor coolant volume, including only the volumes for Mode 4 (hot shutdown), is 130.2 m^3 (4,600 ft^3). A conservatively low reactor coolant mass was assumed by using the cold RCS internal volume. Assuming the coolant temperature of 176.7 °C (350 °F) (the Technical Specification upper limit for hot shutdown), the resulting mass is 115,982 kg (255,697 lbm).

d. The maximum charging flow rate to the RCS of 681.4 L/min (180 gpm), which corresponds to 11.47 kg/sec (25.28 lbm/sec), is used.

e. The critical boron concentration with all rods in except the largest worth rod stuck out and the inverse boron worth are 890 ppm and 74 ppm/%$\Delta\rho$, respectively, including uncertainties. The initial boron concentration for the hot shutdown mode is found by adding the product of the inverse boron worth and the minimum shutdown margin (i.e., 6.5 percent) to the critical boron concentration. The resulting minimum initial boron concentration in Mode 4 is 1,371 ppm. Thus, the change of boron concentration from 6.5 %$\Delta\rho$ subcritical to critical is 481 ppm.

15.4.6.3.3 Results

Using the above conservative parameters in Equation (15.4-3), the minimum possible time interval to dilute from 6.5 %$\Delta\rho$ subcritical to criticality is 72.8 minutes. Utilizing only the redundant, qualified neutron flux alarm, this time period will provide reasonable assurance of detection of an inadvertent decrease in reactor coolant boron concentration event at least 30 minutes prior to criticality.

Inadvertent decrease in reactor coolant boron concentration will then be terminated before loss of shutdown margin by the operator actions discussed in Subsection 15.4.6.1.

15.4.6.4 Barrier Performance

For cases where reactor power does not increase during the transient, the barrier performance during a boron dilution is bounded by the results of the inadvertent chemical and volume control system (CVCS) operation event documented in Subsection 15.5.2.

For cases where the transient is initiated at power and reactor power increases, the barrier performance during the transient is bounded by the results for the uncontrolled CEA withdrawal at power event documented in Subsection 15.4.2.

15.4.6.5 Radiological Consequences

The radiological consequence of this event is bounded by the CEA ejection accident described in Subsection 15.4.8.

15.4.6.6 Conclusions

The inadvertent decrease in reactor coolant boron concentration event meets the following fuel design limits: (1) minimum DNBR greater than or equal to 1.29, and (2) the peak linear heat generation rate is less than 656 W/cm (20 kW/ft).

The reactor coolant system pressure remains below 110 percent of its system design pressure for all cases, so the integrity of the reactor coolant pressure boundary is maintained.

For all cases, when the boron dilution is in progress when the reactor is shut down or tripped, indications are available to alert the operator to the uncontrolled reactivity addition and sufficient time is available for the operators to diagnose the situation and take corrective action before criticality or post-trip return to criticality occurs. This event does not lead to a more serious fault condition.

15.4.7 Inadvertent Loading and Operation of a Fuel Assembly in an Improper Position

15.4.7.1 Identification of Causes and Frequency Classification

The inadvertent loading and operation of a fuel assembly in an improper position event is initiated by interchanging two fuel assemblies in a core. The likelihood of an error in core loading is considered to be extremely remote because of the strict procedural control used during core loading.

This event is conservatively considered as an anticipated AOO. Event frequency conditions are described in Subsection 15.0.0.1.

15.4.7.2 Sequence of Events and Systems Operation

The fuel enrichment within a fuel assembly is identified by a coded serial number marked on the exposed surface of the top end plate of the fuel assembly. This serial number is used to positively identify each assembly in the plant. At the completion of core loading, the exposed surfaces of the top end plates are inspected to verify that all assemblies are correctly located.

If a fuel misloading occurs, the consequences depend on the types and locations of the fuel assemblies that have been interchanged. The misloading of a fuel assembly may affect the core power distribution only slightly, for example, if assemblies of similar enrichments and reactivities are misloaded. If assemblies having very different enrichments or reactivities are misloaded, the core power distribution may be affected enough so that core performance would be degraded.

In the unlikely event that two assemblies of different enrichments would be interchanged, some misloadings would be detected using ex-core startup detectors and the reactivity computer during the low power physics testing. In these tests, a symmetry check is

performed in which the reactivity worths of symmetrically located CEAs are compared with one another. The interchange of two or more fuel assemblies with greatly different K_∞'s destroys the octant symmetry of the core flux distribution and would produce significant variations in the worths of symmetrically located CEAs. This asymmetry would be corroborated by symmetry checks performed for other symmetric rod groups, thereby confirming and possibly even locating a fuel assembly misload.

In addition, many misloadings could be detected by either the ex-core detectors directly or the in-core detector channels, which are analyzed at power levels greater than 20 percent during the power ascension test at beginning of cycle (BOC) and periodically throughout the cycle.

Thus, most of the fuel assembly misloadings that can be postulated are detectable both during the rod symmetry checks and during power range operation. However, there are a small number of misloadings that are undetectable during the rod symmetry testing or even early in the cycle with in-core instrumentation during power range operation. Of this small class, the worst case is the interchange of a shimmed assembly with an unshimmed assembly at the center of the core. This case, although not detectable at BOC, would cause local power peaking as the shims burn out.

Chapter 16, Technical Specifications, requires that the planar radial peaking factor (F^m_{xy}) be measured at least once per 31 effective full power days (EFPDs) and that the measured planar radial peaking factor (F^m_{xy}) be less than or equal to the planar radial peaking factor (F^c_{xy}) used in the core operating limit supervisory system (COLSS) and in the core protection calculator (CPC). Even if the increase in radial peak is not large enough to alert the reactor engineer to the possibility of a misloading, the measured radial peak would be used in the COLSS and the CPC. This would reduce the operating band to compensate for the reduction in the thermal margin caused by these misloads.

15.4.7.3 Core and System Performance

15.4.7.3.1 Evaluation Model

Because no transient occurs for this event, the typical transient analysis codes are not used. The ROCS Code is used to calculate both a normal expected radial power distribution and the radial power distributions resulting from the assumed fuel loading errors. ROCS is a

three-dimensional, two-group diffusion core calculation code based on the nodal expansion method, as described in Subsection 4.3.3.1.

15.4.7.3.2 Input Parameters and Initial Conditions

Several single assembly interchanges of this type were postulated and investigated using the fine-mesh neutronics methods discussed in Subsection 4.3.3.1. Most were shown to be detectable when estimates of the symmetric rod worths were calculated. Of those misloads that were not conclusively demonstrated to be detectable during startup at BOC, the interchange of Assemblies 12 and 24 (see Figure 15.4.7-1) was shown to result in the highest F_{xy} value during subsequent full power operation over the first cycle. This limiting case is determined through spectrum analyses of misloading.

15.4.7.3.3 Results

Maximum F_{xy} increase is less than 15 percent including consideration of increased measurement uncertainties due to the misloading. An increase of 20.5 percent in integrated radial peak is considered in the CEA drop analysis and shown to result in a DNBR greater than the 95/95 DNBR limit (see Subsection 15.4.3). The consequences of this event are less severe than those of the CEA drop event, and the resultant DNBR for this event is greater than the 95/95 DNBR limit.

15.4.7.4 Barrier Performance

This event causes changes only in the local heat flux and distribution of power within the core. The core power, flow, and RCS pressure of the whole core are not changed. Therefore, the integrity of the reactor coolant pressure boundary is not challenged.

15.4.7.5 Radiological Consequences

The radiological consequence of this event is bounded by the CEA ejection accident described in Subsection 15.4.8.

15.4.7.6 Conclusions

Those inadvertent loading of a fuel assembly into the improper position events that are not detected during startup at BOC do not result in fuel cladding failure and are within 10 CFR 50.34 guidelines.

The reactor coolant pressure stays below 110 percent of the design pressure so that the integrity of the reactor coolant pressure boundary is maintained.

15.4.8 Spectrum of Control Element Assembly Ejection Accidents

15.4.8.1 Identification of Causes and Frequency Classification

A control element assembly (CEA) ejection (CEAE) event is postulated to occur as a result of a mechanical failure that causes an instantaneous circumferential rupture of the control element drive mechanism (CEDM) housing or its associated nozzle. This results in the reactor coolant system pressure ejecting the CEA and drive shaft to the fully withdrawn position.

The CEDM housings are capable of withstanding throughout their design life all normal operating loads including the steady-state and transient operating conditions specified for the reactor vessel. The occurrence of such a failure is considered to be incredible, and this event is classified as a PA as defined in Subsection 15.0.0.1.

The CEA ejection accident applies the following acceptance criteria:

a. The maximum reactor pressure during any portion of the assumed excursion is less than the value that result in stresses that exceed the “Service Limit C” as defined in the ASME Code.

b. The total number of failed fuel rods that are considered in the radiological assessment is equal to the sum of all of the fuel rods failing each of the criteria below:

   1) The high cladding temperature failure criterion for zero power conditions is a peak radial average fuel enthalpy greater than 711.8 kJ/kg (170 cal/g) for fuel

rods with an internal rod pressure at or below system pressure, or 628.0 kJ/kg (150 cal/g) for fuel rods with an internal rod pressure exceeding system pressure. For intermediate and full power conditions, fuel cladding failure is presumed if local heat flux exceeds thermal design limits.

2) The pellet cladding mechanical interaction (PCMI) failure criterion is a change in radial average fuel enthalpy greater than the corrosion-dependent limit depicted in Figure B-1 of NUREG-0800 (SRP 4.2, Appendix B).

In addition to the fuel failure and boundary criteria above, the following criteria from NUREG-0800 (SRP, Section 4.2, Appendix B) apply to core coolability.

a. Peak radial average fuel enthalpy remains below 963.0 kJ/kg (230 cal/g).

b. Peak fuel temperature remains below incipient melting conditions.

c. Mechanical energy generated as a result of (1) non-molten fuel-to-coolant interaction and (2) fuel rod burst must be addressed with respect to reactor pressure boundary, reactor internals, and fuel assembly structural integrity.

d. There is no loss of coolable geometry due to (1) fuel pellet and cladding fragmentation and dispersal or (2) fuel rod ballooning.

15.4.8.2 Sequence of Events and Systems Operation

The sequence of events during the fuel performance aspect of the CEAE initiated from various power conditions is presented in Table 15.4.8-1.

The postulated mechanical failure of the CEDM causes the ejection of a CEA, which adds positive reactivity to the core resulting in a rapid increase in reactor core power for a short period of time. This power excursion is terminated by the combination of delayed neutron and Doppler feedback effects. Closely following the CEAE, reactor shutdown is initiated by a core protection calculator (CPC) or reactor protection system (RPS) variable overpower trip (VOPT) on high neutron power. The reactor power decreases rapidly as the shutdown CEAs drop into the reactor core. A loss of offsite power (LOOP) is assumed to be coincident with a turbine trip.

The analysis assumes that operator action is delayed until 30 minutes after event initiation. Plant cooldown is accomplished by using the auxiliary feedwater (AFW) system in conjunction with the atmospheric dump valves (ADVs) until shutdown cooling entry conditions are reached.

This event results in a turbine trip when initiated from at-power conditions. A turbine trip could cause a disturbance to the utility grid, which could cause a loss of offsite power, which could cause a RCP coastdown. The RCS pressure increase caused by turbine trip and LOOP can mitigate fuel failure due to DNB, but the change of RCS pressure is conservatively not considered for DNBR calculation.

None of single failures listed in Table 15.0-4 has any effect on this event. The limiting single failure for this event is one train failure of the RPS. Other trains provide adequate protection. Details on the RPS are provided in Section 7.2.

15.4.8.3 Core and System Performance

15.4.8.3.1 Evaluation Model

The core response to a CEAE is simulated using the method of analysis referenced in Subsection 15.0.2. The evaluation model is used to determine the peak fuel rod temperature and fuel rod enthalpy, which are required for the evaluation of the high cladding temperature failure, the pellet cladding mechanical interaction (PCMI) failure, and the core coolability. The DNBR is calculated using the CETOP and STRIKIN-II computer programs described in Subsection 15.0.2 with the KCE-1 CHF correlation. A matrix relating the initial and ejected CEA radial peaking factors is obtained from ROCS code, which is a three-dimensional, two-group diffusion core calculation code based on the nodal expansion method, as described in Subsection 4.3.3.1. This matrix is used to calculate the number of fuel pins experiencing DNB. Further conservatism is introduced by assuming that clad failure occurs when fuel rods experience DNB.

The nuclear steam supply system (NSSS) response to a CEA ejection is simulated using the CESEC-III computer program described in Subsection 15.0.2.2.1.

Except for radiological release from containment, the analysis of the NSSS response to a CEA ejection does not consider the leakage and the RCS depressurization that would be

caused by the rupture of the primary pressure boundary. This approach does not affect the fuel failure calculation, but it does increase the calculated secondary steam release. Not considering the leakage and the RCS depressurization maximizes the resultant doses from secondary steam release.

15.4.8.3.2 Input Parameters and Initial Conditions

The initial conditions for the principal process variables are varied within the reactor operating space given in Table 15.0-3 to determine the set of conditions that produce the most adverse consequences following a CEA ejection. The initial pressurizer and steam generator water level, as controlled within the operating space, have an insignificant effect on the consequences of the CEA ejection analysis. Table 15.4.8-2 shows the parameters used in the CEA ejection analysis for peak fuel rod temperature and fuel rod enthalpy analysis. The following assumptions, which encompass conditions characteristic of the beginning of cycle (BOC) and end of cycle (EOC), are used to calculate conservative transient results.

a. A spectrum of initial reactor power level is considered as follows: (1) hot full power (HFP), (2) 50 percent power, (3) 20 percent power, and (4) hot zero power (HZP).

b. Thermal-hydraulic parameters (maximum reactor coolant inlet temperatures, minimum reactor coolant system pressure, and minimum reactor coolant flow fraction) are set to maximize the net energy increase in the fuel of hot channel. For DNBR analysis, the most adverse combination of initial conditions (core inlet temperature, reactor coolant system pressure, and core flow) at a power operating limit by COLSS are selected by parametric studies to minimize the DNBR for HFP and 50 percent power case. COLSS is described in Subsection 7.7.1.4.

c. It is conservative to use minimum delayed neutron fraction and minimum neutron lifetime at EOC to make the power increase faster and further.

d. The most positive moderator temperature coefficient (MTC) at BOC is used with varying power level to maximize the positive feedback during the transient.

e. The least negative fuel temperature coefficient (FTC) is used to minimize Doppler feedback during the power excursion. Doppler reactivity weighting factor is assumed to be 1.0 for conservatism.

f. In the three-dimensional modeling, the most reactive CEA ejection is selected with consideration for power dependent rod insertion limit. The magnitude of the enthalpy rise increases with increasing ejected worth.

g. As the hot channel power is obtained by multiplying the average channel power by the three-dimensional post-ejected peaking factor, the maximum three-dimensional post-ejected peaking factor is used to maximize the net energy content in the hottest fuel. Also, the maximum ratio of the three-dimensional post-ejected to pre-ejected peaking factor is used to maximize the prompt enthalpy rise in the hottest fuel.

h. Scram curves corresponding to bottom peaked axial shape are used to minimize the initial negative reactivity insertion. The minimum net scram worth with the most reactive rod stuck out and a CEA ejected is used from HFP to HZP.

i. A top-peaked axial power distribution is set to maximize the energy content in the hottest fuel pellet.

j. The maximum delay time is 0.55 second (including time to open the reactor trip switchgear) for the VOPT and 0.5 second for CEA holding coil decay time.

15.4.8.3.3 <u>Results</u>

For peak fuel rod temperature and fuel rod enthalpy analysis, the results are summarized in Table 15.4.8-3. For the HZP case, the fuel radial average enthalpy of hot spot is well below the high cladding temperature failure criterion. The prompt fuel enthalpy rise is less than 251.2 kJ/kg (60 cal/g), which is the lowest criterion of the PCMI failure depicted in Figure B-1 of SRP 4.2 and the oxide to wall thickness ratio is less than 0.2 (described in Subsection 4.2.3.1.4). The PCMI cladding failure is defined with respect to prompt pulse width for the 20 percent power case and the HZP case. The non-prompt scenarios that do not exhibit a prompt critical or narrow pulse power excursion, such as the HFP case and the 50 percent power case, would be not concerned with PCMI cladding failure.

In the results, there are no fuel failures due to the high fuel enthalpy and PCMI. From a core coolability perspective, the peak fuel radial average enthalpy and the fuel centerline temperature meet the criterion. The fuel cladding temperature does not increase to cause fuel rupture or significant rod ballooning. There is no loss of core coolable geometry. The interim criteria for reactivity-initiated accident (RIA) described in NUREG-0800 (SRP 4.2 Appendix B) are met.

The centerline temperature is increased by 157.2 ºC (315 ºF) in case of considering the thermal conductivity degradation (TCD) effect (Reference 78). However, the maximum centerline temperature is below the melting temperature and met the criterion.

Following a postulated CEA ejection event, 10.0 percent of the fuel is calculated to experience DNB. As all fuel pins that experience DNB are conservatively assumed to suffer clad failure, 10.0 percent of fuel failure is used in the offsite dose evaluation in Subsection 15.4.8.5. The case initiated from HFP initial conditions is expected to result in the greatest potential for offsite dose consequences.

Table 15.4.8-1 contains the sequence of events that occur during a CEA ejection for enthalpy case. Figures 15.4.8-1 through 15.4.8-12 show the core power, heat flux, clad and fuel temperatures, and reactivity effects for HFP and HZP cases.

The limiting secondary system releases for the CEAE event are based on a full power DNBR analysis, with the sequence of events summarized in Table 15.4.8-1. These steam releases are applied to the CEAE radiological consequence assessment presented in Subsection 15.4.8.5. The dynamic behaviors of important NSSS parameters following CEA ejection are presented in Figures 15.4.8-13 and 15.4.8-14.

15.4.8.4 Barrier Performance

15.4.8.4.1 Evaluation Model

The evaluation model is identical to that of core performance as described in Subsection 15.4.8.3.1. The CESEC-III code is used to analyze the RCS pressure transient following CEA ejection.

15.4.8.4.2 Input Parameters and Initial Conditions

The input parameters are similar to the core and system performance analysis described in Subsection 15.4.8.3.2. The initial conditions and NSSS characteristics assumed in this analysis are determined to maximize the primary and secondary system pressures. The input parameters of full power conditions are used with the difference of the initial pressurizer pressure. The initial pressurizer pressure for this case is 163.46 kg/cm^2A (2,325 psia).

15.4.8.4.3 Results

The peak RCS pressure for this event is 177.55 kg/cm^2A (2,525.34 psia). The peak RCS pressure includes the pressure difference between the cold leg at the RCP discharge and the surge line. This value is less than the value that results in stresses that exceed the Service Limit C. The peak main steam system pressure reaches 90.17 kg/cm^2A (1,282.52 psia). The main steam system pressure is not challenged by this event.

The dynamic behaviors of important NSSS parameters following CEA ejection are presented in Figures 15.4.8-15 through 15.4.8-18.

15.4.8.5 Radiological Consequence

The radiological consequences are performed to determine EAB, LPZ, MCR, and TSC doses due to CEA ejection accident using the AST methodology, the TEDE dose criteria, the guidance in SRP 15.0.3, and the plant-specific bounding design information applicable to the APR1400.

The following two release cases are considered:

a. Containment leakage release: activity released from the fuel is assumed to be released instantaneously and homogeneously throughout the containment atmosphere and available for release to the environment.

b. Secondary system release: activity released from the fuel is assumed to be completely dissolved in the primary coolant and available for release to the environment through the secondary system.

15.4.8.5.1 Evaluation Model

Figure 15A-4 in Appendix 15A shows the leakage paths and transport of the activity released to environment, MCR, and TSC during a CEA ejection event.

Containment Leakage Case

For this case, the activity released from the failed fuel is assumed to be instantaneously and homogeneously distributed in the containment following a CEA ejection. This analysis also releases 100 percent of the iodine and noble gases initially present in the RCS. The activity in the containment is subject to be released by the design leak rate specified in the Technical Specifications.

Secondary System Release Case

The preferred means to release steam for the cooldown is by dumping steam to the condenser. To maximize the secondary system release doses, it is assumed that offsite power is lost so that the main steam condenser is not available. Following the CEA ejection event, the reactor is shut down and the plant is cooled down by discharging secondary coolant through the two SGs using the combination of one or more ADVs and MSSVs.

The SG tubes are expected to be uncovered during the first 30 minutes of the CEA ejection event because the MSSVs are open to cool down the RCS. During this period, the P-T-S leakage flashing fraction averages 15.0 percent. After 30 minutes, the SG tubes remain covered during the CEA ejection. During the first 30 minutes, the unflashed P-T-S leakage mixes with the SG secondary coolant, and after 30 minutes all of the P-T-S leakage mixes with the SG secondary coolant. An iodine partition coefficient of 100 is assumed for transporting the iodine from the SG secondary coolant. For the secondary liquid iodine release from the SG, an iodine partition coefficient of 100 is assumed, which is consistent with the value recommended in NRC RG 1.183.

15.4.8.5.2 Input Parameters and Initial Conditions

The design basis CEA ejection accident is analyzed using a conservative set of assumptions and APR1400 design inputs. The CEA ejection analysis is performed using the guidance in NRC RG 1.183, Appendix H.

Per NRC RG 1.183, Appendix H, Section 1, for the CEA ejection accident, the release from the failed fuel is based on the number of fuel rods to experience DNB and the assumption that 10 percent of the core inventory of the noble gases and iodines is in the fuel gap. The expected number of fuel rods in DNB is 10 percent of the core. The failed fuel is modeled with a radial peaking factor of 1.80. Fuel melt is not expected to occur during the CEA ejection. The CEA ejection releases more iodine and noble gases from fuel gap than the other non-LOCA events as specified in NRC RG 1.183, Table 3. The assumed inventory of fission products in the reactor core and available for release to the reactor coolant is based on the maximum power level of 4,062.66 MWt corresponding to current fuel enrichment and fuel burnup, which is 1.02 times the APR1400 licensed thermal power of 3,983 MWt with the cycle burnup of 56.4 GWD/MTU.

The secondary coolant iodine concentration is limited to 3.7×10^3 Bq/g (0.1 μCi/g) DE I-131. The RCS DE I-131 isotopic concentration profile is multiplied by a factor of 0.1, representing ten percent of primary coolant concentration to determine the secondary coolant iodine concentration. The secondary coolant iodine concentration is multiplied by the total coolant mass in both steam generators to calculate the total secondary coolant iodine inventory.

The chemical forms of iodine released from the steam generators to the environment are 97 percent elemental and 3 percent organic. These iodine chemical forms apply to iodine releases from the P-T-S leakage and from the secondary liquid.

Input parameter values used for CEA ejection radiological consequence evaluation are presented in Table 15.4.8-4.

A reduction in the amount of radioactive material available for leakage from the containment that is due to natural deposition, containment sprays, recirculating filter systems, or other engineered safety features can be taken into account. This analysis

credits aerosol removal by natural deposition. No credit is taken for elemental iodine or aerosol removal by containment sprays.

The primary containment leaks at a Technical Specification peak pressure leak rate of 0.1 percent by volume for the first 24 hours. This leak rate is reduced to 0.05 weight percent after 24 hours.

The P-T-S leakage is at the RCS operational leakage limit of 1.14 L/min (0.3 gpm) through any one SG as specified in the Technical Specification. The P-T-S leak exists until shutdown cooling is in operation and releases from the steam generators have been terminated at 8.0 hours. The primary coolant density used in converting the volumetric P-T-S leak rates to mass leak rates is 1.0 g/cm^3 (62.4 lbm/ft^3). All noble gas radionuclides released from the primary system via the P-T-S leaks are released to the environment without reduction or mitigation.

The χ/Q values used in the analysis for EAB, LPZ, MCR, and TSC are described in Subsection 2.3.4 and are provided in Tables 2.3-2 through 2.3-12; breathing rates are given in Table 15A-11.

15.4.8.5.3 Results

The radiological consequences due to a CEA ejection are presented in Table 15.4.8-5. The results of the CEA ejection analyses indicate that the EAB and LPZ doses are within their allowable dose limit, which is 25 percent of the 10 CFR 50.34(a)(1) value, as specified in SRP 15.0.3. The MCR and TSC doses are also within the dose limit in GDC 19.

15.4.8.6 Conclusions

For the spectrum of CEA ejection evaluated, none of the power excursions causes the fuel temperatures to reach the limiting fuel melting temperature or the fuel enthalpy limits. For the events that exceeded the DNBR limit, the number of fuel failures was less than the value allowed for the radiological release limit. The peak RCS pressure remains below 110 percent of the RCS design pressure. The stresses due to the primary pressure response during the transients do not exceed Service Limit C as defined in the ASME Code.

The doses at the EAB, LPZ, MCR, and TSC are within their allowable dose criteria.

15.4.9 Combined License Information

No COL information is required with regard to Section 15.4.

Table 15.4.1-1

Sequence of Events for the Low Power Sequential CEA Withdrawal

Time (sec)	Event	Setpoint or Value
0.00	Withdrawal of CEAs – initiating event	—
29.19	Core power reaches variable overpower reactor trip analysis setpoint, % of design power	25.0
29.64	Variable overpower trip signal generated	—
29.74	Trip breakers open and the turbine is tripped / LOOP occurs	—
30.25	Maximum core power, % of design power	43
30.45	Maximum core average heat flux, % of full power heat flux	21
30.45	Minimum DNBR	3.34
34.48	Maximum pressurizer pressure, kg/cm^2A (psia)	158.2 (2,250)

Table 15.4.1-2

Assumptions and Initial Conditions
for the Low Power CEA Withdrawal Analysis

Parameter	Value
Initial core power level, MWt	0.03983
Core inlet coolant temperature, °C (°F)	295.0 (563)
Core mass flow rate, 10^6 kg/hr (10^6 lbm/hr)	69.64 (153.52)
Pressurizer pressure, kg/cm^{2}A (psia)	152.9 (2,175)
Three-dimensional peaking factor	5.94
Steam generator pressure, kg/cm^{2}A (psia)	81.7 (1,161)
Moderator temperature coefficient, 10^{-4} Δρ /°C (10^{-4} Δρ /°F)	0.9 (0.5)
Doppler reactivity	Least negative
CEA reactivity addition rate, 10^{-4} Δρ /sec	1.175
CEA worth on trip, %Δρ	−5.5
CEA withdrawal speed, cm/min (in/min)	76.2 (30.0)

Table 15.4.2-1

Sequence of Events for the Sequential CEA Withdrawal at Power

Time (sec)	Event	Setpoint or Value
0.00	Withdrawal of CEAs – initiating event	—
22.95	Core power reaches CPC variable overpower trip analysis setpoint, % of design power	115.0
23.50	CPC variable overpower trip signal generated	—
23.60	Trip breakers open and the turbine is tripped/ LOOP occurs	—
23.65	Maximum core average heat flux, % of full power heat flux	113.80
24.15	Maximum core power, % of design power	115.56
25.30	Minimum DNBR	1.31
27.25	Maximum pressurizer pressure, kg/cm^2A (psia)	172.97 (2,460.2)

Table 15.4.2-2

Assumptions and Initial Conditions
for the Sequential CEA Withdrawal Analysis at Power

Parameter	Value
Core power level, MWt	4,062.66
Core inlet coolant temperature, °C (°F)	287.8 (550)
Core mass flow rate, 10^6 kg/hr (10^6 lbm/hr)	69.64 (153.52)
Pressurizer pressure, kg/cm^{2}A (psia)	163.5 (2,325)
Integrated radial peaking factor	1.49
Initial core minimum DNBR	1.72
Steam generator pressure, kg/cm^{2}A (psia)	68.26 (970.9)
Moderator temperature coefficient, 10^{-4} $\Delta\rho$ /°C (10^{-4} $\Delta\rho$ /°F)	0.0 (0.0)
Doppler reactivity	Least negative
CEA worth on trip, %$\Delta\rho$	−8.0
Reactivity addition rate, 10^{-4} $\Delta\rho$ /sec	0.315
CEA withdrawal speed, cm/min (in/min)	76.2 (30.0)

Table 15.4.3-1

Sequence of Events for the Single CEA Drop

Time (sec)	Event	Setpoint or Value
0.0	A single CEA begins to drop	—
0.0	Maximum pressurizer pressure, kg/cm^2A (psia)	152.9 (2,175)
382.5	Minimum DNBR	1.36

Table 15.4.3-2

Assumptions and Initial Conditions for the Single CEA Drop

Parameter	Assumed Value
Core power level, MWt	4,062.66
Core inlet coolant temperature, °C (°F)	295.0 (563)
Core mass flow rate, 10^6 kg/hr (10^6 lbm/hr)	69.64 (153.52)
Pressurizer pressure, kg/cm^{2}A (psia)	152.9 (2,175)
Steam generator pressure, kg/cm^{2}A (psia)	75.86 (1,079)
Axial shape index	−0.3
Initial core minimum DNBR	1. 81
Integrated radial peaking factor	1.37
Dropped CEA reactivity worth, 10^{-2} $\Delta\rho$	−0.13
Time for dropped CEA to be fully inserted, sec	2.0
Moderator temperature coefficient, $\Delta\rho$/°C($\Delta\rho$/°F)	-5.4×10^{-4} (-3.0×10^{-4})
Doppler reactivity	Most negative

Table 15.4.6-1

Assumptions and Results for the Inadvertent Deboration Analysis

Parameter	Assumptions and Results					
Operation Mode	3 (1)	4 (1)	4 (2)	5 (1)	5 (2)	5 (3)
Cold RCS Volume, m^3 (ft^3)	283.1 (10,000)	283.1 (10,000)	130.2 (4,600)	283.1 (10,000)	130.2 (4,600)	107.6 (3,800)
Dilution Flow, L/min (gpm)	681.4 (180)	681.4 (180)	681.4 (180)	681.4 (180)	681.4 (180)	567.8 (150)
Initial Boron Concentration - C_0, ppm	1,250	1,371	1,371	1,386	1,386	1,386
Critical Boron Concentration - C_{crit}, ppm	821	890	890	912	912	912
Total Dilution time, min	124.9	158.3	72.8	165.2	76.0	75.3

(1) In Modes 3, 4, and 5 with RCS full and at least one of the reactor coolant pumps operating

(2) In Modes 4 and 5 with the RCS full and all RCPs idle

(3) In Mode 5 with the RCS partially drained

Table 15.4.8-1 (1 of 3)

Sequence of Events for the CEA Ejection

Power	Time (sec)	Event	Setpoint or Value
HFP	0.00	Mechanical failure of CEDM causes CEA to eject	—
	0.03	Core power reaches variable overpower reactor trip analysis setpoint, % of design power	127.5
	0.05	CEA fully ejected	—
	0.07	Maximum core power, % of design power	156.3
	1.08	CEAs begin to drop into core	—
	3.30	Maximum radial average fuel enthalpy in the hot spot, kJ/kg (cal/gm)	522.1 (124.7)
	3.43	Maximum clad surface temperature in the hot spot, °C (°F)	567.2 (1,053.0)
	3.67	Maximum fuel centerline temperature in the hot spot, °C (°F)	2,490.2 (4,514.3)
50%	0.00	Mechanical failure of CEDM causes CEA to eject	—
	0.03	Core power reaches variable overpower reactor trip analysis setpoint, % of design power	75.0
	0.05	CEA fully ejected	—
	0.08	Maximum core power, % of design power	129.4
	1.08	CEAs begin to drop into core	—
	3.20	Maximum clad surface temperature in the hot spot, °C (°F)	569.2 (1,056.5)
	3.31	Maximum radial average fuel enthalpy in the hot spot, kJ/kg (cal/gm)	504.1 (120.4)
	3.72	Maximum fuel centerline temperature in the hot spot, °C (°F)	2,370.9 (4,299.6)

Table 15.4.8-1 (2 of 3)

Power	Time (sec)	Event	Setpoint or Value
20%	0.00	Mechanical failure of CEDM causes CEA to eject	—
	0.04	Core power reaches variable overpower reactor trip analysis setpoint, % of design power	45.0
	0.05	CEA fully ejected	—
	0.10	Maximum core power, % of design power	140.3
	1.09	CEAs begin to drop into core	—
	3.30	Maximum radial average fuel enthalpy in the hot spot, kJ/kg (cal/gm)	473.5 (113.1)
	3.62	Maximum clad surface temperature in the hot spot, °C (°F)	586.7 (1,088.1)
	3.67	Maximum fuel centerline temperature in the hot spot, °C (°F)	2,331.3 (4,228.4)
HZP	0.00	Mechanical failure of CEDM causes CEA to eject	—
	0.21	Core power reaches variable overpower reactor trip analysis setpoint, % of design power	25.0
	0.05	CEA fully ejected	—
	0.32	Maximum core power, % of design power	141.3
	1.26	CEAs begin to drop into core	—
	2.48	Maximum clad surface temperature in the hot spot, °C (°F)	346.9 (656.5)
	3.04	Maximum radial average fuel enthalpy in the hot spot, kJ/kg (cal/gm)	314.8 (75.2)
	3.67	Maximum fuel centerline temperature in the hot spot, °C (°F)	1,501.5 (2,734.7)

Table 15.4.8-1 (3 of 3)

Time (sec)	Event (System Response at HFP)	Setpoint or Value
0.00	Mechanical failure of CEDM causes CEA to eject	—
0.04	Core power reaches variable overpower reactor trip analysis setpoint, % of design power	127.5
0.05	CEA fully ejected	—
0.16	Maximum core power, % of design power	151.7
0.49	Reactor trip signal	—
0.59	Reactor trip breakers open	—
1.09	CEAs begin to drop into core	—
3.10	Maximum RCS pressure, kg/cm^2A (psia)	177.5 (2,524.7)
3.59	Turbine trip/generator trip/loss of offsite power	—
7.20	Main steam safety valves open, kg/cm^2A (psia)	86.9 (1,235.7)
11.50	Maximum steam generator pressure, kg/cm^2A (psia)	90.1 (1,281.9)
1,800.00	Operator begins plant cooldown	—

Table 15.4.8-2

Assumptions and Initial Conditions for the CEA Ejection Analysis

Parameter	Cases			
	HZP	20%	50%	HFP
Core power level, MWt	1.00	796.60	1991.50	4,062.66
Delayed neutron fraction, β	0.00412	0.00412	0.00412	0.00412
Moderator temperature coefficient, $10^{-4}\ \Delta\rho$ /°C ($10^{-4}\ \Delta\rho$ /°F)	0.90 (0.50)	0.72 (0.40)	0.45 (0.25)	0.00 (0.00)
Doppler temperature coefficient, $\Delta\rho / \sqrt{K}$	−0.00130	−0.00130	−0.00130	−0.00130
Ejected CEA worth, $10^{-2}\ \Delta\rho$	0.4469	0.3711	0.2578	0.1459
Post-ejected 3-d power peaking factor	11.49	10.79	6.49	4.32
Ratio of the 3-d post-ejected to pre-ejected power peaking factor	3.93	3.90	3.49	3.17
Total CEA worth available for insertion on reactor trip, $10^{-2}\ \Delta\rho$	−5.0	−5.0	−5.0	−5.0
Postulated CEA Ejection time, sec	0.05	0.05	0.05	0.05
Core inlet coolant temperature, °C (°F)	295 (563)	295 (563)	295 (563)	295 (563)
Core mass flow rate, 10^6 kg/hr (10^6 lbm/hr)	69.64 (153.52)	69.64 (153.52)	69.64 (153.52)	69.64 (153.52)
Pressurizer pressure, kg/cm^{2}A (psia)	152.9 (2,175)	152.9 (2,175)	152.9 (2,175)	152.9 (2,175)

Table 15.4.8-3

Results of the CEA Ejection Event

Parameter	Power			
	HZP	20%	50%	HFP
Maximum radial average fuel enthalpy at hot spot, kJ/kg (cal/gm)	314.8 (75.2)	473.5 (113.1)	504.1 (120.4)	522.1 (124.7)
Maximum fuel centerline temperature, °C (°F)	1,501.5 (2,734.7)	2,331.3 (4,228.4)	2,370.9 (4,299.6)	2,490.2 (4,514.3)
Maximum prompt enthalpy rise,(1) kJ/kg (cal/gm)	90.9 (21.7)	138.6 (33.1)	160.8 (38.4)	118.9 (28.4)
Maximum cladding surface temperature, °C (°F)	347.0 (656.6)	586.7 (1,088.1)	569.2 (1,056.5)	567.2 (1,053.0)

(1) Maximum energy deposition during the prompt power pulse width. For HFP and 50 percent power case, the prompt enthalpy rise is the value at 1.0 second.

Table 15.4.8-4 (1 of 3)

Parameters Used in Evaluating the Radiological Consequences of a CEA Ejection

Parameter	Value
Source Terms	
Reactor Core Power Level	4,062.66 MWt
Percent of Fuel Assumed to Experience DNB	10 %
Initial RCS Iodine Specific Activity	3.7×10^4 Bq/g (1.0 μCi/g) DE I-131
Initial RCS Noble Gases Specific Activity	2.15×10^7 Bq/g (580 μCi/g) DE Xe-133
Initial Secondary Liquid Iodine Specific Activity	3.7×10^3 Bq/g (0.1 μCi/g) DE I-131
Radial Peaking Factor	1.80
RCS Initial Mass	267,620 kg (590,000 lbm)
Containment Leakage Transport Model	
Containment Net Free Volume	8.86×10^4 m^3 (3.13×10^6 ft^3)
Reactor Coolant Mass Released to Containment	2.68×10^5 kg (5.90×10^5 lbm)
Credit for Radioactive Decay during Hold up in Containment In Transit to Dose Points	 Applicable Not Applicable
Iodine Chemical Form Aerosol (CsI) Elemental Organic	 95.0 % 4.85 % 0.15 %
Containment Aerosol Natural Deposition Removal	Powers model with a 10-percentile probability
Containment Leak Rate	0.1 %/day (0 ~ 24 hrs) 0.05 %/day (24 ~ 720 hrs)

Table 15.4.8-4 (2 of 3)

Parameter	Value
Secondary System Release Transport Model	
Primary-To-Secondary Leak Rate through SGs	2.27 L/min (0.6 gpm) through all SGs 1.14 L/min (0.3 gpm) through any one SG
Steam Generator Liquid Mass	104,326 kg (230,000 lbm)
Primary-To-Secondary Leak Duration	8 hrs
Steam Mass Released from Both Intact SGs to Environment 0 ~ 0.5 hrs 0.5 ~ 2 hrs 2 ~ 8 hrs	 118,660 kg (261,600 lbm) 650,737 kg (1,434,630 lbm) 624,538 kg (1,376,870 lbm)
Primary-To-Secondary Leak Flashing Fraction	15.0 % average for 1,800 sec after onset of accident
SG Liquid Iodine Partition Coefficient for SG Liquid Iodine Release	100
Alkali Material (Cs, Rb) Partition coefficient	5.0×10^{-3}
Chemical Form of Iodine Released from SG Elemental Organic Iodine	 97 % 3 %

Table 15.4.8-4 (3 of 3)

Parameter	Value
MCR and TSC Model Parameters	
Envelope Volume	5,663 m^3 (200,000 ft^3)
Normal Ventilation Flow Rate (unfiltered)	105 m^3/min (3,700 cfm)
Emergency Ventilation Makeup Rate (filtered)	105 m^3/min (3,700 cfm)
Emergency Ventilation Recirculation Flow Rate (filtered)	122 m^3/min (4,300 cfm)
Emergency HVAC Delay Time	5 mins
Emergency Ventilation Charcoal Filter Efficiency (elemental and organic iodine removal)	99 %
Emergency Ventilation HEPA Filter Efficiency (particulate removal)	99 %
Unfiltered Inleakage	8.50 m^3/min (300 cfm)
Occupancy Factors 0 ~ 24 hrs 24 ~ 96 hrs 96 ~ 720 hrs	 100 % 60 % 40 %
Onsite χ/Qs	See Tables 2.3.2 ~ 2.3.12
Offsite Model Parameters	
χ/Qs	See Table 2.3-1
Breathing Rate	See Table 15A-11
Dose Conversion Factors	See Table 15A-10

Table 15.4.8-5

Radiological Consequences of CEA Ejection

Containment Leakage Case

Post-CEA Ejection Activity Release Path	TEDE Dose (mSv)		
	MCR and TSC	EAB	LPZ
Containment Leakage	1.27E+01	3.99E+01	3.77E+01
External Cloud	6.88E-01	0.00E+00	0.00E+00
Emergency Ventilation Filter Shine	1.34E-06	0.00E+00	0.00E+00
Total	1.34E+01	3.99E+01	3.77E+01
Allowable TEDE Limit	5.00E+01	6.30E+01	6.30E+01

Steam System Release Case

Post-CEA Ejection Activity Release Path	TEDE Dose (mSv)		
	MCR and TSC	EAB	LPZ
P-T-S Iodine Release	1.54E+01	1.94E+01	1.35E+01
P-T-S Noble Gas Release	1.30E+01	2.04E+01	8.78E+00
Secondary Liquid Iodine Release	6.62E-02	1.22E-01	4.66E-02
External Cloud	6.88E-01	0.00E+00	0.00E+00
Emergency Ventilation Filter Shine	1.34E-06	0.00E+00	0.00E+00
Total	2.92E+01	3.99E+01	2.23E+01
Allowable TEDE Limit	5.00E+01	6.30E+01	6.30E+01

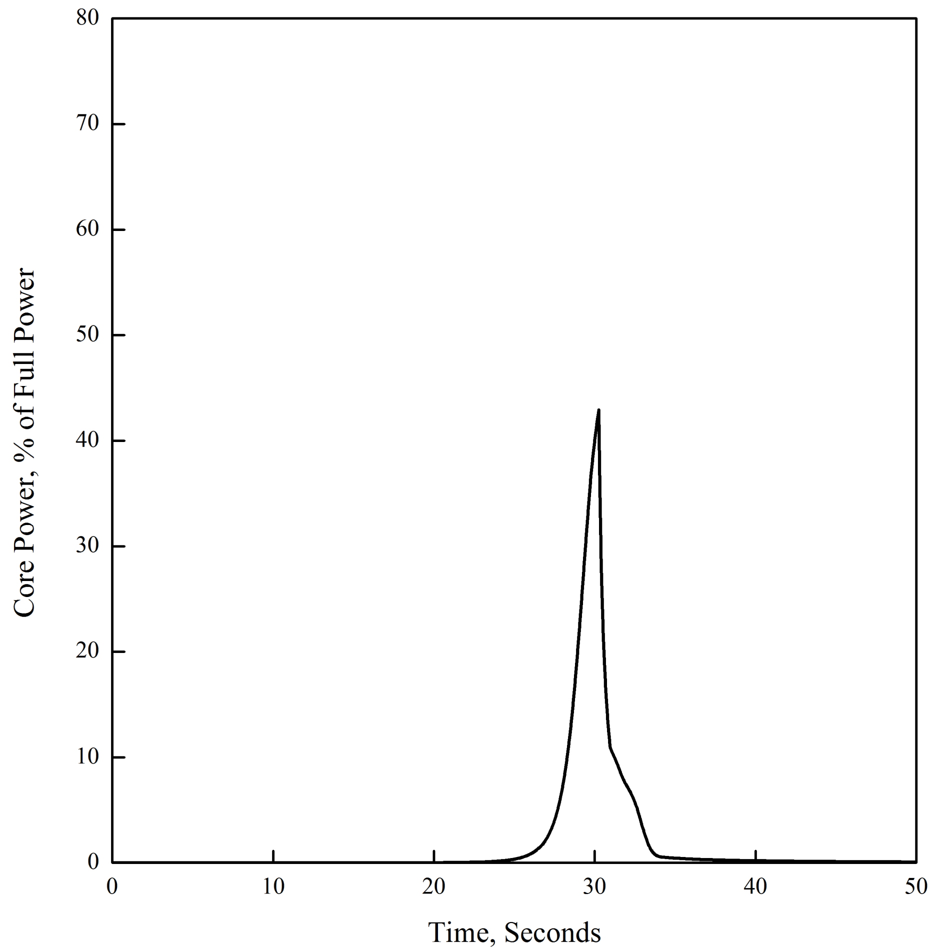

Figure 15.4.1-1 Uncontrolled CEA Withdrawal at Low Power ; Core Power vs. Time

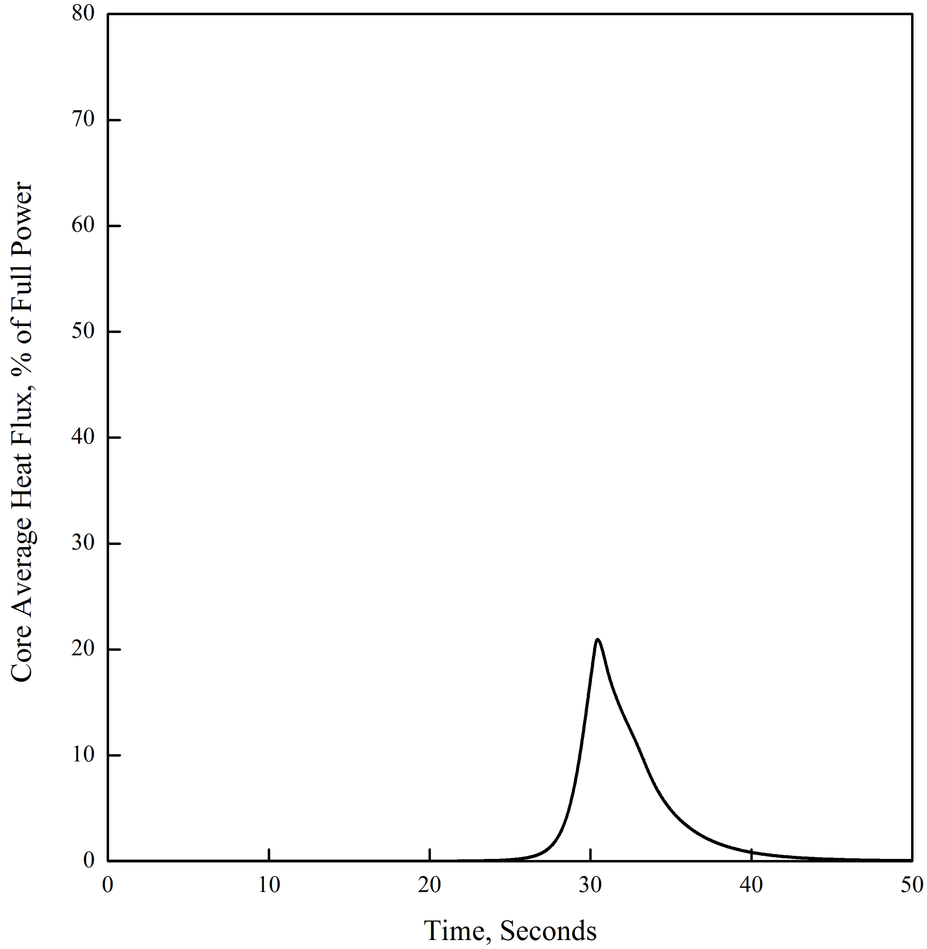

Figure 15.4.1-2 Uncontrolled CEA Withdrawal at Low Power ; Core Average Heat Flux vs. Time

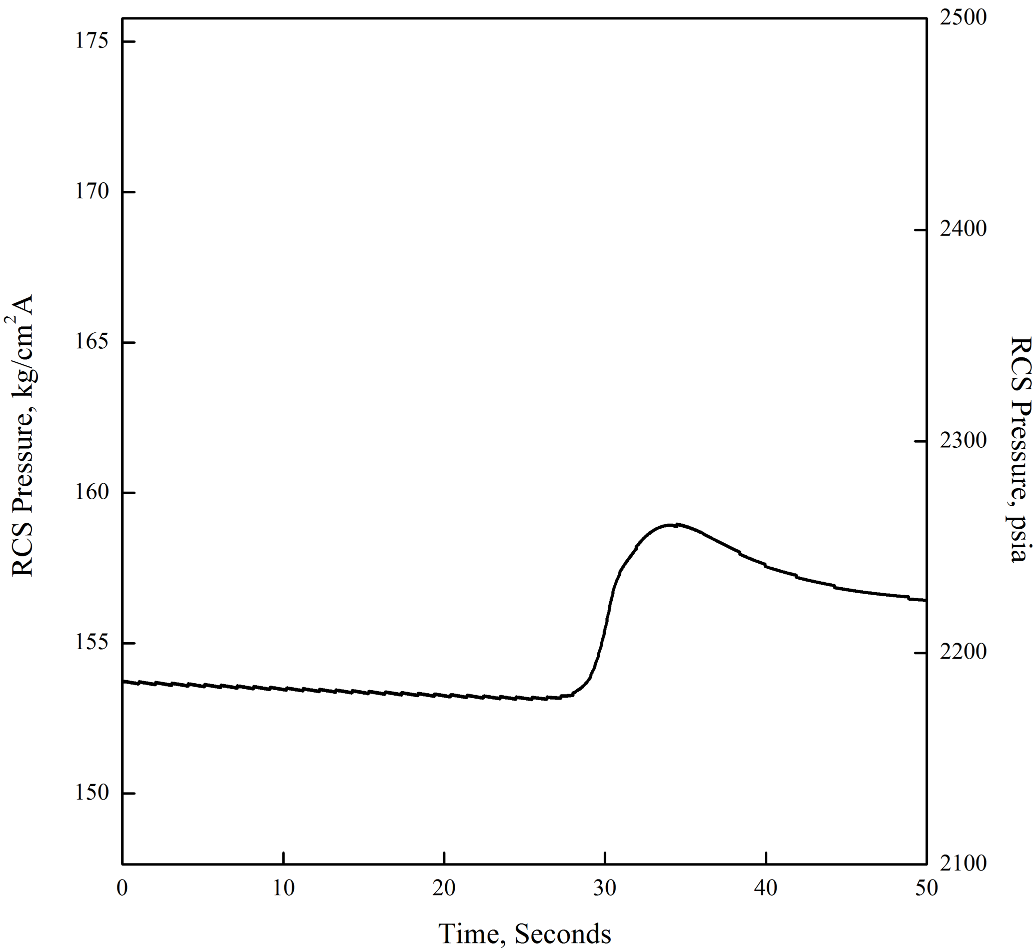

* The pressure difference between cold leg at the RCP discharge and the surge line is not included.

Figure 15.4.1-3 Uncontrolled CEA Withdrawal at Low Power ; RCS Pressure vs. Time

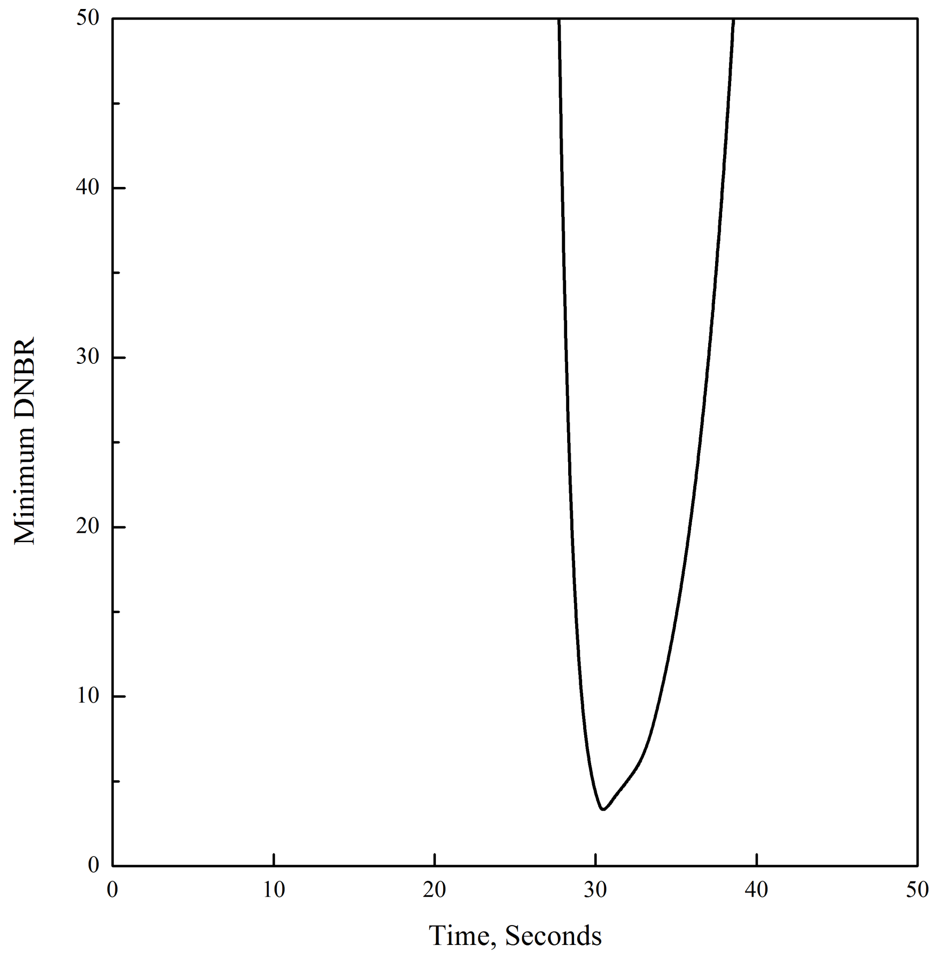

Figure 15.4.1-4 Uncontrolled CEA Withdrawal at Low Power ; Minimum DNBR vs. Time

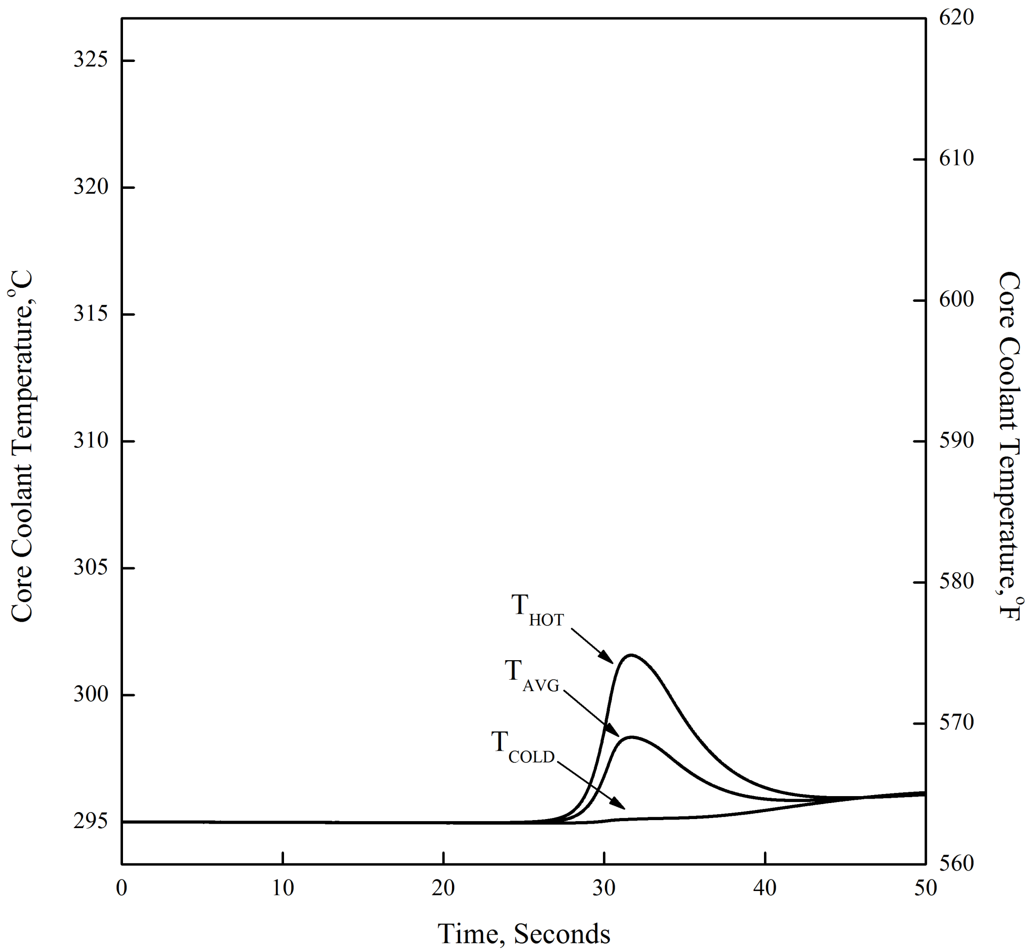

Figure 15.4.1-5 Uncontrolled CEA Withdrawal at Low Power ; Core Coolant Temperature vs. Time

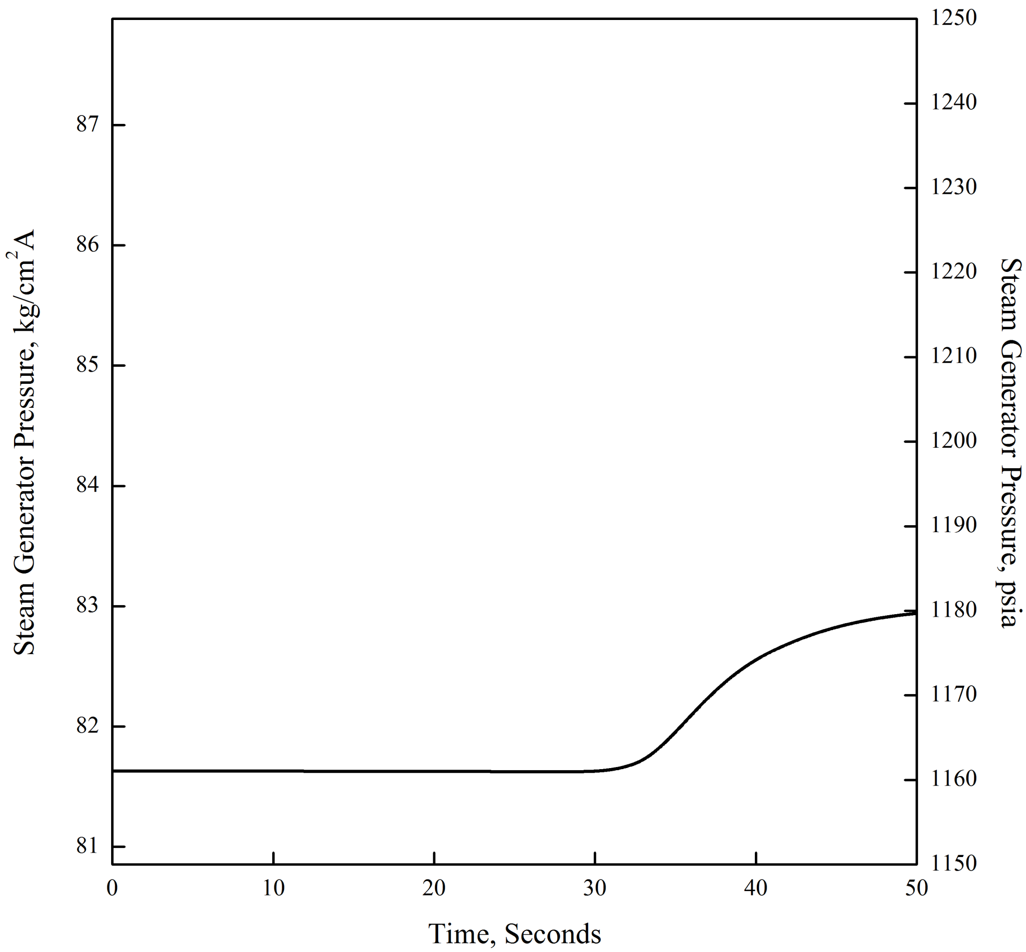

Figure 15.4.1-6 Uncontrolled CEA Withdrawal at Low Power ; Steam Generator Pressure vs. Time

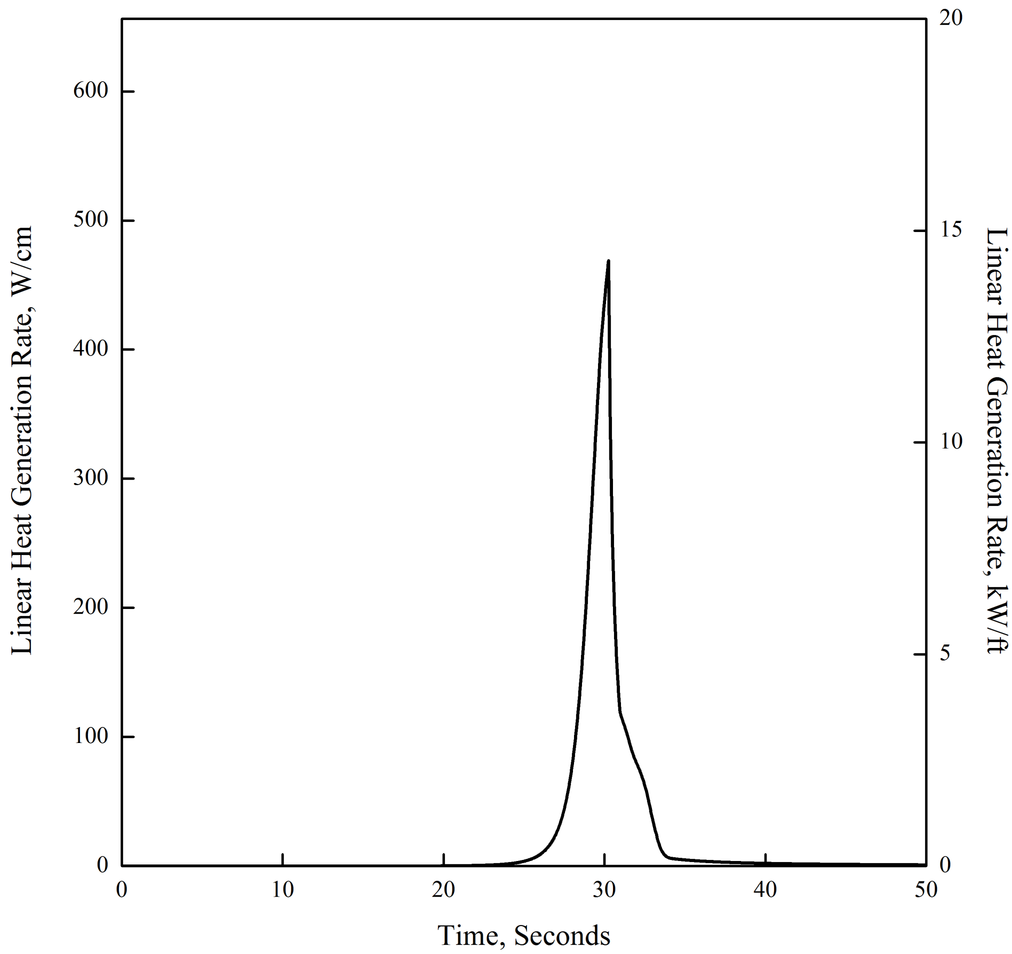

Figure 15.4.1-7 Uncontrolled CEA Withdrawal at Low Power ; Linear Heat Generation Rate vs. Time

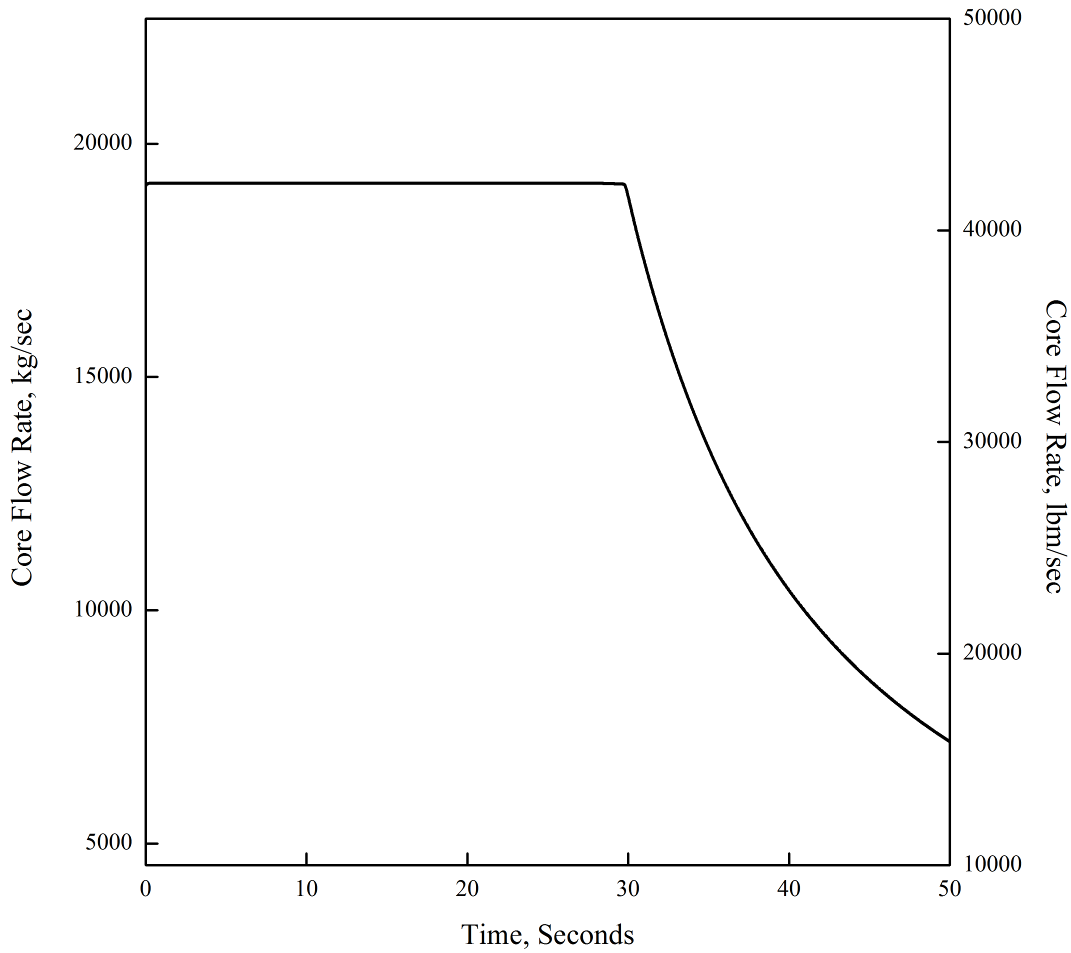

Figure 15.4.1-8 Uncontrolled CEA Withdrawal at Low Power ; Core Flow Rate vs. Time

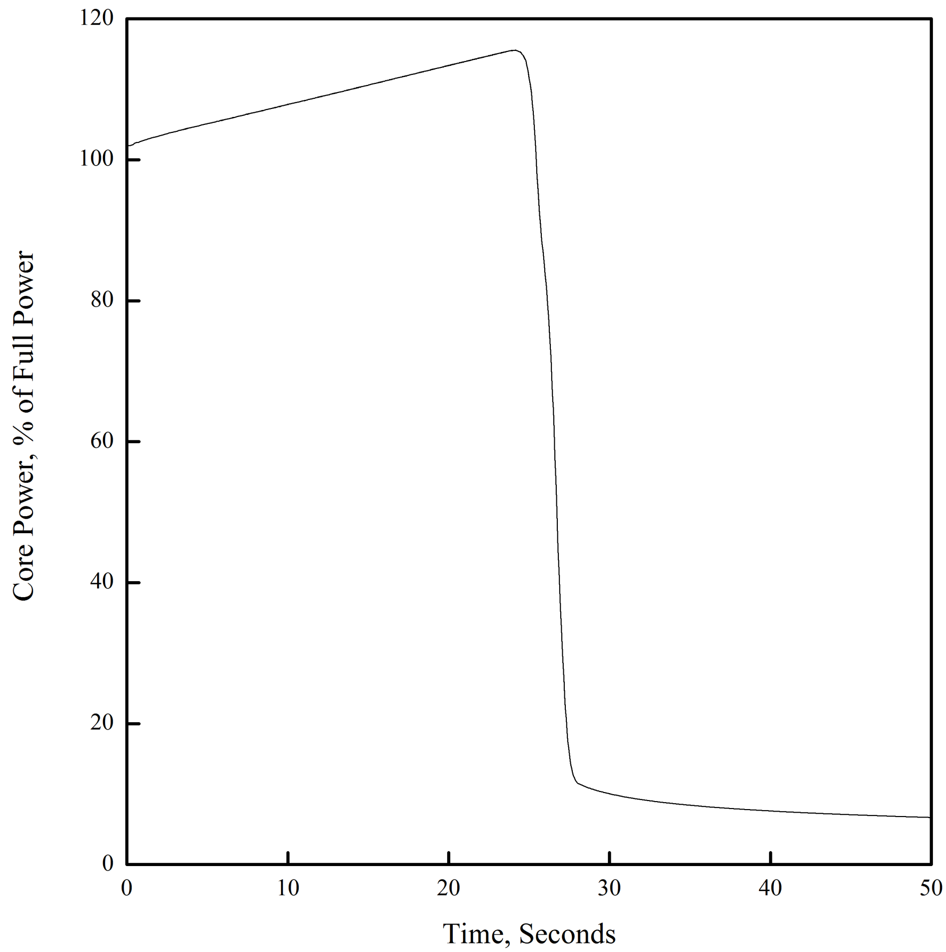

Figure 15.4.2-1   Uncontrolled CEA Withdrawal at Power ; Core Power vs. Time

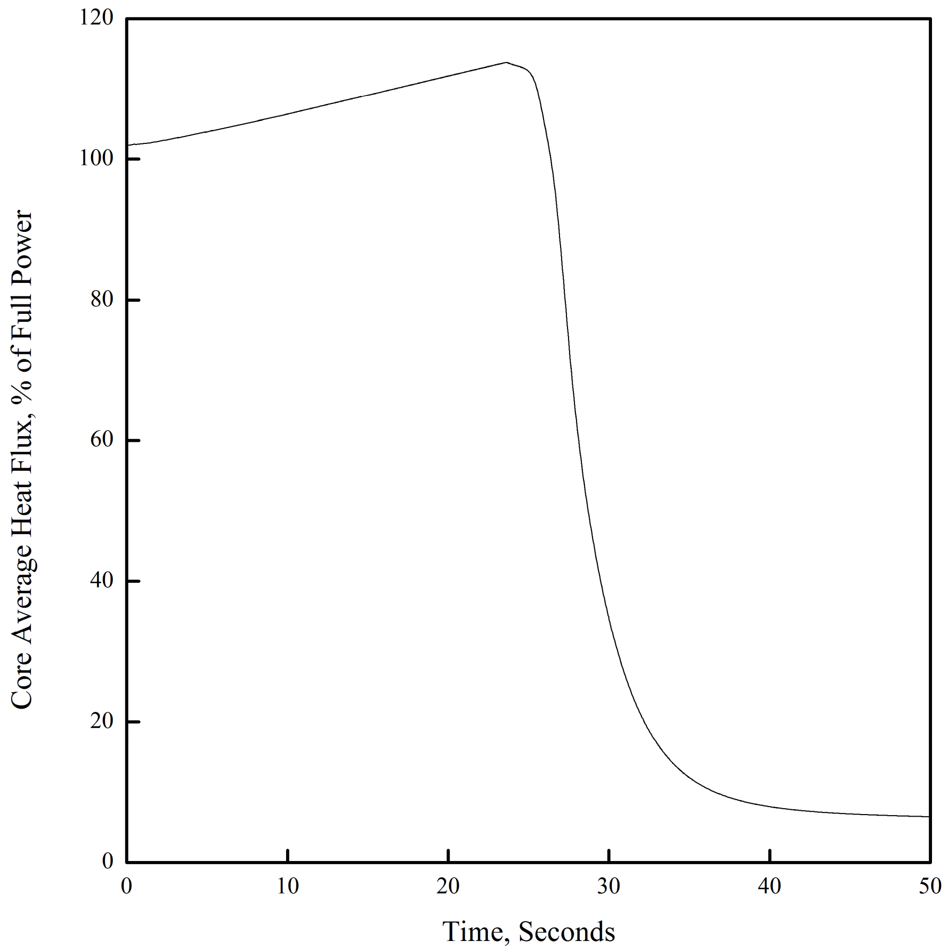

Figure 15.4.2-2 Uncontrolled CEA Withdrawal at Power ; Core Average Heat Flux vs. Time

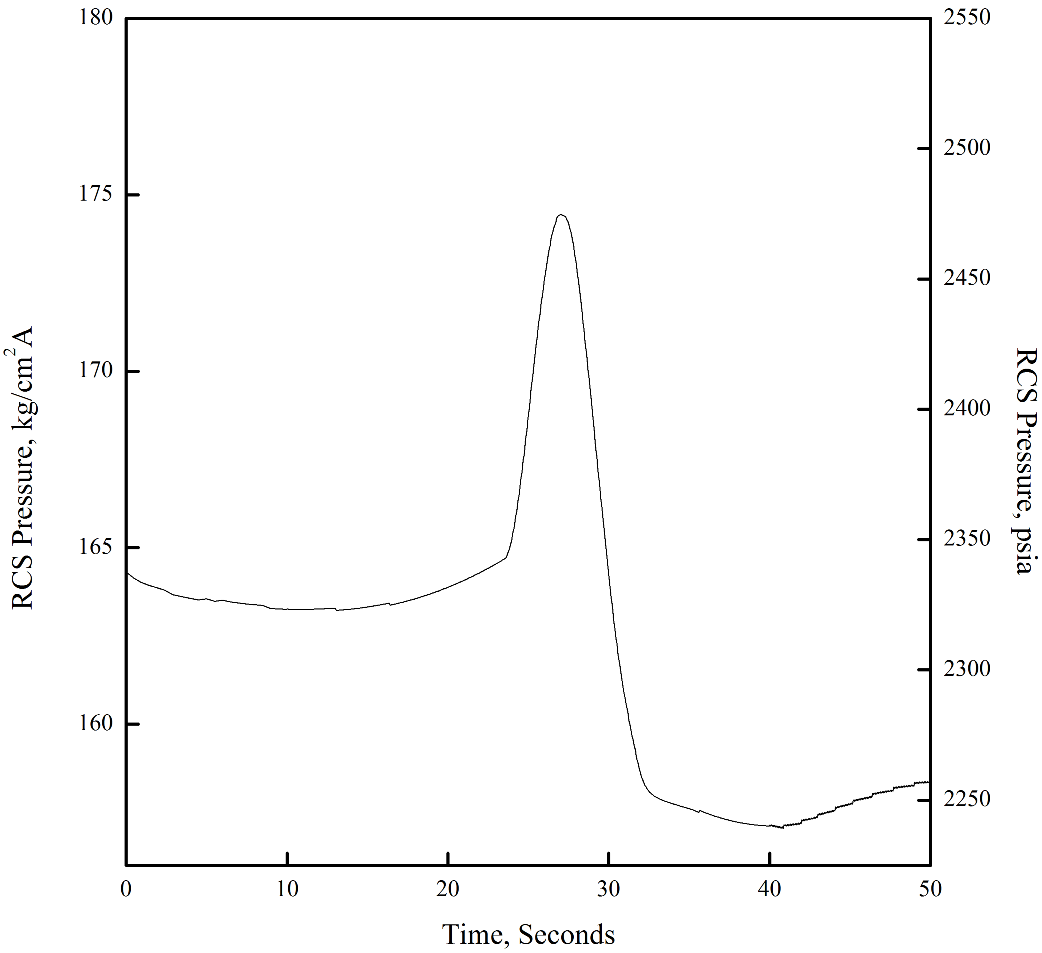

* The pressure difference between cold leg at the RCP discharge and the surge line is not included.

Figure 15.4.2-3 Uncontrolled CEA Withdrawal at Power ; RCS Pressure vs. Time

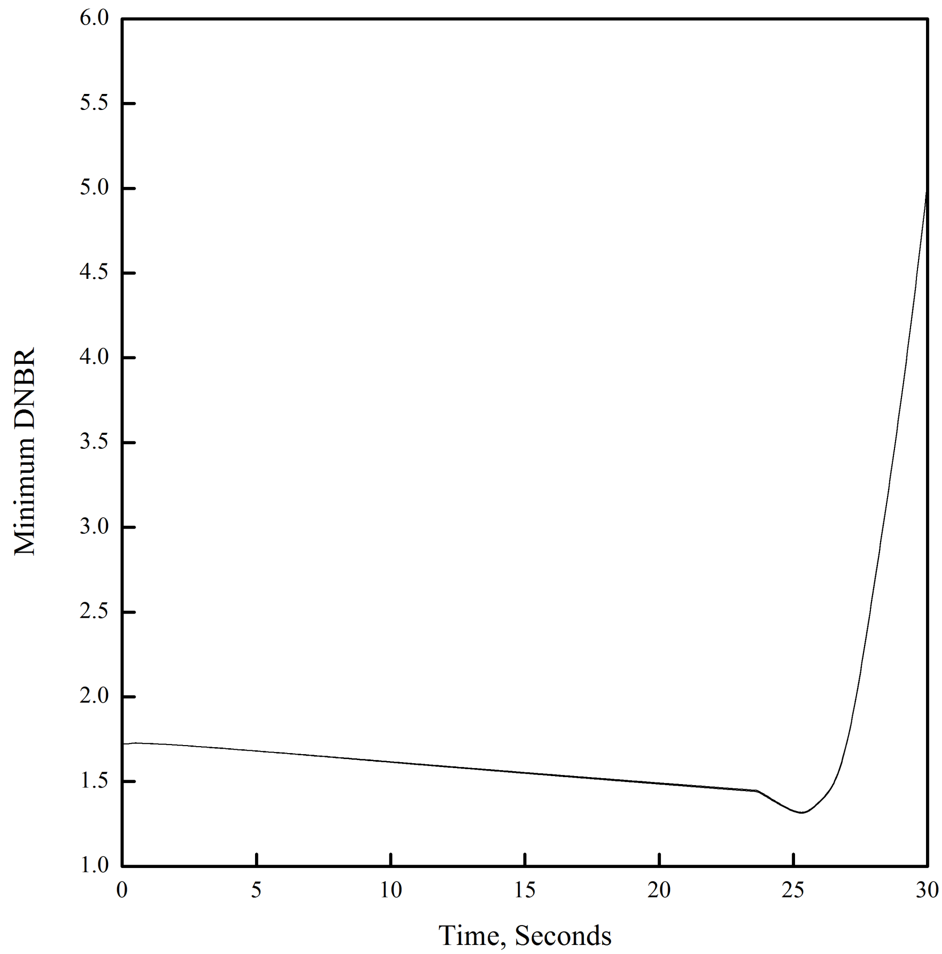

Figure 15.4.2-4 Uncontrolled CEA Withdrawal at Power ; Minimum DNBR vs. Time

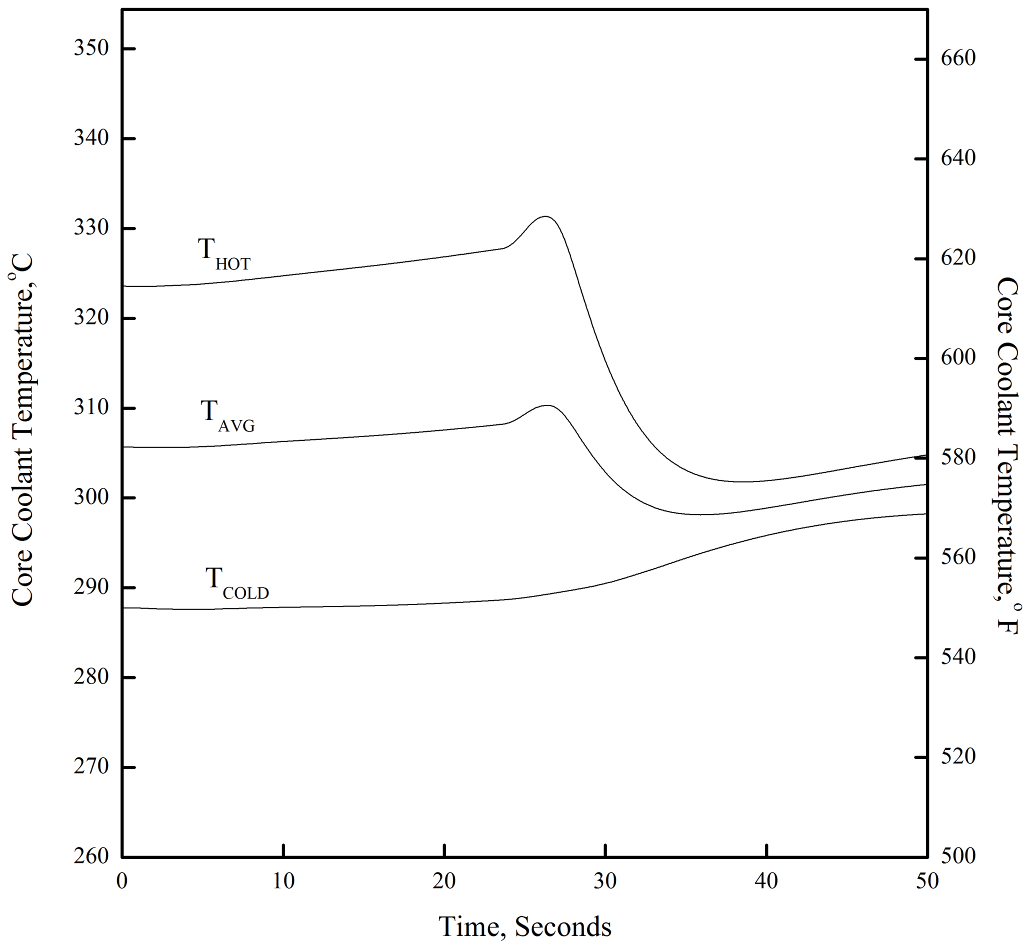

Figure 15.4.2-5 Uncontrolled CEA Withdrawal at Power ; Core Coolant Temperature vs. Time

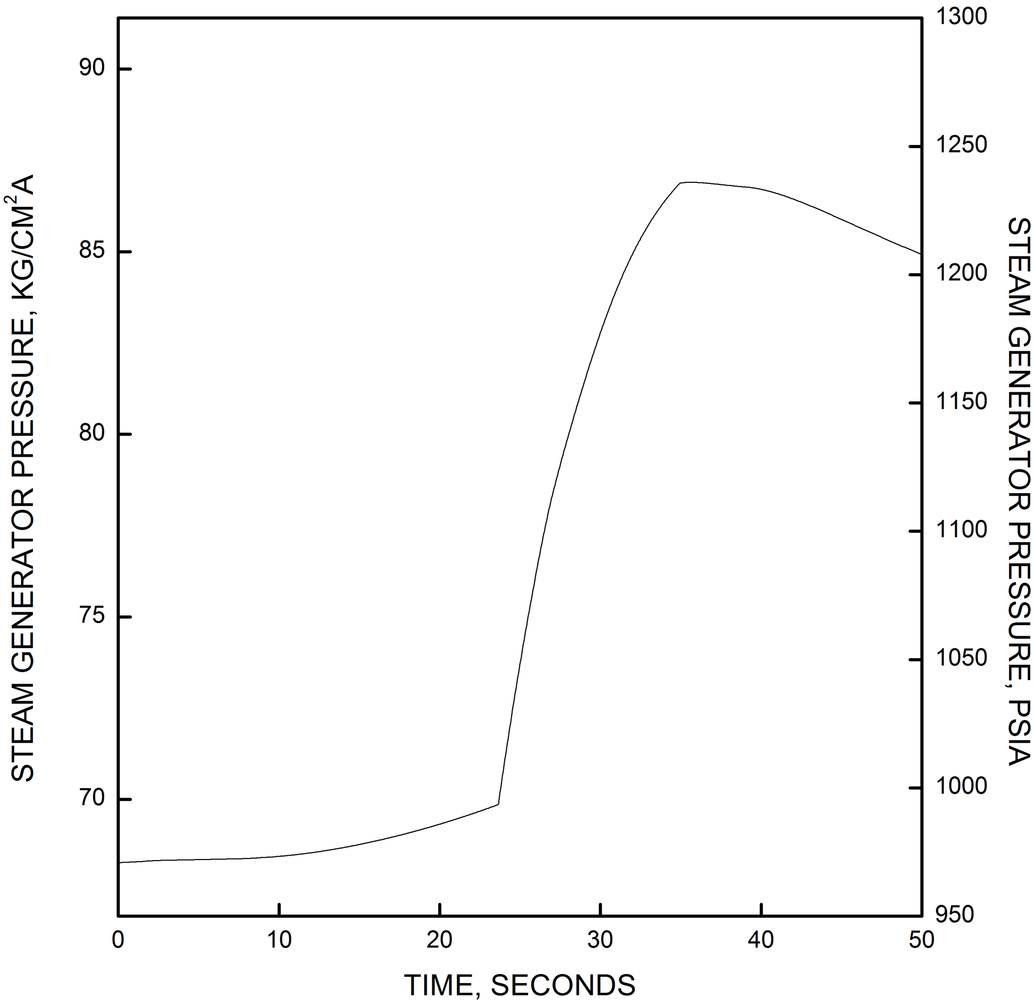

Figure 15.4.2-6 Uncontrolled CEA Withdrawal at Power ; Steam Generator Pressure vs. Time

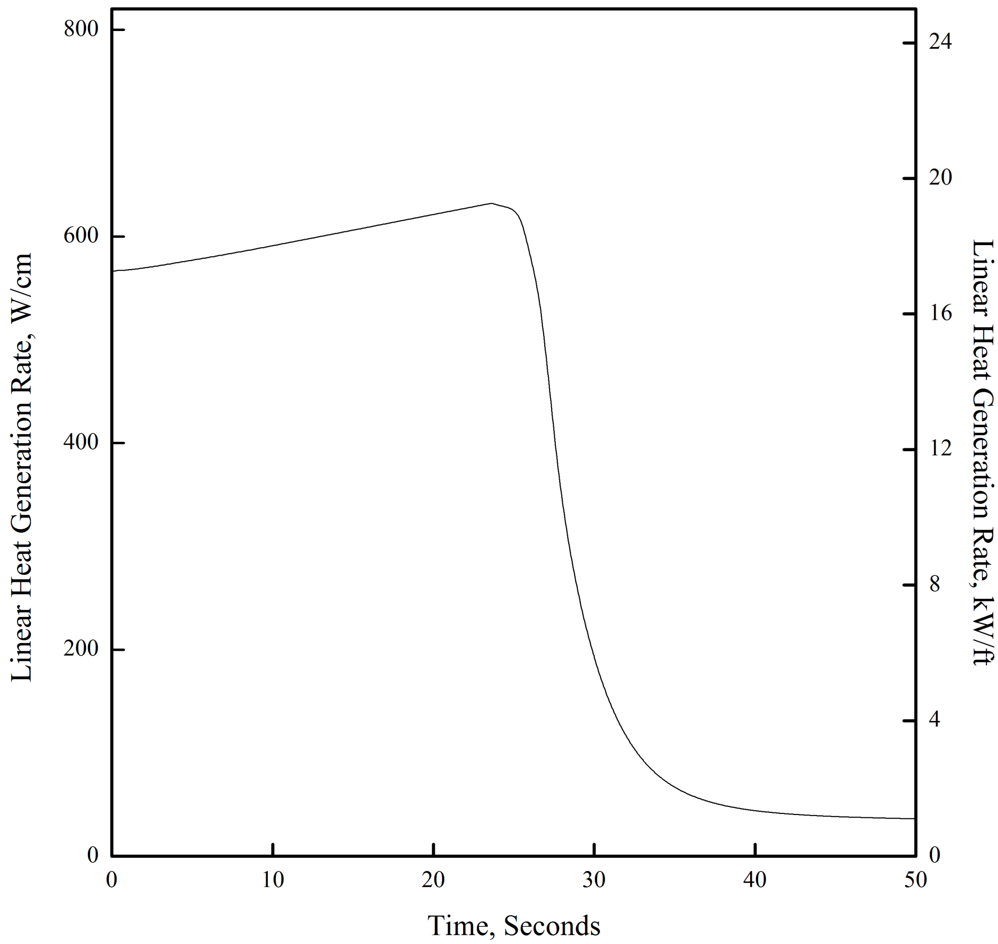

Figure 15.4.2-7 Uncontrolled CEA Withdrawal at Power ; Linear Heat Generation Rate vs. Time

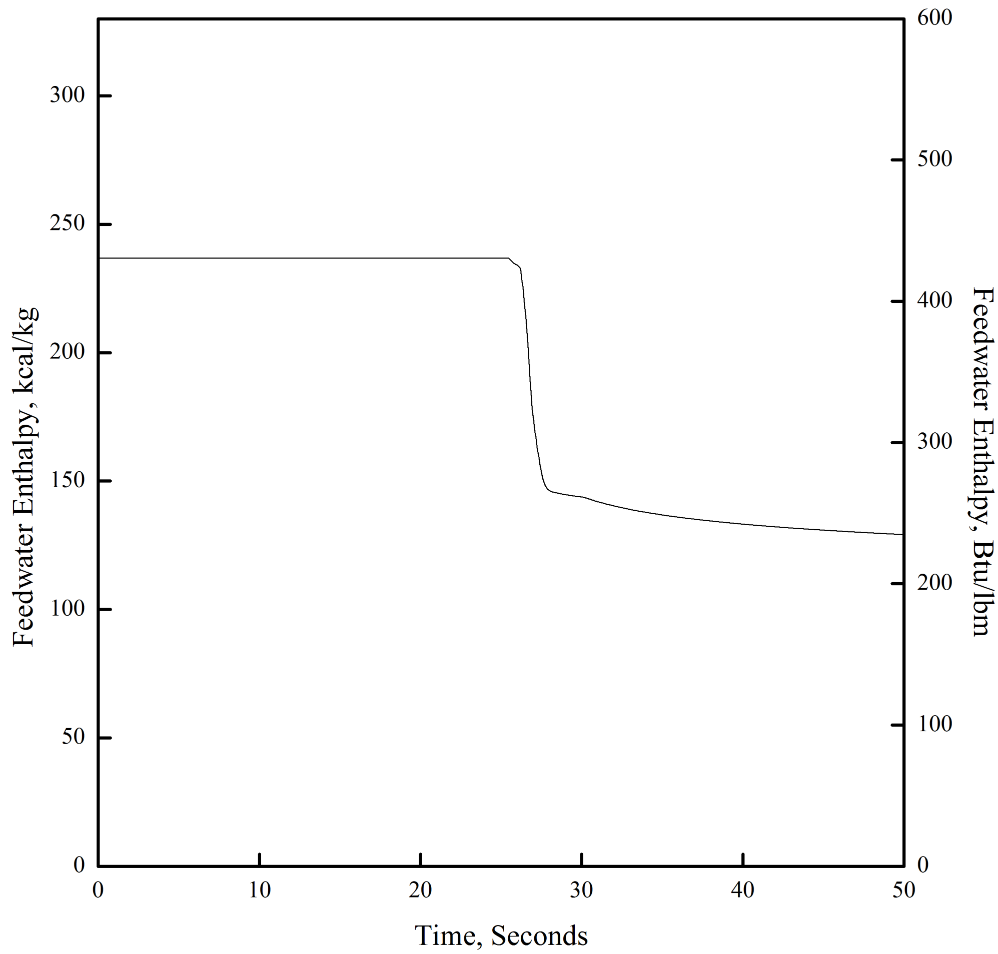

Figure 15.4.2-8 Uncontrolled CEA Withdrawal at Power ; Feedwater Enthalpy vs. Time

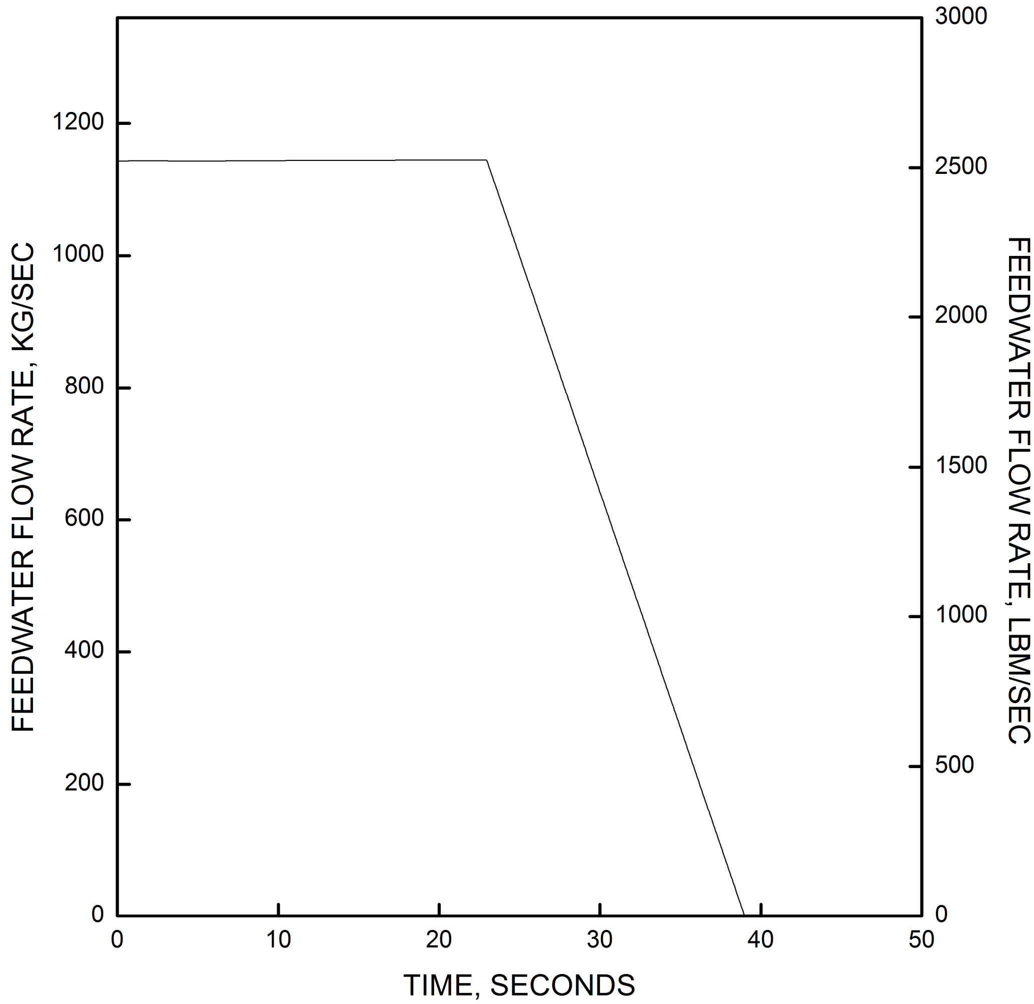

Figure 15.4.2-9 Uncontrolled CEA Withdrawal at Power ; Feedwater Flow Rate vs. Time

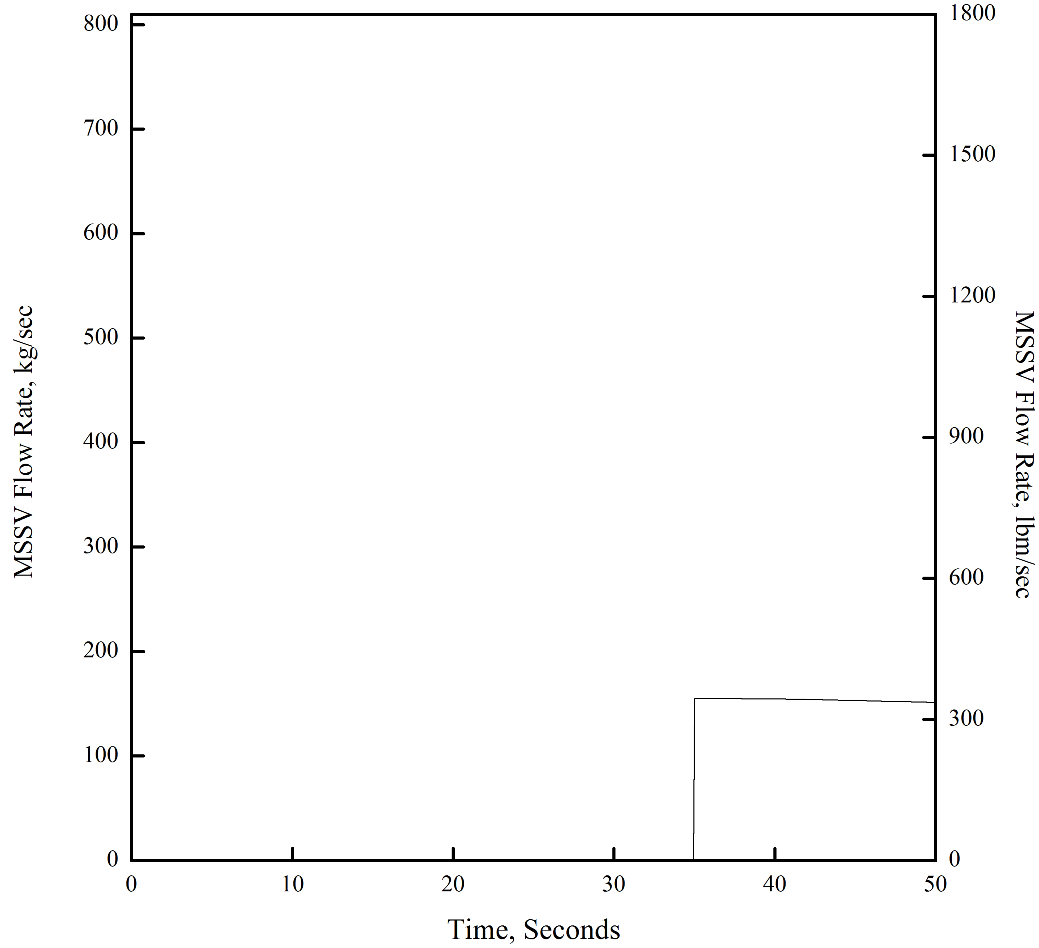

Figure 15.4.2-10 Uncontrolled CEA Withdrawal at Power ; MSSV Flow Rate vs. Time

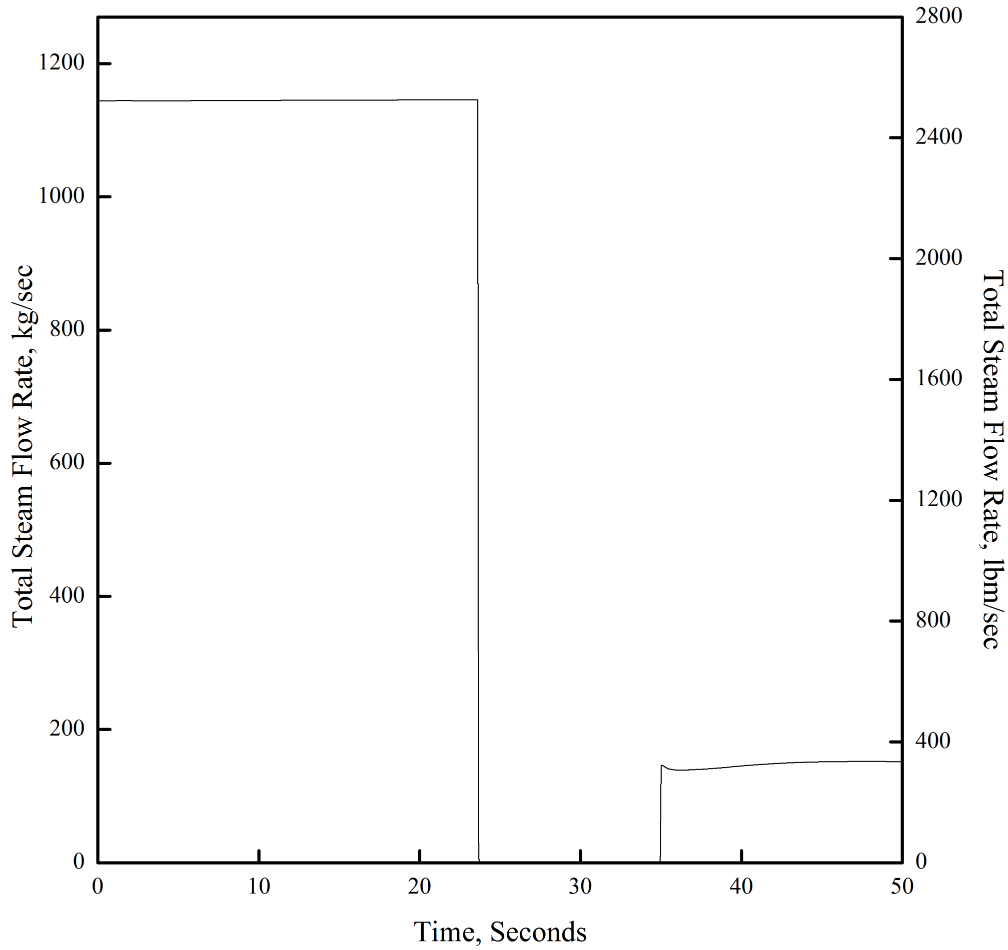

Figure 15.4.2-11 Uncontrolled CEA Withdrawal at Power ; Steam Flow Rate vs. Time

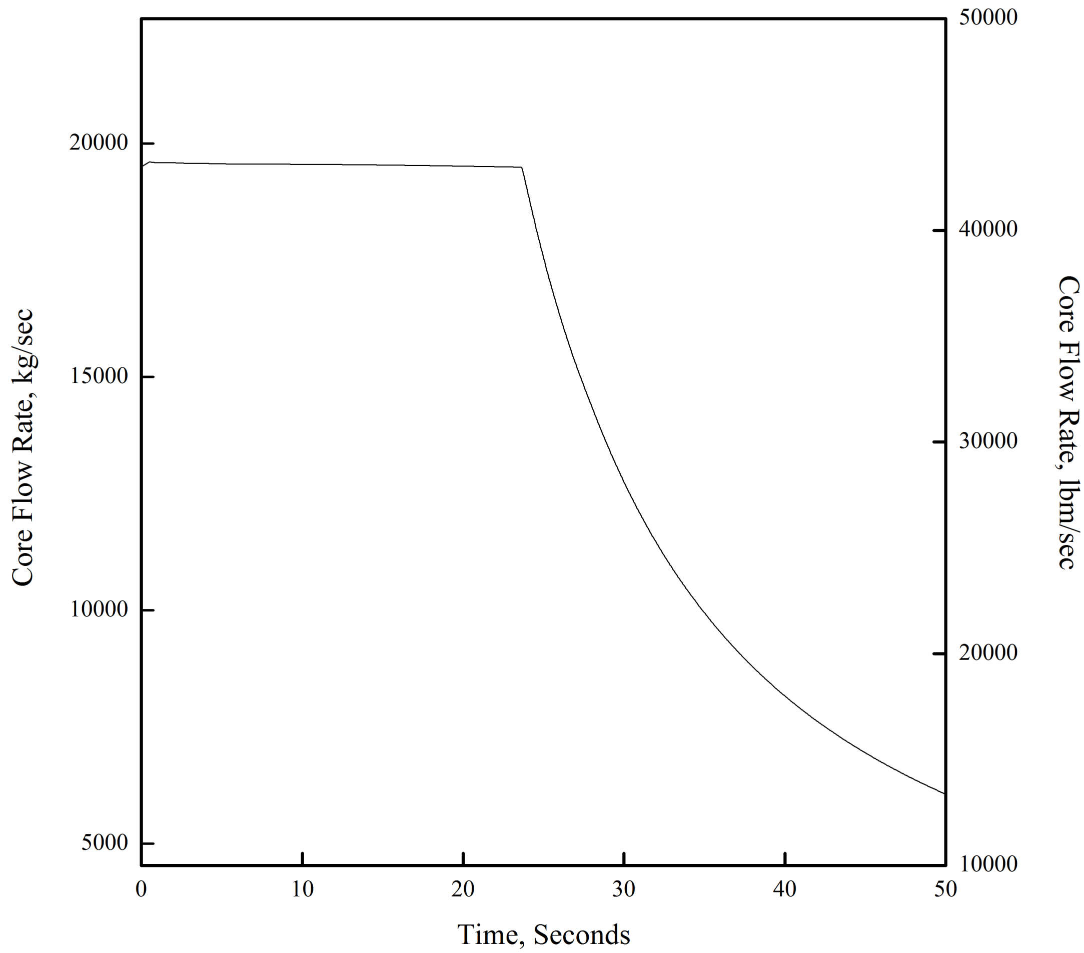

Figure 15.4.2-12 Uncontrolled CEA Withdrawal at Power ; Core Flow Rate vs. Time

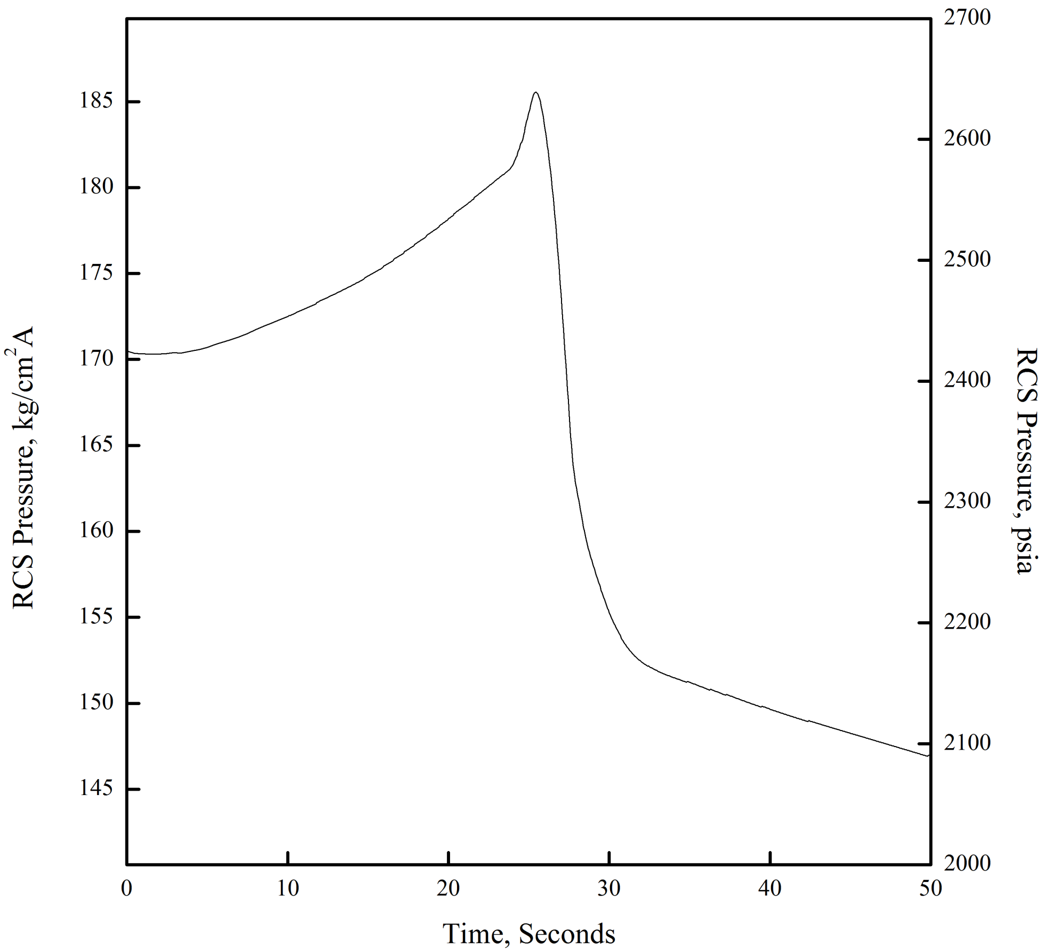

* The pressure difference between cold leg at the RCP discharge and the surge line is included.

Figure 15.4.2-13 Uncontrolled CEA Withdrawal at Power ; RCS Pressure vs. Time (Peak Pressure Case)

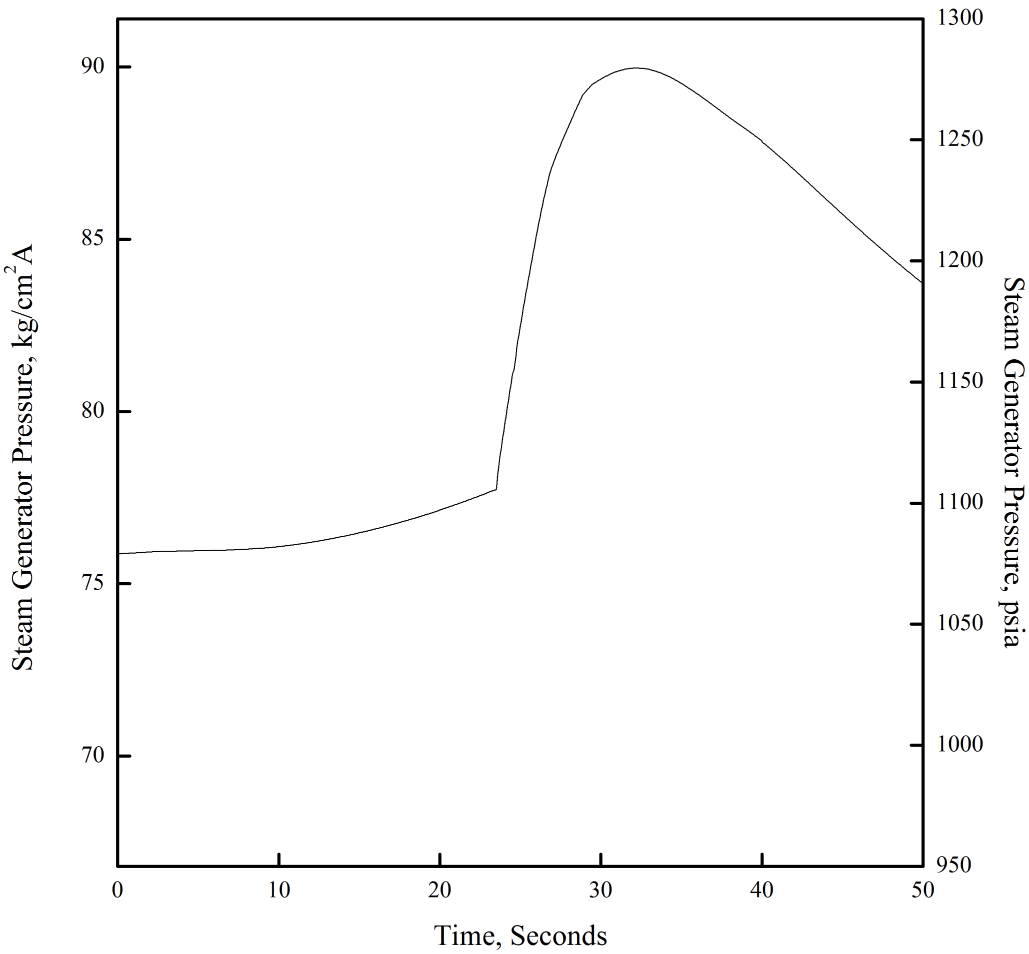

Figure 15.4.2-14 Uncontrolled CEA Withdrawal at Power ; Steam Generator Pressure vs. Time (Peak Pressure Case)

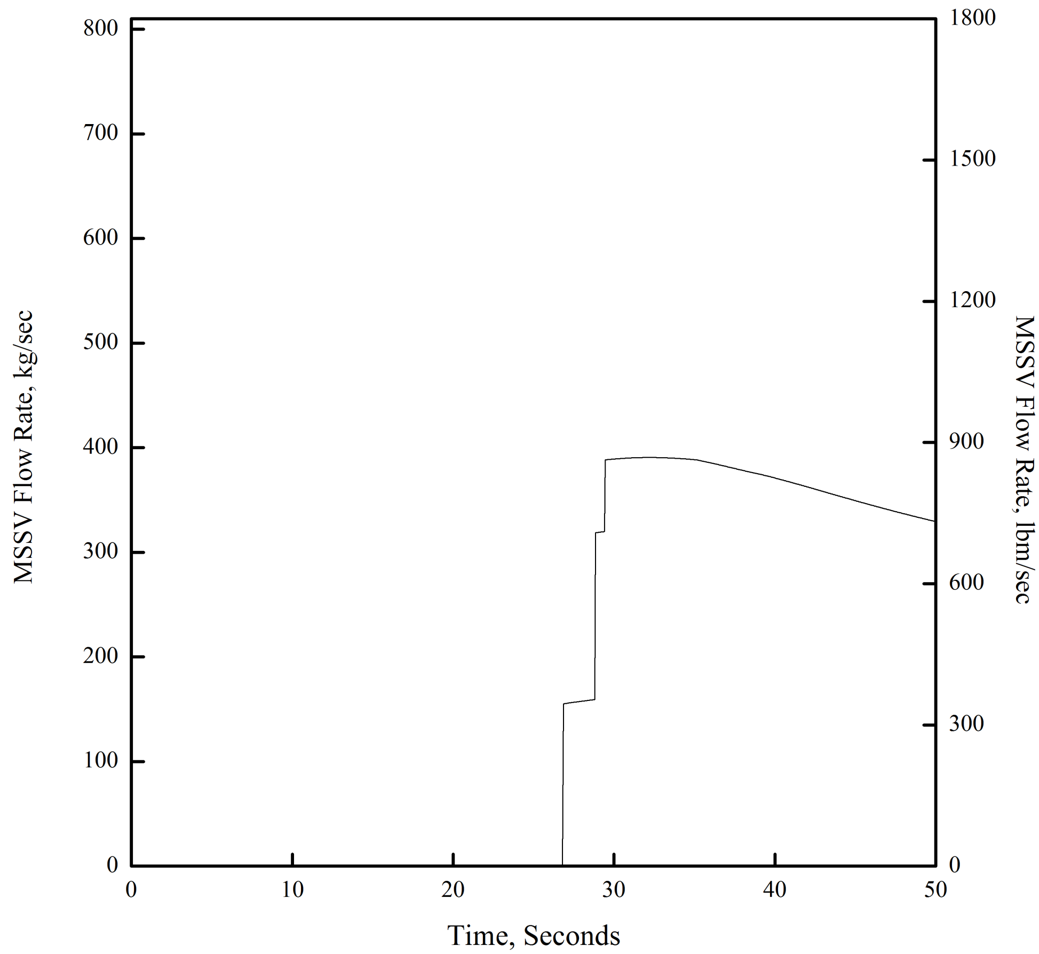

Figure 15.4.2-15 Uncontrolled CEA Withdrawal at Power; MSSV Flow Rate vs. Time (Peak Pressure Case)

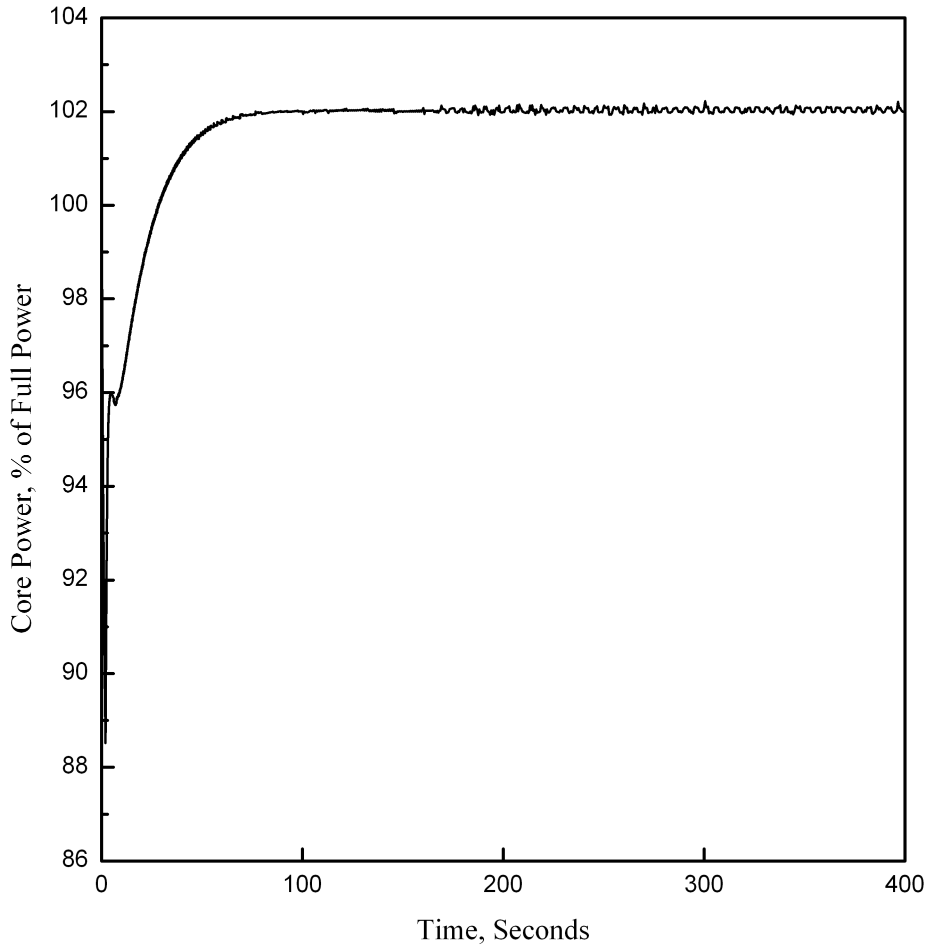

Figure 15.4.3-1 Single CEA Drop ; Core Power vs. Time

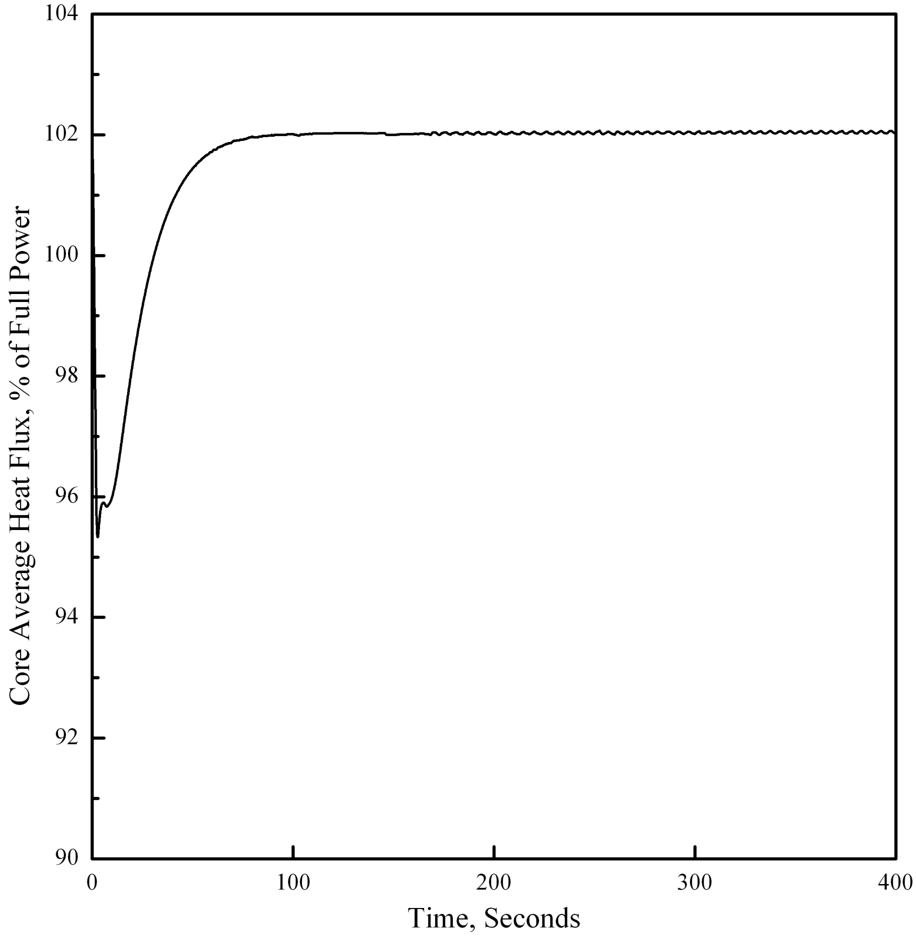

Figure 15.4.3-2 Single CEA Drop ; Core Average Heat Flux vs. Time

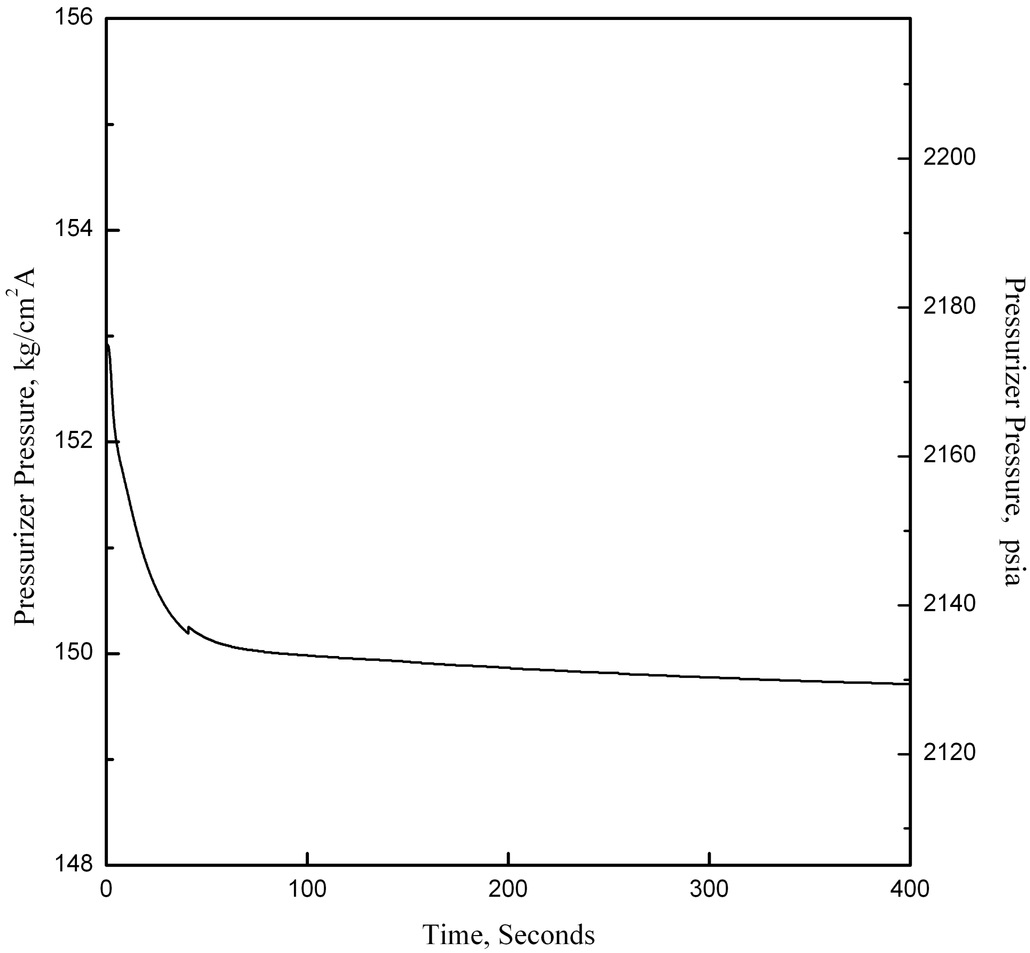

Figure 15.4.3-3 Single CEA Drop ; Pressurizer Pressure vs. Time

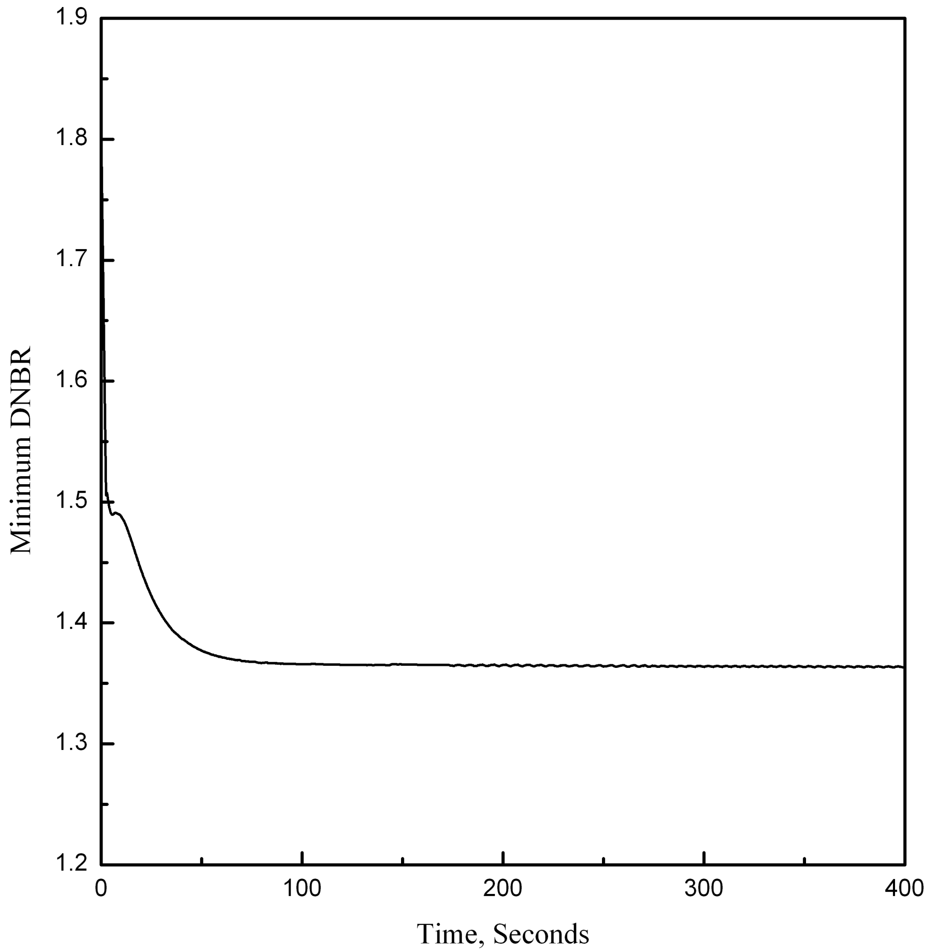

Figure 15.4.3-4 Single CEA Drop ; Minimum DNBR vs. Time

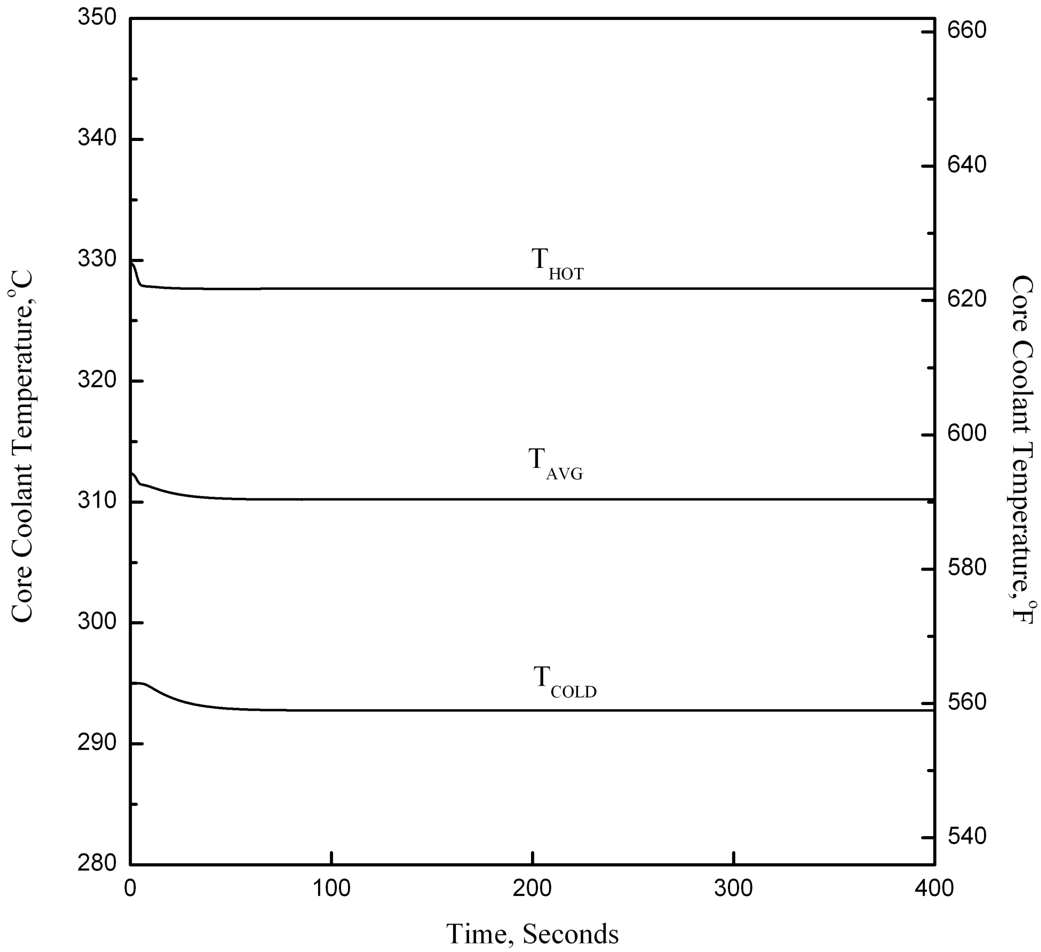

Figure 15.4.3-5 Single CEA Drop ; Core Coolant Temperatures vs. Time

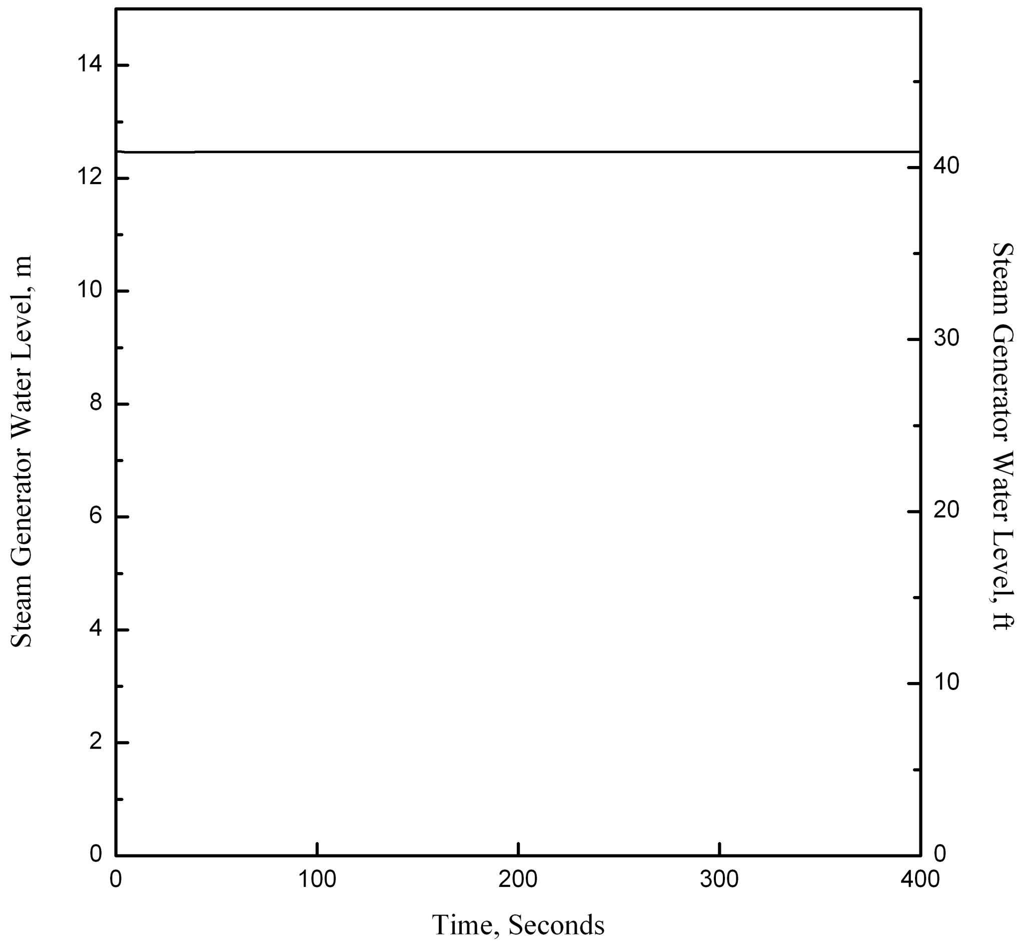

Figure 15.4.3-6 Single CEA Drop ; Steam Generator Water Level vs. Time

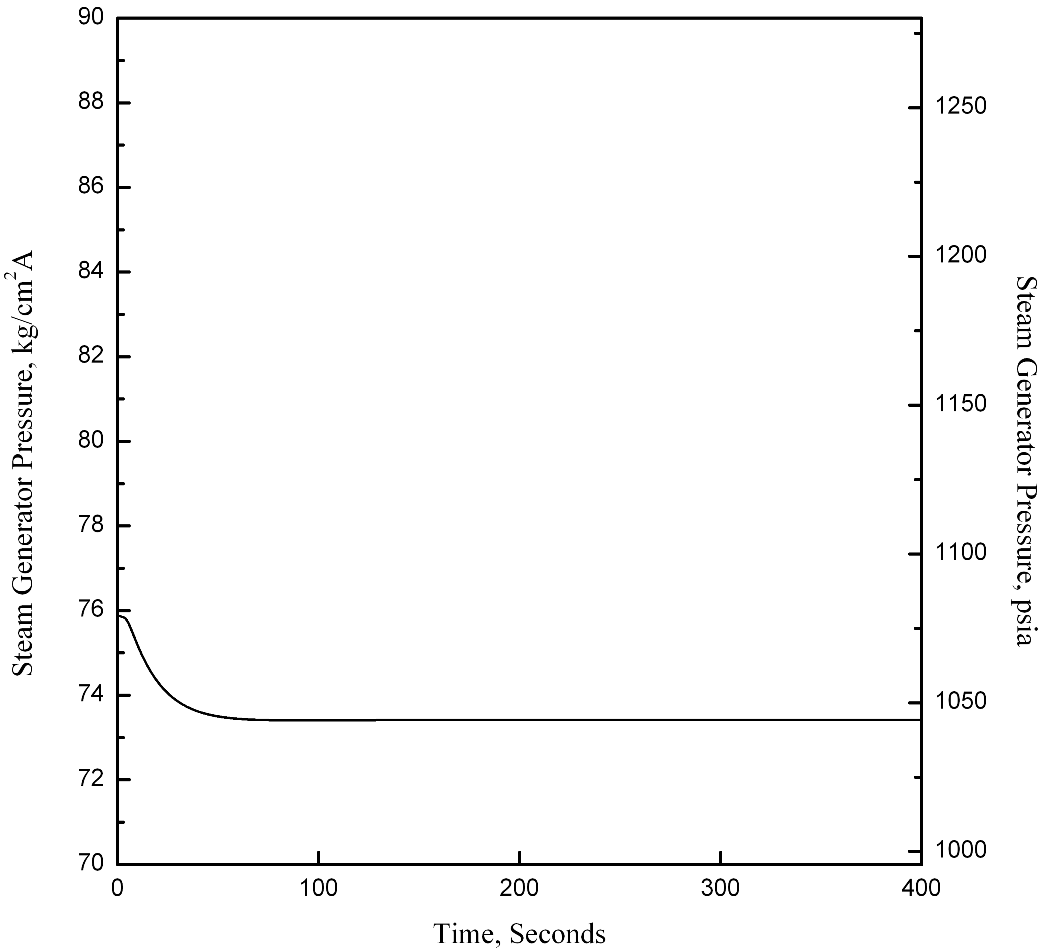

Figure 15.4.3-7   Single CEA Drop ; Steam Generator Pressure vs. Time

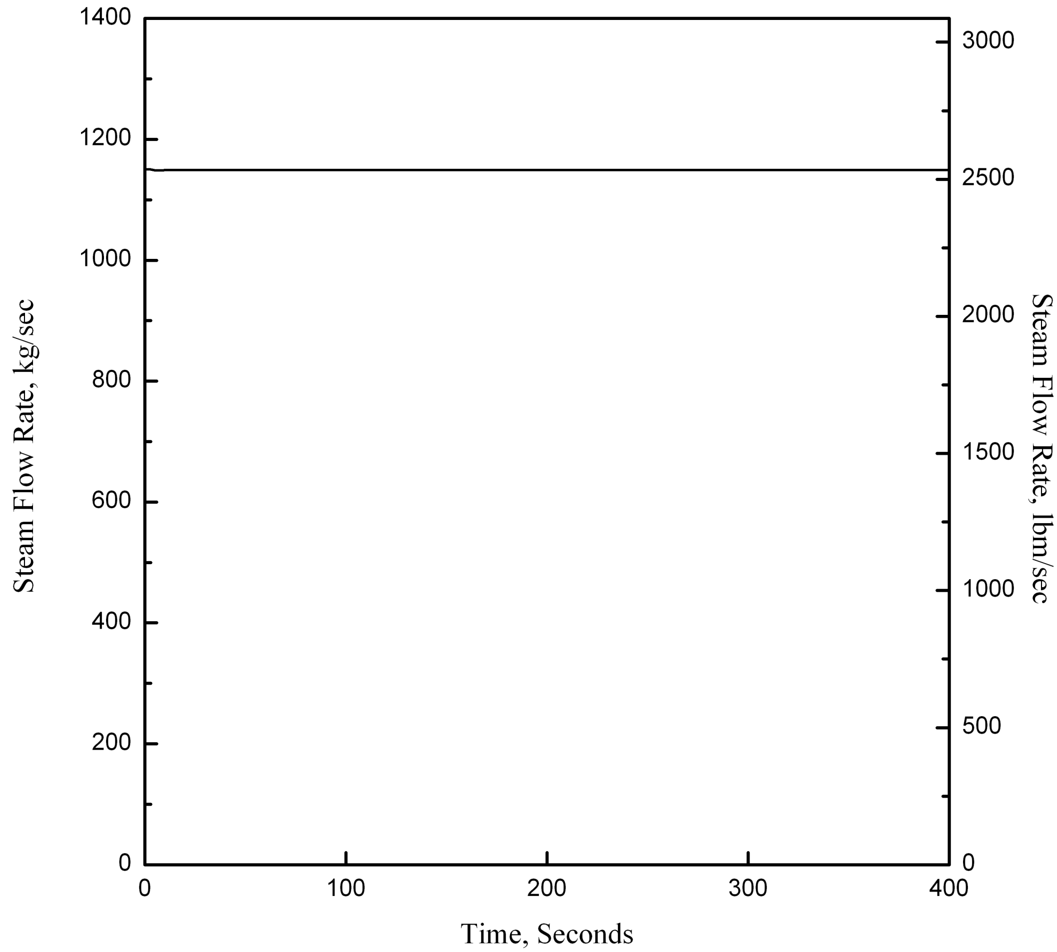

Figure 15.4.3-8 Single CEA Drop ; Steam Flow Rate per Steam Generator vs. Time

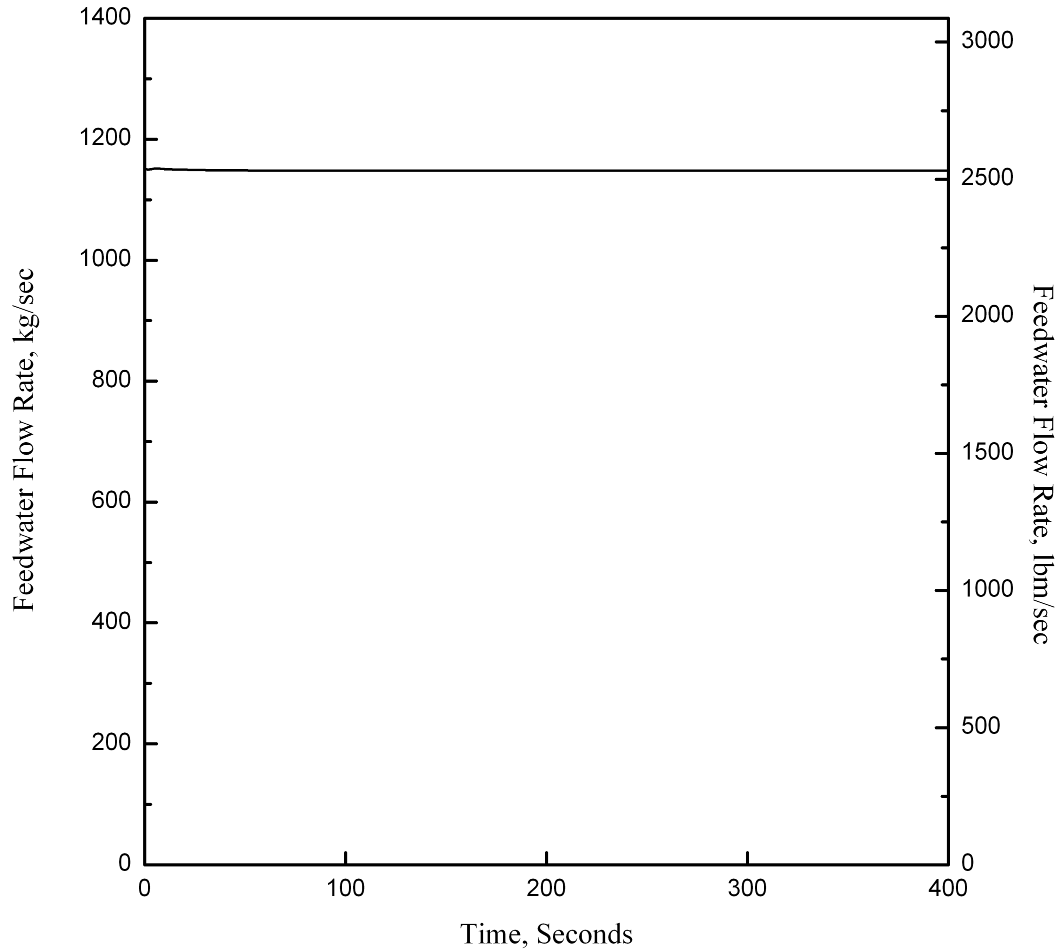

Figure 15.4.3-9 Single CEA Drop ; Feedwater Flow Rate per Steam Generator vs. Time

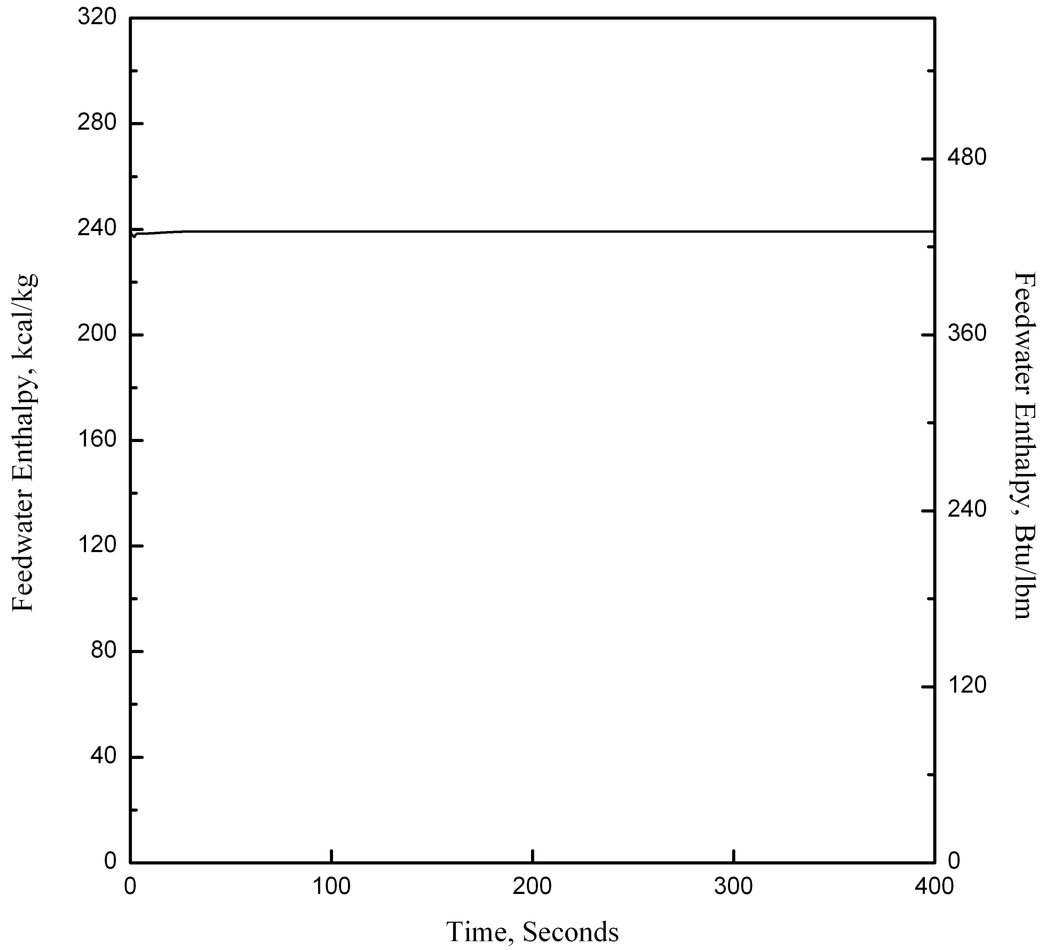

Figure 15.4.3-10 Single CEA Drop ; Feedwater Enthalpy vs. Time

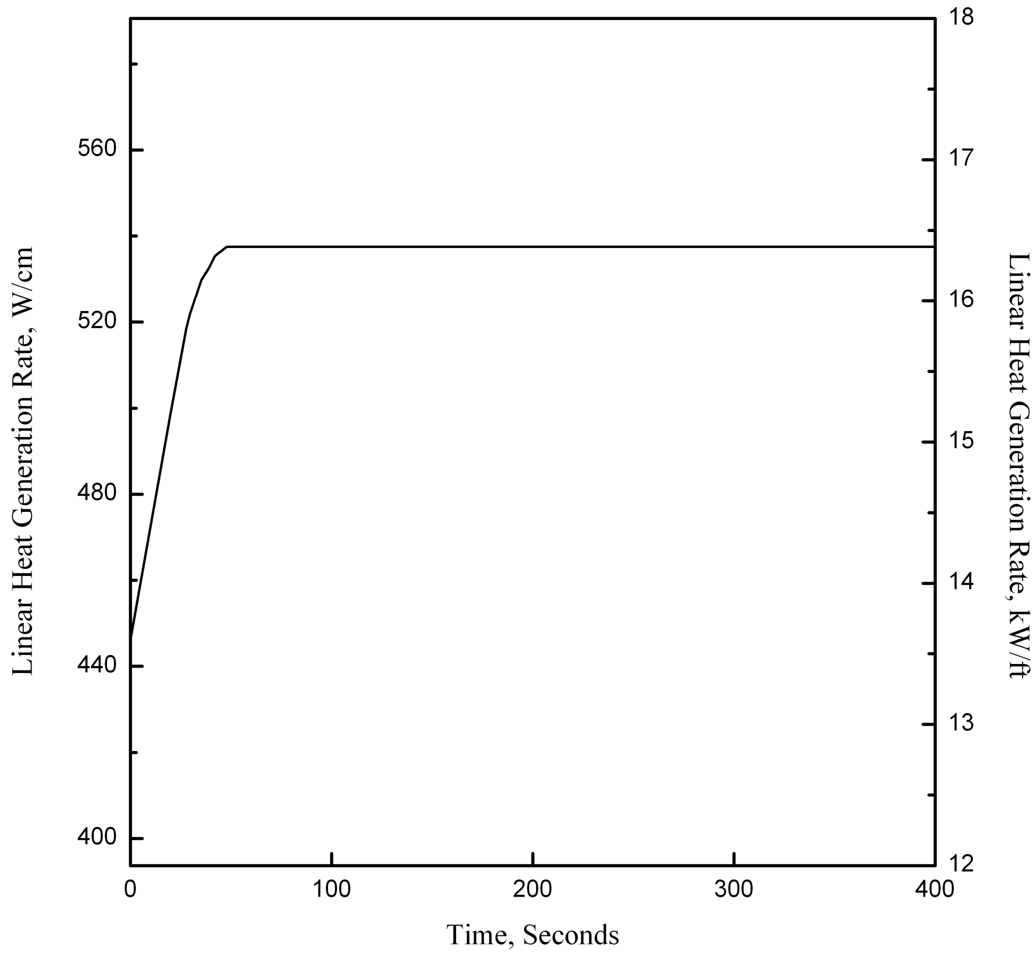

Figure 15.4.3-11 Single CEA Drop ; Linear Heat Generation Rate vs. Time

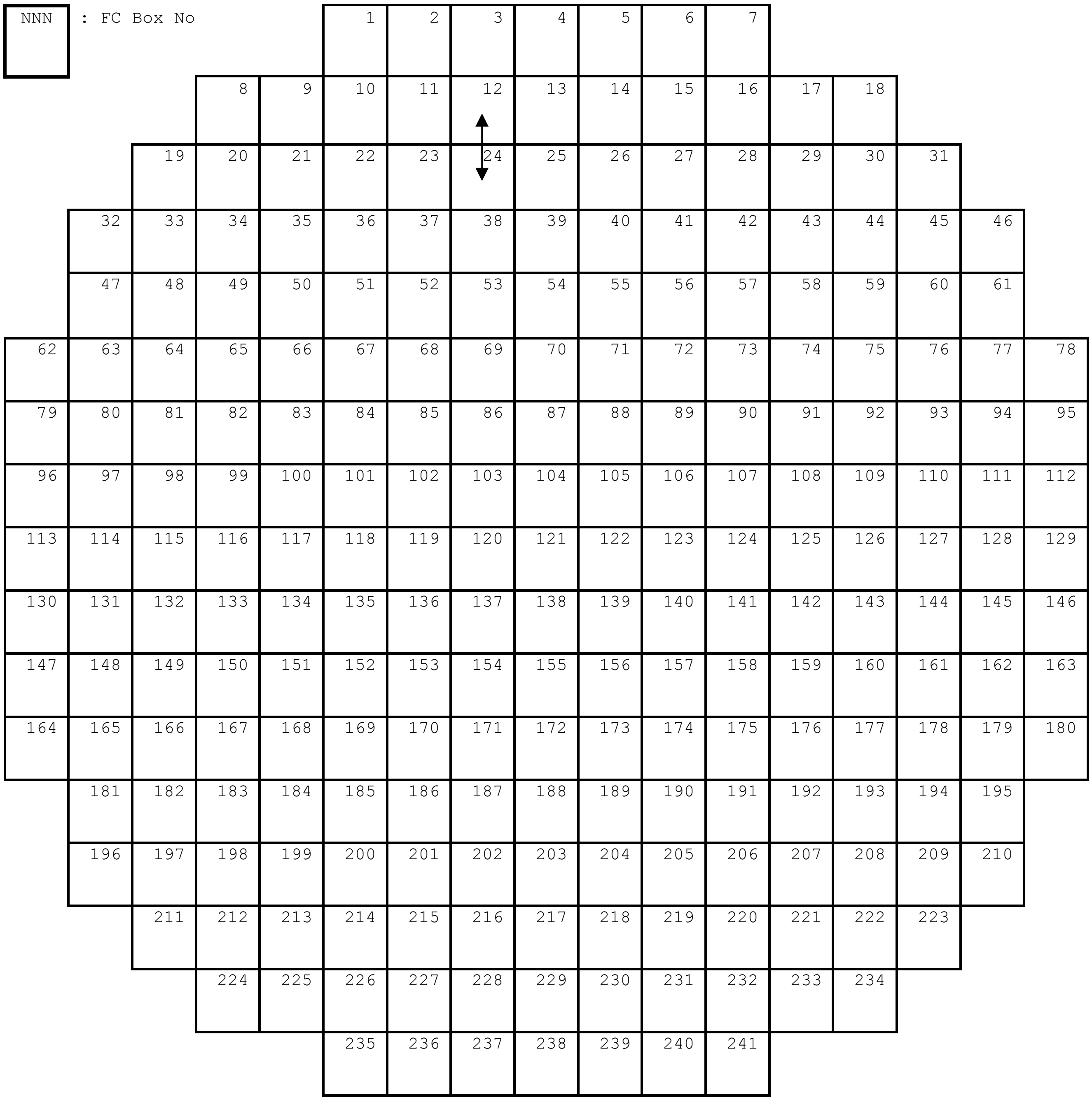

Figure 15.4.7-1 Location of the Worst Case Misloading

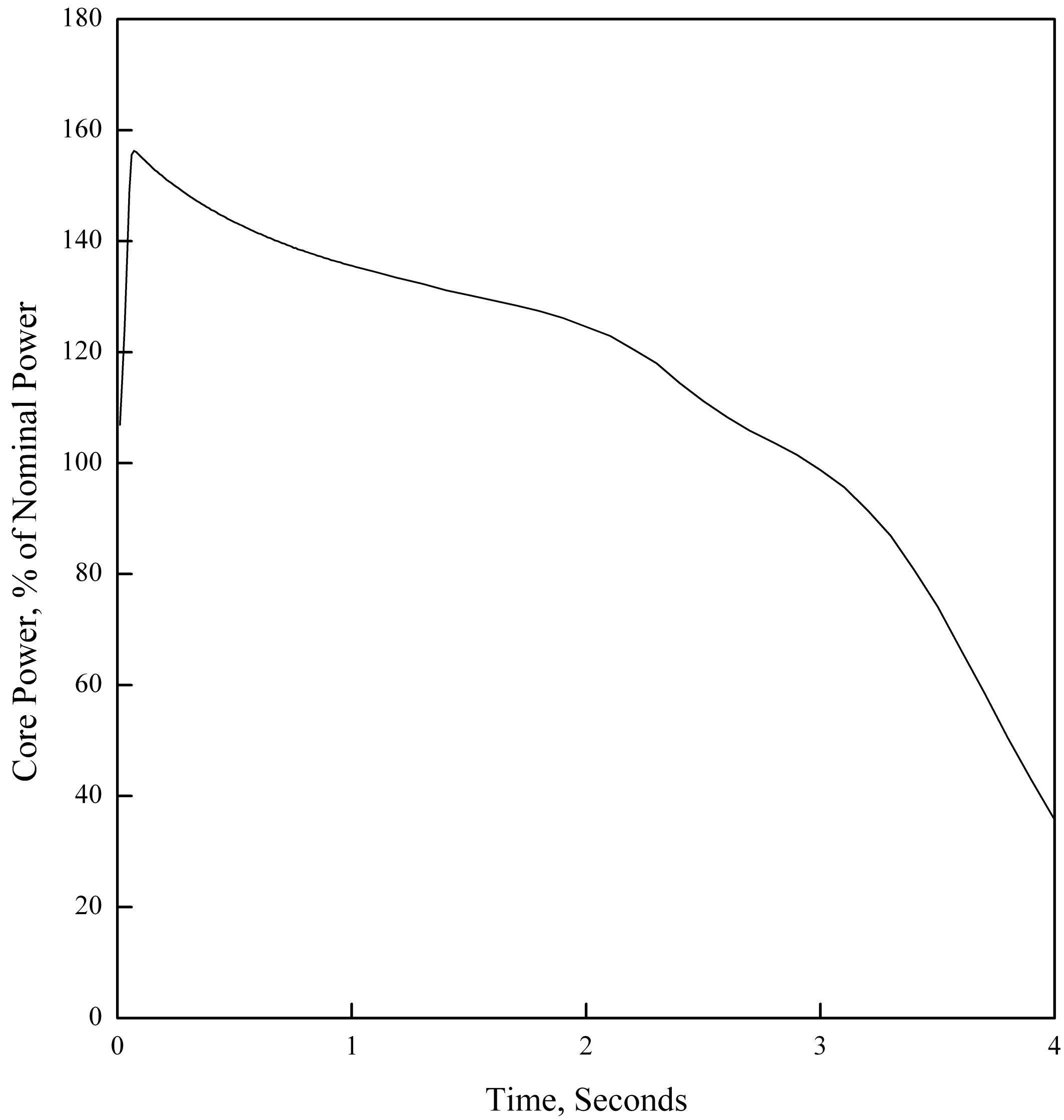

Figure 15.4.8-1 CEA Ejection ; Core Power vs. Time (HFP)

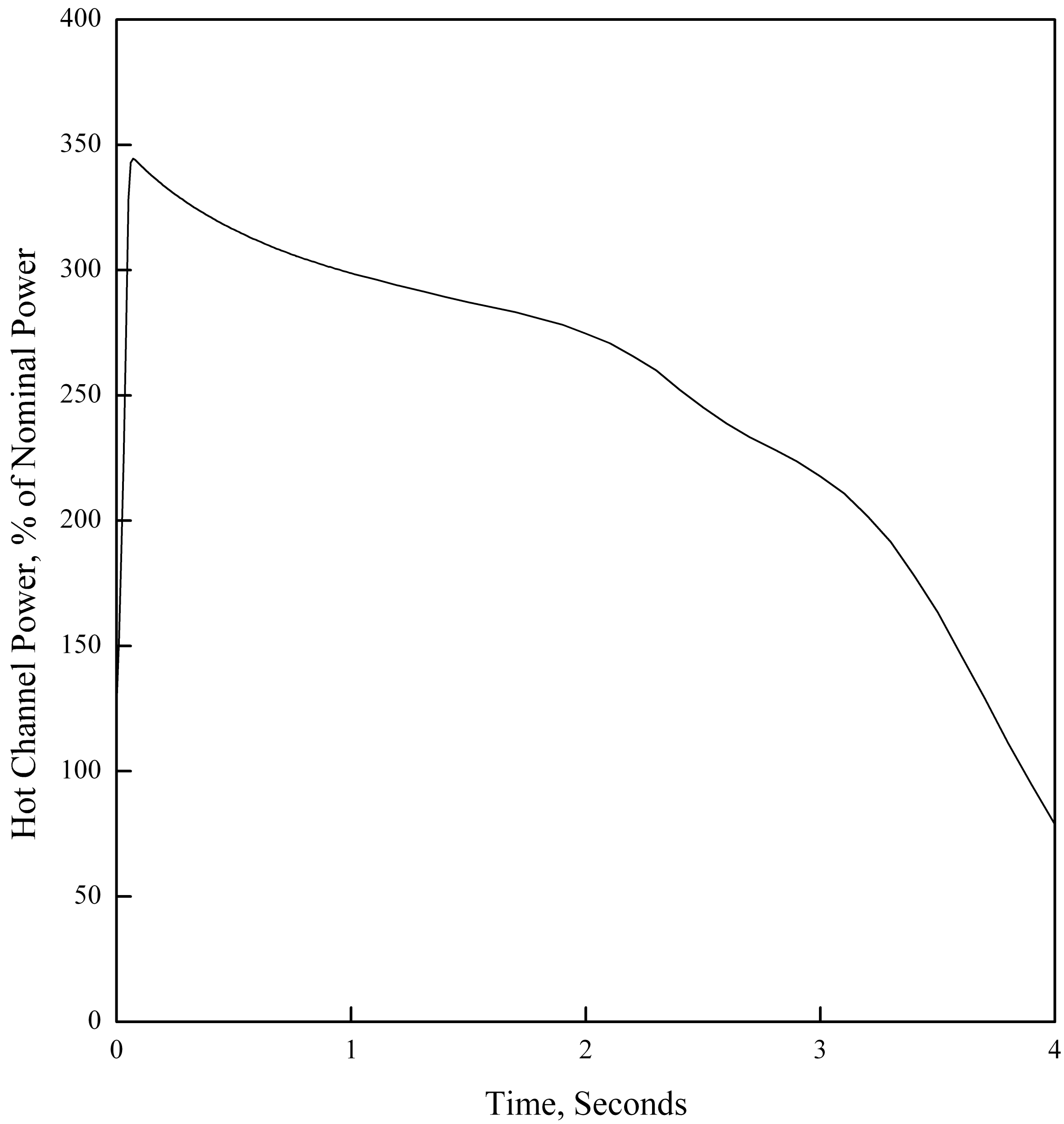

Figure 15.4.8-2 CEA Ejection ; Hot Channel Power vs. Time (HFP)

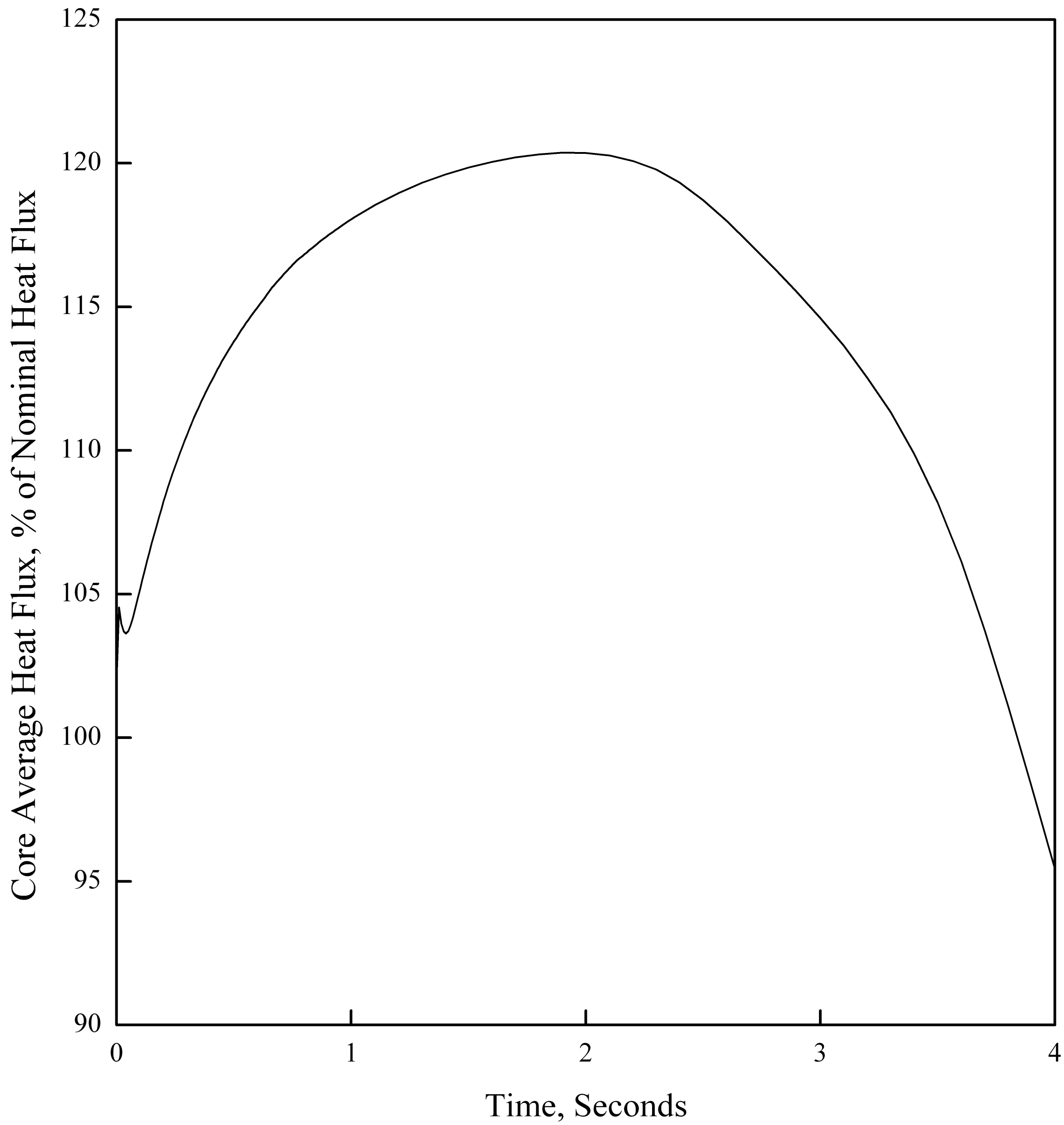

Figure 15.4.8-3 CEA Ejection ; Core Average Heat Flux vs. Time (HFP)

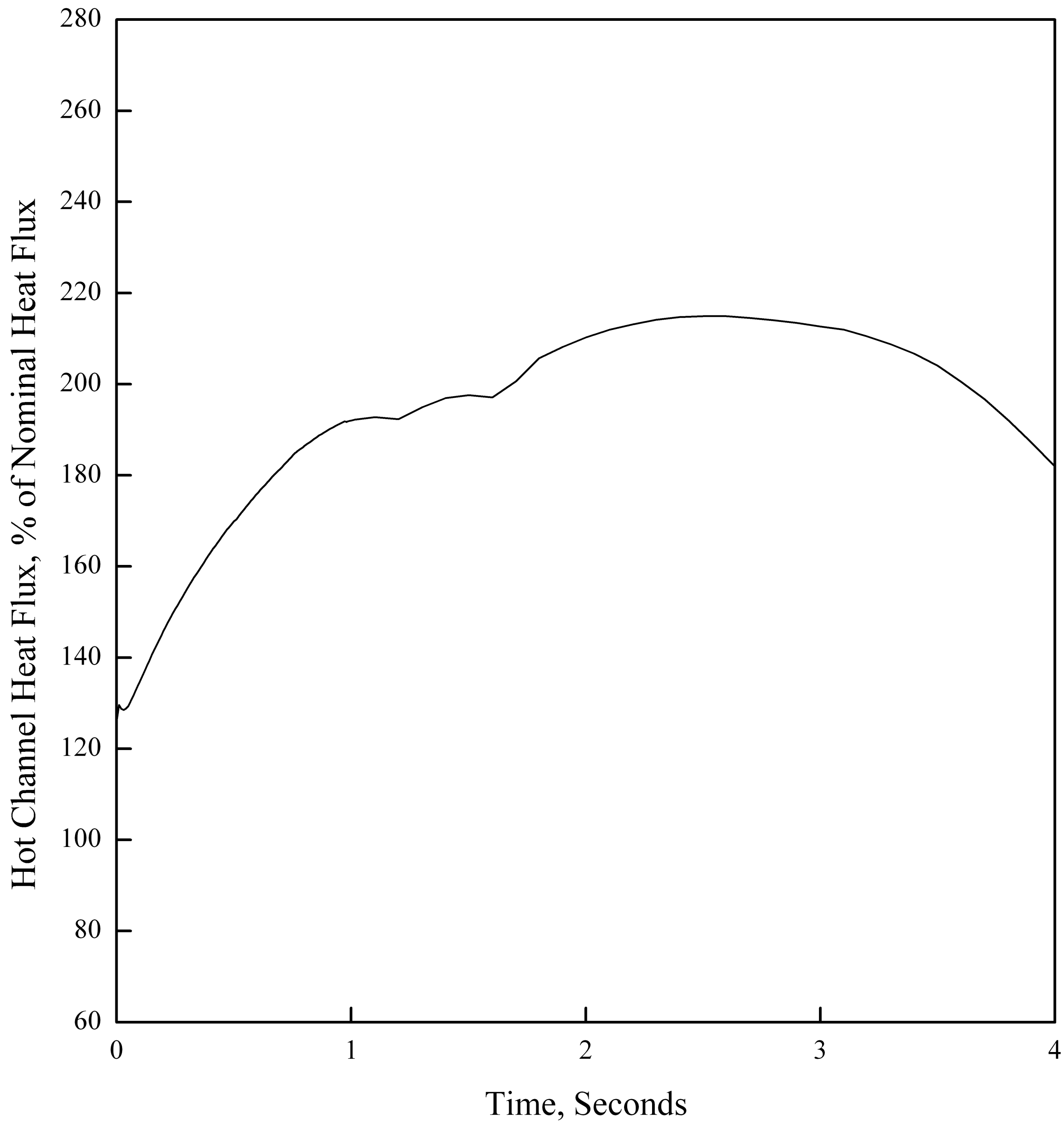

Figure 15.4.8-4 CEA Ejection ; Hot Channel Heat Flux vs. Time (HFP)

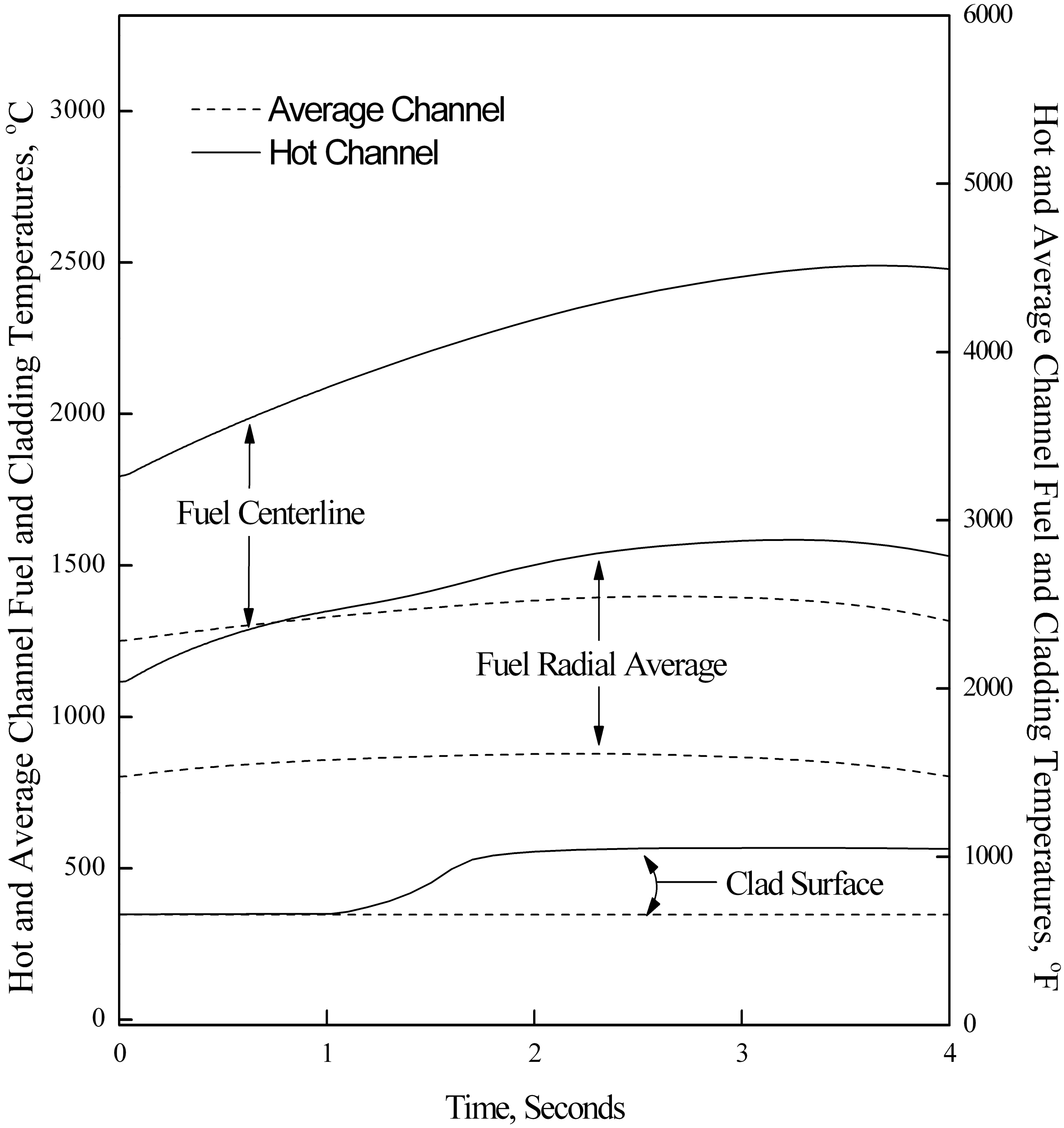

Figure 15.4.8-5 CEA Ejection ; Hot and Average Channel Fuel and Cladding Temperatures vs. Time (HFP)

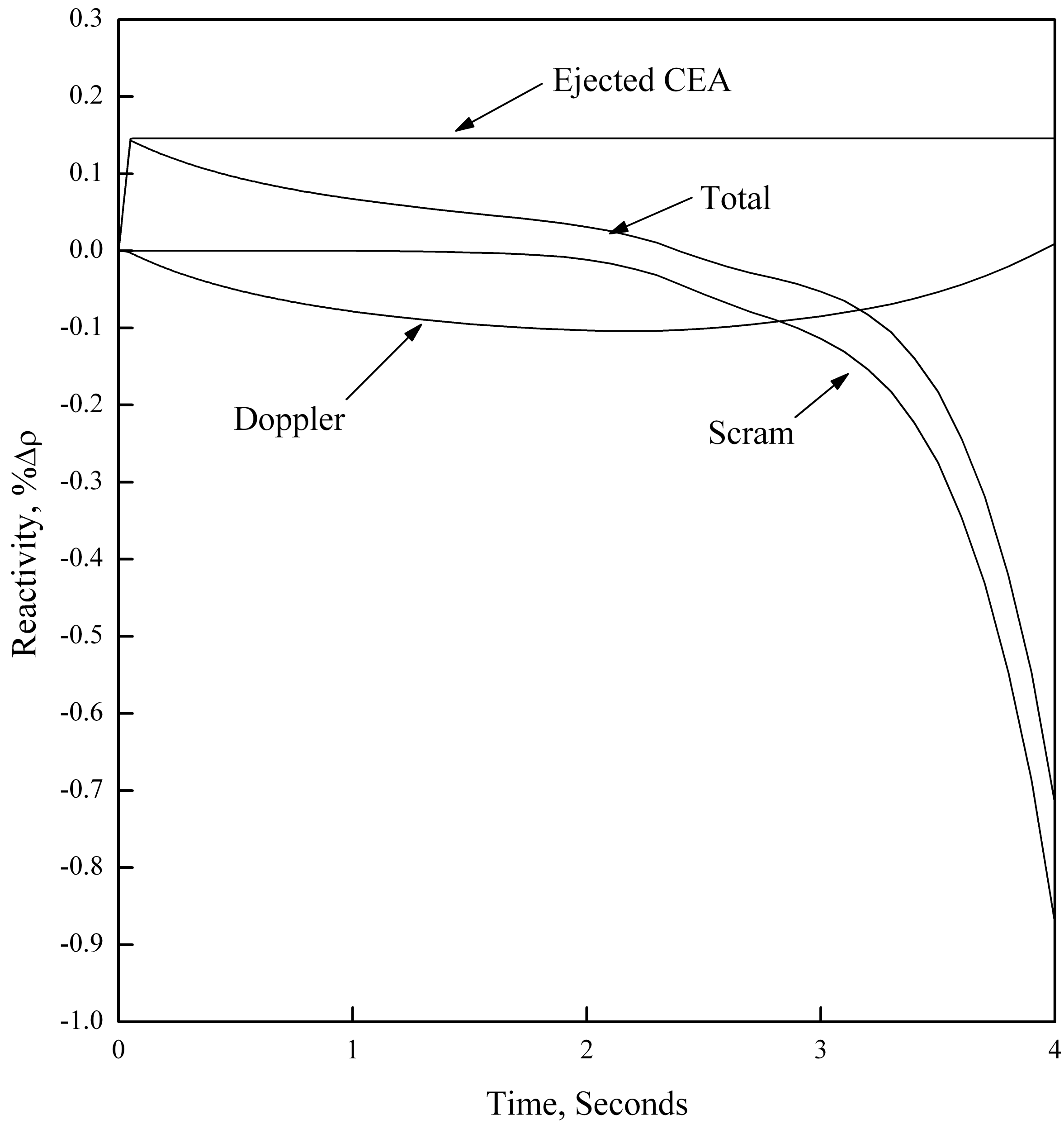

Figure 15.4.8-6   CEA Ejection ; Reactivity vs. Time (HFP)

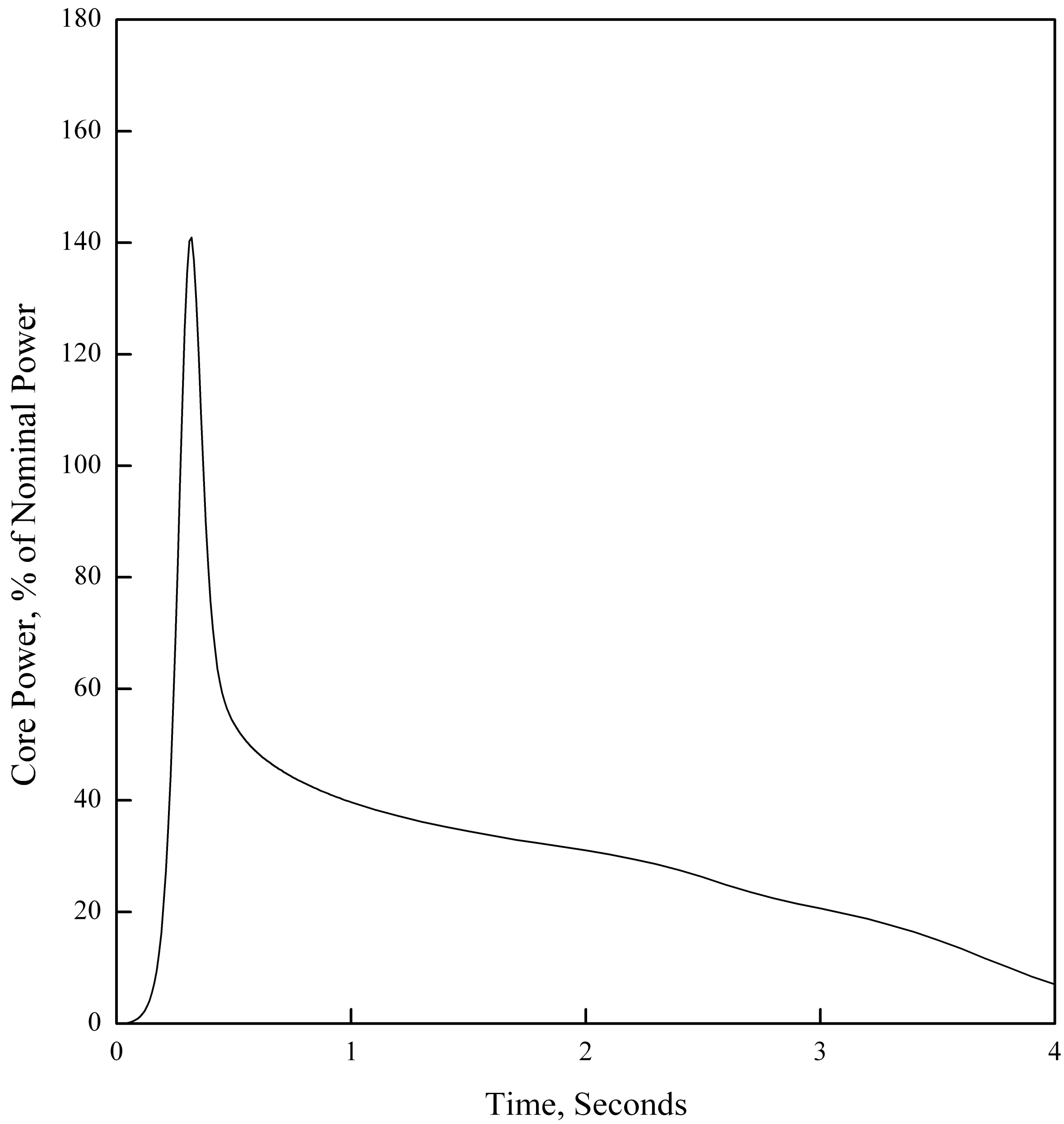

Figure 15.4.8-7 CEA Ejection ; Core Power vs. Time (HZP)

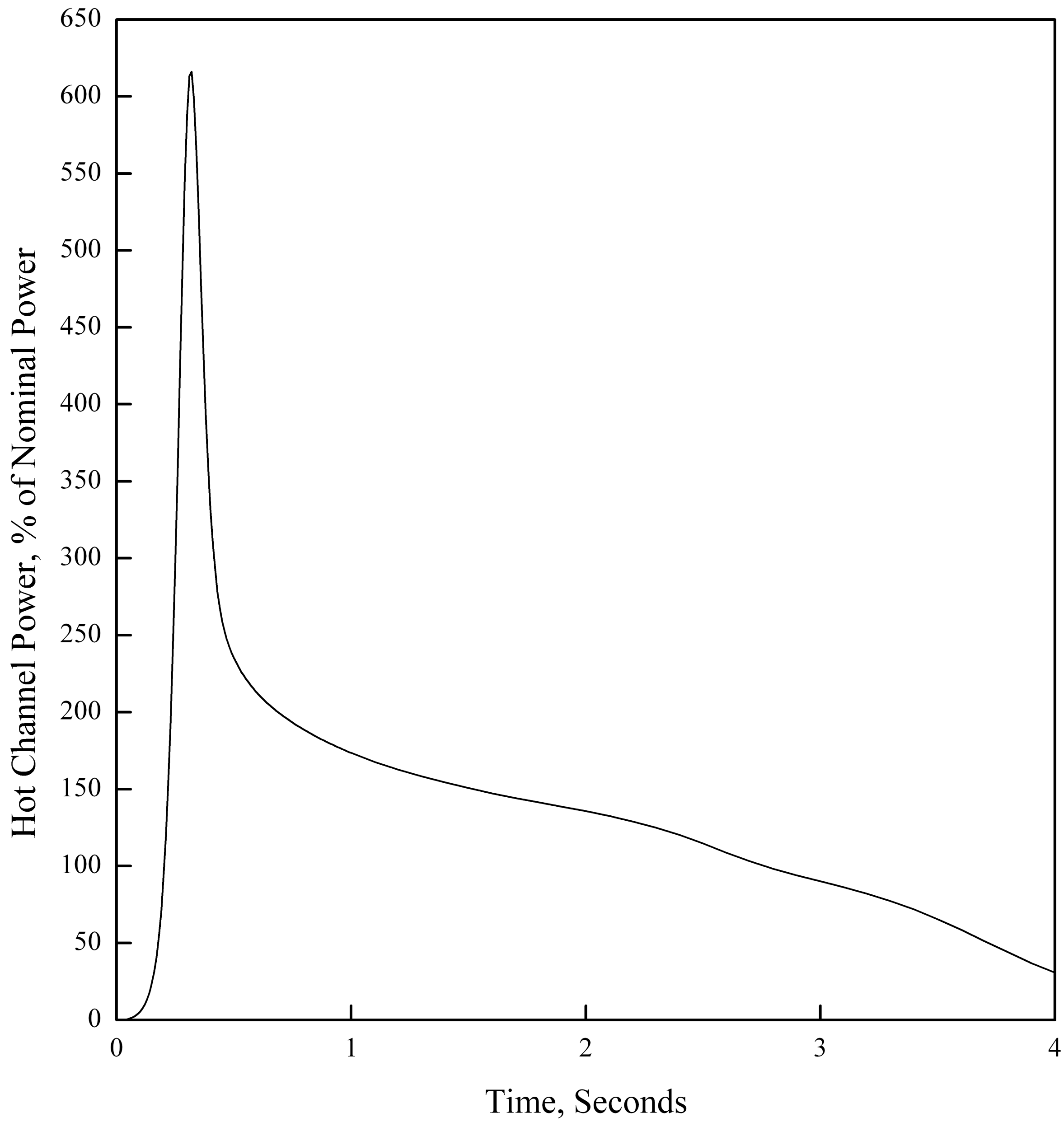

Figure 15.4.8-8 CEA Ejection ; Hot Channel Power vs. Time (HZP)

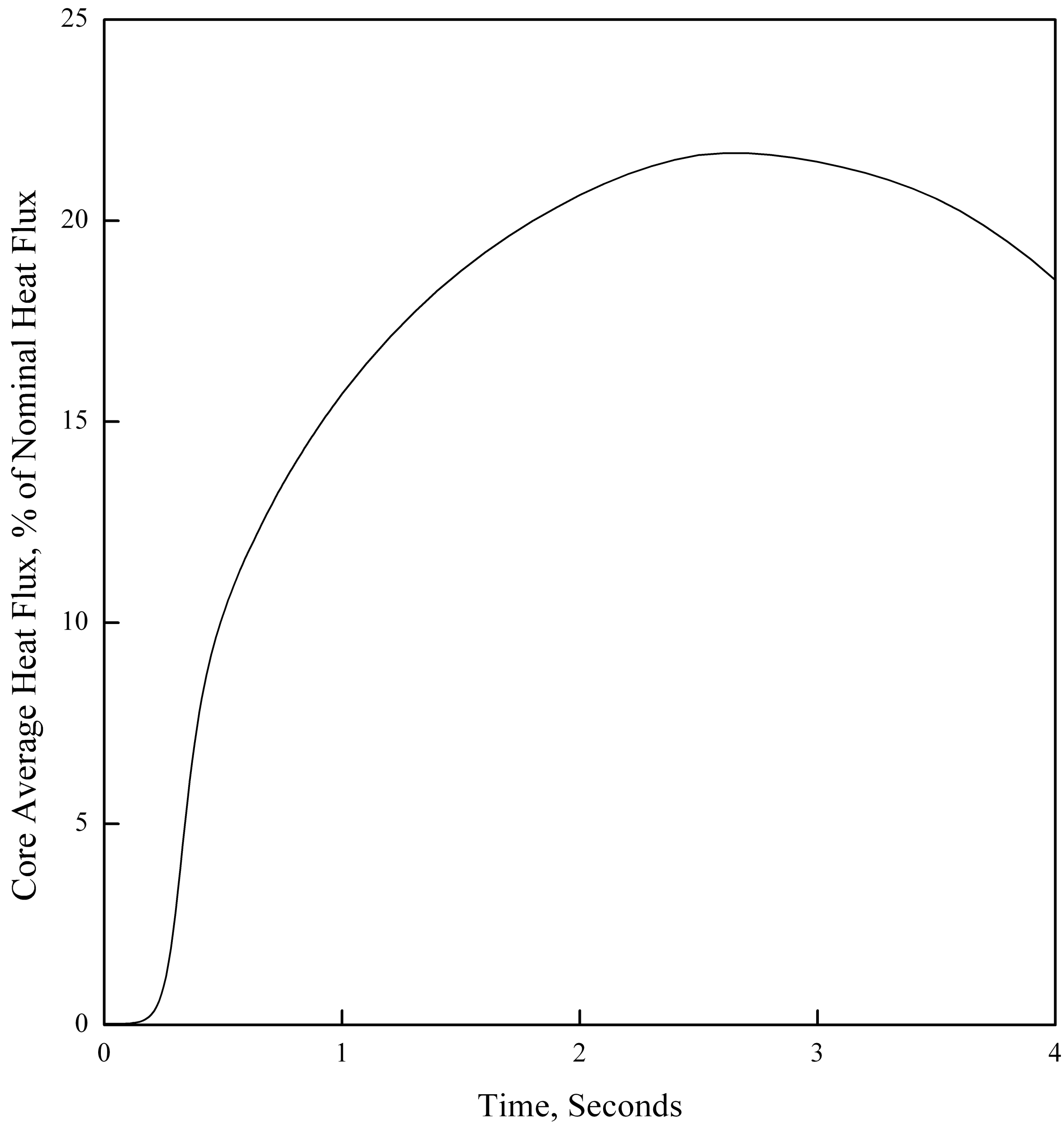

Figure 15.4.8-9 CEA Ejection ; Core Average Heat Flux vs. Time (HZP)

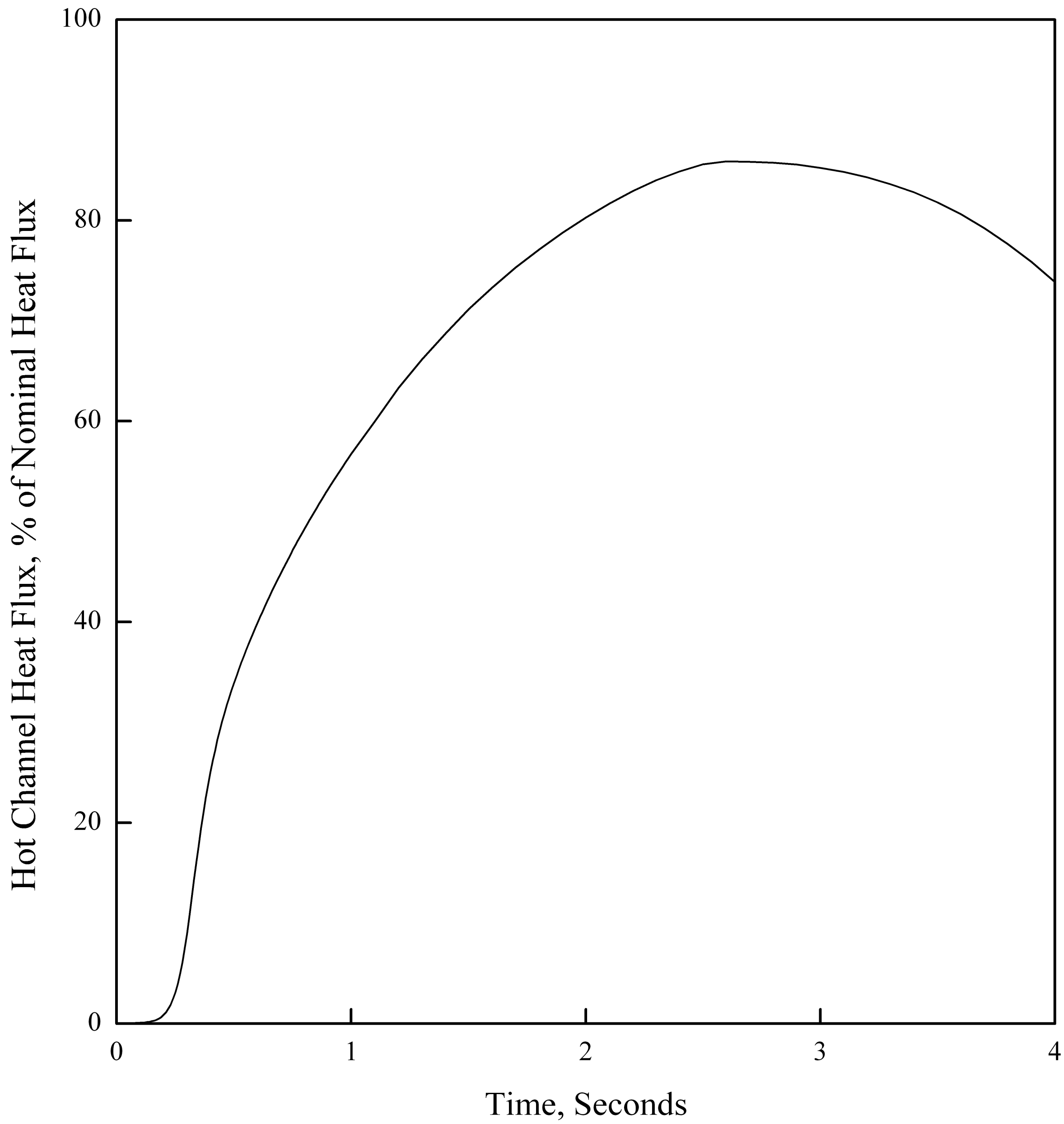

Figure 15.4.8-10 CEA Ejection ; Hot Channel Heat Flux vs. Time (HZP)

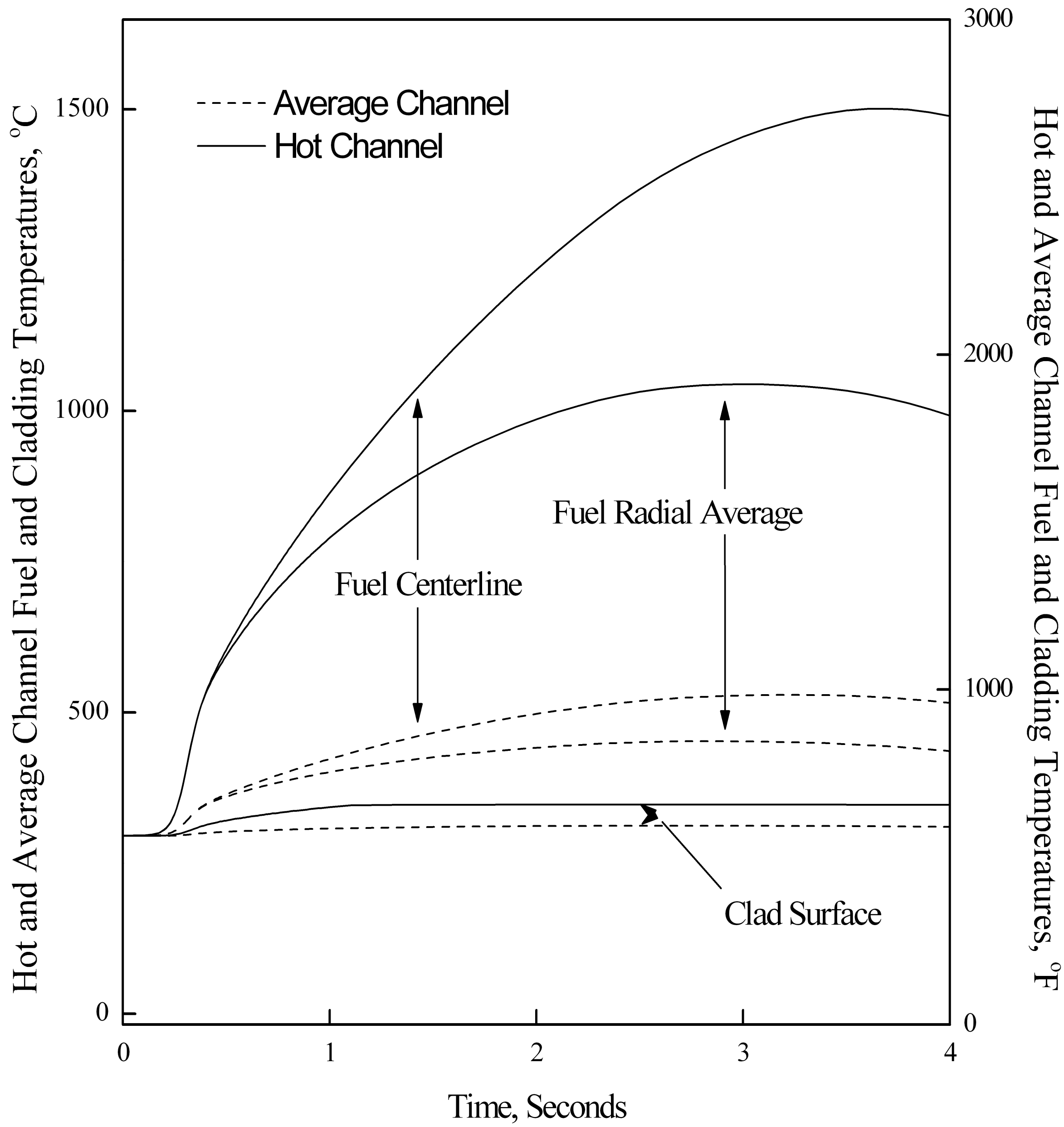

Figure 15.4.8-11 CEA Ejection ; Hot and Average Channel Fuel and Cladding Temperatures vs. Time (HZP)

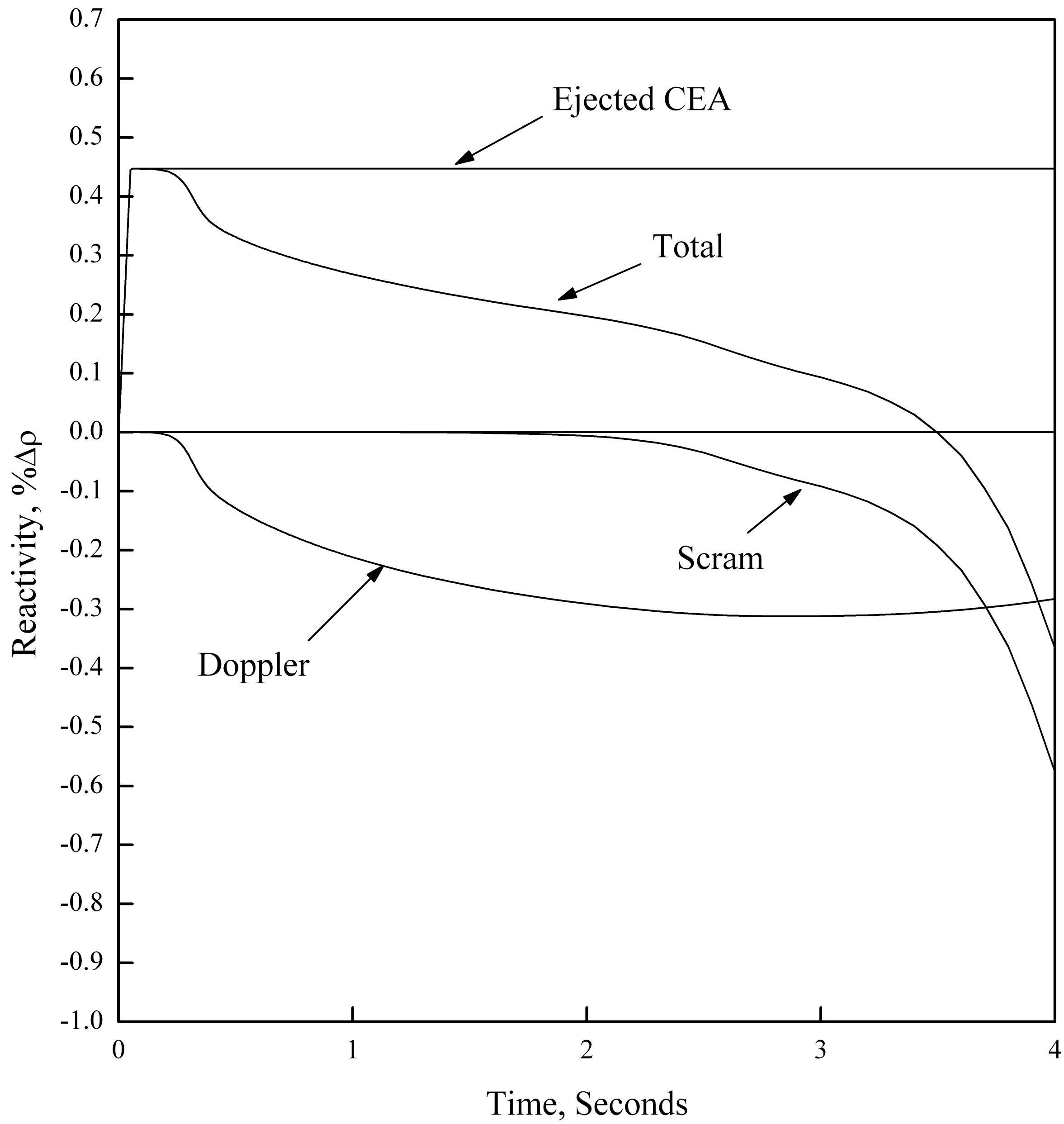

Figure 15.4.8-12   CEA Ejection ; Reactivity vs. Time (HZP)

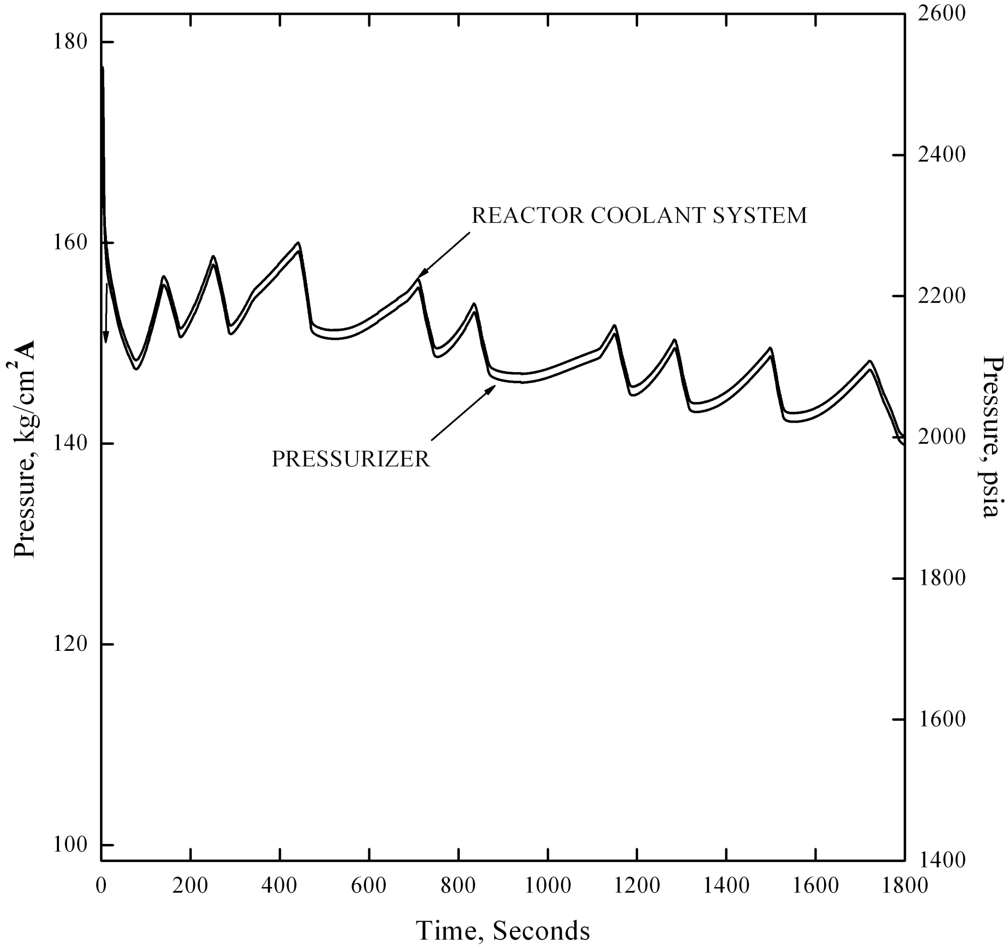

* The pressure difference between cold leg at the RCP discharge and the surge line is not included.

Figure 15.4.8-13 CEA Ejection ; RCS and Pressurizer Pressures vs. Time

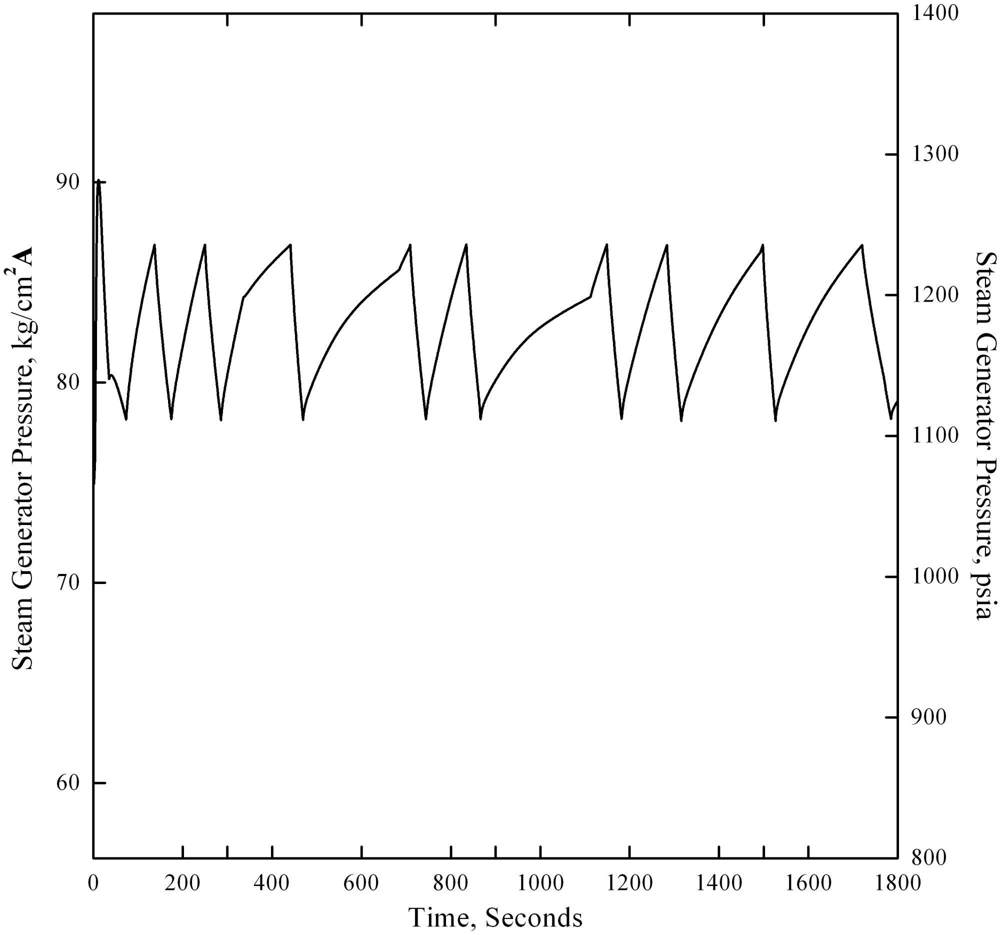

Figure 15.4.8-14 CEA Ejection ; Steam Generator Pressure vs. Time

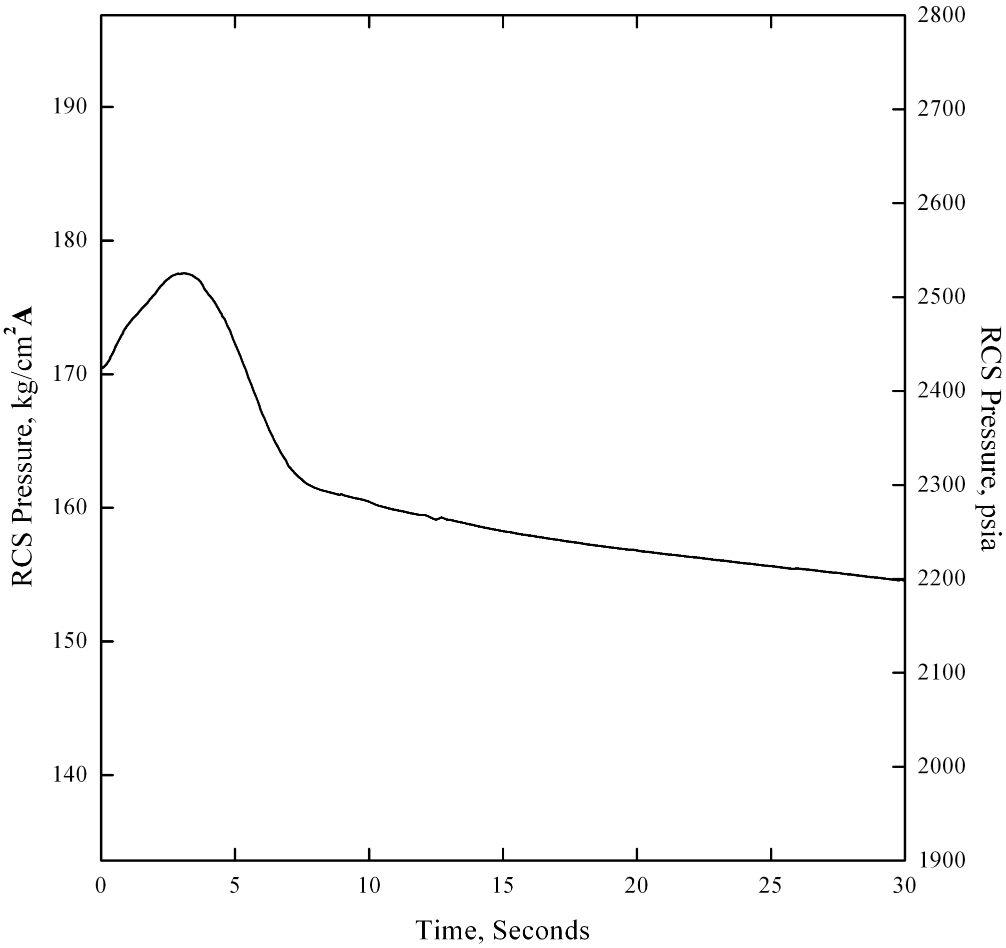

*The pressure difference between cold leg at the RCP discharge and the surge line is included.

Figure 15.4.8-15 CEA Ejection ; RCS Pressure vs. Time (Peak Pressure Case)

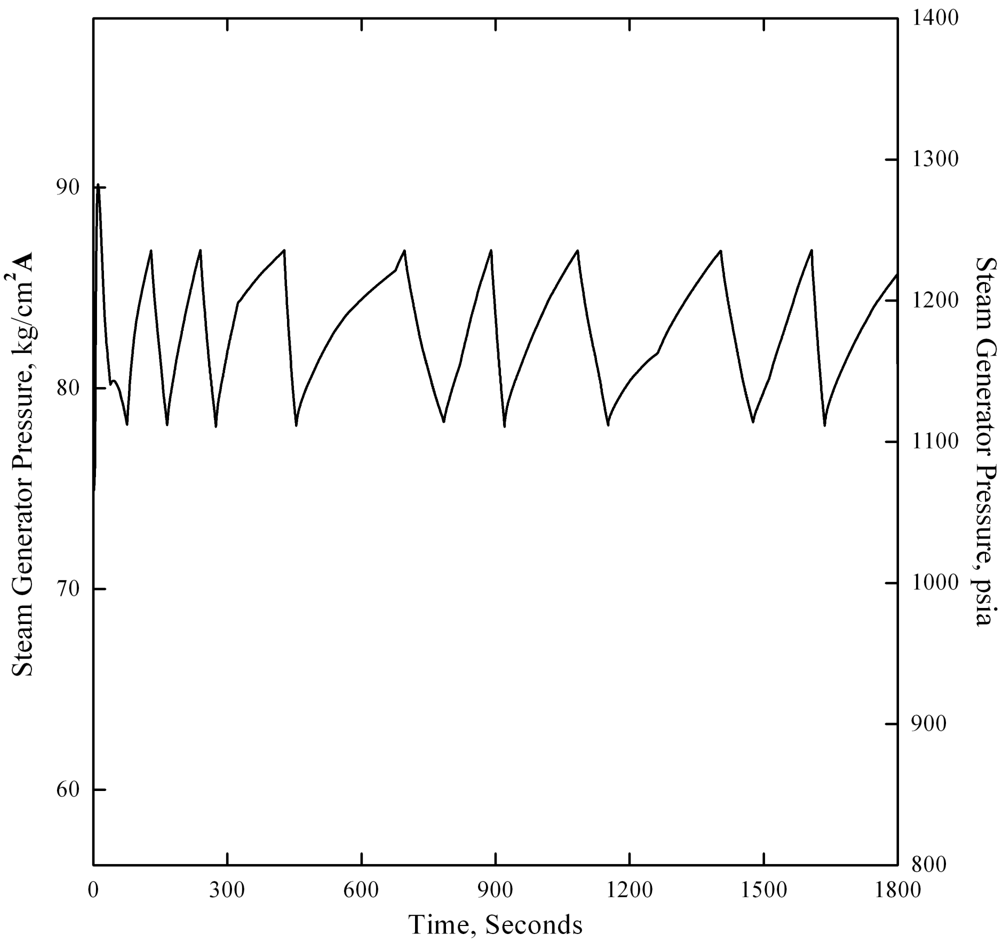

Figure 15.4.8-16 CEA Ejection ; Steam Generator Pressure vs. Time (Peak Pressure Case)

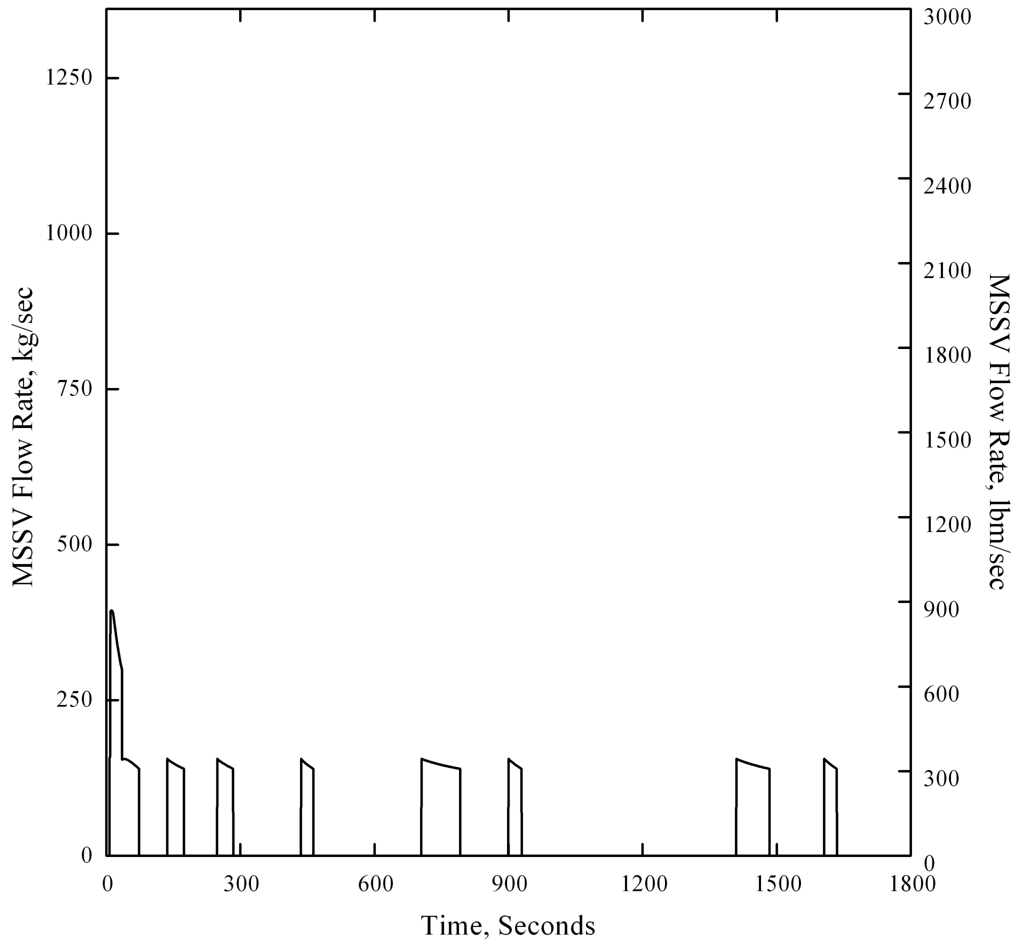

Figure 15.4.8-17 CEA Ejection ; MSSV Flow Rate vs. Time (Peak Pressure Case)

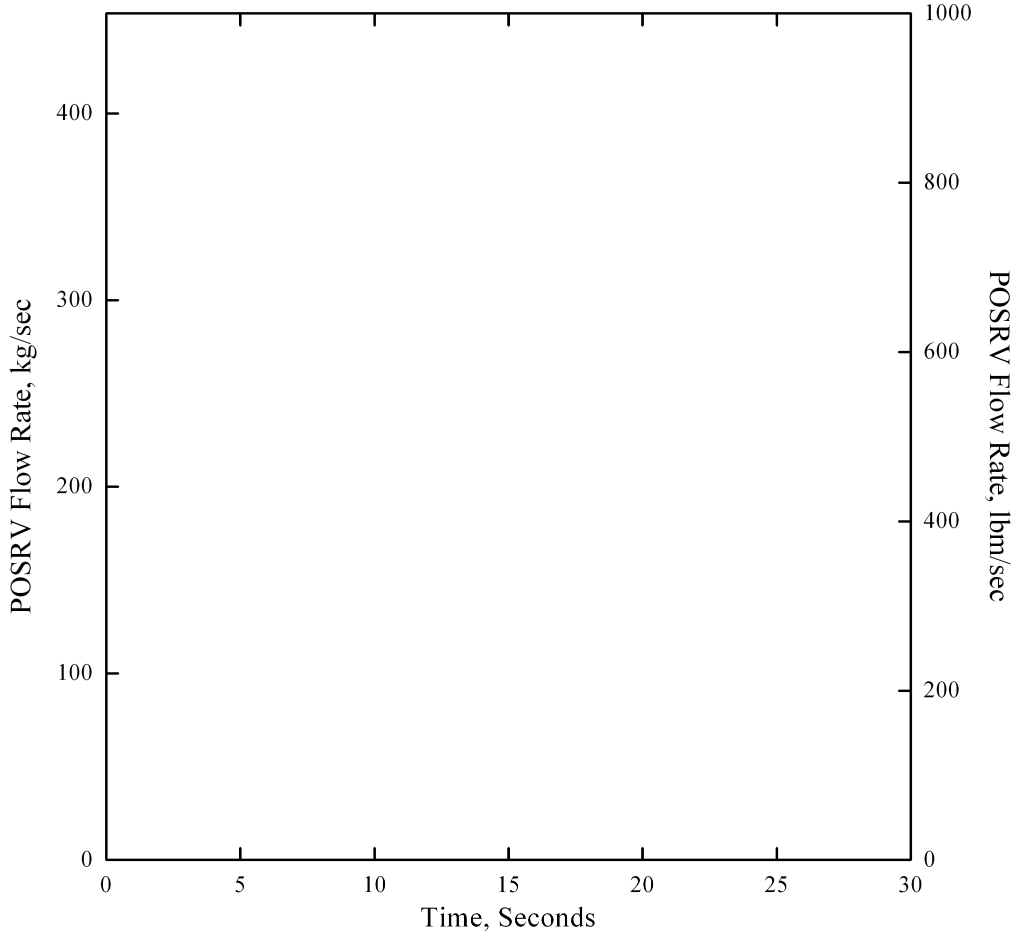

Figure 15.4.8-18 CEA Ejection ; POSRV Flow Rate vs. Time (Peak Pressure Case)

15.5 Increase in Reactor Coolant Inventory

Analyses of the following events are described in this section:

a. Subsection 15.5.1 – Inadvertent operation of emergency core cooling system (ECCS) that increases reactor coolant inventory

b. Subsection 15.5.2 – Chemical and volume control system malfunction that increases reactor coolant inventory

These events are considered anticipated operational occurrences (AOOs) as defined in Subsection 15.0.0.1.

15.5.1 Inadvertent Operation of the Emergency Core Cooling System that Increases the Reactor Coolant Inventory

15.5.1.1 Identification of Causes and Frequency Classification

The inadvertent operation of the emergency core cooling system, which is identified as the SIS for the APR1400, is assumed to actuate the four SI pumps and open the corresponding discharge valves. This operation occurs as a result of a spurious signal to the system or an operator error.

An inadvertent operation of the ECCS event is classified as an AOO. Each frequency condition is described in Subsection 15.0.0.1 and Table 15.0-5.

15.5.1.2 Sequence of Events and Systems Operation

Inadvertent operation of the SIS is only of consequence when it occurs below the SI pump shutoff head pressure. Above that pressure, there will be no injection of fluid into the system. Below the SI pump shutoff head pressure when the shutdown cooling system is isolated, the SI flow will increase RCS inventory and pressure until the pressure reaches the pump shutoff head pressure. During shutdown cooling system operation, the increase in RCS inventory and pressure will be mitigated by the shutdown cooling system relief valves.

15.5.1.3 Core and System Performance

15.5.1.3.1 Evaluation Model

There is no evaluation model for this event because this event is not applicable for the thermal hydraulic analyses.

15.5.1.3.2 Input Parameters and Initial Conditions

There are no input parameters and initial conditions for this event because this event is not applicable for the thermal hydraulic analyses.

15.5.1.3.3 Results

Plant operation above the SI pump shutoff head pressure will not be impacted by the inadvertent operation of the SIS. Below the SI pump shutoff head pressure when the shutdown cooling system is isolated, there will be an RCS inventory and pressure increase. This increase will be terminated when the pressure rises above the shutoff head pressure. Due to the pressure increase caused by this transient at low RCS temperatures, there is an approach to the brittle fracture limits of the RCS. If the SIS inadvertently actuates during shutdown cooling operation, the shutdown cooling relief valves mitigate the pressure transient.

15.5.1.4 Barrier Performance

The peak pressurizer pressure reached during the inadvertent operation of the SIS is well below 110 percent of the RCS design pressure.

15.5.1.5 Radiological Consequences

The fuel integrity is not challenged by this event and no radioactivity is released to the environment.

15.5.1.6 Conclusions

The peak pressurizer pressure reached during the inadvertent operation of the SIS is well below 110 percent of design pressure. Additionally, the pressure-temperature limits for

brittle fracture of the RCS are not violated by this transient. The fuel integrity is not challenged by this event.

15.5.2 Chemical and Volume Control System Malfunction that Increases the Reactor Coolant Inventory

15.5.2.1 Identification of Causes and Frequency Classification

All events and events plus single failure that cause an increase in RCS inventory are examined with respect to the RCS pressure and fuel cladding performance. According to the analyses, the pressurizer level control system malfunction with a LOOP concurrent with a turbine trip following reactor trip is the most severe event.

When in the automatic mode, the pressurizer level control system (PLCS) responds to changes in pressurizer level by changing charging and letdown flows to maintain the programmed level. Normally, one charging pump is running. The other charging pump is key-locked to prevent simultaneous operation of both charging pumps except during pump switching operation. If the pressurizer level controller fails low or the level setpoint fails high, a low level signal can be transmitted to the controller. In response, the controller will control the charging flow control valve for the maximum charging and close the letdown orifice isolation valves for the minimum letdown resulting in the minimum rate of mass discharge of the RCS. The limiting single failure is determined with respect to its impact on fuel performance and system pressure.

Regarding the pressure criteria, the major factors that cause an increase in RCS pressure are as follows:

a. Increasing coolant temperature

b. Decreasing core flow

c. Decreasing primary-to-secondary (P-T-S) heat transfer

The PLCS malfunction causes a reactor trip, on high pressurizer pressure, resulting in the maximum RCS pressure in the first 3 seconds following reactor trip. Any single failure

that would result in a higher RCS pressure during the transient would have to affect at least one of the above parameters during the first 3 seconds following reactor trip.

The single failures that have been postulated are listed in Table 15.0-4. The failures that affect the RCS behavior during this interval are as follows:

a. Failure of the pressurizer pressure control system

b. Failure of the feedwater control system

c. Failure of the steam bypass control system

Failure of the feedwater control system can only result in an excess cooldown, resulting in a lower peak pressure. After turbine trip, a LOOP concurrent with a turbine trip and reactor trip is considered as a basic assumption. The failures of RCPs, condenser pumps, circulation pumps, PLCS, pressurizer pressure control system (PPCS), reactor regulating system (RRS), feedwater control system (FWCS), and steam bypass control system (SBCS) are followed after a LOOP.

The effect of a LOOP on PLCS malfunction is as shown below. Failure of RRS does not have much effect within 3 seconds. However, the failures of SBCS and FWCS increase the pressure and temperature of steam generator. The P-T-S heat transfer decreases and decelerating RCP make the heat transfer decrease more. In addition, pressurizer spray does not work due to a loss of power in RCP and PPCS. It causes an increase in RCS pressure.

Regarding the approach to the fuel design limit, the major parameter of concern is the minimum hot channel DNBR. The major factors that cause a decrease in local DNBR are as follows:

a. Increasing coolant temperature

b. Decreasing coolant flow

c. Increasing local heat flux (including radial and axial power distribution effects)

PLCS malfunction causes the minimum DNBR to be reached within 3 seconds after the reactor trip. No single failure is identified from Table 15.0-4 that would have a significant effect on DNBR prior to the reactor trip. Therefore, any single failure that would result in a lower DNBR during the transient would have to affect at least one of the above parameters during the first 3 seconds following trip. The failures that affect the RCS behavior during this interval are as follows:

a. Failure of the PPCS

b. Failure of the RRS

Failure of the PPCS or RRS cannot appreciably affect any of the major factors that determine DNBR during the first 3 seconds following trip. None of the single failures listed in Table 15.0-4 will result in a lower DNBR than that predicted for the PLCS malfunction with a LOOP coincident with turbine trip.

A PLCS malfunction event is classified as an AOO. Each frequency condition is described in Subsection 15.0.0.1 and Table 15.0-5.

15.5.2.2 Sequence of Events and Systems Operation

Table 15.5.2-1 presents a chronological sequence of events that occurs during a PLCS malfunction in combination with a LOOP until the operator stabilizes the plant and initiates plant cooldown.

The excess of charging over letdown and the assumed PLCS malfunction results in the reactor trip on the high pressurizer pressure. The closing of the turbine stop valves, the interruption of the feedwater flow, and the reduction of reactor coolant flow due to a LOOP concurrent with a turbine trip following reactor trip result in an increase in RCS pressure, which opens the pressurizer POSRVs. SBCS is unavailable due to the LOOP, the MSSVs cycle open and close until auxiliary feedwater is automatically initiated on low steam generator water level signal. At 30 minutes after event initiation, the operator utilizes the AFWS and the atmospheric dump valves to cool down the primary system.

15.5.2.3 Core and System Performance

15.5.2.3.1 Evaluation Model

The NSSS response to a PLCS malfunction with a LOOP coincident with the turbine trip is simulated using the CESEC-III described in Subsection 15.0.2.2.1. The CESEC-III is modified to reflect the centrifugal charging pump model. The minimum DNBR is calculated using the CETOP (Subsection 15.0.2.2.4), which uses the KCE-1 CHF correlation described in Reference 28 of Subsection 15.0.5.

15.5.2.3.2 Input Parameters and Initial Conditions

Table 15.5.2-2 lists the assumptions and initial condition used for this analysis in addition to those discussed in Section 15.0. Additional clarification to the assumptions and parameters listed in Table 15.5.2-2 is provided as follows:

Since the pressure transient is primarily due to an increase in RCS coolant inventory for the significant portion of the event, not to thermal expansion, there will be no significant power transient, coolant temperature transient, or DNB transient prior to reactor trip. The initial conditions for the principal process variables, with the exception of pressurizer pressure, have no significant effect on the consequences. Minimizing the initial RCS pressure maximizes time to reactor trip on high pressurizer pressure and maximizes the increase in RCS inventory. An initial conservatively low pressurizer pressure of 152.92 kg/cm^2A (2,175 psia) is chosen from the parametric studies with respect to the initial condition in Table 15.0-3. The initial water volume in the pressurizer is chosen to be about 60 percent of the total volume.

Since the charging flow through the regenerative heat exchanger exceeds the letdown flow, the temperature of the makeup water added to the RCS by the charging pump is decreased significantly. A negative value of moderator temperature coefficient is selected to maximize the positive reactivity addition from injection of cold makeup water.

The maximum charging flow to the RCS due to one operating pump is 681.37 L/min (180 gpm), and the minimum letdown flow is 151.4 L/min (40 gpm). The PPCS is assumed to be in manual mode with the main sprays off, preventing the PPCS from suppressing the resulting pressure transient.

15.5.2.3.3 Results

The dynamic behavior of NSSS parameters following a PLCS malfunction with a LOOP at turbine trip is presented in Figures 15.5.2-1 through 15.5.2-12.

Failure of the PLCS causes an increase in RCS inventory initiated by maximum charging flow coupled with a decrease in letdown flow to its minimum. With the PPCS in manual mode and the proportional sprays turned off, an increase in RCS inventory results in a pressurizer pressure increase to the reactor trip analysis setpoint of 169.72 kg/cm^{2}A (2,414 psia) at 459.3 seconds. The increase in pressure is also aggravated by the slight power increase that results from the injection of cold charging flow. The trip breakers open at 460.15 seconds.

Since the SBCS is unavailable due to the LOOP after turbine trip and the rate of closure of the turbine stop valves is faster than the rate of control rod insertion, the pressurizer pressure reaches to 177.13 kg/cm^{2}A (2,519.4 psia), which is the pressurizer POSRVs opening setpoint. The decrease in the P-T-S heat transfer due to the four reactor coolant pump loss of flow also contributes to the pressure increase. The RCS pressure reaches a maximum of 186.95 kg/cm^{2}A (2,659 psia) at 463.4 seconds.

A separate set of analyses are performed to determine the minimum DNBR during a PLCS malfunction with a LOOP coincident with turbine trip. This event causes RCS pressure to increase due to an increase in primary system inventory. Consequently, after a slow increase of the minimum DNBR, it rapidly decreases due to a decrease in coolant flow rate following a LOOP concurrent with turbine trip, then suddenly increases again. The result for the DNBR is provided in Figure 15.5.2-12. The minimum DNBR is calculated to be 1.5177. Decreasing core heat flux due to reactor trip and the opening of the pressurizer POSRVs causes the pressure to eventually drop.

The unavailability of the SBCS causes the steam generator pressure to increase, causing the main steam safety valves to open at 463.45 seconds. The decreasing core power and the safety valves function to limit the steam generator pressure to 91.00 kg/cm^{2}A (1,294.34 psia).

The 639.92 kg (1,410.77 lbm) of steam discharged by the pressurizer POSRVs are contained within the IRWST with no releases to the atmosphere. The main steam safety

valves discharge 108,557.8 kg (239,329 lbm) of steam to the atmosphere prior to 1,800 seconds. At 1,800 seconds, the operator stabilizes the plant and initiates plant cooldown, using the AFWS and the atmospheric dump valves.

15.5.2.4 Barrier Performance

For the CVCS malfunction event, the RCS pressure remains below 110 percent of the RCS design pressure, thus providing reasonable assurance of primary system integrity. The maximum SG pressure also is below 110 percent of the SG design pressure.

15.5.2.5 Radiological Consequences

The fuel integrity is not challenged by this event and no radioactivities are released to the environment.

15.5.2.6 Conclusions

The peak RCS and steam generator pressures reached during the PLCS malfunction with a LOOP at turbine trip are 186.95 kg/cm^{2}A (2,659 psia) and 91.0 kg/cm^{2}A (1,294.34 psia), respectively. These pressures are less than 110 percent of the primary and secondary design pressures, 193.34 kg/cm^{2}A (2,750 psia) and 92.83 kg/cm^{2}A (1,320 psia), respectively. The minimum DNBR is calculated to be 1.5117, which is above the DNBR SAFDL value of 1.29. The acceptance criterion regarding fuel performance is met.

15.5.3 Combined License Information

No COL information is required with regard to Section 15.5.

Table 15.5.2-1

Sequence of Events for the PLCS Malfunction with a Loss of Offsite Power Coincident with Turbine Trip

Time (sec)	Event	Setpoint or Value
0.00	Charging flow maximized and letdown flow minimized	—
459.30	Pressurizer pressure reaches reactor trip analysis setpoint, kg/cm^2A (psia)	169.72 (2,414)
460.05	High pressurizer pressure trip signal generated	—
460.15	Turbine trip occurs and trip breakers open	—
460.15	Loss of offsite power occurs	—
463.10	Pressurizer pilot-operated safety relief valves opening setpoint reached, kg/cm^2A (psia)	177.13 (2,519.4)
463.40	Maximum RCS pressure, kg/cm^2A (psia)	186.95 (2,659)
463.45	Main steam safety valves open, kg/cm^2A (psia)	86.88 (1,235.66)
465.00	Pressurizer pilot-operated safety relief valves closing setpoint reached, kg/cm^2A (psia)	159.32 (2,266)
466.40	Maximum steam generator pressure, kg/cm^2A (psia)	91.0 (1,294.34)
736.25	SG water level reaches AFAS analysis setpoint, %WR	19.9
797.70	Auxiliary feedwater flow initiates	—
1,800.00	Operator initiates plant cooldown	—

Table 15.5.2-2

Assumptions and Initial Conditions for the PLCS Malfunction with a Loss of Offsite Power Coincident with Turbine Trip

Parameter	Value
Initial core power level, MWt	4,062.66
Initial core inlet coolant temperature, °C (°F)	296.1 (565.0)
Initial core mass flow rate, 10^6 kg/hr (10^6 lbm/hr)	73.3 (161.6)
Initial pressurizer pressure, kg/cm^{2}A (psia)	152.92 (2,175)
Initial pressurizer water volume, m^3 (ft^3)	39.91 (1,409.44)
CEA worth on trip, 10^{-2} $\Delta\rho$	−8.0
Moderator temperature coefficient, $\Delta\rho$/°C ($\Delta\rho$/°F)	-5.4×10^{-4} (-3.0×10^{-4})
Doppler reactivity	Least Negative

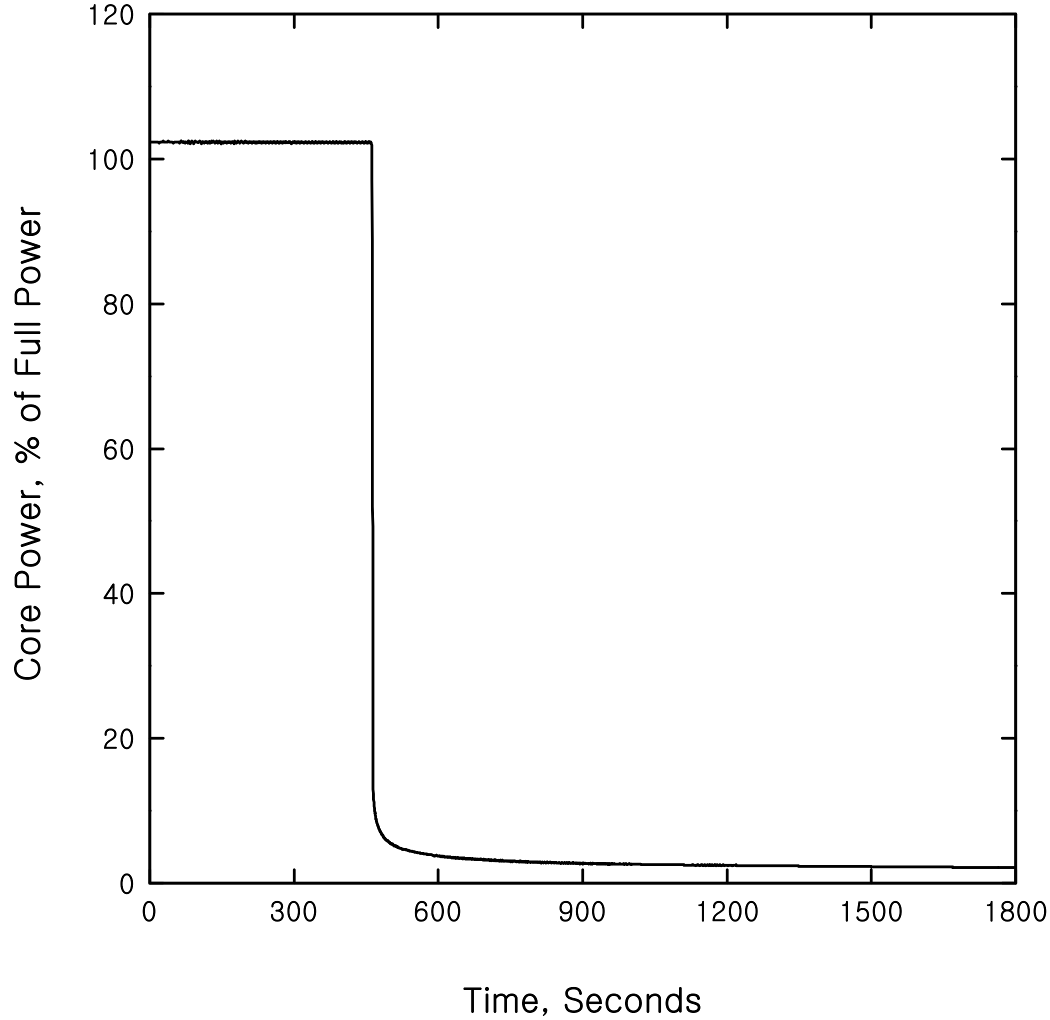

Figure 15.5.2-1 PLCS Malfunction with LOOP : Core Power vs. Time

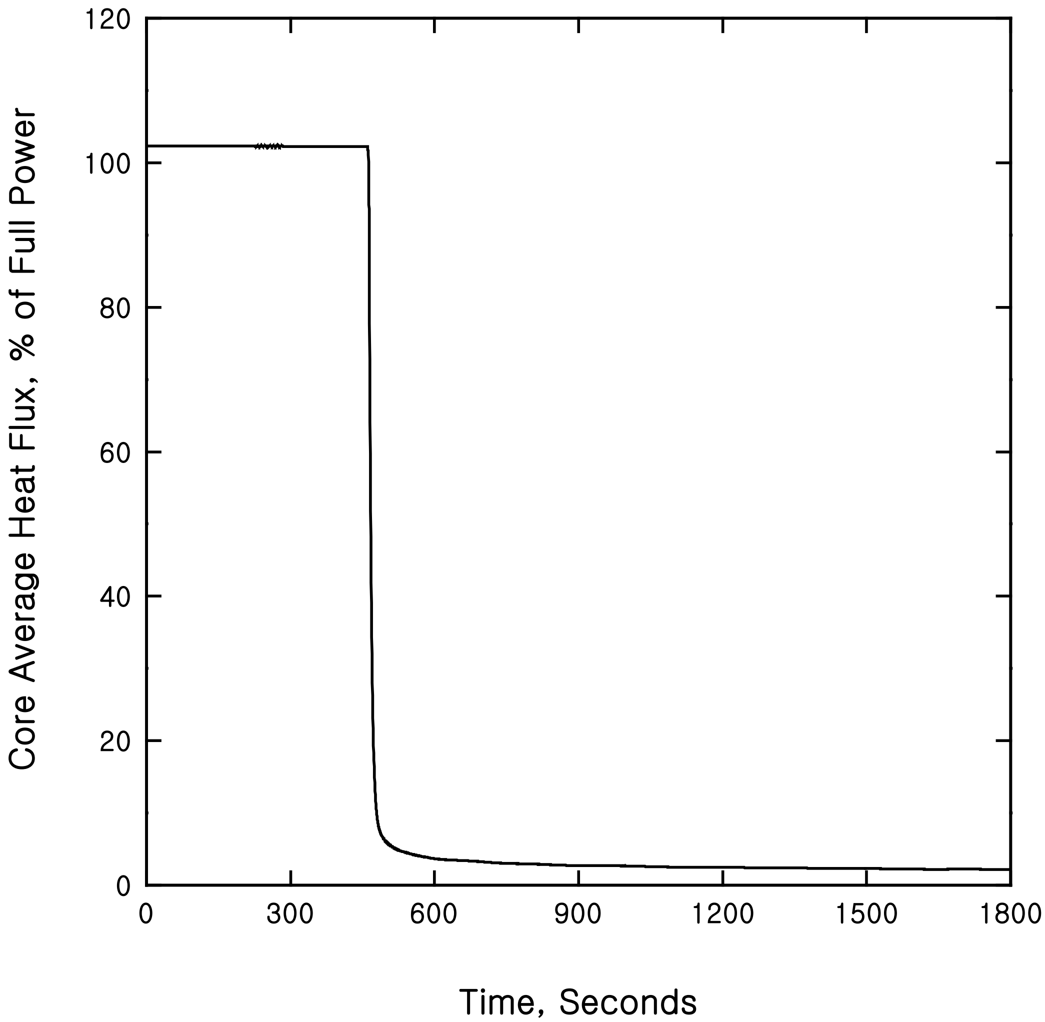

Figure 15.5.2-2 PLCS Malfunction with LOOP : Core Average Heat Flux vs. Time

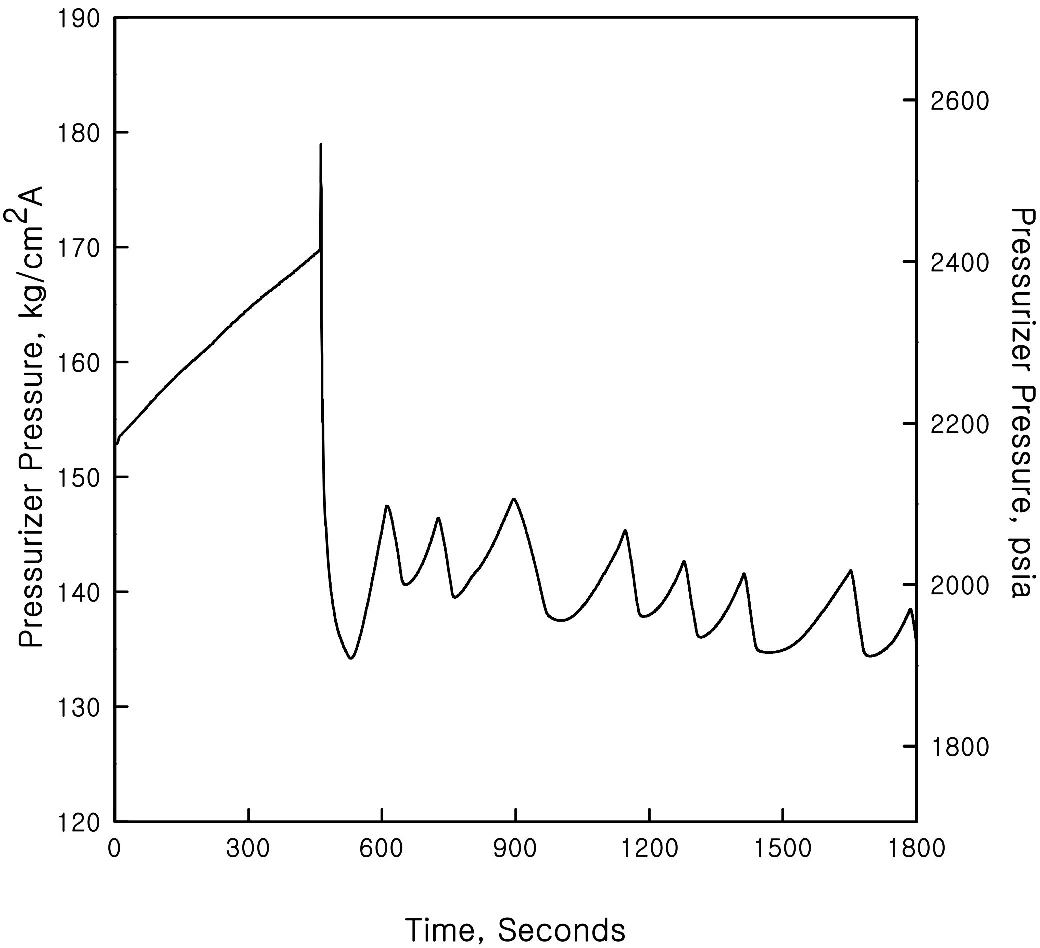

Figure 15.5.2-3 PLCS Malfunction with LOOP : Pressurizer Pressure vs. Time

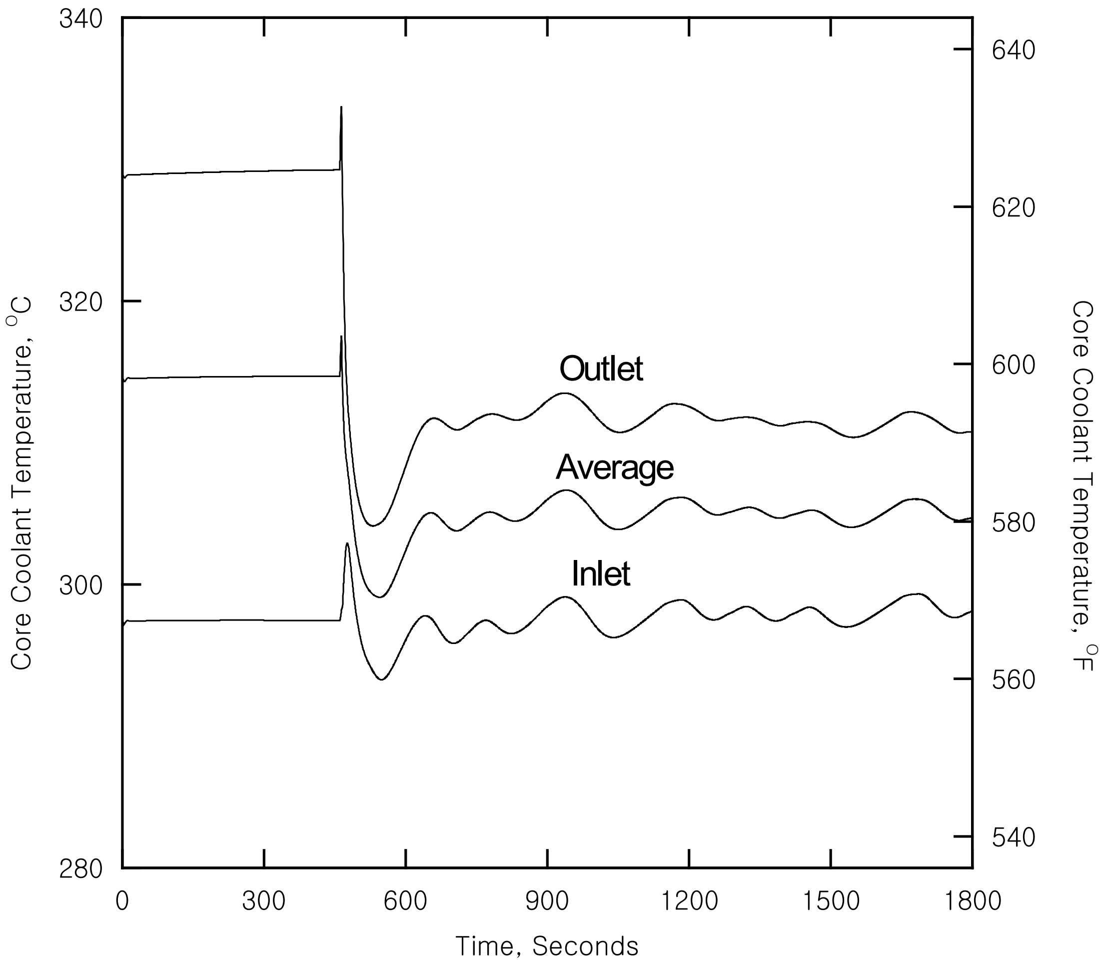

Figure 15.5.2-4 PLCS Malfunction with LOOP : Reactor Coolant Temperature vs. Time

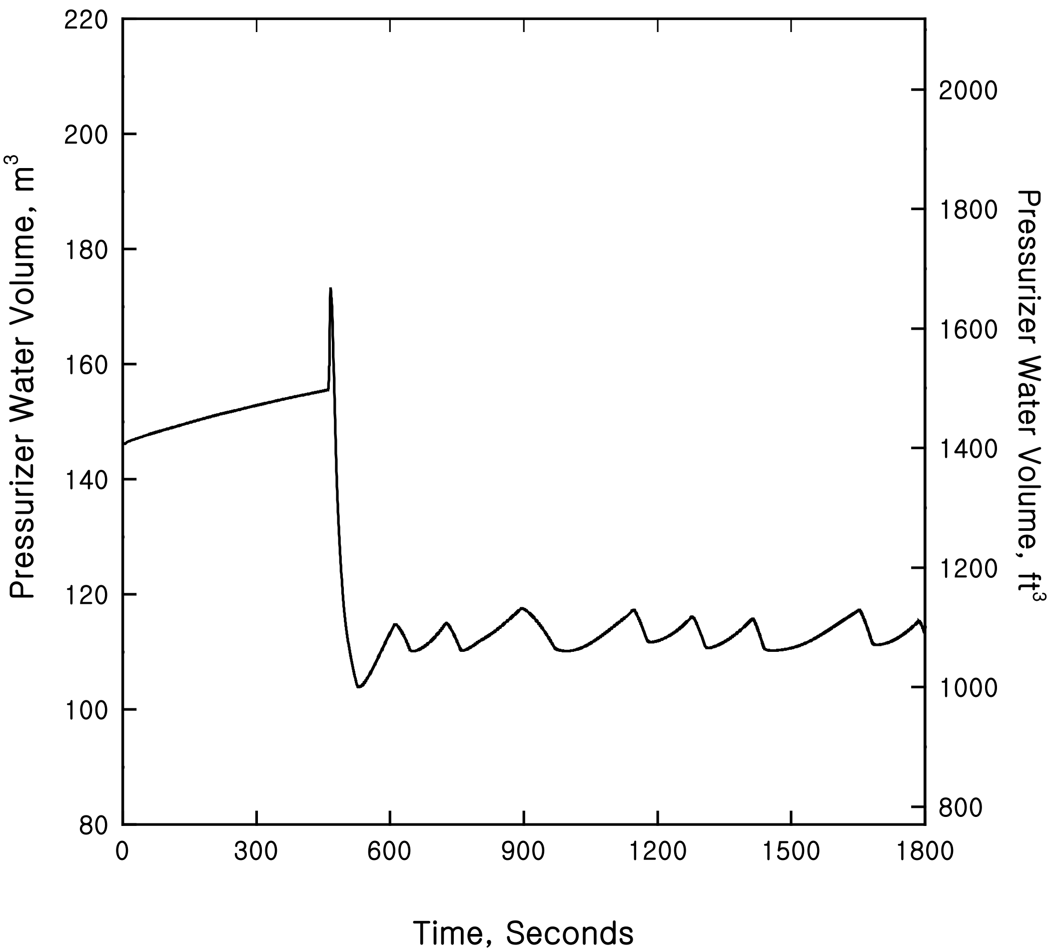

Figure 15.5.2-5 PLCS Malfunction with LOOP : Pressurizer Water Volume vs. Time

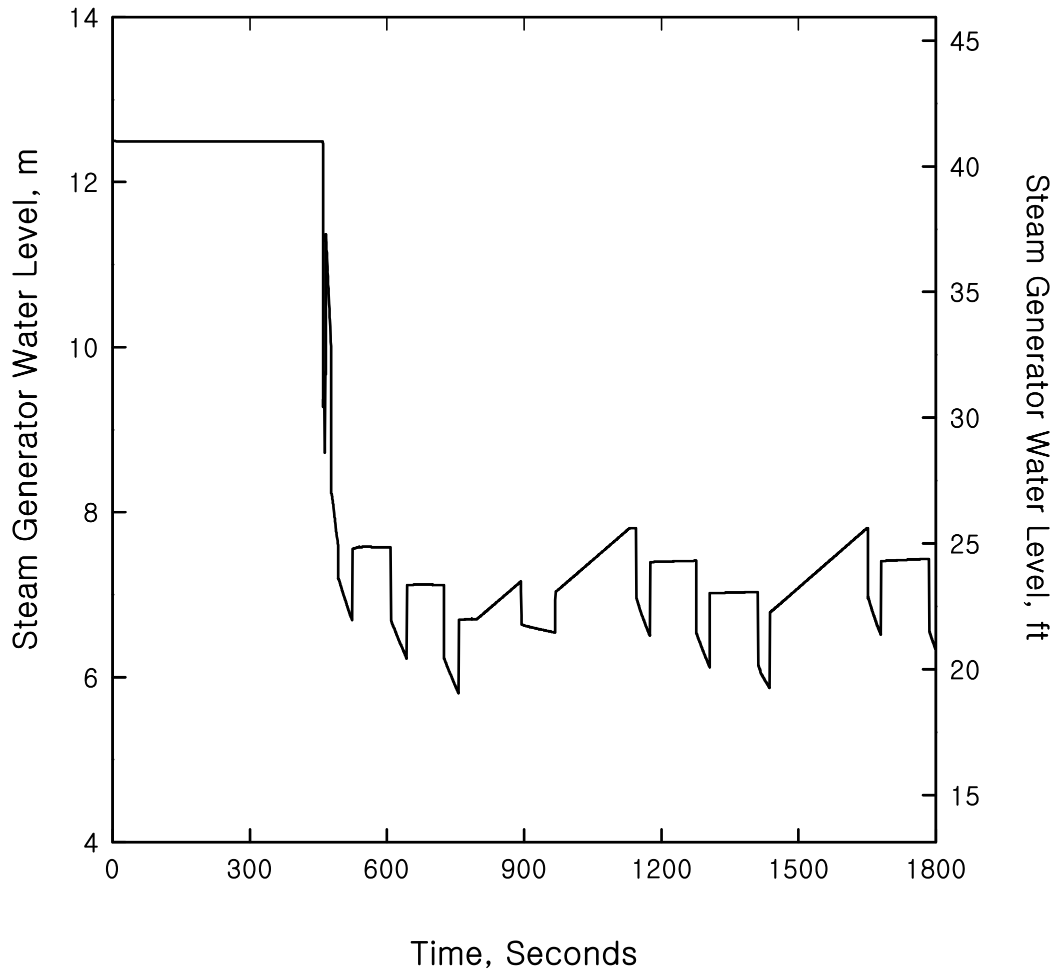

Figure 15.5.2-6 PLCS Malfunction with LOOP : Steam Generator Water Level vs. Time

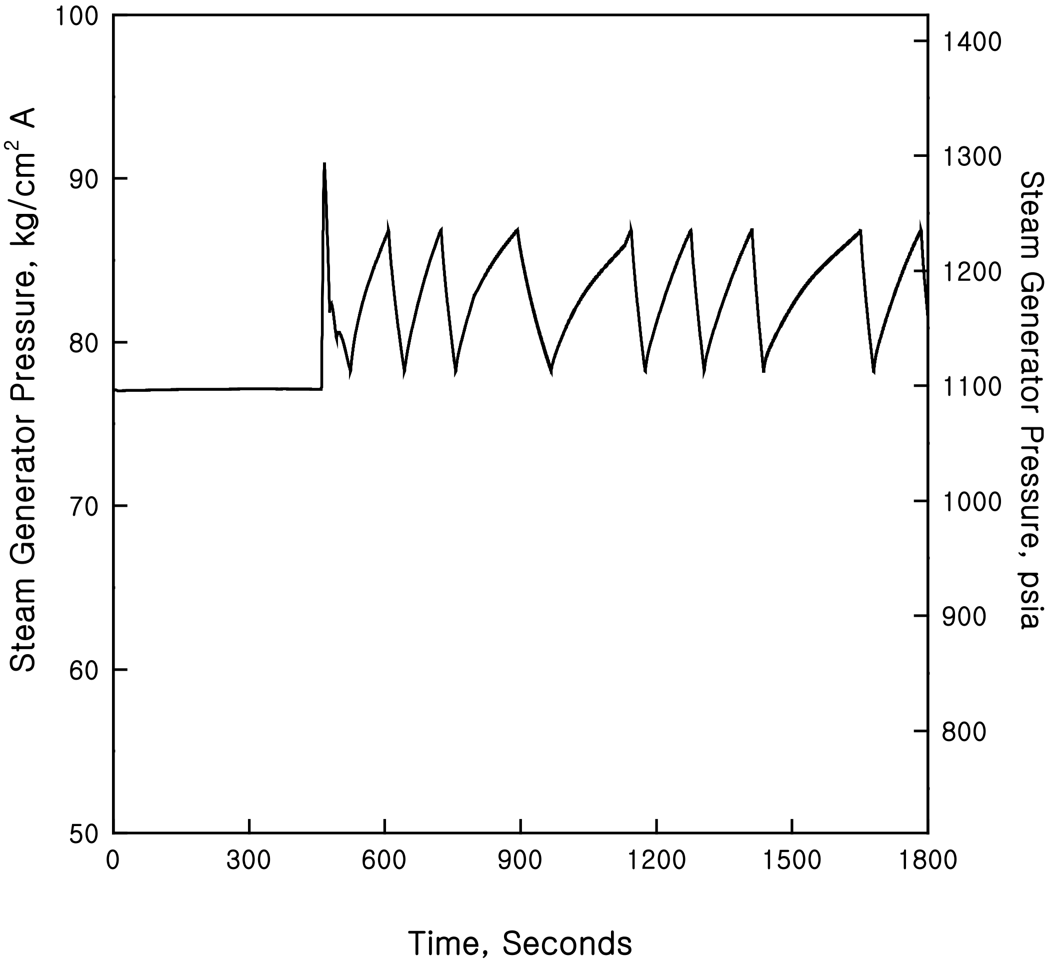

Figure 15.5.2-7 PLCS Malfunction with LOOP : Steam Generator Pressure vs. Time

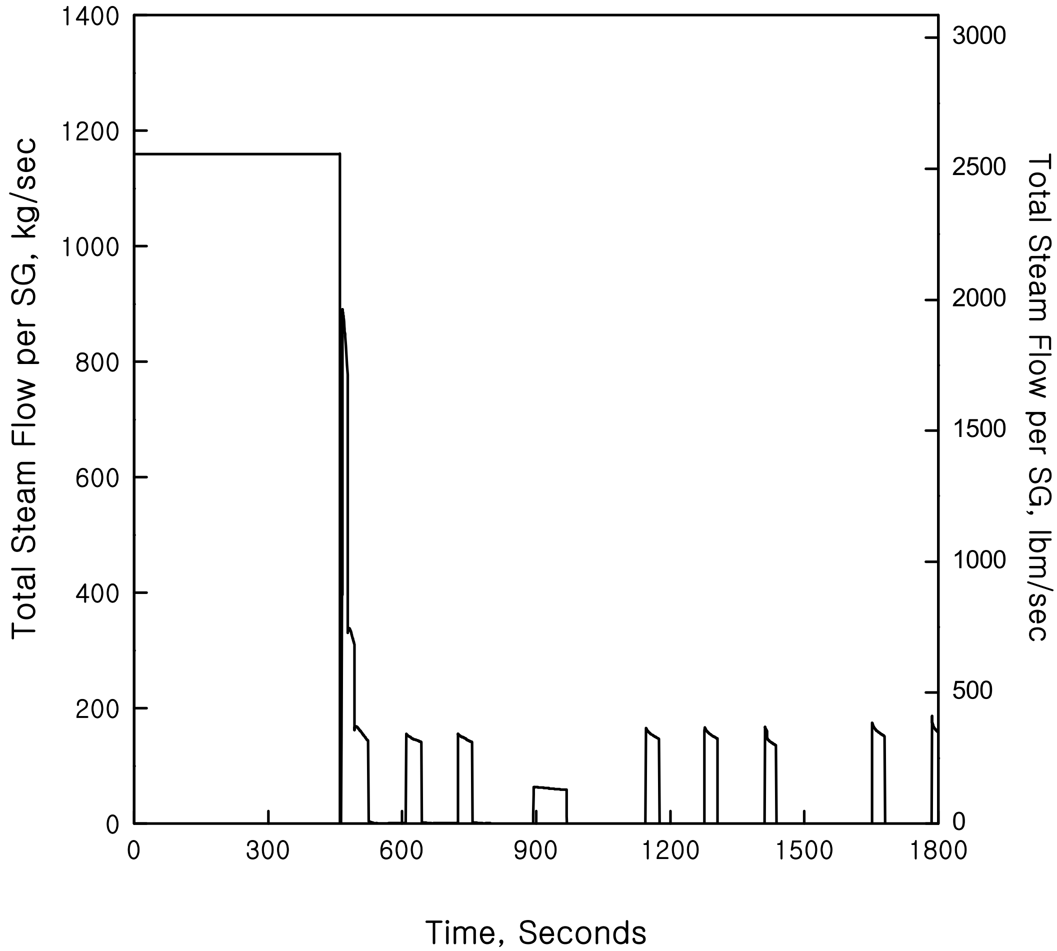

Figure 15.5.2-8 PLCS Malfunction with LOOP : Total Steam Flow Rate vs. Time

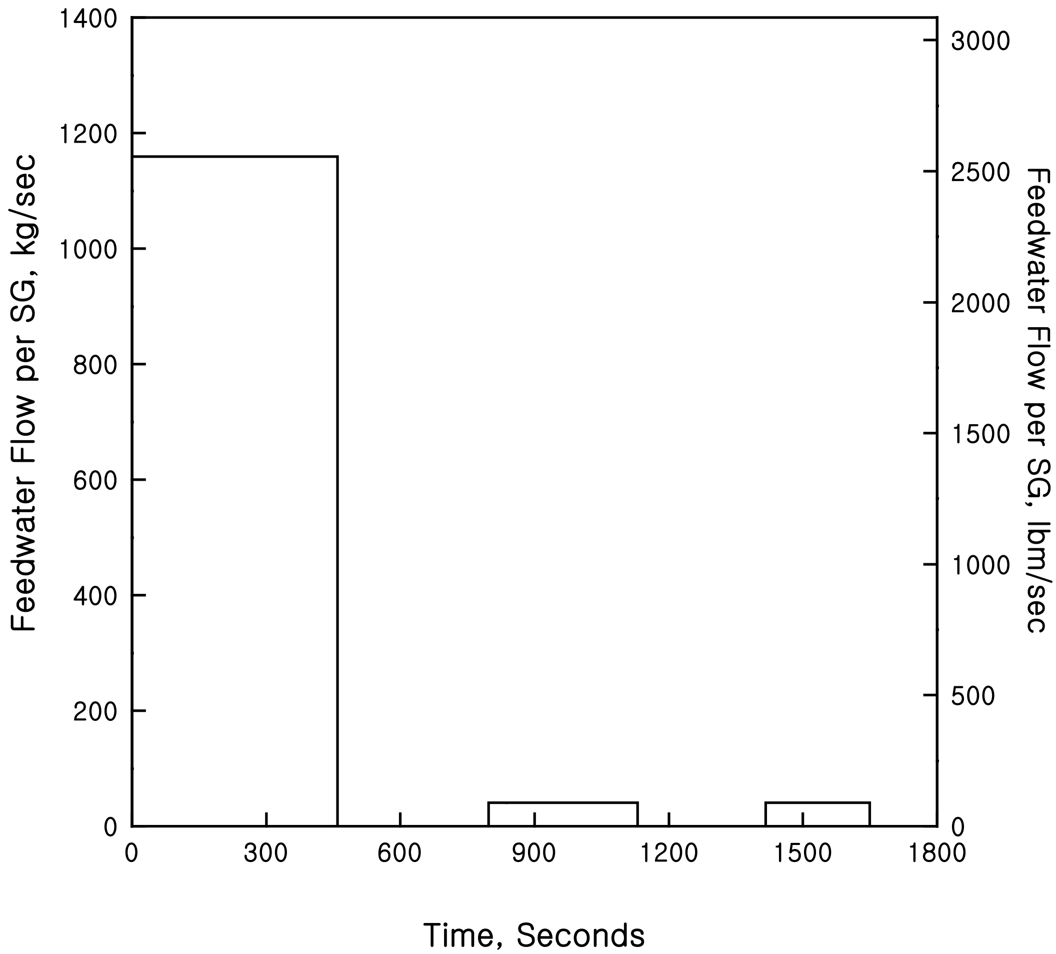

Figure 15.5.2-9 PLCS Malfunction with LOOP : Feedwater Flow Rate vs. Time

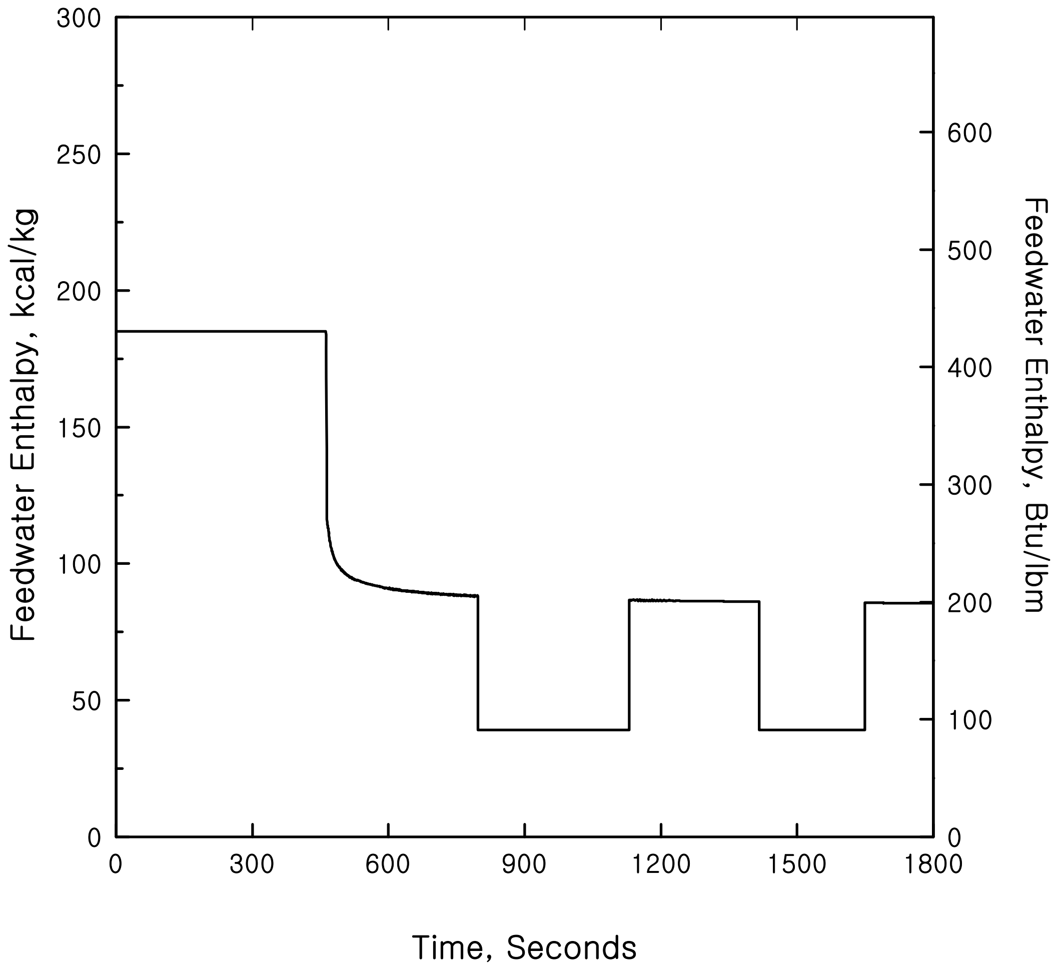

Figure 15.5.2-10 PLCS Malfunction with LOOP : Feedwater Enthalpy vs. Time

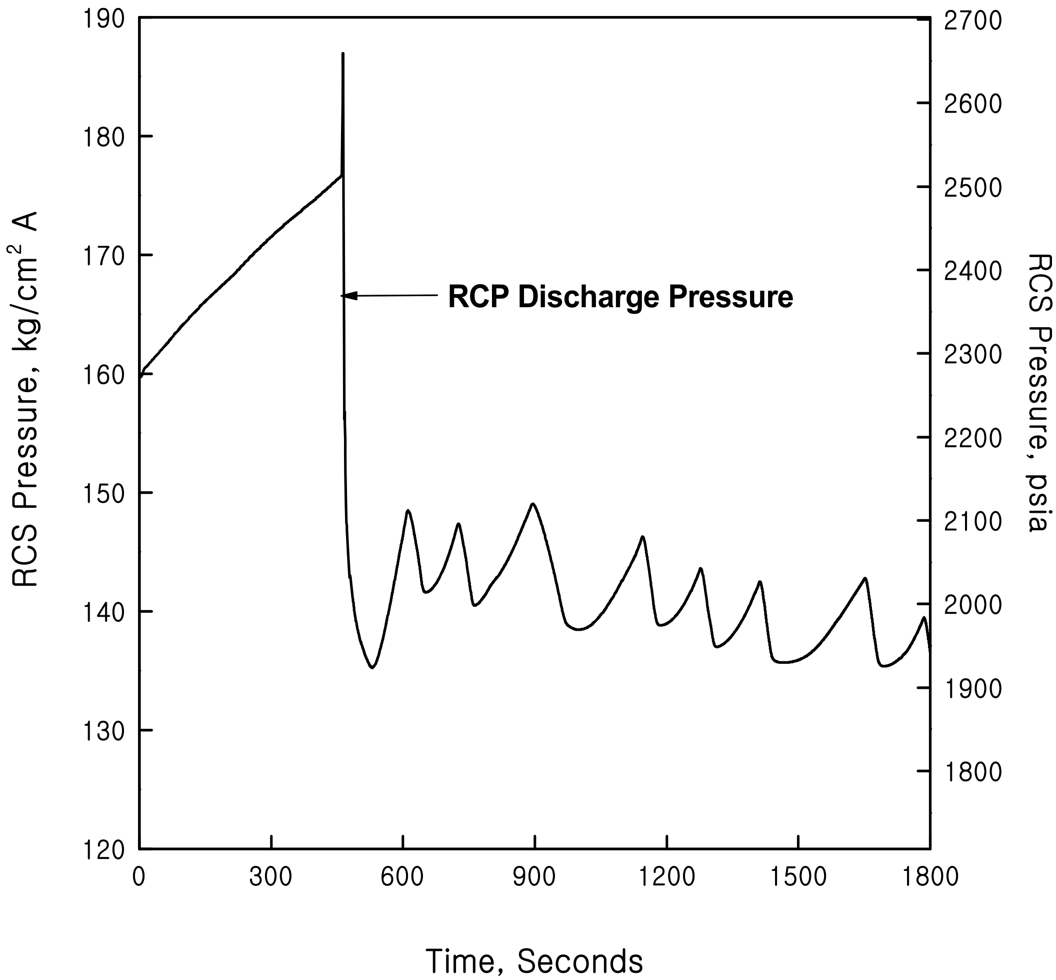

Figure 15.5.2-11 PLCS Malfunction with LOOP : RCS Pressure vs. Time

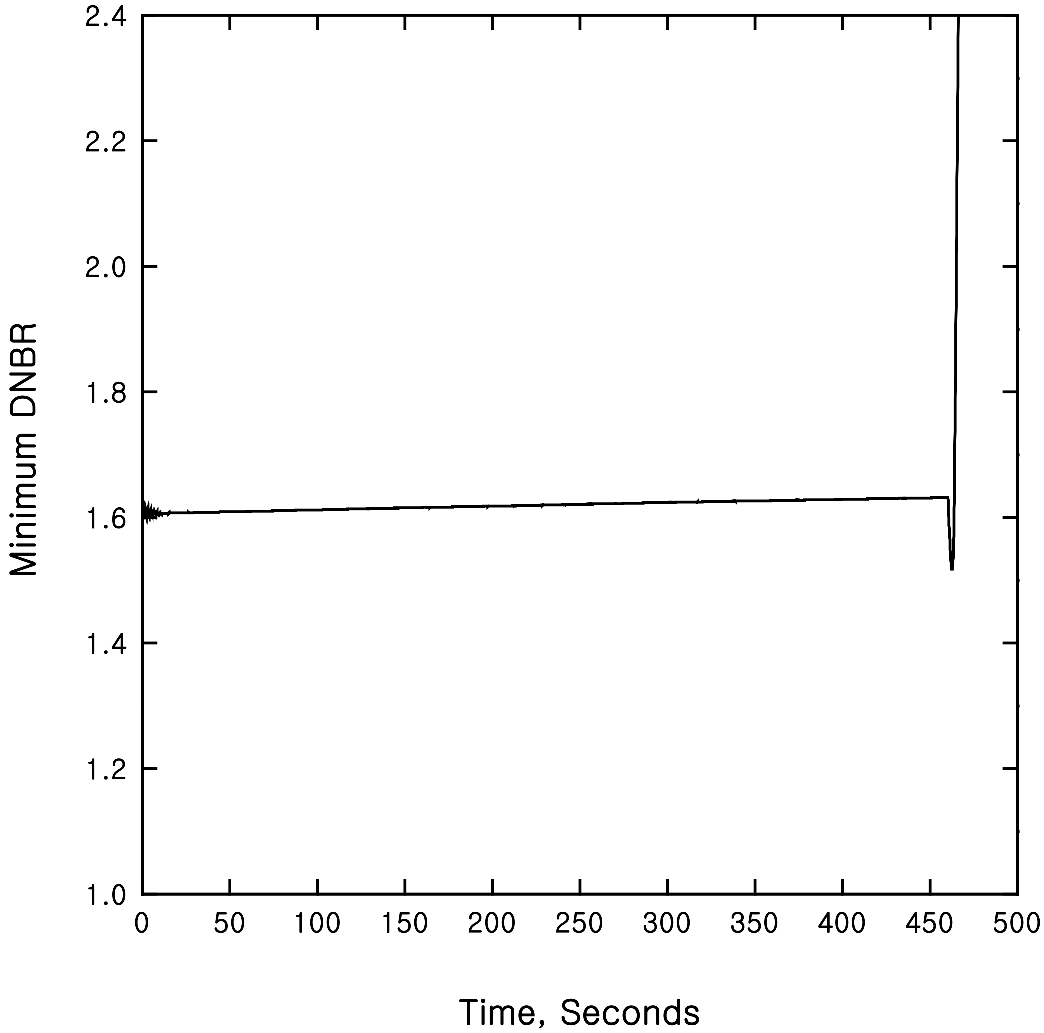

Figure 15.5.2-12 PLCS Malfunction with LOOP : Minimum DNBR vs. Time

15.6 Decrease in Reactor Coolant Inventory

This section describes the analyses that have been performed for events that could result in a decrease in reactor coolant inventory, which can lead to a temperature increase in the reactor coolant system (RCS).

Several anticipated operational occurrences (AOOs) and postulated accidents (PAs) can cause a decrease in reactor coolant inventory. Detailed analyses of these reactor coolant inventory events are described in the following subsections:

a. Subsection 15.6.1 – Inadvertent opening of a pressurizer pressure relief valve

b. Subsection 15.6.2 – Failure of small lines carrying primary coolant outside the containment

c. Subsection 15.6.3 – Steam generator tube failure

d. Subsection 15.6.4 – Radiological consequences of main steam line failure outside the containment for a boiling water reactor (not applicable to the APR1400)

e. Subsection 15.6.5 – Loss-of-coolant accidents (LOCAs) resulting from a spectrum of postulated piping breaks within the reactor coolant pressure boundary (RCPB)

15.6.1 Inadvertent Opening of a PWR Pressurizer Pressure Relief Valve

The evaluation of an inadvertent opening of a POSRV is described in Subsection 15.6.5 presenting SBLOCA.

15.6.2 Failure of Small Lines Carrying Primary Coolant Outside Containment

15.6.2.1 Identification of Causes and Frequency Classification

The direct release of reactor coolant may result from a break or leak outside the containment of a letdown line, instrument line, or sample line. A double-ended break of the letdown line outside the containment upstream of the letdown isolation valve is selected for this analysis because it is the largest line and thus results in the largest release of reactor coolant outside the containment.

The single active failure of an isolation valve is not considered in the analysis because the letdown line includes three isolation valves in series inside the containment. Hence, failure of one isolation valve does not make the consequences of the event more severe.

A letdown line break (LDLB) can range from a small crack in the piping to a complete double-ended break. The cause of the event may be attributed to corrosion that forms etch pits or from fatigue cracks resulting from vibration or inadequate welds.

An LDLB event is classified as an AOO. Each frequency condition is described in Subsection 15.0.0.1 and Table 15.0-5.

15.6.2.2 Sequence of Events and Systems Operation

A double-ended break of the letdown line outside the containment upstream of the letdown isolation valve releases primary fluid to the auxiliary building at a rate of approximately 11.3 kg/sec (25 lbm/sec). The maximum break flow is limited to this value by the letdown orifices inside the containment downstream of the letdown heat exchanger. The event sets off a number of alarms. Table 15.6.2-1 lists the alarms that would be noted by the reactor operator in the main control room (MCR).

Of the alarms listed in Table 15.6.2-1, the letdown line low pressure alarm immediately alerts the operator after the initiation of the event. Additional alarms provide indications of the event at various times. The high temperature, high humidity, and high radiation level alarms in the auxiliary building are expected to be triggered within a few seconds after the event initiation. The pressurizer low-level alarm is expected to alert the operator within a few minutes after the event initiation. The auxiliary building sump high-high level and the volume control tank low-level alarms are expected to be triggered within a few minutes after the event initiation.

The analysis conservatively assumes that operator action is delayed until 30 minutes after the initiation of the event when the operator isolates the letdown line, thereby terminating any further release of primary flow to the auxiliary building. One of three valves in series inside the containment is closed to isolate the LDLB. The design of these valves, relative to their function during a letdown line break, is detailed in Subsection 9.3.4.2. The operator is assumed to take appropriate steps for a controlled reactor shutdown.

Table 15.6.2-2 presents the chronological sequence of events following a double-ended break of the letdown line until the operator takes action to terminate the primary system fluid loss 30 minutes after the initiation of the event. The operator subsequently manually trips the plant and cools it down to shutdown cooling entry conditions.

15.6.2.3 Core and System Performance

15.6.2.3.1 Evaluation Model

The NSSS response to a double-ended break of the letdown line outside the containment upstream of the letdown isolation valve is simulated with the CESEC-III computer program described in Reference 165. The analysis assumes critical flow through the break and accounts for letdown line losses and for operation of the pressurizer pressure control system (PPCS) and pressurizer level control system (PLCS). The model of the LDLB that is used is described in Reference 16 of Subsection 15.0.5.

15.6.2.3.2 Input Parameters and Initial Conditions

Table 15.6.2-3 lists the assumptions and initial conditions used for this analysis in addition to those discussed in Section 15.0. Conditions are chosen to maximize the primary system mass release for an LDLB. These conditions lead to the most conservative predictions of radiological releases.

The initial conditions and NSSS characteristics used in the analysis of the maximum total radiological release for the LDLB are based on parametric studies. The parameters evaluated are initial core inlet temperature, initial power level, initial pressurizer pressure, initial core inlet flow rate, initial pressurizer liquid inventory, and break size.

The maximum total mass release is obtained when the transient is initiated with the following parameters from Table 15.0-3:

a. Maximum core power

b. Maximum allowed core inlet temperature

c. Low core flow rate

d. Maximum pressurizer pressure

e. High pressurizer level

In order to maximize the break flow, a reactor trip is prevented from occurring before operator action at 30 minutes. Because the reactor does not trip, the value of scram rod worth used in the analysis has no impact on the consequences of the event. Similarly, because the core power and core coolant temperature do not vary significantly during the event, the choices of the moderator temperature coefficient and Doppler reactivity functions have little impact on the event consequences.

All control systems are assumed to be in the automatic mode to maximize the total primary mass release. The pressurizer heaters are assumed to be operational during the LDLB event. This is not a mitigative feature. Instead, the primary system pressure is maintained at a higher value due to the operation of the heaters, which maximizes the break flow. The break is assumed to be a full cross-sectional area (double-ended) pipe break.

The PLCS is assumed to be in the automatic mode during the transient. The lower charging flow rate maximizes the fluid temperature at the break, thereby resulting in a higher flashing fraction for the fluid at the break. The higher flashing fraction maximizes the offsite radiological release due to the increased steam release at the break. As a result of an assumed malfunction in the control system, the charging flow rate is conservatively assumed to decrease to the minimum value of 266.50 L/min (70.4 gpm) during the transient.

The PLCS could also fail in such a way as to maximize the charging flow rate (maximum flow rate of about 681.35 L/min [180.0 gpm]). The impact of this high flow rate is to (1) maintain the RCS pressure slightly higher, resulting in slightly larger break flow rates during the transient and (2) decrease the flashing fraction of the fluid at the break due to the increased heat removal realized in the regenerative heat exchanger from the increased charging flow rate. Parametric studies have concluded that the increase in the flashing fraction due to the lower charging flow rate is more limiting with respect to radiological releases than the increase in the break flow rate due to the higher charging flow rate. Consequently, an analysis that assumes the minimum charging flow rate yields a conservatively high offsite radiological release.

15.6.2.3.3 Results

The dynamic behavior of important NSSS parameters following a double-ended break of the letdown line outside the containment is presented in Figures 15.6.2-1 through 15.6.2-12. The minimum DNBR versus time as shown in Figure 15.6.2-13 remains above 1.29 throughout the transient. The decrease in the primary system mass causes the pressurizer pressure to decrease from the initial value of 163.46 kg/cm^{2}A (2,325 psia) to about 159.37 kg/cm^{2}A (2,266.8 psia) at 1,800 seconds. During the same period, the pressurizer liquid volume decreases from an initial value of about 39.91 m^3 (1,409 ft^3) to 12.37 m^3 (437 ft^3).

Thirty minutes into the transient, the operator isolates the letdown line, terminating the release of primary fluid outside the containment. During this period, no more than 20,276 kg (44,700 lbm) of primary system fluid is released outside the containment. Shortly after the termination of the primary system mass release, the operator manually trips the reactor. The minimum DNBR for the LDLB event described here does not decrease below the SAFDL value of 1.29 because the RCS pressure decrease during the event is not sufficient to decrease all of the fuel thermal margin before the operator action at 30 minutes.

For an LDLB with a reactor trip and coincident loss of offsite power (LOOP), the minimum DNBR also stays above the SAFDL because (1) the rate of decrease of RCS pressure during an LDLB event is bounded by the rate for a double-ended steam generator tube rupture (SGTR) accident and (2) as shown in Subsection 15.6.3.2 for an SGTR accident with a LOOP, the minimum DNBR remains above the SAFDL of 1.29.

15.6.2.4 Barrier Performance

The double-ended break of a letdown line outside the containment upstream of the letdown line isolation valve results in below 110 percent of the RCS design pressure. The secondary side pressure does not increase above its initial condition value during the transient and remains below 110 percent of design, providing reasonable assurance of the integrity of the main steam system.

15.6.2.5 Radiological Consequences

The radiological consequences are performed to determine EAB, LPZ, MCR, and TSC doses due to an LDLB accident using the guidance in SRP 15.6.2 and the generic AST

methodology guidance in NRC RG 1.183, the TEDE dose criteria, and the plant-specific bounding design information applicable to the APR1400.

15.6.2.5.1 Evaluation Model

The following transport models of radioactive materials are applied to evaluate radiological consequences due to an LDLB accident.

Release via the Auxiliary Building

RCS fluid is released into the Auxiliary Building (AB) through the letdown line break, and from there, is assumed to be directly released to the environment through the AB exhaust vent without mixing with the AB volume for conservatism. The fraction of iodine assumed to become airborne and available for release to the atmosphere through the AB exhaust vent, without credit for plateout, is equal to the fraction of the coolant flashing into steam in the depressurization process. In addition, a portion of the iodine in the unflashed leakage vaporizes with a partition coefficient. The LDLB iodine is released through the building ventilation system to the environment without any credit for filtration of radioactivity.

Release via the Steam Generators

In order to remove decay heat, the plant begins to release the secondary coolant to atmosphere. After 30 minutes, the SGs are used to cool down the RCS and the contaminated steam present in the SGs is released to the environment through the ADV. The RCS iodine activity entering the SGs via P-T-S leakage is assumed to mix with, and be diluted within, the bulk water in the SGs. The steam release from the SGs continues to 8 hours until the shutdown cooling system is aligned to dissipate heat.

Release via the Condenser

The contaminated secondary steam in the SGs is released to the condenser until operator actions are taken. But the steam release to the condenser is not considered in the post-LDLB activity release to the environment due to the path to the condenser through the turbines and moisture separators, and condenser hold-up time.

Figure 15A-5 in Appendix 15A shows the leakage paths and transport of the activity released to environment, MCR, and TSC during an LDLB event.

15.6.2.5.2 <u>Input Parameters and Initial Conditions</u>

The design basis LDLB accident is analyzed using a conservative set of assumptions and the APR1400 design inputs. Input parameter values used for LDLB radiological consequence evaluation are presented in Table 15.6.2-4.

No fuel damage is postulated for the LDLB accident. Consistent with SRP 15.6.2, it is assumed for the event-generated iodine spike that the primary system transient associated with the LDLB causes an iodine spike in the primary system. The increase in primary coolant iodine concentration is estimated using a spiking model that assumes that the iodine release rate from the fuel rods to the primary coolant increases to a value 500 times greater than the release rate corresponding to the equilibrium primary coolant iodine concentration of 3.7×10^4 Bq/g (1.0 μCi/g) DE I-131. The assumed iodine spike duration is 8 hours. It is assumed that the iodine activity released from the fuel to RCS is mixed instantaneously and homogeneously with the primary coolant. The event-generated iodine spike isotopic iodine activity appearance rates in the RCS are calculated in Table 15A-6.

The maximum RCS noble gas concentration for the APR1400 is 2.15×10^7 Bq/g (580 μCi/g) DE Xe-133 as shown in Table 15A-8.

The RCS flashing fraction is determined to be 0.259 based on the enthalpy difference under circumstance of primary coolant leak by assuming the leakage to be constant enthalpy process. Iodine partition coefficient of 10 is conservatively considered for the unflashed RCS fluid.

The RCS is assumed to leak into the SGs at a P-T-S leak rate of 2.27 L/min (0.6 gpm). It is assumed that the P-T-S leakage into the SGs continues until the primary system pressure is less than the secondary system pressure, or until the temperature of the leakage is less than 100 °C (212 °F) and shutdown cooling is in operation. The RCS is assumed to leak into the SGs for 8 hours until the shutdown cooling system is initialized.

The time required to isolate any break by operator action is conservatively assumed to be 30 minutes.

It is assumed that the chemical forms of iodine released from the steam generators to the environment are 97 percent elemental and 3 percent organic.

All noble gas radionuclides released from the primary system via the P-T-S leak are released to environment without reduction or mitigation. The iodine activity in the bulk water is assumed to become vapor at a rate that is a function of the steaming rate and iodine partition coefficient.

The χ/Q values used in the analysis for EAB, LPZ, MCR, and TSC are described in Subsection 2.3.4 and listed in Tables 2.3-2 through 2.3-12; breathing rates are given in Table 15A-11.

15.6.2.5.3 Results

The radiological consequences due to LDLB accident are presented in Table 15.6.2-5. The results of the LDLB accident analyses indicate that the EAB and LPZ doses due to a LDLB accident with an event-generated iodine spike are within their allowable dose criteria limits, which are 10 percent of the 10 CFR 50.34(a)(1) value as specified in SRP 15.0.3. The MCR and TSC doses are also within the limit in GDC 19.

15.6.2.6 Conclusions

The double-ended break of a letdown line outside the containment upstream of the letdown isolation valve results in a gradual depressurization of the RCS. The minimum DNBR remains above 1.29, thus providing reasonable assurance of fuel cladding integrity. The doses at the EAB, LPZ, MCR, and TSC are within the allowable criteria specified. Also, the RCS pressures remain below 193.34 kg/cm^{2}A (2,750 psia), and the steam generator pressures remain below 92.83 kg/cm^{2}A (1,320 psia).

15.6.3 Steam Generator Tube Failure

The steam generator tube rupture (SGTR) accident is a penetration of the barrier between the RCS and the main steam system and is the result of a double-ended guillotine break of a steam generator U-tube. An SGTR is classified as a PA and is not expected during the lifetime of the plant, but the event is postulated because the consequences include the potential release of significant amounts of radioactivity.

15.6.3.1 SGTR without a Concurrent Loss of Offsite Power

15.6.3.1.1 Identification of Causes and Frequency Classification

The SGTR accident is a penetration of the barrier between the RCS and the secondary system and is the result of the failure of a steam generator U-tube. The integrity of the barrier between the RCS and secondary system is significant in regard to a radiological release. The radioactivity from the leaking steam generator tube mixes with the shell-side water in the affected steam generator (SG). Before the turbine trip, the radioactivity is transported through the turbine to the condenser where the noncondensable radioactive materials are released through the main condenser evacuation system. Following a reactor trip and turbine trip, the main steam safety valves open to control the secondary system pressure. After a reactor trip, the operator begins to cool down the hot leg temperature using the turbine bypass valves to the saturation temperature corresponding to the main steam safety valve (MSSV) opening setpoint. The operator then cools the nuclear steam supply system (NSSS) to shutdown cooling entry conditions using the unaffected SG after isolating the affected SG or verifying that it is isolated. The analysis conservatively assumes that operator action is delayed until 30 minutes after initiation of the event.

Diagnosis of the SGTR accident is facilitated by radiation monitors that initiate alarms and inform the operator of abnormal activity levels and that corrective operator action is required. The detectors are installed in the condenser air ejector exhaust, SG blowdown lines, and main steam line. Additional diagnostic information is provided by RCS pressure and pressurizer level responses indicating a leak and by a level response in the affected SG.

Experience with nuclear SGs indicates that the probability of a complete severance of the Inconel vertical U-tubes is remote. The more probable modes of failure result in considerably smaller penetrations of the pressure barrier. They involve the formation of etch pits or small cracks in the U-tubes or cracks in the welds joining the tubes to the tube sheet.

The most limiting SGTR event is a double-ended rupture of a U-tube at full-power conditions.

A SGTR event is classified as a PA. Each frequency condition is described in Subsection 15.0.0.1. Also see Table 15.0-5.

15.6.3.1.2 Sequence of Events and Systems Operation

Table 15.6.3-1 presents a chronological list of the events that occur during the SGTR transient, from the time of the double-ended rupture of a steam generator U-tube to the attainment of the shutdown cooling entry conditions.

The SGTR event increases the SG level and results in the high steam generator level (HSGL) trip or the generation of a CPC hot leg saturation temperature trip or low DNBR trip due to the decrease in the pressurizer pressure. After the reactor trip, the RCS pressure decreases rapidly, and a safety injection actuation signal is generated on low pressurizer pressure.

After the generation of the main steam isolation signal on HSGL, the main steam isolation valves and the main feedwater isolation valves are closed. The MSSVs are opened to limit secondary system pressure by removing the heat generated or stored in the core and the RCS.

The sequence presented demonstrates that the operator can cool the plant down to the shutdown cooling entry condition during the event.

15.6.3.1.3 Core and System Performance

Evaluation Model

The thermal-hydraulic response of the NSSS to the SGTR without a LOOP is simulated using the CESEC-III code described in Reference 16 of Subsection 15.0.5. The thermal margin on DNBR in the reactor core is determined using the CETOP code described in Reference 7 with the KCE-1 critical heat flux (CHF) correlation described in Reference 28.

Input Parameters and Initial Conditions

The initial conditions and parameters assumed in the analyses of the system response to an SGTR without a concurrent LOOP are listed in Table 15.6.3-2. The values of the initial

conditions are determined to maximize the effect of radioactivity during the SGTR transient with parameter study.

The initial reactor operating conditions are varied over the operating space given in Table 15.0-3 to determine the set of conditions that would produce the most adverse consequences following an SGTR without a concurrent loss of offsite power. The various combinations of initial operating conditions that have been considered include initial core inlet temperature, initial power level, initial RCS pressure, initial core coolant flow rate, initial pressurizer liquid level, initial SG liquid level, and fuel rod gap thermal conductivity.

Decreasing the initial core inlet temperature increases the P-T-S leak rate and integrated leak because of the increase in coolant density. However, a decrease in RCS enthalpy due to a reduced initial core inlet temperature results in decreased flashing fraction and reduced radiological release from the MSSVs. Decreasing the core inlet flow rate results in a higher enthalpy for the fluid entering the SG, resultant increased flashing fraction, and increased radiological release from the MSSVs. Parametric studies indicate that the maximum radiological release is obtained when the transient is initiated with the maximum pressurizer pressure, maximum pressurizer liquid volume, maximum SG secondary liquid volume, maximum core power, minimum core coolant flow, maximum core coolant inlet temperature, and a low fuel rod gap thermal conductivity.

During an SGTR accident, the RCS temperature does not vary significantly after the reactor trip. There are no reactivity feedback effects, and the choice of the moderator temperature coefficient and Doppler reactivity feedback functions is not important. In the SGTR analysis, a scram rod worth of $-8.0\ \%\ \Delta\rho$ is used.

The maximum safety injection increases the primary system pressure and the leakage flow rate. The maximum safety injection has more influence on radiological release than a decrease in flashing fraction due to a decrease in the primary system temperature.

Because the reactor trip occurs earlier, the steam release through the MSSVs increases. The radiological release through the MSSVs is more severe than through the condenser because the partition factor through the MSSVs is assumed to be 1.0 whereas a release through the condenser is assumed to be 100. Therefore, the early trip condition is more conservative because the radiological consequences through the MSSVs are more severe than release paths through the condenser.

The radiological consequences of the SGTR transient are also dependent on the break size. Because the break size is decreased from that of a double-ended rupture, the integral leak is reduced for the 30-minute operator action interval and the radiological consequences are less severe. The radiological consequences of a small tube rupture without the intervention of the reactor protection system (RPS) or the operators would be within the limits of 10 CFR 50.34 because the steam from the affected SG flows through the turbine or steam bypass control system (SBCS) and condenses in the condenser and is cycled back as feedwater to the SG. The major release point for radioactive gases would be the condenser air-ejectors for which a decontamination factor of 100 is applicable. A partition factor of 100 is also applicable in the affected SG. Therefore, a factor of 10,000 is applied on the steam releases to obtain the radiological releases, resulting in significantly small doses. The most adverse break size is a full double-ended rupture of a SG tube combined with a reactor trip.

Results

The dynamic behavior of important NSSS parameters following an SGTR without a concurrent LOOP is presented in Figures 15.6.3-1 through 15.6.3-16.

For a double-ended tube rupture, the P-T-S leak exceeds the capacity of the charging pump. As a result, the pressurizer pressure gradually decreases. The P-T-S leak and the pressurizer level decrease cause the charging flow control valve to increase the charging flow. Even with the maximum charging flow and the pressurizer heaters on, the pressurizer pressure and level continue to drop. At the initiation of the tube rupture, a reactor trip and MSIS are conservatively assumed to be generated due to the SG level reaching an HSGL trip condition. Before the reactor trip, the main feedwater control system is assumed to supply feedwater to SG so that the amount of feedwater can be equal to that of steam entering the turbine.

Following the reactor trip, the secondary system pressure increases until the MSSVs open at 2.4 seconds to control the secondary system pressure. A maximum secondary system pressure of 84.07 kg/cm^{2}A (1,195.76 psia) occurs at 7.95 seconds. Subsequent to this peak pressure, the secondary system pressure decreases, resulting in the temporary closure of the MSSVs. In the absence of feedwater flow due to an MSIS on HSGL at the initiation of the event, the MSSVs cycle open and close to remove decay heat until operator action occurs at 30 minutes after the event initiation.

After 1,800 seconds, the operator identifies and completes isolation of the affected SG. The operator then initiates an orderly cooldown using plant emergency operation procedures. After the pressure and temperature of the reactor coolant are reduced to 31.64 kg/cm^{2}A (450 psia) and 176.67 °C (350 °F) respectively, the operator activates the shutdown cooling system and isolates the unaffected SG.

Figures 15.6.3-1 through 15.6.3-16 represent the results for an SGTR accident without a loss of offsite power. The steam released through the MSSVs and the ADV of the unaffected SG allows the RCS to cool down to shutdown cooling entry condition by removing both sensible heat and decay heat.

Figure 15.6.3-11 gives the MSSV integrated flow versus time for the SGTR without a concurrent loss of offsite power. At 1,800 seconds, when operator action is assumed, no more than 81,193 kg (179,000 lbm) of steam from the affected SG and 66,678 kg (147,000 lbm) from the intact SG is discharged through the MSSVs. During the same time period, approximately 40,715 kg (89,761 lbm) of primary system fluid is leaked to the affected SG. Subsequently, the operator begins a plant cooldown at the Technical Specification cooldown rate (55.6 °C/hr [100 °F/hr]) using the atmospheric dump valves (ADVs) of the unaffected SG or the turbine bypass valves (TBVs). For the first two hours following the initiation of the event, a total of 491,331 kg (1,083,200 lbm) of steam flows from the SG to the condenser. For the 2- to 8-hour cooldown period, an additional 451,778 kg (996,000 lbm) of steam is discharged through TBVs.

15.6.3.1.4 Barrier Performance

The RCS pressure during the event does not exceed 110 percent of the RCS design pressure. Also, the secondary side pressure does not exceed 110 percent of SG design pressure, providing reasonable assurance of the integrity of the main steam system.

15.6.3.1.5 Radiological Consequences

The radiological consequences of the SGTR accident without LOOP are bounded by those of an SGTR accident with a LOOP of Subsection 15.6.3.2.5.

15.6.3.1.6 Conclusions

The radiological releases calculated for the SGTR accident with a LOOP have adequate design margins over the allowable dose limits.

The RCS and secondary system pressures are below 110 percent of the design pressure limits, providing reasonable assurance of the integrity of these systems. The minimum DNBR is greater than the DNBR SAFDL value of 1.29. Therefore, the acceptance criterion regarding fuel performance is met.

The plant is maintained in a stable condition due to automatic actions, and after 30 minutes, the operator uses the plant emergency operating procedure for the SGTR to cool down the plant to shutdown cooling entry conditions.

15.6.3.2 Steam Generator Tube Rupture with a Concurrent Loss of Offsite Power

15.6.3.2.1 Identification of Event and Causes

The significance of an SGTR accident is described in Subsection 15.6.3.1.1. As a result of the loss of normal AC power, electrical power is unavailable for the station auxiliaries such as the RCPs and the main feedwater pumps. Under such circumstances, the plant experiences a loss of load, normal feedwater flow, forced reactor coolant flow, condenser vacuum, and SG blowdown. A LOOP subsequent to the reactor trip and turbine-generator trip is assumed in the analysis because it produces the most adverse effect on the radiological releases. The plant is operating at full power initially before the assumed reactor trip by the RPS. An early reactor trip maximizes radiological releases through MSSVs because the MSSVs open more frequently prior to operator action, releasing radioactive materials to the atmosphere.

The effect of the single failures listed in Table 15.0-4 on the radiological consequences for the SGTR with a LOOP is evaluated. The single failures that may affect the radiological consequences of the SGTR event are the failure on the auxiliary feedwater system, safety injection system, and electrical power system.

With respect to the radiological consequences criteria, there are no single failures that, when combined with the event, result in a more severe radiological consequences than the

SGTR with a LOOP. Therefore, no single failure is considered for the SGTR with a LOOP.

An SGTR event is classified as a PA. Each frequency condition is described in Subsection 15.0.0.1. Also see Table 15.0-5.

15.6.3.2.2 Sequence of Events and Systems Operation

For the SGTR accident with a LOOP, two analyses are performed. The first case is chosen to maximize the impact of the event on the thermal margin, thereby identifying the lowest minimum DNBR during the event. The second case maximizes the offsite radiological release.

Minimum DNBR Case

For this case, the initial conditions are chosen to initiate the tube rupture from a power-operating limit. During the SGTR accident, the pressurizer pressure continuously decreases while the core power, core flow rate, and core average temperature remain constant until a reactor trip is realized. The DNBR also continuously decreases, eroding the thermal margin to DNB. A CPC trip is consequently generated on hot leg saturation temperature trip signal. The turbine trips due to the reactor trip, and a loss of offsite power is assumed concurrent with the turbine trip.

Subsequent to the reactor trip, the core heat flux begins to decrease. The core flow rate also decreases due to the coastdown of the reactor coolant pumps. Since the core flow rate decreases faster than the core heat flux, the DNBR decreases rapidly during a brief period of time subsequent to reactor trip and loss of offsite power.

Maximum Offsite Radiological Release Case

For the maximum offsite radiological release case, the initial conditions and assumptions are chosen to maximize the offsite radiological releases.

Table 15.6.3-3 presents a chronological list of events that occur during the SGTR accident with a LOOP, from the double-ended rupture of a steam generator U-tube to the attainment of cold shutdown cooling entry conditions.

The reactor trip and concurrent turbine trip occur immediately on the HSGL trip signal. No time delay between the turbine trip and LOOP is assumed in the analysis.

Subsequent to a reactor trip, stored and fission product decay energy is dissipated by the RCS and secondary systems. In the absence of a forced reactor coolant flow, heat removal from the reactor core is facilitated by the natural circulation reactor coolant flow. Initially, the residual water inventory in the SGs is used, and the resultant steam is released to atmosphere through the MSSVs. With the availability of standby power, the auxiliary feedwater is automatically initiated on a low steam generator level (LSGL) signal. The operator can identify the affected SG by radioactivity detector or water level variation after the reactor trip. After identifying the affected SG, the operator isolates the affected SG or confirms that it is isolated. Using the plant emergency procedure, the operator continues to cool the NSSS manually using the operation of the auxiliary feedwater system and the ADVs of the unaffected SG. The analysis presented here conservatively assumes that operator action is delayed until 30 minutes after the first indication of the event.

15.6.3.2.3 Core and System Performance

Evaluation Model

The mathematical model used for the evaluation of core and system performance is identical to that described in Subsection 15.6.3.1.3 except for the minimum DNBR calculation. The thermal margin on DNBR in the reactor core is determined using the CETOP.

Input Parameters and Initial Conditions

a. Minimum DNBR case

   The initial conditions and input parameters for this case are chosen to obtain the closest approach to the fuel design limit. The following parametric cases are analyzed to determine the most limiting conditions and parameters: maximum core power, minimum core inlet temperatures, minimum core mass flow rate, and maximum pressurizer pressure. The value of one pin integrated radial peaking factor (F_r) is iterated upon until the power operating limit (POL) conditions are obtained. The maximum Fr value, 1.9786, is used in the analysis.

b. Maximum offsite radiological release case

The input parameters and initial conditions used for this case are identical to those described in Subsection 15.6.3.1.3 and are given in Table 15.6.3-5.

Results

a. Minimum DNBR case

Figure 15.6.3-32 shows the variation of the minimum DNBR during the most limiting SGTR accident with a LOOP with respect to fuel performance. The thermal margin to DNB decreases continuously as a result of the decrease in RCS pressure during the accident. The continuous decrease in RCS pressure is caused by the loss of primary coolant through the ruptured steam generator tube. The reactor trip occurs as a result of a high steam generator level trip signal or hot leg saturation temperature CPC trip signal. Following the reactor trip, the turbine generator is assumed to trip immediately. The offsite power is assumed to be lost concurrent with the turbine generator trips. The reactor trip causes the control rods to drop, resulting in a decrease in the core heat flux. The RCPs begin to coast down in response to the LOOP. Because the core flow rate initially decreases faster (as a result of the RCP coastdown) than the core heat flux, there is a short period during which the DNBR decreases very rapidly (see Figure 15.6.3-32). The core heat flux decreases further, and the imbalance between the heat flux reduction and core flow rate decrease is gradually eliminated. Subsequently, the DNBR increases sharply as the core heat flux is significantly reduced due to the control rods reaching the bottom of the core. As can be seen from Figure 15.6.3-32, the minimum DNBR stays above the specified acceptable fuel design limit of 1.29 throughout the transient. No fuel failure is predicted to occur for the SGTR event with a LOOP.

b. Maximum offsite radiological release case

The dynamic behavior of important NSSS parameters following an SGTR with a LOOP is presented in Figures 15.6.3-17 through 15.6.3-31 for the maximum offsite radiological release case.

Upon a double-ended rupture of a steam generator tube, the steam generator liquid level increases due to the break flow. A reactor trip signal is assumed to be generated on the high steam generator level trip condition to maximize steam releases through MSSVs. Following the reactor trip, the turbine generator is assumed to trip immediately. The offsite power is assumed to be lost concurrent with the turbine generator trips. MSIVs are assumed to close at the same time.

Following the turbine trip and LOOP, the secondary system pressure increases until the MSSVs open at 2.45 seconds to control the secondary pressure. A maximum secondary system pressure of 84.06 kg/cm^{2}A (1,195.55 psia) occurs at 5.55 seconds. Subsequent to this peak in pressure, the secondary system pressure fluctuates around the MSSV opening pressure due to the opening and closing of the valves in order to remove the decay heat until the operator initiates a plant cooldown at 30 minutes after the event initiation.

The primary-to-secondary (P-T-S) leak makes the pressurizer pressure and level continue to drop. The charging flow is terminated due to the LOOP. Due to the LOOP, the reactor coolant pumps begin to coast down, reducing the core coolant flow rate and the mass flow into the upper head region. This region may become thermal-hydraulically decoupled from the rest of the RCS. However, void formation is prevented by maximum safety injection to the RCS.

Prior to the turbine trip, the feedwater control system is assumed to supply feedwater to the SGs to match the steam flow. Following the turbine generator trip and LOOP, the feedwater flow ramps down to zero due to the closing of the MSIVs. Consequently, the SG water levels decrease continuously due to the steam flow out through the MSSVs.

After 1,800 seconds, the operator identifies and isolates the affected SG. The operator then initiates an orderly cooldown by means of the ADVs and auxiliary feedwater flow to the unaffected SG. After the pressure and temperature are reduced to 31.64 kg/cm^{2}A (450 psia) and 176.67 °C (350 °F), respectively, the operator activates the shutdown cooling system and isolates the unaffected SG.

The maximum RCS and secondary pressures do not exceed 110 percent of design pressure following an SGTR event with a concurrent LOOP, providing reasonable assurance of the integrity of the RCS and secondary system.

Figure 15.6.3-27 gives the MSSV integrated flow rates versus the time for the SGTR accident with a LOOP. At 1,800 seconds, when operator action is assumed, no more than 77,600 kg (171,000 lbm) of steam from the affected SG and 64,400 kg (142,000 lbm) from the unaffected SG are discharged through the MSSVs. During the same period, approximately 40,200 kg (88,640 lbm) of primary system mass is leaked to the affected SG. The operator subsequently begins a plant cooldown at the Technical Specification cooldown rate (55.6 °C/hr [100 °F/hr)]) using the intact SG, atmospheric dump valves, and auxiliary feedwater system. For the first 2 hours following the initiation of the event, about 463,000 kg (1,021,000 lbm) of steam is released to the environment through the ADVs. For the 2- to 8-hour cooldown period, an additional 586,000 kg (1,293,000 lbm) of steam is released through the ADVs.

Because of the delayed isolation of the AFW flow in the affected SG, the level in the SG approaches 90 percent wide range. The SG does not overfill during 30 minutes after the initiation of the event.

15.6.3.2.4 Barrier Performance

The RCS pressure during the event does not exceed 110 percent of the RCS design pressure. The secondary side pressure also does not exceed 110 percent of design pressure, providing reasonable assurance of integrity of the main steam system.

15.6.3.2.5 Radiological Consequence

The radiological consequences are performed to determine EAB, LPZ, MCR, and TSC doses due to a SGTR accident using the AST methodology, the TEDE dose criteria, guidance in NRC RG 1.183, Appendix F, and the plant-specific bounding design information applicable to the APR1400 including the maximum allowed accident induced P-T-S leak rate.

15.6.3.2.5.1 Evaluation Model

The following transport models of radioactive materials are applied to evaluate radiological consequences due to SGTR.

Release through the Affected Steam Generator

The post-SGTR thermal hydraulic condition in the affected SG is such that a large amount of RCS coolant released through the ruptured tube increases the secondary side coolant mass inventory, which eliminates the possibility of a steam generator dryout condition. The iodine and noble gas in the P-T-S rupture flow is assumed to flash to vapor in the affected SG and be released to the environment without mitigation. The P-T-S rupture flow that does not flash is assumed to mix with the secondary liquid during the periods of SG tube submergence. The contaminated steam present in the affected SG is released to the environment through the MSSVs until operator action is taken to open the ADV aligned to the unaffected SG. The radioactivity in the bulk water is assumed to become vapor at a rate that is the function of the steaming rate and the partition coefficient.

Release via the Unaffected Steam Generator

With regard to the unaffected SG used for plant cooldown, the P-T-S leakage is assumed to mix with the secondary water without flashing during periods of total tube submergence and become vapor at a rate that is a function of the steaming rate and an assumed iodine partition coefficient. The steam release from the unaffected SG continues to 8 hours until the shutdown cooling system is aligned to dissipate heat.

Release via the Condenser

Prior to the LOOP, the contaminated secondary steam in the unaffected and affected SG is released to the condenser. But the steam release to the condenser is not considered in the post-SGTR activity release to the environment due to the path to the condenser through the turbines and moisture separators, and condenser hold-up time.

Figure 15A-6 in Appendix 15A shows the leakage paths and transport of the activity released to environment, MCR, and TSC during an SGTR event.

15.6.3.2.5.2 Input Parameters and Initial Conditions

The design basis SGTR accident is analyzed using a conservative set of assumptions based on NRC RG 1.183, Appendix F and the APR1400 design inputs. Input parameter values used for SGTR radiological consequence evaluation are presented in Table 15.6.3-5.

Since no fuel damage is postulated for the SGTR event, the activity released is the maximum RCS activity allowed by the Technical Specifications. Two cases of iodine spiking corresponding to a pre-accident iodine spike and an event-generated iodine spike are assumed.

It is assumed for the pre-accident iodine spike that a reactor transient has occurred prior to the postulated SGTR and has raised the primary coolant iodine concentration to the maximum value of 2.22×10^6 Bq/g (60 μCi/g) DE I-131.

For the event-generated iodine spike, the primary system transient associated with the SGTR causes an iodine spike in the primary system. The increase in primary coolant iodine concentration is estimated using a spiking model that assumes that the iodine release rate from the fuel rods to the primary coolant, which is expressed in curies per unit time, increases to a value 335 times greater than the release rate corresponding to the equilibrium primary coolant iodine concentration of 3.7×10^4 Bq/g (1.0 μCi/g) DE I-131. The assumed iodine spike duration is 8 hours. It is assumed that the iodine activity released from the fuel to RCS is mixed instantaneously and homogeneously with the primary coolant.

The maximum RCS noble gas concentration for the APR1400 is 2.15×10^7 Bq/g (580 μCi/g) DE Xe-133.

The total primary coolant break flow into the affected SG is 64,200 kg (141,448 lbm), which is calculated by thermal-hydraulic analysis.

The RCS is assumed to leak into the unaffected and affected SGs at a P-T-S leak rate of 2.27 L/min (0.6 gpm). The total primary coolant flow into the unaffected and affected SG via P-T-S is 1,090 kg (2,404 lbm). The P-T-S leakage into the SG continues until the primary system pressure is less than the secondary system pressure, or until the temperature of the leakage is less than 100 °C (212 °F) and shutdown cooling is in operation.

It is assumed that all noble gas radionuclides released from the primary system are released to environment without reduction or mitigation. The radioactivity in the bulk water is assumed to become vapor at a rate that is the function of the steaming rate and the partition coefficient.

The chemical forms of iodine released from the steam generators to the environment are assumed to be 97 percent elemental and 3 percent organic.

All noble gas radionuclides released from the primary system via the P-T-S leak are released to environment without reduction or mitigation.

The χ/Q values used in the analysis for EAB, LPZ, MCR, and TSC are described in Subsection 2.3.4 and are in Tables 2.3-2 through 2.3-12, and the breathing rates are given in Table 15A-11.

15.6.3.2.5.3 Results

The radiological consequences due to SGTR accident are presented in Table 15.6.3-6. The results of the SGTR accident with pre-accident and event-generated iodine spike analyses indicate that the EAB and LPZ doses due to an SGTR accident with pre-accident and event-generated iodine spike are within their allowable dose criteria limits, which are 100 percent and 10 percent of the 10 CFR 50.34(a)(1) value, respectively. The MCR and TSC doses are also within the dose limit in GDC 19.

15.6.3.2.6 Conclusions

The radiological consequences for the SGTR accident with a LOOP are within the allowable criteria. The RCS and secondary system pressures are below the 110 percent of the design pressure limits, thus providing reasonable assurance of the integrity of these systems. The minimum DNBR is above the DNBR SAFDL value of 1.29. The acceptance criterion regarding fuel performance is met.

For the limiting SGTR event with respect to SG overfill considerations (SGTR with a LOOP), the maximum liquid inventories do not result in an overfill and consequent introduction of liquid water into the steam lines, providing reasonable assurance of the integrity of these steam lines.

After 30 minutes, the operator uses the plant emergency procedure for the SGTR to cool down the plant to shutdown cooling entry conditions.

15.6.4 Radiological Consequences of Main Steam Line Failure Outside Containment (Boiling Water Reactor)

Not applicable to the APR1400.

15.6.5 Loss-of-Coolant Accidents Resulting from the Spectrum of Postulated Piping Breaks within the Reactor Coolant Pressure Boundary

15.6.5.1 Identification of Causes and Frequency Classification

Loss-of-coolant accidents (LOCAs) are hypothetical accidents that result from the loss of reactor coolant at a rate that exceeds the capability of the reactor coolant makeup system. The cause is breaks in the pipes in the reactor coolant pressure boundary up to and including a break equivalent in size to the double-ended rupture of the largest pipe in the RCS.

In the accident analyses for the APR1400, large break and small break LOCAs are both classified as postulated accidents (PAs). They are not expected to occur during the life of the plant but are postulated as a conservative design basis.

15.6.5.2 Sequence of Events and Systems Operation

15.6.5.2.1 Description of Large Break Loss-of-Coolant Accident

A cold leg break between the outlet of the reactor coolant pump (RCP) and the corresponding reactor vessel (RV) inlet nozzle is found to be the most limiting with respect to the peak cladding temperature (PCT) in a large break LOCA. The large break LOCA analysis assumes a LOOP. The RCPs lose ac power and coast down after the LOOP. In order to determine the limiting break size, a guillotine break spectrum of a 100, 80, and 60 percent break area is studied. The blowdown PCT is a maximum when the break area is 100 percent of the cold leg cross-sectional area. The reflood PCT is a maximum when the break area is 80 percent. However, because the reflood PCT is not as high as the blowdown PCT, the 100 percent break size is chosen as the limiting guillotine break case.

In the 100 percent guillotine break, the total break area is two times the cold leg cross-sectional area. A 200 percent slot break shows lower PCT in the blowdown period and the transient is found to be faster by about 4 seconds than that of the 100 percent guillotine break. The PCT of the reflood phase is lower than that of the guillotine break, and the fuel

quenching is somewhat earlier. The 100 percent double-ended guillotine break in a cold leg is determined to be the limiting case.

The scenario is divided into four periods that characterize the events during the transient. The periods are blowdown, refill, early reflood, and late reflood and are defined by the inventory of the reactor pressure vessel and the flow condition of safety injection tank with fluidic device (SIT-FD).

A blowdown is defined as the period from the opening time of the break to the start time of the SIT-FD injection. The refill period is defined as the period from the start time of the SIT-FD injection to the time when the mixture level in the reactor vessel lower plenum reaches the bottom of the active core. The definitions of these two periods are the same as those of the conventional LBLOCA scenario in PWRs.

Unlike the conventional scenario, the reflood period is divided into early reflood and late reflood periods based on the time in which the SIT-FD becomes empty. The division is intended to address any possibility of core heatup during the late reflood period in detail because the APR1400 does not have a low-pressure safety injection pump.

Blowdown Period

The blowdown period starts when the break opens and ends when an SIT-FD injection is initiated; blowdown lasts for approximately 15 seconds. During blowdown, the primary coolant is rapidly expelled into the containment through the break. The reactor coolant changes from a subcooled liquid to a two-phase mixture or pure steam due to fluid flashing. By roughly 6 seconds, the core region begins to dry out.

The initial break flow is very high, reflecting the subcooled critical flow at the break. Mass flow from the reactor vessel side of the break is larger than that from the pump side due to the higher hydraulic resistances of the pump and the SG. As the break flow develops in the reverse direction from the core to the break as well as in the positive direction, the core flow rapidly stagnates and then reverses shortly after the break occurs.

As the primary system depressurizes, flashing occurs first in the hot regions of the system, such as the upper plenum, hot leg, pressurizer, and core, and then proceeds to the relatively

cold regions, such as the lower plenum, downcomer, and cold legs. Extensive voiding occurs in all areas of the reactor pressure vessel. Nucleate boiling develops in the core. Fission power that is calculated by a kinetics model drops to the level of decay heat due to the voiding in the core. The flashing also reduces the primary system depressurization rate.

When the critical heat flux (CHF) condition is reached in the core, heat transfer changes from nucleate boiling to post-CHF heat transfer regimes (i.e., transition boiling, film boiling, and forced convection to vapor), and much of the core dries out. Fuel rod cladding temperatures increase rapidly due to the degrading rod-to-fluid heat transfer. The cladding temperature increase during the early blowdown period is terminated by several processes:

a. First, as the core rapidly voids, the core power immediately decreases via void reactivity insertion.

b. Second, the flow at the core reverses after stagnation.

c. Third, the large coolant inventory of the upper guide structures (UGSs) and upper head moves toward the top of the core by two paths, through the UGS drainage holes in the UGS bottom plate between the UGS and upper plenum and through the guide tube pipes that terminate in the upper inactive core.

As the low pressurizer pressure setpoint is reached, the reactor is tripped. Reactor coolant pumps (RCPs) are modeled to trip and coast down from the beginning of the accident assuming a LOOP. As the primary system pressure continues to decrease, flashing develops in the cold regions of the system. The resultant voiding occurring in the RCP degrades its pumping performance. The break flow rate decreases rapidly as the flow regime changes from subcooled to saturated critical flow at the break.

Four SIT-FDs begin to deliver flow into the four direct vessel injection (DVI) lines when the primary system pressure falls below its actuation setpoint. The coolant flows through the DVI nozzles into the upper annulus and then begins to refill the reactor pressure vessel. Because the reactor coolant system is still depressurizing, some of the coolant entering the upper annulus is swept out to the break along with entrained liquid from the lower plenum and the downcomer. Although the break flow remains high, the coolant is delivered

downward into the downcomer and increases the downcomer water level. Then the coolant injected by the SIT-FD eventually reaches the lower plenum.

Refill Phase

The refill period begins when the SIT-FD injection flow is initiated and ends when the water level in the lower plenum reaches the core inlet.

Emergency core cooling (ECC) water in the reactor vessel downcomer can flow down by gravity or be swept out to the break by the pressure differential and upward-escaping steam flow that levitates the liquid. Reactor vessel walls and internals are considered as the large metal structures at temperatures above saturation. When subcooled ECC water comes into contact with the metal structures in the downcomer, steam is generated by nucleate boiling, reducing the gravitational head of the fluid in the downcomer. The process of liquid penetration and sweep-out repeats in the downcomer and direct-contact condensation of steam on the subcooled ECC water continues in the upper annulus.

The depressurization of the system wanes as the differential pressure between the RCS and the containment reduces. Owing to the gradual reduction of flashing and break flow, the rate of liquid penetration into the lower plenum increases. With a decreasing steam flow rate, a small amount of the ECC injection is bypassed, and most of it flows downward to fill the downcomer and the lower plenum. At this stage, water levels in the downcomer and the lower plenum increase rapidly.

Heatup, which is almost adiabatic, continues in the core during this period because there is no inventory to cool the core.

The refill period ends when the liquid level in the lower plenum reaches the bottom of the active core.

Early Reflood Phase

The early reflood period begins when the lower plenum is completely filled with water and ends when the SIT-FD water is depleted. Near the beginning of the early reflood period,

the safety injection pumps (SIPs) begin to inject water. Initially, the core reflood is quite rapid because of the following:

a. The downcomer remains filled with water by the ECC injection.

b. The high flow injection of SIT-FD continues.

c. There is little loop steam flow and hydraulic resistance in the loop is therefore low.

d. There is no severe steam binding.

The maximum SIT-FD injection flow is reached during this period. High flow injection through the standpipe becomes unavailable, and only the flow through the fluidic-device becomes injected. During the high-flow injection, the downcomer and core liquid levels increase rapidly. As the downcomer liquid level approaches the level of the cold legs, much of the coolant spills out of the break, and the vessel side break flow tends to increase. When the water level in the SIT-FD decreases to below the top of the standpipe, the low-flow injection begins. Water levels in the downcomer and core decrease slightly, but the levels increase again within approximately 10 seconds, maintaining downcomer water level above the level of the cold legs. The combined SIP and SIT-FD flows are injected to maintain the water level in the downcomer and to retard core heatup.

In the core, heat transfer regimes encompass the entire spectrum. The regimes include single-phase liquid convection, nucleate boiling, transition boiling, film boiling, and single-phase vapor convection.

Local quenching could occur due to droplet de-entrainment at the fuel alignment plate and spacer grids. Vapor velocities and liquid entrainment in the central region of the core are higher due to the higher power of this region. The entrained liquid could have a cooling effect on the upper region of the core. Some of the entrained liquid is de-entrained at the fuel alignment plate, and the remainder is carried into the upper plenum, forming a two-phase pool. Liquid from the pool can re-enter the low-powered regions of the core through the fuel alignment plate due to the lower vapor velocities in those regions. A three-dimensional flow pattern can therefore occur: water flows from low-powered to high-powered regions in the core, while the flow is in the opposite direction in the upper plenum.

Liquid from the upper plenum pool may be further entrained and carried over into the hot legs and SGs.

As reflooding progresses upward from the lower core region, more liquid is entrained to the upper plenum, and the level of the two-phase mixture in the pool can reach the hot leg. When the entrained liquid reaches the U-tubes of the SGs, it is vaporized by reverse heat transfer from the secondary side to the primary side. Due to the vaporization in the U-tubes, hot side pressure increases and causes steam binding, which deteriorates the reflooding of the core. Because the steam generation rate in the core decreases due to the lower reflood rate, liquid entrainment and the steam binding effect decrease, causing the reflood rate to increase again. Through this cyclical process, the entire core eventually becomes reflooded. The increase of core pressure due to the steam binding causes manometric oscillations between levels in the downcomer and the core.

The early reflood period ends when SIT-FDs are emptied.

Late Reflood Phase

The late reflood period begins when the SIT-FDs are emptied. ECC water is supplied only by the SIPs during this period.

Water level in the downcomer decreases somewhat as the SIT flow stops at the beginning of the late reflood period and falls below the level of the cold legs. Then the core water level becomes stabilized. Liquid levels in the downcomer and core become balanced within approximately 20 seconds. Due to the decreased flow of coolant into the downcomer, liquid temperature in the downcomer can increase to a near saturation temperature under the influence of the residual heat of the metal structures (i.e., vessel walls in the downcomer). Boiling can occur on the surface of the walls depending on the conditions. ECC water is provided by the four SIPs, the possibility of downcomer boiling is suppressed, and the core is found to remain amenable to cooling.

Because the entire core remains in a quenched state during this period, steam generation in the core is not significant enough to cause any severe ECC water bypass during this period.

Only safety-related systems or components are credited to mitigate the accident, as follows:

a. Normally operating plant instrumentation and controls

   Steady-state conditions of a large break LOCA are calculated at the normal operating plant conditions (e.g., power, flow rate, pressure, temperature).

b. Reactor protection system (RPS)

   The reactor trip signal is generated from the low pressurizer pressure during the large break LOCA. The trip signal also generates the turbine trip and RCP trip automatically. Coastdown of the RCP progresses after the RCP trip. However, because the CEA insertion is not used for large break LOCAs, the negative reactivity of CEA is not credited. For the small break LOCA, the CEA insertion is credited including the signal delay.

c. Engineered safety feature actuation system (ESFAS)

   An ESFAS is generated from the low pressurizer pressure or high-containment pressure during the large break LOCA. Low pressurizer pressure is credited only in the LOCA analysis and actuates the containment isolation actuation signal (CIAS) and safety injection actuation signal (SIAS).

d. Safety injection system (SIS)

   During the LOCA, the SIS provides the direct vessel injection. The discharge of each SI pump and SI tank is piped directly to a reactor vessel nozzle where the flow is directed into the reactor vessel downcomer region. Storage of fluid for the SIS is accomplished by the IRWST, which contains borated fluid.

e. Containment spray system (CSS)

   The containment spray (CS) system is designed to reduce containment pressure and temperature from a main steam line break or LOCA and to remove fission products from the containment atmosphere following a LOCA. The CS system uses the IRWST and has two independent trains. During the large break LOCA, CSS is automatically actuated on a high-high containment pressure signal. Maximum

containment spray capacity is assumed to calculate the minimum containment pressure, which is described in Subsection 6.2.1.5.

15.6.5.2.2 Description of Small Break Loss-of-Coolant Accident

Small break LOCA behavior differs according to the break size. When the break is small, the coolant inventory can be kept by the SIP. In this case, cooling and depressurization using an SG are performed by the operator. If break size increases, release flow cannot be compensated sufficiently by the SIP.

Small break LOCA behavior can also differ according to the break location. A DVI line break LOCA, known as the most limiting, can be generally divided into the following five phases: blowdown, natural circulation, loop seal clearing, core boil-off, and core recovery. The break size and system characteristics determine whether a phase occurs and the duration of the phase

Blowdown Phase

The RCS pressure is abruptly decreased by the break. If RCS pressure reaches the low-pressure steam generator reactor trip setpoint, the reactor is scrammed by control rod dropping. The RCS pressure decreases to the steam generator low-low safety injection signal occurrence setpoint. The safety injection water is injected into the RCS after a delay such as the pump starting time. The RCS is mostly filled with fluid during the blowdown phase. Subcooling and saturation state coolant is released through the break region into the containment. If the RCS pressure decreases and then reaches quasi-equilibrium, the blowdown phase is over.

Natural Circulation

Thermal quasi-equilibrium can last for several hundred seconds according to the break size. RCPs are not operated for this time, and there is therefore no forced circulation. Heat transfer from the primary system to the secondary system is performed by the natural circulation of a single phase of two phases. The coolant is drained gradually from the RCS upper region, and phase separation is then executed in order, beginning with steam generator U-tube upper region, followed by the core upper head and reactor upper plenum. Core decay heat is then removed by break flow and the steam generator. Because the loop

seal is filled with coolant, it cannot make an effective steam release path, so steam generated from the core cannot be released smoothly.

Loop Seal Clearing

The loop seal clearing phase is from the natural circulation cut-off to the loop seal clearing. If the coolant level in the loop seal becomes lower than the top of pump suction horizontal part, the loop seal is cleared, and steam confined in the system is then released through the break region. Before the loop seal clearing, the two-phase fluid level in the core is abruptly decreased for a short period so that core uncovery can occur. After the loop seal clearing, if the pressure unbalance in the RCS is relieved, the core water level is recovered up to cold leg height.

Core Boil-Off

After the loop seal clearing occurs, the coolant in the core is evaporated by decay heat, the core water level is gradually decreased again, and core uncovery can occur. At this time, clad temperature can reach a peak point. If the RCS pressure decreases and the safety injection flow rate exceed the break flow rate, the core water level is started to be recovered.

Core Recovery

Core recovery is continued from the time the core water level reaches the minimum level until the core is filled with water and the core is cooled sufficiently by the recovered water level.

The effects of automatic tripping of the RCPs on small break LOCAs (TMI Action Item II.K.3.5) were reported in CEN-268 (Reference 75), which identifies the RCP trip methodology.

15.6.5.2.3 Description of Post Loss-of-Coolant Accident Long-Term Cooling

Immediately following a LOCA, safety injection is initiated to mitigate the short-term consequences of the event by replenishing the lost coolant. Safety injection is characterized by the automatic actuation of injection pumps and the passive operation of injection tanks. Responses by operators are not required in the short term after a LOCA.

The post-LOCA long-term period is defined as beginning when the core is reflooded and ending when the plant is secured. During the long term, operator action is needed to provide reasonable assurance that the core cooling is maintained until the plant is brought to a cold shutdown condition.

The basic function of long-term cooling (LTC) is to maintain the core at safe temperature levels while avoiding the precipitation of boric acid in the RCS. The capability of performing this basic function is reasonably assured until such time that the fuel assemblies are removed from the reactor vessel.

The analysis procedures account for single-failures to provide reasonable assurance that the performance objectives are met even with this assumption. There is a behavioral difference between large and small break LOCAs in the long term. This difference is that the RCS will remain at high pressure for small breaks and the injection flow rate will be too low for effective cooling; thus, small breaks require cooling of the RCS by the SGs until shutdown cooling (SDC) can be initiated. Large breaks, on the other hand, are adequately cooled by the injection flow because this flow is large due to the low RCS pressure; however, large breaks use simultaneous hot leg and cold leg injection to flush boric acid from the vessel. As a consequence, the LTC large break and small break analyses are different.

15.6.5.3 Core and System Performance

15.6.5.3.1 Evaluation Model

The acceptance criteria for the emergency core cooling system (ECCS) for light water-cooled reactors are provided in 10 CFR 50.46 (Reference 62). The analyses presented in this section demonstrate that the APR1400 design satisfies these criteria.

Analyses are performed for a complete spectrum of break sizes. The most limiting break, which limits the peak linear heat generation rate (PLHGR), is identified as the 1.0 (discharge coefficient) × double-ended guillotine at the pump discharge (DEG/PD) break. The results of the analyses demonstrate that for a PLHGR of 446.2 W/cm (13.6 kW/ft), the APR1400 SIS design meets the acceptance criteria of Reference 62. Requirements are as follows:

a. Criterion 1 – Peak Cladding Temperature

   The calculated maximum fuel element cladding temperature shall not exceed 1,204 °C (2,200 °F).

b. Criterion 2 – Maximum Cladding Oxidation

   The calculated total oxidation of the cladding anywhere shall not exceed 0.17 times (17 percent) of the total cladding thickness before oxidation.

c. Criterion 3 – Maximum Hydrogen Generation

   The calculated total amount of hydrogen generated from the chemical reaction of the cladding with water or steam shall not exceed 0.01 times (1 percent) the hypothetical amount that would be generated if all of the metal in the cladding cylinders surrounding the fuel, excluding the cladding surrounding the plenum volume, were to react.

d. Criterion 4 – Coolable Geometry

   Calculated changes in core geometry shall be such that the core remains amenable to cooling.

e. Criterion 5 – Long-Term Cooling

   After any calculated successful initial operation of the ECCS, the calculated core temperature shall be maintained at an acceptably low value, and decay heat shall be removed for the extended period of time required by the long-lived radioactivity remaining in the core.

<u>Large Break Loss-of-Coolant Accident Evaluation Model</u>

The large break LOCA analysis is performed using the CAREM (Reference 63) realistic evaluation methodology for the criteria of 10 CFR 50.46 (Reference 62). This methodology is based on the model and assumption described in NRC RG 1.157 (Reference 64).

In CAREM, the RELAP5/MOD3.3 Code (Reference 65) is used for the calculation of ECCS thermal-hydraulics behavior and cladding temperature. Containment back pressure and temperature calculations are performed by the CONTEMPT4/MOD5 Code (Reference 66). Containment back pressure affected by the mass and energy release rate, and thermal-hydraulics phenomena is dependent on the containment back pressure. RELAP5/MOD3.3 and CONTEMPT4/MOD5 are merged to exchange their results in every time step.

CAREM quantifies the overall calculation uncertainty by propagating the uncertainty of each parameter. The ranges of uncertainty parameters are determined by auxiliary calculations and literature survey and confirmed by checking experimental data. To quantify the PCT at a 95 percent probability with a 95 percent confidence level, 124 times random sampling calculations are performed adopting non-parametric statistics. This methodology extrapolates the code accuracy to quantify the uncertainty that is applied to plant calculations.

A total of 124 input vectors are generated by random sampling, and simple random sampling (SRS) analyses are performed with the application of each input vector. The code uncertainty parameters and their ranges are determined by the evaluation of the code accuracy and confirmation of data covering processes. PCT is determined by applying Wilks' Formula to the SRS results in a 95 percent tolerance limit at a 95 percent confidence level.

Cases in which the reflood peak clad temperature differences within 100K compared with the highest reflood peak are selected for scale bias calculations, extracting the highest two cases from 124 cases of SRS. Code biases in the prediction of ECC water bypass and steam binding are evaluated separately. Steam binding bias is evaluated by combining the results of two bias evaluations of droplet de-entrainment in the upper plenum of the reactor vessel and droplet evaporation in the steam generator U-tube. The final values of the third PCT considering the uncertainties of the automatic time step control function and data reading frequency of RELAP5 are suggested for the comparison of LOCA criteria.

Small Break Loss-of-Coolant Accident Evaluation Model

The calculations presented in this section are performed using the small break evaluation model, which is described in Reference 67 and approved by the Nuclear Regulatory

Commission (NRC) in Reference 68. The CEFLASH-4AS (Reference 69) computer program is used to determine the primary system hydraulic parameters during the blowdown phase, and the COMPERC-II (Reference 70) computer program is used to determine the system behavior during the reflood phase. Fuel rod temperatures and clad oxidation percentages are calculated using the STRIKIN-II (Reference 71) and PARCH (Reference 72) computer programs. The interface between these programs is described in detail in Reference 67.

The small break evaluation model already met the requirements of TMI action item II.K.3.30 and II.K.3.31. Details are respectively described in Reference 23 and Section 15.6.5.3.

Post Loss-of-Coolant Accident Long-Term Cooling Evaluation Model

Long-term cooling (LTC) initiates when the core is quenched after a LOCA and terminates when the plant is secured. The objectives of LTC are to maintain the core at safe temperature levels and to avoid the precipitation of boric acid in the core region. To accomplish these objectives, an LTC analysis was performed using the codes and methods documented in Reference 73.

The LTC plan uses one of two procedures depending on the break size. The shutdown cooling system (SCS) is used if the break is sufficiently small that reasonable assurance of a successful operation of the SCS is provided. For large break LOCAs, a simultaneous hot leg and direct vessel injection is used to maintain core cooling and boric acid flushing. The plant operator initiates the appropriate procedure based on the indicated RCS pressure.

Figure 15.6.5-34 shows the LTC sequence of events and the schedule for operator actions for the LTC plan. The operator’s first action is to initiate cooldown within 1 hour post-LOCA by releasing steam from the SGs. The steam is released through the turbine bypass system if available or through the atmospheric dump valves. Between 1 and 3 hours post-LOCA, the operator isolates or vents the safety injection tanks (SITs) to avoid injecting a large quantity of nitrogen (noncondensable) gas into the RCS. Between 1 and 4 hours post-LOCA, pressurizer cooldown is initiated. Between 2 and 3 hours post-LOCA, the discharge lines of SIP 3 and 4 are realigned to the hot legs to divide the SIP flow between the hot leg and direct vessel injection connections.

If the RCS pressure is above 31.6 kg/cm^{2}A between 8 to 9 hours post-LOCA, the RCS is filled, which provides reasonable assurance that proper suction is available for entering shutdown cooling. Cooling of the RCS continues until the indicated RCS temperature is lower than the maximum SDC entry temperature including instrument uncertainty. The operator then throttles the SIPs until the RCS pressure is reduced to shutdown cooling entry pressure, including instrument uncertainty, and initiates shutdown cooling.

A prerequisite to throttling or terminating SI flow is that the RCS is in a subcooled condition for the indicated RCS pressure. While reducing RCS pressure to initiate SCS operation, the operator maintains subcooling of the RCS consistent with the emergency operating procedures.

If the SCS is inoperable, the alternative for decay heat removal is the continued use of the SGs. This requires the continued availability of auxiliary feedwater and the atmospheric dump valves or the turbine bypass system. If the SCS becomes operable later, it is put into operation. This path is indicated by the dashed lines in Figure 15.6.5-34.

If the indicated RCS pressure falls below 31.6 kg/cm^{2}A at 8 to 9 hours, the break may be too large for absolute assurance that proper suction is available for the shutdown cooling mode. In this event, a simultaneous hot leg and direct vessel injection by itself cools the core and also flushes the reactor vessel indefinitely.

15.6.5.3.2 Input Parameters and Initial Conditions

Large Break Loss-of-Coolant Accident

The SIS consists of four safety injection pumps (SIPs) and four safety injection tanks (SITs). Automatic operation of the SIPs and valves is actuated by a low pressurizer pressure signal or a high containment pressure signal. Flow is initiated from the SITs by the opening of a check valve when the reactor vessel downcomer pressure drops below the SIT pressure. A fixed internal device in the SI tank regulates the flow rate with changing level and pressure. SI flow is delivered by DVI connections.

The most limiting single failure for a large break LOCA is the loss of one SIP train. However, two of the four SIPs are conservatively assumed to be available. The available

SIP injection located near the broken cold leg with another available injection located on the opposite side of broken cold leg is the limiting condition for the large break analysis.

The operating parameters and ranges for the plant uncertainty evaluation determined in large break LOCA analysis are listed in Table 15.6.5-1. Core and system parameters are prepared by using measurement uncertainty ranges or determined to cover the minimum and maximum ranges of the design data or the limit of the Technical Specifications.

The large break analysis accounts for 10 percent tube plugging of the steam generator tubes that may occur during the life of the plant.

The accidents are assumed to occur at the initial burnup for the large break analysis. The stored energy is the maximum value because the fuel elements show the most densification at the initial burnup (BOC), and the burnup yields the highest cladding temperature in the large break LOCA.

Subsection 6.2.1.5 presents the minimum containment pressure analysis that is performed in the analysis of ECCS performance. The analysis identifies the containment parameters used in the large break analysis. The values for the containment parameters are chosen to minimize containment pressure to minimize the core reflood rate.

The worst break in the large break analysis is the double-ended guillotine at the RCP discharge leg (Reference 63). To determine the limiting break size, a guillotine break spectrum of 100 percent, 80 percent, and 60 percent break areas are analyzed, and the limiting break size is applied for 124 cases of SRS calculation.

Small Break Loss-of-Coolant Accident

The safety injection system (SIS) consists of four direct vessel injection lines, each supplying flow from one SIT and one SIP. Offsite power is conservatively assumed to be lost upon reactor trip, and the SIPs therefore await diesel startup and load sequencing before they can start. The total time delay assumed is 40 seconds from when the SIAS setpoint is reached to when the full SI flow is delivered to the RCS. For breaks in the DVI line, all safety injection flow delivered to the broken line is assumed to spill out of the break.

An analysis of the possible single failures that can occur within the SIS shows that the worst single failure for the small break spectrum is the failure of one SI pump train. This failure causes a loss of two of the four SIPs with additional conservativeness, thereby minimizing the safety injection available to cool the core.

Based on the above assumptions, the following safety injection flows are credited for the small break analysis:

a. For a break in the pump discharge leg, the SI flow credited is full flow from two SIPs and four SITs.

b. For a break in a DVI line, the SI flow credited is full flow from one SIP and three SITs. The flow from the remaining active SIP and from one SIT is assumed to spill out of the break.

Table 15.6.5-6 presents the SI pump flow rates assumed at each of the four injection points as a function of RCS pressure.

The significant core and system parameters used in the small break calculations are presented in Table 15.6.5-7. PLHGR of 492.0 kW/m (15.0 kW/ft) is assumed to occur 15 percent from the top of the active core. A conservative beginning-of-life moderator temperature coefficient of 0.0×10^{-4} $\Delta\rho$/°C (0.0×10^{-4} $\Delta\rho$/°F) was used in all small break calculations.

The initial steady-state fuel rod conditions are obtained from the FATES3 (Reference 74) computer program. The small break analysis uses a hot rod average burnup, which maximizes the amount of stored energy in the fuel.

The small break analysis uses the containment parameters of the initial containment pressure and the maximum containment volume. Containment parameters do not influence the small break analysis because the break flow stays critical.

Post Loss-of-Coolant Accident Long-Term Cooling

The major assumptions used in performing the LTC analysis are as follows:

a. No offsite power is available.

b. The worst single failure is the loss of two SI pump trains with additional conservativeness. This results in the following:

   1) Two SIPs are operable.

   2) One motor-driven auxiliary feedwater pump is operable.

c. One atmospheric dump valve on each SG is available to cool down the RCS.

d. RCS cooldown begins at 2 hours post-LOCA.

e. The SITs are vented or isolated before establishing shutdown cooling conditions for the small break LTC procedure.

f. The pressurizer is depressurized to establish shutdown cooling conditions for the small break LTC procedure.

g. RCS cooldown is terminated when the hot leg temperature is below the maximum shutdown cooling entry temperature including instrument uncertainty.

h. Pump flow rates and initial water source inventories used in the large break LOCA boric acid precipitation analysis are selected to maximize the boric acid concentration in the core.

i. A boric acid precipitation limit of 29.3 weight percent (Reference 73) is used in the large break LOCA boric acid precipitation analysis. This limit is based on a conservative containment pressure of 1.03 kg/cm^2A.

Significant core and system parameters used in the post-LOCA long-term cooling analysis are presented in Table 15.6.5-12.

The IRWST sump strainer related to GSI-191 is designed to provide reasonable assurance that debris quantities are maintained within the bounds of a post-LOCA long-term cooling analysis. See Subsection 6.8.2.2 for further information.

15.6.5.3.3 Results

Large Break Loss-of-Coolant Accident Analysis Results

Major input variables used in the performance evaluation of the SIS in a large break LOCA are summarized in Table 15.6.5-2. The important results such as the PCT, PCT location, and time results for large break LOCA spectrum analyses are listed in Table 15.6.5-3. Major times of interest are listed in Table 15.6.5-4. The transient behaviors of the NSSS parameters are shown in Figures 15.6.5-2 through 15.6.5-23.

The most limiting break is a 100 percent of double-ended guillotine at the pump discharge break. Hence, a SRS calculation is performed for a 100 percent double-ended guillotine break.

The cladding temperature behavior result obtained from 124 times SRS calculations is shown in Figure 15.6.5-23. In the 124 times calculations, the highest two PCT cases are excluded. The third highest PCT is 991.3 °C (1,816.4 °F) and maximum cladding oxidation is 3 percent with exceeding the 95 percent at 95 percent confidence level.

The cases in which the clad temperature differences in the second peak are within 100 °C (180 °F) compared with the highest second peak are selected for scale bias calculations. Code biases in the prediction of ECC water bypass and steam binding are evaluated separately. Steam binding bias is evaluated by combining the results of two separate bias evaluations of droplet de-entrainment in the upper plenum of the reactor vessel and droplet evaporation in the steam generator U-tube. Even though reflood cladding temperatures are increased by the biases, they do not exceed the blowdown PCT of 991.3 °C (1,816.4 °F). Total PCT bias is evaluated as +0 °C, as shown in Table 15.6.5-5. The maximum cladding oxidation with bias evaluation is 3 percent as shown in Table 15.6.5-5.

Uncertainties from sources other than code models or plant operation conditions, such as automatic time step control function and data reading frequency of RELAP5/MOD3.3, are considered of maximum 10 °C. The hot rod average oxidation is calculated lower than one percent. The final PCT, maximum cladding oxidation, and core-wide hydrogen generation combining all the biases are as follows:

Peak cladding temperature = 991.3 °C + 10 °C
= 1,001.3 °C (1,834.3 °F)
= 1,274.5 K < 1,477.15 K (2,200 °F)

Maximum cladding oxidation = 3.09 % < 17 %

Maximum hydrogen generation << 1 %

The highest cladding temperature in the large breaks analyzed is 1,001.3 °C (1,834.3 °F), which is 202.7 °C (365.7 °F) lower than the acceptance criterion of 1,204 °C (2,200 °F).

The final PCT considering the effect of thermal conductivity degradation is still satisfied the acceptance criteria. Details are given in Reference 78. The PCT increase is ended when the core is maintaining a coolable geometry. The heat generated from the fuel is able to be removed properly for a long period.

Based on the results of this analysis, it is concluded that the APR1400 SIS satisfies the all SRP acceptance criteria of References 62 and 64 (Subsection 15.0.5) for a complete spectrum of large break LOCAs and is adequate to perform its intended function of maintaining the integrity of the core, thereby limiting radiation release to the environment.

<u>Small Break Loss-of-Coolant Accident Analysis Results</u>

The nine breaks analyzed at 4,062.66 MWt, 102 percent of nominal, include reactor coolant pump discharge leg breaks ranging in size from 465 cm^2 (0.5 ft^2) to 46.5 cm^2 (0.05 ft^2) and DVI line breaks from 372 cm^2 (0.4 ft^2) to 18.6 cm^2 (0.02 ft^2). One break, equal in area to a fully open PRSRV, 27.9 cm^2 (0.03 ft^2), is postulated to occur in the top of the pressurizer. The 465 cm^2 (0.5 ft^2) discharge leg break is also analyzed for the large break spectrum and is defined as the transition break size (Reference 67). Table 15.6.5-8 lists the various break sizes and locations examined for this analysis.

The transient behavior of important NSSS parameters is shown in the figures listed in Table 15.6.5-9. Table 15.6.5-10 summarizes the important results of this analysis. Times of interest for the various breaks analyzed are presented in Table 15.6.5-11. A plot of PCT versus break size is presented in Figure 15.6.5-33. The 372 ft^2 (0.4 ft^2) DVI break results in the highest cladding temperature 624 °C (1,156 °F) of the small breaks analyzed, which is 580 °C (1,044 °F) lower than the acceptance criteria of 1,204 °C (2,200 °F). Of the pump discharge leg and DVI line break locations, the DVI line break is limiting due to the assumed loss of all safety injection flow to the broken line.

For the DVI line break location, as the break size becomes progressively smaller than 372 cm^2 (0.4 ft^2), the inner vessel two phase level follows a definite pattern:

a. The time of initial core uncovery is later.

b. The depth of core uncovery is less.

c. The rate of level decrease and increase becomes slower.

This trend continues until the core does not uncover at all. These trends predictably affect the PCT.

As the break size decreases, both the later time of the initial core uncovery and the shallower depth of uncovery tend to mitigate the temperature transient. This trend continues until the core does not uncover as typified by the 18.6 cm^2 (0.02 ft^2) break. By analyzing several break sizes over this range, the behavior of PCT versus break size is adequately determined.

The above behavior of core uncovery with break size results from the design characteristics of the SIS. For DVI break sizes below 93 cm^2 (0.1 ft^2), the RCS pressure remains above the SIT pressure and coolant flow injection to the reactor vessel is accomplished entirely by one SIP. For break sizes greater than 93 cm^2 (0.1 ft^2), the transient is terminated by the action of both the SITs and SI pumps.

For the cold leg breaks, the additional SIS flow resulting from being able to credit two SIPs precludes core uncovery to break sizes up to 93 cm^2 (0.1 ft^2). In addition, the core

uncovery for break sizes greater than 93 ft^2 (0.1 ft^2) is delayed, and the depth and duration of uncovery decreased relative to DVI breaks, which credit only one SIP. This more favorable behavior results in lower cladding temperatures relative to breaks in a DVI line.

In addition to the break locations discussed above, the rupture of an in-core instrument tube is considered. A break equal in size to a completely severed instrument tube (2.8 cm^2 [0.003 ft^2]) is postulated to occur in the reactor vessel bottom head.

Following rupture, the primary system depressurizes until a reactor scram signal and safety injection actuation signal (SIAS) are generated due to low pressurizer pressure at 109.3 g/cm^2A (1,555 psia). The assumed LOOP causes the primary coolant pumps and the feedwater pumps to coast down. After the 40-second delay, required to actuate the emergency diesel and the SIPs following the SIAS, safety injection flow is initiated to the RCS. Four SITs are available but do not inject due to the high RCS pressure.

The primary side depressurization continues accompanied by a rise in secondary side pressure until the secondary side pressure reaches the lowest setpoint of the steam generator safety valves. The primary system pressure continues to fall until it is just slightly greater than the secondary side pressure. At this point, the flow from the two operating SIPs (63 kg/sec [139 lbm/sec]) exceeds the leak flow (12 kg/sec [26 lbm/sec]). Therefore, the RCS fills. The decay heat generated in the core is removed in the SGs by steam flow through the secondary side safety valves. The core remains covered and cooled in this condition.

Based on the results of this analysis, it is concluded that the APR1400 SIS satisfies the all SRP acceptance criteria of References 1 and 62 (Subsection 15.0.5) for small break LOCAs.

<u>Post Loss-of-Coolant Accident Long-term Cooling Evaluation Results</u>

An evaluation of the various break locations showed that the double-ended (9,104.5 cm^2 [9.8 ft^2]) cold leg break was confirmed to be the limiting break geometry for the boric acid precipitation analysis (Reference 73). The long-term loop seal refilling with a slot break at the top of the cold leg does not significantly affect the boric acid precipitation analysis. For a cold leg break, the core flushing flow is the difference between the hot leg injection flow rate and the core boiloff rate. The initiation of a simultaneous hot leg and direct vessel SIP injection flow at 3 hours post-LOCA provides a substantial and time-increasing core flushing flow as shown in Figure 15.6.5-35. Figure 15.6.5-36 shows that with no

core flushing flow, boric acid does not begin to precipitate until 3.2 hours post-LOCA. The margin provided for the prevention of boric acid precipitation by the core flushing flow of 113.6 L/min (30 gpm) is also shown in Figure 15.6.5-36. The analyses also show that all hot leg steam entrainment of injection water is terminated in less than 3 hours post-LOCA. When the operator initiates simultaneous hot leg and direct vessel injection by 3 hours, there is no potential for the hot leg entrainment and boric acid precipitation.

The left branch of the LTC plan in Figure 15.6.5-34 applies to the break sizes for which the RCS refills. The LTC analysis predicts that the RCS will refill at various times depending on break size, as shown in Figure 15.6.5-37. As shown, for a break size as large as 37.2 cm^2 (0.04 ft^2), the RCS refills within 8 hours. The LTC analysis determines that more than 14 hours is required to exhaust all of the auxiliary feedwater during cooldown of the RCS. To allow a substantial time margin to avoid exhausting the auxiliary feedwater, a period of 8 to 9 hours is selected for the operator to decide whether the small break LTC procedure is appropriate. These results demonstrate that breaks as large as 37.2 cm^2 (0.04 ft^2) are able to use SCS for the long-term cooling and flushing of the core. The LTC analysis determines that the large break procedures can flush the core for break sizes down to 3.7 cm^2 (0.004 ft^2). The overlap in break sizes for which either the large break or small break procedures can be used is illustrated in Figure 15.6.5-38.

The operator chooses the appropriate procedure on the basis of the indicated RCS pressure between 8 and 9 hours. Figure 15.6.5-38 lists the RCS pressure at 8 hours for a wide range of break sizes, and Figure 15.6.5-39 presents this information graphically. The decision pressure is selected as 31.6 kg/cm^2A (450 psia) so that, with consideration of the maximum RCS pressure measurement error up to ± 21.1 kg/cm^2 (± 300 psia), reasonable assurance is provided that the operator selects the proper procedure for any break size.

The natural circulation cooldown analysis that is performed as part of the LTC analysis determines that the SCS entry temperature of 193 °C (379 °F) is reached at approximately 6.7 hours after the start of the LOCA. The analysis simulates a conservatively slow cooldown rate and consequently, a maximum value for the earliest time that the SCS entry temperature is reached. The analysis takes credit only for safety grade systems, namely, the safety injection system, the auxiliary feedwater system, and the atmospheric dump valves. Reaching the SCS entry temperature at 6.7 hours leaves sufficient time for the operator to depressurize the RCS to the SCS entry pressure and initiate shutdown cooling.

Based on the results of this analysis, it is concluded that the APR1400 SIS satisfies the all SRP acceptance criteria of References 1 and 62 (Subsection 15.0.5) for LTC.

15.6.5.4 Barrier Performance

In Section 6.2, the barrier performance is described in detail, and the containment vessel pressure that affects the performance of the barriers is evaluated.

15.6.5.5 Radiological Consequence

The radiological consequences for large-break LOCAs are performed to determine the post-LOCA doses at the EAB, LPZ, MCR, and TSC using the AST guidance in NRC RG 1.183, plant-specific design inputs, and TEDE dose criteria for the following post-LOCA release paths:

a. Containment leakage

b. Engineered safety feature (ESF) leakage

c. Low volume purge release

d. Back leakage to the IRWST leakage

The following regulatory requirement and guidance are applied as the acceptance criteria for the receptors at EAB, LPZ, MCR, and TSC:

a. NRC RG 1.183

b. 10 CFR 50.34

c. Standard Review Plan, Subsection 15.0.3

15.6.5.5.1 Evaluation Model

For the design basis accident LOCA, all fuel assemblies in the core are assumed to be affected, and the maximum core fission product inventory is used. The maximum core

fission product inventories are listed in Appendix 15A, Table 15A-1. The remaining isotopes are not accounted for in the analysis. The dose analysis is based on a core thermal power of 4,062.66 MWt including the 2 percent power level measuring instrument uncertainty. The following evaluation models of radioactive materials are applied to evaluate radiological consequence due to a LOCA.

15.6.5.5.1.1 Containment Leakage

Containment Air Mixing

The APR1400 containment spray covers 75 percent of the containment volume, and the remaining 25 percent of containment free volume is considered to be unsprayed volume. Because the reactor containment fan coolers (RCFCs) are non-safety-related, the forced mixing between the sprayed and unsprayed regions due to the RCFCs is not credited. Instead, consistent with NRC RG 1.183, the mixing rate attributed to natural convection between the sprayed and unsprayed regions of the containment building is assumed to be two turnovers of the unsprayed region per hour. This containment mixing rate is used in the analysis to transport the post-LOCA activity between the sprayed and unsprayed regions.

Containment Spray Operation

Although the APR1400 containment spray system (CSS) is designed to operate throughout the design basis event, the spray operation period is assumed to be 4 hours. Containment spray removal of iodine and aerosols is assumed to be initiated at 110 seconds after the start of the LOCA event. The CSS is automatically initiated by a safety injection actuation signal (SIAS) or a containment spray actuation signal (CSAS) to comply with the SRP, Subsection 6.5.2, Acceptance Criterion 1.A. The APR1400 does not have a recirculation mode of operation during the CSS operation period because the CSS takes suction from IRWST for the entire duration of the design basis event.

The containment spray elemental iodine removal coefficient λ_E is calculated to be 20 hr^{-1} using the APR1400 plant-specific containment spray parameters, which meets the SRP Subsection 6.5.2 limitation of 20 hr^{-1}. Consistent with the SRP, Subsection 6.5.2, the effectiveness of the spray in removing elemental iodine is presumed to end when the maximum elemental iodine DF value of 200 is reached. The total elemental iodine atoms when a DF of 200 is reached in the sprayed region are calculated by using the elemental

iodine of 4.85 percent of the total 40 percent iodine activity released from the core into the sprayed region volume and a DF of 200. This means that when the total elemental iodine atoms in the sprayed region reach a value corresponding to the DF of 200, the containment spray cannot be credited for further removal of elemental iodine. Based on the RADTRAD calculation for the post-LOCA containment leakage, the sprayed region elemental iodine removal coefficient reaches a value of DF at 2.25 hours. Therefore, the containment spray is not credited beyond 2.25 hours for the removal of elemental iodine.

The containment spray aerosol removal coefficient λ_P is calculated to be 6.25 hr^{-1} as given in Subsection 6.5.2. This containment spray aerosol removal coefficient is modeled until a DF of 50 is reached, and then the removal coefficient is reduced to 0.625 hr^{-1}. According to the RADTRAD calculation, the containment spray aerosol removal is reduced to 0.625 hr^{-1} at 2.40 hours. The containment spray is not credited beyond 4.0 hours for the removal of the aerosols.

During the initial 24 hours, the total leakage of 0.1 volume percent per day directly leaks to the outside environment. From 24 hours to 30 days, the initial total leakage is halved to a value of 0.05 volume percent per day.

Containment Natural Deposition

Reduction in particulate radioactivity in containment by natural deposition is credited. The natural deposition model is based on the Powers model that is incorporated into RADTRAD code, and the aerosol removal coefficient is determined with a 10-percentile probability as described in Subsection 6.5.2.3.3.

Long-Term Iodine Partition

The IRWST water is assumed to contain fission products washed from the reactor core and removed from the containment atmosphere. If the solution is acidic, the radiation absorbed by the IRWST water generates enough hydrogen peroxide to react with both iodide and iodate ions and make elemental iodine revolution possible. For IRWST water with a pH of less than 7, molecular iodine vapor is conservatively assumed to evolve into the containment atmosphere. NRC RG 1.183 requires evaluation of the re-evolution of iodine for an IRWST pH value of less than 7. As presented in Subsection 6.5.2.3, the

IRWST water pH remains at greater than 7.0 for duration of the accident including the effect of acids and bases created during the LOCA event and the radiolysis products. Consequently, the re-evolution of dissolved iodine from the IRWST is not credible and is therefore not considered in the analysis.

15.6.5.5.1.2 Engineered Safety Feature (ESF) System Leakage

The ESF systems that recirculate IRWST water outside containment are assumed to leak during their intended operation. This release source includes leakage through valve packing glands, pump shaft seals, flanged connections, and other similar components. The radiological consequences from the postulated ESF leakage are analyzed and combined with consequences postulated for other fission product release paths to determine the total radiological consequences from the LOCA.

Post-LOCA Sump Water Iodine Source Term

NRC RG 1.183 requires that, with the exception of noble gases, all of the fission products released from the fuel to the containment are assumed to instantaneously and homogeneously mix in the IRWST water. Consistent with this guidance, a total of 40 percent of the core iodine released during the gap and early in-vessel phases is assumed to mix in the IRWST water.

ESF Leakage Release Path

The ESF pumps including the containment spray (CS), safety injection (SI), and component cooling water (CCW) pumps are located in the auxiliary building (AB). The ESF leakage is assumed to be retained on the floor of the equipment compartments in the AB and the iodine in the ESF leakage flashes and becomes airborne in the AB and the iodine is released to the environment through the AB ventilation exhaust system.

Flashing of Iodine from ESF Leakage

NRC RG 1.183 requires that if the temperature of the ESF leakage exceeds 100 °C (212 °F), the fraction of total iodine in the liquid that becomes airborne is assumed to be equal to the fraction of the leakage that flashes to vapor. This flash fraction (FF) is determined using a

constant enthalpy process based on the maximum time-dependent temperature of the IRWST water circulating outside containment.

The post-LOCA sump water temperature for the APR1400 is higher than 107 °C (225 °F) between 11,000 seconds (≈ 3.0 hours) and 60,000 seconds (16.67 hours), and it reaches the maximum values of 113 °C (235.5 °F) at 27,500 seconds (7.64 hours). Assuming the IRWST water temperature is 107 °C (225 °F) yields an iodine FF of 1.35 percent. The iodine FF of 2.39 percent is calculated for the maximum IRWST water temperature at 113 °C (235.5 °F), and an average FF of 2 percent is calculated for the IRWST water temperature between 3.0 hours and 16.67 hours. For the remainder of the accident, the IRWST water is conservatively assumed to remain at less than 100 °C (212 °F), and the FF of 10 percent is used during this period to be consistent with NRC RG 1.183. The post-LOCA ESF leakage release rates based on the calculated FF and an assumed design basis ESF leakage of 18.9 L/hr (5 gal/hr) (doubled to 37.8 L/hr [10 gal/hr]) are used to calculate the resulting dose consequences.

15.6.5.5.1.3 Containment Low Volume Purge System Release

If the primary containment is routinely purged during power operations, releases through the purge system prior to containment isolation are analyzed, and the resulting doses are summed with the postulated doses from other release paths. The containment low volume purge system (CLVPS) release occurs following the large-break LOCA and before containment isolation. The isolation valves of the CLVPS are closed by the containment isolation actuation signal (CIAS) after a LOCA with a LOOP within 5.0 seconds. The CLVPS release evaluation assumes that 100 percent of the radionuclide inventory in the RCS liquid is released to the containment at the initiation of the LOCA and homogeneously mixed in the containment atmosphere. A release of gap activity into the containment is not considered because the CLVPS release terminates within 5 seconds, which is before the onset of the gap release, which occurs at 30 seconds.

CLVPS Release Source Term

The RCS isotopic iodine concentrations are based on the Technical Specification for RCS equilibrium activity and the thyroid dose conversion factors specified in Federal Guidance Report 11 (Reference 55). The noble gas concentrations are based on 1 percent failed fuel. Consistent with NRC RG 1.183, iodine spiking is not considered.

CLVPS Release Path

The CLVPS release point is located at the highest level in the AB. The main steam valve room is located near the MCR and AB air intakes. Therefore, the main steam valve room release point is conservatively selected for the CLVPS release for the MCR, TSC, and AB air intake χ/Qs.

15.6.5.5.1.4 Post-LOCA Back-Leakage to In-Containment Refueling Water Storage Tank

The IRWST is located inside the containment, and a minimum flow line is provided on each CSS pump discharge line, which is connected to the CSS suction line. Any post-LOCA leakage that occurs from the minimum flow line components is confined within the containment pressure boundary and not directly released to the environment.

15.6.5.5.2 Input Parameters and Initial Conditions

The radiological consequences of the LOCA are analyzed using a conservative set of assumptions and the APR1400 design inputs. Input parameter values used in the analysis are presented in Table 15.6.5-13.

Credit is taken only for the accident mitigation features that are classified as safety-related, are required to be operable by the Technical Specifications, are powered by emergency power sources, and are either automatically actuated or, in limited cases, have actuation requirements addressed in emergency operating procedures. The operations of the containment spray system, containment purge valve isolation, and main control room HVAC system, including filtration efficiencies credited in the analysis to mitigate the dose consequences, are operable by the Technical Specifications. The control room HVAC system intake radiation monitor capability to align with the less contaminated air intake is also credited in the analysis.

The numeric values used in this analysis are chosen as inputs with the objective of maximizing the postulated dose. The use of a control room HAVC system recirculation flow rate; use of the actually tested (99 percent) charcoal filtration efficiencies; use of a ground release that leads to the most conservative MCR and AB air intake χ/Q values regardless of actual source-receptor configuration; and the use of the most limiting U.S.

meteorological hourly data demonstrate the inherent conservatisms in the analysis. Many of the design input parameter values used in the analysis are those specified in the Technical Specifications.

The χ/Q values used in the analysis for EAB, LPZ, MCR, and TSC are described in Subsection 2.3.4 and are listed in Tables 2.3-1 through 2.3-12; breathing rates are given in Table 15A-11.

15.6.5.5.3 Results

The radiological consequences due to large break LOCA are presented in Table 15.6.5-14. The results of large break LOCA analyses indicate that the EAB and LPZ doses are within their allowable dose limits in 10 CFR 50.34(a)(1). The MCR and TSC doses are also within the limit in GDC 19.

15.6.6 Combined License Information

No COL information is required with regard to Section 15.6.

Table 15.6.2-1

Alarms Actuated Upon the Event for a Double-Ended Break of a Letdown Line Outside the Containment

1	Letdown line low pressure alarm (downstream of the break)
2	Auxiliary building high radiation alarm
3	Auxiliary building high temperature alarm
4	Auxiliary building high humidity alarm
5	Pressurizer low level alarm
6	Auxiliary building sump high-high level alarm
7	Volume control tank low level alarm

Table 15.6.2-2

Sequence of Events for a Double-Ended Break of the Letdown Line Outside Containment Upstream of the Letdown Isolation Valve

Time (sec)	Event	Setpoint or Value
0.0	Letdown line rupture occurs	—
274.9	Pressurizer backup heaters turned on, kg/cm^2A (psia)	159.95 (2,275)
514.5	Pressurizer backup heaters turned off, kg/cm^2A (psia)	161.71 (2,300)
> 662.0	Pressurizer backup heaters cycle on, kg/cm^2A (psia) Pressurizer backup heaters cycle off	159.95 (2,275)/ 161.71 (2,300)
1,800.0	Pressurizer pressure prior to manual reactor trip, kg/cm^2A (psia)	159.37 (2,266.8)
1,800.0	Minimum pressurizer liquid level, m (ft)	2.66 (8.73)
1,800.0	Operator isolates the letdown line, trips the reactor and takes steps for a controlled cooldown of the reactor	—

Table 15.6.2-3

Assumed Input Parameters and Initial Conditions for the Double-Ended Break of the Letdown Line Outside Containment Upstream of the Letdown Isolation Valve

Parameters	Assumed Value
Initial core power level, MWt	4,062.66
Initial core inlet temperature, °C (°F)	296.11 (565)
Initial pressurizer pressure, kg/cm^2A (psia)	163.5 (2,325)
Initial core mass flow, 10^6 kg/hr (10^6 lbm/hr)	69.64 (153.52)
Initial pressurizer liquid volume, m^3 (ft^3)	39.91 (1,409)
CEA worth at trip, 10^{-2} $\Delta\rho$	−8.0
Break size (double-ended), m^2 (ft^2)	0.001446 (0.01556)

Table 15.6.2-4 (1 of 2)

Parameters Used in Evaluating the Radiological Consequences of a Double-Ended Break of the Letdown Line Outside Containment

Parameter	Value
Source Terms	
Reactor Core Power Level	4,062.66 MWt
Percent of Fuel Assumed to Experience Departure from Nucleate Boiling (DNB)	0 %
Percent of Fuel Assumed to Melt	0 %
Initial RCS Mass	292,431 kg (644,700 lbm)
Initial Steam Generator Liquid Mass per SG	89,086 kg (196,400 lbm)
Initial RCS Iodine Specific Activity	3.7×10^4 Bq/g (1.0 μCi/g) DE I-131
Initial Secondary Liquid Iodine Specific Activity	3.7×10^3 Bq/g (0.1 μCi/g) DE I-131
Initial Noble Gas Specific Activity	2.15×10^7 Bq/g (580 μCi/g) DE Xe-133
Event-generated Iodine Spiking Factor	500
Duration of Event-generated Iodine Spike	8 hrs
Chemical Forms of Iodine Released from the SG to the Environment	97 % elemental and 3 % organic
Secondary System Activity Transport Model	
Primary-to-secondary Leak Rate through SG	2.27 L/min (0.6 gpm) for two SGs
Integrated P-T-S Leakage 0 ~ 2 hrs 2 ~ 8 hrs	 272 kg (601 lbm) 818 kg (1,803 lbm)
Total Steam Mass Release from Both SGs 0 ~ 0.5 hrs 0.5 ~ 2 hrs via ADV 2 ~ 8 hrs via ADV	 0.00 kg (0.0 lbm) 461,000 kg (1,016,000 lbm) 54,600,000 kg (1,203,000 lbm)
LDLB Isolation Time	30 mins
Unaffected SG P-T-S Leak Duration, and Termination of Release from Unaffected SG	8 hrs
SG Liquid Iodine Partition Coefficient	100
Alkali Material (Cs, Rb) Partition coefficient	5.0×10^{-3}
Letdown System Flow Rate	18,100 kg/hr (39,842 lbm/hr)

Table 15.6.2-4 (2 of 2)

Secondary System Activity Transport Model (cont.)	
RCS Mass Release Outside Containment	20,300 kg (44,700 lbm)
RCS Fluid Flashing Factor	0.259
Unflashed Letdown Line Break Fluid Iodine Partition Coefficient	10
Auxiliary Building Controlled Area Exhaust System Filter Efficiencies Elemental and Organic Iodine Particulate	 0 % 0 %
MCR and TSC Model Parameters	
Envelope Volume	5,663 m^3 (200,000 ft^3)
Normal Ventilation Flow Rate (unfiltered)	105 m^3/min (3,700 cfm)
Emergency Ventilation Makeup Rate (filtered)	105 m^3/min (3,700 cfm)
Emergency Ventilation Recirculation Flow Rate (filtered)	122 m^3/min (4,300 cfm)
Emergency HVAC Delay Time	5 mins
Emergency Ventilation Charcoal Filter Efficiency (elemental and organic iodine removal)	99 %
Emergency Ventilation HEPA Filter Efficiency (particulate removal)	99 %
Unfiltered Inleakage	8.50 m^3/min (300 cfm)
Occupancy Factors 0 ~ 24 hrs 24 ~ 96 hrs 96 ~ 720 hrs	 100 % 60 % 40 %
Onsite χ/Qs	See Tables 2.3.2 ~ 2.3.12
Offsite Model Parameters	
χ/Qs	See Table 2.3-1
Breathing Rate	See Table 15A-11
Dose Conversion Factors	See Table 15A-10

Table 15.6.2-5

Radiological Consequences of a Double-Ended Break of the Letdown Line Outside Containment

Post-LDLB Activity Release Path	TEDE Dose (mSv)		
	MCR and TSC	EAB	LPZ
LDLB Iodine and Noble Gas Release	3.96E-01	1.31E+01	2.88E+00
P-T-S Iodine Release	2.95E-01	4.53E-01	2.73E-01
P-T-S Noble Gas Release	1.32E-02	1.19E-02	8.54E-03
Secondary Liquid Iodine Release	2.95E-02	5.99E-02	2.52E-02
External Cloud	6.88E-01	0.00E+00	0.00E+00
Emergency Ventilation Filter Shine	1.34E-06	0.00E+00	0.00E+00
Total	1.42E+00	1.36E+01	3.18E+00
Allowable TEDE Limit	5.00E+01	2.50E+01	2.50E+01

Table 15.6.3-1

Sequence of Events for a Steam Generator Tube Rupture without a Loss of Offsite Power

Time (sec)	Event	Setpoint or Value
0.0	Tube rupture occurs	—
0.55	Trip breakers open due to high steam generator level trip signal	—
0.55	Turbine trip: turbine stop valves start to close	—
0.55	MSIS generated on high steam generator level and MSIVs and MFIVs are closed	—
2.4	Main steam safety valves open, kg/cm^2A (psia)	80.27 (1,141.74)
7.95	Maximum steam generator pressure, kg/cm^2A (psia)	84.07 (1,195.76)
211.55	Pressurizer pressure reaches safety injection actuation signal setpoint, kg/cm^2A (psia)	132.53 (1,885)
251.55	Safety injection flow begins	—
1,800	Operator cools the NSSS using plant emergency procedure after isolation of affected steam generator or confirmation of isolation	—
28,800	Shutdown cooling entry conditions are assumed to be reached; RCS pressure, kg/cm^2A (psia) / RCS temperature, °C (°F)	31.6/176.7 (450/350)

Table 15.6.3-2

Assumptions and Initial Conditions for a Steam Generator Tube Rupture without a Loss of Offsite Power

Parameters	Assumed Value
Initial core power level, MWt	4,062.66
Initial core inlet coolant temperature, °C (°F)	295 (563)
Initial pressurizer pressure, kg/cm^2A (psia)	163.5 (2,325)
Initial core mass flow rate, 10^6 kg/hr (10^6 lbm/hr)	69.64 (153.52)
One pin integrated radial peaking factor, with uncertainty	1.8236
Moderator temperature coefficient, 10^{-4} $\Delta\rho$/°C (10^{-4} $\Delta\rho$/°F)	0.0 (0.0)
Doppler coefficient	Least negative
CEA worth at trip, % $\Delta\rho$ (most reactive CEA fully withdrawn)	−8.0

Table 15.6.3-3

Sequence of Events for a Steam Generator Tube Rupture with a Loss of Offsite Power

Time (sec)	Event	Setpoint or Value
0.0	Tube rupture occurs	—
0.55	Trip breakers open due to high steam generator level trip signal	—
0.55	Turbine trip: turbine stop valves start to close	—
0.55	Loss of offsite power	—
0.55	MSIS generated on high steam generator level Main steam isolation valves closed	—
2.45	Main steam safety valves open, kg/cm^2A (psia)	80.27 (1,141.74)
5.55	Maximum steam generator pressure, kg/cm^2A (psia)	84.06 (1,195.55)
215.35	Pressurizer pressure reaches safety injection actuation signal setpoint, kg/cm^2A (psia)	132.53 (1,885)
255.35	Safety injection flow begins	—
1,800	Operator cools the NSSS using plant emergency procedure after isolation of affected steam generator or confirmation of isolation	—
28,800	Shutdown cooling entry conditions are assumed to be reached, RCS pressure, kg/cm^2A (psia) / temperature, °C (°F)	31.6/176.7 (450/350)

Table 15.6.3-4

Assumptions and Initial Conditions for the Steam Generator Tube Rupture with a Loss of Offsite Power

Parameters	Assumed Value
Initial core power level, MWt	4,062.66
Initial core inlet temperature, °C (°F)	295 (563)
Initial pressurizer pressure, kg/cm^2A (psia)	163.47 (2,325)
Initial core mass flow, 10^6 kg/hr (10^6 lbm/hr)	69.64 (153.52)
Maximum radial peaking factor (including uncertainty)	1.9786
Moderator temperature coefficient, 10^{-4} $\Delta\rho$/°C (10^{-4} $\Delta\rho$/°F)	0.0
Doppler coefficient	Least negative
CEA worth at trip, % $\Delta\rho$ (most reactive CEA fully withdrawn)	−8.0

Table 15.6.3-5 (1 of 3)

Parameters Used in Evaluating the Radiological Consequences of the Steam Generator Tube Rupture with a Loss of Offsite Power

Parameter	Value
Source Terms	
Reactor Core Power Level	4,062.66 MWt
Percent of Fuel Assumed to Experience Departure from Nucleate Boiling (DNB)	0 %
Percent of Fuel Assumed to Melt	0 %
Initial RCS Mass	290,680 kg (640,840 lbm)
Initial Steam Generator Liquid Mass	117,688 kg/SG (259,457 lbm/SG)
Initial RCS Iodine Specific Activity	3.7×10^4 Bq/g (1.0 μCi/g) DE I-131
Secondary Liquid Iodine Specific Activity	3.7×10^3 Bq/g (0.1 μCi/g) DE I-131
Initial RCS Noble Gas Specific Activity	2.15×10^7 Bq/g (580 μCi/g) DE Xe-133
Used for Pre-accident Iodine Spike Case RCS Iodine Specific Activity	2.22×10^6 Bq/g (60 μCi/g) DE I-131
Event-generated Iodine Spiking Factor	335
Duration of Event-generated Iodine Spike	8 hrs
Chemical Forms of Iodine Released from the Steam Generators to the Environment	97 % elemental and 3 % organic

Table 15.6.3-5 (2 of 3)

Parameter	Value
Secondary System Activity Transport Model	
Primary-to-secondary Leak Rate through SG	2.27 L/min (0.6 gpm) for two SGs
Integrated P-T-S Leakage 0 ~ 2 hrs 2 ~ 8 hrs	 272 kg (601 lbm) 818 kg (1,803 lbm)
Integrated Break Flow into Affected SG 0 ~ 0.5 hrs 0.5 ~ 2 hrs 2 ~ 8 hrs	 40,200 kg (88,640 lbm) 24,000 kg (52,808 lbm) 0 kg (0.0 lbm)
Integrated Flashed Break Flow into Affected SG 0 ~ 0.5 hrs 0.5 ~ 2 hrs 2 ~ 8 hrs	 2,450 kg (5,400 lbm) 2,900 kg (6,400 lbm) 0 kg (0.0 lbm)
Steam Mass Release from Affected SG 0 ~ 0.5 hrs via MSSV 0.5 ~ 2 hrs 2 ~ 8 hrs	 77,600 kg (171,000 lbm) 0 kg (0.0 lbm) 0 kg (0.0 lbm)
Steam Mass Release from Unaffected SG 0 ~ 0.5 hrs via MSSV 0.5 ~ 2 hrs via ADV 2 ~ 8 hrs via ADV	 64,400 kg (142,000 lbm) 463,000 kg (1,021,000 lbm) 586,000 kg (1,293,000 lbm)
Termination of Release from Affected SG by Operator Action	30 min
Unaffected SG P-T-S Leak Duration, and Termination of Release from Unaffected SG	8 hrs
SG Liquid Iodine Partition Coefficient	100
Letdown System Flow Rate	18,100 kg/hr (39,842 lbm/hr)
Total RCS Leak Rate	41.6 L/min (11 gpm)

Table 15.6.3-5 (3 of 3)

Parameter	Value
MCR and TSC Model Parameters	
Envelope Volume	5,663 m^3 (200,000 ft^3)
Normal Ventilation Flow Rate (unfiltered)	105 m^3/min (3,700 cfm)
Emergency Ventilation Makeup Rate (filtered)	105 m^3/min (3,700 cfm)
Emergency Ventilation Recirculation Flow Rate (filtered)	122 m^3/min (4,300 cfm)
Emergency HVAC Delay Time	5 mins
Emergency Ventilation Charcoal Filter Efficiency (elemental and iodine removal)	99 %
Emergency Ventilation HEPA Filter Efficiency (particulate removal)	99 %
Unfiltered Inleakage	8.50 m^3/min (300 cfm)
Occupancy Factors 0 ~ 24 hrs 24 ~ 96 hrs 96 ~ 720 hrs	 100 % 60 % 40 %
Onsite χ/Qs	See Tables 2.3-6 and 2.3-7
Offsite Model Parameters	
χ/Qs	See Table 2.3-1
Breathing Rate	See Table 15A-11
Dose Conversion Factors	See Table 15A-10

Table 15.6.3-6

Radiological Consequences of the Steam Generator
Tube Rupture with a Loss of Offsite Power

Pre-accident Iodine Spike Case

Post-SGTR Activity Release Path	TEDE Dose (mSv)		
	MCR and TSC	EAB	LPZ
P-T-S Iodine Release	3.25E+00	8.38E+00	1.93E+00
P-T-S Noble Gas Release	9.84E-01	2.46E+00	5.45E-01
Secondary Liquid Iodine Release	8.79E-02	1.42E-01	5.87E-02
External Cloud	6.88E-01	0.00E+00	0.00E+00
Emergency Ventilation Filter Shine	1.34E-06	0.00E+00	0.00E+00
Total	5.01E+00	1.10E+01	2.53E+00
Allowable TEDE Limit	5.00E+01	2.50E+02	2.50E+02

Event-generated Iodine Spike Case

Post-SGTR Activity Release Path	TEDE Dose (mSv)		
	MCR and TSC	EAB	LPZ
P-T-S Iodine Release	1.19E+00	3.72E+00	9.70E-01
P-T-S Noble Gas Release	9.84E-01	2.46E+00	5.45E-01
Secondary Liquid Iodine Release	8.79E-02	1.42E-01	5.87E-02
External Cloud	6.88E-01	0.00E+00	0.00E+00
Emergency Ventilation Filter Shine	1.34E-06	0.00E+00	0.00E+00
Total	2.95E+00	6.32E+00	1.57E+00
Allowable TEDE Limit	5.00E+00	2.50E+01	2.50E+01

Table 15.6.5-1

<u>Uncertainty Parameter Ranges and Distributions</u>

No.	Parameter	Distribution	Parameter Ranges Min.	Parameter Ranges Max	Component
1	Fq	Uniform	1.94	2.41	Fuel
2	Gap conductance	Uniform	0.75	1.50	
3	Fuel conductivity	Normal	0.8455	1.1545	
4	Core power	Normal	0.9691	1.0309	
5	Decay heat	Normal	0.89803	1.10197	
6	Burst temperature dial	Uniform	0.90	1.10	
7	Burst strain dial	Uniform	0.30	1.70	
8	Oxidization dial	Normal	0.961	1.039	
9	Groeneveld CHF dial	Normal	−0.17111	2.17111	Core
10	Chen nucleate boiling dial	Normal	0.382	1.618	
11	Zuber CHF dial	Normal	0.5365	1.4635	
12	Dittus Boelter, liquid dial	Normal	0.606025	1.393975	
13	Dittus Boelter, vapor dial	Normal	0.606025	1.393975	
14	Bromley dial	Normal	0.42835	1.57165	
15	Weber number dial	Uniform	1.350	7.0	
16	F. Rohsenow dial	Uniform	0.5	1.5	
17	Weismann dial	Uniform	0.40	1.60	
18	1-Phase Cd	Normal	0.7821	0.9979	
19	2-Phase Cd	Normal	0.7026	1.4374	
20	Pump K-factor	Uniform	0.239	0.577	Loop
21	Pump head multiplier	Uniform	0.0	1.0	
22	Pump torque multiplier	Uniform	0.0	1.0	
23	Pressurizer pressure, bar	Normal	152.47	157.80	Pressurizer
24	SIT pressure, bar	Uniform	40.31	44.59	SIT/Cold Leg
25	SIT water volume, m3	Uniform	50.69	54.57	
26	SIT water temp, K	Uniform	283.0	321.9	
27	SIP flow multiplier	Uniform	−0.5	0.5	
28	IRWST water temp, K	Uniform	283.0	321.9	
29	Thermal Conductivity	Uniform	1.0	2.0	Downcomer Wall
30	Heat Capacity	Uniform	1.0	1.5	

Table 15.6.5-2 (1 of 2)

General System Parameters and Initial Conditions Large Break ECCS Performance

Plant Parameters	Reference Conditions
Core	
1. Core power, MWt 2. Power peaking factor 3. Fuel type 4. Power output pattern 5. Decay heat	3,983 2.258 16 × 16 Figure 15.6.5-1 ANS79 model
Reactor Coolant System	
1. Initial core flow rate, kg/hr	73.3×10^6
Pressurizer	
1. Pressure, bar	155.1
Steam Generator	
1. Feedwater temperature, K 2. Tube plugging rate, %	505.23 10
Safety Injection System	
1. Safety injection tank coolant volume, m^3 2. Safety injection tank gas pressure, bar 3. Safety injection tank coolant temperature, K 4. FD K-factor for high injection flow (including piping K) 5. FD K-factor for low injection flow (including piping K) 6. IRWST temperature, K	52.63 42.45 302.5 25 120 302.5

Table 15.6.5-2 (2 of 2)

Plant Parameters	Reference Conditions
Containment Building	
1. Initial pressure, bar	0.98
2. Initial temperature, K	283.15
3. Free volume, m^3	97,239
4. Number of spray	2
5. Delay time for spray actuation, s	0
6. Spray flow rate (2 pumps), L/min (gpm)	10,000

Table 15.6.5-3

Summary of Fuel Rod Performance Large Break Spectrum

Variable		100 % Break	80 % Break	60 % Break
Blowdown	PCT, °C	892.0	870.0	768.9
	PCT Location, m	2.57	2.57	2.76
	PCT Time, sec	6.5	36.5	36.5
Reflood	PCT, °C	798.9	869.5	762.5
	PCT Location, m	2.57	2.76	2.76
	PCT Time, sec	36.5	64.0	71.5
Peak Local Oxidation, %		1.50	1.92	1.24
Peak Zr-H_2O location, m		2.57	2.76	2.76
Maximum Hydrogen Generation, %		< 1.0	< 1.0	< 1.0
Hot Fuel Rod Rupture		N/A	N/A	N/A

Table 15.6.5-4

Sequence of Events for Representative LBLOCA

EVENT	100 % Break (sec)	80 % Break (sec)	60 % Break (sec)
Break Occurs	0	0	0
Reactor Trip signal Occurs	6.2	6.2	7.3
SI Injection signal Occurs	6.2	6.2	7.3
SIT Discharge Begins			
SIT 1 (Broken Cold Leg Side)	14.4	16.2	22.2
SIT 2 (Broken Loop Intact Cold Leg Side)	14.4	16.2	22.2
SIT 3 (Intact Loop Intact Cold Leg Side 1)	14.4	16.2	22.2
SIT 4 (Intact Loop Intact Cold Leg Side 2)	14.4	16.2	22.2
Pumped SI Injection	46.2	46.2	46.4
Core Water Level Recovery	44.2	40.6	45.51
SIT Empty Time			
SIT 1 (Broken Cold Leg Side)	201.5	207.5	206.7
SIT 2 (Broken Loop Intact Cold Leg Side)	201.5	207.5	206.8
SIT 3 (Intact Loop Intact Cold Leg Side 1)	201.5	207.5	206.7
SIT 4 (Intact Loop Intact Cold Leg Side 2)	201.5	207.5	206.6

Table 15.6.5-5

Summary of SRS and Bias Evaluation Results

SIT Empty Time, °C		Value
SRS Results	Highest PCT Highest Reflood PCT	991.3 982.9
Scale BIAS Evaluation Results	Final BIAS Reflood PCT Max. BIAS Case Reflood PCT – ECC Bypass BIAS – Steam Binding BIAS	982.9 982.9 +0.0 +0.0
Final PCT (w/ BIAS)		991.3 [(1)]
Max. Cladding Oxidation, %		Value
SRS Results	Max. Cladding Oxidation	3.00
Scale BIAS Evaluation Results	Final BIAS Reflood PCT Max. BIAS Case Reflood PCT – ECC Bypass BIAS – Steam Binding BIAS	3.09 2.56 +0.14 +0.39
Final Max. Cladding Oxidation (w/ BIAS)		3.09

(1) The final PCT with considering thermal conductivity degradation effect is still satisfied the acceptance criteria.

Table 15.6.5-6

Safety Injection Pumps Minimum Delivered Flow to RCS
(Assuming Two SI Pump Trains Failed)

RCS Pressure, kg/cm^2 (psig)	Flow Rate Per Injection Point,[(1)] L/min (gpm)	
	A	B
112 (1,600)	0 (0)	0 (0)
105 (1,500)	1,096 (290)	1,096 (290)
98 (1,400)	1,524 (403)	1,524 (403)
91 (1,300)	1,843 (487)	1,843 (487)
84 (1,200)	2,107 (557)	2,107 (557)
77 (1,100)	2,337 (617)	2,337 (617)
70 (1,000)	2,542 (672)	2,542 (672)
63 (900)	2,730 (721)	2,730 (721)
56 (800)	2,903 (767)	2,903 (767)
49 (700)	3,064 (810)	3,064 (810)
42 (600)	3,216 (850)	3,216 (850)
35 (500)	3,360 (888)	3,360 (888)
32 (450)	3,429 (906)	3,429 (906)
28 (400)	3,496 (924)	3,496 (924)
25 (350)	3,562 (941)	3,562 (941)
21 (300)	3,627 (958)	3,627 (958)
18 (250)	3,690 (975)	3,690 (975)
14 (200)	3,752 (991)	3,752 (991)
11 (150)	3,812 (1,007)	3,812 (1,007)
7 (100)	3,872 (1,023)	3,872 (1,023)
4 (50)	3,929 (1,038)	3,929 (1,038)
0 (0)	3,986 (1,053)	3,986 (1,053)

(1) For breaks assumed at the DVI location, Injection Point A is assumed to be the broken line. Injection Point B is the intact injection line. There is no flow delivered to the two injection points in the other loop due to the assumed failure of one emergency generator.

Table 15.6.5-7

General System Parameters and Initial Conditions;
Small Break ECCS Performance Analysis

Quantity	Value
Core Power Level (102 % of Nominal), MWt	4,062.66
Average Linear Heat Generation Rate, kW/m (kW/ft)	18.75 (5.715)
Peak Linear Heat Generation Rate (PLHGR), kW/m (kW/ft)	49.2 (15.0)
Gap Conductance at PLHGR, kcal/hr-m^2-°C (Btu/hr-ft^2-°F)	10,289 (2,107)
Fuel Centerline Temperature at PLGHR, °C (°F)	1,965 (3,568)
Fuel Average Temperature at PLHGR, °C (°F)	1,200 (2,192)
Hot Rod Gas Pressure, kg/cm^{2}A (psia)	52.0 (740)
Moderator Temperature Coefficient, Δρ/°C (Δρ/°F)	0.0×10^{-4} (0.0×10^{-4})
Initial RCS Flow Rate, kg/hr (lbm/hr)	75.6×10^6 (166.6×10^6)
Initial Core Flow Rate, kg/hr (lbm/hr)	73.3×10^6 (161.6×10^6)
Initial RCS Pressure, kg/cm^{2}A (psia)	158.2 (2,250)
Initial Reactor Vessel Inlet Temperature, °C (°F)	290.6 (555.0)
Initial Reactor Vessel Outlet Temperature, °C (°F)	324.4 (615.9)
Low Pressurizer Pressure Reactor Trip Setpoint, kg/cm^{2}A (psia)	109.3 (1,555)
SIAS Setpoint on Low Pressurizer Pressure, kg/cm^{2}A (psia)	109.3 (1,555)
SIT Gas Pressure, kg/cm^{2}A (psia)	41.1 (584.7)

Table 15.6.5-8

Small Break Spectrum

Break Size and Location	Abbreviation	Figure No.
465 cm^2 (0.5 ft^2) break in pump discharge leg	465 cm^2/PD	15.6.5-14
325 cm^2 (0.35 ft^2) break in pump discharge leg	325 cm^2/PD	15.6.5-15
93 cm^2 (0.1 ft^2) break in pump discharge leg	93 cm^2/PD	15.6.5-16
46.5 cm^2 (0.05 ft^2) break in pump discharge leg	46.5 cm^2/PD	15.6.5-17
372 cm^2 (0.4 ft^2) break in DVI line	372 cm^2/DVI	15.6.5-18
93 cm^2 (0.1 ft^2) break in DVI line	93 cm^2/DVI	15.6.5-19
46.5 cm^2 (0.05 ft^2) break in DVI line	46.5 cm^2/DVI	15.6.5-20
18.6 cm^2 (0.02 ft^2) break in DVI line	18.6 cm^2/DVI	15.6.5-21
27.9 cm^2 (0.03 ft^2) break in top of pressurizer	27.9 cm^2/HL	15.6.5-22

Table 15.6.5-9

Variables Plotted as a Function of Time for Each Small Break in the Spectrum

Variable	Figure Symbol
Normalized total core power	A
Inner vessel pressure	B
Break flow rate	C
Inner vessel inlet flow rate	D
Inner vessel two-phase mixture level	E
Heat transfer coefficient at hot spot	F
Coolant temperature at hot spot	G
Hot spot clad surface temperature	H

Table 15.6.5-10

Peak Cladding Temperature and Oxidation Percentage
for the Small Break Spectrum

Break	Peak Cladding Temperature, °C (°F)	Maximum Cladding Oxidation, %	Maximum Core-Wide Oxidation, %
465 cm^2/PD	498 (929)	0.0017	< 0.0003
325 cm^2/PD	492 (917)	0.0015	< 0.0002
93 cm^2/PD	565 (1,049)	0.0010	< 0.0001
46.5 cm^2/PD	568 (1,054)	0.0008	< 0.0002
372 cm^2/DVI	624 (1,156)	0.0195	< 0.0029
93 cm^2/DVI	569 (1,056)	0.0069	< 0.0009
46.5 cm^2/DVI	571 (1,059)	0.0018	< 0.0003
18.6 cm^2/DVI	616 (1,140)	0.0029	< 0.0006
27.9 cm^2/HL	568 (1,055)	0.0006	< 0.0002

Table 15.6.5-11

Times of Interest for the Small Break Spectrum
(Seconds after Break)

Break	SI Pump Flow Delivered to RCS	SI Tank Flow Delivered to RCS	Hot Spot Peak Cladding Temperature Occurs
465 cm^2/PD	57	150	167
325 cm^2/PD	62	218	105
93 cm^2/PD	138	1,128	100
46.5 cm^2/PD	248	2,984	208
372 cm^2/DVI	60	192	239
93 cm^2/DVI	138	1,092	100
46.5 cm^2/DVI	250	N/A (1)	210
18.6 cm^2/DVI	624	N/A (1)	1,184
27.9 cm^2/HL	795	N/A (1)	750

(1) Calculation terminated before initiation of SI tank discharge

Table 15.6.5-12

General System Parameters and Initial Conditions
Long-Term Cooling SIS Performance

<table>
<tr><th colspan="2">Quantity</th><th>Value</th></tr>
<tr><td colspan="2">Reactor Power Level (102 % of Nominal), MWt</td><td>4,062.66</td></tr>
<tr><td colspan="2">SCS Entry Temperature, °C (°F)</td><td>193 (380)</td></tr>
<tr><td colspan="2">SCS Entry Pressure, kg/cm^2A (psia)</td><td>28.1 (400)</td></tr>
<tr><td colspan="2">Atmospheric Dump Valve Capacity, per Valve at 70.3 kg/cm^2A (1,000 psia), kg/hr (lbm/hr)</td><td>430,900 (950,000) (min)</td></tr>
<tr><td colspan="2">Auxiliary Feedwater Storage Tank Capacity, per tank, L (gal)</td><td>1,870,000 (494,000) (min)</td></tr>
<tr><td rowspan="3">Boric Acid Concentration, wt% (ppm)</td><td>RCS</td><td>0.94 (1,650) (max)</td></tr>
<tr><td>IRWST</td><td>2.52 (4,400) (max)</td></tr>
<tr><td>SIT</td><td>2.52 (4,400) (max)</td></tr>
</table>

Table 15.6.5-13 (1 of 3)

Major Input Parameters Used in Radiological Consequences Analysis for Large Break LOCA

Parameter	Value	
Containment Leakage Parameters		
Reactor Core Power Level	4,062.66 MWt	
Core Inventory	See Table 15A-1	
Radionuclide Composition		
Group	Elements	
Noble Gases	Xe, Kr	
Halogens	I, Br	
Alkali Metals	Cs, Rb	
Tellurium	Te, Sb, Se, Ba, Sr	
Noble Metals	Ru, Rh, Pd, Mo, Tc, Co	
Lanthandies	La, Zr, Nd, Eu, Nb, Pm, Pr, Sm, Y, Cm, Am	
Cerium	Ce, Pu, Np	
Timing of Release Phases		
Phase	Onset	Duration
Gap Release	0.0083 hr	0.5 hrs
Early In-Vessel Release	0.5083 hr	1.3 hrs
Fraction of Core Inventory Released into Containment		
Group	Gap Release Phase	Early In-Vessel Release Phase
Noble Gases	0.05	0.95
Halogens	0.05	0.35
Alkali Metals	0.05	0.25
Tellurium Metals	0.00	0.05
Ba, Sr	0.00	0.02
Noble Metals	0.00	0.0025
Cerium	0.00	0.0005
Lanthanides	0.00	0.0002

Table 15.6.5-13 (2 of 3)

Parameter	Value
Activity Transport Parameters in Primary Containment	
Containment Net Free Volume	8.86×10^4 m^3 (3.13×10^6 ft^3)
Sprayed Volume	6.64×10^4 m^3 (2.35×10^6 ft^3)
Unsprayed Volume	2.21×10^4 m^3 (7.82×10^5 ft^3)
Primary Containment Leak Rate	0.1 v/o/day (0 ~ 24 hrs) 0.05 v/o/day (24 ~ 270 hrs)
Flow Rate Between Sprayed and Unsprayed Regions	736 m^3/min (26,000 cfm) (Mixing Flow) 2 turnovers of unsprayed volume/hr
Spray Initiation Time	110 sec (Delay time)
Spray Recirculation Phase Initiation Time	Spray water is circulated from IRWST for entire duration of accident (IRWST→CS→HVT→IRWST)
Containment Spray Removal Coefficients Elemental (λ_E) Particulate (λ_P)	20 hr^{-1} (0 ~ 2.25 hrs until DF is 200) 6.25 hr^{-1} (0 ~ 2.40 hrs until DF is 50) 0.625 hr^{-1} (2.40 ~ 4 hrs)
ESF Leakage Parameters	
Minimum IRWST Water Volume	2.44×10^3 m^3 (8.61×10^4 ft^3)
ESF Leakage Rate	8.08 L/hr (2.13 gal/hr)
ESF Leakage Initiation Time	0.0 min
Long-term Minimum IRWST Water pH	> 7
ESF Leakage Flashing Factor	10 % (0 ~ 3 hrs) 2 % (3 ~ 16.67 hrs) 10 % (> 16.67 hrs)
Post-LOCA Sump Water Temperature 3.0 hr 7.64 hr 16.67 hr	 107 °C (225 °F) 113 °C (235.5 °F) 107 °C (225 °F)

Table 15.6.5-13 (3 of 3)

Parameter	Value
Chemical Form of Iodine in ESF Elemental Organic	 97 % 3 %
Fraction of Core Iodine in Sump Water	40 %
MCR Parameters	
MCR Wall Thickness East West North South Ceiling	 0.91 m (3.0 ft) 0.91 m (3.0 ft) 0.91 m (3.0 ft) 0.91 m (3.0 ft) 0.46 m (1.5 ft)
Minimum MCR Envelope Concrete Shielding	0.46 m (1.5 ft)
Emergency Ventilation HVAC Filter Charcoal Density	0.45 g/cc (28.1 lb/ft^3)
Emergency Ventilation HVAC Filter Charcoal Tray Dimension	1.65 m (L) × 1.65 m (W) × 2.34 m (H) 1.65 m (L) × 1.65 m (W) × 1.65 m (H)
Other MCR Parameters	See Table 15.3.3-3
Containment Low Volume Purge System (CLVPS) Release Parameters	
CLVPS Valve Closure Time	5.0 sec
Volume Flow Rate of CLVPS Release	11 m^3/sec (2.34 × 10^4 cfm)
Reactor Coolant Mass	300,000 kg (661,000 lbm)
Reactor Coolant Specific Activity	≤ 3.7 × 10^4 Bq/g (1.0 μCi/g) DE I-131
Onsite χ/Qs	See Tables 2.3.2 ~ 2.3-12
Offsite Model Parameters	
χ/Qs	See Table 2.3-1
Breathing Rate	See Table 15A-11
Minimum Concrete Density	2,240 kg/m^3 (140 lb/ft^3)

Table 15.6.5-14

Radiological Consequences of a Large Break LOCA

Post-LOCA Activity Release Path	TEDE Dose (mSv)		
	MCR and TSC	EAB	LPZ
Containment Leakage	3.26E+01	2.03E+02	1.01E+02
ESF Leakage	9.77E+00	2.38E+01	1.35E+02
CLVPS Release	2.81E-02	5.68E-03	1.25E-03
Containment Shine	0.00E+00	0.00E+00	0.00E+00
External Cloud	6.88E-01	0.00E+00	0.00E+00
Emergency Ventilation Filter Shine	1.34E-06	0.00E+00	0.00E+00
Total	4.31E+01	2.27E+02	2.37E+02
Allowable TEDE Limit	5.00E+01	2.50E+02	2.50E+02

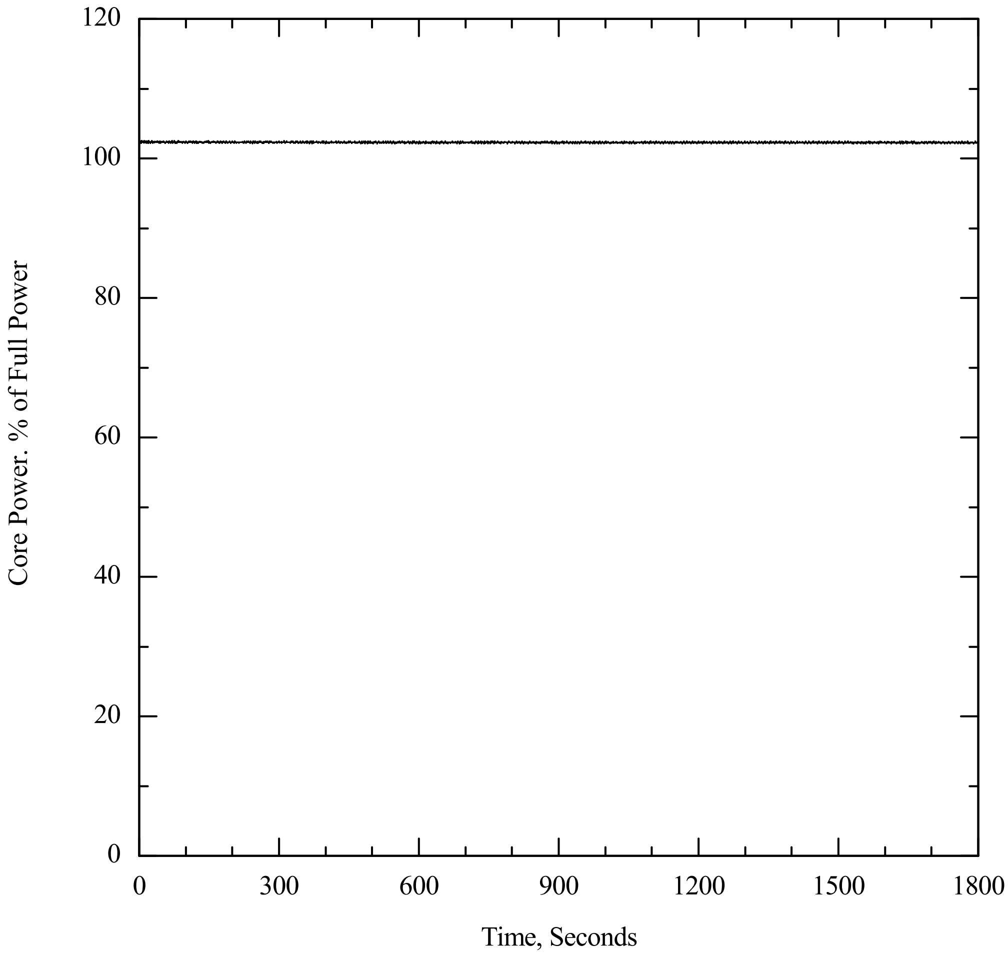

Figure 15.6.2-1 Letdown Line Break, Outside Containment Upstream of Letdown Isolation Valve:Core Power vs. Time

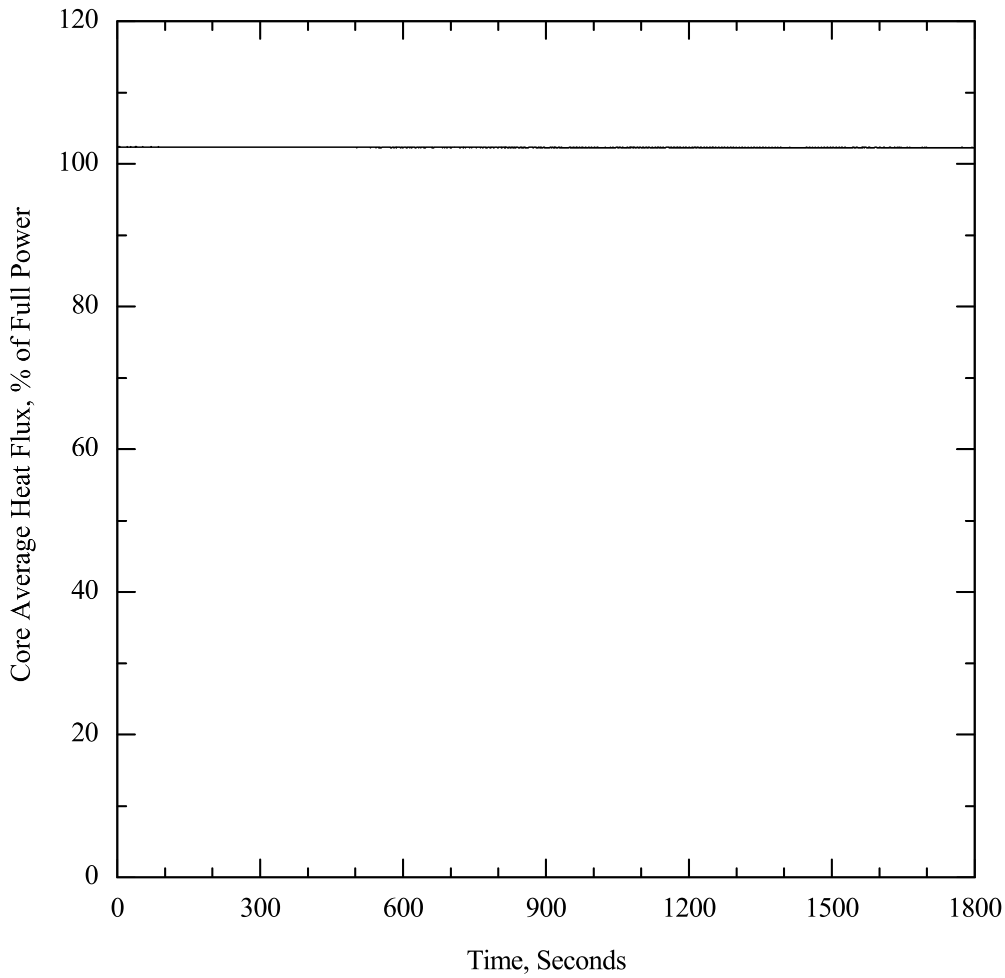

Figure 15.6.2-2 Letdown Line Break, Outside Containment Upstream of Letdown Isolation Valve : Core Average Heat Flux vs. Time

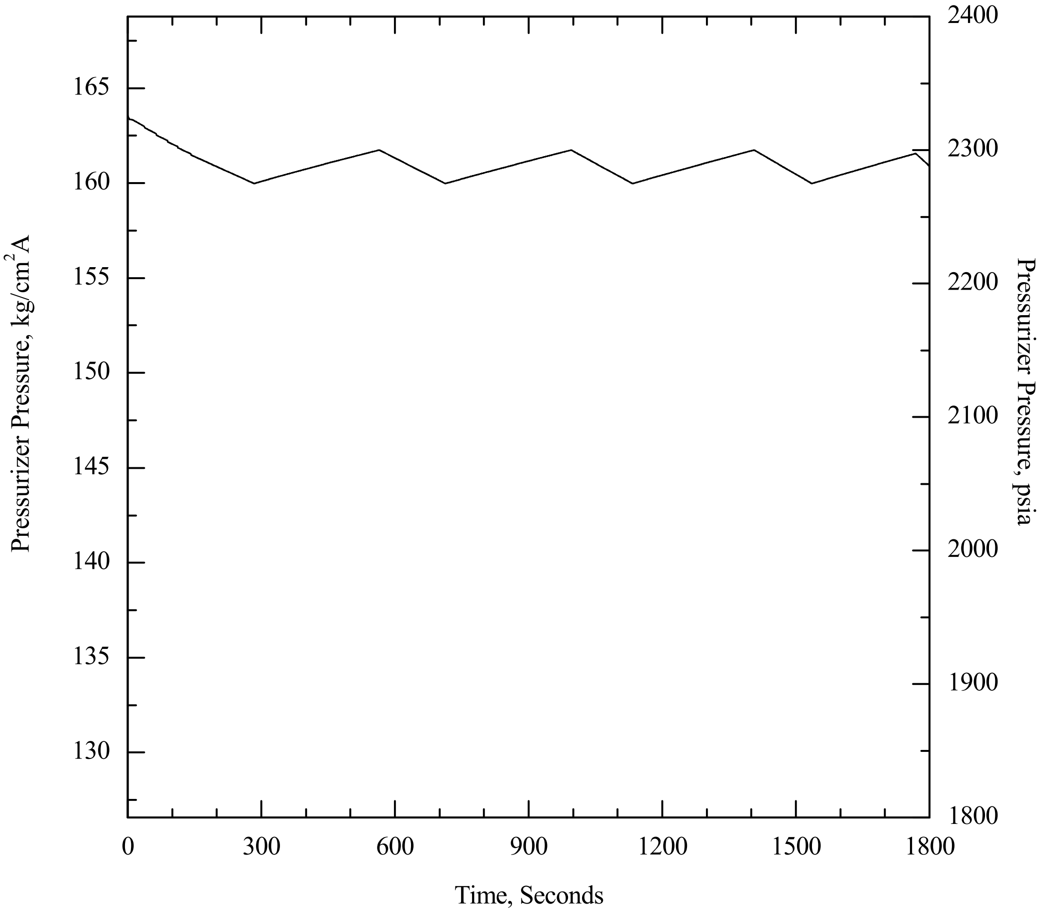

Figure 15.6.2-3 Letdown Line Break, Outside Containment Upstream of Letdown Isolation Valve : Pressurizer Pressure vs. Time

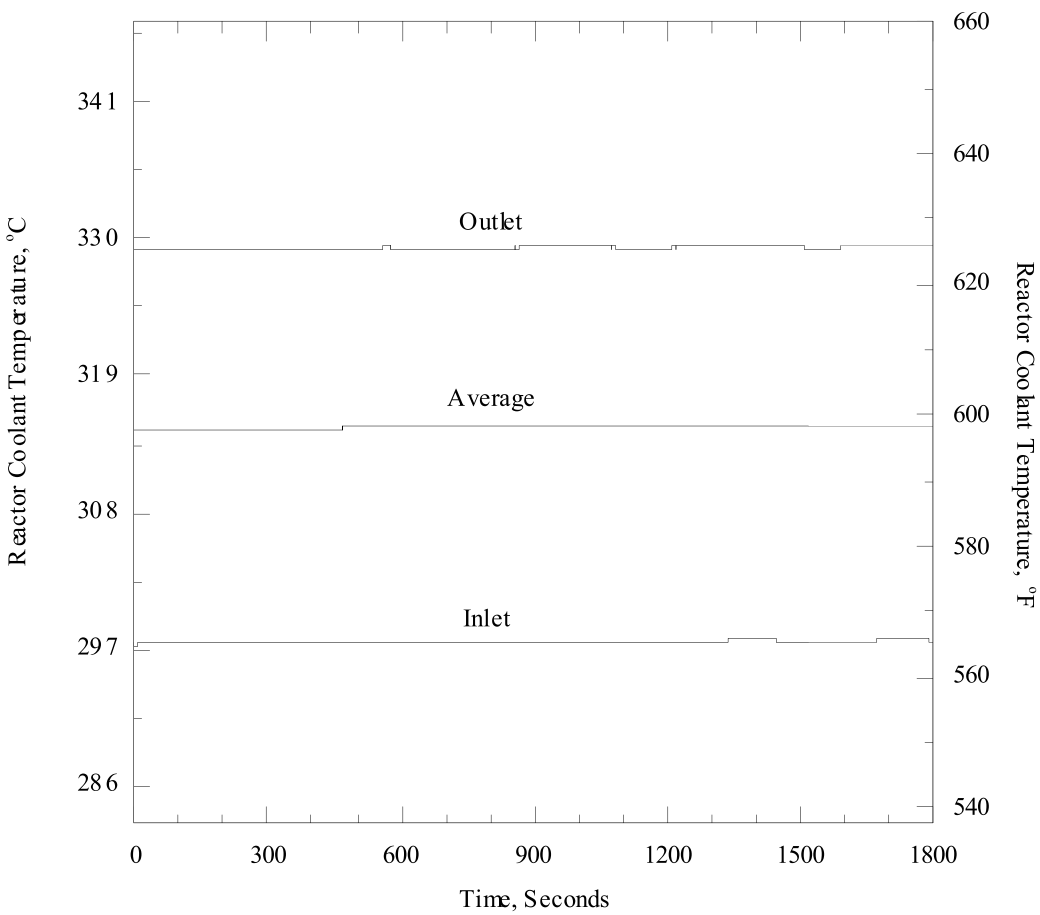

Figure 15.6.2-4 Letdown Line Break, Outside Containment Upstream of Letdown Isolation Valve : Reactor Coolant Temperatures vs. Time

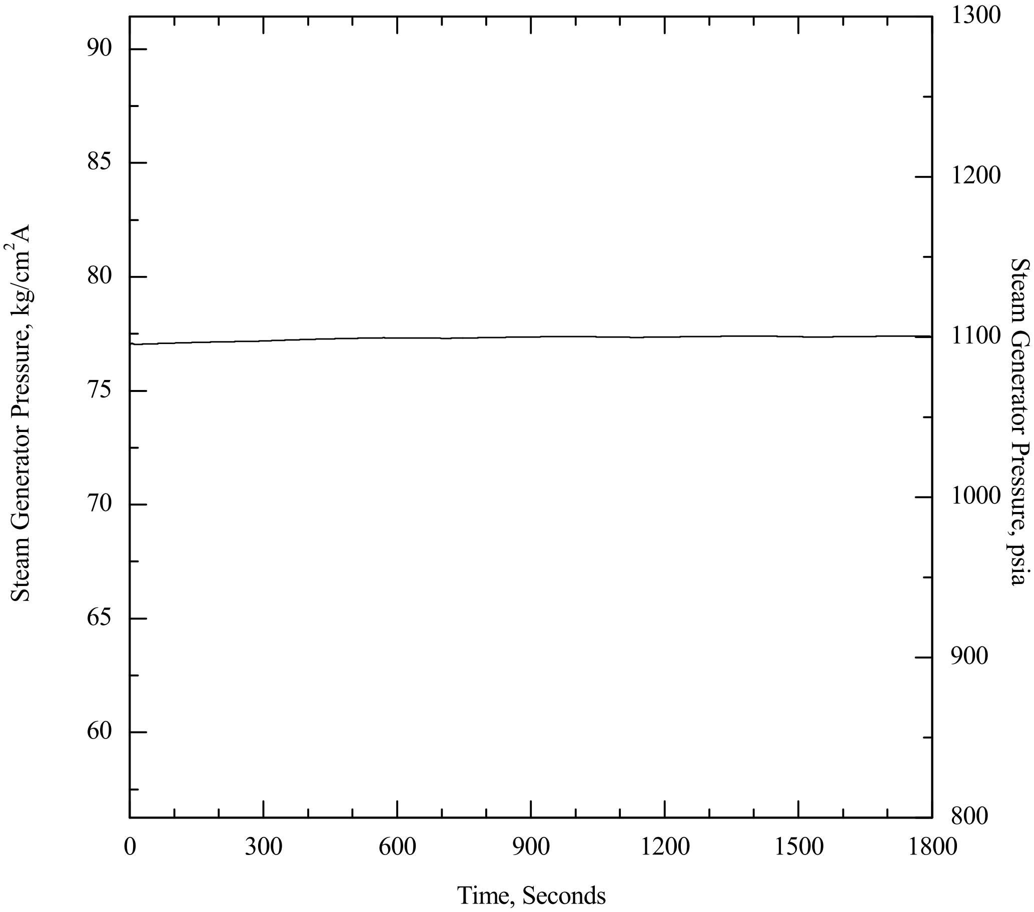

Figure 15.6.2-5 Letdown Line Break, Outside Containment Upstream of Letdown Isolation Valve : Steam Generator Pressure vs. Time

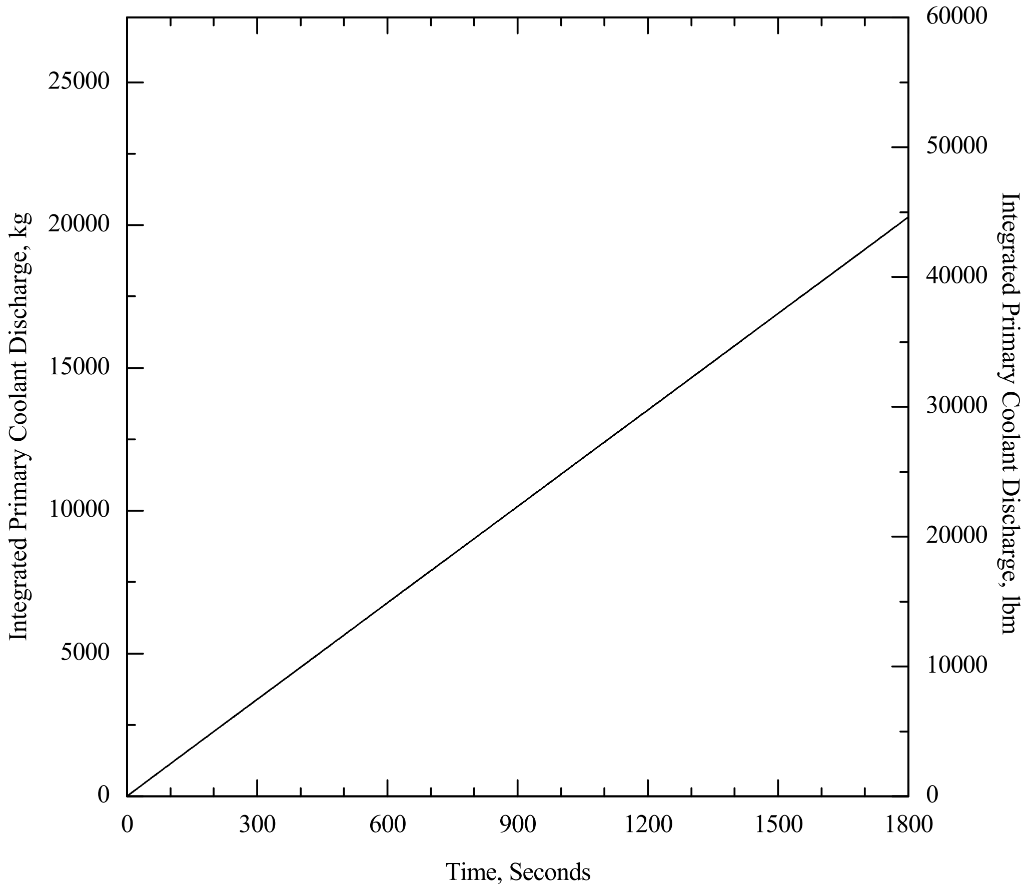

Figure 15.6.2-6 Letdown Line Break, Outside Containment Upstream of Letdown Isolation Valve : Integrated Primary Coolant Discharge vs. Time

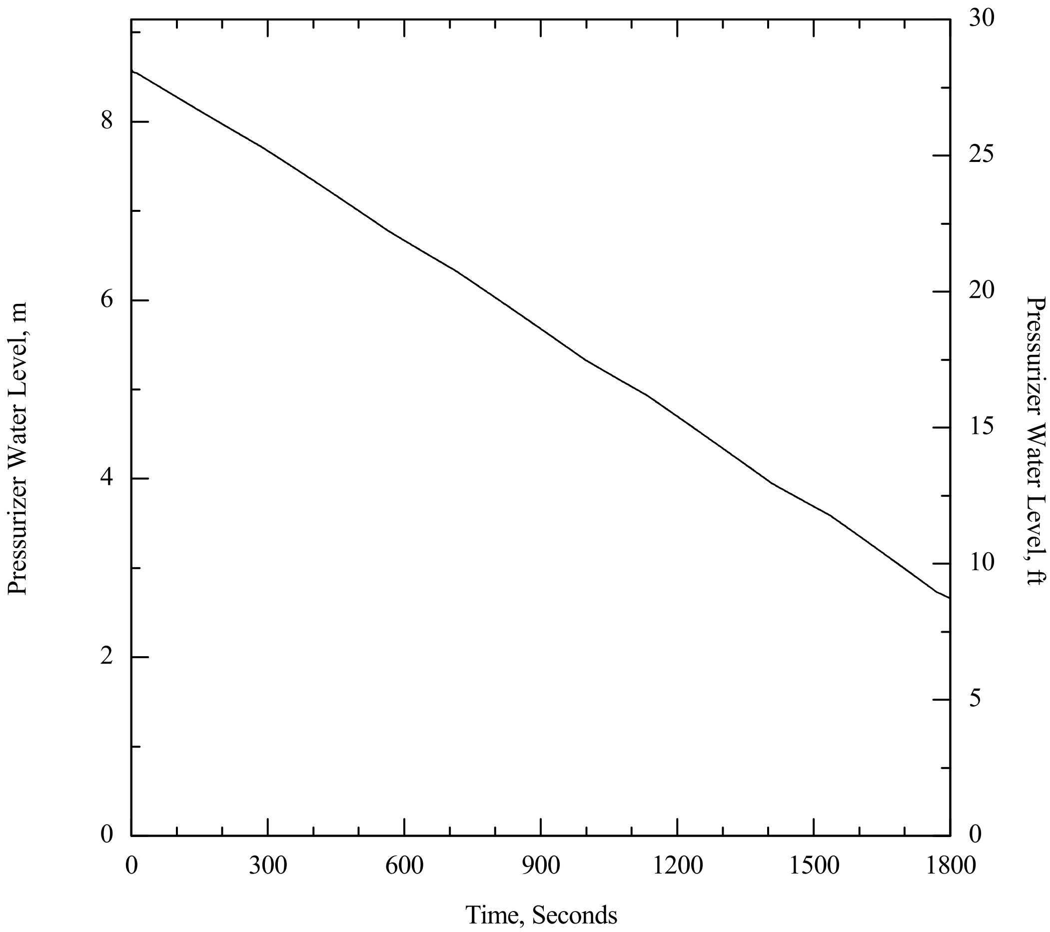

Figure 15.6.2-7 Letdown Line Break, Outside Containment Upstream of Letdown Isolation Valve : Pressurizer Water Level vs. Time

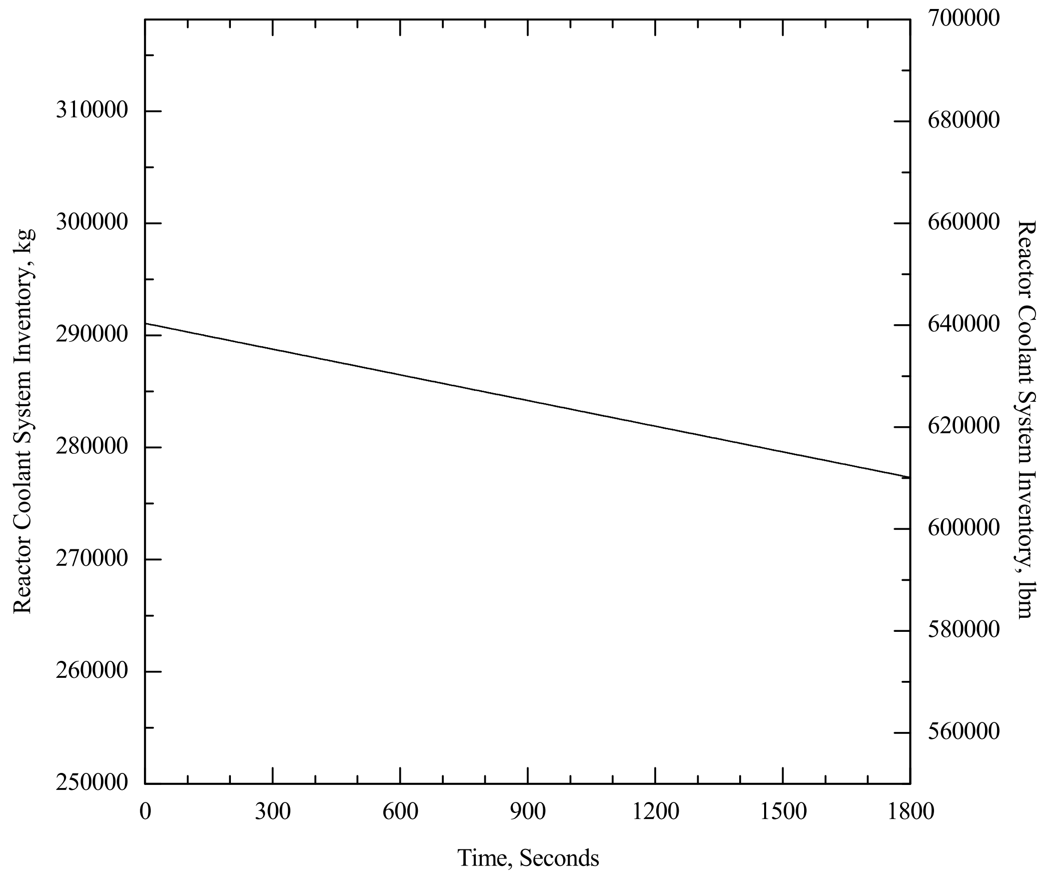

Figure 15.6.2-8 Letdown Line Break, Outside Containment Upstream of Letdown Isolation Valve:RCS Mass Inventory vs. Time

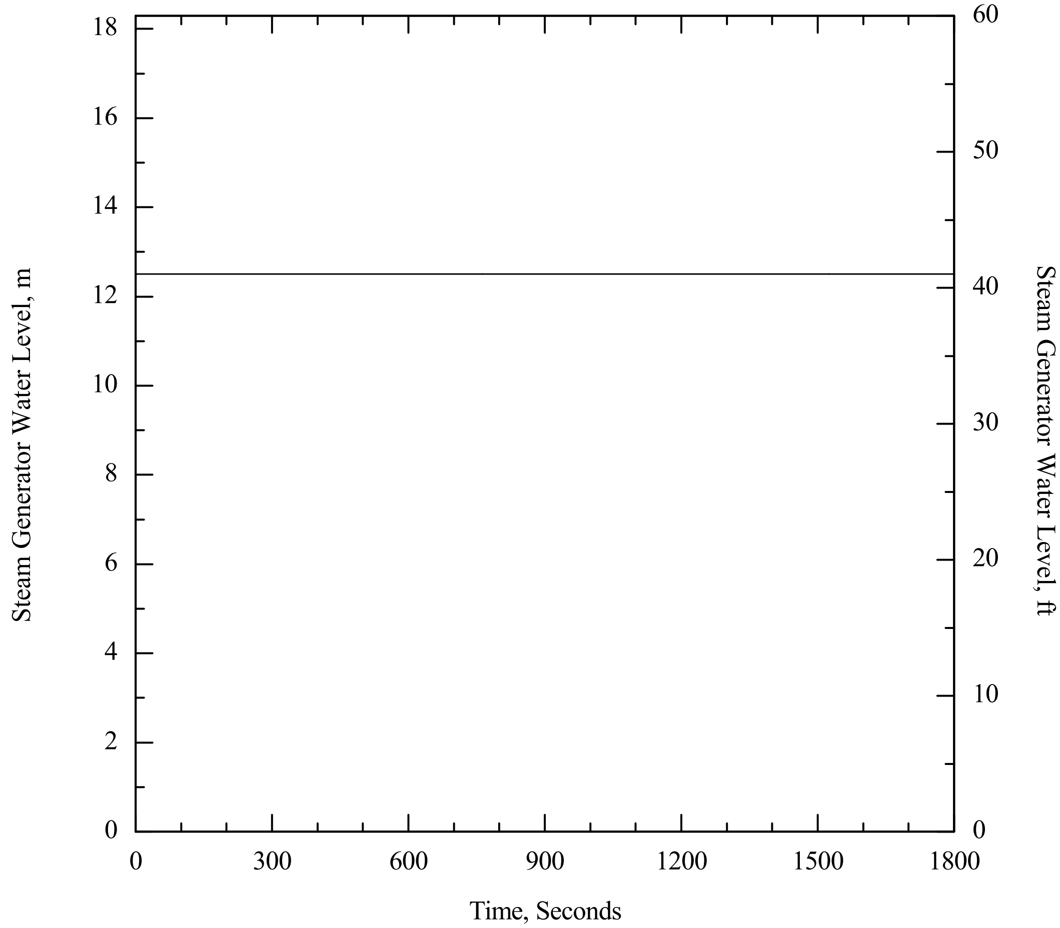

Figure 15.6.2-9 Letdown Line Break, Outside Containment Upstream of Letdown Isolation Valve:Steam Generator Water Level vs. Time

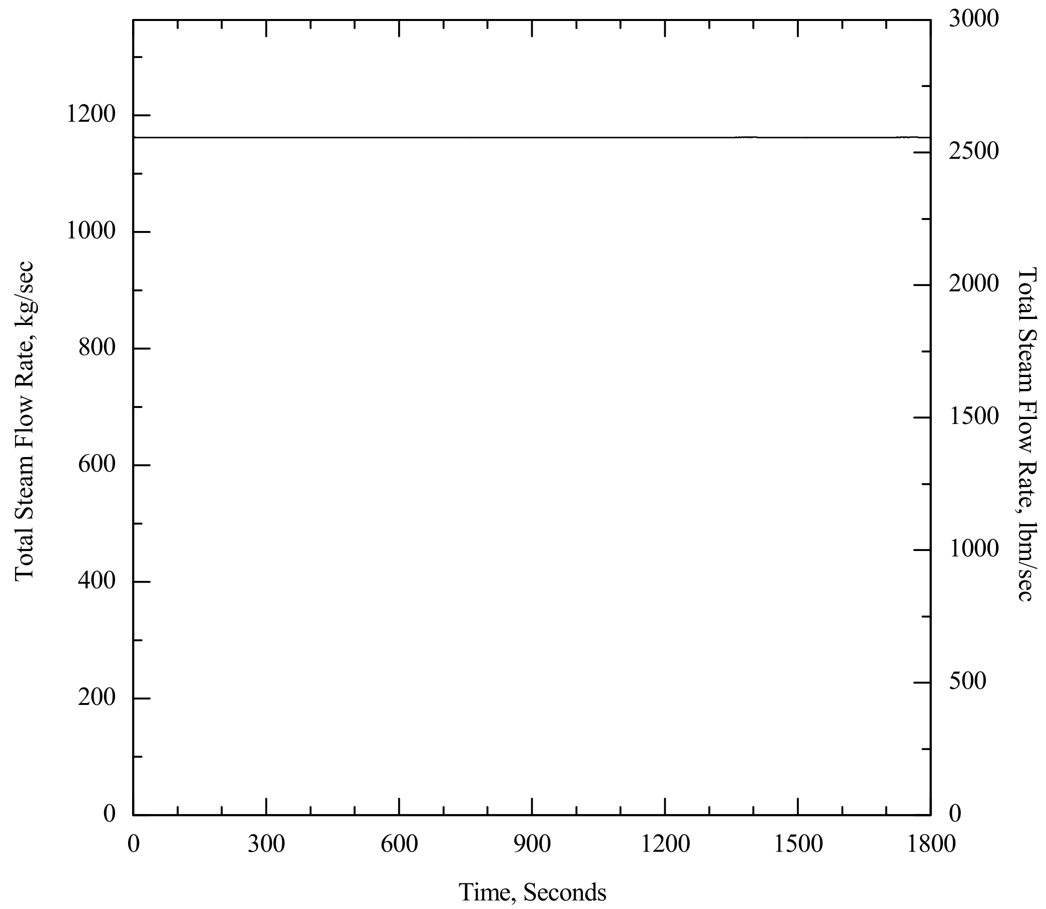

Figure 15.6.2-10 Letdown Line Break, Outside Containment Upstream of Letdown Isolation Valve:Total Steam Flow Rate vs. Time

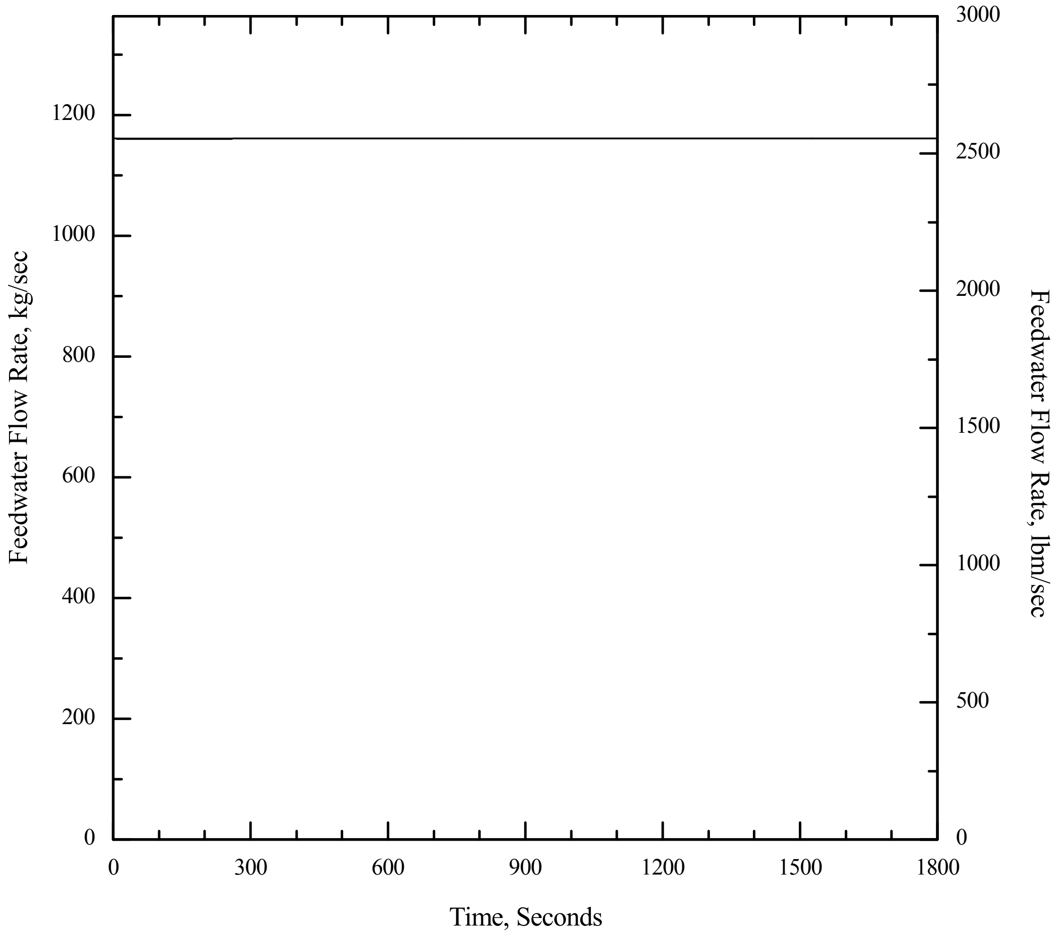

Figure 15.6.2-11 Letdown Line Break, Outside Containment Upstream of Letdown Isolation Valve:Feedwater Flow Rate vs. Time

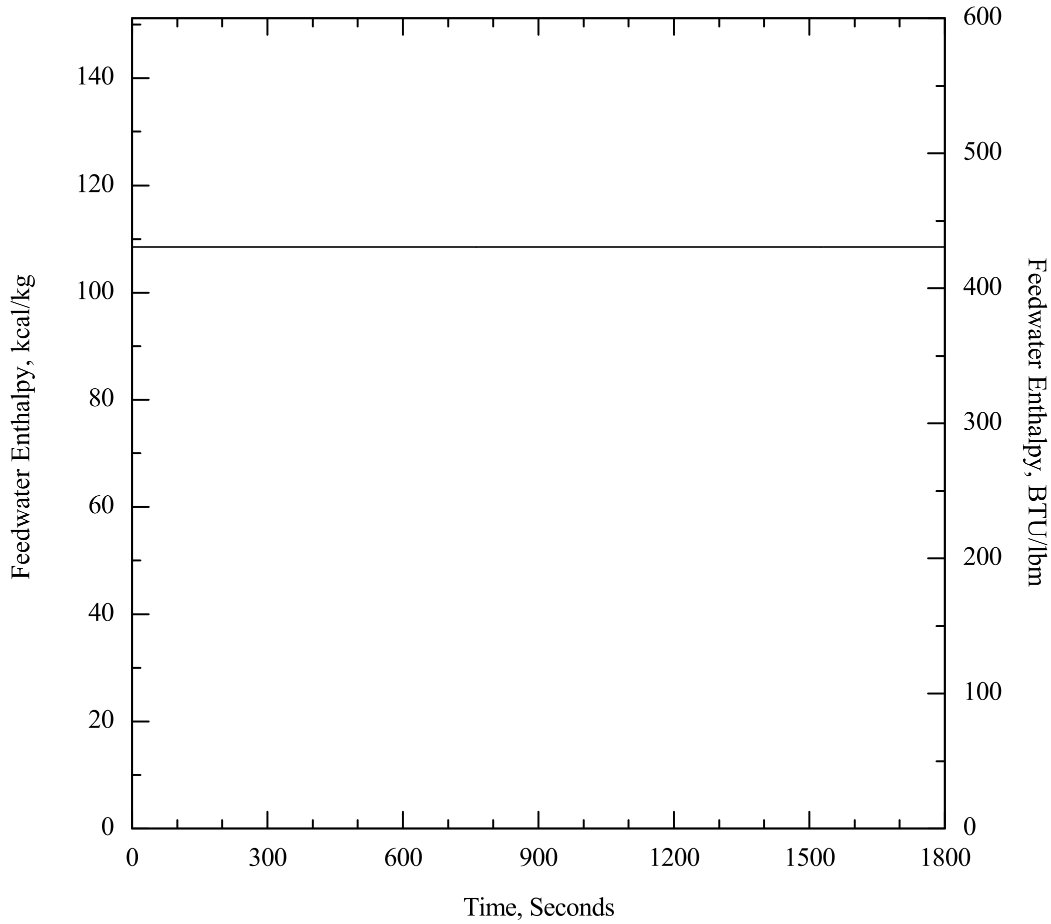

Figure 15.6.2-12 Letdown Line Break, Outside Containment Upstream of Letdown Isolation Valve:Feedwater Enthalpy vs. Time

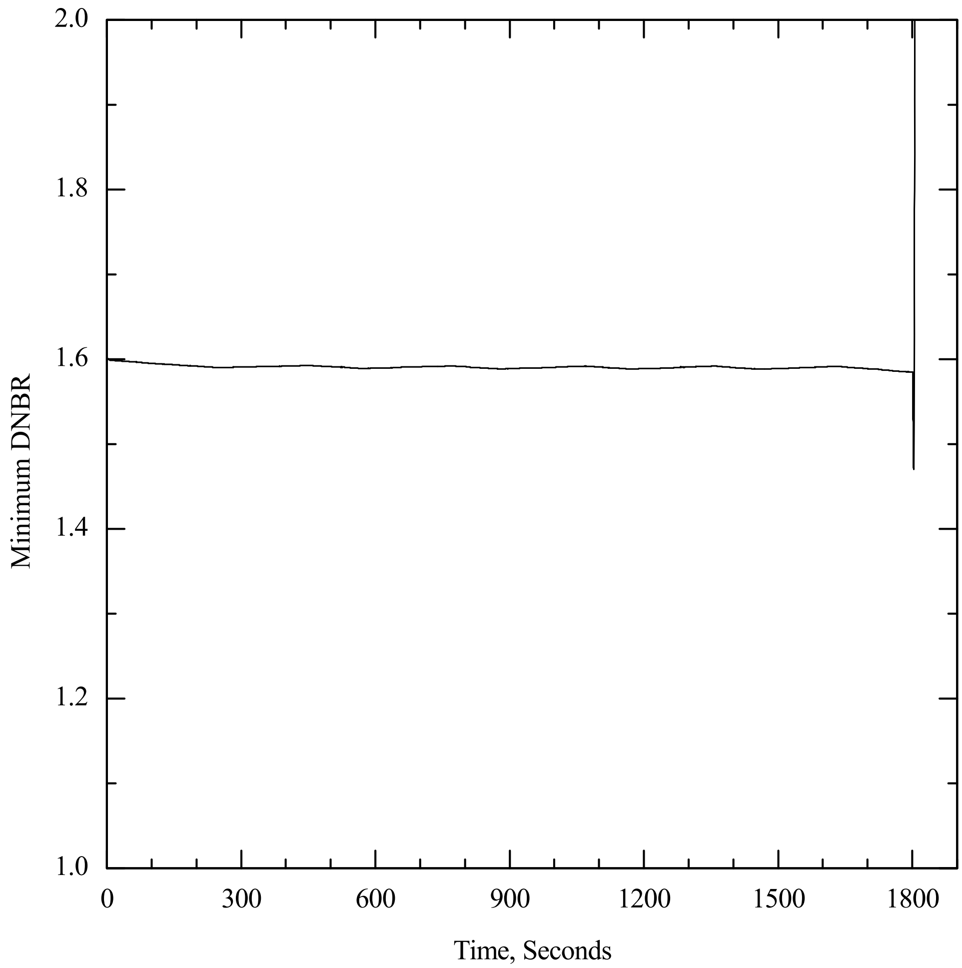

Figure 15.6.2-13 Letdown Line Break, Outside Containment Upstream of Letdown Isolation Valve : Minimum DNBR vs. Time

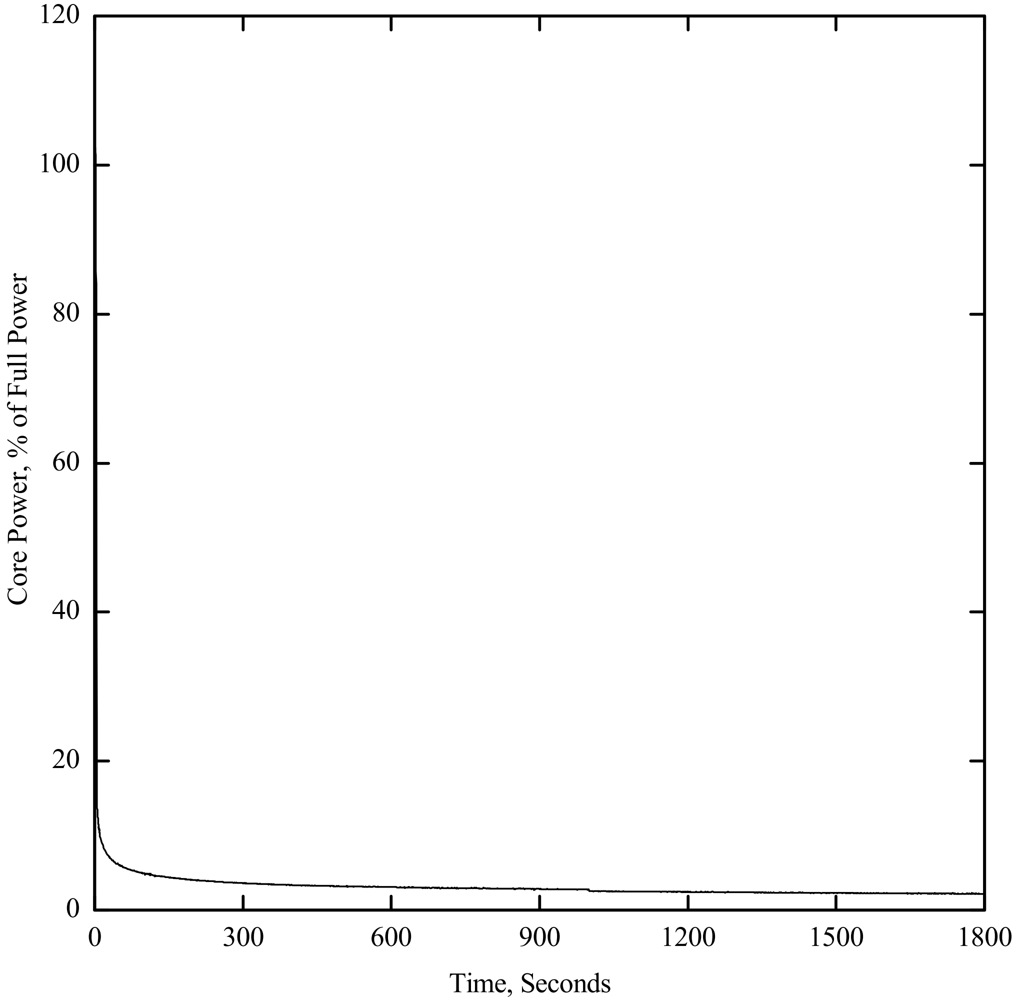

Figure 15.6.3-1 SGTR Without LOOP: Core Power vs. Time

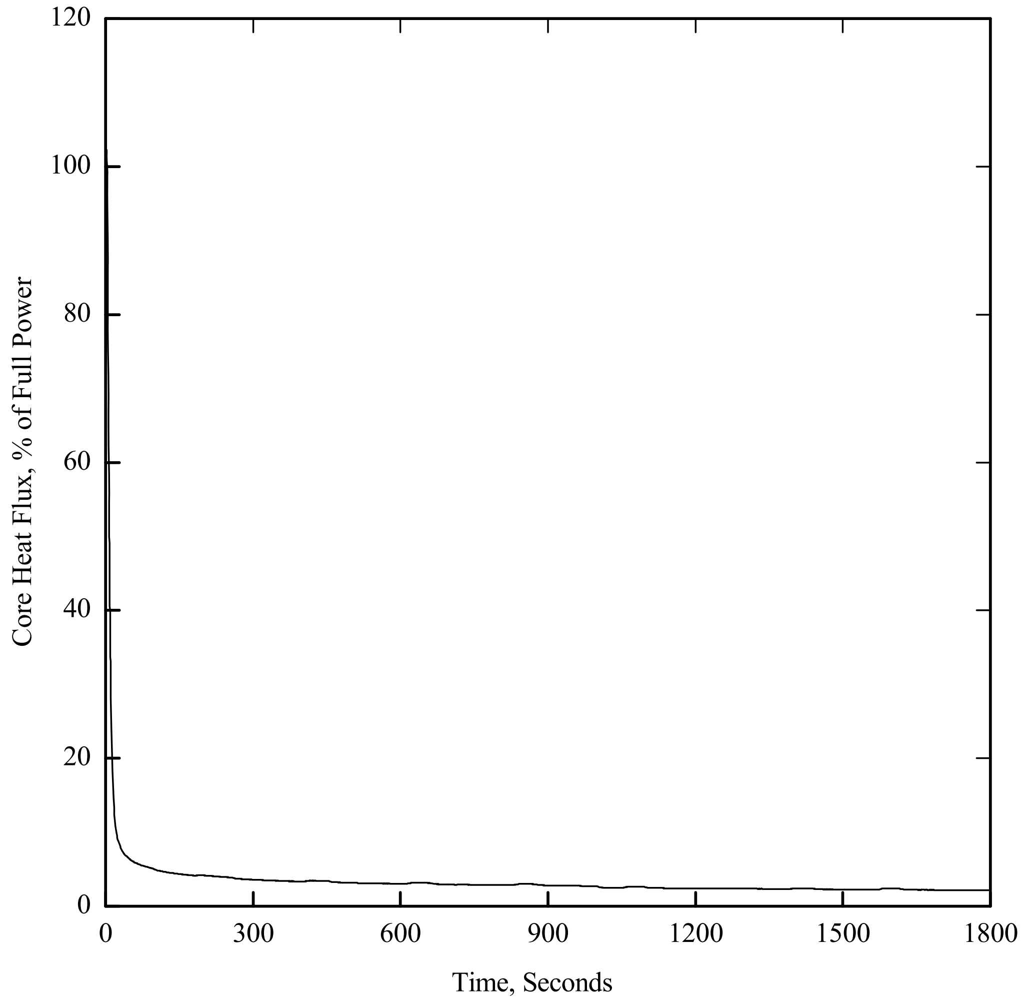

Figure 15.6.3-2 SGTR Without LOOP:Core Average Heat Flux vs. Time

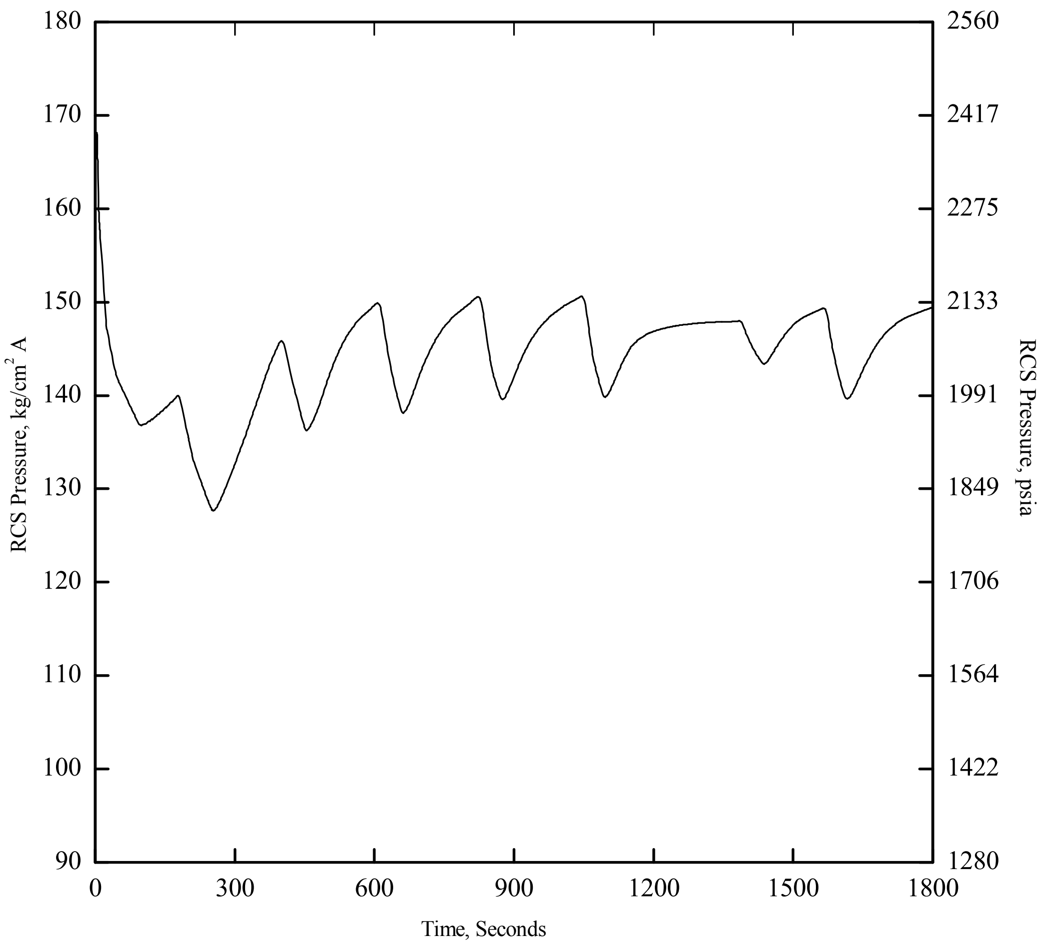

Figure 15.6.3-3 SGTR Without LOOP:RCS Pressure vs. Time

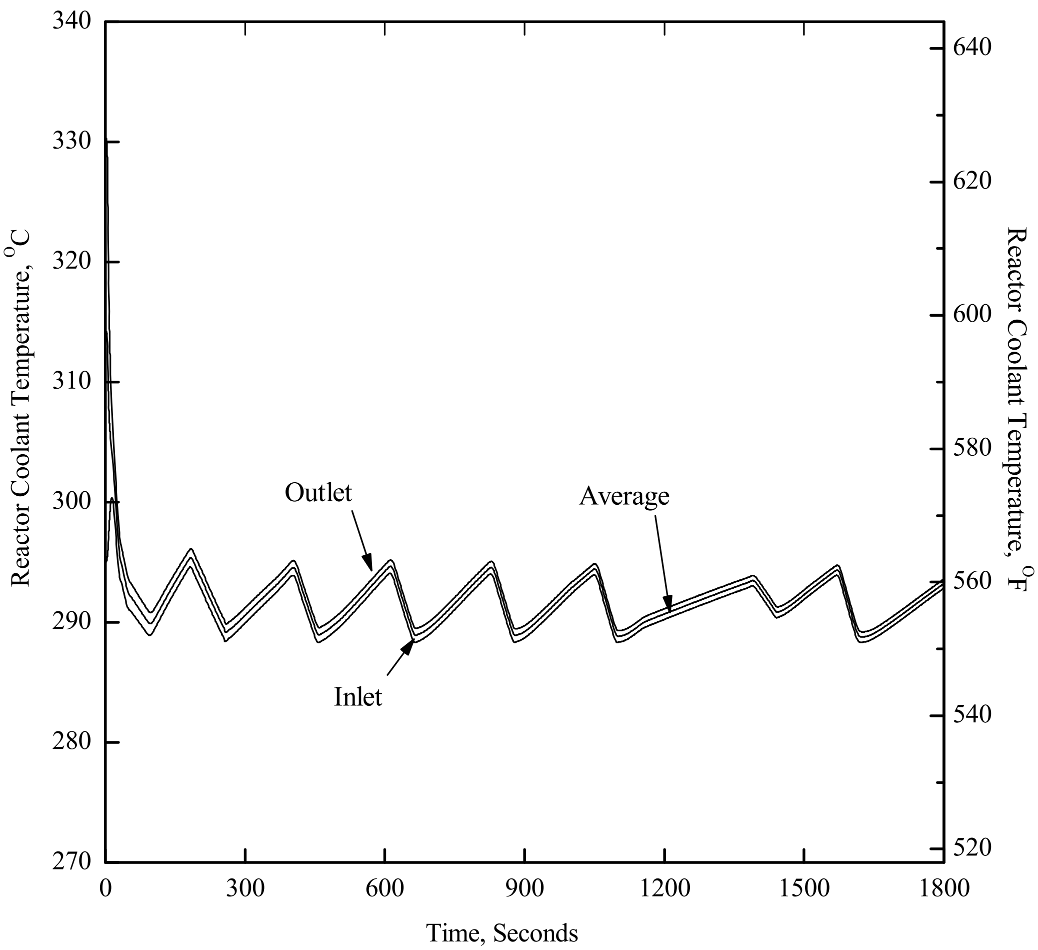

Figure 15.6.3-4 SGTR Without LOOP:Reactor Coolant Temperature vs. Time

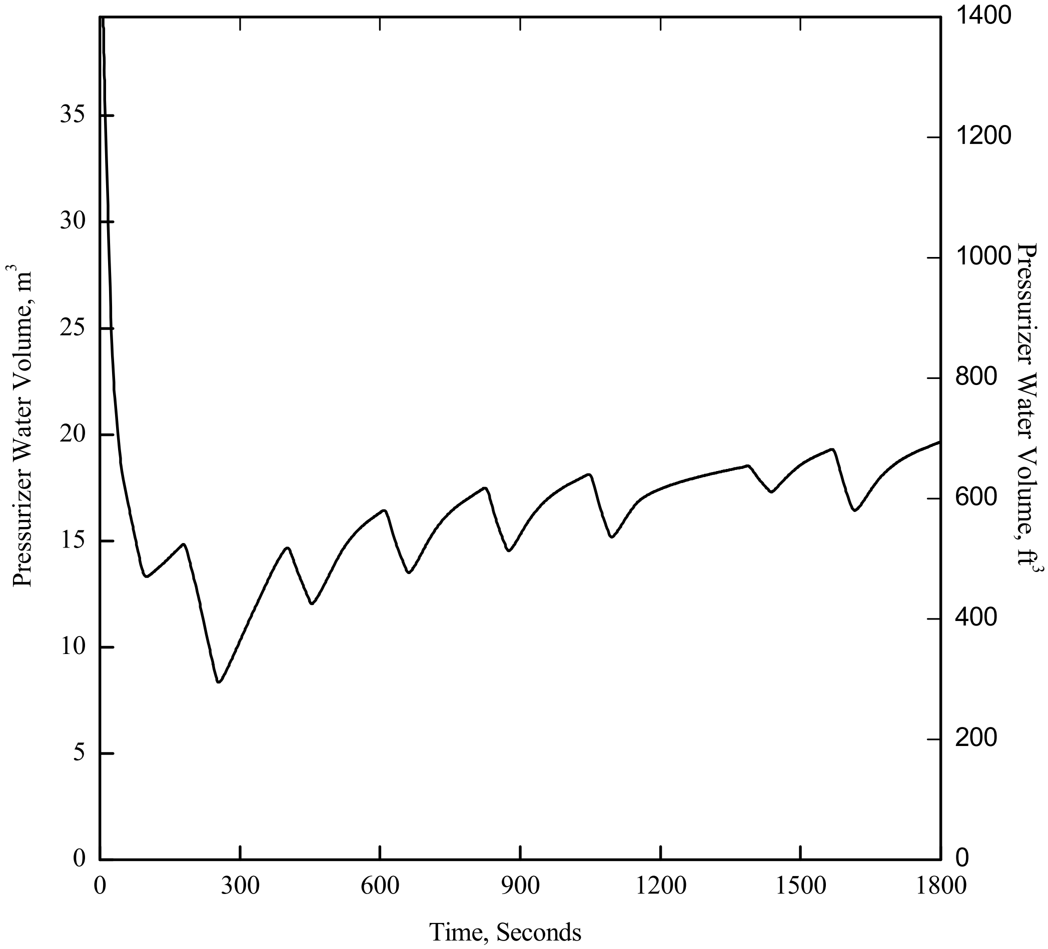

Figure 15.6.3-5   SGTR Without LOOP : Pressurizer Water Volume vs. Time

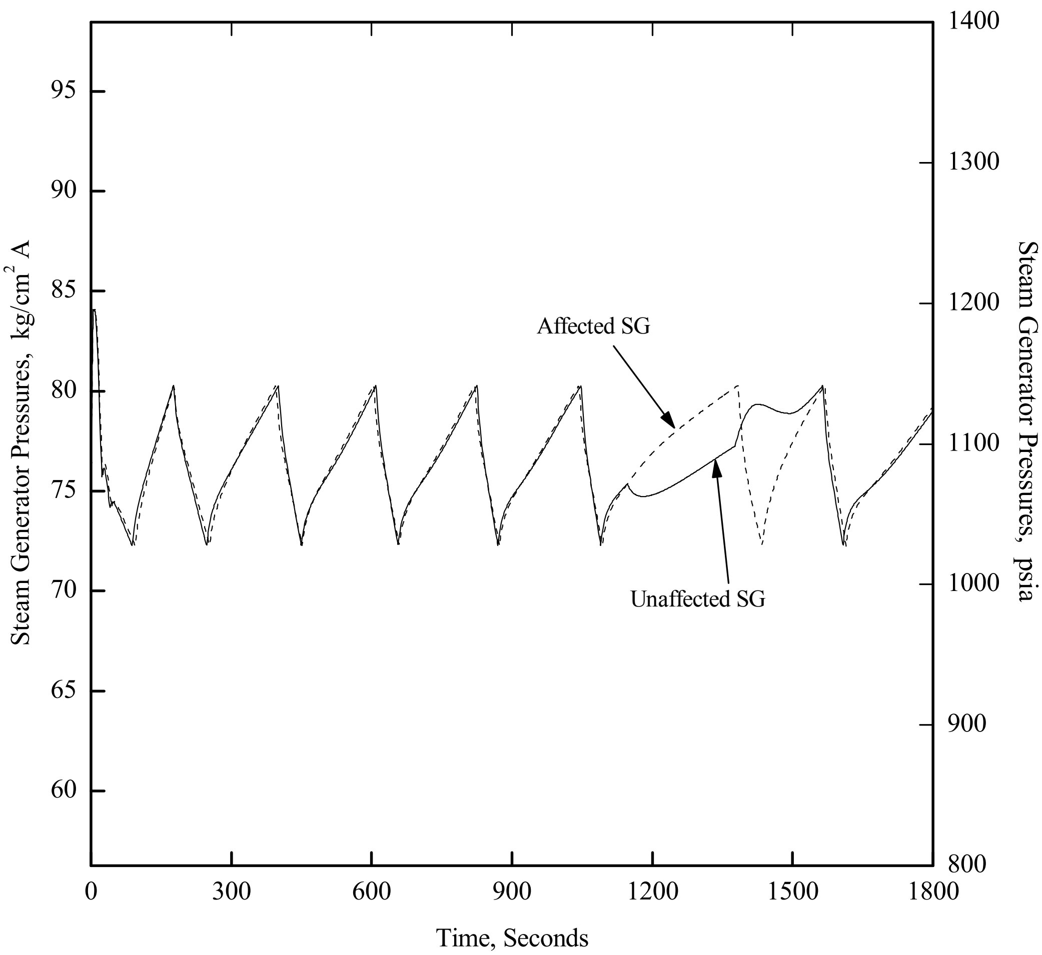

Figure 15.6.3-6 SGTR Without LOOP : Steam Generator Pressure vs. Time

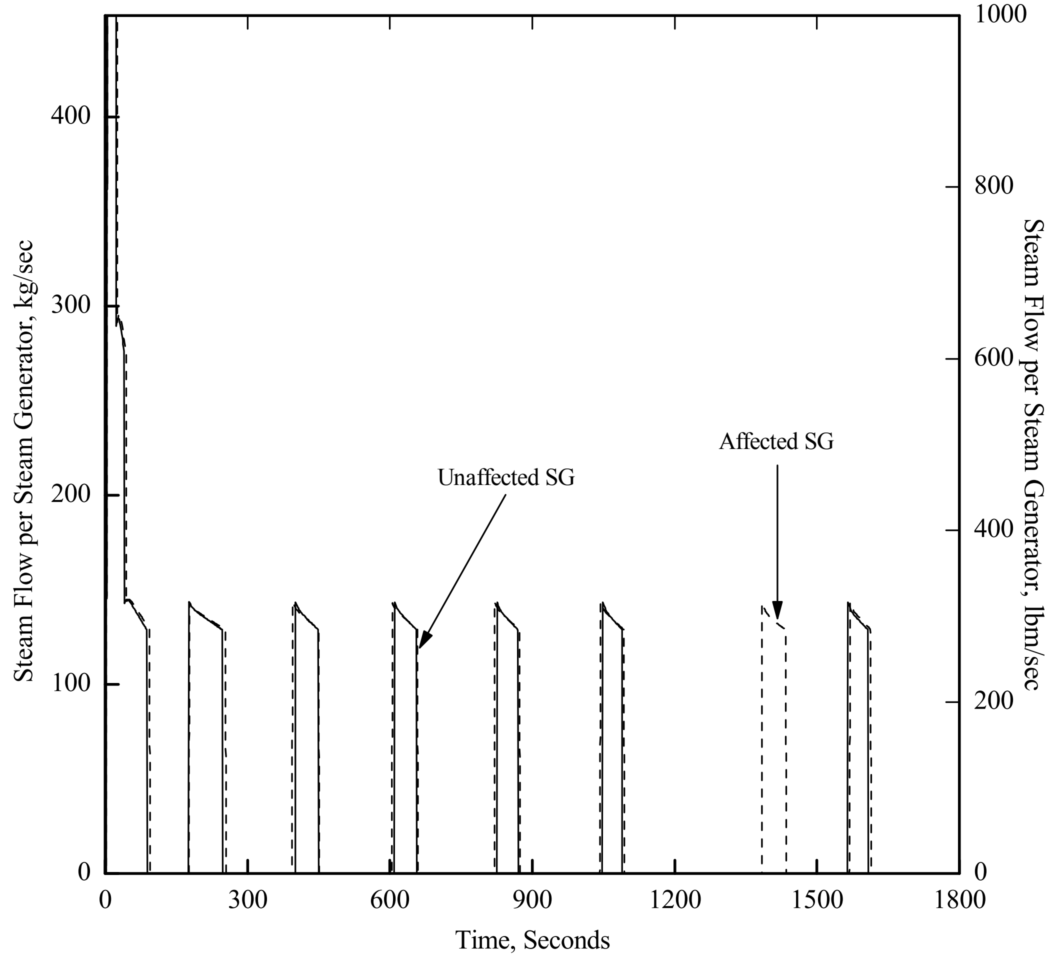

Figure 15.6.3-7 SGTR Without LOOP : Steam Flow Rate vs. Time

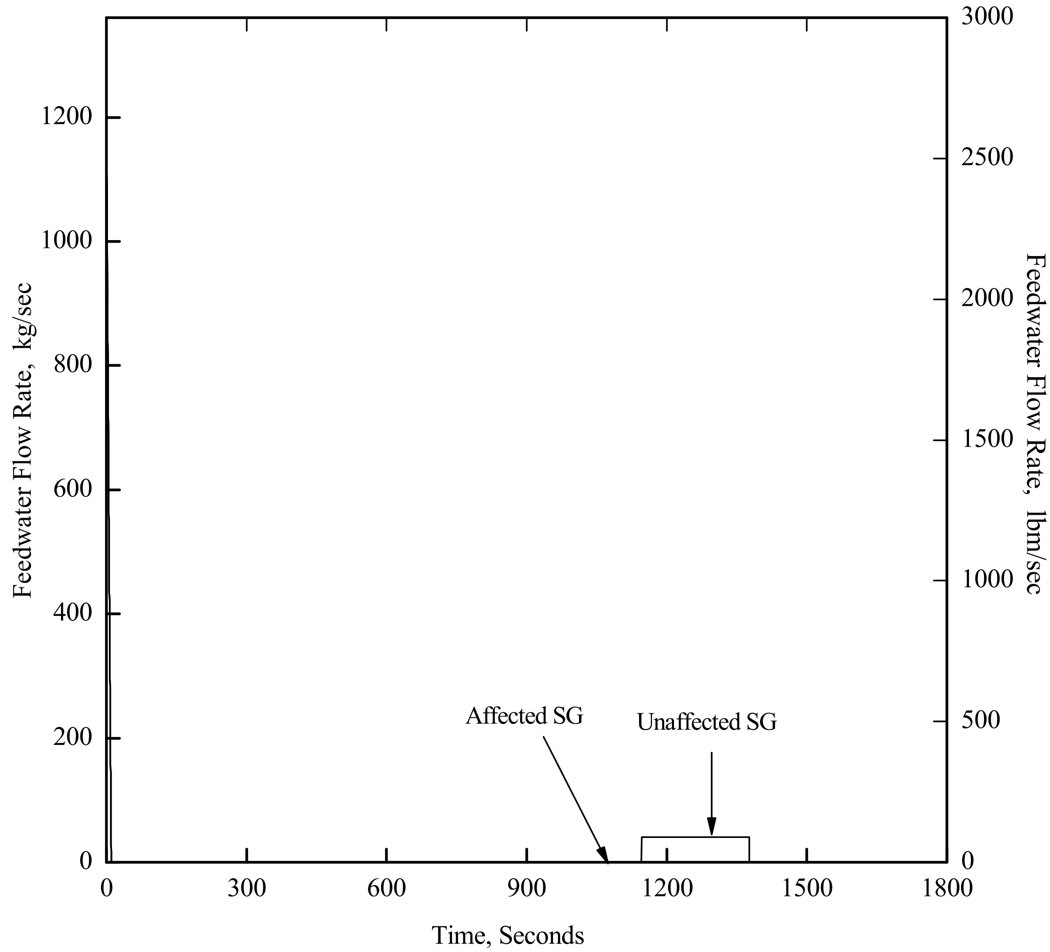

Figure 15.6.3-8 SGTR Without LOOP : Feedwater Flow Rate vs. Time

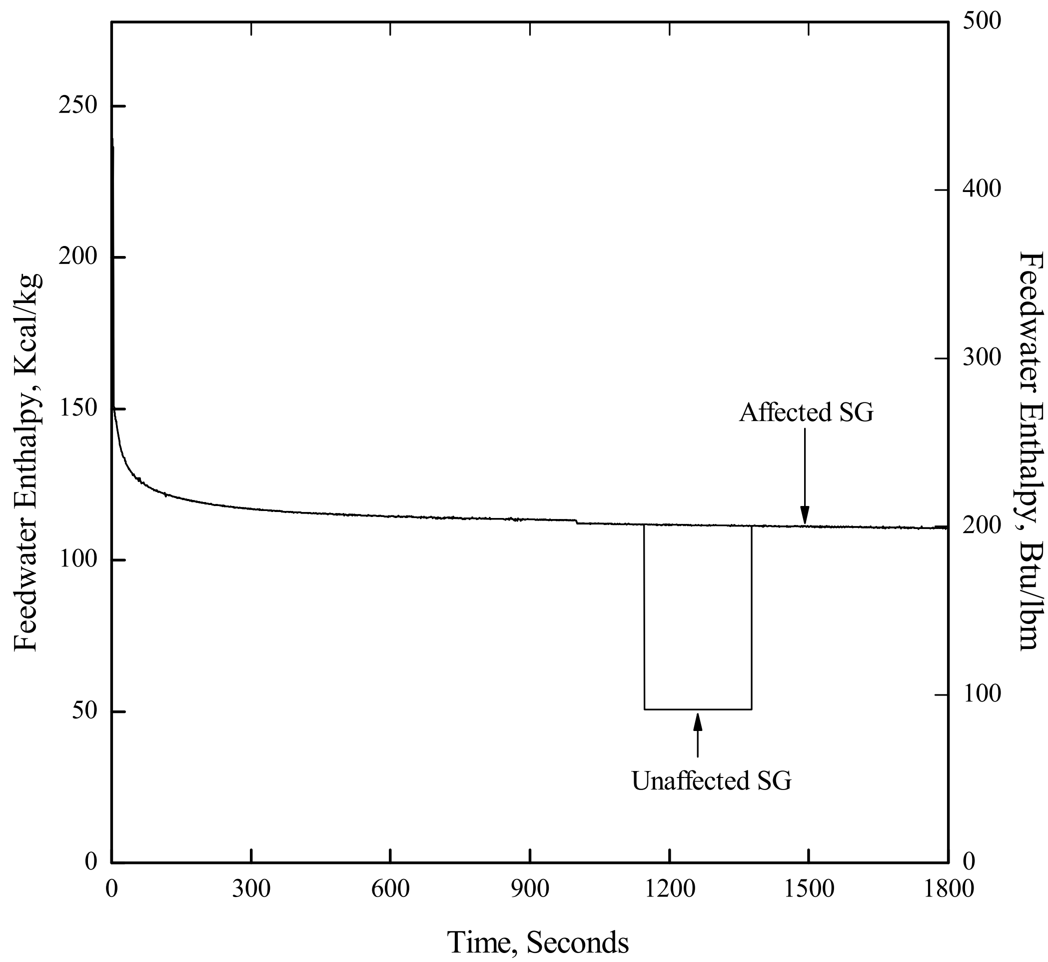

Figure 15.6.3-9 SGTR Without LOOP : Feedwater Enthalpy vs. Time

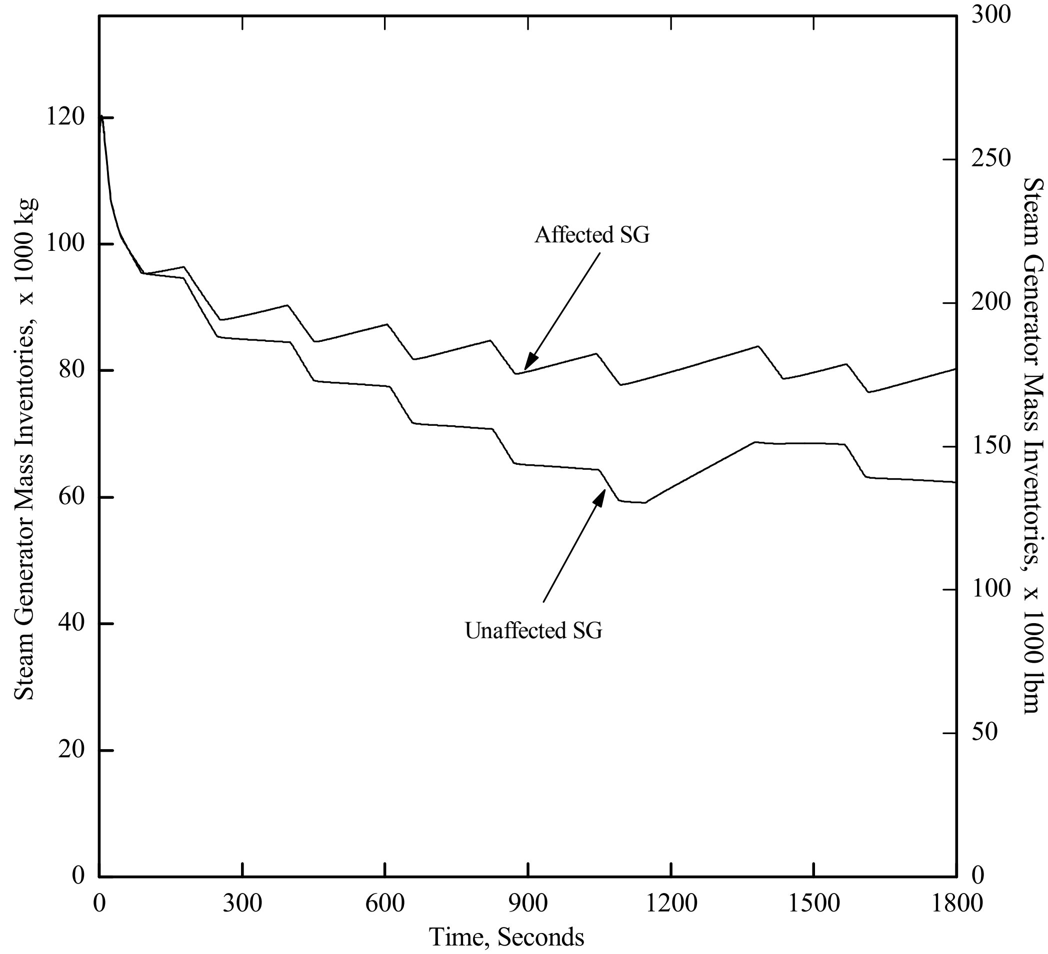

Figure 15.6.3-10 SGTR Without LOOP : Steam Generator Mass Inventories vs. Time

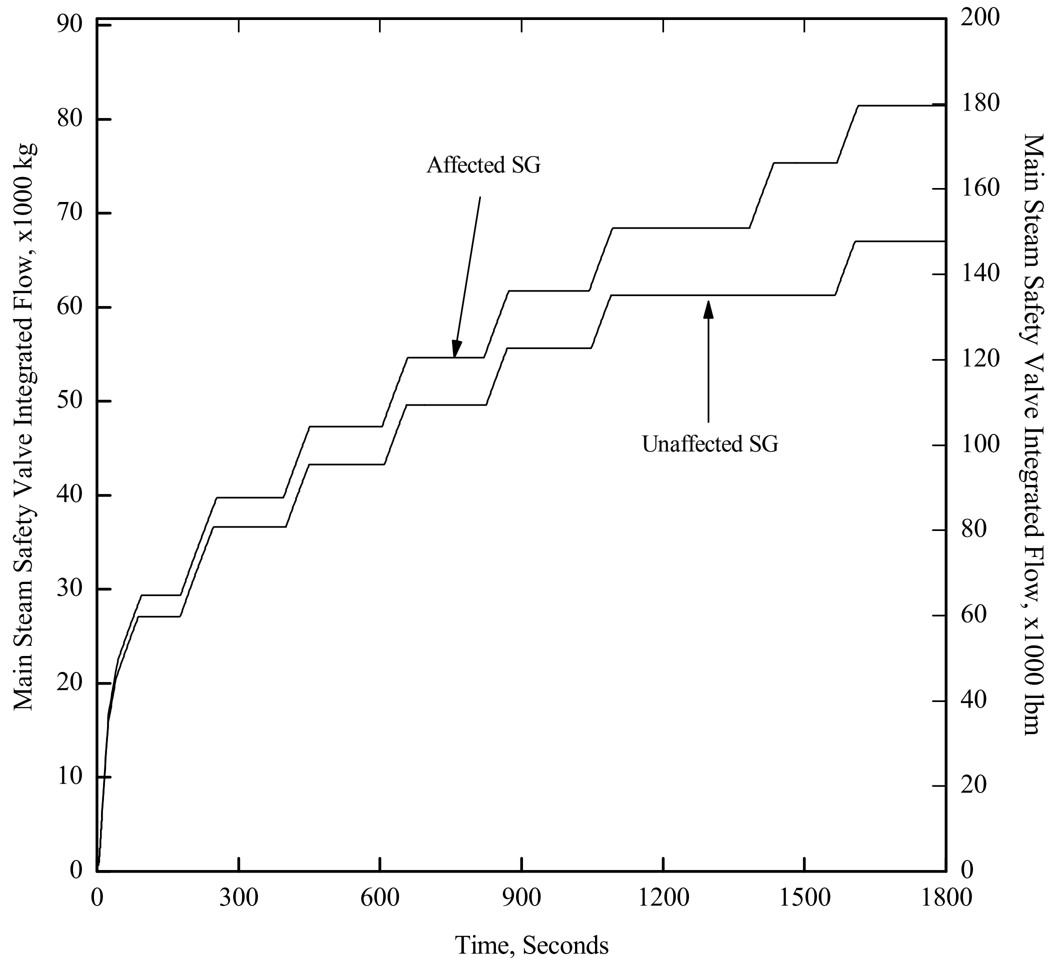

Figure 15.6.3-11 SGTR Without LOOP : MSSV Integrated Flow vs. Time

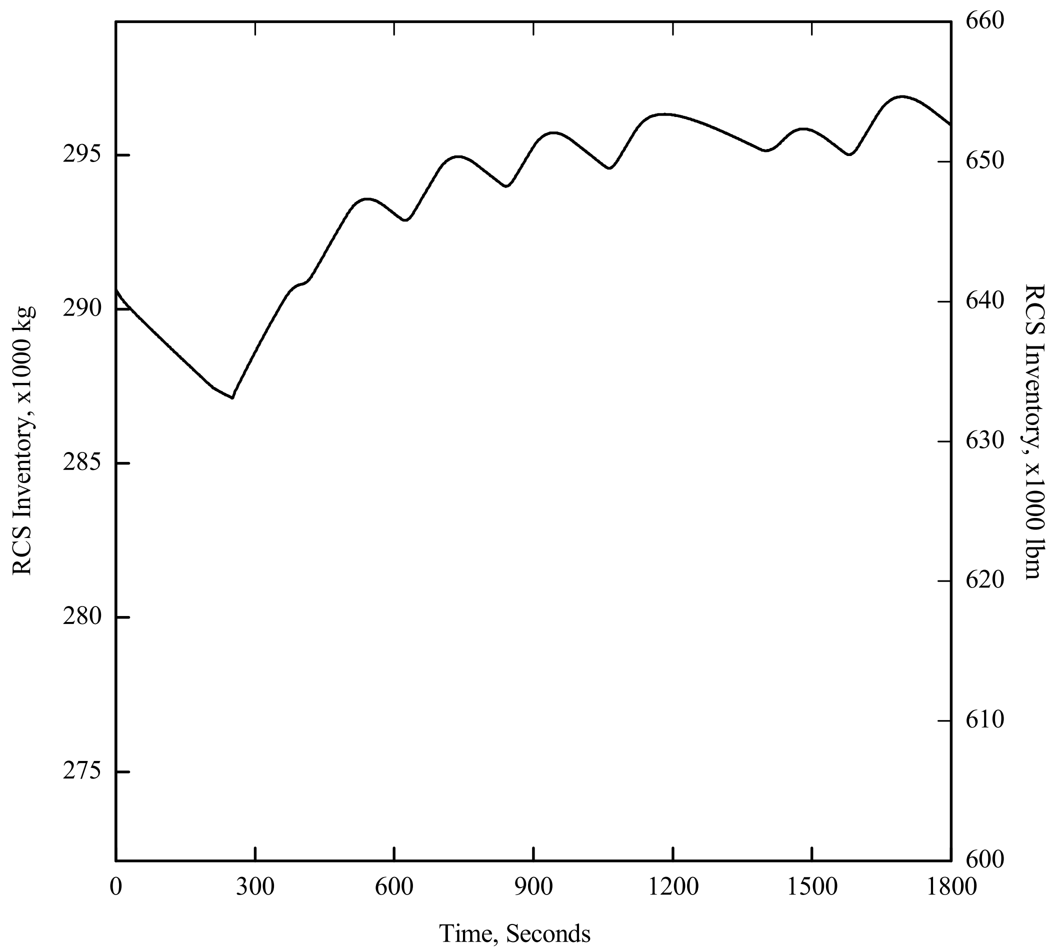

Figure 15.6.3-12 SGTR Without LOOP : RCS Mass Inventory vs. Time

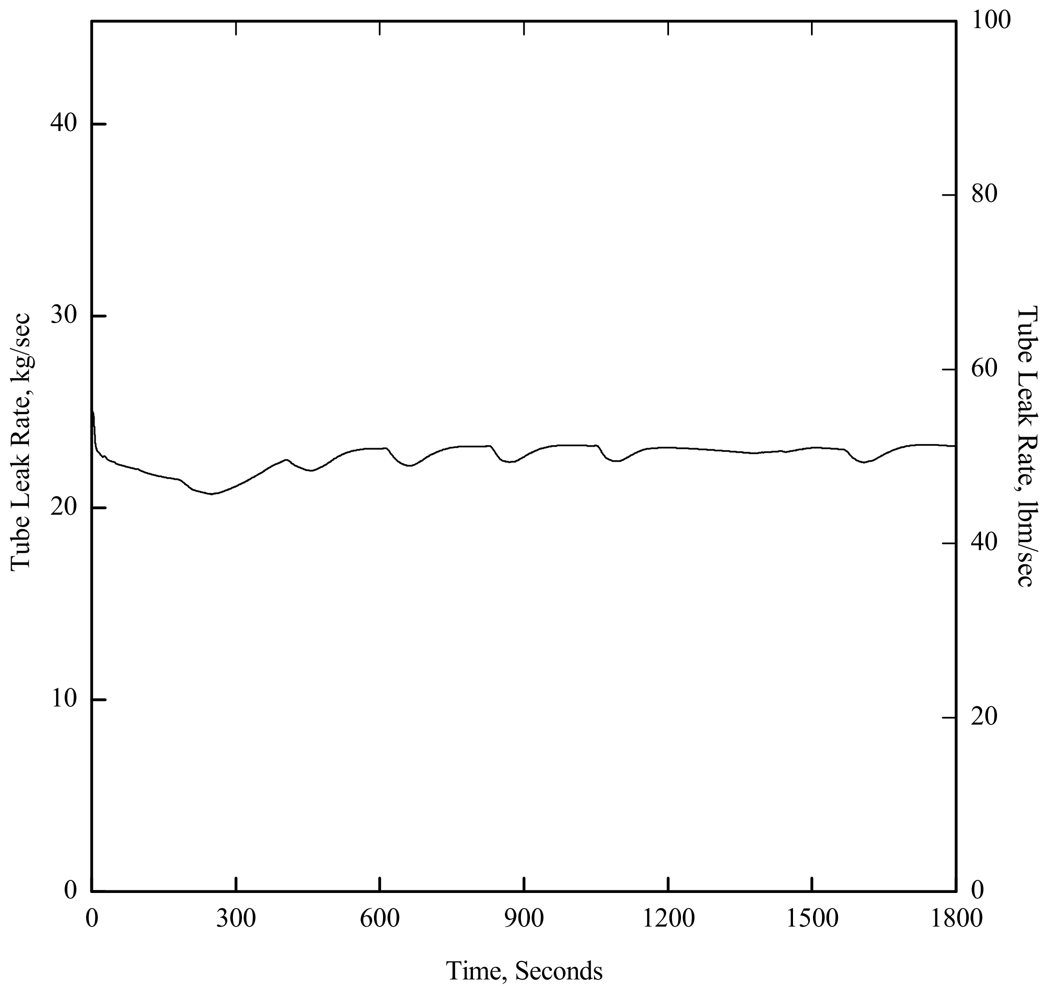

Figure 15.6.3-13 SGTR Without LOOP : Tube Leak Rate vs. Time

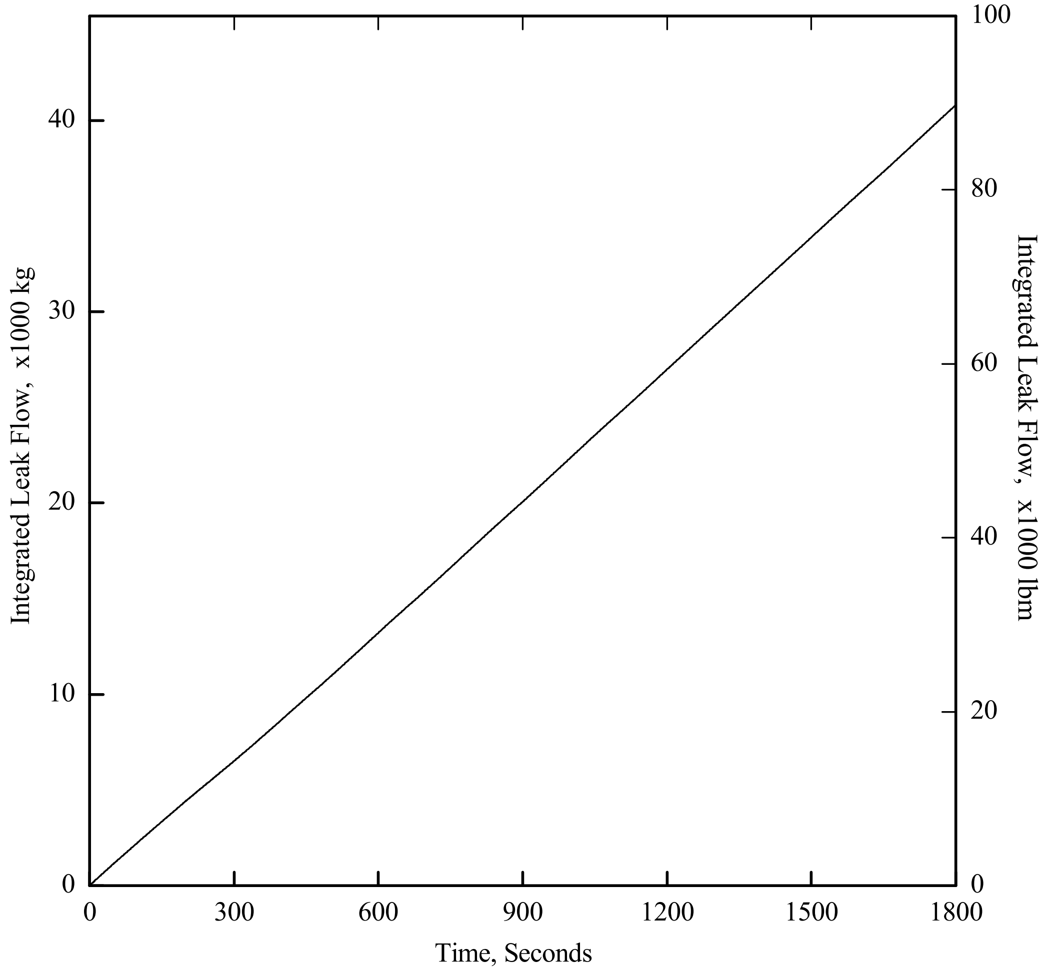

Figure 15.6.3-14 SGTR Without LOOP:Integrated Leak Flow vs. Time

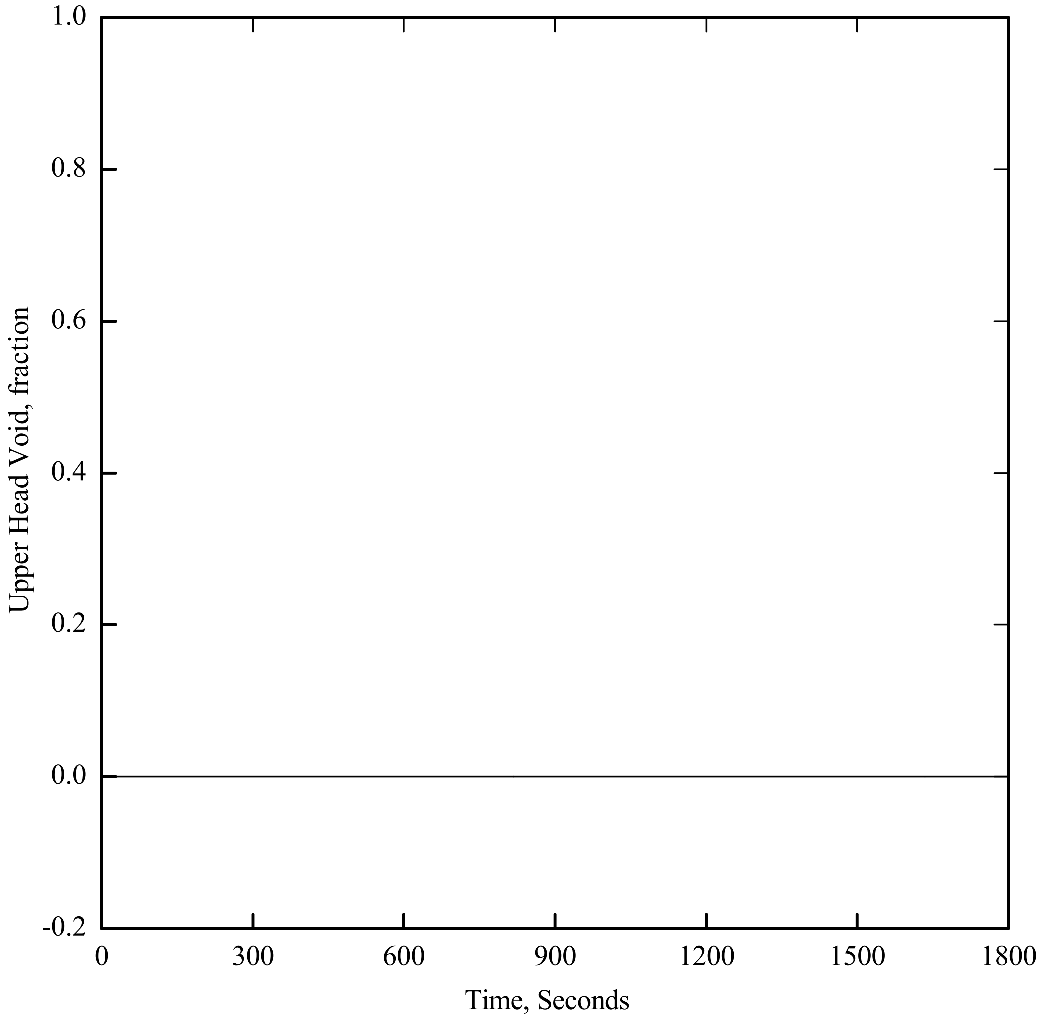

Figure 15.6.3-15 SGTR Without LOOP:RV Upper Head Void Fraction vs. Time

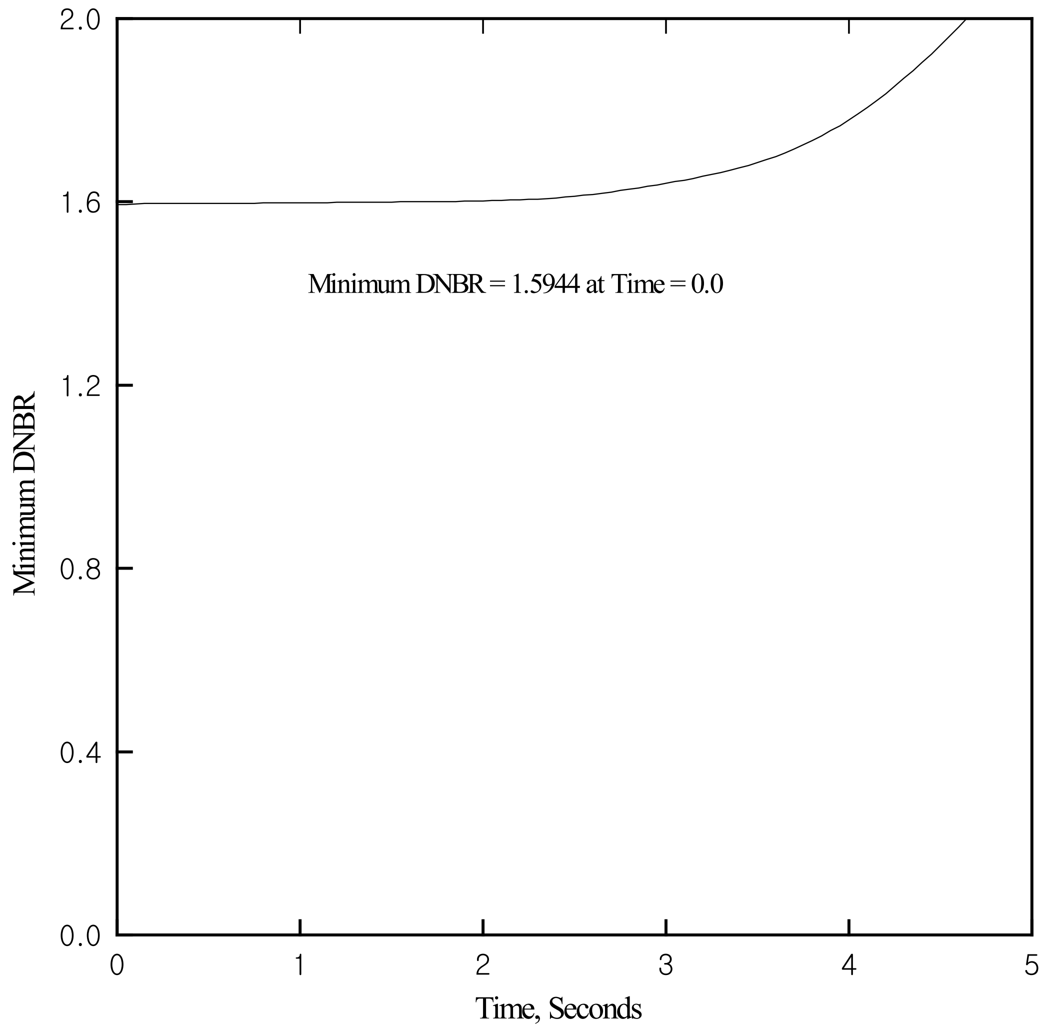

Figure 15.6.3-16 SGTR Without LOOP:Minimum DNBR vs. Time

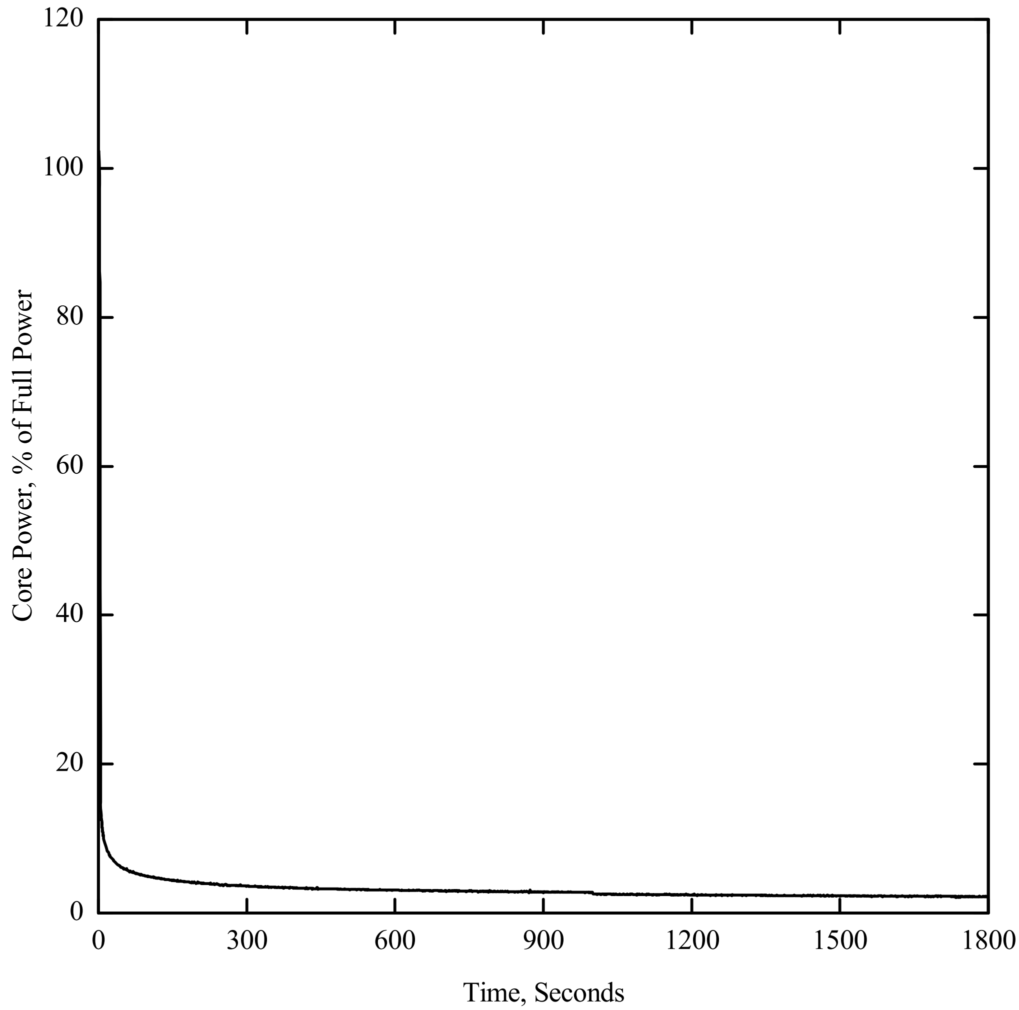

Figure 15.6.3-17 SGTR With Concurrent LOOP:Core Power vs. Time

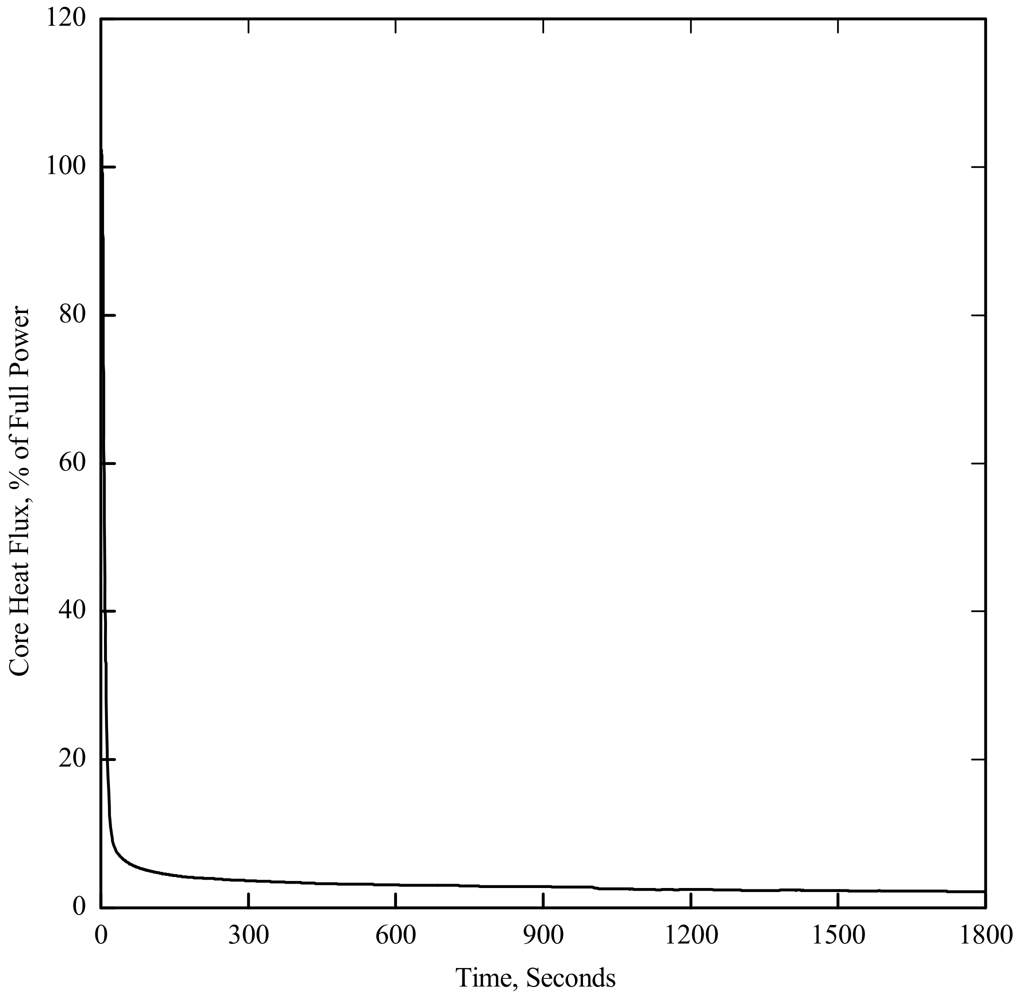

Figure 15.6.3-18 SGTR With Concurrent LOOP:Core Average Heat Flux vs. Time

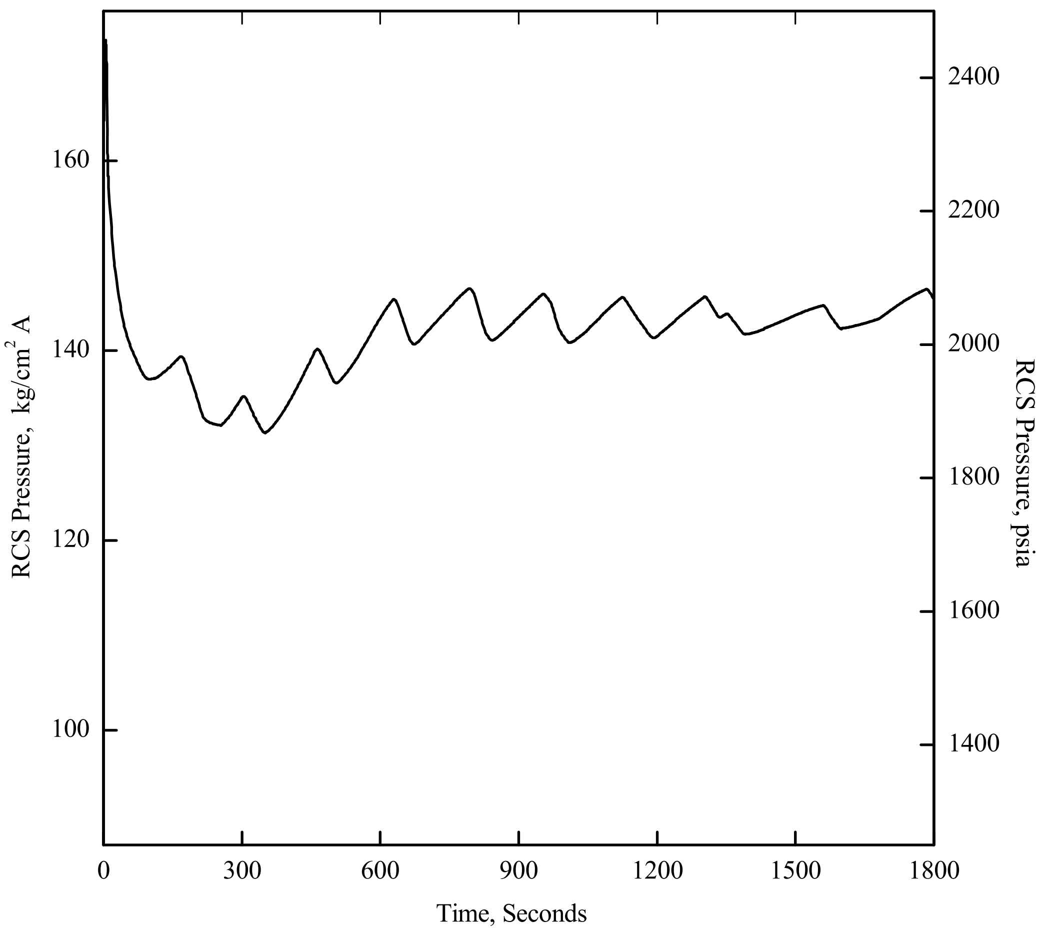

Figure 15.6.3-19 SGTR With Concurrent LOOP:RCS Pressure vs. Time

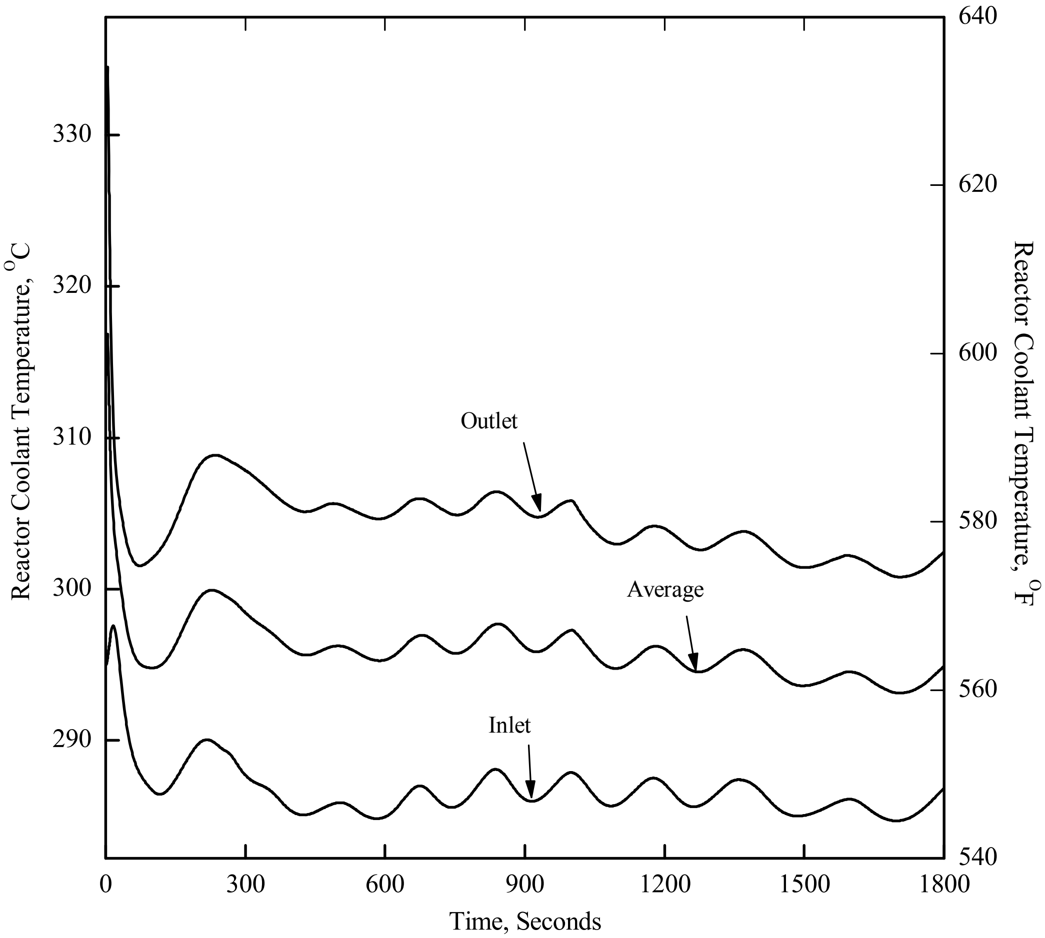

Figure 15.6.3-20 SGTR With Concurrent LOOP:Reactor Coolant Temperature vs. Time

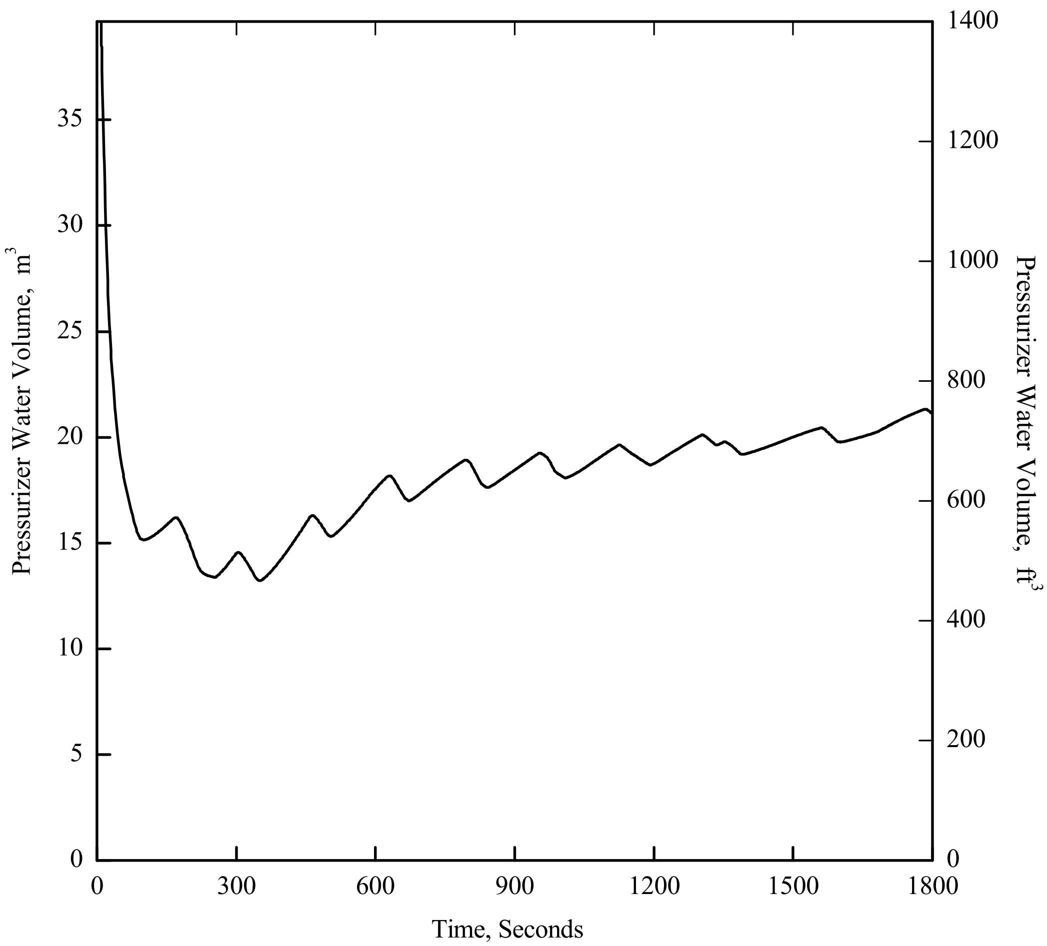

Figure 15.6.3-21 SGTR With Concurrent LOOP:Pressurizer Water Volume vs. Time

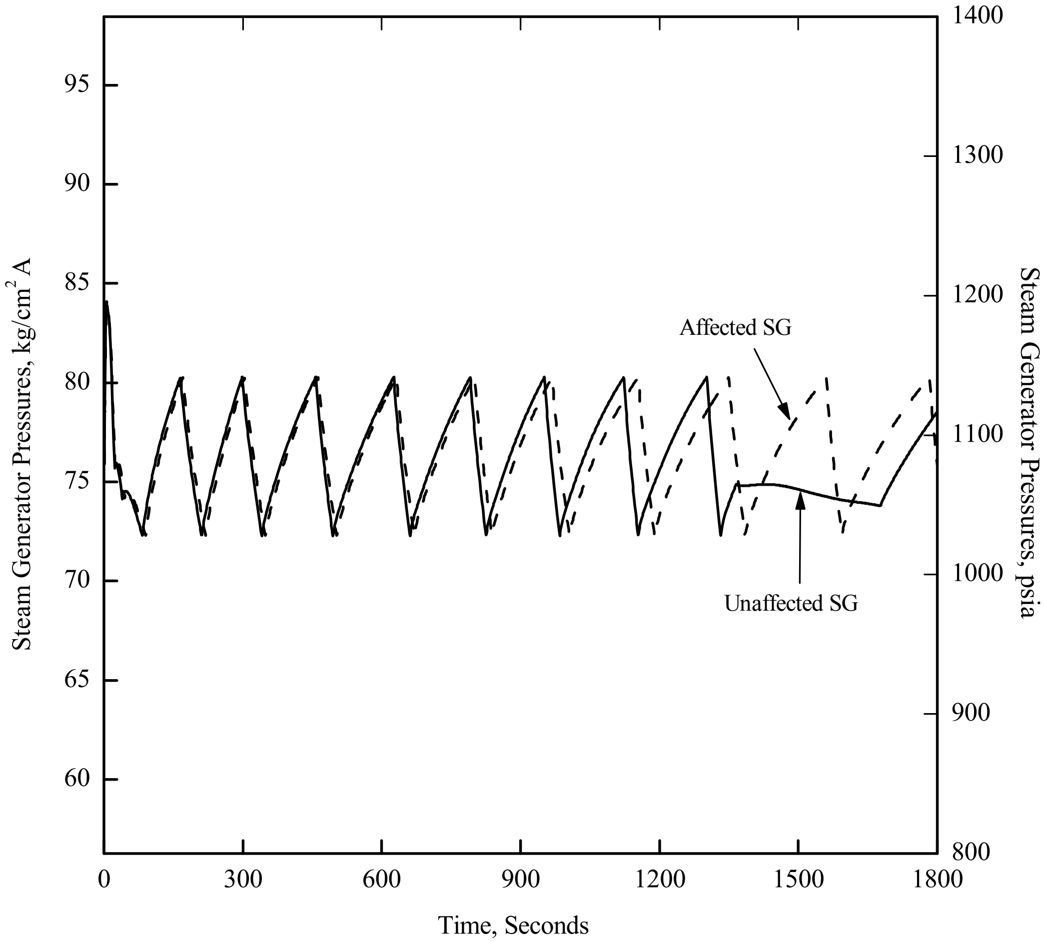

Figure 15.6.3-22 SGTR With Concurrent LOOP : Steam Generator Pressure vs. Time

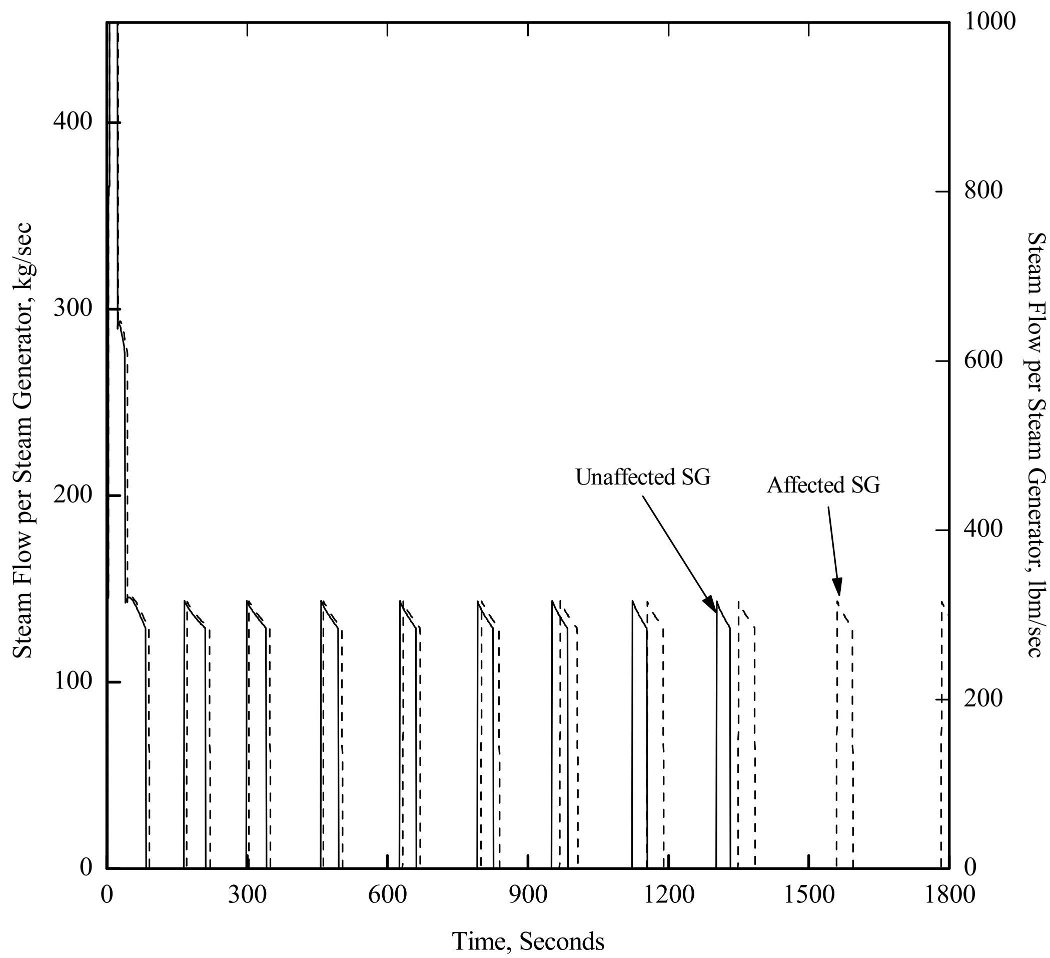

Figure 15.6.3-23 SGTR With Concurrent LOOP : Steam Flow Rate vs. Time

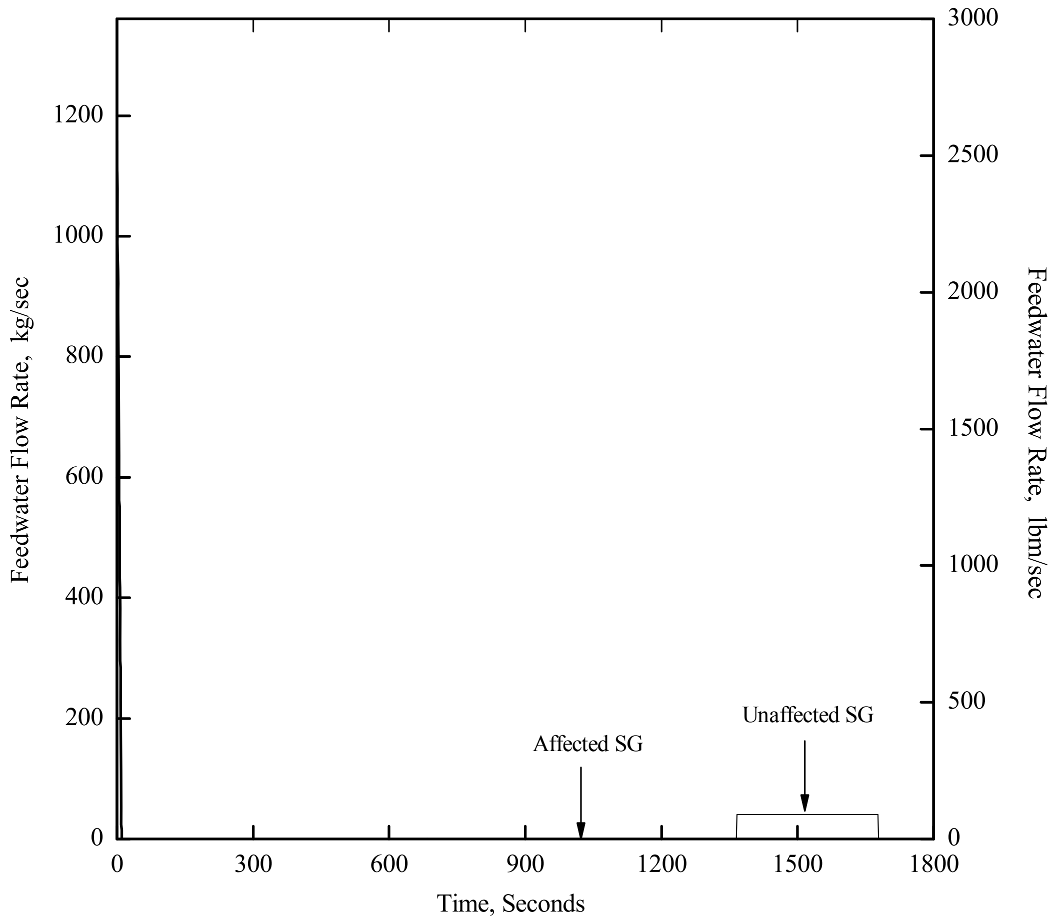

Figure 15.6.3-24 SGTR With Concurrent LOOP : Feedwater Flow Rate vs. Time

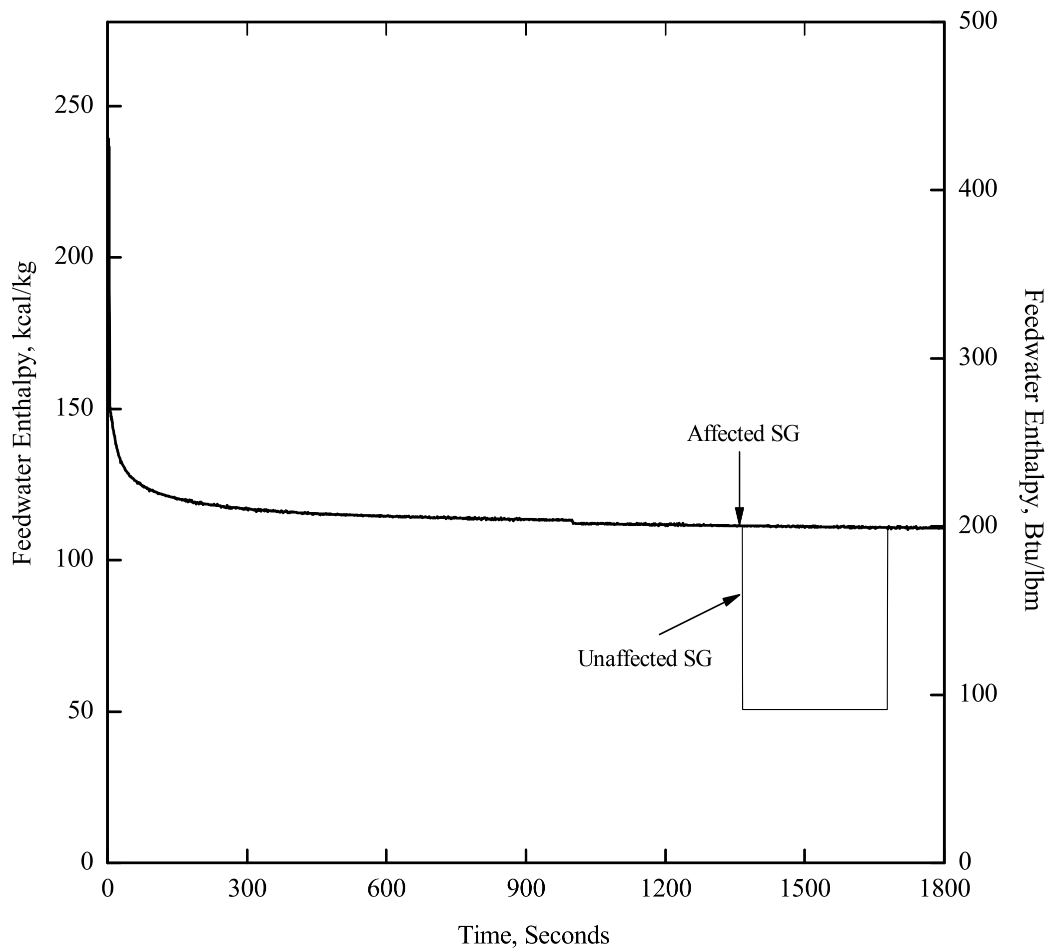

Figure 15.6.3-25 SGTR With Concurrent LOOP: Feedwater Enthalpy vs. Time

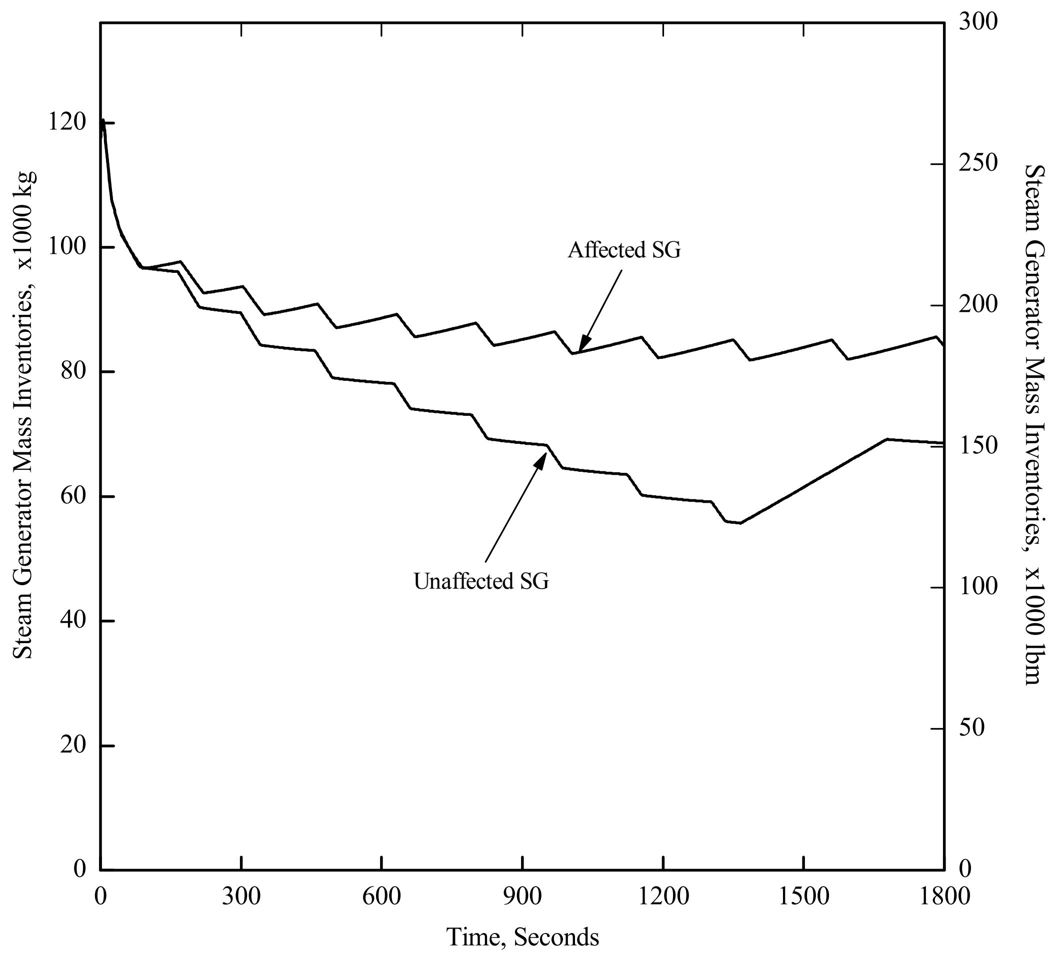

Figure 15.6.3-26 SGTR With Concurrent LOOP:Steam Generator Mass Inventories vs. Time

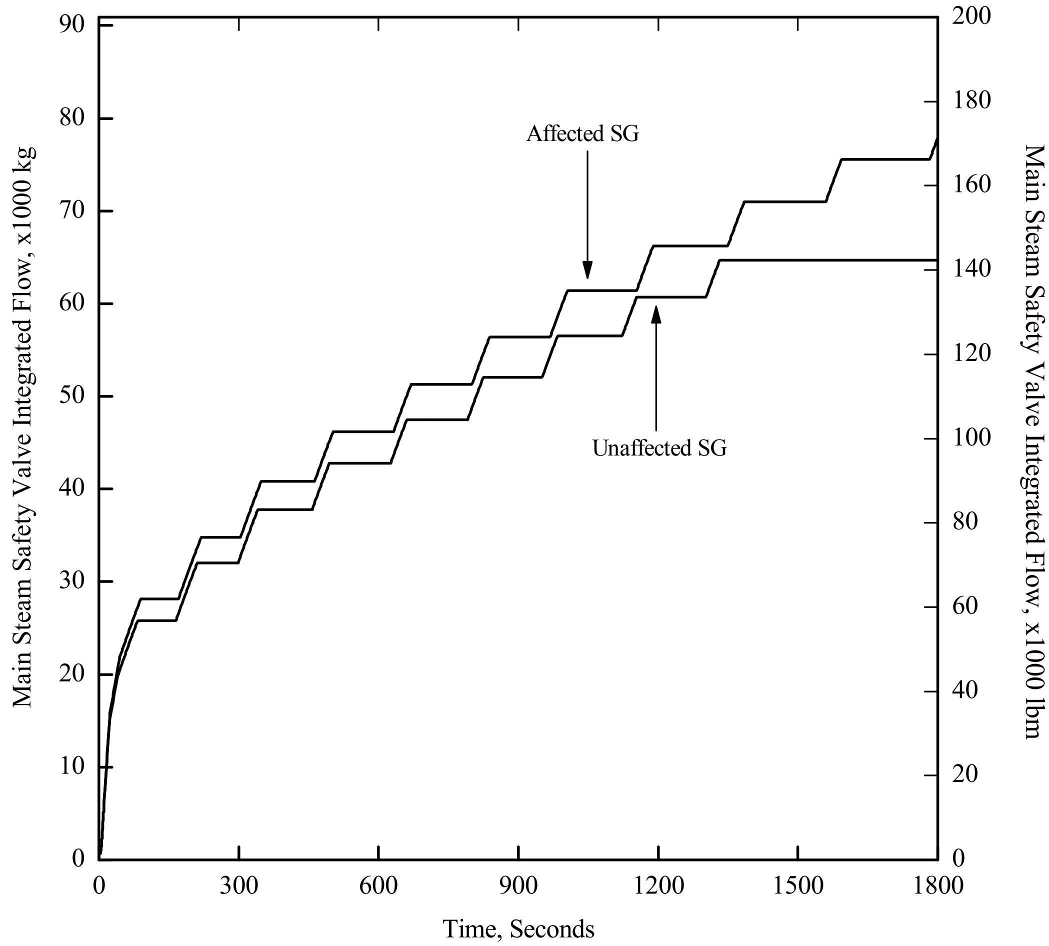

Figure 15.6.3-27 SGTR With Concurrent LOOP : MSSV Integrated Flow vs. Time

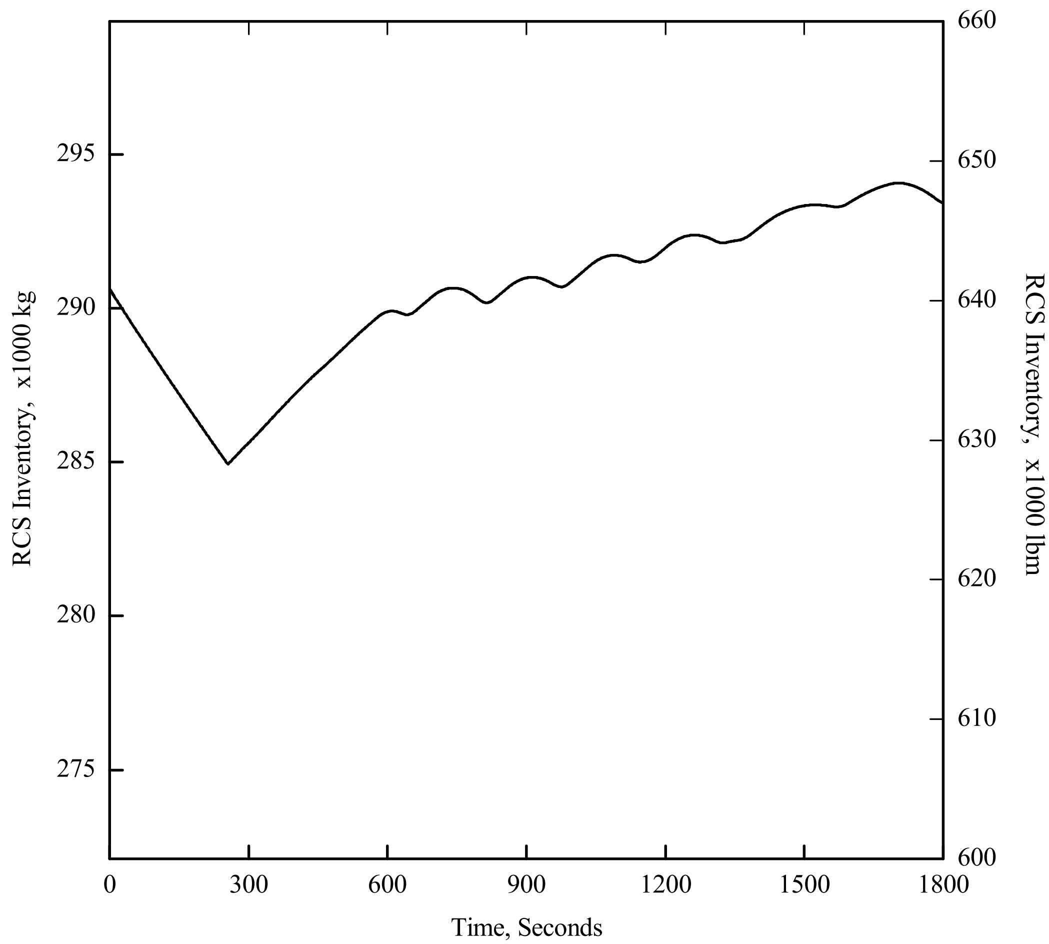

Figure 15.6.3-28 SGTR With Concurrent LOOP : RCS Mass Inventory vs. Time

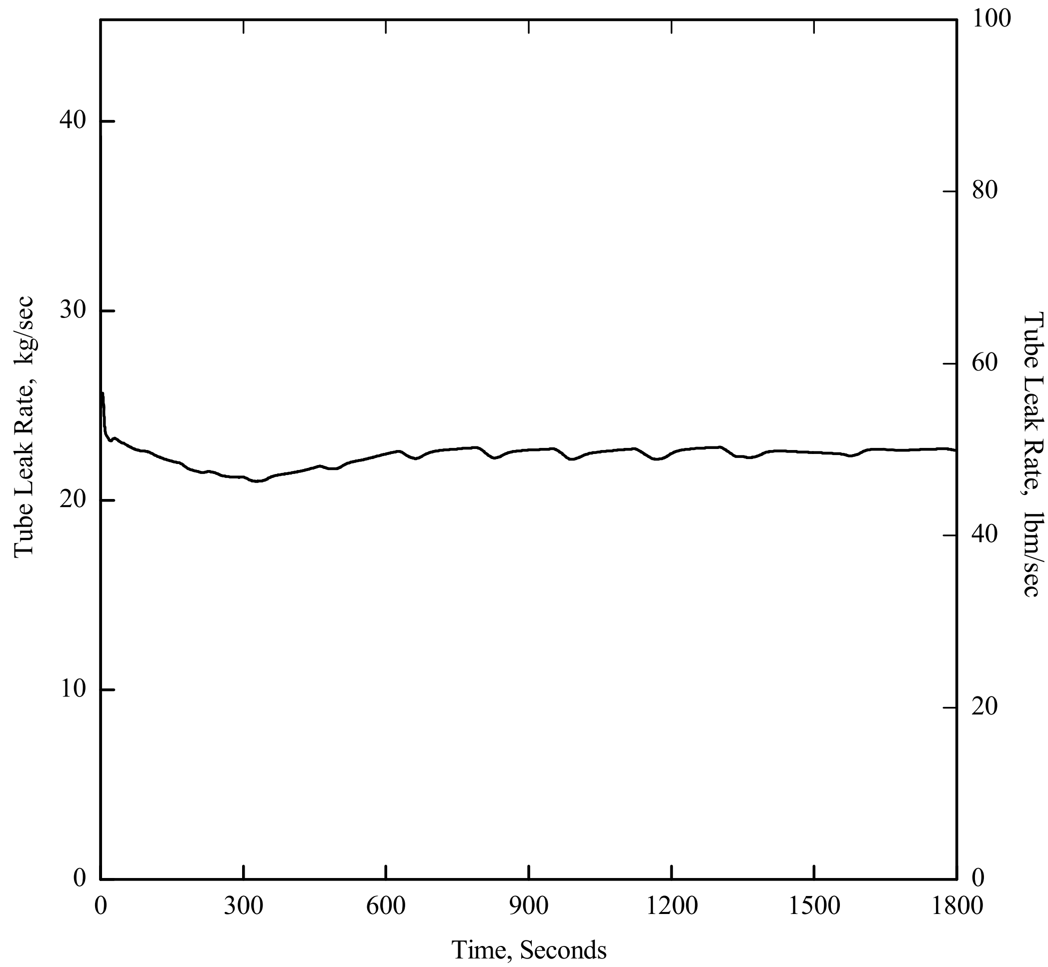

Figure 15.6.3-29 SGTR With Concurrent LOOP : Tube Leak Rate vs. Time

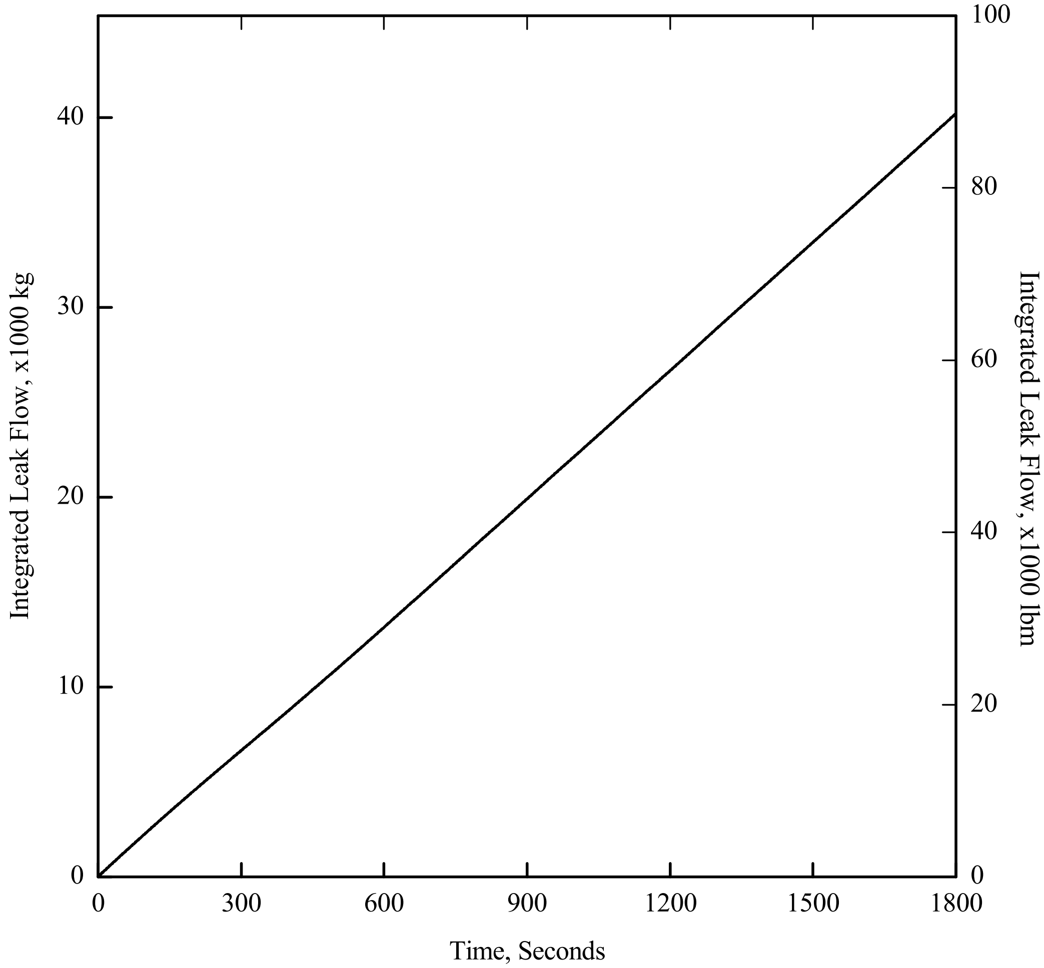

Figure 15.6.3-30 SGTR With Concurrent LOOP : Integrated Leak Flow vs. Time

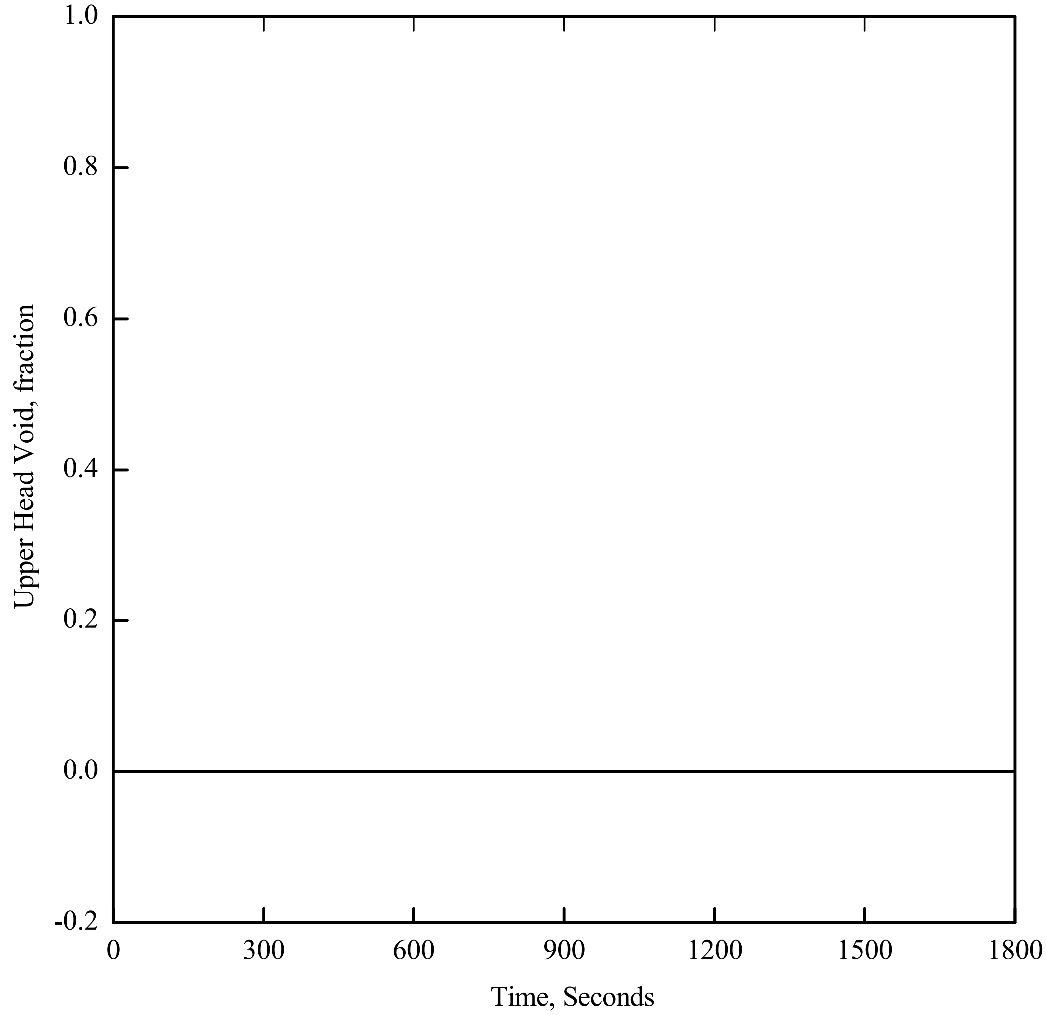

Figure 15.6.3-31 SGTR With Concurrent LOOP: RV Upper Head Void Fraction vs. Time

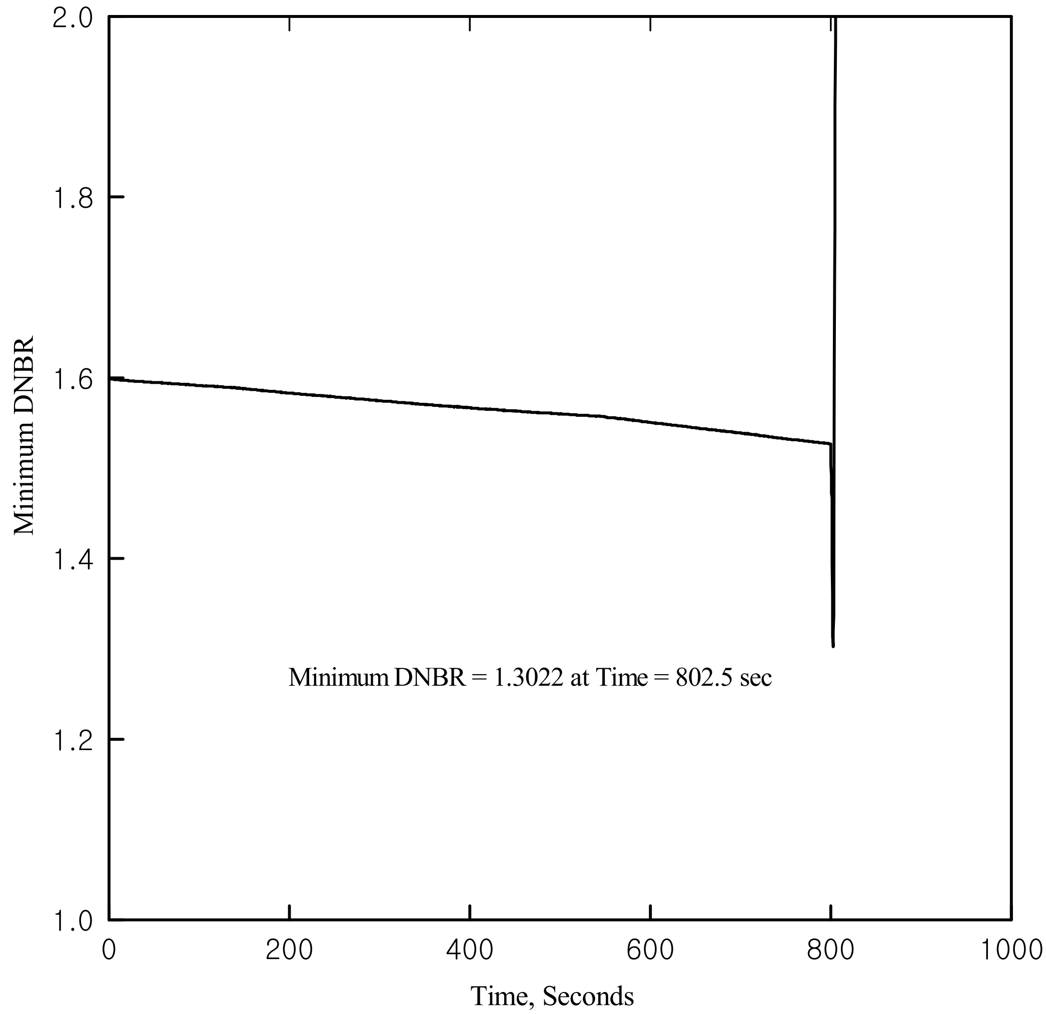

Figure 15.6.3-32 SGTR With Concurrent LOOP : Minimum DNBR vs. Time

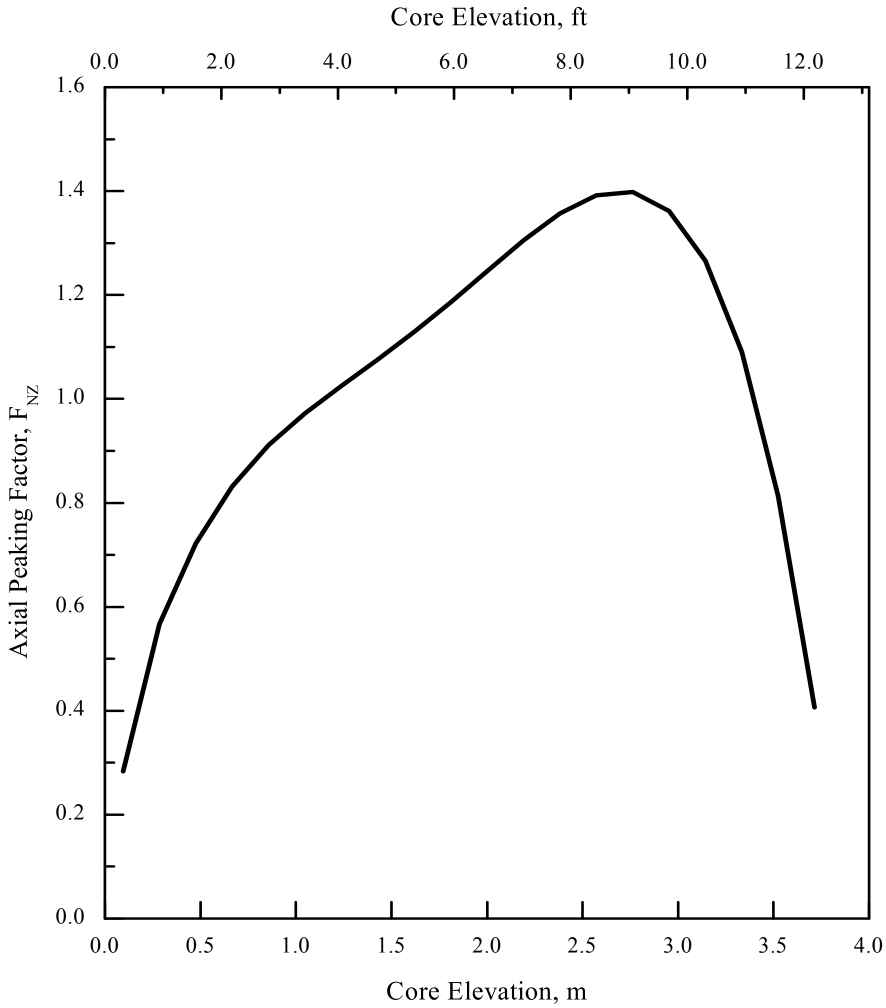

Figure 15.6.5-1 Axial Power Distribution at Large Break

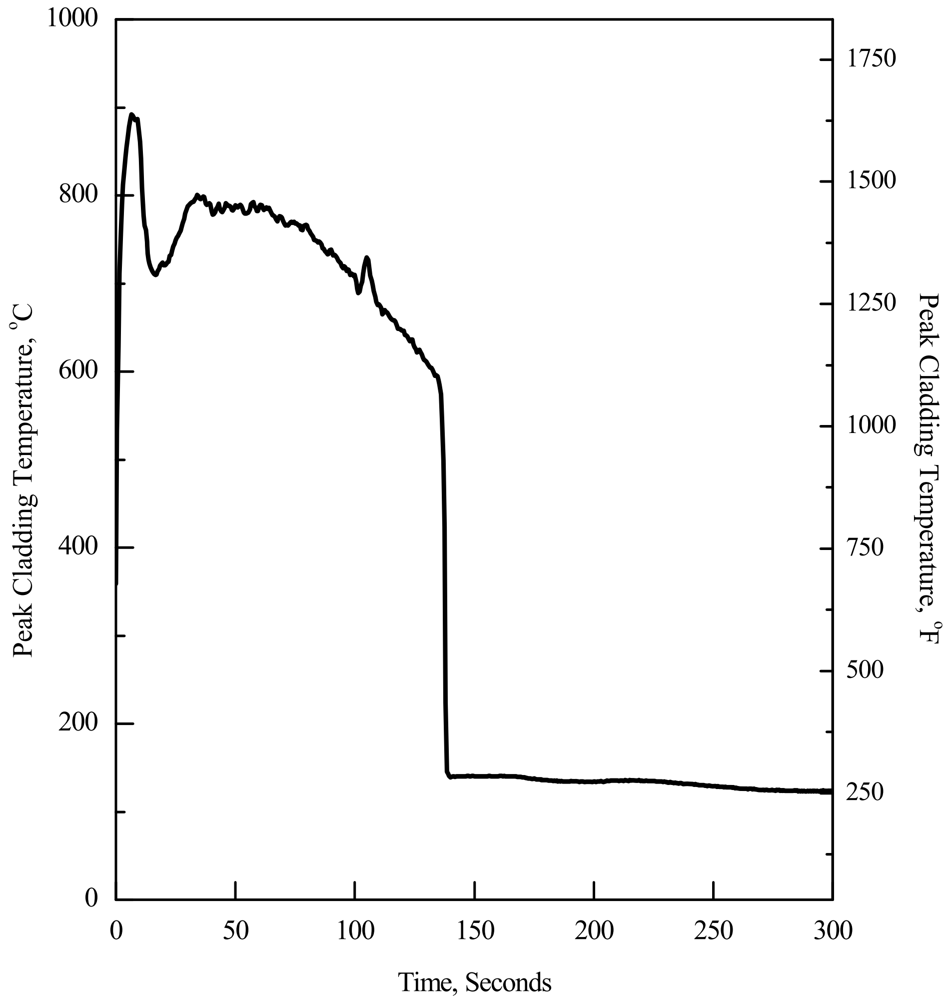

Figure 15.6.5-2 1.0 × Double-ended Guillotine Break in Pump Discharge Leg (Peak Cladding Temperature) (1 of 4)

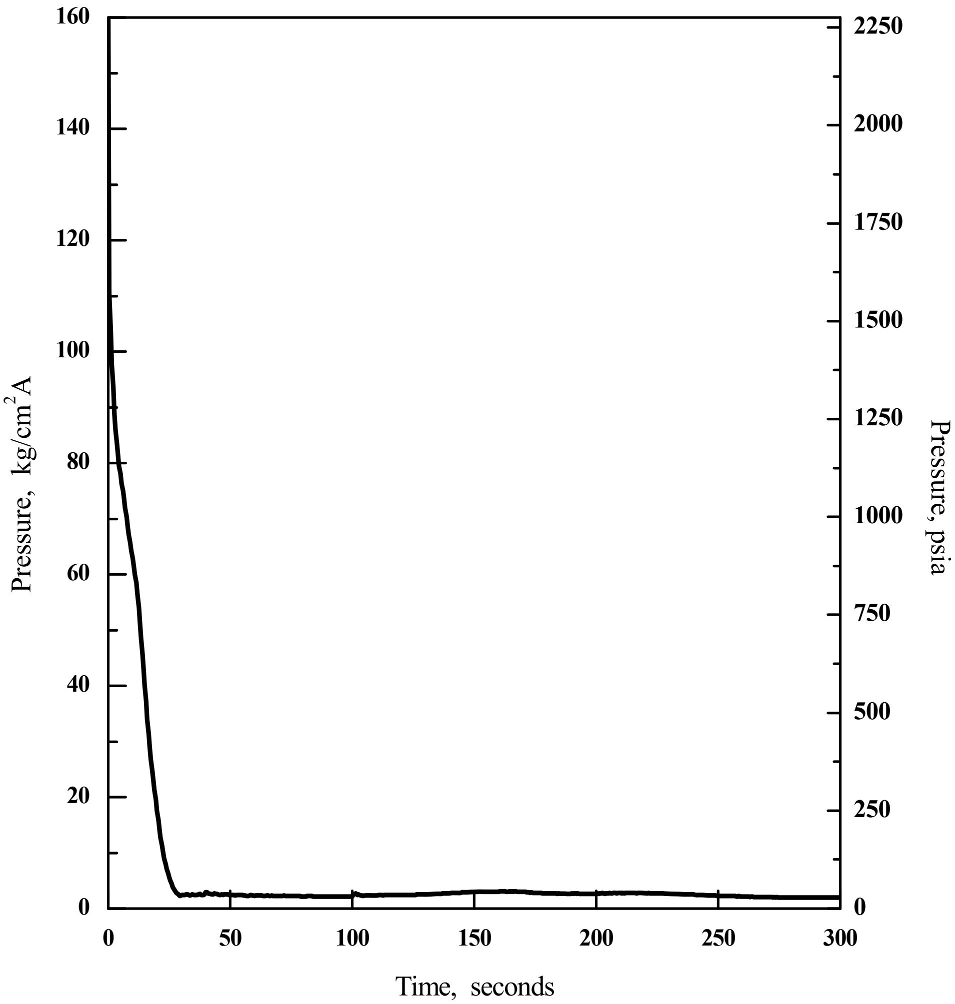

Figure 15.6.5-3 1.0 × Double-ended Guillotine Break in Pump Discharge Leg (Core Pressure) (2 of 4)

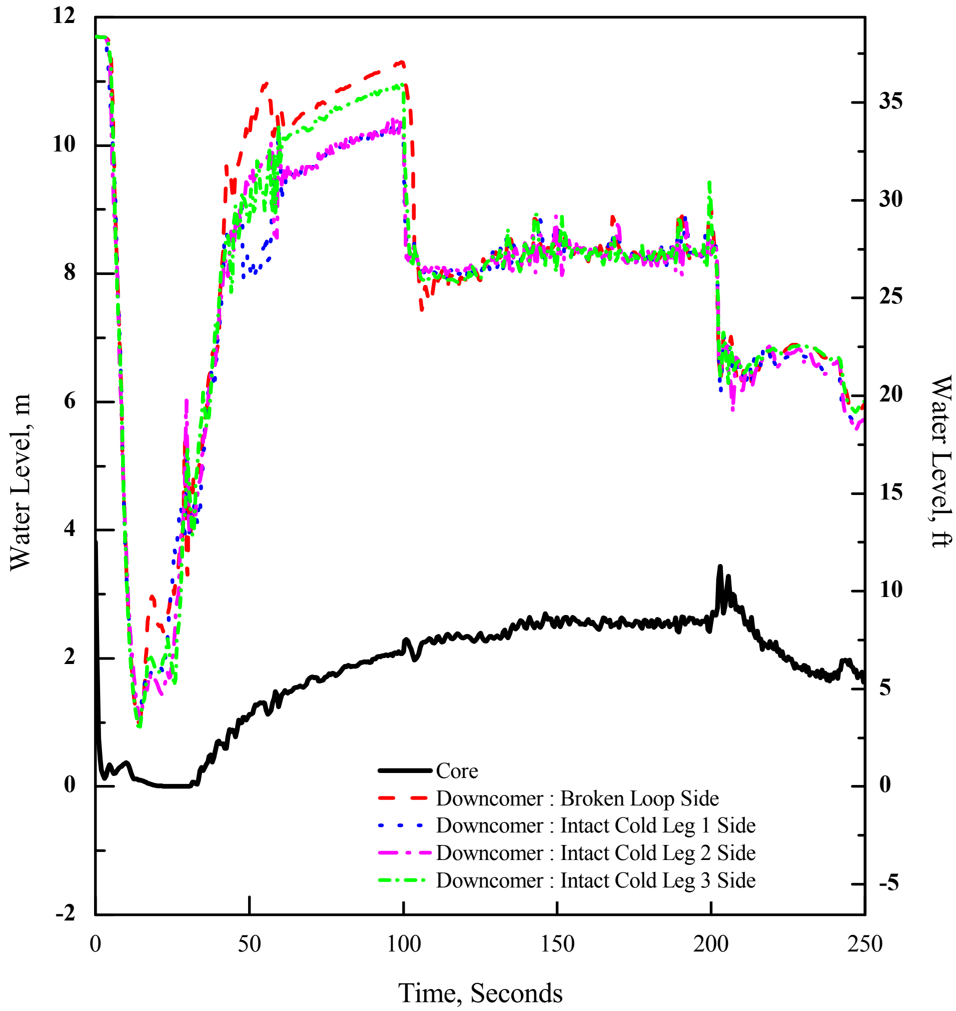

Figure 15.6.5-4 1.0 × Double-ended Guillotine Break in Pump Discharge Leg (Water Level in Core and Downcommer) (3 of 4)

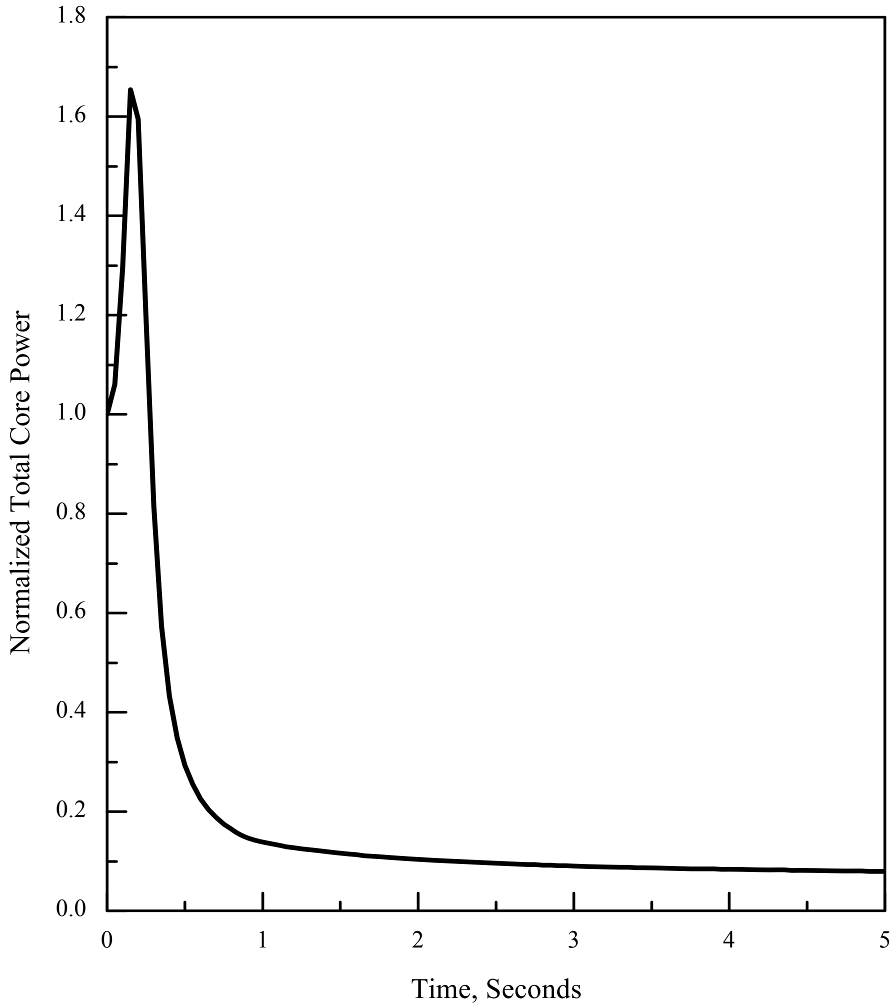

Figure 15.6.5-5 1.0 × Double-ended Guillotine Break in Pump Discharge Leg (Normalized Core Power) (4 of 4)

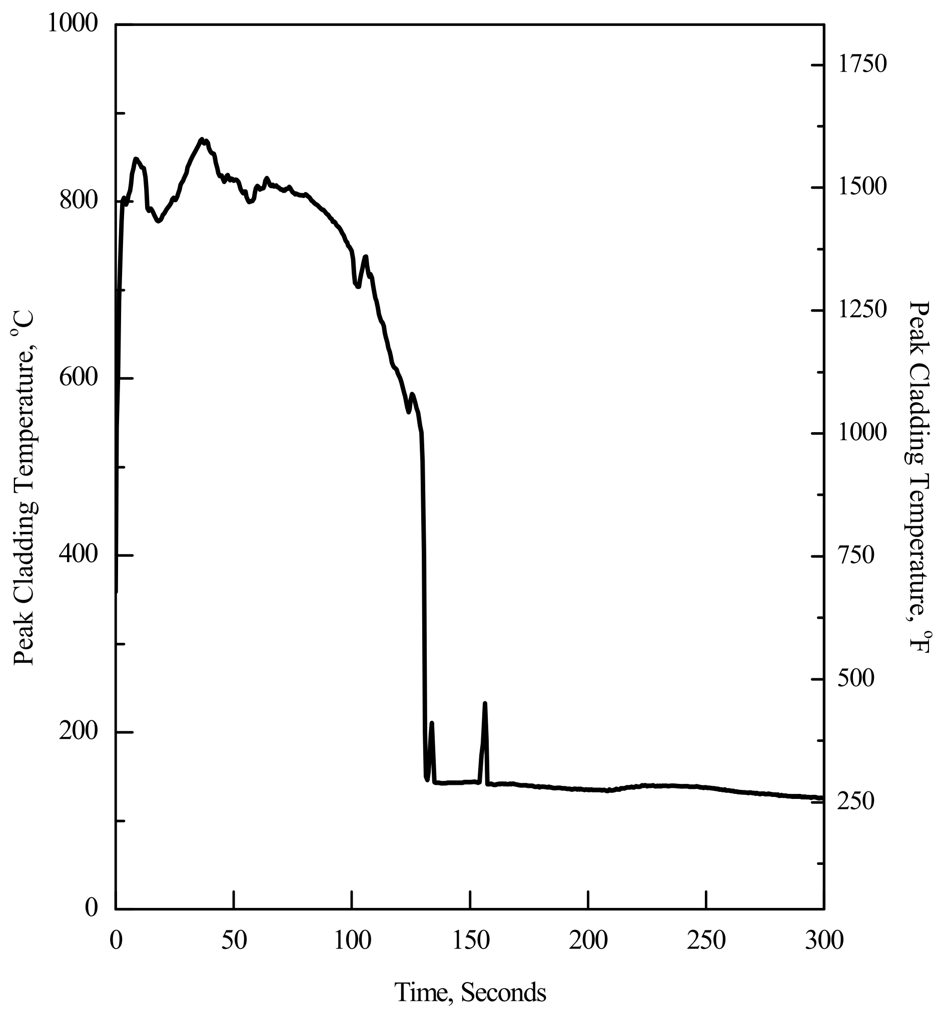

Figure 15.6.5-6 0.8 × Double-ended Guillotine Break in Pump Discharge Leg (Peak Cladding Temperature) (1 of 4)

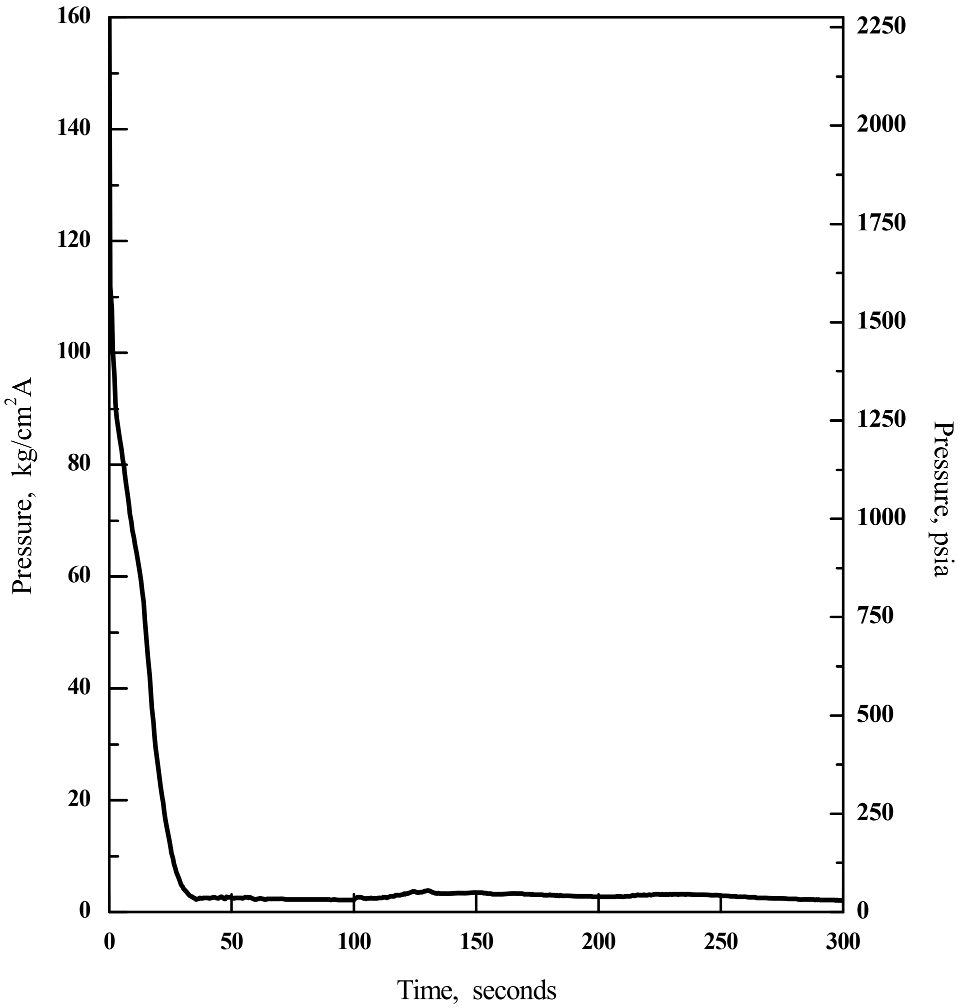

Figure 15.6.5-7 0.8 × Double-ended Guillotine Break in Pump Discharge Leg (Core Pressure) (2 of 4)

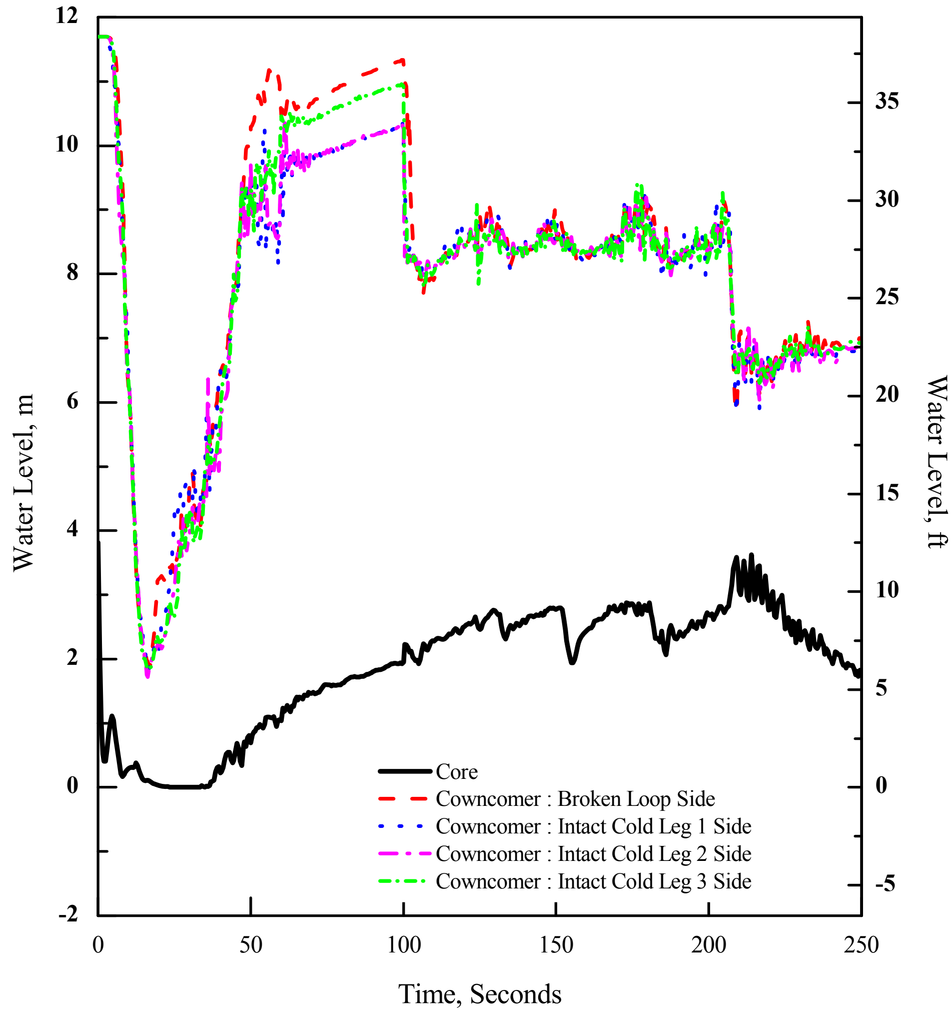

Figure 15.6.5-8 0.8 × Double-ended Guillotine Break in Pump Discharge Leg (Water Level in Core and Downcommer) (3 of 4)

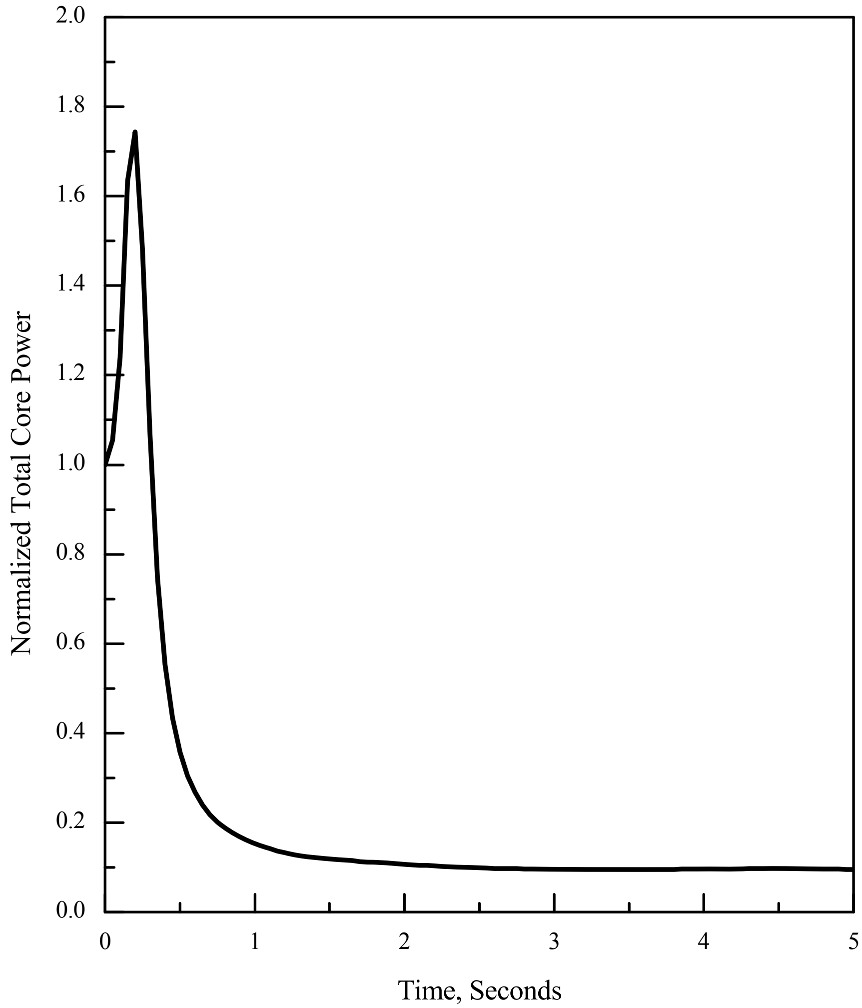

Figure 15.6.5-9 0.8 × Double-ended Guillotine Break in Pump Discharge Leg (Normalized Core Power) (4 of 4)

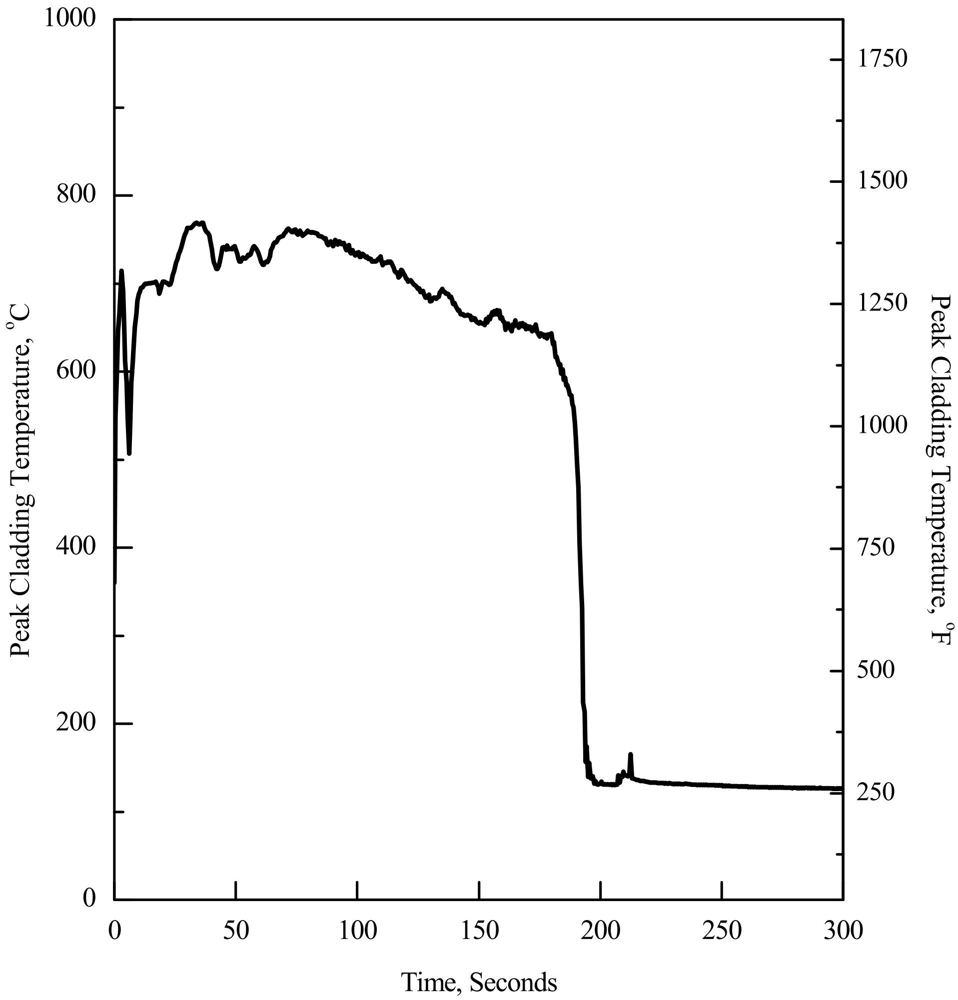

Figure 15.6.5-10 0.6 × Double-ended Guillotine Break in Pump Discharge Leg (Peak Cladding Temperature) (1 of 4)

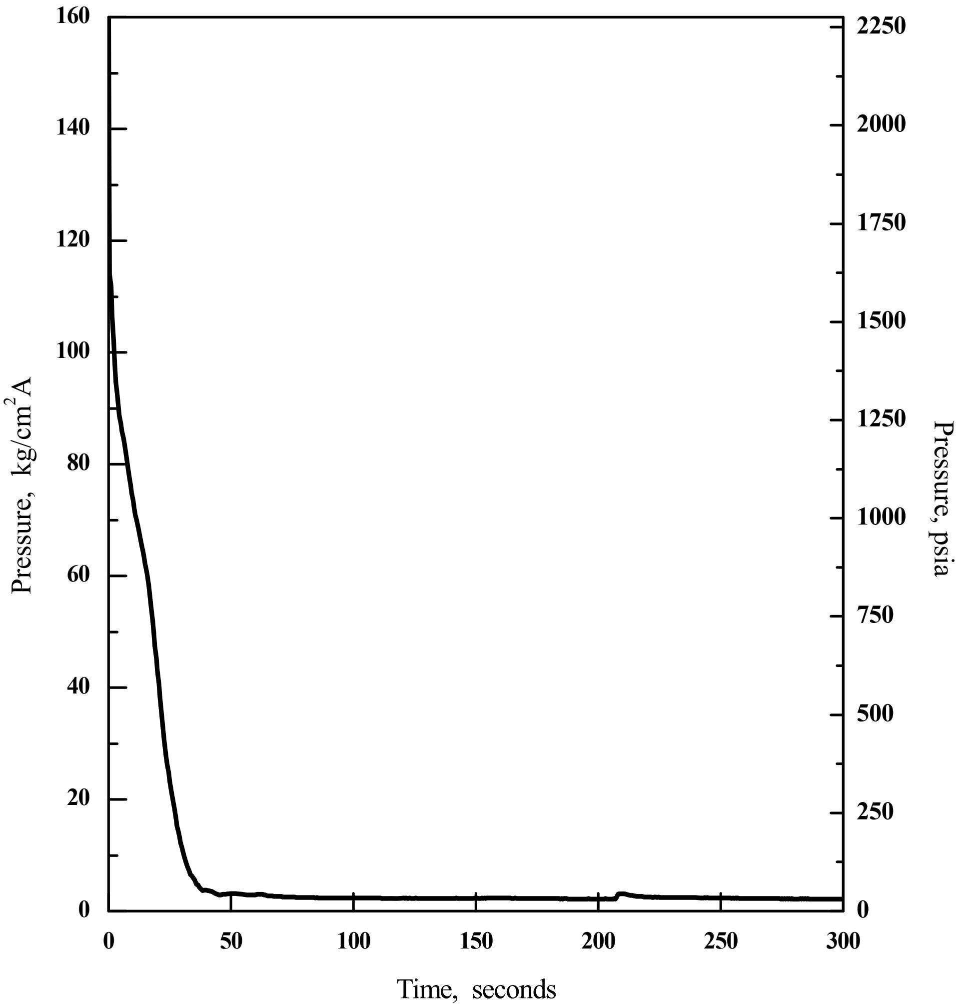

Figure 15.6.5-11 0.6 × Double-ended Guillotine Break in Pump Discharge Leg (Core Pressure) (2 of 4)

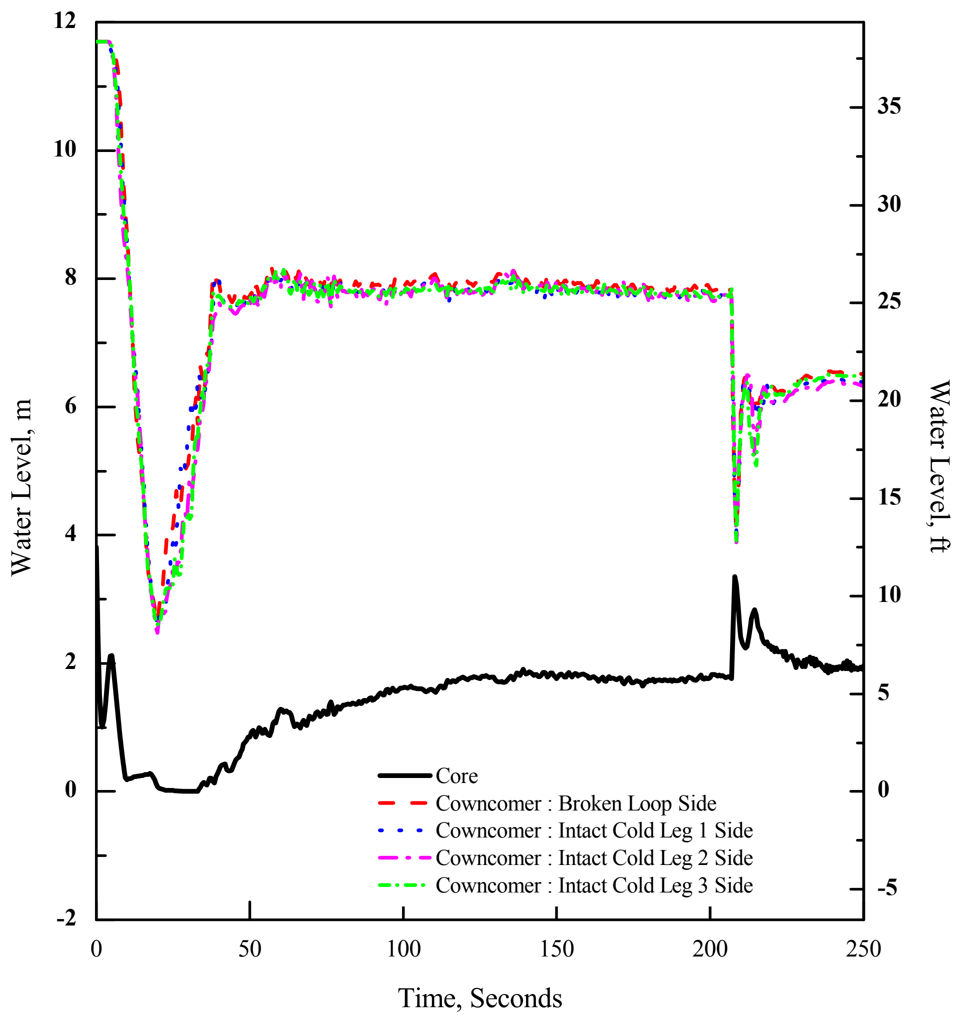

Figure 15.6.5-12 0.6 × Double-ended Guillotine Break in Pump Discharge Leg (Water Level in Core and Downcommer) (3 of 4)

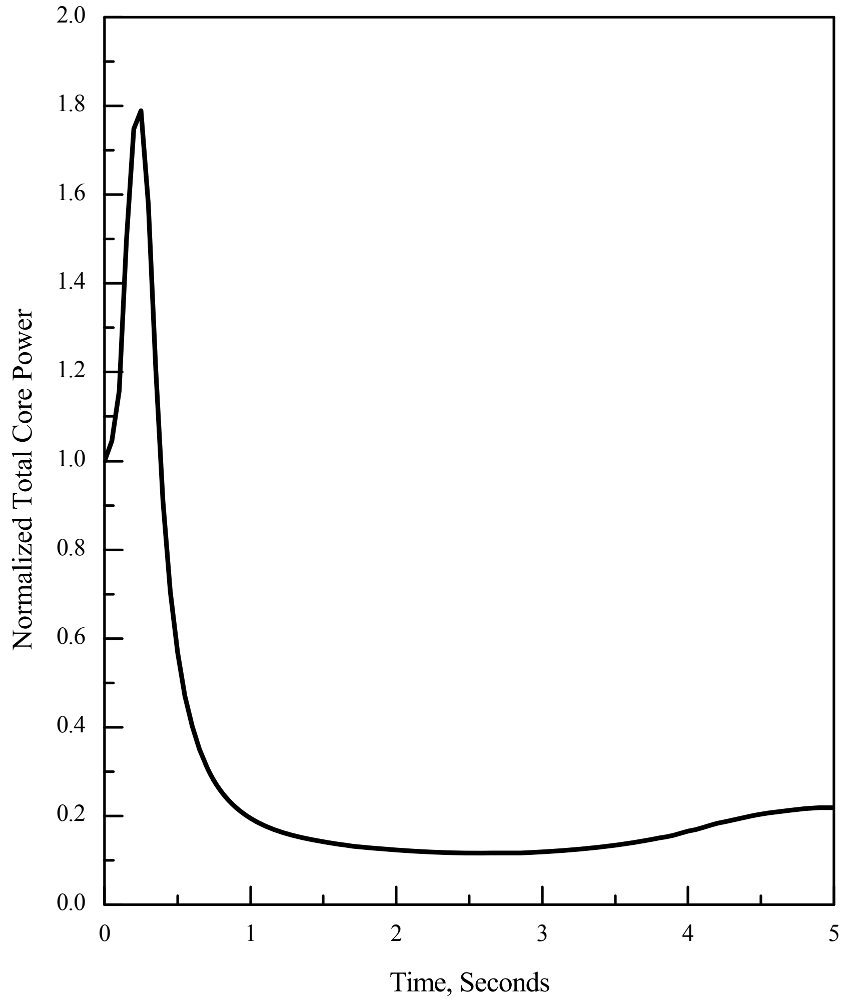

Figure 15.6.5-13 0.6 × Double-ended Guillotine Break in Pump Discharge Leg (Normalized Core Power) (4 of 4)

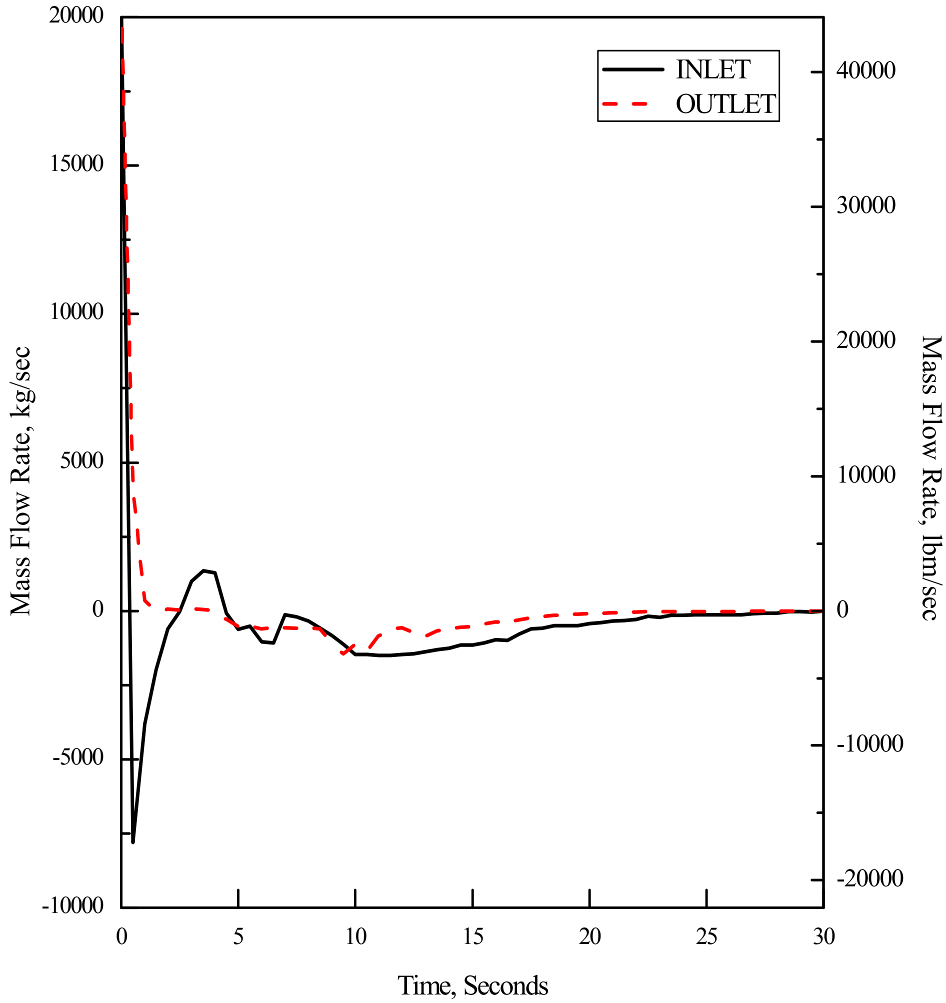

Figure 15.6.5-14 1.0 × Double-ended Guillotine Break in Pump Discharge Leg (Core Inlet and Outlet Mass Flow) (1 of 9)

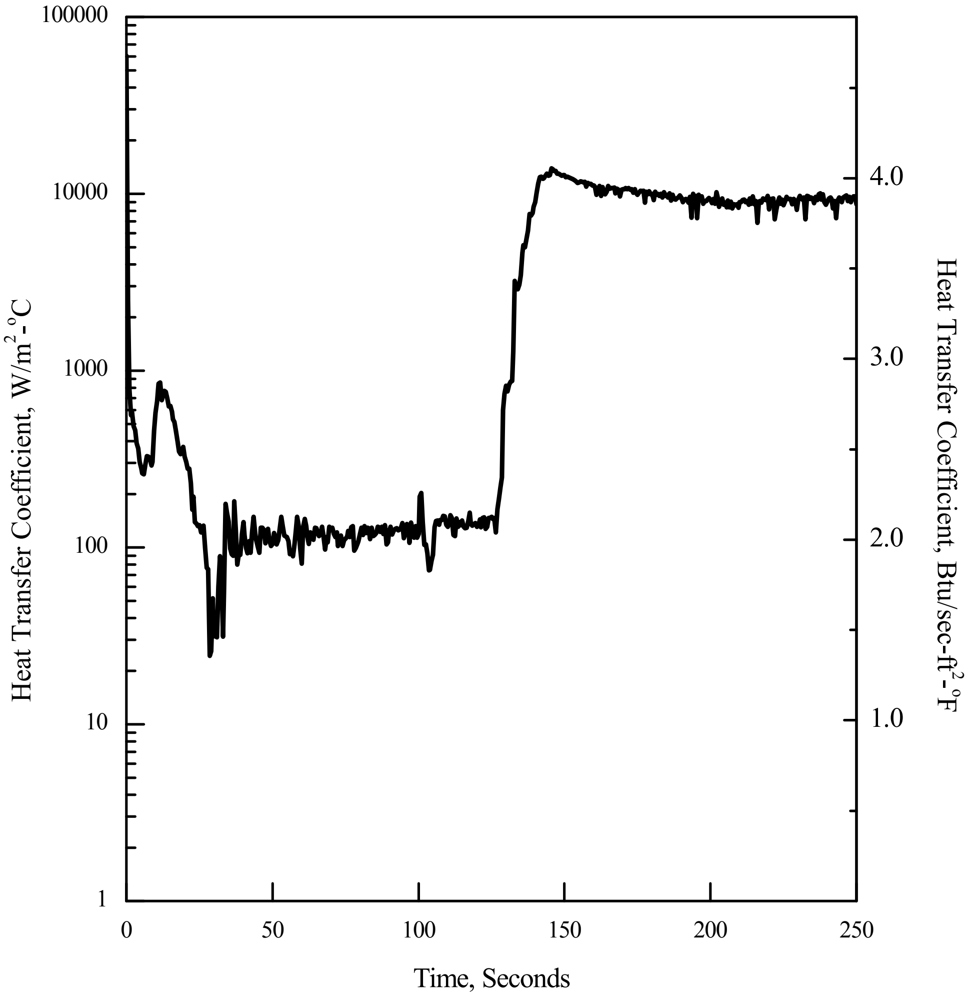

Figure 15.6.5-15 1.0 × Double-ended Guillotine Break in Pump Discharge Leg (Hot Spot Heat Transfer Coefficient) (2 of 9)

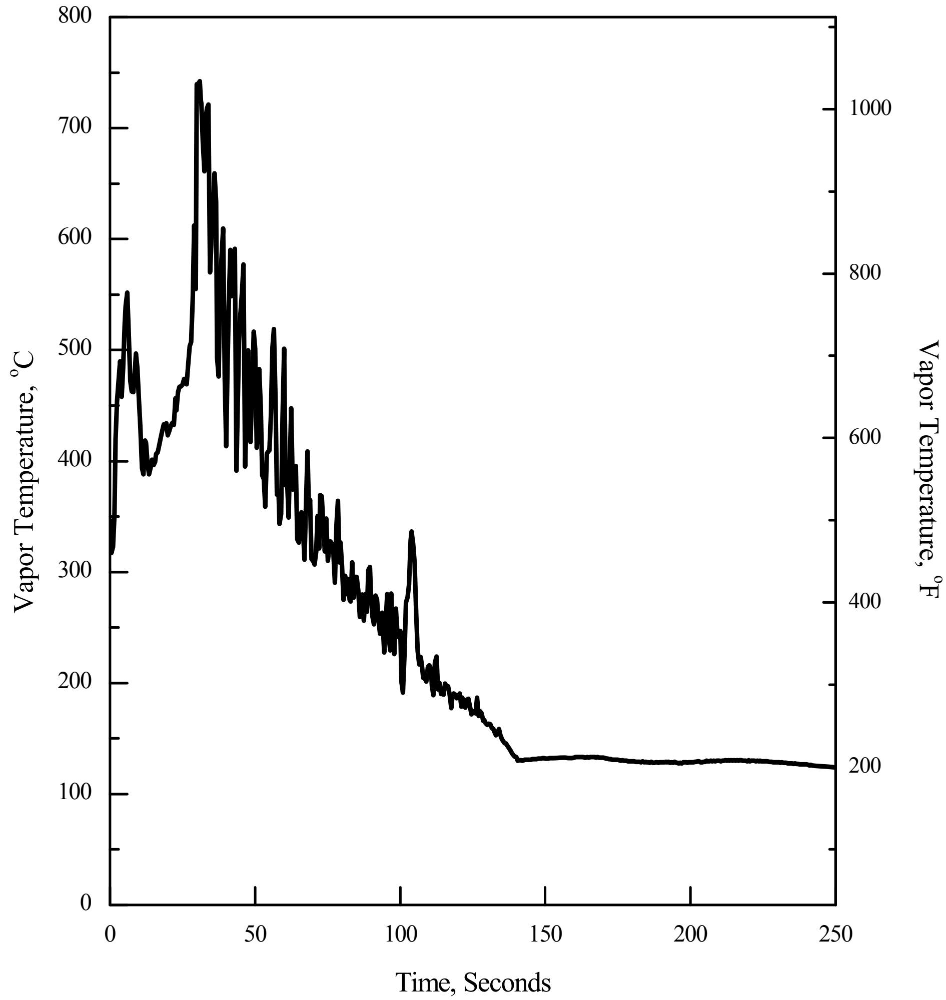

Figure 15.6.5-16 1.0 × Double-ended Guillotine Break in Pump Discharge Leg (Hot Spot Vapor Temperature) (3 of 9)

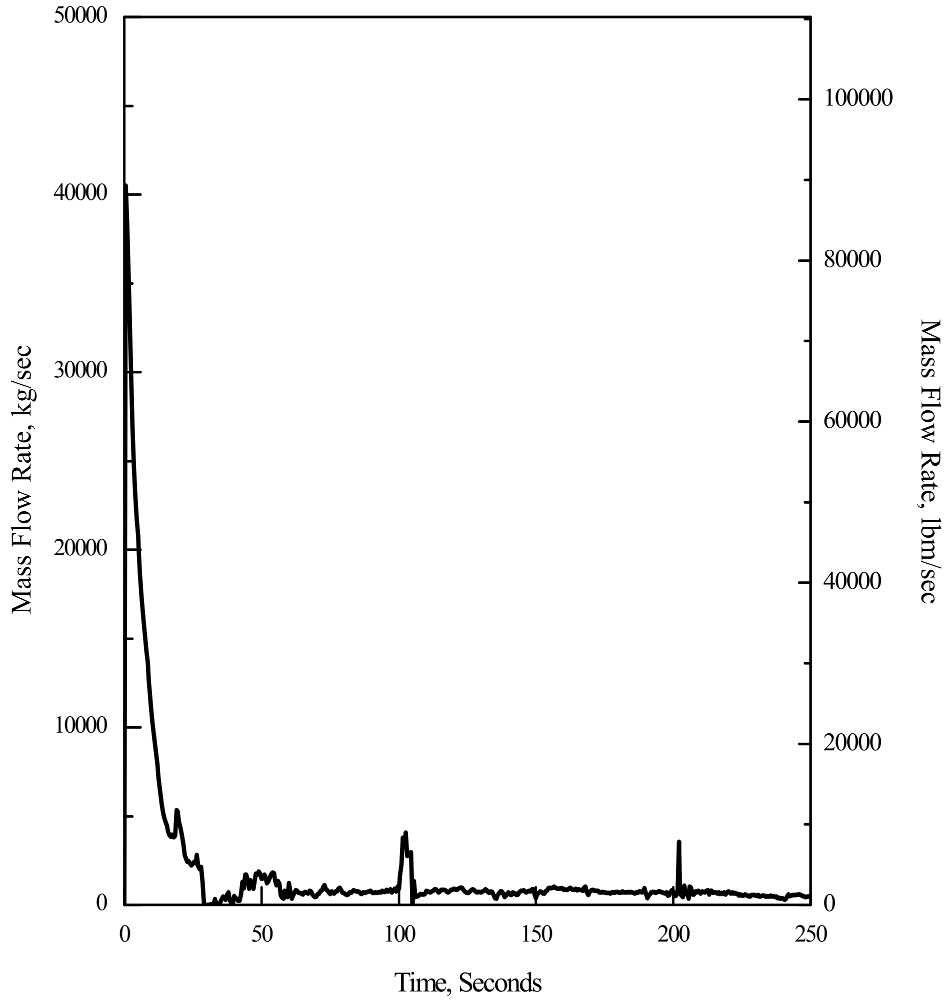

Figure 15.6.5-17 1.0 × Double-ended Guillotine Break in Pump Discharge Leg (Break Flow) (4 of 9)

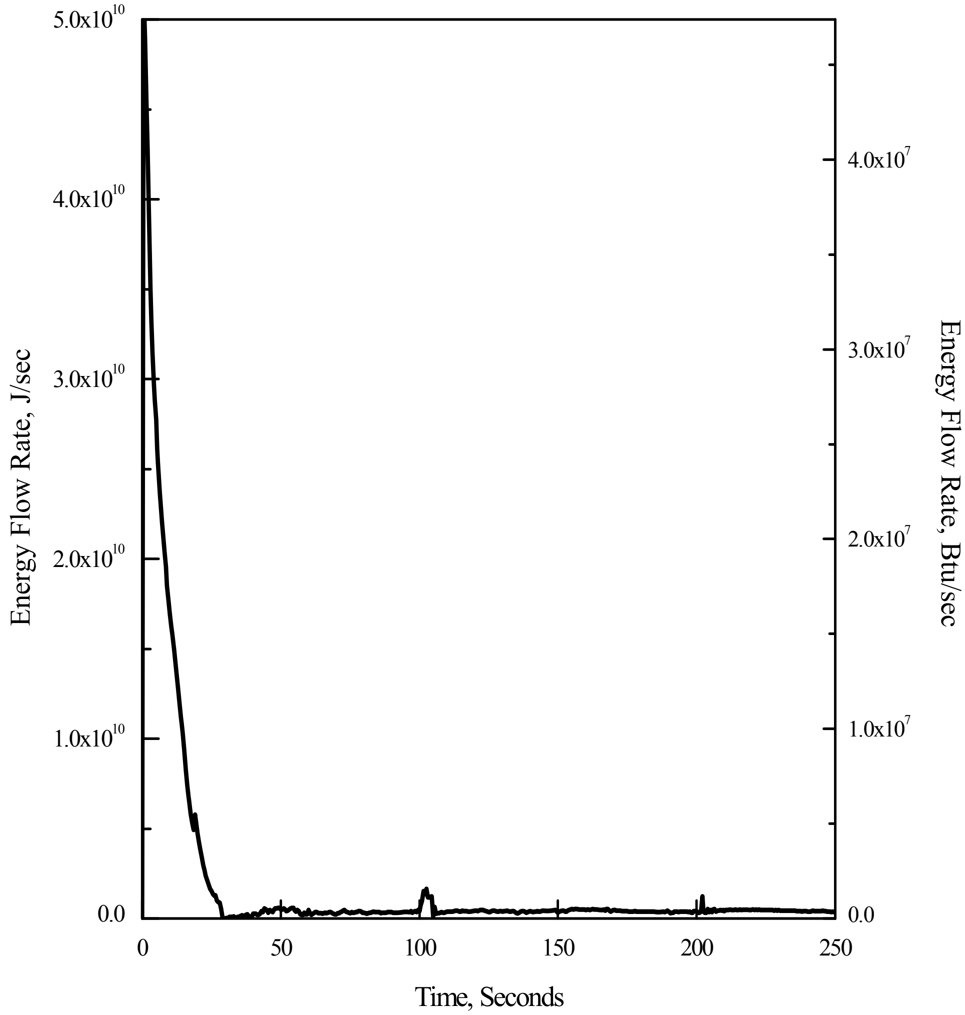

Figure 15.6.5-18 1.0 × Double-ended Guillotine Break in Pump Discharge Leg (Break Energy Flow) (5 of 9)

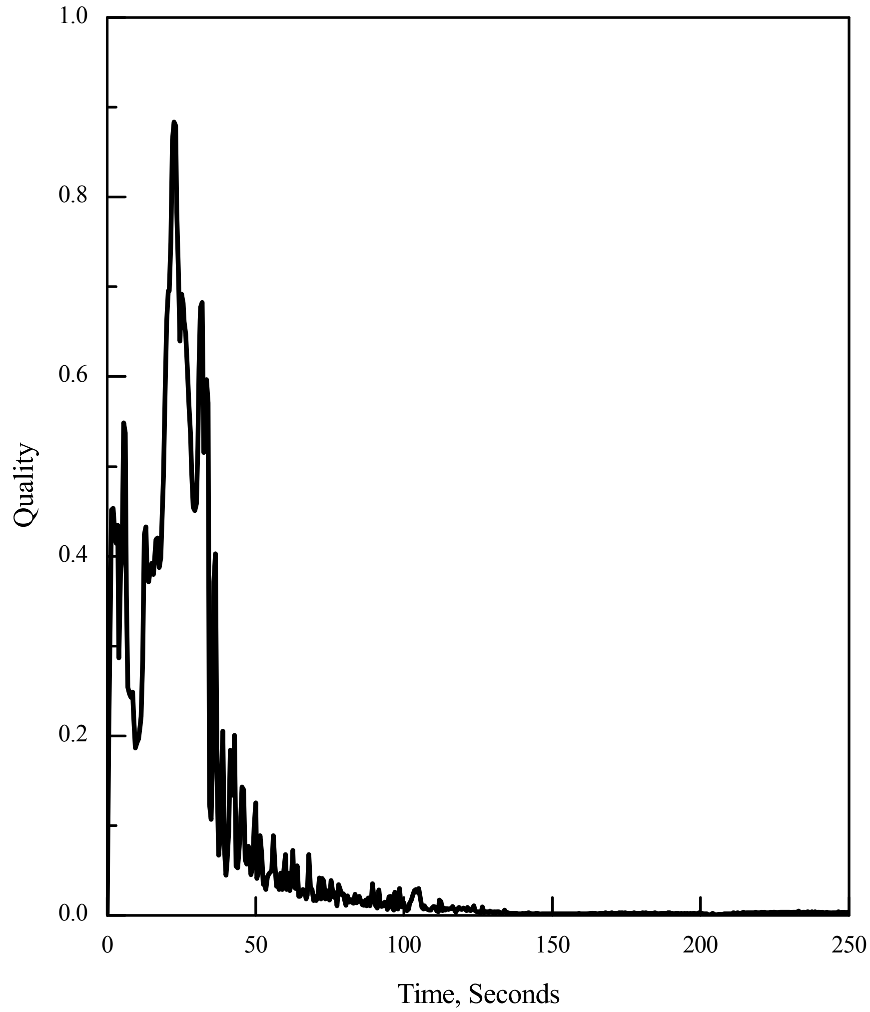

Figure 15.6.5-19 1.0 × Double-ended Guillotine Break in Pump Discharge Leg (Hot Assembly Quality) (6 of 9)

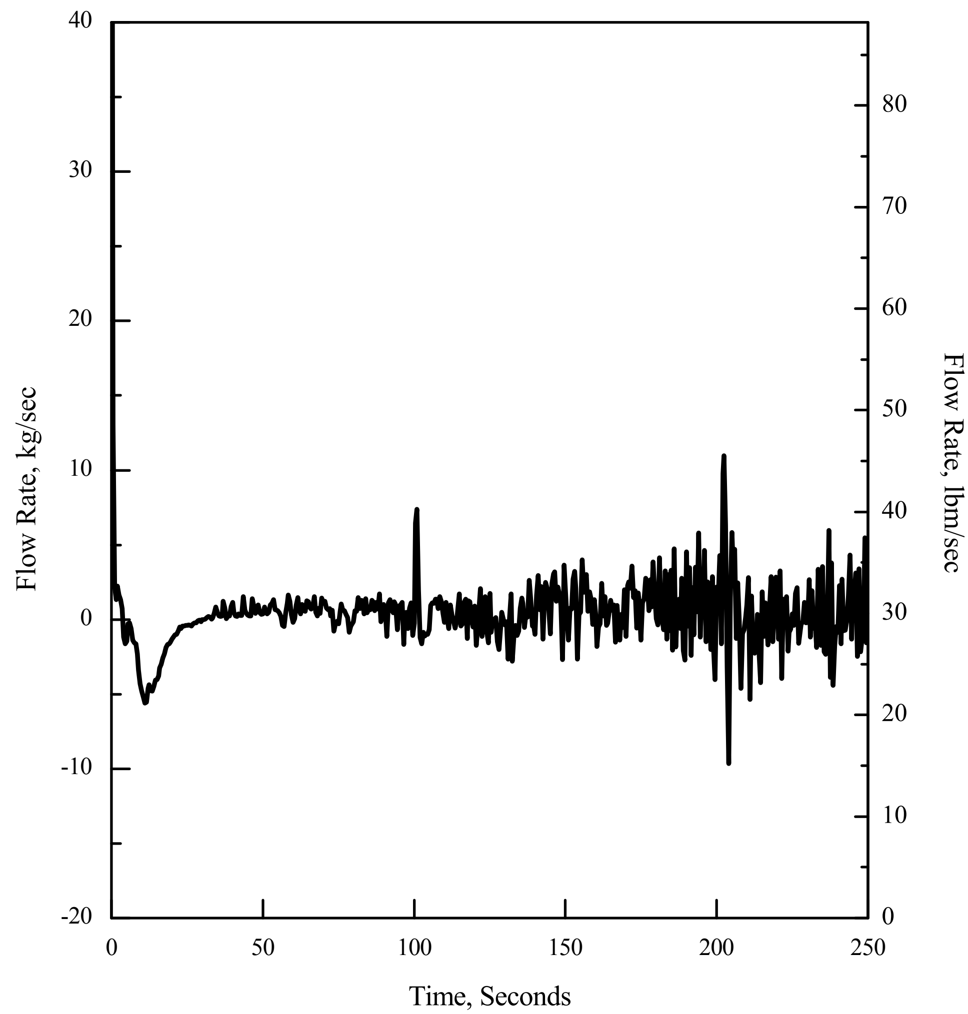

Figure 15.6.5-20 1.0 × Double-ended Guillotine Break in Pump Discharge Leg (Hot Assembly Mass Flow Rate) (7 of 9)

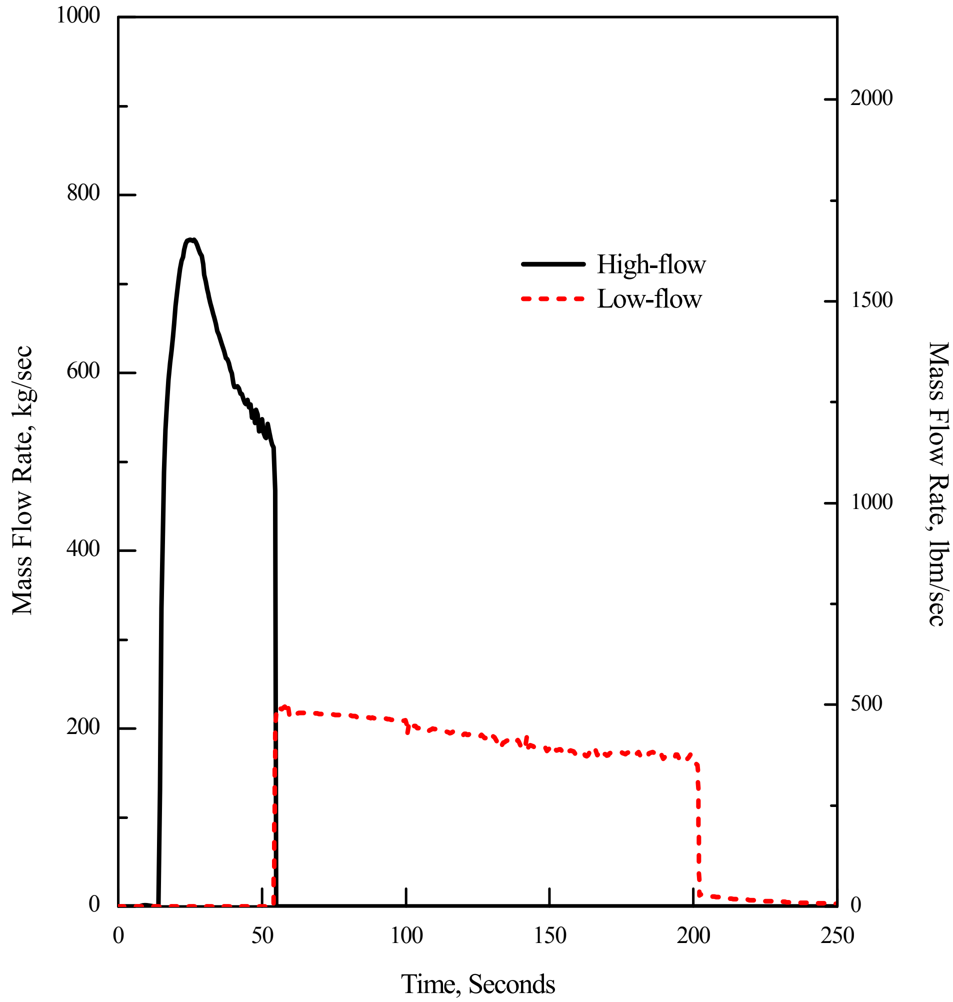

Figure 15.6.5-21 1.0 × Double-ended Guillotine Break in Pump Discharge Leg (Safety Injection Tank Flow) (8 of 9)

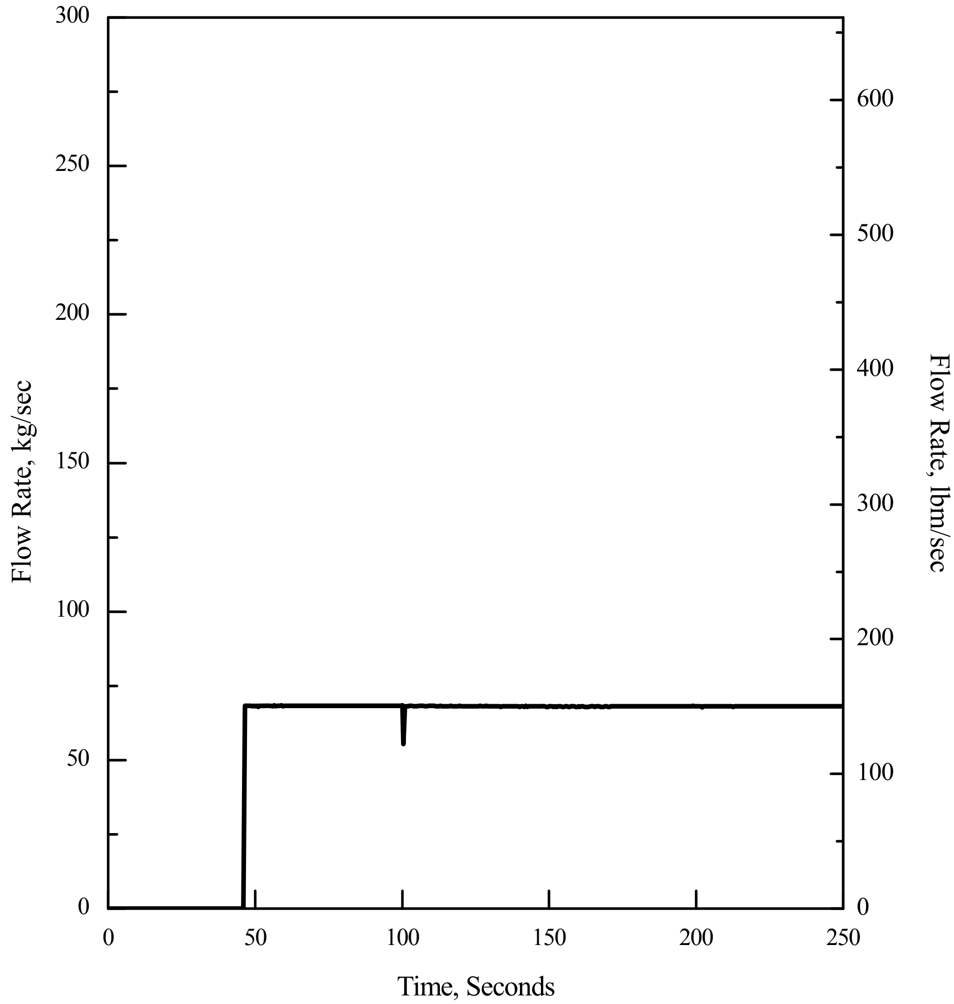

Figure 15.6.5-22 1.0 × Double-ended Guillotine Break in Pump Discharge Leg (SI Pump Flow Rate) (9 of 9)

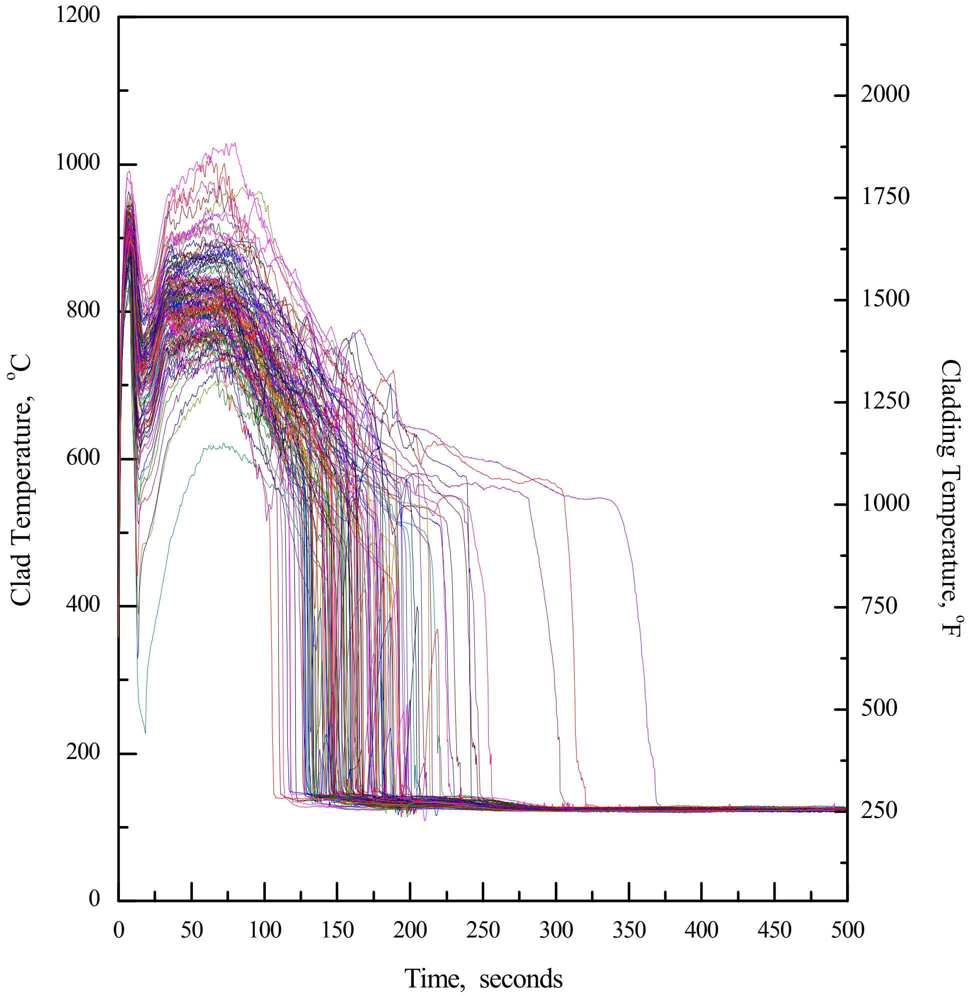

Figure 15.6.5-23 SRS Peak Cladding Temperature

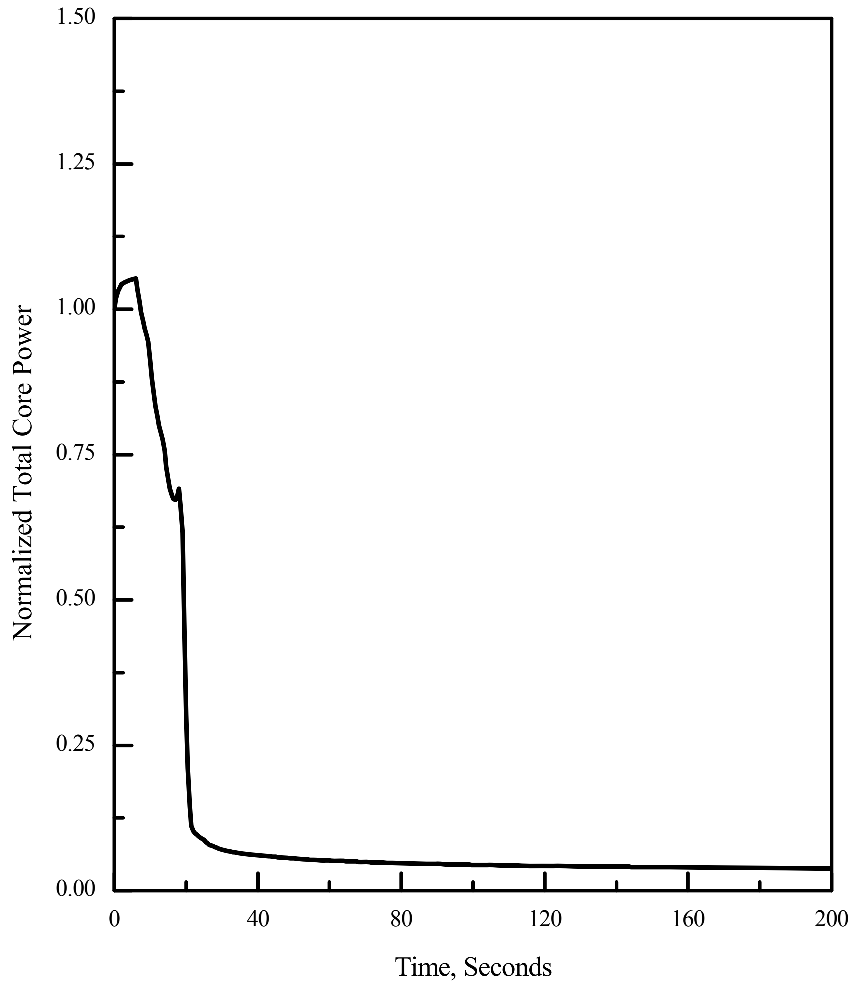

Figure 15.6.5-24A 465 cm^2 (0.5 ft^2) Break in Pump Discharge Leg ; Normalized Total Core Power

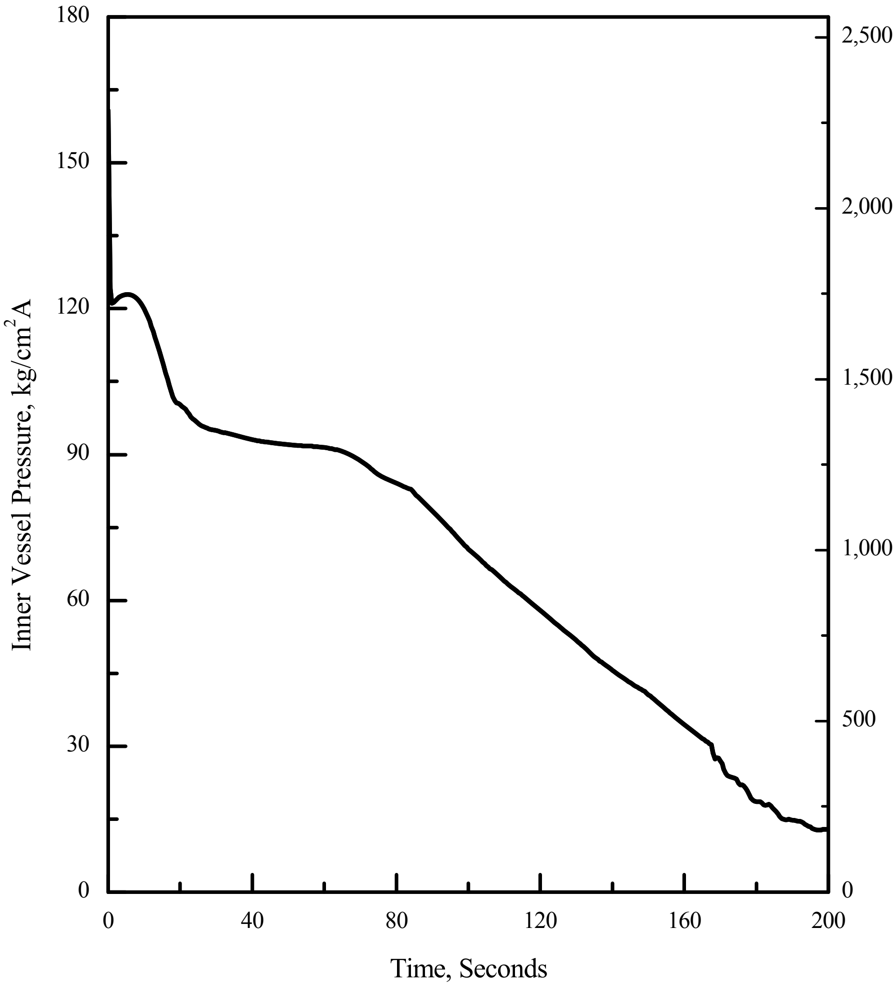

Figure 15.6.5-24B 465 cm^2 (0.5 ft^2) Break in Pump Discharge Leg ; Inner Vessel Pressure

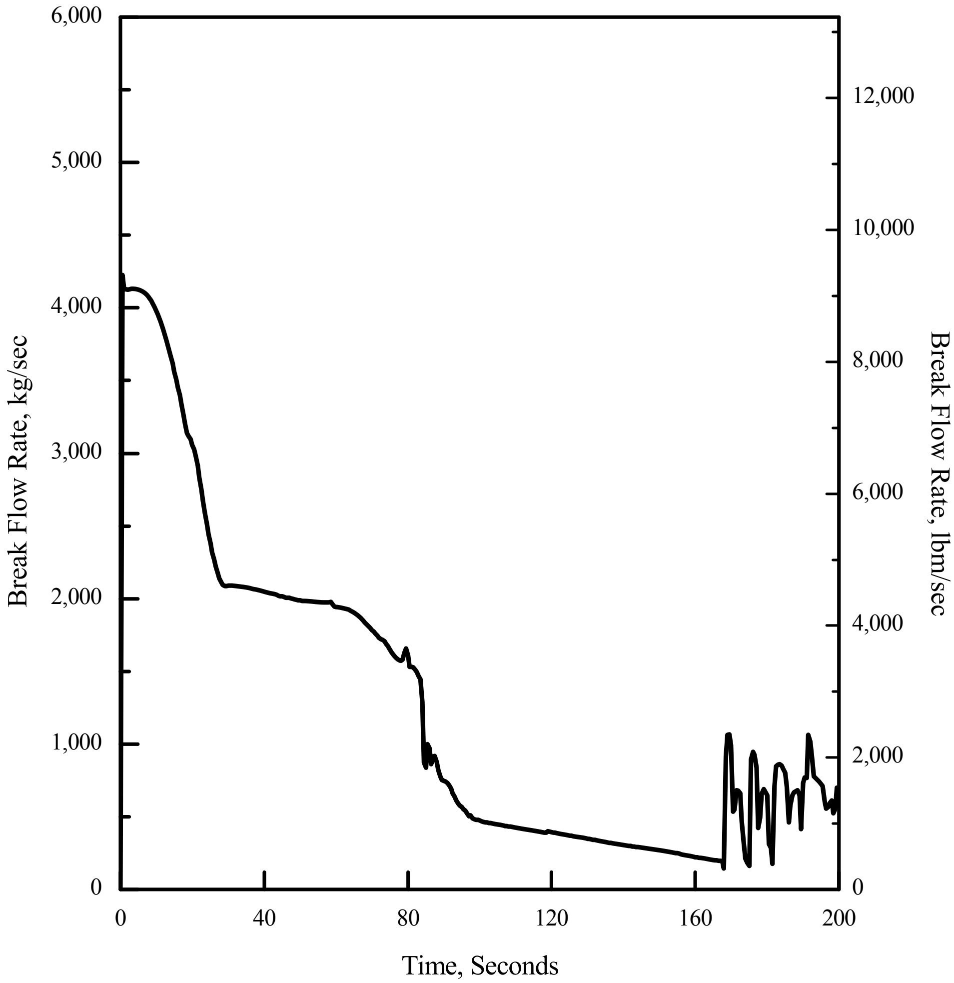

Figure 15.6.5-24C 465 cm^2 (0.5 ft^2) Break in Pump Discharge Leg ; Break Flow Rate

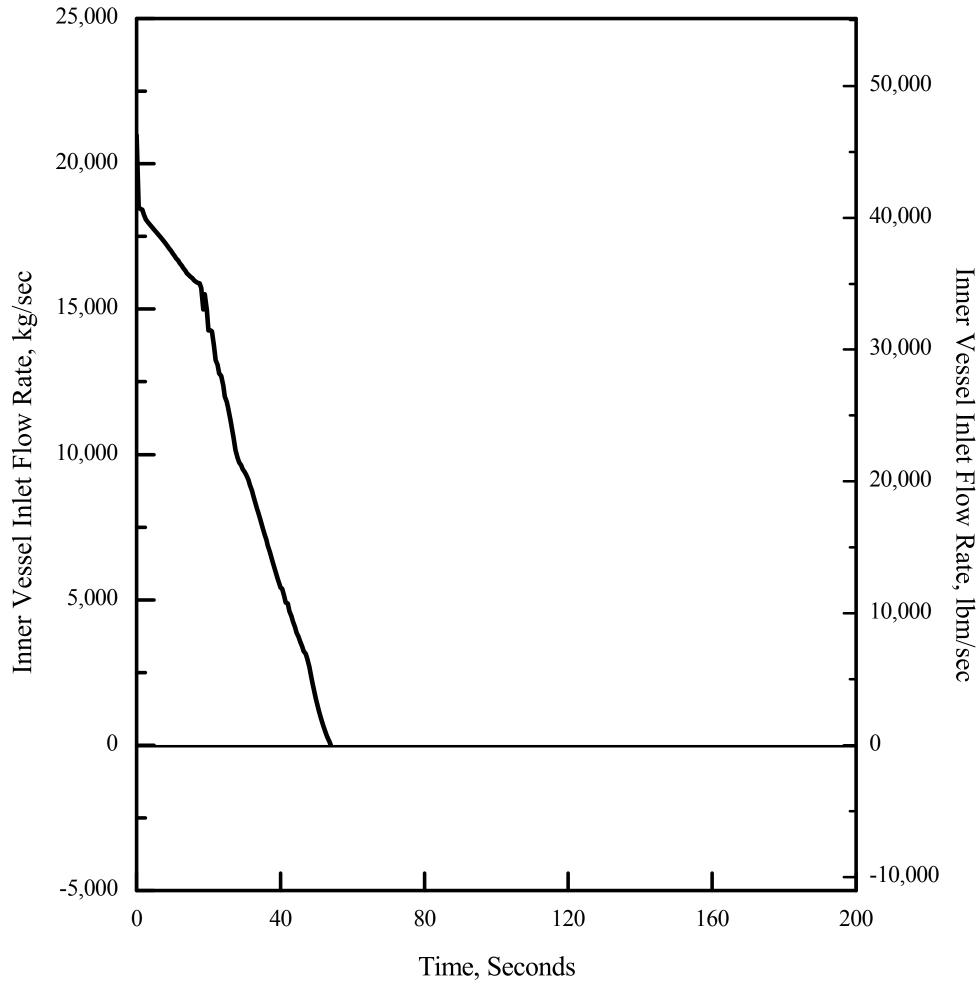

Figure 15.6.5-24D 465 cm^2 (0.5 ft^2) Break in Pump Discharge Leg ; Inner Vessel Inlet Flow Rate

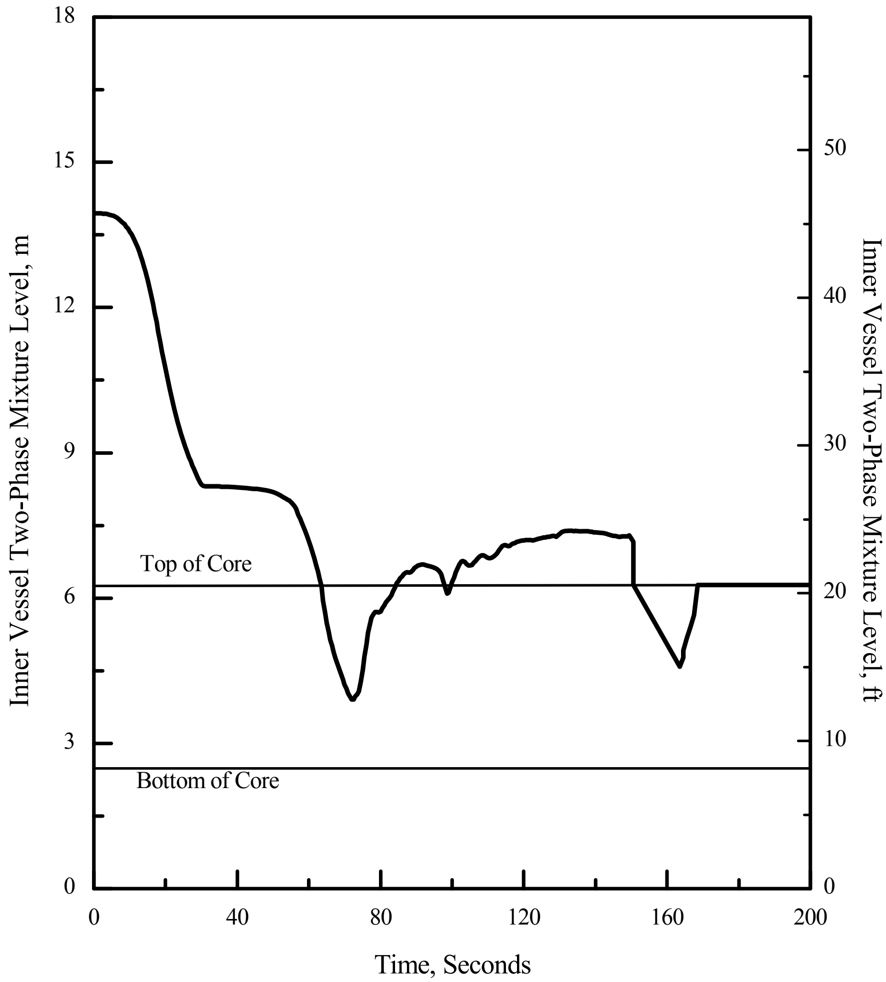

Figure 15.6.5-24E 465 cm² (0.5 ft²) Break in Pump Discharge Leg ; Inner Vessel Two-Phase Mixture Level

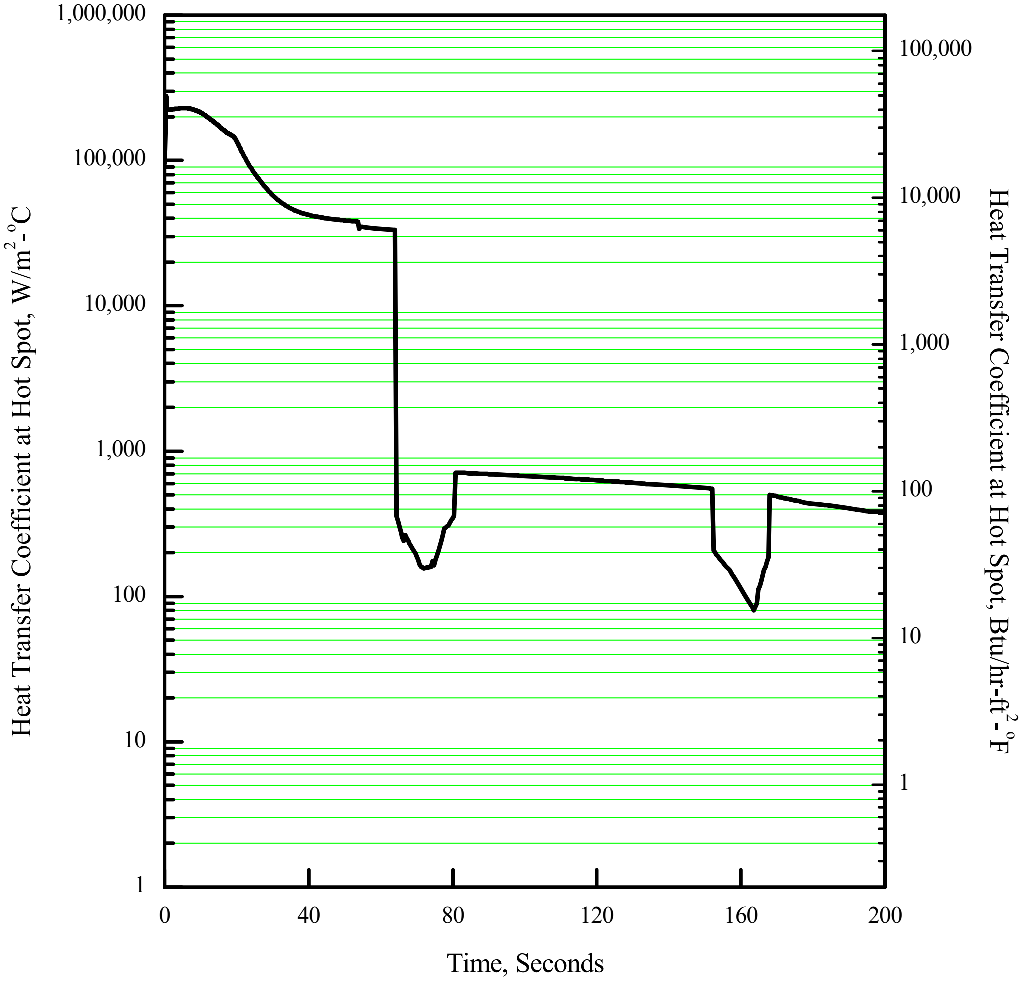

Figure 15.6.5-24F 465 cm^2 (0.5 ft^2) Break in Pump Discharge Leg ; Heat Transfer Coefficient at Hot Spot

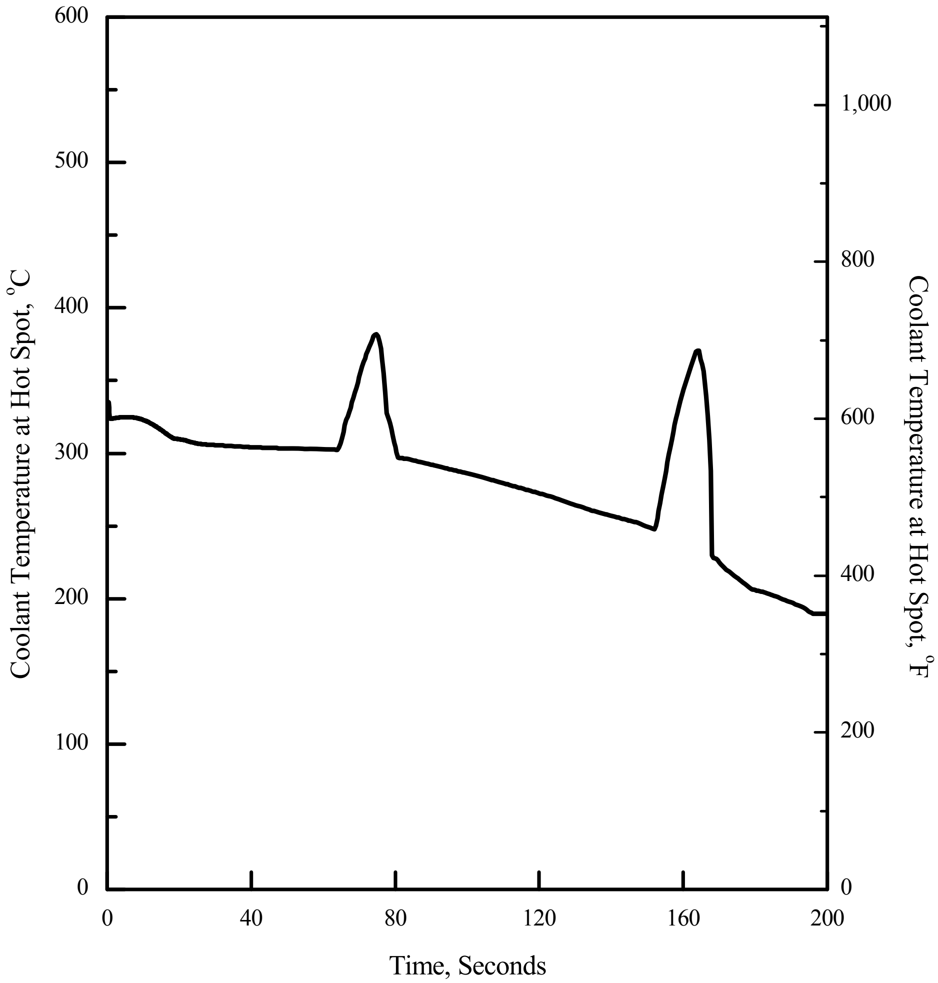

Figure 15.6.5-24G 465 cm^2 (0.5 ft^2) Break in Pump Discharge Leg ; Coolant Temperature at Hot Spot

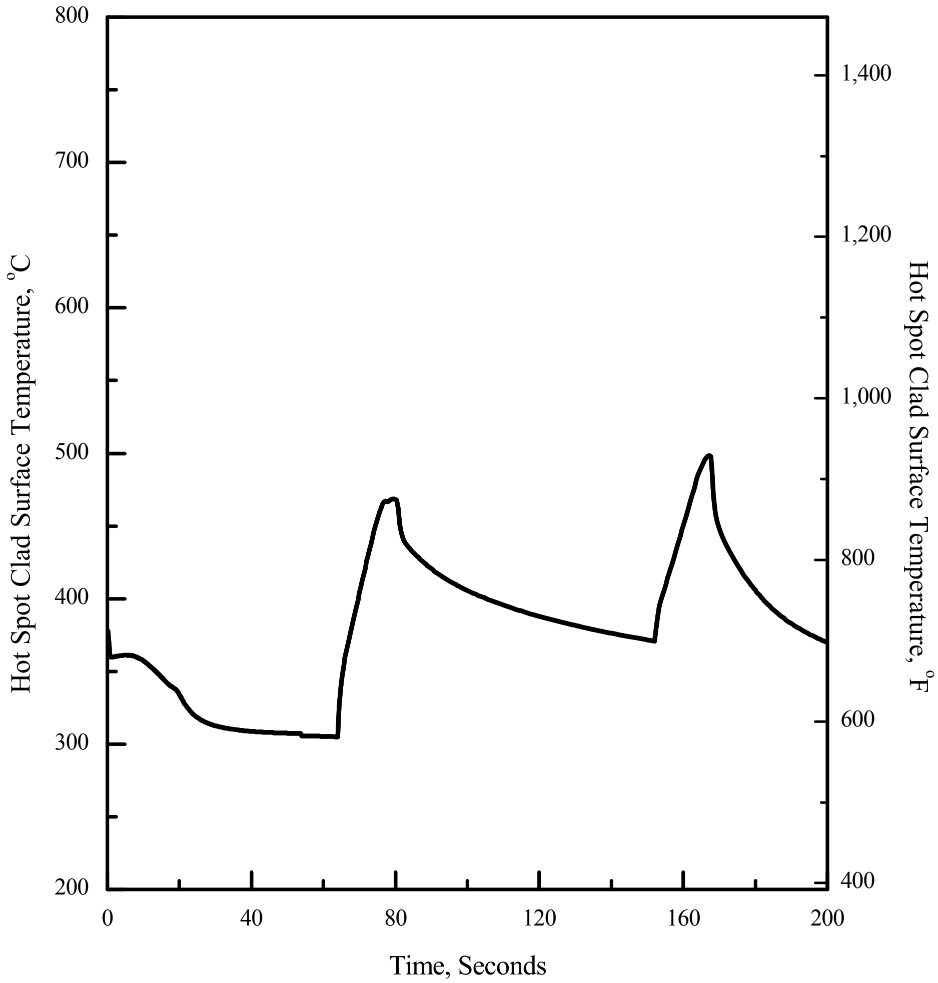

Figure 15.6.5-24H 465 cm^2 (0.5 ft^2) Break in Pump Discharge Leg; Hot Spot Clad Surface Temperature

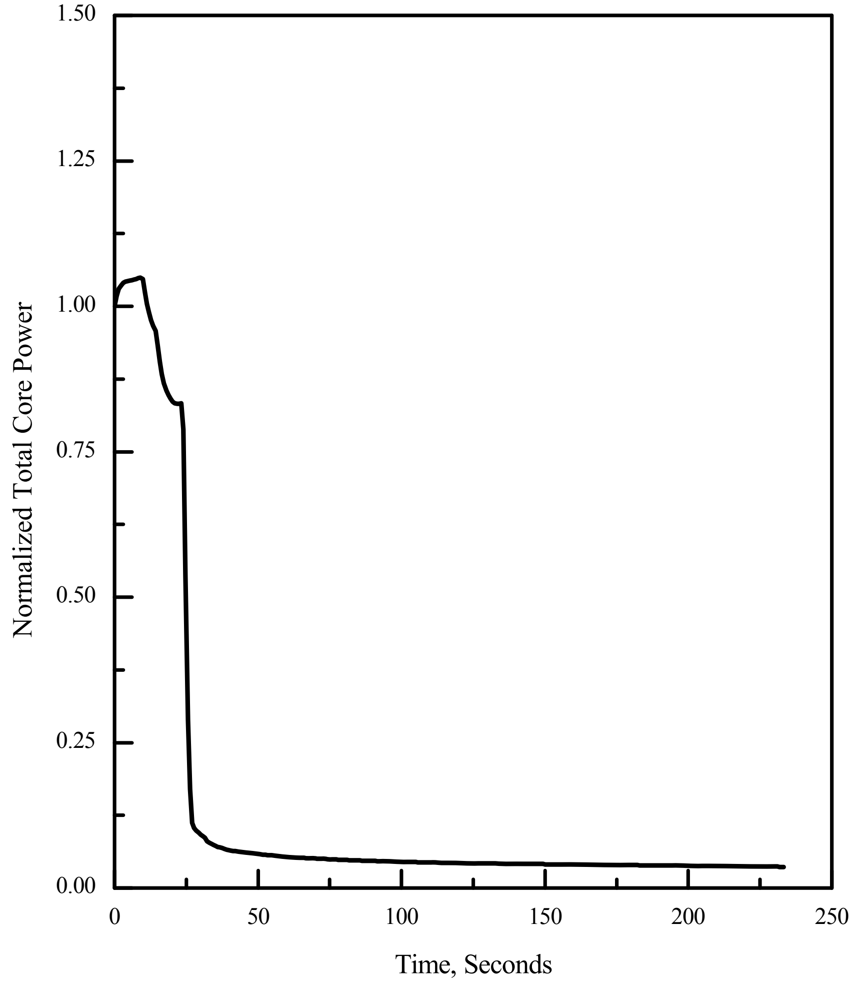

Figure 15.6.5-25A 325 cm^2 (0.35 ft^2) Break in Pump Discharge Leg ; Normalized Total Core Power

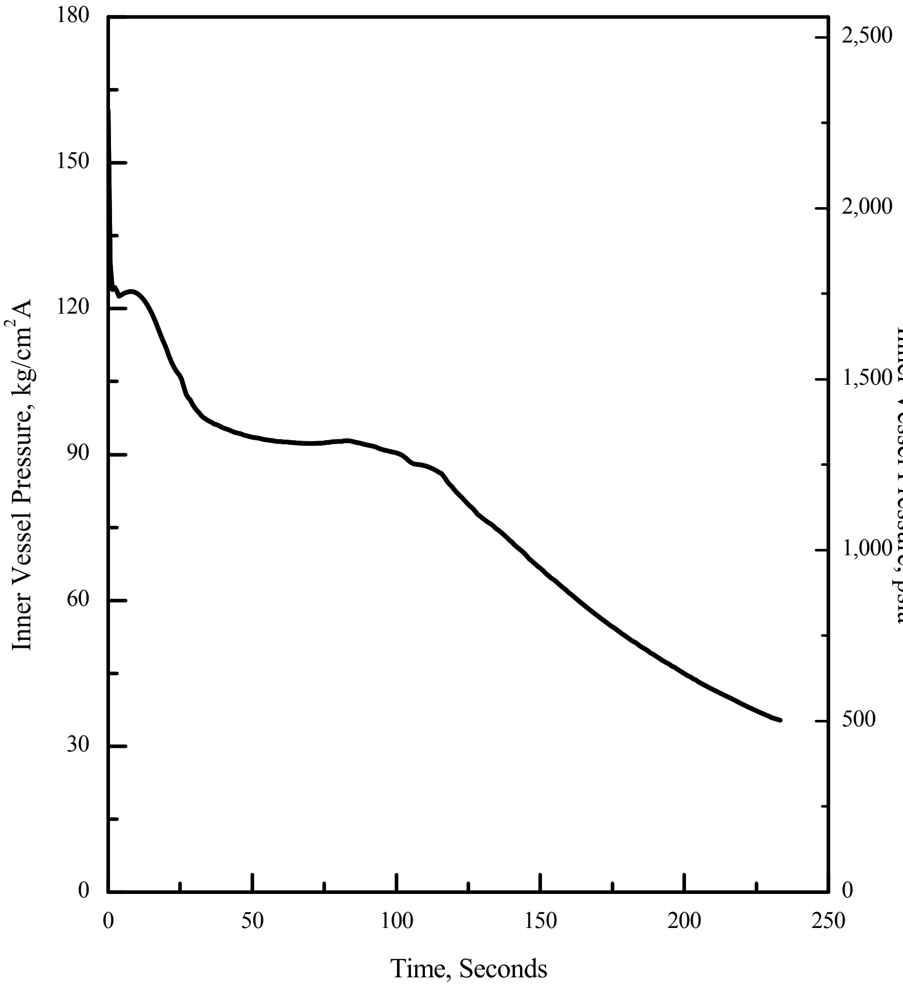

Figure 15.6.5-25B 325 cm^2 (0.35 ft^2) Break in Pump Discharge Leg ; Inner Vessel Pressure

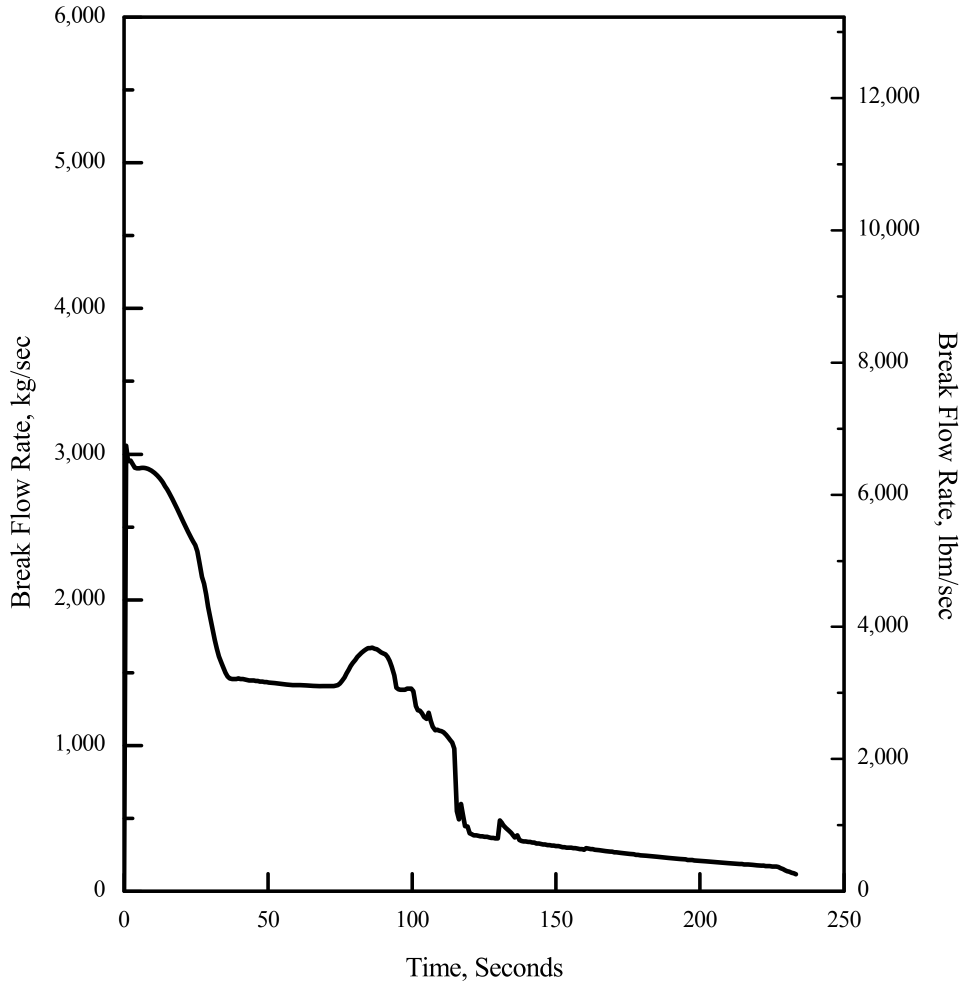

Figure 15.6.5-25C 325 cm^2 (0.35 ft^2) Break in Pump Discharge Leg ; Break Flow Rate

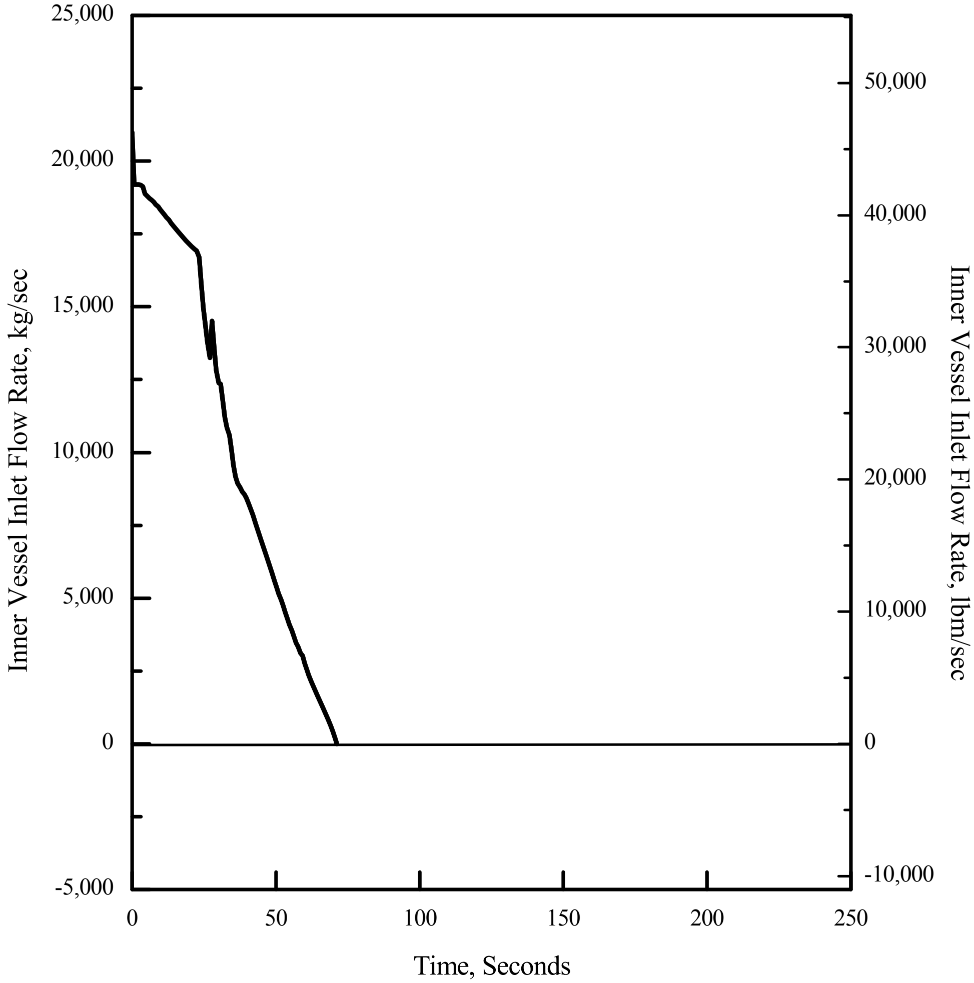

Figure 15.6.5-25D 325 cm^2 (0.35 ft^2) Break in Pump Discharge Leg ; Inner Vessel Inlet Flow Rate

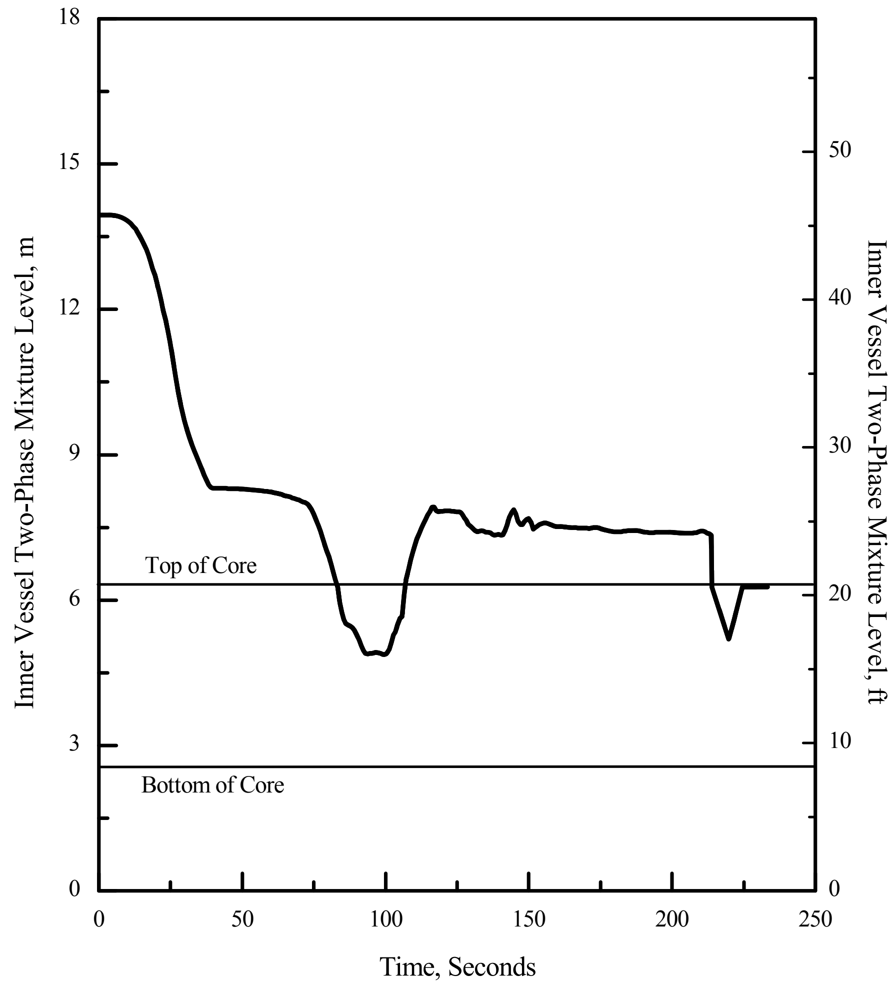

Figure 15.6.5-25E 325 cm^2 (0.35 ft^2) Break in Pump Discharge Leg ; Inner Vessel Two-Phase Mixture Level

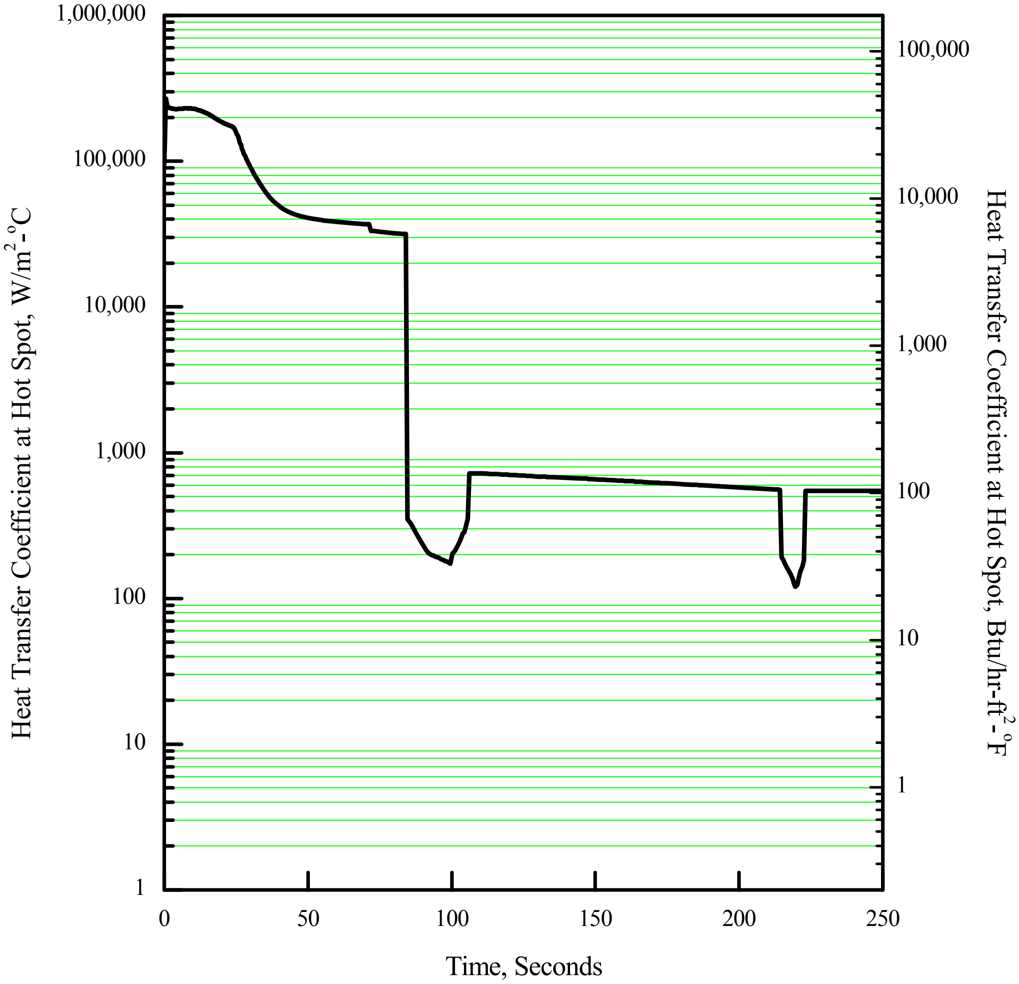

Figure 15.6.5-25F 325 cm^2 (0.35 ft^2) Break in Pump Discharge Leg ; Heat Transfer Coefficient at Hot Spot

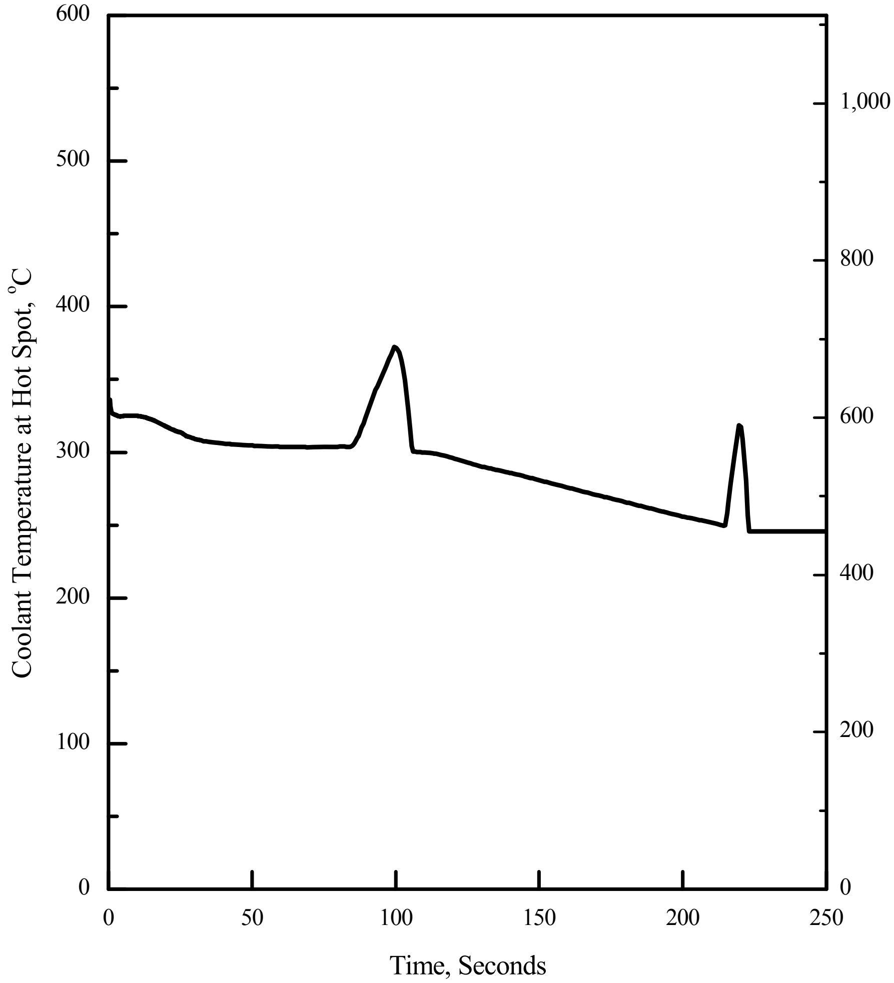

Figure 15.6.5-25G 325 cm^2 (0.35 ft^2) Break in Pump Discharge Leg ; Coolant Temperature at Hot Spot

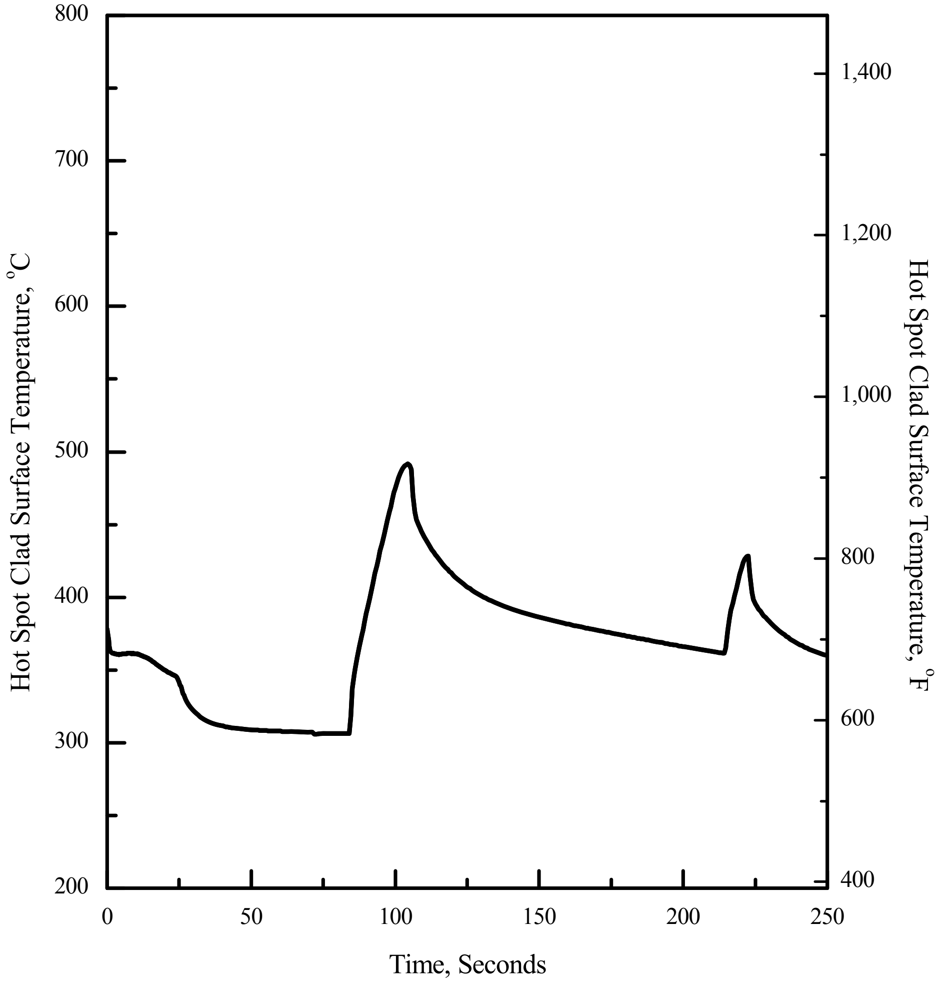

Figure 15.6.5-25H 325 cm^2 (0.35 ft^2) Break in Pump Discharge Leg; Hot Spot Clad Surface Temperature

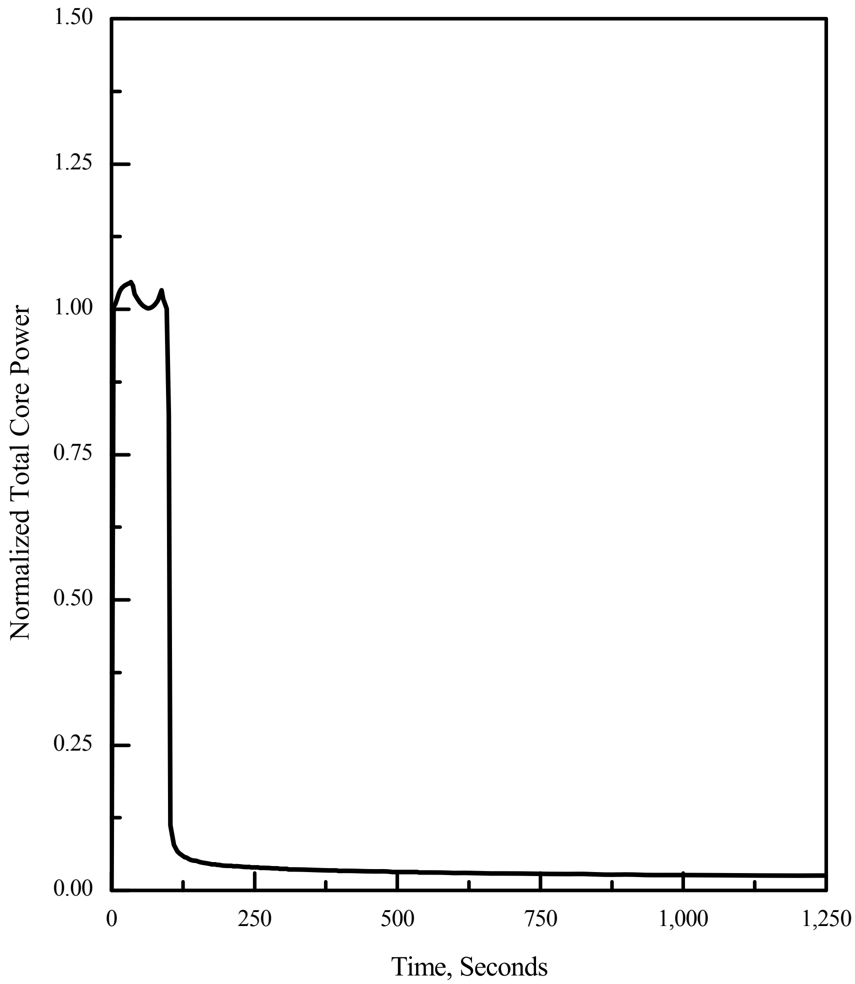

Figure 15.6.5-26A 93 cm^2 (0.1 ft^2) Break in Pump Discharge Leg ; Normalized Total Core Power

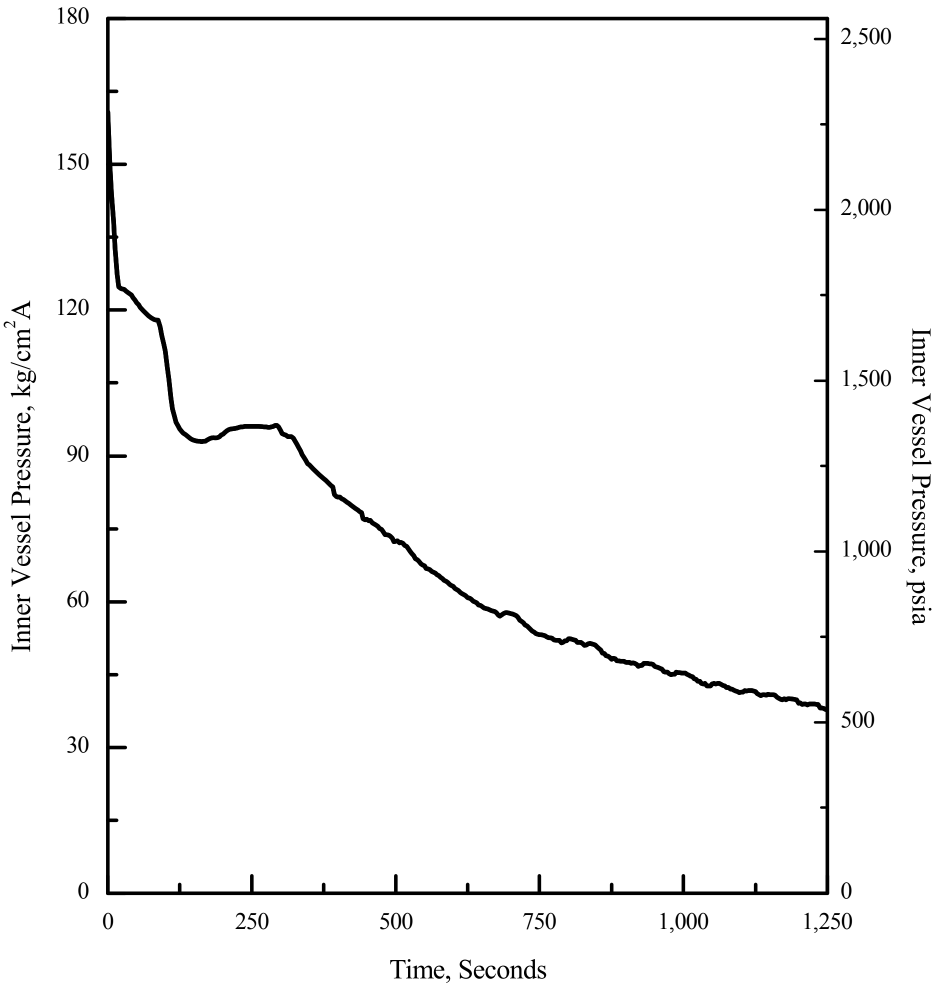

Figure 15.6.5-26B 93 cm² (0.1 ft²) Break in Pump Discharge Leg ; Inner Vessel Pressure

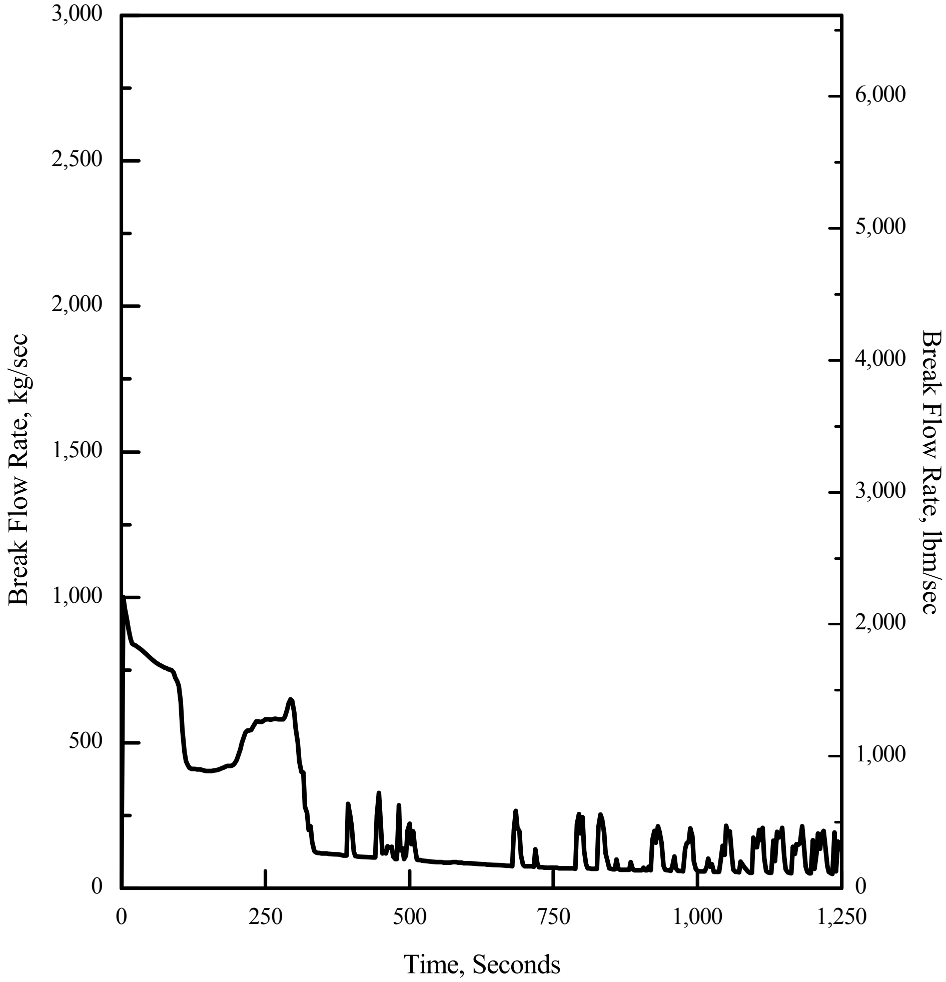

Figure 15.6.5-26C 93 cm^2 (0.1 ft^2) Break in Pump Discharge Leg ; Break Flow Rate

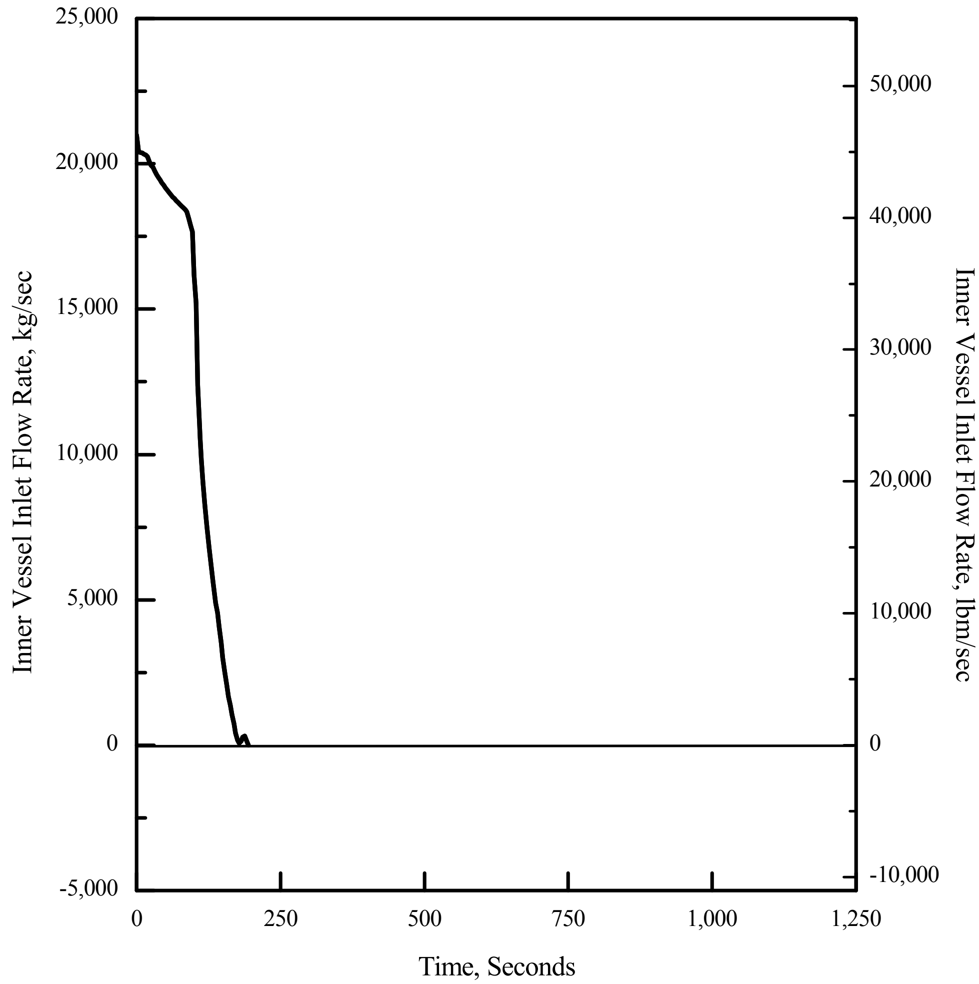

Figure 15.6.5-26D 93 cm² (0.1 ft²) Break in Pump Discharge Leg ; Inner Vessel Inlet Flow Rate

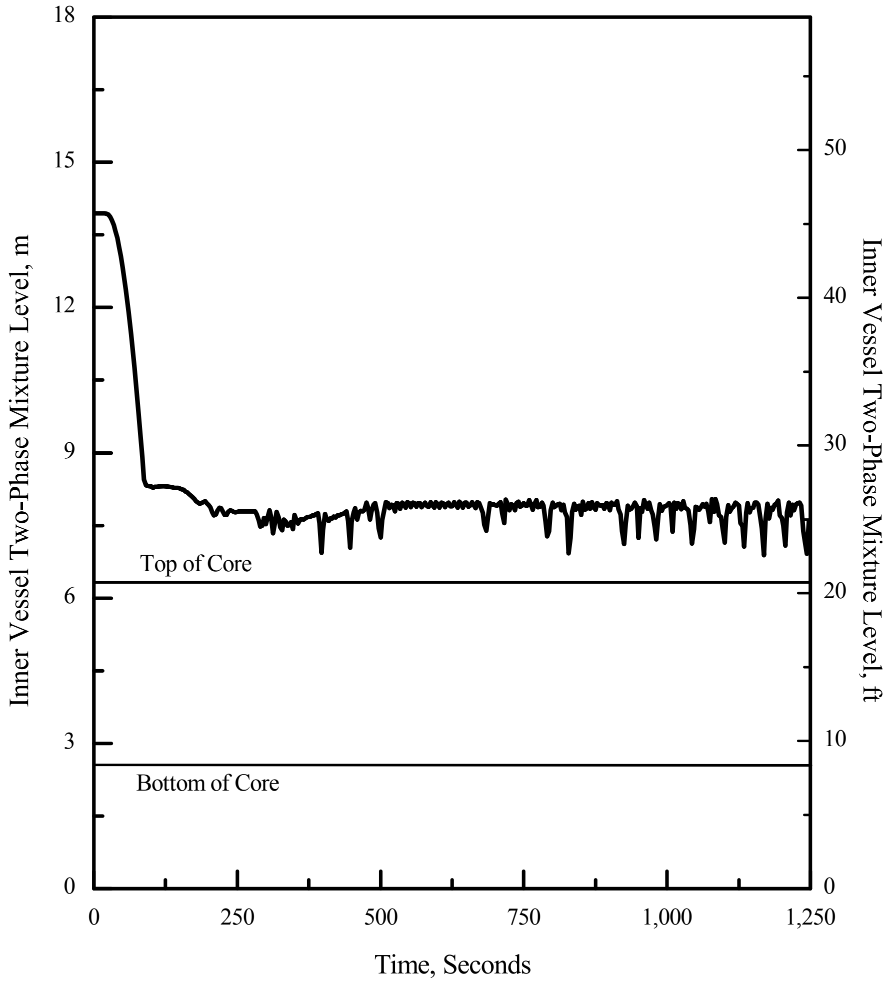

Figure 15.6.5-26E 93 cm^2 (0.1 ft^2) Break in Pump Discharge Leg ; Inner Vessel Two-Phase Mixture Level

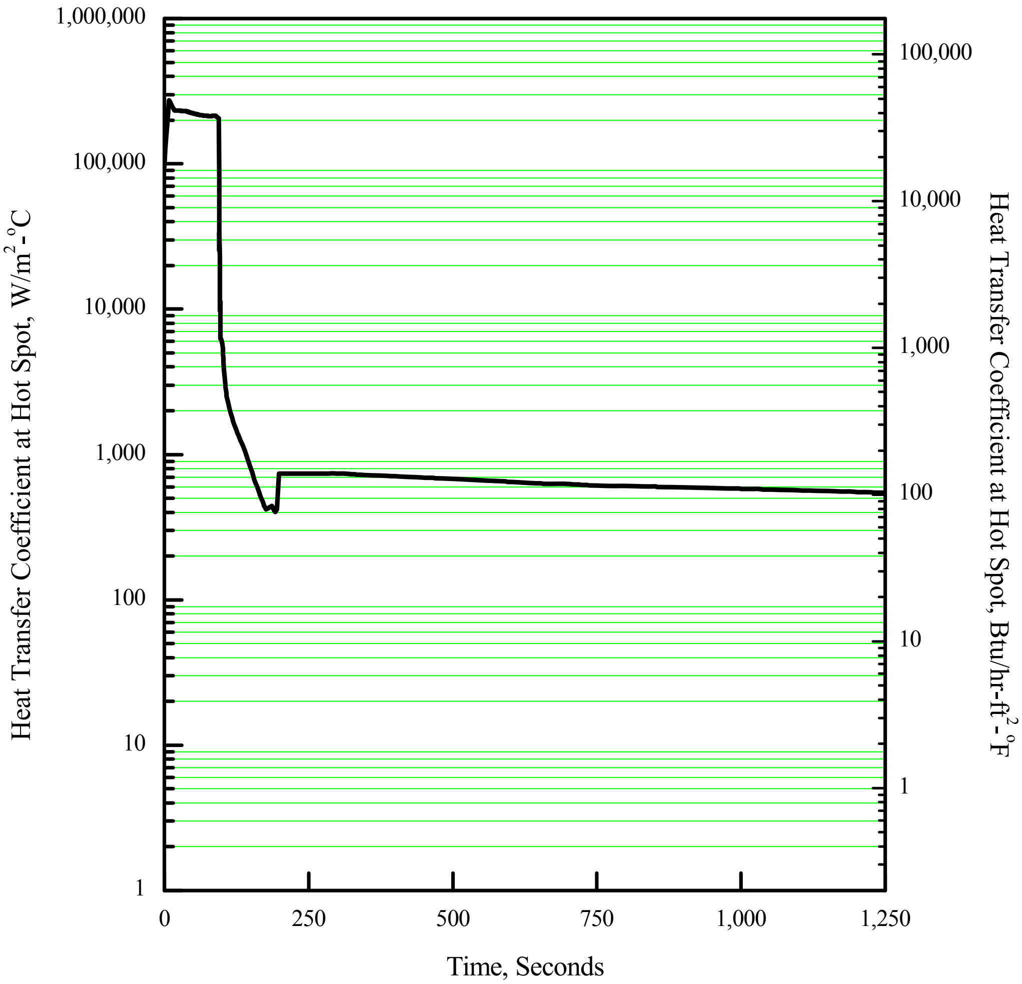

Figure 15.6.5-26F 93 cm^2 (0.1 ft^2) Break in Pump Discharge Leg ; Heat Transfer Coefficient at Hot Spot

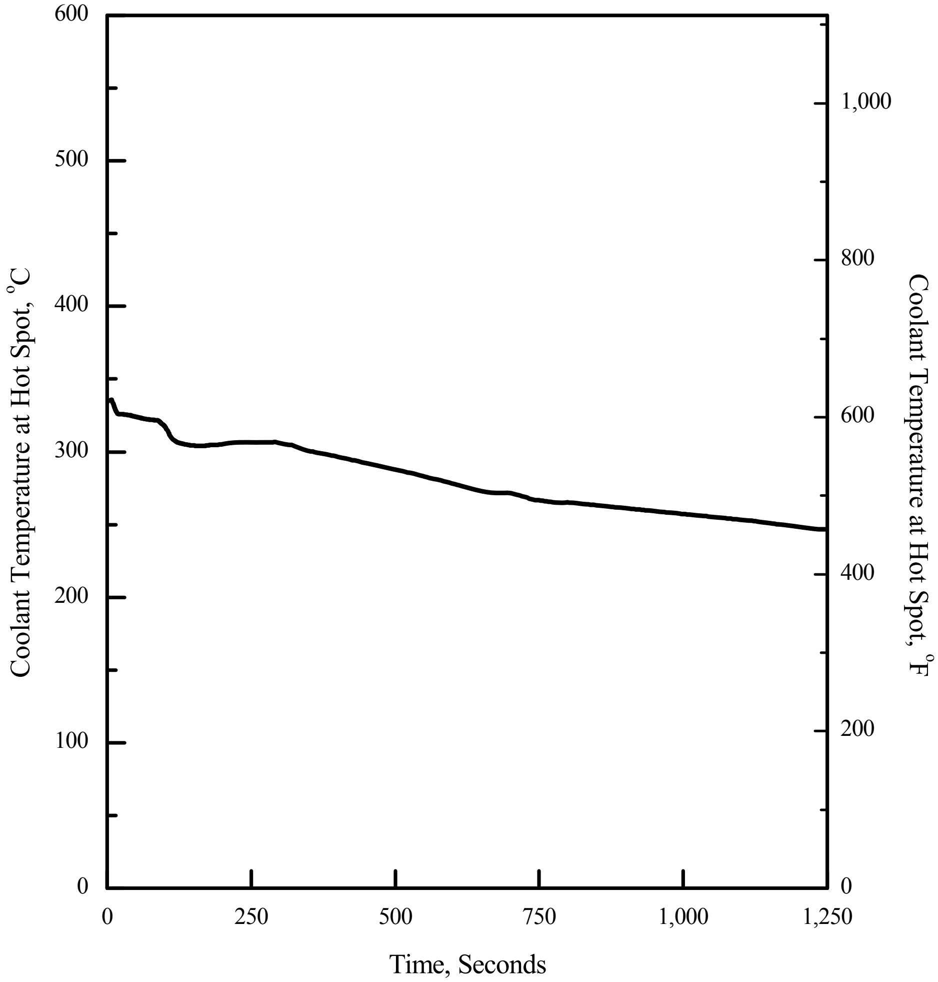

Figure 15.6.5-26G 93 cm^2 (0.1 ft^2) Break in Pump Discharge Leg ; Coolant Temperature at Hot Spot

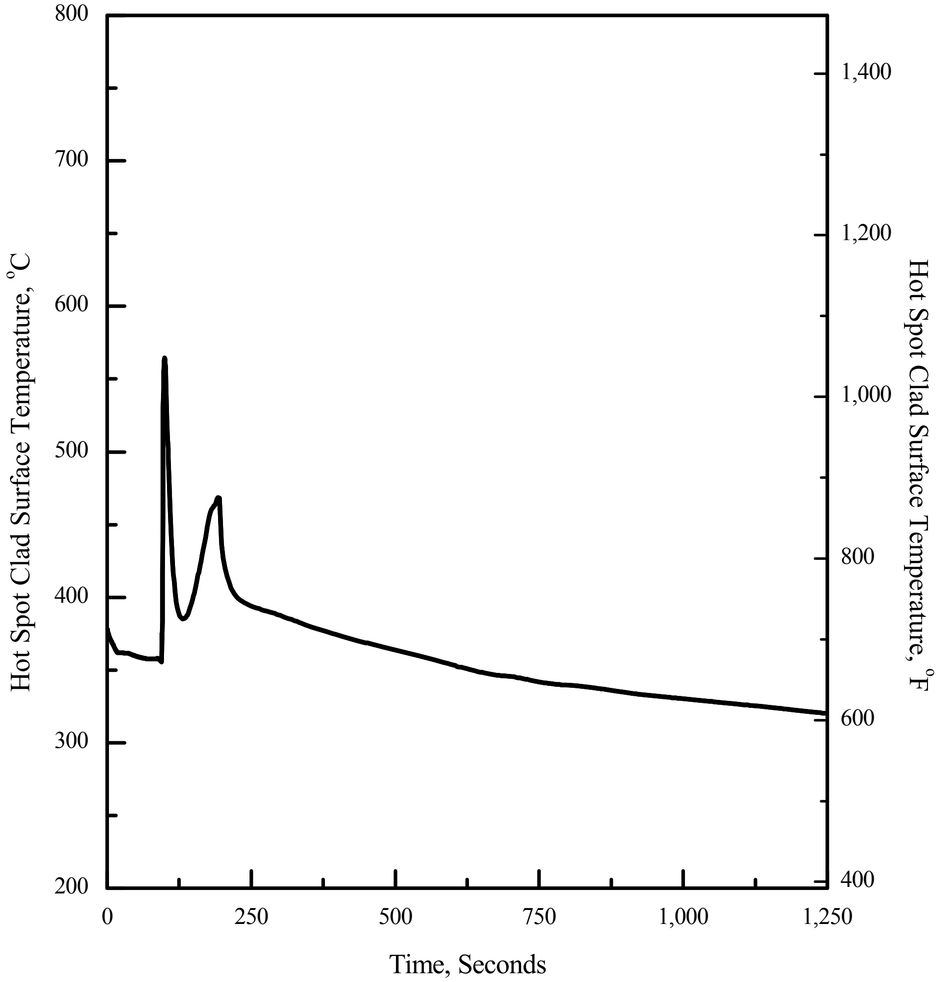

Figure 15.6.5-26H 93 cm^2 (0.1 ft^2) Break in Pump Discharge Leg ; Hot Spot Clad Surface Temperature

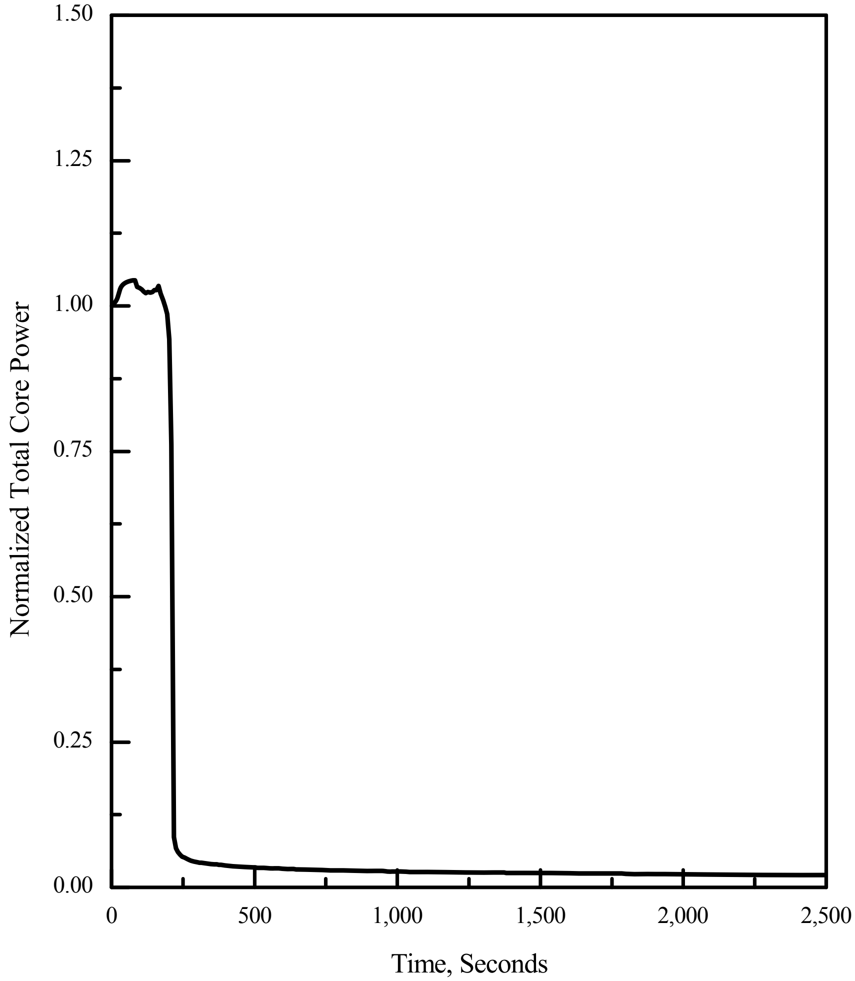

Figure 15.6.5-27A 46.5 cm^2 (0.05 ft^2) Break in Pump Discharge Leg ; Normalized Total Core Power

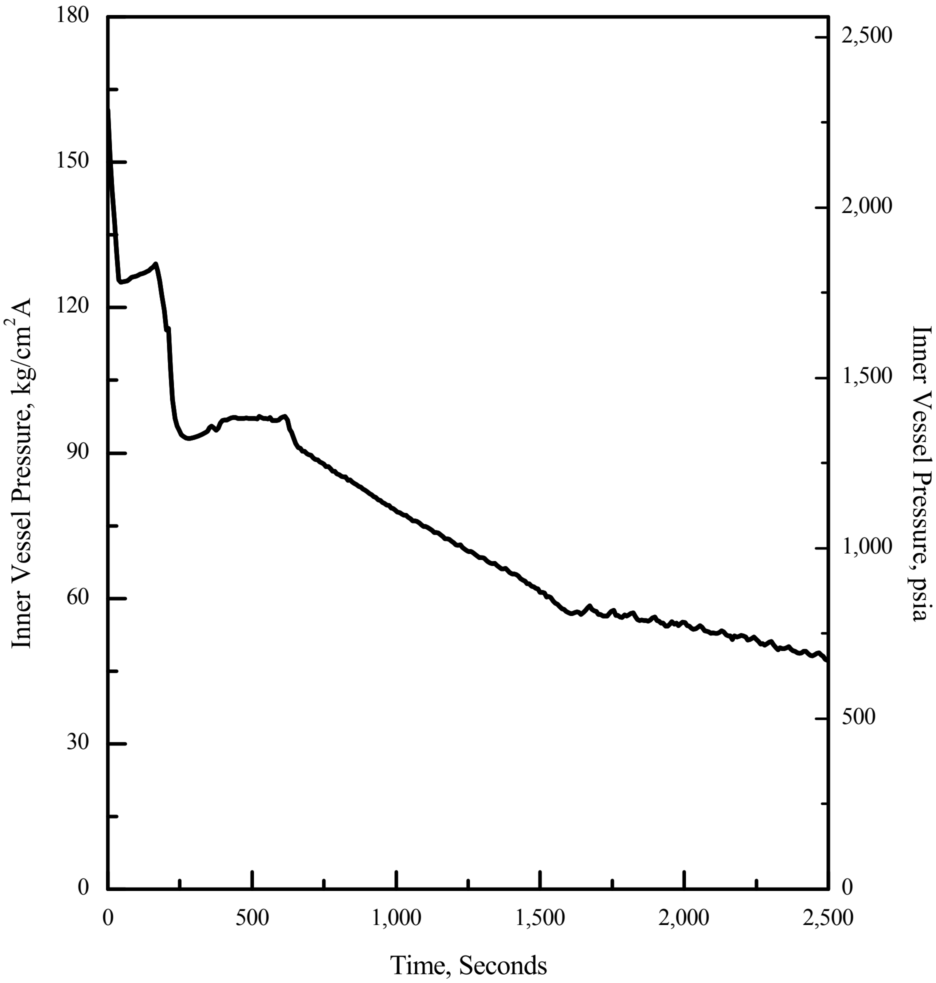

Figure 15.6.5-27B 46.5 cm^2 (0.05 ft^2) Break in Pump Discharge Leg ; Inner Vessel Pressure

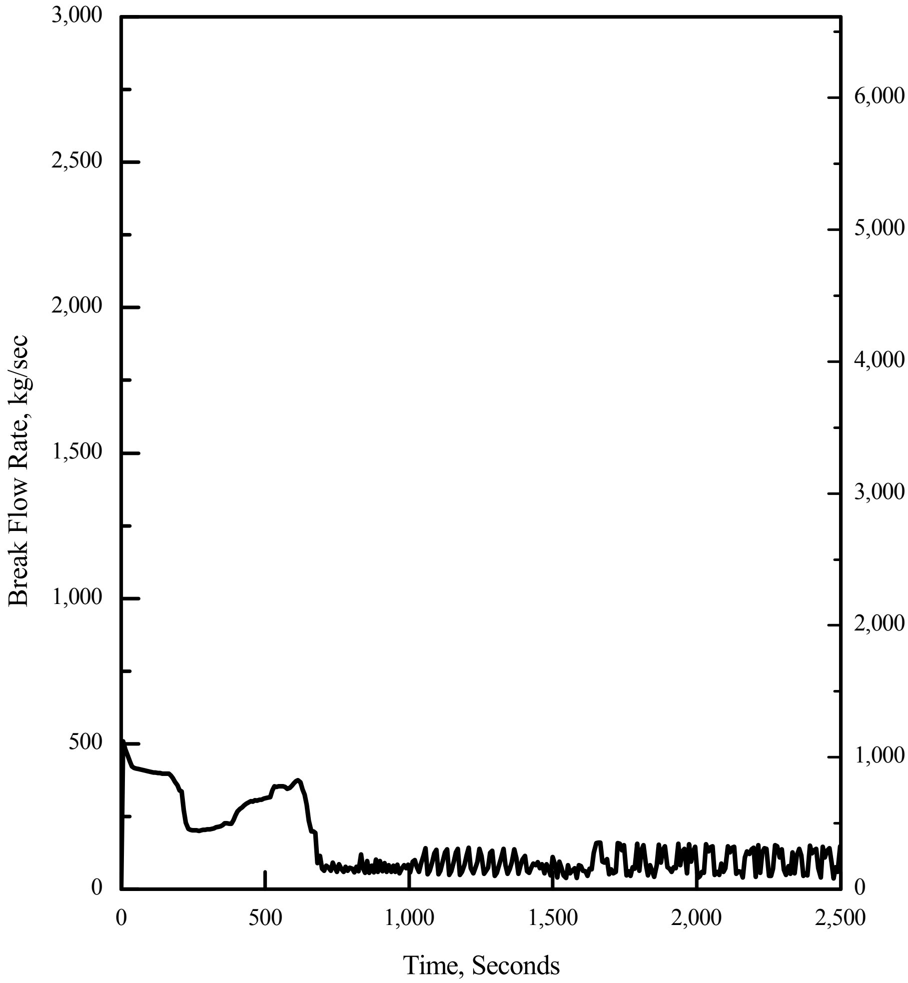

Figure 15.6.5-27C 46.5 cm^2 (0.05 ft^2) Break in Pump Discharge Leg ; Break Flow Rate

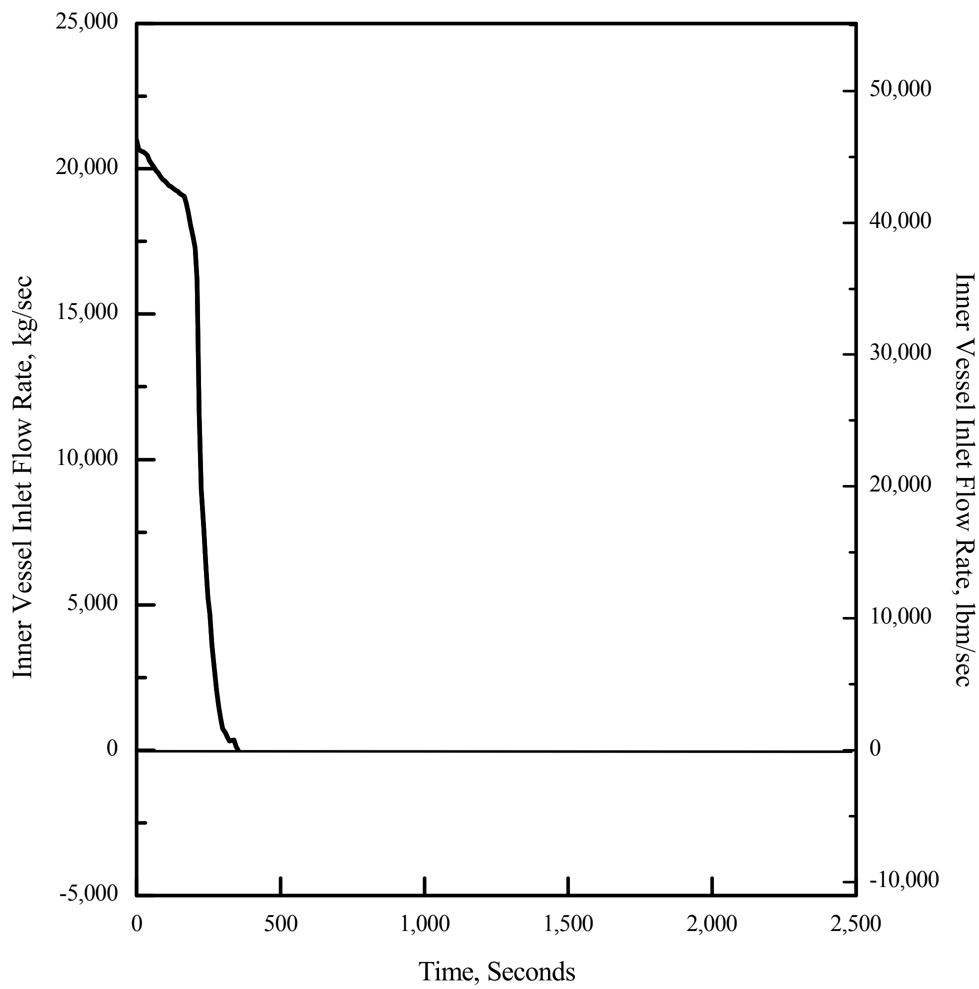

Figure 15.6.5-27D 46.5 cm^2 (0.05 ft^2) Break in Pump Discharge Leg ; Inner Vessel Inlet Flow Rate

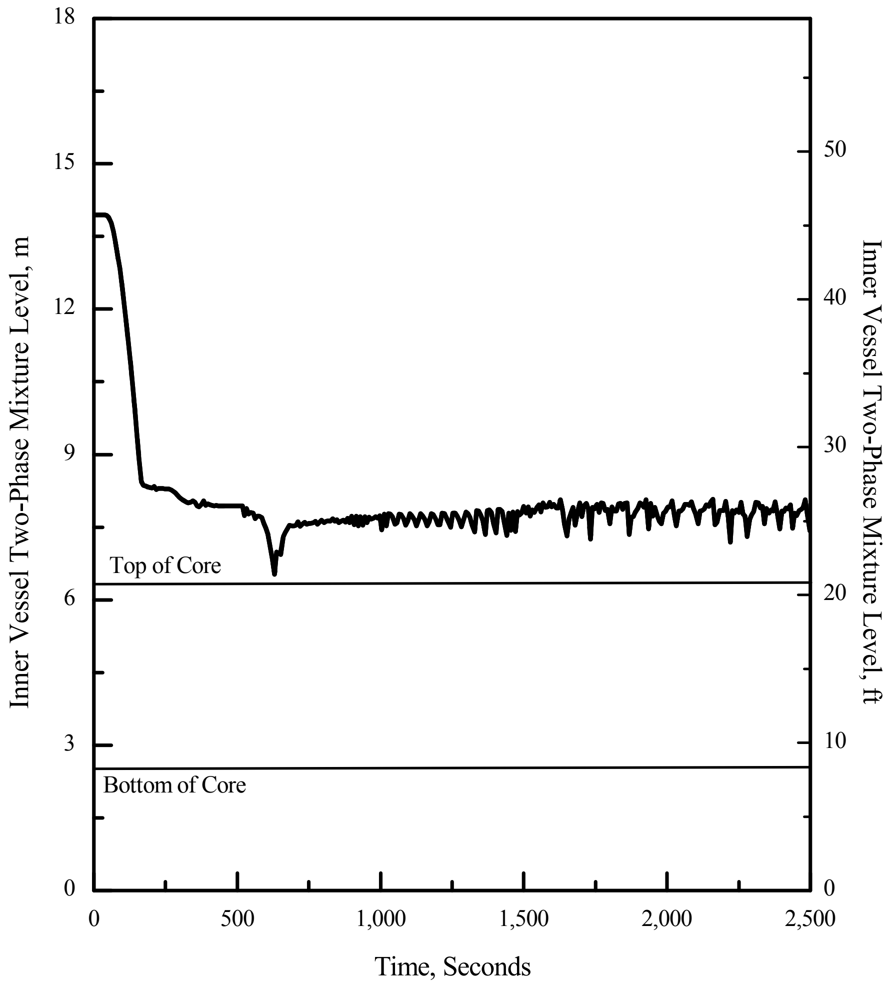

Figure 15.6.5-27E 46.5 cm² (0.05 ft²) Break in Pump Discharge Leg ; Inner Vessel Two-Phase Mixture Level

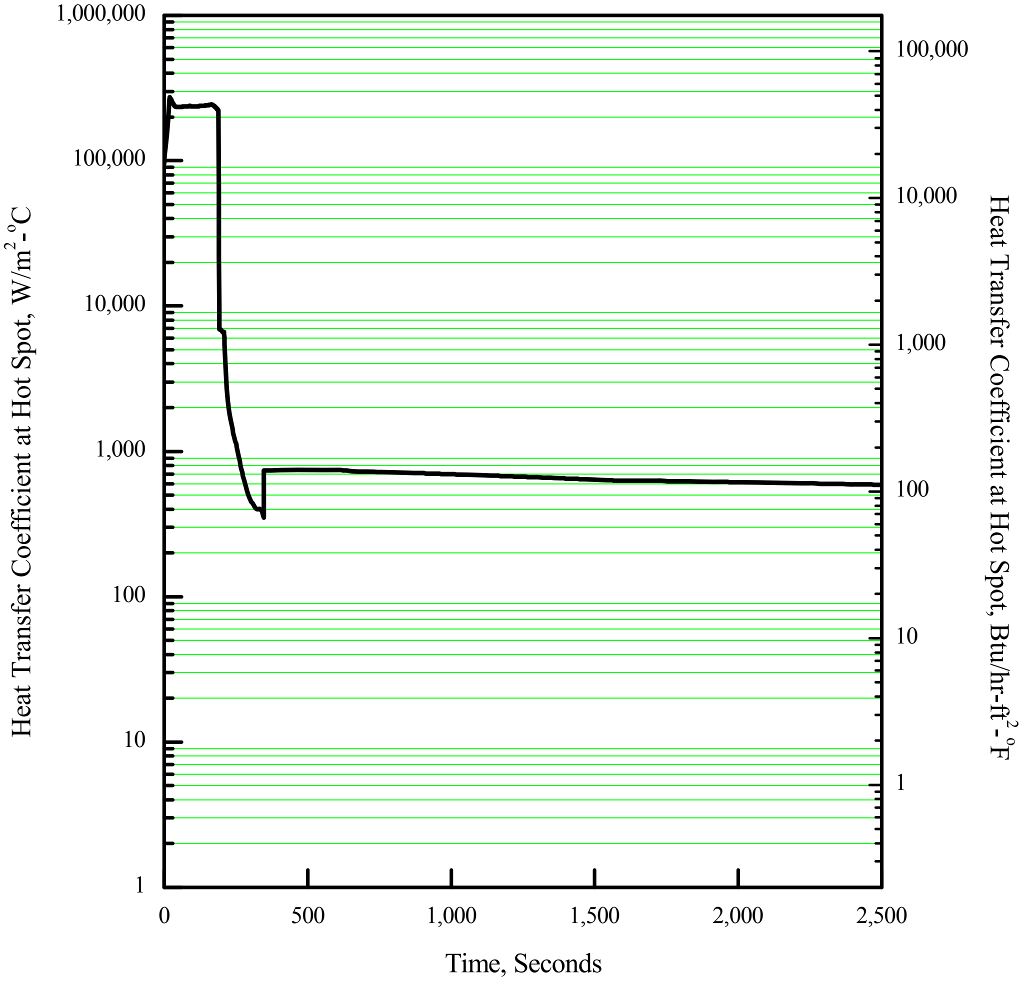

Figure 15.6.5-27F 46.5 cm^2 (0.05 ft^2) Break in Pump Discharge Leg ; Heat Transfer Coefficient at Hot Spot

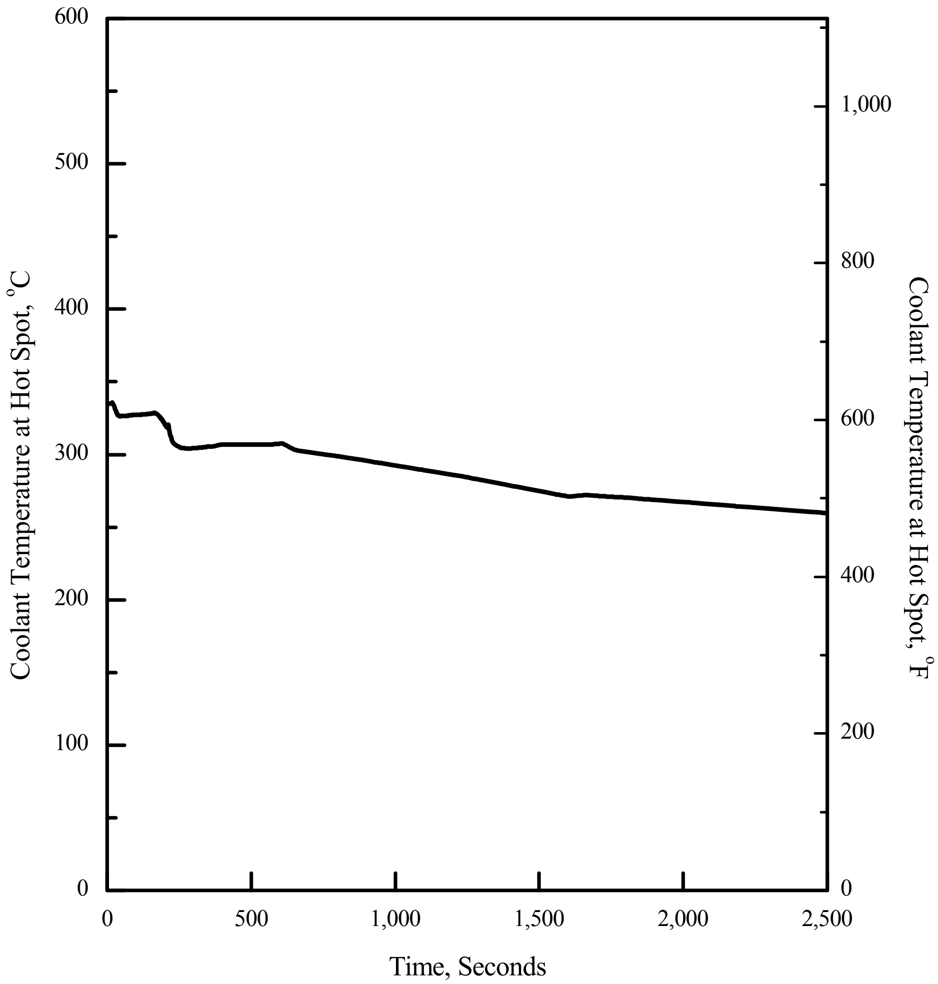

Figure 15.6.5-27G 46.5 cm^2 (0.05 ft^2) Break in Pump Discharge Leg ; Coolant Temperature at Hot Spot

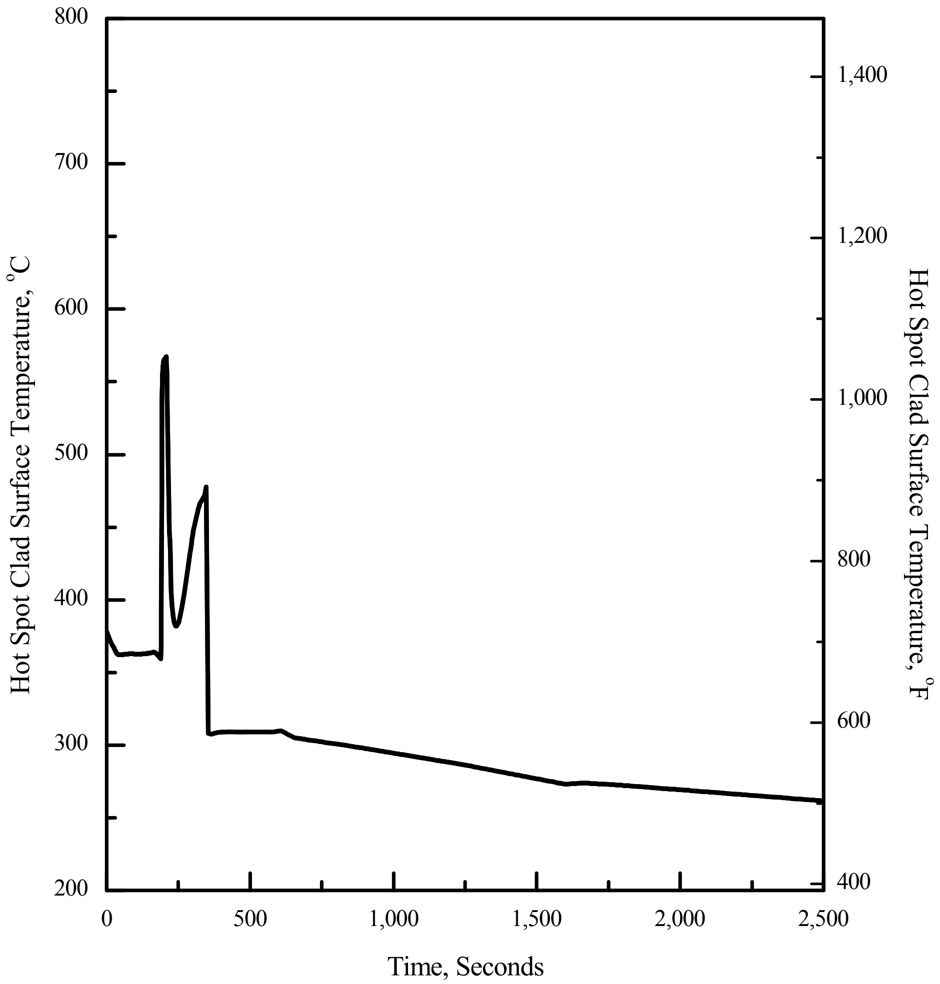

Figure 15.6.5-27H 46.5 cm² (0.05 ft²) Break in Pump Discharge Leg ; Hot Spot Clad Surface Temperature

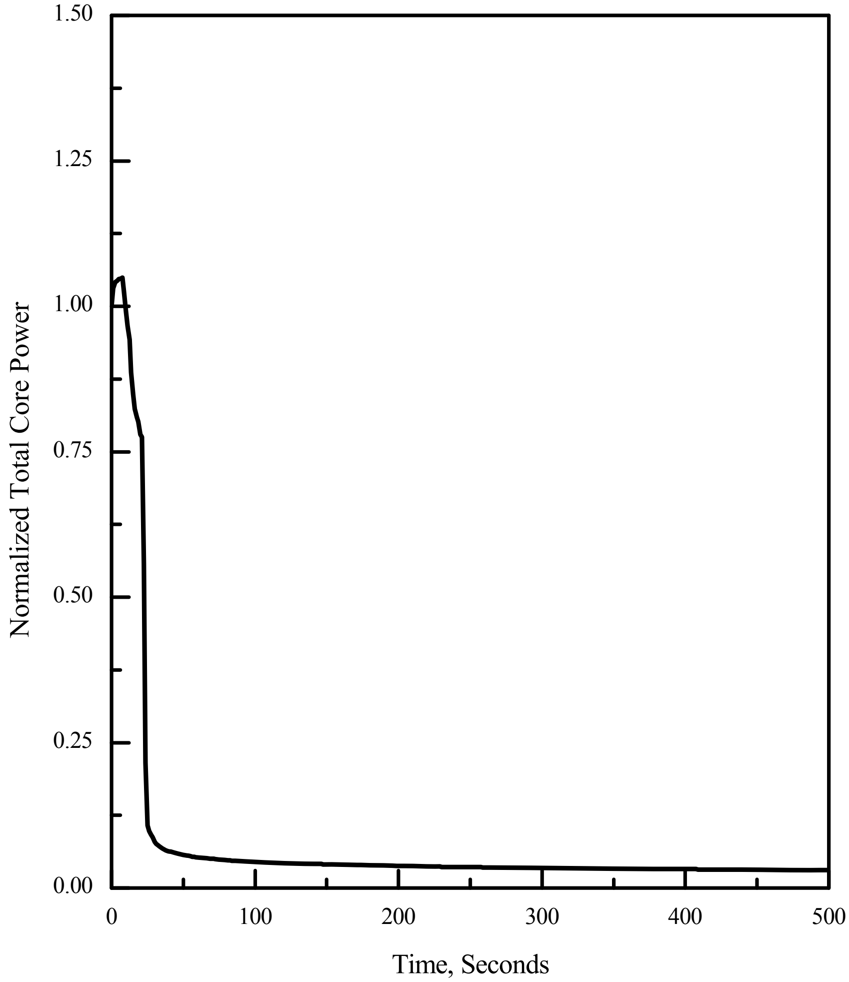

Figure 15.6.5-28A 372 cm^2 (0.4 ft^2) Break in DVI Line ; Normalized Total Core Power

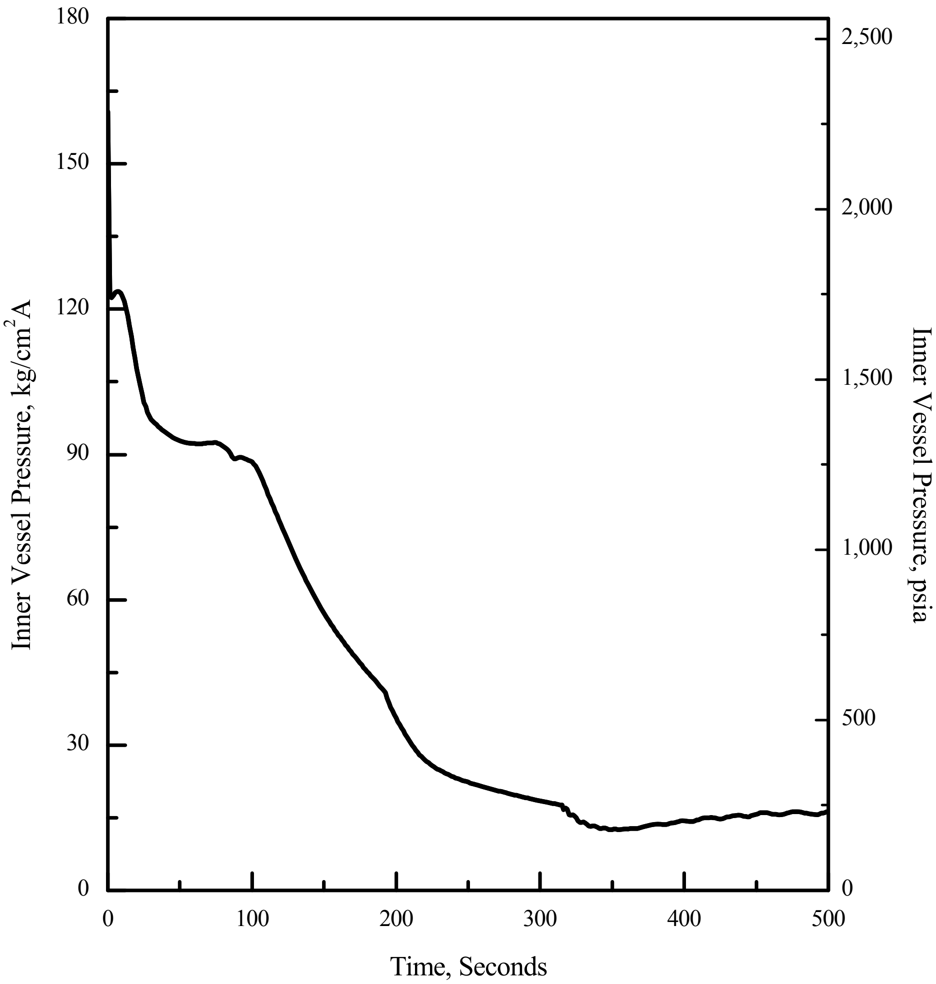

Figure 15.6.5-28B 372 cm^2 (0.4 ft^2) Break in DVI Line ; Inner Vessel Pressure

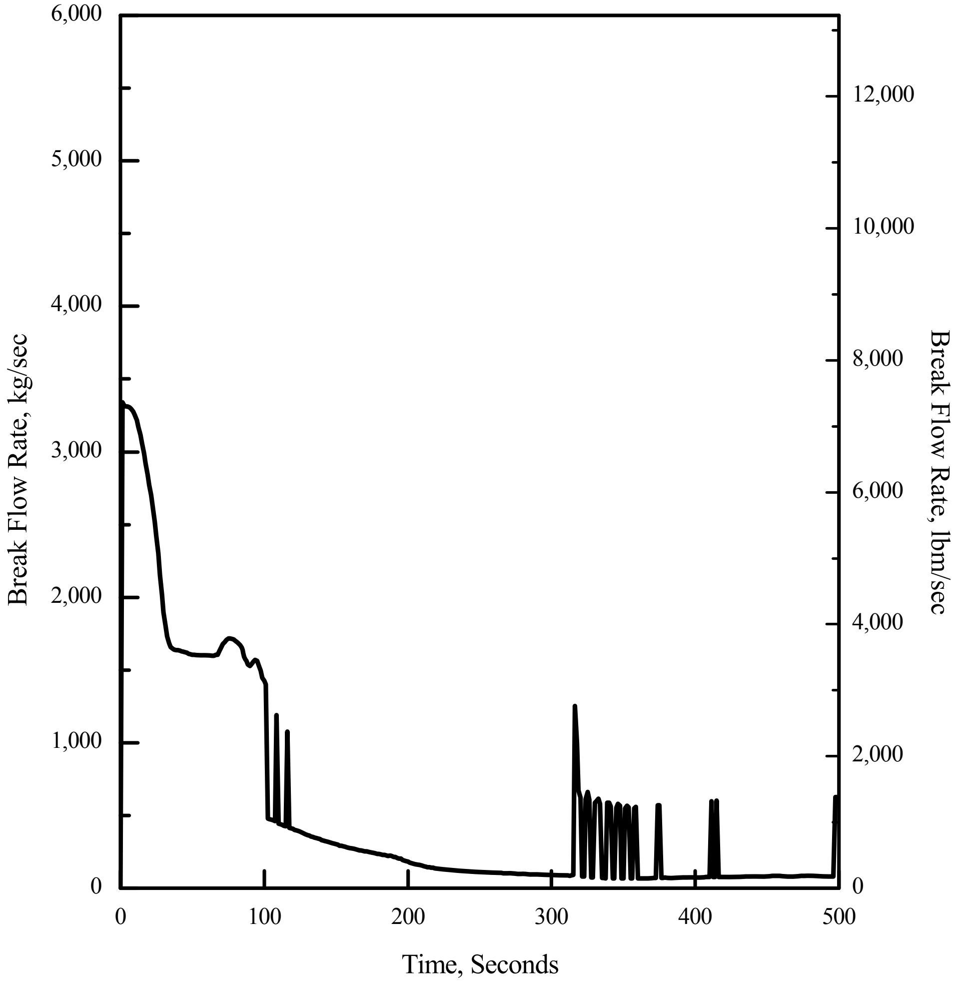

Figure 15.6.5-28C 372 cm^2 (0.4 ft^2) Break in DVI Line ; Break Flow Rate

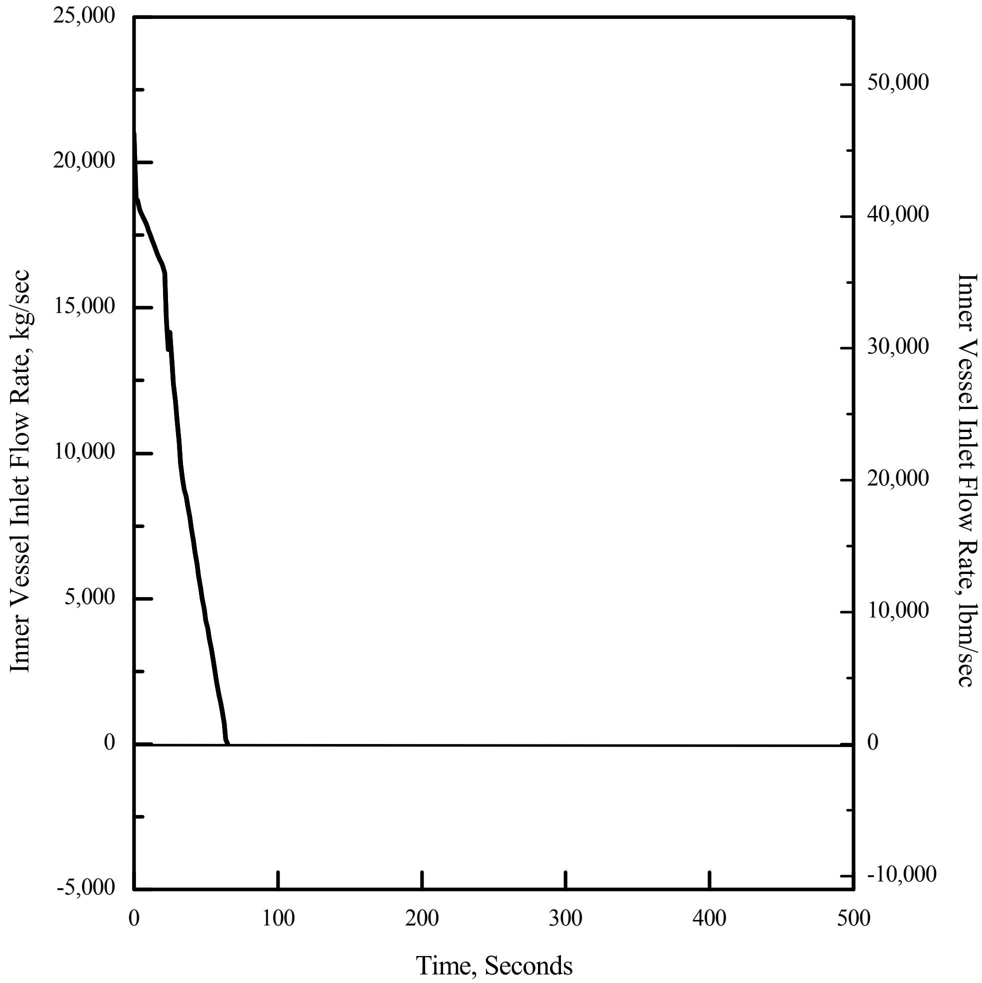

Figure 15.6.5-28D 372 cm^2 (0.4 ft^2) Break in DVI Line ; Inner Vessel Inlet Flow Rate

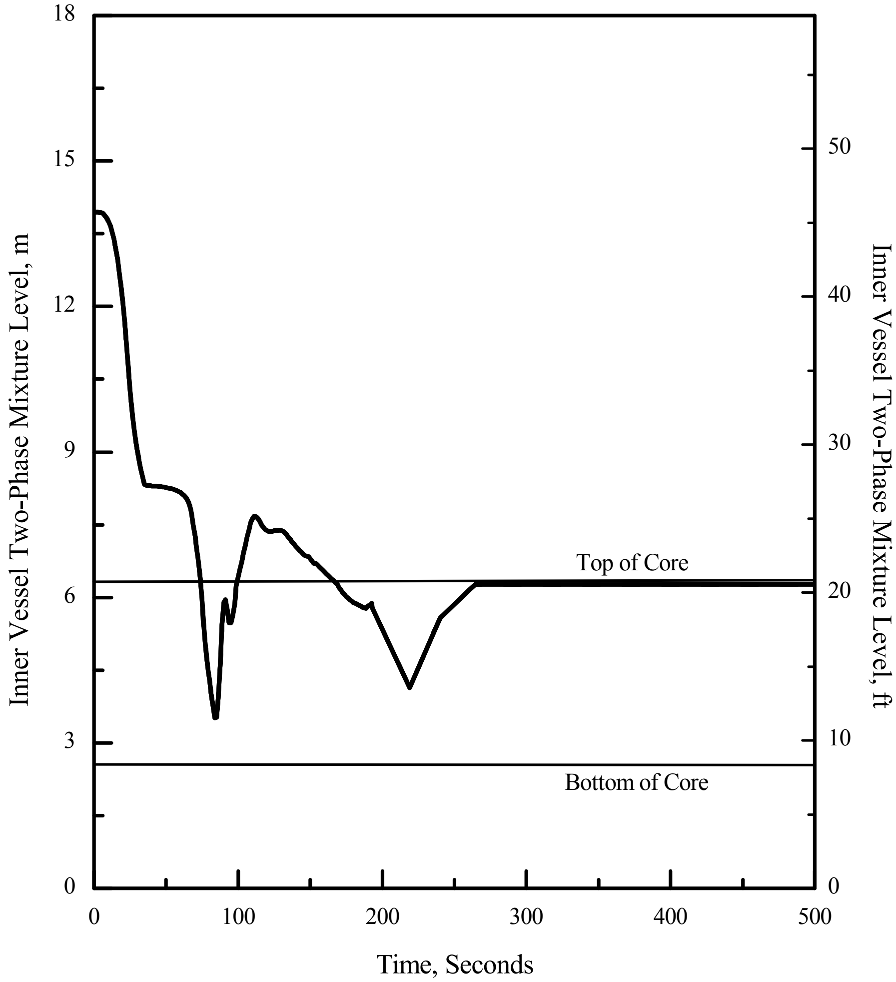

Figure 15.6.5-28E 372 cm^2 (0.4 ft^2) Break in DVI Line ; Inner Vessel Two-Phase Mixture Level

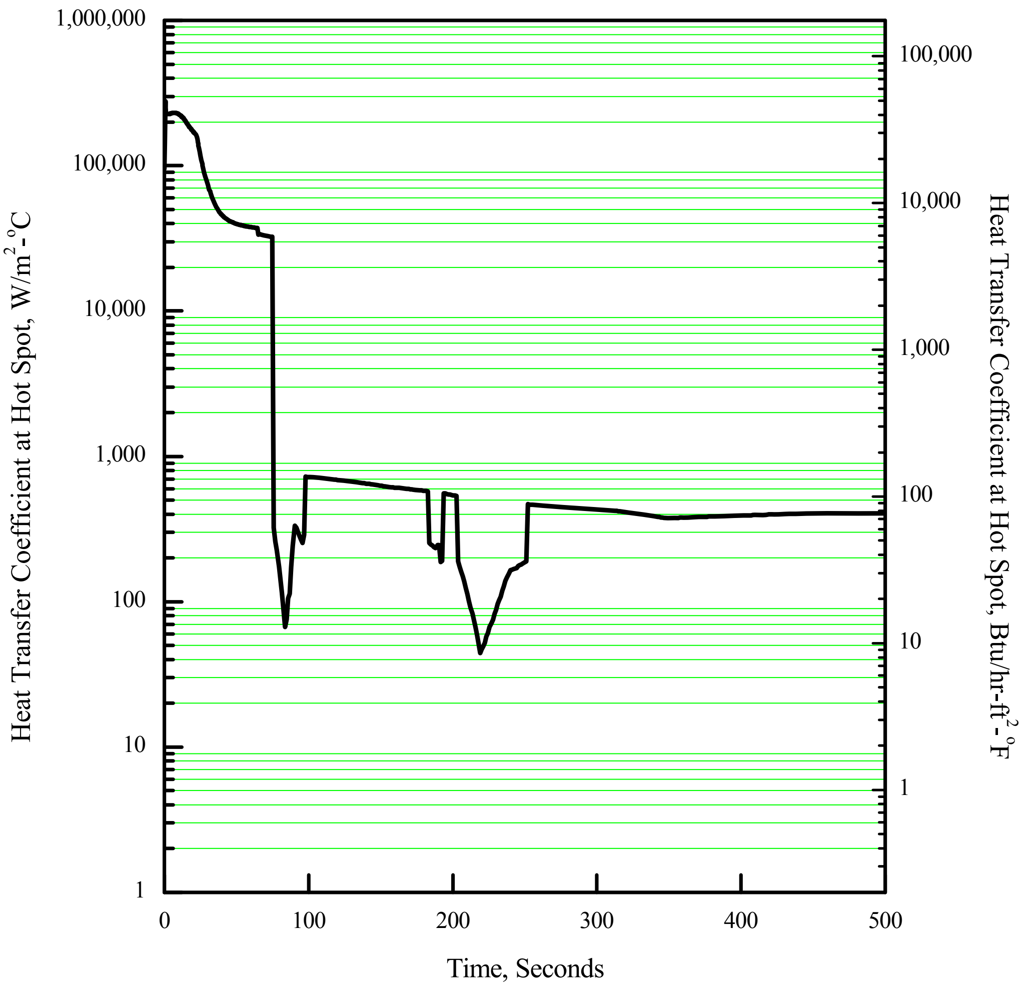

Figure 15.6.5-28F 372 cm^2 (0.4 ft^2) Break in DVI Line ; Heat Transfer Coefficient at Hot Spot

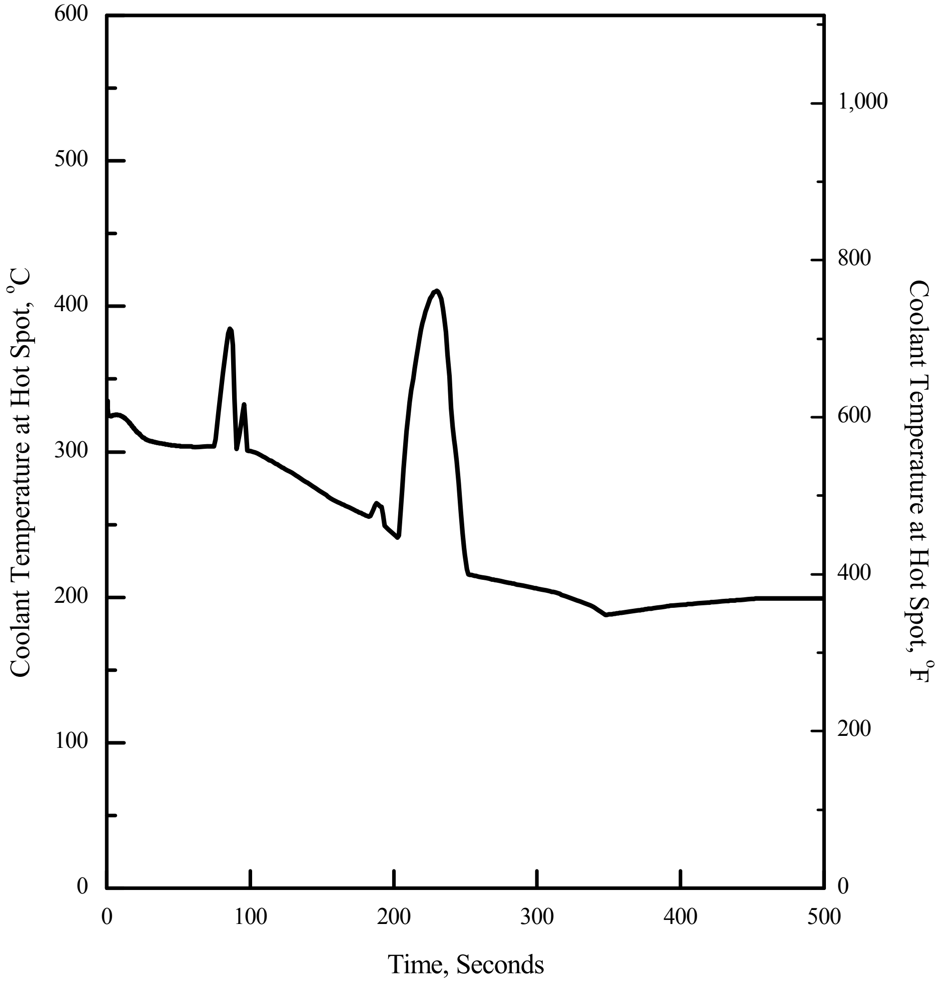

Figure 15.6.5-28G 372 cm^2 (0.4 ft^2) Break in DVI Line ; Coolant Temperature at Hot Spot

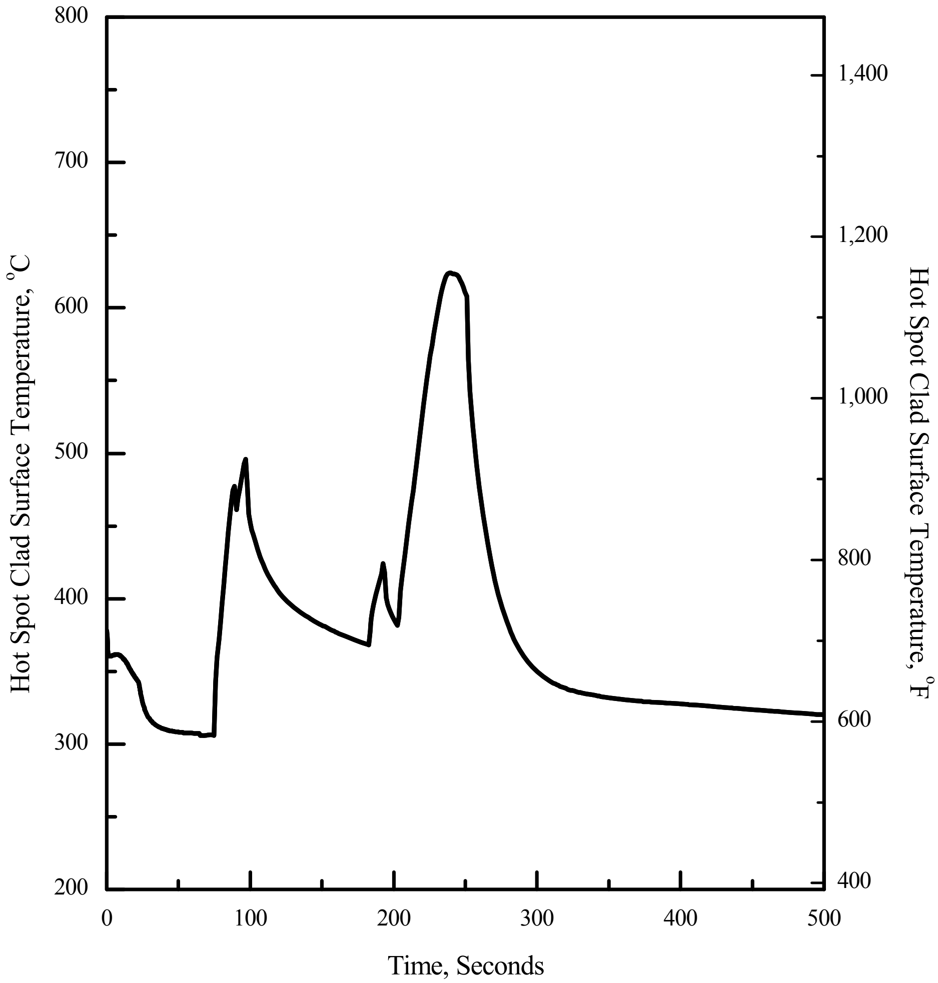

Figure 15.6.5-28H 372 cm^2 (0.4 ft^2) Break in DVI Line ; Hot Spot Clad Surface Temperature

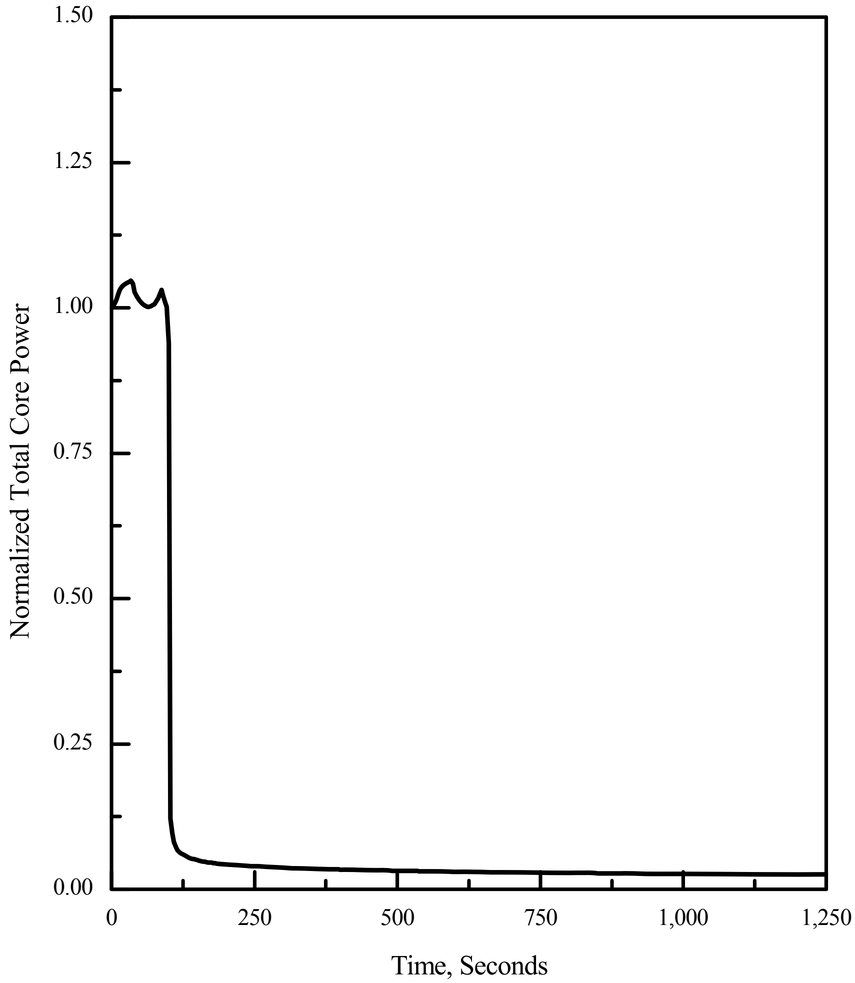

Figure 15.6.5-29A 93 cm^2 (0.1 ft^2) Break in DVI Line ; Normalized Total Core Power

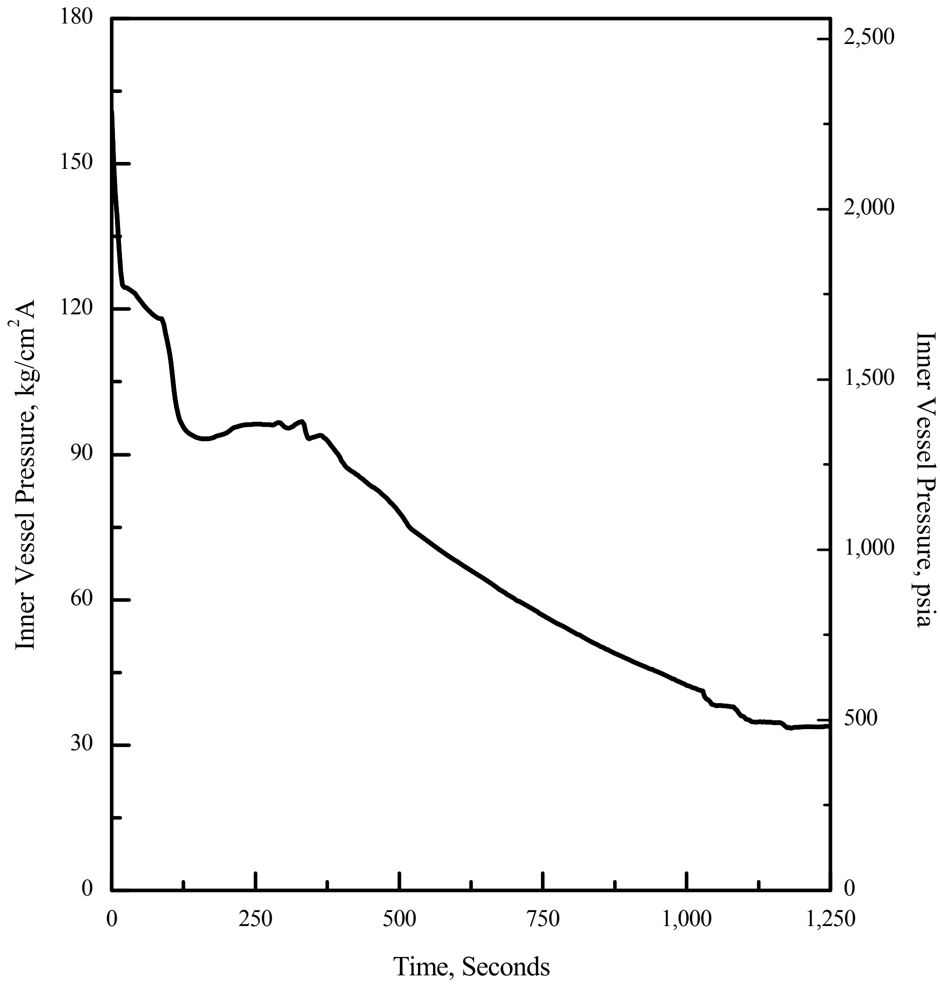

Figure 15.6.5-29B 93 cm^2 (0.1 ft^2) Break in DVI Line ; Inner Vessel Pressure

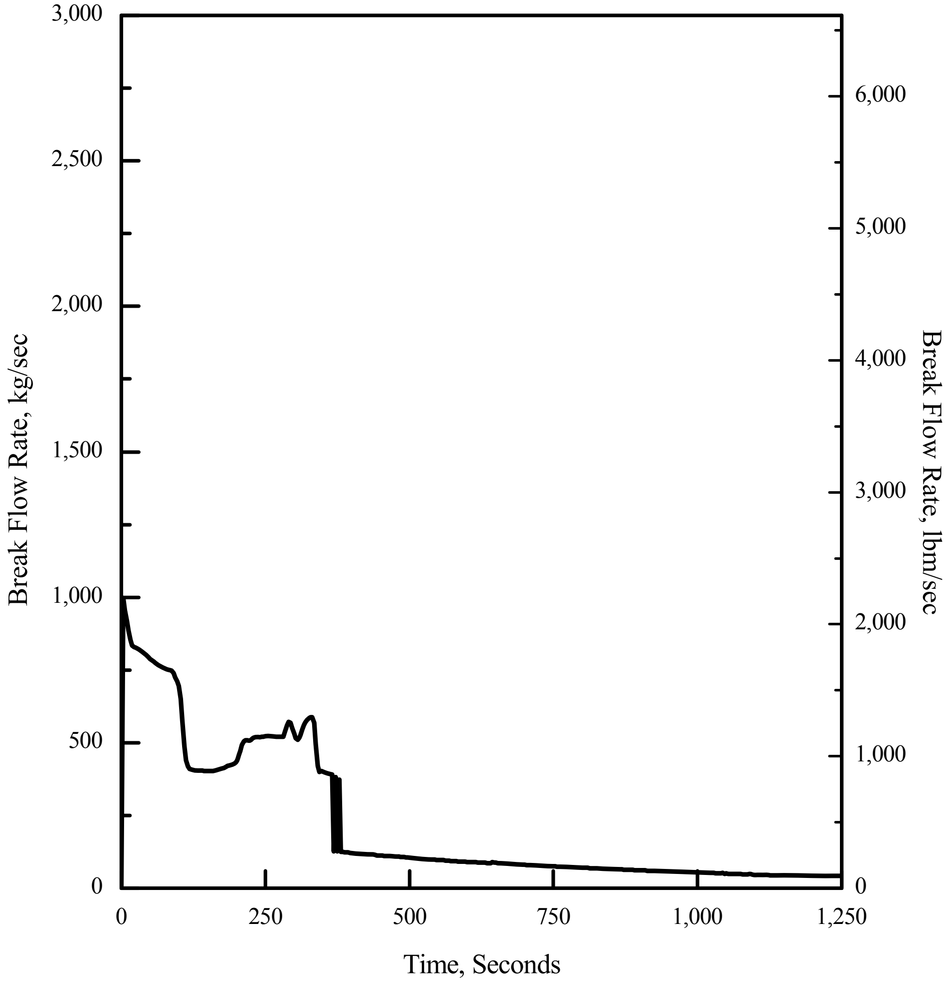

Figure 15.6.5-29C 93 cm^2 (0.1 ft^2) Break in DVI Line ; Break Flow Rate

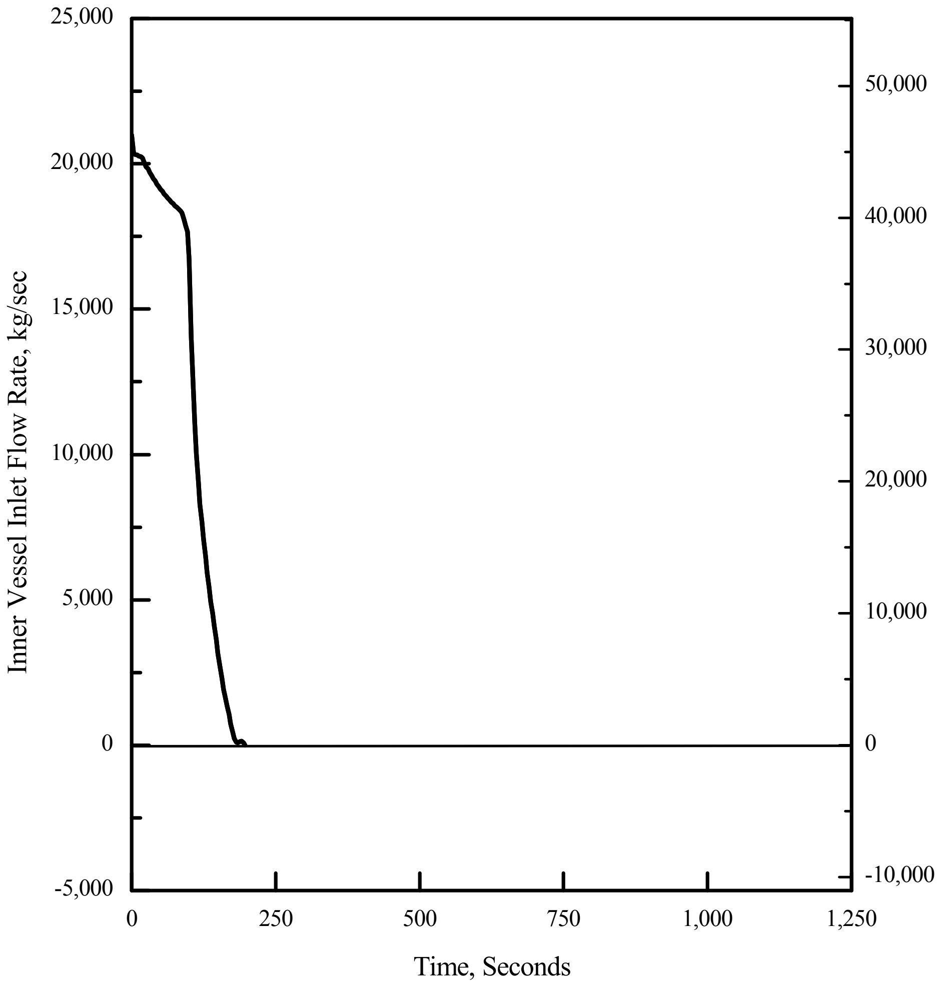

Figure 15.6.5-29D 93 cm^2 (0.1 ft^2) Break in DVI Line ; Inner Vessel Inlet Flow Rate

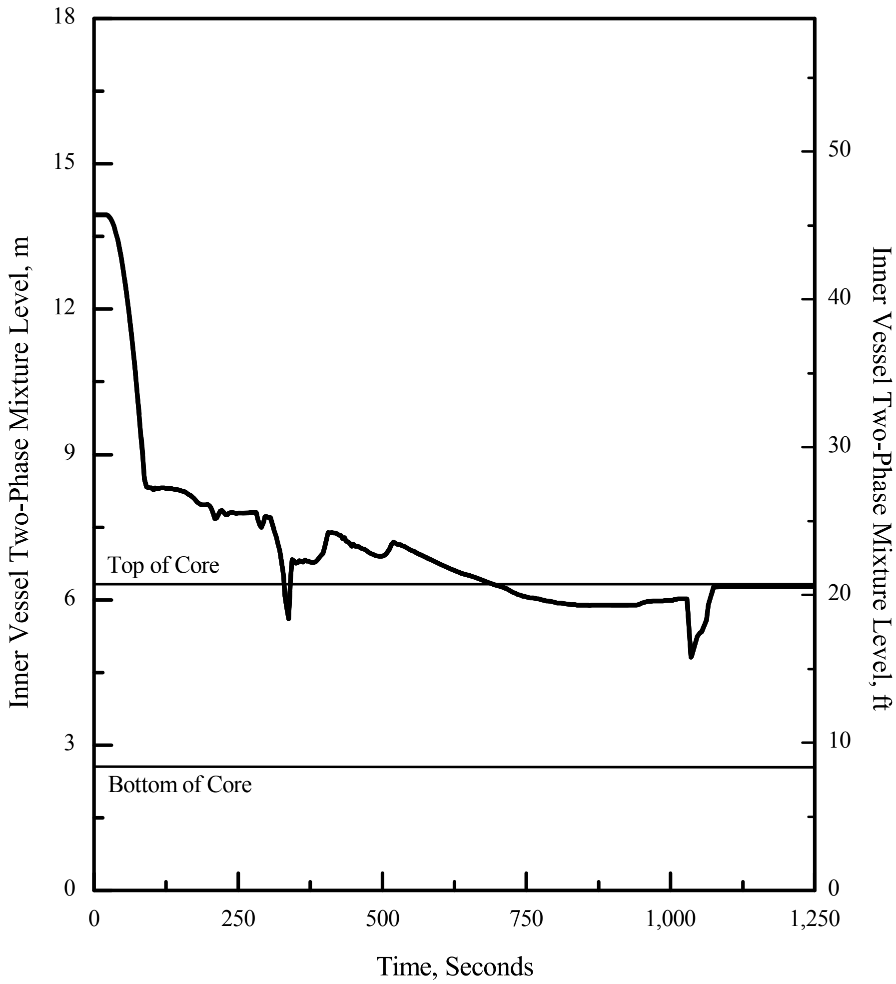

Figure 15.6.5-29E 93 cm^2 (0.1 ft^2) Break in DVI Line ; Inner Vessel Two-Phase Mixture Level

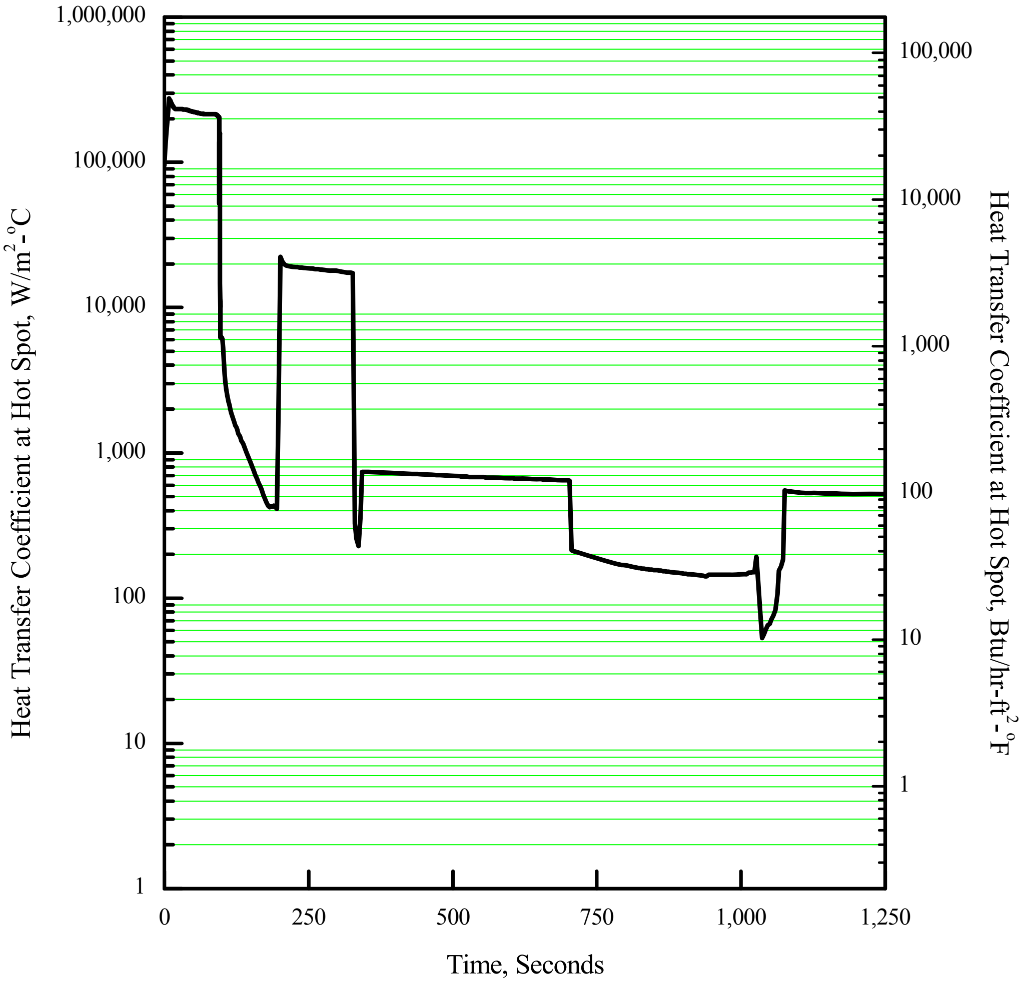

Figure 15.6.5-29F 93 cm^2 (0.1 ft^2) Break in DVI Line ; Heat Transfer Coefficient at Hot Spot

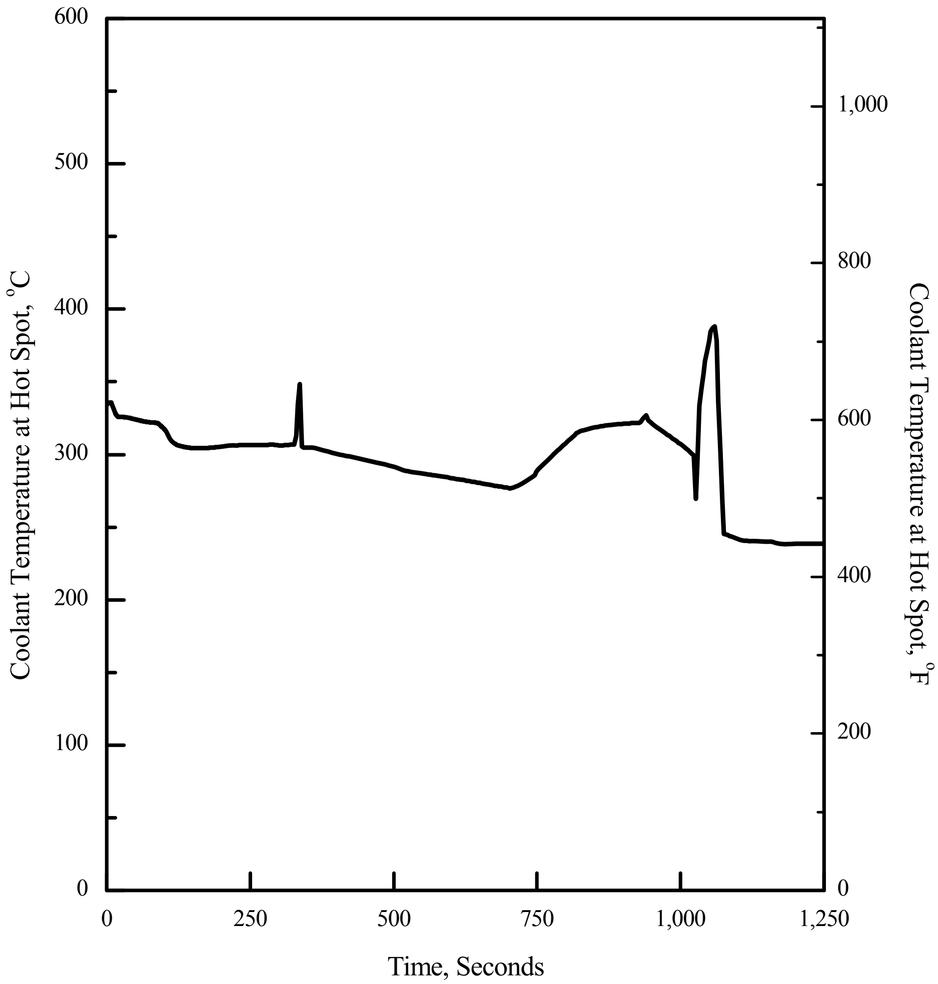

Figure 15.6.5-29G 93 cm^2 (0.1 ft^2) Break in DVI Line ; Coolant Temperature at Hot Spot

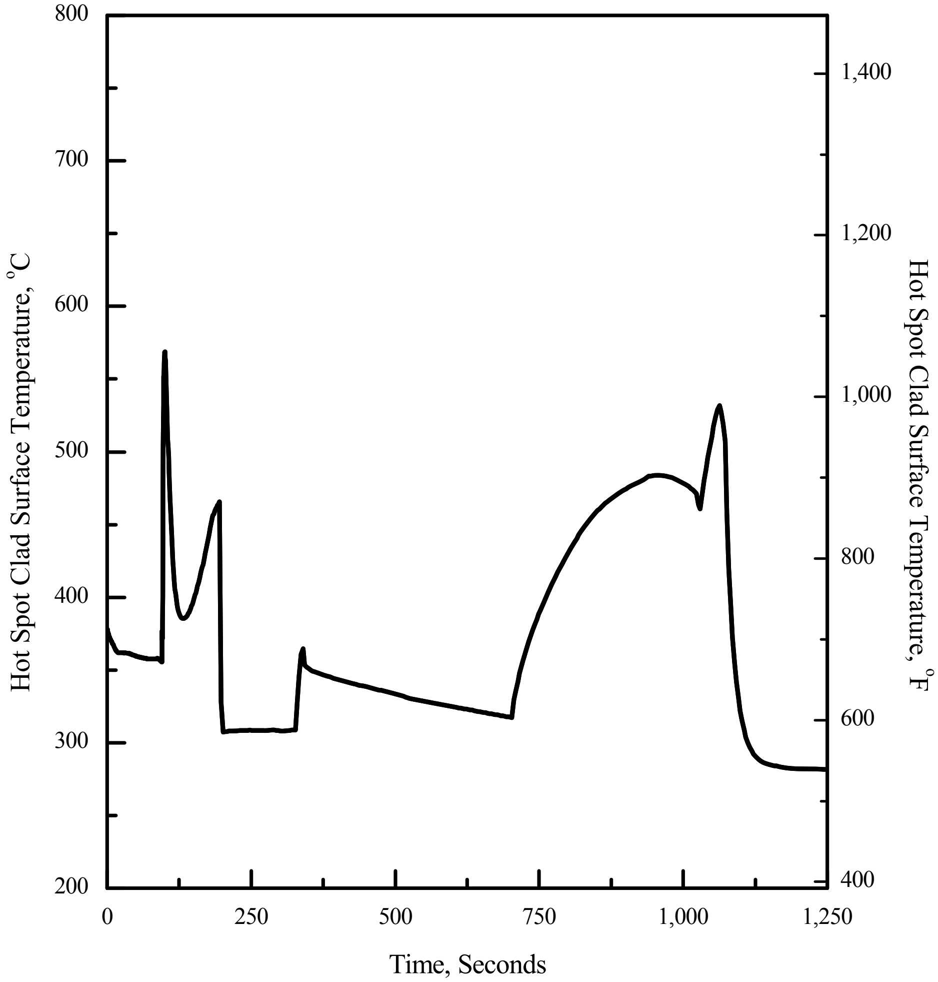

Figure 15.6.5-29H 93 cm² (0.1 ft²) Break in DVI Line ;
Hot Spot Clad Surface Temperature

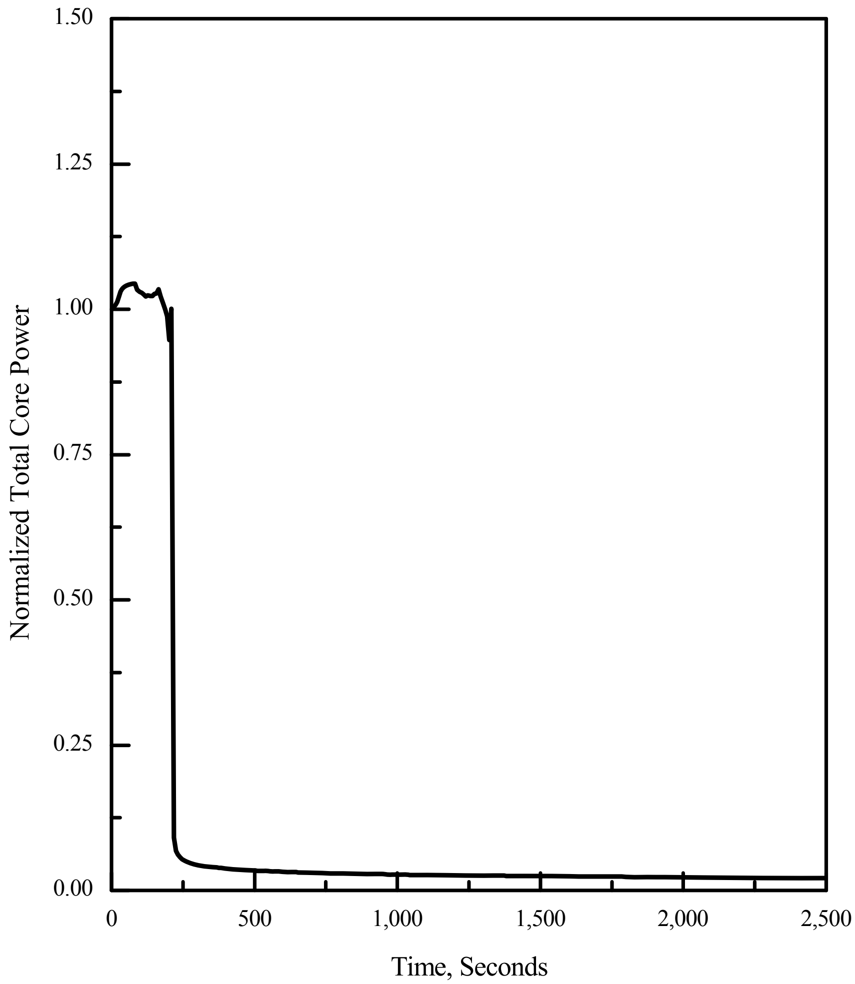

Figure 15.6.5-30A 46.5 cm^2 (0.05 ft^2) Break in DVI Line ; Normalized Total Core Power

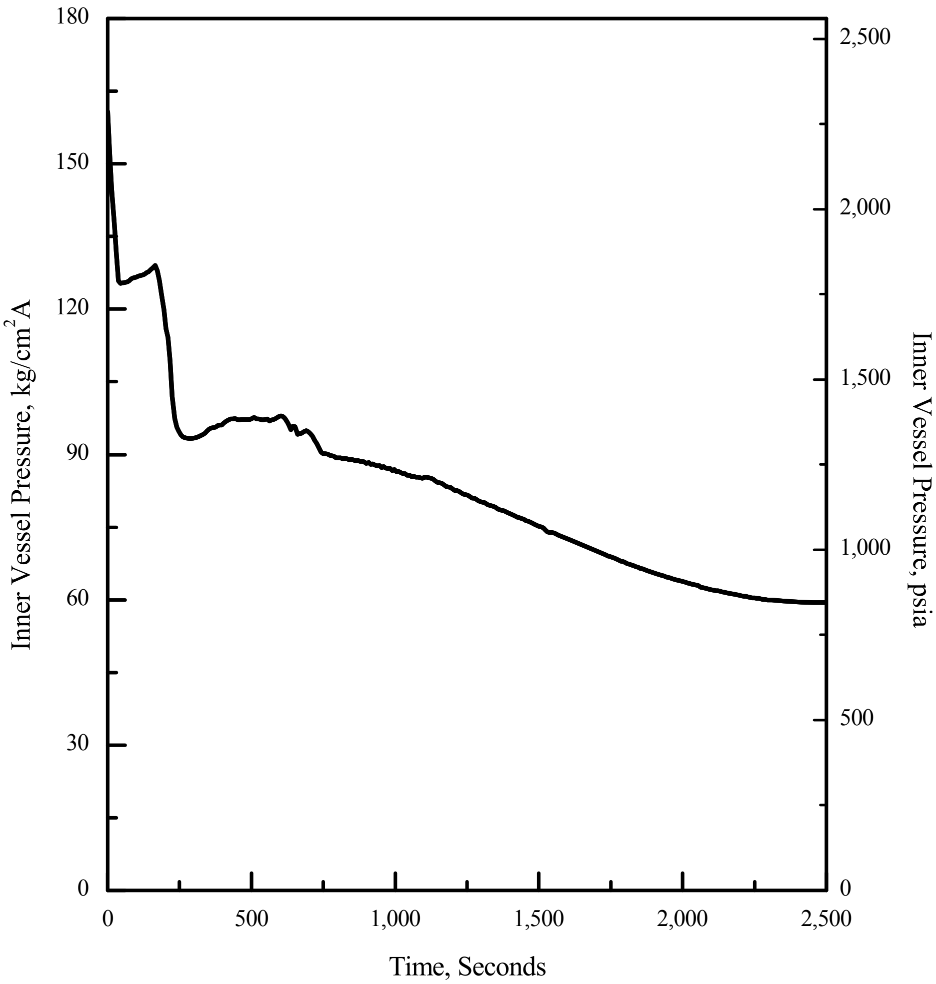

Figure 15.6.5-30B 46.5 cm^2 (0.05 ft^2) Break in DVI Line ; Inner Vessel Pressure

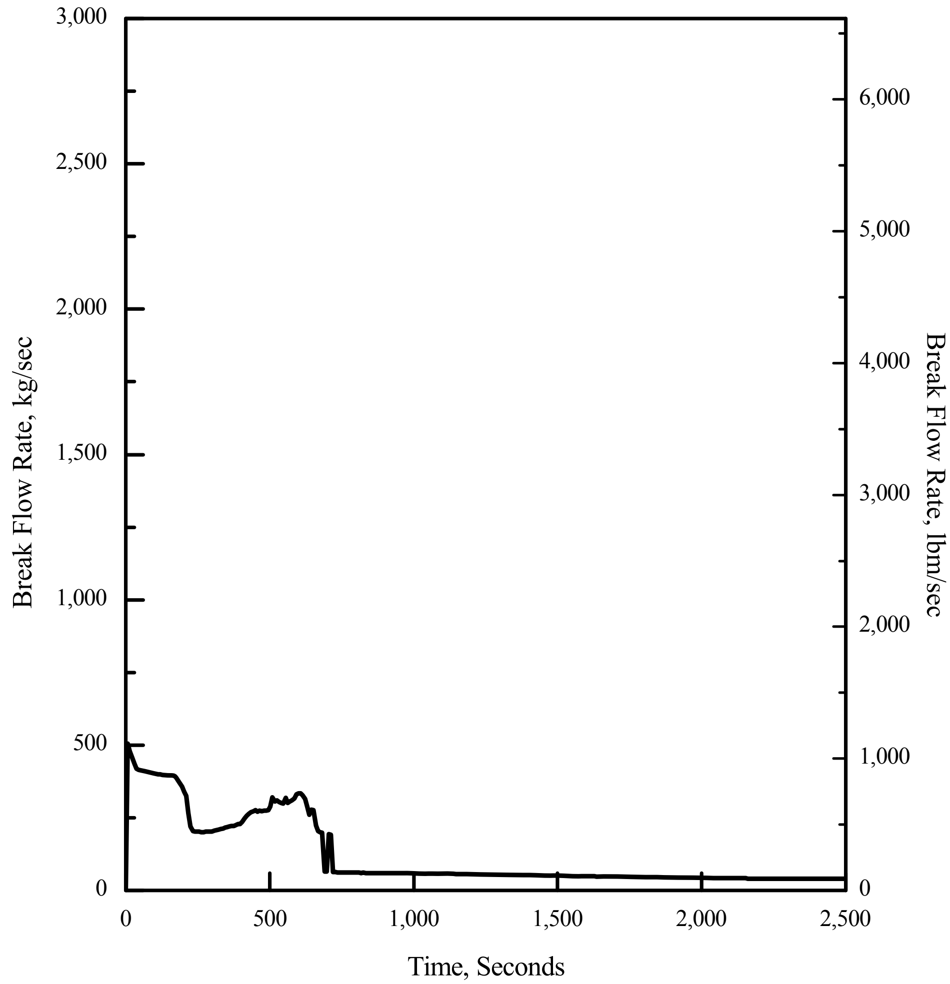

Figure 15.6.5-30C 46.5 cm^2 (0.05 ft^2) Break in DVI Line ; Break Flow Rate

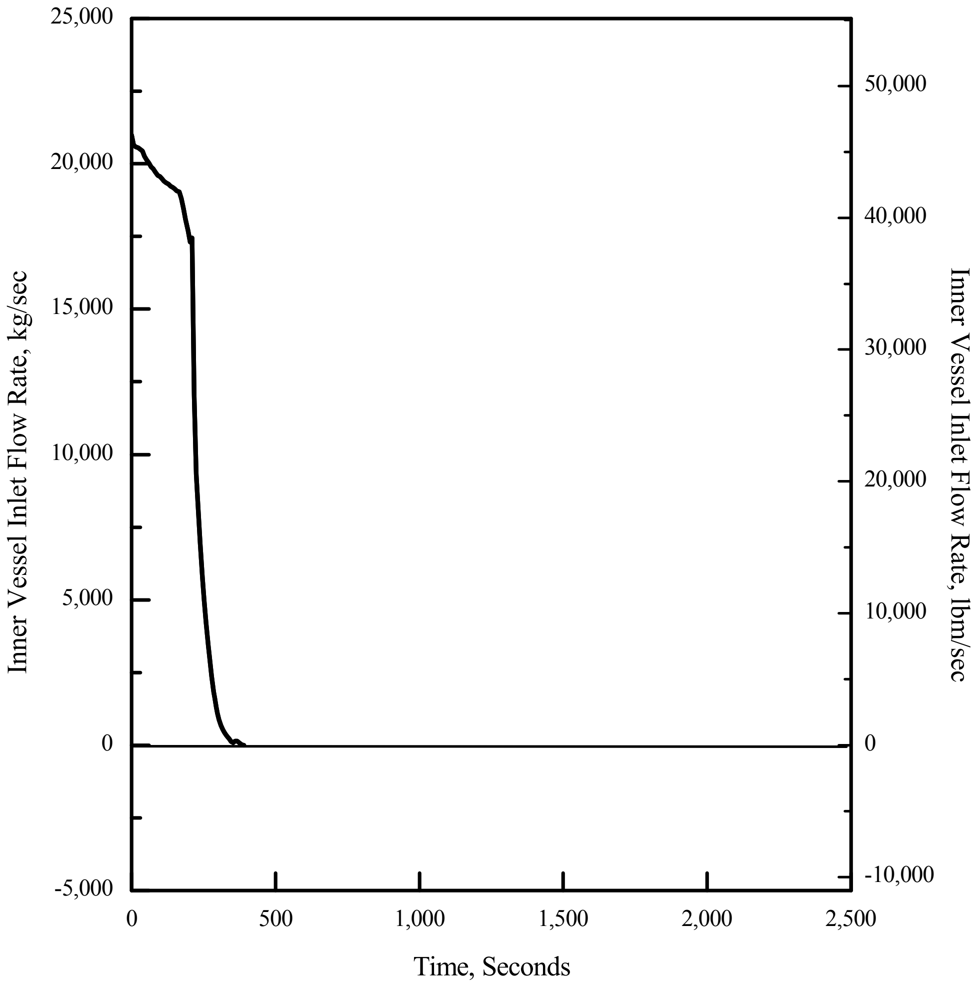

Figure 15.6.5-30D 46.5 cm^2 (0.05 ft^2) Break in DVI Line; Inner Vessel Inlet Flow Rate

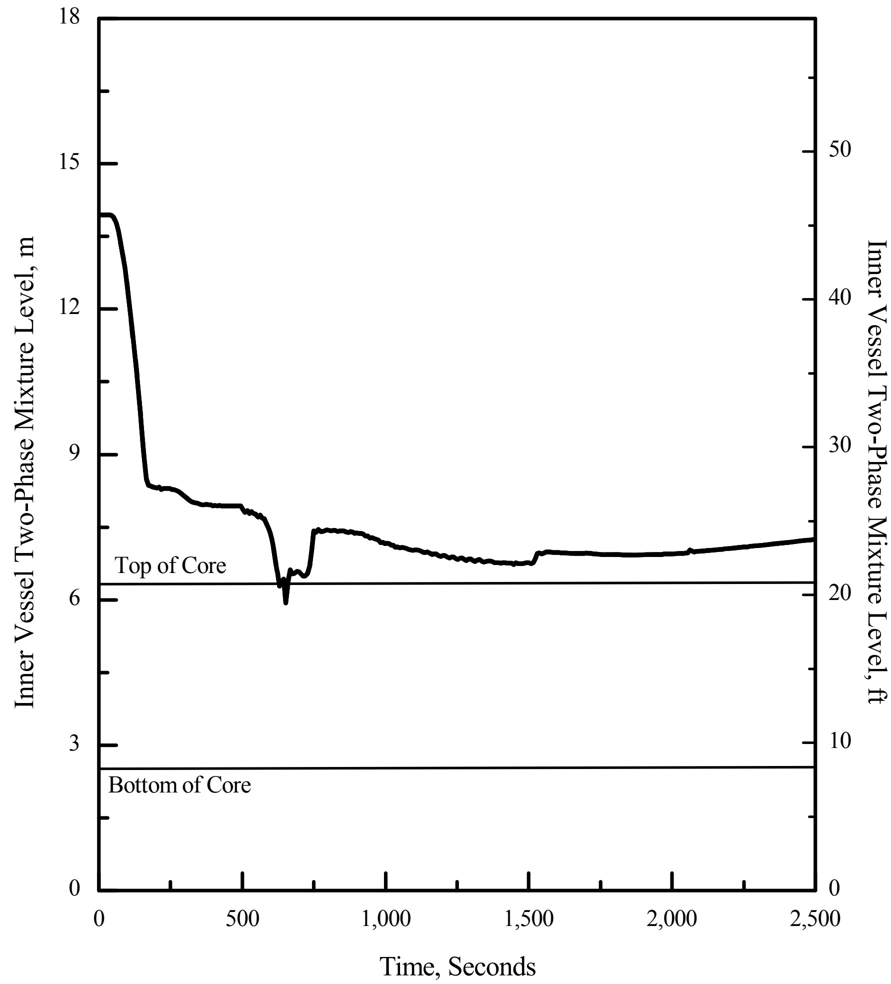

Figure 15.6.5-30E 46.5 cm^2 (0.05 ft^2) Break in DVI Line ; Inner Vessel Two-Phase Mixture Level

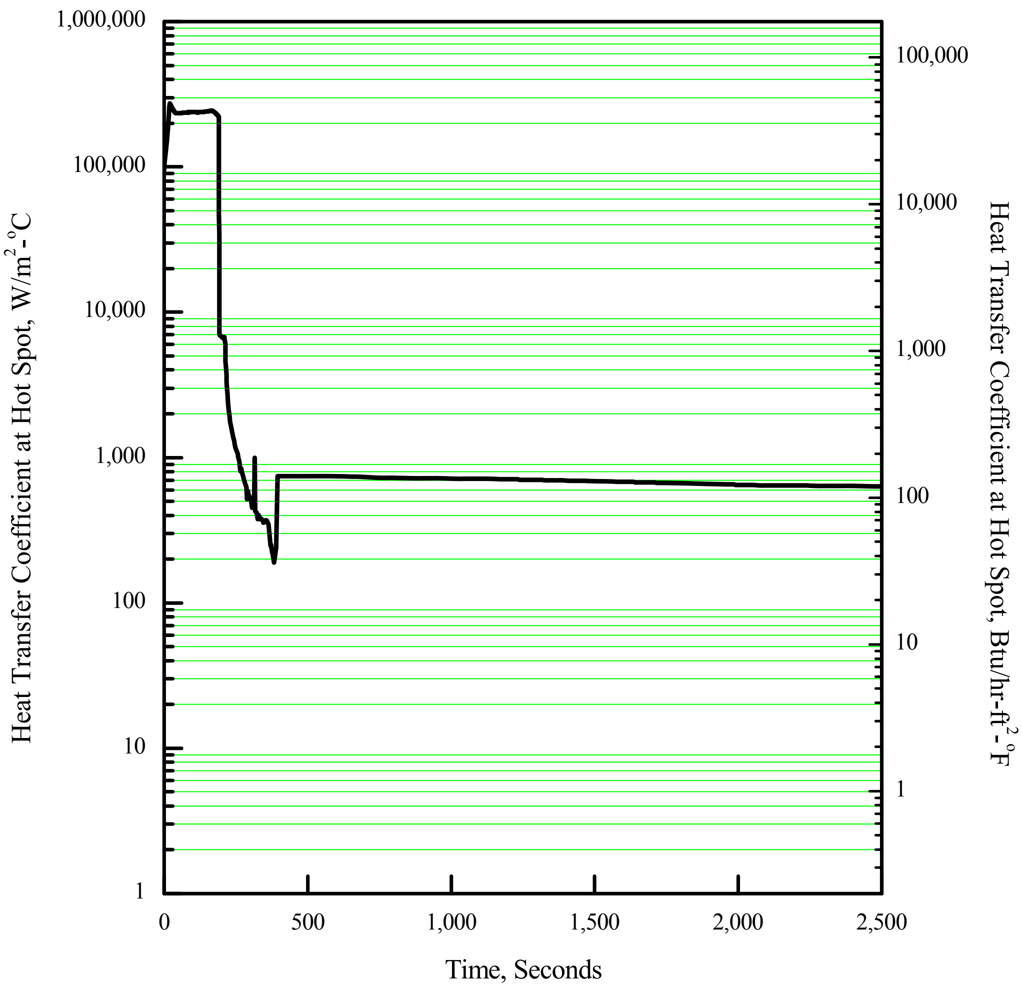

Figure 15.6.5-30F 46.5 cm^2 (0.05 ft^2) Break in DVI Line ; Heat Transfer Coefficient at Hot Spot

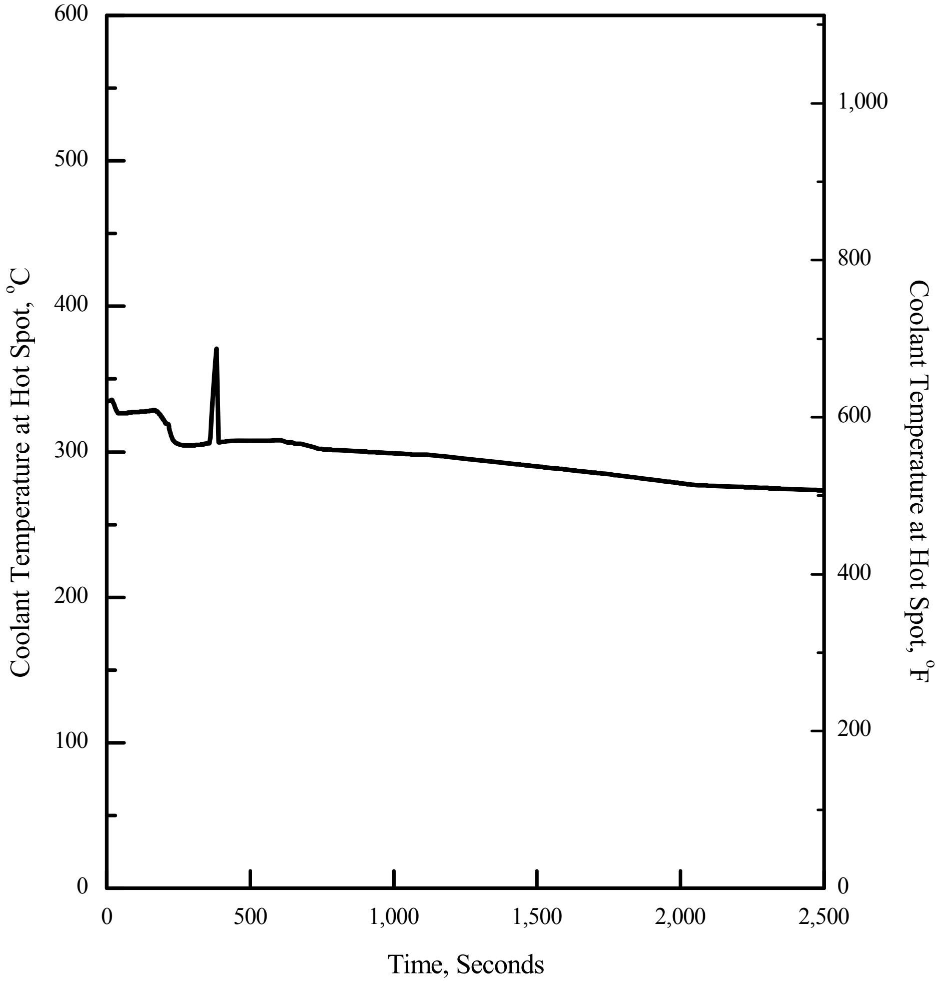

Figure 15.6.5-30G 46.5 cm² (0.05 ft²) Break in DVI Line ; Coolant Temperature at Hot Spot

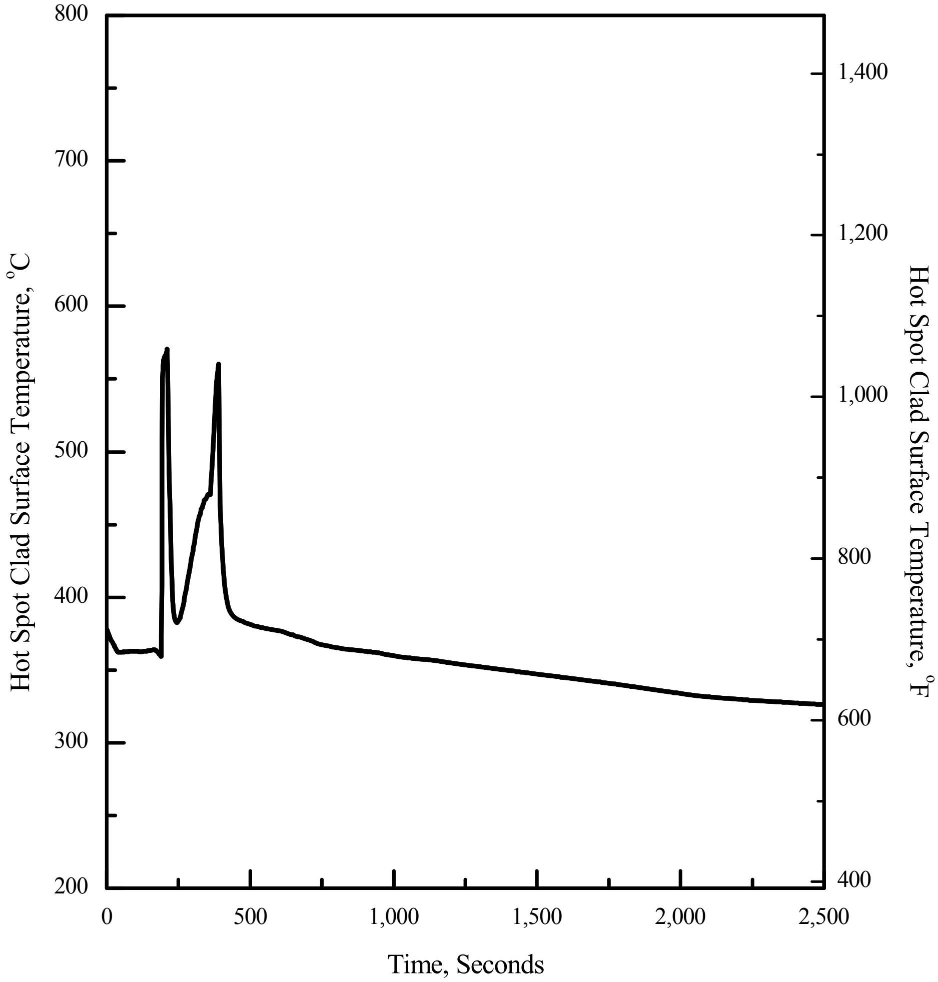

Figure 15.6.5-30H 46.5 cm^2 (0.05 ft^2) Break in DVI Line ; Hot Spot Clad Surface Temperature

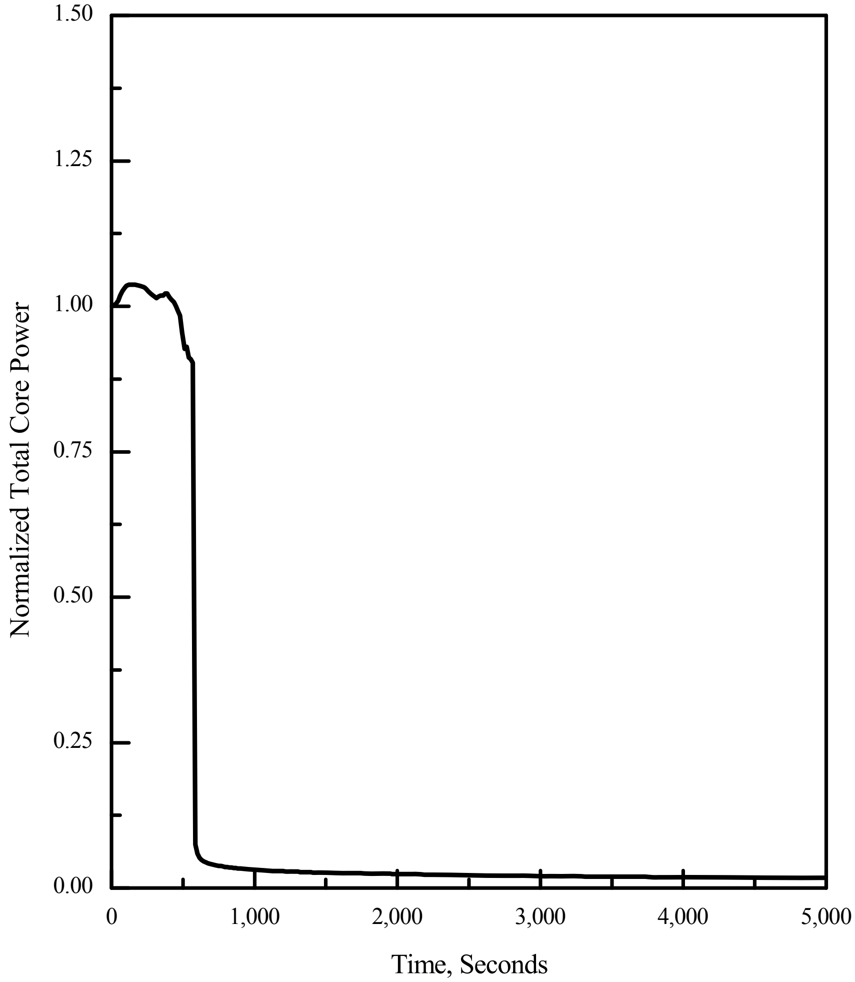

Figure 15.6.5-31A 18.6 cm^2 (0.02 ft^2) Break in DVI Line ; Normalized Total Core Power

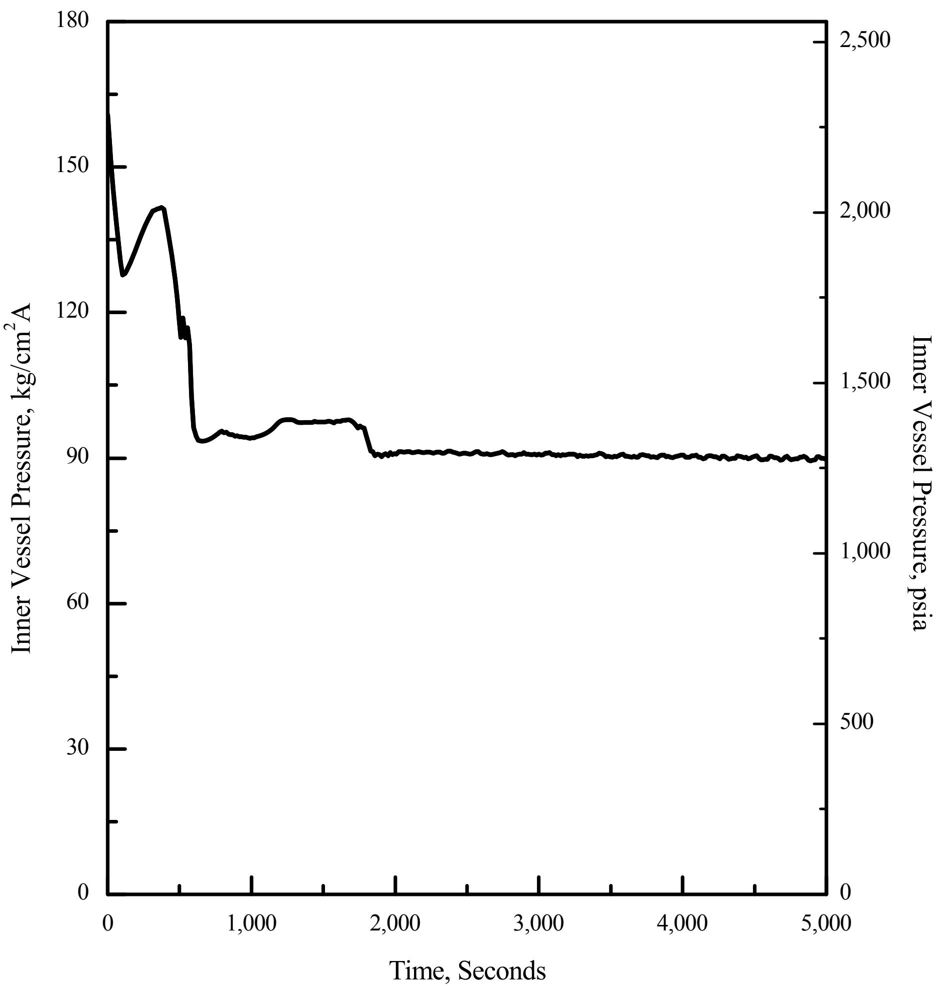

Figure 15.6.5-31B 18.6 cm^2 (0.02 ft^2) Break in DVI Line ; Inner Vessel Pressure

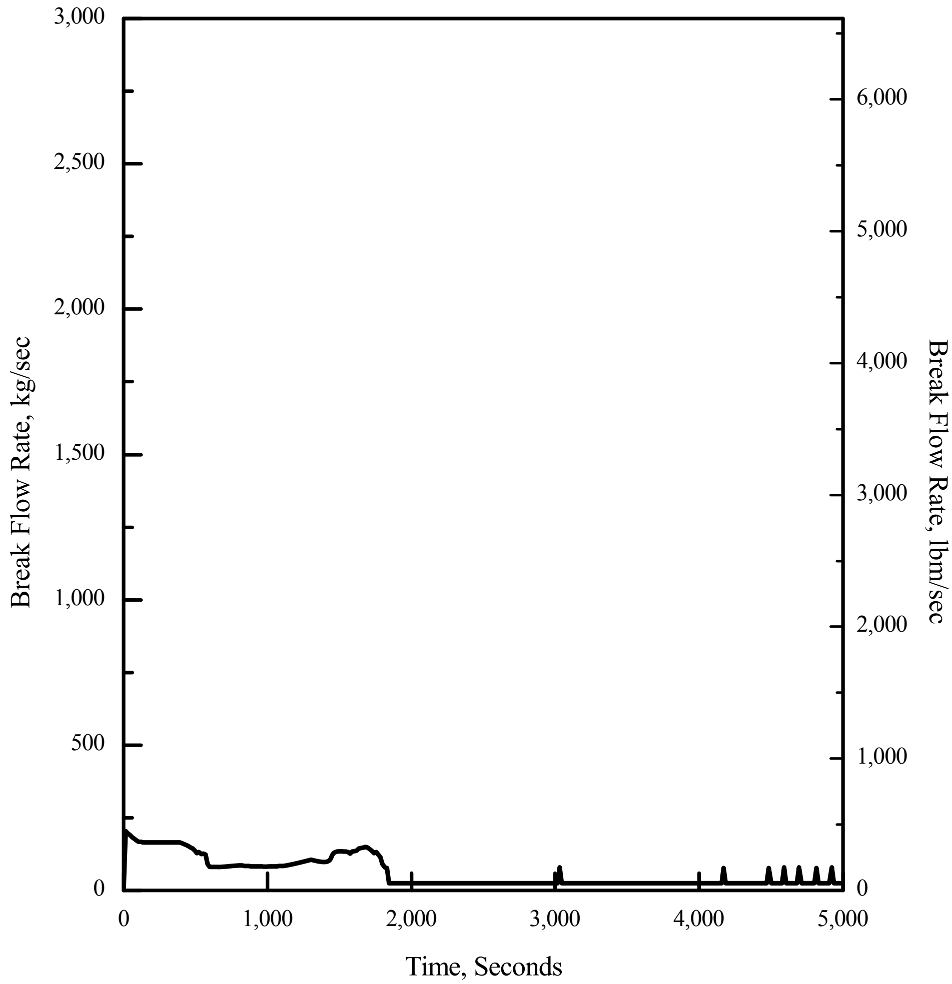

Figure 15.6.5-31C 18.6 cm^2 (0.02 ft^2) Break in DVI Line ; Break Flow Rate

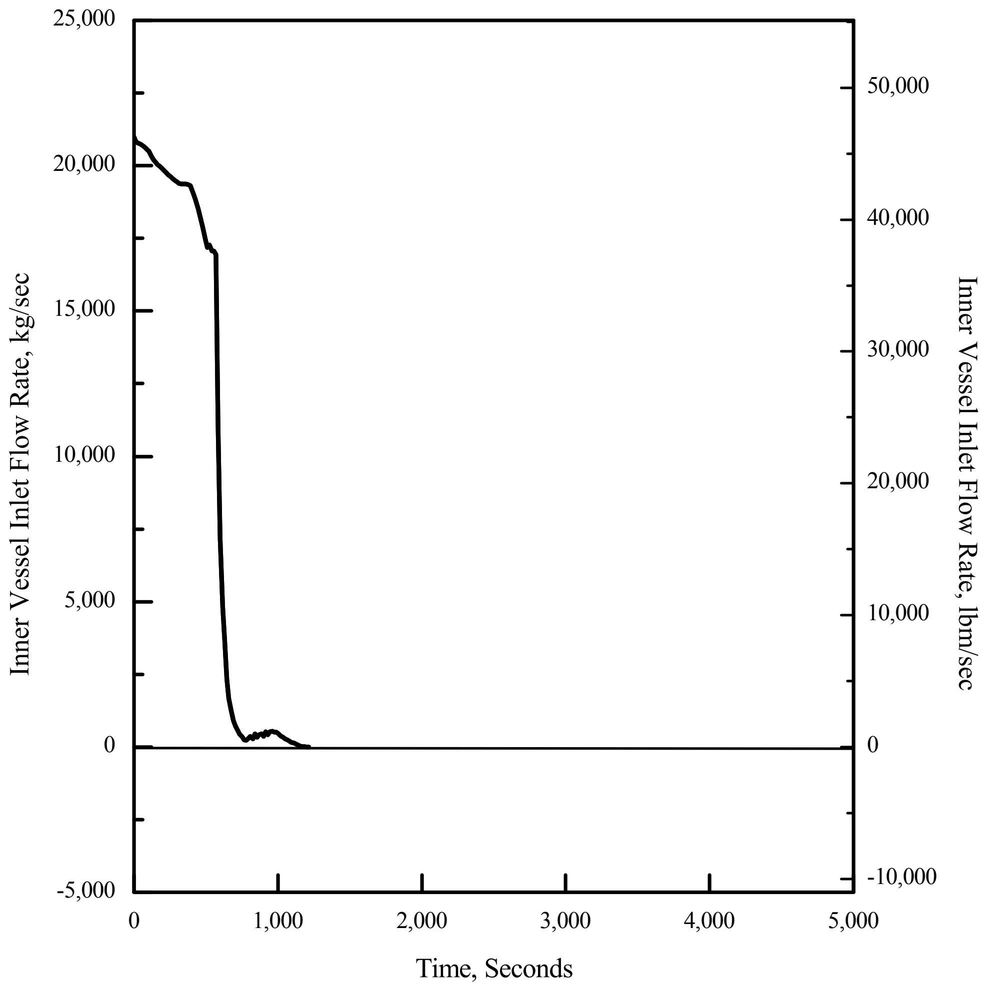

Figure 15.6.5-31D 18.6 cm^2 (0.02 ft^2) Break in DVI Line ; Inner Vessel Inlet Flow Rate

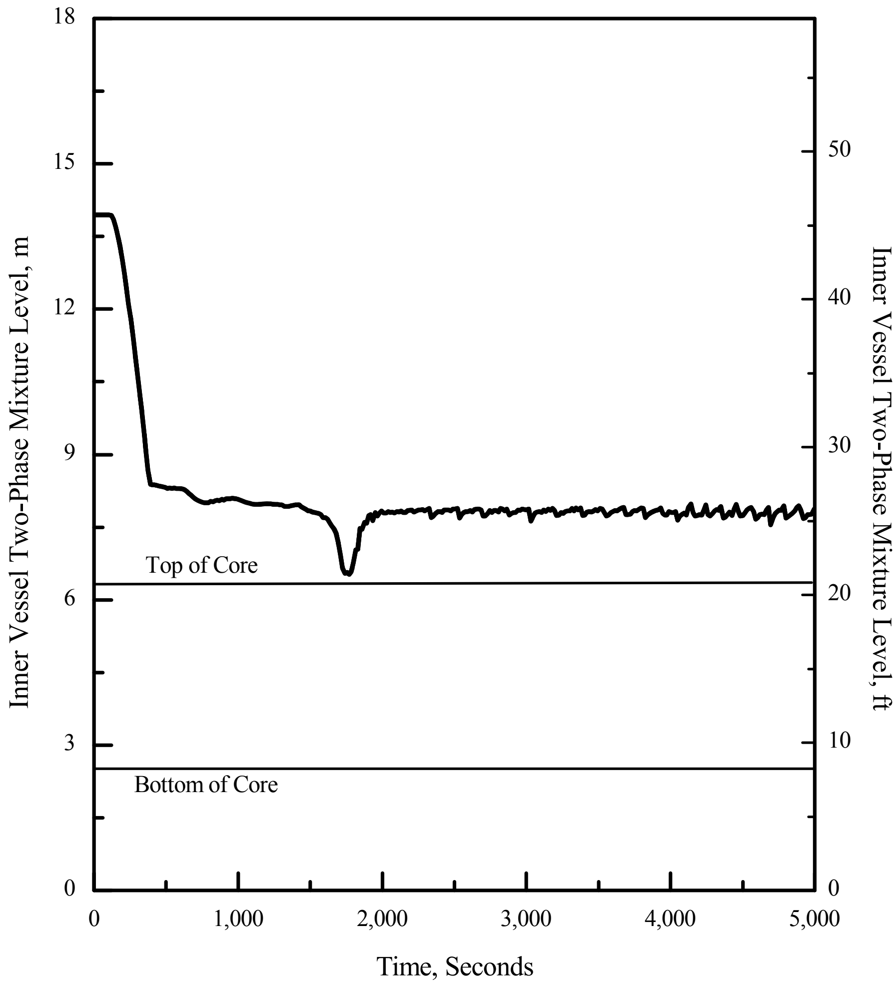

Figure 15.6.5-31E 18.6 cm^2 (0.02 ft^2) Break in DVI Line ; Inner Vessel Two-Phase Mixture Level

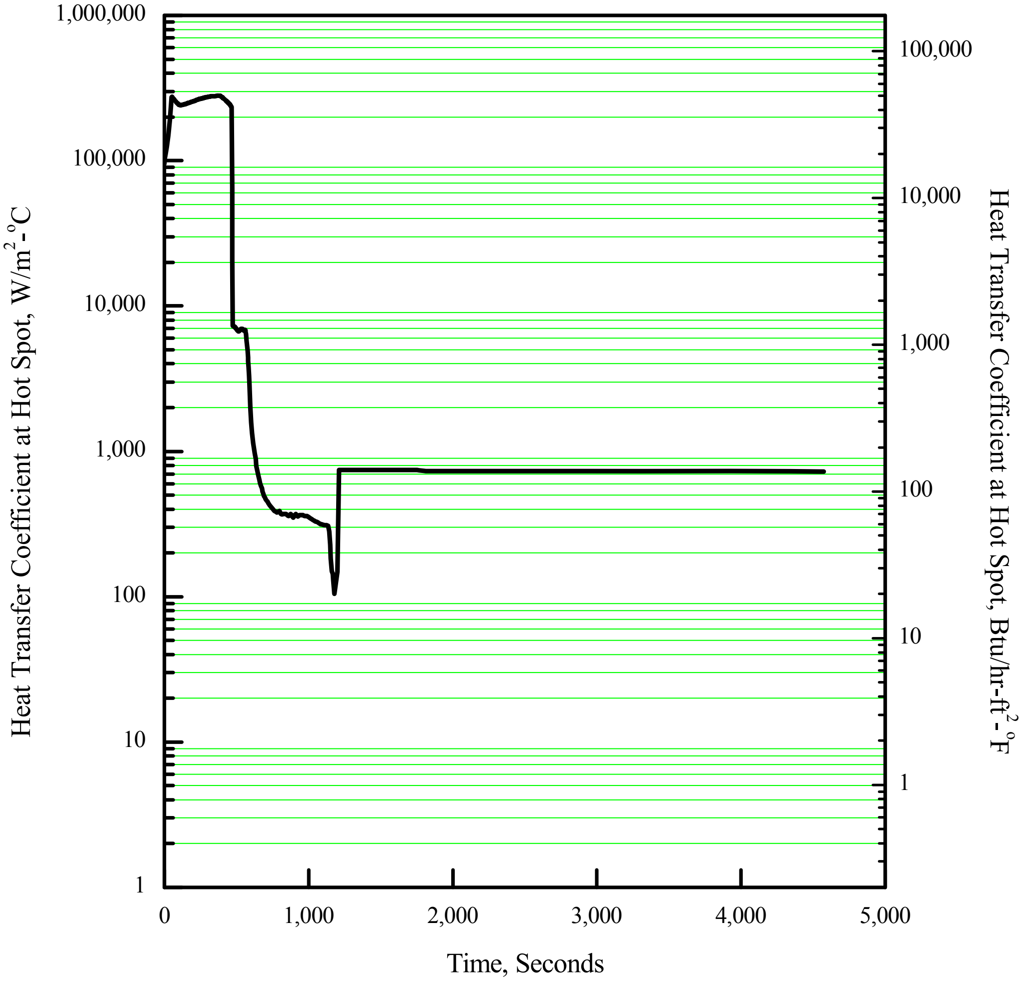

Figure 15.6.5-31F 18.6 cm^2 (0.02 ft^2) Break in DVI Line ; Heat Transfer Coefficient at Hot Spot

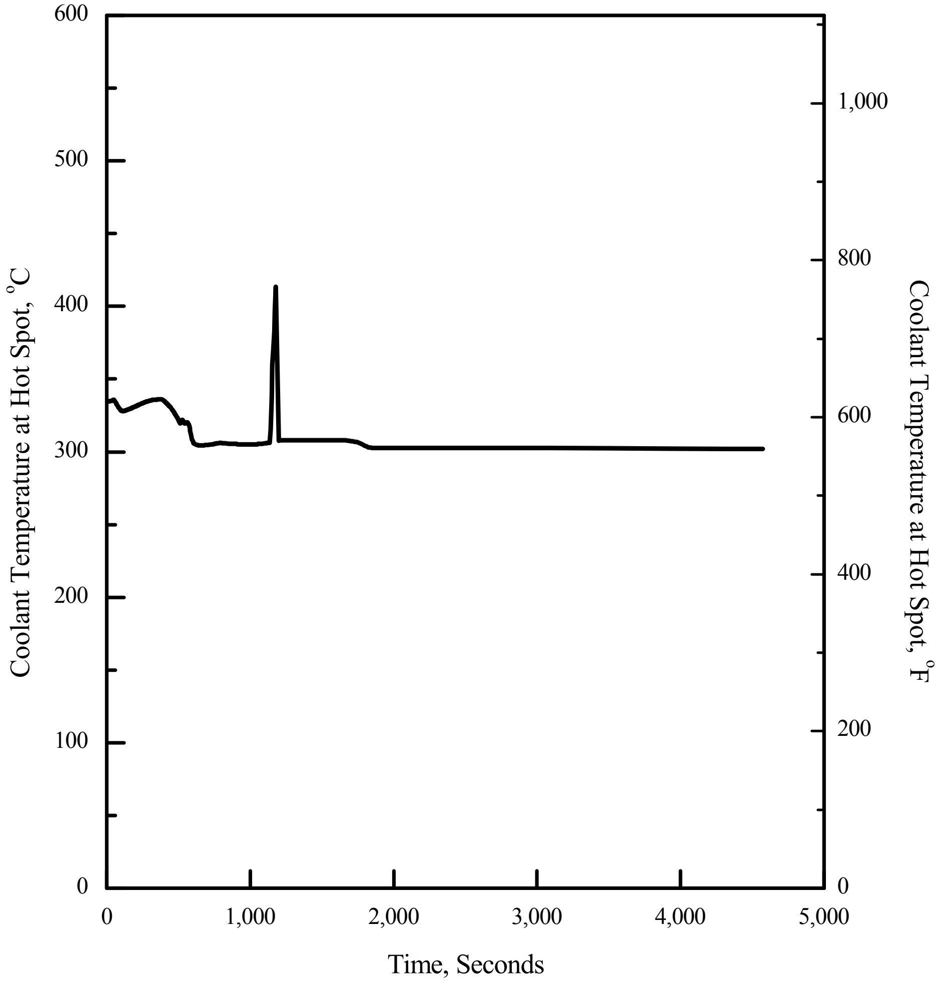

Figure 15.6.5-31G 18.6 cm^2 (0.02 ft^2) Break in DVI Line ; Coolant Temperature at Hot Spot

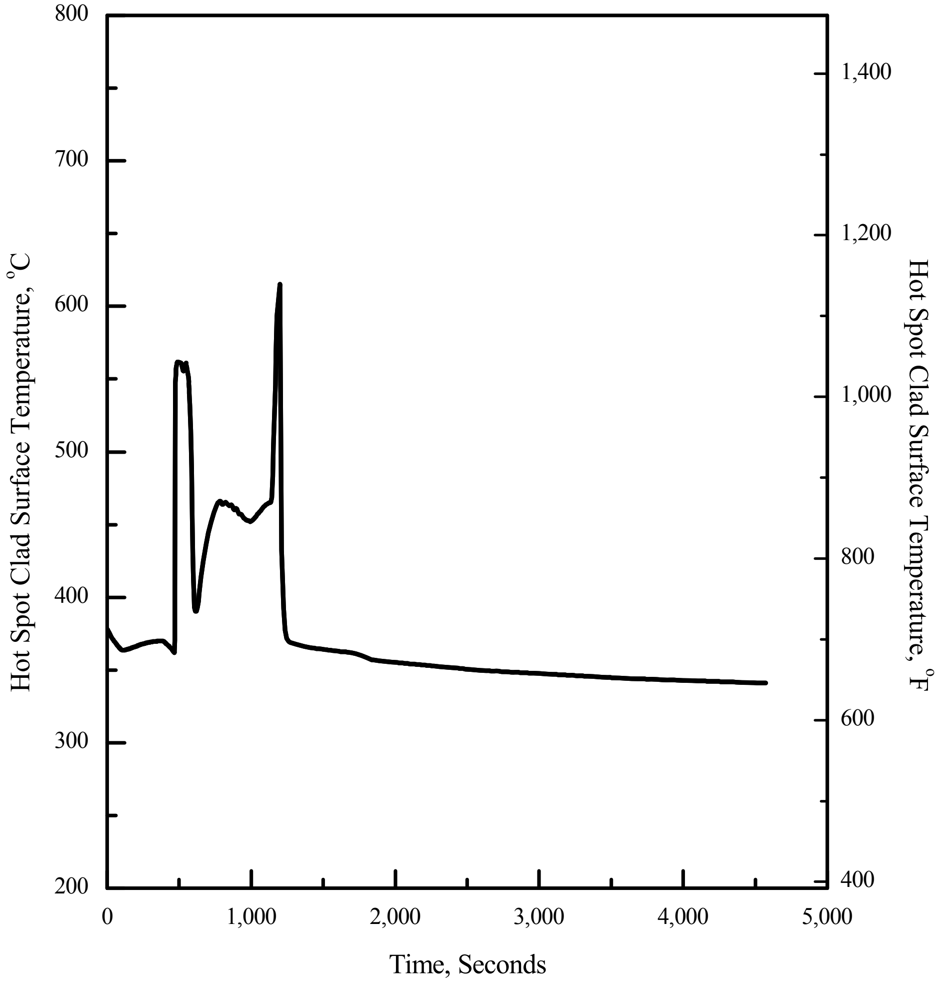

Figure 15.6.5-31H 18.6 cm^2 (0.02 ft^2) Break in DVI Line ; Hot Spot Clad Surface Temperature

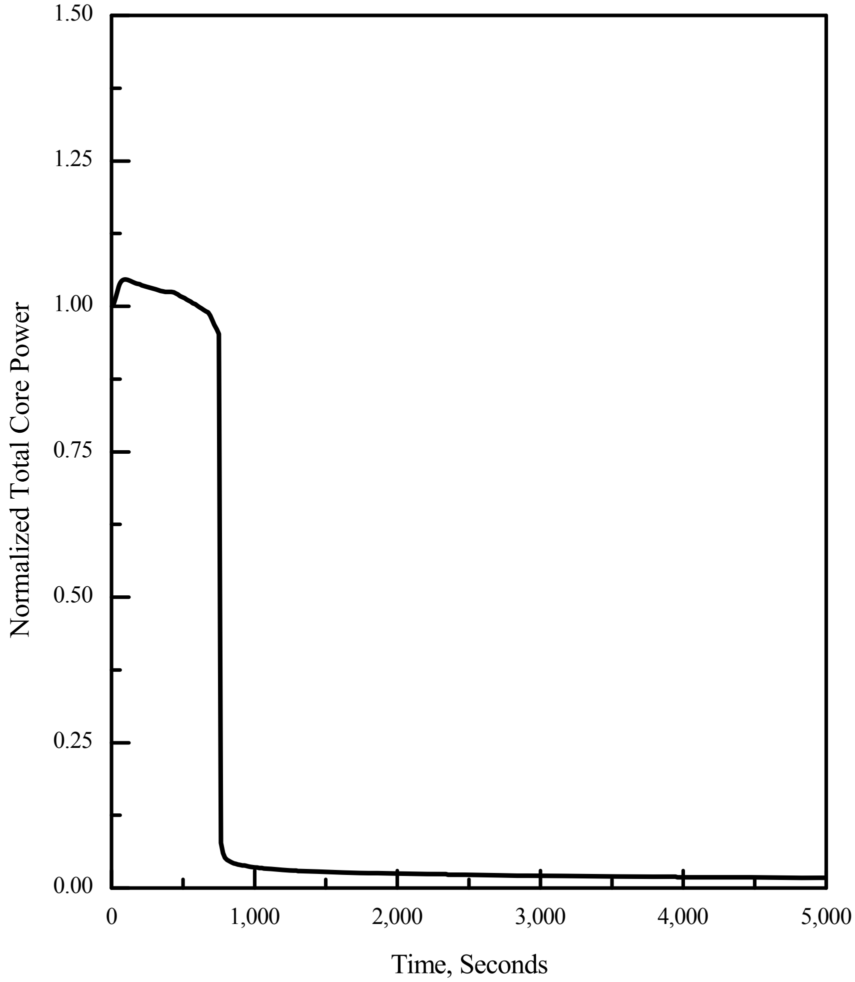

Figure 15.6.5-32A 27.9 cm^2 (0.03 ft^2) Break in Top of Pressurizer ; Normalized Total Core Power

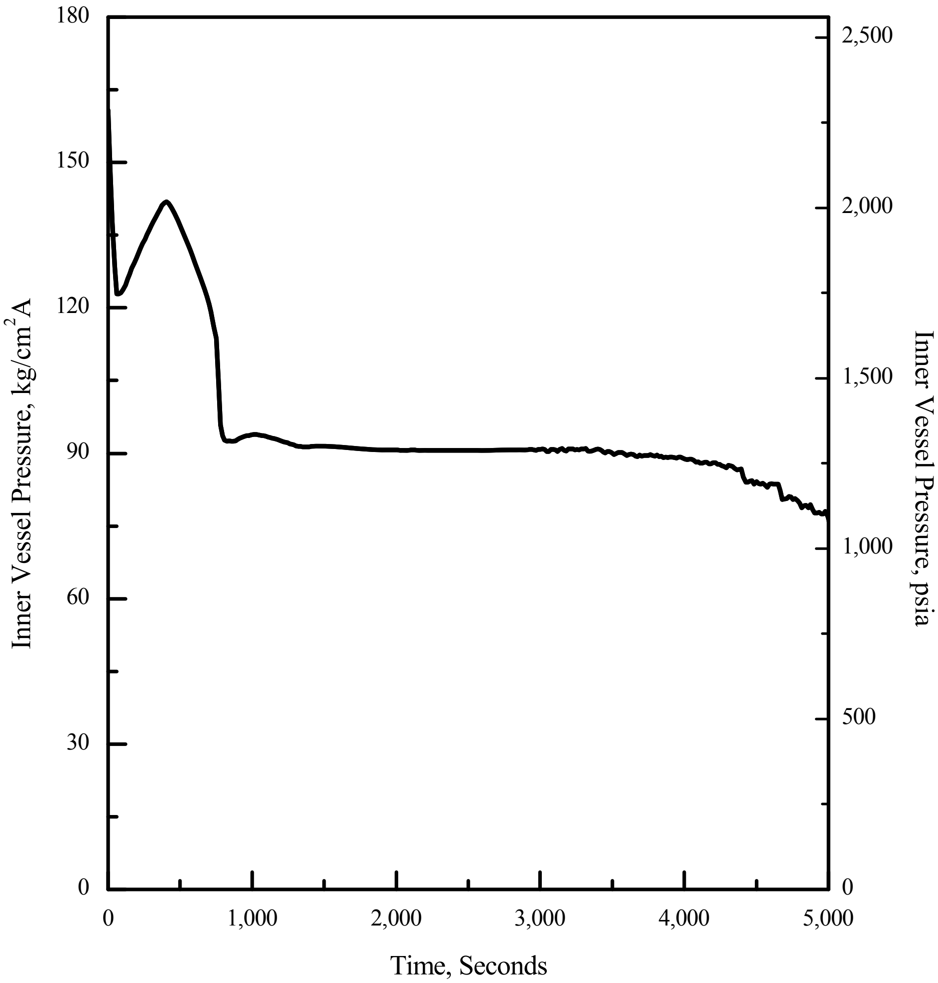

Figure 15.6.5-32B 27.9 cm^2 (0.03 ft^2) Break in Top of Pressurizer ; Inner Vessel Pressure

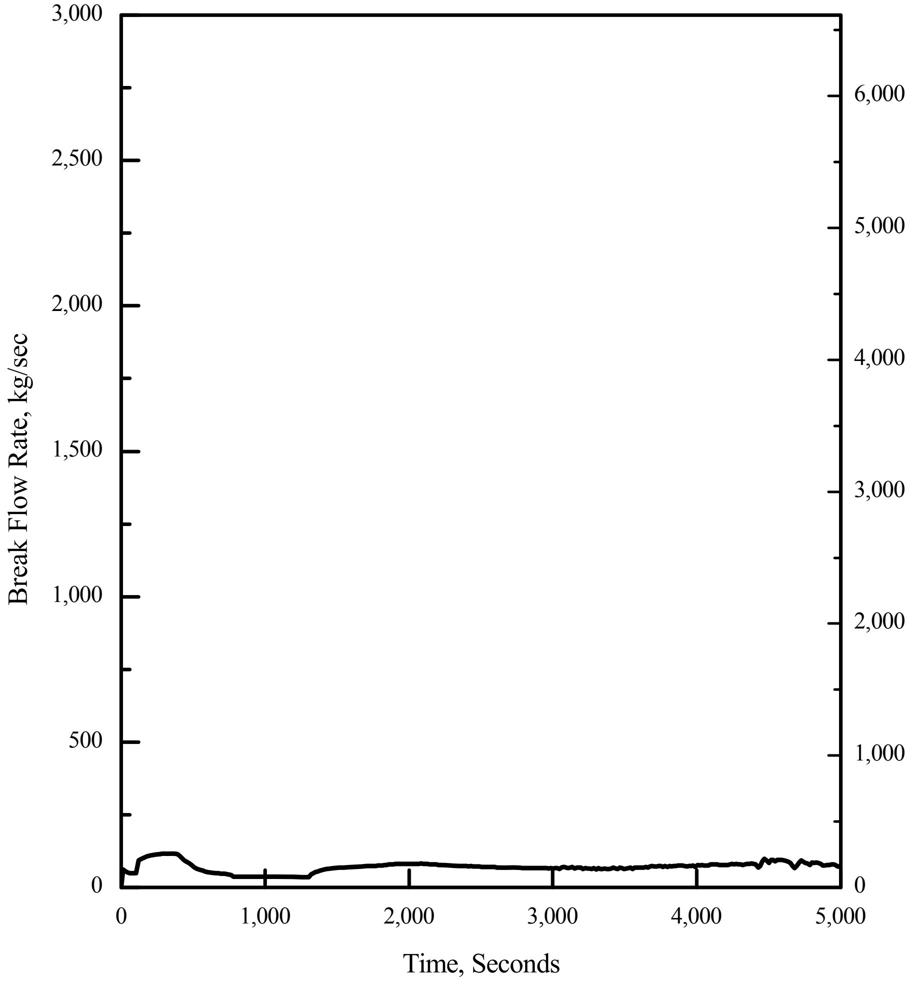

Figure 15.6.5-32C 27.9 cm^2 (0.03 ft^2) Break in Top of Pressurizer ; Break Flow Rate

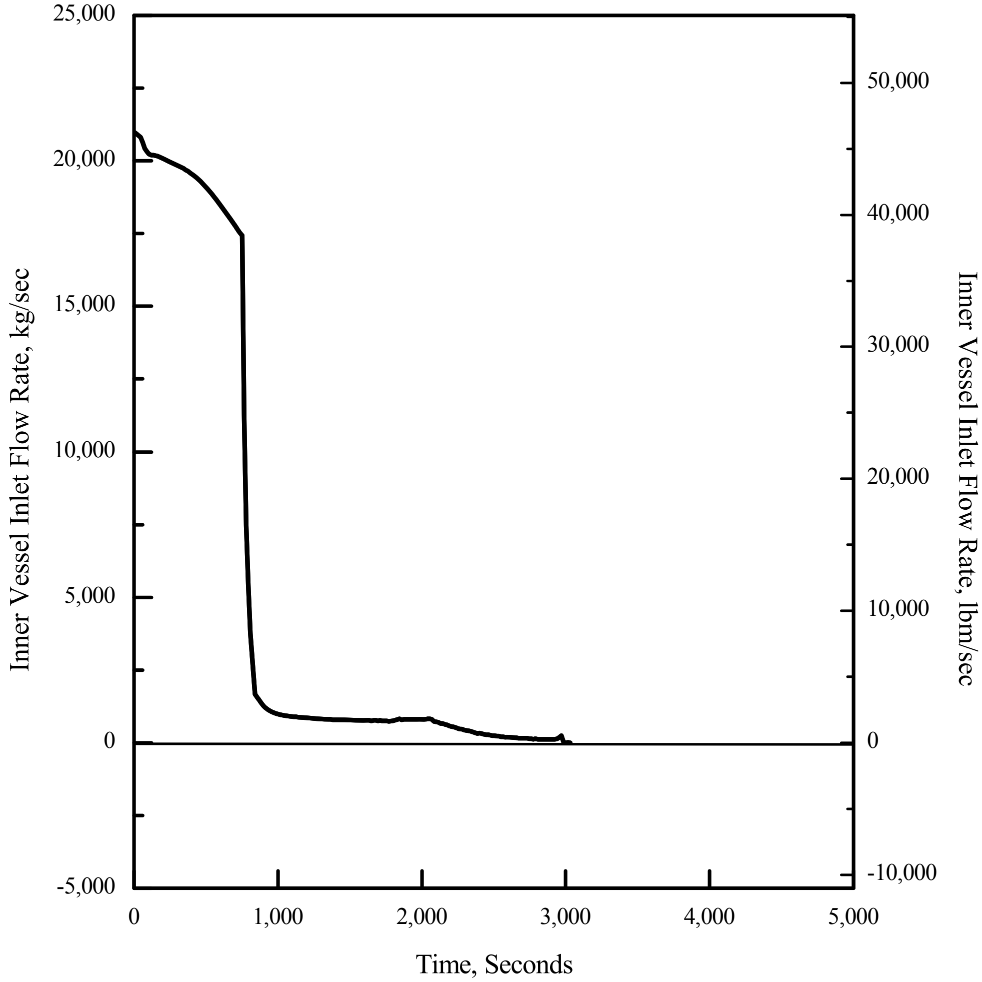

Figure 15.6.5-32D 27.9 cm^2 (0.03 ft^2) Break in Top of Pressurizer ; Inner Vessel Inlet Flow Rate

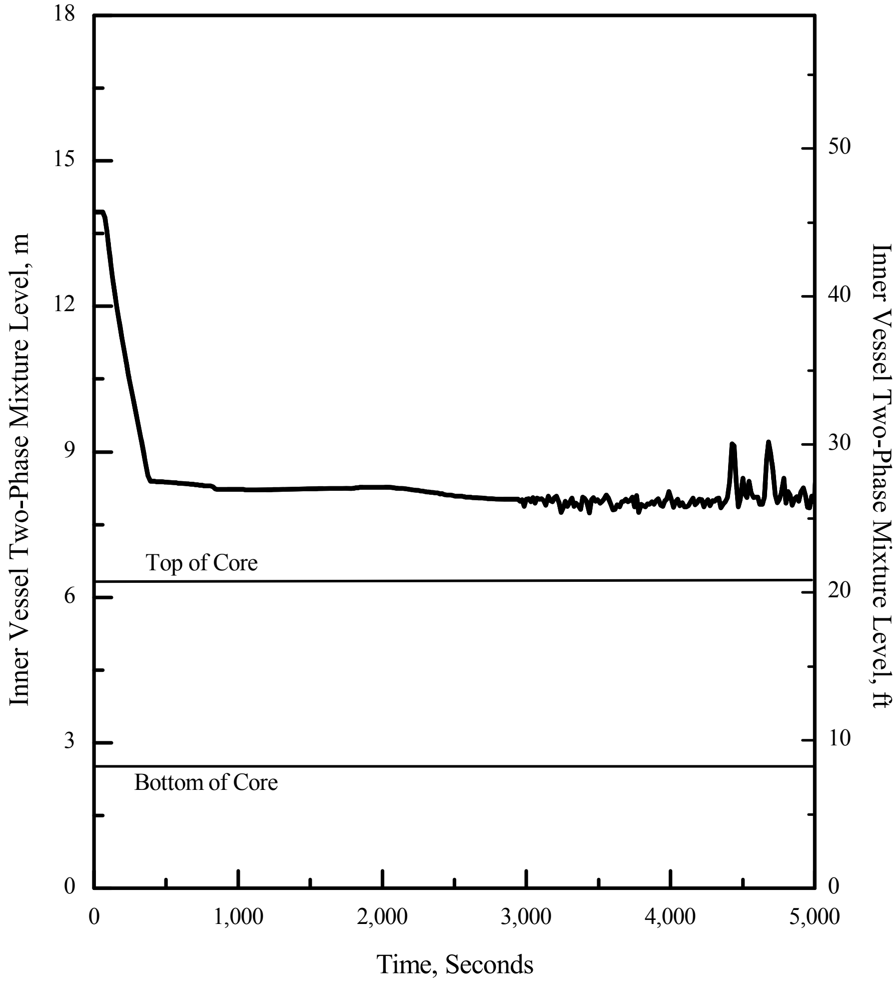

Figure 15.6.5-32E 27.9 cm^2 (0.03 ft^2) Break in Top of Pressurizer ; Inner Vessel Two-Phase Mixture Level

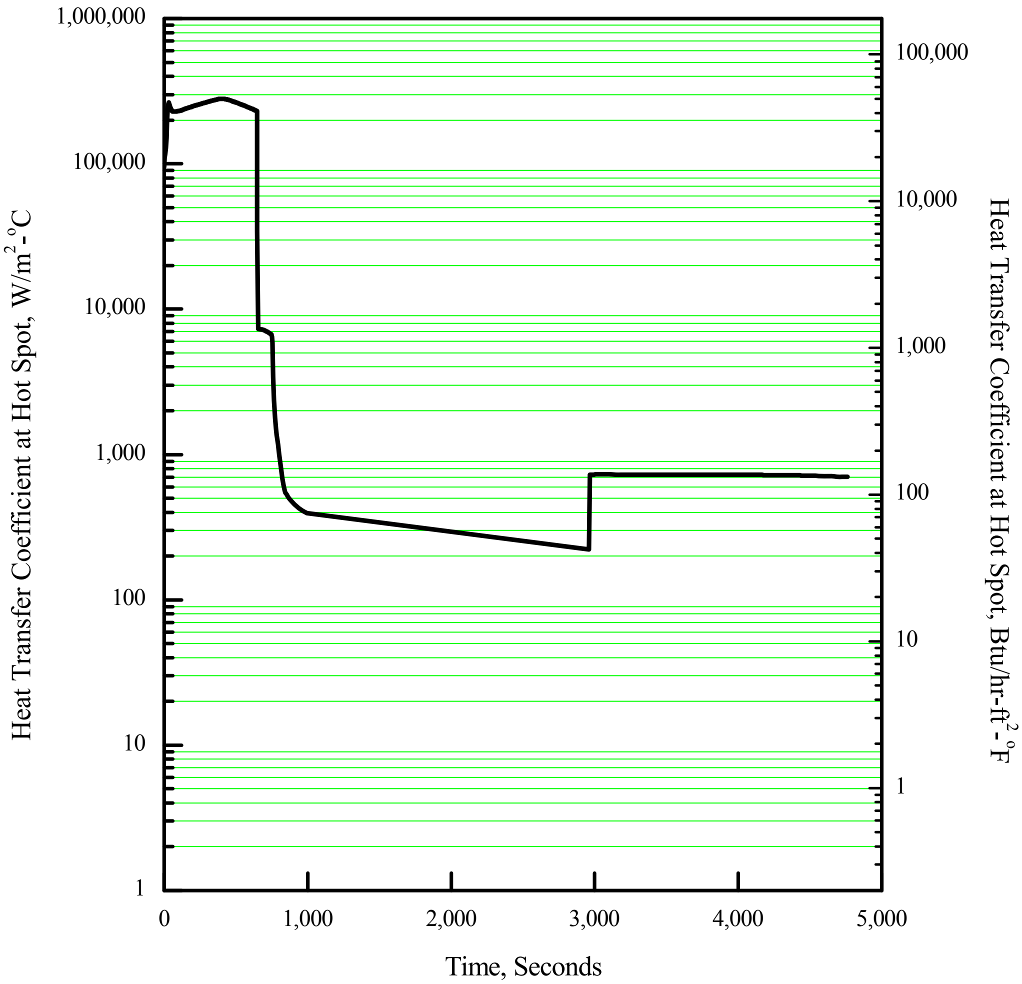

Figure 15.6.5-32F 27.9 cm^2 (0.03 ft^2) Break in Top of Pressurizer ; Heat Transfer Coefficient at Hot Spot

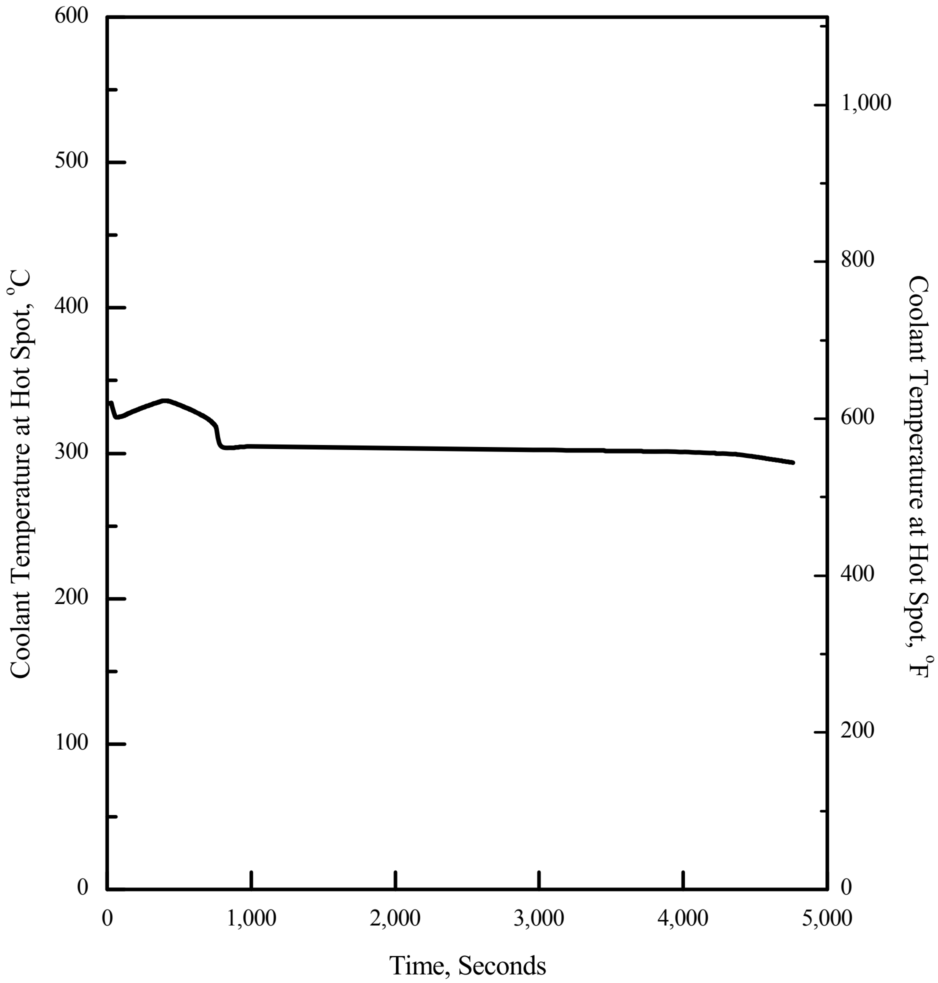

Figure 15.6.5-32G 27.9 cm^2 (0.03 ft^2) Break in Top of Pressurizer ; Coolant Temperature at Hot Spot

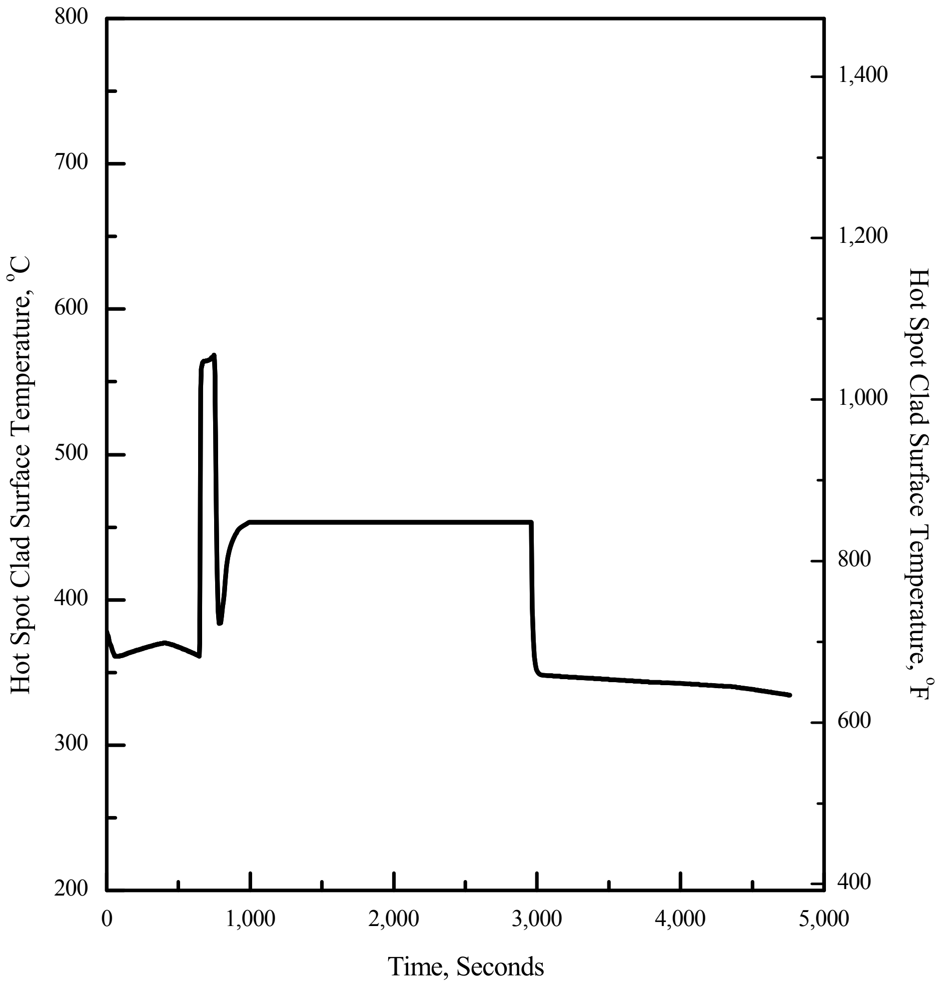

Figure 15.6.5-32H 27.9 cm^2 (0.03 ft^2) Break in Top of Pressurizer ; Hot Spot Clad Surface Temperature

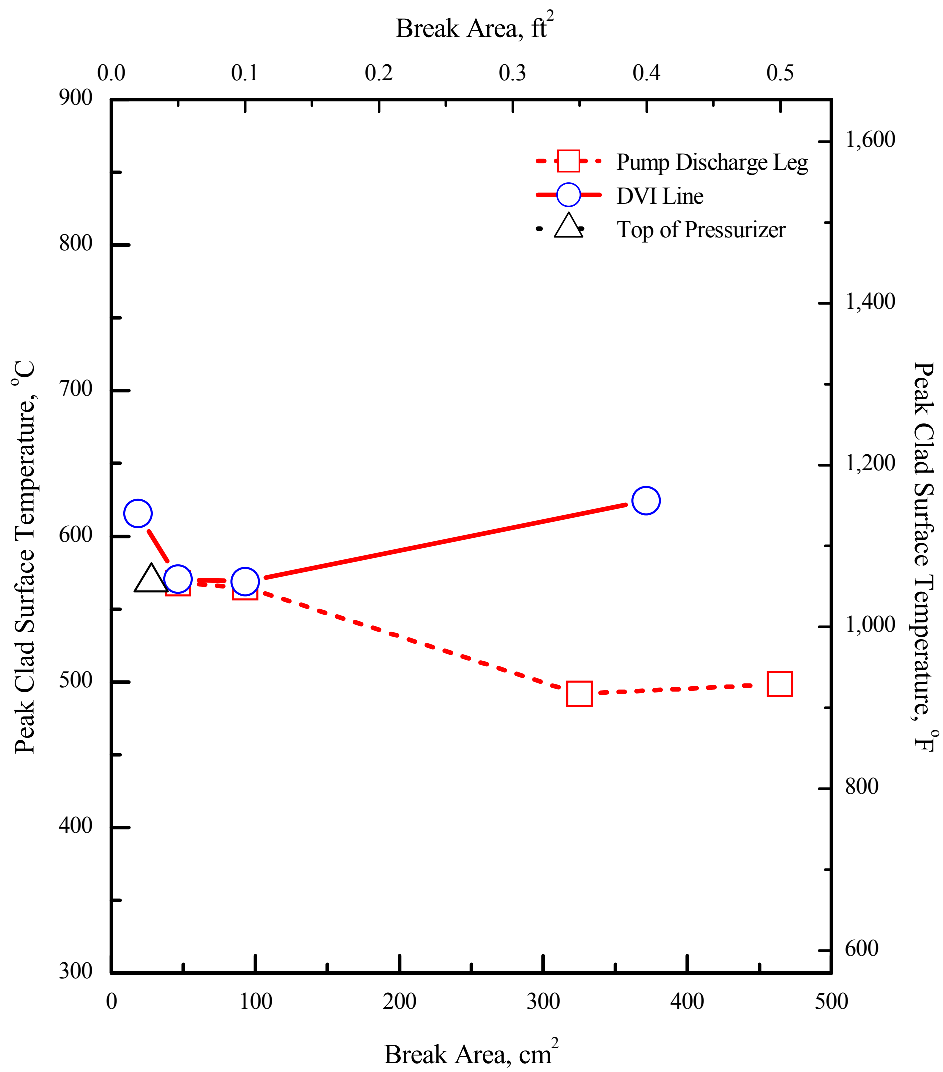

Figure 15.6.5-33 Peak Cladding Temperature vs. Break Size

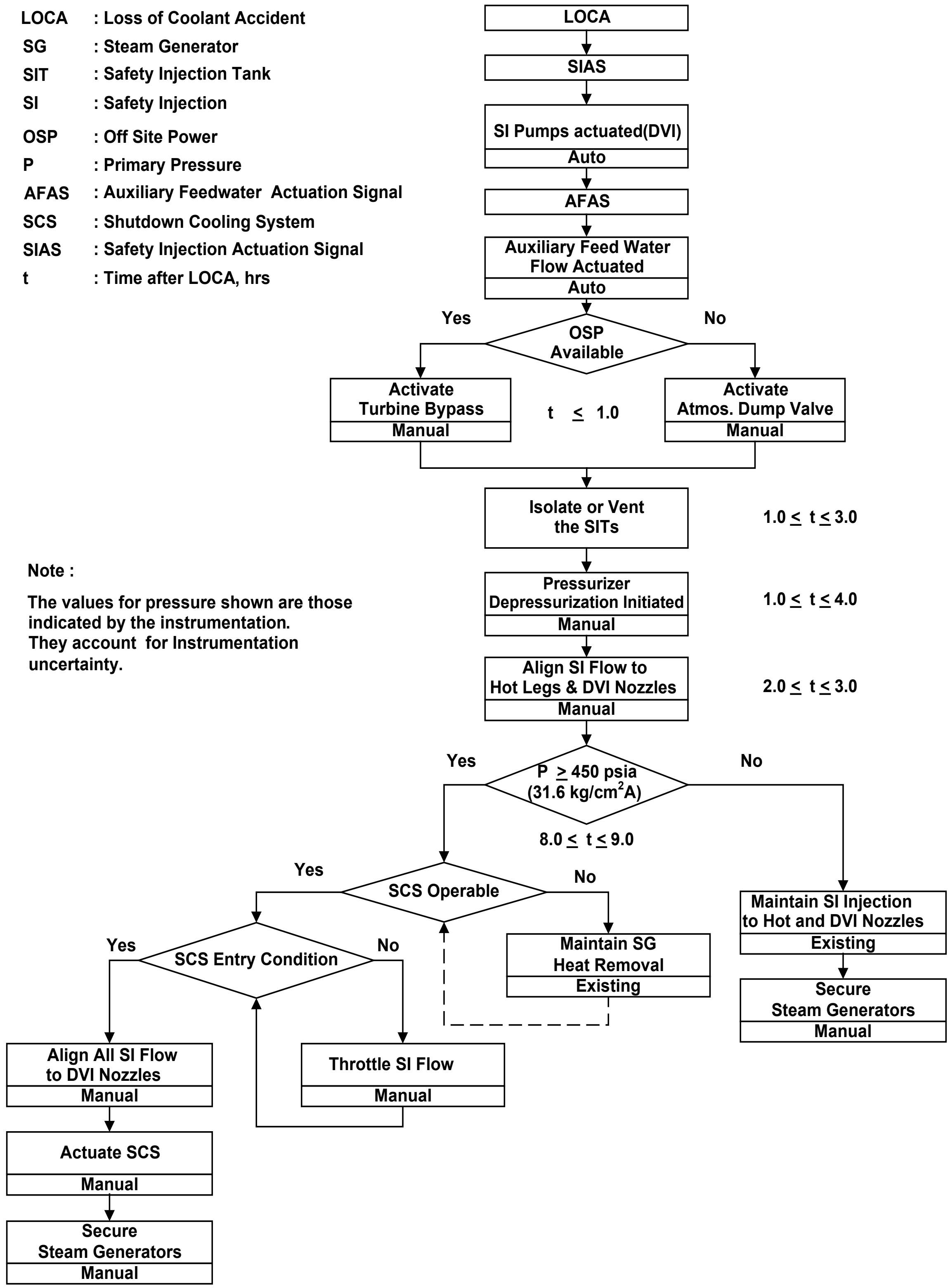

Figure 15.6.5-34 Long Term Cooling Plan

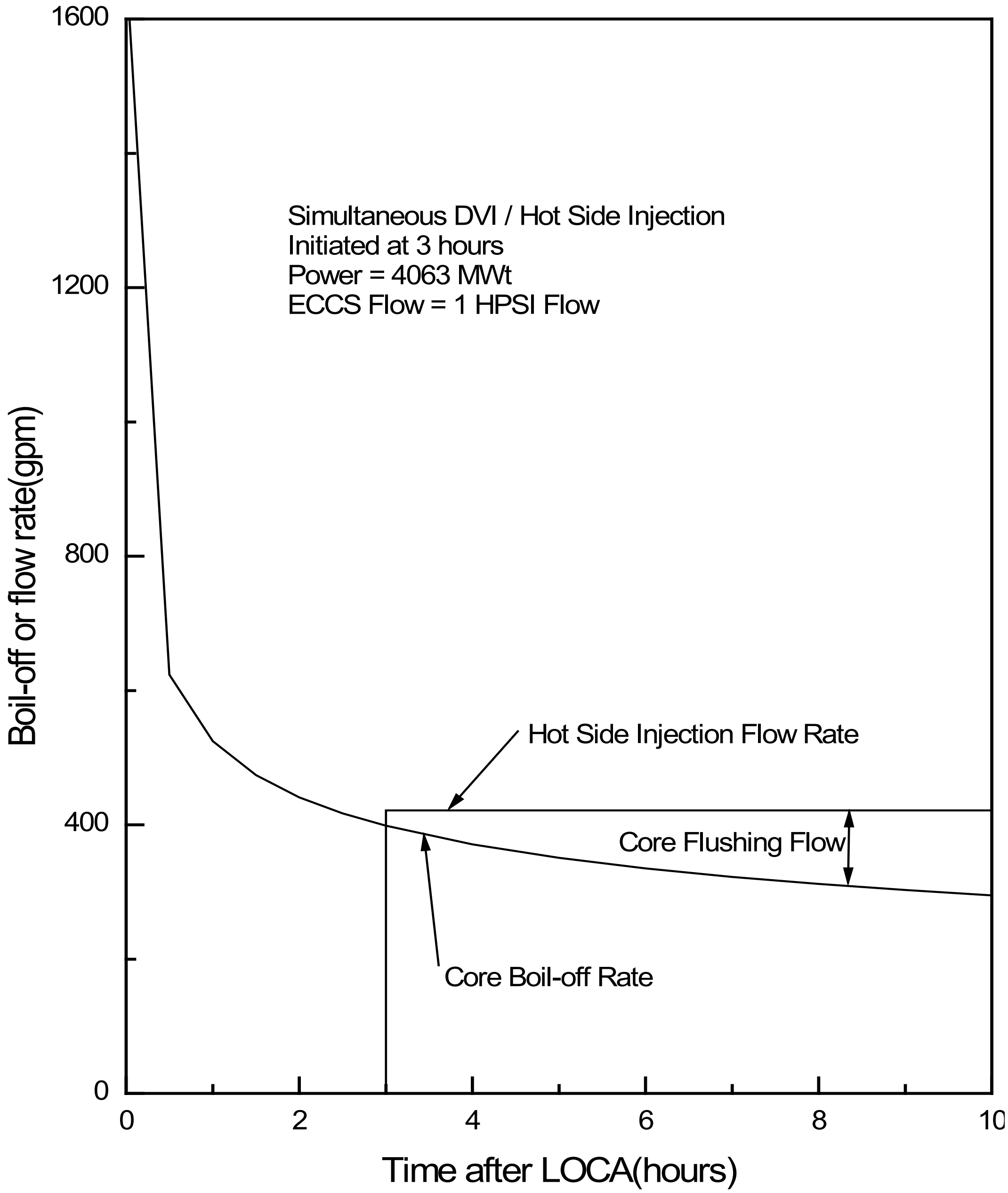

Figure 15.6.5-35 Core Flush by Hot Side Injection for 9,104.5 cm^2 (9.8 ft^2) Cold Leg Break

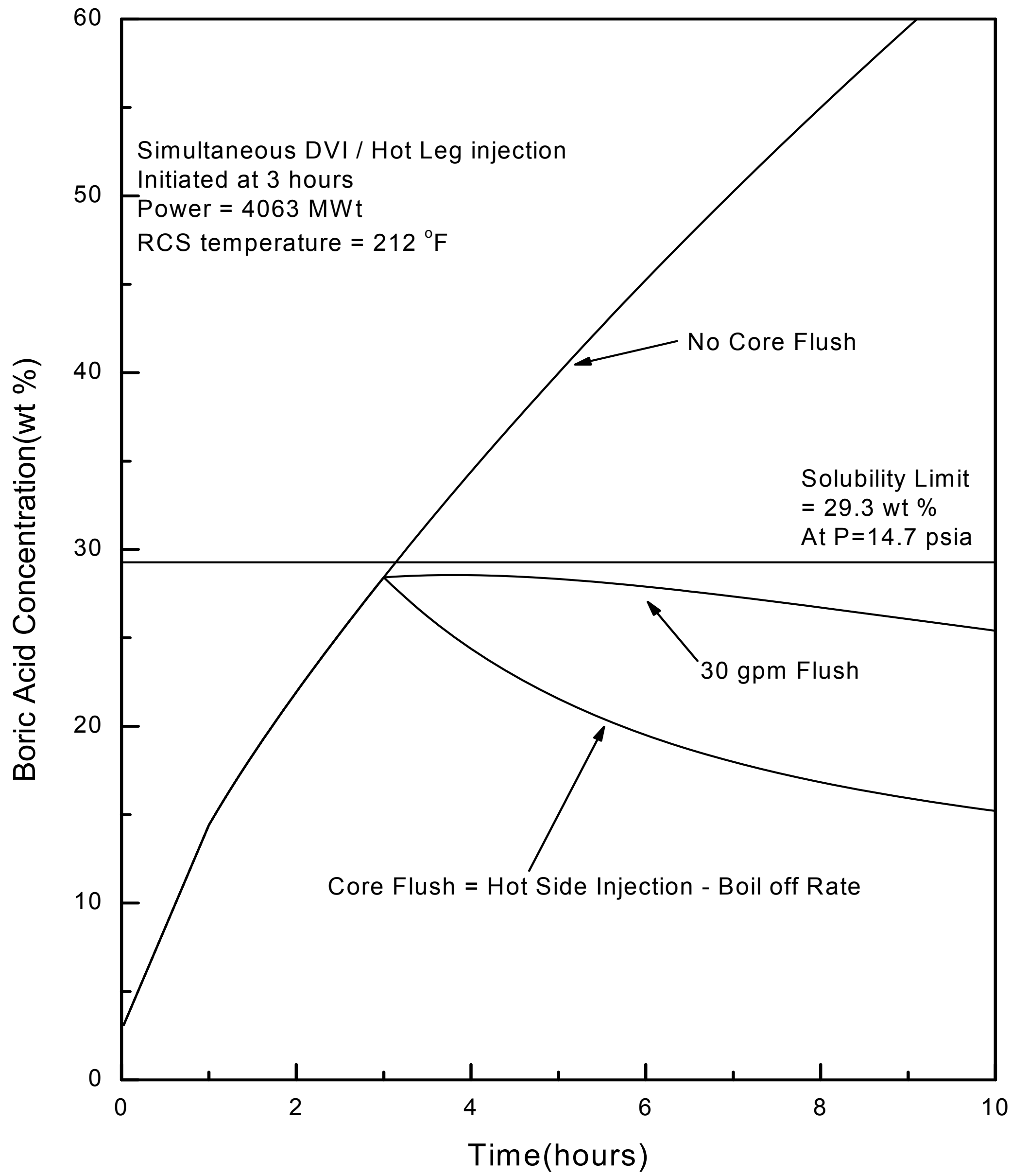

Figure 15.6.5-36 Inner Vessel Boric Acid Concentration vs. Time

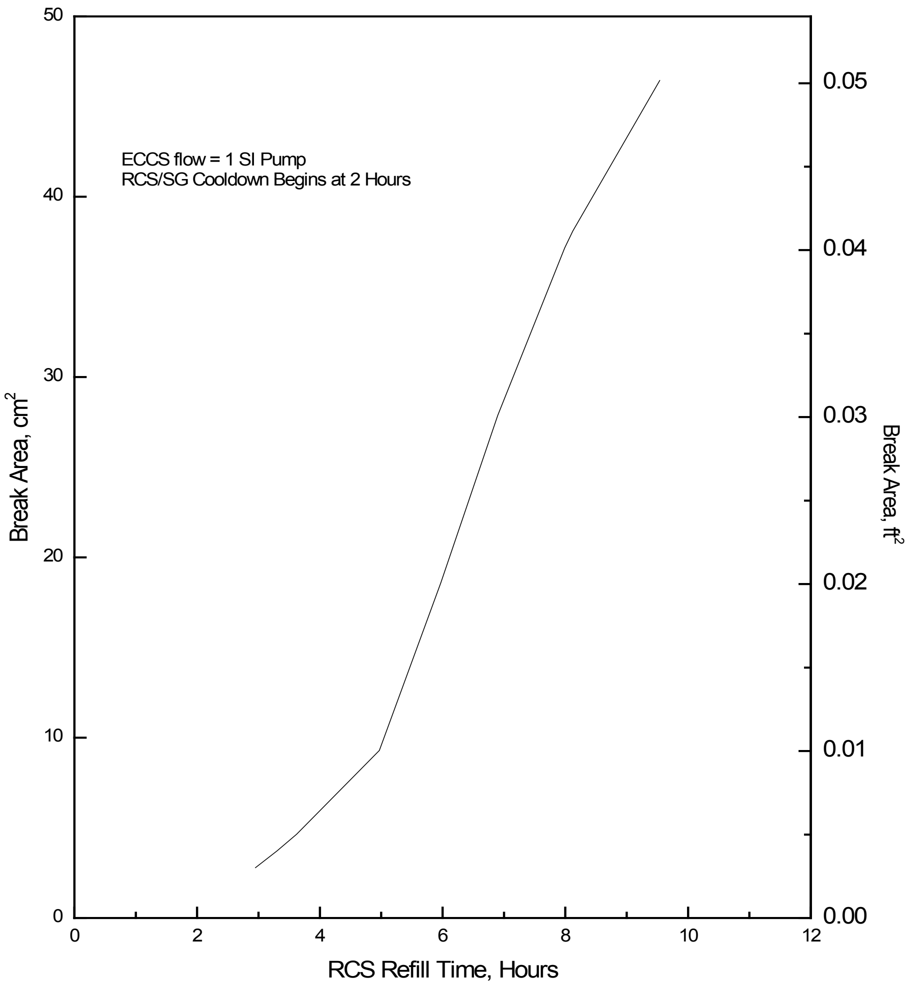

Figure 15.6.5-37 RCS Refill Time vs. Break Area

Break Area cm^2 (ft^2)	RCS Pressure at 8 Hours kg/cm^{2}A (psia)
464.5 (0.500)	2.5 (36)
92.9 (0.100)	5.3 (75)
46.5 (0.050)	5.3 (76)
38.1 (0.041)	5.3 (76)
37.2 (0.040)	6.5 (92)
27.9 (0.030)	7.9 (113)
18.6 (0.020)	11.7 (167)
9.3 (0.010)	27.3 (388)
4.6 (0.005)	60.8 (865)
3.7 (0.004)	73.3 (1042)
2.8 (0.003)	86.8 (1234)

Simultaneous Hot Leg/DVI Nozzles Injection Cools Core and Flushes Boric Acid from Vessel.

Refill of RCS Disperses Boric Acid throughout System and SGs are able to cool RCS to SDC Entry Temperature.

Figure 15.6.5-38 Overlap of Acceptable LTC Modes in Terms of Cold Leg Break Area

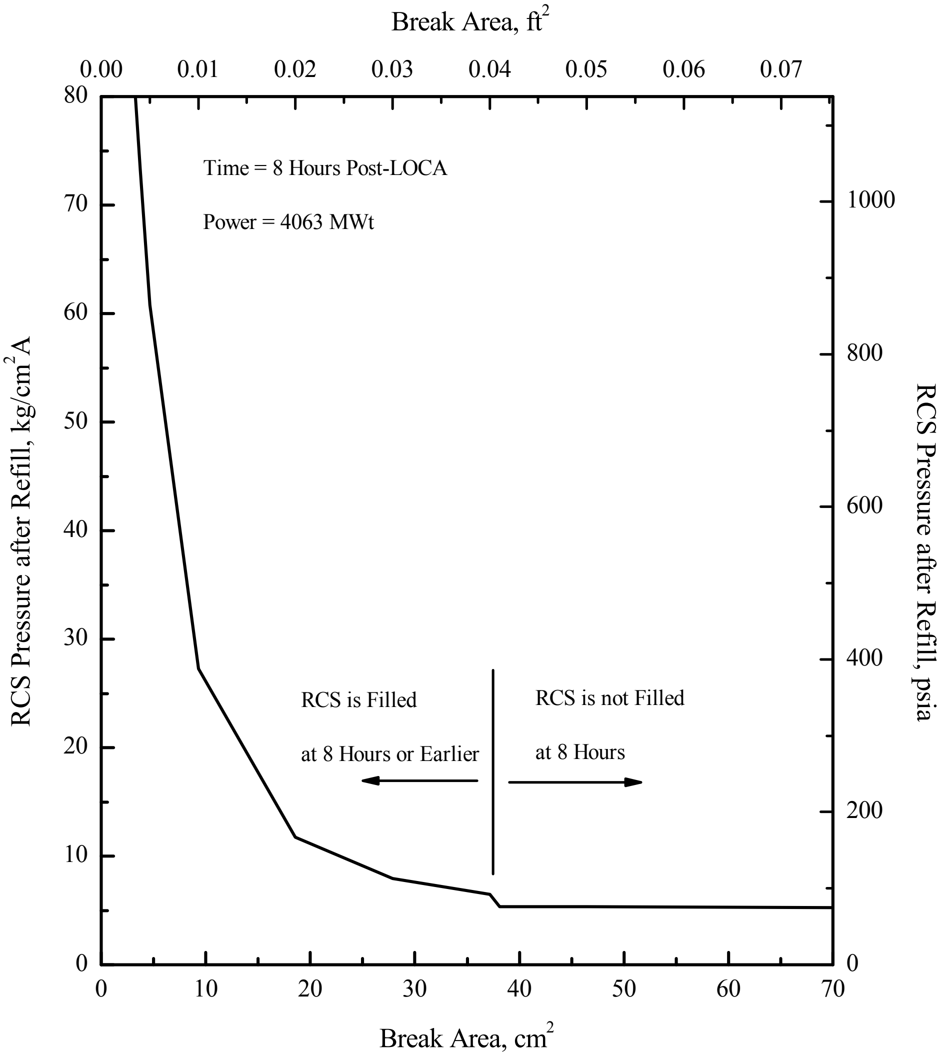

Figure 15.6.5-39   RCS Pressure after Refill vs. Break Area

15.7 Radioactive Material Release from a Subsystem or Component

The accidents that could result in a radioactive material release from a subsystem or component are discussed in the following subsections:

a. Subsection 15.7.1 – Radioactive gas waste system leak or failure

b. Subsection 15.7.2 – Radioactive liquid waste system leak or failure

c. Subsection 15.7.3 – Postulated radioactive releases due to liquid-containing tank failures

d. Subsection 15.7.4 – Fuel handling accident

e. Subsection 15.7.5 – Spent fuel cask drop accident

15.7.1 Radioactive Gas Waste System Leak or Failure

In the version of US NRC SRP Rev. 3, the section corresponding to a radioactive gas waste system leak or failure event has been deleted. Branch Technical Position 11-5 (Reference 60) has been added to Section 11.3 and provides detailed guidance on evaluating the radiological consequences due to a gaseous radioactive waste system leak or failure event.

The analysis method and radiological consequences of the gaseous radioactive waste system leak or failure event are described in Subsection 11.3.3.

15.7.2 Radioactive Liquid Waste System Leak or Failure

In the version of US NRC SRP Rev. 3, the section corresponding to a radioactive liquid waste system leak or failure event has been deleted, and the SRP no longer includes a radioactive liquid waste system leak failure event. Therefore, no radiological consequence analysis for this event is performed.

15.7.3 Postulated Radioactive Releases Due to Liquid-Containing Tank Failures

Branch Technical Position 11-6 (Reference 61) has been added to Section 11.2 and provides detailed guidance on evaluating the radiological consequences due to the liquid-containing tank failure.

The analysis method and release of radioactivity to the environment resulting from the liquid radwaste system leak of failure are described in Subsection 11.2.3.

15.7.4 Fuel Handling Accident

In the postulated fuel handling accident (FHA), a fuel assembly is assumed to be dropped and damaged during fuel handling. The accident takes place in the containment or in the spent fuel pool (SFP) inside the fuel handling area in the auxiliary building (AB). The analysis design inputs and assumptions are chosen so that the results of a single FHA analysis are bounding for an accident occurring in either the containment or SFP.

15.7.4.1 Evaluation Model

The radiological consequences of an FHA to determine EAB, LPZ, MCR, and TSC doses use the guidance in NRC RG 1.183, Appendix B, TEDE criteria, and the bounding design information applicable to APR1400. Since there is no active failure of a component that can worsen the radiological consequence, a single failure is not considered in this analysis. The following transport models of radioactive material are applied to evaluate radiological consequences due to an FHA.

FHA in the Containment Building

The containment boundary has one equipment hatch, two personnel air locks, and containment piping and electrical penetrations. The Technical Specification requires the equipment hatch to be closed and held in place by four bolts, one door in each airlock to be closed, and each penetration providing direct access from the containment atmosphere to the outside atmosphere to either be closed by a manual or automatic isolation valve, blind flange, or equivalent or to be capable of being closed by an operable containment purge system. The containment is opened when the high volume purge system is operating. If the FHA happens in this state, the containment purge isolation actuation signal (CPIAS) is actuated by the safety-related radiation monitoring system (RMS), which provides prompt

signal of high airborne radiation. The containment purge system is also designed to close the isolation valve of the low volume exhaust system with shorter time than the transit time of radioactive materials through the inner damper of low volume exhaust system. These requirements are applicable when irradiated fuel is moved in the containment (i.e., during a refueling outage) to confine the post-FHA release inside the containment and eliminate any potential activity release to the environment. If LOOP is assumed in the FHA analysis, the radioactive materials may escape to the environment for certain duration before the purge system is isolated because the isolation may be delayed until the emergency power is actuated. This case, however, is bounded by the FHA occurring in the fuel handling area, which assumes the release of all the radioactive materials to the environment. It is not required to analyze the radiological consequence of FHA in the containment.

FHA Outside Containment

The spent fuel pool (SFP) is located in the fuel handling area inside the auxiliary building. After the FHA in the SFP, the fission products released from the breached fuel assembly are scrubbed in the SFP water with a depth of 7 m (23 ft) from the top of the SFP racks to the SFP surface. Escaped radioactivity is detected by the fuel handling area radiation monitors so that the fuel handling area emergency ventilation actuation signal (FHAEVAS) is actuated. The post-FHA activity from the SFP is then drawn by the safety-grade fuel handling area emergency ventilation system equipped with HEPA and charcoal prior to being released to the environment. The release from the FHA in the SFP is terminated when all the radioactivities released from the breached fuel assembly are discharged to the environment with the flow capacity of the emergency fuel handling area ventilation system.

15.7.4.2 Input Parameters and Initial Conditions

The fractions of the core inventory assumed to be in the gap for the various radionuclides are given in NRC RG 1.183. The release fractions are used in conjunction with the core fission product inventory with the maximum core radial peaking factor of 1.80.

It is assumed that all gap activity in the damaged rods is instantaneously released to the pool water. The gap radionuclides included are xenons, kryptons, and iodines. It is further assumed that the irradiated fuel is not removed from the reactor until the unit has been shut down for at least 72 hours.

Non-iodine halogen isotopes (e.g., bromine) are not modeled due to their short half-lives, which leave a negligible activity in the fuel source term at 72 hours. Alkali metal (i.e., particulate) isotopes are not modeled because they are not released from the water. The assumed inventory of fission products in the reactor core and available for release to the containment or fuel handling area is based on the maximum power level of 4,062.66 MWt corresponding to current fuel enrichment and fuel burnup, which is 1.02 times the APR1400 rated thermal power of 3,983 MWt.

For FHA in which fuel damage is projected, the release from the fuel gap is assumed to occur instantaneously with the onset of the projected damage (i.e., 72 hours after reactor shutdown).

The chemical form of radioiodine released from the fuel to the surrounding water is assumed to be 95 percent cesium iodide (CsI), 4.85 percent elemental iodine, and 0.15 percent organic iodine. The CsI released from the fuel is assumed to completely dissociate in the pool water. Because of the low pH of the pool water, the iodine re-evolves as elemental iodine. The re-evolution as elemental iodine is assumed to occur instantaneously.

Since the depth of water above the damaged fuel for APR1400 is 7 m (23 ft), the overall effective iodine decontamination factor of 200 is used. The iodine above the water is composed of 57 percent elemental and 43 percent organic species.

The retention of noble gases in the water in the fuel pool or refueling pool is negligible (i.e., decontamination factor of 1). Particulate radionuclides are assumed to be retained by the water in the fuel pool or refueling pool (i.e., infinite decontamination factor).

A reduction in the amount of radioactive material released from the fuel pool by engineered safety features (ESF) filter systems may be taken into account since these systems meet the guidance of NRC RG 1.52 and Generic Letter 99-02. Delays in radiation detection, actuation of the ESF filtration system, or diversion of ventilation flow to the ESF filtration system are determined and accounted for in the radioactivity release analyses. However, although the APR1400 provides the safety-grade filtration system by the fuel handling area emergency ventilation system, no credit is taken for conservatism in this analysis. The main control room HVAC system charcoal and HEPA filtration is credited.

The radioactivity release from the fuel pool is assumed to be drawn into the ESF filtration system without mixing or dilution in the fuel building. If mixing can be demonstrated, credit for mixing and dilution may be considered on a case-by-case basis. In this analysis, no dilution or mixing is credited in the fuel handling building.

The χ/Q values used in the analysis for EAB, LPZ, MCR, and TSC are described in Subsection 2.3.4 and listed in Table 15.7.4-1; breathing rates are given in Table 15A-11.

15.7.4.3 Results

The radiological consequences due to FHA are presented in Table 15.7.4-2. The results of the FHA analyses indicate that the EAB and LPZ doses are within their allowable dose limit, which is 25 percent of the 10 CFR 50.34(a)(1) value as specified in SRP 15.0.3. The MCR and TSC doses are also within the criterion in GDC 19.

15.7.4.4 Conclusion

The potential radiological consequences of a postulated FHA have been conservatively analyzed, using the assumptions and models described in the preceding subsections. The calculated doses are within the criteria specified in SRP 15.0.3.

15.7.5 Spent Fuel Cask Drop Accident

A spent fuel cask handling accident is evaluated if the spent fuel cask can be dropped from a height exceeding 9.14 m (30 ft) onto a hard unyielding surface or if it can be dropped or tipped onto stored irradiated fuel.

The fuel handling system and plant layout of the APR1400 is designed to meet the following criteria:

a. All spent fuel cask lifts from the cask transporter to the cask laydown area are limited to less than 9.14 m (30 ft)

b. The spent fuel cask handling crane operating procedures establish the requirements for operator training, crane inspections, and approved cask handling procedures

c. The cask handling crane is provided with mechanical stops and electrical interlocks to prevent its movement near the spent fuel pool after the pool contains irradiated fuel

d. The fuel handling area is arranged so the spent fuel cask does not pass over critical components during passage from the cask transporter to the cask laydown area

Radiological evaluations for a cask handling accident are not required because plant design features and cask handling procedures of the APR1400 meet all applicable criteria.

15.7.6 Combined License Information

No COL information is required with regard to Section 15.7.

Table 15.7.4-1 (1 of 2)

Parameters Used in Evaluating Radiological Consequences of Fuel Handling Accident

Parameter	Value
Source Terms	
Reactor Core Power Level	4,062.66 MWt
Fraction of Fission Product Inventory in Gap	
Group	Fraction
I-131 Kr-85 Other Noble Gases Other Halogens Alkali Metals	0.08 0.10 0.05 0.05 0.12
Number of Damaged Fuel Assembly	1 Fuel Assembly
Number of Fuel Assemblies in Core	241
Radial Peaking Factor	1.80
Iodine Chemical Form Released from Fuel to Water	
Aerosol (CsI) Elemental Organic	95.0 % 4.85 % 0.15 %
Activity Transportation	
Minimum Refueling Pool and Pool Water Depths	7 m (23 feet)
Credit for Dilution or Mixing in Fuel handling area	No Dilution of Mixing in FHB
Overall Effective Decontamination Factor (DF) for Iodine	200
Chemical Form of Iodine Released from Pool Water	
Elemental Organic	57 % 43 %
Spent Fuel Pool Volume	28.32 m^3 (1000 ft^3)
DF of Particulates	Infinite

Table 15.7.4-1 (2 of 2)

Parameter	Value
MCR and TSC Model Parameters	
Envelope Volume	5,663 m^3 (200,000 ft^3)
Normal Ventilation Flow Rate (unfiltered)	105 m^3/min (3,700 cfm)
Emergency Ventilation Makeup Rate (filtered)	105 m^3/min (3,700 cfm)
Emergency Ventilation Recirculation Flow Rate (filtered)	122 m^3/min (4,300 cfm)
Emergency HVAC Delay Time	5 mins
Emergency Ventilation Charcoal Filter Efficiency (elemental and organic iodine removal)	99 %
Emergency Ventilation HEPA Filter Efficiency (particulate removal)	99 %
Unfiltered Inleakage	8.50 m^3/min (300 cfm)
Occupancy Factors	
0 ~ 24 hrs	100 %
24 ~ 96 hrs	60 %
96 ~ 720 hrs	40 %
Limiting Onsite χ/Qs for MCR Air Intake (s/m^3)	
0 ~ 2 hrs	2.59E-04
2 ~ 8 hrs	2.04E-04
8 ~ 24 hrs	8.98E-05
24 ~ 96 hrs	5.93E-05
96 ~ 720 hrs	4.58E-05
Limiting Onsite χ/Qs for MCR Unfiltered Inleakage (s/m^3)	
0 ~ 2 hrs	1.04E-03
2 ~ 8 hrs	8.18E-04
8 ~ 24 hrs	3.59E-04
24 ~ 96 hrs	2.37E-04
96 ~ 720 hrs	1.83E-04
Offsite Model Parameters	
χ/Qs	See Table 2.3-1
Breathing Rate	See Table 15A-11
Dose Conversion Factors	See Table 15A-10

Table 15.7.4-2

Radiological Consequences of Fuel Handling Accident

Activity Release Path	TEDE Dose (mSv)		
	MCR and TSC	EAB	LPZ
Fuel handling area vent release	6.25E+00	3.89E+00	8.56E+00
Allowable TEDE limit	5.00E+01	6.30E+01	6.30E+01

15.8 Anticipated Transient without Scram

15.8.1 Identification of Causes and Frequency Classification

An anticipated transient without scram (ATWS) is an anticipated operational occurrence (AOO) as defined in Appendix A of 10 CFR 50 followed by the failure of the reactor trip portion of the protection system as specified in General Design Criteria (GDC) 20.

Because the protection system satisfies the single failure criterion, multiple failures or a common cause mode failure cause the assumed failure of the reactor trip. The possibility of an AOO, in coincidence with multiple failures or a common cause failure, is much lower than the probability of any of the other events that are evaluated under the SRP, Chapter 15. An ATWS event cannot be classified as either an AOO or a PA and has historically been considered a beyond-design-basis event.

15.8.2 Anticipated Transient without Scram Rule (10 CFR 50.62) Design Requirements

The requirements for the reduction of risk from ATWS events are given in 10 CFR 50.62, "Requirements for Reduction of Risk from Anticipated Transients without Scram Events for Light-Water-Cooled Nuclear Power Plants." The requirements in 10 CFR 50.62 are as follows:

a. "Each pressurized water reactor must have equipment from sensor output to final actuation device, that is diverse from the reactor trip system, to automatically initiate the auxiliary (or emergency) feedwater system and initiate a turbine trip under conditions indicative of an ATWS. This equipment must be designed to perform its function in a reliable manner and be independent (from sensor output to the final actuation device) from the existing reactor trip system."

b. "Each pressurized water reactor manufactured by Combustion Engineering or by Babcock & Wilcox must have a diverse scram system from the sensor output to interruption of power to the control rods. This scram system must be designed to perform its function in a reliable manner and be independent from the existing reactor trip system (from sensor output to interruption of power to the control rods)."

An integrated approach is applied to the APR1400 to prevent and mitigate an ATWS. The approach results in the incorporation of diverse and redundant backup systems to provide reasonable assurance of a reactor trip and the delivery of auxiliary feedwater under ATWS conditions according to the requirements described above.

NUREG-0460 also states that an ATWS can be accommodated by reducing the probability of occurrence of an ATWS event to the extent that it is unnecessary to consider it as a design basis or alternatively, by providing features to mitigate the consequences of an ATWS event if it occurs.

15.8.3 Anticipated Transient without Scram Design for the APR1400

The requirements for the reduction of risk from ATWS are provided in 10 CFR 50.62 "Requirements for Reduction of Risk from Anticipated Transients without Scram (ATWS) Events for Light-Water-Cooled Nuclear Power Plants." The APR1400 design includes digital safety system and a diverse protection system (DPS) to comply with the ATWS rule.

The plant protection system (PPS) is normally available to prevent and mitigate an ATWS. The PPS includes the electrical and mechanical devices and circuitry required to perform the functions of the reactor protection system (RPS) and the engineered safety features-component control system (ESF-CCS). The RPS is the portion of the PPS that trips the reactor when required. A coincidence of two signals from the two-out-of-four trip logic is required to generate a reactor trip signal. This signal de-energizes the control element drive mechanism (CEDM) coils, allowing all control element assembly (CEAs) to drop into the core. The ESF-CCS is the portion of the PPS that activates the engineered safety feature systems. Additionally, the reactor trip system includes the RPS portion of the PPS, reactor trip switchgear system, and components that perform a reactor trip after receiving a signal from the RPS (either automatically or manually). Upon removal of power to the CEDM power supplies, the CEAs fall into the core by gravity. Additionally, two sets of manual trip switches are provided to open the trip circuit breakers. The manual trip completely bypasses the trip logic.

The DPS provides a diverse backup to the PPS. The DPS initiates a reactor trip signal on high pressurizer pressure to decrease the possibility of an ATWS and provides an auxiliary feedwater actuation signal (backup to the ESF-CCS of the PPS) to provide reasonable assurance that an ATWS event is mitigated if it occurs.

The DPS for the APR1400 complies with 10 CFR 50.62 requirements and provides a method of initiating reactor trip and auxiliary feedwater that is diverse and independent from the reactor protection system (Section 7.8). Moreover, the design, analysis, and testing of the RPS, as described in Section 7.2, provides reasonable assurance that the RPS itself is reliable.

The complete loss of main feedwater without turbine trip was considered for the reference APR1400, because it produced the highest primary pressure during an ATWS condition (References 21 and 22) with respect to the thermal hydraulic responses. Reference 22 analyzed a wide range of ATWS events for CE-fleet plants, and the study concluded that the most adverse conditions occurred during the loss of main feedwater event with the failure of the reactor to trip.

15.8.4 Conclusions

The APR1400 has met the intent of the ATWS rule for the ATWS transient with a diverse protection system.

15.8.5 Combined License Information

No COL information is required with regard to Section 15.8.

APPENDIX 15A

ANALYTICAL MODEL FOR DETERMINING RADIOLOGICAL CONSEQUENCES OF ACCIDENTS

APPENDIX 15A – ANALYTICAL MODEL FOR DETERMINING RADIOLOGICAL CONSEQUENCES OF ACCIDENTS

TABLE OF CONTENTS

LIST OF TABLES

LIST OF FIGURES

APPENDIX 15A - ANALYTICAL MODEL FOR DETERMINING RADIOLOGICAL CONSEQUENCES OF ACCIDENTS

This appendix presents assumptions, parameters, and models used in radiological consequences analysis for the APR1400 design basis accidents.

15A.1 Source Term

15A.1.1 Core Source Term

The radioactivity inventory in the core is used as an input into the events that cause failure of the fuel cladding or melting, which releases fission products from the fuel gap or pellets. This inventory is calculated using ORIGEN-S computer code (Reference 1), which is widely used in the nuclear industry. The core power is assumed to be 4,062.66 MWt, which is 2 percent higher than the expected power of 3,983 MWt. The core loading for the APR1400 is assumed to be 103.8 MT of uranium, and a three-cycle burnup of 56.4 GWD/MTU is assumed to calculate the maximum core inventory. This burnup is a conservative approach because the three-batch fuel assemblies are assumed to have been burned at full power for three cycles.

The maximum core fission product inventories in the APR1400 reactor are listed in Table 15A-1 for 60 essential isotopes. The remaining isotopes are not accounted for in the radiological consequences analysis for the following reasons:

a. Short-lived

b. Initial activities that are smaller than the activities of the essential isotopes

c. Non-gamma parent nuclides or they decay into non-gamma daughters

d. Inhaled dose conversion factors that are smaller (more than two orders of magnitude) than those of the essential isotopes

15A.1.2 Reactor Coolant Source Term

15A.1.2.1 Fuel Pellet Clad Gap Inventory

For the events that experience fuel cladding damage, the fission products in the gap are assumed to be released to the primary coolant. The fractions of the core inventory assumed to be in the gap for the various radionuclides are based on NRC RG 1.183 (Reference 2) and given in Table 15A-2. The release fractions are used in conjunction with the fission product inventory calculated with the maximum core radial peaking factor for the non-LOCA accidents inducing the fuel damage.

For reactivity initiated accidents (RIAs) such as CEA ejection accident, it is assumed that the total fission product gap fraction available for release following any RIA includes the steady-state gap inventory during normal operation (present prior to the event) listed in Table 15A-2 plus any transient fission gas released during the event. The transient fission gas release is considered based on Appendix B of SRP 4.2 (Reference 8).

15A.1.2.2 Iodine Spike Concentration

Iodine spike phenomenon occurs because of pre-existing tube defects as a result of rapid depressurization of RCS and subsequent power transient, attributed to excessive cooldown, resulting in the augment of the iodine concentration in primary coolant.

As recommended in Appendix E of NRC RG 1.183, if no or minimal fuel damage is postulated for the limiting event, the released activity is the maximum coolant activity allowed by the Technical Specifications, and pre-accident and event-generated iodine spikes are evaluated.

Pre-Accident Iodine Spike (PIS)

The pre-accident iodine spike concentrations are determined by increasing the primary coolant iodine concentrations to 60 times the maximum value of 3.7×10^4 Bq/g (1.0 μCi/g) dose equivalent (DE) I-131, as permitted in the Technical Specifications, which is the transient Technical Specifications limit for full power operation. The nuclide profile of the iodine concentration corresponds to that of 1 percent fuel defect. It is assumed that all of the spike activity is instantaneously and homogeneously mixed in the primary coolant

prior to the initiation of the event. The resulting primary coolant iodine concentrations are given in Table 15A-3.

Event-Generated Iodine Spike (GIS)

There is an iodine appearance rate that is applied in the radiological source term analysis to calculate the event-generated iodine spike (GIS) in events such as an SGTR or an MSLB. The assumptions used for calculating the appearance rate are as follows:

a. Prior to the occurrence of an event, the RCS iodine appearance rate is assumed to be equal to the iodine removal rate due to RCS purification.

b. No removal by the purification flow is considered during the spike.

c. The appearance rate and the removal constant are assumed to be constant during the spike.

d. Since the purification flow is small compared to the RCS coolant mass, it is assumed that the reactor coolant mass is a constant.

The appearance rate of iodine during the event-generated iodine spike is calculated using the following equation and is given in Tables 15A-4 through 15A-7.

$$\text{Iodine appearance rate } (\text{sec}^{-1}) = A_i \left(C \frac{P}{M} + \lambda_{decay} \right)$$

Where:

A_i	=	Total iodine activity at equilibrium condition as specified in the Technical Specifications
P	=	Purification flow rate (gal/min) (includes unidentified and identified RCS leakage)
M	=	RCS mass (g)
C	=	Conversion factor (62.51 g•min/gal•sec)
λ_{decay}	=	Radioactive decay constant of iodines (sec^{-1})

15A.1.2.3 Noble Gas Inventory

For pre-accident noble gas concentrations, the initial concentration is assumed to be at 2.15 $\times 10^7$ Bq/g (580 μCi/g) DE Xe-133 in the primary system, based on one percent fuel defect. This assumption is conservative because the Technical Specifications restrict the noble gas concentrations in the RCS to less than 1.11 x 10^7 Bq/g (300 μCi/g). The resulting activities are presented in Table 15A-8.

15A.1.2.4 Alkali Metal Inventory

It is possible that alkali metal activities in the RCS are ignored because the dose contribution from alkali metals is insignificant compared to the dose contribution from noble gases that are released directly to the environment without holdup. The alkali metals have a low partition coefficient from the coolant to steam phase so the alkali metal activities released to the environment are significantly reduced and the dose contribution is also negligible.

15A.1.3 Secondary Coolant Source Term

The iodine activity of the secondary coolant system is assumed to be at the Technical Specification limit of 3.7 $\times 10^3$ Bq/g (0.1 μCi/g) DE I-131. This is one-tenth of the maximum equilibrium reactor coolant activities and is given Table 15A-9.

15A.2 Chemical Form

15A.2.1 Containment Airborne Iodine Form

Consistent with NRC RG 1.183, the chemical form of radioiodine released to the containment atmosphere is assumed to be 95 percent cesium iodide (CsI) (i.e., particulate), 4.85 percent elemental iodine, and 0.15 percent organic iodide.

15A.2.2 Steam Generator Release Iodine Form

Consistent with NRC RG 1.183, the iodine releases from the steam generators to the environment are assumed to be 97 percent elemental and 3 percent organic.

15A.3 General Activity Transport Model

15A.3.1 Activity Transport from Containment

For LOCA and CEA ejection accidents, radionuclides are released within the containment and are assumed to mix instantaneously and homogeneously throughout the free air volume of the primary containment. Radionuclides within the containment escape to the environment through leakages. During the first 24 hours the containment is assumed to leak at its maximum Technical Specification leak rate of 0.1 volume percent per day and at 50 percent of this leak rate (i.e., 0.05 volume percent per day) for the remaining duration of the accident.

15A.3.2 Activity Transport from Steam Generators

The amount of the P-T-S leakage through the SG tubes is assumed to be 2.27 L/min (0.6 gpm) as specified as an LCO in the Technical Specifications. For the events that the P-T-S leakage through any one SG is used, a value of 1.135 L/min (0.3 gpm) is applied because the TS LCO also limits the leakage from each SG below a half of the total allowable limit.

When the primary coolant is discharged through the leaking SG tubes, the radioactivity released to the environment is dependent on the extent of submergence of the SG tubes. During the transient, the SG U-tubes can be at one of the following conditions:

a. Dryout

b. Partial uncovery

c. Total submergence

During the period of steam generator dryout such as MSLB, all of the P-T-S leakage is assumed to flash to vapor and be released directly to the environment with no concurrent mitigation at the initiation of the event.

If the secondary side water uncovers the SG tubes a portion of the P-T-S leakage flashes to vapor. The flashing fraction is determined based on the thermal hydraulic conditions in

the primary and secondary coolant. The leakage that flashes to vapor is assumed to rise through the bulk water of the SG and enter the steam space without any credit for removal.

For the cases of unaffected SG, of which tubes are fully submerged by the secondary water, the P-T-S leakage is assumed to mix with the secondary water without flashing during period of total tube submergence. The radioactivity in the bulk water is assumed to become vapor at a rate that is the function of the steaming rate and the partition coefficient. A partition coefficient for iodine of 100 is assumed.

15A.3.3 Activity Transport from Spent Fuel Pool

The DFs for the elemental and organic iodine in the pools are 500 and 1, respectively, because the depth of water above the stored spent fuel is designed to be 7.0 m (23 ft) or greater. This DFs result in overall effective DF of 200, which means that 99.5 percent of the total iodine released from the failed fuel rods is retained in the pool water.

Noble gases are released out of the pool surface without scrubbing. Particulate radionuclides are assumed to be retained by the water in the fuel pool or refueling pool (i.e., infinite decontamination factor).

15A.3.4 Flashing Fraction

The flashing fraction, the portion of discharged fluids that flashes to vapor, is calculated based on the enthalpy difference under circumstance of coolant leakage by assuming the leakage to be constant enthalpy process and expressed as follows:

$$\text{Flashing fraction (FF)} = \frac{h_{f_1} - h_{f_2}}{h_{fg}}$$

Where,

h_{f_1} = Enthalpy at system temperature and pressure before leaking from a component

h_{f_2} = Enthalpy at saturation condition after leaking from a component

h_{fg} = Enthalpy of steam at saturation condition after leaking from a component

The fraction of total iodines and alkalis in the liquid that becomes airborne and is available for release to the atmosphere without credit for plateout is conservatively assumed to be equal to the fraction of the coolant leakage that flashes to vapor in the depressurization process.

If the temperature of the leakage is less than 100 °C or the calculated flashing fraction is less than 10 percent, the amount of iodine that becomes airborne is assumed to be 10 percent of the total iodine activity in the leaked fluid.

All noble gases released from the primary system are assumed to be released to the environment without reduction or mitigation.

15A.3.5 Airborne Radioactivity Removal Mechanism

Airborne radioactivity removal coefficients are addressed in Subsection 15.6.5.5.

15A.4 Event-specific Activity Transport Model

15A.4.1 Steam Line Break

Radioiodines initially contained in the primary coolant transfer to the SG through the SG tube leaks,. The secondary coolant releases directly to the environment through the ruptured steam line. A portion of the iodine activity initially contained in the unaffected SG, and noble gas and iodine activities due to SG tube leakage is released to environment through ADVs or MSSVs. The primary coolant discharged to IRWST through POSRV during the accident is released to the environment due to containment leakage. The appropriate partitioning coefficient, flashing fraction, and iodine spiking effects are considered for dose calculation. More specific evaluation model, assumptions, and input data used for this event are discussed in Subsection 15.1.5.5. The activity transport paths from containment, the affected and unaffected SGs to the environment (or the main control room) for the event are illustrated in Figure 15A-1.

15A.4.2 Feedwater Line Break

For the affected SG, radioiodines contained in the primary leaking through SG tubes and those in the secondary coolant are released to the containment through the break in the feedwater line. Throughout the event, P-T-S leakage entering the affected SG is conservatively assumed to be directly released to the environment through the MSSVs. The unaffected SG releases steam when the intact SG MSSVs and ADVs open. The RCS fluid is released to the IRWST located inside containment through POSRV during the accident and from there is released to the environment due to the containment leakage. The appropriate partitioning coefficient, flashing fraction, and iodine spiking effects are considered for dose calculation. More specific evaluation models, assumptions, and input data used for this event are discussed in Subsection 15.2.8.5. The activity transport paths from the feedwater line break through the containment building, and the P-T-S leakage through the two SGs and to the environment (or the main control room) through MSSV and ADV steaming are illustrated in Figure 15A-2.

15A.4.3 Reactor Coolant Pump Rotor Seizure

Prior to a LOOP following an RCP rotor seizure event, the contaminated secondary steam in the unaffected and affected SGs is released to the environment through the condenser. The contaminated secondary steam is then released to the environment through the ADVs or the MSSVs because the condenser is unavailable. Activity release from the secondary system is based on the initial activity of the secondary side in the SGs plus the initial primary activity and the failed fuel gap activity resulting from the SG tube design leakage. The appropriate partitioning coefficient, flashing fraction, and fuel failure rate are considered for the dose calculation. More specific evaluation model, assumptions, and input data used for this event are discussed in Subsection 15.3.3.5. The activity transport paths from the affected and unaffected SGs to the environment (or the main control room) for the event are illustrated in Figure 15A-3.

15A.4.4 CEA Ejection Accident

Radiological consequences for this event are calculated for two release cases: containment leakage and release through the secondary system. For containment leakage, all of the activities in the gap of the failed fuel clad are assumed to be instantaneously mixed throughout the containment and available for leakage to the environment. Reduction in airborne radioactivity in the containment by the ESF systems or by natural deposition within containment may be credited to mitigate airborne radioactive material within the containment. For release through the secondary system, activity release from the secondary system is based on the initial activity of the secondary side in the SGs plus the initial primary activity and the failed fuel gap activity resulting from the SG tube design leakage. The appropriate partitioning coefficient, flashing fraction, and fuel failure rate are considered for the dose calculation. More specific evaluation models, assumptions, and input data used for this event are described in Subsection 15.4.8.5. The activity transport paths from the containment or both SGs to the environment (or the main control room) for the event are illustrated in Figure 15A-4.

15A.4.5 Failure of Small Lines Carrying Primary Coolant Outside Containment

Primary coolant activities from a double-ended break of the letdown line outside the containment are discharged into the auxiliary building. The primary coolant is then released from the auxiliary building. The analysis does not take credit for the filtration of

radioactivity by the auxiliary building ventilation system or for ground deposition of the activity that escapes the auxiliary building. Prior to the manual trip for the reactor and the turbine by operators, the contaminated secondary steam in both SGs is released to the environment through the condenser. The secondary inventories from the SGs are conservatively assumed to be released to the environment even though offsite power is available. The appropriate partitioning coefficient, flashing fraction, and iodine spike effects are considered for dose calculation. More specific evaluation models, assumptions, and input data used for this event are addressed in Subsection 15.6.2.5. The activity transport paths from the containment or both SGs to the environment (or the main control room) for the event are illustrated in Figure 15A-5.

15A.4.6 Steam Generator Tube Rupture

Prior to the LOOP following an SGTR event, the contaminated secondary steam in the unaffected and affected steam generators is released to the environment through the condenser. The steam is then released to the environment through the ADVs or MSSVs because the condenser is unavailable. The radioactivities released to environment contain the secondary-side activity, primary coolant activity leaked from the ruptured SG, and SG design leakage from the unaffected SG. The appropriate partitioning coefficient, flashing fraction, and iodine spiking effects are considered for the dose calculation. More specific evaluation models, assumptions, and input data used for this event are addressed in Subsection 15.6.3.5. The activity transport paths from the affected and unaffected SGs to the environment (or the main control room) for the SGTR event are illustrated in Figure 15A-6.

15A.4.7 LOCA

Following a LOCA event, radioactivity is released from the fuel into the containment using the timing and release fractions from Table 15.6.5-13, which is followed by release from the containment into the environment through the containment low-volume purge system and containment leakage. Once the ESFs are actuated, radioactivity in the IRWST solution may be released to the environment by means of leakage from ESF equipment into the auxiliary building. A reduction in airborne radioactivity in the containment by ESF systems or natural deposition within the containment may be credited to mitigate airborne radioactive material within containment. More specific evaluation models, assumptions,

and input data used for this event are addressed in Subsection 15.6.5.5. The activity transport paths are illustrated in Figure 15A-7.

15A.4.8 Fuel Handling Accident

This accident may take place either in the containment or in the spent fuel pool (SFP) inside the fuel handling area inside the auxiliary building. The same accident scenario is used for the two potential locations of the fuel handling accident (FHA). Radioactive material that escapes the spent fuel pool is assumed to be released to the environment without any credit for the filtration of radioactivity from the fuel handling area emergency ventilation system. More specific evaluation models, assumptions, and input data used for this event are described in Subsection 15.7.4. The activity transport paths from fuel pool to the environment (or the main control room) for the event are illustrated in Figure 15A-8.

15A.5 Dose Calculation Methodology

15A.5.1 Atmospheric Dispersion Factor

Accident atmospheric dispersion factors (χ/Q) for the exclusion area boundary and the low population zone are used to calculate the potential offsite doses. The representative χ/Q values are determined as described in Subsection 2.3.4 and are given in Table 2.3-1. Main control room χ/Q values are also addressed in Subsection 2.3.4 and given in Tables 2.3-2 through 2.3-13.

15A.5.2 Dose Conversion Factor

15A.5.2.1 Immersion Dose Conversion Factor

Consistent with NRC RG 1.183, effective dose equivalent (EDE) is used in determining the contribution of external dose to the TEDE. This calculation models the EDE dose conversion factors in the column headed "effective" in Table III.1 of Federal Guidance Report 12, "External Exposure to Radionuclides in Air, Water, and Soil," (Reference 3). The dose conversion factors for calculation of EDE doses are shown in Table 15A-10.

15A.5.2.2 Inhalation Dose Conversion Factor

Consistent with NRC RG 1.183, the exposure-to-committed effective dose equivalent (CEDE) factors for inhalation of radioactive material are derived from the data provided in ICRP Publication 30, "Limits for Intakes of Radionuclides by Workers." This calculation models the CEDE dose conversion factors in the column headed "effective" yield doses in Table 2.1 of Federal Guidance Report 11, "Limiting Values of Radionuclide Intake and Air Concentration and Dose Conversion Factors for Inhalation, Submersion, and Ingestion," (Reference 4). The dose conversion factors for calculation of CEDE doses are shown in Table 15A-10.

15A.5.3 Breathing Rate

Consistent with NRC RG 1.183, for the first 8 hours, the receptor offsite breathing rate is assumed to be 3.5×10^{-4} m^3/sec after the initiation of the event. From 8 to 24 hours after

the accident, the breathing rate is assumed to be 1.8×10^{-4} m^3/sec. After 24 hours and until the end of the accident, the rate is assumed to be 2.3×10^{-4} m^3/sec. For the control room, the breathing rate of the individual is assumed to be 3.5×10^{-4} m^3/sec during the entire period of the accident. These breathing rates are listed in Table 15A-11.

15A.5.4 Offsite Dose Calculation Method

15A.5.4.1 Assumptions

The following assumptions are used in modeling the external effective dose equivalent from immersion in a cloud of radioactivity and the internal effective dose equivalent from inhalation of radioactivity.

a. The dose contribution of direct radiation from sources other than the leakage cloud is negligible compared to the dose due to immersion in the leakage cloud

b. All radioactivity releases are treated as ground level releases regardless of the point of release

c. Radioactive decay from the point of release to the dose receptor is neglected

15A.5.4.2 Immersion Dose

The EDE is obtained by considering the dose receptor to be immersed in a radioactive cloud which is infinite in all directions above the ground plane (i.e., a semi-infinite cloud).

The concentration of radioactive material within this cloud is considered to be uniform and equal to the maximum centerline ground level concentration.

The external effective dose equivalent is a result of exposure to external gamma radiation. The EDE due to immersion in a semi-infinite cloud is given by the following equation:

$$D_E = \chi/Q \cdot \sum_i (Q_i \cdot DCF_{E,i})$$

Where:

D_E = external effective dose from immersion in a semi-infinite cloud for a given time period, Sv

Q_i = activity of isotope i released during a given time period, Bq

χ/Q = atmospheric dispersion factor for a given time period, sec/m^3

$DCF_{E,i}$ = external effective dose conversion factor for isotope i, Sv-m^3/Bq-sec

15A.5.4.3 Inhalation Dose

The CEDE from inhalation is obtained from the following expression:

$$D_c = \chi/Q \cdot B \cdot \sum_i (Q_i \cdot DCF_{C,i})$$

Where:

D_c = internal effective dose due to inhalation, Sv

χ/Q = atmospheric dispersion factor for a given time period, sec/m^3

B = breathing rate for a given time period, m^3/sec

Q_i = activity of isotope i released for a given time period, Bq

$DCF_{C,i}$ = internal effective dose conversion factor for isotope i, Sv/Bq inhaled

15A.5.4.4 Total Effective Dose Equivalent

The total effective dose equivalent (TEDE) doses are the sum of the EDE and the CEDE doses.

15A.5.5 Main Control Room Dose Calculation Method

The CEDE and EDE models for the major contributors to the main control room (MCR) dose are described below. The dose to the MCR occupants due to a postulated accident is calculated on the basis of source strength, atmospheric transport, and MCR emergency pressurization and filtration as illustrated in the following equations.

15A.5.5.1 Immersion Dose

The EDE due to inflow into MCR is calculated using the following equation:

$$D_{EL} = CV^{0.338} \sum_{i} DCF_{E,i} \cdot A_i$$

Where:

D_{EL}	=	external effective dose due to inflow into MCR, Sv
V	=	volume of MCR, m^3
A_i	=	time integrated concentration of isotope i, Bq-sec/m^3
$DCF_{E,i}$	=	external effective dose conversion factor for isotope i, Sv-m^3/Bq-sec
C	=	conversion constant (8.525E-04)

The EDE to MCR personnel due to a cloud external to the MCR is calculated using the following equation:

$$D_{EC} = \sum_{j} \left(\chi/Q_j \cdot \sum_{i} A_{ij} \cdot CF_i \right)$$

Where:

D_{EC}	=	external effective dose due to external cloud shine, Sv
χ/Q_j	=	atmospheric dispersion factor for the time period j, sec/m^3
A_{ij}	=	total activity of isotope i released during time period j, Bq
CF_i	=	a dose rate response function for a unit concentration of nuclide i, Sv-m^3/Bq-sec

15A.5.5.2 Inhalation Dose

The CEDE from inhalation is obtained from the following expression:

$$D_c = \sum_{i} BR \cdot DCF_{C,i} \cdot A_i$$

Where:

D_c	=	internal effective dose from inhalation, Sv
BR	=	breathing rate, m^3/sec
$DCF_{c,i}$	=	internal effective dose conversion factor for isotope i, Sv/Bq inhaled
A_i	=	time integrated concentration of isotope i, Bq-sec/m^3

15A.5.5.3 Total Effective Dose Equivalent

The TEDE doses are the sum of the EDE and the CEDE doses.

15A.6 RADTRAD Computer Code

For the analysis of the radiological consequences, RADionuclide Transport, Removal, And Dose (RADTRAD) computer code Version 3.03 (Reference 5) is used. RADTRAD Code is designed to calculate doses at offsite locations, as well as onsite locations such as main control room due to postulated radioactivity releases from design basis accident conditions. The code calculates dose consequences for different time intervals based on user-input information on the amount, form, and species of the radioactive material released in the nuclear power plant.

RADTRAD Code has two optional source terms to describe fission product release from the RCS to the containment: those from TID-14844 (Reference 6) and those from NUREG-1465 (Reference 7). The code uses a compartment model and simulates radioactive material transport through the containment and related systems, structures, and components. The user can account for sprays and natural mechanisms that would reduce the quantity of radioactive material that is transported out of the reactor complex and to various specified offsite and onsite locations. Material can flow between buildings, from buildings to the environment, or into the main control room through filters, piping, or other connectors. An accounting of the amount of radioactive material retained due to these tortuous pathways is maintained. Decay and in-growth of daughters can be calculated over time as the material is transported.

The governing equation for the number of atoms of nuclide n, in compartment i, during time step m is provided with all source and sink terms as given in the equation below.

$$\frac{d}{dt}N_{n,i}^{m} = \sum_{v=1}^{n-1}\beta_{n,v}\, N_{v,i}^{m}\, \lambda_v + S_{n,i}^{m}$$

$$-\left[\sum_{\substack{j=1\\ j\neq i}}^{L}\left|F_{i,j(conv)}^{m} + \frac{Q_{i,j(s)}^{m}}{Vol_i} + \frac{Q_{i,j(p)}^{m}}{Vol_i}\right| + \lambda_n + \lambda_{spr,n}^{m}(t) + \lambda_{dep,n}^{m}(t) + \frac{\eta_{n:i,j}^{m}}{100}F_{i,j(forced)}^{m}\right]N_{n,i}^{m}$$

$$+\sum_{\substack{j=1\\ j\neq i}}^{L}\left[\left(1-\frac{\eta_{n:i,j}^{m}}{100}\right)F_{i,j(forced)}^{m} + F_{i,j(conv)}^{m} + \frac{Q_{i,j(s)}^{m}}{Vol_j DF_{n(s)}^{m}} + \frac{Q_{i,j(p)}^{m}}{Vol_j DF_{n(p)}^{m}}\right]N_{n,j}^{m}$$

$$\lambda_n = ln(2)\,/\,T_n^{1/2}$$

Where:

$N_{n,i}^{m}$ = number of atoms of nuclide n in compartment i during time step m

$\beta_{n,v}$ = fraction of nuclide that decays to nuclide n (dimensionless)

λ_n = radiological decay constant for nuclide n (s^{-1})

$T_n^{1/2}$ = half-life of nuclide n (s)

$F_{i,j(conv)}^{m}$ = volume-normalized convective (leakage) air flow rate from compartment j to i (s^{-1})

$F_{i,j(forced)}^{m}$ = volume-normalized forced air flow rate from compartment j to i (s^{-1})

L = number of compartments defined in the plant model

$Q_{i,j(s)}^{m}$ = volumetric flow rate from compartment j to i through a suppression pool (m^3/s)

$Q_{i,j(p)}^{m}$ = volumetric flow rate from compartment j to i through a pipe (m^3/s)

Vol_k = volume of compartment k (m^3)

$DF_{n(s)}^{m}$ = suppression pool decontamination factor for nuclide n during time step m (dimensionless)

$DF_{n(p)}^{m}$ = piping decontamination factor for nuclide n during time step m (unitless)

$\lambda_{spr,n}^{m}(t)$ = time-dependent spray removal coefficient for nuclide n (s^{-1})

$\lambda_{dep,n}^{m}(t)$ = time-dependent natural deposition removal rate coefficient for nuclide n (s^{-1})

$S_{n,i}^{m}$ = source injection rate of nuclide n to compartment i during time step m (atoms/s)

$\eta_{n:i,j}^{m}$ = filter efficiency associated with nuclide n and the pathway from j to i (percent)

15A.7 References

1. NRC NUREG/CR-0200, “ORIGEN-S: SCALE System Module to Calculate Fuel Depletion, Actinide Transmutation, Fission Product Buildup and Decay, and Associated Radiation Source Terms,” Rev. 6, ORNL, September 1998.

2. NRC RG 1.183, “Alternative Radiological Source Terms for Evaluating Design Basis Accidents at Nuclear Power Reactors,” July 2000.

3. U.S. EPA, Federal Guidance Report No. 12, EPA 402-R-93-081, “External Exposure to Radionuclides in Air, Water, and Soil,” September 1993.

4. U.S. EPA, Federal Guidance Report No. 11, EPA 520/1-88-020, “Limiting Values of Radionuclide Intake and Air Concentration and Dose Conversion Factors for Inhalation, Submersion, and Ingestion,” September 1993.

5. U.S. NRC NUREG/CR-6604, “RADTRAD: A Simplified Model for RADionuclide Transport and Removal and Dose Estimation,” SNL, December 1997.

6. TID-14844, “Calculation of Distance Factors for Power and Test Reactor Sites, U.S. Atomic Energy Commission,” 1962.

7. U.S. NRC NUREG-1465, “Accident Source Terms for Light Water Nuclear Power Plants,” February 1995.

8. U.S. NRC NUREG-0800, U.S. Nuclear Regulatory Commission, Standard Review Plan, Section 4.2, Revision 3, Appendix B, Fuel System Design, March 2007.

Table 15A-1 (1 of 2)

Maximum Core Fission Product Inventories
(Core Power: 4,062.66 MWt, Burnup: 56.4 GWD/MTU)

Nuclides	Core Inventory (Bq)	Nuclides	Core Inventory (Bq)
Co-58(1)	-	Sb-127	4.32×10^{17}
Co-60(1)	-	Sb-129	1.48×10^{18}
Kr-85	5.86×10^{16}	Te-127	4.28×10^{17}
Kr-85M	1.58×10^{18}	Te-127M	7.21×10^{16}
Kr-87	3.23×10^{18}	Te-129	1.41×10^{18}
Kr-88	4.57×10^{18}	Te-129M	2.88×10^{17}
Rb-86	1.29×10^{16}	Te-131M	9.42×10^{17}
Sr-89	5.71×10^{18}	Te-132	6.28×10^{18}
Sr-90	5.13×10^{17}	I-131	4.43×10^{18}
Sr-91	7.68×10^{18}	I-132	6.42×10^{18}
Sr-92	7.75×10^{18}	I-133	9.37×10^{18}
Y-90	5.41×10^{17}	I-134	1.07×10^{19}
Y-91	7.00×10^{18}	I-135	8.84×10^{18}
Y-92	7.82×10^{18}	Xe-133	9.33×10^{18}
Y-93	5.61×10^{18}	Xe-135	2.80×10^{18}
Zr-95	8.18×10^{18}	Cs-134	1.38×10^{18}
Zr-97	7.77×10^{18}	Cs-136	3.55×10^{17}
Nb-95	8.15×10^{18}	Cs-137	7.65×10^{17}
Mo-99	8.53×10^{18}	Ba-139	8.77×10^{18}
Tc-99M	7.51×10^{18}	Ba-140	8.68×10^{18}
Ru-103	5.89×10^{18}	La-140	8.70×10^{18}
Ru-105	3.48×10^{18}	La-141	8.00×10^{18}
Ru-106	5.27×10^{18}	La-142	7.81×10^{18}

(1) Co-58 and Co-60 activities, 2.55×10^2 Ci/MW_t and 1.95×10^2 Ci/MW_t, respectively, are conservatively assumed to be added into the LOCA radiological consequence analysis, which is obtained from the RADTRAD User's Manual, Table 1.4.3.2-2.

Table 15A-1 (2 of 2)

Nuclides	Core Inventory (Bq)	Nuclides	Core Inventory (Bq)
Rh-105	5.27×10^{18}	Ce-141	7.81×10^{18}
Ce-143	7.98×10^{18}	Pu-239	1.40×10^{15}
Ce-144	5.67×10^{18}	Pu-240	2.63×10^{15}
Pr-143	7.80×10^{18}	Pu-241	7.40×10^{17}
Nd-147	3.13×10^{18}	Am-241	7.96×10^{14}
Np-239	1.03×10^{20}	Cm-242	3.99×10^{17}
Pu-238	2.91×10^{16}	Cm-244	5.68×10^{16}

Table 15A-2

Fraction of Fission Product Inventory in Gap

Nuclides		Fraction of Core Inventory		
		LOCA	Non-LOCA	
			Non-CEA Ejection	CEA Ejection
Noble gases	Kr-85	0.05	0.10	0.10
	Others	0.05	0.05	0.10
Halogens	I-131	0.05	0.08	0.10
	Others	0.05	0.05	0.0
Alkali metals	All	0.05	0.12	0.0

Table 15A-3

Reactor Coolant Iodine Concentrations for Various Conditions

Nuclides	1.0 % Failed Fuel RCS Iodine Activity Concentration (Bq/g)	3.7×10^4 Bq/g (1.0 μCi/g) DE I-131 Activity Concentration (Bq/g)	2.2×10^6 Bq/g (60 μCi/g) DE I-131 Activity Concentration (Bq/g)
I-131	9.92×10^4	2.93×10^4	1.76×10^6
I-132	2.66×10^4	7.88×10^3	4.72×10^5
I-133	1.41×10^5	4.16×10^4	2.50×10^6
I-134	1.63×10^4	4.81×10^3	2.89×10^4
I-135	7.99×10^4	2.37×10^4	1.42×10^6

Table 15A-4

Iodine Appearance Rates for Event-generated Iodine Spike (Steam Line Break)

Nuclides	3.7×10^4 Bq/g (1.0 μCi/g) DE I-131 Activity (Bq)	Decay Constant (sec^{-1})	Letdown Purification Removal Rate (sec^{-1})	500 Times of Iodine Appearance Rate (Bq/sec)
I-131	8.05×10^{12}	9.98×10^{-7}	2.00×10^{-5}	8.43×10^{10}
I-132	2.16×10^{12}	8.37×10^{-5}	2.00×10^{-5}	1.12×10^{11}
I-133	1.14×10^{13}	9.26×10^{-6}	2.00×10^{-5}	1.67×10^{11}
I-134	1.32×10^{12}	2.20×10^{-4}	2.00×10^{-5}	1.58×10^{11}
I-135	6.49×10^{12}	2.91×10^{-5}	2.00×10^{-5}	1.59×10^{11}

Table 15A-5

Iodine Appearance Rates for Event-generated Iodine Spike
(Steam Generator Tube Rupture)

Nuclides	3.7×10^4 Bq/g (1.0 μCi/g) DE I-131 Activity (Bq)	Decay Constant (sec^{-1})	Letdown Purification Removal Rate (sec^{-1})	335 Times of Iodine Appearance Rate (Bq/sec)
I-131	8.80×10^{12}	9.98×10^{-7}	1.90×10^{-5}	5.91×10^{10}
I-132	2.36×10^{12}	8.37×10^{-5}	1.90×10^{-5}	8.14×10^{10}
I-133	1.25×10^{13}	9.26×10^{-6}	1.90×10^{-5}	1.18×10^{11}
I-134	1.44×10^{12}	2.20×10^{-4}	1.90×10^{-5}	1.15×10^{11}
I-135	7.10×10^{12}	2.91×10^{-5}	1.90×10^{-5}	1.15×10^{11}

Table 15A-6

Iodine Appearance Rates for Event-generated Iodine Spike
(Failure of Small Lines Carrying Primary Coolant Outside Containment)

Nuclides	3.7×10^{4} Bq/g (1.0 μCi/g) DE I-131 Activity (Bq)	Decay Constant (sec^{-1})	Letdown Purification Removal Rate (sec^{-1})	500 Times of Iodine Appearance Rate (Bq/sec)
I-131	8.58×10^{12}	9.98×10^{-7}	1.89×10^{-5}	8.55×10^{10}
I-132	2.30×10^{12}	8.37×10^{-5}	1.89×10^{-5}	1.18×10^{11}
I-133	1.22×10^{13}	9.26×10^{-6}	1.89×10^{-5}	1.72×10^{11}
I-134	1.41×10^{12}	2.20×10^{-4}	1.89×10^{-5}	1.68×10^{11}
I-135	6.92×10^{12}	2.91×10^{-5}	1.89×10^{-5}	1.66×10^{11}

Table 15A-7

Iodine Appearance Rates for Event-generated Iodine Spike (Feedwater Line Break)

Nuclides	3.7×10^4 Bq/g (1.0 μCi/g) DE I-131 Activity (Bq)	Decay Constant (sec^{-1})	Letdown Purification Removal Rate (sec^{-1})	500 Times of Iodine Appearance Rate (Bq/sec)
I-131	8.45×10^{12}	9.98×10^{-7}	1.92×10^{-5}	8.54×10^{10}
I-132	2.27×10^{12}	8.37×10^{-5}	1.92×10^{-5}	1.17×10^{11}
I-133	1.20×10^{13}	9.26×10^{-6}	1.92×10^{-5}	1.71×10^{11}
I-134	1.39×10^{12}	2.20×10^{-4}	1.92×10^{-5}	1.66×10^{11}
I-135	6.82×10^{10}	2.91×10^{-5}	1.92×10^{-5}	1.65×10^{11}

Table 15A-8

Primary Coolant Noble Gas Concentration at Various Conditions

Nuclides	1.0 % Fuel Defect RCS Noble Gas Concentration[(1)] (Bq/g)	1.1 × 107 Bq/g (300 μCi/g) DE Xe-133 Noble Gas Concentration (Bq/g)
Kr-85	1.78×10^5	9.19×10^4
Kr-85M	4.14×10^4	2.14×10^4
Kr-87	3.26×10^4	1.68×10^4
Kr-88	9.03×10^4	4.67×10^4
Xe-131m	1.78×10^5	9.19×10^4
Xe-133	1.15×10^7	5.97×10^6
Xe-133m	1.08×10^4	5.59×10^3
Xe-135	2.37×10^5	1.22×10^5
Xe-135m	2.37×10^4	1.22×10^4
Xe-138	2.07×10^4	1.07×10^4

(1) Values for 1.0 % fuel defect are equivalent to 2.15×10^7 Bq/g (580 μCi/g) DE Xe-133.

.

Table 15A-9

Secondary Coolant Iodine Concentrations

Nuclide	Secondary Coolant Activity of 3.7×10^3 Bq/g (0.1 μCi/g) (Bq /g)
I-131	2.93 × 103
I-132	7.88 × 102
I-133	4.16 × 103
I-134	4.81 × 102
I-135	2.37 × 103

Table 15A-10 (1 of 4)

Dose Conversion Factors

Nuclide	EDE Dose Conversion Factor (Sv-m^3/Bq-sec)	CEDE Dose Conversion Factor (Sv/Bq)
Noble Gases		
Kr-85	1.19×10^{-16}	—
Kr-85 m	7.49×10^{-15}	—
Kr-87	4.11×10^{-14}	—
Kr-88	1.02×10^{-13}	—
Xe131m	3.89×10^{-16}	—
Xe133m	1.37×10^{-15}	—
Xe-133	1.56×10^{-15}	—
Xe135m	2.04×12^{-14}	—
Xe-135	1.19×10^{-14}	—
Xe-138	5.76×10^{-14}	—
Halogens		
I-131	1.82×10^{-14}	8.89×10^{-9}
I-132	1.12×10^{-13}	1.03×10^{-10}
I-133	2.95×10^{-14}	1.58×10^{-9}
I-134	1.30×10^{-13}	3.55×10^{-11}
I-135	7.97×10^{-14}	3.32×10^{-10}
Alkali Metals		
Rb-86	4.81×10^{-15}	1.79×10^{-9}
Cs-134	7.57×10^{-14}	1.25×10^{-9}
Cs-136	1.06×10^{-13}	1.98×10^{-9}
Cs-137	7.74×10^{-18}	8.63×10^{-9}

Table 15A-10 (2 of 4)

Nuclide	EDE Dose Conversion Factor (Sv-m^3/Bq-sec)	CEDE Dose Conversion Factor (Sv/Bq)
Barium and Strontium		
Sr-89	7.73×10^{-17}	1.12×10^{-8}
Sr-90	7.53×10^{-18}	3.51×10^{-7}
Sr-91	3.45×10^{-14}	4.55×10^{-10}
Sr-92	6.79×10^{-14}	2.18×10^{-10}
Ba-139	2.17×10^{-15}	4.64×10^{-11}
Ba-140	8.58×10^{-15}	1.10×10^{-9}
Tellurium Group		
Sb-127	3.33×10^{-14}	1.63×10^{-9}
Sb-129	7.14×10^{-18}	1.74×10^{-10}
Te-127	2.42×10^{-16}	8.60×10^{-9}
Te-127m	1.47×10^{-16}	5.81×10^{-9}
Te-129	2.75×10^{-15}	2.09×10^{-11}
Te-129m	1.55×10^{-15}	6.48×10^{-9}
Te-131m	7.01×10^{-14}	1.76×10^{-9}
Te-132	1.03×10^{-14}	2.55×10^{-9}
Noble Metals		
Co-58	4.76×10^{-14}	2.94×10^{-9}
Co-60	1.26×10^{-13}	5.91×10^{-8}
Mo-99	7.28×10^{-15}	1.07×10^{-9}
Tc-99m	5.89×10^{-15}	8.80×10^{-12}
Ru-103	2.25×10^{-14}	2.42×10^{-9}

Table 15A-10 (3 of 4)

Nuclide	EDE Dose Conversion Factor (Sv-m^3/Bq-sec)	CEDE Dose Conversion Factor (Sv/Bq)
Ru-105	3.81×10^{-14}	1.23×10^{-10}
Ru-106	1.04×10^{-14}	1.29×10^{-7}
Rh-105	3.72×10^{-15}	2.58×10^{-9}
Lanthanides		
Y-90	1.91×10^{-16}	2.28×10^{-9}
Y-91	2.61×10^{-16}	1.32×10^{-8}
Y-92	1.30×10^{-14}	2.11×10^{-10}
Y-93	4.80×10^{-15}	5.82×10^{-10}
Zr-95	3.60×10^{-14}	6.39×10^{-9}
Zr-97	9.02×10^{-15}	1.17×10^{-9}
Nb-95	3.74×10^{-14}	1.57×10^{-9}
La-140	1.17×10^{-13}	1.31×10^{-9}
La-141	2.39×10^{-15}	1.57×10^{-9}
La-142	1.44×10^{-13}	6.84×10^{-11}
Pr-143	2.10×10^{-17}	2.19×10^{-9}
Nd-147	6.19×10^{-15}	1.85×10^{-9}
Am-241	8.18×10^{-16}	1.20×10^{-4}
Cm-242	5.69×10^{-18}	4.67×10^{-6}
Cm-244	4.91×10^{-18}	6.70×10^{-5}

Table 15A-10 (4 of 4)

Nuclide	EDE Dose Conversion Factor (Sv-m^3/Bq-sec)	CEDE Dose Conversion Factor (Sv/Bq)
Cerium Group		
Ce-141	3.43×10^{15}	2.42×10^{-9}
Ce-143	1.29×10^{-14}	9.16×10^{-10}
Ce-144	8.53×10^{-16}	1.01×10^{-7}
Np-239	7.69×10^{-15}	6.78×10^{-10}
Pu-238	4.88×10^{-18}	7.79×10^{-5}
Pu-239	4.24×10^{-18}	8.33×10^{-5}
Pu-240	4.75×10^{-18}	8.33×10^{-5}
Pu-241	7.25×10^{-20}	1.34×10^{-6}

Table 15A-11

Breathing Rates

Time from Start of Accident	Breathing Rate (m^3/sec)
Offsite	
0 ~ 8 hrs	3.5×10^{-4}
8 ~ 24 hrs	1.8×10^{-4}
1 ~ 30 days	2.3×10^{-4}
Main Control Room (MCR)	
0 ~ 30 days	3.5×10^{-4}

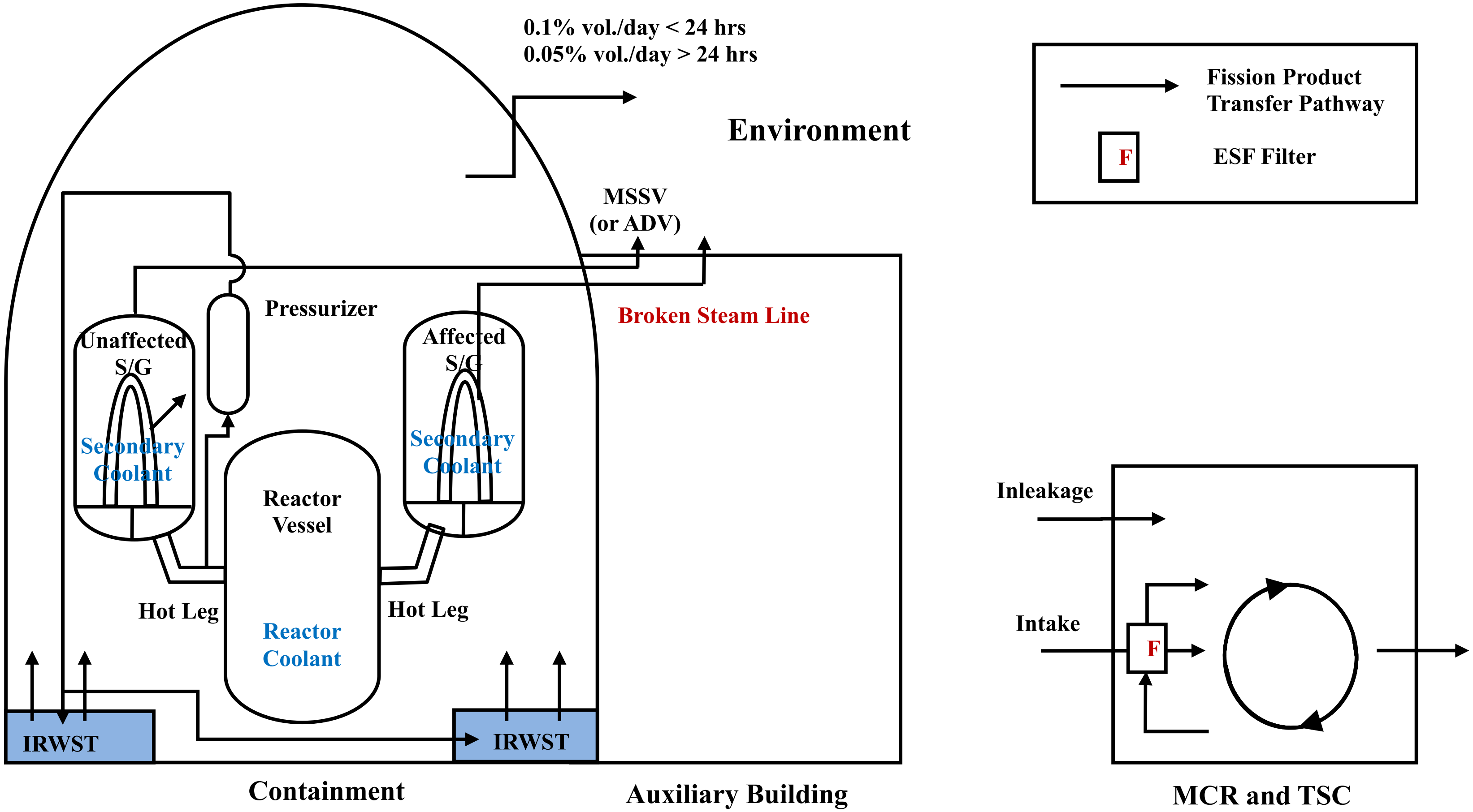

Figure 15A-1 Radioactivity Transport Model for Steam Line Break

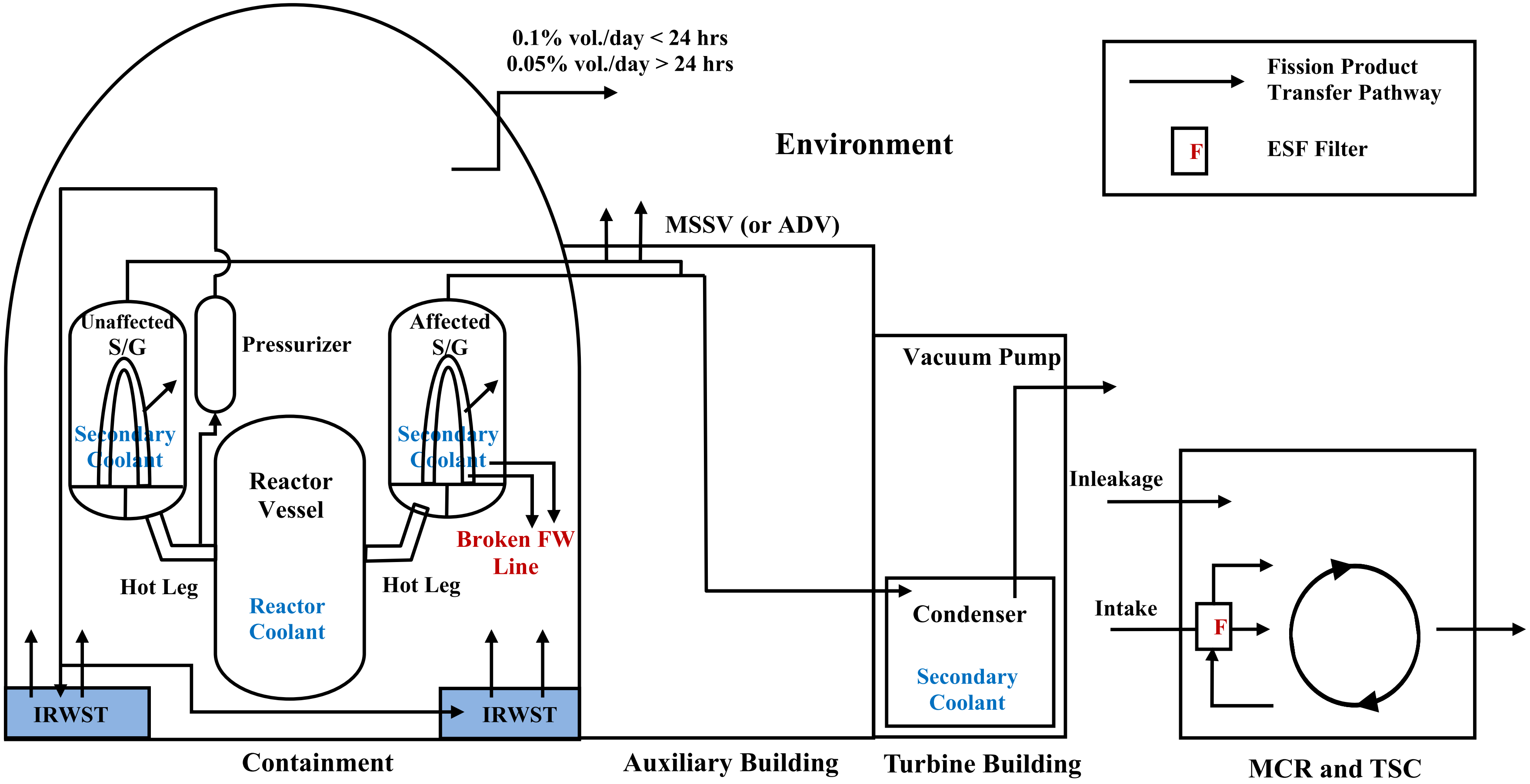

Figure 15A-2 Radioactivity Transport Model for Feedwater Line Break

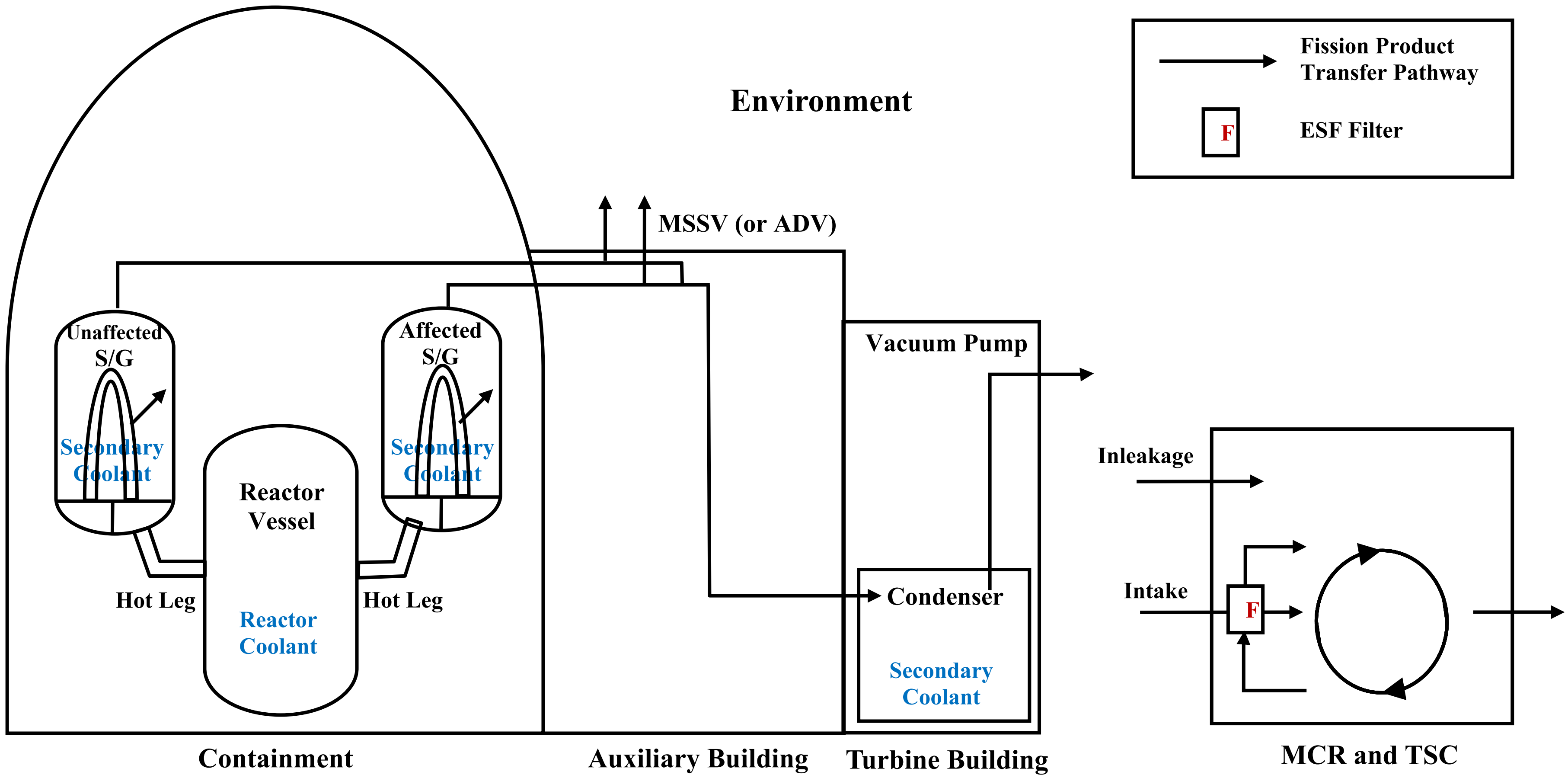

Figure 15A-3   Radioactivity Transport Model for RCP Rotor Seizure

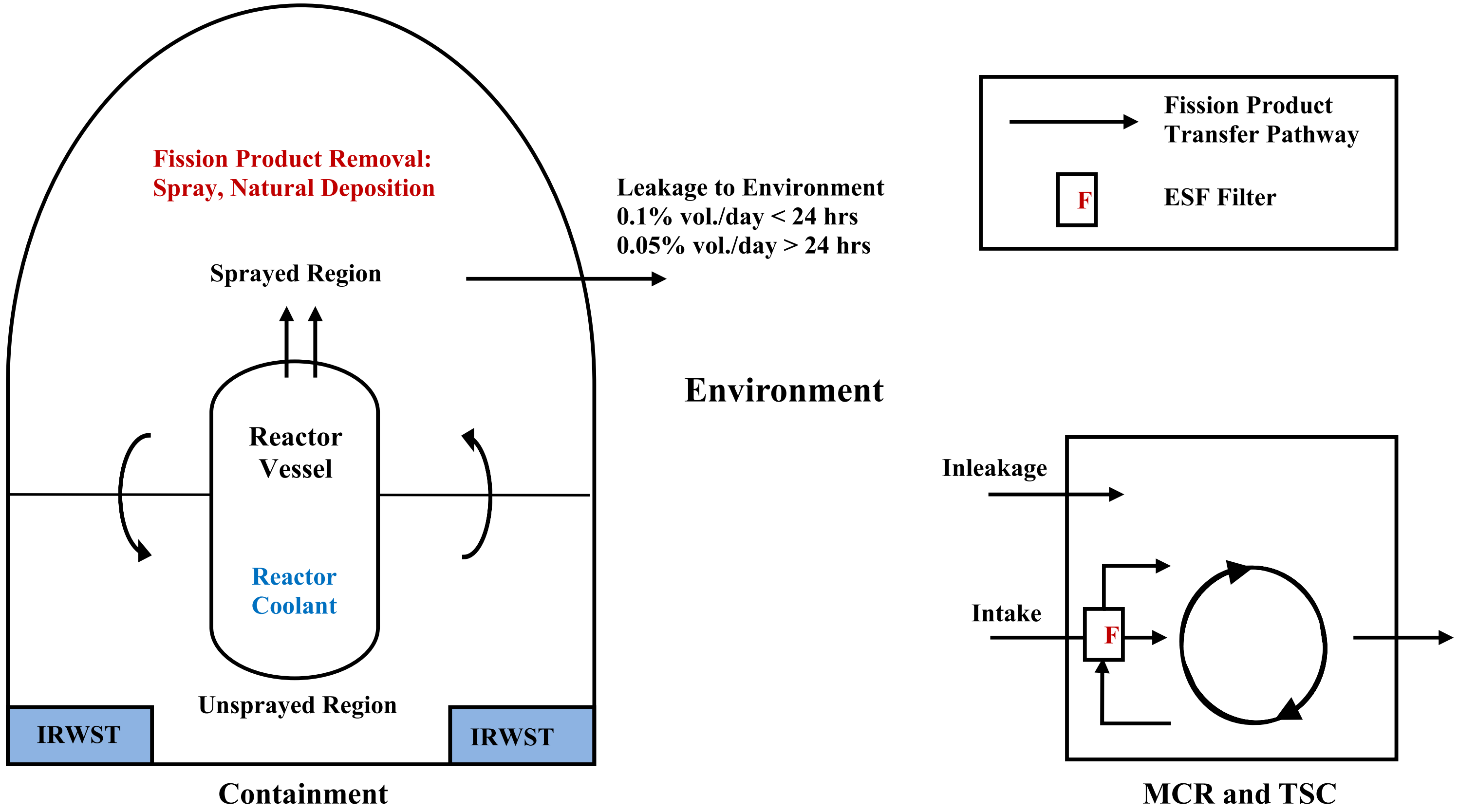

Figure 15A-4 Radioactivity Transport Model for CEA Ejection (1 of 2)

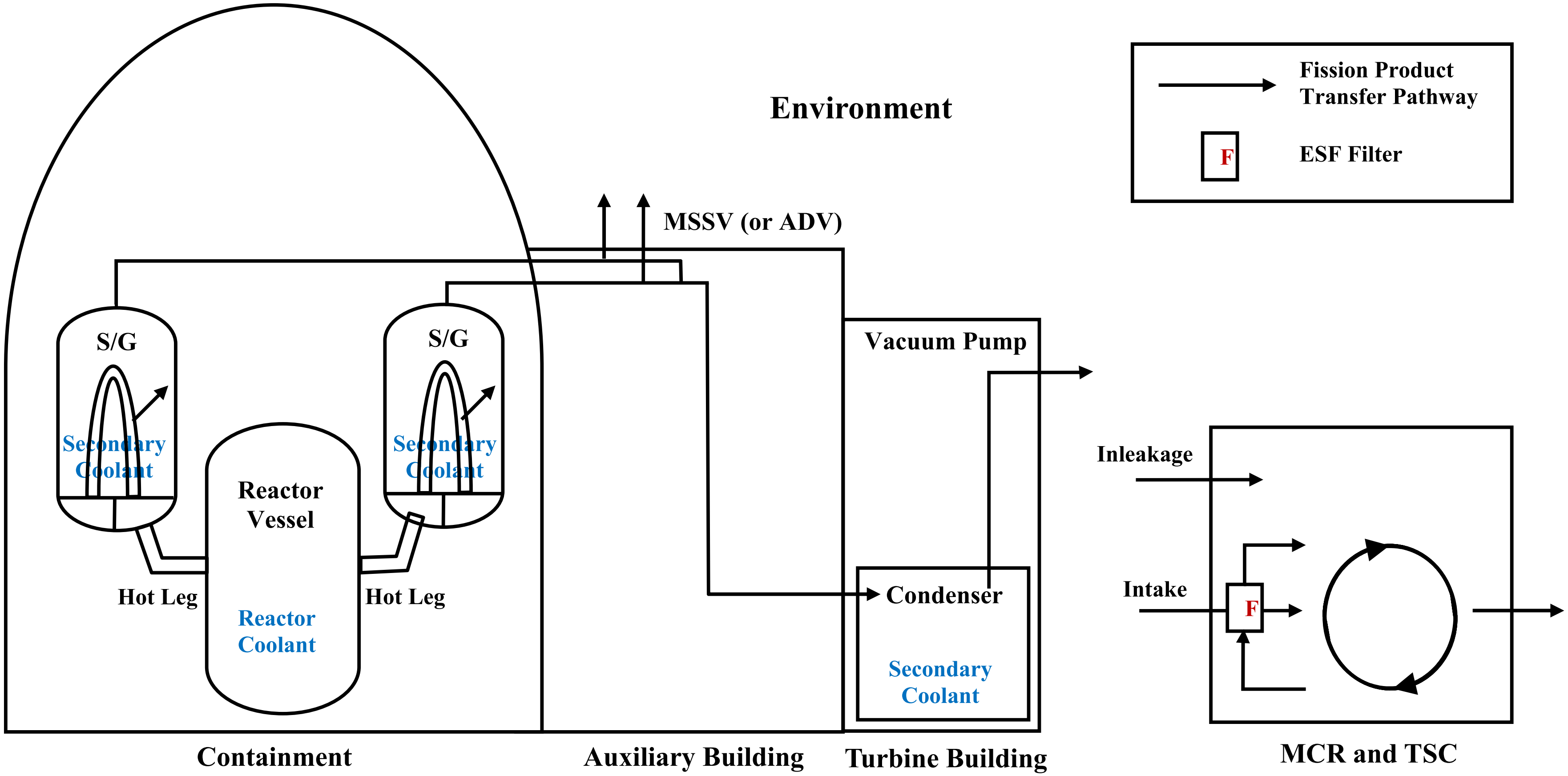

Figure 15A-4 Radioactivity Transport Model for CEA Ejection (2 of 2)

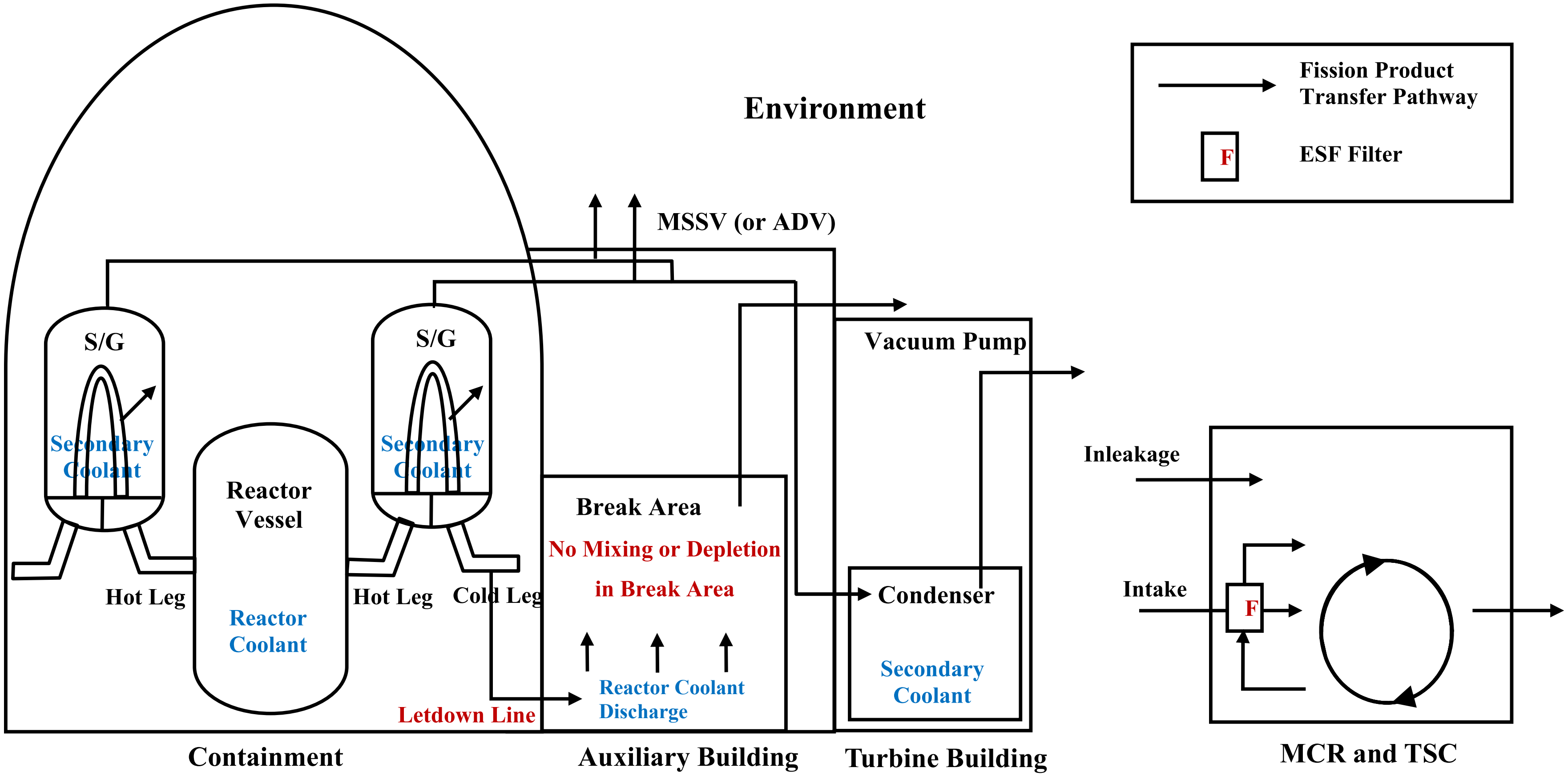

Figure 15A-5 Radioactivity Transport Model for Failure of Small Lines Carrying Primary Coolant Outside Containment

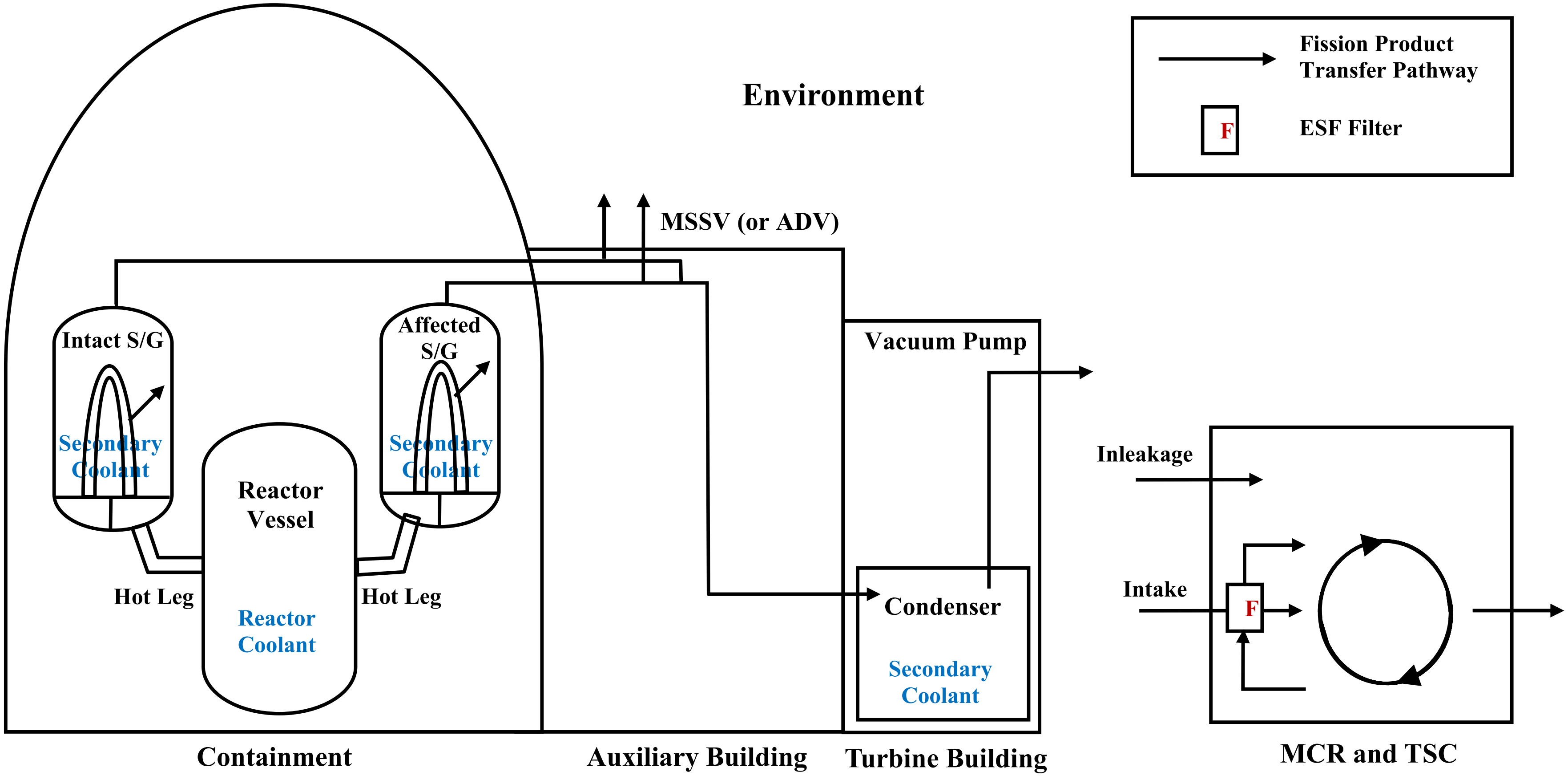

Figure 15A-6 Radioactivity Transport Model for Steam Generator Tube Rupture Accident

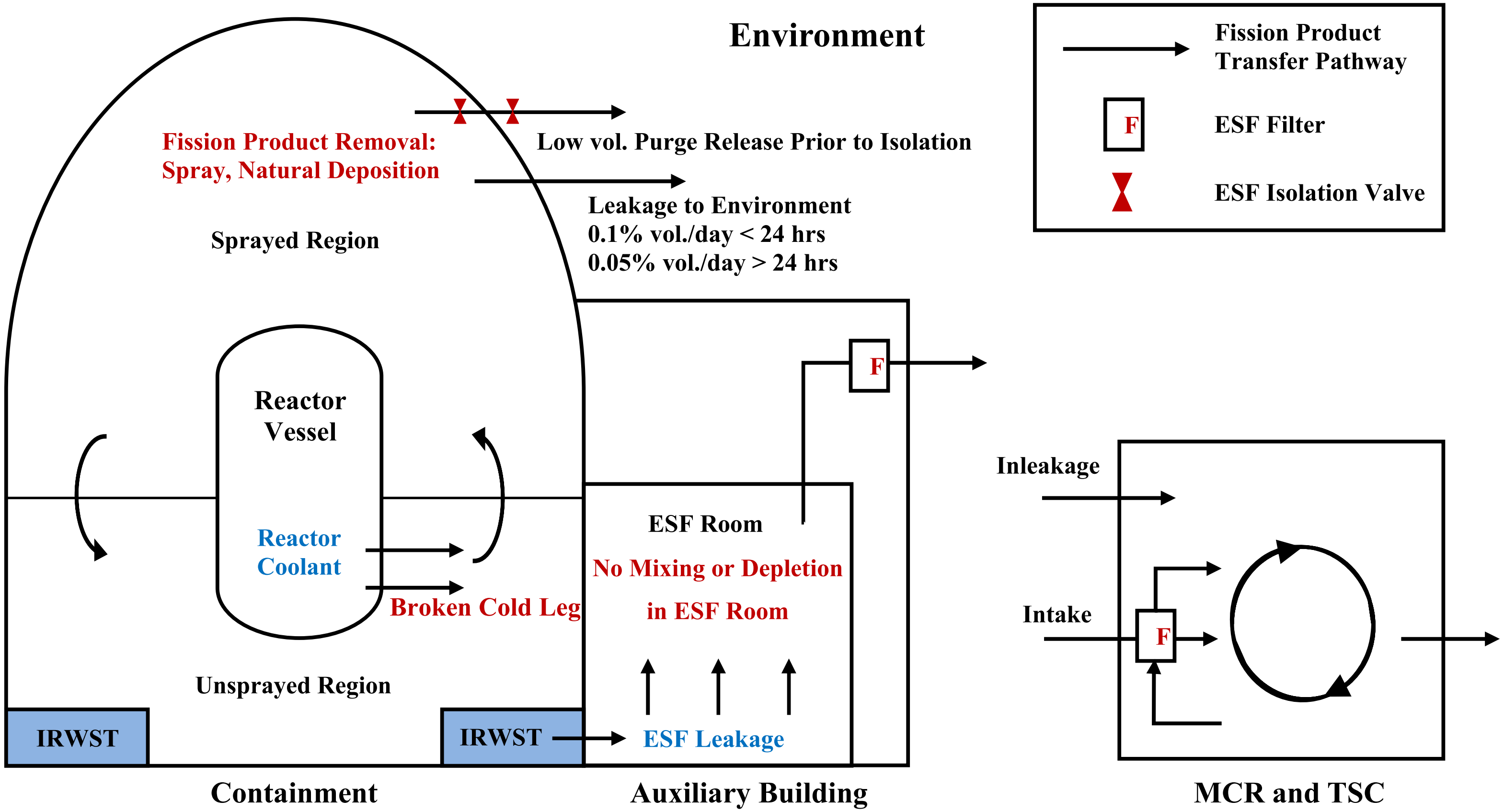

Figure 15A-7 Radioactivity Transport Model for Loss of Coolant Accident

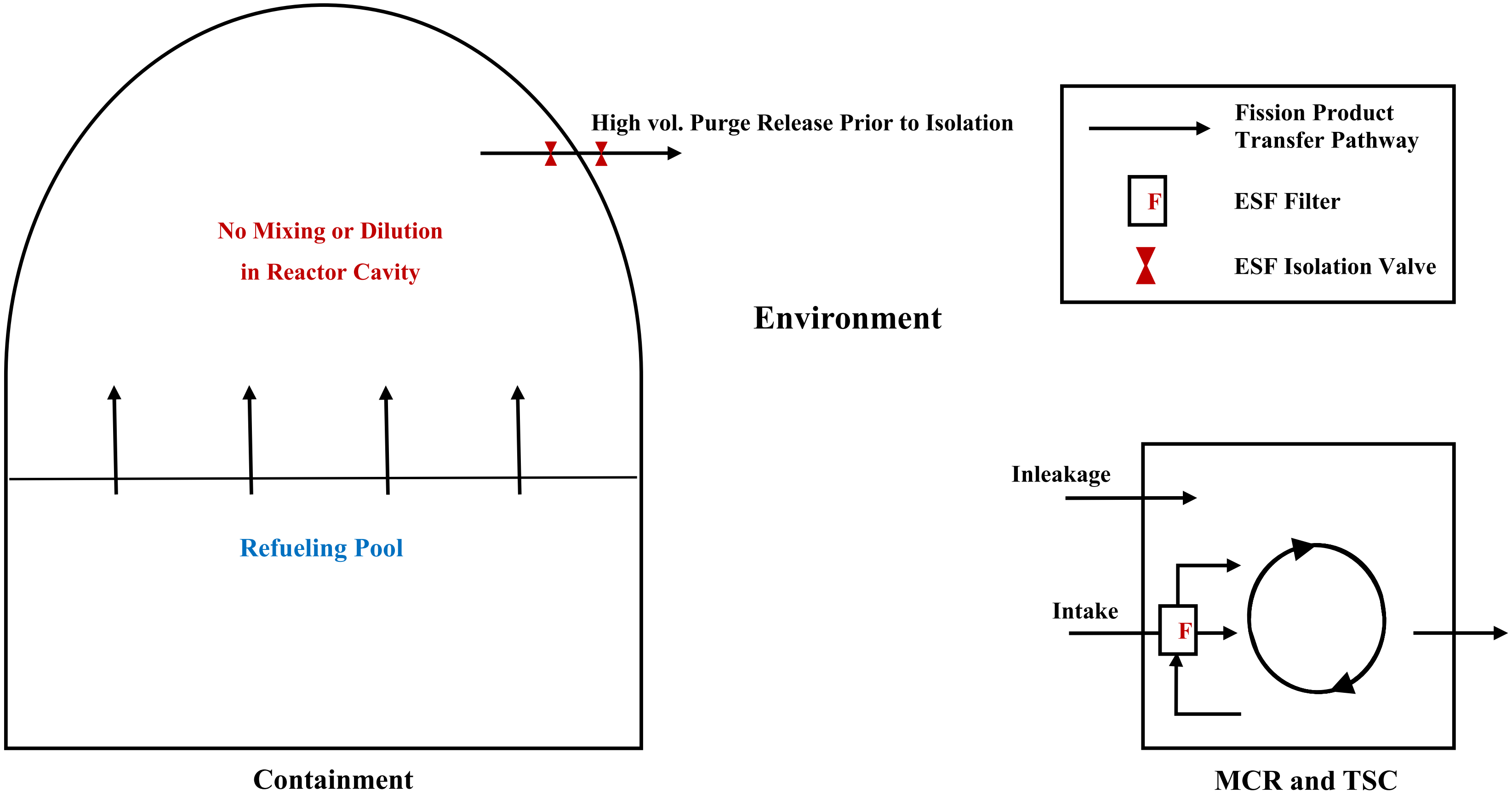

Figure 15A-8 Radioactivity Transport Model for Fuel Handling Accident (1 of 2)

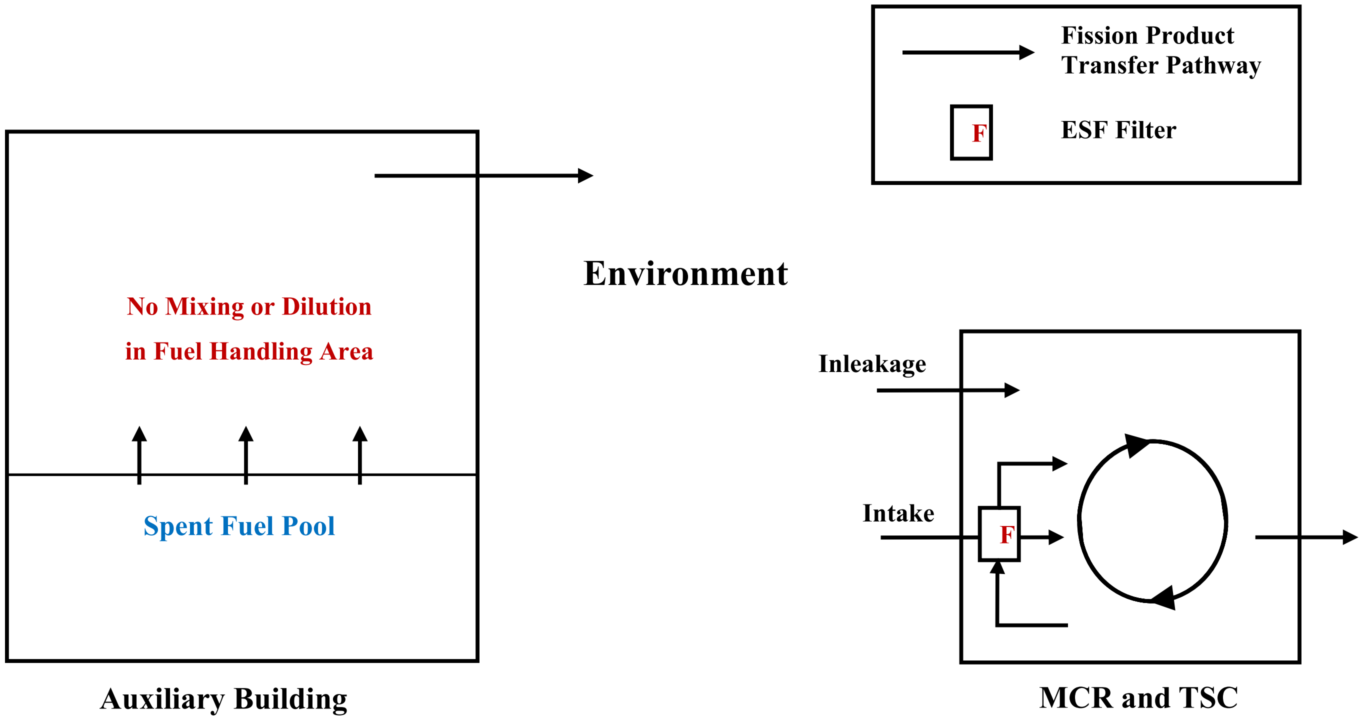

Figure 15A-8 Radioactivity Transport Model for Fuel Handling Accident (2 of 2)